# CHAPTER 1

## INTRODUCTION

### By L. J. Haworth

The cathode-ray tube is a form of visual indicator that permits an interpretation of electrical phenomena in terms of a picture painted on a phosphorescent screen by a sharply focused beam of electrons which is controlled in position and intensity by electrical signals. Under the proper conditions it paints this picture in an extremely facile way, being capable of utilizing many millions of separate data per second. Because of this facility and the ease and accuracy with which observations and measurements can be made, the device has had great importance in many diverse applications. As a laboratory and factory instrument, it is widely used for both qualitative and quantitative studies of electrical phenomena and of other phenomena that can be reduced to electrical terms. The geometrical picture that it presents makes it peculiarly appropriate as an indicator for television and radar.

The picture seen on the phosphorescent screen is called the "display," the "indication" or the "presentation." The tube itself is referred to as the "indicator," "indicator tube," "display tube," "CRT" or "scope."

Often when a tube presenting a particular form of display is to be identified, a descriptive adjective or code designation is prefixed to "scope." The words "indicator" and "scope" are often extended to include devices and circuits auxiliary to the cathode-ray tube proper.

This volume will describe displays and techniques of display production which were developed to provide indicators primarily for radar applications and secondarily for use in the electronics laboratory, although their usefulness is by no means confined to these fields. The cathode-ray tubes themselves will be discussed more from the functional than from the developmental standpoint although the latter will receive some emphasis in connection with screens and screen materials. A rather full account will be given of the methods of combining vacuum-tube circuits and other devices that provide the necessary voltages and currents for producing the displays. Other volumes of this series give more detailed descriptions of the component parts (Vol. 17) and of the fundamentals of the basic circuits (Vols. 18, 19, 20, 21). The application of the displays to operational radar is discussed in Vol. 1.

**1·1. The Cathode-ray Tube.**—A cathode-ray tube is an elongated vacuum tube with a cylindrical neck and an enlarged section or bulb that has a flattened front surface, containing or having associated with it as external components an electron gun, an electron-beam-deflecting system, and a phosphorescent screen (Fig. 1·1).

The *electron gun* comprises those electrodes that create, control, and focus the beam of electrons. It is placed axially within the neck of the tube, and consists of a heated *cathode* as the source of electrons, and one or more electrodes that form these electrons into a beam that travels axially down the tube at high velocity. The beam is controlled in
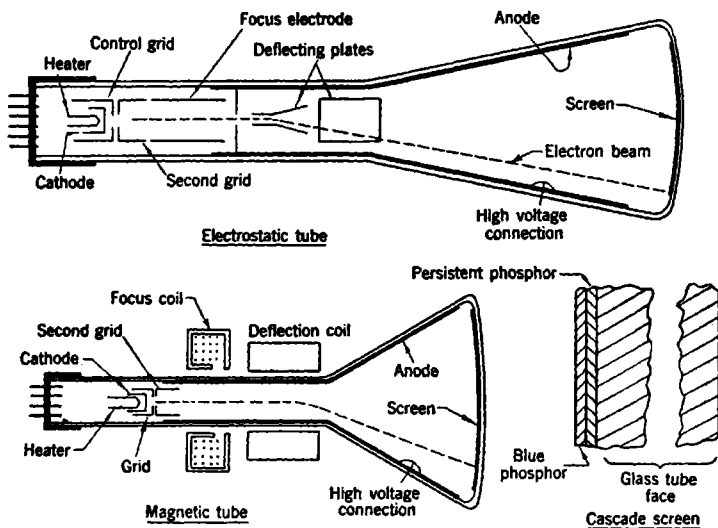


Fɪɢ. 1·1.—Elements of cathode-ray tubes.

intensity by a negative *control grid* consisting of a pierced diaphragm immediately in front of the cathode. Immediately in front of this grid may be an *accelerating grid* (sometimes called the *second grid*), which is either at a potential of several hundred volts positive with respect to the cathode or at full anode potential. If present, this electrode serves to make the beam current independent of variations in the potentials of subsequent electrodes. The electron beam is given its final high velocity by virtue of a potential difference of from 500 volts to several thousand volts maintained between the cathode and an anode formed by a conducting coating (usually Aquadag or Dixonite) on the inner glass surface over the region indicated. An additional element of the gun consists of a focusing *electron lens,* which makes this beam converge to a small area or spot at the front of the bulb. This electron lens may be either

*electrostatic* or *magnetostatic.*  If it is electrostatic, it is formed by the electric field distribution between the *focus electrode* (or *first anode*), which is maintained at an intermediate potential, and the high-voltage *second anode.*  Adjustment of focus is made by controlling the potential of the focus electrode.  If the focusing lens is magnetostatic, it is formed by the magnetic-field distribution along the axis of the tube set up by a focus coil or permanent magnet external to the tube.  In this case, focus adjustment is provided by varying either the current through the coil, or the position of a shunt in the case of a permanent-magnet focusing device.

*Deflection* is produced by transverse electric or magnetic fields in the region indicated in Fig. 1·1.  The same type of field is usually used for both deflection and focus; although electrostatic focus sometimes is combined with magnetic deflection.  In any case tubes are classified as "electrostatic" or "magnetic" in accordance with the method of deflection.

Electrostatic deflection is accomplished by passing the beam between each of two orthogonal pairs of *deflecting electrodes* or *plates* mounted in succession in the neck of the tube.  The deflection due to each pair is accurately proportional to the potential difference between them, and the two orthogonal deflections add vectorially.  If the deflections are to be large, best focal conditions are achieved by applying equal and opposite deflecting potentials to the two members of a pair so that the mean potential between them is independent of the deflection, and the electrons experience a minimum of longitudinal acceleration in passing through.

Magnetic deflection is accomplished by passing currents of the desired waveforms through a coil or a combination of coils surrounding the tube neck.  Permanent magnets are sometimes used to provide fixed deflections.  The deflection due to each coil is proportional to the current through it, and the individual deflections add vectorially.  Good focal conditions demand that all of the deflecting fields occupy the same axial region in the tube.

A single deflection coil[1] can be used to provide a polar display by mounting it on bearings so that a radial deflection in any desired direction can be produced.

Multiple coils are used in many different ways.  Often two are arranged orthogonally either to produce entirely independent deflections in a rectangular display or to provide the two cartesian components of the radial deflection in a polar display.  Occasionally two coils are used

----

[1] A "coil" usually consists of at least two separate windings that are symmetrically placed with respect to the tube and are connected either in series or in parallel.

to provide additive deflections in the same direction, especially if the frequencies involved are widely different.

A rotatable coil is frequently surrounded by an orthogonal pair of fixed coils or by a separately orientable single coil or magnet in order to provide a displacement of the origin of the polar display.

The design of deflection coils that can produce displays accurate in geometry and of good resolution is an exacting task, especially when this design must also incorporate maximum efficiency in driving power. Hand in hand with the design of the coils must go a consideration of the associated vacuum-tube or other electrical circuits that must accurately provide the necessary currents with a minimum of cost in size, weight, and power. A number of advances in both coil and circuit design, which have been made in connection with radar indicator development, will be described in later chapters.

*Comparison of Tube Types.*—At the present state of development, magnetic tubes produce sharper images than do electrostatic tubes of the same screen diameter. This fact is especially true at the higher electron beam currents.

Electrostatic tubes are far easier and cheaper to deflect than magnetic tubes at any except the lowest frequencies because of the induced voltages in the deflection coils of the latter.

The weight and size of an indicator are greater with a magnetic than with an electrostatic tube, partly because of the weight of magnetic-focusing and deflecting systems themselves and partly because of the power they require.

The particular size of tube to be used in a given application depends principally upon the conditions under which it is to be viewed and the requirements for *dispersion* of the picture, especially when measurements are to be made. The relative spot size, which determines the attainable resolution, is relatively independent of the size for each of the two varieties. Furthermore the operating cost is the same for all magnetic tubes and has no systematic dependence on size for electrostatic tubes.

*The Screen.*—The important characteristics of the screen are its efficiency, its color, its decay properties and the manner in which it "integrates" or "builds up" the effects of repeated signals.

Since the strength of the electron beam has definite upper limits set by a tendency to defocus at high intensities, and since the focal properties are seldom all that could be desired, it is important that the excitation efficiency of the screen should be as high as possible. This requirement is particularly vital when a given spot is being excited only a small fraction of the time as in many cases of complex or interrupted displays. It is important, of course, that the emitted light be in a spectral region

of high visual efficiency or, if the screen is to be photographed, that it be proper for that purpose.

The screen must have sufficient persistence ("afterglow") to permit observations and measurements and, in the usual case of a repeating picture, to make the picture as nearly continuous as possible. On the other hand the image must not persist so long as to cause confusion if the picture is a changing one. For photographic purposes a "fast," high-intensity blue screen is best. For visual observations three cases may be considered.

1. Those in which little or no persistence is needed, either because the picture repeats itself in a time less than the retentivity time of the eye (about $\frac{1}{20}$ sec), or because the spot moves so slowly that ample time is afforded for observation without persistence.

   Screens incorporating the familiar green willemite phosphor used in ordinary oscilloscopes and known as type P1 (phosphor number one) are widely used in such applications. This material has an exponential type of decay with a time constant of a few milliseconds and is extremely efficient in terms of light intensity.



FIG. 1·2.—Cathode-ray tube screen characteristics.

2. Applications in which persistence is needed to smooth out the effects of flicker. As will be seen in Sec. 18·8, a recently developed screen of zinc-magnesium fluoride with an exponential decay time of between 60 and 100 milliseconds (Fig. 1·2) and designated P12 serves quite well for this purpose except that its efficiency leaves something to be desired.

3. Applications in which the picture repeats itself so infrequently that considerable persistence is needed to afford viewing time and, in so far as possible, to provide a composite picture. This classification is especially important in radar applications where scanning periods may be as long as 20 or 30 sec. Exceedingly long persistence screens were developed for this purpose during the recent war. They incorporate the "cascade" principle in which the persistent phosphor, placed next to the glass, is principally excited by the light from a coating of a blue-emitting phosphor that receives its excitation directly from the electrons. For reasons to be explained
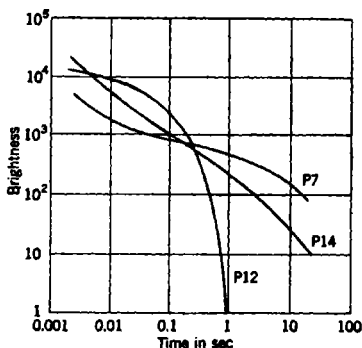
in Chap. 18 persistent phosphors excited in this way have much better "buildup" and decay properties for the uses intended than they would have if directly excited by the electrons.    Two such screens are commercially available—the P14, which is suitable for frame times up to a very few seconds, and the P7, which has a much longer persistence (Fig. 1·2).    Since the decay of these cascade screens is an inverse-power rather than an exponential function of the time, the disappearance of old signals is less clean-cut than with the P1 and P12 types.    Unfortunately no satisfactory phosphors with exponential decays of more than about 100 milliseconds have as yet been developed.

The problem of obtaining sufficient light from these long-persistence screens is a serious one, partly because the screens are not so very efficient and partly because they are usually excited only an extremely small fraction of the time.

The influence of the buildup and decay properties of the screens on the visibility of repeated signals, especially in the presence of disturbing interferences, can best be discussed after some of the applications involved have been more fully described.

A special type of persistent screen, known as the "skiatron" or "dark trace" screen, which has the property of darkening under electron excitation and is used principally for projection purposes, will be described in Chap. 18.

**1·2. The Geometry of Displays.**—In a majority of cathode-ray-tube applications one particular quantity, *the signal*, is to be studied as a function of one or more independent variables.    The signal may represent a voltage or current in an electrical circuit, an audio signal detected by a microphone, the "video" signals of television, the "echo" signals of radar, or almost any quantity that can be represented electrically. The independent variables may be any quantities, including time, on which the signals explicitly or implicitly depend.    In forming the displays the signal is used either to displace (*deflection-modulate*) or intensify (*intensity-modulate*) the electron beam (Fig. 1·3).    Independent variables are in general used only to displace the beam.    The motion resulting from one such variable is referred to as a "sweep."    The tracing of the pattern in response to all of the variables is called "scanning," and a pattern applied once is called a "single scan" or a "frame."    A particular method of scanning is often designated by prefixing a descriptive or a coded expression to the word scan (B-scan, PPI-scan).

In a *deflection-modulated display* the signal deflection is applied at right angles to an axis or *baseline*, determined by a *sweep*.    The result is a graphical representation that affords precise information on the

(a)                                    (b)

(c)                                    (d)

(e)                                    (f)
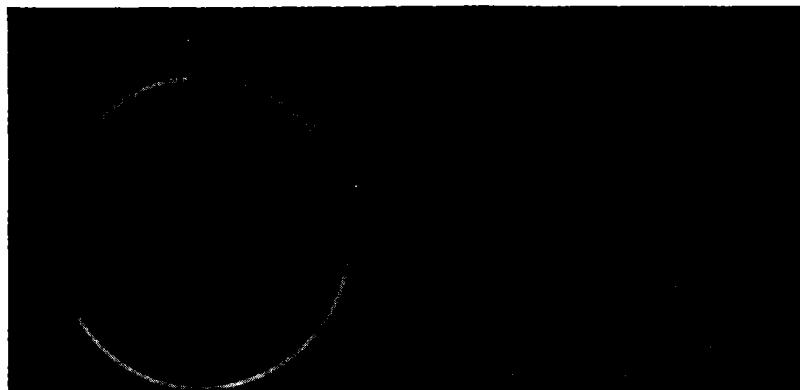
Fɪɢ. 1·3.—Typical cathode-ray tube displays.

strength and character of the signals in terms of a single variable.  In an *intensity-modulated* display each of the two coordinates of the tube face (cartesian or polar) represents an independent variable and the signals are applied to intensify the spot so that the display resembles a picture or a map.  Outstanding characteristics of the signals can be accurately located with respect to the independent variables but infor-

mation on their strength and character is only qualitative. In most laboratory applications, the display is deflection-modulated, the independent variable usually being time. In television, intensity modulation provides a "picture" in the ordinary sense. Both deflection and intensity modulation are used in radar, the echo signals being displayed in terms of one or two geometrical coordinates.

A *sweep* may be continuously *controlled* by *information* or *data* provided by an external source, or it may be an explicit function of time, with or without dependence on external parameters. The *data* pertinent to a *controlled sweep* may consist of voltages that are utilized, directly or through amplifiers, to deflect the beam proportionally; alternatively they may consist of means for controlling the orientation of a deflection coil used in a polar display.

A motion that is an explicit function of time is called a "time-base sweep." Such sweeps are of great importance in two ways. In many cases time itself is one of the desired display coordinates as, for example, when observing waveforms. In other applications a time base can be used to represent some other variable whose time dependence is known. For example, in radar a linear-time-base sweep is linear in radar range and is usually spoken of as a "range sweep." Similarly, in television, time serves as the connecting link between the linear scanning of the image tube in the "camera" and the identical scanning of the cathode-ray ("picture") tube in the receiver. The waveforms required to provide a time-base sweep are generated by some sort of electrical network in the indicator circuits. When the displacement represents some quantity other than time the initiation of the waveform must usually be "synchronized" with some external sequence of events in order that the zero of the coordinate be properly fixed. Often when time itself is the coordinate a similar synchronization with the signals must be provided.

Sometimes the characteristics of a time-base sweep are made responsive to the values of external parameters. Such a sweep is said to be *modulated* by the pertinent external data.

In a majority of applications continuity is supplied to the display by repeating the scan at more or less regular intervals. In many applications, such as radar and television, the repetition results from periodicities in the independent variables; in others, involving a time-base coordinate, repetition is "synchronized" with an explicit periodicity of the signals in time. If, in either case, the signals are identical from cycle to cycle the display pattern is stationary ("frozen") as in a photograph or a drawing (Fig. 1·3a) and observations and measurements can be easily and accurately made. If the pattern is a changing one, its progress can be readily followed unless the changes are of a random nature. Even if the signal is a transient one it is frequently possible to excite it again

and again in order to provide time for study.    Often the exciting stimulus is provided or initiated by a signal from the indicator itself.

In a deflection-modulated display the periodicity of the scan and of the sweep are the same.    A two-dimensional intensity-modulated display involves two sweep periodicities, the one of lower frequency determining the periodicity of the scan.    The appearance of the pattern depends upon the coordinates of the display, the periodicities involved, the relative time occupied by each sweep, and the form of the explicit or implicit dependence of the sweep speeds on time.    Consider, for example, the important case in which both sweeps are linear and the period of the faster sweep is short compared to the total frame period. A cartesian display will then consist of a set of parallel straight lines with a slope determined by the relative sweep speeds and a spacing determined by the ratio of the fast-sweep period to the total-frame period.    A polar display will consist of a set of radial but slightly spiraled "spokes" if the angular sweep period is the longer, or a continuously expanding spiral if the reverse is true.    In any of these cases successive scans will exactly superpose only if the two frequencies are commensurate. In a vast majority of cases, however, the ratio between the sweep periodicities is so great that neighboring traces overlap, giving a solid pattern that approximately superposes regardless of the exact frequency ratio.

**1·3.  Laboratory Instruments.**—The nature of most laboratory applications is such that the most useful displays are deflection-modulated. Electrostatic tubes are invariably used for this purpose because they are far easier to deflect than magnetic tubes and because the nature of the display is such that low electron-beam intensities with their attendant good focus can usually be used.

*The Synchroscope.*—Although special equipments are frequently used, most of the requirements for a laboratory instrument can be illustrated by the so-called "synchroscope."    This instrument consists of an electrostatic cathode-ray tube in a case that also encloses a variety of electronic circuits and power supplies for operating both the tube and the circuits.

Included in the circuits are means for providing a linear range sweep whose speed can be adjusted (usually in steps) over a wide range of values.    The sweep circuit is so arranged that the electron beam rests, with zero intensity, at one side of the tube until the receipt of a "trigger pulse," at which time the sweep begins and the beam is intensified by a square voltage wave applied to the control grid.    After passing across the tube the electron beam is cut off in intensity and is then quickly returned to the origin where it remains until the next trigger pulse. The trigger pulses may be supplied externally or they may be derived from an internal oscillator of variable frequency.    Pulses from the internal oscillator can be brought out of the synchroscope through an

external connection. The circuit that derives pulses from the internal oscillation can perform the same function for sinusoids or other regular or random external waveforms. Usually, means are provided for "scaling down" the pulses in a regular way so that only a fraction are used to trigger the sweep. When desired, the sweep can be triggered by a *delayed pulse* derived from a variable-time-delay circuit. Often the instrument contains sources of precise timing indices, which consist of very short pulses used to produce sharp pips at right angles to the base line of the sweep. These may consist of a set of discrete, uniformly spaced (in time) indices, or a continuously variable index, or both. The delay circuit and the time indices are not available in all synchroscopes.

Signals may be applied directly or through an amplifier to the deflecting plates orthogonal to those used by the sweep.

By means of these facilities the instrument can be used to study the sequence of signals following any regular or random external trigger pulse or following any particular phase of a more complex waveform. Several cycles of the signals may be viewed along the sweep by making use of the scaling circuit. If the delay circuit is available, any desired time interval can be examined in detail by using a fast, delayed sweep.

The internally derived trigger can be used to initiate any desired external sequence of events, the scaling and delay circuits serving the same roles as before. By means of a switch it is possible to interchange the role of the delayed and the undelayed triggers so that the sweep begins before a trigger is delivered to the outside. In this way it is possible to obtain a clear view of the initial stages of the signal resulting from the externally delivered trigger.

This device is much more flexible than the oscilloscope so familiar before the recent war. By comparison the latter suffers from the facts that it can be used only for regularly spaced signals, that it is difficult and often impossible to view a selected time interval on a fast sweep, and that there is no way of viewing a "single sweep." The presence of these features on the synchroscope render the oscilloscope obsolete except for very limited applications.

*The J-scope.*—A second extremely useful laboratory instrument, the J-scope, is used principally when very precise time measurements are desired. In this device the time base sweep is "wrapped" into a circle and the signal deflections are applied radially by means of a central electrode (Fig. 1·3c). The sweep is derived by applying a properly phased precision sinusoid applied in quadrature to the two pairs of deflecting plates. The frequency of the oscillation is made very high, but lower frequencies are made available through frequency-reducing circuits. For each signal sequence the tube is blanked on all but one sweep cycle so that a delayed sweep is effectively produced. Measure-

ments are made with the aid of fixed indices or by shifting the phase of the oscillation with respect to the signal sequence and using a single fixed index.   In either case the control knob must determine the phase (in whole and part cycles) at which the tube must be brightened.

<div align="center">RADAR DISPLAYS</div>

**1·4. Digression on Pulsed Radar.**—Since most of the displays to be described in this volume were originally developed for radar use, they can most easily be classified in that connection.   A brief description of the operation of pulsed radar will therefore be helpful.[1]

Radar operates on the echo principle.   Short, regularly spaced bursts (*pulses*) of radio-frequency waves are generated by an oscillator (*magnetron*) excited by a short pulse of d-c power from a modulator (Fig. 1·8). These are transmitted into space in a more or less narrow beam from a directional antenna.   An object (*target*) in the path of the beam scatters the radiation and some of it is returned to the antenna whence it is directed to a sensitive receiver and finally to an indicator such as a cathode-ray tube.   Since the radiation has a known velocity, equal to that of light, the range to a given target can be determined by measuring the time elapsing between the transmission of a pulse and the receipt of the corresponding echo.   The elapsed time and the range are related by the factor 10.8 $\mu$sec/statute mile, or 12.2 $\mu$sec/nautical mile; or, put in another way, $R/t = 167$ yd/$\mu$sec.   In order to avoid confusion, the time between pulses is made greater than that required for receipt of an echo from the maximum expected range.   The direction of the target is also known from the orientation of the antenna when the echo is received. Thus by "scanning" the beam about, it is possible to observe each target within range and, in principle, to plot its position.

Since maximum ranges lie between approximately 20 and 200 miles, depending upon the application, the range of pulse-repetition frequencies (PRF) is from a few hundred to a few thousand per second.   Pulse lengths vary from 0.1 to 5.0 $\mu$sec, 0.5 and 1.0 $\mu$sec being the most common. The *range resolution*, that is, the minimum distinguishable separation of targets in range is 167$\tau$ yd where $\tau$ is the pulse length in microseconds. The range of a resolvable target can be determined to a small fraction of this value, however, by timing some particular part of the echo pulse such as its leading edge.

The duration of the echo pulses range from the value $\tau$ in the case of a point target to much greater values for extended targets.   Thus the frequencies involved in the demodulated signals are in the range from a few times 1/$\tau$ down to very low values.

---

[1] The principles and design of radar are described in Vol. 1 of this series.

Resolution in angle depends upon the width of the r-f beam.  In microwave radar this varies from 0.5° to 10°.

Scanning is usually accomplished by rotating the antenna mount or *scanner* about one or two axes, although in some cases limited angles are scanned by mechanical or by electrical means internal to the antenna. During most operations, scanning proceeds continuously but in some circumstances the motion is stopped and the beam points (*searchlights*) in a manually controlled direction.

Many different scanning motions are used.  The most commonly used scan is a rotation about a vertical axis.  The r-f beam is made narrow in azimuth and has a vertical extension sufficient to cover the required sector in elevation.  The latter may vary from a few degrees when observing the earth's surface from a low level, to 45° or more when observing the surface from a high level, or aircraft from any location. A huge antenna used for long-range aircraft detection may rotate continuously through 360° as slowly as 2 rpm; a small one used at close range may rotate as rapidly as 100 rpm.  Smaller sectors can be covered in oscillatory fashion at approximately the same angular velocities. "Electrical" scanners cover a few degrees at rates as high as 10 or 20 scans per second.

With such antennas it is possible to obtain the azimuth angle (*bearing*) of each target.

Often elevation as well as azimuthal information is needed.  In one widely used method of acquiring this, a vertically narrow beam, fanned horizontally through a limited angle, is scanned rapidly about a horizontal axis.  In some cases the antenna is manually oriented in azimuth to point at the target, using information from a second radar set that is scanning horizontally.  In other cases a continuous azimuthal rotation is provided so that the beam executes a "vertical sawtooth" type of scan.

Other types of two-dimensional scanning include:

1.  The "spiral scan," in which a limited sector is covered by slowly tilting the antenna beam through an angle about a rapidly rotating axis;

2.  The "helical scan," a special case of the spiral scan in which the axis of rotation is vertical;

3.  The "horizontal sawtooth" in which the rapid azimuthal rotation of the helical scan is replaced by a rapid oscillation; and

4.  The "V-beam scan" in which a V-shaped beam with apex at the ground and one leg vertical is rotated in azimuth.  The azimuthal position of targets can be determined from the vertical lobe and the height from a combination of the range and the relative scanner orientations at which the target is detected by the two beams.

Those characteristics that concern the displays are given in Table 1·1 for a few typical radar sets.

TABLE 1·1.—CHARACTERISTICS OF SOME TYPES OF RADAR SETS

| Characteristic | Ground-based air search | Airborne sea search | Shipborne sea search | Airborne high-resolution (over land) | Height finder |
|---|---|---|---|---|---|
| Wavelength........ | 10 cm | 3 cm | 3 cm | 1 cm | 10 cm |
| Pulse length........ | 1 μsec | 0.5 and 1.0 μsec | 0.5 μsec | 0.25 and 1.0 μsec | 1 μsec |
| Repetition rate..... | 300/sec | 1200 and 600/sec | 800/sec | 2000 and 500/sec | 600/sec |
| Horizontal-beam width.......... | 0.5° | 2° | 1° | 0.6° | 5° |
| Vertical-beam width. | * | * | 6° | * | 1.3° |
| Scanning rate...... | 2 to 4 rpm | 30 rpm | 10 rpm | 20 to 60 rpm | 4/sec 2/min |
| Maximum range.... | 200 miles on aircraft | 75 miles on ship 100 miles on land | Horizon on ships 80 miles on mountains | 25 miles and 40 miles | 50 miles |

\* The beam in these cases is "fanned" vertically and is "shaped" in such a way that the energy is more concentrated in the horizontal direction where it is most needed.

**1·5. General Features of Radar Displays.**—The information available from a radar receiver may contain as many as several million separate data per second.   From these and other data, such as the orientation of the antenna, the indicator should present to the observer a continuous, easily understandable, geometrical picture of the radar targets under study, giving the size, shape, and, in so far as possible, the nature of each to any desired degree of accuracy.   A cathode-ray tube, the only available device that can begin to fulfill these requirements, does so to an astonishing degree.   Its principal shortcoming is that it cannot present a true three-dimensional picture.   Under very simple conditions it is possible to present a third dimension in an understandable, though unnatural way, but in any complicated three-dimensional situation, more than one display must be used.

The fundamental geometrical quantities involved in radar displays are the spherical coordinates—range, azimuth angle (or bearing), and elevation angle—relating the position of the target to the origin at the antenna.   Almost every radar display includes one or two of these quantities directly as coordinates of the tube face or is a simple modification of a display that does.

A vast majority of displays use as one coordinate the value of slant

range, its horizontal projection (ground range), or its vertical projection (altitude). Since slant range is involved in every radar situation, it inevitably appears in at least one display on every set. It is the coordinate that is duplicated most often when more than one type of display is used, partly because displays presenting range have the highest signal-to-noise discrimination (Sec. 1·11) and partly for geometrical reasons.

Range is displayed by means of a linear[1]-time-base sweep starting from a given point or line at a definite time in each pulse cycle. Thus distances along this *range sweep* are proportional to increments of slant range. The sweep speed determines the *scale factor*, relating distance on the tube to actual range, and the *sweep length*, or total distance represented. Distances are expressed in miles (statute or nautical) or yards. The origin of range may be on or off the tube face. Sometimes it is made virtual by delaying the start of the sweep for some time after the instant of transmission.

An angle at which the scanner is pointing, either in azimuth or elevation, may enter into a display (1) directly as a polar angle, (2) directly as a cartesian coordinate, or (3) as a basis for resolving a range sweep in a particular direction. These various methods will be better understood in connection with the specific display types.

Many considerations enter into the choice of the display geometry. In a three-dimensional problem the designer must decide how to divide the coordinates between two displays or how to arrange them in a single display, if this method is feasible. Even when reduced to two dimensions the problem is a complicated one, often involving conflicting requirements, such as the need for high resolution and dispersion without sacrificing the field of view. In some cases the needs can best be met by deliberately deforming the picture; in others it becomes necessary to use more than one display, either alternately on a single tube or simultaneously on different ones.

Many different display schemes have been employed to resolve these questions. The following summary includes the important geometries that have actually been used. (Many more permutations and combinations are possible but they have had little or no practical application to date. The various types will be described in detail in the next section.)

1. *One-dimensional Deflection-modulated Displays.* The independent variable is always range (type A, type J, etc.). Two such displays on a single tube are sometimes compared to obtain directional

---

[1] The range sweep must be nonlinear when range is to be projected in a plane not containing the radar set as, for example, in the case of true ground mapping on the indicator of an airborne radar.

information by comparing signal intensities from two different antenna-beam lobes (types K and L).

2. *Two-dimensional Intensity-modulated Displays.*    The signals appear as bright spots or patches against a background that is usually partially illuminated by the receiver noise.    These may be classified as follows:

a. The representation of a horizontal or vertical plane.

(1) True plots of a plane surface in which range and an angle are combined as polar coordinates (PPI).

(2) Deformed displays.

(a) Radial deformation of a polar plot, created by a shift of the range origin (open-center PPI, delayed PPI).

(b) Linear deformation created by "stretching" a polar plot along one rectangular axis ("stretched" PPI, the RHI).

(c) Rectangular plots of the polar coordinates range and angle (type B, type E, V-beam display).

b. Rectangular plots of azimuth and elevation.

(1) True displays that follow the antenna orientation (type C).

(2) Error indicator (type F.    Such displays are not always intensity-modulated.)

3. *Three-dimensional Intensity-modulated Displays.*    These are all modifications of two-dimensional displays in which one or more coordinates of the tube face present, in a formalized way, information about the third dimension being displayed.

*Indices.*—It is always desirable and usually mandatory to provide some form of index or marker for making geometrical measurements on the display.    Often these consist simply of a gridwork of regularly spaced lines from which fairly accurate values can be read at a glance. If high precision is required these are supplemented by a continuously movable interpolating index in each coordinate.    Often their controls are connected to devices providing remote data transmission, and movable markers are sometimes used for this reason alone.

The indices may be provided either by placing a transparent surface containing them as nearly as possible in optical superposition on the display or by modulating the electron beam in such a way that the marks appear as part of the display itself.

Lines ruled on a fixed transparency over the tube face are the simplest to provide but their use results in errors due to display inaccuracies and to parallax as well as to faulty interpolation.    Furthermore, in general, they do not lend themselves to changes in the origin of the scale factors of the display unless they are discrete and few enough in number so that multiple scales are not confusing.    Mechanical motions can be

introduced to provide for interpolation and for a moving display, but this method is usually cumbersome. Parallax may be largely overcome by methods of optical superposition (Chap. 16) but in their simplest form these indices are likely to be confusing, and the more elegant ones are bulky. Their principal usefulness is in connection with plotting and with superposing maps or charts on the display.

Electronic markers, produced by modulating the electron beam, reduce or eliminate most of these difficulties. They completely eliminate parallax and, because they can be generated by precision means that are independent of the sweeps, they automatically fall in their proper place on the display regardless of its position, its scale factor, or any deliberate or unintended distortion. In general the methods of producing interpolation indices are far less cumbersome than the mechanical methods but in many cases, especially on slow scans, the intermittency with which the display is "painted in" hinders the process of setting the index on the echo unless rather complicated switching methods are introduced to provide the markers at more frequent intervals.

Electronic indices are invariably used in range determinations. They consist of sharp pulses, generated by a precision timing circuit, that are introduced into the display along with the echo signals at the proper times on each pulse cycle. Almost every display entails a set of discrete markers derived from a precision oscillator that is properly phased with respect to the transmission of the r-f pulse. Since the radar data are inherently capable of providing very great accuracy in range determinations, and since fixed markers must be rather few in number to avoid confusion, an interpolating index is very often used. Fairly simple circuits providing an amazing degree of precision have been developed for this purpose.

In the case of angle determinations, the fundamental data are not so precise as in range determinations, and, in general, inaccuracies introduced by the display are less. For these reasons and in the interests of simplicity it has been most usual in the past to use a set of fixed indices engraved on a transparent overlay. In the particular case of a polar display (PPI) concentric with the tube face, these indices are often supplemented by a rotatable cursor. More recently, as the inherent accuracy of the data and the accuracy requirements have increased, electronic indices have been replacing mechanical angle markers. These can be produced most simply by brightening a few range sweep traces by means of a signal generated when the scanner passes through the position in question. This method is satisfactory for fixed, discrete indices and for a variable index on a fairly rapid scan. On slower scans the intermittency makes adjustment so slow that the switching methods alluded to above must be used. These are more costly and in the case of a mechanically rotating coil they cannot be used at all.

**1·6. One-dimensional Deflection-modulated Displays.**—Since one-dimensional displays yield little geometrical information, their only justification in radar is that they permit the use of deflection modulation, thereby yielding a maximum of information about the intensity and form of the echo signals. For this purpose it is best to display the signals as a function of time or range; therefore, the only radar displays using deflection modulation are those in which the deflections are applied perpendicular to a range sweep (Fig. 1·3b). As in the synchroscope, the sweep may represent part, or nearly all, of the period between pulses. In the former case the particular interval appearing on the display is determined by the delay elapsing between transmission of the outgoing pulse and the starting of the range sweep.

*The A-scope.*—The general classification *type A* is applied to describe such displays. An "A-scope" is universally used for observing the radar signals and the various circuit waveforms in a radar set during test and alignment. For this reason an A-scope is an indispensable adjunct to every radar set, either as a part of the permanent installation or as a piece of portable test equipment.

As an operational radar indicator the A-scope is, with modern narrow beam sets, used only when "searchlighting" and then chiefly as an instrument on which to make accurate range determinations or occasionally for decoding IFF or beacon signals.

*Range Scopes.*—The generic name "R-(for range) scope" is applied to several forms of modified A-scope used for accurate ranging. In all of them a greatly expanded display is combined with a precision timing device. In some cases the delay is only crudely calibrated, the entire precision being incorporated in a marker timing circuit. In others the delay circuit itself is a precision device and forms part of the complete timing equipment. The displays used are sometimes subclassified in terms of the particular type of electronic marker used (Sec. 6·3).

Sometimes an R-sweep and an A-sweep are shown simultaneously on the same tube by switching between them on alternate pulses. The A-sweep is used for general utility and for determining the proper delay for the R-sweep, either by inspection of the range scale or by displaying on the A-sweep an electronic marker that indicates the setting of the R-sweep delay. Such an indicator is called an "A-and R-scope" or an "A/R-scope" (Sec. 7·6).

A "J-scope" or a combination of a fast and a slow J-scope is often used for extremely accurate range determinations.

**1·7. Two-dimensional Intensity-modulated Displays.**—Most radar sets use a simple azimuth scan and present their data on an intensity-modulated display of the horizontal plane. Even when height (or elevation angle) is important some sort of range-azimuth display is usually basic to the indication system. The third coordinate usually appears in
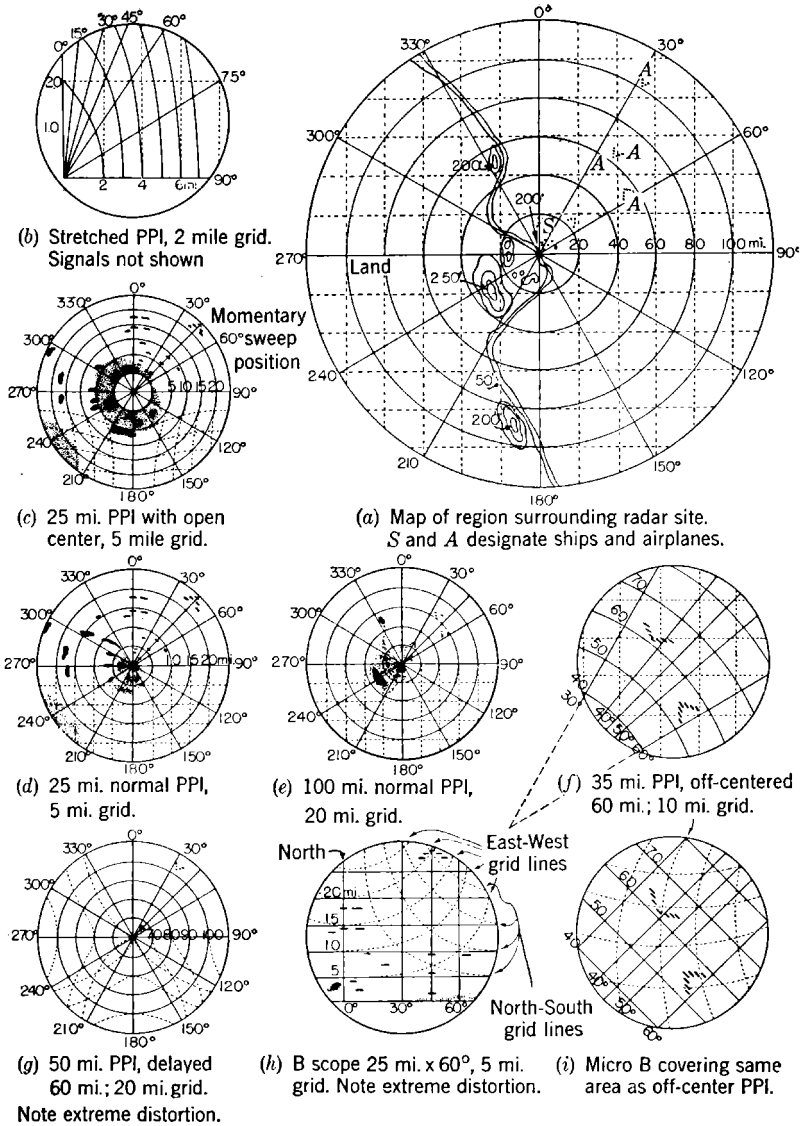
(b) Stretched PPI, 2 mile grid. Signals not shown

(c) 25 mi. PPI with open center, 5 mile grid.

(a) Map of region surrounding radar site. S and A designate ships and airplanes.

(d) 25 mi. normal PPI, 5 mi. grid.

(e) 100 mi. normal PPI, 20 mi. grid.

(f) 35 mi. PPI, off-centered 60 mi.; 10 mi. grid.

(g) 50 mi. PPI, delayed 60 mi.; 20 mi. grid. Note extreme distortion.

(h) B scope 25 mi. x 60°, 5 mi. grid. Note extreme distortion.

(i) Micro B covering same area as off-center PPI.

Fig. 1·4.—Radar display types.

a separate display on another tube, most frequently in a presentation of a vertical plane into which all the targets in a given azimuthal sector are projected. Thus intensity-modulated displays of plane surfaces, particularly the horizontal one, are the most important of those used in radar. Several such displays are diagrammed in Fig. 1·4.

*The Plan-position Indicator.*—If the ground range and azimuth angle of each target are represented respectively by the distance from a fixed origin and by azimuth angle on the tube face the result is a map with the radar site at the origin. Except when aircraft targets are observed at large elevation angles or when ground mapping is done from a very-high-flying aircraft, the difference between ground range and slant range is small and slant range is therefore usually used in the display.

An indicator used for such a display is known as a "plan-position indicator" or "PPI"[1] (Figs. 1·3e, 1·4d and 1·4e). It is achieved by rotating a range sweep about the range origin in synchronism with the azimuthal scanning of the antenna. The various targets then appear in the proper directions as well as at the proper relative distance from this origin and the result is a map.

The origin of the PPI may be at the center of the cathode-ray tube giving an equal field of view in all directions. Frequently, however, it is displaced, sometimes far off the tube face, in order to give a maximum expansion to a given region (Fig. 1·4f). Such a display is called an "off-center PPI." If the displacement is extreme it is frequently called a "sector" display.

The PPI is the most widely used and versatile of all displays. In presenting the information with which it deals, its only fundamental shortcoming is that, in common with all maps or charts, it cannot simultaneously possess a highly expanded scale and a large field of view.

The vertical analogue of the PPI may, of course, be formed by substituting elevation for azimuth angle but it is more customary to use deformed displays for this purpose.

In spite of the usefulness of a true display such as the PPI, occasions arise in which it is not ideal. These occasions usually involve the need for providing high resolution or dispersion in some particular coordinate without restricting the field of view too severely in other dimensions. A number of types of deformed displays have been devised for such purposes; they are particularly useful when dealing with point targets.

*Radial Deformation.*—Two types of radial deformation of the PPI have been widely used. In the *open-center PPI* (Fig. 1·4c), the origin is expanded into a circle in order that more accurate bearing determinations

[1] The abbreviation "PPI" is used interchangeably to represent both the *indicator* and the *indication*. The same double usage applies to abbreviations used for other types of indicators.

may be made on a nearby target, as, for example, when "homing." Range and bearing scales remain linear but relative target positions and the shapes of extended targets are deformed, especially near the origin. The *delayed PPI* (Fig. 1.4*g*), so-called because of the technique used, collapses an annulus ring into a solid circle. By this means, high resolution and dispersion can be provided on distant targets without sacrificing an all-around view as an off-center PPI would do. The extent of the resulting deformation depends upon the amount of the delay relative to the range interval covered by the display. It is most serious near the center of the display.

*Linear Deformation (the "Stretched" PPI, the RHI).*— A deformed display of considerable utility, especially in the vertical plane, can be formed by "stretching" a polar plot in one rectangular dimension as
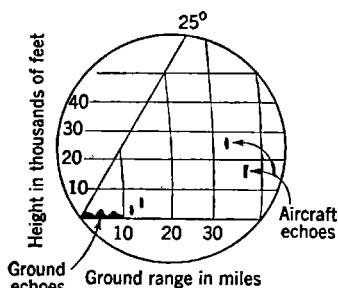


Fig. 1·5.—Range-height indication.

though it were on a sheet of rubber. On such a display the cartesian coordinates parallel and perpendicular to the axis of stretch retain their original meaning and their linearity but they have different scale factors. Straight lines remain straight but, except for those parallel to the coordinate axes, their directions are changed. Circles of equal range appear as ellipses with their major axes in the direction of the stretching.

This technique finds its greatest use in the determination of the height of aircraft. For this purpose the display, known as "range-height indication" (RHI) (Fig. 1·5) represents a vertical plane on which all of the aircraft in any desired azimuthal sector are shown. Because the maximum height of aircraft is much less than the range interval usually of interest, and because it is usually required that height be measured to a high degree of accuracy, a vertically stretched display is extremely desirable. The amount of stretching which may be effectively used is determined by the ground-range interval portrayed as compared to the airplane ceiling. The RHI is always used in conjunction with a PPI or other horizontal display, which often obtains its data from another radar set. Correlation of the echoes between the displays is made partly by azimuthal position and partly by range. If the height-finding antenna scans rather than searchlights in azimuth, the RHI is usually blanked except during a narrow azimuthal interval that may be chosen at will.

The horizontal counterpart of the RHI, sometimes called the "stretched" PPI (Fig. 1·4*b*), is used principally in connection with the

ground control of aircraft approaching a landing.   The stretching is done perpendicularly to the landing strip and aids greatly in detecting slight deviations from the proper course.

*Rectangular Presentation of Range and Angle (Type B, Type E).*—A plane surface is often represented in a deformed manner by combining range and angle in cartesian rather than polar coordinates.   This display is obtained by moving a range sweep laterally across the tube face in synchronism with the antenna motion so that the origin is stretched out into a straight line.

In range and azimuth these rectangular displays, known as "Type B," are of two different sorts.

1. Displays in which no attempt is made to minimize the deformation, either because it is unimportant in the particular circumstances or because certain advantages can be gained by neglecting it (Figs. 1·3d and 1·4h).   Any desired range interval and azimuthal sector may be covered, although in practice more than 180° is rarely used. The display is normalized to make optimum use of the tube face. At short range the angular resolution and dispersion are far greater than in the PPI.   The display is used in situations in which the chief considerations are the range and bearing of point targets or groups of targets with little or no importance attached to the shapes of extended targets or the relative locations of widely separated targets.   It is of special usefulness in homing operations, and in determining range and bearing.

2. Displays in which the desired angular field of view is so small that the distortion can be made negligible by properly normalizing the range and angle scales (Fig. 1·4i).   Such a display, known as a "micro-B," is simply a substitute for a PPI sector and is used either because it is technically easier to attain or because the same indicator is alternately used for a regular B display.   Proper normalization requires that the angular dispersion be kept proportional to the range to the center of the display.

The vertical analogue of these displays, known as "type E," is used instead of the RHI when elevation angle rather than height is desired. In some older sets, it is also used to determine height by means of an engraved hyperbolic scale, but in modern practice the RHI is used for this purpose.   The analogue of the micro-B is never used because deformation does no particular harm in this case and its use permits both a large field of view in range and a high dispersion in angle.   A modification of the type E display, which is used with the V-beam antenna, is described in Sec. 15·5.

*Azimuth-elevation (Type C) Indication.*—Azimuth and elevation angle are used as rectangular coordinates of the tube face in the type C indication (Fig. 1·6). The electron beam scans the tube face in synchronism with the two-dimensional antenna motion and the video signals are applied as intensity modulation in the usual way. This display has the great disadvantage that the signal discrimination is very poor if an appreciable fraction of the pulse cycle is used for the reception of signals. For this reason the cathode-ray tube is activated during only the short time interval that includes the signal. The proper delay is determined from another display that involves range. The C-scope is used principally in connection with homing or firing on a point target.
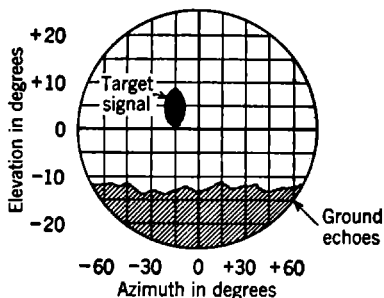

Fig. 1·6.—Type C indication.

**1·8. Three-dimensional Displays.**—Two conventionalized three-dimensional displays have been successfully used in situations involving relatively few targets.

*The "Double Dot" Display.*—This is a modified type B presentation on which the elevation angle is roughly indicated. On alternate range
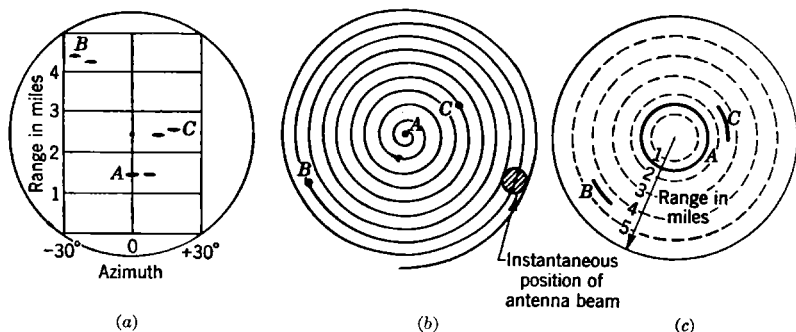


Fig. 1·7.—Three-dimensional displays. *A, B* and *C* are targets. (*a*) Double-dot display. (*b*) Spiral scan. (*c*) Radial-time-base indicator.

sweeps the origin of the pattern is moved to the right and left respectively by a fixed amount (Fig. 1·7a). On the sweeps corresponding to the right-hand position, the origin is simultaneously shifted vertically by an amount proportional to the sine of the elevation angle. Any single echo therefore appears in two neighboring positions, and the slope of the line joining the two "dots" is a rough measure of elevation angle

which is accurate to two or three degrees under the usual circumstances of use. This display has been used in air-to-air homing.

*Three-dimensional "Radial Time Base."*—A radial time base can be used as a three-dimensional display, most easily with a spiral scan. A range sweep moves from the center of the tube in a direction corresponding to the projection of the antenna beam on a plane perpendicular to the axis of scanning (Fig. 1·7c). The echoes therefore appear at radial distances corresponding to their range. If the target is on the symmetry axis of the scan, it is equally illuminated at all "spin" angles and the echo appears as a full circle (Target *A*). If it is far off axis it is illuminated only through a narrow spin angle (Target *B*) and the arc on the display is short. Target *C* indicates an intermediate case. The display is surprisingly easy to interpret after a short period of observation. The technique of providing this display is exactly the same as that for one PPI, the spin angle taking the place of azimuth angle.

**1·9. Error Indicators.**—A cathode-ray tube may be used as a radar indicator in a very different way from those so far described, that is, as a meter on which to display various forms of intelligence. One common application of this type is its use to indicate accuracy of pointing in connection with a conical scan. The signal intensity is combined electrically with the scanning information to provide voltages proportional to (or at least increasing with) the pointing error in both azimuth and elevation, and these voltages are used to deflect the spot. A departure of the spot from the tube center indicates the direction and, to a qualitative degree at least, the magnitude of the pointing error. The radar signal is sometimes used to intensify the spot in order to be able to distinguish between perfect pointing and no target. Range can be indicated by causing the spot to grow "wings" whose length is some rough inverse measure of the range. In this form the indication gives to a surprising degree the illusion of an actual aircraft that apparently grows larger as it approaches.

**1·10. The Elements of Complete Indicators.**—The equipment auxiliary to the cathode-ray tube varies widely with different situations but a few general statements can be made. Those parts concerned with the pulse repetition cycle are collectively called the "timer" (Fig. 1·8). The timer provides synchronization with the modulator, sweeps, and markers for the display and measurement of range, blanking of the cathode-ray tube during unused portions of the pulse cycle, and other related operations that may arise in special cases. The remaining equipment, other than the necessary power supplies, is mainly concerned with the display and measurement of geometrical quantities other than range.

Because time is always measured with respect to the instant at which the modulator fires, synchronization between the modulator and the
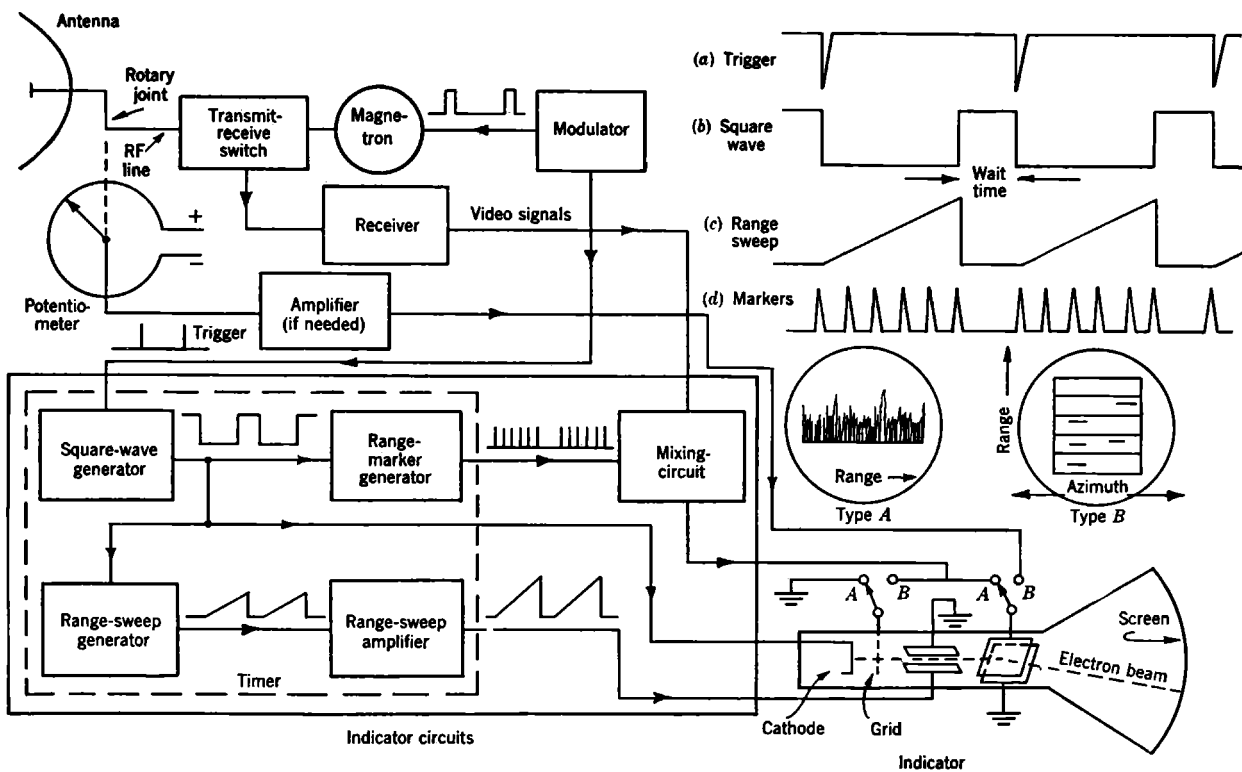
FIG. 1·8.—Typical radar indicator and its relationship to other components.

timer is of basic importance.    In some cases, the timer exerts precise control of the exact firing time of the modulator by sending it a trigger pulse; in others, it responds to a trigger from the modulator.    In the latter case, the system is said to be "self-synchronous."[1]    Although certain advantages can often be derived by giving control to the timer, this method cannot always be used,[2] and it is sometimes inconvenient in a multiple-display system.    Figure 1·8 illustrates a self-synchronous system.    Some of the departures possible when the timer does the synchronizing will be pointed out later.

The cathode-ray tube must be turned on only during the fraction of the pulse cycle in which it is used.    One portion of the timer generates a square wave (Waveform *b*, Fig. 1·8) that performs this function and usually finds other applications within the timer.

If the display includes a range sweep, as is nearly always the case, the timer generates the waveform that ultimately produces it.    This waveform usually consists of a linearly increasing voltage wave that begins at the initiation of the sweep and returns to the initial condition at its end (Waveform *c*, Fig. 1·8).    This method of operation involves a switching action, which (as indicated in Fig. 1·8) is usually provided by the same square wave that turns on the cathode-ray tube.

The timer generates a set of discrete range markers: sharp video pulses occurring at regular, precisely known intervals.    In a self-synchronous system, the markers must be recycled on each transmitter pulse; a transient oscillator is therefore required.    In the simple example illustrated, the square wave *b* provides the necessary switching voltage. Often the discrete range markers are supplemented by a continuously variable range marker that may be generated in any of several ways. As indicated in Fig. 1·8, the markers are usually mixed with the radar video signals and the combination applied to the cathode-ray tube.    In some cases, however, the signals and the markers are applied separately to different electrodes of the cathode-ray tube.

The equipment illustrated does not provide for the use of a delayed sweep.    If one is to be used, separate square-wave generators are necessary to switch the range-marker circuit and to perform the other functions.    The generator used to switch the range-marker circuit must be triggered directly as before.    The other generator must be provided with

[1] A trigger generator for the modulator is sometimes housed with the indicator equipment for convenience, but the actual synchronization is accomplished by transmitting the modulator pulse to the timer proper.    This case is functionally identical with that in which the trigger source is physically part of the modulator.

[2] Certain modulators, such as the rotary gap, cannot be triggered at all.    Other types can be triggered, but have so variable a response time that the modulator pulse itself must be used for synchronization in order to provide the necessary precision.

a delayed trigger that may come from a continuously variable timing circuit or may be one pulse of a discrete set, often the range-marker pulses themselves.    The continuous type of delay is frequently associated with a continuous precision range marker.

Many deviations from Fig. 1·8 are possible if the timer provides the synchronizing pulse.    In particular, the discrete range markers can then be derived from a high-precision c-w oscillator, one of the marker pulses being selected as the modulator trigger by a scaling-down process.    A continuous marker may also be provided from this oscillator by means of a continuous phase-shifting device.    Other advantages of the timer-controlled synchronization entail the use of a "pretrigger" by means of which the actions of certain circuits can be initiated somewhat in advance of the firing of the modulator.

Many other functions, some of which will appear in later sections, are performed by the timer in complex situations.

Before proceeding farther in the discussion of the indicating equipment, it is necessary to specify the type of display.    For illustrative purposes, Fig. 1·8 has been arranged to illustrate a simple A-scope or, alternatively, a simple B-scope.    The former requires no equipment beyond that already described.    The connections to the cathode-ray tube are shown as position *A* of the switch.    The range-sweep voltage is applied to one pair of deflecting plates and the signal- and range-mark voltages to the other.    The square wave controlling the cathode-ray-tube intensity is applied to the cathode in proper polarity to brighten the tube during the range sweep.    The same arrangement forms the basis of most synchroscopes.

In the B-scope display, the range sweep is applied to a deflection plate just as before.    Signal modulation is applied to the control grid, and the second set of deflecting plates receives a voltage that produces the azimuthal deflection.    This voltage may be furnished, in simple cases, by a linear potentiometer geared to the scan axis.    Amplification may sometimes be necessary before applying the azimuth sweep voltage to the cathode-ray tube.    The circuits shown are equally applicable to a magnetic tube, the only appreciable changes being in the deflection amplifiers.

The timer of Fig. 1·8 can be used in the production of many other types of indication.    For example, Fig. 1·9 shows the additional parts necessary to generate one type of PPI, and Fig. 1·10 those necessary for a (technically) different PPI or, alternatively, for one form of RHI.

The PPI of Fig. 1·9 is of the so-called "rotating coil" type.    A single deflection coil driven by the range-sweep amplifier produces a radial range sweep.    By means of some form of electro-mechanical repeater, this sweep is made to take the direction on the tube face which corre-

sponds to the instantaneous antenna orientation.   Except for this modification in the deflection system, the display circuits may be identical to that of the B-scope of Fig. 1·8.
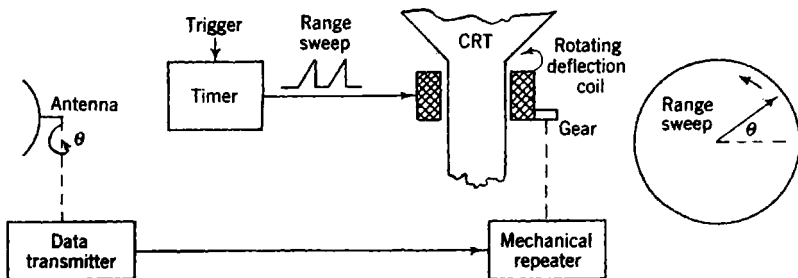


FIG. 1·9.—Rotating-coil PPI.

Figure 1·10 shows the parts necessary to convert Fig. 1·8 to an "electronic" PPI without moving parts, or, by a slight variation, to an RHI.   The range sweep of a PPI can be considered to be made up of two orthogonal sweeps with speeds proportional to $\sin \theta$ and $\cos \theta$ (see sketch in Fig. 1·10).   In this particular form of PPI, these sweep
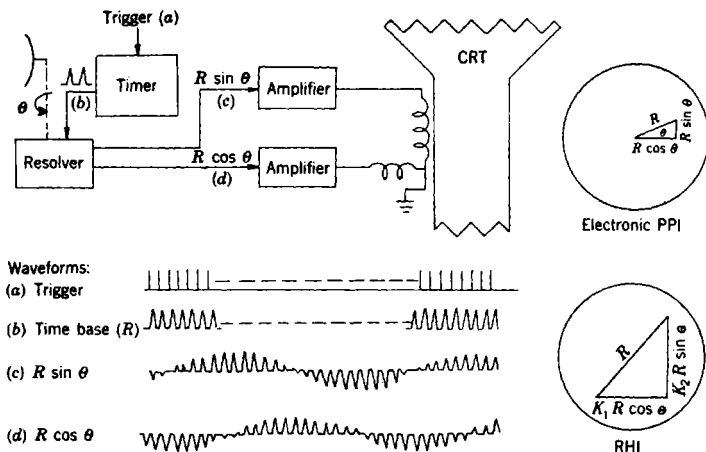


FIG. 1·10.—Electronic PPI and RHI.

components are formed by passing a sawtooth waveform through a sine-cosine resolver on the scanner.   The resolver is a variocoupler or a sine-cosine potentiometer that, when excited by a given waveform, produces two components of the same waveform but proportional respectively to the sine and the cosine of the orientation angle of the resolver.   Proper

amplifiers are provided for driving either a pair of orthogonal coils (as indicated in Fig. 1·10) or the deflecting plates of an electrostatic tube.

If elevation angle is substituted for azimuth angle, the device becomes an RHI. Usually, in this case, the gain of the vertical amplifier is made greater than that of the horizontal amplifier, and the display is therefore "stretched" in the vertical direction. Since direct-coupled push-pull sweep amplifiers are usually used, they can be biased in such a way as to produce the off-centering shown.

## SIGNAL DISCERNIBILITY AND RESOLUTION

In order that the radar operator may obtain a maximum of information, it is essential that the display aid in every possible way his ability to detect weak echoes and to distinguish details when the echo pattern is a complex one. These problems, which are closely related, involve principally such display characteristics as the type of display, the spot size, the sweep speed, and the properties of the screen.

**1·11. Signal Discrimination.**—The ultimate limitation in detecting weak echo signals is nearly always set by the inherent noise of the radar receiver. The noise energy, which is generated in the input circuits of the receiver, is distributed uniformly throughout the whole frequency spectrum. One of the major problems of radar-set design is to maximize the discernibility of weak signals in the presence of this noise. The broad aspects of this problem are discussed elsewhere in these volumes.[1] Those factors that concern the display will be considered briefly here and in Chap. 18. The signal discernibility depends on a great number of intimately related factors involving almost all of the components and many of the design parameters of the radar set. One of the most important of these factors is the *signal-to-noise ratio*, that is, the ratio of the power contained in the video signal to the average noise power. Within the radar set this ratio is determined by the power delivered to the antenna by the transmitter, the antenna characteristics, the losses in the various r-f components, the noise generated in the receiver, and the frequency response of the receiver and the video amplifier. Of these, only the frequency response needs to be discussed here. Both theory and experiment have shown that for this type of signal, the maximum signal-to-noise ratio is attained when the i-f bandwidth $\mathcal{B}$ is approximately 1.2 times the reciprocal of the pulse length $\tau$; that is, when $\mathcal{B} = 1.2/\tau$, where $\mathcal{B}$ is in Mc/sec if $\tau$ is in $\mu$sec. If $\mathcal{B}$ is appreciably less than this optimum value, the loss in signal energy through rejection of its higher-frequency components is proportionally greater than the accompanying rejection of noise. For $\mathcal{B}$ greater than the optimum value the energy contained in the frequency spectrum of the signal is

[1] Chap. 2, Vol. 1 and Chaps. 8 and 9, Vol. 24 of the Radiation Laboratory Series.

not sufficiently great to compensate for the linear increase in the noise energy passed when the bandwidth is increased. However, the maximum is a rather broad one and therefore little sacrifice is made in signal-to-noise ratio if the bandwidth is made, for example, twice as great as the optimum value. This, then, is the bandwidth usually chosen in order to make the receiver tuning less critical and to preserve the pulse shape in the interests of good range resolution.

Thus in the signals delivered to the detector and video amplifier, appreciable energy is contained in frequency components as high as two or three times the reciprocal of the pulse length. In the case of a 1-$\mu$sec pulse, these frequency components are 2 or 3 Mc/sec. It is the function of the video amplifier and the display proper to so treat these signals that the signal-to-noise discernibility is as great as possible within the limits set by other requirements.

An extremely important aspect of this problem is the fact that the receiver noise is entirely random in character; therefore the problem is a statistical one. Since, as in all such cases, the ability to draw a correct conclusion is enhanced by making a large number of observations, it is desirable to average or sum measurements over as many pulse cycles as possible. Before the implications of this fact are examined in detail, another consideration arising from the random nature of the noise will be discussed.

Because in pulsed radar the echo from a small target lasts for only a very small fraction of the pulse repetition cycle, it is obvious that the greatest signal discernibility will be achieved if the observations can be made in such a way that the output signal of the receiver is examined not in terms of the average power over the entire pulse cycle, but rather in terms of the average power during time intervals comparable with the pulse length.

Fortunately, a cathode-ray-tube display that includes a *range sweep* provides an excellent means for making these observations. Comparisons are made in terms of elementary units of the tube face, the size of which is determined by the spot size of the tube or the visual acuity of the observer. The time interval included in each observational element is, of course, inversely proportional to the speed of the sweep. If the latter is low the data are integrated over a time interval that is long compared to the pulse length, and the signal must compete against an unnecessary amount of noise. For very slow sweeps, the power necessary for the signal to be discernible is inversely proportional to the square root of the sweep speed. As the speed is increased, further changes become less and less important and an optimum condition is reached when the speed is such that the beam moves approximately 1 mm (or one spot size if it is greater than 1 mm) during the duration of the signal.

Beyond this point the discernibility slowly decreases although not enough to be of practical importance. The reasons for this behavior are not clearly understood but they are probably connected with the fact that, as the signal is smeared out on the display, the contrast gradient between it and its surroundings is lessened, and with the fact that the randomness of the data results in graininess in the display.

An idea of the magnitude of the above effects can be gathered from the fact that if a 1-$\mu$sec signal is displayed on a 7-in. PPI tube the minimum discernible signal power must be approximately 2 db (60 per cent) higher on a 50-mile sweep than under the optimum conditions of an 8- or 10-mile sweep.

It is clear from this discussion that a type C display provides extremely poor discernibility because the receiver output signal is integrated over the entire pulse cycle. Since there is no range sweep the motion that determines the observational interval is the much slower one provided by the antenna scan, although this interval is determined in a somewhat different way than in the case of the range sweep.

Considerations such as the preceding ones place requirements on the bandwidth of the video amplifier. If its bandwidth is too small, it effectively integrates the data over an unnecessarily long time interval with much the same effect as that produced by a slow sweep. For this reason and for the sake of good range resolution, the bandwidth of the video amplifier in a well-designed set is always made appreciably higher than half the i-f bandwidth.

It has been stated earlier that the signal discernibility depends upon the number of pulse cycles included in the observation. Statistical considerations predict and experiment has proved that the power necessary in a "minimum detectable" signal is inversely proportional to the square root of the number of pulses included in the observation, provided that all of the elements concerned in the integration are linear. The number of pulses included is proportional to the pulse-repetition rate of the transmitter and to the time over which evidence accumulates. The factors determining the latter depend upon the particular situation involved.

In the case of a deflection-modulated display with the antenna stationary, the integration time is determined by the eye and mind of the operator or by the cathode-ray-tube screen, depending upon which can average the signals over the longer interval. Experiments testing the operator's memory have been performed by applying the signals at a fixed PRF for a definite time interval to an A-scope with a short persistence (P1) screen. For reasons of simplicity of analysis the signal was confined to some one of six known positions on the sweep. It was found that as the time interval was increased the inverse-square-root law

was obeyed up to almost 10 sec and even then broke down only slowly. This "memory time" may well be somewhat shorter in the practical case where the whole trace must be considered.   On the other hand it is
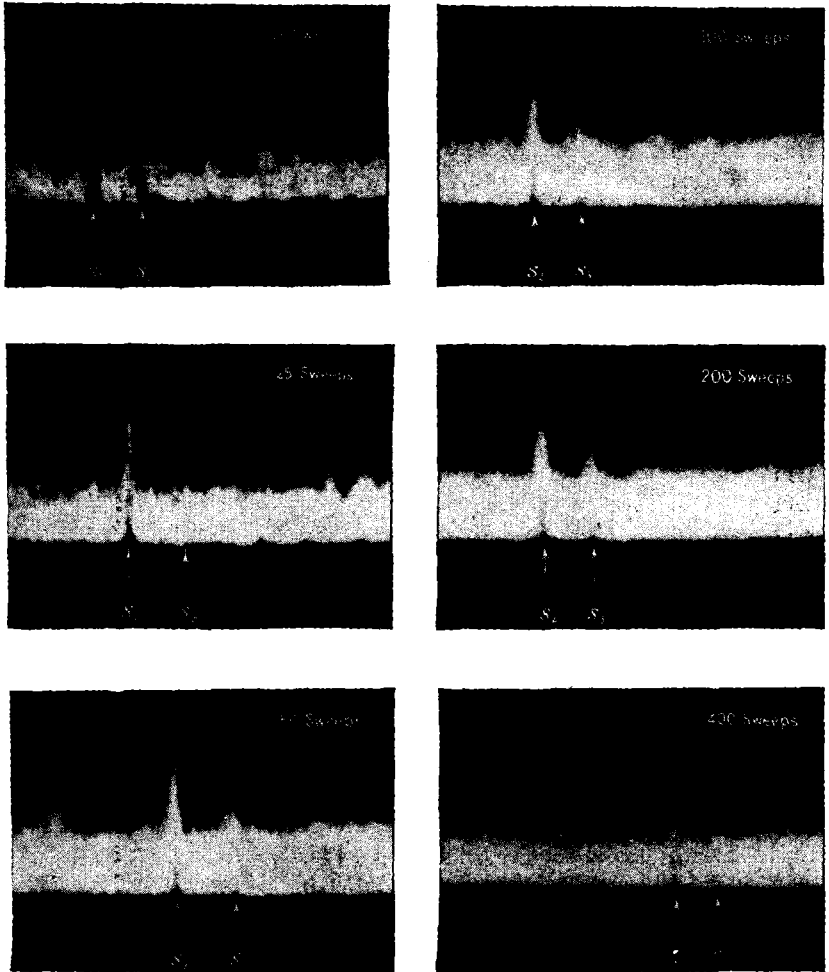


FIG. 1·11.—Effects of pulse repetition on signal visibility.   In this series of photographs the number of A-scope sweeps recorded during each exposure was varied from 12 to 400. Artificial signals were injected at the locations marked, with the following strength relative to average noise power: $S_1$: +10 db; $S_2$: +5 db; $S_3$: 0 db; $S_4$: −5 db.

usually true that in the final stages of an observation the operator concentrates on a region where he suspects that a signal is manifesting itself. The effect of increasing the number of pulses is clearly shown in Fig. 1·11

where the camera has been substituted for the eye and mind of the observer.

Since the memory time of the observer is so long, it can be aided appreciably only by a very long persistence screen. The preceding experiments, repeated with a P7 screen, indicated a decrease of about 1.5 db (40 per cent) in the necessary signal power as compared to the P1 screen when the signals were applied indefinitely.[1] This rather small improvement is offset by the poorer resolution of the cascade screen (Sec. 18·9) and by the confusion resulting if the picture is changing. For this reason and because signal discernibility is not, in the case of modern radar sets, of very great importance on type A displays, persistent screens have not been widely used for this purpose in the United States.

It should be pointed out that when certain forms of man-made interference are present, the improvement obtained by using a long-persistent screen is much greater than when the random receiver noise is the limiting factor. Indeed, it was for this application that the cascade screen was originally developed in England.

In an intensity-modulated display the number of integrated pulses is determined by the PRF and by the method and rate of scanning, the memory of the observer, the screen characteristics, or some combination of these factors. From this standpoint alone the ideal screen would be one on which the intensity of each spot would represent the average of all the excitations received over a very long time in the past. The limits within which this requirement can be met are set by (1) the achievable properties of the screen and (2) the degree to which past information can be retained without causing confusion as the picture changes.

The screen properties of importance in this connection are the type of decay and the manner in which the light intensity "builds up" under successive excitations.

In order to examine these effects, consider first a scan that is so slow that either the limitations of achievable persistence or the requirements of freedom from confusion prevent appreciable storage of information from one scan to the next. In such a case the averaging is to be done over a single pulse group occurring in a time that, with modern narrow antenna beams and customary scanning rates, is always short compared to the total scanning time and to the achievable decay times. In order, then, to give the operator a composite picture and time to make observations, the screen chosen will have sufficient persistence so that there

---

[1] Experiments in England showed somewhat greater improvement with a small fraction of the tubes used.

is no appreciable decay[1] during the process of scanning across the target, and the entire echo arc will be observable at one time. In order, however, that the average intensity of this arc shall represent all of the data, it is essential that the screen integrate the effects of all the pulses that overlap on a given focal spot; that is, it should not saturate too quickly. The number of overlapping pulses, which is often large, is given for a PPI by the expression $NS/\omega r$ at the center of the arc, where $N$ is the PRF, $S$ is the spot size, $\omega$ is the angular velocity of the scan and $r$ is the distance from the origin of the display to the echo spot. For example, with a 30-sec scan and a PRF of 300 there are about 7 overlapping pulses at "ranges" corresponding to the tube radius, $R$ (assuming $S/R = \frac{1}{180}$). The number increases with decreased distance until the entire pulse group, consisting in this case of 25 pulses, is included. The property of buildup in intensity from the excitation by such a group of successive pulses is possessed to an adequate degree by all cascade screens if the excitation is not at too high a level.

At faster scanning rates it becomes possible to provide screens having carry-over from one scan to the next. Within the requirements set by clarity on a changing picture the longest obtainable persistence should, in general, be used in order to average over the largest possible number of pulses. If, however, the permissible decay time is so short that the operator and not the screen has the longer memory, the persistence should be determined entirely by the requirements of freedom from flicker on the one hand and freedom from blurring due to motion on the other. This condition usually obtains with very rapid scans because their use implies rapid relative motion.[2] If a set has several indicators involving different scale factors their persistences should theoretically be graded, fast screens being used on the expanded displays where the picture changes rapidly and slower ones being used on those displays covering large areas. Fortunately, it is usually the latter on which the signal-to-noise discernibility is of most importance because the expanded displays are usually confined to near-by regions.

In connection with excitation by successive scans, a peculiar property of certain cascade screens becomes involved. If the scanning is not too slow (that is, if it is approximately one scan per second) many screens will, if initially unexcited, display more than twice as much intensity

[1] Except for that involved in the disappearance of the so-called "flash," which occurs within a very short time interval during and immediately after each excitation.

[2] When extended observations are to be made on a single target or region, the display is frequently "frozen"; that is, the relative motion is removed so that the picture remains stationary. It is then, of course, possible to use longer persistences without blurring. Since, however, observation of the frozen display is usually part of the "tracking" operation that controls the removal of the motion, the persistence must not be so long as to inhibit the ability to detect small changes.

after two scans than after one, and so on even though, in the time
between scans, the intensity may have decayed many fold.    This
property of "supernormal" buildup was at one time believed by many
to be very desirable from the signal-discernibility standpoint on the
hypothesis that it would enhance the brightness of the repeating signal
as compared to the random noise.    However, the property is most
exaggerated on an initially unexcited screen, whereas in actual cases of
successive scan integration the screen is initially excited by previous
scans.    Furthermore, it is not evident a priori that the readjustment in
the weighting of the successive pulse groups which the phenomenon
introduces is a desirable one.    In any case careful observation has not
detected any appreciable advantage in this respect for screens with very
high super-normal buildup.    This fact does not imply, of course, that
this property is not connected with other definitely desirable ones.
Indeed, those screens with highest buildup are in general those with the
longest persistence.

**1·12. Resolution.**—In order to distinguish between objects or between
parts of the same object, it is necessary that they be resolved.    The
characteristics of the receiving equipment which influence resolution
most importantly are the bandwidth of the signal channel, which affects
range resolution, and the spot size and scale factor of the display, which
also affect range resolution and to a lesser extent angular resolution as
well.

The "spot size" of a cathode-ray tube depends upon the tube type,
the individual tube, the voltages employed, the design of focus and
deflection coils, and the intensity level at which the tube is operated.
In the series of magnetic tubes used for radar it is roughly proportional
to the tube radius and is usually such that from 150 to 200 spots can
be resolved along the display radius.    As a convenient figure in this dis-
cussion, the number will be taken as 180.    Now, on a range sweep of
length $R$ in nautical miles, the number of radar pulse lengths is $12.2R/\tau$,
where $\tau$ is the pulse length in microseconds.    Thus, on a centered PPI
the fundamental pulse-length resolution and the spot-size resolution are
equal when $12.2R/\tau = 180$ or $R \approx 15$.    Accordingly, on a set with a
1-$\mu$sec pulse, a 15-mile centered PPI will halve the inherent range reso-
lution; a 100-mile PPI will reduce it approximately seven fold, and so on.
This disadvantage can be overcome by the use of expanded displays, but
the accompanying restriction in the field of view is often undesirable.
Fortunately, this is not the entire story.    For one thing the operator
could not, except on the fastest sweeps, realize the fundamental range
resolution without optical aids, even if the display made it available; in
fact, on a 5-in. tube the spot-size resolution is nearly as good as the
visual acuity of the observer, although on a 12-in. tube it is three or

four times worse.   Secondly, range resolution alone is of limited usefulness if it is accompanied by poor angular resolution, and, in this regard, the fundamental limitation is usually not the indicator but the r-f beam width.   The angular width of the cathode-ray-tube spot on any PPI is given in radians by $R/180r$ where $R$ is the radius of the tube and $r$ is the distance from the range origin to the spot in question.   The beam-width $\Delta\theta$, measured in degrees, is given by $57R/180r = \Delta\theta$ or $R/r \approx 3\Delta\theta$.   Thus, even for a 1° beam the display resolution exceeds the fundamental resolution for all points further from the origin than one third of a tube radius.   Therefore, the cathode-ray tube is usually not the limiting factor in over-all angular resolution.   In certain cases of accurate range measurements or of observing groups of aircraft or ships, however, better range resolution on long-range displays would be useful.   Frequently, the need for high *dispersion* requires expanded displays apart from question of resolution.

This discussion shows that, in general, the cathode-ray tube imposes a severe restriction in range resolution on any but the fastest sweeps. It is therefore apparent that unless fast sweeps are to be used, there is no point in going to extreme bandwidths in the receiver.   Indeed, in most cases the latter need not be so great as seriously to impair the signal-to-noise discrimination.   It should be borne in mind, however, that with too small a bandwidth, a signal far in excess of the limit level has a much greater length after limiting than would have been the case had it been weak in the first place.

**1·13. Contrast.**—The contrast of the display depends upon the characteristics of the screen and upon the way in which it is excited.   Unfortunately, present screens of the persistent type have serious shortcomings in this respect.   The screen material has a natural color not far from that of the phosphorescent light so that contrast is reduced by reflected light.   The necessary thickness of the screen tends to blur the edges of the signals, reducing contrast "gradient" as do also limitations in the sharpness of focus of the electron beam.   Many screens also have a certain amount of graininess, which contributes to this effect.

Contrast between signals of different intensities is especially important in overland flying where it is essential to be able to distinguish land from water and at the same time to have good contrast between echoes from ordinary terrain and the much stronger ones from built-up areas.   Unfortunately, the range of echo intensities is so great that, if the receiver has gain high enough to render the terrain visible, the signals from built-up urban areas must be drastically limited to avoid "blooming" of the cathode-ray tube, and detail is destroyed.   If the gain is low enough to preserve detail in the strong signals, the land background is not visible.

This difficulty is made worse by the nonlinear response of the cathode-
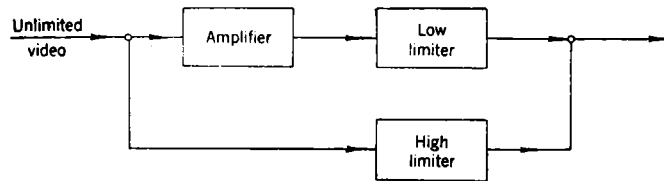
(a) Split video channel
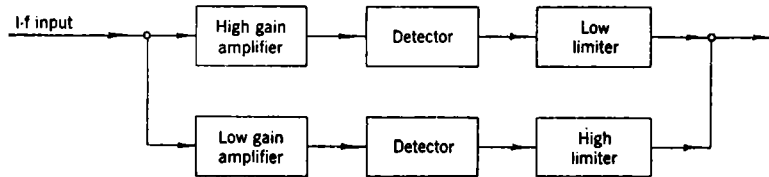
(b) Split i-f channel
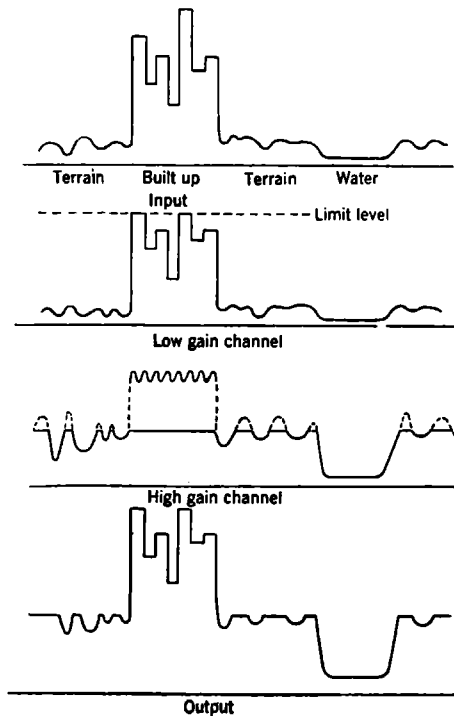
FIG. 1·12.—Three-tone method.
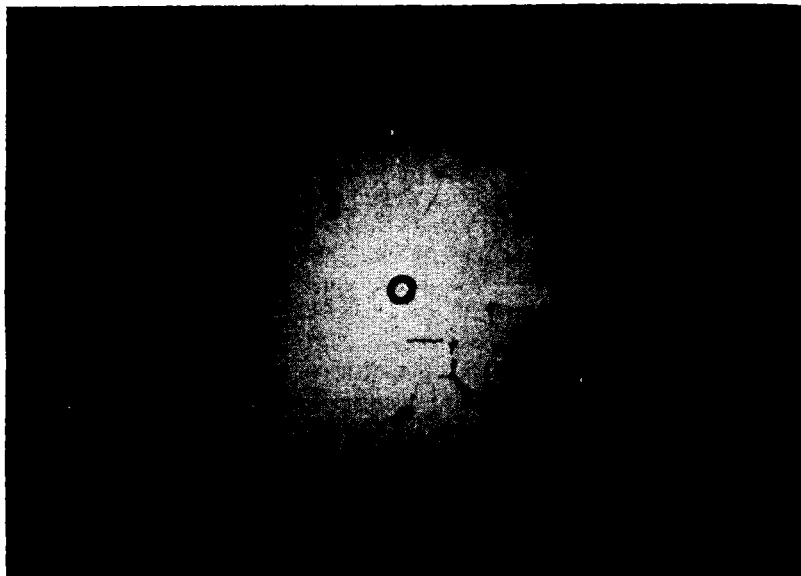
(a)



(b)

Fig. 1·13.—Photographs of three-tone normal indication.

ray tube. Since the beam current in a magnetic tube is proportional to the cube of the grid swing as measured from cutoff (which is near the operating point in the absence of signal and noise), a signal of, for example, half the voltage of a limited signal will, in principle, give only one-eighth as much light intensity. In actual fact the difference is not so great as this because of the tendency of the screen to saturate on strong signals. This nonlinearity reduces considerably the difference in signal voltage between those signals that are just strong enough to produce a visible result and the level at which strong signals must be limited. Thus the choice between a land background with no detail in built-up areas and the reverse is an even more necessary one than if the cathode-ray-tube response were linear. It is possible, of course, to introduce a nonlinear element in the video amplifier to compensate for the tube characteristic. This method has been used with some success, but no really satisfactory circuit has been devised, partly because the need was not fully appreciated until comparatively recently.

*The "Three Tone" Method.*—A simple but extremely effective method of retaining detail on high-intensity echoes while still providing a land-to-water contrast is illustrated in Figure 1·12. At some point in the signal channel ahead of any saturation or limiting, the signals are split into two channels. In one of these they are amplified much more than in the other, which may not contain any amplification at all. If the signals are not already in video form, each channel includes a detector. In any case each contains a limiter, the one in the low-gain channel being set at approximately twice the level of the other. Following the limiters, the two sets of signals are mixed and passed through a standard video amplifier. As can be seen by the waveform diagrams the net result is to enhance the strength of the land echoes but without destroying the detail in echoes from the built-up areas. A "before and after" picture is shown in Figure 1·13. The aptness of the name "three tone" given to this method is vividly shown by the three shades—black, gray, and white.[1] The method can, of course, be extended to more than two channels.

Many variations of this technique are possible. One, which has been applied to existing sets in which an additional channel is difficult to install, consists of switching the gain up and the limit level down on alternate pulse cycles by means of a scale-of-two multivibrator,[2] the signals being added on the cathode-ray-tube screen. The results are almost indistinguishable from those utilizing two channels.

[1] The name "Three-tone PPI" is frequently applied because of the type of indication usually used.

[2] See Sec. 4·4.

# CHAPTER 2

## CATHODE-RAY TUBES

### By T. Soller

A very brief discussion of the elements of a cathode-ray tube has been given in Sec. 1·1. This chapter gives an elementary treatment of the electron-optical principles involved in the formation of the focused spot on the cathode-ray-tube screen, and of the effects on the electron beam of the variation of certain parameters of the electron gun. Later sections discuss more specifically the electrical characteristics of the electrostatic and magnetic types of cathode-ray tubes, and the operating conditions necessary to achieve optimum performance.

### BEHAVIOR OF THE ELECTRON BEAM OF A CATHODE-RAY TUBE

**2·1. Electron Optics.**—The theory and design of electron guns used in cathode-ray tubes are based on well-defined electron optical principles. A field of research and development, designated as "electron optics," has arisen out of the analogy between the behavior of light rays in passing through media of different indexes of refraction and that of the trajectories of electrons in electric and magnetic fields. Although it is beyond the scope of this volume to give a comprehensive résumé of electron-optical systems,[1] a brief discussion of a few electron-optical principles is nevertheless needed for an understanding of the performance of cathode-ray tubes.

The electron guns used in cathode-ray tubes always involve axial symmetry, being composed of coaxial cylindrical elements or apertured disks to which various electric potentials are applied. Figure 2·1 illustrates the construction of a typical gun. A series of equipotential lines have been drawn for the specific potential distribution on the electrodes as indicated by the figures. Any region of the gun in which an

---

[1] The reader interested in electron-optical design is referred to the following literature on the subject: L. M. Myers, *Electron Optics, Theoretical and Practical*, Van Nostrand, New York, 1939; I. G. Maloff and D. W. Epstein, *Electron Optics in Television*, McGraw-Hill, New York, 1938; O. Klemperer, *Electron Optics*, University Press, Cambridge, England, 1939; V. K. Zworykin and G. A. Morton, *Television*, Wiley, New York, 1940; H. Moss, "The Electron Gun of the Cathode-ray Tube, Part 1," *J. Brit. Inst. Rad. Eng.*, **5**, 10–26 (1945); H. Moss, "The Electron Gun of the Cathode-ray Tube, Part 2," *J. Brit. Inst. Rad. Eng.*, **6** (1946).

appreciable nonuniformity in the axial potential distribution occurs may be considered to be an "electron lens." It is apparent that the gun illustrated involves essentially two lenses: one near the cathode, the other in the region of the junction of Anode No. 1 and Anode No. 2. This latter lens, whose performance is less complicated than that of the cathode lens, is the main focusing lens of the gun.
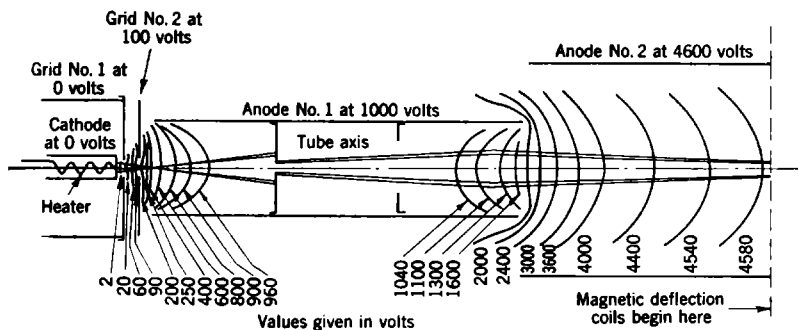


Fig. 2·1.—Typical electron-gun diagram, beam outline, and equipotential line plot.

The action of all electrostatic electron lenses is based on the elementary fact that the force acting upon an electron traveling in an electric field is in a direction normal to the lines of equal potential, and has a magnitude proportional to the potential gradient. This fact may be expressed as follows:
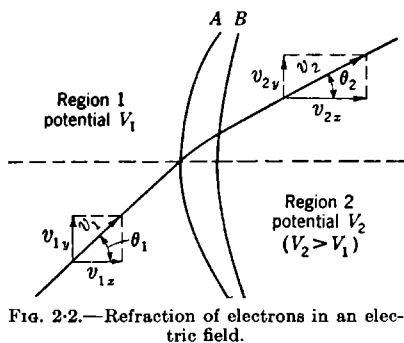


Fig. 2·2.—Refraction of electrons in an electric field.

$$F = \frac{dV}{dn}.$$

The passage of an electron through a portion of the field, as indicated in Fig. 2·2, will be considered in some detail. In this figure and in the subsequent analysis, the following simplifying assumptions are made: $A$ and $B$ are two adjacent equipotential surfaces having the potentials $V_1$ and $V_2$ respectively; the region 1 to the left of $A$ is field-free, that is, at the potential $V_1$; and the region 2 to the right of $B$ is similarly field-free, that is, at potential $V_2$.

The kinetic energy of an electron is proportional to the potential at any given point, and is given by the equation

$$\tfrac{1}{2}mv^2 = V \cdot e. \tag{1}$$

Consequently, in Region 1,

$$v_1^2 = 2 \frac{e}{m} \cdot V_1, \tag{2}$$

and, in Region 2,

$$v_2^2 = 2 \frac{e}{m} V_2. \tag{3}$$

Since the only force acting on the electron as it crosses from Region 1 to Region 2 is normal to the equipotential surfaces, only the $x$-component of the velocity is affected, the $y$-component remaining constant, as indicated by the equation

$$v_{1y} = v_{2y}. \tag{4}$$

But $v_{1y} = v_1 \sin \theta_1$, and $v_{2y} = v_2 \sin \theta_2$. Hence, Eq. (4) becomes

$$v_1 \sin \theta_1 = v_2 \sin \theta_2, \tag{4a}$$

and substituting for $v_1$ and $v_2$ their values from Eqs. (2) and (3),

$$\sqrt{V_1} \cdot \sin \theta_1 = \sqrt{V_2} \cdot \sin \theta_2. \tag{5}$$

Snell's law of optics for the bending of a ray of light traveling from a region of index of refraction $n_1$ to one of index $n_2$ is

$$n_1 \sin i = n_2 \sin r, \tag{6}$$

where $i$ is the angle of incidence and $r$ is the angle of refraction. The similarity between Eqs. (5) and (6) leads to the conclusion that the behavior of an electron (originally starting from rest) in an electrostatic field may be described in optical terms by assigning to every region in the field an index of refraction $n = \sqrt{V}$.

In the extended field region indicated in Fig. 2·1 the trajectory of each electron will be a curved path, and it is apparent qualitatively that a divergent bundle of electrons entering the focusing lens will be made convergent, roughly as shown in the diagram. The region therefore acts as a convergent lens.

The conditions in ordinary optics are somewhat different from those in electron optics. In the case of optical image formation, the index of refraction changes abruptly from one fixed value to another at the boundaries of the lens surfaces; whereas, in the electron-optical case, no such definite boundaries exist, and the index changes gradually over a wide region. In order to calculate the electron trajectories, a knowledge of the spatial distribution of the potential is therefore necessary. In certain cases the potential distribution may be expressed mathematically as a second-order differential equation, whose solutions determine the trajectories sought; in other cases, measurement of the equipotential surfaces is done experimentally in an electrolytic tank, and approximate

step-by-step methods of ray-tracing are employed to yield the trajectories. Fortunately, the solutions are simplified by the fact that in electron optics the trajectories are never far removed from the axis, nor do they make large angles with the axis. Therefore, only paraxial electrons need be considered.

In describing the performance of electron lenses, it is convenient to follow the analogy to ordinary optics, and to use the optical terminology. Since electron lenses in general spread out over a considerable space, they are most closely analogous to thick optical lenses. For the latter the laws of image formation are most simply expressed in terms of distances measured not from the lens surfaces but from what are known as the "cardinal points" of the lens system. These are four in number: two "focal points" $F_1$ and $F_2$, and two "principal points" $H_1$ and $H_2$, whose positions can be calculated from the radii and positions of the various boundary surfaces and from the appropriate indexes of refraction. The performance of the entire lens system, regardless of the number and location of the glass surfaces, may be determined from the equivalent optical system as defined by these points.

In an analogous manner, the image-forming properties of an electron lens may most simply be described in terms of its cardinal points. Two forms of lens generally employed in cathode-ray tubes are those formed by (1) two cylinders, either of the same diameter or of diameter ratios between 1 and 3, with the larger cylinder at a higher potential than the smaller; and (2) two adjacent apertured disks.

For an analysis of the problem of determination of the cardinal points for various electron optical systems, the reader is referred to the work of Maloff and Epstein.[1]   Their calculations show that, for coaxial cylinders, the focal length of the lens decreases, that is, the "power" of the lens increases, with increasing voltage ratio, and that the inverse is true for an increasing ratio of the diameters of the cylinders forming the lens. The focal length in the image space $f_2$ is greater than that in the object space $f_1$ when the electron is accelerated in going through the lens. In fact, the ratio $f_2/f_1 = \sqrt{V_2/V_1}$. Their analysis also shows that the principal points for the conditions illustrated in Fig. 2·1 are located at some distance inside the first-anode cylinder.

It is apparent that, in the case of the focusing lens here discussed, both object and image are at relatively great distances from the principal points. In this case the lens may be considered as a "thin lens," whose center is midway between the principal points, for which the familiar LaGrange law of optics, illustrated in Fig. 2·3, states that

$$n_1 h_1 \sin \theta_1 = n_2 h_2 \sin \theta_2. \tag{7}$$

[1] Maloff and Epstein, op. cit.

In the equation, the subscripts 1 and 2 refer to the object and image space, respectively, $n$ = index of refraction, $h$ = object or image height, and $\theta$ refers to the semiangle subtended at the object or image by the lens aperture.

In the case of electron-optical image formation, the angles $\theta_1$ and $\theta_2$ are always so small that $\sin \theta$ may be replaced by $\tan \theta$, and Eq. (7) then becomes

$$n_1 h_1 \tan \theta_1 = n_2 h_2 \tan \theta_2, \qquad (8)$$

or

$$n_1 h_1 \frac{R}{u} = n_2 h_2 \frac{R}{v}, \qquad (9)$$

whence the magnification is

$$m = \frac{h_2}{h_1} = \frac{v}{u} \cdot \frac{n_1}{n_2} = \frac{v}{u} \sqrt{\frac{V_1}{V_2}}. \qquad (10)$$
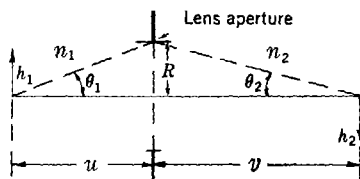


Fig. 2·3.—Geometry illustrating object-image relationship.

**2·2. Focusing-lens Systems.**—The lens system just described is the main focusing system in the electrostatically focused cathode-ray tubes. There are many variations of this electrostatic focusing system, one of which comprises adjacent apertured disks instead of cylinders. There are no simple formulas that represent the performance of a given lens because its optical constants depend on the nature of the potential distribution along the axis. This distribution, in turn, is a complicated function of the shape and size of the various elements. In addition, the various aberrations that afflict an optical system are also present in electron-optical systems. Some of these are the results of misalignment of adjacent elements, or of asymmetry in the elements themselves. Others arise from spherical aberration caused by the shape of the potential distribution. In order to obtain a completed design that gives satisfactory performance, it is necessary to supplement theoretical design information with a good deal of empirical data obtained from experimental guns.

In cathode-ray tubes of some types, the focusing is done by a magnetostatic lens rather than by an electrostatic lens. This magnetostatic lens usually takes the form of a short coil surrounding the tube neck. The coil itself is housed in a soft-iron shell having an air gap so located that it produces a fairly localized axial magnetic field, through which the electron beam must pass. The focal length of such a lens is given to a fair approximation by the equation[1]

$$\frac{1}{f} = \frac{1}{8} \frac{e}{m} \frac{1}{V} \int_{-\infty}^{+\infty} H_z^2 \, dz, \qquad (11)$$

where $f$ is the focal length, $e$ is the electronic charge, $m$ is the electronic

[1] Maloff and Epstein, *op. cit.*

mass, $V$ is the electrical potential (assumed to be uniform in the region occupied by the lens), and $H_z$ is the axial component of the magnetic field produced by the coil.   The focal length of such a lens is easily adjusted by varying the current through the coil, to which $H$ is proportional. The magnetic lens, as usually constructed, can be considered as a "thin lens," and Eq. (10) also holds for the magnetostatic focusing lens.

In order to reduce spherical aberration, the cross section of the electron bundle is usually limited by the introduction into the gun of apertured disks that act as stops.   This method is particularly applicable to guns used in tubes in which both focusing and deflection are done by electrostatic means.   If the focus is to be electrostatic, aberration due to the focusing lenses may also be reduced by making the geometrical size of the lens larger, that is, by using a gun of larger diameter.   In the case of magnetic focusing, the size of the focus coil is usually adequate to reduce the aberration to a satisfactory degree, because the coil itself is external to the tube.[1]

*Focusing of Ions.*—The electrical particle of chief importance in the operation of a cathode-ray tube is the electron.   However, the presence of even a minute percentage of heavy ions may affect the useful life of the tube.   Particularly, a focused beam of negative ions may produce a localized screen deterioration or "ion spot" at the center of the tube face. In Eq. (11) the focal length of a magnetic lens is shown to be a function of the mass as well as the charge of the particle, and hence, when electrons are focused on the screen, ions will not be focused.   On the other hand, the trajectory of charged particles in an electrostatic field turns out to be the same both for electrons and for singly charged ions provided that all particles start with zero velocity.   Hence, with electrostatic focusing, ions which originate at or near cathode potential as well as electrons will be brought to a focus at the screen.   Magnetic focusing is therefore superior to electrostatic focusing in this respect.

**2·3. Cathode- or Immersion-lens System.**—The bundle of electrons focused on the fluorescent screen by the focusing lens originates from the cathode and is controlled by a modulating or control grid.   The emitting surface of the cathode is usually a small plane area immediately behind the central opening in the modulating grid.   In the region just beyond the modulating grid there is usually another electrode at a relatively high positive potential.   This electrode serves to draw the electrons from the cathode and accelerate them along the axis, as indicated in Fig. 2·1.   This combination of electrodes forms the cathode-lens system.   This is an immersion-lens system because the object is not external to the lens, but immersed in it, in a manner analogous to the case of the well-known immersion objectives used in microscopes.

[1] See Sec. 3·1 for aberrations of focus coils.

The electrical fields in this region are much more complicated than in the region of the main focusing lens.    Furthermore, they change when the beam is controlled in intensity by varying the potential of the modulating grid.    For a typical gun this variation is indicated in Fig. 2·4 by the series of equipotential plots in the region of the cathode for four values of grid voltage between −10 and −165 volts, the latter corresponding to beam cutoff.[1]
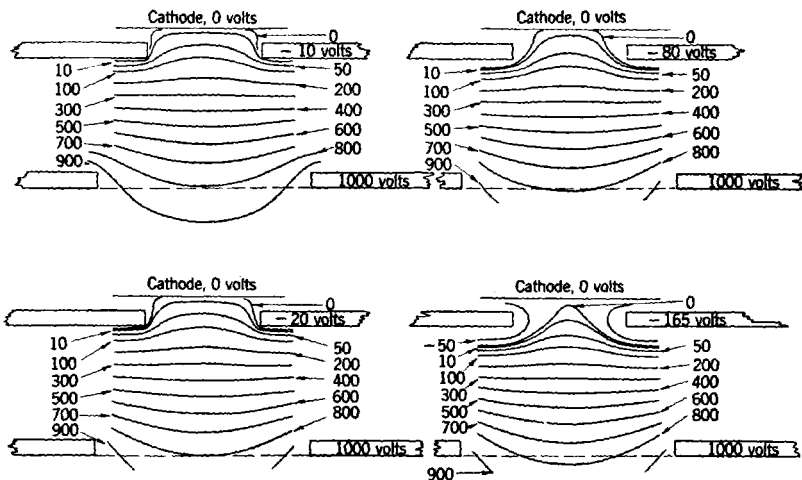


Fig. 2·4.—Equipotential plots of cathode lens, for several values of grid bias.

In addition to the changes in the constants of the cathode lens produced by the changes in the potential of the control grid, the cathode-lens problem is further complicated by three facts.

1. The electrons may leave the cathode in any direction, and the analysis of this region cannot therefore deal simply with paraxial electrons (see Sec. 2·1).

2. Since the electrons are emitted from a hot cathode, they leave the cathode with random speeds (a Maxwellian distribution).    At any given point, the index of refraction for electrons that enter the field with any but zero velocity is determined by the variable velocity of the electron at this point.    Therefore, even in the case of paraxial electrons, there is no single set of cardinal points for this lens for any given distribution of equipotential surfaces.

3. Space-charge effects in this region are appreciable because the current density may be fairly high, and the average velocity is usually low.

[1] These plots were obtained through the courtesy of Dr. L. B. Headrick, Lancaster Engineering Department, RCA.

Figure 2·5a shows in a schematic way the trajectories followed, under the influence of field conditions such as are represented in the plot for −80-volt grid bias in Fig. 2·4c, by electrons leaving the cathode in various directions from (1) a point on the axis, and (2) a point at some distance from the axis. These trajectories cross the axis at a relatively short distance from the cathode, in a region designated as the "crossover," and thereafter proceed to form an enlarged image of the cathode some distance beyond. All the electrons leaving the cathode form a bundle of variable cross section, which reaches a minimum value at the crossover and thereafter expands, as shown by the schematic beam envelope in Fig. 2·5b. The location of the cardinal points of the immersion lens has been found by Maloff and Epstein.[1] For the particular case considered it was determined that the image of the cathode would be formed at a distance of approximately 2 cm from the cathode, and that its magnification would be approximately 5. This image, however, is of secondary importance, the chief function of the immersion lens being to form a crossover of minimum size. Because of the change in lens constants, the position of the crossover moves away from the cathode as the grid is made less negative, thereby increasing the beam current.



Fig. 2·5.—Formation of crossover and beam envelope.

**2·4. The Complete Electron Gun.**—The complete electron gun of the cathode-ray tube embodies in various forms both electron lenses described in Secs. 2·2 and 2·3. One of these has already been illustrated in Fig. 2·1. Figure 2·6 illustrates two other gun types, more generally used. Figure 2·6a shows an electrostatic-focus gun used in a typical oscilloscope tube, in which the deflection is also produced by electric fields. Figure 2·6b illustrates a typical gun used in an all-magnetic tube, in which both focusing and deflection are produced magnetically. The focusing lens in this case is physically placed outside the tube, but it snould definitely be considered as part of the gun. In all types of tubes illustrated, the cathode lens is essentially the same.

[1] Maloff and Epstein, *op. cit.*

The conventional analysis of the process of image formation in all types of cathode-ray tubes is in terms of the action of two lenses and may be summarized as follows.   Electrons are emitted from the cathode in
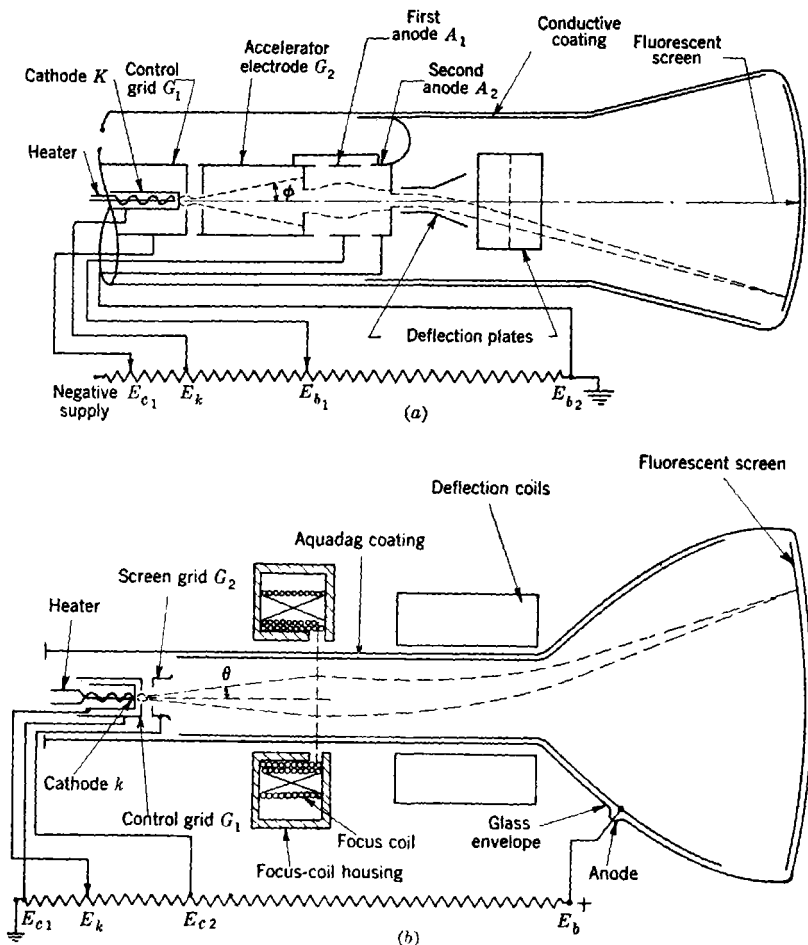


FIG. 2·6.—Two common forms of cathode-ray tubes.   (a) Electrostatic deflection-type cathode-ray tube with electron gun designed for zero current to focusing electrode (first anode).   (b) Magnetic deflection-type cathode-ray tube with tetrode electron gun.

an amount determined by the potential of the control grid $G_1$, and accelerated by the field due to the positive potential applied to the accelerating electrode $G_2$; the shape of the beam is controlled by the constants of the cathode lens formed by these elements, resulting first

in a constriction near the cathode, known as the "crossover," and thereafter in a divergence of the beam; either the entire bundle (Fig. 2·6b) or the central part of it (Fig. 2·6a) then passes through the region of a second lens, called a "focusing lens," at a considerable distance from the cathode, and is there made to converge toward the tube axis, reaching a focus at the screen of the tube.    Obviously the crossover described in the previous section cannot be observed directly, but from the constants of the focusing lens and the size of the image formed on the screen, it can be shown that the object that is imaged on the screen is very near the cathode, and that its size is considerably smaller than that of the emitting area of the cathode.    It is much smaller than that which would result if the enlarged image of the cathode were considered to be the "object" for the focusing lens.    Consequently it is concluded[1] that the object focused may be considered to be the virtual image of this crossover, which also turns out to be smaller than the emitting part of the cathode, and the position of which is in the vicinity of the cathode, and slightly behind it.

A somewhat different analysis of the electron optical system involved in the formation of the image has been made by Liebmann,[2] who considers the image to be formed by three rather than two lenses.    By replacing the single cathode-lens field distribution mentioned in the previous paragraph by two relatively closely spaced lenses, he arrives at the conclusion that because of the combined action of these two lenses there is formed, not far from the modulating grid, a virtual, reduced, inverted image of the cathode.    The main focusing lens then forms an image of this at the screen (see also page 56).

The conditions existing in this region of the cathode-ray tube are so complicated that the theoretical analyses necessarily employ greatly oversimplified conditions.    Further investigations toward a clearer understanding of this complicated electron-optical problem are necessary and important.

A discussion of (1) the effect of various parameters on the beam current, (2) the area from which this current originates, (3) the angle that this beam subtends at the cathode, and (4) the current density of the beam at the screen will contribute to an understanding of the properties of complete cathode-ray tubes.

*Beam-current–grid-bias Relations.*—The characteristics that an input amplifier must have in order properly to drive the cathode-ray tube are determined by the tube's modulation or transfer characteristic, which is the relation between the current to the screen of the cathode-ray tube and the voltage applied to the control grid.

[1] Maloff and Epstein, *op. cit.*

[2] G. Liebmann, "Image Formation in Cathode-ray Tubes," *Proc. I.R.E.*, **33**, 381–389 (1945).

This relation is expressed by

$$i_{sn} = A(E_{c1} - E_{co})^n \equiv AE_d^n, \tag{12}$$

in which $i_{sn}$ = screen current, $E_{c1}$ = voltage of control grid (a negative number), $E_{co}$ = voltage on control grid to produce tube cutoff (a negative number), $E_d$ = "grid drive" above cutoff, in volts ($E_d$ is positive, since $|E_{co}|$ must be greater than $|E_{c1}|$ in order to have any beam current), $A$ = grid-drive factor, a constant, and $n$ = a constant (positive, and not necessarily an integer). For constant tube geometry and anode voltage, $A$, $n$, and $E_{co}$ will be constant. However, the value of $E_{co}$ is not specific because cutoff may be defined in various ways. Since the value of grid potential for which the screen current is judged to be zero depends upon the sensitivity of the measuring instrument, this definition of cutoff is not employed. Instead, the grid bias necessary to produce some arbitrary small current, for example, 0.5 or 1.0 $\mu a$, may be used to define $E_{co}$. A much more commonly used definition for $E_{co}$, however, is that known as the "visual cutoff" voltage. Even this value is not too well defined since it depends, for any given electron gun, on the condition of the eye of the observer, the external illumination falling on the screen, the efficiency of the phosphor, and the area of the screen being bombarded by electrons. Thus the cutoff voltage for the visual extinction of a stationary, sharply focused spot will be considerably greater than that corresponding to extinction of the line pattern of a television raster.

*Method* 1 *for Determination of Constants in Eq.* (12).—One customary method of determining the constants $A$ and $n$ in Eq. (12) involves plotting $i_{sn}$ and $E_d$ on a log-log plot, with $E_d$ measured from the visual cutoff as determined by some arbitrary criterion. The slope of the line best fitting the experimental points then gives the value of the exponent $n$, and the value of $A$ can be determined by choosing some one point on the line and substituting its coordinates in Eq. (12). Experimental data compiled by Moss[1] and others indicates that the relation between cathode current $i_k$ and grid drive, determined by this method, is

$$i_k = KE_d^{3.5}, \tag{13}$$

where $K$ is a function of the visual cutoff of the tube, and is given approximately by the expression

$$K = 3E_{co}^{-2}. \tag{14}$$

Thus, combining Eqs. (13) and (14),

$$i_k = \frac{3E_d^{3.5}}{E_{co}^2}. \tag{15}$$

[1] H. Moss, "The Electron Gun of the Cathode-ray Tube, Part 1," *J. Brit. Inst. Rad. Eng.*, **5**, 10–26 (1945).

At zero bias, the cathode current is

$$(i_k)_{E_g=0} = 3E_{co}^{1.5} \tag{16}$$

In Eqs. (13), (14), and (15), $i_k$ is measured in microamperes, $E_{co}$ and $E_d$ in volts.

For many magnetic-focus guns, almost no current is intercepted by apertures in the gun. Consequently Eq. (15) holds as the relation between screen current and grid voltage as well, and indicates that the value of the exponent $n$ in Eq. (12) is 3.5. On the other hand, for tubes employing electrostatic focusing, beam stops are almost universally introduced. They take a considerable portion of the cathode current, and the screen current is consequently considerably less than in the case of magnetic focusing. The value of $n$ is therefore less than 3.5. Moss indicates that, over most of the characteristic, $n$ has the value 1.5.

*Method 2 for Determination of Constants in Eq.* (12).—A second method of determination of the constants in Eq. (12), which does not depend on the determination of the visual cutoff, consists of considering $n$ as a parameter and plotting $i_{sn}^{1/n}$ as a function of $E_{c1}$ for several arbitrarily chosen values of $n$.[1] The correct value for $n$ in Eq. (12) is the one that gives the best straight line in these plots. The intercept on the $E_{c1}$ axis then gives the value of $E_{co}$, which is called the "extrapolated cutoff," and which differs from the $E_{co}$ used in Method 1. The constant $A$ is the slope of the line raised to the $n$th power. For magnetic tubes not containing limiting apertures, the value of $n$ thus found is very near 3. Using this method, Eq. (12) becomes

$$i_{sn} = A(E_{c1} - E_{co})^3 \equiv AE_d^3. \tag{17}$$

The value of $A$ is found to vary with cutoff, but not so simply as expressed by Eq. (14) (see also Sec. 2.12).

For tubes of the electrostatic focus and deflection type, in which the masking of the beam is severe, this method indicates that the value of $n$ is approximately 2, and the screen current is then given by

$$i_{sn} = A(E_{c1} - E_{co})^2 \equiv AE_d^2. \tag{18}$$

Because of variations in size, location, and alignment of apertures in this type of tube, wider variations result in $n$ and especially in $A$ than in the case of magnetic tubes.

The exact evaluation of the values of $n$ and $A$, and the reasons for their variation, are of primary interest to the designer of the cathode-ray tube. In using the tube, it is probably sufficient to know that in general the screen-current vs. grid-drive curves are roughly cubic for magnetic

---

[1] W. B. Nottingham, RL Report No. 62-7, May 14, 1943.

deflection-type tubes, and roughly square-law curves for electrostatic deflection-type tubes.   In some cases this is not true, since some magnetostatic focus tubes employ beam masking, and some electrostatic focus tubes may have no masking of the beam.

*Emitting Area of Cathode and Cathode Loading.*—The area of the cathode from which the current indicated by Eq. (12) originates is of considerable interest.   At cutoff, this area is zero, whereas for zero grid voltage, Moss[1] has shown that the emitting diameter is equal to that of the control-grid aperture $D$, regardless of the spacing between grid and accelerating electrode (see Fig. 2·1) or of the voltage applied to this electrode.   For values of grid voltage between these extremes, Moss found that the curve of emitting diameter $d$ as a function of grid drive $E_d$ was a somewhat S-shaped curve, which can, to a first approximation, be considered linear, so that

$$d = \frac{E_d}{E_{co}} \cdot D. \tag{19}$$

Furthermore, the emission current density has been found to vary over the emitting area in a manner roughly illustrated by Fig. 2·7.   Both the peak and the mean current density are seen to increase with increasing grid drive.   The ratio of peak density to mean density also increases with increasing current.   The cathode loading is defined as the cathode current per unit emitting area.   A very rough assessment of the cathode loading for any value of grid drive $E_d$ may be made as follows.   From Eq. (15),

$$i_k = \frac{3E_d^{3.5}}{E_{co}^2}, \tag{2·15}$$

From Eq. (19),

$$A = \frac{\pi d^2}{4} = \frac{\pi \cdot E_d^2}{4E_{co}^2} \cdot D^2. \tag{20}$$



FIG. 2·7.—Cathode current density as function of grid voltage.

Therefore, the mean cathode loading is

$$\bar{\rho}_c = \frac{i_k}{A} = \frac{12}{\pi} \cdot \frac{E_d^{1.5}}{D^2}. \tag{21}$$

From experimental data, Moss arrives at a semiempirical relation for the peak cathode loading $\rho_c$ as follows:

$$\rho_c = \frac{0.015}{D^2} \cdot E_d^{1.5}, \tag{22}$$

[1] Moss, *op. cit.*

in which $\rho_c$ is expressed in ma/mm²; $D$, the grid-hole diameter, in mm; and the drive $E_d$ in volts. This equation gives only an approximate estimate of the peak loading. In practice, the diameter of the grid hole of a cathode-ray tube is between 0.75 and 1.0 mm. From Eq. (22) the estimated peak cathode loading for a 50-volt drive on a tube having a 1-mm grid hole is found to be approximately 5 ma/mm². For satisfactory cathode life, conservative designers estimate that the maximum peak loading should not be far above 10 ma/mm².

*Beam Divergence.*—The angle of divergence $\phi$ of the conical bundle of electrons, after they have passed through the grid aperture, determines the cross section of the beam at the focusing lens, and consequently it affects the magnitude of spherical aberration in this lens as well as the amount of deflection defocusing.
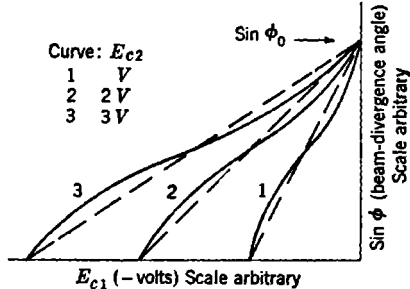


FIG. 2·8.—Relationship between grid drive and beam divergence.

For a given geometry of gun, the experimentally determined relation between beam-divergence angle $\phi$ and control-grid potential $E_{c1}$ is illustrated in Fig. 2·8. In this figure, each curve applies to a specific value of $E_{c2}$, the potential applied to the accelerating grid, with the further condition that all electrodes beyond the accelerating grid are maintained at the same potential as this grid, that is, that the region beyond the accelerating grid is equipotential. The cutoff of the tube increases with increasing $E_{c2}$, but the interesting fact is evident that at zero grid bias the beam-divergence angle is independent of $E_{c2}$. This fact is to be expected from the principle of voltage similitude, which states that the trajectories are unaltered by multiplication of all electrode potentials by a constant factor.[1] To a first approximation,

$$\sin \phi = \frac{E_d}{E_{co}} \cdot \sin \phi_0, \qquad (23)$$

where $E_d/E_\infty$ is the voltage drive expressed as a fraction of the drive to zero bias. The value of $\phi_0$, however, varies with the gun geometry, increasing with an increase in size of the grid aperture and with a decrease in the distance between control and accelerating grids.

In a complete tube, under normal operating conditions, the region beyond $G_2$ is generally not field-free, and hence the beam divergence will be altered somewhat. For example, in the case of the magnetic gun

[1] Maloff and Epstein, *op. cit.*, p. 187; H. Moss, *J. Brit. Inst. Rad. Eng.*, **5**, 204 (1945); **6** (1946).

illustrated in Fig. 2·6b, the potential difference between $G_2$ and the conducting coating of the anode causes some electrostatic focusing and thereby reduces the beam divergence (see also Sec. 2·13).

Whenever a gun contains beam-limiting apertures, as in Fig. 2·6a, for example, a very small grid drive $E_d$ suffices to make the cone $\phi$ fill the aperture. In practice, then, the values of grid drive employed are considerably larger, with the result that the effective beam angle is determined by the size and location of the masking aperture, and the increase in beam current to the screen with grid drive is due to the increase in current density from the cathode.

*Effects of Beam Convergence on Image Current Density.*—The problem of the designer of a cathode-ray tube is to achieve as bright and as small a spot as possible, with the use of a minimum of input power both to create and to deflect the spot. This requirement necessitates the incorporation within the tube of a screen of maximum efficiency together with an electron gun that can produce an electron beam that converges at the screen into a minimum diameter. The two principal elements of this gun have been briefly described. It is now of interest to consider the effects of beam convergence on the current density.

A fundamental law, derived by Langmuir,[1] is that given by Eq. (24):

$$\rho_i = \rho_c \left( \frac{Ve}{kT} + 1 \right) \sin^2 \theta, \tag{24}$$

in which $\rho_c$ = current density at the cathode, $\rho_i$ = current density at the image, $V$ = potential at the image, $e$ = electronic charge, $k$ = Boltzmann constant, $T$ = temperature of cathode (degrees Kelvin), and $\theta$ = semiangle of convergence of the beam at the screen.

In order to consume a minimum of power, $V$ should be kept as low as possible. Also, to keep $T$ as low as possible, oxide-coated cathodes are used. The value of $\rho_c$ is not constant over the whole emitting area, but, as was indicated in Fig. 2·7, decreases exponentially with the distance from its center. The peak density at the center increases with increasing total current. However, the maximum current density that can safely be drawn from the cathode, the peak cathode loading previously discussed, is also subject to practical limitations.

Thus the only variable in Eq. (24) which is not essentially severely restricted is $\theta$. The current density at the image may therefore be increased by making $\theta$ larger. For a fixed location of gun and screen, this increase can be attained by altering the gun so that the divergence of the beam from the first lens is increased; and $\theta$ will then increase in

[1] D. B. Langmuir, "Theoretical Limitations of Cathode-ray Tubes," *Proc. I.R.E.*, **22**, 977 (1937).

direct proportion to the diameter of the beam at the focusing lens. Alternatively, with no changes in the gun, $\theta$ may be increased by shortening the tube, that is, by decreasing the distance between focusing lens and screen. This decrease must be accompanied by a simultaneous increase in the power of the focusing lens. Obviously, the process of shortening the tube means a loss in deflection sensitivity because the distance from deflecting system to screen is also reduced.

The increase in current density obtained by increasing $\theta$ has definite limitations, which are intimately associated with the mechanism used to deflect the beam, and which pertain specifically to the problem of deflection defocusing.
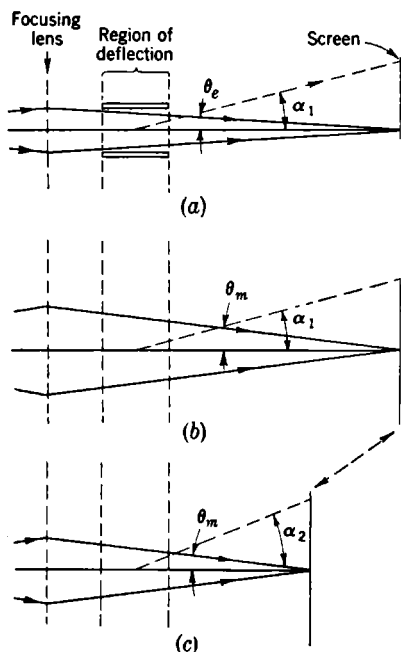


Fig. 2·9.—Comparison between deflection by electric and magnetic fields. (a) Deflection by electric field. (b) Deflection by magnetic field. (c) Shortened tube.

This deflection defocusing is a function of the angle of deflection, the cross section of the electron bundle in the region of deflection, and the type of deflection system used. A comparison may be made between magnetic deflection produced by coils of good form external to the tube, and electric-field deflection produced by carefully designed plates, with identical distances between deflecting systems and screen, as illustrated in Figs. 2·9a and b. For a deflecting angle $\alpha_1$, chosen to be roughly the maximum angle for good performance with electric-field deflection, the deflection defocusing becomes serious in the case of deflection produced by the action of deflection plates when the beam diameter at the plates exceeds 2 or 3 mm; whereas, for magnetic deflection with the same deflection angle, this diameter may be as large as 6 or 7 mm before it produces an equivalent amount of defocusing. Consequently, the ratio between the maximum values of $\theta_m$ and $\theta_e$ is roughly between 2/1 and 3/1. The ratio of current densities, which varies as $\theta^2$, then comes out to be roughly 6 to 1 in favor of magnetic deflection. The reasons for this are (1) that the area of uniformity of field is considerably greater in the magnetic case because the dimensions of the parts producing the field can be much greater and (2) that the energy of the electrons

is constant during the magnetic deflection, and is not constant for electric-field deflection.

A further possible advantage of a tube of the magnetic-deflection type, namely, a shorter over-all length, immediately becomes apparent; for, keeping $\theta_m$ constant, a decrease in the distance from focusing lens to screen, illustrated in Fig. 2·9c, results in a smaller beam diameter in the deflecting region. Therefore, with the same over-all defocusing, a greater deflecting angle $\alpha_2$ may be used. The deflecting angle employed in almost all magnetic tubes developed for radar use is 27°; and for the most widely used screen size, namely 5 in., the ratio of the over-all lengths of the electrostatic type to that of the magnetic type is approximately 1.5 to 1 (namely, $16\frac{3}{4}$ in. for the 5CP1 vs. $11\frac{1}{8}$ in. for the 5FP7).

The preceding discussion indicates the superiority of magnetic deflection over electric deflection in several respects, but it does not indicate the degree to which experiment checks the Langmuir equation for current density. Even in the most carefully designed and constructed tubes, the measured current density at the screen[1] is roughly only 10 per cent of that predicted by the Langmuir theory. The discrepancy between these values is, without doubt, due to the combined effects, principally in the region of the immersion lens, of space charge, the finite velocity of emission of electrons, and aberrations in the lens. The problem is by no means completely understood.

*Variation of Spot Size with Electrical Parameters $E_g$, $E_{c2}$, $E_b$.*—Since the current distribution to the screen and, to a first approximation, the luminance of the spot follow a Gaussian distribution, it becomes difficult to define just what should be called the "spot size." Thus the term "spot size" must be arbitrarily defined, and is taken to be the diameter of that circle at which the luminance has reached some definite fraction of the peak value at the center of the distribution curve. Because of the finite thickness of the screen and the scattering of light therein, the light output of the screen will have a somewhat broader distribution than that of the beam current that strikes the screen. In the following paragraphs, this difference is neglected, and "current density" and "spot-size" distributions will be considered as being identical.

In making an analysis of the effects of the various parameters on the

[1] In order to avoid the difficulties that scattering of light in the phosphor and possible nonlinearity between the current density and the resulting light output would introduce, it is necessary in making measurements of current density to work directly with the electron beam, rather than to observe the characteristics of the luminous spot in a conventional cathode-ray tube. Therefore, the screen is replaced by a specially designed electrode containing either a small circular aperture or a narrow slit in front of a Faraday cage by means of which the current passing through the aperture may be measured as the beam is moved across it by the deflecting system. For a discussion of this method, see L. Jacob, *Phil. Mag.*, **28**, 81 (1939).

experimentally determined current distribution using the Faraday cage method, simplifying assumptions are made.   These are

1. The focusing lens, and the immersion lens, are considered to be free from aberrations.
2. The effects of space charge are neglected.

Under these conditions the measured current density distribution at the screen, which appears as $d_2$ in Eq. (21), $d_2/d_1 = (v/u)\ \sqrt{V_1/V_2}$, gives information of the conditions existing at the crossover, which is assumed to be the "object" whose "image" is measured.   Note that the crossover cannot be measured directly.   Under experimental conditions in which the effective area of the cathode is limited to avoid the introduction of excessive aberrations, Moss[1] found (1) that the diameter of the crossover is independent of $E_g$, at least over a limited range, and (2) that the diameter of the crossover is proportional to $1/\sqrt{V_1}$, where $V_1$ is the voltage at the crossover; that is,

$$d_1 = \frac{k}{\sqrt{V_1}}. \tag{25}$$

Therefore it would seem that it would be advantageous to have the crossover formed at as high a potential as possible.   However, since, in Eq. (23), $\sqrt{V_1}$ appears in the numerator, the diameter of the image should be independent of $V_1$ and, as is readily seen by combining Eqs. (23) and (25), should be inversely proportional to $\sqrt{V_2}$, where $V_2$ is the final-anode potential; that is,

$$d_2 = \frac{k}{\sqrt{V_2}}. \tag{26}$$

In reality, however, the simple conditions under which these results obtain are not met in practice.   Space charge in the cathode region is not negligible, and neither lens is free from aberration, particularly in the complicated cathode region.   Therefore, the observed spot size increases with increasing current.   Also, the spot size decreases with increasing voltage on the accelerating grid, probably because of (1) the reduction of space-charge effects, and (2) the increase in the cathode loading.   Finally, the observed variation of spot size with increasing anode voltage does not uniformly agree with Eq. (26).   This last fact has led Liebmann[2] to discount this crossover theory, and to propose an analysis based on three lenses rather than on two.   This analysis results in a deemphasis of the crossover as such and indicates that the spot size should be independent

[1] Moss, *op. cit.*
[2] Liebmann, *loc. cit.*

of $V_2$.   A complete understanding of the many factors entering into the exact behavior of the cathode-ray-tube spot is thus not at hand.[1]

### ELECTROSTATIC CATHODE-RAY TUBES[2]

Cathode ray tubes in which both the focusing and deflection are electrostatic are the most common types of tubes.   For brevity, these will be designated in Secs. 2·5–2·9 simply as "electrostatic" cathode-ray tubes.   Several typical ones are illustrated in Fig. 2·10.   The principal
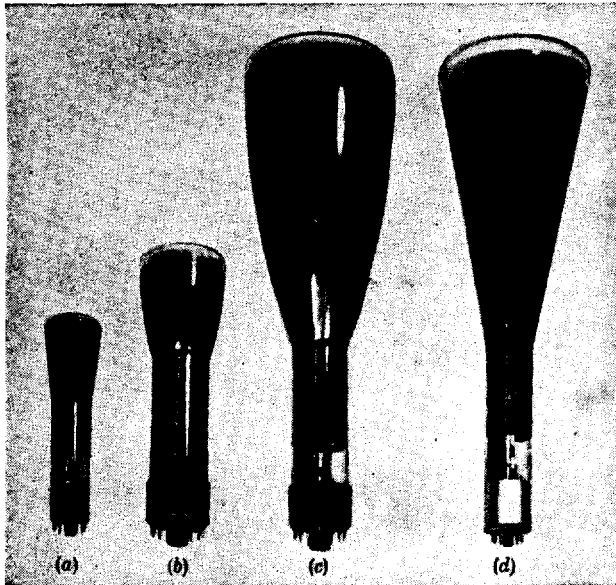


Fig. 2·10.—Typical electrostatic cathode-ray tubes: (a) 2AP1; (b) 3BP1; (c) 5CP1; (d) 5BP1.

advantages of these tubes employing deflection by electrostatic fields lie in the high impedance of the deflection elements, the extremely fast writing speeds that may be obtained, and the linearity of the deflection with respect to the voltages applied to the deflection elements.

**2·5. Gun Types Used in Electrostatic Cathode-ray Tubes.**—The guns used in cathode-ray tubes of the electrostatic focus and deflection type currently available in the United States are of three types.   The latest one of these to come into use has already been briefly described in

[1] Further experimental data in regard to various methods of measurement of spot size in complete cathode-ray tubes, and spot-size relationships for various conditions of operation, are given in Chap. 17.

[2] The assistance of A. Y. Bentley in the compilation of data and material for this section is gratefully acknowledged.

Sec. 2·4 and in Fig. 2·6a. The three guns differ principally in regard to the arrangement of the focusing lens. These variations introduce changes in the control characteristic, as well as in the total light output available, and in the quality of the focus. Photographs of typical samples of the three types of electron gun are shown in Fig. 2·11, with
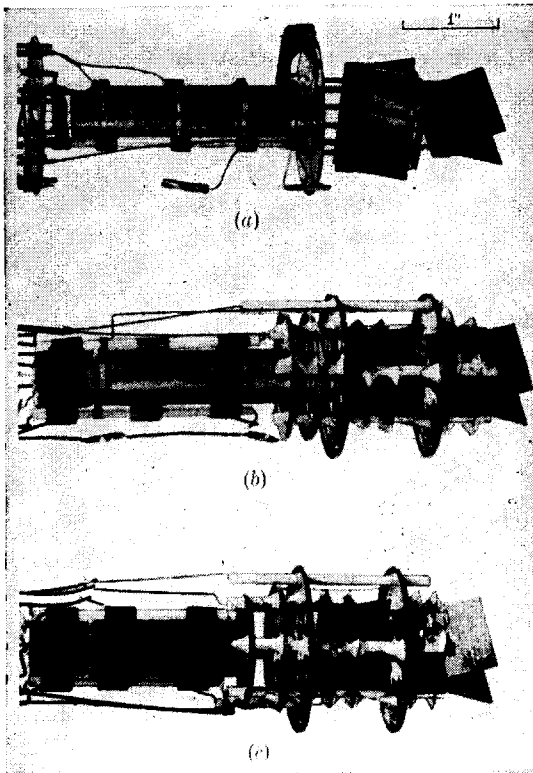


Fig. 2·11.—Photographs of typical electrostatic electron guns used in electrostatic deflection cathode-ray tube. (a) Triode type. (b) Accelerator type. (c) Zero-first-anode-current type.

cross sections as indicated in Fig. 2·12. In all these, the cathode and control-grid construction are not essentially different.

*Cathode.*—The thermionic cathode of almost all cathode-ray tubes is a nickel cylinder or cup, indirectly heated by an internal heater that is electrically insulated from the cathode by a ceramic covering. The emitting portion of the cathode is a small area on the closed end surface of this cylinder which is coated with barium and strontium oxides. The emitting surface is usually a plane perpendicular to the axis of the cup.

The input power to the heater is customarily 4 watts, and most heaters are designed for operation at 6.3 volts.

*Control or Modulating Grid.*—The element controlling the flow of electrons from the cathode is a nickel cylinder, usually $\frac{1}{2}$ in. in diameter, coaxial with the cathode cylinder. With the exception of an approximately 1-mm-diameter circular central opening immediately opposite the emitting portion of the cathode, the forward end of the cylinder is closed. The spacing between cathode and grid is about 0.005 to 0.010 in. and must be closely controlled.

Sometimes the grid cylinder extends a short distance beyond the plane containing the aperture. This extension is known as the "grid skirt" and is introduced to effect the proper degree of control of the beam. The grid skirt also introduces some additional focusing action. It is very important for good image formation that the planes of the cathode and grid aperture be parallel, and that the grid hole be truly circular and free from burrs. If any cathode material gets onto the grid aperture, the elevated temperature of the grid due to its proximity to the hot cathode may result in emission of electrons from the grid. These electrons are accelerated toward the screen by the high positive potential on other electrodes and cause uncontrollable stray light emission



FIG. 2·12.—Typical electron guns used in electrostatic cathode-ray tubes. (*a*) Triode type. (*b*) Accelerator type. (*c*) Zero-first-anode-current type.

known as a "ghost." To eliminate this effect, it is customary to reduce the emissivity of the grid either by gold-plating it, or by adding radiating fins to the grid cylinder to reduce its temperature, or both.

The rest of the gun structure is composed of an arrangement of coaxial cylindrical and apertured disk elements that differ in the three types of guns.

*Triode Guns.*—In the oldest type of gun, which is sometimes called a "triode gun" although it contains four essential elements (see Fig. 2·12*a*), the electrons after passing through the control-grid aperture enter the first anode, or focusing electrode. This electrode is in the form of a long cylinder containing one or more apertures of various sizes. The field

between the first anode and control grid forms part of the immersion or cathode lens discussed in Sec. 2·3, and is not considered to contribute any focusing action. Because the region within the focusing electrode is almost field-free, the electrons travel essentially in straight lines. The purpose of the apertures is to mask off the outer portion of the conical bundle of electrons. Immediately beyond the focusing electrode is the second anode. This electrode usually consists of a short cylinder closed at the far end by a disk containing a small central circular aperture. This aperture further masks off part of the exterior portions of the electron bundle. The second anode is maintained at or near ground potential and is connected electrically to a conducting coating that lines the inner wall and bulb of the cathode-ray tube to a point extending almost up to the forward end, which contains the fluorescent screen. Thus, the volume beyond the second anode forms an essentially field-free region.

The principal focusing action of the electron gun takes place in the region between the focusing electrode and the second anode because of the strong lens formed by the potential difference between these two elements. As is indicated in the figure, the potential of the focusing electrode is negative with respect to the second anode. For the construction usually employed, the voltage needed on the focusing electrode in order to bring the electron beam into focus at the screen is roughly one-fourth the total voltage applied to the electrons. One characteristic of a gun of this type is that the act of focusing the beam by varying the potential of the focusing electrode simultaneously changes the constants of the cathode lens and causes a change in the beam current. This unwanted change in brightness of the trace must be corrected by a manipulation of the control-grid potential, and the process of securing proper adjustment of the beam is thus made more complex. The maximum beam current that reaches the screen is relatively low; hence, although the focused spot has small size, the available brightness is only moderate.

*Accelerator Type of Electron Gun.*—This electron gun type is a modification of the one just described, containing an additional electrode that is interposed between the control grid and the focusing electrode or first anode (see Fig. 2·12b). This new electrode usually consists of an apertured disk or a shallow cup, which is connected internally to the second anode. This electrode accelerates the electrons in the region immediately in front of the grid to the velocity corresponding to second-anode potential, increasing the maximum current that may be drawn at zero grid bias. It further acts as a screen grid and prevents variation of the potential of the focusing electrode from affecting the constants of the cathode lens, which now is formed between the control grid and the accelerating electrode. Therefore the beam current is essentially

unaffected by variations in focusing voltage. Thus two desirable improvements have been effected by the introduction of the accelerator electrode: (1) freedom from interaction between focusing voltage and beam current, and (2) an appreciable increase in the modulation sensitivity. The latter is desirable for intensity modulation applications because the video amplifier may then have a lower gain, resulting in considerable saving in power. It should be noted, however, that this higher modulation sensitivity is obtained at the cost of some impairment of focus.

In both types of electron gun described thus far, an appreciable fraction of the total current is intercepted by the apertures in the focusing electrode. In practically all electrostatic deflection tubes the second anode also contains a masking aperture that collects a fraction of the current. The purpose of the aperture in the second anode is to assure a well-defined beam centrally located with respect to the deflection plates. In both electron guns described, the current flowing to the focusing electrode is usually considerably greater than that flowing to the second anode. Hence, to secure reasonably good voltage regulation of the first anode, it is necessary to make the resistance of the bleeder circuit relatively low, thus wasting power in the bleeder. A small amount of regulation of the first-anode voltage is desirable since the voltage of this electrode should decrease somewhat with increasing beam current in order to maintain focus (see Sec. 2·8). Such compensation by means of the regulation afforded in the bleeder circuit is, however, complicated by the fact that the variation in first-anode current existing from tube to tube is considerable, and therefore no universal regulation can be applied in this manner.

*Zero-first-anode-current Type of Electron Gun.*—In order to overcome the focusing-electrode regulation difficulties, a further modification of the gun has been made, in which the focusing electrode draws essentially no current.[1] A gun of this type is sketched in Fig. 2·12c. The accelerator electrode is in the form of a long cylinder, with a masking aperture at its forward end. As before, the focusing electrode is interposed between the accelerator and the second anode. However, it is now relatively short, and consists either of an open cylinder, as illustrated, or of an apertured disk with aperture diameter greater than that of the apertures in the adjacent parts of the accelerator and second anode. The electron lens formed in the region of the focusing electrode then makes the beam converge to a focus at the screen, as in the previous types. By masking the beam in $G_2$ instead of in $A_2$, secondary electrons emitted from the

[1] This type of gun structure was first produced by RCA. Its advantages have been clearly demonstrated, so that the more recently designed tubes of practically all manufacturers employ this type of gun.

masking aperture are less apt to reach the screen. Also, the smaller diameter of the beam in the focusing field is advantageous in that it reduces the effects of spherical aberration in the focusing lens.

Cathode-ray tubes of a given type number may contain any of the three types of guns. Specifications, particularly on older tube types, have been so lax that they could be met by any of the existing gun types. Therefore, the gun type used was a matter of preference with individual manufacturers. However, it is possible to identify tubes having their electron guns changed to the zero-focus-current guns because these are uniformly designated by the addition of the letter "A" after the tube type number. These and other newer zero-focus-current types which do not have the A designation may be identified in table D-1 by reference to the values pertaining to Anode No. 1 current.

The gun proper may be considered to end at the second anode. A converging bundle of electrons, well defined by the aperture in the second anode, and traveling with a speed that is determined by the total voltage difference between cathode and second anode, then passes through the region of two orthogonal sets of plates, where it is acted upon by the deflecting electrostatic fields.
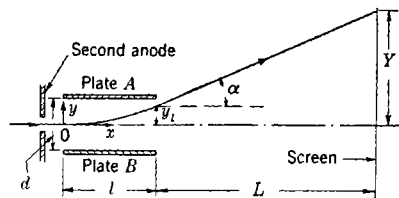


FIG. 2·13.—Deflection of electron beam in an electrostatic field.

**2·6. Theory of Deflection in an Electrostatic Field.**—The equations for the deflection of the beam at the fluorescent screen due to the electrostatic field between the plates between which the beam passes will now be derived. In this derivation, the simplifying assumptions are made that the plates are parallel, that the electrostatic field between the plates is uniform and normal to the plane of the plates, and that the field is zero everywhere else; that is, fringing fields are neglected.

The origin of the coordinates may be taken to be at the point at which the electron enters the field, with the $x$- and $y$-axes as indicated in Fig. 2·13. In this figure, $l$ = length of plates (cm), $d$ = separation of plates (cm), $L$ = distance from end of plates to screen, and $Y$ = position of deflected spot on screen. Also, let

   $V$ = potential of second anode with respect to cathode,

   $V_A$ = potential of top plate,

   $V_B$ = potential of bottom plate (for the direction of deflection shown, $V_B < V_A$),

   $V_d = V_A - V_B$ = deflecting voltage,

   $e$ = electronic charge,

   $m$ = electronic mass.

The kinetic energy of an electron as it enters the deflecting region will be

$$\tfrac{1}{2}mv^2 = V \cdot e. \tag{27}$$

Therefore, its speed $v$ is given by

$$v = \sqrt{\frac{2eV}{m}}, \tag{28}$$

and it is initially directed along the $x$-axis. Therefore, the initial conditions existing at point $O$ are $t = 0$, $x = 0$, $y = 0$, and $v_y = dy/dt = 0$.

Because of the potential difference existing between the plates, an electric field

$$E = \frac{V_d}{d} \qquad \text{volts/cm}, \tag{29}$$

which exerts a uniform force on the electron in the direction of the $+y$-axis, exists between the plates. By the time the electron reaches the end of the plates, this force has displaced it from the axis by an amount $y_l$, and its path at this point is inclined at an angle $\alpha$ with respect to the $x$-axis. The desired expression for the displacement is simply determined from the geometry illustrated, because

$$Y = y_l + L \tan \alpha. \tag{30}$$

The problem is to find $y_l$ and $\tan \alpha$.

The equation of motion for an electron in the electric field $E$ is

$$m \cdot \frac{d^2y}{dt^2} = E \cdot e. \tag{31}$$

When Eq. (31) is integrated twice, and the initial conditions already mentioned are used, both constants of integration are zero, and the equation for the displacement $y$ becomes

$$y = \frac{e}{m} \cdot E \cdot \frac{t^2}{2}. \tag{32}$$

To a first approximation, the electrons travel at the uniform speed $v$. The relation for the time $t$ required to travel a distance $x$ is given by $t = x/v$. Equation (32) may therefore be written in terms of the distance $x$ rather than in terms of time.

$$y = \frac{e}{m} \cdot E \cdot \frac{x^2}{2v^2}. \tag{33}$$

Using Eq. (27), Eq. (33) reduces to

$$y = \frac{1}{4} \frac{E}{V} \cdot x^2. \tag{34}$$

At the end of the plates, $y = y_l$ and $x = l$; hence

$$y_l = \frac{1}{4}\frac{E}{V} \cdot l^2. \tag{35}$$

Also, from Eq. (32), the inclination of the beam at any point is

$$\frac{dy}{dx} = \frac{1}{2}\frac{E}{V} \cdot x. \tag{36}$$

In Fig. 2·13 the value of $dy/dx$ at the end of the plates is represented as $\tan \alpha$; therefore from Eq. (36)

$$\tan \alpha = \frac{1}{2}\frac{E}{V} \cdot l. \tag{37}$$

Substituting Eqs. (35) and (37) into Eq. (30),

$$
\begin{aligned}
Y &= \frac{1}{4}\frac{E}{V} \cdot l^2 + \frac{1}{2}\frac{E}{V} \cdot l \cdot L \\
  &= \frac{1}{2}\frac{El}{V}\left(L + \frac{l}{2}\right) \\
  &\approx \frac{1}{2}\frac{E}{V} \cdot L \cdot l
\end{aligned}
\tag{38}
$$

for the case where $l \ll L$. This condition exists in most cathode-ray tubes.

Replacing the $E$ in Eq. (38) by its constituent factors, from Eq. (29),

$$Y = \frac{1}{2} \cdot \frac{V_d}{V}\frac{l}{d} \cdot L. \tag{39}$$

The deflection sensitivity

$$\text{DS} \equiv \frac{Y}{V_d} = \frac{1}{2}\frac{l}{d} \cdot \frac{1}{V}L. \tag{40}$$

A more customary method of stating the deflection characteristics is in terms of the deflection factor DF, which is the reciprocal of the deflection sensitivity and is usually expressed in deflecting volts per inch of deflection; that is,

$$\text{DF} \equiv \frac{V_d}{Y} = \frac{2dV}{lL} \equiv k \cdot V \qquad \text{(volts/inch)}. \tag{41}$$

The more sensitive the tube, the smaller will be its deflection factor. It is evident from Eq. (41) why short tubes, in which the plates are relatively near the screen, have large deflection factors. The plates nearest the screen are designated as $D_1$ and $D_2$, and those nearer the base as $D_3$ and $D_4$. Generally the deflection factor for plates $D_1$ and $D_2$ is considerably greater than that for plates $D_3$ and $D_4$ because of the decreased

value of $L$ for the former set of plates. This difference can be partially counteracted by a decrease in the spacing or an increase in length, or both, for the set nearer the screen.

In practice, the deflecting plates used in cathode-ray tubes do not consist of the straight parallel plates here described. Rather, they are either curved or bent to improve the sensitivity and still prevent the beam from striking the forward end of the plates.

In operation, the deflection factor of the cathode-ray tube is directly proportional to the operating voltage $V$ of the second anode. This voltage is limited by the difficulty in producing the peak deflecting voltage needed to deflect the spot to the edge of the screen.

**2·7. Postdeflection Acceleration.**—The light output of a phosphor increases roughly as the square of the voltage through which the electrons striking the screen have been accelerated. Therefore it is advantageous to use as high a total voltage as possible. However, doubling the total voltage also doubles the deflection factor, as is evident from Eq. (38). In order to secure the advantages of higher brightness without a corresponding sacrifice in deflection sensitivity, the possibility of using post-deflection acceleration has been introduced in several types of cathode-ray tubes. In these tubes, the electrons may be accelerated through a potential difference approximately equal to that existing between cathode and second anode after they have passed the region of the deflection plates. The required accelerating field is achieved by splitting the conducting coating that usually extends almost to the screen. The annular gap between the resulting two conducting sections is $\frac{1}{4}$- to $\frac{1}{2}$-in. wide, and is located on the bulb a short distance beyond deflection plates $D_1$ and $D_2$. The section of the coating surrounding the deflection plates is connected internally with the second anode, whose lead comes out through one of the pins in the base of the tube. The conducting surface between the annular gap and the screen is called the "third anode" or "intensifier," to which electrical connection is made by means of a separate contact on the bulb. In order to eliminate flashover between the second and third anode due to sharp points that may exist in the adjacent edges of the two coatings, the space between them is usually bridged by a semiconducting coating having a high resistance. The coating serves to insure a uniform field distribution in this region.

In order to accelerate the electrons after they leave the deflection plates without affecting the deflection sensitivity of the tube, it would be necessary that the equipotential surfaces of the accelerating field be everywhere normal to the direction of the incident electrons. This condition has not been achieved in practice, and the shape of the equipotential surfaces in the region between second and third anodes is such as to alter the trajectories of the electrons. Consequently, for a voltage

difference between second and third anodes $(E_{b3} - E_{b2})$ equal to that between cathode and second anode $(E_{b2} - E_k)$, there is an increase in deflection factor of approximately 20 per cent over that which would exist if the third anode were connected directly to the second anode.

In addition to the effect of the postdeflection field on the deflection sensitivity, this field introduces aberrations in the deflected spot, so that the maximum useful ratio of $E_{b3}$ to $E_{b2}$ is approximately 2 to 1.

With careful design, it should be possible to achieve the deflection sensitivity and light output obtained when using postdeflection acceleration in a conventional type of tube not employing this feature. However, the problem of obtaining voltage insulation through the base of
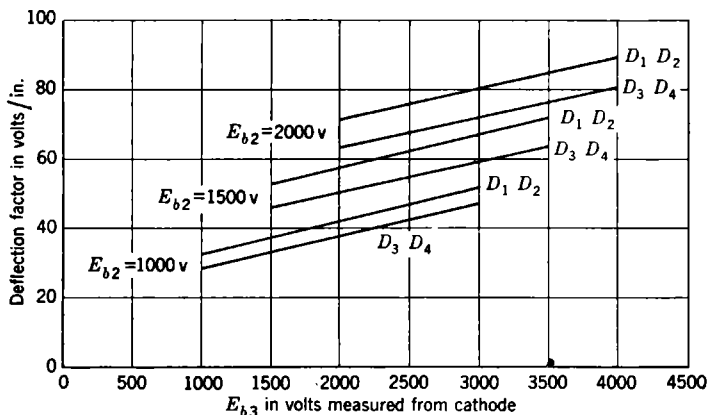


FIG. 2·14.—Variation of deflection factors with second- and third-anode voltage, for 5CP1-type tube.

such a tube is considerable, and the postdeflection-acceleration principle reduces these insulation difficulties very considerably. A further factor in favor of the use of postdeflection acceleration is that the total accelerating voltage may be applied half below ground potential and half above ground potential, thus reducing the problem of insulation of all supply voltages. Several 3-in., 5-in., and 12-in. electrostatic tubes employ the postdeflection-acceleration principle.[1]

**2·8. Electrical Characteristics of Standard Cathode-ray Tubes.** *Deflection Characteristics.*—As indicated by Eq. (41), the deflection factor of a tube is proportional to the accelerating voltage applied to the second anode. Using the customary terminology for second anode voltage, namely $E_{b2}$,

$$\mathrm{DF} = k \cdot E_{b2}. \tag{42}$$

[1] For further particulars consult Appendix D. This same principle, but applying the total voltage in several steps, is used in the special type 5RP tube described in Sec. 2·9.

If allowance is made for the introduction of postdeflection acceleration and its effect on the deflection factor, the deflection-factor equation is, in the general case,

$$DF = k_1(E_{b2}) + k_2(E_{b3} - E_{b2}). \qquad (43)$$

Figure 2·14 illustrates the behavior of the deflection factor with variation in the accelerating voltages for a common type of cathode-ray tube (5CP1). For this tube type, the constants $k_1$ and $k_2$ in Eq. (43) have the following values when $E_{b2}$ and $E_{b3}$ are expressed in kilovolts, and the deflection factor is in volts per inch: for deflection by $D_1$ and $D_2$, $k_1 = 35$, $k_2 = 9$; for deflection by $D_3$ and $D_4$, $k_1 = 30$, $k_2 = 10$.[1]

*Transfer Characteristics.*—From Eq. (18) in Sec. 2·4, the relation between screen current and grid drive for electrostatic tubes is

$$i_{sn} = A \cdot (E_{co} - E_{c1})^2 = A \cdot E_d^2. \qquad (2·18)$$

As noted in Sec. 2·4, the method of measurement adopted affects the evaluation of the constants $n$ and $A$ in Eq. (12). Figure 2·15 presents data for tubes having the same cutoff bias, but which have electron guns of the three types discussed in Sec. 2·5 but made by different manufacturers. For elec-



FIG. 2·15.—Transfer characteristics of various gun types used in electrostatic cathode-ray tubes: (1) accelerator; (2) zero-focus-current; and (3) triode type. Test conditions: $E_{b2} = 1500$ volts, $E_{b3} = 3000$ volts.

trostatic tubes made during the war years, those made with triode guns generally had the lowest grid-drive factor $A$, whereas those made with the accelerator type have the highest. This does not imply that the three types of gun necessarily differ so widely in their transfer characteristics. For any specific tube, the cutoff bias, as well as the transfer characteristic, varies with changes in the operating voltages applied to the tube.

Figure 2·16 represents transfer characteristics for an accelerator-type gun. The cutoff bias increases roughly linearly with increasing second-anode voltage, and the grid-drive factor $A$ decreases as the cutoff bias increases. This behavior is characteristic of all guns.

The variation in geometry from tube to tube makes it impossible to

[1] For deflection factors of all common tubes, as well as tolerances in these factors, see the table in Appendix D.

express the grid-drive factor $A$ specifically in terms of the cutoff bias measured under some standard condition. In practice, the specification limits on transfer characteristics are expressed in terms of the maximum grid drive required to produce a stated change in screen current. The transfer characteristic is specified only for a relatively restricted number of tube types. Since many tube types do not provide means for measurement of the screen current, the more customary specification is in terms of a "modulation characteristic," which is the relation between grid drive and light output.



FIG. 2·16.—Transfer characteristics as a function of accelerating voltage, for type 5CP1 tube.

| Curve | $E_{b2}$, volts d-c | $E_{b3}$, volts d-c |
|-------|---------|---------|
| 1 | 2250 | 4500 |
| 2 | 2000 | 4000 |
| 3 | 1750 | 3500 |
| 4 | 1500 | 3000 |
| 5 | 1250 | 2500 |
| 6 | 1000 | 2000 |

*Focus-voltage Characteristics.*— The guns used in all common types of electrostatic cathode-ray tubes are so designed that the voltage needed on the focusing electrode, the first anode, to focus the beam at a specified grid drive is approximately one-fourth that applied to the second anode. Specified tolerances on this fraction are usually $\pm 20$ per cent.

For any given tube, the focusing voltage varies with the grid drive. A typical curve illustrating this variation is shown in Fig. 2·17. If
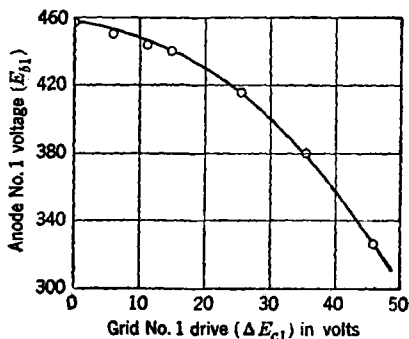


FIG. 2·17.—Focusing-anode voltage for best focus as a function of grid drive from cutoff. Curve is typical of that obtained with 3BP1A tube.

optimum focus is to be maintained
in the case of an intensity-modu-
lated display, the focusing voltage
must vary in the manner illus-
trated over the range of grid
voltages applied to the tube. As
briefly discussed in Sec. 2·5, this
variation may be obtained by pro-
viding a certain amount of regula-
tion in the bleeder supply, but
this method is not flexible enough
to compensate properly for varia-
tions from tube to tube. There-
fore, in critical applications, the
focusing voltage may be varied by
applying to the focusing electrode
a waveform similar to that intro-
duced upon the control grid, but
suitably amplified and inverted.
In some cases, it is practical to use a
pulse transformer for this purpose.



Fig. 2·18.—Variation of line width with
anode voltage. Curve $A$: light output ad-
justed to 5 foot-lamberts. Curve $B$: light
output adjusted to 10 foot-lamberts.

*Line-width Characteristics.*—The spot size, or the width of the line
traced out on the screen of an electrostatic cathode-ray tube, increases
with increasing screen current or light output, and decreases with increas-



Fig. 2·19.—Typical line-width versus
screen-current curves for 5CP1 cathode-ray
tubes. Curves 1: $E_{b2} = 1500$ volts; $E_{b3}$
$= 3000$ volts. Curves 2: $E_{b2} = 2000$ volts;
$E_{b3} = 4000$ volts. Solid curve is measured
at Position $A$, and dotted curve is measured
at Position $B$.

ing over-all accelerating voltage.[1]
For a given beam current, with the
focusing voltage adjusted for best
focus at the center of the tube face,
the line width is found to increase
with increasing distance from the
center of the tube. This increase
is, in general, different for orthog-
onal deflections produced by the
two sets of deflecting plates. The
specifications for line width are
based upon the "shrinking raster"
method described in Sec. 17·4.
The ordinates of Figs. 2·18 and
2·19 refer to this method of

[1] Proper adjustments of operating
voltages and use of push-pull deflection
are necessary for optimum spot size.
See Sec. 2·10.

measurement. Fig. 2·18 illustrates the decrease in spot size with increasing accelerating voltage, for two light-output levels. Figure 2·19 illustrates the variation of line width with screen current for two values of accelerating voltage.

**2·9. Special Types of Cathode-ray Tubes.** *Central-electrode–radial-deflection Type* (3DP1).—The purpose of this type of tube is to provide an increased length of time base without increase in the tube size for A-scope applications. This condition is met by making the time base a large circle concentric with the tube axis instead of the customary straight line across the diameter of the tube. When so used, the tube is called a "J-scope." The electron gun used in this tube is standard, being identical to that used in the 3BP1 type. The circular time base is produced by applying voltages in quadrature to the two sets of deflection plates. The signal is applied to an electrode in the form of a tapered rod sealed into the center of the tube face; the electrode extends axially toward, but not as far as, the region of the deflection plates. Contact to this electrode is made by a button that extends through the tube face. A difference of potential between this central electrode and the conducting coating on the bulb produces a radial electric field. Hence, signals applied to the central electrode appear on the trace as inward or outward deviations from the circular trace.

A tube of this type is not adapted to the measurement of the strength of the signal applied to the central electrode because the radial deflection sensitivity is a function of the sign of the voltage applied to the central electrode, the radius of the base circle, and the instantaneous position of the spot on this circle. The electric-field strength at any point in the radial field between the central electrode and the second-anode coating varies as the reciprocal of the distance of the point from the axis of the tube. Hence, the deflection sensitivity decreases in the same manner. Accordingly, the deflection factor, which is the reciprocal of the deflection sensitivity, increases linearly with distance from the central electrode. This behavior is illustrated in Fig. 2·20, which also illustrates that the deflection factor is greater when the radial deflection occurs along the line corresponding to the deflection produced by plates $D_3$ and $D_4$ than when it is along the line corresponding to the orthogonal set of plates $D_1$ and $D_2$. Radial deflection along the line $D_1D_2$ results in a lower deflection factor because, for unit deflection produced on the tube face by either set of deflecting plates in the absence of any signal voltage on the central electrode, the average position of the electron beam is nearer the central electrode when deflected by plates $D_1$ and $D_2$ than when the deflection is by the plates farther removed from the screen, $D_3$ and $D_4$. The radial field distribution also accounts for the nonsymmetry between the curves shown in Fig. 2·21 for radial deflection toward the center and those for

radial deflection away from the center of the tube face, particularly for the base circle of 15-mm radius.   Because of the complications illustrated
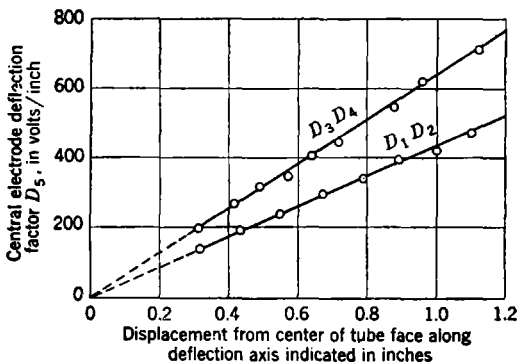


FIG. 2·20.—Variation of deflection factor for central electrode of type 3DP1 cathode-ray tube, deflection produced by deflecting plates $D_1D_2$ and $D_3D_4$.
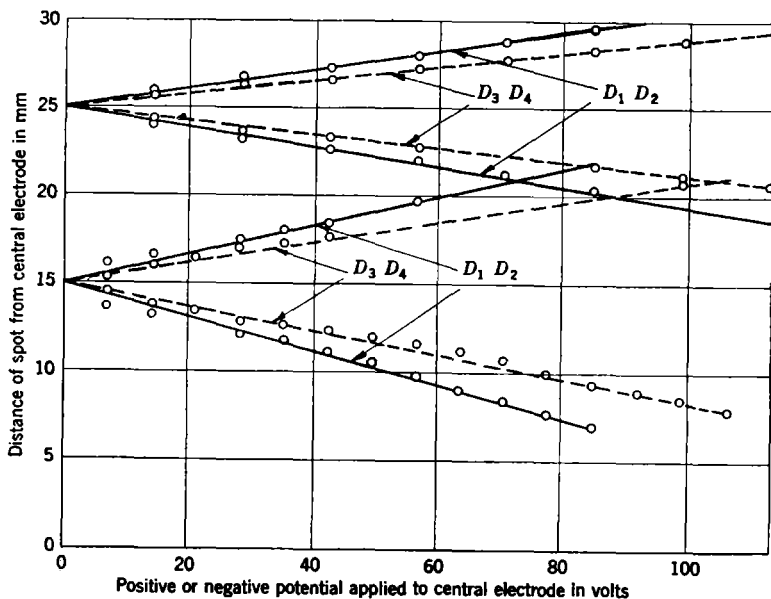


FIG. 2·21.—Radial deflection as a function of central-electrode potential for a type 3DP1 tube with $E_b = 2000$ volts.   Note asymmetry when base circle has a radius of 15 mm.

in Figs. 2·20 and 2·21, the use of the 3DP1 cathode-ray tube is restricted to the measurement of time relationships.

*Multigun Electrostatic Cathode-ray Tubes.*—It is often desirable to present simultaneously on a cathode-ray-tube screen either several related

quantities, such as current and voltage, as a function of time, or two sweeps of different speeds, displaced vertically. Cathode-ray tubes incorporating more than one electron gun and deflecting system have been designed for these applications.

The 5SP1, a tube of the two-gun type, consists essentially of two complete 5CP1 electrical systems in one envelope. All elements of each gun and deflecting system are completely independent and have separate pins. The eight leads to the deflection plates and two to the second anodes are brought out through the glass neck. The two gun structures are so mounted that their axes intersect at the screen. Electrostatic shielding of the two deflection systems from one another is provided, so that there is practically no interaction between them. The maximum coupling between any two plates, one in each system, is approximately 0.03 $\mu\mu$f. The capacitance between the two modulating grids is approximately 0.075 $\mu\mu$f. The two traces may be shifted at will by separate centering controls; only the results of deviation from perfect parallelism of the two sets of corresponding deflection plates cannot conveniently be compensated. This deviation may amount to as much as 3°.

More than two guns may be mounted in a single tube. Also, some corresponding elements must usually be connected internally, in order to reduce the number of leads through the base.

The multiple-gun tubes are particularly useful when the phenomena to be observed are nonrecurrent. If the phenomena recur at regular intervals, and if the conditions of writing speed and recurrence rate are not extreme, conventional single-gun tubes may be used for the observation of two phenomena by employing electronic switching of the two waveforms, each of which is presented on alternate sweeps. Usually the use of a multiple-gun tube is to be preferred to the added circuit complexities necessary for the electronic switching.

*High-intensity Cathode-ray Tubes.*—In order to obtain a useful intensity of trace when very fast single sweeps are to be observed, the energy of the cathode-ray beam must be considerably higher than in the customary tube types. This increase in energy is obtained by raising the voltage rather than the current since a high current usually makes the spot size too large.

The best method of achieving the desired result is by extending the postdeflection-acceleration principle discussed in Sec. 2·7. It was there pointed out that the voltage on the third anode could not be increased more than a limited amount if excessive deflection defocusing was to be avoided. A much higher ratio of total accelerating voltage to that existing in the region of deflection has been made possible by controlling the shape of the equipotential surfaces, by altering the shape of the bulb from the curved wall of the 5CP1 type to a cylindrical section of the

same diameter as the face, and by introducing into this cylindrical section three intensifier bands held at specific voltages. The type 5RP tube incorporates this feature, and, with it, a ratio for $E_{b3}/E_{b2}$ (with respect to the cathode) of 10/1 is possible with a final voltage of 25 kv. Under these conditions, it is possible to photograph traces for which the maximum writing speed is approximately 250 cm/μsec.[1]

*Ultrahigh-frequency Cathode-ray tubes.*—The amplitude $A$ of the deflection produced by a parallel-plate type of deflecting system varies with the frequency of an applied sinusoidal voltage of constant peak amplitude according to the relation

$$A = A_0 \frac{\sin \omega t/2}{\omega t/2}, \tag{44}$$

where $A_0$ is the amplitude of deflection for frequencies approaching zero, $\omega$ is the angular frequency of the applied deflecting voltage in radians per second, and $t$ is the transit time of the electron through the deflecting field in seconds. Accordingly, as the frequency increases, $A$ will be reduced to 50 per cent of $A_0$ when $\omega t/2 = 2$, will be zero when $\omega t/2 = \pi$, and thereafter will alternate in sign in the manner of a damped oscillation.

For nonsinusoidal transient phenomena containing very-high-frequency components, serious distortion may take place because the sensitivity will be different for the various harmonics, and some components may even produce reversed deflections. Hence, in order to reproduce an exponential waveform without appreciable distortion, the time constant of the exponential should be at least five times the electron transit time.

From these considerations, it is evident that the transit time of the electrons through the deflecting region of the cathode-ray tube should be reduced to a minimum when observations of phenomena involving ultrahigh frequencies, such as oscillations in the microwave region, or transient phenomena containing ultrahigh-frequency components, are to be made.

Lee[2] has constructed an oscillograph using very short deflection plates (5 mm) and a high accelerating voltage (50 kv). If an effective plate length of 7 mm is allowed for, the transit time under these conditions is $5.5 \times 10^{-11}$ sec and the reduction of deflection sensitivity is therefore only 4 per cent at 3000 Mc/sec and 40 per cent at 10,000 Mc/sec. Lee's oscillograph requires continuous pumping, and records the trace by means of direct electron impact on a photographic plate. Optical enlargement of 100 times of these minute traces is possible, and, at this magnification, the sensitivity of the oscillograph at 50 kv is 0.1 mm per volt. This sensitivity corresponds to a deflection factor of 250 volts per inch.

[1] Additional information on the 5RP type will be found in Appendix D.

[2] G. M. Lee, "A Three-Beam Microoscillograph for Recording at Frequencies up to 10,000 Mc/sec," *Proc. I.R.E.*, **34**, 121W (1946).

About 10 min are required for changing the photographic plate and for reestablishment of operating vacuum; eight sets of three oscillograms may be recorded on a single plate.

The desire for a sealed-off tube of reasonable deflection sensitivity suitable either for direct viewing or for photography at high writing
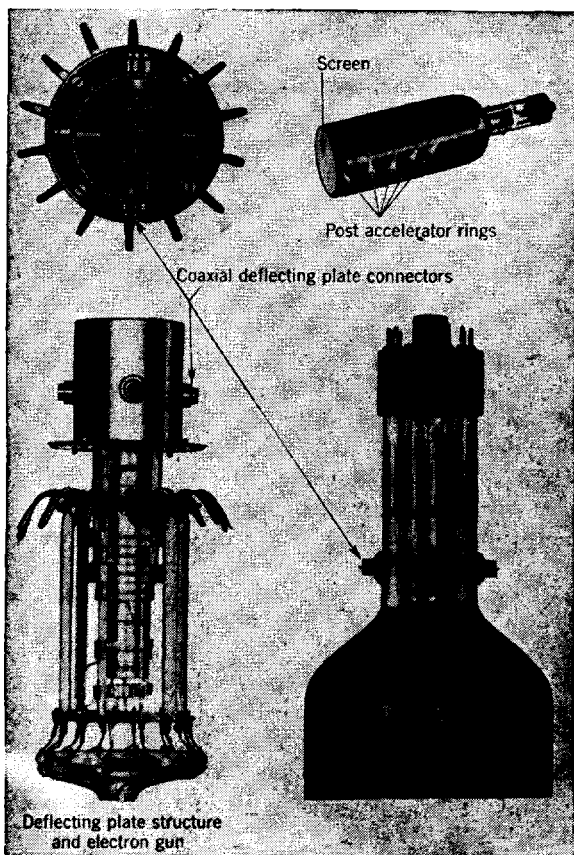


FIG. 2·22.—Special cathode-ray tube, Du Mont type K1017. (*Courtesy of Du Mont Laboratories.*)

speeds, to be incorporated into a high-speed oscilloscope developed at the Radiation Laboratory (see Sec. 7·7), led to the development by Du Mont of the type K-1017 ultrahigh-frequency cathode-ray tube.

This tube has two orthogonal sets of deflection plates 8 mm long, each set enclosed in a shielding structure to prevent electrostatic coupling, with plates directly connected to coaxial-type fittings attached to the

glass tube neck. The speed of the electron beam as it passes through the deflecting region is limited for continuous operation to that corresponding to an accelerating potential of 4.5 kv. For pulsed operation, a somewhat higher potential may be used. After deflection, the beam is accelerated by a series of five intensifying bands. With $E_{b2} = 3$kv, the calculated transit time through one set of plates is $3 \times 10^{-10}$ sec, for which 2000-Mc/sec sine waves will be recorded at half amplitude. With $E_{b2} = 3$ kv, and $E_{b3} = 25$ kv, the deflection factor is approximately 125 volts per inch. The screen normally used is the P11, and with this screen and the above voltages applied to the tube, sufficient light intensity is available to enable photographic recording of single-trace writing speeds up to 300 in./$\mu$sec with orthochromatic film (Eastman 5211) and a coated lens of aperture f/1.5.

Figure 2·22 shows several views of the tube. Additional electrical and mechanical details will be found in Table D·1.

**2·10. Remarks Concerning Operating Conditions for Electrostatic CRT's.** *Adjustment of Mean Potential of Deflection Plates.*—The mean
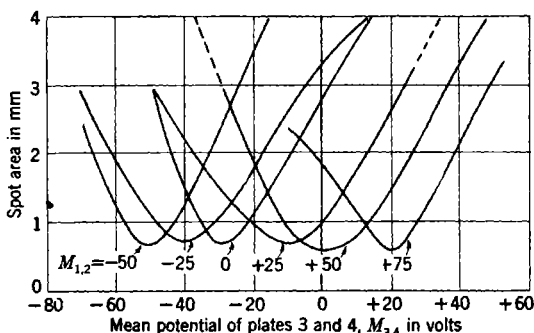


Fig. 2·23.—Spot area as a function of the mean potential of the deflection plates with respect to that of the second anode.

potential of the two pairs of deflection plates with respect to the potential of the second anode must be properly adjusted if optimum spot size is required. Normally one would expect that the optimum results would be obtained when the mean potential of these plates is the same as that of the second anode. In practice it is found that values other than zero are often necessary in order to obtain good focus. The reason is that misalignments in the deflection-plate structures often introduce into the electric fields asymmetries that can be at least partially compensated by proper adjustment of the mean potentials. Figure 2·23 gives experimental results for a particular cathode-ray tube. Each of the series of curves here represented gives the area of the spot, measured in square millimeters, for a fixed value of the mean potential $M_{12}$ of plates 1 and 2,

when the mean potential $M_{34}$ of the other set is allowed to take on various values. For each value of $M_{12}$ there corresponds a specific value of $M_{34}$ which produces a spot of minimum area, and the minimum area of spot is not sensitive to the exact values of the set of potentials chosen. The minima of the curves of Fig. 2·23 are indicated as circles in Fig. 2·24. There is considerable variation in the optimum value of $M_{12}$ and $M_{34}$ from tube to tube of a given type, as well as a systematic difference between specific tube types. The lines plotted in Fig. 2·24 indicate averaged data for a large number of tubes for three typical tube types. From these curves, it is apparent that provision should be made for
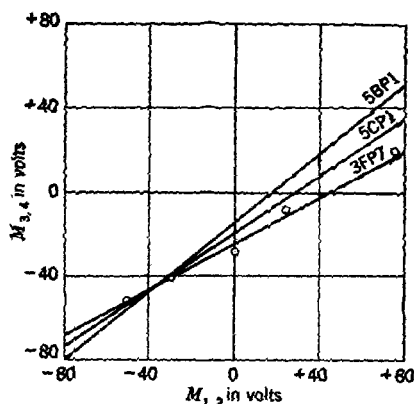


Fig. 2·24.—Average value of mean potentials $M_{1,2}$ and $M_{3,4}$ of deflecting plates for optimum focus. Potentials are measured with respect to that of the second anode.

adjustment of the mean potential of at least one set of deflection plates, and that its range of operating values will depend upon the mean potential of the other "fixed" set. One method of making this adjustment is to set the mean potential of Plates $D_1$ and $D_2$ at the second-anode potential, and to provide means for the adjustment of the mean potential of $D_3$ and $D_4$ between 0 and 50 volts below the second-anode potential. For any given tube, the adjustment of mean potential for optimum focus should be made when the tube is installed; it will usually not require further adjustment. This control, often called an "astigmatism control" does not therefore need to appear on the panel containing operating adjustments.

*Push-pull Deflection.*—As the spot is deflected from the center of the tube face by the action of one pair of deflection plates, it is subject to deflection defocusing, in which a round spot is distorted into an elliptical shape with the major axis of the ellipse along the direction of deflection. Because the electron beam has an appreciable cross section, the portion

of the beam that is nearer the positive deflection plate is traveling at a higher speed than that portion on the opposite side, and it is therefore deflected less by the electric field. In addition, the fringing fields around the deflection plates contribute an appreciable focusing action. For least disturbance of the focus, this fringing field should be as symmetrical as possible.[1] In order to insure symmetry, and thus to minimize deflection defocusing, the deflecting field should be produced in such a way that the mean potential of the pair of plates remains constant. Push-pull driver tubes, which provide symmetrical voltage swings of the two deflection plates, may be used. In fact, for cathode-ray tubes having a high deflection factor, the method of driving a single plate of a pair with an ordinary receiving-type tube, besides causing serious defocusing, would require operating the tube beyond the voltage limit for a tube of this type.

For optimum performance both the sweep and the signal plates should have push-pull drive. However, if the amplitude of the signal is restricted to a small fraction of the screen radius, single-sided drive for the *signal* will give reasonably satisfactory results.

*Push-pull Centering.*—For the same reasons discussed in the preceding paragraph, the centering controls for the two pairs of deflection plates should apply symmetrical voltages, so as to maintain a constant mean potential.[2]

*Choice of Operating-voltage Levels.*—For maximum light output and sharpness of trace, the cathode-ray tube should be operated at as high an accelerating voltage as possible, consistent with power-supply and driving-circuit limitations.

In Fig. 7·17 the cathode is at a negative potential, the second anode at, or slightly above, ground potential, and the third anode at a high positive potential (+2000 volts). The ground of the system could be at the cathode or at the third anode without altering its performance. However, it is desirable to have the greatest possible number of the electrodes that must accept signals near ground potential. Therefore, the second anode and the deflection plates are kept near ground, as shown.

*Shielding.*—Magnetic shielding of electrostatic cathode-ray tubes is almost a necessity in order to reduce the effect on the pattern of small alternating magnetic fields.[3]

## MAGNETIC CATHODE-RAY TUBES

The principal advantages of tubes of the magnetic-deflection type as compared with those of the electrostatic-deflection type are their better

---

[1] For an extensive discussion, see I. G. Maloff and D. W. Epstein, *Electron Optics in Television*, McGraw-Hill, New York, 1938.

[2] A typical circuit illustrating both push-pull centering and deflection is given in Fig. 7·17.

[3] For a discussion of magnetic shields, see Sec. 16·4.

spot size at high luminance levels and their shorter length. The shorter length is primarily due to the greater practicable deflection angle. The reduction in length is greatest for medium-sized tubes, and becomes relatively small for tubes with very large face diameters. Several typical magnetic cathode-ray tubes are illustrated in Fig. 2·25.

In order to attain these advantages, external focus and deflection coils must be introduced. The use of these coils involves greater complexity of both deflection and focus control circuits than in the case of electrostatic deflection and focusing, with consequent increases in weight both in the tube mount and in the larger power supplies required. It
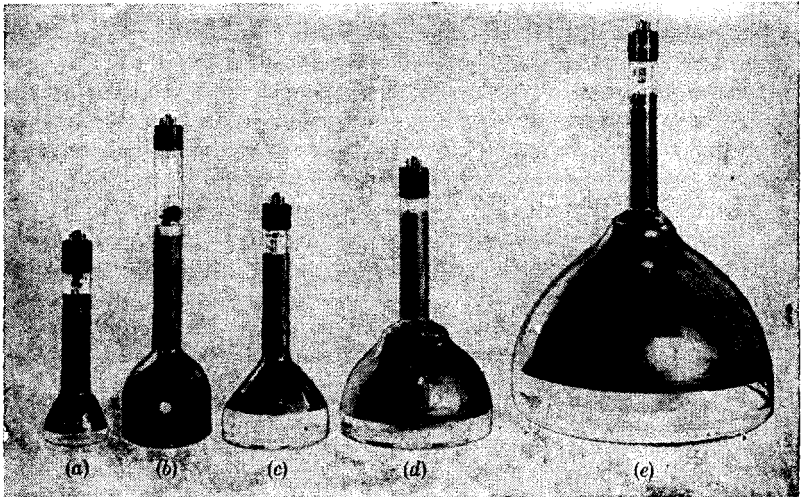


FIG. 2·25.—Typical magnetic cathode-ray tubes. (a) 3HP7; (b) 4AP10; (c) 5FP7; (d) 7BP7; (e) 12DP7.

should also be pointed out that the cost in driving power could be considerably reduced if the advantage of short over-all length were sacrificed to some extent. If the beam deflection angle of 55° commonly used for military-type tubes could be decreased to 35° to 40°, a significant saving in power, as well as a reduction in the deflection defocusing, could be attained.

Magnetic cathode-ray tubes are the logical choice for high performance only when the display involves intensity modulation of the traces. For oscilloscopes, the use of an electrostatic tube is far less cumbersome, and, in general, gives just as satisfactory performance.

**2·11. Triode Gun.**—This simplest of all gun types consists of cathode, control grid, and high-voltage anode. It has been used extensively in British cathode-ray tubes during the war, and is capable of giving

excellent performance.    Its chief disadvantages are a considerable variation in cutoff bias and transfer characteristic, both of which are functions of the accelerating voltage.    It is not a common gun type in the United States; therefore it will not be discussed further.

**2·12. Tetrode Gun.**—The tetrode gun, sketched in Fig. 2·6b, is the basic type used in cathode-ray tubes manufactured in the United States. It has an extra electrode, known as the "second grid, $G_2$" (sometimes also called a "first anode"), located immediately in front of the modulating grid $G_1$.    This grid is usually in the form of a shallow cylinder with a relatively small aperture at the end nearest the control grid, and
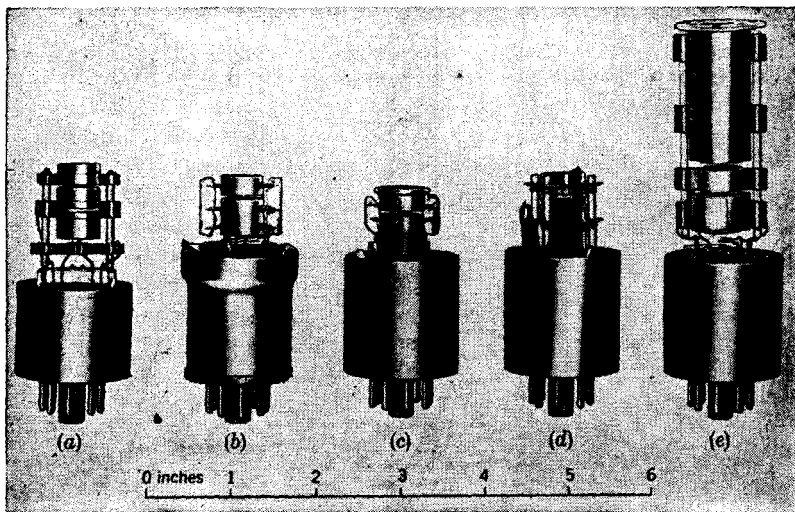


FIG. 2·26.—Several versions of guns used in magnetic tubes.

with its forward end either wide open or with an outwardly rolled edge. The chief purpose of this electrode is to act as a screen grid, and thus make the cutoff voltage independent of the anode voltage.    It is also possible to utilize this electrode for blanking the trace.    Although the normal operating voltage on $G_2$ is $E_{c2} = +250$ volts, an improvement in spot size results if this grid is made more positive (see Sec. 17·8).    It should therefore be operated at as high a voltage as possible, but the changes in cutoff bias and modulating characteristics which occur with changing $E_{c2}$ must be considered.[1]

Figures 2·26a to d illustrates several versions of this type of gun as made by various manufacturers.

[1] The increase in cathode loading which results when $E_{c2}$ is raised will shorten the life of the cathode.    Whether this will be significant or not depends upon the specific conditions of operation, such as the average operating current, etc.

*Transfer Characteristic of Tetrode Gun Type.*—As stated in Sec. 2·4, the beam-current—grid-bias relation for a magnetic tube, as obtained by the "extrapolated cutoff" method, is

$$i_{\text{sn}} = A(E_{c1} - E_{\text{co}})^3 = AE_d^3 \tag{2·17}$$

A condition for Eq. (2·17) is that all potentials except $E_{c1}$ be held constant. From Fig. 2·27, which gives experimental data on three tubes differing in cutoff voltage, it is evident that the cubic law holds closely, and also that the grid-drive factor $A$, which is determined from the slope of curves, decreases with increasing $E_{\text{co}}$. Measurements of the transfer
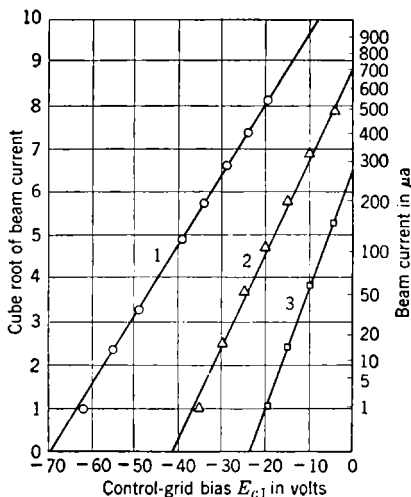


Fig. 2·27.—Static characteristics of three 5FP7 cathode-ray tubes at $E_b = 4\text{kv}$, $E_{c2} = 25\text{C}$ volts.

characteristic of a large number of tubes of various manufacturers give the distribution of points shown in Fig. 2·28, in which the factor $A$ is plotted against the extrapolated cutoff voltage $E_{\text{co}}$. A mean-value curve has been drawn through these points, but this curve follows no simple mathematical relationship. Very roughly,

$$A \approx 1.5E_{\text{co}}^{-1.3}. \tag{45}$$

This curve indicates (1) a wide range of $E_{\text{co}}$ for production tubes, (2) considerable scattering in the value of $A$ for a given $E_{\text{co}}$, and (3) a factor of approximately 5 in the range of values of $A$ to be expected in production tubes. Accordingly, the grid drive required to produce a given beam current may vary by a factor of $\sqrt[3]{5}$, or 1.7. This fact must be considered in the design of amplifiers to drive the tube.

Factors that affect the cutoff bias and transfer characteristic are the size of the $G_1$ aperture, the spacing between cathode and grid, and the effects of the field distribution immediately in front of the $G_1$ aperture. In the case of a simple triode gun, this distribution is determined by the value of $E_b$; for the tetrode guns, it is determined by the shape, location, and potential of the screen grid $G_2$, and *is almost independent of the value of $E_b$*. Once a choice in cutoff, normal operating value of $E_{c2}$, etc., has been decided upon, the spread in cutoff values illustrated in
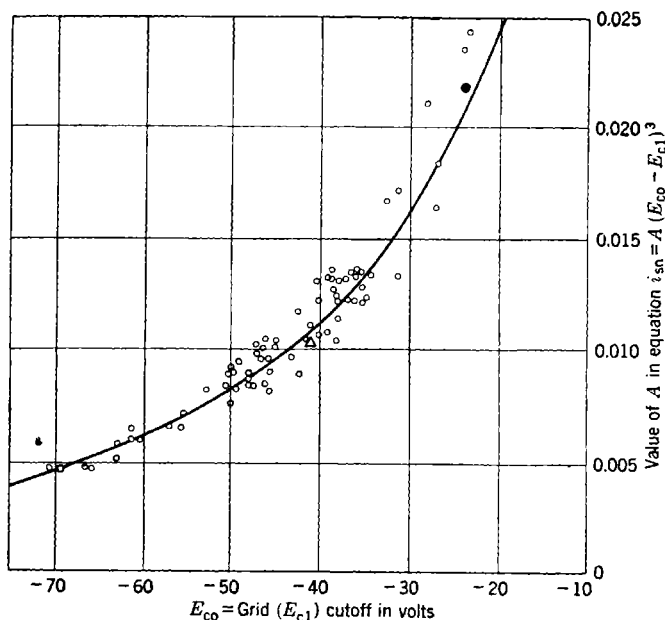


FIG. 2.28.—Variation of grid-drive factor $A$ with extrapolated cutoff voltage.

Fig. 2.28 results primarily from variations (0.001 in. to 0.002 in.) in the normal cathode-to-grid spacing, which normally is about 0.005 in.

The variation in $A$ for a given $E_{co}$ for tubes of the same manufacturer is caused by variations in cathode emissivity.   For any given tube, a value of $A$ far below the line indicated in Fig. 2.28 indicates an unsatisfactory cathode.   Usually such a tube will be found to have the central part of the cathode inactive because of gas in the tube, which causes positive-ion bombardment of the cathode.   Such a tube will almost always be unsatisfactory in operation because of aberrations in the focused spot.

For a given tube, both the cutoff and transfer characteristic are affected by the value of $E_{c2}$.   Figure 2.29 illustrates this behavior for a

single tube.   For comparison, the dashed line in this figure refers to one of the tubes whose data are given in Fig. 2·27.
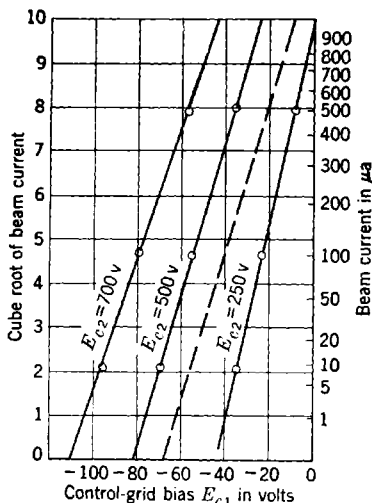


FIG. 2·29.—Variation of static characteristics with change in second-grid voltage $E_{c2}$.

Measurements on a series of different tubes indicate that a linear relation exists between cutoff bias ($E_{co}$) and the second-grid voltage ($E_{c2}$), as illustrated in Fig. 2·30.[1] The curves intersect the $E_{c2}$ axis at approximately $-75$ volts, indicating that this negative value is required on the second grid if the tube is to be cut off with zero volts on the control grid.   Care must therefore be exercised with regard to signal level on the grid in order to secure blanking of the return trace by gating the second grid.   If the second grid goes only to zero potential, the curves indicate the necessary negative potential of the control grid to obtain cutoff.

In most specifications, the limits of cutoff bias are specified at some standard value of $E_{c2} = E_s$, usually $+250$ volts.   If the tube is to be
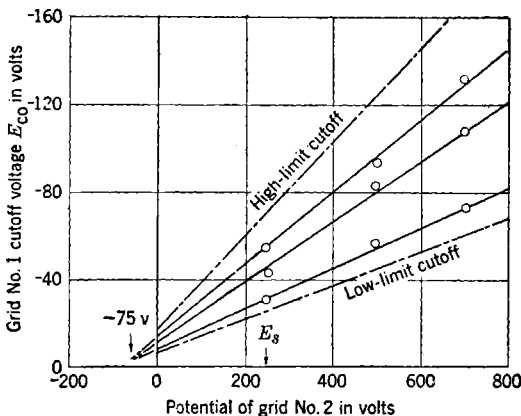


FIG. 2·30.—Variation of cutoff bias with change in second-grid voltage $E_{c2}$.

operated at any arbitrary value of $E_{c2}$, the corresponding value of cutoff

[1] A relationship of this form, derived from the principle of voltage similitude, is given by H. Moss, *J. Brit. Inst. Radio Eng.*, **5**, 204 (1945).

voltage $(E_{co})_{c2}$ can be found from the empirical equation

$$(E_{vo})_{c2} = (E_{vo})_s \frac{(E_{c2} + 75)}{(E_s + 75)}, \tag{46}$$

where $(E_{co})_s$ is the value of cutoff voltage when $E_{c2}$ has the standard value of $E_s$.

The figure also indicates that if the tubes are to be operated at a high value of $E_{c2}$, the actual tolerance limits on cutoff bias are increased greatly above those that exist under normal specification conditions, and adequate bias-voltage control must be provided.

The strong similarity between the family of plots of Fig. 2·29 and Fig. 2·27 suggests that any given tube may be caused to have any specified $E_{co}$, with a corresponding specific slope, by suitable control of
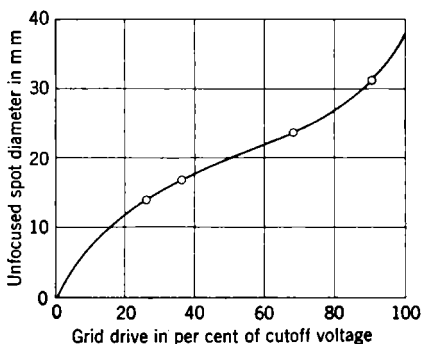


FIG. 2·31.—Typical increase in beam divergence with grid drive.

the parameter $E_{c2}$, and therefore that the operation of all tubes may be "normalized" by this procedure. This process can be carried out as far as $E_{co}$ and slope are concerned, but the beam-divergence angle will not thereby be normalized.

*Beam-divergence Angle of Tetrode Gun.*—The parameters $E_{c2}$ and $E_b$ affect the strength of the electron-optical lenses in the gun, which determine the cone angle $\phi$ of the electron bundle passing down the tube axis.

The beam angle can be determined experimentally by measuring the diameter of the unfocused beam at the screen. Since the edges of the spot are relatively well defined, reasonably accurate measurements are possible. The diameter at the screen divided by the distance from the control grid to the screen gives to a first approximation the cone angle $\phi$ of the beam as it leaves the gun. Figure 2·31 illustrates the variation of the unfocused-spot diameter with grid drive for a typical 7BP7 tube. The similarity between this curve and that of Fig. 2·8 is apparent, although the region beyond the accelerating grid in the case here described

is not field-free.    The curves of Fig. 2·32 are obtained when a log-log
plot of the beam angle $\phi$ as a function of beam current rather than
control-grid voltage is made for a series of values of the accelerating grid
voltage $E_{c2}$ and of the total final voltage $E_b$.    The points fall on reason-
ably straight lines, whose slopes are almost independent of the values of
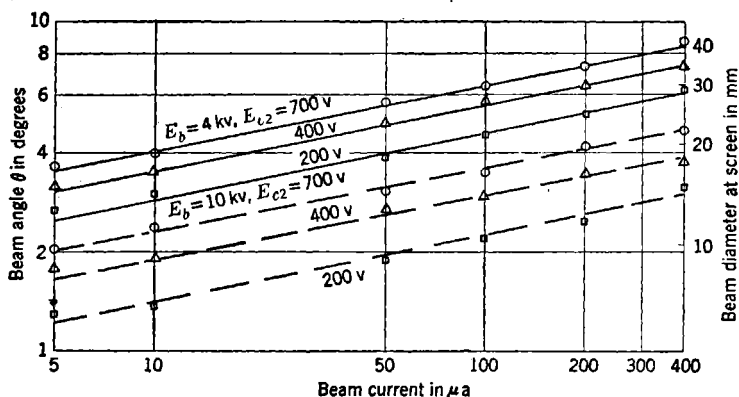


FIG. 2·32.—Beam angle as a function of beam current, for various values of $E_b$ and $E_{c2}$, for a
type 7BP7 cathode-ray tube.

$E_{c2}$ and of $E_b$, and have a value of approximately 0.2; therefore, the
relation

$$\phi = k \cdot i_{sn}^{0.2} \tag{47}$$

over the range of screen currents encountered in actual operation of the
tubes is indicated.[1]    This relation may be put in terms of the grid drive
$E_d$ because, if the fifth root of Eq. (17) is taken,

$$i_{sn}^{0.2} = k' E_d^{0.6}, \tag{48}$$

whence

$$\phi = k'' E_d^{0.6} \tag{49}$$

A curve of the form of Eq. (49) will fit the experimental curve shown in
Fig. 2·31 up to a point represented by a drive of 70 per cent of cutoff
voltage, which is the region of interest.

The curves of Fig. 2·32 indicate that, for any given beam current at a

[1] Curves similar to those of Fig. 2·32, which have been obtained for several other
tubes of the same and other gun constructions, lead to the following general
conclusions:

   1. For the tetrode gun type used in 7BP7 tubes, variations in cutoff bias under
      standard conditions affect the beam angle slightly, the beam being larger for
      larger values of cutoff.
   2. For triode-type guns, the logarithmic plot is a line concave upwards, indicat-
      ing an increasing slope with increasing beam current.    The average slope in
      the region 2 to 200 $\mu$a is, however, not far from 0.2 to 0.25.

fixed total voltage, the beam-divergence angle *increases* with increasing voltage applied to the accelerating grid $G_2$. This action is the net result of two opposing electron-optical effects arising from the change in accelerating grid voltage $E_{c2}$ alone:

1. The strength of the lens formed by the field between $G_2$ and the conducting anode coating in its vicinity decreases as $E_{c2}$ increases because the ratio of $E_b$ to $E_{c2}$ is thereby decreased. Hence the effect of the lens in decreasing the divergence of the electron bundle as it passes through this region is diminished.
2. Increasing $E_{c2}$ increases the cutoff bias and the cathode loading. Therefore, for a given cathode current, the fractional drive to zero bias is thereby decreased, and thus the initial beam-divergence angle $\phi$ is decreased, as is evident from Fig. 2·8.

The experimental curves of Fig. 2·32 indicate that the first effect predominates.

The spherical aberration in the focusing lens increases with the cross section of the electron bundle that it is required to focus. Hence the curves of Fig. 2·32 seem to indicate that increasing $E_{c2}$, for constant $E_b$, would result in a deterioration of the focused spot. The reverse is actually true (see Sec. 17·8). The improvement in spot size is undoubtedly due primarily to the very great reduction in the aberrations of the cathode lens because of the progressive elimination of space-charge effects.

**2·13. Modified Tetrode.**—A modification of the tetrode gun illustrated in Fig. 2·6b consists of placing in front of the second grid



Fig. 2·33.—Tetrode gun with anode cylinder.

a cylinder of the same diameter as that of the second grid. This cylinder is electrically connected to the anode coating by stiff spring clips, and it is rigidly attached to the other parts of the gun by means of supports to two or more insulating rods. Figure 2·33 indicates the general arrangement of this gun and a photograph of a gun of this type is given in Fig. 2·26e.

This type of construction produces almost no change in the transfer characteristic because the anode cylinder does not intercept any of the

beam. The power of the $G_2$-to-anode lens, which is formed by the $G_2$ and anode cylinders, is increased by reducing the diameter of the anode from that of the conducting coating (as in the common tetrode type previously described) to that of the anode cylinder having the same diameter as the $G_2$ cylinder. Measurements of the type illustrated in Fig. 2·32 indicate that the beam angle is reduced by a small amount by this change in gun construction, with a resultant improvement in spot size, but extensive quantitative data are not available. The chief advantages gained by this modification, however, are the possibility of a more accurate alignment of the component parts of the gun (that is, better centering of the electron axis of the gun in the tube neck) and much greater rigidity. Both of these improvements result in better performance under operating conditions.

**2·14. Magnetic Guns with Limiting Apertures.**—A logical modification of the gun described in Sec. 2·13 consists of the introduction of an apertured disk into the anode cylinder, either at the emergent end or within the cylinder. By proper choice of the size of aperture and its
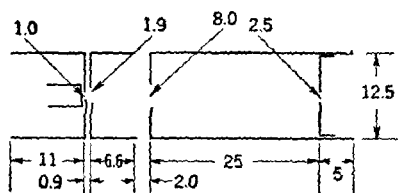


FIG. 2·34.—Typical limiting-aperture electron gun. All dimensions in millimeters.

location, any desired degree of masking of the beam is attainable. The effects of increased masking are (1) a reduction in spherical aberration due to the focusing lens, (2) a reduction of deflection defocusing because of smaller beam cross section in the region of the deflection coils, and (3) a change in the transfer characteristic from a cubic law to one that approaches a square law, for reasonable amounts of masking. These effects are desirable from the standpoint of improvement in spot size and in the dynamic range of signals reproduced. Qualitatively, these improvements have been noticed in operating systems utilizing limiting-aperture guns having dimensions approximating those shown in Fig. 2·34. A quantitative assessment of the improvement in performance requires the development of better methods of measurement and many more experimental data.

**2·15. Electrostatic-focus Guns for Magnetic-deflection Cathode-ray Tubes.**—There are ample reasons, particularly in airborne radar applications, why a gun utilizing an electrostatic-focusing lens rather than a magnetic lens is desirable. These are (1) a saving in weight since focus coils weigh about 2 lb, (2) elimination of the power required to operate the focusing coil, (3) elimination of defocusing caused by the changing resistance of the focus coil with change in ambient temperature, (4) decrease in mechanical complexity and cost to provide means for neces-

sary adjustments of the focusing coil, and (5) elimination of time-consuming adjustments.

The chief reason why electrostatic-focus tubes were not widely used in the United States is that the design of such tubes was not sufficiently advanced to give performance equal to that obtainable from magnetically focused tubes, particularly at the low anode voltages normally used.    In order to get good spot size, it is necessary that the elements of the gun be

extremely well aligned. The alignment achieved in experimental tubes has not been adequate to produce spots free from excessive aberrations, especially at the high deflection angles customarily used.  Progress in the design of such tubes is encouraging, and it is hoped that the performance of this type of gun will soon be comparable with that of the magnetic-focus guns.



Fig. 2·35.—Comparison between transfer characteristics of typical magnetic- and electrostatic-focus guns.

In guns of the electrostatic-focus magnetic-deflection type, a large fraction of the current leaving the cathode is usually intercepted by the apertures in the focusing element.  At an operating voltage of 4 to 6 kv, and for the range of normal operating beam currents, most electrostatic-focus guns deliver approximately 25 per cent of the total cathode current to the screen.   Hence the grid drive necessary to achieve a given current to the screen is considerably larger than that required for the magnetic-focus tetrode commonly used. Figure 2·35 gives curves for the grid drive plotted against beam current for the common magnetic-focus gun and for a typical electrostatic-focus gun, for normal gun variations.   The video amplifier required to drive electrostatic-focus guns will therefore require roughly double the gain of that required for magnetic-focus guns.

The efficacy of electrostatic-focus tubes for projection purposes, where the accelerating voltage is very high, improves both because the relative performance improves at higher voltage and because the power required to focus magnetic tubes becomes considerable.

**2·16. Special Types of Guns and Tubes.** *Ion-trap Guns.*—Particularly for television applications, it is desirable to eliminate negative ions

from the beam that reaches the screen because these cause a dark spot known as an "ion spot." The effect of any ions present is less serious when the focusing is magnetic rather than electrostatic, as discussed in Sec. 2·2. The complete removal of the ions from the beam may be accomplished by specially designed guns. In one of these a "bent" gun is used, in which the initial direction of the electron beam makes an angle of roughly 30° with the tube axis. A localized magnetic field normal to the tube axis then bends the electron beam until it travels axially, but it has almost no effect on the ions which are intercepted by the wall of the cylinder.
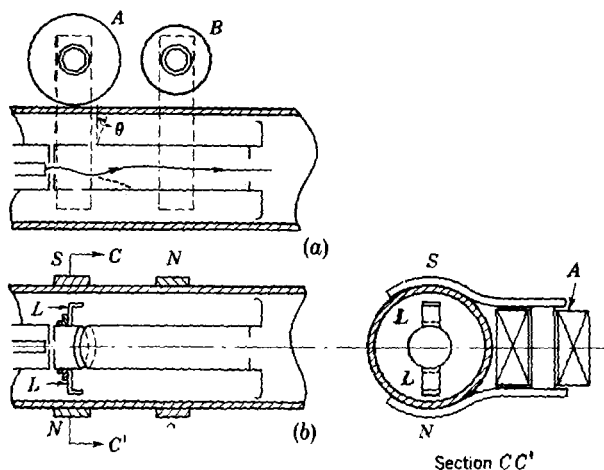


Fig. 2·36.—Ion-trap gun.

A second form of gun, shown in Fig. 2·36, incorporates a different kind of ion trap, involving both magnetic and electrostatic fields. The paths of electrons and ions in this gun are indicated by the solid and dotted lines, respectively, in Fig. 2·36a. The magnetic field in the region of the second-grid cup is produced by an electromagnet $A$ whose pole pieces form arcs fitting closely around the tube neck, as shown in Fig. 2·36c. Its field is directed to the proper region of the gun by the two soft-iron lugs $L$ welded to the second-grid cup by means of a non-magnetic angle piece. The adjacent ends of the second-grid and anode cylinders are cut at an angle $\theta$ with the normal and cause the axis of the electric field between them to be similarly oriented with respect to the tube axis. A second electromagnet, $B$, with pole pieces similar to those of $A$, is located over the midsection of the anode cylinder, as shown. Soft-iron lugs are not used with this second magnet. It is not imperative to use the lugs $L$ associated with the first magnetic field. If used, they

must be accurately located and of very good magnetic material, so as not to cause an unsymmetrical field.

The action of the device is as follows. The magnetic field due to $A$, when the polarity is as indicated in Fig. 2·36c, will bend electrons as indicated in Fig. 2·36a, but it will have little effect on the direction of the ions. The subsequent electric field across the gap between the cylinders bends both electrons and ions in the opposite direction, so that both would strike the side wall of the anode cylinder. However, the path of the electrons is bent in the reverse direction by the action of the magnetic field due to $B$. This field does not so affect the ions, which are trapped within the cylinder.

It is necessary that the electron beam emerging from the gun be traveling along the axis of the gun. This positioning of the beam can be accomplished by the proper adjustment of the field strengths of magnets $A$ and $B$. With slight redesign of the gun, it should be possible to achieve trapping of the ions and an axial course for the electron beam by making use of only a single magnetic field.

Ion-trap guns may be used with either electrostatic or magnetic focusing. The 7DP4 type uses the former, and the 10BP4, the latter.

*Projection Cathode-ray Tubes.*—Projection tubes have been designed to be used with lens or reflective optical systems to provide large displays that are useful in radar as aids to plotting, and in television to provide more comfortable viewing, or to enable many people to see a single display. Tubes whose greatly magnified images are to be projected must have luminances many times those of conventional tubes and should possess resolution at least as good as that of tubes used for direct viewing.

To achieve high luminance it is necessary to apply much higher accelerating voltages (10 to 70 kv) to the projection cathode-ray tube. At relatively low voltages, the luminance of a phosphor, for constant current density, increases as $E_b^n$, where $E_b$ is the applied accelerating voltage, and $n$ varies between 1.5 and 2. As the applied voltage approaches the limiting or "sticking" potential of the particular phosphor used, a further increase in applied potential results in little further increase in luminance (see Sec. 18·6). Consequently, the development of methods of eliminating this limitation is receiving much attention. One method that has proved to be both practical and effective is that of covering the phosphor on the vacuum side with a film of evaporated aluminum, whose thickness is between 500 A and 5000 A. This film is connected to the high-voltage source, and has good conductivity; therefore it effectively eliminates the sticking potential. If the phosphor is first covered with an organic material to provide a smooth surface, the evaporation of the aluminum film onto this material results in an efficient

mirror that reflects toward the observer a large fraction of the light that, in an unfilmed tube, would be directed backward into the bulb. Relatively low velocity electrons will not penetrate such a film, but at 15 kv the efficiency of an Al-backed screen is approximately 4 cp/w, which is roughly twice that of an unbacked screen at the same voltage. A further advantage of the aluminum backing is the elimination of the ion spot, for the thickness of film used completely stops any ions present in the beam.[1]

The requirements of high beam currents with minimum spot size, and the high potential differences in adjacent gun parts call for special care in the design and construction of the electron guns used in projection tubes. These guns may have either magnetic or electrostatic focusing. The former type allows the use of a larger-aperture beam with less aberration than is possible with an electrostatic-focus gun. However, the power required to focus a high-voltage beam by means of a magnetostatic lens is considerable. This requirement and the added complexity of the external focusing arrangement make an electrostatic-focus gun desirable. In either case, the guns require an especially good alignment and, if electrostatic focus is used, a focusing electrode of large diameter and a high degree of symmetry, in order to minimize aberrations. High-voltage electrodes must have no sharp points, and their edges should be rolled, in order to prevent corona.

A gun of the magnetic focus type for operation up to 10 kv has been designed by R. R. Law.[2] The only projection tube designed for radar use, the 4AP10, also utilizes magnetic focusing. Since this tube is used at 9 kv, the construction of the gun differs very little from that shown in Fig. 2·34.[3]

An electrostatic focus gun is used in the 5TP4 tube, designed for the projection of television images by means of a reflective optical system. This tube is designed to operate at 27 kv. It utilizes a second grid between the control grid and focusing electrode to prevent interaction of the fields produced by these electrodes. The focusing electrode intercepts a maximum of 27 per cent of the total current, at an Anode No. 2 current of 200 $\mu$a. In order to maintain focus, the regulation of the supply to the focusing electrode should be such that its voltage will drop by about 125 volts in the range of Anode No. 2 current between 0 and 200 $\mu$a. This tube also contains the Al-backed screen previously mentioned.

[1] For a more complete discussion, see D. W. Epstein and L. Pensak, "Improved Cathode Ray Tubes with Metal-backed Luminescent Screens," *RCA Review*, **7**, 5–10 (March 1946); C. H. Bachman, *Gen. Elect. Rev.*, **48**, 13–19 (Sept. 1945).

[2] R. R. Law, "High Current Electron Gun for Projection Kinescopes," *Proc. I.R.E.*, **25**, 954–976 (1937).

[3] See Sec. 16·16 for a discussion of the use of this tube in a projection indicator.

**2·17. Remarks Concerning Operating Conditions for Magnetic Cathode-ray Tubes.**—Since it is desirable to have the maximum number of signal-receiving electrodes near ground potential, magnetic tubes are usually operated with the cathode near ground. The focus and deflection coils may be held at any convenient potential without affecting the behavior of the tube because the internal conducting coating on the glass of the tube neck provides electrostatic shielding.

This method of operation places the screen of the tube at a high positive potential, often greater than 5 kv. This screen potential causes no difficulty when the humidity is low, and good electrical insulation of the tube face is maintained, and when the normal procedure requires only visual observation of the display. When plotting must be done on or near the tube face, or when a scale must be moved relative to it, a local disturbance of the potential of the screen may be caused by contact with the glass, or by the electric charge on the moving scale. This disturbance will result in a shift or distortion of the pattern, unless suitable precautions are taken (see Secs. 16·5 and 16·9).

The required range of bias voltage depends upon the choice of operating level of the second grid, as discussed in Sec. 2·12. For the normal value of $E_{c2}$, namely 250 volts, the normal value of cutoff bias is $-45$ volts. This value is subject to a tolerance of $\pm 50$ per cent, resulting in cutoff limits for this value of $E_{c2}$ of $-22\frac{1}{2}$ and $-70$ volts. On the other hand, if a higher value of $E_{c2}$ is used in order to obtain better spot size, the normal value of cutoff will be determined by Eq. (42). Thus if the maximum allowable value of $E_{c2}$, namely 750 volts, is used, the normal cutoff at this voltage will be $-115$ volts, which will result in cutoff limits of $-60$ and $-175$ volts. For other values of $E_{c2}$, corresponding cutoff limits will be required.

The maximum signal voltage required will also depend upon the choice of the operating level of $E_{c2}$, and will increase with increasing voltage on the second grid. For a given operating value of $E_{c2}$, the maximum useful grid drive or signal level will depend upon the amount of defocusing permissible in the display. Since this defocusing depends upon the properties of both the tube itself and of the focus and deflection coils used with it, no specific numbers can be definitely stated. However, a rough approximation can be made by an arbitrary assumption of a maximum beam current of 200 $\mu a$. Using this value as a basis for determining the maximum limited signal voltage required (see Sec. 4·8), a high-cutoff-limit tube operating at $E_{c2} = 250$ volts would require approximately a 33-volt signal, whereas the same tube operated at $E_{c2} = 750$ volts would require a 50-volt signal. These figures then give rough values for the signal output voltage required of the video amplifier that drives the cathode-ray tube. In all cases, a smooth

attenuation control, having good frequency-response characteristics, is required to permit reducing to zero volts the actual voltage supplied to the cathode-ray tube.

A blanking voltage sufficient to cut off all beam current during the time interval between sweeps must be provided.    This voltage may be applied either to the cathode, the control grid, or the second grid.    The most common method consists of the application of a blanking gate to the second grid.    The upper limit of the voltage of such a blanking gate is limited to that of the B+ supply voltage.    The curves of Fig. 2·30 will be helpful in determining the actual voltage to which this blanking gate must drive the second grid in order to ensure complete blanking, when the limiting voltage of the signal actually appearing on the cathode or grid during this blanking interval is known.

When the second grid is to be operated at a potential higher than that of the normally available power-supply voltage, it is usually operated from a bleeder across the high-voltage supply.    In this case, it is advisable to apply the blanking voltage either to the cathode or to the control grid, mixing the blanking voltage with the signals, if necessary.

# CHAPTER 3

## FOCUS COILS AND FOCUS MAGNETS

### By R. D. Rawcliffe

#### FOCUS COILS

**3·1. Focus-coil Theory.**—The theory of the focusing action of an axially symmetrical magnetic field is discussed elsewhere[1] and only a brief statement of the results needed for a discussion of the focus coils and magnets used in practice will be given here. The focusing action is much more complicated than that of an electrostatic field because the electrons do not stay in one plane. The electron trajectories are amenable to solution only in a few simple cases, one of which is that of the "short" field. In the solution of the "short" field, the following assumptions are made:

1. The field is negligible except within an interval, $\overline{AB}$, which is small compared with the object and image distances. If such is the case, the radial distance of the electrons from the axis does not change much within this interval, but the radial velocity does change.

2. Within the interval $\overline{AB}$ the electrostatic field is zero, that is, the electrons have reached their final speed before entering the focusing field.

3. The diameter of the electron beam is small. Therefore, if $\theta$ is the angle between an electron path and the axis, then $\sin \theta \approx \theta$ and $\cos \theta \approx 1$, that is, only paraxial electrons are considered.

The short field, then, will behave as a "thin" optical lens (see also Sec. 2·2) whose focal length is given by the following equation:

$$\frac{1}{f} = \frac{e}{8mE_b} \int_A^B H_z^2 \, dz, \tag{1}$$

where $f$ is the focal length, $e$ is the electronic charge, $m$ is the electronic mass, $E_b$ is the accelerating voltage applied to the tube, and $H_z$ is the $z$ component of the magnetic field on the $z$-axis, which is chosen to be the axis of symmetry.

[1] V. K. Zworykin and G. A. Morton, *Television*, Wiley, New York, 1940, p. 117; I. G. Maloff and D. W. Epstein, *Electron Optics in Television*, McGraw-Hill, New York, 1938, Chap. 8.

The approximations that have been made in deriving Eq. (1) are not, however, accurate for practical focus coils. The field-distribution curves of Fig. 3·2 show that the field is considerable over a longer interval than is justified under Assumption 1. Assumption 2 is usually fulfilled, but, if the beam current is not small, Assumption 3 is not justified. In light optics, if the diameter of the light beam striking an uncorrected lens is large, aberrations result and the image "points" are distorted. Similar defocusing occurs in electron optics if the electron beam is too large. In this case, however, corrections to the lenses are extremely difficult to apply. Enlarged or distorted images therefore occur if the beam currents are too large.

In spite of the fact that the assumptions used in developing Eq. (1) do not apply accurately to practical focus coils, the equation does indicate several important facts that are borne out by experiment:

1. As the field is everywhere proportional to the current $I$ through the coil, provided that any iron in the magnetic circuit is not operated near saturation, $\int_A^B H_z^2 \, dz$ is proportional to $I^2$. Consequently, $I$ is proportional to the square root of $E_b$ if the focal length is constant (as it would be for a fixed position of the focus coil).
2. The focal length is independent of the sign of $H$ or of $I$.
3. If electrons are focused, heavy ions will not be focused. Hence there will be no "ion spot" or small burned area near the center of the screen, such as is formed with electrostatically focused beams.

A second equation usually derived in connection with Eq. (1) gives the rotation $\phi$ of the electron beam. It is

$$\phi = \sqrt{\frac{e}{8mE_b}} \int H_z \, dz. \tag{2}$$

The rotation arises because the force on the electron is perpendicular both to its velocity and to the magnetic field, and the electrons tend to follow a helical path. Although a study of this rotation is sometimes useful in studying the action of focus coils, it is of no significance in most cathode-ray tubes because the image is a "point" whose orientation is of no interest. In other applications of magnetic focusing such as in the electron microscope, the rotation is important.

A rotation of the pattern shown on a cathode-ray-tube screen exists, however, and although it arises in a manner somewhat similar to that of the spot rotation, these two rotations should be distinguished. Both the focusing and deflecting fields spread out along the $z$-axis, over-

lapping each other over a large interval.   The deflection starts before the focusing is complete, but, as far as the focus field is concerned, deflected electrons are the same as nonaxial electrons in an electron beam.   The focus field causes them to spiral around and the pattern is rotated.[1]

**3·2. Types of Focus Coils.**—A focus coil consists of a number of turns of wire, wound into a cylindrical form.   The winding is usually mounted in an iron shield that concentrates the field.   Cross-sectional views of a few types of coils are shown in Fig. 3·1.   These are repre-
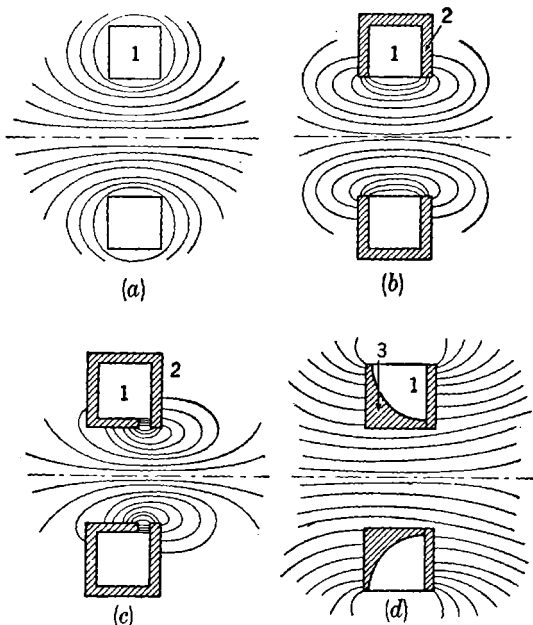


FIG. 3·1.—Cross-sectional views of several types of focus coils, showing magnetic-field distributions (1) winding; (2) iron; (3) nonmagnetic material.

sentative of the varieties of winding and shield construction.   The general contours of the field distribution in a transverse plane are shown on each drawing.   Figures 3·1a, b, and c consist of a simple coil with different degrees of magnetic shielding.   Figure 3·1d is a coil designed for projection cathode-ray tubes used in television[2] in an attempt to reduce spherical aberration.   In order to control the field distribution, the winding is placed on a form shaped to follow a parabolic curve.

Graphs of $H_z$ as a function of $z$, for the coils shown in Fig. 3·1, are

[1] Discussed in Chap. 9.

[2] R. R. Law, "Some Observations on the Spherical Aberrations of Magnetic Final Focusing Lenses for Use with Cathode-ray Tubes," RCA Report No. LR-34.

shown in Fig. 3·2. The curves have been displaced along the z-axis to make their maxima coincide. It is evident that Coil c gives the sharpest field, and that the curve for type d is asymmetrical with a long tail in the direction of the gun.
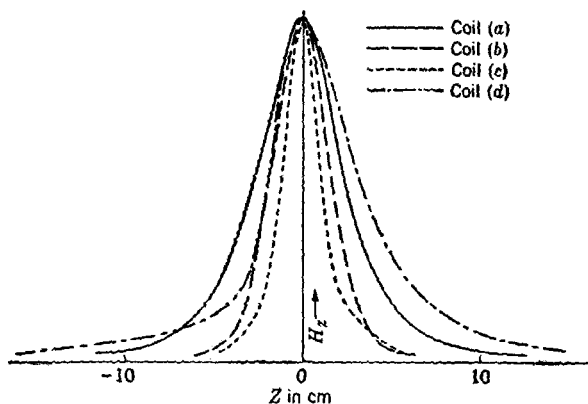


FIG. 3·2.—Intensity of axial component of focus field along axis for focus coils shown in Fig. 3·1.

When used with magnetic cathode-ray tubes of the type considered here, a type d coil wound according to the RCA specifications gives slightly superior focus at high beam currents, but at medium or low beam currents the focus is definitely poorer than that of the type c coil.
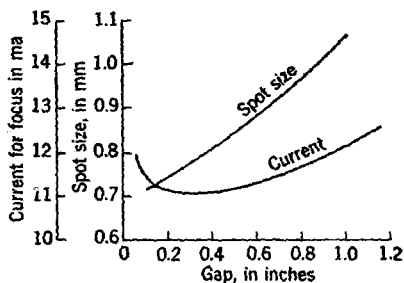


FIG. 3·3.—Spot size and focus current for various focus-coil gap widths; average for seven 7BP7 tubes; $E_b = 5$kv; $I_b = 250$ $\mu$a.

Probably this characteristic is due to the longer field, which extends back too far and interferes with the electrostatic lenses in the electron gun. In radar equipment, type c coils have been used with all magnetic cathode-ray tubes except those in which permanent-magnet focus units have been employed.[1]

**3·3. Focus-coil Performance Curves.**—The performance of the type c focus coil is illustrated in Figs. 3·3 to 3·7. Except where otherwise stated, the dimensions are those given in Appendix A. Spot-size measurements have all been made with the shrinking-polka-dot-raster method.[2]

---

[1] Details of the construction of a coil of this type are given in Appendix A.

[2] Described in Chap. 17.

Figure 3·3 shows the effect of varying the width of the gap on the average spot size and on the required current.    Measurements were made on type 7BP7 tubes but the graph should apply to all tubes with an appropriate change in the ordinate scales.    (See Fig. 3·6.)    The gap width most commonly used is $\frac{1}{4}$ in.    If the gap width is reduced, the

spot size can be improved a few per cent at the expense of an increase in the electric power required for focusing.    As the gap is narrowed, however, the alignment becomes more critical and the best compromise value of gap width is probably between 0.2 and 0.25 in.

Spot size is affected also by the position of the focus coil on the tube neck.    As the position is changed, two factors act to change the spot size.    The spot is a mag-



FIG. 3·4.—Focused spot on type 12DP7 tube for various coil positions.    Numbers indicate the distance from focus-coil gap to the reference line.

nified image of the crossover (see Secs. 2·1 to 2·3) in the gun.    The magnification equals the ratio of the image to object distances; therefore, as the coil is moved forward toward the screen the magnification decreases. However, as the coil is moved forward, the diameter of the electron beam entering the focus coil becomes larger.    As the aberrations increase, distortion of the spot occurs.    The optimum position of the focus coil is the point at which the magnification is as small as possible without objectionable aberrations. The spot-size variation is illustrated by the series of photographs in Fig. 3·4.    The "tails" on the spots, presented when the focus coil is too far forward of the optimum position, are a characteristic spot deformation.    The loss in resolution caused by these tails is difficult to evaluate accurately. A direct examination of the spot would indicate a gross enlarge-



FIG. 3·5.—Variation of spot size with focus-coil position.

ment.    However, if spots are shrunk together in the polka-dot-raster method (see Chap. 17) the presence of tails does not seem to have much effect.    This fact is illustrated in Fig. 3·5 in which spot-size measurements for a given tube for different coil positions are shown as circles, and spot

sizes calculated from the magnification and normalized at one point are shown by the curve. The close agreement between these two sets of
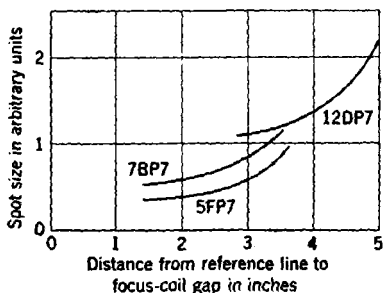


FIG. 3·6.—Variation of spot size with focus-coil position for commonly used tube types.

values indicates that the aberrations have little effect on the spot size as measured by this method. Evidently the tails usually contain only a small fraction of the total light in the spot. Average spot-size curves for the three commonly used tube types are given in Fig. 3·6, but these measurements do not tell the whole story. For instance, tails on strong signals may mask weak signals; moreover, clean cut, round spots have a certain aesthetic appeal. In Fig. 3·7 are shown the focus currents required for the focus-coil position of Fig. 3·6.

**3·4. Focus-coil Current Control.**—Figure 3·8 illustrates the effect on the required voltage and current of changing the wire size in a focus coil but winding enough turns in each case to fill the available volume. The wire size for most efficient focusing from a given power supply should be so chosen that, after an adequate safety factor has been allowed, the voltage across the coil is as large a fraction of the total supply voltage as possible. The safety factor may have to be much larger than one would expect. The most important variations to be allowed for are as follows:

1. *Tolerances in the Coil Itself.* Variations of $\pm 10$ per cent for the focus current and voltage may reasonably be expected. They are due to such things as changes in wire size, wire tension in winding, number of turns in the coil, and gap width and permeability of the case.

2. *Tube Tolerance.* The JAN-1 specified tolerances on the number
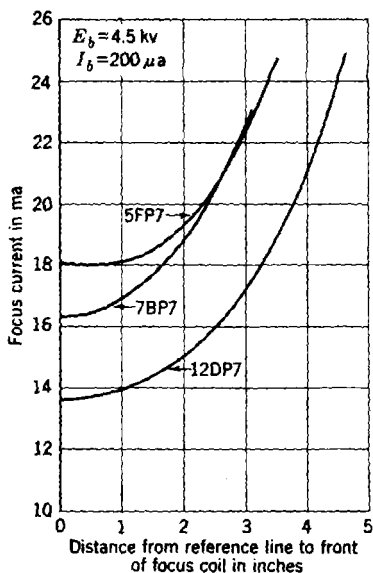


FIG. 3·7.—Variation of focus current with focus-coil position. Focus coil is type shown in Fig. A·1.

of ampere-turns required to focus a cathode-ray tube using a standard focus coil under standard conditions are $\pm 15$ per cent for the 5FP7, $\pm 21$ per cent for the 7BP7, and $\pm 25$ per cent for the 12DP7. In general, for existing tube types, the tolerance tends to be larger for larger diameter tubes.

3. *Line-voltage Variations.* The effect of line-voltage variations depends on whether the focus and anode voltages are regulated. As
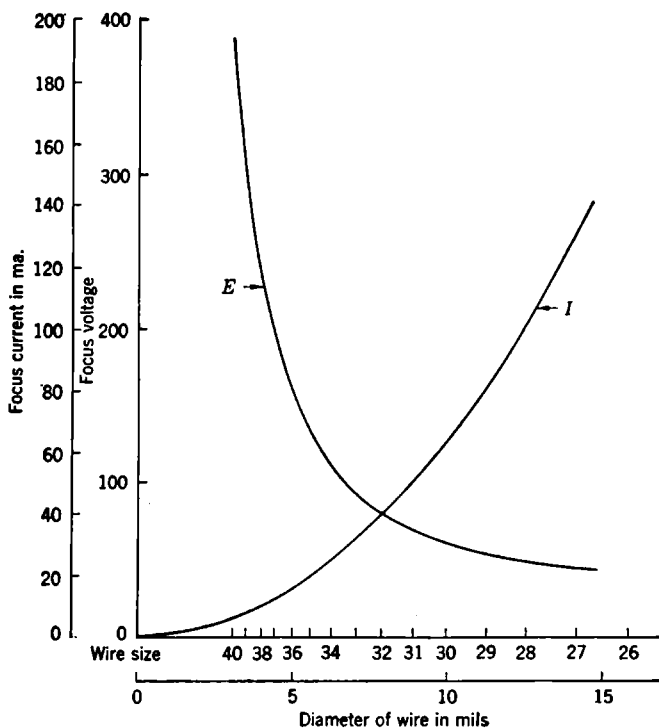


FIG. 3·8.—Focus current and voltage plotted against wire size.

was shown in connection with Eq. (1), the required focus current is proportional to the square root of the anode voltage. Therefore, for small voltage changes, the focus voltage (or current) should change half as much as the anode voltage in order to maintain focus. If the anode voltage is proportional to the line voltage, the usual $\pm 10$ per cent change in line voltage should be accompanied by a $\pm 5$ per cent change in focus voltage.

4. *Power-supply Tolerances.* With a given input voltage and load, power-supply voltages will vary among different equipments, perhaps

by ±10 per cent in ordinary production units.   The variation is probably larger in the anode supply voltage than in the focus supply voltage.

5. *Temperature Variations.*   The resistance of copper wire varies approximately 0.4 per cent/°C, and hence the focus voltage (but not the current) also varies in the same manner,   The temperature change is the change in the temperature of the wire itself and includes heating due to the focus current, to the remainder of the equipment, and to ambient temperature changes.

If the preceding tolerances are all considered, the possible over-all variation is alarmingly large: namely, a required variation in the voltage across the focus coil by a factor of 3 or 4 is indicated.   There is small probability, however, that all the variations will be extreme and in the same direction.   Nevertheless, if a rheostat is used in series with the focus coil to control the current, it must be a power rheostat with a rating of perhaps more than 25 watts.   Its resistance will also have to be high if a high-resistance coil is used.



FIG.   3·9.—Circuit   for   focus-coil control.

Much better control of the focus-coil current is obtained with a pentode vacuum-tube regulator.   The circuit shown in Fig. 3·9 permits 20 per cent change in plate voltage with negligible change in focus current.   The current is then unaffected by resistance changes in the coil due to temperature changes.

In order to simplify the operation of the equipment, it is usually worth while to eliminate the focus-control knob from the front panel, and to have a "screwdriver control" inside the chassis.   Neither a rheostat nor the circuit of Fig. 3·9 will allow this simplification because anode-voltage variations due to line-voltage changes cause defocusing and a readjustment of the focus control is necessary.   The defocusing occurs because the focal length of the coil depends upon the anode voltage.   In the discussion of Eq. (1) it was shown that the focus current is proportional to the square root of the anode voltage, $I \propto \sqrt{E_b}$, or for small changes in anode voltage,

$$\frac{\Delta I}{I} = \frac{1}{2}\frac{\Delta E_b}{E_b}.$$

The effects on spot size of variations in $I$ and $E_b$ such as might occur with anode-voltage variations are shown in Fig. 3·10.   Curve $A$ would normally be followed if unregulated voltage supplies were used and both

the focus and anode voltages were proportional to the line voltage, or
if the focus coil were either run from a regulated voltage or used in a
circuit such as Fig. 3·9. The two curves obtained (1) with the focus
voltage unregulated and (2) with the focus voltage regulated actually
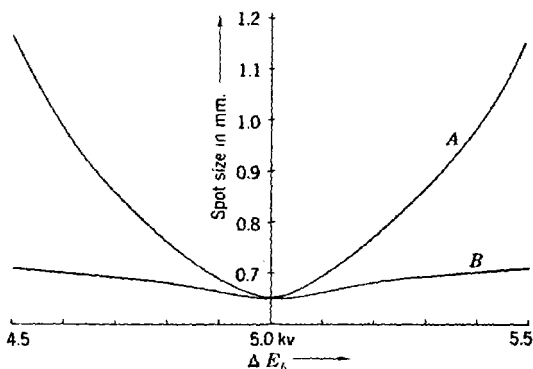


FIG. 3·10.—Observed values of spot size vs. anode voltage on a 7BP7 tube. Curve $A$:
average curve for constant focus current and for focus current proportional to anode volt-
age. Curve $B$: curve for focus current varying half as fast as the anode voltage.

do not coincide, but the difference between them is small and they have
been averaged to obtain Curve $A$. The much smaller variation shown
in Curve $B$ results if the focus voltage is made to vary only half as fast
as the anode voltage by means of
the modified form (Fig. 3·11) of the
circuit of Fig. 3·9. In the circuit
of Fig. 3·11, the anode voltage $E_b$ is
mixed with a regulated voltage $E_r$
through the resistors $R_b$ and $R_r$.
The voltage $E_0$ at the junction of
these resistors is applied through a
potentiometer to the grid of the
pentode focus-control tube. The
necessary condition that $\Delta E_0/E_0$
$= (\frac{1}{2})\Delta E_b/E_b$ is that $E_b/R_b = E_r/R_r$.
This condition is independent of the
resistance of the potentiometer.

The condenser $C$ is used to by-
pass ripple voltage from the high-



FIG. 3·11.—Compensated focus-coil-control
circuit.

voltage supply. The resistor $R_k$ in the cathode circuit provides degener-
ation to improve the linearity of the tube response.

A simple circuit, which corrects for line-voltage variations but which
is sensitive to variations in temperature, is shown in Fig. 3·12. In this

circuit, regulated and unregulated voltages are mixed as before to obtain a semiregulated voltage $E_0$. The assumption is made that the anode
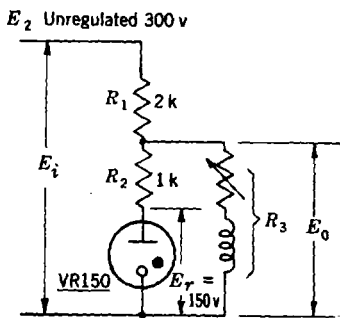


Fig. 3·12.—Partially compensated focus-coil-control circuit.

voltage and the unregulated voltage $E_i$ vary proportionally. The mixing circuit must have a low impedance because the focus current flows through it. The regulation is independent of $R_3$—that is, the load has no effect on the regulation of $E_0$ as long as there is enough current through the VR tube for it to maintain regulation. In addition to the focus compensation, the size of the pattern can be made independent of the line voltage by using the voltage $E_0$ to supply the sweep-generation circuits because the deflection varies inversely as the square root of the anode voltage. (See Sec. 8·1.)

**3·5. Compensation for the Defocusing Due to Deflection.**—In most magnetic tubes, the center of curvature of the tube face is farther away from the screen than is the center of deflection. Consequently, even in the absence of defocusing caused by the deflection coil, the beam will not be focused both at the center and at the periphery of the tube. In order to maintain focus, the focus current should be reduced linearly by about 4 per cent as the beam is deflected from the center to the edge of the screen. Without such focus-current correction the normal focusing procedure is to adjust for optimum focus not at the center of the tube face, but half way along the radius so that the over-all focus may be best. A 15 to 20 per cent improvement in spot size, both at the center and at the edge, may result when focus-current correction is used. This gain is small, but it is large enough to justify a correcting circuit in precision equipment, especially if a centered radial sweep



Fig. 3·13.—Focus coil for focus compensation with deflection.

(PPI) is used. The correction circuit for a PPI is simple; if a rectangular scan is used, the circuit may well be too complicated.

The field produced by the focus coil must be varied a small amount in synchronism with the sweep. Because the ordinary focus coil has

too large an inductance to produce this variation, an auxiliary coil such as that shown in Fig. 3·13 must be used. This coil is inserted in the gap of a standard focus coil. A 600-turn coil of No. 40 wire will fit into the available space.[1] It has an inductance of 25 mh and requires about 15 ma for focus compensation.

The same waveform that controls the main sweep driver can conveniently be used to control the driver for this coil. One triode section of a 6SN7 is adequate for driving this compensating coil at sweep speeds up to about 50 $\mu$sec/radius.

**3·6. Mechanical Adjustment of Focus Coils.**—In most cathode-ray-tube mounts it is necessary to provide adjustments to correct for misalignments both of the tube electrodes and of the coils. The unfocused, undeflected electron beam does not normally hit the center of the screen, but, as in the 12DP7 for instance, may hit anywhere within a 1-in radius of the center. This misalignment is usually corrected by moving the focus coil. One of the simplest methods of doing this is shown in Fig. 3·14. The outside surface of the focus coil is a section of a sphere. This surface mounts against a spherical section in the tube mount, which has slots for the three mounting screws, so that



FIG. 3·14.—Simple mount for focus-coil adjustment.

the coil can be tilted through an angle of about 10° about any axis perpendicular to the tube axis. This action tilts the focus-coil "lens" and displaces it laterally, and results in a displacement of the image.

Sometimes the method of tilting the focus coil is used to provide off-centering of the electron beam. This method, however, results in a rapid deterioration in both focus and pattern as the amount of off-centering increases. Off-centering should, therefore, be done with the deflection system.

For optimum focus, the focus-coil axis should coincide with the axis of the electron beam. Aberrations will then be reduced to a minimum. If this alignment is to be achieved, it is necessary that means be provided for tilting the focus coil as before, and also for adjusting its position along the horizontal ($x$) and vertical ($y$) axes. One such arrangement is shown in Fig. 3·15. A necessary and sufficient condition that the coil be aligned with the beam is that the focused spot coincide with the center of the unfocused spot when the current passes through the coil

[1] Standard Coil, type *c*. See Appendix A for the dimensions of this coil.

in either direction.    Under these circumstances, the spot may not be
centered on the screen, but centering can be achieved by passing current
through the deflection coil, or, better, by the use of the precentering ring
described in Sec. 9·2.

If a low-voltage coil is used, it is convenient to connect the coil to
an adjustable 60-cps voltage so that the two focused spots and the
unfocused spot are all seen at once.    If a high-voltage coil is used, the
inductance of the coil will be too large for focusing at 60 cps with a
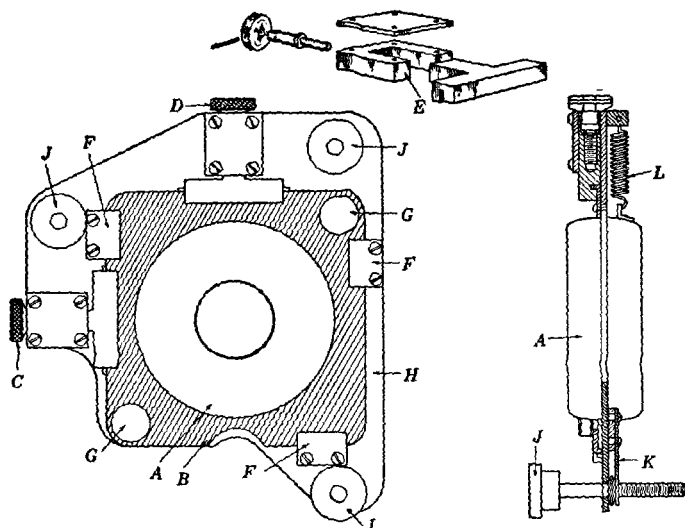


FIG. 3·15.—Adjustable support for focus coil.    *A*, focus coil in case; *B*, sliding plate
onto which focus coil is mounted; *C*, adjusting screw for horizontal motion of coil; *D*,
adjusting screw for vertical motion of coil; *E*, detail of adjusting mechanism of *C* and *D*; *F*,
retaining clamps for *B*; *G*, clamping screws for *B*; *H*, main plate; *J*, adjusting screws for
tilting main plate to be threaded into fixed plate (not shown); *K*, spring clip support for
*J*; *L*, tension spring (antibacklash).

reasonable voltage and it is therefore necessary to have a d-c focus
voltage connected to the coil through a reversing switch that has an
OFF position.    To avoid coil breakdown due to the large surge voltages
that occur when the switch is opened, a condenser[1] should be connected
across the coil.

The alignment procedure is somewhat tedious but, if carried out sys-
tematically, should not be difficult.    When the reversing switch is flipped
back and forth, the undeflected spot on the screen of the tube changes
as the current in the focus coil changes, and one of the shapes shown in
Figs. 3·16 is created.    Alignment may be achieved by using either the

---

[1] 0.01-$\mu$f, 400-volt for a 200-volt coil.

$x$- or the $y$-positioning control to bring this pattern to a symmetrical crescent shape, as illustrated in Fig. 3·16$d$.    The choice of $x$- or $y$-positioning control may be determined by trial.    Only small changes at a time should be made and the results checked by flipping the switch through one complete cycle.    After the crescent shape has been acquired, the tilting controls should be used to reduce the size of the crescent, but its symmetrical shape should be preserved by adjusting the $x$- and $y$-controls. If only small systematic adjustments are made, the three spots can gradually and steadily be brought into coincidence as illustrated in



(a)                 (b)                 (c)                 (d)

(e)                 (f)                 (g)                 (h)
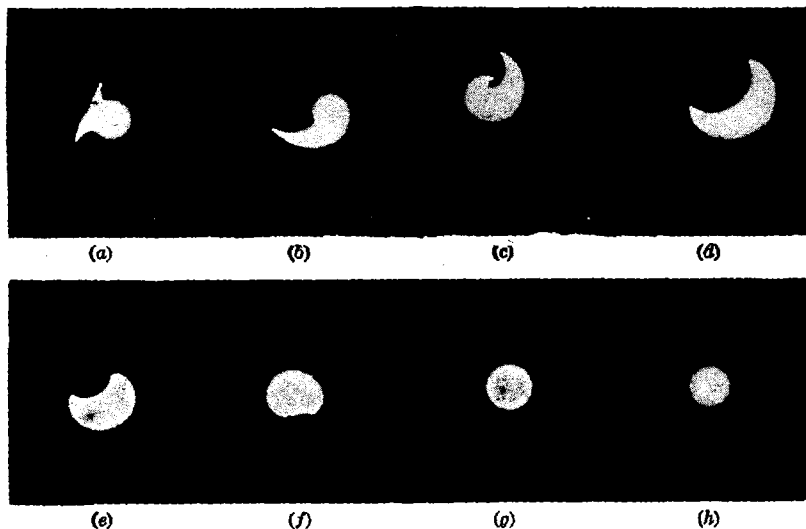
FIG. 3·16.—Focus-coil-alignment steps.

Figs. 3·16$e$, $f$, $g$, and $h$.    This procedure will probably require considerable time in the first attempt, but, after a little practice, it will be possible to achieve correct alignment in a few minutes.

### FOCUS MAGNETS

**3·7. Theory and Operation of Focus Magnets.**—The axially symmetrical field needed for focusing the beam of a cathode-ray tube can also be produced by a hollow cylindrical permanent magnet.    Figure 3·17 is a cross section of the magnetic parts of a typical focus magnet with the field distribution sketched in.[1]    The distribution is considerably different from that produced by a focus coil (Figs. 3·1, 3·2).    Note the large amount of flux outside the magnet, the long spread of the field along the axis, and the two reversals of the field along the axis.    A

[1] A. M. Skellett, "Permanent Magnet Focusing Yoke," BTL Report No. 469.

graph of $H_z$ plotted against $z$, in which the field reversals are clearly evident, is shown in Fig. 3·18.
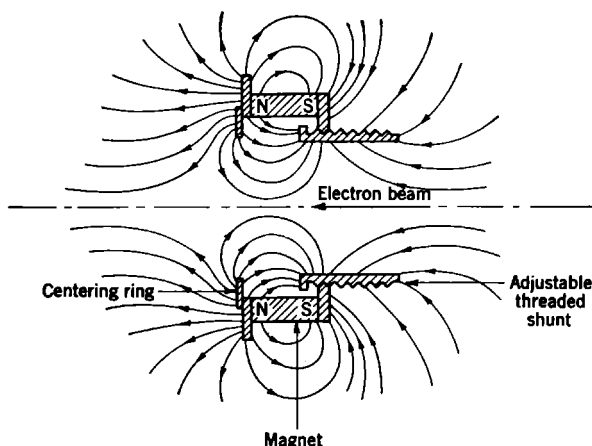


FIG. 3·17.—Focus magnet showing the magnetic-field distribution.

In order to adjust the magnet for best focus of the cathode-ray beam, it is necessary that the strength of the field be varied. This variation is obtained by moving the threaded shunt shown in Fig. 3·17. As the



FIG. 3·18.—Intensity of the axial component $H_z$ of the focus field along the axis for the focus magnet shown in Fig. 3·17.

shunt is moved, the gap width varies. Hence, both the field strength and the field configuration are changed. It is also possible to use a fixed gap of optimum width inside the magnet, and to control the field strength by adjusting an external shunt that provides a variable-reluctance shunt path for the flux. If the external shunt is used, however, the magnet must be considerably stronger than is necessary when the threaded shunt of Fig. 3·17 is used. Figure 3·19 is a graph of the gap width needed to obtain a focus with different anode voltages. The voltage scale depends on the degree of magnetization of the magnet. If the magnet were twice as strong, for instance, the voltage scale would need to be multiplied by four. To correct for tube and coil misalignments, the centering ring

(Fig. 3·17) is provided instead of the tilt adjustments used with focus coils. This ring is the front member of the magnetic gap, and its displacement along a line perpendicular to the axis is more or less equivalent to tilting the whole unit. Pattern displacements of the order of magni-
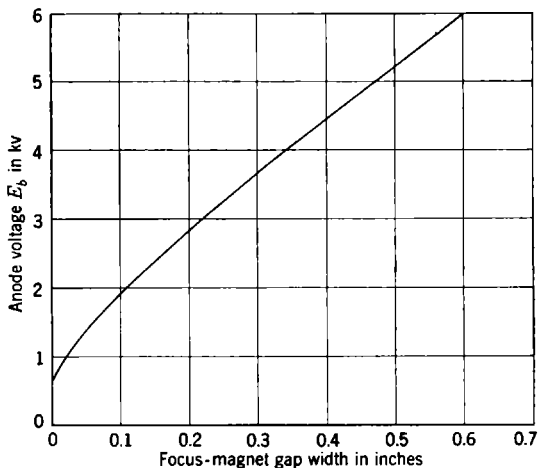


Fig. 3·19.—Anode voltage vs. gap width for optimum focus.
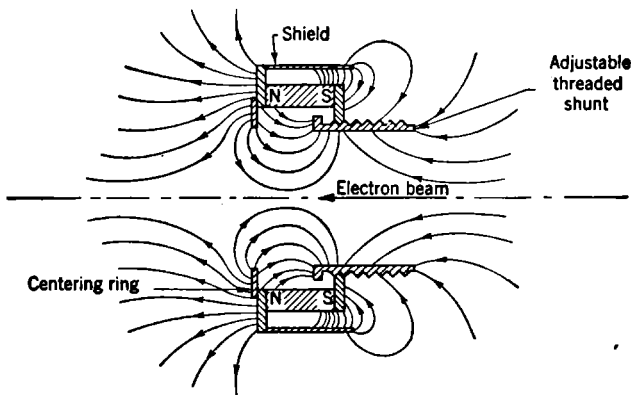


Fig. 3·20.—Field distribution around a shielded magnet.

tude of half a radius can be produced in this manner. Here again, however, it is very bad practice to use the focus unit for deflection of the beam, except when correcting for tube misalignments. Otherwise, poor focus and pattern distortion result.

The field distribution can be controlled somewhat by the proper placement of magnetic materials in the field. Frequently a shield of the form shown in Fig. 3·20 has been used. The new field distribution

is shown in this figure and in Fig. 3·21. The field is weaker in the region of the deflecting field and also in the surrounding space, but it is somewhat stronger in the neighborhood of the electron gun. Since the shield shunts a great deal of flux away from the internal gap, however, the magnet must be considerably stronger than is otherwise necessary.

Reducing the flux in the neighborhood of the deflection coil is advantageous.[1] In addition, if a cathode-ray-tube mount of the rotating-deflection-coil type is used, the focus field gets into the bearings supporting the deflection coil. If these are made of magnetic material, they may become magnetized and their field may deflect the electron beam. As the bearing rotates, this deflecting field also rotates, causing a distortion of the pattern. Nonmagnetic bearings are obtainable but they are expensive and difficult to make; they do not run so freely as steel bearings, and their resistance to wear is considerably less. (See Sec. 16·3.)



Fig. 3·21.—Intensity of the axial component of the focus field as a function of the distance along the axis for shielded (Curve A) and unshielded (Curve B) focus magnets.

The stray field at the rear of the magnet spreads into the neighborhood of the electron gun and distorts the electron trajectories in the electrostatic lenses of the gun. "Tails" are produced on the focused spots. Modified tetrode guns have been used in some tubes partially to overcome this. (Chapter 2, Fig. 2·33.) The electrostatic field between the second grid and the anode cylinder is much more concentrated than it is when no such cylinder is used. The electrons reach their final velocity more quickly. Hence the magnetic field has a shorter distance in which to interfere with the action of the electrostatic lens. The distortion of the focused spot is thereby considerably reduced.

The large external field surrounding the magnet may interfere with other apparatus and thus necessitate the use of a shield. The shield of Fig. 3·20, however, is insufficient to do more than to alter the field distribution by a small amount. The external field is then strong enough, for instance, to spoil completely the operation of a magnetic compass located within about two feet of the magnet. As it is sometimes necessary to mount a cathode-ray tube and a compass on the same instrument panel in an airplane, a method of reducing the stray field to a minimum is desirable.

[1] The troubles arising because of interactions of the deflecting and focus fields will be discussed in Chap. 9.

In Curve *A* of Fig. 3·22, the field strength, in units of the earth's field, is plotted against the distance from the center of the magnet along a line perpendicular to the axis. The positions on this curve roughly correspond to possible locations of a compass. Curve *B* was measured with a 1-in. long permalloy shield similar to that shown in Fig. 3·20. A $\frac{1}{32}$-in. thick cylindrical Armco iron shield, 4-in. diameter by 4-in. long, was used for Curve *C*. The shield used in obtaining Curve *D* is similar to that used for Curve *C* except that it is 6 in. long. The maximum at $4\frac{1}{2}$ in. in Curve *C* shows that much of the flux leaks out of the open ends of the shield, not through it. Hence little is to be gained by improving the permeability of the shield material unless longer shields can be used. A 4-in. ID shield is far enough from the magnet so that the flux in the interior is not seriously weakened.[1]

**3·8. Comparison of Focus Coils and Magnets.**—The most obvious advantage of a focus magnet is the saving in current. The second big advantage is the increased stability, as a result of which the cathode-ray tube will stay focused indefinitely if a regulated anode voltage is used. This feature is important in aircraft applications where large, rapid, temperature fluctuations are encountered.

The performance of focus magnets is somewhat inferior to that of



FIG. 3·22.—External field around a focus magnet with and without shielding.

focus coils, probably because of the spread-out field. Roughly, the focus with a magnet under the best conditions is about as good as the focus with a coil under average conditions. It is fundamentally impossible to align a magnet so that its axis coincides with the electron-beam axis as was described for focus coils in Sec. 3·6. In aligning a focus coil, it is necessary to turn off the current through the coil, and to reverse it. This procedure cannot be followed with a permanent magnet. In addition, the troubles caused by the large stray field of the magnet have already been described. In weight, the magnet has a small advantage over the coil; that is, $1\frac{1}{2}$ lb against $2\frac{1}{2}$ lb. When produced in quantity a focus magnet should cost about $50.00, whereas a focus coil costs about a tenth as much. To the cost of the coil itself must be added the cost of the electrical parts used in controlling the focus current, and the added expense in constructing a larger power supply.

In general, the focus magnet should never replace the focus coil

[1] See Appendix A for construction details of focus magnets.

except in a few special cases where the saving in weight and power, and the stability of the magnet are important enough to overcome the disadvantages of poorer performance and increased cost.

**3·9. Composite Focus Units.**—The cathode-ray beam can be focused by a composite focus unit (see Fig. 3·23) consisting of a coil similar to the ordinary focus coil except that the periphery of the case is a perma-
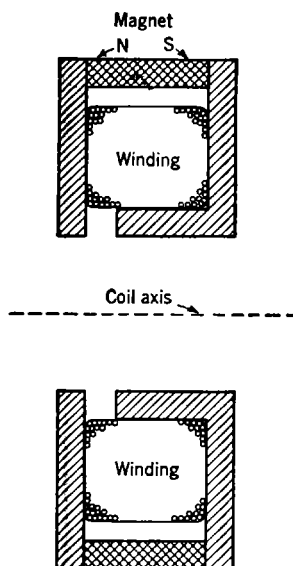


FIG. 3·23.—Focus coil with auxiliary magnet in the case.

nent magnet instead of soft iron.   The magnet is adjusted so that half the focus field is due to the magnet and half is due to the current in the coil.   Then, if both the anode and focus voltages are unregulated, the pattern remains in focus as the line voltage varies.   The saving in focus power is not very great because the magnet introduces a large gap in the magnetic path for the field from the coil.   As this unit has the disadvantages of both focus coils and focus magnets, it is not likely to find wide application.

# CHAPTER 4

## CIRCUIT TECHNIQUES

By F. N. Gillette and C. A. Washburn

To perform a linear analysis of a circuit it is necessary to replace all vacuum tubes by equivalent networks consisting of generators and impedances. This method involves the assumption that all signals are of small enough amplitude to permit the use of constants for the tube parameters. It is not always convenient to deal with display circuits in this way, since in many cases a tube is driven rapidly from a condition of zero current to one of saturation. Usually a sufficiently accurate
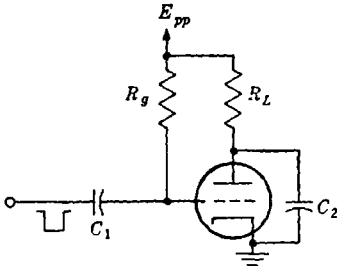


Fig. 4·1.—Triode amplifier.
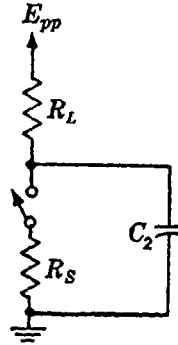
Fig. 4·2.—Equivalent circuit of an over-driven triode.

picture of the performance of such a circuit is obtained by treating the tube as a switch in series with certain elements that have approximately the same characteristics as the tube.

A triode (Fig. 4·1) is reasonably well represented by making the series element a resistance, as in Fig. 4·2. The value of the resistance depends upon the tube type and upon the bias condition that prevails when the tube is conducting. In the example shown, grid current will prevent the potential of the grid from rising much above that of the cathode, but the equivalent resistance of the tube may be reduced by drawing more grid current. As the switch opens, the time constant of the plate circuit is determined entirely by the external components. As it closes, the equivalent impedance of the tube is in parallel with these components and the time constant is therefore much smaller.

111

A pentode is more conveniently represented[1] by assuming the series element to be a constant-current generator as in Fig. 4·3. The magnitude of the current is a function of the tube type, the grid bias, and the screen voltage. It may range in value from a few to several hundred milliamperes. When the switch opens, the plate time constant again is
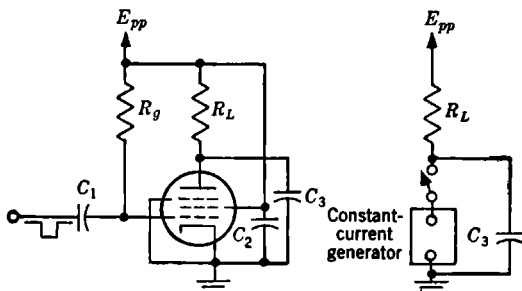


Fig. 4·3.—Equivalent circuit of an overdriven pentode.

determined by the external components. When it closes, the plate voltage wave is not exponential since the current into the plate circuit is constant. In many cases the shape of the plate voltage wave is determined largely by the capacitive portion of the plate load with the resistive portion serving to determine the final equilibrium level. The equilibrium condition may leave the current unchanged, or it may prove necessary to assume a discontinuity of the current as the plate reaches the potential level of the cathode.
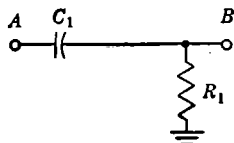


Fig. 4·4.—$RC$-coupling.

**4·1. Condenser Coupling and D-c Restoration.**—A coupling condenser between stages is conventionally regarded as an impedance that forms part of an attenuator, the attenuation ratio varying with the frequency of the sine wave involved. It is more convenient in dealing with nonsinusoidal waves to think in terms of the time constant. As a general illustration a rectangular wave as in Fig. 4·6b is applied to the input terminal $A$ in each of the following examples.

For the first case (Fig. 4·4) the wave is assumed to be symmetrical; that is, $t_1$ equals $t_2$. Because of the exponential discharge of the condenser the rectangular wave is distorted at $B$ to an extent determined by the time constant $R_1C_1$. A very short time constant "differentiates" the rectangular wave, producing the pulses shown in Fig. 4·5a. Increas-

---

[1] The dynamic resistance of the tube, which should be included in parallel with the load, has been omitted since it will generally be large with respect to the load resistance.

ing the time constant reduces the "droop" as shown in Figs. 4·5b, c, and d.

In this example the wave at $B$ has been symmetrical with respect to ground potential.   In the more general case of $t_1$ not equal to $t_2$ the con-
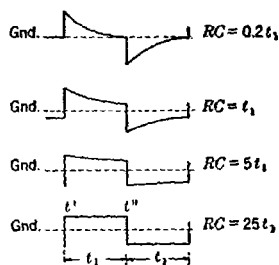


FIG. 4·5.—Rectangular wave after passing through $RC$-coupling.
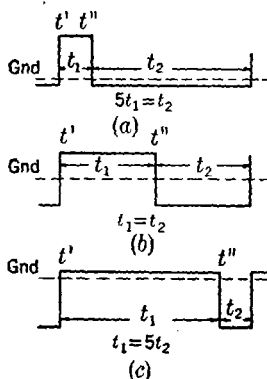


FIG. 4·6.—Shift in d-c level produced by long-time-constant $RC$-coupling.

dition for equilibrium is that the charge lost by the condenser during $t_1$ must be equal to the charge regained during $t_2$.   In other words, the area under the voltage wave above ground potential must equal the area below ground.   Figure 4·6 shows the equilibrium condition for various ratios of $t_1$ and $t_2$, if the time constant is assumed to be very long.

This shift in level with duty ratio,[1] which also occurs with any other form of nonsymmetrical wave, must frequently be avoided.   The simplest
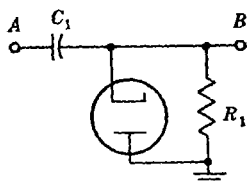


FIG. 4·7.—Simple d-c restorer.
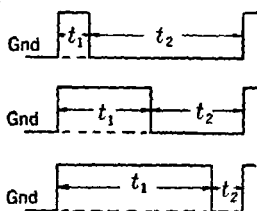


FIG. 4·8.—Level  stabilization  by  d-c restoration.

method of maintaining a chosen d-c level is shown in Fig. 4·7.[2]   A diode is connected in parallel with the resistor $R_1$.   During $t_1$ the cathode of the diode is at higher potential than the plate and no current flows through it.   The condenser then discharges only through $R_1$.   During $t_2$

[1] The duty ratio is defined as $t_1/(t_1 + t_2)$ or as $t_2/(t_1 + t_2)$.   The choice between the two depends upon events that take place in the two intervals.

[2] See Sec. 4·5 for other methods.

the cathode becomes negative with respect to the plate, and the diode conducts. The condenser is recharged through the diode, which has an impedance of perhaps a thousand ohms. Thus the condition of equal charge and discharge is maintained, but the condition of equal area is not. The waves of Fig. 4·6 then appear as in Fig. 4·8. Reversal of the diode would shift the level so that $B$ would be at ground potential during $t_1$ and below ground during $t_2$.
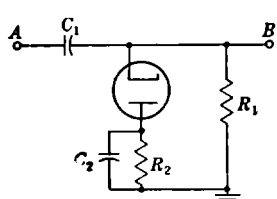


FIG. 4·9.—Diode d-c restorer.

If the voltage to which the wave is restored is not ground, the resistance of the bias-voltage supply will be in series with the diode during the recharge time. The quality of the restoration will depend upon the relative values of $t_1$ and $t_2$ and also upon the ratio of $R_1$ to $R_2$, where $R_2$ is the total resistance through which the recharge current must flow. The condition to be satisfied is

$$\frac{t_1}{R_1} \ll \frac{t_2}{R_2}.$$

When the diode closes at $t''$ (Fig. 4·6) the potential at $B$ must fall below the bias level in order to cause recharge current to flow through $R_2$. The amplitude of this overshoot may be reduced by means of a large bypass condenser $C_2$, as shown in Fig. 4·9. The conditions for good restoration then become

$$
\begin{aligned}
&C_1 \ll C_2, \\
&V\,\frac{t_1}{R_1} \ll \frac{t_2}{R_2}, \\
&R_2 C_2 \ll t_1 + t_2,
\end{aligned}
\tag{1}
$$

where $V$ is the amplitude of the rectangular wave.

If the grid of any vacuum tube is positive with respect to its cathode, current flows to the grid. Thus the grid and cathode form a diode of sorts which, in many cases, automatically provides d-c restoration to the cathode level.

**4·2. Cathode Followers.**—The cathode follower (Fig. 4·10) is an amplifier stage with the load in the cathode circuit. It is widely used in display circuits to provide (1) an impedance changer to match the impedance of a transmission line, (2) a low-



FIG. 4·10.—Cathode follower.

impedance path for rapid charging of a condenser, (3) an inexpensive voltage regulator of fair quality for low voltages and moderate currents,

and (4) a voltage takeoff that causes little loading of the driving circuit, and yet can deliver considerable power at its output terminal.

These and other possible uses depend on the following properties of the circuit:

1. The voltage gain of the circuit is given by

$$\mathcal{G} = \frac{E_0}{E_i} = \frac{\mu}{\mu + 1} \cdot \frac{R_k}{R_k + \left(\dfrac{1}{g_m + \dfrac{1}{r_p}}\right)}, \qquad (2)$$

where $\mu$, $g_m$, and $r_p$ are the amplification factor, the transconductance, and the plate resistance of the tube respectively. The term $\mu/(\mu + 1)$ multiplied by the input voltage is the generator voltage, and the quantity in parenthesis is the generator impedance for the equivalent circuit of Fig. 4·11. For large values of $\mu$ and $R_k$ the gain will be very nearly equal to, but less than one.
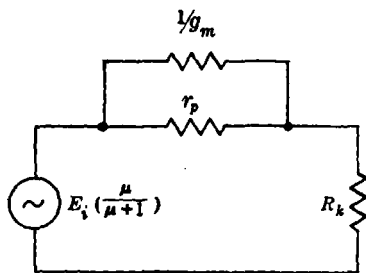


FIG. 4·11.—Equivalent circuit of cathode follower.

If the tube is a pentode, $1/r_p$ is small with respect to $g_m$, and $\mu$ is large. Therefore, the expression for $\mathcal{G}$ reduces to

$$\mathcal{G} \approx \frac{R_k}{R_k + \dfrac{1}{g_m}}. \qquad (3)$$

In this case the equivalent generator voltage is approximately $E_i$ and the internal impedance is $1/g_m$.



Internal impedance too high.    Internal impedance too low.
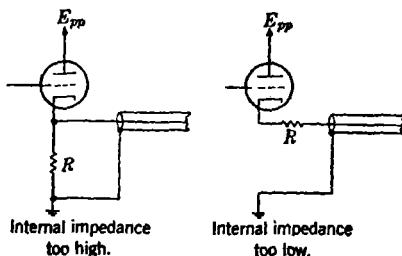
FIG. 4·12.—Matching cathode-follower output impedance to transmission-line impedance

2. The output impedance has a value between 100 and 500 ohms for most tube types. It can be matched exactly to a cable impedance

by adding a small resistance either across the cable or in series with it as in Fig. 4·12.

3. The low output impedance affords good high-frequency response even with considerable capacitive loading. For example, with 300-$\mu\mu$f loading and 100 ohms output impedance, the circuit has a bandwidth[1] of about 5 Mc/sec.
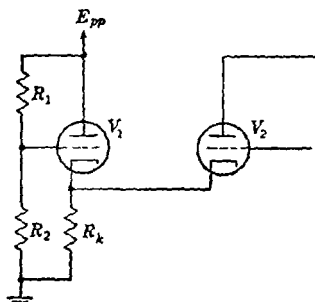


Fig. 4·13.—Cathode-follower voltage regulator.

4. A cathode follower may be used to provide a regulated voltage as in Fig. 4·13 where $V_1$ provides for $V_2$ a cathode bias voltage that is relatively independent of the current through $V_2$. If the current through $V_2$ increases, the bias on $V_1$ increases and the current through $V_1$ is reduced to keep approximately the same voltage drop across $R_k$.

5. The input resistance may be very high. If the maximum grid resistance permitted for a given tube type is not high enough for some application, the effective input resistance of the circuit may be made larger than the actual value of the grid resistor by returning the grid resistor as shown in Fig. 4·14. Here $R_1$ provides self-bias for the tube and might in some cases be zero. The effective input resistance of this circuit is

$$R_{in} = \frac{R_g}{1 - \mathcal{G}\left(\dfrac{R_2}{R_1 + R_2}\right)}. \qquad (4)$$



Fig. 4·14.—Method of increasing effective input resistance.

6. The input capacity is very low. In a carefully designed circuit most of the input capacity will be due to the interelectrode capacities of the tube. The effective capacity between any electrode and the grid depends upon the signal voltage between that electrode and the grid. Thus, if the load is in the plate circuit the plate-to-grid capacity is multiplied in its effect by $(1 + \mathcal{G})$ since the two signals are out of phase. For the cathode follower all electrodes are either fixed or move in phase with the grid. Thus no interelectrode capacity is amplified and some are reduced by a factor of $(1 - \mathcal{G})$.

[1] Defined in Sec. 4·8.

The input capacity of a 6AC7 with screen bypassed to cathode may be as low as 2 $\mu\mu f$.

The preceding conclusions are all based on the assumption of small-amplitude grid signals. The derivation of equations that are not subject to this restriction is difficult, but much useful information can be obtained by a less rigorous analysis.

First, the cathode load may be assumed to be a pure resistance; then the output signal corresponding to any input signal may be determined without great difficulty from the characteristic curves of the tube. The addition of capacitive loading does not alter this picture so long as the grid signal contains no components of frequency high enough to make the cathode susceptance significant.

Now a second case may be considered for which the capacitive loading is large, and a positive signal such as the solid line of Fig. 4·15 is applied. As a further simplification the cathode resistance and the voltage drop across it may be made such that the static current is almost the same at both initial and final levels. This condition is fulfilled if the cathode resistor is returned to a large negative supply voltage, or if the cathode follower is operated with a large cathode voltage during the initial state.



Fig. 4·15.—Response of cathode follower with capacitive load.

The flow of current into the condenser must pass through the tube output impedance; hence, a voltage difference will exist between the input and output voltages, as shown by the dashed line in Fig. 4·15, during the time the condenser is being charged. The cathode wave is normalized to the grid wave at the two constant levels.

If the rate of rise and the capacity are such that the tube cannot deliver the current required to charge the condenser without entering the region of positive bias, the result will depend upon the nature of the grid driving circuit. If this circuit can supply the necessary grid current the action will be as already stated. If it cannot, the grid wave will be distorted as zero bias is reached, and the subsequent rise of both grid and cathode will take place at a rate determined by the zero-bias current of the tube. In this situation two cathode followers are sometimes used in series. The second drives the output capacity and the first supplies the grid current required by the second.

For a third case the signal shown by Curve 1 of Fig. 4·16 is applied to the grid. Here the condenser is assumed to be large and the resistor fairly small. In the initial condition the voltage drop across the resistor is determined solely by the current through the tube. As the grid voltage drops, the tube current is reduced and an increasing portion of the

current through the resistor is furnished by discharge of the condenser; the cathode voltage will lag until the tube current has reduced enough to increase the condenser discharge current to the value required by the instantaneous condenser voltage and the cathode resistor.

In an extreme case the tube will be completely cut off and the discharge of the condenser will follow an exponential curve with a time constant $RC$. The exponential discharge continues until either the condenser is discharged or the tube again begins to conduct. If the tube turns on, the condenser current diminishes and the rate of descent decreases until once again the entire current through the cathode resistance is flowing through the tube.
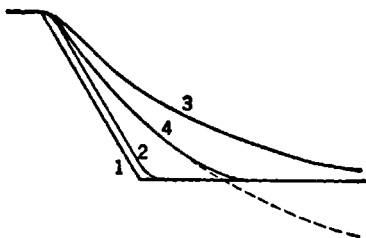


FIG. 4·16.—Response of cathode follower to negative signal.

For Curve 2 the initial current is made so high that the tube does not cut off at any time. For Curve 3 the initial current is lower and the tube does reach cutoff. It is further assumed that the initial drop across the cathode resistor is just equal to the amplitude of the cathode signal, and the tube does not turn on again. For Curve 4 the initial current is the same as that for Curve 3, but the initial drop across the cathode resistor is much larger than the signal amplitude. The cathode wave then follows the dotted exponential curve for a time and leaves it as the tube starts to conduct. Again the curves have been normalized to the same initial and final levels.

From this discussion it follows that the response of a cathode follower to negative signals can be improved by (1) using a sharp-cutoff tube, (2) increasing the initial current, and (3) increasing the voltage drop across the cathode resistor so that only the steep portion of the exponential wave is followed. The operating conditions of a cathode follower must always be arranged with great care if it is to exhibit the highly useful properties claimed for it.

**4·3. Trigger Generators.**—This book is concerned primarily with displays utilizing information that is repeated at definite intervals. The repetition rate is determined by some oscillatory circuit or by a mechanical timer such as a rotary spark gap. The various events in the display cycle are then initiated in proper synchronism by voltage waves appearing in or derived from the primary timing device.

Figure 4·17 shows various trigger waveforms commonly encountered, of which $a$ is the most useful. With $b$ the disturbances following the main trigger pulse may prevent normal operation of the triggered circuit, either by feeding through and distorting the output signal, or by actually

causing it to shut off because of the positive overshoot. The sharp trailing edge of *c* is a disadvantage. A wide pulse of the form of *c* may be differentiated by a coupling condenser and give a second pulse of opposite sign at the point of termination; whereas a narrow one demands very rapid response in the triggered circuit lest the trigger disappear before the circuit has responded.

Transmission of a trigger pulse over a long cable requires a very low output impedance for the trigger generator in order either to maintain the sharp leading edge in spite of the capacity of the cable, or to match the impedance of a terminated cable. If the same trigger generator is used for parallel triggering of several circuits, a low output impedance helps to reduce interaction between the various circuits. For the rare circumstance when a trigger pulse is applied to just one near-by circuit, a much higher impedance may be used.

However, a trigger generator that has other desirable characteristics need not be discarded because of high output impedance. It is always



(a) Ideal trigger pulse

(b) Oscillatory trigger pulse

(c) Rectangular trigger pulse

FIG. 4·17.—Typical trigger waveforms.

possible to add buffer stages to provide any required isolation or output impedance. The cathode follower is particularly suited to the transmission of positive trigger pulses. In this case it can have a very low quiescent current because only a fast leading edge is required and a slow fall is desirable. The negative trigger pulse is more economically obtained from the plate signal of an amplifier stage. The amplifier is



FIG. 4·18.—Deriving a trigger pulse from a sine wave.

biased to a very low current and turned on abruptly by a positive pulse from the trigger generator. If the tube is of the high-current type the plate will descend rapidly even though working into a low impedance. The trailing edge may be much less steep, but usually this is an advantage.

The well-known art of designing very stable sine-wave oscillators

suggests the use of such a circuit as the frequency source. Figure 4·18 shows one method of deriving a trigger pulse from a sine wave. The sine wave is amplified in overdriven amplifiers until it becomes essentially rectangular, and is then differentiated to give a positive and a negative trigger pulse. If the circuit to be activated will respond to both pulses, the undesired pulse may be eliminated by means of a diode or a suitably biased amplifier stage.

Complete phasing of the output trigger pulse may be accomplished by any of the familiar methods of shifting the phase of a sine wave. A more limited control is obtained by adjusting the bias on one of the early amplifier stages.
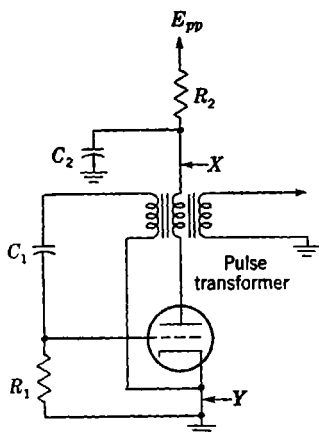


Fig. 4·19.—Simple blocking oscillator.

The term "blocking oscillator" has been applied to many different circuits, but here its use will be restricted to variations of the basic circuit shown in Fig. 4·19. This circuit provides a sharp trigger pulse and also determines the repetition rate. It is a high-frequency sine-wave oscillator in which the grid is driven positive during half of the cycle. Sufficient grid current flows into $C_1$ during this half cycle to block further oscillation until the charge on the grid leaks off through $R_1$ and the tube again conducts. Thus the output is a series of narrow pulses separated by the grid recovery time.

The pulse appearing on the plate or across the third winding of the transformer[1] is shown in Fig. 4·17b. Its width is largely determined by the characteristics of the pulse transformer although certain variations in the circuit permit a limited control of pulse width. Transformers are available to give pulses varying in width from perhaps 10 $\mu$sec to a fraction of a microsecond.

The pulse appearing at the transformer is seldom used directly, partly because of its bad overshoot and partly because of the fact that any load on the transformer affects the pulse shape and the repetition frequency. A trigger pulse like that of Fig. 4·17c may be obtained by inserting a small resistance, perhaps 100 ohms, at either $X$ or $Y$ of Fig. 4·19. Since the signals obtained in this way are proportional to the current in the tube, they are free from overshoot. Better trigger pulses are also obtained by applying the signal from the third winding to the grid of a cathode follower or an amplifier. By means of a large

[1] Transformers appropriate for this application are of a special group called "pulse transformers," which have excellent response at high frequencies.

load resistor and some capacitive loading the output signal can be made to resemble Fig. 4·17a.

Since the peak currents drawn may be several hundred milliamperes, it is essential that additional filtering be provided to decouple the blocking oscillator from the power supply.   Although the peak current is very high, the duty ratio is so low that the blocking oscillator is the most economical form of trigger generator.

Unfortunately the repetition rate depends not only upon the grid time constant $R_1C_1$, but upon the cutoff level of the tube and the charge accumulated by the condenser during the pulse.   Because cutoff is widely variable for many tube types, replacing the tube may cause a large change
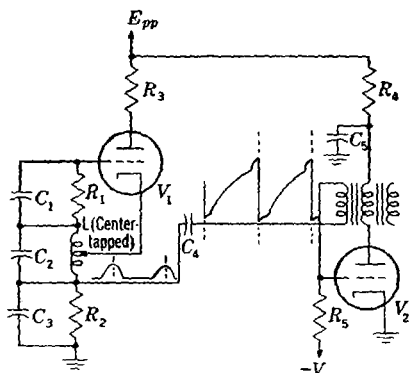


FIG. 4·20.—Blocking oscillator controlled by Hartley oscillator.

in frequency.   Also the charging of the condenser may vary from one cycle to the next, resulting in unequally spaced pulses.

The lack of frequency stability in the blocking oscillator leads directly to a different usage of the circuit.   If the grid resistor of Fig. 4·19 were returned to a voltage below cutoff for the tube, the circuit would be stable and would fire only if some outside agency caused the tube to conduct momentarily.   Thus a sine-wave oscillator might be used to control the firing of the blocking oscillator.   Figure 4·20 shows this method of operation.   Tube $V_1$ is a Hartley oscillator in which a current pulse appears across $R_2$ during a portion of the cycle.   This pulse is coupled to the grid of the blocking-oscillator tube $V_2$, which is normally biased below cutoff.   The result is a trigger pulse that has the sharpness and low impedance of a blocking oscillator and the stability of a sine-wave oscillator.   The addition of $C_3$ provides a bypass across $R_2$ for the high frequencies contained in the blocking-oscillator pulse.

If the output of a given circuit is not sharp enough for direct use as a trigger pulse it may still be sharp enough to activate a blocking oscil-

lator.   The biased-off blocking oscillator can then be employed as an inexpensive trigger pulse sharpener.

By making the recovery time of the blocking oscillator longer than the period between successive input pulses the circuit can be made to operate as a frequency divider.   After the blocking oscillator has fired, its grid will not return to the firing potential until some chosen number of succeeding triggering pulses have passed.   Thus the output frequency is a submultiple of the input frequency.

The multivibrator circuit (see Sec. 4·4) is also useful as a trigger source.   The circuit shown in Fig. 4·21 provides the optimum frequency
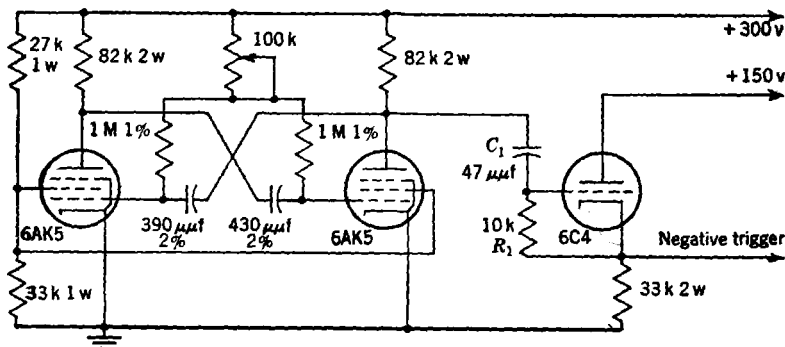


Fig. 4·21.—Multivibrator designed for maximum stability; 1600 cps.

stability attainable with a multivibrator.   In designing this circuit, the following restrictions on its operation have been taken into account:

1. The signals applied to the grids must be large and of constant amplitude.   The size of the plate resistors and the fact that the tubes are pentodes insure that the plate signal will be virtually equal to the supply voltage and that variations in tube emission will have little effect on its size.

2. The slope of the grid wave must be as great as possible as the grid potential enters the conducting region.   For this reason the grid resistors are returned to the plate supply voltage.   The point of conduction is thereby effectively shifted to a steeper portion of the exponential curve, and some compensation is provided for variation in that supply level.

3. Variations in tube cutoff level must be small with respect to the signal applied to the grid.   The operation of sharp-cutoff pentodes at low screen potential meets this requirement.

4. The recovery of each plate during the nonconducting period of that tube must be as nearly complete as possible.   For this reason

the period is approximately equally divided between the two states of the circuit.

5. The cross-coupling condensers and the grid resistors must be of the best quality so that temperature and aging variations will be minimized.    These are the only critical components involved.
6. The output coupling must place little load on the circuit.    In the diagram the output coupling is a very small condenser $(C_1)$ that produces negligible load compared to that due to the cross-coupling condensers.    The output wave is differentiated by this condenser and $R_1$.    The cathode follower is biased to saturation and the resulting positive trigger pulse is therefore suppressed and only the negative one is transmitted.

Other frequencies may be obtained by adding a ganged switch and different cross-coupling condensers.    The potentiometer in series with the two grid resistors permits fine adjustment of any one of the frequencies; the other frequencies will then be accurate within the tolerances of the condensers employed.

Certain applications require a trigger pulse that is accurately phased with respect to a sine wave of frequency much higher than the repetition frequency of the trigger pulse.    Where the frequency-stability requirements on the sine wave are such as to require crystal control of the oscillator it is difficult to pulse the oscillator at the repetition frequency.    In such cases it is customary to permit the sine-wave oscillator to run continuously and to derive the trigger pulse from the sine wave by means of successive counting stages.

**4·4. Rectangular-wave Generators.**—The ideal rectangular wave is characterized by an instantaneous change in voltage, followed after a time by an equally abrupt change back to the original value.    Between these points of discontinuity the voltage is constant.

Fortunately, considerable departure from the ideal is acceptable in most applications.    If the rectangular wave is to be used as a time index, only the rapid transition must be stressed, in order that trigger and marker pulses may be derived from the change in voltage.    If it is used as a gating signal, that is, for turning a circuit on or off for a given time, the emphasis may fall on the flatness of the wave during one of the intervals.

Rectangular waves may be produced by all forms of switches or contacts if the time intervals are fairly long.    For short time intervals some form of electronic switch is required.

It is possible to form a rectangular wave from a sine wave, or almost any waveform, by successive amplification and limiting stages.    If such an input wave is available this may be the practical solution to the

problem, but in general it is necessary to generate the wave before amplifying it, and the net cost is therefore rather high.

There are various one-tube circuits that involve a transfer of the cathode current from the screen grid to the plate and back again, which give out approximately rectangular waves. Since these circuits are useful only under fairly special conditions they will not be described here. One that has been widely used as a delay circuit is described, however, in Sec. 6·3.

The most common rectangular-wave generator consists of two amplifier stages with the output terminal of each coupled to the input terminal of the other so as to cause regeneration. It differs from similar sine-wave generators by the absence of resonant elements in the circuit. The loop gain[1] is high if both tubes are conducting; therefore, a signal applied at almost any point in the circuit is amplified and reamplified until some limiting condition of zero gain for one of the stages is reached. The circuit cannot long remain in the region between limits because the random fluctuations in cathode emission provide a sufficient signal to start the regenerative process. The operation then consists of successive rapid transitions from one limit to the other.

Many of the characteristics of the circuit depend upon the nature of the limiting conditions. If the limiting condition is saturation of one of the stages while the other stage remains in the conducting region, the circuit is completely unstable and any small disturbance sends it to the other limit. Consequently circuits are not so designed. If the limiting condition is cutoff of one tube, with the cutoff voltage supplied by a condenser that will gradually discharge, the plate currents are constant for the length of time required for the cutoff tube to return to the conducting region. Temporary stability is therefore attained. If the cutoff bias is supplied by a resistive network or by a fixed-bias source, the circuit is completely stable and stays put until some outside influence disturbs it.

Several factors limit the sharpness of the changes in plate voltage. Clearly the speed of fall is improved by reducing either the capacitive loading or the effective resistance of the tube. A faster rise time results from a reduction of the plate load resistor or the capacitive loading. Loading due to any actual condensers can be removed by insertion of a cathode follower. Only the stray capacity remains and this can be reduced somewhat by careful design and construction.

Various circuits differ widely in their speed of recovery. At each transition the charges in various condensers must change to new values. Until this change has taken place the circuit will not respond in a normal

[1] Loop gain is determined by breaking the circuit at some point and calculating the gain from the break through the loop and back to the break.

fashion to an incoming signal. If fast recovery is important all condensers must be small, or their charging impedances must be low.

The multivibrator, shown in Fig. 4·22, is a well-known rectangular-wave generator. It has condenser coupling from each plate to the grid of the other tube, and the grid resistor is returned to cathode potential or to a positive bias. Thus both limits represent conditions of temporary stability and the circuit generates a train of waves without being triggered. The off time of $V_1$ is proportional to $R_1C_2$ and that of $V_2$ to $R_2C_1$. Both times are affected by the amplitude of a negative signal acting on the grid, the level of bias at which the tube begins to conduct, and the voltage to which the grid resistors are returned. Thus many forms of frequency control are possible.
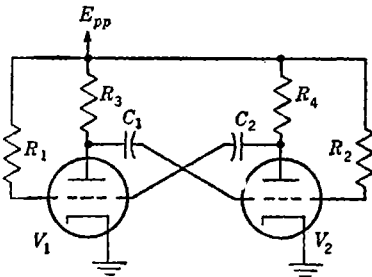


FIG. 4·22.—Multivibrator circuit.

The plate time constant during most of the rise is given by $R_3C_1$ (or $R_4C_2$). Since the coupling condensers may be very large the rise time will be long unless cathode followers are used to drive the condensers.

Synchronizing pulses may be introduced to lock in the multivibrator at the trigger frequency or at a lower frequency.
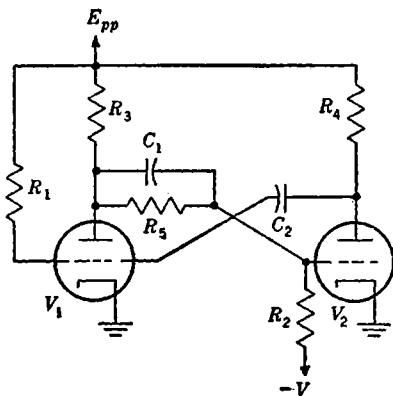


FIG. 4·23.—Flip-flop circuit.

In the circuit of Fig. 4·23 a resistance network returned to a negative bias replaces one of the coupling condensers of the multivibrator. ($C_1$ is very small and serves only to improve the high-frequency gain of the loop.) Thus one of the limits is stable and the circuit requires an external trigger to flip it out of this condition. Then, at a time determined by $R_1C_2$, it flops back to the stable condition. This circuit will be called a "flip-flop."

Since $C_1$ is small the rise of the plate of $V_1$ may be rapid. If $R_4C_2$ is not large, or if $C_2$ is driven through a cathode follower, the recovery time will be short.

Other small changes in the multivibrator may also make it a flip-flop circuit. For example, the introduction of a fixed bias for one of the tubes

makes one of the limits stable so that the circuit will not operate unless triggered.

Resistance networks are used for both couplings in Fig. 4·24, and both limits are therefore stable. Thus the circuit will remain in either condition until triggered. This circuit will be called a "scale-of-two" since one cycle corresponds to two input-trigger pulses. Strictly speaking this name would be reserved for the case in which the same trigger pulse, coupled to both grids, shuts off the tube that is conducting at the moment and causes a transition to occur. Although this is the only case in which the input frequency is truly scaled down, the name will be used here for any circuit of this type which requires two input signals per cycle.



FIG. 4·24.—Scale-of-two circuit.

Both $C_1$ and $C_2$ are small, and thus either plate may rise rapidly. Also the recovery time is very short, so that the operation of the circuit is virtually independent of the interval between triggers. The circuit is therefore extremely useful where this interval may vary over wide limits or in a random fashion.

The circuit of Fig. 4·25 has a resistance coupling from the plate of $V_1$ to the grid of $V_2$ and a second coupling from cathode to cathode, which completes the loop. Since all connections are direct, both limiting conditions are stable, and the circuit remains in one state or the other depending upon the value of $E_g$. Thus the circuit is able to form a rectangular wave from a very slowly changing input voltage. When so used it is called a "flopover" circuit.

Because no large condensers are used, both rise time and recovery time may be made short. Since the voltage wave across $R$ does not enter into the action of the circuit, it is possible to replace $R$ by a transformer winding, the coil of a relay, or any other impedance that is not so large as to limit the current in $V_2$.
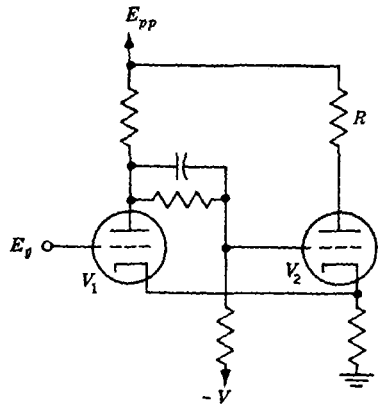


FIG. 4·25.—Cathode-coupled flopover circuit.

By returning the grid of $V_1$ to a fixed voltage through a grid resistor

and by introducing triggers to both grids, the circuit is changed into a scale-of-two circuit.

Figure 4·26 shows the same basic circuit in which the plate-to-grid coupling has been changed to a condenser. The circuit is now a flip-flop for which the off time of $V_2$ is very accurately proportional to the grid voltage of $V_1$. It is very useful as a delay circuit because the delay time can be determined by a high-impedance circuit.

The first three elements of a pentode, the cathode, grid, and screen, constitute a triode and may be so used. If one of the triodes of a rectangular-wave generator is replaced by a pentode in this way, the operation of the circuit will be unchanged. The plate of the pentode, which is coupled to the circuit only



Fig. 4·26.—Cathode-coupled flip-flop circuit.

by the electrons flowing through the tube, provides another element from which a very sharp rectangular wave may be taken. Since the plate is not involved in the coupling of the circuit it may be used for the generation of other waveforms as well. An example may be seen in Fig. 7·1.
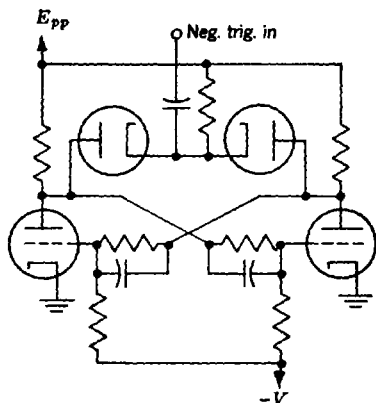


Fig. 4·27.—Scale-of-two circuit triggered through diodes.

Trigger pulses may be introduced to the circuits (multivibrator, flip-flop, or scale-of-two) across any element used in coupling one stage to the other provided, first, that the trigger-source impedance is low enough to drive the impedance presented by the chosen element, and second, that the polarity and amplitude of the trigger pulse are such as to produce a transition under the conditions existing in the circuit at that instant. The second requirement does not apply if the circuit is being used to scale down the trigger frequency.

Often the trigger pulse is applied to a plate or grid through a small condenser. However, the coupling condenser, although small, does load down the triggered element to some extent. Also, if the trigger pulse is inferior in shape, any disturbances that follow the sharp leading edge are coupled into the circuit and may either prevent normal triggering or cause a reverse transition to occur before it is wanted. Thus trigger isolation is sometimes necessary.

Diodes are frequently used to provide isolation. Figure 4·27 shows

a scale-of-two circuit with a negative trigger pulse introduced to the two plates through diodes. The drop in the plate load resistor of the conducting tube provides a bias for one diode which prevents transmission of the trigger pulse. Thus the trigger pulse is applied only to that grid upon which it will have an effect, and a great improvement in the dependability of the triggering results.

Figure 4·28 shows a flip-flop circuit with the trigger introduced
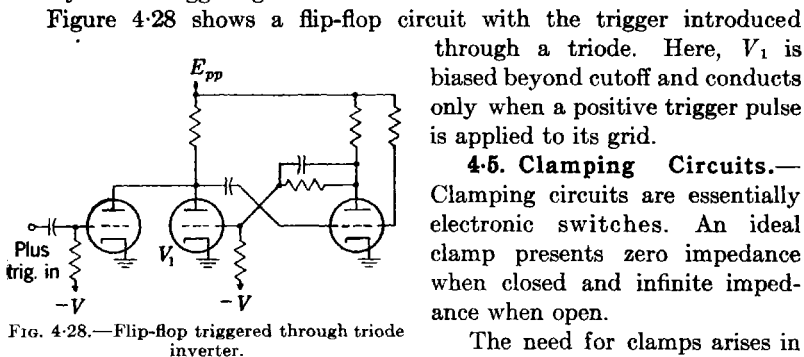


FIG. 4·28.—Flip-flop triggered through triode inverter.

through a triode. Here, $V_1$ is biased beyond cutoff and conducts only when a positive trigger pulse is applied to its grid.

**4·5. Clamping Circuits.**— Clamping circuits are essentially electronic switches. An ideal clamp presents zero impedance when closed and infinite impedance when open.

The need for clamps arises in various situations. For example, some of the waveforms used in display circuits are simple functions of time which can be generated by networks if the voltages and currents of the network have specified initial values. Clamps may be used to hold the network at the initial values. Opening the clamps then permits the waveform to develop according to the characteristics of the circuit. Clamps are also used to create a momentary connection between some terminal of a circuit and a reference voltage in order to establish the voltage level of that terminal. Examples of this use are found in ordinary d-c restoration and in certain forms of carrier-demodulation systems.

Clamps may be classified as either two-way or one-way clamps. These descriptive terms are defined by the following statements: A one-way clamp will conduct in only one direction, and hence can bring Terminal $A$ to the potential of Terminal $B$ only if $A$ is always more positive than $B$ or if $A$ is always more negative than $B$, depending on the polarity with which the clamp is put between $A$ and $B$. A two-way clamp will conduct in either direction, and will restore the potential at $A$ to that at $B$ whether $A$ is positive or negative with respect to $B$.

*One-way Clamps.*—The following examples will be simplified by using ground potential as the reference voltage. The diode d-c restorer discussed in Sec. 4·1 may be regarded as a special form of clamp which is opened or closed by the action of the voltage at the terminal to be clamped. Its use is limited to cases in which clamping is to occur at the maximum or minimum of the voltage wave.

The general characteristics of clamping circuits will be discussed in

connection with the simple triode clamp of Fig. 4·29,[1] which acts as a switch between the point $A$ and ground. In this circuit the clamp is normally closed and a steady current flows through it to ground. The voltage drop across the clamp is determined by this current and the effective resistance of the clamp.

Often the current is fixed by other considerations so that improvement in the clamping can be achieved only by a reduction of the clamp resistance. Therefore the use of a tube type having a low effective resistance is helpful. Usually a tube with a low plate resistance also has a low effective resistance when used as a clamp. The use of several tubes in parallel also improves the clamping action. For a given tube the effective resistance will be reduced if more current is drawn through the grid circuit; that is, if the grid is driven more positive.

The clamp may be opened by applying a negative signal, usually a rectangular wave, to the grid. Any high-frequency components in the grid wave will be coupled to the plate circuit by the interelectrode capacity and may be very objectionable. This effect is minimized by using a grid wave that has a slow leading edge and that is just large enough to keep the clamp open. The amplitude required depends upon the maximum voltage on the plate. If the gating signal provided is very sharp, its high-frequency components can be kept from reaching the grid by inserting the simple RC-network shown by the dotted components of Fig. 4·29.
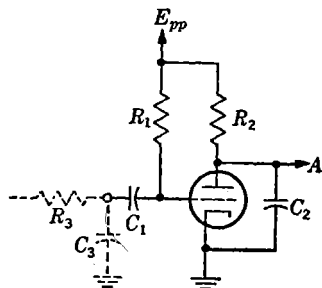


FIG. 4·29.—One-way triode clamp for positive signal.

The triode of this circuit may be replaced by a pentode in order to effect a further reduction in grid-to-plate coupling, although, in general, triodes provide a lower clamp resistance. Not only is the interelectrode capacity of the pentode smaller, but the sharper cutoff characteristic permits the use of a much smaller grid signal.

When the clamp closes, the circuit returns to the normal condition. The speed with which it recovers is determined by the ability of the clamp to discharge $C_2$ rapidly. Thus, a low-resistance clamp permits quicker recovery. If $C_1$ is permitted to discharge appreciably while the clamp is open, the grid will be overdriven when it closes, and a very low clamp resistance will be produced during the time $C_2$ is being discharged. However, too much overdrive may be worse than too little because it can

---

[1] The circuit used for illustrative purposes in this and the following figures is a simple sawtooth generator. which will be described in Sec. 4·6.

cause the plate voltage to fall below the equilibrium value for a short time.

Figure 4·30 shows the way the triode clamp may be used if Terminal *A* is negative with respect to the reference voltage. The grid signal must now be much larger in order that the cathode excursion may not cause current to flow through the tube. The recovery may be slightly more
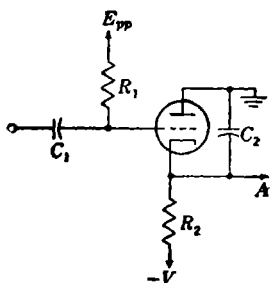


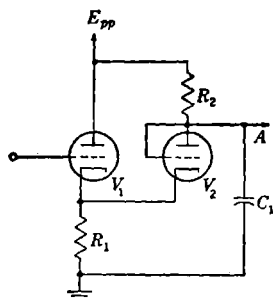Fig. 4·30.—One-way triode clamp for negative signal.



Fig. 4·31.—One-way cathode-follower diode clamp.

rapid in this case since the tube acts as a cathode follower, although the plate voltage on the tube is too low for very good cathode-follower operation. The grid current also helps to discharge $C_2$.

The cathode follower and diode clamp of Fig. 4·31 closes when $V_1$ cuts off, and may be opened by a positive signal applied to the grid of $V_1$. Both the recovery and the action of clamping of this circuit are adversely affected by the presence of $R_1$ in series with the diode. Resistor $R_1$
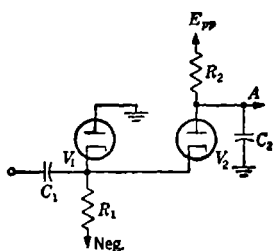


Fig. 4·32.—One-way double-diode clamp.
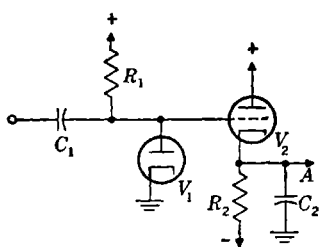


Fig. 4·33.—One-way diode-cathode-follower clamp.

can seldom be made as small as might be desired because the signal at *A* can be no larger than the voltage developed across $R_1$ when the clamp is opened. Unless $V_1$ is to draw a very high current, $R_1$ must thus be fairly large. Nevertheless, this clamp is preferable for some applications where the output signal is small since it will not cause an overshoot in the wave at *A*.

Figure 4·32 shows a two-diode clamp. The clamp may be considered to consist of $V_2$, with $V_1$ acting as a d-c restorer that holds the cathode of $V_2$ at the reference level. The effective resistance of the clamp is that of the two diodes in series. For the d-c restoration to be effective, the current through $R_1$ must be greater than that through $R_2$. Thus, $R_1$ may be fairly small. Since the positive signal that opens the clamp is applied across $R_1$, the source impedance of the signal must be low with respect to $R_1$. If Terminal $A$ in Fig. 4·32 is negative with respect to the reference voltage, the circuit is simply inverted as in Fig. 4·35 and no new complications arise.



FIG. 4·34.—Two-way double-triode clamp.

The diode and cathode-follower clamp of Fig. 4·33 is useful only if $A$ is negative with respect to the reference voltage. The diode is a d-c restorer on the grid of the cathode follower. The clamp is opened by a sufficiently large negative signal on the grid of $V_2$ to allow for the negative excursion of the cathode. An advantage of this clamp is its extremely rapid recovery since $C_2$ is discharged through the very low impedance of the cathode follower. However, the quiescent level of the cathode of $V_2$ will be higher than the reference voltage unless suitable allowance is made in selecting the return voltage of $V_1$, and this property is often a disadvantage.



FIG. 4·35.—Two-way four-diode clamp.

*Two-way Clamps.*—The two-triode clamp of Fig. 4·34 consists of the two circuits of Fig. 4·29 and Fig. 4·30 in combination. The voltage applied to $R_2$ may be either positive or negative. When the clamp closes, $V_1$ will conduct if $A$ is below ground and $V_2$ will conduct if it is above ground. The clamp is opened by a negative signal applied to the grids. This signal must be fairly large since the cathode of $V_1$ may go negative. Also the interelectrode coupling may be very bad with this circuit since the capacities in the two tubes add.

The four-diode circuit of Fig. 4·35 contains the two-diode clamp of

Fig. 4·32 plus the inverted version of the same circuit.    In the absence of
signals at $C_1$ and $C_2$, the diodes conduct so that $A$ is brought to the
voltage at the reference point $B$, which may be at ground or any other
potential.    Again the voltage $V$ applied to $R_3$ may be either positive or
negative with respect to $B$.    The currents through $R_1$ and $R_2$ must each
be greater than that through $R_3$ in order to close the restoring tubes $V_1$
and $V_2$.    The clamp is opened by simultaneous application of a negative
signal to $C_1$ and a positive signal to $C_2$.    Each signal must be at least as
large as the maximum excursion of $A$ in the direction of that signal.
However, the large signal will not necessarily be coupled through the
clamp.    If the two gating signals are alike in shape, the signals coupled



FIG. 4·36.—Two-way trans-
former-coupled double-triode
clamp.

through $V_3$ and $V_4$, being equal and op-
posite, will cancel out.

The use of ground as the reference
voltage produces an oversimplification in
this discussion.    In general, this voltage
level will not be at ground, and the volt-
age source will present an impedance that
must be included in the circuit in series
with the clamp.    Since this series imped-
ance will impair the speed of recovery and,
as part of a resistance divider, will affect
the voltage at which clamping is effected,

every effort should be made to provide a source of reference voltage which
has a low output impedance.

If it is impossible to reduce the output impedance of the source of
reference voltage, it becomes necessary to reduce the current drains on
the source to a minimum.    Reduction to zero of the current into the
clamped terminal may still leave a considerable drain on the reference
source in each of the circuits described above, by way of some channel,
such as $R_1$ in Fig. 4·34, involved only in activating the clamps.    Figure
4·36 shows a variation of the double-triode clamp in which this extraneous
current has been eliminated.    The activating signals are transformer-
coupled to the grids, and each grid circuit is then a closed loop that takes
no current from the reference point or from Terminal $A$.    A common use
of this circuit in the demodulation of a sine-wave carrier is discussed in
Sec. 5·5.

A circuit with similar properties may also be derived from the four-
diode clamp.

**4·6. Sawtooth-wave Generators.**—Any voltage waveform that resem-
bles Fig. 4·37 will be called a "sawtooth wave."    That portion of the
wave in which the change of amplitude is roughly proportional to time
will be called the "rise" whether the change in voltage is positive or

negative. The flat portion is the "quiescent" voltage and the portion that follows the rise is the "return" or "flyback." A waveform may differ considerably from Fig. 4·37 and still be called a sawtooth wave. For example, the quiescent period may be of any length down to zero and the return may occupy more time than the rise.

Each of the sawtooth-wave generators to be considered here contains the basic components shown in Fig. 4·38. There is a switch of internal resistance $R_s$ (this switch might be any of the clamping circuits discussed in Sec. 4·5), a current-controlling element, $X$, and a condenser $C$.
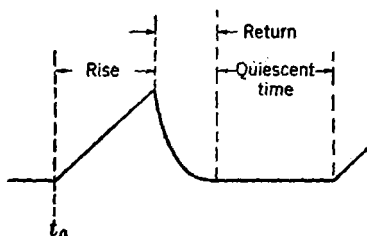


FIG. 4·37.—Sawtooth waveform.

When the switch is closed the condenser is short-circuited if the switch resistance can be assumed to be negligibly small. At a time $t_0$ the switch opens and current flows into the condenser. The instantaneous voltage $e$ at the output terminal is given by

$$e = \int_{t_0}^{t} \frac{i}{C} \, dt. \tag{5}$$

Thus, the slope and linearity of the sawtooth wave depend entirely on the



FIG. 4·38.—Equivalent circuit of current-integration type of sawtooth wave generator.

size of the condenser and the current flowing into it. If the current is constant the output voltage will be exactly proportional to time. Thus, the problem of producing a linear sawtooth wave is simply that of obtaining a constant charging current.

When the switch closes it not only diverts the charging current from the condenser, but discharges the condenser. During this interval the current will be large and the switch resistance must be considered because it determines to a very great extent the return time of the circuit.

The slope of the sawtooth wave can be changed in several obvious ways. Changing the size of the condenser in discrete steps provides a coarse control. Fine control is usually obtained by adjustment of the charging current. The charging current is determined by the characteristics of the control element and, in some cases, by the voltage applied to it. The possibility of

voltage control is particularly useful for display circuits since many of the data-transmission systems provide position information in the form of slowly varying voltages from which sawtooth waves of amplitude proportional to the position voltage are to be formed.

In many applications of the sawtooth wave a waveform like that shown in Fig. 4·39 is required. This wave may be regarded as the sum of



Fig. 4·39.—Trapezoid waveform consisting of sawtooth and step waves.

a sawtooth wave and a rectangular wave. The rectangular component may be added to the output signal of any of the circuits described below by inserting a small resistor, known as the "step" resistor, in series with the charging condenser. While the switch is open the current flowing into the condenser causes an IR-drop across the step resistor. This drop appears at the output terminal and adds to the signal produced by the charging of the condenser.

The simplest current-controlling element ($X$ in Fig. 4·38) is a resistor returned to a relatively high potential. Since the charging current is proportional to the voltage across the resistor, the sawtooth wave will be exponential rather than linear. Any desired degree of linearity may



Fig. 4·40.—Pentode-charging sawtooth-waveform generator.
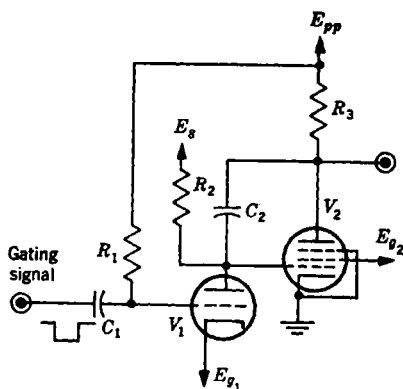


Fig. 4·41.—"Miller run-down" sawtooth-waveform generator.

be obtained by limiting the ratio of maximum sawtooth amplitude to initial voltage across the resistor. A ratio of 1 to 10 will be small enough for any sweep application, and larger ratios may sometimes be accepted. If the available supply voltage is high enough to meet the linearity requirement, this form of sawtooth generator should be used because of its simplicity and because its recovery time may be very short.

As long as the plate voltage of a pentode is above the knee of the

characteristic curves, the plate current varies only slightly with changes in plate voltage.    The variation is still less if the tube is biased by means of an unbypassed cathode resistor.    Thus, a pentode may be used as the current-controlling element of a sawtooth-wave generator.    In this way a sawtooth amplitude of perhaps 75 per cent of the supply voltage may be obtained with acceptable linearity.

Figure 4·40 shows the pentode used to produce a negative sawtooth wave.    Unfortunately the clamping tube is in the plate circuit so that a floating heater supply may be required and the gating signal must be large.    If the pentode is used to generate a positive sawtooth wave a floating screen supply returned to the cathode is required to keep the current constant.

The "Miller run-down" circuit of Fig. 4·41 may be resolved into two familiar circuits.    A simple resistance-charging circuit ($V_1$, $R_2$, and $C_2$) develops a small-amplitude sawtooth wave at the grid of an amplifier.    The amplifier is a high-gain pentode with enough negative voltage feedback to insure linear amplification of the grid signal. The element of strangeness in the circuit arises from the dual function of $C_2$, which not only provides the



Fig. 4·42.—Generalized circuit of bootstrap sawtooth-wave generator.

feedback but also acts as the charging condenser.

This circuit requires very precise clamping because any error in clamping is greatly amplified by the pentode.    The amplification of the error is reduced if a triode is used but this change also reduces the linearity of the output wave.

The linearity of the sawtooth wave produced by the resistance-charging method may be greatly improved by another scheme involving positive feedback.    If, as in Fig. 4·42, the sawtooth wave is the input signal for a noninverting power amplifier with a voltage gain of one, and the output signal is applied to the supply end of the charging resistor, the voltage across the resistor remains constant and the sawtooth wave is linear.    Circuits of this type are called "bootstrap" sawtooth-wave generators.

If the gain $\mathcal{G}$ of the amplifier is less than unity, the rise will be exponential rather than linear.    The shape of the sawtooth wave may still be determined by assuming an effective supply voltage equal to $(1/1-\mathcal{G})E$ and a correspondingly increased charging resistor.    A gain of 0.95 thus gives an effective supply voltage of $20E$ and the sawtooth wave
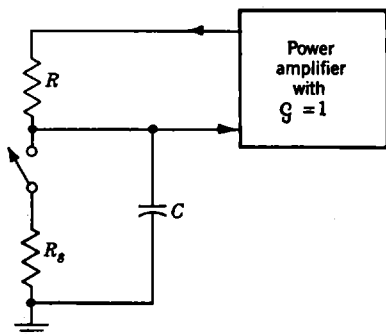
will remain linear enough for use as a sweep voltage of amplitude of at least 2*E*. This statement is not valid, however, if the amplifier saturates in the process.

By making the gain greater than one, a sawtooth wave of increasing slope may be obtained. This waveform is used in certain data-transmission systems to compensate for low-frequency losses.

A cathode follower has all the characteristics required of the amplifier, and, in addition, is economical. Although its gain is always less than one, it can be made to approach one very closely. For example, a medium-μ triode may have a gain of 0.95, and a pentode such as a 6AC7 with screen bypassed to cathode may have a gain of 0.995.



FIG. 4·43.—Simple bootstrap circuit with cathode follower as power amplifier.

The principal disadvantage of the cathode follower in this application is the small potential difference between input and output levels. It is thus impossible to use direct connection throughout unless a battery or a floating power supply is included in the circuit to provide the proper d-c relations. Although this is sometimes justified for a laboratory circuit, it is too inconvenient for field equipment. More often a condenser is used for the feedback channel with the d-c component of the charging current supplied through another channel. Since the coupling condenser must be large enough to transmit the sawtooth wave without appreciable distortion, it is difficult to insure complete recovery of the circuit.

Figure 4·43 shows a common version of the bootstrap circuit, in which the d-c component of charging current is supplied through the decoupling resistor $R_1$ and the feedback signal through $C_1$. The charging condenser is $C_2$, and $R_2$ is the charging resistor. The slope of the rise is proportional to the potential difference across $R_2$. While the switch is open $C_1$ loses through $R_1$ some charge that must be regained before the circuit returns to a stable condition. Since the time allowed for recovery is almost always insufficient, the voltage across $R_2$ will change until an equilibrium condition is reached in which the charge lost equals the charge regained in each cycle. This equilibrium is affected both by the amplitude of the sawtooth wave and its duty ratio, and therefore the slope is sensitive to variations in either quantity. This form of the circuit cannot be used

where the response must be exact, unless the operating conditions are all constant or the duty ratio is very small.

Figure 4·44 shows another form of the circuit in which the d-c component of the charging current is supplied through a diode. When the switch is open, $C_1$ loses charge only through $R_1$ since the diode is open during this part of the cycle. During the recovery period $V_1$ is conducting, holding one end of the condenser at the supply level while charge flows back into $C_1$ through $R_2$. By either reducing the value of $R_2$ or returning it to a negative potential, the recovery time can be shortened
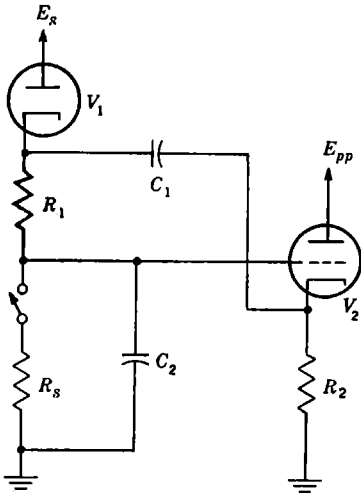


FIG. 4·44.—Bootstrap circuit with diode recharge path.
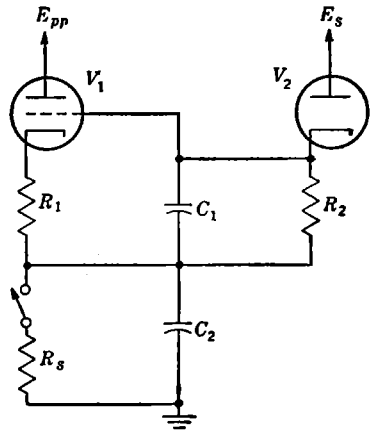
FIG. 4·45.—Variation of bootstrap circuit.

so that the slope is independent of amplitude and repetition rate for duty ratios up to perhaps 75 per cent.

In the circuit of Fig. 4·45 the charging resistor $R_1$ is supplied directly by the cathode follower $V_1$. The signal is coupled to the grid of the cathode follower through $C_1$. During the quiescent period $V_2$ holds the grid of $V_1$ at the potential $E_s$, and since this voltage appears across $R_1$, it determines the slope of the sawtooth wave. Condenser $C_1$ discharges only through the resistor $R_2$, which may be made quite large. Thus, $C_1$ can be much smaller in this circuit than in the preceding examples, and the recharge problem is therefore less difficult. If $E_s$ is supplied from a low-impedance source the recovery can be made very rapid. A major defect of this circuit is the initial high level of the cathode of $V_1$. For a given supply voltage, saturation of $V_1$ will occur at a smaller amplitude of the sawtooth wave than in the preceding circuits.

If any of these three circuits is used to generate a sawtooth wave proportional to a variable control voltage, trouble will be encountered if the variation of the control voltage is at all rapid.    The recharge mechanism may be unable to establish the proper charge in the coupling condenser in the time allowed.    Although nothing much can be done to improve the performance of the circuit of Fig. 4·43, substitution of two-way clamping circuits for the diodes and switches of the circuits of Figs. 4·44 and 4·45 will greatly increase their ability to follow rapid changes.

Some applications of sawtooth waves for the determination of a time interval demand very high linearity of the sawtooth signal.    This linearity can be obtained with a bootstrap circuit by means of a more expensive amplifier than the cathode follower, or by adding to the sawtooth wave a correction term that compensates for the imperfections of the circuit.    Adding a correction term that is proportional to the integral of the sawtooth voltage will compensate not only for an amplifier gain of less than unity, but also for loss of charge by the bootstrap coupling condenser.    Figure 7·17 shows a method of introducing this correction term, which is generated by $R_4$ and $C_6$.    The diode across $R_4$ is required to insure proper initial conditions.

Although the presence of a cathode follower in each of these bootstrap circuits seems to provide an excellent output terminal for the sawtooth wave, it must be remembered that the cathode wave may lag slightly behind the grid wave if the rise of the sawtooth wave is sufficiently rapid.    The result appears as a delay at the start of the cathode wave.    If a fast start is required, the output waveform must be taken directly from the charging condenser.



Fig. 4·46.—Common charging condenser for positive and negative sawtooth waves.

In many applications a push-pull sawtooth wave is required.    When conditions permit the use of a simple generator and duplication is not too expensive, the push-pull signal may be obtained by independent generation of positive and negative waves.    Some simplification of the switching problem may be achieved by using a single charging condenser for generating both signals, as is illustrated in Fig. 4·46.

Alternatively, a single-ended signal of small amplitude might be produced and applied to the input terminal of a phase-splitting amplifier. The "floating-paraphase" circuit of Fig. 4·47 is widely used for this purpose and is satisfactory for all but the most steeply rising waves. Another common phase splitter, which has the load resistor divided between the plate and cathode circuits, is particularly applicable to the bootstrap circuit.    If the supply levels and signal amplitudes are appropriate, a resistor equal to the cathode resistor may be inserted as a plate load of the cathode follower (in Fig. 4·43 or Fig. 4·44) without material
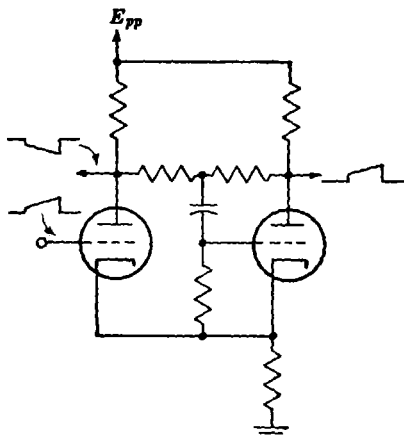


Fig.   4·47.—Floating-paraphase   phase
splitter.
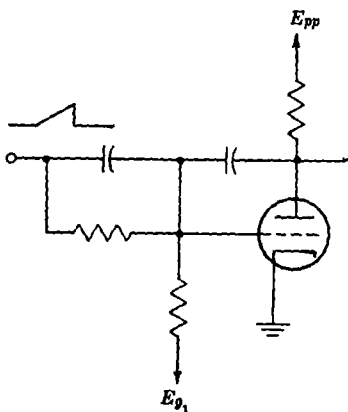
Fig.   4·48.—Sawtooth   inverter   with
feedback.

effect on the cathode signal.    The push-pull output signal is then taken from the plate and cathode of this tube.

A third method first generates a single-ended signal of large enough amplitude to serve as one of the output signals.    The other signal is derived from the first, which is attenuated and applied to the input terminal of an inverting amplifier.    The amplifier used here must have a very linear response which is most easily obtained by means of negative voltage feedback.    Figure 4·48 shows an example in which the feedback channel is part of the attenuating network.

**4·7. Automatic-shutoff Circuits.**—Some displays require a sawtooth wave of constant amplitude which has a number of different slopes to be selected by means of a switch.    This waveform may be obtained by combining a rectangular-wave generator and a sawtooth generator as shown in Fig. 4·49.    The switch that selects the constants for the sawtooth circuit must also select appropriate time-constant components for the rectangular-wave generator so that its output wave will terminate

just as the sawtooth wave reaches the required amplitude.  Several close-tolerance components and probably a few trimming resistors are therefore required.  Crosstalk difficulties are also increased by the sharp-edged waves carried by the switch leads.

If the display requires that the slope of the sawtooth wave vary continuously between certain limits, new complications arise.  Although it is very easy to vary both the slope of the sawtooth wave and the time



Fig. 4.49.—Combination of rectangular-wave and sawtooth generators.

constant of the rectangular-wave generator by means of potentiometers, it is far from simple to design a single control coupling these two potentiometers so as to maintain the required relationship between slope and time constant.

A better method of terminating the sawtooth wave is to employ an "automatic shutoff" circuit in which the sawtooth wave, or some portion of it, is applied to the input terminal of the shutoff circuit (see Fig. 4·50).  When the sawtooth signal reaches the required amplitude, the shutoff circuit causes a transition of the rectangular-wave generator.  The rectangular wave then closes the switch tube and causes the sawtooth wave to return to the quiescent level.

For the sake of brevity in the following discussion the two conditions of the rectangular-wave generator will be called "*A*" and "*B*".  The circuit is in Condition *B* while the sawtooth wave develops, and it is in Condition *A* during the return time and the quiescent period.

Its use in an automatic-shutoff circuit places the following special requirements on the rectangular-wave generator:
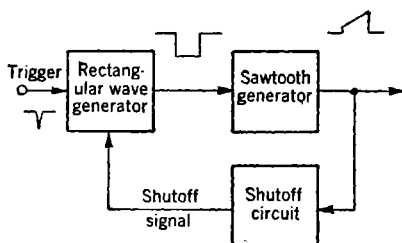


Fig. 4·50.—Alternative combination providing automatic shutoff.

1. In Condition *A* it should be stable so that its operation is not too dependent on repetition frequency.

2. The transition to Condition *B* should be followed by a rapid recovery to a state that permits the circuit to respond to the shutoff signal.  Once this state is attained no major change should take place for a time longer than the duration of the longest sawtooth wave required.

3. The circuit must eventually return to Condition *A* even though the shutoff signal should fail to arrive.  This requirement is partic-

ularly important if a condenser coupling exists anywhere in the loop. In the transient conditions associated with turning on the power, the rectangular-wave generator may be forced into Condition $B$ with the coupling condenser so charged that no shutoff signal will be generated. The return provision gives assurance that the circuit will not stall.

The "scale-of-two" circuit (Fig. 4·24) meets these requirements very well except for the one requiring eventual return to Condition $A$. However, it is only necessary to apply the initiating trigger to both tubes of the circuit to remedy this defect. Then, if the circuit should stall in Condition $B$, the first input trigger to arrive sends it back to Condition $A$ where it remains until the next trigger starts it off correctly. Thus only one cycle of operation is lost.

The flip-flop circuit is imperfect for use in an automatic-shutoff circuit in that conditions do not remain constant during the time it is in Condition $B$. Figure 4·51$a$ shows the waveform on the grid of $V_1$ of Fig. 4·23. Initially the grid is driven far negative, and then it moves slowly positive. At $t'$ only



Fig. 4·51.—Grid waves of various flip-flop circuits.

a very large signal on this grid will cause a transition, but at $t''$ a small signal is sufficient. Some improvement results from applying only a portion of the plate signal to this grid and making the grid time constant very long. The result is the wave shown in Fig. 4·51$b$. Here the signals required at $t'$ and $t''$ are nearly equal, but the loop gain has been reduced by the reduction ratio of the plate signal. A superior circuit, which produces the grid waveform of Fig. 4·51$c$, may be obtained by connecting a diode to the grid as shown in Fig. 4·52. Although the entire plate signal is applied to the grid, its negative excursion is stopped by the diode at a level slightly below the cutoff level for $V_1$. The grid time constant is made very long so that the grid of $V_1$ will remain essentially at the diode level until the shutoff signal arrives. The response of the circuit to the shutoff signal is both excellent and uniform. Since the grid voltage is limited in one direction by grid current in $V_1$ and in the other direction by diode current in $V_2$, $R_1$ is not necessary to the operation of the circuit. It is included simply to insure eventual return to Condition $A$.
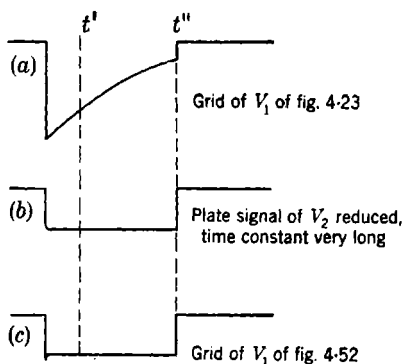
The multivibrator circuit needs the same refinement as the flip-flop circuit. In addition, its ability to operate without an input trigger rules it out for some applications.

The numerous devices that have been used to generate the shutoff signal fall into two classes. The first class involves the formation of a shutoff trigger that is applied to the rectangular-wave generator in the normal fashion. The second requires the introduction of a disturbance into the rectangular-wave generator. This disturbance increases steadily until a point of instability is reached and a transition occurs.

Some of the many circuits capable of forming a trigger pulse from a sawtooth wave have been discussed in earlier sections. For example, a blocking oscillator normally biased beyond cutoff may be used, provided that the sawtooth wave has a slope greater than the minimum value required to activate the blocking oscillator. Also a flopover circuit (Fig. 4·25) might be used with the sawtooth wave applied to the controlling grid. The output will be a rectangular wave from which a trigger pulse may be obtained by differentiation.

The second method requires more detailed treatment since no satisfactory circuits have yet been discussed. The specific problem is assumed to be the attainment of a transition of the flip-flop circuit of Fig. 4·52 without generating a trigger to do this.
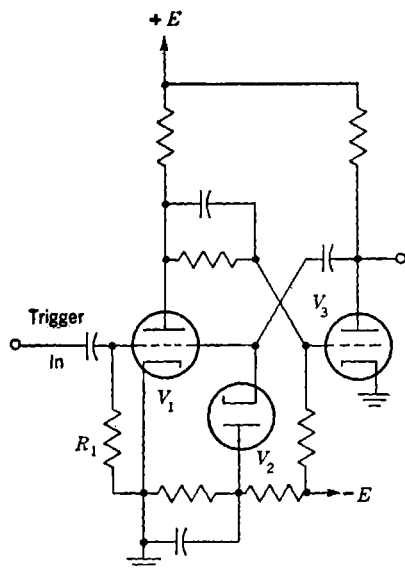


Fig. 4·52.—Improved flip-flop circuit for use with automatic shutoff.

It must be remembered that $V_1$ is biased beyond cutoff, and that $V_3$ is at zero bias while the sawtooth voltage is developing. Thus the transition condition may be reached by causing positive movement of the grid of $V_1$ or negative movement of the grid of $V_3$. Because of the cross coupling both ways, equivalent effects are produced by driving the plate of $V_1$ negative, or the plate of $V_2$ positive. A transition can be produced by applying an appropriate signal to any one of these four points. The means of application must not inhibit the transition; that is, if the grid of $V_1$ is forced positive by a slow signal, it must be free to move upward

much more rapidly once the transition starts.   The coupling must also not interfere with the initial transition from Condition $A$ to Condition $B$.

Figure 4·53 shows a number of one-tube circuits, any one of which might be added to Fig. 4·52 as indicated with satisfactory results.   In each case the added tube is biased so that it does not conduct until the sawtooth wave reaches a certain critical amplitude.

The diode circuits place some load on the source of the signal and so cannot always be used.   The pentode is very useful if the amplitude of the signal is small since the pentode can be operated with high gain and sharp cutoff.

Any of these circuits causes some disturbance at the electrode to which it is coupled (and perhaps elsewhere), prior to the transition. If this electrode provides an output signal, the preliminary disturbance may cause undesirable effects in the associated circuit.   Thus it is preferable to take output signals, particularly the one that operates the clamping circuit, from points in the circuit which are not affected until the transition takes place.   If the clamping tube starts to conduct before the transition takes place,



Fig. 4·53.—Various circuits for introducing shutoff signal to flip-flop circuit of Fig. 4·52.

increase of the sawtooth voltage will stop and the transition may not occur.

If the sawtooth signal must be directly coupled to the shutoff circuit, some adjustment of the supply levels of the various circuits will be required.   The use of a resistance divider, such as that from the plate of $V_1$ to the grid of $V_3$ in Fig. 4·52, may be helpful, but care must be taken that the frequency response of the divider be uniform to avoid variation in the amplitude of the sawtooth wave.   In most cases the voltage levels can be dealt with by coupling the sawtooth wave in through a condenser and d-c restoring it to an appropriate level.

Occasionally, in a particular set of circumstances, a very simple feedback connection will provide automatic shutoff.   Figure 4·54 shows an example of this sort.   The operation becomes obvious once the conditions on the voltage at the point $X$ are stated.   During the quiescent period of the sawtooth wave, this potential must be low enough to allow the scale-of-two circuit to operate in a normal fashion.   When the
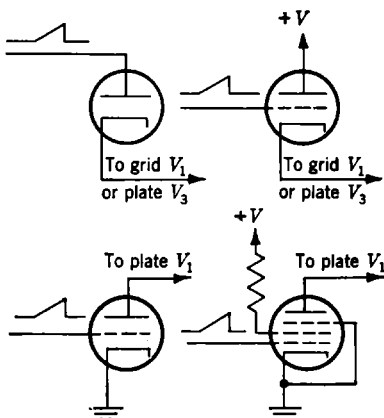
initiating trigger pulse[1] arrives, $V_1$ is cut off and its grid settles down to its stable level. The sawtooth voltage then develops and causes an increase in the voltage at $X$. The signal at $X$ must be great enough eventually to push the grid of $V_1$ into the conducting region, and thus cause the circuit to return to the initial condition. The high-frequency coupling from the cathode of $V_4$ to the grid of $V_1$ is very poor so that the amplitude of the sawtooth wave will not be independent of slope.

There are various special circuits that perform the same function as the automatic-shutoff circuit, but which have the sawtooth generator and the rectangular-wave generator so interlocked that it is very difficult
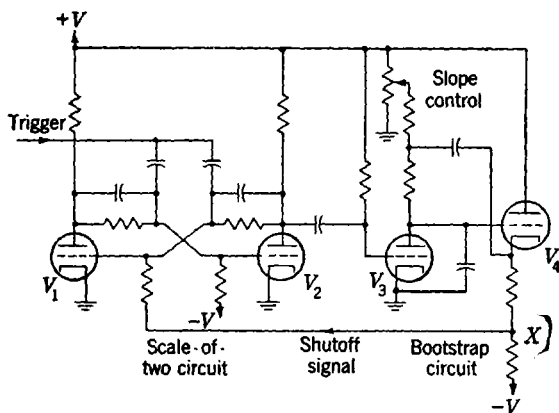


FIG. 4·54.—Automatic shutoff circuit using scale-of-two and bootstrap circuits.

to make any general statements about them. One group of these circuits makes use of the fact that the derivative of a sawtooth wave is a rectangular wave. An input trigger pulse opens a switch tube momentarily and permits the sawtooth wave to start. The derivative of the sawtooth wave is then coupled back to the switch tube in such a way as to hold it open as long as the sawtooth voltage continues to increase. When the rise of the sawtooth wave is stopped, either by saturation of some tube or by conduction in a diode added for the purpose, the derivative becomes zero and the switch tube closes.

A type used more often, which is particularly suited to the generation of a high-duty-ratio sawtooth wave, uses a gas-filled tube as a self-activated switch. Such a tube does not conduct until the potential across it reaches a critical level called the "striking potential." At this point, a gaseous discharge starts in the tube and continues until either

---

[1] Note that the input trigger is also coupled to the grid of $V_1$ to insure proper starting of the circuit.

the plate-to-cathode potential becomes negative, or the current through the tube is reduced below a critical level that quenches the discharge. During the discharge the internal impedance of the tube is very low,[1] and any capacity that may be across the tube can therefore be very rapidly discharged.  A small series resistor must always be used with the tube to prevent damage due to excessive discharge current.

Although a simple neon tube can be used as a switch tube, it is more common to use a tetrode type which has a control grid that determines the striking potential.   The presence of ions of both signs in the discharge means that the grid will draw a large current regardless of the potential to which it is returned unless a large series resistance is used to limit this current.

If the high duty ratios of which the gas tube is capable are to be realized, the associated sawtooth generator must be one that has a short recovery time.   Thus, some of the bootstrap circuits are not appropriate.   Figure 4·55 shows the gas-filled tube as used with a resistance charging circuit.   The output waveform is shown in the accompanying sketch.   The maximum slope of the sawtooth wave in this and similar circuits is
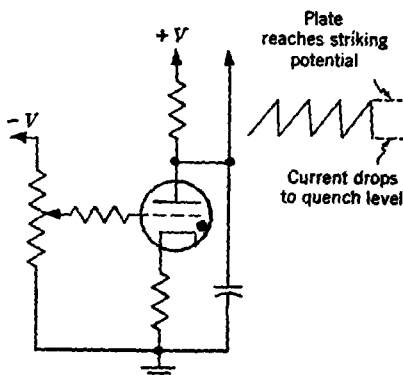


Fig. 4·55.—Gas-filled tube sawtooth generator.

determined by the deionization time of the tube.   If the plate rises too rapidly, the discharge will be reestablished before the striking level is reached because of the presence of residual ions from the preceding discharge.

The output wave may be synchronized at frequencies higher than the free-running frequency by introducing pulses on either the grid or cathode.   If the plate voltage is near the striking potential, a small change in bias will initiate the discharge.

**4·8   Video Amplifiers.**—The term "video amplifier," which originated in television work, has been extended to cover any device that is designed to amplify signals of transient character and to preserve their waveforms with reasonable fidelity.   In addition to the usual amplifier requirements a relatively large pass band with a fairly constant time delay for all frequencies within the band is desired.

[1] If the gas-filled tube is represented by a switch, the additional circuit elements required are a battery of about 10 volts output and a series resistance of less than 100 ohms.

*Nature of the Video Signal.*—The individual signals obtained at the detector stage in a radar receiver have a width dependent on the radar-modulator pulse length (a typical value is 1 $\mu$sec) and amplitudes dependent on the strengths of the individual target echoes. A nearby target gives such a strong echo that some stage in the video amplifier following the detector is likely to reach saturation, whereas many distant and small targets give echoes so small that their signal amplitudes are less than that of the "noise" generated in the receiver.

When such signals are displayed on an A-scope,[1] they appear as in Fig. 1·3b, where the strong signals have reached a limiting value and a number of weak signals barely are visible in the noise. For detection on the A-scope of the weakest possible signal, the receiver gain may be increased until the noise peaks are about 0.5 mm high. Greater amplitude than this possibly may make observation less tiring, but will reveal no additional signals. It is more or less immaterial whether strong signals are limited, provided that the limiting does not paralyze the video amplifier after reception of a strong signal.

In an intensity-modulated display[2] such as the PPI or the B-scope, the signal intensity controls the cathode-ray-tube beam current. If the receiver gain is adjusted so that weak signals and noise "specks" are just visible on the tube face, then strong signals will be so large that the grid-cathode voltage in the CRT will be driven above zero bias. It is impossible to maintain beam-focusing over such a wide range of signal level. In addition to this difficulty, excessively bright areas in the display interfere greatly with the perception of weak signals. Hence signal-limiting can be used to advantage in these displays. Extensive measurements show that the greatest amount of information can be obtained from the intensity-modulated display if the limiting value is set at about two or three times the average noise peak amplitude and if the cathode-grid bias is set so that, without video signals, the sweep is just visible on the tube face. The video gain is adjusted to give a reasonable brightness at which limited signals do not cause defocusing of the beam. Under these conditions, noise shows as a general speckled background, but because of the nonlinear grid-bias–beam-current characteristic of the cathode ray tube (Fig. 2·27), signals slightly greater

[1] Time, or range, is plotted horizontally and signal amplitude vertically, with a cathode-ray-tube beam of constant intensity.

[2] The position of the cathode-ray-tube beam is synchronized so as to represent the position in space of the transmitted radar pulse (actually half the distance to the pulse, to allow for echo return time) and the presence of a target at any given point is indicated by using the signal from the target to increase the cathode-ray-beam current from a nominal zero value.

than noise are preferentially amplified, and because of the superproportional response of the phosphor[1] to repeated signals, real signals give brighter response than random noise fluctuations.

Linearity of the video amplifier is required in very few display systems, and then only if it is desired to measure signal strength on a deflection-modulated display. Hence for most of the circuits shown in this section and in Appendix E, no attempt has been made to produce an output voltage proportional to the input voltage.

*Frequency-response Characteristics.*—In order that the output signal may rise to full amplitude in the duration of the input signal, it is required that the minimum bandwidth be $1/T$ Mc/sec, where $T$ $\mu$sec is the width of the input pulse. Another consideration in the determination of bandwidth is that the spread of the pulse along the time base imposes a limitation on the resolution of adjacent pulses, which would seem to call for very wide bandwidth in the amplifier since the pulses may occur very close together. However, two spots on the cathode-ray tube whose center-to-center distance is less than the spot diameter will overlap and at some point will become indistinguishable. This factor also limits the resolution and determines a value of amplifier bandwidth beyond which no gain in resolution is realized. This upper limit for a display using a time-base sweep is given by

$$\text{Bandwidth in Mc/sec} = \frac{L}{3St},$$

where $S$ is the spot size in cm and $L$ is the spot displacement in cm taking place in $t$ $\mu$sec. For any display system, two or three times the larger of these two values of bandwidth should be used as a basis for design of the video amplifier.

Unfortunately the mathematical and computing tools now available require that many of the problems of the multistage amplifier be handled from a steady-state viewpoint to determine the characteristics of the complete amplifier. The result may then be used to predict in a qualitative way the transient behavior of the device.

For a brief summary of the methods and results of steady-state analysis, consider the resistance-coupled pentode amplifier stage shown in Fig. 4·56. Over a limited range of frequencies it is permissible to assume the impedance of all bypass and coupling condensers to be zero and that of all shunt capacities to ground to be infinite. In this region the gain of the amplifier, called the midfrequency gain, is $\mathcal{G}_m = g_m R_L$.

At higher frequencies the impedance of the shunt capacities in parallel with $R_L$ causes the gain to drop off as frequency increases. The high-

---

[1] The CRT screen is usually long persistent, P-7 or P-14. See Chap. 18.

frequency limit of the amplifier is arbitrarily defined as the frequency, $f_h$, for which the voltage gain drops to $0.707\mathcal{G}_m$. This value corresponds to a reduction in power gain of 50 per cent or 3 db from the midfrequency value. Very often $f_h$ is called the "bandwidth" of the amplifier.

At lower frequencies the cathode and screen bypass condensers have appreciable impedance, which has a degenerative effect on the amplifier gain. Also, because of the impedance of the coupling condenser, the signal applied to the next stage is less than that appearing at the plate of the amplifier. These various effects together cause a reduction in gain
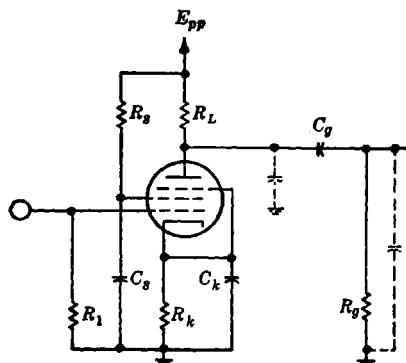


Fig. 4·56.—Resistance-coupled pentode amplifier stage. $R_L \ll R_g$; $R_L \ll$ plate impedance of tube.

with decreasing frequency. The low-frequency limit of the amplifier is similarly defined as the frequency, $f_l$, for which the voltage gain reduces to $0.707\mathcal{G}_m$.

The frequency range between $f_l$ and $f_h$ is called the "pass band" of the amplifier and is one of the important quantities that determine the transient response of the amplifier. Good transient response often requires a pass band that extends from about a hundred cycles per second to several megacycles per second.

The phase-shift characteristic of the amplifier is the second important factor in transient response. Over a region of constant gain the angular phase shift in a resistance-coupled amplifier is proportional to frequency. There is, therefore, equal time delay for all input frequencies within the band. For frequencies in the end regions where the gain is changing rapidly, the phase shift is not proportional to frequency and the time delay is not constant. The output signal may therefore be distorted.

The subsequent discussion of the method of improving the transient response of a circuit will be simplified by stating the definition of some

terms that measure the quality of the transient response.    Figure 4·57 shows first a step function that is applied to the input terminal of a video amplifier.    The following figures show output waves that might result. For each the time scale has been selected to emphasize the characteristic illustrated by the figure.

1. Rise Time.    To avoid the ambiguity of deciding just when a wave starts to rise and when it stops rising, the rise time is taken to be the time in which the signal rises from 10 per cent to 90 per cent of its final amplitude. Over this range the slope is usually steep enough to permit reasonably accurate measurements.    For the amplifier of Fig. 4·56 the rise time is related to $f_h$ by the equation

$$\text{Rise time} = \frac{0.35}{f_h}. \qquad (6)$$

Equation (6) holds approximately for any resistance-coupled amplifier.

2. Delay.    This term needs no definition.    Delay does little harm, except that it must be taken into account if time relationships are important.    Its magnitude is determined by the slope of the phase-shift–frequency curve of the amplifier.



FIG.   4·57.—Terms defining transient response of a video amplifier.

3. Overshoot.    This quantity is a measure of the maximum amount by which the output signal momentarily exceeds its nominal amplitude.    It is usually stated as a percentage of the nominal amplitude.    Overshoot is related to nonlinearity of the phase-shift–frequency characteristic.    The simple amplifier of Fig. 4·56 will not produce overshoot.

4. Droop.    The droop is a measure of the failure of a circuit to maintain the flatness of the top of an input signal.    It corresponds to inadequate low-frequency gain.    A common specification restricts the droop to a maximum value of 10 per cent of the nominal signal amplitude.    In this case the quality of the amplifier may be indicated by the time required for the droop to reach this value.
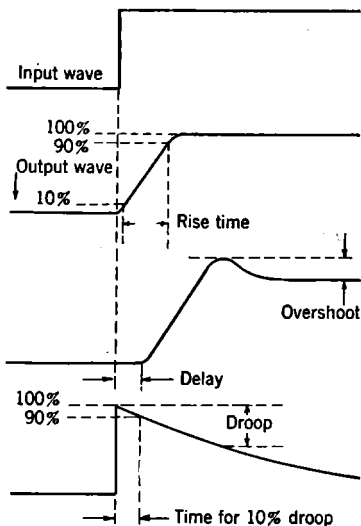
The steady-state response of an amplifier can be improved by certain modifications of the basic circuit of Fig. 4·56. The success of any alteration should be judged in the light of its effect on rise time, overshoot, or droop.

*Low-frequency Response.*—There are several ways of extending the pass band to lower frequencies. Each one amounts to an increase, either actual or effective, in the time constant of a bypass or coupling circuit, that serves to reduce the droop caused by that circuit. The obvious approach would be that of simply increasing $C_k$, $C_s$, and $C_g$ until the droop is as small as need be. However, more practical means are available in each case.

The effect of $C_k$ might be eliminated by removing it completely. This step results in a reduced value of $G_m$ but is sometimes worth while. Also it is possible to ground the cathode and to supply grid bias from a negative supply. This change introduces a greater dependence of gain on tube characteristics than was present, because self-bias tends to minimize the dependence of gain on tube characteristics.

The simple approach may be very successful when applied to $C_s$ because the effective resistance across it is usually large enough to give a sufficiently long time constant with practical values of $C_s$. For extreme cases the screen might be returned directly to a regulated-supply-voltage source, or its voltage might be stabilized by a voltage-regulator tube.
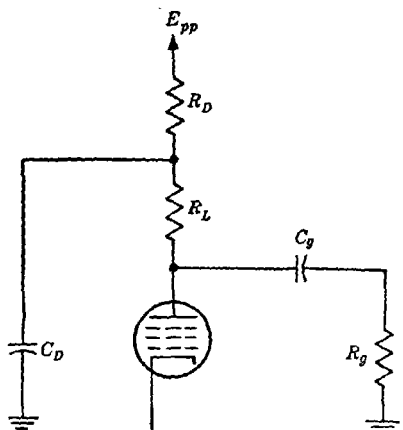


Fig. 4·58.—Plate decoupling used to compensate for droop produced by $C_gR_g$. $R_D \ll R_g$; $R_L \ll R_D$; $C_DR_D = C_gR_g$.

The time constant $C_gR_g$ could be eliminated by means of direct coupling using a resistance divider between the plate and some negative voltage, but the amplifier then becomes extremely sensitive to bias voltage. Direct coupling is to be avoided unless flat response down to zero frequency must be provided. If $R_g$ has been made as large as the tube specifications will permit, a larger value of $C_g$ is required to increase the grid time constant. The maximum value of $C_g$ is determined by the shunt capacity associated with large condensers, which will limit the high-frequency response of the amplifier. Up to perhaps 0.01 $\mu$f the increase in shunt capacity is not serious because this and smaller values are available in the form of "postage-stamp" mica condensers.

A larger effective grid time constant is obtained by adding the decoupling elements shown in Fig. 4·58 to the plate circuit of the amplifier.    If

$$C_D \cdot \frac{R_L R_D}{R_L + R_D} = C_g R_g, \tag{7}$$

the steady-state response is equivalent to that provided by a grid time constant of $C_D R_D$.    A slightly better transient response is obtained by making

$$C_D R_L = C_g R_g. \tag{8}$$

If $R_D \gg R_L$ the two conditions are equivalent.    This form of compensation functions by providing a plate signal that increases in amplitude for some time after the initial step at a rate that precisely cancels the droop due to the grid time constant. Should the grid of the next stage be d-c restored, the cancellation provided depends upon duty ratio and this dependence leads to uncertain operation.

The plate-decoupling elements are sometimes used to compensate for droop due to cathode or screen effects although this use is perhaps less satisfactory.  Since the conditions for compensation depend upon certain tube parameters, the effectiveness of the compensation may change when tubes are replaced.   No

Fig. 4·59.—Effective amplifier circuit at high frequencies.

such effect arises when plate decoupling is used to compensate for grid time constant.

*High-frequency Response.*—Improvement of the high-frequency response involves very different considerations.  Figure 4·59 is a diagram of the same pentode amplifier with all the low-frequency elements deleted since they have little effect in this discussion.  The high-frequency response is limited by the various shunt capacities in the plate circuit.  These capacities are represented by $C_t$, which consists of the output capacity of the amplifier, the input capacity of the next stage, socket capacities, and wiring capacities.  By careful construction the wiring capacities can be reduced to a very small value that may be considered constant for any simple amplifier.  If the next stage uses the same type of tube, then $C_t$ can be considered as a parameter of the tube
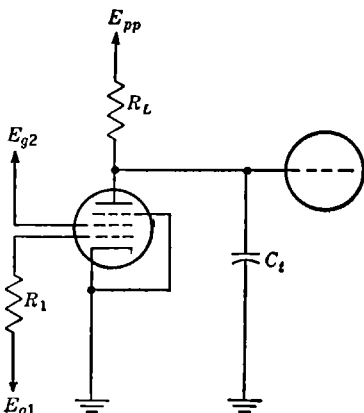
type equal to input capacity plus output capacity plus about 10 $\mu\mu f$[1] to allow for sockets and wiring.

For an amplifier with resistance load $f_h$ is the frequency for which the impedance of the shunt capacity equals the load resistance. That is,

$$f_h = \frac{1}{2\pi C_t R_L}. \tag{9}$$

Since $\mathsf{G}_m = g_m R_L$ this equation can be written

$$\mathsf{G}_m f_h = \frac{g_m}{2\pi C_t} \cdot K, \tag{10}$$

with $K$, in this case, equal to one.

Equation (10) shows that the product of bandwidth and midfrequency gain is a constant for any given type of tube and may be considered to be a figure of merit for tubes used in this way. It has the dimensions of frequency and is equal to the value of $f_h$ obtained by making the midfrequency gain of the stage unity. Table 4·1 lists the figure of merit for

TABLE 4·1.—FIGURE OF MERIT OF PENTODES COMMONLY USED IN VIDEO AMPLIFIERS

| Tube type | $\dfrac{g_m}{2\pi C_t}$ (Mc/sec) |
|-----------|-------------|
| 6AC7 | 57.3 |
| 6AG7 | 58.3 |
| 6AK5 | 66.2 |
| 6AG5 | 56.9 |

several commonly used tube types. These values represent excellent amplifier construction and will be very difficult to realize in practice.

Higher gain-bandwidth products may be obtained with other methods of coupling. The constant $K$ in Eq. (10) is a factor of relative quality for various coupling networks and, as stated, its value is unity for simple resistance coupling. Increasing the value of $K$ requires the plate impedance of the amplifier to diminish less rapidly as frequency increases. This requirement can be met by means of shunt peaking, which consists of inserting a small inductance in series with $R_L$, as in Fig. 4·60. Then for higher frequencies as the reactance of the shunt capacity decreases, the total impedance of the $R$-$L$ branch increases, tending to reduce the variation of total plate impedance.

If

$$L = mC_t R_L^2, \tag{11}$$

then $m$ is a parameter that determines the performance of the circuit. Critical damping of the plate circuit corresponds to $m = 0.25$. This is the largest value of $m$ for which the transient response will have no

---

[1] For miniature tube types this figure is about 6 $\mu\mu f$.

overshoot. For this case $K = 1.41$. For $m = 0.4$ the value of $K$ is 1.70 and the overshoot is only 2.5 per cent. This value is not objectionable in a single stage, but the cumulative effect of several stages with this value of peaking may be troublesome.

Many types of two- and four-terminal network have been used to provide high-frequency compensation.[1] However, the improved performance with a more complex network must be balanced against the fact that components must be held to somewhat closer tolerances and malfunction is more difficult to correct.

If $\mathcal{G}_m$ is not changed as the value of $K$ is increased, the rise time is reduced in inverse proportion to the factor by which $K$ is increased.

Another, and very simple, form of high-frequency compensation is available if the cathode bias resistor is not bypassed. The addition of a very small condenser $C_k$ across $R_k$ tends to increase the gain of the stage at higher frequencies and partially to counteract the effects of lower plate impedance. No overshoot will be produced if

$$C_k R_k = C_t R_L. \tag{12}$$



FIG. 4·60.—Shunt peaking.

When a video amplifier contains several stages of the type described above, the overall performance is inferior to that obtained with a single stage since the total gain is the product of the gains for each stage. The over-all characteristics of the amplifier may be computed by combining the individual stage-gain–frequency curves, but in special cases the over-all characteristics may be determined more easily. For example, if the droop in each stage is small (approximately 1 per cent for the longest pulse transmitted), then the over-all droop is very nearly equal to the sum of the individual values, provided that the total does not exceed 10 per cent. At high frequencies the over-all gain-bandwidth product for $n$ identical shunt-peaked stages (up to $n = 10$) may be determined from Table 4·2 which lists an effective $K$ for stages having $m = 0$ (that is, no peaking), $m = 0.25$, and $m = 0.4$. The over-all gain-bandwidth product is then equal to the $n$th power of the product of the figure of merit and the appropriate effective $K$.

Thus far only one type of video amplifier stage, which is intended to provide a certain voltage gain and pass band when working into the relatively high impedance of another grid circuit, has been considered.
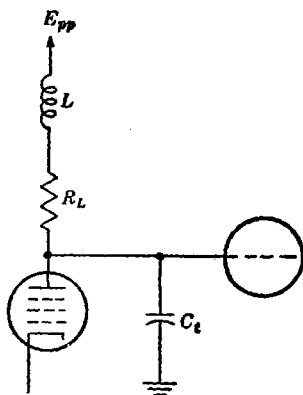
[1] See Fig. 1·26 of Vol. 18 of the Radiation Laboratory Series.

A complete video amplifier ordinarily consists of one or more stages of this sort followed by an output stage. In most cases the output stage drives a much lower impedance and so is designed differently.

TABLE 4·2.—EQUIVALENT $K$ FOR $n$ SHUNT-PEAKED STAGES

| Number of stages | Value of $m$ (peaking parameter) | | |
|---|---|---|---|
| | 0 | 0.25 | 0.4 |
| 1 | 1 | 1.41 | 1.70 |
| 2 | 0.64 | 0.94 | 1.30 |
| 3 | 0.51 | 0.76 | 1.13 |
| 4 | 0.44 | 0.64 | 1.03 |
| 5 | 0.39 | 0.57 | 0.95 |
| 6 | 0.35 | 0.52 | 0.89 |
| 7 | 0.32 | 0.48 | 0.84 |
| 8 | 0.30 | 0.45 | 0.80 |
| 9 | 0.28 | 0.42 | 0.76 |
| 10 | 0.27 | 0.40 | 0.74 |

*Video Output Amplifiers.*—Often the video signal must be transmitted over a considerable distance. To eliminate reflections a concentric line terminated in its characteristic impedance is used. The output stage must be capable of generating a signal of the required amplitude across this impedance, which may be approximately 50 or 100 ohms. The prime requisite of the tube in this case is its ability to deliver high peak currents. Capacity is of less importance here because the load resistance is small.

Although a power amplifier to drive a cable can be designed with the load in the plate circuit, it is generally better to use a cathode follower because (1) its output impedance is low and therefore can be matched with the load impedance; and (2) a high d-c potential is not applied to the cable. Most video signals are unidirectional (that is, the signal consists of a temporary departure in a given direction from a fixed base voltage) and have a duty ratio somewhat less than 50 per cent. For transmitting a positive-going signal average power may be reduced by use of a cathode follower.

If the signal is transmitted at large amplitude the peak current required may necessitate the use of several driver tubes in parallel. Therefore it is economical to transmit video signals at low level[1] and to provide additional amplification at the receiving end of the line.

A second form of output stage is needed to apply video signals to a cathode-ray tube. An output signal of 30 to 100 volts in amplitude may

[1] Designers of radar equipment have recently attempted to standardize on 2-volt positive video voltage for transmission over lines.

be required, but the voltage gain is not very important since preceding stages can compensate for any lack of gain in the output stage. One type of output stage, which should be used whenever possible, has the load in the plate circuit very close to the cathode-ray tube so that the total capacity on the output terminal is little greater than that on the plate of an intermediate stage in the amplifier. The general design considerations are then the same as those stated for the intermediate stage except for the greater signal amplitude. Actually the transition from one type to the other is very gradual in this case and it may well be that the last two or even three stages of a particular amplifier should be considered as large-amplitude stages.

The maximum plate signal $E_m$ that can be produced in the midfrequency region with a given amplifier is $E_m = \Delta I \cdot R_L$, where $\Delta I$ is the maximum change in plate current that can be produced under the existing operating conditions. Substituting this relation into Eq. (9), which defines $f_h$ for this case also, gives

$$E_m f_h = \frac{\Delta I}{2\pi C_t}. \tag{13}$$

The product $E_m f_h$, denoted by $K_1$, can be used as the figure of merit for large-amplitude stages. The value of $K_1$ depends not only on the tube type, but also on the conditions of operation since $\Delta I$ may have many values according to the bias of the stage. However, there are three values of $\Delta I$ that cover most situations.

1. If the video signal is unidirectional and the output signal is negative, the initial bias may be nearly at cutoff. Then $\Delta I$ is the maximum peak current allowed by the duty ratio of the video signal.
2. If the video signal is unidirectional and the output signal is positive, the tube will be conducting in the absence of signal. Then $\Delta I$ equals the maximum continuous current the tube can conduct.
3. If the output signal has equal amplitudes in both directions, $\Delta I$ lies between one-half and one times the maximum continuous current.

Table 4·3 shows the values of $K_1$ for common tube types operating under Condition 2, which involves the fewest assumptions on the nature of the video signal. For these calculations the total capacity was assumed to be 30 $\mu\mu$f larger than the output capacity of the tube.

Clearly Condition 1 provides the maximum value of $\Delta I$ and hence of $K_1$. On this basis it is highly profitable to apply unidirectional video signals to the cathode-ray tube as negative signals. To obtain optimum results an accurate bias in the region of cutoff must be provided for the output stage and the bias level must not shift with change in duty ratio

or signal amplitude.    Thus it is often necessary to provide d-c restoration for the grid of the output stage.

Similarly the d-c level of the signal applied to the cathode-ray tube is likely to be critical.    If it is not possible to couple the cathode-ray tube directly to the plate of the output stage, d-c restoration at the cathode-ray tube is advisable and the additional stray capacity of the restorer must be included in the design calculations.

For this particular situation the addition of a cathode follower between output stage and cathode-ray tube would have little, if any,
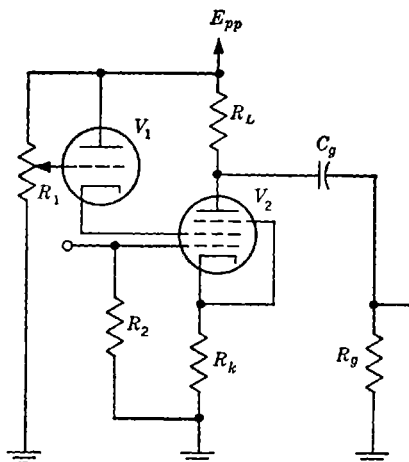


Fig. 4·61.—Gain controlled by screen voltage.

advantage since the output stage would still drive about the same total capacity and would be required to supply a somewhat larger signal. However, there are other situations in which the output stage is not adjacent to the cathode-ray tube and the stray capacity is large with respect to the output capacity of the amplifier.    Insertion of a cathode follower to drive the stray capacity may then be advantageous.    For this case it seems preferable to operate the output stage in Condition 2 if the video signal is unidirectional, and thus permit the cathode follower to operate under more favorable conditions.

TABLE 4·3.—FIGURE OF MERIT FOR LARGE-AMPLITUDE STAGES

| Tube type | $K_1$(Mc/sec) |
|---|---|
| 6AK5 | 48 |
| 6AC7 | 68 |
| 6AG7 | 170 |
| 6V6GT/G | 212 |
| 6L6G | 318 |

*Amplifier Gain Control.*—For controlling the gain of the amplifier the following general methods are in common use.

1. The characteristics of the vacuum tubes can be controlled over a certain range by changing the operating voltages. Figure 4·61 shows an amplifier stage $V_2$ with the screen voltage supplied by a cathode follower $V_1$ whose output is determined by $R_1$. It is practical to vary the gain by a factor of 2 by this method. For greater variation several stages may be similarly treated.

2. If negative feedback is used, variation of the feedback signal controls the gain. Figure 4·62 shows a variable cathode resistor that changes the gain without altering the bias on the stage. The maximum value of $R_2$ is limited by the stray capacitance on the cathode which will eventually cause overcompensation at high frequencies. The gain of the stage can usually be varied by a factor of 5.

FIG. 4·62.—Gain controlled by cathode degeneration.

3. The signal produced at any point in the circuit can be attenuated. Figure 4·63 shows a step attenuator for which attenuation is
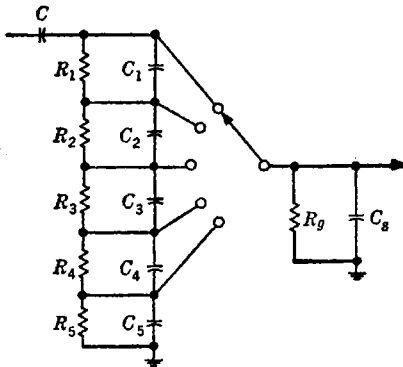
FIG. 4·63.—Compensated step attenuator, $C_s$ is total stray capacity on arm of switch.

independent of frequency if $R_g C_s = R_1 C_1 = R_2 C_2$, etc. Unlimited control of gain is provided by this method. Figure 4·64 shows a low-resistance potentiometer used as the load resistor of an amplifier stage. This method also provides a wide variation

in gain.   A potentiometer of higher resistance can sometimes be used if it is compensated as shown in Fig. 4·65.   If the condenser $C_1$ is equal to the stray capacity on the arm of the potentiometer, a marked improvement in frequency response is provided over a certain range of adjustment.   The compensation is not good as the arm approaches ground potential.
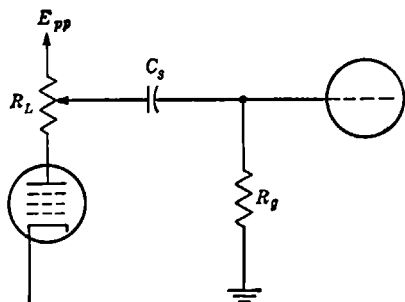


FIG. 4·64.—Low-resistance potentiometer as plate load.

The gain control may be intended to vary the output amplitude, to permit variation of the input signal, or to provide a precise gain despite a considerable variation of tube characteristics from the nominal values.   The point at which the gain control is inserted depends upon its function, but it should usually be so placed that it is able to prevent overloading of any stage in the presence of the largest input signal expected.

This statement does not apply if the overdrive is intentional as it might be if a "limited" output signal is required.   A limited output signal is one that increases in amplitude with increasing input signal amplitude up to a certain critical level and after that remains constant. Limiting is usually accomplished by setting the bias on a stage that receives a negative signal so that the tube is cut off by an input signal of the critical amplitude.   A larger input signal then produces no additional effect at the output terminal.



FIG. 4·65.—Compensated potentiometer.

*General Remarks.*—For some applications it is important that the gain of the amplifier be independent of signal amplitude.   In general this independence will not be obtained because of nonlinear vacuum-tube characteristics.   By means of negative feedback it is possible virtually to eliminate these vacuum-tube effects.   The use of an unbypassed cathode resistor constitutes the simplest form of negative feedback. Other practical methods create a feedback loop that includes one, two, or three stages of the amplifier.   Inclusion of more than three stages in the feedback loop may make it difficult to prevent the amplifier from oscillating.

The voltage supply line provides a possible coupling between various
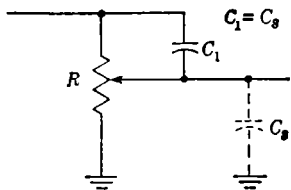
stages of the amplifier. If the impedance of this line to ground is not extremely low at all frequencies in the pass band of the amplifier a regenerative feedback coupling through the power supply may exist. A good electronic regulator or a very large output condenser in the power supply will prevent oscillation at low and medium frequencies. At very high frequencies the inductance of the supply lines may cause trouble unless additional bypass condensers, which need not be large, are added at the video amplifier.

Switches are sometimes required in a video amplifier circuit, either to alter the characteristics of the circuit or to shift the input or output terminals to a different circuit. The switching mechanism must be so designed that the generation of large switching transients is avoided (since several seconds may be required for some amplifiers to return to normal) and that the switch and its leads shall not provide a regenerative feedback loop.

**4·9. Blanking.**—There are various circumstances that make it necessary to prevent the display of information during a portion of the cycle. A signal known as the "blanking gate," or with equal justice as the "intensifying gate," may be used to do this by increasing the bias of the cathode-ray tube during the "off" portion of the cycle so that a maximum-amplitude signal does not cause current to flow. In general it is necessary that the regions of transition be made as narrow as possible, and that the blanking wave be absolutely flat during the "on" portion of the cycle. The first requirement is satisfied by using a rectangular wave from some form of multivibrator, either directly or through a buffer stage. The second is met by taking the wave from some circuit element in which the current goes to zero during the "on" time of the display since this value is easy to maintain at a constant level. To preserve the flatness of the wave thus obtained, the coupling to the cathode-ray tube should be direct, or else a d-c restorer that functions during the "on" time should be used. Occasionally a long-time-constant a-c coupling will be sufficient. The amplitude of the blanking wave for grid or cathode blanking must be slightly greater than the amplitude of the maximum applied signal.

In the case of the magnetic tube it is common practice to apply the blanking signal to the second grid. The amplitude required is much greater since the second grid must be at a potential of several hundred volts during the "on" time, and must be at or slightly below the level of the cathode during the "off" time. Because of the difficulty of generating a 500-volt rectangular wave, a compromise with good focus is usually made by accepting an amplitude of perhaps 250 volts. Although this method is widely used in the examples cited later, it is probably not the best method.

In special cases blanking may be done by gating the information generator or some intervening amplifier stage, but this method will not be discussed here.

**4·10. Signal Mixing.**—The signals that are to be applied as intensity modulation may include the primary information of the display (such as radar video signals), a blanking signal, and various of the indices and markers whose generation is discussed in Chap. 6. In all cases the method of mixing the signals must be such as to meet the individual bandwidth requirements.

This superposition of signals may be either additive or nonadditive. In the first case the coincidence of two signals produces a net signal equal to the sum of the two. This method is required for mixing the blanking wave and the primary information. In the second case the net signal is equal to the larger one, or nearly so.

A ready-made facility for additive mixing exists in the various intensity-controlling electrodes of the cathode-ray tube. If the number of signals does not exceed the number of such electrodes, one signal may be applied to each electrode and each signal may therefore be treated completely independently. The first and second grids present very high input impedances and can be driven by almost any signal generator. However, the input impedance of the cathode is about 50,000 to 100,000 ohms, and the driving circuit must have an output impedance low enough to handle this load in parallel with any external loads that may be present.

Additional mixing provision is required if (1) the number of signals exceeds the number of electrodes, (2) nonadditive mixing of any combination of signals is required, (3) polarities of the signals cannot be fitted to the available electrodes, or (4) several signals are generated at the same location remote from the display and transmission would be simplified by mixing them at the source.

Network-mixing is highly economical only if the signals to be mixed are widely different in frequency characteristics so that a circuit like that of Fig. 4·66a may be used. If the two signals should be a series of 1-μsec pulses and a low-frequency sine wave, the values of $R$ and $C$ can be so chosen that each signal is almost unaffected by the existence of the other.

If the signals have about the same frequency characteristics, and therefore require the circuits of Fig. 4·66b and c, then the mixing elements will constitute attenuators that increase the amplitude required of the signal generator. Also the generators must have output impedances low enough to prevent the first signal from affecting the operation of the second generator and vice versa.

More versatile mixing is obtained by the use of vacuum tubes. Figure 4·67 shows various vacuum-tube mixers. The first circuit is appropriate when an amplifier stage is already present. In addition to

the normal signal to the grid, another from a low-impedance source is applied to the cathode.  Occasionally a signal may be mixed in on the screen as well.  The output signal in this case is the amplified grid or cathode signal modulated by the screen signal.

The second circuit may be extended by adding parallel tubes to accept any number of high- or low-impedance signals.  The output signal is
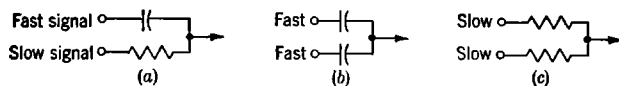


FIG. 4·66.—Network-mixing.

almost perfectly additive if pentodes are used but is only partially so with triodes.  If the input signals are negative, the various biases may be adjusted to give independent amplitude limiting for each signal.

The third circuit is also able to mix many signals and can be arranged to be very nearly nonadditive.

In any particular display it will probably be possible to introduce all necessary signals in more than one way.  The choice of the method to be used will be determined by the answers to such questions as the following: Is any circuit already present from which a suitable blanking signal may
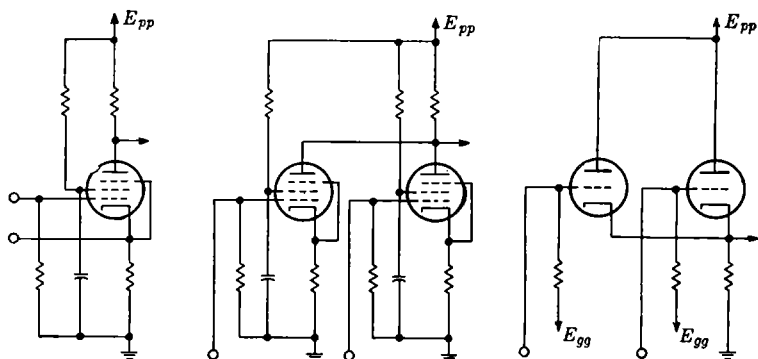


FIG. 4·67.—Circuits for signal-mixing.

be taken?  Is the polarity of one of the input signals irrevocably fixed? Is the amplitude provided on the borderline so that no attenuation is tolerable?  Does one of the alternatives provide a simpler transmission problem?  All this simply indicates that no decision can be reached until the entire display problem has been outlined.

**4·11. Power-supply Considerations.**—In the design of a display system and its attendant rectifier and regulator circuits, considerable effort should be expended on the reduction of total power consumed to the minimum value that will permit the circuit to perform as required.

In some cases the expense of providing the input power is important, as is also the size, weight, and cost of high-power components. Even when these considerations are not significant there remains the problem of dissipating the heat produced. Some components fail at high temperatures whereas others exhibit marked variation in characteristics. Higher input power increases the difficulty of holding the temperature at acceptable levels.

It should not be necessary to present design information for low-voltage rectifier and regulator circuits since this subject is a familiar one, but it might be profitable to consider some of the possible steps that will reduce input power.

First, and most obvious, is the reduction of the power consumed in each circuit. The reduction of input current is naturally considered by any designer, but often little thought is given to the supply voltage. From force of habit the supply level is set at 250 or 300 volts and no attention is paid to the fact that many of the circuits involved will operate as well at 100 or 150 volts.

Second is the choice of voltage levels to be provided. If the total current required is small a single supply is most economical, but at higher currents several levels, each providing the correct voltage for a group of circuits, should be considered. A calculation of the total input power involved in each method may clearly decide the issue. If the two powers are about equal the decision can be based on relative convenience.

Third is the avoidance of regulated voltage supplies, or the reduction of current taken from them. The mere fact that some portion of the current at a particular voltage level must be regulated does not always justify the regulation of the total current supplied at that level. Here again a calculation of input power will decide whether the addition of an extra rectifier is less expensive than the larger regulator tubes required to supply the entire current. This decision is complicated by the fact that less filtering is needed if the output voltage is to be regulated. The possible saving in weight must also be considered.

Fourth is the combination of a regulated and an unregulated level with the same rectifier.

Fifth is the use of an independent negative supply level to provide bias voltages. Often the power used to provide cathode bias from an existing positive supply is greater than the total power input to a low-voltage negative supply. In any event the greater flexibility provided by a negative supply justifies its inclusion in all but the smallest of display systems.

A sixth point is sometimes applicable. It may be that some circuits use very little current during one portion of the cycle, but during the remainder they use a current that is a very large portion of the total

taken from a particular supply level. The average current may then vary by some large factor as the duty ratio changes, and this variation will alter the voltage level of the supply. An electronic regulator capable of supplying the very large peak-current requirements of these circuits may be so costly that a cheaper solution is the addition of another tube that equalizes the current drain throughout the cycle by conducting when the original circuits shut off and vice versa. Often this tube can also be utilized to perform some other useful function in the system, such as to provide a blanking signal.

**4·12. High-voltage Power Supplies for Cathode-ray Tubes.**—A relatively high d-c voltage is needed to accelerate the electron beam of a cathode-ray tube. Because the power supply from which this voltage is obtained is required to supply only a low current, its design presents problems different from those of other vacuum-tube power supplies, particularly when close control of the output voltage is required.

The required voltages vary from less than 1 kv for the smallest tubes up to 50 kv for tubes of the projection type and those employing extremely fast writing speeds. Of more common interest are the electrostatic cathode-ray tubes requiring from 1.5 to 3 kv, electrostatic tubes with post-deflection acceleration requiring 4 to 5 kv, and magnetic deflection tubes requiring from 4 to about 10 kv.

The beam current required for a cathode-ray tube is low and does not vary so much between tube types as does the accelerating voltage. The design of a high-voltage supply must allow for maximum load currents, for leakage currents (particularly where extensive cabling is required between the supply and the cathode-ray tube), and for bleeder or voltage-divider current.

A bleeder is generally required to discharge the filter condensers of magnetic-tube supplies. In electrostatic-tube supplies a voltage divider also provides bias, anode, and focus-electrode potentials. For this purpose its impedance must be low enough to prevent excessive shift of these potentials with beam-current modulation because part of the beam is attracted to these electrodes. From 1 to 2 ma of current is required for the electrostatic-tube supply, but 500 $\mu$a plus bleeder current generally is ample for the magnetic tube.

Because accelerating-potential supplies are used in conjunction with and generally placed close to low-voltage circuits, particular attention must be paid to safety. Five milliamperes is generally recognized as the maximum allowable continuous current for safety against human fatality. For a condenser from which the initial short-circuit current may be high but the discharge time limited, an energy storage above one joule is considered dangerous. Careful shielding of high-voltage components helps but is never a complete safeguard. A more desirable solution lies in

control of the output characteristic of the supply so that the short-circuit current is limited to a low value.

*Unregulated A-c Power-line Supplies.*—Unregulated rectifier circuits include half-wave, full-wave, bridge, half- and full-wave voltage doublers,
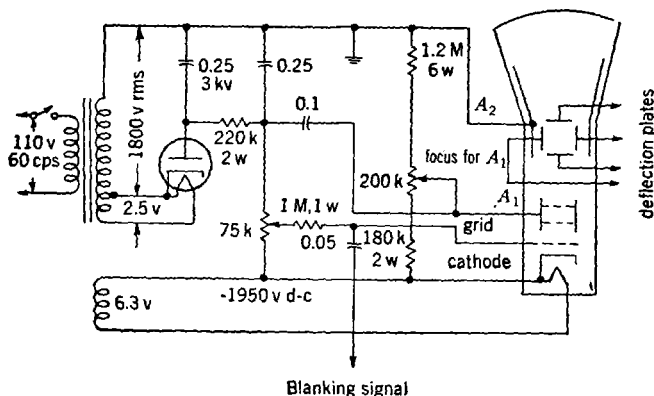


**Blanking signal**

FIG. 4·68.—Typical negative 2-kv supply for electrostatic cathode-ray tube. The divider constants given are only approximate as they depend upon the tube type employed.

voltage triplers, quadruplers, etc. Considerable recent literature has appeared on the characteristics of voltage-multiplier circuits.[1] Of these circuits, the half-wave rectifier and the full-wave voltage doubler have had the widest application. Voltage multipliers occasionally find use



FIG. 4·69.—Typical positive-voltage supply for magnetic tubes, using half-wave rectifier and two-section *RC*-filter.

where elimination of the high-voltage transformer can be effected. Figures 4·68, 4·69, and 4·70 show some of the unregulated supplies most commonly used in display systems.

The popularity of the half-wave circuit is due to its simplicity, especially when a vacuum-tube rectifier is used. The complication introduced by additional rectifier tubes and particularly that due to insulation of their heater transformer windings, discourages the use of multipliers. Metallic (selenium) contact rectifiers, which have recently become available for this type of application, eliminate this difficulty, and future use of such circuits will undoubtedly increase.

[1] See O. H. Schade, "Analysis of Rectifier Operation," *Proc. I.R.E.* (July, 1943), also *Proc. I.R.E.* (July, 1945).

For the same conditions of output voltage, current, regulation, and ripple, the full-wave doubler is the most efficient of the rectifier circuits. It requires half the transformer-secondary voltage and half the filter capacity needed with a half-wave rectifier. Although two rectifier elements are required, their peak inverse voltages are halved. The use of miniature rectifier tubes also makes the application of the voltage doubler more favorable.

Table 4·4 lists the characteristics of the more common rectifier tubes suitable for high-voltage applications.

Selenium rectifiers suitable for high-voltage, high-temperature applications are available with peak inverse-voltage ratings of 1, 2, 3, and 4 kv (see Fig. 4·71) and with a current rating of 5 ma at 55°C or 1 ma at 90°C. They have an extremely nonlinear conduction characteristic and also exhibit leakage in the inverse direction. Figure 4·72 shows these charac-



Fig. 4·70.—Cathode-ray-tube supply of +6 kv using selenium rectifiers in full-wave doublers and with +700-volt tap for $A_1$ or $G_2$ supply.

teristics for a 4-kv rectifier. The curves represent maximum values of inverse-current leakage and forward-voltage drop and are similar to those obtained for lower-voltage units, provided that the voltage scale factor is changed to correspond to the required inverse-voltage ratings.

TABLE 4·4.—CHARACTERISTICS OF HIGH-VOLTAGE RECTIFIER TUBES

| Type | Filament | | Inverse peak voltage, kv | Peak anode current, ma | Average d-c output current, ma | Resistance, 10 ma current | Base |
|------|------|-----|------|------|------|------|------|
| | Volts | Amp | | | | | |
| 2X2 | 2.5 | 1.75 | 12.5 | 45 | 7.5 | 7.5k | 4 pin |
| 2V3 | 2.5 | 5.0 | 16.5 | 12.0 | 2.0 | | 4 pin |
| 8016 | 1.25 | 0.2 | 10.0 | 7.5 | 2.0 | 20 | Octal |
| 1Z2 | 1.5 | 0.3 | 20.0 | 10.0 | 2.0 | 7.5 | Miniature 7 pin |
| 3B24 | 2.5–5 | 2.5 | 20.0 | 150–300 | 30–60 | 4–2 | 4 pin |

The selenium rectifiers illustrated in Fig. 4·71 are hermetically sealed in $\frac{1}{2}$-in. glass tubes and may be operated in oil. They have long life, particularly at low temperatures. These factors make it feasible to seal the entire high-voltage unit in an oil-filled container.

Since ripple voltage is of higher frequency than variations due to bad

voltage regulation, it is in general much more noticeable. It must therefore be held to closer limits than is necessary for regulation variations.
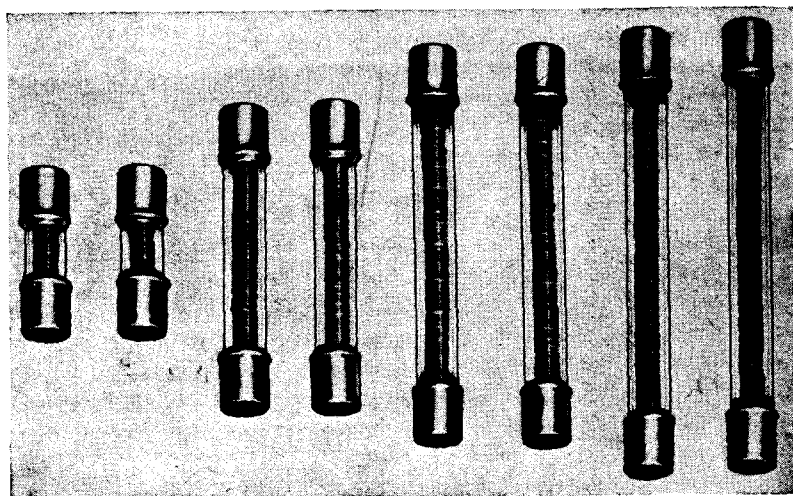


Fig. 4·71.—Selenium rectifiers for cathode-ray-tube applications.

For most magnetic- and electrostatic-tube applications, 0.5 per cent peak-to-peak ripple is a reasonable design figure, and 0.1 per cent represents the point of diminishing returns.
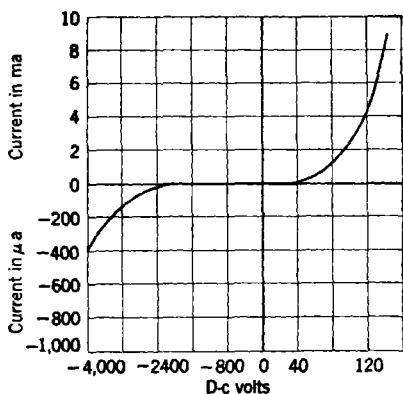


Fig. 4·72.—Selenium-rectifier characteristic, 110-disk-assembly high-temperature type.

Although ripple voltages are ordinarily thought of as originating from the a-c input voltage, they may also be caused by variations in output current. In general, if beam-current variations are of much higher frequency than those of the a-c input voltage, their effect will be negligible. If they are lower in frequency, they may be the predominating factor in the filter design.

Most filter-circuit requirements are met either by a single condenser or by a two-section $RC$-filter. The single condenser is applicable at relatively high frequencies (several thousand cycles per second) and the two-section filter is preferable at power-line and aircraft (400 cps) supply frequencies. Inductances are seldom used because the

high impedance required (250,000 ohms at 60 cps is 500 henrys) makes them expensive and bulky. Figures 4·73$a$, $b$, $c$, and $d$ show these filters with half-wave and with full-wave-doubler rectifier circuits.

A simple formula that expresses peak-to-peak ripple voltage for the single-condenser filter and is applicable to either half-wave or voltage-doubler circuits may be developed as follows:

If $p$ is defined as the ratio of discharge time per cycle to the period $(1/f)$, then the discharge time is $t = p/f$. The percentage ripple voltage is $\mathcal{E}_r = \Delta V(100)/E_o$, where $\Delta V$ is the discharge of condenser $C_1$ in time $t$. But $\Delta V = It/C_1$ and $I = E_o/R_L$. Then, $\Delta V = E_o p/R_L C_1 f$, and

$$\Delta V/E_o = p/fT_1$$

where $T_1$ is the filter time constant. Therefore,

$$\mathcal{E}_r = \frac{100p}{fT_1}. \tag{14}$$

For most purposes, the factor $p$ may be either assumed equal to unity or estimated.

Stray-capacity coupling due to $C_s$ as shown in Fig. 4·73$a$ and $b$ introduces a ripple component. In Fig. 4·73$b$ $C_s$ is the effective stray capacity of the transformer secondary to ground, and the ripple component is given by $\mathcal{E}_c = 100C_s/(C_1 + C_s)$. [It is $\mathcal{E}_c = 200C_s/(C_1 + C_s)$ for Fig. 4·73$a$.] It may be balanced out by applying a condenser $C_s'$ as shown in Fig. 4·73$b$ for the voltage-doubler circuit.

An equation for the ripple of a two-section filter may be developed in a manner similar to the derivation of Eq. (14). It is

$$\mathcal{E}_r = \frac{T_1}{T_2}\left[\frac{1}{T_1 f(1 - e^{-\frac{1}{ft}})} + \ln fT_1\,(1 - e^{-\frac{1}{ft}}) - 1\right], \tag{15}$$

where $T_1 = R_o C_1$ and $T_2 = C_2 R_L$. This development neglects the rectifier conduction time and, in calculating input voltage, assumes the output voltage to be constant.

Variations of output voltage of the high-voltage supply may be due either to input-voltage or to load-current variations. The amount of regulation required for this voltage depends on the amount of pattern distortion, variation in intensity, and defocusing that can be tolerated.

For an electrostatic tube, proportional variations of the high-voltage, focus, and deflection potentials result in no defocusing[1] but do change the beam intensity and deflection factor of the tube. The latter effect is undesirable when the tube is used as a direct measuring device. The

---

[1] See Sec. 2·8 for focus-voltage characteristics.

variations will be proportional if all potentials are derived from the same primary source and if the time constants of high-voltage and low-voltage supplies are identical.

For a magnetic tube the voltages across the focus and deflection coils must vary as the square root of the accelerating potential in order to maintain focus and pattern size. The deflection is, then, less sensitive to changes in accelerating potential but, at the same time, it is more
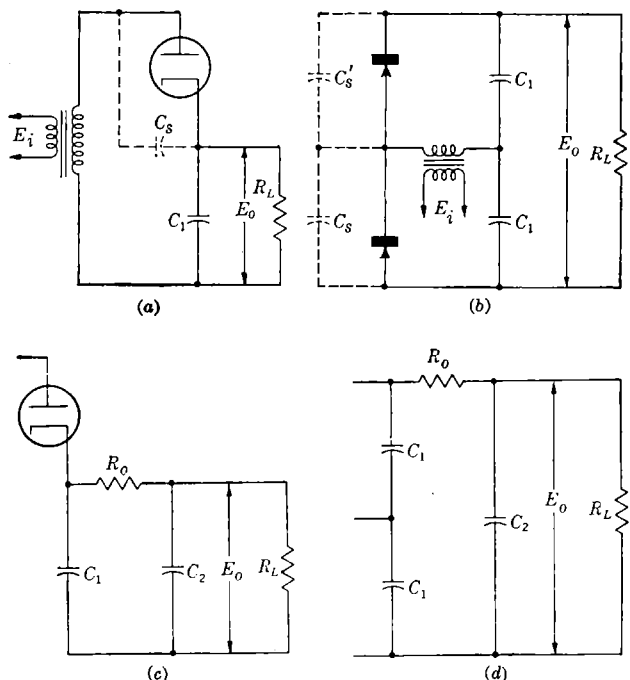


Fig. 4·73.—(a) Half-wave rectifier; (b) voltage doubler; (c) two-section filter on half-wave rectifier; (d) two-section filter on voltage doubler.

difficult to correct for variations in voltage than in the case of the electrostatic tube. For normal power-line variations of $\pm 10$ per cent, correction of the focus voltage as outlined in Sec. 3·4 or complete regulation of all voltages is desirable. The latter method is to be preferred.

The voltage-regulation factor $k_v$ of a circuit is here defined as the ratio of the per cent change in output voltage to the corresponding per cent change in input voltage. Denoting percentage changes by $\mathcal{E}_o$ and $\mathcal{E}_i$ respectively,

$$\mathcal{E}_o = k_v \mathcal{E}_i = \frac{\Delta E_o}{\Delta E_i} \cdot \frac{E_i}{E_o} \cdot \mathcal{E}_i. \tag{16}$$

The load regulation factor $k_L$ of a supply is defined as the percentage change in output voltage per unit change in load current.   Thus

$$k_L = \frac{100\,\Delta E_o}{E_o\,\Delta I_L} = \frac{100 R_S}{E_o}, \tag{17}$$

where $R_S$ is the internal resistance and $E_o$ the open-circuit output voltage of the supply.   The percentage change in output voltage $\mathcal{E}_L$ for a given change in load current $\Delta I_L$ is then given by

$$\mathcal{E}_L = k_L\,\Delta I_L = \frac{100 R_S\,\Delta I_L}{E_o}. \tag{18}$$

It is convenient to express $k_L$ in per cent per 100 $\mu$a for high-voltage supplies.

Load-regulation requirements range from perhaps as high as 7 to 8 per cent per 100 $\mu$a for applications requiring constant beam current, to as low as 0.1 per cent per 100 $\mu$a.   From the focus standpoint 3 per cent per 100 $\mu$a is tolerable for a magnetic-tube application requiring as much as 200 $\mu$a change in beam current at frequencies too low to be absorbed by the power-supply filter.   The relation between focus (spot size) and accelerating potential is illustrated in Fig. 3·10.   Inspection of this curve indicates that, for a 5FP7 or 7BP7 magnetic tube, a $\pm 3$ per cent change in accelerating potential results in a change in spot size of 12 per cent.

*Regulated Supplies.*—Methods of regulating the input voltage of a-c power-line supplies include the use of a variety of commercially available line regulators that use nonlinear-impedance networks.   Voltage-regulation factors of from about 0.2 to 0.05



Fig. 4·74.—Nonlinear resistance regulator.

are generally achieved by these devices, but load regulation is not provided.   In fact, their use can increase the effective output impedance of the supply, and the output wave shape is so distorted from a sine wave that the output of a peak voltage rectifier is not necessarily held constant by such a device.

Use of a nonlinear element in an output voltage regulator is illustrated in Fig. 4·74 in which $R_T$ is a Thyrite block.   For Thyrite $I = bE^n$ where $b$ is primarily determined by the shape of the material and $n$ is a constant whose value is between 2.5 and 6.   The small improvement in regulation obtained with this circuit seldom justifies its use.

The $\mu$-bridge circuit has been used as a high-voltage regulator but poor load regulation, circuit complexity, and the requirement of a floating
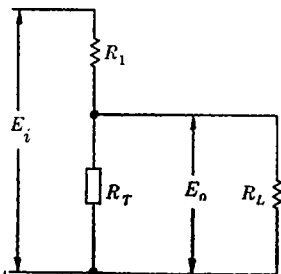
grid-bias power supply make it inferior to the series and shunt regulators for this type of application.

The series and shunt regulators are degenerative circuits in which the change in output voltage is amplified and applied to the circuit in such a manner as to decrease its value. The value of $\Delta E_o$ is obtained by comparing a portion of $E_o$ to a constant source of potential, referred to as the standard, or $E_s$. In most applications requiring regulation of the high voltage, a regulated low-voltage supply is available and is used for $E_s$. Any degree of regulation may be obtained by varying the amplification of $\Delta E_o$. Because of the requirement that the bulk of the regulator
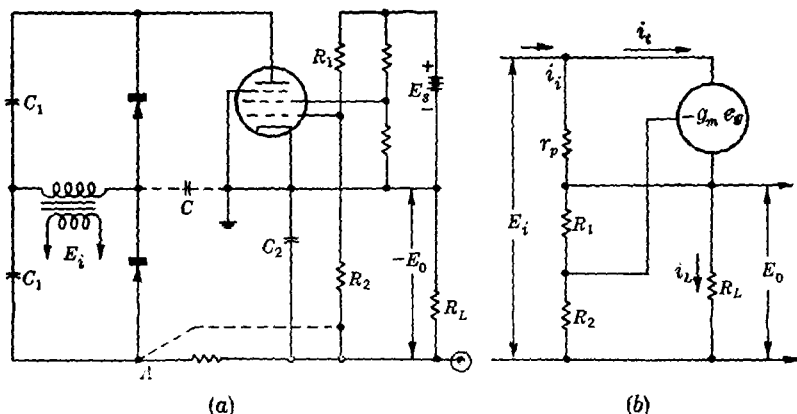


Fig. 4·75.—Series regulator circuit. (a) Actual circuit. (b) Equivalent circuit.

circuit be at or near ground potential, the shunt regulator is applicable only to positive output supplies and the series regulator only to negative supplies.

Figure 4·75a shows the circuit for a series-regulator supply, the equivalent circuit for which is shown in Fig. 4·75b. Choice of the rectifier circuit is arbitrary.

In practice the apparent resistance of the tube $(R_1 + R_2)/R_1 g_m$ is small compared to the other terms comprising the internal impedance of the regulator and is therefore the primary term in determining the output impedance. The factor $R_1/(R_1 + R_2)$ is very nearly equal to $E_s/(E_o + E_s)$; hence regulation is improved by choosing $E_s$ as large as possible as well as by employing a tube with a high amplification factor.

In a typical design using a 6SJ7 for the regulator tube, $E_o = 1800$ volts, $E_1 = 2250$ volts, $E_s = +300$ volts, $R_L = 1$ megohm, $R_1 = 1$ megohm, $R_1 + R_2 \approx 7$ megohm, $r_p = 0.5$ megohms, and $g_m \approx 0.35$ ma/volt at $E_{sc} = 100$ volts. The apparent resistance of the tube is 20,000 ohms, and hence $R_s$, the internal resistance of the regulator circuit,

is very little less than this. The load regulation $k_L$ as defined in Eq. (17) is then 0.11 per cent/100 $\mu a$. The voltage regulation factor $k_v$ is 0.05.

Stray-capacity coupling of the transformer secondary to ground (as shown by $C$ in Fig. 4·75a) may sometimes cause excessive ripple. In such cases it may be desirable to connect $R_2$ to $A$ (as shown dotted) rather than to the output terminal, thus effectively introducing an additional filter stage but increasing the output impedance.

Safety is achieved by adjusting the screen voltage so that the tube draws grid current when the cathode current is about three milliamperes. An excessive load may then cause the tube to stop regulating, and the output voltage may therefore go rapidly to zero without an appreciable increase in output current. For this application a tube designed for full
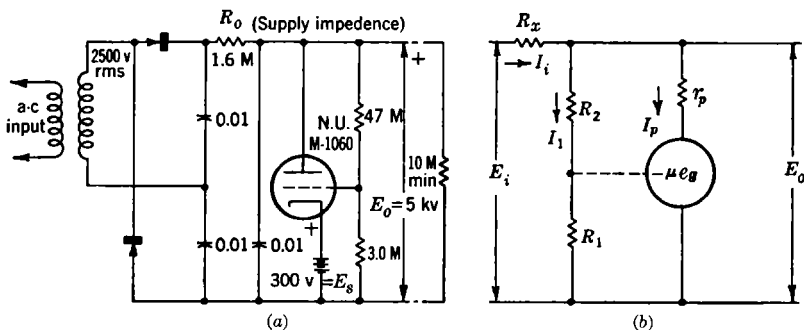


FIG. 4·76.—Shunt-regulator circuit. (a) Actual circuit. (b) Equivalent circuit.

output voltage across its plate would be desirable. Plate voltage restrictions on receiver-type tubes limit their application to supplies of not more than about 1700 volts negative.

The shunt regulator (Fig. 4·76a and b) comprises a tube essentially in parallel with the load. The input voltage is coupled to this tube through a series resistor $R_o$ and the internal resistance of the rectifier circuit. The sum of these two resistances is indicated by $R_x$ in Fig. 4·76b. An increase in output voltage causes an amplified increase in regulator tube current. This current flowing through $R_x$ produces a voltage drop that tends to compensate for the change in input voltage, thus stabilizing the output voltage.

The plate of the shunt regulator tube must operate at full output voltage and the amplification factor must be rather high ($\mu = 500$–$650$). A high-voltage, low-power triode[1] still in the developmental stage at this writing has satisfactory electrical characteristics. They are tabulated in Table 4·5, and a plate-voltage, plate-current characteristic is shown in

---

[1] National Union No. M-1060.

Fig. 4·77. Life-test performance of this tube is as yet unsatisfactory for commercial production and some tubes exhibit instability due to excessive grid current.

TABLE 4·5.—ELECTRICAL CHARACTERISTICS OF NATIONAL UNION No. M-1060 TRIODE

| | |
|---|---|
| Max. plate voltage............................... | 10 kv |
| Max. plate power.................................. | 10 w |
| Amplification factor.............................. | 500–650 (approx.) |
| Transconductance................................. | 500–650 $\mu$mho |
| Plate resistance.................................. | 1 megohm |
| Filament voltage.................................. | 6.3 v |
| Filament current.................................. | 0.3 amp |

In practice $R_x$ and $R_1 + R_2$ shown in the equivalent circuit (Fig. 4·76b) are very large compared to the reflected resistance of the regulator tube. Hence, the internal impedance and regulation of the circuit are determined primarily by $g_m$ and by $E_s/E_o$. It is desirable therefore to choose $g_m$ and $E_s$ as large as possible. A minimum current of about 200 $\mu$a is required through the tube in order to keep $g_m$ at a reasonably high value. This current and the power rating of the tube limit the range of regulation. However, for output voltages of 5 to 6 kv the range is ample to control variations of $\pm 10$ per cent in the line voltage for normal loads. Measurements with a number of experimental tubes in the circuit shown, with a load current of 500 $\mu$a, gave values of load regulation of from 0.052 to 0.064 per cent/100 $\mu$a and values of voltage regulation of from 0.026 to 0.032.



FIG. 4·77.—National Union M-1060 high-voltage triode characteristics.

Because it is often desirable to have freedom of choice of the operating frequency or of the type of operation, tube oscillators or pulse generators are particularly useful for supplying power to high-voltage rectifiers. Thus the use of operating frequencies high compared to power-line frequencies results in smaller, more compact, and lighter filter and transformer components. This is an advantage when space and weight are at a premium as in aircraft. Actually an increase in operating frequency does not result in a linear decrease in component size because of the requirement for output-current as well as input-voltage filtering. It is also true of components in general, since high-voltage-insulation requirements soon become the major factor in determining the size of the component. Thus, although considerable saving over low-frequency (60 to

400 cps) operation may be obtained, an increase in frequency above several thousand cycles per second does not result in appreciable further saving in weight or space.

Tube-oscillator high-voltage generators are divided into four classifications, depending on the type of operation: (1) r-f oscillators operating at several hundred kc/sec and using an air-core transformer; (2) a-f oscillators using an iron-core transformer and operating at several kc/sec; (3) pulse or blocking-oscillator generators; and (4) inductance-charging high-voltage generators. The first two types are essentially sine-wave oscillators although most efficient operation is obtained at relatively low $Q$ and large harmonic distortion. The difference between (2) and (3) is primarily one of method of operation since the same circuit may be made to operate either way. With a blocking oscillator, rather sharp voltage pulses of short duration are produced. The generator has very low impedance during the period of operation and does not draw current between pulses. In (4) the high voltage is generated by allowing current to build up in an inductance at low voltage. The current flow is then interrupted and the resultant high inverse voltage is used to charge a filter condenser.

These generators all have rather high load-regulation factors ranging from about 1 to 6 per cent/100 $\mu$a depending on output voltage, etc. They depend for voltage regulation on regulation of their d-c input voltage. When improved load regulation is required, control of the input regulator may be obtained from the high-voltage d-c output.

Radio-frequency oscillators have been used to produce voltages as high as 35 kv. The circuit diagram for a typical 5-kv supply is shown in Fig. 4·78.[1] The transformer comprises two tuned coupled circuits. Optimum load regulation requires that the coupling coefficient $K$ be much greater than $K_c$ for critical coupling, where $K_c = 1/\sqrt{Q_1 Q_2}$. Because $K$ is limited to approximately 0.25 by insulation requirements, this condition must be met by achieving values of $Q_1$ and $Q_2$ of from 10 to 20 under full load conditions. Open-circuit $Q$ values must be much greater than this in order to reduce transformer losses. The output voltage is dependent on the tuning of the input circuit; hence it may be adjusted by means of the primary tank condenser. The grid feedback winding is placed on the opposite side of the secondary or output winding from the primary. Its coupling is therefore principally to the secondary, and the mode of oscillation is determined by the polarity connection of this winding. With the connection as in a conventional single-tuned circuit, best regulation is obtained with operation at the lower-frequency peak. Coupling

[1] For detailed discussion of the theory, method of operation, and design considerations involved in this type of supply see O. H. Schade, "R-f Operated High-voltage Supplies for Cathode-ray Tubes," *Proc. I.R.E.* (April, 1943).

of the grid feedback winding to the primary winding results in an unstable frequency characteristic and cannot be used.

A well-designed r-f supply may have an over-all efficiency (ratio of d-c output to d-c input power) of as high as 50 per cent for an output-voltage drop of 12 per cent at full load. The design involves a compromise between efficiency and load regulation.

An iron-core stepup transformer may be used in a Hartley-oscillator circuit to provide an a-f oscillator high-voltage supply. The transformer
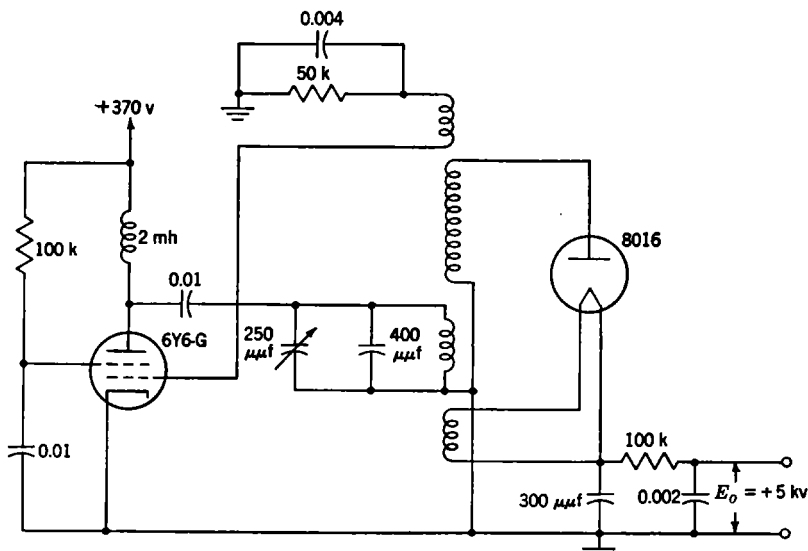


FIG. 4·78.—Cathode-ray-tube supply of the r-f oscillator type.

supplies the necessary tank-circuit inductance of the oscillator circuit. A 6V6 tetrode is satisfactory as a driver tube for producing voltages up to 7 or 8 kv. Typical circuits are shown in Figs. 4·79 and 4·80.

Figure 4·79 is a supply designed for use with a post-acceleration electrostatic tube. It supplies 2 kv and uses 4-kv peak-inverse-voltage selenium-rectifier elements in half-wave rectifier circuits. Polarity of the transformer is such that the oscillator tube and the negative rectifier element conduct at the same portion of the cycle. This arrangement results in best regulation from the negative supply. Since the tube is nonconducting during the positive half cycle, the positive-supply regulation is determined primarily by the tank-circuit impedance and is several times worse than the negative-supply regulation. The negative supply is thus capable of delivering 1 to 1.5 ma to a divider for bias and focus control purposes without undue voltage drop. The only load on the

positive supply is the beam current of the cathode-ray tube and the rectifier leakage current. The leakage current is satisfactory as a means of discharging the filter condenser in applications where the energy storage is considerably below the danger limit. Hence, a bleeder resistor is not provided on the positive supply.

Measured characteristics of the supply shown in Fig. 4·79 are as follows: for an input voltage of 250 volts, the input current varies from 16.1 ma at no load to 25.5 ma for a negative-load current of 1.3 ma and 100-μa positive load; under full-load conditions, output voltages are −1970 volts and +2120 volts; negative regulation is 1.25 per cent per 100 μa and positive regulation is 4 per cent per 100 μa; ripple voltages are
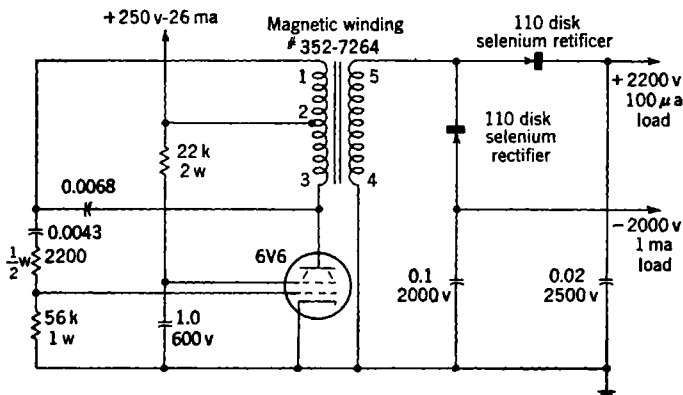


FIG. 4·79.—Audio-frequency voltage supply at ±2 kv.

0.12 per cent for the negative supply (full load) and 0.2 per cent for the positive supply (mostly due to capacitive coupling); the operating frequency is about 2600 cps, and over-all efficiency is 44 per cent. The transformer has a primary (open-circuit) inductance of 0.42 henry and a turns ratio (total primary to secondary) of 7.85. The ratio of grid drive to plate voltage is 1 to 5.

The circuit shown in Fig. 4·80 uses, in a full-wave–doubler circuit, a transformer similar to that used in the circuit of Fig. 4·79. An open-circuit output voltage of 5 kv is obtained for an input voltage of 300 volts. The current requirements are 18.5 ma at zero load to 28 ma at 500-μa load. Regulation over this range is about 3 per cent per 100 μa. Regulation, input current, and efficiency characteristics of this circuit are shown in Fig. 4·81. The regulation for a 60-cps unregulated supply (Fig. 4·69) is shown in comparison.

The single-section filter has a full-load ripple of less than 0.5 per cent. Similar supplies have been built for operation from 4 to 7 kv and from

500 cps to 10 kc/sec with varying degrees of efficiency and regulation. Most typical figures include input current variations from 15 ma at zero
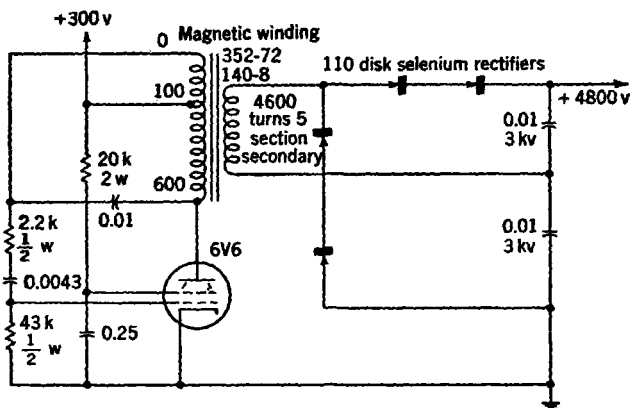


Fig. 4·80.—Audio-frequency voltage supply at 5 kv.

load for the lower voltage units to 35 ma at full load for the higher volt-
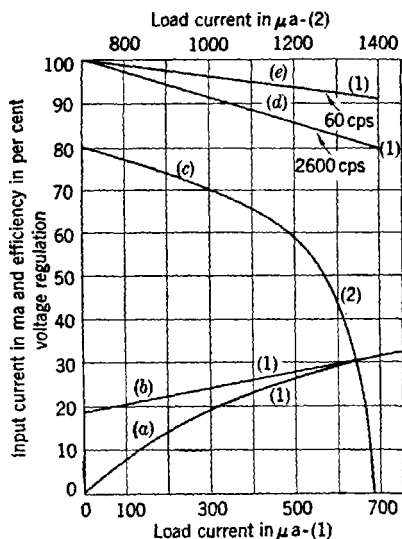


Fig. 4·81.—Characteristics of an audio-frequency oscillator: (a) efficiency; (b) input current; (c) short-circuit characteristic; (d) regulation; (e) for comparison, the regulation of 60-cps unregulated supply is shown.

ages. Regulation figures from 2 per cent per 100 μa to 3.5 per cent per 100 μa are typical. The optimum-frequency design figure for most applications is 3000 cps. The design involves a compromise between good regulation, high efficiency, and small transformer size.

Since the full-wave voltage doubler conducts on both halves of the cycle, regulation is somewhat more dependent on the impedance of the tank circuit than it is in a half-wave circuit. Use of selenium rectifier elements also results in somewhat poorer regulation than is obtained when diodes are used. This difference may amount to from 0.1 per cent per 100 μa to 1 per cent per 100 μa depending on whether the units are operated near their peak

maximum-inverse-voltage rating, and on the amount of current drawn.

The voltage-doubler circuit and selenium rectifiers are useful because of the saving in weight and space achieved although the saving is achieved at the expense of regulation.   Use of the voltage doubler is also effective in increasing the oscillator stability.

Figure 4·82 shows an equivalent circuit diagram of the oscillator supply; $L_p$ and $L_s$ are the primary and secondary leakage inductances, $L_M$ is the mutual inductance, $C_s$ the secondary stray capacitance, $N$ the turns ratio and $C_p$ the tank-circuit plus primary stray capacitance. From this diagram it is evident that the circuit has two possible modes of operation.   In the first, $L_p$, $L_M$, and $C_p$ form the resonant circuit.   In the second the resonant circuit is composed of $C_p$, $C_s$, and the primary and secondary leakage inductance, essentially a capacitive-divider arrange-
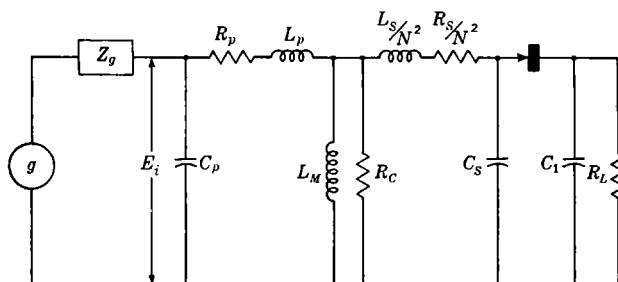


Fig. 4·82.—Equivalent circuit diagram of the a-f oscillator, showing two possible resonant frequencies.

ment in which $E_{sec} = E_i C_p / N C_s$.   Although the circuit is not normally operative in the second or high-frequency mode, it may be so excited by application of a shock such as results when the high-voltage output rectifier conducts under heavy load conditions.   The shift in frequency is accompanied by an abrupt change in output voltage, and oscillation may continue at this frequency when the load is removed.

High-frequency oscillations may be prevented by reducing $C_s$, $L_p$, and $L_s$, and by increasing $C_p$; or by obtaining the grid voltage in such a fashion that the circuit is degenerative at the higher frequency.   The first method results in a wider separation of the two frequencies, higher output voltage and lower $Q$ at the high frequency.   For the purpose of lowering the leakage reactance and effective $C_s$, and for high efficiency and small size at relatively high operating frequencies, use of high-permeability low-loss transformer materials is indicated.   The value of $C_s$ may also be decreased by sectionalizing the secondary winding, as illustrated by the power-supply design of Fig. 4·86.

Degeneration at the higher frequency may be achieved by placing the grid-excitation winding on the outside of the secondary winding and by using capacitive coupling from the secondary to the grid winding.   A

circuit that used a combination of the latter methods and conventional transformer construction had good efficiency and regulation; it required 21 to 31 ma of input current at 300 volts for a 0 to 500-μa load at 7 kv open-circuit output voltage and had a regulation factor of 2.3 per cent per 100 μa. Excellent stability has been achieved in circuits using both methods, for it is then possible to short-circuit the output terminal to ground without exciting the circuit to high-frequency oscillation.

Operation of the blocking-oscillator circuit is discussed in Sec. 4·3. A generator using such an oscillator gave a regulation factor of $k_L = 3$ per cent per 100 μa, and required an input current of 34 ma at 350 volts for an output voltage of 5 kv at 100 μa. A typical circuit diagram is shown in Fig. 4·83. Efficiency and regulation factors are a function of transformer design and choice of driver tube. Application of recent developments in the art of pulse-transformer design would undoubtedly
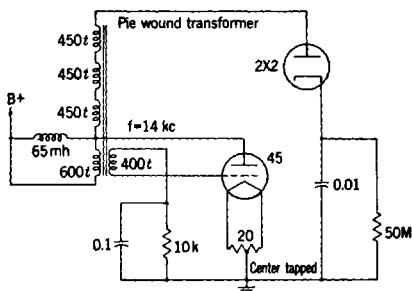


Fig. 4·83.—Pulse-generator or blocking-oscillator high-voltage supply. (*Courtesy of Hazeltine Corporation.*)

improve the performance figures cited. Although past usage has been limited, application of the circuit as a combination trigger and high-voltage generator appears to offer possibilities.

A generator of the inductance-charging type is illustrated in Figs. 4·84a and b. A rectangular voltage is applied to the grid of a driver tube, preferably a pentode to reduce the loading due to $r_p$. When the tube is turned on, current increases through $L$ at a rate determined by

$$\frac{di_L}{dt} = \frac{(E_b - E_p)}{L},$$

where $E_p$ is the voltage at the plate of the pentode while it is conducting. Shunt and series resistance and stray capacitance are for the moment neglected. When the tube is turned off, the voltage at the plate goes instantaneously positive until the high-voltage diode begins conducting at the voltage $E_0$. The rate of decrease of $i_L$ is given by

$$\frac{di_L}{dt} = \frac{(E_0 - E_b)}{L}.$$

Since the total change in $i_L$, given by $\Delta i_L = di_L/dt \cdot t$, must be the same for the charge and discharge periods, there results,

$$\frac{(E_b - E_p)t_2}{L} = \frac{(E_0 - E_b)t_1}{L}, \quad \text{or} \quad E_0 = \frac{E_b(t_1 + t_2)}{t_1} - \frac{E_p t_2}{t_1}.$$

Efficient operation requires that $L/R \gg 1/f$, and that $\sqrt{LC_s} \ll t_1$ or that stray capacitance be kept to a minimum.    Idealized waveforms are shown in Fig. 4·84c.

The process involved is essentially that required to generate a linear current waveform for magnetic deflection as required in a television-type line scan.    Advantage is taken of this fact in combining the two processes
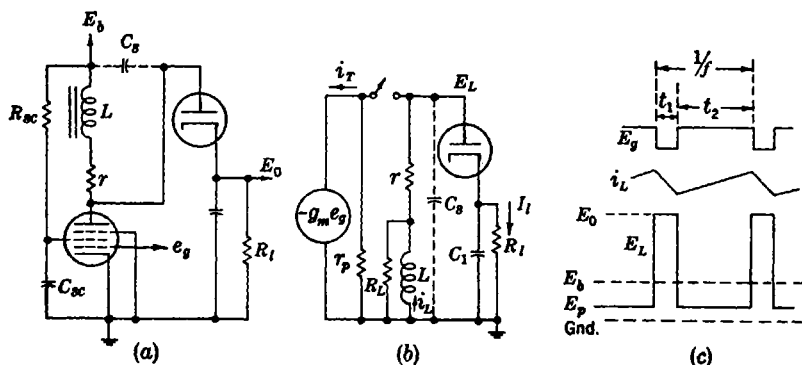


FIG. 4·84.—Inductance-charging generator.  (a) Complete circuit.  (b) Equivalent circuit.
(c) Idealized waveforms.

in a single sweep-circuit and high-voltage generator with resultant saving in power and components.    The combination is limited to applications where the ratio $t_1/t_2$ is constant, and is most efficient where the power dissipation required for the backswing of the deflection yoke and for the high-voltage supply are about equal.    The rapid drop in output voltage of the a-f oscillator for load currents above 1 ma is characteristic of all the vacuum-tube oscillators discussed and is an important safety feature.

*Load Regulation of Oscillator-type Power Supplies.*—Although vacuum-tube high-voltage generators are characterized by high internal impedance, good load regulation may be obtained by controlling the oscillator voltage.    The control voltage is obtained by comparing a portion of the output voltage to a standard voltage $E_s$, and may be applied to the input terminal or to one of the electrodes such as the screen, suppressor, or grid of the oscillator tube.    Screen control has been used in connection with the a-f and r-f oscillators.    A satisfactory range of control for load regulation may be obtained by simple means.    The additional compli-

cations involved in extending this range to cover both input voltage and load variations indicate that direct control of the input voltage is more desirable. A typical circuit of the latter type is shown in Fig. 4·85. Regulation constants for this circuit in conjunction with the a-f oscillator of Fig. 4·82 are well within the limits required for cathode-ray-tube applications. In the typical application, inclusion of load regulation only requires addition of the amplifier tube $V_2$ and the high-voltage divider $R_1 + R_2$. The high-voltage generator is shown as a block indicating that the method applies to any of the circuits discussed.



FIG. 4·85.—Voltage regulation with load feedback.

*Mechanical Construction.*—Many applications require the high-voltage supply to operate under adverse conditions such as dirt, humidity, extremes of temperature, fungus, and high altitude. These conditions are particularly troublesome in high-voltage applications because they tend to break down high-voltage insulation or increase the flashover distances required. The further requirement of shielding the high-voltage components against accidental contact and electrostatic pickup suggests the desirability of hermetic sealing of the complete high-voltage supply. Common practice for high-altitude applications is to put the supply in a pressurized container. Figures 4·86 and 4·87 indicate the advantage to be gained by the use of selenium-rectifier elements, which allow hermetic sealing of the complete high-voltage unit in a metal, oil-filled container. Advantage is taken of the high insulating qualities of oil in compact assembly of the components. The resultant saving in weight and space is appreciable.

Figure 4·86 is the a-f supply shown in Fig. 4·80. The assembly contains the a-f transformer, rectifiers, and output filter. A high-voltage output terminal and three transformer input terminals are provided. The container measures $2\frac{3}{4}$ by 3 by $5\frac{1}{8}$ in. outside dimensions exclusive of the bushings and expansions bellows mounted on one end. The unit
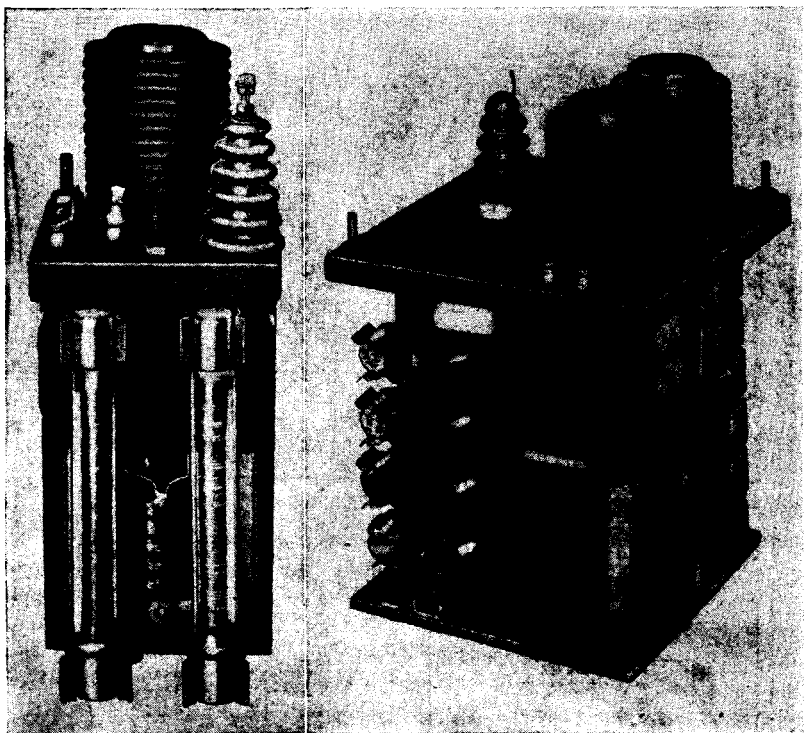


FIG. 4·86.　　　　　　　　　FIG. 4·87.

FIG. 4·86.—Internal construction of a +5-kv audio-frequency oil-filled hermetically sealed power supply for cathode-ray-tube applications.

FIG. 4·87.—Unregulated +15-kv 60-cps cathode-ray-tube supply—oil-filled hermetically sealed unit using selenium rectifiers.

is normally mounted on a 3-in.-depth chassis with the bushings below the chassis.

Figure 4·87 shows the same type of construction applied to a 15-kv, 60-cps, a-c unregulated supply. As before, the only exposed point is the single high-voltage d-c output bushing. The method is applicable to any a-c unregulated supply, to such a supply in conjunction with the series and shunt regulator circuits, and to the lower-frequency oscillator circuits discussed previously.
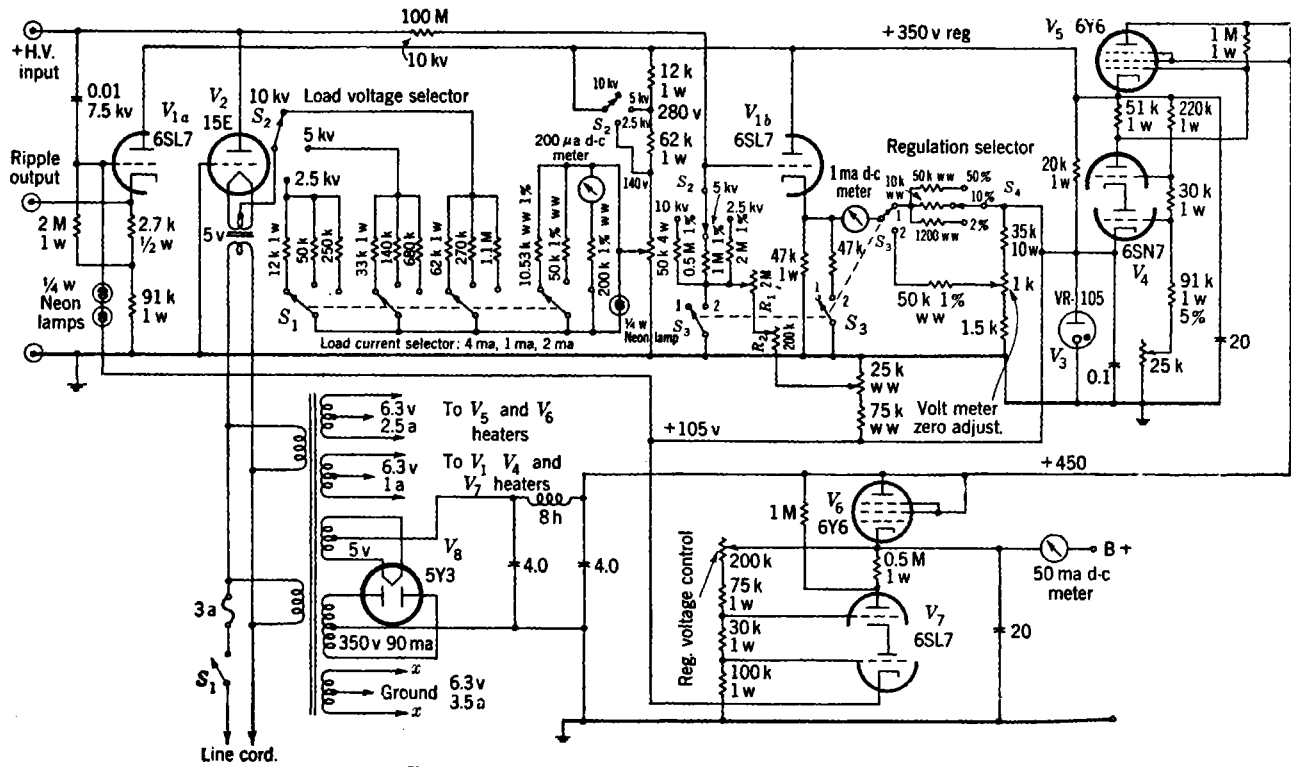
Fig. 4·88.—Testing unit for high-voltage power supply.

*Testing of High-voltage Power Supplies.*—High-voltage power-supply testing presents special problems. They include methods of measurement without loading the supply, control of the output voltage or load from a vantage point near ground, and accurate measurement of small changes in output voltage (regulation) without subjecting the measuring equipment and the operator to the voltage involved.

The test unit diagram in Fig. 4·88 should serve as a suggestion as to methods that may be used in solving these problems. The unit is designed for measuring the four characteristics of interest—voltage, current, regulation, and ripple—for positive supplies from 0 to 10 kv and 0 to +4 ma load. Full-scale regulation of 2 per cent, 10 per cent, and 50 per cent is provided.

Ripple measurements are obtained by coupling the output voltage through a high-voltage condenser to $V_{1a}$, to supply high-impedance input and low-impedance output for observing ripple on a "scope" or measuring on a suitable meter. A high-voltage triode (15E) is used as a controllable load. A suitable potentiometer and resistor in the cathode circuit serve as a means of varying the load current for the current and voltage ranges supplied. The load-current meter in this cathode circuit has ranges of 0.2, 1.0, and 4 ma. The highest range is useful for obtaining overload characteristics such as the a-f regulation curve, Fig. 4·81*d*. The voltage and regulation meter employs a form of electronic vacuum-tube voltmeter circuit. For the voltmeter it consists of an approximately 50-volt meter in the cathode circuit of $V_{1b}$. Switch $S_3$ is turned to Position 2 so that the meter is placed between the cathode and a bias or zero-adjustment point. Grid voltage is obtained from a high-voltage divider whose resistance is 100 megohms. Switching of ranges is accomplished on the low side of the divider. The divider current is small, although not negligible. Because the total divider resistance remains almost constant, correction may be applied where necessary.

The regulation meter circuit is put into operation by turning switch $S_3$ to Position 1. The meter with suitable scale multipliers and selector switch is connected with the polarity indicated between a standard source of potential and a cathode follower. If it is assumed for simplicity that the voltage $E_s$ is 100 volts and the multiplier is of such value that a 10-volt change in $E_g$ produces full-scale meter deflection, the meter then reads 10 per cent regulation. In practice $R_1$ and $R_2$ are adjusted so that the meter reads zero for a no-load voltage of $E_0$. Then as load is applied, the percentage change in output voltage is indicated on the regulation meter.

Additional circuits in the test unit include a regulated power supply for the test instrument and a variable-voltage regulated supply for furnishing power to oscillator-type supplies.

# CHAPTER 5

## POSITION-DATA TRANSMISSION[1]

### By F. B. Berger and Warren F. Goodell

The fundamental problem of data transmission is to obtain at a remote point a signal that is a given function of a primary signal at another point. In the applications of particular interest in this book the primary signal is generally mechanical and the remote signal may be either mechanical or electrical. The means of transmitting the signal have been classified arbitrarily into three groups: mechanical methods, which are used when the remote signal is a shaft rotation; electro-mechanical methods, for which the remote signal is a voltage or a set of voltages; and synchronized methods, which offer a cheaper solution for some applications of each sort, but which are not easily made very accurate.

#### MECHANICAL TRANSMISSION OF ANGULAR DATA

Examples of mechanical transmission of angular data are rotating-coil-PPI radar indicators where the deflection coil rotates in synchronism with the antenna, and azimuth-stabilization schemes in which the stabilizing element is controlled remotely by a fluxgate compass. The principles and circuits to be discussed here may be applied to almost any situation requiring transmission of mechanical rotation.

**5·1. Direct Mechanical Drive.**—If the shaft to be driven is located near the antenna or driving source, it is possible to couple the two by a flexible shaft, but this method is bulky and comparatively inaccurate. Although much of the error may be eliminated by gearing the shaft up to a multiple speed, the maximum speed of shaft rotation is limited because of the friction between the shaft and its protective conduit, especially if the shaft is not straight. Since the shaft is not rigid, only low accelerations may be followed with any degree of accuracy. It is also difficult to control more than one shaft when using this method. Flexible-shaft coupling has been rarely used in the devices described in this book.

In almost all data-transmission systems there is some gearing involved. Special mathematical functions may be introduced by the use of suitable cams.

---

[1] Secs. 5·1 through 5·4 by Warren F. Goodell, remainder of the chapter by F. B. Berger.

**5·2. Synchro Drive.**—The simplest system using synchros[1] (Fig. 5·1) for angular-data transmission consists of a synchro generator and a synchro motor connected as shown in Fig. 5·2. The generator and motor are both rotary transformers and are electrically and mechanically identical except for the addition to the motor of a damper flywheel.
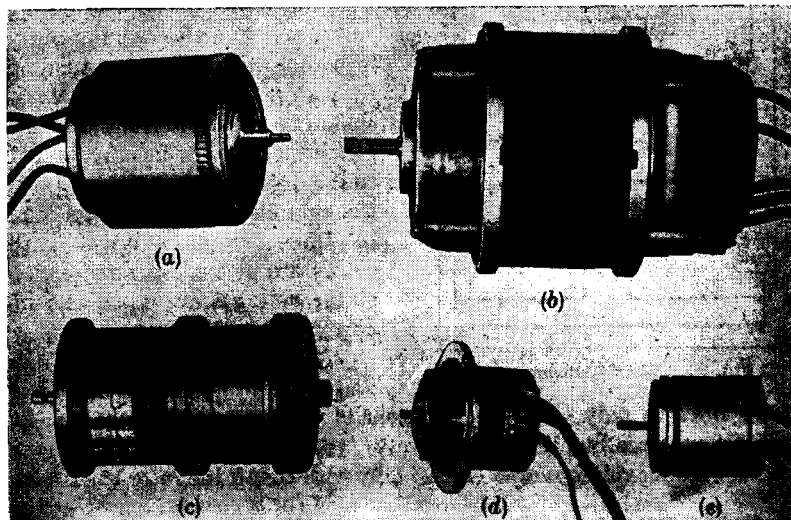


Fig. 5·1.—Typical synchros: (a) Diehl FPE-43-1; (b) GE size 5, 60 cps; (c) GE, 2J, 400 cps; (d) Pioneer Bendix AY-30; (e) Pioneer Bendix AY-100, 400 cps.

In each unit, a-c excitation power is applied to a single-phase primary winding (usually the rotor) that induces voltages in three secondary windings (usually the stator) that are $Y$-connected and are mechanically spaced 120° apart. Another type of synchro often used as a resolving

[1] "Synchro" is a generic term applied to a multitude of similar devices manufactured by several companies under different trade names; for example, the General Electric "Selsyn," the Kollsman Instrument "Teletorque," and the Pioneer-Bendix "Autosyn." In addition, many companies manufacture "Synchros" to Army and Navy specifications. A report (Radiation Laboratory Report No. 740) compiled in June, 1945 lists 225 available standard synchro-type instruments. There are approximately as many more that are not listed there. Chapter 10 in Vol. 17 of this series discusses the available types in much more detail than can be gone into here. Synchros considered as modulating devices are discussed also in Vol. 19, Sec. 12·6.

Normal life expectancy of most synchros in an aircraft installation is between 1000 and 20,000 hr. Most of the available types will pass the standard Navy shock and vibration tests; they will operate satisfactorily from −65°C to +95°C; and when the windings are properly impregnated, they will withstand moisture.

Synchros vary considerably in size and weight. The Bendix "autosyn" AY-100, for example, weighs 5 oz and is 1.4 in. in diameter and 2 in. long over all; whereas Navy synchro 7DG weighs 18 lb, is 5.75 in. in diameter, and 9.2 in. long.

device has but two separate secondary windings mechanically spaced at 90°.

Any lack of correspondence between the positions of the generator



FIG. 5·2.—Simple synchro system.

and motor causes the voltages in the stator windings to be unequal. This inequality causes circulating currents to flow through the windings and produces torques tending to restore the rotors to corresponding positions. Because the generator rotor is usually geared to the driving source, the motor is the only element that can respond to these torques. When both rotors are in correspondence, the stator voltages are equal and no currents flow.

The voltages induced in the stator windings are all in time phase because only single-phase power is applied to the rotor and the synchro revolves but slowly. However, the peak amplitude of a given stator-winding voltage varies sinusoidally with time if the rotor turns with
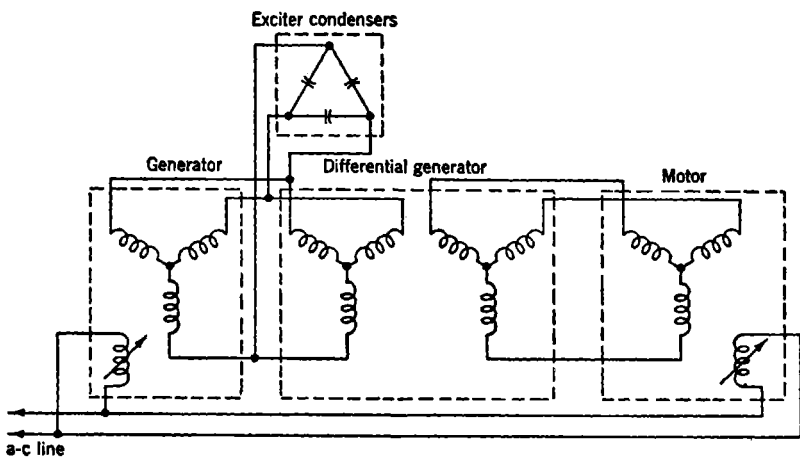


FIG. 5·3.—Synchro system with differential.

uniform angular velocity. Thus, since the three stator windings are mechanically spaced by 120°, the envelopes of the stator voltages will be 120° out of phase.

Differential-generator synchros may be used to add or subtract other angular displacements from that of the generator. As is indicated in Fig. 5·3, a differential generator consists of a three-phase primary winding (usually the stator) and a three-phase secondary winding (usually the rotor). When voltages from the stator of a generator are applied to the primary of the differential generator, new voltages are induced in the secondary of the differential. These voltages correspond to those that would appear in the generator secondary if the generator rotor shaft were turned by an additional amount equal to the shaft rotation of the differential. Because of losses inherent in the construction of differential generators, there is usually a small stepup ratio between its primary and secondary. A differential should, therefore, be connected as shown with the stator connected to the generator stator. Capacitors for power-factor correction are used in parallel with the primary of the differential generator in order to reduce heating.

The angular error by which the synchro motor will lag the generator is roughly proportional to the required output torque at the motor shaft. Because this torque depends upon the magnitude of the restoring currents flowing in the motor-stator windings, its value is limited by the current-carrying capacity of the motor. Therefore, to obtain the required accuracy in following, it is often necessary to gear the synchros to a multiple speed.[1]

In a geared system using ordinary synchros, the maximum speed of rotation of the synchros is limited to from 200 to 400 rpm. Another disadvantage of such a system is the fact that any differential generators used must also be geared to the same multiple speed as the generator.

**5·3. Servo System Drive.**—If greater accuracy and torque than can be obtained from a simple synchro are required, a servo system such as is shown in Fig. 5·4 may be used.[2]

In a servo system the rotor voltage from a control-transformer synchro is amplified and used to control a motor so as to bring both the load and the synchro to a null position. A control transformer consists of a high-impedance three-phase stator and a single-phase rotor. The rotor must be specially wound so that its position with respect to the stator windings will not change the input impedance to those windings. When the stator windings of one of these instruments are connected to the stator windings of a synchro generator, a magnetic field corresponding to that in the generator can be set up in the control transformer. An a-c voltage proportional to the sine of the angle between the positions of the two rotor shafts is induced by this field in the winding of the control-trans-

[1] See Sec. 16·3 for an example of multiple-speed-synchro data transmission.

[2] See Vol. 21 of the Radiation Laboratory Series for design factors in servo-mechanisms; also Chap. 4, Vol. 25, of the Series.

former rotor.    Thus, when the control-transformer shaft is rotated 90°
with respect to the generator shaft, the induced voltage is zero.    The
voltage in the control-transformer rotor is known as the error voltage
because it is a measure of the difference between the two rotor positions.
The servoamplifier and drive motor serve to keep the error voltage as low
as possible, and therefore to keep the two shafts in synchronism.

A differential generator may be introduced into the generator-
control-transformer circuit.    Multiple speed may be used to reduce
errors as was mentioned in the preceding section.    In all cases capacitors
should be used with the control transformers to reduce out-of-phase
currents.    If an "*n*"-speed system is used, microswitch phasing, or an
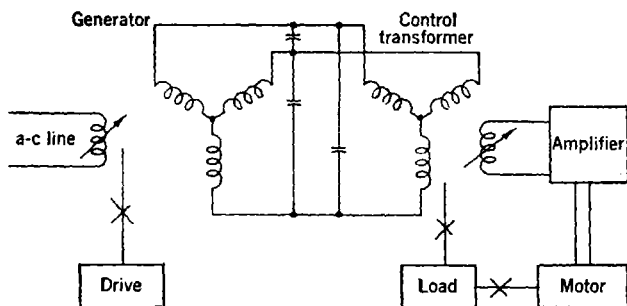


FIG. 5·4.—Servo system block diagram.

additional pair of synchros revolving at "one"-speed may be used to
prevent phase ambiguity.    The voltage from the rotor of the one-speed
transformer may either be added to that of the *n*-speed rotor, or be put
through auxiliary circuits that switch the input terminals of the servo-
amplifier from the *n*-speed rotor to the one-speed rotor whenever the
error voltage becomes too large.

The amplifier used depends upon the type of motor (which determines
whether a-c or d-c output voltage is required), and upon the accuracy
and speed requirements of the system.    If a-c output voltage is required,
the amplifier may consist of one or two stages with suitable phase com-
pensation, or of a phase detector and inverter.    If d-c output voltage is
required, the output stage may be a vacuum tube with the drive-motor
armature or field winding in the plate circuit, or it may be a pair of vibrat-
ing relays.    Servomechanisms that employ vacuum-tube-controlled a-c
motors seem to provide the smoothest and most accurate control for
rotating-coil PPI displays.

The effect of the inertia of the gear train and load on the following
of high accelerations may be partially compensated for by the use of
anticipation networks.    These networks effectively allow the amplifier

to work at higher gain during periods of high acceleration and reduce the gain for continuous operation to a value sufficiently low to prevent unwanted oscillations.

The gear train used must be carefully designed to give the proper output speed and torque with the minimum inertial load on the motor. The first few gears are the most important in this respect and should be light.   Backlash should be eliminated as much as possible to prevent hunting and oscillation.   If more than one synchro is driven from the same gear train, precision gearing should be used between the synchros.

If more power than can easily be furnished by a completely electronic amplifier is desired, the output signal of such an amplifier may be used
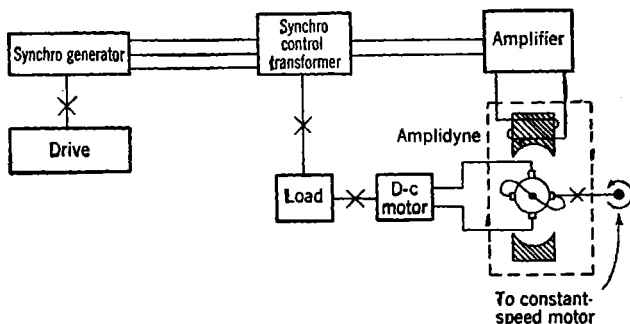


FIG. 5·5.—Amplidyne servo system.

to control an Amplidyne as shown in Fig. 5·5.   An Amplidyne is a controlled d-c generator that acts as a power amplifier with a gain of about 500.[1]

Figure 5·6 shows a 1- and 36-speed 60-cps servo system.   When the difference in position of the input and output shafts (the "following error") is small, the 36-speed synchro signal is amplified, passed through a phase-advance network, amplified again, phase-inverted, and used to drive two 6V6 beam-power tetrode output tubes.   The plates of these tubes are connected differentially to the split field of an a-c motor that drives the load and the synchros coupled to it.

Whenever the following error becomes larger than about 2°, the system may lock in one of 35 extraneous stable positions.   To prevent this, the one-speed signal is amplified enough at 2° error to cause the small neon bulb to strike.   This one-speed signal then takes over control of the amplifier until the error is reduced sufficiently to permit operation in the correct 10° sector, at which time the 36-speed signal again takes over for fine control.   This system follows both continuous rotations of

[1] See Vols. 21 and 25 of the Radiation Laboratory Series.
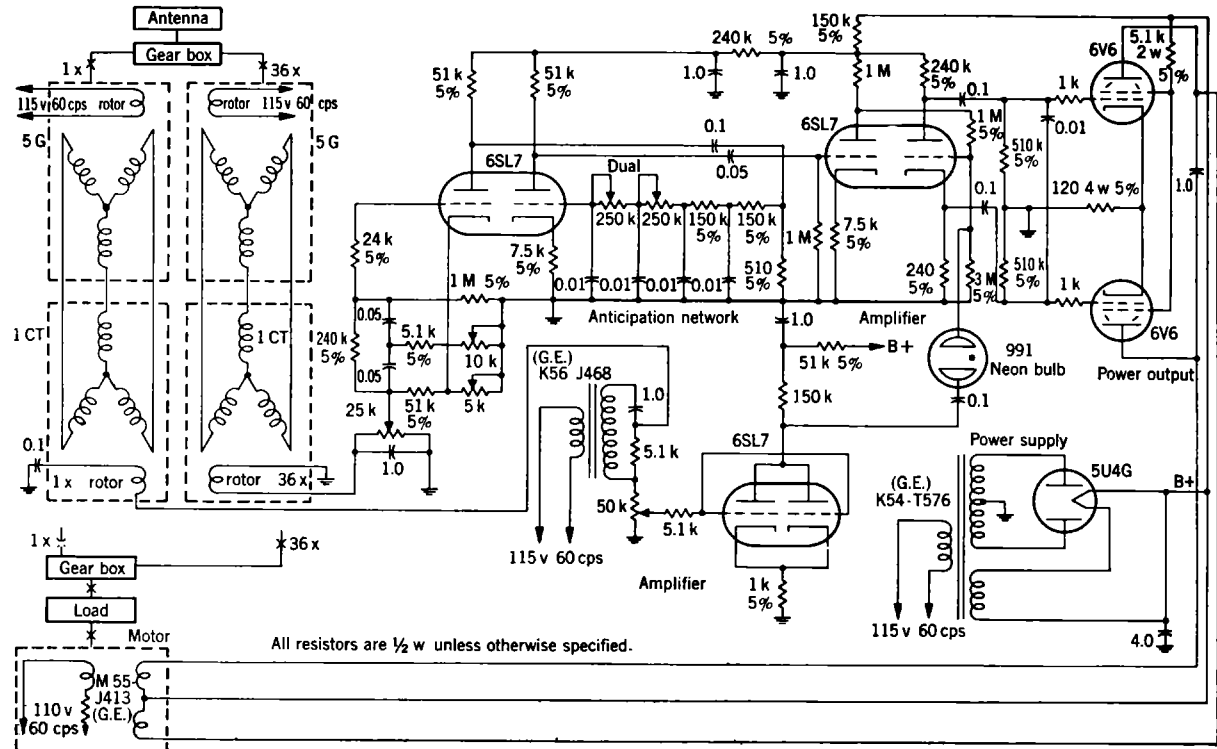
FIG. 5·6.— A 1- and 36-speed servo system.

the antenna at 6 rpm and slow sector-scanning with a maximum error of 0.5°.

Figure 5·7 shows a typical remote-indicator servomechanism, which is also designed for 60-cps use and which employs a one-speed synchro system. The error voltage is put through a phase-advance network, amplified, and applied to the grid of the type 807 driver tube. The output transformer is connected to one phase of a 2-phase induction motor that turns the control transformer and the load. A sample of the output voltage of the transformer is fed back to the amplifier stage to serve as negative feedback. Speeds up to 20 rpm can be followed with an error of less than ± 1°.
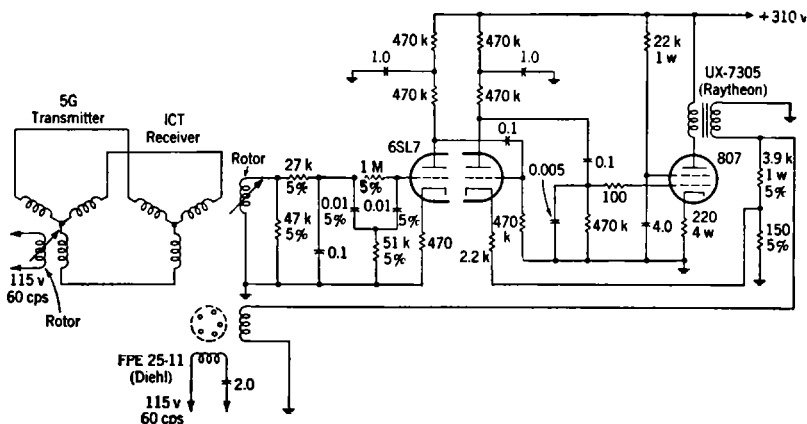


FIG. 5·7.—1-speed servo system. The 2-phase induction motor is geared to the receiver rotor and to the load.

Figure 5·8 shows a typical 400-cps servo system. The synchro system consists of a generator, differential generator, and control transformer, all at one-speed. The error signal is applied to a phase inverter and a phase detector. The resultant push-pull d-c voltages proportional to the error signal are then used to control the biases of the two output 6L6 drivers. The plates and screens of these tubes are run on alternating currents and the plates are differentially connected through an output transformer to one phase of a two-phase induction motor. A differentiating network is inserted just after the phase detector to give the required anticipation.

The system is designed to follow rotations of 6 rpm with an error of less than 0.5° and to follow angular accelerations due to sector-scanning of not greater than 90°/sec² with an error not exceeding 0.7°.

Figure 5·9 shows a 400-cps servo system that uses a pair of vibrating
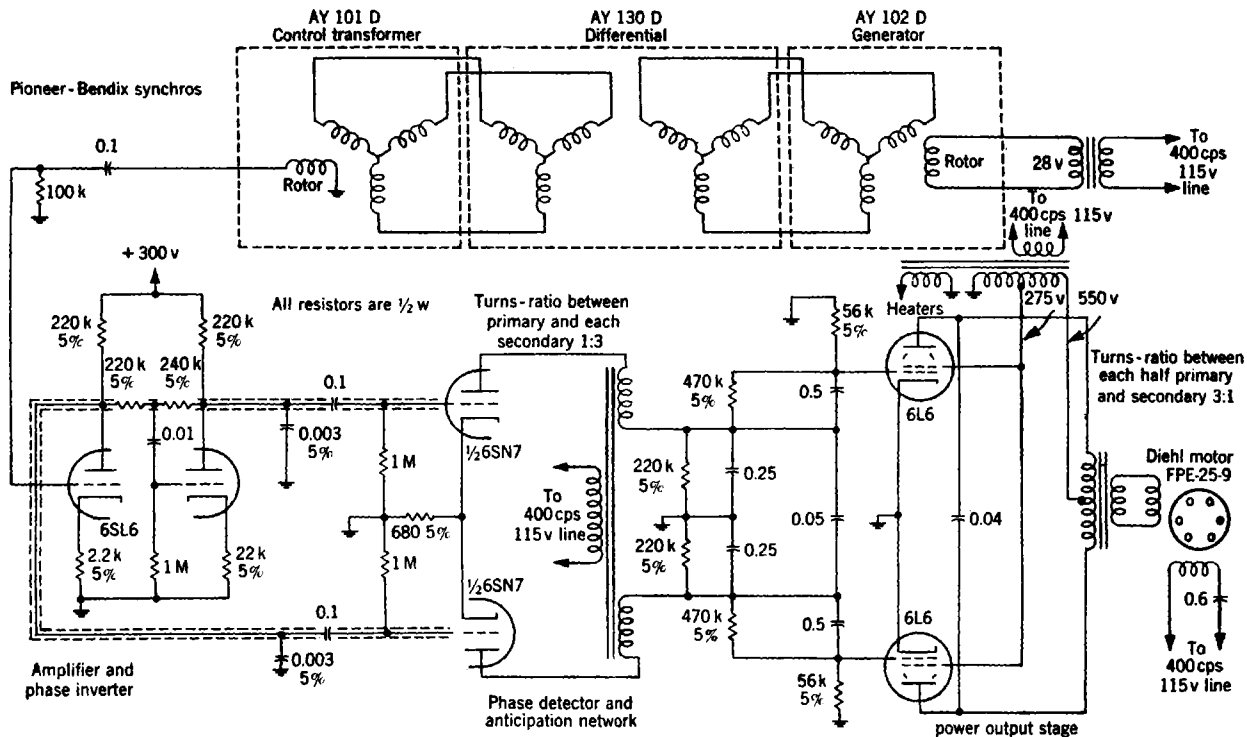
FIG. 5·8.—A 1-speed 400-cps servo system.

mercury relays as the output stage. A feedback loop from the output
terminals of the relays to the phase-detector tubes keeps the relays oscil-
lating at about 100 cps. If the relays open and close in synchronism,
both sides of the armature of the small d-c permanent-magnet-field drive
motor are either at ground or at +27.5 volts and so no power is delivered
to the motor.
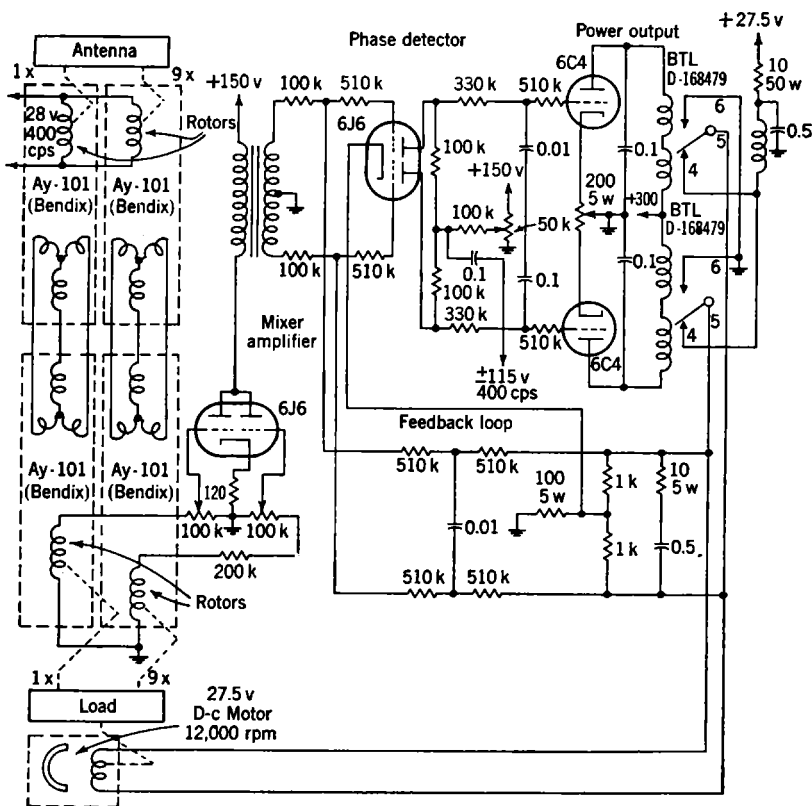


Fig. 5·9.—Airborne 400-cps relay servo.

If an error signal is present, it is amplified and applied to the grids of
the phase-detector tubes. The plates of these tubes are returned to a
source of a-c voltage with a d-c component. Any a-c error signal will
therefore cause more average current to flow through one section than
through the other, and will result in a difference of average bias on the
grids of the output 6C4's. The voltage fed back around the loop to
sustain the relay oscillations is originally a square wave, but is rounded
off by the constants of the feedback loop. Therefore a shift in the

average bias of one of the output tubes causes the tube with the more positive bias to conduct first, thus allowing one relay to close before the other. When the relay closes, one side of the motor armature is connected to ground and the other to $+27.5$ volts. Therefore, current flows and the motor revolves. The tube that conducted first will also conduct after the other tube has been cut off because its average bias is more positive. The motor therefore has two pulses of current for each cycle of oscillation of the relays.

These pulses are smoothed by a series $RC$ filter across the motor terminals to prevent excessive heating of the motor because of high-frequency current components. An $LCR$ filter also limits the current surges for the protection of the relay contacts.

The circuit was designed to follow, with an error of less than $\frac{1}{2}°$, rotations up to 30 rpm and sector scanning at the same angular speed.

**5·4. Errors and Other Operating Characteristics.**—Errors in gearing can be held to $\pm 0.1°$ although in many cases "precision" gears are required. All gearing should have as little backlash as possible. Flexible shafts will probably follow to about $\pm 1°$, depending upon their length and diameter. However, this error may be reduced to as low a value as desired by gearing the flexible shaft to a multiple speed. When a flexible shaft is used for sector scanning, the errors in following only nominal accelerations may be as high as $\pm 20°$ for a single-speed shaft.

Complete tables of synchro errors may be found in Vol. 17.[1] These range from $\pm 0.2°$ for a large generator and $\pm 0.1°$ for a control transformer to more than $7°$ for some types of motor. When used in a straight synchro drive, the torque required of the motor will cause the errors to increase, but this difficulty may be overcome by the use of a multiple-speed system. When used in a servo system as a voltage indicator, the accuracy of a pair of synchros can be held to $\pm 0.2°$. In this application, however, the synchro error must be considered. If a differential generator is inserted in the line, the error is usually 50 to 75 per cent greater.

Servomechanisms may, in general, be made as accurate as desired, but this process involves large and heavy equipment if carried to extremes. Accuracies usually range from $\pm 0.25°$ to $\pm 1.5°$ for constant-velocity applications and from $\pm 0.25°$ to $\pm 3.0°$ for sector scanning. The static errors of such systems are very small; furthermore this type of error is sometimes unimportant. Even errors that are large but constant are unimportant for some applications.

The rotational speed range of display systems extends from almost zero for some azimuth stabilization schemes, to about 60 rpm for a few fairly rapid scanning systems. Sector scanning up to about 30 rpm must also be followed. Accelerations are as high as several thousand degrees

[1] Chap. 10 of Vol. 17, of the Radiation Laboratory Series.

per second per second.    The torque output required is usually less than 15 to 20 oz-in. at the one-speed shaft.

<center>ELECTRO-MECHANICAL DEVICES</center>

**5·5. Some Circuit Considerations.**    *The Nature of the Waveform to Be Modulated.*—There are two methods of using a synchro resolver for

the transmission of angular data, and these differ in the nature of the carrier.   In one method, the carrier is used simply as a medium for the transmission of information supplied by the resolver or modulator, and the waveform of the carrier is not of fundamental importance.   It is usually a sinusoid with a frequency between several cycles per second and several megacycles per second. In the second method the carrier waveform conveys some other intelligence[1] in addition to that imparted to it by the resolver or modulator.   This method may be further divided into those cases in which the intelli-

Fig. 5·10.—Triode peak detector.

gence is transmitted as a voltage waveform, and those in which it is transmitted as a current waveform.

*Sine-wave Carriers, Demodulation, and Filtering.*—The information imparted to a sine-wave carrier by a modulator is generally utilized by the display circuits only after the waveform has been demodulated.    The peak-detector circuit shown in Fig. 5·10 is a simple form of demodulator,

Fig. 5·11.—Idealized peak-detector output waveform.

in which the input waveform to the grid of $V_1$ may be the sinusoid of frequency $f$ shown in Fig. 5·11. For detection, the $RC$ time constant is chosen so large that the time rate of change of cathode voltage when the tube is cut off, $dE_k/dt$, is much smaller than the maximum slope of the sine wave.

The output waveform is then like that shown as a solid line in Fig. 5·11.

In detecting a constant-amplitude sinusoid, the ripple in the output voltage may be made as small as required by further filtering.   For a modulated sinusoid, however, a lower limit to the peak-to-peak ripple is set by the maximum value of the change in the modulated amplitude per carrier period.   Other conditions remaining the same, the ripple amplitude is inversely proportional to the carrier frequency.   When the input

[1] See Chap. 13 for examples.

amplitude is reduced to a value such that the maximum slope of the sine wave is less than the filter decay rate, there will be no detection, but rather the output will follow the input waveform.

*Detecting Circuits.*—The following four types of demodulators include most of the circuits that have been used in radar data-transmission applications.
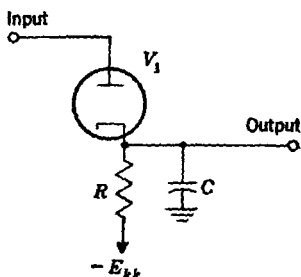


FIG. 5·12.—Diode peak detector.

1. *Peak Detector.* The triode of Fig. 5·10 has been widely employed as a peak detector. A second circuit, which uses a diode, is shown in Fig. 5·12. Its operation is very similar to that of the cathode follower detector, but it presents a greater load to the modulator.

If a sine-wave carrier is modulated by a synchro to give the waveform shown in Fig. 5·13, the phase of the carrier shifts abruptly by 180° at each zero of this sinusoidal envelope because of the reversal of the synchro coupling. When the waveform is demodulated by a peak detector of the type just discussed, the output voltage is proportional to the absolute value of the sine (Fig. 5·13). A detector giving such an output waveform may be spoken of as being "phase insensitive."

2. *Phase-sensitive Detectors.* The phase sense may be preserved either by carrier addition and peak detection or by keyed[1] detection.

If to the modulated carrier of amplitude $A$ shown in Fig. 5·13 is added a carrier of constant amplitude $B$ at the same frequency, a new wave-form is obtained whose amplitude modulation is sinusoidal. The waveform may be represented by
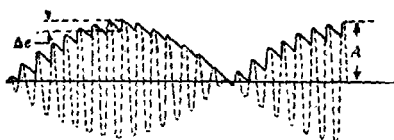


FIG. 5·13.—Sinusoidal carrier modulated by a sinusoid of lower frequency, after demodulation by peak detection.

$$e = (B + A \sin 2\pi f_2 t) \sin 2\pi f_1 t, \qquad (1)$$

where $f_1$ is the carrier frequency and $f_2$ is the modulation frequency. The modulation need not be a sinusoidal function of time.

The composite waveform together with the carrier of amplitude $B$, where $B$ is greater than $A$, is shown in Fig. 5·14. If this wave-form is applied to the detector shown in Fig. 5·10, the demodulated

[1] See Chap. 14, Vol. 19 of the Radiation Laboratory Series.

or output waveform will be a constant $B$, plus a complete sinusoid of amplitude $A$.

$$e_o' = B + A \sin 2\pi f_2 t. \tag{2}$$

A convenient push-pull circuit for performing both the adding and detecting operations is shown in Fig. 5·15. For proper operation this circuit must be loaded symmetrically.
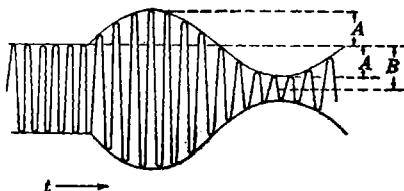


FIG. 5·14.—Sine-wave-modulated carrier $A$ added to constant-amplitude carrier $B$.
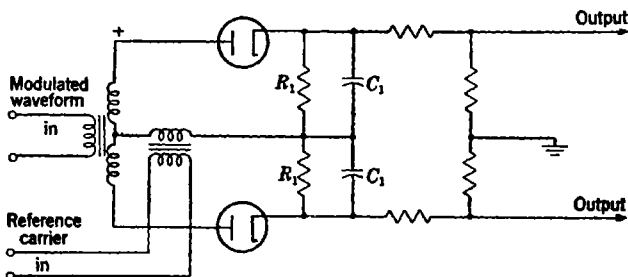


FIG. 5·15.—Detector which adds modulated waveform and reference carrier.

3. *Keyed Detectors.* The phase-sensitive keyed detector may be thought of as a device in which the output terminal is intermittently tied to the input terminal by a switch that is controlled in synchronism with the carrier. The switch is keyed so that it closes for a short time near the peaks of the carrier wave form. The output circuit generally has a time constant long compared with the carrier period.
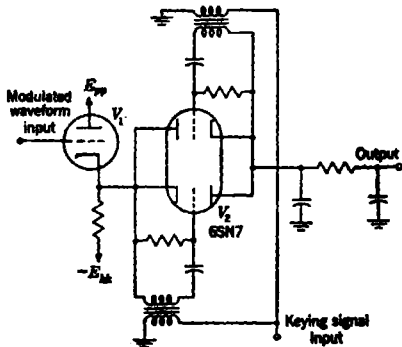
A widely used circuit of this type is shown in Fig. 5·16. The cathode follower



FIG. 5·16.—Keyed detector.

$V_1$ is used in order not to load the modulator. The twin triode $V_2$ is the switch tube. Both of its grids are raised in potential for

a short time near the positive peaks of the carrier or keying signal, and both triodes are nonconducting during the rest of the carrier cycle.    This circuit is a phase-sensitive detector; that is, the output signal will go negative if the modulated carrier is shifted 180° in phase with respect to the unmodulated carrier.

4. *The "Boxcar" Detector.* The "boxcar" detector, illustrated in Fig. 5·17, is particularly well suited to pulse demodulation.    Immediately preceding each pulse of the modulated pulse train, the output terminal is tied to ground through $V_2$, which is made
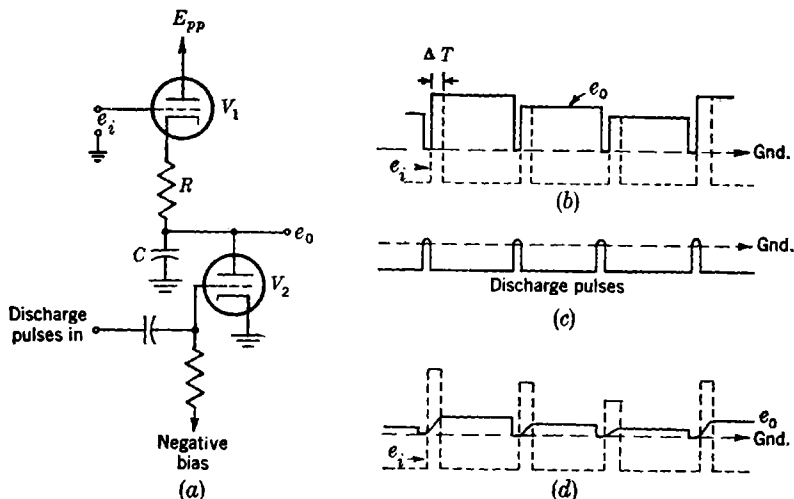


Fig. 5·17.—The boxcar demodulator.  (a) Circuit schematic diagram.  (b) Input and output waveforms for the case where $(R + R_{KF})C \ll \Delta T$.  (c) Discharge pulses on grid of discharge tube $V_2$.  (d) Input and output waveforms for the case where $(R + R_{KF}) C \gg \Delta T$.

conducting at such times by suitable discharge pulses (Fig. 5·17c). In the case shown in Fig. 5·17b where $(R + R_{KF})C \ll \Delta T$, ($R_{KF}$ being resistance of the cathode follower) the peak-pulse amplitude determines the amplitude of the associated "boxcar" waveform. In the case where $(R + R_{KF})C \gg \Delta T$ (Fig. 5·17d) it is the area of the pulse lying above the cutoff potential of $V_1$ which determines the boxcar amplitude.    The chief advantage of the method lies in the fact that, except for the gaps between boxcars, the output amplitude has a magnitude determined by the latest available information and that it can follow a rapid rate of change of pulse amplitude.    The amount of carrier-frequency component due to the gaps between the boxcars is appreciable, but for many appli-

rations it is of little consequence.   Filtering can be used but the advantages peculiar to the system are then largely lost.

*Selection of a Carrier.*—It is generally necessary that the amplitude of the oscillator output voltage be reasonably constant.   The modulator output voltage is proportional to the amplitude of the input waveform as well as to a function of the modulator control signal.   The disturbances against which the modulator output voltage must be stabilized are fluctuations in heater current, ripple and other variations in the power-supply voltages, changes in temperature, and changes in the characteristics of the circuit elements due to aging.   In most of the applications discussed in this book, changes that are slow compared to a cycle of the modulator control signal can be tolerated; but changes occurring in a time comparable to the carrier period are objectionable.   Over-all short-time stability of the order of $\frac{1}{4}$ per cent is commonly attained.

The frequency stability of the oscillator is sometimes of importance, particularly in systems in which the display timing signals are derived from or are synchronized with the carrier.

The 60-cps and 400-cps line voltages can be used as sinusoidal carriers.   If the fluctuations in carrier amplitude are not negligible, they can sometimes be minimized by a comparison system in which the carrier amplitude provides a reference level with which the modulator output voltage can be controlled.

The distance from oscillator to modulator to detector over which the carrier is transmitted may be anything from a few inches to tens of yards.   In cases where the connecting cable is long, properties of the cable may affect the modulated waveform.   A commonly used coaxial cable is RG-62/U for which the attenuation is about 0.25 db/100 ft at frequencies below 1 Mc/sec.   The d-c resistance of the inner conductor of this cable is 60 ohms/1000 ft and its capacity per foot is 13.5 $\mu\mu$f.   If the cable is properly driven and is terminated in its characteristic impedance, the capacitance in itself presents no problem.   However, with some electromechanical devices, notably variable condensers, lead and other stray capacitances must be kept to a minimum.

The frequency response of the electromechanical device itself must be considered, primarily because high attenuation is objectionable and also because of the attendant phase shift.   In general, variable condensers are useful over the frequency range from a few kilocycles per second to a few megacycles per second.   Synchros have been used from 30 cps to 20 kc/sec and potentiometers have been employed with carriers up to 1 kc/sec.

Whenever a phase-sensitive detector is employed, the phase shift of the carrier by the modulator must be either minimized or compensated

for.   This phase shift results in a sometimes objectionable delay in the transmission of the intelligence.

A consideration of filtering shows that a lower limit to the carrier frequency is prescribed by the maximum allowable time rate of change of the intelligence signal, and that a higher frequency than this may be necessary to reduce ripple to an acceptable value.   The acceptable "coarseness" of the data, in general, sets a lower limit on the frequency that can be employed.   This acceptable coarseness or measure of the discreteness of the intelligence in the case of radar displays is determined primarily by the spot size of the cathode-ray tube, the sweep speed, and the width and scan speed of the radio-frequency beam.
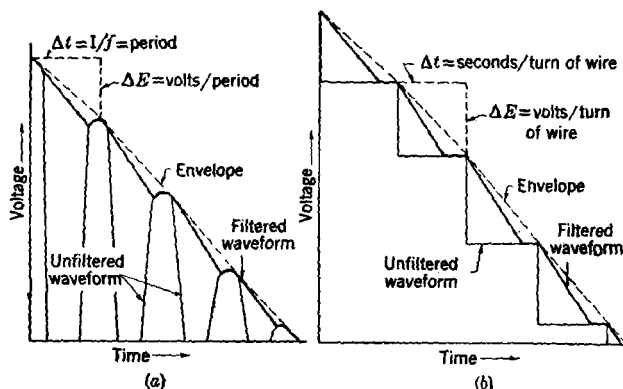


Fig. 5·18.—Comparison of filtered and unfiltered waveforms in the case (a) of a constant-frequency sinusoidal carrier, and (b) of a constant-speed linear potentiometer.

It has been found that if a carrier frequency and a periodicity of the display are almost harmonically related, but not synchronized, annoying beat-frequency intensity and magnitude disturbances frequently are evident on the cathode-ray-tube display and are difficult to suppress.

The detection and filtering of a modulated carrier wave-form is analogous to the filtering problem encountered with the output voltage of a rotating potentiometer.   As illustrated in Fig. 5·18 the amount of ripple in the output voltage depends, for a given filter time constant and time rate of change of voltage of the envelope, upon the coarseness of the data.   In the case of the sinusoid the period of the carrier is a measure of coarseness, which corresponds in the case of the potentiometer to the time per turn of wire.

**5·6. Linear Potentiometers.**—When a voltage proportional to a shaft rotation is desired, a linear potentiometer[1] is generally the most satis-

[1] See Vol. 17, Chap. 8 for a discussion of the manufacture of potentiometers and a listing of available types.   In Vol. 21 will be found a discussion of potentiometers as

factory device to use.   However, an examination of the specifications of
available types of potentiometers shows that they can be used only if the
speed of rotation does not exceed 1 rps, if a life of approximately $10^6$ cycles
is adequate, and if a resolution of approximately $\frac{1}{3}°$ is satisfactory.

In the example shown in Fig. 5·19 the mechanical signal is the oscil-
lation of a shaft over a sector not exceeding 180° and at a rate not exceed-
ing 1 cps.   The potentiometer signal is used to control the horizontal or
azimuth position of the cathode-ray-tube beam (B-scan).   The deflection
coil requires a current of about 40 ma to cover the display area, and this
current is obtained with a 30-volt change on the grid of $V_1$.   The greatest
accuracy is required when the presentation is an expanded sector, map-
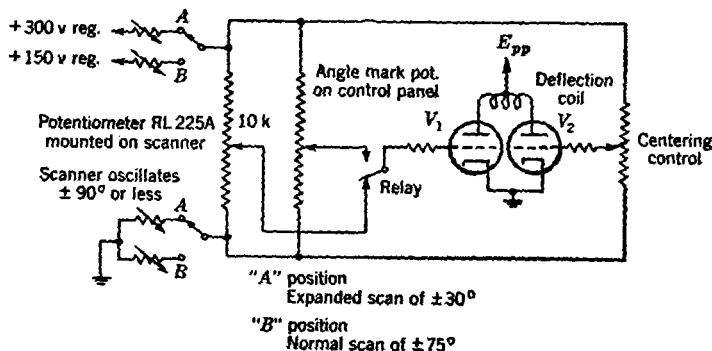


FIG. 5·19.—A radar application of a data-transmission system using a linear potentiometer
rotating less than 360°.

ping only ±30° of azimuth on the cathode-ray tube.   Consequently the
potentiometer is designed to be linear to ±1° in the middle 60° sector of
the winding, with a departure from linearity of as much as ±3° being
acceptable over the remainder of the winding.   A typical potentiometer
has a life of about half a million cycles for 1 ma of brush current.   It is
wound with 505 turns of 0.00275-in.-diameter nichrome wire and has an
angular resolution of 0.37°.

The information from the potentiometer controls the horizontal
position of the cathode-ray beam when the relay switch contacts are in
the position shown in Fig. 5·19.   Whenever the switch is in the other
position, the cathode-ray-tube beam deflection is determined by the
position of the angle-index potentiometer arm.   The relay can be
activated by a push button at any time and it is automatically activated
once per cycle when the expanded sector presentation is being used.
The potentiometer in the grid circuit of $V_2$ serves as a centering control

elements in computing circuits.   Information on potentiometers as modulators will
be found in Vol. 19, Chap. 11.

since the difference in the potentials of the grids of $V_1$ and $V_2$ determines the deflection-coil current. The rheostats are provided to adjust the sensitivity (volts/degree) of the data potentiometer and the d-c level of the amplifier grids. Filtering, in spite of the electrical noise and the wire-to-wire jumps, was not found necessary in this system.

A second example is shown in Fig. 5·20. The potentiometer is turned by a servomechanism at three times the scanner speed. Half a 6SN7W[1] is used as a cathode follower to afford a low-impedance source of the information for the display circuits. To compensate for the nonlinearity of the cathode follower,[2] the potentiometer is driven from the plate of the
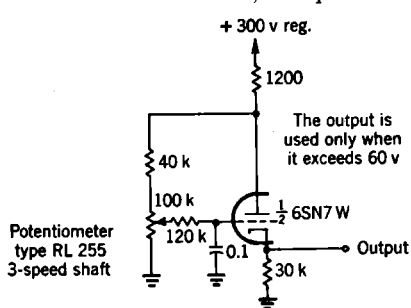
tube. As the potentiometer output voltage goes more positive with respect to ground, the output volts per degree of rotation of the potentiometer decreases, correcting for the increasing cathode-follower gain. This principle can be extended to introduce a desired departure from linearity. A typical potentiometer for this purpose is a General Radio 433A[3] 5-in. unit modified to turn continuously through 360° and supplied with special contactors and slip rings. The winding consists of approximately 250 turns per inch of No. 41 nichrome wire extending over 322° of the rotation and having a total resistance of about 10,000 ohms. The unit is rated at 25 watts and is good for more than $10^7$ rotations at 60 rpm. The potentiometer is operated without lubrication on the sliding electrical contacts in order to reduce the electrical noise. Both the resolution and the linearity of the potentiometer are about 0.1° of potentiometer rotation or about 0.03° of scanner rotation. This value is consistent with the requirement that the display be good to 0.08° under certain conditions.

**5·7. Sinusoidal Potentiometers.** *Requirements and Types.*—The primary function of these potentiometers is to provide four d-c potentials that vary sinusoidally with the angle of rotation of the shaft of the potentiometer. These four sinusoidally varying potentials have the

[1] The reasons dictating the use of the 6SN7W in this application are unrelated to the data-transmission problem. This tube has a heater-cathode rating of 200 volts. If a 6SN7 is used instead, the heater should be operated 100 volts or so above ground.

[2] See Fig. 15·8 for an application to elevation data.

[3] Muter makes an almost identical potentiometer.

same amplitude and are phased at 90° intervals with respect to each other. The potentiometers can turn continuously in either direction.

*A Detailed Example.*—One of the most widely used of the sinusoidal potentiometers[1] is the RL 14.

The sinusoidal variation of the output voltage of the potentiometer is obtained by moving a small point-contact brush in a circle upon a family of straight parallel equipotential lines that lie in a single plane and which have a constant potential gradient. The equipotential lines are provided by the wires of the linear resistance winding illustrated in Fig. 5·21. Four brush contacts like the one shown in Fig. 5·22 rotate in the same circle relative to the resistance card and are always 90° apart from each other. Actually the card and not the brushes is rotated in order to decrease the number of slip rings required.



FIG. 5·21.—Wire-wound resistance card for potentiometer type RL 14. Nichrome wire, diameter 0.0025 in. enameled or coated with Formex. Approximately 305 turns per inch. Winding is varnished with GE clear varnish No. 1170. Varnish and enamel are removed from top of wire on entire convex side of card, using special buffing procedure that cleans and polishes tops of wires without removing insulation from between turns.

The camber, as shown in Fig. 5·21, is deliberately imparted to the resistance card to hold the wires taut and in place and to enable a relatively wide brush to contact no more than two turns of wire at one time.
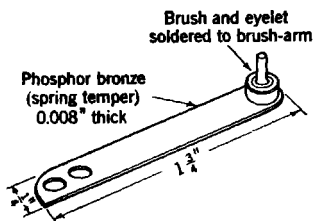


FIG. 5·22.—Brush arm in potentiometer type RL 14.

The curved card abrades the tip of the brush in such a fashion that the brush becomes convex, forming a small point contact.

The resolution expressed in terms of rotation angle varies from 0.17° when the brush is moving at right angles to the turns of wire to infinity when the brush is moving parallel to the wire. The resolution that is ultimately of interest, however, is the angular resolution of the rotation of the PPI sweep vector,[2] that is, the angle of the small but finite step

[1] For a description of other types together with much construction information the reader is referred to Chap. 8 of Vol. 17 of the Radiation Laboratory Series.

[2] The use of this potentiometer in PPI circuit is discussed in Secs. 13·8 and 13·13 of this volume.

with which the PPI vector rotates. This angle varies from 0.17° when two of the brushes are moving normally to the wires, to 0.24° when all four are crossing the wires at 45°.

A simple single-section $RC$-filter is included in the circuit in series with each output lead as shown in Fig. 13·30 in order to suppress potentiometer noise. Both calculations and observations for one-section and two-section filters failed to show any appreciable advantage in using more than a single section. The filter introduces a small delay between the scanner rotation and the rotation of the PPI sweep.

**5·8. Nonlinear Potentiometers.** *Nonlinear Output Signals Obtained by Use of Inherently Linear Potentiometers.*—In Fig. 5·23 two linear
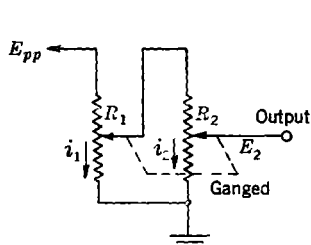


FIG. 5·23.—A means of obtaining an output voltage proportional to the square of a shaft rotation with a dual linear potentiometer. If $R_2 \gg R_1$, $i_1 = \dfrac{E_{pp}}{R_1}$ and $i_2 = \dfrac{E_1}{R_2}$.
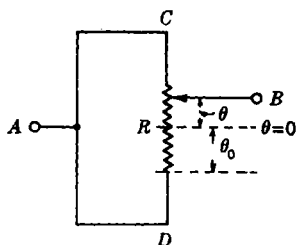
FIG. 5·24.—Method of obtaining a resistance variation proportional to the square of the rotation of the arm of a linear potentiometer.

potentiometers are ganged together, the output voltage of one being the input voltage to the other. If $R_2 \gg R_1$, or if an isolating linear amplifier is inserted between the potentiometers, the output voltage is proportional to the square of the common shaft displacement.

In Fig. 5·24 is shown a method of obtaining a resistance variation proportional to the square of the rotation of the shaft of a single linear potentiometer. If the rotation $\theta$ is measured from the center of the winding of resistance R, the resistance between points $A$ and $B$ will be given by

$$\frac{1}{R_{AB}} = \frac{1}{R_{ACB}} + \frac{1}{R_{ADB}}, \tag{3}$$

where $R_{ACB}$, the resistance above the sliding contact, is $\dfrac{R}{2}\left(1 - \dfrac{\theta}{\theta_0}\right)$; and $R_{ADB}$, the resistance below the brush, is $\dfrac{R}{2}\left(1 + \dfrac{\theta}{\theta_0}\right)$; and $\theta_0$, in turn, is the maximum angle, which corresponds to $R/2$. Expressed as a function of $\theta$,

$$R_{AB} = \frac{R}{4}\left[1 - \left(\frac{\theta}{\theta_0}\right)^2\right]. \tag{4}$$

An application of this "quadratic potentiometer" for approximating the secant function is shown in Fig. 5·25. A simple calculation shows that

$$\frac{E_o}{E_i} = \frac{r_1}{r_1 + r_2\left(1 - \dfrac{\delta^2}{\Delta^2}\right)}, \tag{5}$$

$$\frac{E_o}{E_i} = \frac{r_1}{r_1 + r_2}\left[1 + \frac{1}{2}\left(\frac{2r_2}{r_1 + r_2}\frac{\delta^2}{\Delta^2}\right) + \frac{1}{4}\left(\frac{2r_2}{r_1 + r_2}\frac{\delta^2}{\Delta^2}\right)^2 + \cdots\right], \tag{6}$$

Now,

$$\sec x = 1 + \tfrac{1}{2}x^2 + \tfrac{5}{24}x^4 + \cdots. \tag{7}$$

Comparing Eqs. (6) and (7) it is seen that

$$\frac{E_o}{E_i} \approx \frac{r_1}{r_1 + r_2}\sec\sqrt{\frac{2r_2}{r_1 + r_2}\frac{\delta^2}{\Delta^2}}, \tag{8}$$

the approximation being off about $\frac{1}{24}$ part of the argument to the fourth power. To give an output proportional to sec $\delta$ it is necessary that

$$\sqrt{\frac{2r_2}{r_1 + r_2}\frac{1}{\Delta^2}} = 1.$$

If the maximum angle $\Delta$ is 1 radian and if $r_1 = r_2$, this relation will be satisfied. Under these conditions the circuit shown in Fig. 5·25 gives an approximation to the secant of the shaft rotation good to 1 per cent or better in the range $\pm 40°$.



FIG. 5·25.—Use of linear potentiometer to approximate the secant function.

Figure 5·26 shows another useful circuit using a linear potentiometer to give an output voltage proportional to the reciprocal of the shaft displacement as measured from the proper zero, which is $R_2/k$ less than $\theta = 0$.

From Fig. 5·27 it can be seen that $r = (\theta/\theta_0)(r_0)$, and

$$\frac{E - e}{r_0 - r} = \frac{e}{E} + \frac{E + e}{r_0 + r}. \tag{9}$$

These relations yield

$$\frac{e}{E} = \frac{2R}{2R + r_0}\left(\frac{\theta}{\theta_0}\right)\frac{1}{1 - \dfrac{R}{2R + r_0}\left(\dfrac{\theta}{\theta_0}\right)^2}$$

$$= \frac{2R}{2R + r_0}\frac{1}{\theta_0}\left[\theta + \left(\frac{R}{2R + r_0}\frac{1}{\theta_0^2}\right)\theta^3 + \left(\frac{R}{2R + r_0}\frac{1}{\theta_0^2}\right)^2\theta^5 + \cdots\right]. \tag{10}$$

Now,

$$\tan \theta = \theta + \tfrac{1}{3}\theta^3 + \tfrac{2}{15}\theta^5 + \cdots . \tag{11}$$

Comparing Eqs. (10) and (11) it is seen that if $\dfrac{R}{2R + r_0} \dfrac{1}{\theta_0^2} = \dfrac{1}{3}$, the output

approximates $\tan \theta$ to within $\dfrac{\theta^5}{45} + \cdots$ . If $\theta_0 = 1$ radian, for example,
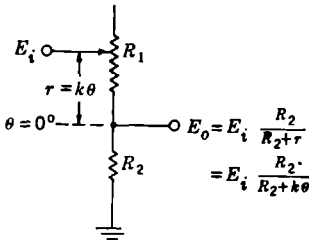
this condition is satisfied for $r_0 = R$.



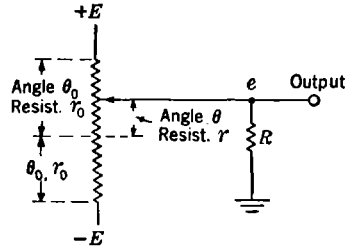FIG. 5·26.—Use of a linear potentiometer to obtain a voltage inversely proportional to the shaft displacement.



FIG. 5·27.—Use of a linear potentiometer to obtain an output voltage approximating the tangent function.

*Nonlinearly Wound Potentiometers.*—Potentiometers are available in which the variation of the resistance between the sliding contact and one end of the winding is a nonlinear function of the displacement of the sliding contact. They are made by winding the cards with variable wire spacing or with wire of variable resistivity, by winding the wire on cards of nonuniform width, or by a combination of these procedures. High-precision nonlinear potentiometers are used rather widely in computing circuits but they have not found much use in data-transmission systems of the type being discussed in this chapter. Only one example of the application of a nonlinear potentiometer will be discussed.
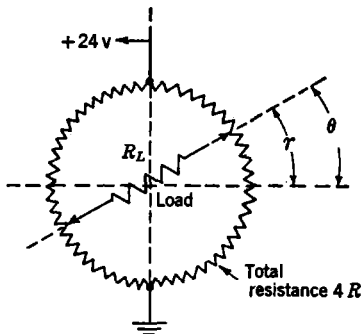


FIG. 5·28.—A nonlinear potentiometer.

This application is for a rectangular display in which azimuth angle is plotted against range (B-scan) and it is desirable that the beam move linearly with the scanner rotation. A direct drive of the azimuth cathode-ray-tube deflection coil is employed in the present case, which is illustrated in Fig. 5·28. The load, represented by $R_L$, "turns through" an angle $\theta$ of $\pm 75°$. It can be shown that, if the current through $R_L$ is to be proportional to $\theta$, the potentiometer must be wound so that

$$\theta = \frac{\pi}{2} \frac{r}{R} \frac{1}{1 + \frac{R}{R_L}\left(1 - \frac{r^2}{R^2}\right)}. \tag{12}$$

If the value of $R/R_L$ were equal to 1, the width of a card that would satisfy Eq. (12) would change by a factor of 7 over a 90° range. Not only would such a tapered card be difficult to wind but it would also be more difficult to approximate with several linear sections (stepped card) than if $R/R_L$ were smaller. From these considerations and from consideration of power drain and power dissipation, the value of $\frac{1}{2}$ for $R/R_L$ was chosen as being optimum. A composition resistance element is not suitable for the present use because manufacturing tolerances are too broad, humidity and temperature would affect it unduly, and it would wear too rapidly.

The potentiometer, as manufactured, is wound with a single size and type of wire with uniform spacing on a toroidal frame (see Fig. 5·29) which is stepped to give a number of linear resistance sections. These different linear sections afford a sufficiently close approximation to the required resistance taper. The production unit has four linear sections in each 90° section.

The potentiometer resistance $R$ was chosen to be 100 ohms. The



FIG. 5·29.—Potentiometer, type RL-B See Fig. 11·16 for an application. *A*, shaft of potentiometer mechanically connected to shaft of scanner; *B*, resistance winding tapered to correct for load of 200 ohms, so that output voltage is linear with respect to angle of rotation of shaft of potentiometer.

load, which should be 200 ohms, is not too critical; the current in $R_L$ departs by an amount equivalent to 1.2° at $\theta = 45$° if $R_L$ is 220 ohms. The brush contacts three or four wires at one time. Other pertinent data are: linearity, 1.8°; 70 wires per inch, 520 wires total; resolution, 0.7°; wire, 0.012-in.-diameter nichrome; torque, 5 in.-oz; maximum voltage, 24 volts; life, $10^6$ cycles.

**5·9. Sinusoidal Carriers.** *General Discussion.*—Generally when a synchro is used as a resolver, the output information is desired in the form of two orthogonal components. When the synchro secondary has a 2-phase winding the output intelligence is in this form. Many of the available synchros have 3-phase windings, however, and although a 3-phase deflecting system can be used, 2-phase output signals are gen-
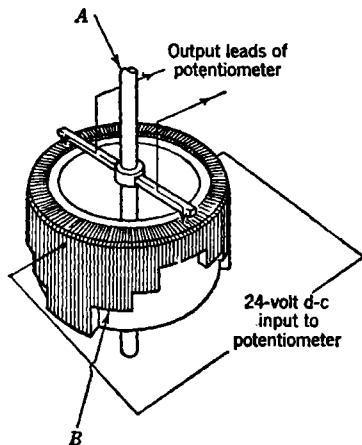
erally required.   Figure 5·30 shows one method in which the desired output signals can be obtained.   The center tap (*C* in Fig. 5·30) is not brought out on any of the standard synchros, hence a center-tapped



FIG. 5·30.—2-phase output from 3-phase synchro.



FIG. 5·31.—Synchro data transmission for 30° quadrant.

resistance must be used.   If the tap *P* is made adjustable, moreover, the cosine output can be shifted a few degrees in phase while the amplitude is kept almost constant.   To get output voltages of the same peak amplitude the transformer should have a voltage stepdown of 1.15 to 1. This procedure is of value as an alternative to a mechanical zero-set

adjustment if only one component is needed.    Three-phase-primary 2-phase-secondary synchros can also be used for this purpose.

A simple data-transmission system designed to operate in one quadrant only (0° to 30° was actually used) is shown in Fig. 5·31.    The synchro stator winding forms part of the 20-kc/sec oscillator tank circuit.    The leads to the synchro were 50 ft long in the system from which this example is taken.    Both the autosyn (at maximum coupling) and the UTC 0–6 are roughly 1:1 transformers.    The 50-$\mu\mu$f condenser across the transformer secondary tunes the transformer to approximately 20 kc/sec,
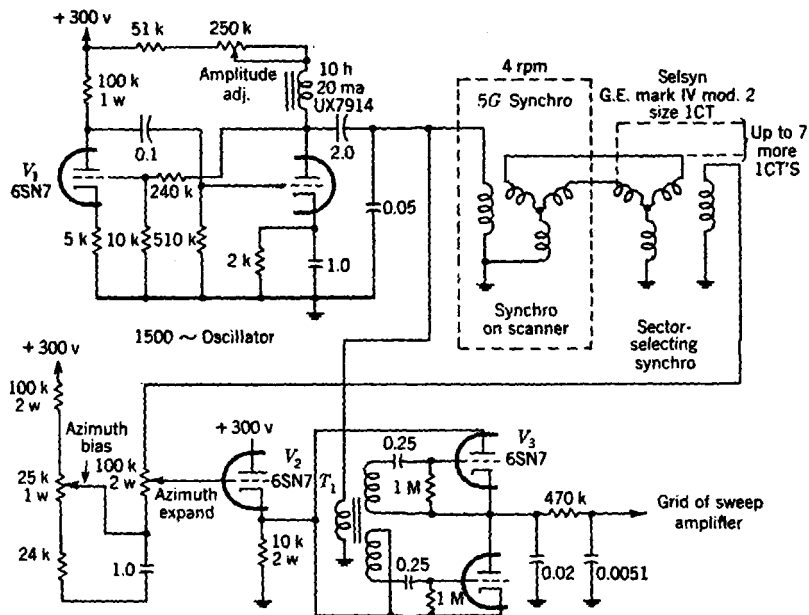


Fig. 5·32.—Synchro data transmission.

and provides a better waveform and somewhat more amplitude than is obtained without the condenser.    The amplitude is substantially independent of frequency over a considerable frequency range.    The maximum angular velocity of the rotor is 150°/sec.    The time constant of the detector is twenty times smaller than the maximum allowable (see Sec. 5·5), and gives a maximum peak-to-peak ripple in the demodulator output of $\frac{1}{4}$ volt or 1 per cent.

A somewhat more complicated example is shown in Fig. 5·32.    The primary of the synchro mounted on the scanner is part of the tank circuit of the 1500-cps two-stage tuned-plate oscillator $V_1$.    The synchro is a Navy 5G synchro designed for 60-cps operation at 115 volts input and

90 volts output. The primary can be operated at 6 watts dissipation. This synchro has an average angular error of 0.2° and a peak angular error of 0.6°.

The secondary output voltage is not utilized directly but is applied to a second synchro,[1] which serves as a sector selector. It may be regarded simply as a transformer. A fraction of the output voltage of the second synchro is applied to the grid of the cathode follower $V_2$. This fraction is chosen by the "azimuth expand" potentiometer to give the desired volts output per degree rotation. The reference d-c level of the output voltage is determined by the setting of the "azimuth bias" potentiometer. The keyed detector comprised of $V_3$ and associated components is the type described in Sec. 5·5.

In this application the scanner turns continuously in one direction and the output information is utilized only during some 50° each side of zero as the output voltage is increasing. During the remainder of the cycle the video signals to the cathode-ray tube are suppressed. The circuit shown in Fig. 11·7 incorporates this method of sector selection.

**5·10. Fundamental Characteristics of Synchros Used as Electromechanical Modulators.**—If a sinusoid is applied to the rotor winding of a synchro, the waveform observed at the stator or output terminals (open circuit) will ideally be a sinusoid of the same frequency as the input waveform but with an amplitude that varies as the sine of the displacement angle between rotor and stator. If the stator has a second winding displaced 90° from the first winding, a second sinusoidal output waveform whose amplitude varies as the cosine of the shaft displacement may be obtained. The two output waveforms may be said to differ in amplitude phase by 90°. The electrical phases of the two output waves and of the input or carrier wave are the same to a first approximation; they differ only in amplitude. For some rotor positions, one or both of the output amplitudes are negative and this condition is equivalent to a 180° shift in electrical phase.

*Angular Accuracy.*—There are several factors to be considered in specifying the accuracy of a synchro. As has been mentioned, the output amplitude should be, ideally, directly proportional to the sine of the angle of rotation of the shaft. The departure of the actual output from such an ideal output gives a measure of the accuracy of the device. The accuracy so measured depends not only on the synchro itself but also on the impedance loading of the stator windings, and upon the amplitude of the input wave because the iron, which is used in the construction of almost all

---

[1] This synchro is a General Electric, Mark IV, Model 2, size 1CT instrument designed for 60-cps operation. With 90 volts on the primary (stator) the maximum rotor voltage will be 55 volts. This synchro is rated at 1.5 watts dissipation; it has average and maximum errors of 0.2° and 0.6° respectively.

synchros, will show saturation effects at high flux densities. Accuracy measurements, to be of much value, must, moreover, be determined with an input source or "driver" of the same impedance characteristics as that to be employed in any given application. Since synchros have both leakage inductance and distributed capacitance that, in general, depend on shaft position, the frequency chosen for the carrier, or the harmonic components of a complex-waveform carrier, will have a determining effect on the accuracy.

The accuracy is sometimes stated as an angular error: namely, the difference between an actual shaft displacement and the displacement that would ideally give the observed output. The angular errors observed frequently show a tendency to vary periodically with shaft rotation. For example, they are a maximum at 60° intervals for most 3-phase synchros. The absolute accuracy obtainable varies widely, being confined to less than $\pm 0.1°$ in the case of the Bendix AY-100 Autosyn and being as large as $\pm 7°$ for an Army Mark XVII synchro. If a synchro is improperly used, much larger errors may result.

The nature and magnitude of the angular error, in so far as it is determined by the synchro itself, is dependent on numerous design factors. Some of the most important are the number of poles on the stator and rotor, whether or not the slots are diagonal, the uniformity of the stator-to-rotor air gap, the method in which the coils are wound and the degree to which they are matched, and the degree of magnetic isotropy of the iron.

*Generator Effect.*—A synchro is not basically different in construction from a generator. Therefore, if the primary current has a d-c component, there will be superimposed on the desired output voltage a component of the output voltage proportional in magnitude to the speed of rotation. This effect cannot be ignored for applications involving relatively fast shaft rotations.

It might be mentioned that the quality of the display is dependent indirectly upon the angular velocity and acceleration of the electromechanical data-transmission device, as determined by the transient response of the associated circuits.

*Waveform Distortion.*—The previous paragraphs discuss errors that are characteristic of synchros considered as rotating devices. Synchros must also be considered as transformers when their performance is evaluated. The transformer affects the waveform in several respects other than amplitude, frequently in ways that are independent of rotor-stator displacement. Because of the leakage inductance between rotor and stator and because of distributed capacitances, an induced sinusoid will, in general, be shifted in phase with respect to the primary sinusoid. This consequence is of importance in some applications. Complex

waveforms, such as a triangular wave, will be distorted on passing through a synchro in a way dependent on the frequency-response characteristics of the device and on the amplitude of the waveform.   Waveform distortion is, of course, dependent upon output loading and driver characteristics as well as on the synchro itself.

*Applicability.*—Because of their sinusoidal angular response, synchros are particularly adapted to the role of resolvers, that is, to produce output voltages proportional to the sine and cosine, respectively, of the angular shaft displacement.

They can be used as data-transmitting devices in cases where the required electrical signal is some function other than the sine or cosine of the primary mechanical displacement.   One method is to use a nonlinear mechanical link preceding the synchro, for example, a suitable cam arrangement on the synchro shaft.   Another is to synthesize the required electrical signal from the available sinusoids.   For example, an electrical output approximately proportional to the shaft rotation may be obtained by using two synchros.   One synchro is driven in harmony with the mechanical signal $\theta$, the other as $2\theta$, and both are driven with a constant-amplitude carrier.   The output voltage of the first synchro less $\frac{1}{8}$ that of the second gives a composite signal

$$
\begin{aligned}
e_o &= (A \sin \omega t) \ (\sin \theta - \tfrac{1}{8} \sin 2\theta) \\
&= (A \sin \omega t) \left( \frac{3}{4} \theta - \frac{\theta^5}{40} + \cdots \right),
\end{aligned} \tag{13}
$$

where $A$ is a constant.   It is seen that $e_o$ is a linear function of $\theta$ to within 1 per cent for values of $\theta$ up to 42°, whereas $\sin \theta$ departs from $\theta$ by 1 per cent at 14°.

A related method useful for obtaining a tangent relationship is illustrated by the following example.   Suppose there are two synchros, as above, the second being geared to have twice the angular displacement of the first.   Let the input voltage to the second be a constant-amplitude carrier.   If the output voltage of this synchro is added to a carrier voltage of the proper constant amplitude and the sum applied to the first synchro, it may be shown that the output voltage of the first synchro has an amplitude proportional to the tangent of its shaft displacement accurate to 1 per cent at 30°.

Another method, which is possible for certain applications, is to distribute the rotor and stator windings in such a way as to make the synchro output voltage the desired function of shaft rotation.

**5·11. Fundamental Characteristics of Variable Condensers Used as Electromechanical Modulators.**—A variable condenser, used generally as part of a voltage-divider circuit, can serve as a modulator to change a

mechanical signal into an electrical signal.[1]   The simplest and most common case is illustrated by $C_1$ and $C_2$ in Fig. 5·34a.   If an alternating voltage signal $e_1$, such as a sinusoid, is applied across $C_1$ and $C_2$ in series and the output voltage $e_2$ taken across $C_2$, then

$$\frac{e_2}{e_1} = \frac{C_1}{C_1 + C_2}.$$   (14)

Let the desired output signal be a function of $\theta$, the shaft rotation of the variable condenser, expressed by

$$e_2 = [A + kf(\theta)] \frac{e_1}{2A}.$$   (15)

Equation (14) shows that this output signal will be obtained if

$$C_2 = C_1 \frac{A - kf(\theta)}{A + kf(\theta)}.$$   (16)

The way in which $C_2$ depends on $\theta$ is determined by the shape and size of the condenser rotor and stator plates.   In designing a condenser for a precision application, edge effects must be considered and particular care must be given to the mechanical design.[2]

The variable condenser as a position-data-transmission device has some advantages and some limitations when compared to other electromechanical devices.   For applications where the angular speed is high, condensers are decidedly better than potentiometers and are better than most synchros, almost all of which have been designed for low-speed operation.   The condensers, which in almost all applications to date have been designed specifically for the job in question, are built to withstand high accelerations.   They withstand shock, vibration, humidity, and long use very well.   Unlike synchros, they can readily be designed to give almost any desired variation of output voltage as a function of shaft rotation.

A variable condenser, if it is to be kept to a reasonable size and be of good mechanical design, cannot have a maximum capacitance greater than a few hundred micromicrofarads.   Because of the small capacity of the device, considerable care must be exercised in the wiring, and the use of short leads to and from the condenser is almost imperative.   Stray and lead capacitances may cause undesirable variations of output voltage with angle and will result in attenuation of the output signal.   Because of the necessity of having the carrier generator and the detector close to the condenser, and because the manufacture of suitable variable con-

---

[1] See Vol. 19, Chap. 11 of the Radiation Laboratory Series.

[2] Chap. 9, of Vol. 17 of the Radiation Laboratory Series discusses the design problems in detail.

densers is very expensive, the variable condenser as a data-transmission device is generally less satisfactory than a potentiometer or a synchro.

**5·12. Use of a Condenser Modulator with a Sinusoidal Carrier.** *General Discussion.*—It is possible with condensers, as with synchros, to use any a-c waveform as the input signal. For example, for a PPI display a variable condenser may be used either with a pre-time-base-resolution system or with a resolved-time-base system (see Sec. 13·9).
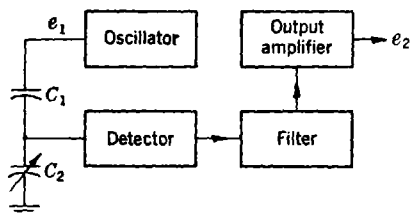


Fig. 5·33.—Block diagram of a condenser-divider data-transmission system.

Either the pre-time-base-resolution method or a combination of the two methods is almost always used because any practicable condenser divider presents a very high impedance to the lower frequencies that are present in most time-base waveforms.

Figure 5·33 shows a block diagram of a data-transmission system employing a sinusoidal carrier wave. In the way in which the condenser is generally driven by the oscillator (for example, Fig. 5·3*f*) the frequency shifts somewhat as $C_2$ is varied, but if the circuit has a fairly high "$Q$" the amplitude will remain constant. This slight frequency shift is of no consequence in most applications.

Two push-pull condenser networks are shown in Fig. 5·34 in which the total capacitance, and hence the frequency, does not change. The



Fig. 5·34.—Push-pull condenser voltage divider.

capacitances are designed to follow the relationships

$$C_2 = C_1 \frac{B + kf(\theta)}{A - kf(\theta)}, \tag{17}$$

$$C_2' = C_1 \frac{B - kf(\theta)}{A + kf(\theta)}, \tag{18}$$

where $A$ and $B$ are constants, giving output voltages

$$e_2 = [A - kf(\theta)]\left(\frac{e_1}{A + B}\right),$$

$$e_3 = [A + kf(\theta)]\left(\frac{e_1}{A + B}\right). \tag{19}$$

The total capacitance $C_T$ is

$$C_T = \frac{C_1C_2}{C_1 + C_2} + \frac{C_1C_2'}{C_1 + C_2'} = C_1\frac{2B}{A + B}, \tag{20}$$

and is seen to be constant.   The analysis shows that equations of the form of Eq. (19) hold for both Figs. 5·34a and 5·34b.   Network b is generally preferred in practice because cable and other stray capacitances from the output terminals to ground are generally much larger than the stray capacitance between input and output terminals.   Stray capacity across the output terminals of network b may simply be considered as part of $C_1$.   Experience with a push-pull network of this type led to the conclusion that in practice it would not be capable of the accuracy of a single divider primarily because of the great difficulty of accurately aligning the two variable condensers.



Fig.  5·35.—Condenser-divider network.

The condenser network shown in Fig. 5·35 has been found useful for producing output voltages that are certain nonlinear functions of condenser-shaft rotation.   For this network

$$\frac{e_o}{e_i} = \frac{C_1}{C + C_1 + C_2}, \tag{21}$$

from which $e_o$ as a function of $\theta$ may be determined when $C$ as a function of $\theta$ is specified.   Bendix condenser No. 74747-1 for which $C = A + k\theta$ has been used in this way to produce a desired nonlinear output.   In one such production application, $C_1 = 122$ $\mu\mu f$, $C_2 = 194$ $\mu\mu f$, and $C$ varies linearly with $\theta$ from nearly 0 to 110 $\mu\mu f$.   Other condenser networks with still different characteristics can be used.   A condenser for which $f(\theta)$ in Eqs. (17) and (18) is $\sin \theta$ has been designed but not put into production.[1]

*Example.*—Two condensers have been designed which yield an output voltage for which $f(\theta)$ in Eq. (15) is linear in $\theta$, that is,

$$e_2 = A + k\theta. \tag{22}$$

One is Bendix OAR 971-30-1; the other is Rauland CV-11.   The following data pertain specifically to the latter: Temperature coefficient of

[1] See Chap. 9, Vol. 17, of the Radiation Laboratory Series.

capacitance is 100 parts per million per degree centigrade; output voltage is linear to $\pm\frac{1}{4}$ per cent; the condenser is operable from $-40°C$ to $+70°C$ and with 95 per cent humdity at $45°C$; it withstands the salt-spray test, 10g-shock test, and 0.03-in. amplitude of vibration from 10 to 55 cps. It is designed for 400 volts rms input. It will last for 10,000 hr at speeds in the range from 10 to 2000 rpm, and it requires 4 in.-oz of torque. It
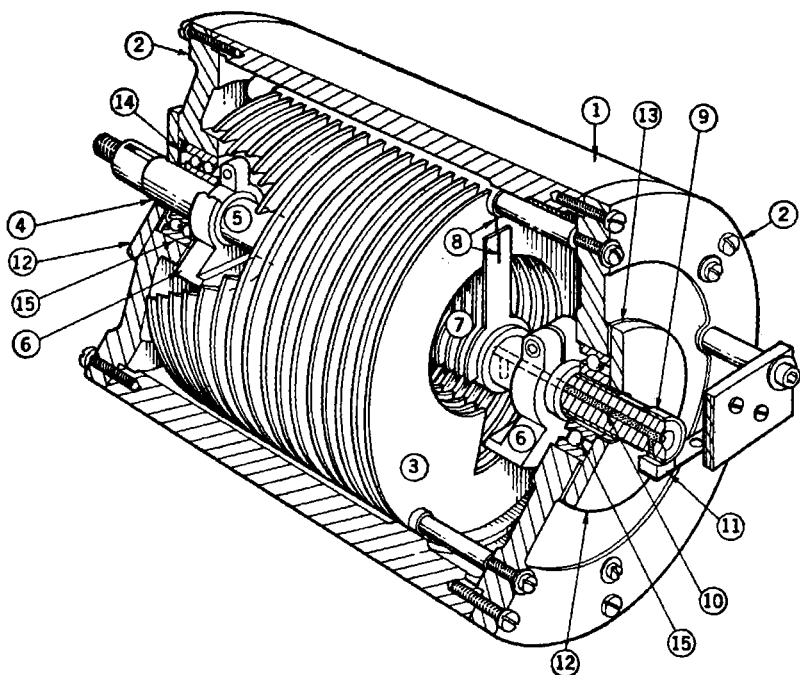


FIG. 5·36.—Rauland CV-11 sweep condenser: (1) housing; (2) end plates; (3) stator plate assembly; (4) stub steel driving shaft; (5) ceramic main shaft; (6) counterweights; (7) rotor plate assembly; (8) index marks for zeroing rotor; (9) slip ring; (10) solder connection from slip ring to stator plates; (11) brush; (12) bearing retainer plates; (13) shims for longitudinal rotor position adjustment; (14) loading spring; (15) ball bearings.

is constructed (see Fig. 5·36) of 17 fixed, and one adjustable, stator plates that are 0.160 in. $\pm 0.001$ in. apart, and of 17 rotor plates, each plate being 0.04 in. thick. The capacitance varies from 50 to 200 $\mu\mu f$ in the usable 320° of rotation. Mechanically the shaft turns continuously.

In Fig. 5·37 is shown a circuit that makes use of a condenser divider that satisfies Eq. (22). The condenser divider forms part of the tank circuit of the 1-Mc/sec Hartley oscillator $V_1$. The peak-to-peak output of 575 volts does not change appreciably even when the heater supply changes over the range from 4 to 8 volts. The tank circuit and all

radiating components including $V_1$ are shielded in copper, and the entire oscillator is mounted only a few inches from the variable condenser and is connected to it by a shielded cable. The trimmer condenser $C_1$ is adjusted so that $C_1$ plus $C_2$ is equal to $C_3$ plus the stray capacitance (about 15 $\mu\mu f$) for $\theta = 0°$. The proper adjustment is ascertained by comparing the observed output vs. angle curve with the calculated curve.

The 6SL7 $V_2$ and $R_1$ and $C_4$ serve as a detector. The shift in d-c level of the output voltage with heater voltage for a 6SL7 is only about half that observed with a 6SN7. Tube $V_3$ is a cathode follower that affords the low output impedance necessary in this case to drive the several feet of cable to the indicator circuits. Both the detector and the
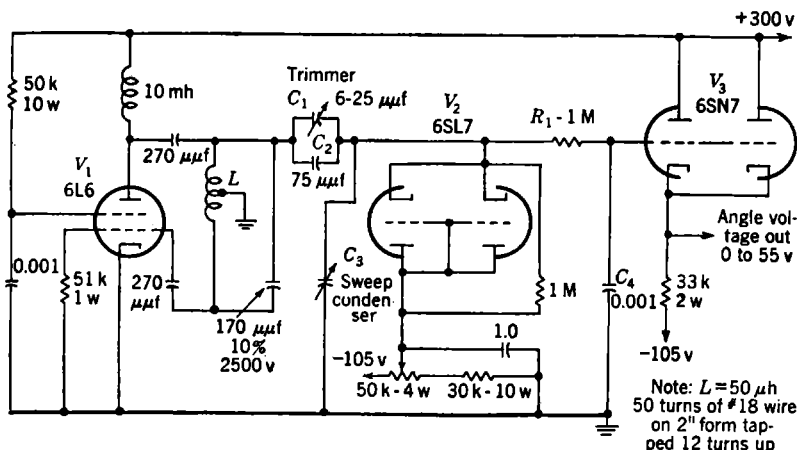


FIG. 5·37.—Angle-voltage generator.

cathode follower are mounted very close to the slip rings of the variable condenser to minimize the stray capacity. With the Rauland condenser in use the output voltage varies from 0 to $\pm 55$ volts for a variation in shaft rotation from $-160°$ to $+160°$.

The calculated peak-to-peak carrier ripple in the output is less than 0.05 volt and the calculated phase shift for 10 rps is about 4°. Since, in this particular application, the condenser is geared up 32 to 1 with respect to the scanner, this delay is permissible. Replacing $R_1$ by a 0.25 henry choke reduces the phase shift to 0.02°.

**5·13. Resolved-time-base Applications Using Condensers.** *General Discussion.*—If a time-base waveform is to be attenuated by a condenser divider, frequencies as low as the repetition rate of the time base must be passed. With available condensers and for ordinary radar applications, the divider must have an impedance of about a megohm for the low-frequency components. At this level, leakage resistance becomes partic-

ularly troublesome. Consequently, variable condensers are unsuited for most resolved-time-base applications of the type commonly employing synchros. Laboratory models have, however, been constructed. Another laboratory system that used a synchro and a sinusoidal condenser in parallel as a resolver for a PPI system was tried. The system worked satisfactorily, but it was felt that a lower-inductance synchro was better for the fast sweep waveforms in question.
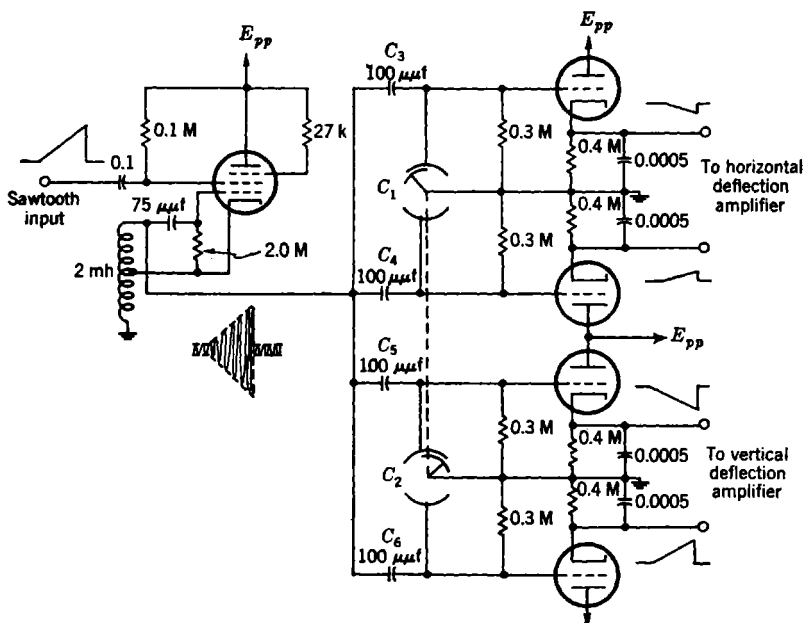


Fig. 5·38.—Circuit of resolved-time-base PPI using a condenser for data transmission.

*Use of a High-frequency Carrier.*—Resolved-time-base systems that employ high-frequency carriers have been built and have performed satisfactorily. Figure 5·38 shows the schematic diagram of a PPI data-transmission system using Cardwell-type sinusoidal condensers. Section $C_1$ is the cosine condenser, and $C_2$, the rotor of which is 90° out of phase with that of $C_1$, is the sine condenser.

Section $C_1$, together with $C_3$ and $C_4$, constitutes a push-pull voltage-divider network similar to that shown in Fig. 5·34. For the Cardwell condenser, $C_1 = A + k \sin \theta$ and $C_1' = A - k \sin \theta$. From Eq. (14) it is seen that the difference in the output voltage is

$$e_3 - e_2 = e_1 \frac{2kC_1 \sin \theta}{(C_1 + A)^2 - k^2 \sin^2 \theta}. \tag{23}$$

If $C_1$ is about 10 times as large as $k$, the $\sin^2 \theta$ term introduces a departure from true sinusoidal push-pull output of less than 1 per cent. A cosine output is similarly obtained from $C_2$ with $C_5$ and $C_6$. In order that a balanced output signal may be obtained, $C_3$, $C_4$, $C_5$, and $C_6$ may be made adjustable. The input waveform is a modulated sinusoid of about 2-Mc/sec frequency.[1] The envelope of the waveform is a sawtooth wave and the modulation is accomplished by applying a triangular wave to the screen of the oscillator.[2] An automatic amplitude-control circuit has been used successfully with this oscillator, the control voltage being applied to the suppressor grid. The detectors are bypassed cathode follower circuits. The output signals are push-pull sawtooth waveforms varying in amplitude as the sine and cosine of the condenser-shaft dis-
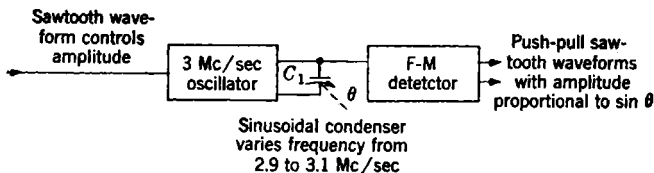


FIG. 5.39.—Modulation of sawtooth waveform by means of sinusoidal condenser.

placement. The circuit shown, together with suitable auxiliary circuits and equipment, gives a PPI presentation of suitable quality for shaft rotations as high as 30 rps. Additional intelligence can be transmitted by frequency modulation of the carrier.

*Frequency-modulated-carrier Examples.*—Figure 5.39 is the block diagram of another system of the resolved-time-base type which employs a carrier; in this case, the carrier is amplitude-modulated by a sawtooth waveform as in the previous example and also frequency-modulated by the variable condenser. A frequency-sensitive detector produces push-pull sawtooth waveforms of amplitude proportional to the frequency deviation and, since the frequency varies linearly with $C_1$, proportional to $\sin \theta$. Since the output is proportional to the input amplitude also, the wave shape is preserved. Such a circuit can be used in the generation of a B-scan presentation (no amplitude modulation), or together with another similar unit with the condenser shifted 90° in phase, to produce a PPI display. Such a system performed satisfactorily in a laboratory test.

**5.14. Generators.**—Generators have been used in two different ways as data-transmission devices. In some applications the generator is used as a tachometer: the output voltage, whose amplitude is proportional

---

[1] Linear electrical modulation is assumed. See Vol. 19, Chap. 12 of the Radiation Laboratory Series.

[2] See Vol. 19, Chap. 11 of the Radiation Laboratory Series.

to the speed of the driving source, is most often utilized by the so-called "triggered" display system to be discussed in Sec. 5·17. The other way in which a generator may be employed makes use of the fact that, for constant angular velocity, the output voltage of an a-c generator varies sinusoidally with shaf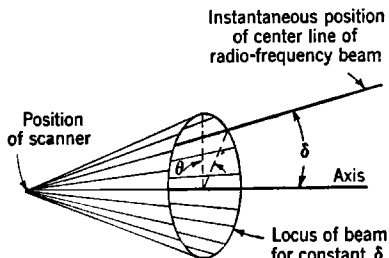t displacement. In an application of the first kind the intelligence is conveyed by the amplitude of the output waveform. This amplitude is a measure of the shaft speed and is used as a means of compensating for variation in shaft speed. In contrast to this, if a generator is employed in the second way, it is assumed that either the angular velocity is constant, in which case the instantaneous value of the output voltage is proportional to the sine of the shaft displacement, or any variation in rate is compensated.



FIG. 5·40.—Geometry of conical scanning.

A simplified version of a radar application of the second (displacement information) method is illustrated in Figs. 5·40 and 5·41. In this instance the radio-frequency beam is rotated at 20 cps making a small angle $\delta$ with respect to a fixed axis, the locus of the "pencil" beam thus tracing out a
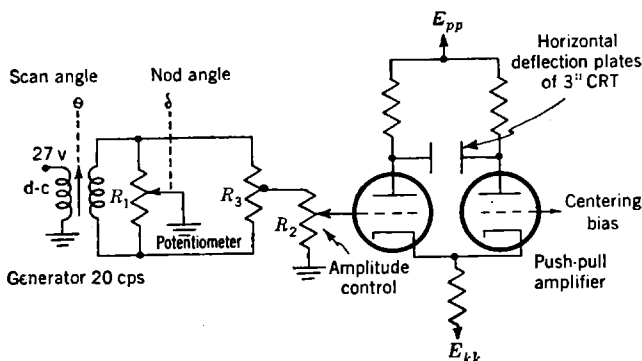


FIG. 5·41.—Data-transmission system using a generator and potentiometer.

cone. The received radar signals are presented as an azimuth angle vs. range, or B-scope. The azimuth position of the beam is $\delta \sin \theta$ measured from a vertical plane passing through the axis of the conical scan. The output of the generator, mounted to rotate as $\theta$, is proportional to $\sin \theta$, and, for a fixed value of $\delta$, therefore, to $\delta \sin \theta$, the azimuth angle.

In order to search all the space lying within an angle $\delta_0$ of the axis, within the range of the set, the angle $\delta$ is continuously varied between

limits of $+\delta_0$ and $-\delta_0$. The amplitude of the cone half-angle $\delta$ goes through one complete cycle in about 4 sec. The fact that $\delta$ actually goes negative means that the phase of the generator output curve must be effectively shifted by 180° each time the amplitude goes through zero. The amplitude of the output sine wave is varied proportionally to $\delta$, and cognizance is taken of the sign by means of the linear potentiometer $R_1$. When $\delta$ is zero the potentiometer winding is grounded at the center. The output from the center-tapped resistor $R_3$ is zero under these circumstances. The amplitude of the output waveform increases linearly with $\delta$ as the brush of $R_1$ moves downward, and reaches a maximum when the lower end of the potentiometer is grounded. As the brush moves in the opposite direction the amplitude increases, approaching the same maximum value but with the phase changed by 180°.
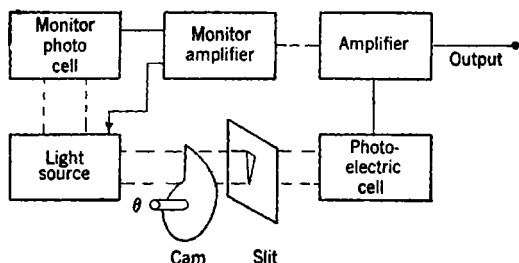


FIG. 5·42.—Electromechanical data-transmission system consisting of a cam and photoelectric cell.

Both a permanent-magnet-field and a d-c excited-field generator[1] have been used in this application. The output waveform shows a variation from sinusoidal shape indicative of the number of poles of the generator. A 1-$\mu$f filter condenser across the generator output terminals has sometimes been used. The generator output is about 60 volts rms at 20 cps.

**5·15. Photoelectric-mechanical Data Transmission.**—An electromechanical data-transmission system that has been used in experimental systems consists of a cam turned by a shaft (the mechanical signal) that modulates the light falling on a photoelectric cell,[2] which, in turn, produces an electrical signal. Such a system is illustrated in Fig. 5·42.

One such system employed a "constant"-intensity light source, a lens system for controlling the light beam, and an RCA 929 high-vacuum photoelectric cell. The output voltage of this photoelectric cell is very nearly proportional to the light intensity. Since it was required that the

[1] Production generator is type 1401 made by Electrical Engineering and Manufacturing Co., Los Angeles.

[2] John Strong, *Procedures in Experimental Physics*, Prentice-Hall, New York, 1939, Chap. 10.

output voltage indicate the shaft position even when the shaft was at rest, a direct-coupled amplifier had to be used. Considerable difficulty was encountered in making an amplifier with an output that did not "drift" excessively.[1] A monitor photoelectric cell was used to obtain a signal proportional to the intensity of the light source. Such a signal could be used to vary the gain of the amplifier and thus compensate completely for light-intensity fluctuations. In this case, however, the monitor signal and the main signal were the two input signals to a differential amplifier; the output for a given (midrange) value of $\theta$ was thus kept fixed. Another, and generally a better, method of monitoring is to control the light intensity in accordance with the monitor output to make that output a given value.

In a second laboratory model neither a lens nor a monitor was employed; an a-c amplifier was used. The use of an a-c amplifier requires that the cam be rotating (600 rpm normally), but the use of an intermittent light source obviates this difficulty.

For certain applications, the photocell compares favorably with other electromechanical devices. It has the advantage that the cam can be cut to give almost any desired functional relationship between the rotation angle and the output signal. Inherently it is capable of applications analogous to those using a "d-c carrier" (a constant-intensity light source), a sinusoidal carrier (intermittent light source), or to resolved-time-base applications (light intensity controlled by a time base).

### SYNCHRONIZED TRANSMISSION OF ANGULAR DATA

In almost all of the foregoing discussion the remote signal was derived directly from the primary signal by mechanical or electromechanical devices. In applying such techniques the primary signal is generally thought of as being an independent variable and the remote signal as being a dependent variable. In some cases, however, both the primary and the remote signal may be considered dependent; dependent, generally, on time. Two techniques have been used in such cases. One is the use of synchronous motors to drive the primary shaft and the remote shaft; the other is the use, as the remote signal source, of an electrical circuit giving an output signal that varies in time in some prescribed way in synchronism with the primary signal, which is assumed to be a prescribed function of time. In both applications, generally the only data actually "transmitted" is a synchronizing signal.

**5.16. Synchronous Motors.**—A means of synchronizing the rotation of two shafts is by the use of synchronous motors, an example of which is shown in Fig. 5.43. Its advantages are very light weight, high accuracy for continuous rotation, and the lack of necessity for an auxiliary ampli-

[1] See Chap. 11, Vol. 18 of the Radiation Laboratory Series.

fier. On the other hand, it is difficult to phase the motors initially, and any slipping of the motor or momentary loss of power requires rephasing of the entire system. In the example shown, the switch is manually adjusted until the antenna and the rotating coil are in phase. Because the phasing feature of this system is not positive, the system is very rarely used. Another disadvantage of this method is its inability to sector scan with any accuracy.

**5·17. Triggered Circuits.**—If the primary signal is a function of time which repeats itself periodically or upon the reception of a triggering or initiating signal, then a remote electrical signal can be derived from an appropriate waveform generator that oscillates or that is triggered in synchronism with the primary signal. For example, if the primary signal is the displacement angle of a uniformly rotating shaft, an electrical
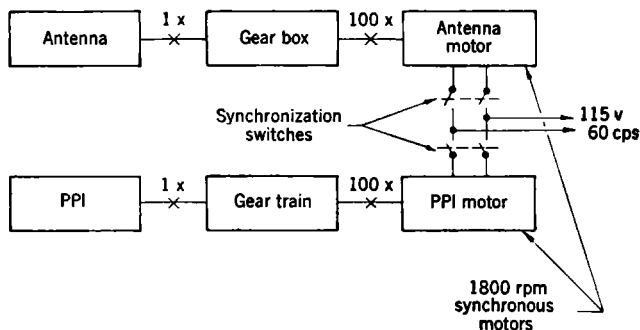


FIG. 5·43.—Synchronized data transmission with synchronous motors.

signal proportional to this displacement can be derived from a sawtooth generator that is triggered by a synchronizing signal from a switch operated by a cam on the shaft. The duration of the sawtooth waveform must be somewhat shorter than the period of the shaft rotation.

*Methods of Triggering and Gating.*—Several methods have been employed for obtaining the synchronizing signal, and two types of synchronizing signal have been employed. One type of synchronizing signal is a trigger or initiating pulse (Figs. 5·44b or c) which serves to start the waveform generator. The other is a gating or switching waveform (Fig. 5·44d) which is a signal having one value for the duration of the required voltage waveform and another value for the rest of the time.

When the trigger pulse is obtained from a switch controlled by a cam on the shaft, the closing or opening time of the switch, or of a relay controlled by it, is of the order of magnitude of a few milliseconds—which is too long for many applications. Another disadvantage is that it is often inconvenient to use cams and switches because proper adjustment is generally difficult.

A disk containing a magnetic "slug" may be fixed to the shaft in question.   A signal derived from a coil held near the surface of the disk can be used to synchronize the waveform generator with the shaft rotation.   The waveform of the pulse, shown in Fig. 5·44b, has an amplitude proportional to the shaft speed and consists of both a positive and a negative part.   It is not very steep at any part, and therefore it is difficult to derive a "jitter free" narrow synchronizing pulse from the coil output.
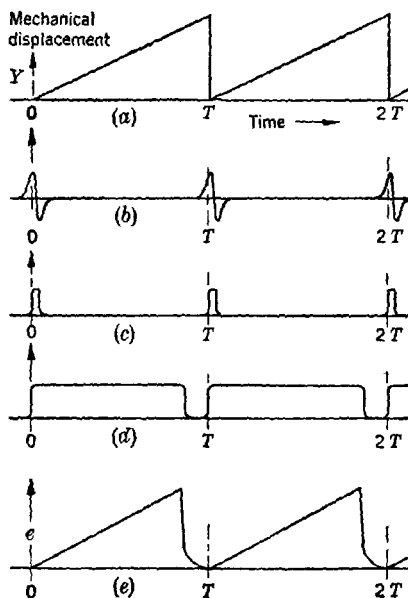


Fig. 5·44.—Some waveforms illustrating triggered-circuit data transmission.

A third method consists of a rotating slotted disk or cam that interrupts a beam of light to a photocell.   This method (see Sec. 6·2), which is the most suitable for most applications, can give either a synchronizing pulse (Fig. 5·44c) or a switching waveform (Fig. 5·44d).   The output signal is, moreover, independent of shaft speed and has a faster rise time than the voltage waveform obtained with the magnetic-slug method.

The output-signal waveform generator must be turned off in time to allow adequate recovery of the circuit before the initiation of the next cycle.   If a gating waveform is used, the shutoff is automatic.   If pulses are used, the shutoff can be effected by a second pulse derived in the same manner as the first, or by an automatic timing circuit at a fixed time after the start.

*Use of a Tachometer.*—The output signal waveform $e(t)$ (Fig. 5·44e) will have a value at any time which is proportional to the mechanical displacement $y(t)$ of the shaft only if both $de/dt$ and $dy/dt$ are constant or vary proportionally. If the mechanical system is such that $dy/dt$ cannot be held constant within the desired limits, a tachometer generator can be connected to the shaft and its output can be used to modulate the slope or amplitude of the time-base waveform.

Figure 5·45 shows the circuit used in one experimental system employing a d-c tachometer generator to correct for rate variations. The gener-
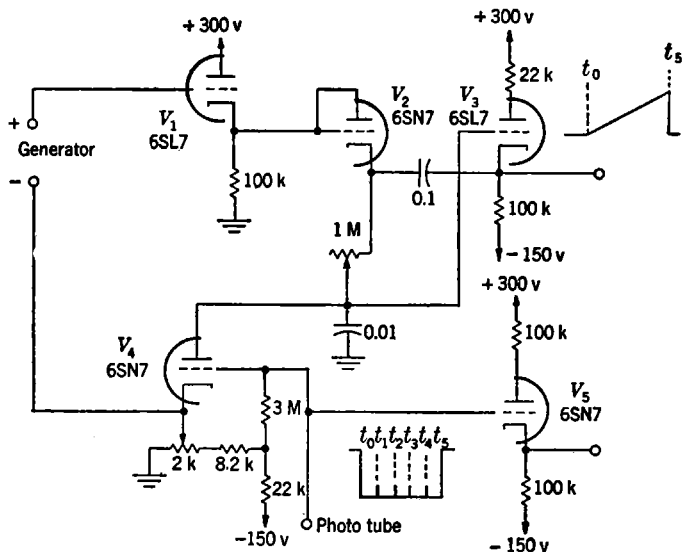


FIG. 5·45.—Triggered data-transmission circuit using tachometer generator and phototube blanking disk.

ator is geared to turn at five times the cam shaft speed, the latter being about 10 rps. The positive generator output is applied to the cathode follower $V_1$. Tubes $V_2$ and $V_3$ and the associated parts form a "bootstrap" sawtooth-generator circuit (see Sec. 4·6). The slope of the output sawtooth waveform is proportional to the initial current flowing through the 1-megohm resistor. This current, in turn, is proportional to the generator output voltage since $V_4$ is conducting before the start of the sawtooth waveform. Thus, if the speed of rotation increases, the sawtooth slope increases proportionately. The voltage waveform on the grid of $V_4$ is shown. The time from $t_0$ to $t_5$ is the duration of the sawtooth, and the bias on the cathode of $V_4$ is adjusted so that the tube is nonconducting from $t_0$ to $t_5$. The cam that interrupts the light beam

introduces smaller modulations of the light intensity at regular intervals. The corresponding fluctuations in output voltage are below the cutoff potential for $V_4$ but are present in the output of $V_5$. These signals serve to brighten the trace on the associated cathode-ray-tube display and thus produce angle marks. The switching signal from $V_4$ serves, through circuits not shown, to blank the cathode-ray tube beam from $t_5$ to the next $t_0$.

# CHAPTER 6

## ELECTRONIC MARKERS AND INDICES

### By H. O. Marcy, III

**6·1. Introduction.**—A display index is commonly a line indicating a particular value of a function that may or may not be one of the coordinates of the display. Either a number of indices that allow interpolation, or a single movable index may be employed. The latter is especially convenient for automatic data transmission. In general, it is desirable that the indices be more sharply defined and more accurately fixed than the particular signal to be evaluated. For example, a sharp line may be used to bisect a broad signal with an error of less than one-tenth the width of the signal.

Overlays are the simplest means for applying indices to a display (see Sec. 16·5). They consist of dark lines or illuminated scratches engraved on a transparent plate placed directly in front of the display tube. They are not always satisfactory because parallax errors are usually present, and because it is essential that the display be stable in position and size in spite of line-voltage or tube-characteristic fluctuations. Greater accuracy can usually be achieved by the use of electronic indices, which appear in the display area as brightened lines or dots, because these may be made independent of any variability or distortion in the display and are not subject to parallax. Unfortunately, circuits for the generation of electronic markers are often costly and complex.

With most two-dimensional displays, scanning is much more rapid in one coordinate than in the other. The B-scope of a radar display is an example of a cartesian-coordinate display with the fast scan in the $y$-coordinate representing range, and the slow scan in the $x$-coordinate representing the azimuth angle of the antenna. As the x-scan progresses across the tube, the y-scan, sweeping successively across, forms a series of parallel slanting lines. All values of $y$ are covered in each y-scan, but only discrete values of $x$ are displayed for each x-scan, the separation of the lines being determined by the ratio of the scanning repetition rates of $x$ and $y$. An index for a particular value $y_1$, made by intensifying each y-scan for a short interval at the value $y_1$, will then appear in the display as a row of brightened dots as shown in Fig. 6·1a. On successive x-scans, when there is no synchronization between the $x$ and $y$

repetition rates, this row of dots will move bodily to the right or left at random and the dots will merge into a smooth line because of the persistence of the observer's vision or of the screen.   The vertical width of the
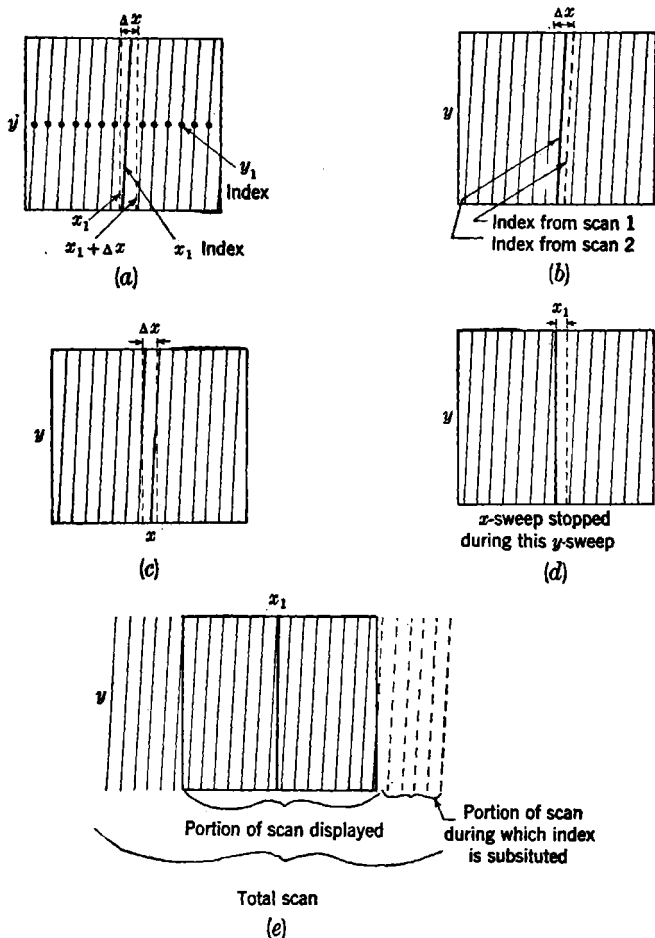


FIG. 6·1.—Diagram of a cartesian-coordinate display.

line depends only on the steadiness of the y-scan and on the interval of time during which each scan is intensified.

An index for a particular value $x_1$, on the other hand, is more difficult to obtain with a clean-cut appearance, especially when the separation of y-scans is large.   In this situation the value $x_1$ may fall where no y-scan is present during a given x-scan, but is present during the next

x-scan because of the random relation between the $x$ and $y$ repetition rates. This fluctuation will cause the index to fade in and out of view or to flicker in an annoying manner. The difficulty can be avoided by broadening the index to include values of $x$ from $x_1$ to $x_1 + \Delta x$ where $\Delta x$ is greater than the separation between successive y-scans. In this way, there is certain to be a y-scan during the intensified portion of each x-scan, but such broadening of the index can introduce other defects if $\Delta x$ is much more than the spot size of the cathode-ray beam. The random position of the y-scan in the interval $\Delta x$ may cause the intensified line to move about from one x-scan to the next (Fig. 6·1b) or the intensified line may start in the middle of one y-scan and continue into the next (Fig. 6·1c). With a persistent screen, these effects may not be noticed individually, but they do cause the index to waver and to appear defocused.

To avoid these difficulties, it is possible to stop the x-scan at $x_1$ until there is a complete y-scan (Fig. 6·1d). After the index has been formed, the x-scan is made to catch up to its correct position.

Another method of generating slow-scan indices, useful with persistent cathode-ray-tube screens, is to remove the normal x-scan and momentarily replace it by substitution of the single value $x_1$. The fast y-scans are allowed to continue and may be intensified to give a bright line index of value $x_1$. This method may be used to advantage if a portion of the slow-scan cycle is not used. An example is an expanded display in which only a portion of the x-region observed by the scanning device is displayed on the tube. During the undisplayed part of the scan a relay may switch the presentation to the particular value $x_1$ of the index. Figure 6·1e shows this diagrammatically. If all of the scan should be displayed, a sacrifice of duty ratio is necessary.

**6·2. Slow-scan Indices.**—These indices may be subdivided into two classes, flashing indices and substitution indices. To obtain flashing indices the fast sweep may be intensified in one of several ways.

*Mechanical Switching.*—Figure 6·2 shows the generation of an angle mark on a PPI display by the use of a cam coupled to the device that rotates the position of the radial sweep on the cathode-ray tube. At the proper position the cam closes a microswitch which, in turn, actuates a two-circuit relay. As soon as the first relay closes, it energizes a second relay. This relay opens the circuit that was closed by the first relay. The net result, shortly after the microswitch is closed by the cam, is a circuit closed during a short interval that is determined by the "actuation time" of the second relay. This closed circuit is used to change the grid bias of the cathode-ray tube in such a way that the trace is brightened. The duration of the angle mark is determined only by the actuation time of the second relay and is independent of the shape of the cam. By the choice of a suitable relay, the interval may be varied.

In general, this method is applicable only to angular scan rates less than 5 rpm. Its accuracy is determined by mechanical considerations and by the uncertain delay in closing the microswitch and the first relay. Easy phasing of the index is accomplished by the use of a mechanical differential between the antenna and the cam.

*Photoelectric Method.*—This is the most precise method of generating indices. A slotted disk, mechanically coupled to the scanning device, is so placed that it intercepts a collimated light beam that would otherwise fall on the sensitive surface of a photocell. Whenever the light beam passes through a slot in the disk, the photocell signal is generated.
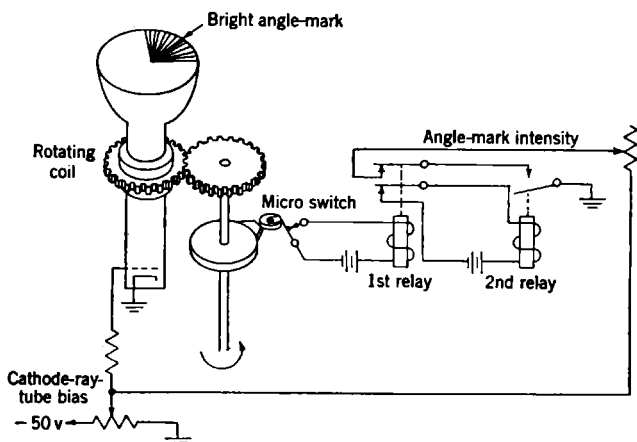


Fig. 6·2.—Mechanical switching to intensify sweeps at a particular angle.

After suitable amplification, this signal may be applied to the cathode or grid of the cathode-ray tube and thereby change the brightness of the trace. The electrical circuit is shown in Fig. 6·3. A gas-filled phototube is used because of its greater sensitivity, and because the linearity of response is unimportant. Collimation of the light from a six-candle-power bulb is accomplished by using a narrow slit placed in the light shield surrounding the bulb. Accurate alignment of this slit with the slit in the rotating disk is required. With good alignment the width of the index is proportional to the width of the light beam plus the width of the slot in the disk. By rotating the disk at several times the speed of the scanning device, multiple indices of proportionately narrower width may be generated. The errors of this method, subject to the provision that the interval between fast scans be sufficiently small, are only those introduced by the mechanical coupling to the scanning device and the errors inherent in the scanning device itself. Phasing of the index may be done mechanically. This process will prove cumbersome if the scan-

ning device and the photocell unit are remote from the display, and therefore photoelectric indices are usually fixed.

*Synchro-null Methods.*—When a carrier is applied to the rotor of a steadily rotating synchro there will appear across any two output terminals a sine modulated-carrier wave. For a complete revolution of the synchro there are two positions, 180° apart, at which the phase of the carrier reverses and the amplitude passes through a minimum. If this carrier is demodulated by means of some type of peak detector, the resulting wave consists of a series of positive sine-wave half cycles. At the minimum value there is a rapid reversal of the slope of the demodulated waveform and both the negative and positive slopes are at their greatest values on either side of this minimum. Narrow pulses that
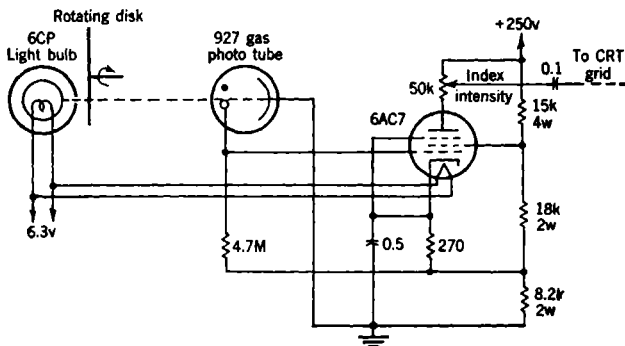


Fig. 6·3.—Photocell index circuit.

occur at two definite angular positions 180° apart can therefore be formed from the demodulated waveform.

The advantage of this method is that the phase of the index may be controlled at a position remote from the scanning device to which the rotating synchro is attached. The stator of another synchro located on the control panel may be connected to the stator of the first synchro. Rotation of the second synchro rotor will phase the index to any position desired since the second synchro acts as an electrical differential.

The carrier energizing the synchro must be of a sufficiently high frequency to furnish information to the demodulator at intervals more frequent than those corresponding to the maximum allowable error of the index. In general an upper frequency limit to the carrier is set by the transfer characteristic of the synchro at high frequencies and the stray capacity in the synchro itself and in the transmission lines. Capacity unbalance frequently causes the minimum values of the carrier to vary for different settings of the second phasing synchro. A change in the d-c level of the minima of the demodulated wave then results. In most

circuits this change in turn causes a variation of the angular width of the index itself.    A circuit for generating indices by the synchro-null method is shown in Fig. 6·4.    An oscillator (4·5 kc/sec) is used to excite the rotor of a synchro mechanically coupled to the antenna.    Although the fre-
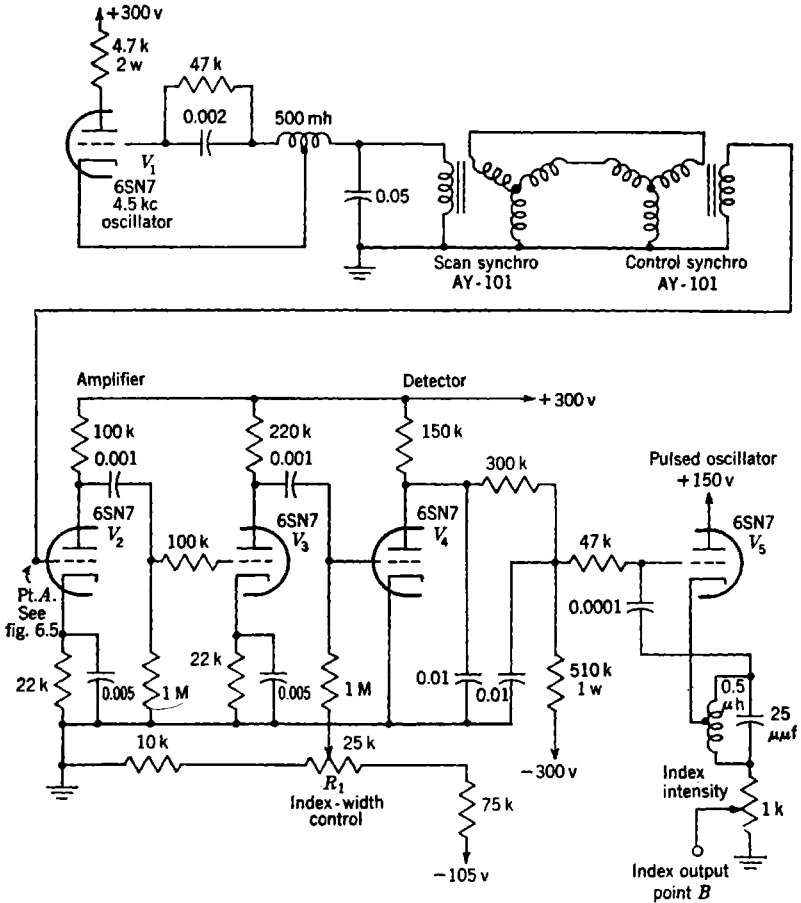


Fig. 6·4.—Synchro-null indices.

quency stability of this oscillator is of no consequence, amplitude variation in the oscillator will cause a proportional increase in the width of the index.    For any position of the control synchro there are two corresponding positions of the scan synchro in which the output from the secondary of the control synchro goes to zero.    At all other positions of the scan synchro there is an appreciable carrier signal.    This signal is amplified

by a two-stage amplifier and coupled into a peak detector that is biased just beyond cutoff. When there is any appreciable signal, the peak detector conducts over part of the cycle and the condenser in the plate circuit discharges. During a null, the detector tube fails to conduct and the plate condenser is charged to B+ voltage. The amount of input signal required before the detector tube conducts depends upon the bias, controlled by $R_1$. The bias thereby controls the width of the positive plateau in the plate waveform, which is generally used to cut off a cathode

follower, an amplifier, or an oscillator[1] at all times when the plate voltage is not at B+. Thus $R_1$ is the width control for the index. Indices with a width of 2° out of the 360° rotation of the antenna synchro may be obtained with ease; sharper indices require stable amplifiers, stable power supplies, and care in the reduction of stray-capacity effects. Variations of the circuit shown in Fig. 6·4 may be deduced from the data on de-modulation in Chap. 5. Lower-frequency carriers have been successfully used for the genera-tion of indices by this method.

Elimination of alternate indices may be accomplished if desired by the addition of the circuit shown



Fig. 6·5.—Elimination of alternate index.

in Fig. 6·5. The control transformer synchro used to phase the index in Fig. 6·4 is replaced by a differential synchro. By suitable connections a carrier whose modulation envelope is 90° in scan angle behind that used for the generation of the index may be obtained from this differential synchro. This carrier is added to a suitable fraction of the unmodulated carrier, and the sum is then demodulated to give a wave proportional to the cosine of the scan-synchro rotation angle. When the cosine wave is near a maximum, a vacuum tube driving a relay conducts and thereby actuates the relay, which allows the index to be transmitted to the display tube.

*Indices Derived from the Cathode-ray-tube Sweep-control Potential.*— A varying voltage, related to the position of the scanning device, is usually generated as the means of controlling the cathode-ray-tube

[1] An oscillator, $V_5$ of Fig. 6·4, is used to allow passage of the index signal through video circuits.

sweep. A particular value of this voltage usually corresponds to a single position of the scanner. It is, therefore, possible to generate an index by a circuit that reacts discontinuously at this particular voltage. The circuit shown in Fig. 6·6 makes use of a "flopover" $V_2$ and $V_3$, which fires when the $V_2$ grid potential changes from negative to positive with respect to the grid of $V_3$. The cathode follower $V_1$ isolates the sweep-control from the index circuit and offers a low impedance to the divider $R_1$ and $R_2$. The potential at the junction of $R_1$ and $R_2$ can be varied by means of the low-impedance potentiometer $R_3$. The value of the sweep-control voltage at which the flopover circuit fires may thus be selected at will. Since the potential at the plate of $V_2$ shifts abruptly negative whenever the grid of $V_2$ changes from a potential below that of the grid
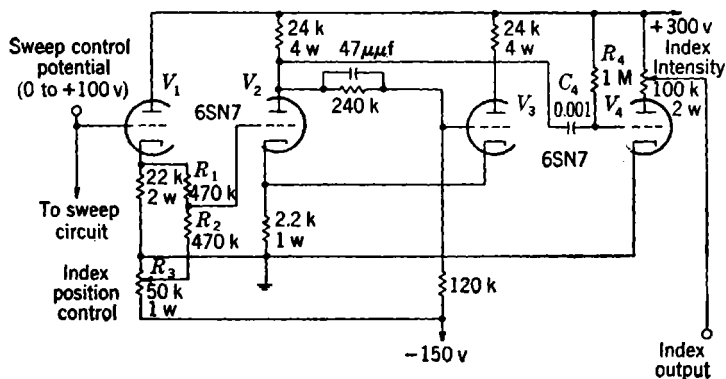


Fig. 6·6.—Index from sweep-control potential.

of $V_3$ to one above, $V_4$ is cut off instantaneously. After an interval, determined by $R_4C_4$, $V_4$ again becomes conducting as $C_4$ is charged positively through $R_4$. There will appear, therefore, at the plate of $V_4$ a positive pulse whose start corresponds to a particular value of the scan-control potential, determined by the setting of $R_3$, and whose duration is determined by $R_4C_4$. When the sweep-control potential decreases to the critical value, the flopover will return to the initial condition. No index will be generated since only a positive pulse appears at the grid of $V_4$. If an index were generated at each transition of the flopover, a slight difference in the potentials corresponding to the indices produced by alternate transitions would be observed. This method of generating indices is therefore restricted to scan-control voltages that vary unidirectionally during the useful portion of the scan.

*Sweep-stopping Circuit.*—Variations of the position and intensity of a slow-scan index $x_1$ that are due to a variation of the discrete values of $x$ corresponding to the start of the fast scans will occur in some cases.

It is therefore often desirable to stop the slow scan momentarily at the value $x_1$. After intensification of a fast y-sweep at $x_1$, the slow x-scan is allowed to catch up to the correct value. The block diagram, Fig. 6·7, shows a sweep-stopping circuit for the special case of sawtooth sweeps. At a time corresponding to the value $x_1$, a negative trigger pulse, generated by any of the methods already described for the generation of indices, flips a scale-of-two circuit, which unclamps a sawtooth generator. The resulting positive sawtooth voltage is then resistance-mixed with the negative sawtooth waveform from the scanner. If the positive sawtooth voltage is adjusted to the correct slope, the sum of the two sawtooth
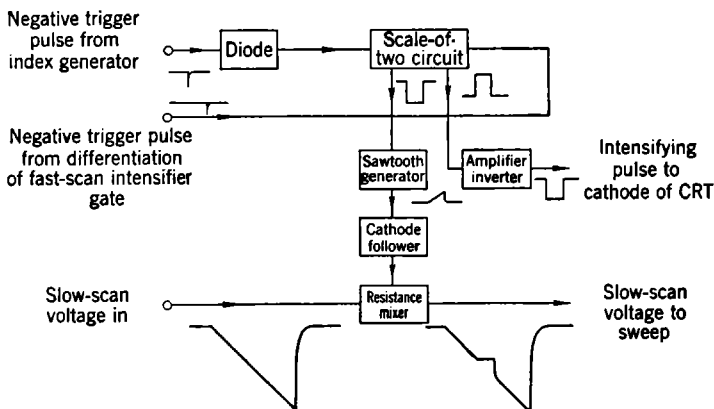


FIG. 6·7.—Block diagram of sweep-stopping circuit.

waveforms will not change during the interval in which the scale-of-two circuit is in this state. To cause a transition of the scale-of-two circuit back to the original state a negative trigger pulse, derived from the end of the intensifier-gate circuit associated with the fast scan, must be applied to the grid of the second tube. As soon as the scale-of-two circuit flips back, the sawtooth generator is clamped. The sum of this sawtooth waveform and the scanner sawtooth waveform immediately becomes equal to the value of the scanner sawtooth voltage alone. The scan is therefore in the same position in which it would have been if the sweep had not been momentarily stopped. To intensify the cathode-ray-tube beam during the index, a pulse is developed from the scale-of-two circuit and applied to the cathode of the cathode-ray tube.

Figure 6·8 shows the actual sweep-stopping circuit. The scale-of-two circuit uses a pentode, $V_2$, and a triode, $V_3$. The screen of the pentode acts as the anode in the scale-of-two circuit. The plate of the pentode is an electron-coupled switch used to clamp $C_1$. The rate of charge of $C_1$

is determined by $R_1$ and the potential $E_1$ to which $C_1$ charges. $E_1$ may be controlled by means of a potentiometer.

*The Use of Carriers to Allow Amplification by Video Amplifiers.*— Very often the indices of slow-scan sweeps must be comprised of long intensifying pulses. The duration of these pulses may be as much as a tenth of a second. In many types of displays, particularly radar displays, the signal amplifiers do not have a low-frequency response sufficient to pass such a long pulse. The long pulse may be used to modulate a carrier in order that the index signal may be mixed with the video



Fig. 6·8.—Sweep-stopping circuit.

signals before amplification. In Fig. 6·4 the circuit involving $V_5$ is a Hartley oscillator that is gated at the grid by the index pulse and provides a frequency high enough to pass through the video amplifier. This signal will be demodulated by the nonlinear response of the cathode-ray-tube gun.

*Substitution Indices.*—Figure 6·9 shows a circuit in which the index is placed on the screen of the cathode-ray tube during the interval when the normal slow sweep would cause the cathode-ray beam to be deflected off the face of the tube. When the sweep-control voltage $E_1$ is sufficiently positive to sweep the cathode-ray beam off the screen, the relay switch tube $V_3$ conducts and thus actuates the relay. This relay switches the grid of the sweep amplifier tube from the scanner potentiometer to a fixed potentiometer, which is adjusted so that the cathode-ray-tube sweep is

in the correct position for the desired index.   The relay also switches the cathode-ray-tube grid bias so that it intensifies all fast scans occurring while the slow sweep is held in the index position.   At the same time signals are removed.   As soon as the sweep control voltage falls below the critical value, the relay is released and normal operation is restored.

This method of generating indices requires that only a portion of the scan be presented, and that the unused portion of the scan be sufficiently long to allow the relay to operate.   It requires further that the display-tube screen have sufficient persistence.
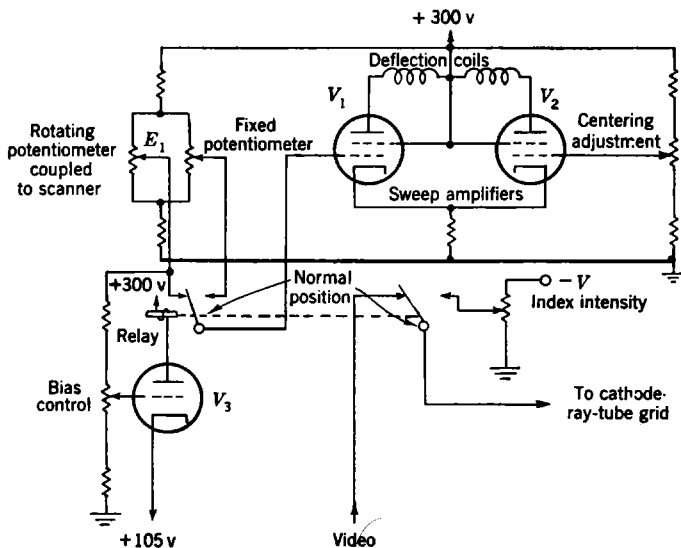


FIG. 6·9.—Substitution index using relay.

For relatively rapid scans an index may be generated in a somewhat analogous manner using electronic switches to clamp the sweep amplifiers momentarily to the desired value.   Transients in the deflection system, especially with magnetic deflection, become troublesome when the clamping interval is small, but these transients may be reduced if clamping is done at a time when the sweep is near the desired index position.   A portion of the scan is sacrificed under this condition, but an index is not usually required for every scan.

*Summary of Slow-scan Indices.*—Five general methods of generating electronic indices directly from the mechanical position of the scanner have been described.   The choice of a suitable method will depend on (1) the number of indices required, (2) the phasability of the indices, (3) the accuracy needed, (4) the speed of the scanner, (5) the amount of scan displayed, and (6) the type of scan.

Multiple indices may easily be obtained by photoelectric methods, certain mechanical-switching methods, and, if submultiple spacing is assumed, by synchro-null methods. Substitution methods, on the other hand, are in general not suitable for generating more than a single index. The fifth method, pickoff of several indices from the sweep waveform, requires duplication of the pickoff circuit and may therefore become uneconomical.

The mechanical-switching method and the photoelectric method are relatively difficult to phase. All the other schemes described are designed to be phasable by a simple remote control.

The most accurate indices may be generated by the photoelectric method. The synchro-null method has the inherent inaccuracy of the synchro, about 1° if the synchro is geared 1 to 1 to the scanner. Pickoff of an index from the sweep waveform has the errors inherent in generating the waveform. Substitution indices depend upon the stability of the sweep amplifiers, and are therefore less accurate than the photoelectric or synchro-null methods.

Mechanical switching to brighten particular sweeps, as well as substitution indices, requires low scanner speeds, but the other methods are limited in scanning speed chiefly by mechanical considerations.

All substitution methods also require the sacrifice of a portion of the scan. Unidirectional scanning is desirable with mechanical switching and with methods utilizing the sweep control voltage. Photoelectric and synchro-null methods may have a small amount of backlash, but are otherwise indifferent to reversal of the scan.

**6·3. Timing Indices.**—In many cathode-ray-tube displays such as are used for test oscilloscopes and radar sets, time is one of the principal coordinates. It is nearly always represented by the faster sweep in a two-coordinate display. Since every sweep will present all values of time throughout the desired interval, the problems arising from the discontinuities in the slower sweep of a two-dimensional scan are absent. The $y_1$ time index consists of a series of dots, each of which is generated by the intensification or deflection of a small section of each y-sweep. With the faster time sweeps, the interval that this section represents may have to be as short as 0.1 $\mu$sec. The generation of such short pulses presents problems in itself.

Usually, it is desirable to generate time indices entirely independently from the sweep. Stable oscillators employing crystals or $LC$ tank circuits are often used. These oscillators may be pulsed at the start of the sweep, or the start of the sweep may be synchronized with the phase of the oscillations. Precise sawtooth delay circuits, often measuring time from a value other than that at the start of the sweep, provide an alternative means of accurately measuring time intervals. The particular method

used for generating the index will depend on whether it is desired to measure a single variable-time interval or to use multiple fixed indices equally spaced. The latter method requires interpolation to determine the time of any signal.

Presentation of the time index will depend on the display used. With a one-dimensional time scan and signals presented as deflection modulation, it is usual to indicate a particular value of time by means of a rapid transverse deflection such as a step or notch. Indication of this type gives the greatest precision, but care must be taken to prevent distortion of the signal by the deflection of the time index. Intensity modulation is always used with two-dimensional scans and often with one-dimensional scans in which the use of fixed indices is likely to cause distortion of the signals to be observed. Such intensity-modulated indices have the disadvantage of poor focus when bright marks require high instantaneous beam currents.

*Movable Time Indices.*—A "flip-flop," the circuit for which is described in Sec. 4·4, may be used to measure a time interval. However, the changes of tube characteristics caused by aging, tube replacement, and variations of heater voltage lead to considerable inaccuracy. It is therefore usual to calibrate the time intervals corresponding to particular potentiometer settings of the $RC$ time constant involved against a more reliable delay circuit. However, the economy of such a multivibrator recommends its use when great accuracy is not required. The particular circuit shown in Fig. 4·23 holds its calibration, for extremes in normal operating conditions and for reasonable lengths of time, to $\pm 5$ per cent.[1] In some cases the tendency of the multivibrator delay time to vary rapidly over a small interval or to "jitter" will broaden the index enough to confuse the observer.

Greater accuracy and stability may be obtained at considerably greater expense with the sawtooth delay circuit shown in Fig. 6·10. The switch tube $V_1$ holds $C_1$ and $C_2$ discharged until a negative square wave starting at time $t_0$ cuts off this tube. To insure a linear sawtooth waveform both "bootstrapping" and compensation by means of $R_2C_2$ are used. At the end of the sawtooth waveform $V_2$ and $V_4$ allow a rapid return to initial conditions. When, at time $t_1$, the plate of the diode $V_5$ becomes positive with respect to the cathode, the remainder of the sawtooth waveform is transmitted through the diode to the grid of the pentode amplifier $V_6$. The pulse transformer in the plate of $V_6$ differentiates and inverts the amplified segment of the sawtooth wave. After further amplification by $V_7$ this waveform triggers a pulse oscillator $V_8$. The resulting sharp pulse may be used directly as an index of the time

[1] See the Radiation Laboratory Series, Vol. 20, Chap. 5 for a more detailed discussion of this circuit and its stability.
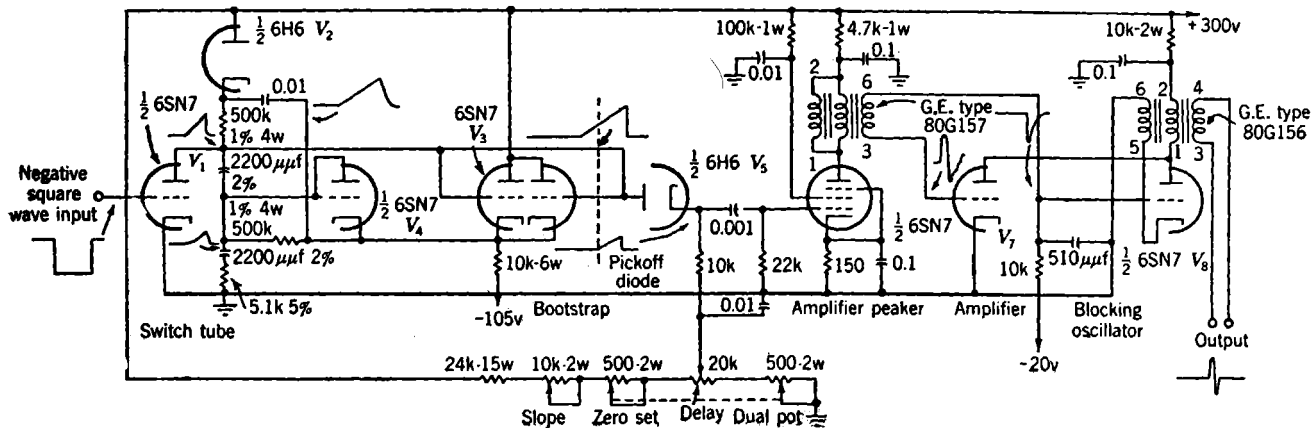
FIG. 6·10.—Sawtooth delay circuit.

interval $t_1$-$t_0$.    The critical parts in this circuit are $V_1$, which determines
the voltage at the start of the sawtooth wave; $V_5$, which may require
slightly varying plate-to-cathode potentials for conduction; the critical
time constants, $R_1C_1$ and $R_2C_2$; and the voltage at the arm of the delay
potentiometer.    Variation of this voltage causes a linear variation of the
time interval.    This circuit will hold its calibration to about $\pm 0.5$ per
cent for extremes of normal operating conditions.    A detailed discussion
of its stability appears in Vol. 20, Chap. 4.
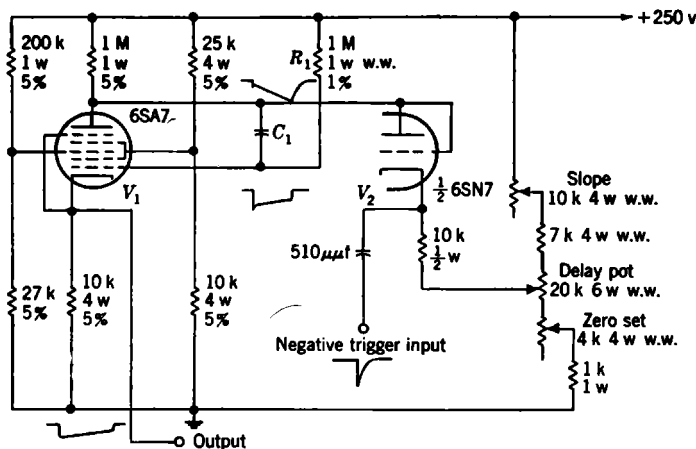


FIG. 6·11.—Phantastron delay circuit.

Another delay circuit, similar in some respects to a multivibrator but
controlled by a linear sawtooth waveform, is shown in Fig. 6·11.[1]    Nor-
mally, both $g_1$ and the cathode of $V_1$ are held positive with respect to $g_2$.
Screen current flows, but the plate is cut off by $g_2$.    The plate potential
of $V_1$ is controlled by the delay potentiometer through the diode $V_2$.    If
a negative trigger pulse is allowed to reduce the cathode potential below
that of $g_2$, plate current will flow momentarily and thus cause $g_1$ to be held
at a lower potential by the integrating condenser $C_1$.    After a small
initial drop, the plate potential will be able to become more negative only
as $C_1$ discharges through $R_1$.    The plate continues to become more nega-
tive with a sawtooth waveform until it reaches the potential of $g_2$.    At
this point $g_1$ rapidly becomes positive until it exceeds the potential of
$g_2$; the plate current is then cut off and the circuit returned to the original
conditions.    The time interval is determined by the potential at which
the negative plate sawtooth waveform starts and by the conditions for
which plate current can no longer increase.    The initial plate voltage

---

[1] The action of this circuit, known as the "phantastron" delay circuit, is described
in detail in Chap. 5, Vol. 20 of the series.

may be varied by the delay potentiometer to give an almost linear variation of delay.    Critical parts of the circuit are $R_1C_1$, which determines the slope of the plate sawtooth wave, the screen potential of $V_1$, and the suppressor potential of $V_1$.    The output waveform may be taken from either the screen or the cathode.    Since the screen has a steeper negative wavefront, a shorter minimum delay time is available there.

More elaborate circuits employing stable oscillators, phase shifters, and a delay circuit to allow selection of a particular sine-wave cycle relative to some other previous sine-wave cycle are described in Vol. 20, Chap. 5.    By the use of continuous crystal oscillators and accurately made phase shifters, errors may be reduced to less than 0.1 $\mu$sec.
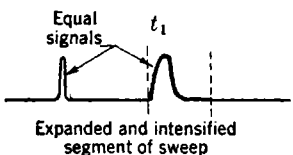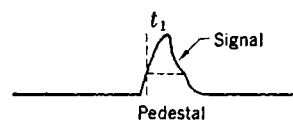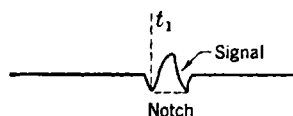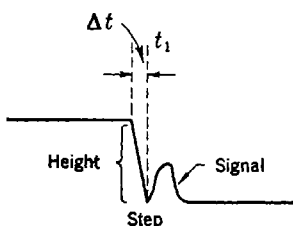
*Deflection Presentation of a Single Time Index.*—To allow very accurate setting of an index on a particular signal, a section of the time sweep in the vicinity of the signal may be expanded.    On an A-scope a step, notch, or pedestal can accomplish this expansion by a deflection transverse to the time sweep.    Since the signal is also indicated by a transverse deflection, care must be taken that the signal is set only to the edge of the step.    For best accuracy the slope of the step must be a maximum at this edge.    A good step will, therefore, break sharply.    Figure 6·12 shows how the position of a pulse may be measured by a step, a notch, or a pedestal.    Experience indicates that for a step 1 in. high a sharp signal may easily be set to one-tenth of $\Delta t$.

An alternative method of expansion employs a sharp increase in the rate of the time sweep for a short interval starting at $t_1$ (Fig. 6·12).    During this interval the CRT beam is intensified for easy identification.    The accuracy of measurement is thus increased without distorting the signal amplitude.    However, this distortion of the time base may be objectionable, and, in general, this method does not yield such accurate results as the step method.



Fig. 6·12.—Methods of setting a signal to a time index $t_1$ from radar A-scopes.

Figure 6·13 shows one form of step-generating circuit.    The sawtooth waveform used for the delay will cause $V_1$ to conduct when the sawtooth potential reaches a value equal to the potential $E_1$ from the delay poten-

tiometer minus the cutoff bias voltage of $V_1$. When $V_1$ conducts, a sawtooth voltage appears at the cathode. This sawtooth waveform is amplified by $V_2$, until $V_2$ reaches saturation. The negative step that appears at the plate of $V_2$ is further amplified by the wideband amplifier $V_3$ and is applied directly to the cathode-ray-tube deflection plate.

A much sharper step may be obtained by the use of a flip-flop fired by a precisely delayed trigger pulse (Fig. 6·14). The start of the step is very sharp because of the large amount of regeneration in the flip-flop circuit. The screen of $V_2$ is used as the anode in the second stage of the flip-flop. The plate of $V_2$ is electron-coupled to the flip-flop and acts as a
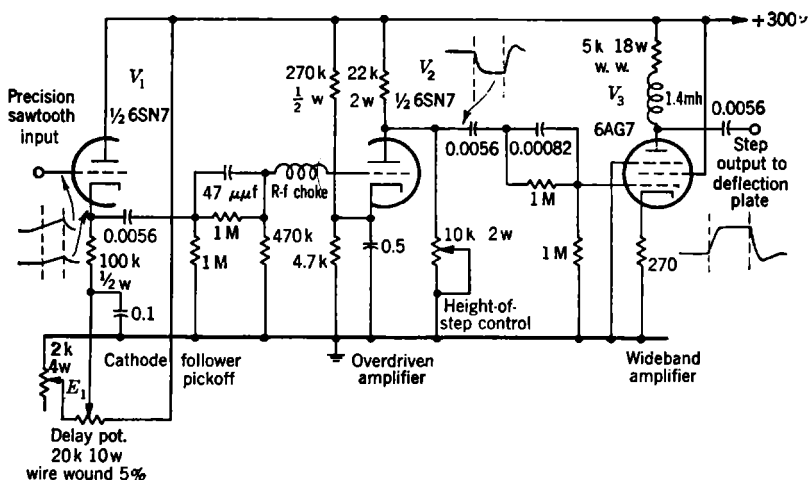


FIG. 6·13.—Step-generator circuit with sawtooth-waveform input.

constant-current source to discharge the stray capacity $C_2$ in parallel with the load resistance $R_2$. Condenser $C_2$ will be discharged almost linearly with time until the plate potential of $V_2$ has fallen to a relatively low value. The remainder of the discharge of $C_2$ will continue at a gradually decreasing rate. The automatic clamp tube $V_3$ sharply arrests the step appearing at the plate of $V_2$ at a potential set by the step-height potentiometer. This relatively expensive circuit will give a steep break of 1 in. in 0.1 μsec with a typical electrostatic cathode-ray tube. The break of the step at $t_1$ is almost instantaneous and the step can therefore be reset to a particular signal with a precision of approximately 0.01 μsec. If $R_1C_1$ is adjusted to a low value the step will become a notch. Only the step appears on the time sweep when the value of $RC$ is made large.

*Periodic Time Indices.*—When multiple indices are used, they are usually required to be equally spaced. Therefore, they may be economi-

cally generated with the aid of a stable sine-wave oscillator. The sine-waves are amplified, clipped, and differentiated to give sharp indices. Crystal oscillators are the most stable but, unfortunately, are difficult to pulse if it is required that the indices start at an arbitrary time. Shock excitation of an *LC* resonant circuit will easily generate a train of sine waves starting at any time, but regeneration, as by the use of a Hartley oscillator circuit, is advisable if more than three or four oscillations are required. In addition, lower-*Q* tank circuits, which recover more rapidly and therefore allow higher duty ratios, may then be used.
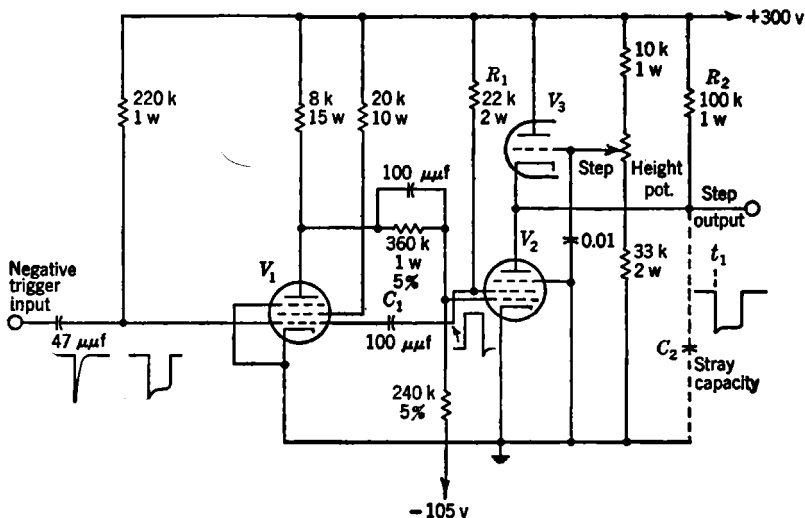


FIG. 6·14.—Fast-step generator with delayed input trigger.

A typical circuit is shown in Fig. 6·15. The shock-excited *LC*-circuit in the cathode circuit of $V_1$ should be temperature compensated and shielded. Care should be taken that the negative gate used to cut off $V_1$ is larger than the peak of the sine wave by at least the amount of the cutoff bias required by $V_1$. Otherwise, $V_1$ will conduct over a portion of the oscillation, thereby damp the tank circuit, and alter the period of the first few oscillations. The amount of regeneration from the Hartley oscillator tube $V_2$ is adjusted by changing the value of $R_1$ until the oscillations are maintained at the natural peak amplitude of the first oscillation. This amplitude is approximately $I_1 \sqrt{L/C}$ where $I_1$ is the current flowing through the tank circuit just before application of the negative gate to the grid of $V_1$. With approximately the correct value for $R_1$, changes in $V_2$ will have very little effect on the frequency of oscillation. Changes in the value of $R_1$, however, will affect the frequency appreciably.

If the value of $C$ in the tank circuit is reduced to approximately 100 $\mu\mu f$, a change of the interelectrode capacity between cathode and heater of $V_1$, which might occur if $V_1$ were replaced, will affect the tuning of the $LC$ tank circuit and alter the interval between the indices.

Tubes $V_3$ and $V_4$ form a cathode–coupled flip-flop circuit. With $V_1$ conducting, $V_3$ conducts because the grid of $V_3$ is held positive with respect to the grid of $V_4$ by the current from $V_1$ and $V_2$ passing through $R_2$. When $V_1$ is cut off, the grid of $V_3$ goes negative and thus causes the plate of $V_3$ to rise until $V_4$ becomes conducting. Thereafter the regeneration between $V_3$ and $V_4$ greatly increases the rate at which the plate potential of $V_3$ increases. The heavy pulse of current required to charge
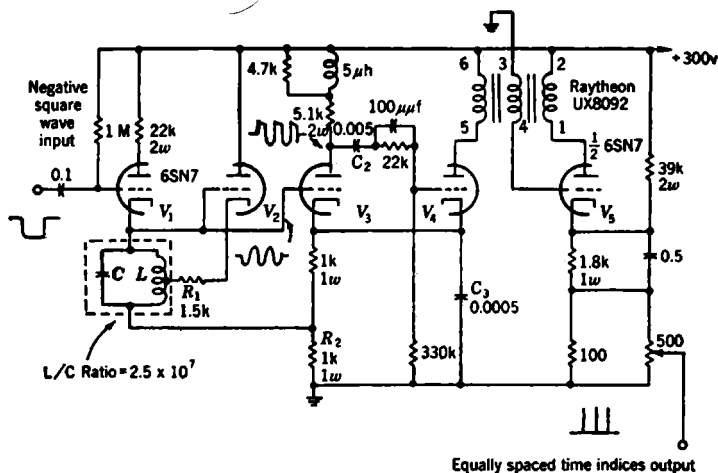


FIG. 6·15.—Generator of multiple time indices.

$C_3$ is drawn through $V_4$ and the pulse transformer, and hence triggers the pulse-sharpening tube $V_5$. When the sine wave at the grid of $V_3$ goes positive, $V_3$ again conducts and $V_4$ is cut off. The pulse appearing across the pulse transformer is now of the wrong polarity to trigger $V_5$. When the sine wave again goes negative, $V_3$ and $V_4$ regenerate at precisely the same value of the sine-wave potential if the voltage across $C_2$ has not changed. This voltage is approximately constant if $C_2$ is sufficiently large and if the grid current from $V_4$ is limited. All indices are then generated at the same sine-wave voltage. Since this voltage occurs near the zero value of the sine wave, variations in sine-wave amplitude do not greatly affect the phase of the sine wave at which the index is generated. The sine waves generated by the Hartley oscillator are, moreover, fairly constant in amplitude, a condition that could not be achieved if they were obtained merely by shock-exciting a simple $LC$

resonant circuit as has sometimes been done.  It will be apparent that a small delay, before the "zero" time index is generated, is inherent in this circuit.

*Intensity Modulation.*—The spot diameter of a 5-in. magnetic cathode-ray tube is approximately 0.5 mm.  If the sweep speed is 1.5 mm per μsec, a typical figure for a fast sweep, the duration of a pulse equivalent to one spot diameter will be about 0.33 μsec.  A sharp intensity-modulated index requires that the duration of the intensifying pulse applied to the cathode-ray tube correspond to less than one spot diameter. Such a short pulse requires very good peaking circuits.

In the circuit of $V_5$ in Fig. 6·15, the pulse sharpener is triggered through the third winding of the pulse transformer.  The voltage across a small resistor in the cathode circuit of $V_5$ is used for the index.  It is proportional to the current pulse.  Since the latter is unidirectional, there is no overshoot at the end of the index.  The rate of rise of the pulse depends upon the mutual conductance of the tube, the transfer characteristics of the pulse transformer, and the rate of rise of the trigger pulse. The length of the pulse is almost entirely dependent on the pulse transformer.  Series grid or plate resistance will decrease the rate of rise and increase the length of the pulse.

Since it is often necessary to use short pulses for intensity-modulated indices, difficulty in obtaining sufficient light intensity without defocusing the cathode-ray beam is common, especially when the repetition rate of the time base is low.  For best results the pulse length should be increased when changing from a fast sweep of high repetition rate to a slower sweep of necessarily lower repetition rate.

*Presentation of Multiple Markers.*—Either deflection- or intensity-modulated indices, short in duration compared with the signal-amplitude changes, may be used with A-scopes.  With displays presenting two coordinates, intensity modulation is always used.  When many indices are used, it is helpful to have every fifth or every tenth index brighter than the others.  This contrast may be obtained by selecting every fifth or tenth index by means of a dividing circuit.  An additional intensifying pulse from this index may then be mixed with the other indices before they are applied to the cathode-ray tube.

**6·4. Special Types of Indices.**  *Indication of Two Coordinates Simultaneously.*—Although a grid made up of separate indices is ordinarily used to indicate two coordinates, it is sometimes convenient to use a single specialized index.  An example is the index on a radar B-scope display shown in Fig. 6·16.  In this case the range and bearing of a signal are measured by terminating an angle index of a particular bearing at a particular range.

A second type of specialized index is the intensification of a small
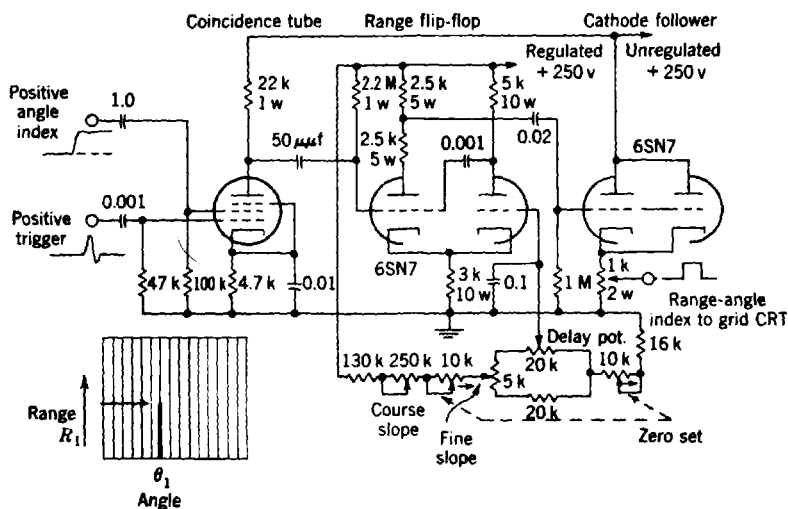
FIG. 6·16.—Range-angle index generator.
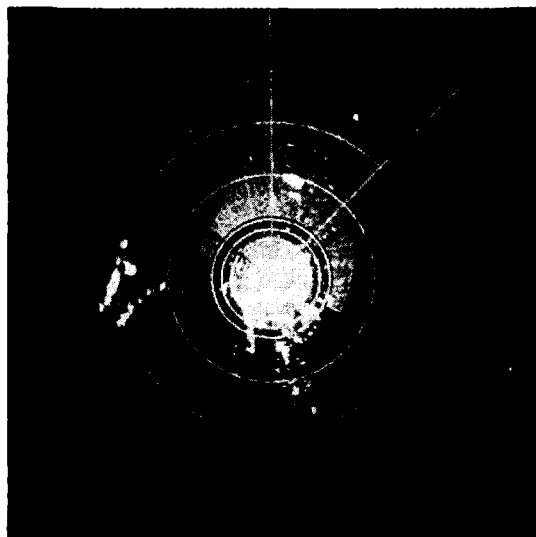


FIG. 6·17.—Area intensification to indicate the position of a sector display.

area of a display.    Often it is desired to center an expanded sector display
on a particular point of a second more generalized display.    The area
covered by the expanded sector can be indicated by brightening this
portion of the second display.    Figure 6·17 is a photograph of a radar

FIG. 6·18.—Height-index circuit.

PPI scope on which is shown the position of an expanded sector scope. The intensification of the PPI is economically accomplished by mixing a portion of the intensifier for the sector display with the signals applied to the PPI.   Figure 6·17 also illustrates the use of range and angle indices.

*Derived Indices.*—Indices that are functions of one or both of the coordinates used in scanning the display tube are often useful, but these functions may be too complicated to be generated by simple electrical or mechanical computation from the fundamental scanner information. These indices may be more easily generated by the method of video mapping described in Chap. 16.

Other indices may be computed directly from information generated by the scanning device.   An example of such an index is a height marker on a radar display of elevation angle versus slant range.   The height marker is a function of both coordinates, given by $R \sin \theta$, where $R$ is slant range and $\theta$ is the elevation angle of the radar beam.   A circuit that will generate a variable height index is shown in Fig. 6·18.   The input waveforms to the circuit are a voltage proportional to $\sin \theta$, generated by means of a sine potentiometer attached to the radar antenna, and a negative square wave starting at the instant the radar pulse is trans-



FIG. 6·19.—Height index on display of range vs. elevation angle.

mitted.   This negative square wave cuts off the switch tube $V_1$ so that $C_1$ becomes charged through $R_1$ toward a voltage proportional to $\sin \theta$.   To insure a linear sawtooth wave with a slope proportional to $\sin \theta$, a bootstrap circuit, $V_3$ and $V_5$, is required.   A cathode-follower buffer tube $V_8$ then applies the sawtooth voltage to a flopover amplifying circuit. The flopover fires when the sawtooth waveform at the cathode of $V_8$ reaches a critical voltage.   Then $V_9$ conducts and $V_{10}$ is rapidly cut off; thus there is generated an overpeaked square wave, which may be differentiated to give a useful positive index.   Since the flopover fires at a constant value of $kt \sin \theta$ for a given setting of the height potentiometer, the index is generated at a constant value of $R \sin \theta$ or height.   To vary the value of $kt \sin \theta$ that corresponds to the index, the initial value of the a-c–coupled sawtooth voltage at the cathode of $V_8$ is adjusted by means of the height potentiometer.   This potentiometer may be calibrated to read directly in height.   The diodes $V_3$ and $V_7$, together with the triode clamp tubes $V_4$ and $V_6$, are required to insure that the initial conditions at the start of the sawtooth waveform are independent of repetition rate or values of $\sin \theta$.

The constant-height index may be presented on an E-scope as shown in Fig. 6·19, where elevation angle is plotted against slant range. With this display the index is nearly a segment of a hyperbola for values of elevation angles up to 35°. (If the sine of the elevation angle were plotted against slant range, constant-height lines would be rectangular hyperbolas.) Figure 6·20 is a photograph of a display with height plotted against range. Since the sweeps, however, are generated as radial lines, the height index cannot be formed by intensifying a single sweep. The photograph shows the straight constant-height line and
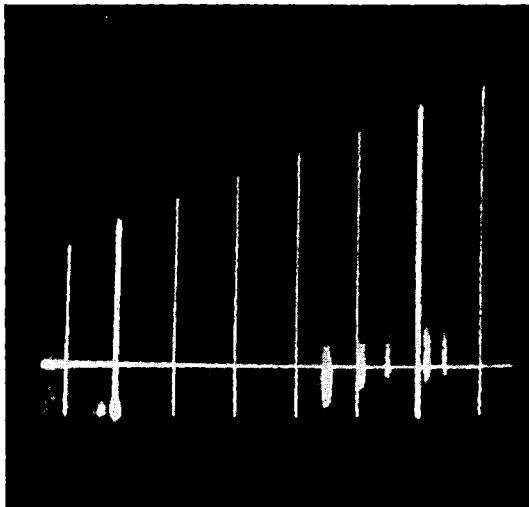


Fig. 6·20.—Range-height-index display showing constant-height index.

also range indices in which every fifth index is intensified. The start of the display is delayed.

*Indices Transformed to New Coordinates.*—If indices referred to some new set of coordinates are desired, it is sometimes convenient to transform the scan intermittently to the new set of coordinates. Indices may then be generated by simple means while scanning is taking place in these coordinates.

An example of this method is a radar PPI in which range and angle are to be measured from some point off the center of rotation. It is possible intermittently to shift the center of rotation of the scan to this point. The normal signals are removed, and range or angle indices, generated in the usual way, are then applied. With rapid angular scans it may be convenient to apply the indices every fourth or fifth scan. With slow scans every few range sweeps may be shifted to the new center of rotation.

# CHAPTER 7

## DEFLECTION-MODULATED DISPLAYS

BY R. P. ABBENHOUSE, P. F. BROWN, AND D. F. WINTER

**7·1. A Simple Test Scope.** *Purpose.*—This simple test scope was designed as a test instrument to be permanently installed in a radar equipment. Since great accuracy was not required, very simple circuits could be used to provide deflecting voltages for the cathode-ray tube. Figure 7·1 is the complete circuit diagram of this scope. All the necessary power was obtained from the parent radar equipment.

*Circuits.*—The positive input trigger pulse (at least 50 volts in amplitude, and rising to 90 per cent in at most 0.5 $\mu$sec) is applied to the grid of one half of a 6SL7 tube that is normally nonconducting (the "off" tube of the flip-flop). The grid and screen circuits of the following 6AC7 combined with this portion of the 6SL7 form the complete flip-flop whose action provides a rectangular voltage wave initiated by the input trigger pulse. The repetition frequency must be between 100 and 2500 pps. The positive output wave, taken from the screen of the 6AC7, is applied as the intensifier signal to the grid of the type 2AP1 cathode-ray tube. The plate of the 6AC7 acts as a clamp in the sawtooth generator. Between sweeps the grid is at zero bias and the plate potential is therefore firmly fixed slightly above ground. Since the grid of the 6AC7 is held negative for the duration of the pulse because of the time constant $(R_1C_1)$, the plate moves toward B+ at a rate determined by the RC time constant of the plate load resistor $(R_2 + R_3)$ and the capacity to ground consisting of either $C_2$ or the distributed wiring capacity. The resultant waveform is a fairly linear sawtooth wave, which is applied directly to one horizontal plate of the 2AP1.

The other half of the single 6SL7 acts as a sweep amplifier and inverter to provide a negative sawtooth waveform for the other horizontal plate of the cathode-ray tube. The input voltage to this half of the 6SL7 is that fraction of the sawtooth voltage at the plate of the 6AC7 which, when amplified by the 6SL7, will give a reversed-polarity sawtooth wave of the same amplitude. This input is provided from a tap in the charging resistor $(R_2$ and $R_3)$. Negative feedback from a cathode resistor helps to maintain linearity of response.

Two sweep speeds are provided. The long sweep, as determined by $C_2$, provides a range of approximately 300 $\mu$sec. With the switch $S_1$ in

the alternate position a short sweep of about 5 μsec (as determined by the distributed capacity at the plate of the 6AC7) is obtained.

The circuit is simplified by dispensing with centering controls. The deflecting plates are direct-coupled to the source of sweep voltage. The d-c voltage levels of the source automatically center the sweep in the horizontal plane while a fixed d-c voltage applied to one vertical plate provides for vertical positioning of the trace.
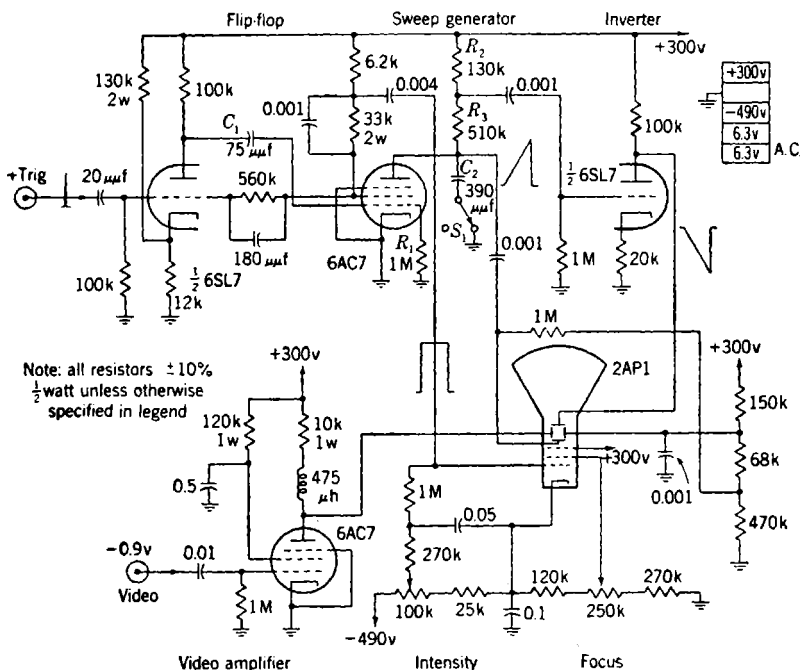


Fig. 7·1.—Circuit diagram of simple test scope.

A single stage of video amplification couples the input signal to the other vertical deflecting plate. The input voltage is required to be negative and not more than 0.9 volts.

**7·2. P-4 Synchroscope.** *Purpose.*—The P-4 synchroscope was designed primarily as a general-purpose test scope for the laboratory study of short pulses.

The following are its characteristics:

1. Time-base speeds are 0.04, 0.166, 0.5, and 2 in./μsec.
2. Synchronizing voltages:
   a. It will accept either a positive or negative external signal or trigger pulse at a range of repetition frequencies of from 150 to

4000 cps.    There is about a 0.05-$\mu$sec delay from this signal to the start of the time base.

*b.* It will accept a sine wave from an external oscillator (approximately 15 volts rms) of from 200 to 4000 cps, and derive from it a trigger pulse of positive polarity and 135 volts amplitude. This output trigger pulse is phasable with respect to the start of the time base by plus or minus nearly 90° of a cycle of the oscillator voltage.

*c.* An internal sine-wave oscillator whose frequency can be fixed by a selector-switch circuit at either 500, 1000, 2000, or 4000 cps is available.    Trigger pulses can be derived from the internal sine wave in the same manner as from an external sine wave.

3. Signal input to a deflecting plate of the cathode-ray tube is either direct or through an r-f detector and video amplifier.    This attachment is described at the end of this section.

4. Time-base calibration within 5 per cent is provided for the sweeps on Positions 1 and 2 of the sweep-selector switch by means of a damped oscillation from a simple *LC*-circuit operating at 2 Mc/sec.

Figure 7·2 is a block diagram of circuit operation.

When fitted with an r-f detector and video amplifier this equipment also serves as an r-f envelope viewer.    Figure 7·3*a* shows the P-4 synchro-
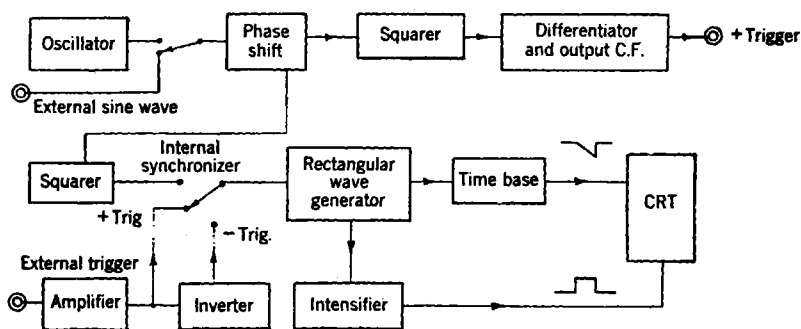


FIG. 7·2.—Block diagram of circuit operation.

scope so modified by the installation of the video attachment beside the cathode-ray-tube socket support.

*Circuits.*—The P-4 synchroscope includes the following circuits: (1) an internal oscillator for setting the repetition rate of the system under observation; (2) a delay or phasing network that can vary the time position with respect to the start of the time base of an output trigger pulse derived from a sine wave; (3) squaring and differentiating circuits for deriving rectangular waveforms and trigger pulses for synchronizing
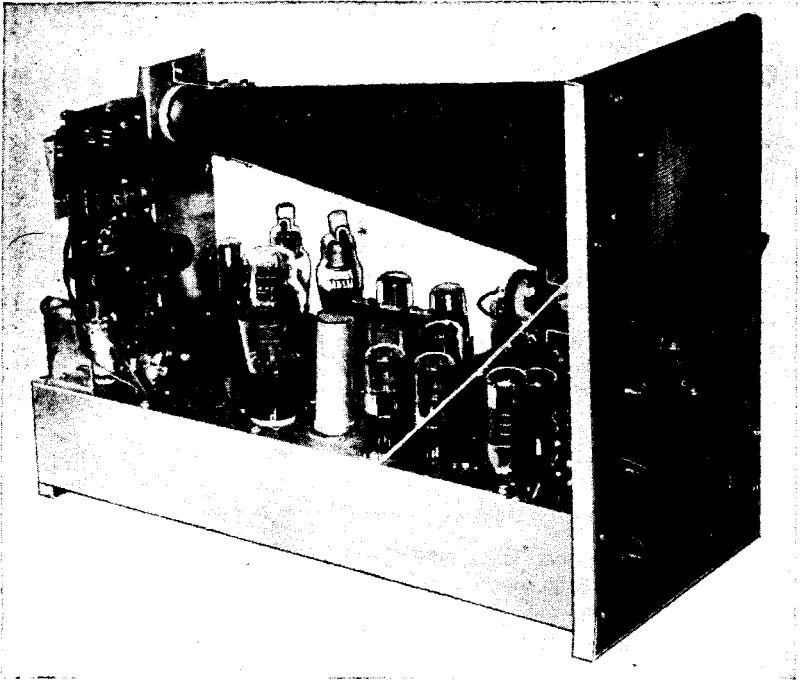
(a)
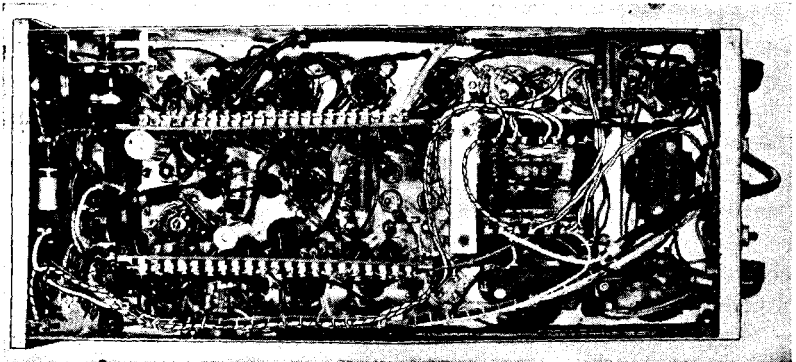


(b)

Fig. 7·3.—P4E synchroscope.   (a) Left interior view.   (b) Bottom view.   (*Courtesy of Sylvania Electric Products, Inc.*)

external apparatus and other internal circuits from the sine-wave oscillator; (4) a time-base generator; (5) an intensifying circuit for the cathode-ray tube; (6) input-trigger-pulse amplifiers and inverters. A conventional power supply furnishes these circuits and the cathode-ray tube with the necessary d-c voltages. See Fig. 7·4 for the complete circuit diagram.

*Trigger Generator and Associated Circuits.*—If the repetition frequency is determined by either an internal or external sine-wave oscillator, then phasing, squaring, and peaking circuits are used to derive the trigger pulse. The internal oscillator consists of a Wien-bridge circuit and a 6SN7 tube $V_1$, which provide a sinusoidal voltage having a high degree of frequency stability. The lamp in the cathode circuit of $V_1$ acts as a nonlinear element to stabilize the amplitude. The oscillator operates at four frequencies: 500, 1000, 2000, and 4000 cps. Its output is amplified by $V_{2A}$, and a conventional $RC$ phasing network in the secondary of the plate transformer of $V_{2a}$ furnishes two sinusoidal voltages, one of which is of variable phase with respect to the other. The reversing switch in the output of the phasing network alternates the variable-phase voltage between the output trigger circuit and the internal time-base-triggering circuits. By means of this switch, it is thus possible to start the time base either before or after the output trigger pulse is generated, and at a time determined by the setting of the phasing controls located on the front panel. Hence, any portion of the signal from the external circuit under observation can be superimposed on the time base.

The generation of trigger pulses from the phased sine waves is accomplished by two separate channels. One of these contains a rectifier, three amplifiers, and a cathode follower: $V_{2b}$, $V_{3a}$, $V_{3b}$, $V_{4a}$, and $V_{4b}$, respectively. Peaking is used between $V_{3b}$ and $V_{4a}$ (1-$\mu$sec time constant of $C_1R_1$) to provide a sharp output trigger pulse. The other channel contains only a rectifier and two amplifier stages, $V_{5a}$, $V_{5b}$, and $V_{6a}$, respectively. The output of this channel is actually a negative rectangular wave that is further differentiated to form a synchronizing trigger pulse on the grid of $V_{7a}$.

If external trigger pulses are used for synchronizing, they are peaked, amplified, and inverted (either once or twice) to produce negative trigger pulses. These trigger pulses are coupled from the trigger amplifier $V_{10}$ to the multivibrator. A peaked portion of the input trigger pulse is coupled to the intensifier tube $V_9$ to produce a rapidly rising intensifying pulse. (Less than 0.05-$\mu$sec delay is desirable.)

The selection of the synchronizing voltage is accomplished by a three-position three-gang switch $S_1$. The three positions correspond to sine wave, negative-trigger in, and positive-trigger in. Gang $A$ on the switch connects the input terminal of the rectangular-wave generator to the
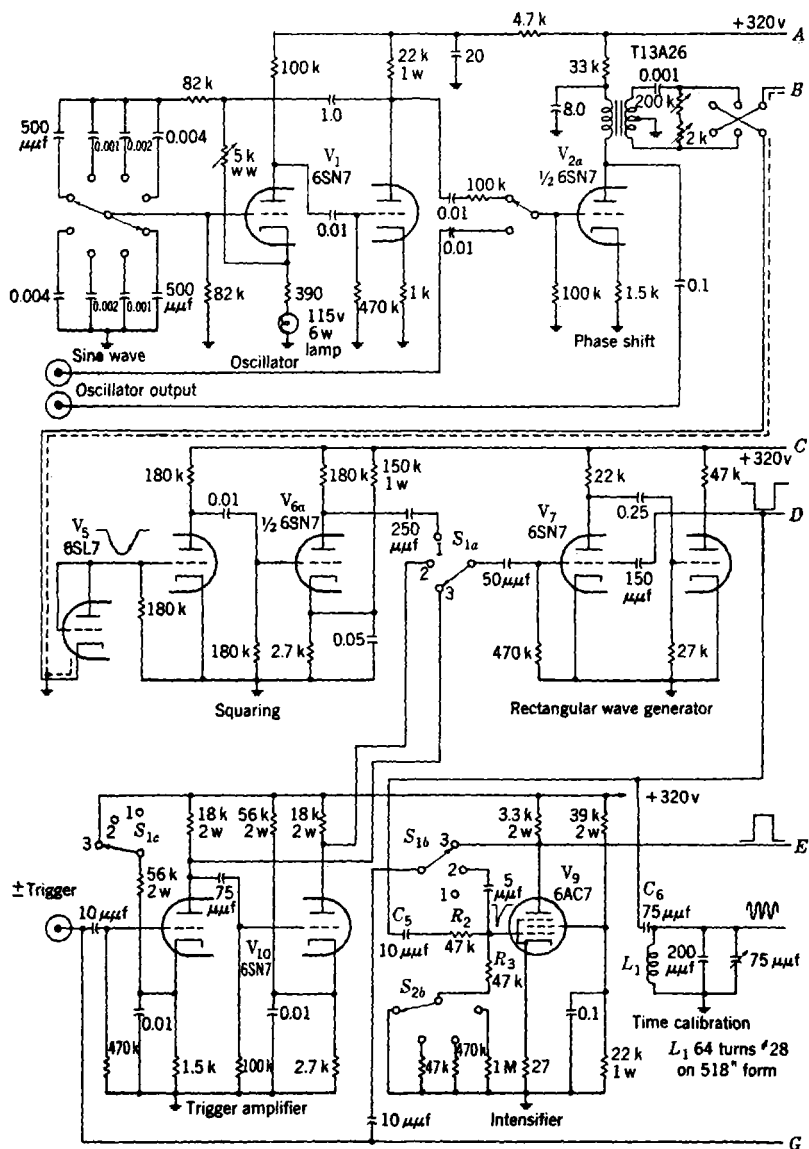
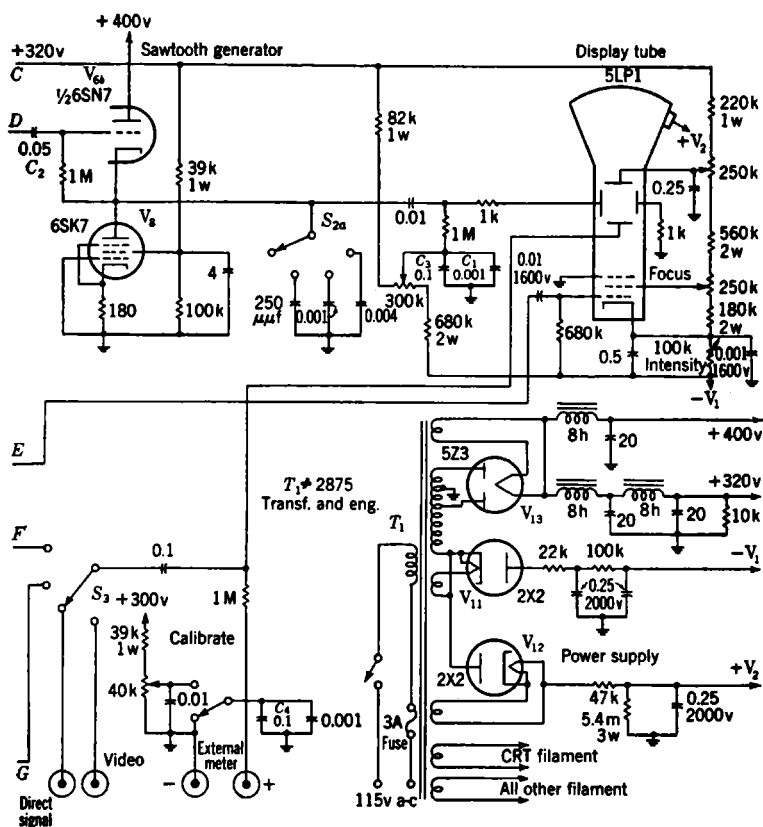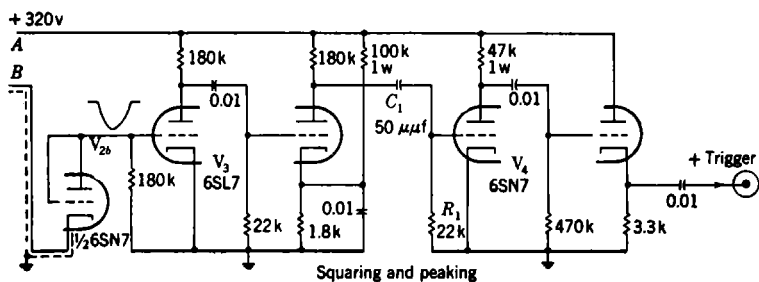Fig. 7·4a.—Schematic circuit diagram of P-4 synchroscope.

Fig. 7·4b.—Schematic circuit diagram of P-4 synchroscope (*continued*).

proper point, Gang $C$ is used to bias the trigger-pulse inverter, and Gang $B$ is used to supply the peaking to the intensifier tube. Sine-wave synchronization requires about 15 volts rms of input signal, which can be of any frequency from 200 to 4000 cps. The input trigger pulses can be from 10 to 150 volts in amplitude.

*Time-base Generator.*—The time-base-generating circuits include a multivibrator $V_7$ operating as a flip-flop, and a constant-current discharging circuit $V_{6b}$ and $V_8$ for the capacitors associated with switch $S_{2a}$. A circuit of this type is discussed in detail in Sec. 4·4. The multivibrator runs freely at a low frequency but readily "locks on" to the frequency of the trigger pulse applied to it through the switch $S_{1a}$.

The output of $V_7$ is a negative rectangular wave that is about 200 $\mu$sec long. This length is longer than the longest sweep and is not changed with sweep speed. (The length of the intensifier pulse and the amplitude of the sweep sawtooth are switched with changes in sweep speed.) The negative rectangular wave is used for three circuits: the sweep generator (through $C_2$), the intensifier (through $C_5$), and the calibration markers (through $C_6$).

The time base is started by applying the negative rectangular wave to the grid of $V_{6b}$, thus its plate current is cut off and the capacitor selected by switch $S_{2a}$ discharges linearly through $V_8$. The plate voltage applied in this circuit is high enough to result in a negative-going sawtooth waveform of sufficient amplitude to deflect the cathode-ray beam across the cathode-ray-tube screen. Although the discharge continues for the duration of the negative rectangular wave, the length of time required to reach full screen deflection is changed by switching condensers by means of $S_{2a}$.

At precisely the same time that the time base is applied to the deflecting plates, the cathode-ray beam is intensified by a positive rectangular-voltage pulse applied to the grid of the cathode-ray tube. The length of the intensifier pulse is set to equal the length of the sweep (that is, the time it takes for the sweep trace to travel across the entire tube face). This pulse is obtained from $V_9$, which acts as a sharp-cutoff amplifier. The negative differentiated front edge of the rectangular wave from $V_7$ is applied to the grid. This edge cuts off tube $V_9$ and the tube remains cut off until the condenser $C_5$ is charged. Thus, the grid rises exponentially with a time constant of $C_5$, $R_2$, $R_3$ and the resistor chosen by $S_{2b}$. When the grid goes above cutoff the plate voltage decreases, thereby ending the intensification.

The time base can be calibrated by a sinusoidal voltage of 2-Mc/sec frequency obtained from the $LC$-circuit on one position of switch $S_3$. This circuit is excited into a damped oscillation by the negative rectangular wave from the time-base multivibrator $V_7$.

*Cathode-ray Tube.*—Conventional circuits involving a voltage-doubler rectifier furnish the necessary operating potentials for the type 5LP1 cathode-ray tube. These potentials are such that the vertical deflection factor is about 60 volts per inch. A voltage from the low-voltage supply and a potentiometer with connections for a voltmeter are supplied for d-c voltage calibration of the amplitude of signals being observed.

*General.*—It will be noted that the time base is applied to only one horizontal deflecting plate of the cathode-ray tube. Because this instrument was not designed for extreme precision in measurements of observed signals, this feature was not considered a great disadvantage. Excessive astigmatism of the trace and an apparent deceleration of the beam, which
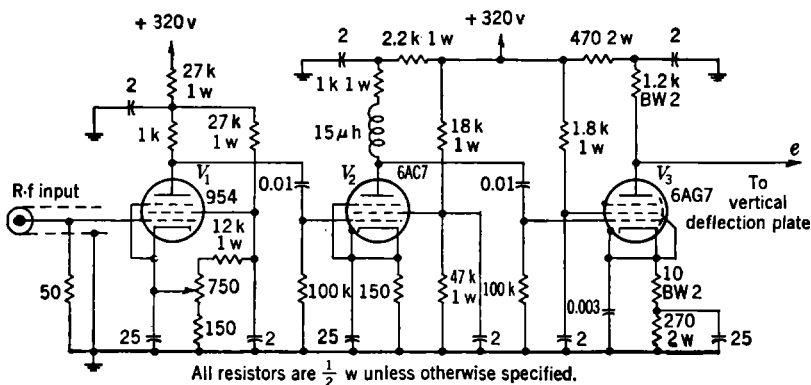


Fig. 7·5.—R-f detector and video amplifier.

causes a slight but perceptible rotation of the trace when it is moved appreciably above or below the center of the screen, limit the accuracy attainable when a single-ended time base is used.

The 1000-ohm resistors in series with the horizontal deflecting plates minimize the effects of cross coupling from the vertical plates when voltage pulses having a very steep wave front are being observed. The 0.001-$\mu f$ condensers in parallel with the 0.1-$\mu f$ condensers ($C_3, C_4$) are present because they are higher-quality condensers and will bypass the high frequencies better than the large tubular 0.1-$\mu f$ condensers can.

*Video Attachments.*—If an r-f detector and video amplifier are installed, a specially designed input connector is used to couple the r-f power to the grid of a 954 acorn tube operating as a square-law detector (see Fig. 7·5). A concentric-disk resistor of 50 ohms, located inside the coupling, terminates the coaxial transmission line. The vertical deflection of the trace on the cathode-ray tube is then proportional to the input power. The two-stage resistance-coupled video amplifier shown in Fig.

7·5 has a gain of about 100 over a band of from about 200 cps to 4.5 Mc/sec.

Other video attachments have been used with this synchroscope. A wider-band higher-gain video amplifier having four resistance-coupled stages has been frequently used where greater sensitivity was required. This attachment is shown in Fig. 7·6. It has a maximum bandwidth of
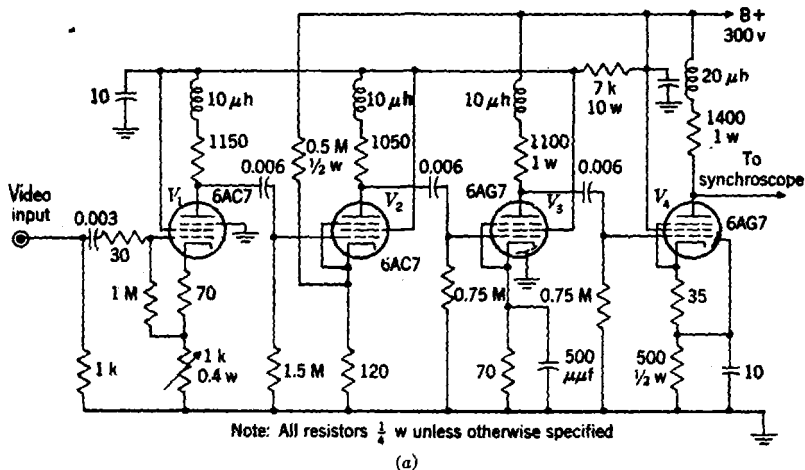
(a)

(b)
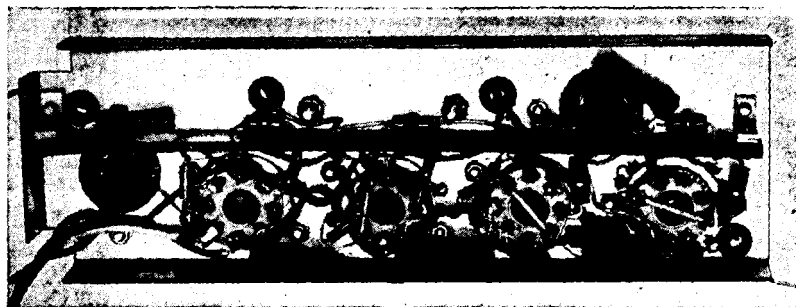
Fig. 7·6.—High-gain video circuit. (a) Circuit diagram. (b) Inside view.

from approximately 120 cps to 5·4 or 8·2 Mc/sec in accordance with the setting of the gain control. Maximum gain is about 2000 and minimum gain about 200. The wider bandwidth is available at the lower value of gain.

As seen in the circuit diagram, shunt peaking is used in all four stages to compensate for loading effects of the output shunt capacities. Input voltage to the amplifier may be from +0.16 to −0.8 volts without serious

saturation effects.    Saturation occurs when the output amplitude reaches
+140 volts.    If a crystal detector is connected to the input terminal,
with not over 12 in. of video cable, this amplifier may be used as an r-f
envelope detector.    The output voltage is then nearly proportional to
r-f input power when the gain control is at the medium setting.

Another attachment that has been used with the P-4 synchroscope is
a cavity-type r-f envelope detector.[1]    With this device, the input imped-
ance of the synchroscope is no longer the limitation on the rise time of a
pulse being viewed.

**7·3. Model 5 Synchroscope.** *Purpose.*—This synchroscope was
designed in order to meet the requirements for more precise studies of
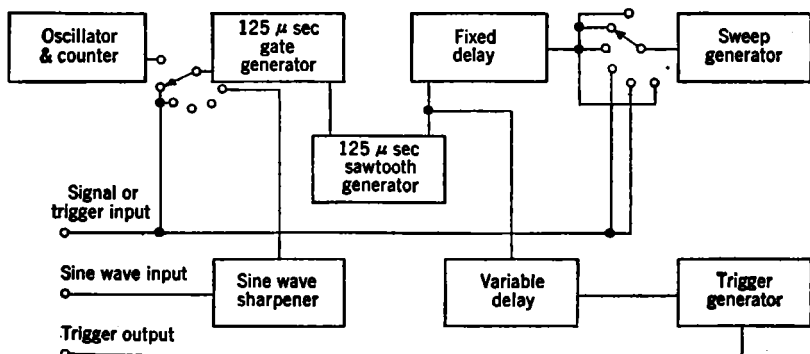


FIG. 7·7.—Block diagram of circuit operation.

pulse-type waveforms.    To meet these needs, faster sweep speeds with
increased freedom from "jitter" (random displacement) of the observed
signal were required.    The application of this instrument to production
testing of radar components has been widespread but, because of its bulk,
it is essentially a laboratory instrument.

*General Description.*—The Model 5 synchroscope is an oscilloscope
intended primarily for determining the amplitude, duration, and shape
of short video pulses.    The horizontal-time-base writing speeds are 0.01,
0.05, 0.2, 1, 2, and 5 in. per $\mu$sec with a sweep amplitude of 4 in. or more
on a type 5JP1 cathode-ray tube.

*Vertical Deflection.*—The vertical deflection sensitivity is approxi-
mately 65 volts per inch.    A vertical-deflection-sensitivity calibration
circuit is provided with connectors for a voltmeter, which should have a
sensitivity of at least 1000 ohms per volt.    Space and power are available
in the synchroscope for a video amplifier requiring not more than 2.2 amp
at 6.3 volts a-c and 70 ma at 360 volts d-c, and for an r-f envelope viewer.

_____
[1] See Vol. 11 of the Radiation Laboratory Series.

FIG. 7·8a.—Schematic circuit diagram of Model 5 synchroscope.
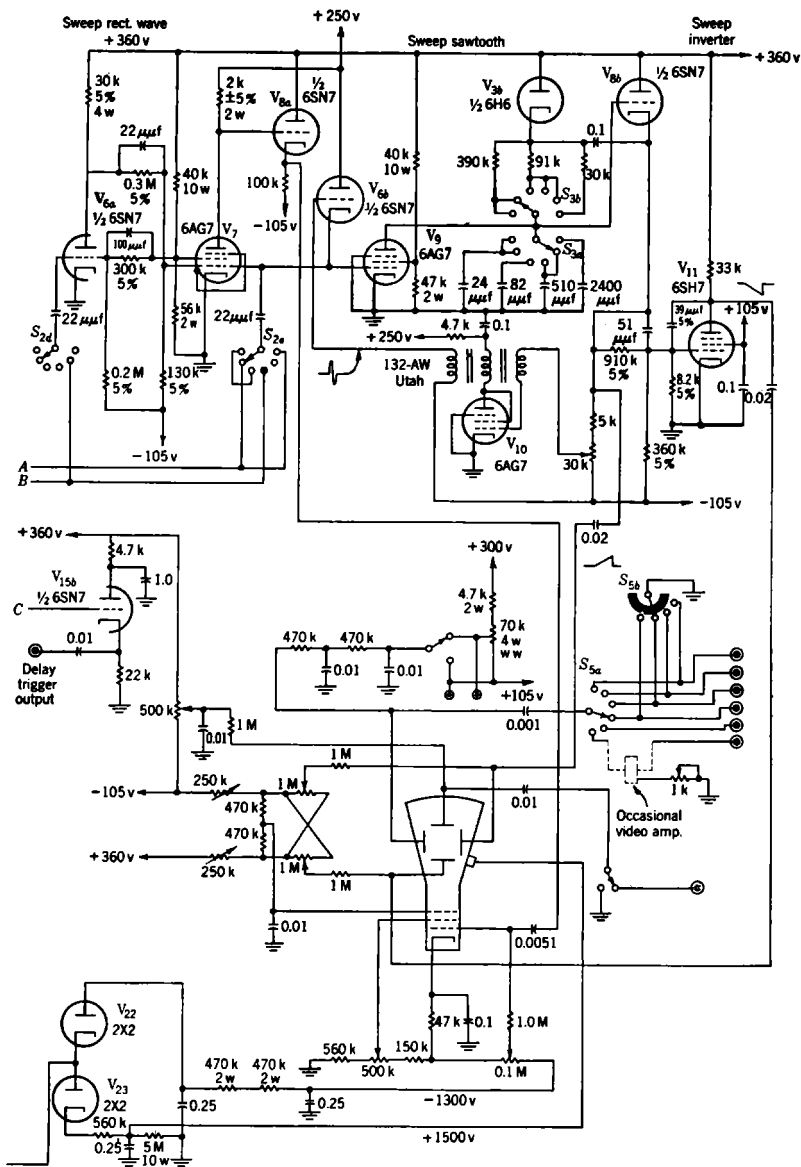
FIG. 7·8b.—Schematic circuit diagram of Model 5 synchroscope (continued).

Seven input connectors and a selector switch are provided so that the operation of any one of seven external circuits can be observed.

Time-delay circuits are incorporated in the synchroscope to give the following facilities:

1. A sweep that can be started by a positive or negative external trigger pulse.
2. A sweep that is delayed 90 $\mu$sec with respect either to the internal trigger pulse or to an external positive or negative trigger pulse; a positive output trigger pulse adjustable in time from 75 $\mu$sec before to 25 $\mu$sec after the start of the sweep.   The positive output trigger pulse reaches an amplitude of at least 200 volts in 0.3 $\mu$sec.

The delay circuits may be synchronized with the following trigger pulses:

1. The internal trigger generator, with repetition frequencies of 500, 1000, 2000, or 4000 cps.
2. A positive or negative external trigger pulse of at least 50 volts amplitude rising to 35 volts in not more than 0.5 $\mu$sec and having a repetition frequency of from 50 to 5000 cps.
3. A sinusoidal voltage having a peak-to-peak amplitude of at least 30 volts and a frequency of 50 to 5000 cps.

A connector is provided at the back of the chassis so that an external trigger generator similar to the internal delayed-trigger generator may be operated from the delay sawtooth waveform in the synchroscope to give another trigger pulse adjustable in time phase.   The synchroscope is designed to operate (without video attachments) at a power input of 200 watts from an a-c source of 105 to 125 volts at 50–60 cps.

*Circuits.*—The circuits used in each of the separate functional blocks achieve a higher degree of stability and resolution than those used in the P-4 synchroscope.   Figure 7·7 is a block diagram showing the various possible combinations of circuit functions available by suitable switching. Figure 7·8 is a complete circuit diagram of the instrument.

*Trigger Generator.*—The internal synchronizing trigger pulse is generated by means of a conventional Hartley oscillator $V_{1a}$ operating at either of two fixed frequencies of 1000 or 4000 cps in conjunction with a blocking-oscillator frequency divider $V_{1b}$.   Thus, an internal trigger pulse is available at 500, 1000, 2000, and 4000 cps, the frequency being determined by the time constants in the grid circuit of the blocking oscillator.

*Delay Circuits.*—Since, for many applications, it is desirable to adjust the time relationship between the sweep and the synchronizing trigger pulse. it is necessary to introduce time delay in the operation of both the

sweep generator and the trigger generator that supplies the trigger pulse for external synchronizing. In this instrument two delay circuits are used for this purpose; one to supply a fixed delay for the sweep circuit, and the other to apply to the output trigger circuit a continuously variable delay that overlaps the fixed delay. Figure 7·9 shows these time-delay relationships.

The operation of these delay circuits depends on a sawtooth voltage of approximately 125–μsec duration and approximately 100 volts amplitude, generated in a "bootstrap" circuit $(V_{3a}, V_4)$. A "flip-flop" circuit
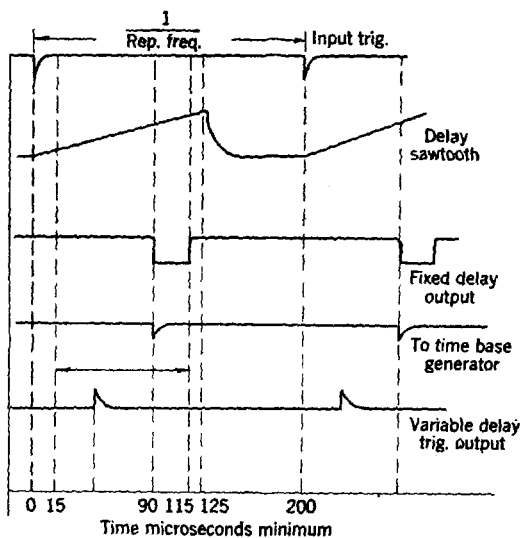


Fig. 7·9.—Time relationships in delay circuits.

$V_2$, whose operation is initiated by a trigger pulse obtained from either the internal trigger generator, an internal sine-wave squaring circuit, or an external trigger source, produces the negative rectangular-voltage wave that controls the bootstrap circuit.

The purpose of external triggering through the delay circuits is to provide over-all synchronization at frequencies other than those available from the internal trigger generator. The synchroscope is designed to operate in this manner over a range of from 50 to 5000 cps.

In both the fixed- and variable-delay circuits, cathode-coupled flip-flop circuits regenerate at a particular amplitude of the sawtooth wave. The duration of the variable delay $(V_{14})$ is controlled by adjusting the bias of the "on" grid $(V_{14b})$ to change the value at which the flip-flop regenerates.

The leading edge of the fixed-duration negative rectangular-voltage

wave from the fixed-delay flip-flop $V_5$ is differentiated and is used as a trigger pulse to initiate the operation of the sweep generator. Figure 7·9 shows the time relationship of this leading edge with respect to the original trigger pulse.

The positive-going variable-duration rectangular-voltage wave from the variable-delay flip-flop $V_{14}$ is applied to the blocking oscillator $V_{15a}$. This oscillator generates a trigger pulse corresponding to some point on the leading edge of the rectangular pulse. A cathode follower $V_{15b}$ delivers the positive swing of the cycle at a low-impedance level to the trigger output terminal. The rise time of this trigger pulse is about 0.25 μsec between 20 and 200 volts of amplitude.

The important feature of this type of time or phasing control is that almost complete freedom from jitter (random variation of time between output trigger pulse and sweep) is achieved when a well-regulated supply voltage is used for the delay circuits. Particularly when a fast sweep of about 5 in. per μsec is used, a displacement corresponding to the width of the vertically deflected trace (due to a signal) cannot ordinarily be tolerated. From consideration of nominal trace width, this width corresponds to a time displacement of about 0.006 μsec. The jitter in this instrument is somewhat less than this.

Pickup of hum by the cathodes of either $V_5$ or $V_{14}$ from the heater supply is primarily responsible for the jitter. It was found that this pickup is greatly reduced when tubes having a spirally constructed heater such as, for example, the RCA type of 6SN7 are used. This necessary tube selection may be considered as objectionable under some circumstances.

*Sweep Generator.*—The sweep generator ($V_{3b}$, $V_9$, and $V_{8b}$) also utilizes the "bootstrap" principle. Its operation is controlled by a negative rectangular-voltage wave from a "flop-over" circuit ($V_{6a}$ and $V_7$). The waveform is initiated by a negative trigger pulse from the fixed-delay circuit, and it is terminated by a positive trigger pulse from the automatic-shutoff circuit, $V_{10}$ and $V_{6b}$. The writing speeds available from this sweep circuit are 0.01, 0.05, 0.2, 1, 2, and 5 in. per μsec. Push-pull deflection of the cathode-ray trace is obtained by inverting in a unity-gain amplifier $V_{11}$ the sawtooth waveform obtained from the cathode follower $V_{8b}$. The automatic-shutoff circuit $V_{10}$ derives a trigger pulse from this sawtooth wave when it reaches an amplitude determined by the setting of the 50,000-ohm potentiometer in the cathode circuit of $V_{8b}$. Thus, the length of the sweep on the cathode-ray-tube scale can be set to any value within limits determined by the operating conditions of the shutoff. This circuit is less effective on the faster sweeps since, because of the dependence of the transformer action on the slope of the sawtooth wave, the sweep is not terminated at the same amplitude in each case. But

this feature is not objectionable because it is seldom necessary to see the termination of the sweep when it is possible to delay or advance the operation of the circuit or equipment under test with respect to the start.

It is also possible to initiate the operation of the sweep generator directly from an external trigger pulse or the observed signal itself independently of the delay circuits. Operation of this type is sometimes referred to as "self-synchronous." Since operation of this type requires that the sweep be started as quickly as possible after the initiating signal is applied, it is necessary that the regenerative action of the sweep flopover ($V_{6a}, V_7$) be as rapid as possible. This rapid change is made possible by using a 6AG7 pentode tube as the "on" tube ($V_7$). Tests have shown that the sweep will start approximately 0.01 μsec after $V_7$ is cut off by a negative signal. The positive rectangular pulse at the plate of $V_7$ and, hence, at the grid of the cathode-ray tube will reach 90 per cent of maximum amplitude at about the same time. Since only about 0.01 μsec is lost in circuits associated with $V_7$, the starting time of the sweep depends on how quickly $V_7$ is cut off. If the input signal is of positive polarity, an additional time is lost, the magnitude of which depends on how long it takes for the plate of $V_{8a}$ to cut off $V_7$.

*Cathode-ray Tube.*—This synchroscope employs a type 5JP1 cathode-ray tube, characterized by low shunting capacities (of the order of 3 μμf) at the deflecting plates. Therefore, transient voltages of about 50 Mc/sec, or higher, in frequency can be observed. However, when the cathode-ray-tube deflecting plate is connected through the selector switch in the scope this input capacity is increased to approximately 15 μμf.

No video-amplification or sweep-calibration circuits are provided, but space and power are available in the synchroscope for such attachments. However, in the case of sweep calibration, it has been customary to use external equipment of a more elaborate and precise design than could be included in the synchroscope.

*Power Supplies.*—Conventional circuits are used to furnish the necessary d-c voltages and current for the various tubes and circuits. Included is an electronically regulated supply circuit that furnishes a stable d-c voltage for the delay control circuits, since any variations of voltage there would vary the operating conditions of the circuits and, hence, cause variations or jitter in the synchronizing of the output trigger pulse and the sweep.

*Video Attachments.*—Space and power for various video attachments are available in the Model 5 synchroscope. The space was designed for the same attachments that are available for the P-4 synchroscope, but an improved amplifier was designed.

This amplifier was specifically designed for this unit to take advantage

FIG. 7·10.—Schematic diagram of wideband video amplifier for Model 5 synchroscope.
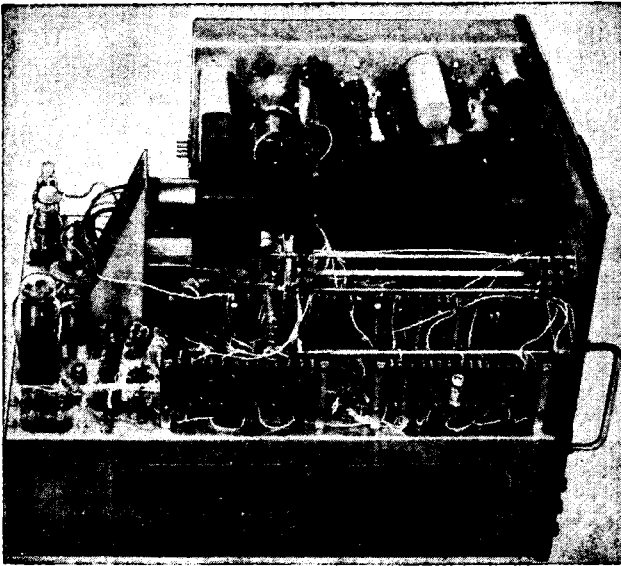
(a)
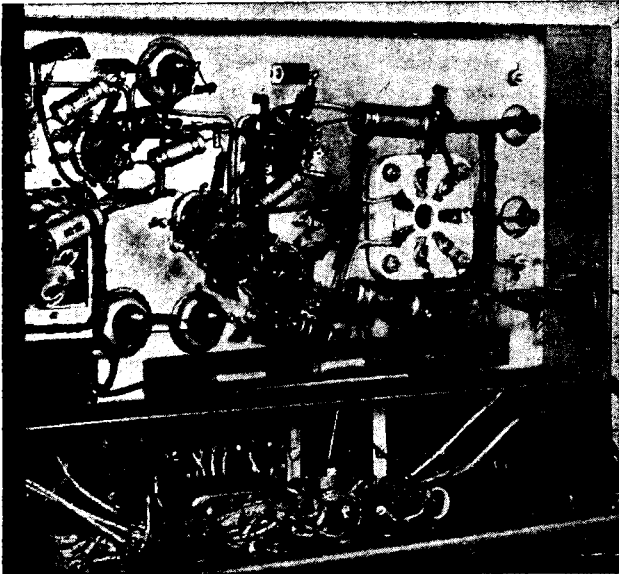


(b)

Fig. 7·11.—Model 5 synchroscope.   (a) Left interior.   (b) Video amplifier in Model 5 synchroscope.   (*Courtesy of Sylvania Electric Products, Inc.*)

of the low capacity of the deflecting plates of the type type 5JP1 CRT. Figure 7·10 is the schematic circuit diagram and Fig. 7·11 shows the method of installation. It is seen that the push-pull output circuit is coupled to the deflecting plates by very short leads.

The characteristics of the amplifier are as follows: Frequency response is flat within 3 db between 20 cps and 18 Mc/sec; gain is approximately 180; input impedance is 1 megohm; attenuator provides total attenuation of 500 to 1 in steps of between 3 and 4 to 1; maximum input voltage allowable at grid of first stage, 6AC7, is 0.3 volt; maximum output voltage, plate-to-plate, without overloading is approximately 55 volts; power requirements are 225 volts of direct current at 290 ma and 6.3 volts of alternating current at 7 amp, obtained from a separate power supply.
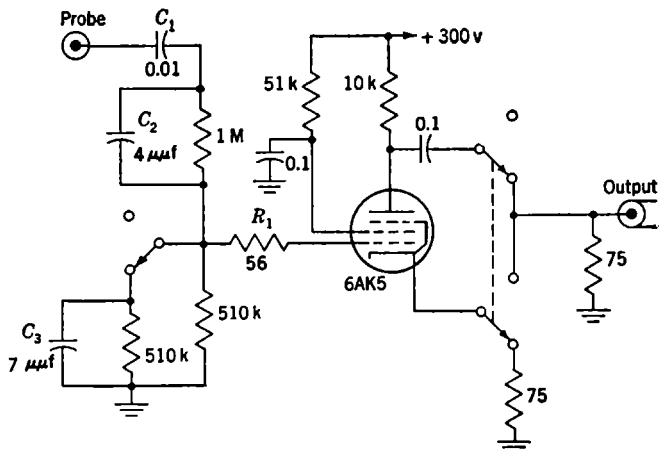


Fig. 7·12.—Video test probe, schematic diagram.

The unusually wide pass band was obtained by careful consideration of the layout of components and compensation for the effects of loading due to tube and wiring capacities. Since these factors are very closely interrelated, very careful design is required in order to obtain optimum results in gain and bandwidth at a given input power. It is seen in the circuit diagram, Fig. 7·10, that for optimum performance with the layout as illustrated in Fig. 7·11 both shunt- and series-peaking networks are used to take care of the compensation problem.

**7·4. High-frequency Test Probe.**—Figures 7·12 and 7·13 illustrate a test probe that is particularly useful for viewing rapid phenomena. It has a very high input impedance ($C = 8 \ \mu\mu\text{f}$, $R > 1$ megohm), a low output impedance (75 ohms), and a gain of 0.12 or 0.08; it can be built very compactly. The tube used is a 6AK5 pentode, which is small and has a high input impedance. The output signal can be obtained from

either the plate or the cathode depending on the polarity desired. The pass band is 70 Mc/sec wide; therefore $C_2$ and $C_3$ are needed for frequency compensation. If the attenuation is changed, it is necessary to change these condensers so that the ratio of the reactances remains equal to the ratio of the resistances in the attenuator. Any decrease in the attenuation will decrease the input impedance (provided that the frequency compensation is maintained) because of the existent distributed capacity from the grid of the tube to ground. Too little attenuation will also result in the overloading of the tube by large signals. As shown, the probe can accommodate signals up to 10 volts. To prevent parasitic oscillations, $R_1$ is inserted. The low-frequency response is limited by $C_1$.
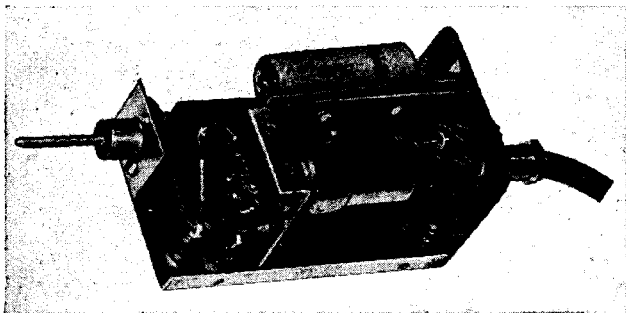


FIG. 7·13.—Video test probe, inside view.

**7·5 Model G Synchronizer.** *Purpose.*—The Model G synchronizer is designed primarily to convert an ordinary oscilloscope into an A-scope for laboratory use. It provides a linear time base controlled by a synchronizing trigger from a source either internal or external to the synchronizer in very much the same manner as are the time bases in the equipments already described in this chapter, and differs from a synchroscope only by the absence of the usual cathode-ray tube.

A feature of the synchronizer is its versatility. The input and output terminals of the various functional blocks are all located on the front panel. In order to eliminate complex switches, patch cords are used to connect these circuits as desired for a particular application. This type of construction enables the individual circuits to be used independently.

*General Description.*—The operating characteristics of the Model G synchronizer are as follows:

1. *Internal Trigger Generator.* A free-running blocking oscillator supplies positive and negative trigger pulses of approximately 200 volts amplitude, rising to 90 per cent in 0.25 μsec, at a continuously variable repetition frequency of from 250 to 2500 cps.

2. *Delay Circuits.*

   a. A fixed-delay circuit requiring a negative trigger pulse that reaches at least a 45-volt amplitude in 0.25 $\mu$sec provides positive and negative triggers delayed 20 $\mu$sec from the input trigger and having the same characteristics as the output trigger pulse of the trigger generator.

   b. A variable-delay circuit with the same input requirements and output characteristics as the fixed-delay circuit provides a continuously variable time delay of from approximately 15 to 1200 $\mu$sec between output and input trigger pulses.

3. *A calibrating circuit*, requiring a negative rectangular-voltage wave, provides sinusoidal voltages of 100 kc/sec and 500 kc/sec for sweep calibration.

4. *A utility circuit* is available for use as an amplifier, inverter, or cathode follower.

5. *Sweeps.*

   a. The nine sweep speeds available range from 0.2 to 600 $\mu$sec per inch if the direct horizontal deflection factor of the CRT is 40 volts per inch. The sweep output is push-pull.

   b. The initiating trigger for the sweep may be either positive or negative; it must be at least 50 volts in amplitude and rise to 90 per cent in at least 0.5 $\mu$sec.

   c. Positive and negative rectangular voltage waves are available for intensifying the cathode-ray beam or for external use.

*Circuits.*—A complete diagram of this equipment is shown in Fig. 7·14.

*Variable-frequency Trigger Generator.*—This circuit furnishes positive and negative trigger pulses. The output signal from a blocking oscillator, consisting of $V_{9a}$ and a pulse transformer $T_1$, whose frequency is variable from about 250 cps to about 2500 cps, is applied to a cathode-follower inverter $V_{9b}$. The output signal from the plate of $V_{9b}$ is then brought to $J_1$ and $J_2$, and the output from the cathode is brought to $J_3$.

*Trigger-delay Circuits.*—Two trigger-delay circuits are incorporated in the synchronizer; one provides a fixed delay of about 20 $\mu$sec, and the other provides a continuously variable delay from a minimum of about 15 to a maximum of about 1200 $\mu$sec. These circuits each consist of a flip-flop and a blocking oscillator. The latter fires at a time corresponding to the return of the flip-flop to its stable quiescent condition.

In the case of the fixed delay, the time constant controlling the duration of the unstable condition of the flip-flop is fixed and is determined by $R_4$ and $C_1$. In the variable-delay circuit, the corresponding time constant is determined by the adjustment of both $R$ and $C$; that is,

FIG. 7·14.—Schematic circuit diagram of Model G synchronizer.

by using a variable resistor $R_5$ and varying the capacity by means of the selector switch $S_1$. The capacitors that are switched into the circuit by $S_1$ are chosen so that successive positions of the switch provide delay ranges that overlap when $R_5$ is turned through its range of values. Continuous variation of delay from minimum to maximum is therefore provided.

This type of delay control is not completely jitter-free. In fact, the amount of jitter is very nearly a constant fraction of the amount of delay being used and is approximately 0.02 per cent. The jitter can be reduced by a factor of about two if a well-regulated plate supply is used for $V_7$, as shown in the circuit diagram. A switch and a terminal for applying this power is located on the rear panel. The chief advantage of this method of generating a delay is its simplicity and low cost in space and power. The performance of this circuit is perfectly adequate for general applications where calibrated delay controls are not required.

*Sweep Generator.*—The sweep generator is very much like the corresponding circuit in the Model 5 synchroscope and differs only in the method of terminating the sweep. A flop-over ($V_{1b}, V_2$) is used to develop a rectangular-voltage wave for the pentode switch tube $V_3$. A unity-gain amplifier $V_4$ inverts the sawtooth sweep voltage so that push-pull deflection can be applied to the external cathode-ray tube. The sawtooth voltage is terminated by coupling a fraction of it, determined by $R_1$, $R_2$, and $R_3$, back to the grid of the pentode $V_2$. Thus the rectangular wave is initiated by a trigger from an external source and is terminated by a positive-going fraction of the sweep sawtooth wave.

The electron-coupled plate circuit of $V_2$ furnishes a positive rectangular voltage, which is applied to the grid of $V_{1a}$. This tube acts as a cathode follower to supply a positive rectangular voltage as an intensity gate for the external cathode-ray tube, and a negative rectangular voltage for general use.

The operation of this circuit can be initiated by either a positive or negative trigger of at least 50-volt amplitude. There are two equal output sawtooth waveforms of opposite polarity, each of 80-volt amplitude. The slopes of these vary from 0.033 volts/$\mu$sec to 100 volts/$\mu$sec. The sweeps available when used with a CRT having a horizontal deflection factor of 40 volts/in. are 600 to 0.2 $\mu$sec/in. in 9 steps of approximately 3-to-1 ratio.

*Auxiliary Circuits.*—A simple sweep calibration and a utility amplifier circuit are also included in this instrument. The calibrator is a Hartley oscillator, associated with $V_{11}$ and $V_{10b}$, which can be keyed by the negative rectangular output voltage from the sweep sawtooth-generator circuit. Two frequencies, 100 kc/sec and 500 kc/sec, are available at the output terminal of a cathode follower for rough calibration of the

sweep speeds of the sawtooth generator. The utility circuit $V_{10a}$ is useful as a cathode follower, an amplifier, or inverter, depending on the positions of the associated switches.

The connections to the CRT circuit should be as indicated in the diagram of Fig. 7·15. Usually, simple modifications are required in average oscilloscopes such as the Du Mont types 208, 224A, and 241, and others in which push-pull deflection is possible. The impedance looking into the horizontal deflecting plates should be symmetrical and should have as low a shunt capacitance as possible. Considerations of
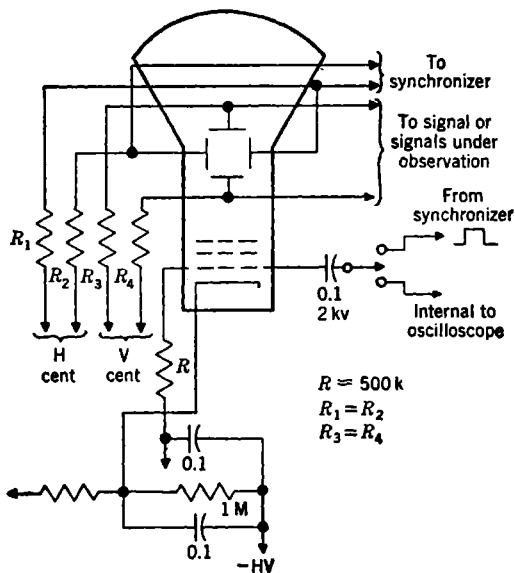


FIG. 7·15.—Connections to cathode-ray tube from Model G synchronizer.

this input impedance become more important as the sweep speed is increased. When the synchronizer is used in conjunction with an oscilloscope having only one deflecting plate available for horizontal deflection, it would be preferable to use the positive sawtooth waveform from the cathode of $V_{4a}$ for the sweep since the impedance level at this connection is low.

**7·6. A/R Range Scope.** *General Information.*—This instrument has the following characteristics:

1. Any portion of the 1200-$\mu$sec A-sweep can be expanded by using sweeps of 4000, 2000, or 8000 yd, that is, 7, 3.3, and 1.0 $\mu$sec/in., respectively. These sweeps, known as R-sweeps, are continuously

movable in time by a delay circuit and a calibrated dial. A strobe marker is provided on the A-sweeps to indicate the time interval covered by the R-sweeps.

2. The delayed trigger pulse that starts the R-sweep may be used externally as a precision time marker, or to indicate the position of the R-sweep on another indicator.

3. Range accuracy of $\pm 0.1$ per cent of full scale is attainable. Range is read directly from the delay dial by moving the target to the left edge of one of the expanded R-sweeps.
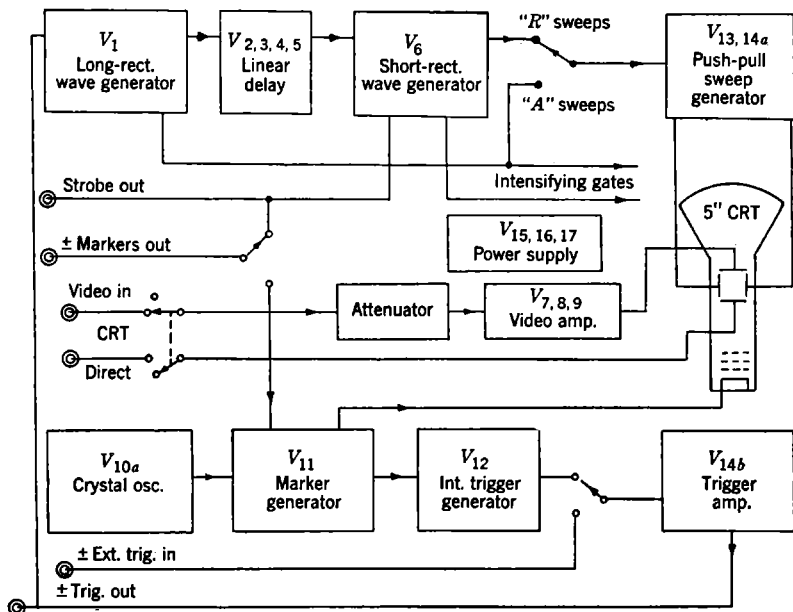


FIG. 7·16.—Block diagram of A/R range units Model 3.

4. Crystal-controlled calibration markers, either 2000 yd or 10,000 yd apart, and accurately phased to the trigger pulse, are provided. Because of the phase-lock circuit, the first 10,000-yd marker is 8000 from zero and the succeeding markers therefore are at 18,000 yd, 28,000 yd, etc. However, this same phase-lock circuit makes the trigger pulse coincident with the 2000-yd markers and thus eliminates any zero factor.

5. The repetition frequency of the internal trigger generator is variable in discrete steps of submultiples of 16.39 kc/sec between 80 and 2000 cps on the 120-$\mu$sec scale, and between 80 and 200 cps

on the 1200-$\mu$sec scale. Both positive and negative polarity trigger pulses of approximately 100 volts are available for external use. The unit also may be switched to operate from either a positive or a negative external trigger having at least a 15-volt amplitude and a minimum rate of rise of 100 volts/$\mu$sec. Slower rising triggers may affect the range calibration.

*Block Diagram.*—The sweep generator driver $V_{13}$ and $V_{14a}$ is gated either by the long undelayed rectangular wave from $V_1$ or by the short delayed rectangular wave from $V_6$.

A quartz-crystal oscillator $V_{10a}$ controls the 2000-yd marker generator $V_{10b}$. These marks are counted 5 to 1 by $V_{11a}$ to give the 10,000-yd markers. The repetition-rate generator $V_{11b}$ further divides this frequency, and $V_{12}$ applies either the internal or external trigger pulse to the other circuits. Tube $V_{14b}$ is the trigger output driver amplifier. Figure 7·17 is a complete schematic diagram of the A/R-scope.[1]   Figures 7·18$a$ and 7·18$b$ show the internal construction.

*Long-rectangular-wave Generator.*—This is a d-c coupled cathode-biased flip-flop circuit. Tube $V_{1a}$ is normally conducting and is turned off by a negative trigger applied to the plate of $V_{1b}$.

The time duration of the rectangular wave (time during which $V_{1a}$ is off and $V_{1b}$ is conducting) is determined by the grid time constant $R_1C_1$ or $R_1C_2$ and is set slightly greater than the time to be covered by the delay circuit. For repetition frequencies higher than 250 cps the entire time interval between successive trigger pulses may be observed by throwing switch $S_1$ to Position 8. The length of the long rectangular pulse is then controlled by $C_3$ instead of $C_1$. Its length is thereby increased from 1200 $\mu$sec to 4500 $\mu$sec. The plate load resistors are divided so that only portions of the positive and negative output pulses are applied to the other circuits. The positive pulse is used to intensify the cathode-ray tube during the A-sweeps. The negative pulse is used to gate the delay circuit (through $C_4$) and the sweep generator (through $C_{14}$), when the A-sweep is used.

*Precision Delay Circuit.*—This bootstrap sawtooth delay circuit is notable for its linearity (better than $\pm 0.1$ per cent) and for its stability.

When the clamp $V_{3a}$ is cut off by a negative pulse on its grid, the condensers $C_5$ and $C_6$ begin to charge exponentially through $R_2$ and the diode $V_{2a}$. The exponential voltage rise is linearized by two feedback circuits. The voltage appearing across $C_5$ and $C_6$ is applied to the grid of a cathode follower $V_{3b}$ whose cathode signal is fed back through $C_9$ to the top end of $R_2$. This feedback path keeps the voltage drop across $R_2$ nearly constant, and thereby linearizes the sweep to about 1 per cent. Complete lineari-

---

[1] The transformers, not described in the drawing, are $T_2$, $T_5$—Utah X-154-T-1; and $T_3$, $T_4$, $T_6$—Utah X-124-T-3.
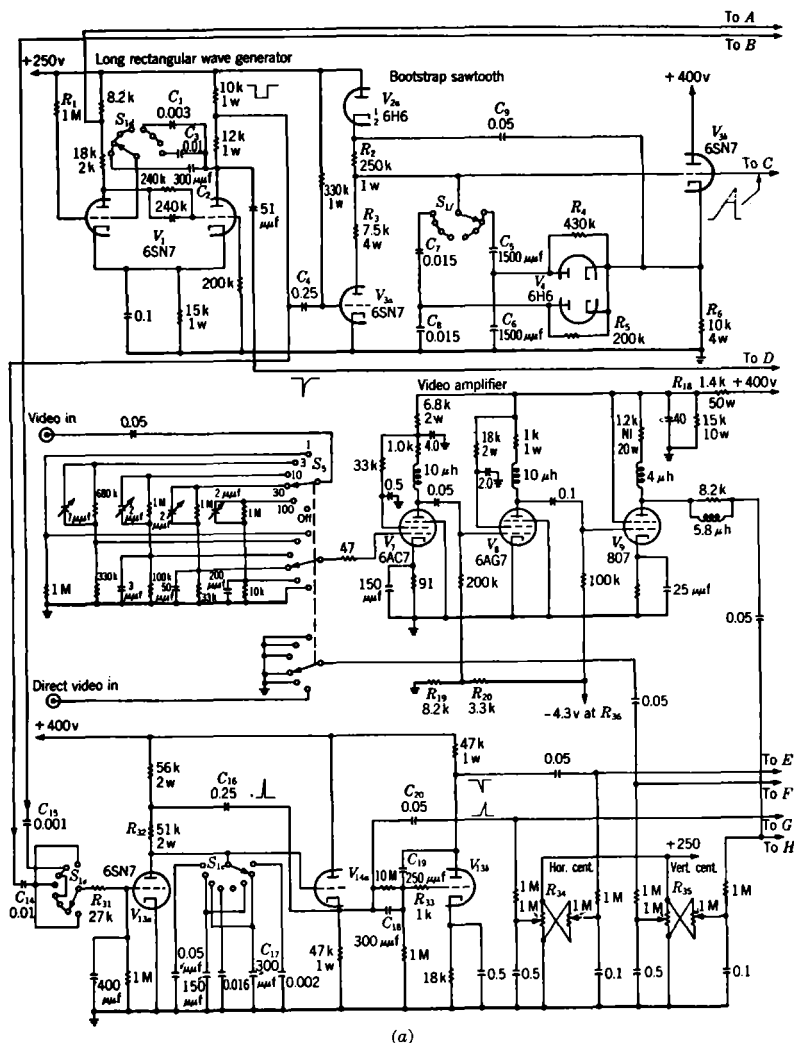
FIG. 7·17.—Schematic dia-

zation is achieved by integrating the sawtooth wave by means of $R_4C_6$ and feeding the resultant voltage across $C_6$ back in series with the existing sawtooth voltage. This process results in a sawtooth wave linear to $\pm 0.1$ per cent or better.

The diodes $V_4$ are used to discharge the condensers at the end of the sawtooth wave and thus increase the maximum duty ratio.
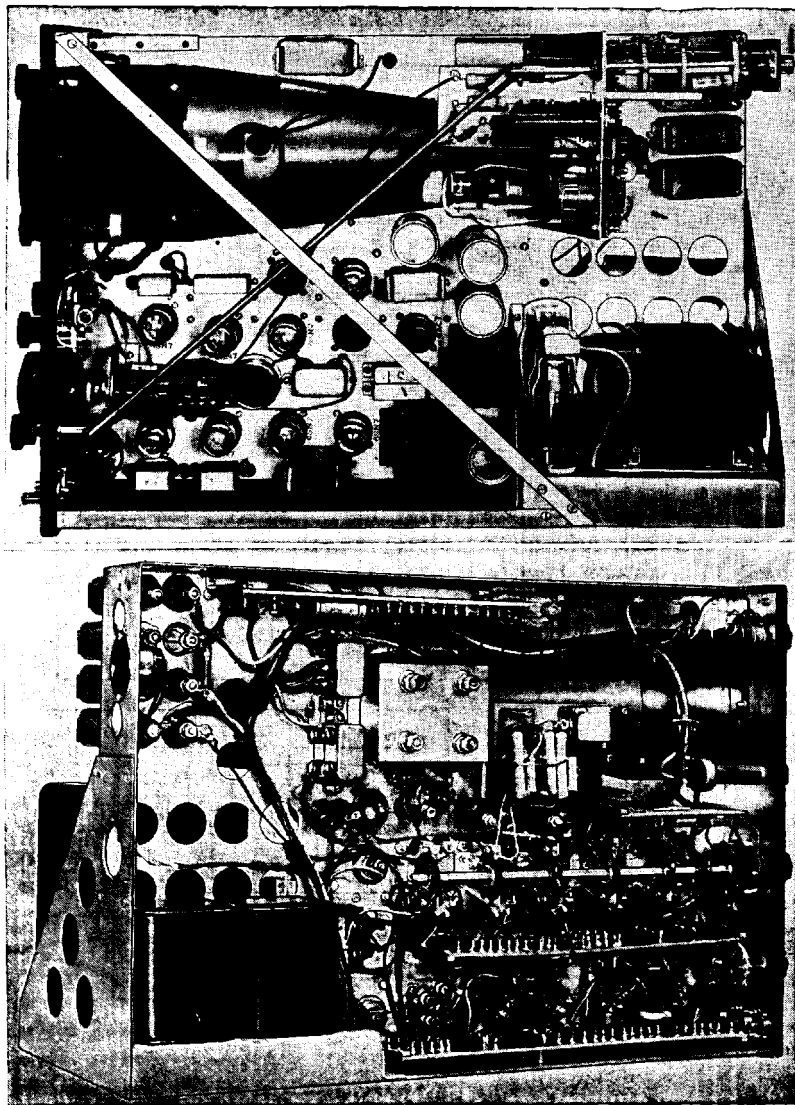
(b)

gram of A/R-scope.

The waveform on the grid of $V_{3b}$ is a sawtooth voltage of slightly more than 100 volts peak amplitude whose slope is determined by $R_2$, $C_5$, and $C_6$. The full sawtooth waveform also appears on the plate of the pickoff diode $V_{2b}$. The point at which the diode starts to conduct is determined by the d-c bias on the cathode of $V_{2b}$. This level is determined by the delay potentiometer $R_{10}$, and its minimum and maximum value are set

FIG. 7·18.—Right and left inside views of A/R-scope.

by the "zero" potentiometer $R_{11}$ and "slope" potentiometer $R_8$.  These potentiometers are used to calibrate the delay dial on the front panel for the 120-μsec range.  A similar set of potentiometers ($R_{12}$ and $R_9$) are used to calibrate the dial for the 1200-μsec range.  To obtain high precision from the delay circuit, a precision potentiometer[1] and a special counter dial are used.  Resistor $R_3$ in the sawtooth-generator clamp circuit $V_{3a}$ sets the potential of the plate of $V_{2b}$ at a level that will permit the zero control to set the minimum voltage of $R_{10}$.

For temperature compensation, wire-wound resistors are used for $R_2$ to $R_{12}$ inclusive, $R_2$ and $R_3$ being made of manganin.  Also a portion of each of the capacity values designated by $C_5$, $C_6$, $C_7$, and $C_8$ is of the
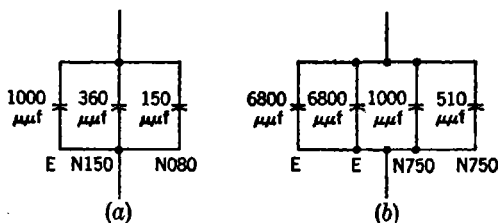


FIG. 7·19.—Temperature compensation of capacities obtained by making $C_5$ and $C_6$ in Fig. 7·17 like (*a*), and $C_7$ and $C_8$ like (*b*).  All capacitors have 5 per cent tolerance.

best silver-mica type available, that is, Grade $E$, and the rest is made up of commercially available negative-coefficient ceramic condensers.

The operation of the delay circuit may be observed on the scope itself by using one of the A-sweeps.  The full 100-volt linear sawtooth wave will be applied to the grid of $V_{3b}$ only when the delay is a maximum; otherwise the top of it is cut off when the pickoff diode $V_{2b}$ conducts.

Only that portion of the sawtooth wave immediately following conduction will appear on the cathode of the pickoff diode $V_{2b}$.  As the dial is turned to increase the delay, the start of this wave moves to the right on the A-scope.

*Amplifier and Delayed-trigger Generator.*—This amplifier is used to sharpen the voltage wave from the cathode of $V_{2b}$ and to derive a trigger at a time corresponding to the initial conduction of this diode.  From the plate of the amplifier $V_{5a}$ is obtained a negative signal at the conduction point and a positive signal at the end of the sawtooth wave.  Since the positive signal is of much greater amplitude it must be eliminated to prevent its returning edge from generating a trigger pulse and thus producing an additional R-sweep.  The discrimination against the large positive signal is accomplished by tying the grid of $V_{5b}$ to B+ voltage through $R_{13}$.  A series resistor is inserted to decrease grid-current

[1] "Helipot" made by National Technical Laboratories, Pasadena, Calif. or "Micropot" made by Thomas B. Gibbs and Co., Delavan, Wis.

effects. The desired negative signal from the $V_{5a}$ plate is, however, amplified by $V_{5b}$ in the normal manner and appears as the delayed-trigger pulse to drive the next circuit. The amplitude of this trigger pulse depends on the range used because the original sawtooth slope is different for the two ranges. It is about $+100$ volts for the 120-$\mu$sec scale and $+40$ to $+50$ volts for the 1200-$\mu$sec scale. Although this much amplitude is not necessary to trigger the next circuit, the size does contribute to the stability of the delayed trigger by increasing the rate of rise.

*Short-rectangular-wave and Delayed-trigger Generator.*—Amplifier $V_{6a}$ fires a special blocking oscillator consisting of $V_{6b}$ and $T_2$. The positive signal on the grid causes $V_{6a}$ to draw current through one winding of $T_2$. This current drives the grid of $V_{6b}$ to conduction because of the transformer coupling. The blocking-oscillator circuit is such that the grid is held positive for about 24 $\mu$sec instead of immediately being driven negative in the usual manner. This action is obtained by a special transformer $T_2$ and the condenser $C_{10}$, which receives the positive cathode signal and thus aids in holding the grid positive for the 24-$\mu$sec period. Normally $V_{6b}$ is kept from firing by the network $R_{14}$, $R_{15}$, and $R_{16}$, which biases the cathode above cutoff. The front edge of the blocking-oscillator signal represents the delayed trigger pulse. The overshoot pip at this front edge is not eliminated because it provides a sharp, clear-cut edge at the start of the R-sweep.

The 24-$\mu$sec output pulse of the blocking oscillator is used as:

1. A movable negative marker on the two A-sweeps (from $R_{17}$ and $S_4$).
2. A positive strobe for any associated indicator (from $R_{18}$).
3. A positive intensifier pulse for the cathode-ray-tube trace during the delayed sweeps (from $R_{16}$).
4. A negative pulse (through $C_{15}$) to start the 4000-, 2000-, or 800-yd R-sweeps.

Since the delay cannot be reduced to zero, the expanded sweeps cannot be moved in to zero. The minimum delay is 500 yd on the 20,000-yd scale and 1000 yd on the 200,000-yd scale. However, a front-panel toggle switch $S_2$ is provided on the grid circuit of $V_{5a}$ to start the fast sweeps from the undelayed trigger.

*Bootstrap Sawtooth-sweep Generator and Sweep Driver.*—The sweep generator is a cathode-follower bootstrap circuit. The sweep clamp $V_{13a}$ prevents the sweep condenser $C_{17}$ from charging, but when the negative gating pulse is applied to the grid, this condenser begins to charge. To compensate for the nonlinearity of exponential voltage rise, feedback is obtained from the cathode follower $V_{14a}$ through $C_{16}$ to the top of the charging resistor $R_{32}$. The proper gating pulse for the clamp, and the

desired sweep-charging condenser are selected by separate gangs (E and C respectively) of $S_1$. The A-sweeps (Switch Positions 1, 5, and 8) use the undelayed long rectangular wave (from $V_{1b}$ through $C_{14}$). The R-sweeps (Switch Positions 2, 3, 4, 6, and 7) get a gating pulse from the short-rectangular-wave generator ($V_{6b}$ through $C_{15}$).

The sweep sawtooth wave drives one of the cathode-ray-tube deflection plates through the cathode follower $V_{14a}$ and $C_{20}$, while $V_{13b}$, an inverter, drives the opposite plate. This tube is kept at unity gain by the capacity divider $C_{18}$ and $C_{19}$. Oscillations are suppressed by $R_{31}$ and $R_{32}$.

*Crystal Oscillator.*—Although this crystal oscillator employs only a triode ($V_{10a}$), stability tests show that it is reliable. Variations within the specified tolerance in tubes and components do not change the frequency by more than $\pm 9$ cps and the crystals are made to an accuracy of $\pm 25$ cps or better. Thus the usual accuracy is 0.02 per cent. The oscillator output wave is not a sine wave because it is peaked by the transformer winding in the plate circuit and also by feedback from the 2000-yd marker generator.

*2000-yd Marker Generator.*—The output of the crystal oscillator goes to a blocking-oscillator circuit $V_{10b}$ that makes the markers sharp and well defined. Their rise time is 0.2 μsec, and the width at the base is 0.6 μsec. The output is in the form of positive and negative current pulses taken from the small resistors $R_{22}$ and $R_{21}$ respectively. Because of coupling through $C_{11}$, some of the 10,000-yd marker pulse may be seen mixed with the 2000-yd markers. This mixing aids in distinguishing every fifth 2000-yd mark.

*10,000-yd Marker Generator.*—This circuit produces 10,000-yd markers by counting five 2000-yd markers. The cathode-coupled-type blocking oscillator $V_{11}$ and $T_4$ is used here to provide stability against changes in heater voltages in the frequency divider. It is fired by every fifth 2000-yd marker through condenser $C_{11}$. The adjustable grid resistor $R_{23}$ has a latitude of division from 3 to 6 to cover tolerances in the transformers and other components. This potentiometer is on the chassis and is locked at the factory after being set for the desired 5-to-1 division ratio. The positive and negative output signals are taken off small resistors in the cathode and plate circuits.

The operation of the divider may be observed by looking at the grid of $V_{11a}$ where a sawtooth wave together with the 2000-yd marker superimposed on it appears. The capacity of the scope lead used in observing this waveform may change the division ratio. Hence $R_{23}$ should not be set under these conditions, but it may easily be adjusted by superimposing the two types of output markers on any type of display.

*Repetition-rate Divider.*—The signal for the trigger amplifier $V_{12}$ is taken from the cathode of $V_{10b}$ in order that it may be in perfect phase

with the crystal markers. However, the markers occur at a frequency of 82 kc/sec, and only certain ones are selected to produce the repetition-rate frequency of 80 to 2000 cps. Tube $V_{11b}$ is, therefore, used as both a divider to count down from 82 kc/sec and a coincidence-gate generator to drive the cathode of the trigger-selector tube $V_{12a}$.

Signals obtained from the cathode of $V_{11a}$ through $C_{12}$ have already been divided by 5, hence the grid-circuit time constant of $V_{11b}$ is so designed as to give the rest of the necessary division. This time constant, and therefore the division, is changed by varying $R_{26}$. To count down to the trigger's repetition rate, $R_{25}$ is inserted in the circuit when the 200,000-yd scale is used in order to prevent the repetition rate from exceeding the maximum (400 cps) for this scale.

The use of transformer $T_5$ widens the output pulse of $V_{11b}$ to about 3000 yd, that is, 18 $\mu$sec. This pulse appears as an approximately rectangular wave across the 220-ohm resistor $R_{24}$. The occurrence of this rectangular wave determines the repetition frequency by selecting a particular 2000-yd marker as the trigger. This selection is accomplished by using $V_{12a}$ as a coincidence circuit. It conducts only when the rectangular wave on the cathode and the 2000-yd marker on the grid occur simultaneously.

The values of $R_{27}$ and $R_{28}$ are such that $V_{12a}$ is biased to about twice cutoff. The pulse from $V_{11b}$ raises it to cutoff and the particular 2000-yd marker occurring in the 3000-yd interval causes it to conduct and fire the $V_{12b}$ blocking oscillator. Thus, a particular marker starts the 3000-yd rectangular wave in $V_{11b}$ and the next succeeding one causes $V_{12a}$ to conduct.

When the trigger selector switch $S_3$ is in the NEGATIVE EXTERNAL position, $V_{12a}$ is self-biased by $R_{21}$ alone, the grid is held to ground by $C_{18}$, and the negative external trigger is applied to the cathode in order to make $V_{12a}$ conduct.

When the trigger-selector switch is in the POSITIVE EXTERNAL position, the cathode is held by $C_{13}$ and the trigger applied to the grid of $C_{12a}$.

*Trigger Shaper.*—A trigger pulse of constant shape is provided for the ranging circuits by $V_{12}$ no matter what the shape and amplitude of the input trigger. Tube $V_{12b}$ is an ordinary blocking oscillator biased beyond cutoff by the network $R_{29}$ and $R_{30}$. It therefore fires only when triggered by $V_{12a}$. The width of this standardized output trigger is set at an optimum of 1.0 $\mu$sec.

*Trigger Buffer.*—The trigger pulse, of either internal or external origin, is provided on front-panel connectors for external use and is isolated from the rest of the circuits by $V_{14b}$. Its width is 1 $\mu$sec, rise time 0.2 $\mu$sec, and amplitude approximately 100 volts.

*Video Amplifier and Attenuator.*—The amplifier $V_7$, $V_8$, and $V_9$ consumes 120 ma. A negative supply voltage is obtained from $R_{36}$ and divided by $R_{19}$ and $R_{20}$ for the $-3.0$-volt tap. The circuits operate from $+250$ volts supplied through the dropping resistor $R_{18}$ rather than from the common $+250$-volt supply.

The pass band is 8 Mc/sec wide. Further peaking could increase this bandwidth but the circuit would be difficult to design because of the variations likely to occur in production units. The response curve goes down gradually, dropping by 6 db at 11 Mc/sec. Perceptible response is obtained up to 30 Mc/sec. The low-frequency response (or response to long signals) results in a 10 per cent "droop" on a 1000-$\mu$sec pulse (Sec. 4·8). With the 8-Mc/sec bandwidth and the 120-ma current consumption, a gain of 100 is obtained. Since the deflection factor of the cathode-ray tube is 80 volts per inch, the deflection factor through the amplifier is 0.8 volts per inch. Maximum deflection before limiting occurs is more than $\pm 1$ inch.

To provide for use with either positive or negative signals the video amplifier was designed to operate as a Class A amplifier, although operation of this type involves some sacrifice in output voltage. If greater deflection is desired and the input polarity is known, the circuit may be changed to give greater deflection. If more power were available, the final stage could be returned to a higher voltage and the output voltage could be increased.

The amplifier is protected against overloading by means of cathode degeneration. Limiting is prevented by using a step attenuator for signals between 1 and 100 volts. Its steps of voltage ratio are 1, 3, 10, 30, and 100, and each step is capacity-compensated to improve the frequency response.

*Intensity Control.*—Since the sweeps are intensified only for their duration, the spot is not visible during its rest time at the left edge of the cathode-ray tube. Special attention should be given to the fact that the intensity control $R_{38}$ (see Fig. 7·20) may easily be set too high, especially on the R-sweeps. On these sweeps the proper level is set by turning the control nearly to the position of maximum intensity and then diminishing the intensity until the spot and the first bright $\frac{1}{2}$ in. or so disappear from view. The remaining visible edge is consequently that intensified by the delayed intensifier pulse. This is the edge to which signals may be accurately set in order to read their range, or to which the markers may be set for calibration. The brightness of the trace is proportional to the repetition rate.

The use of a light shield on the fast sweeps is always recommended, in order to enable one not only to see the sweep but also to observe

details in the waveform being viewed.   A No. 260 green Plexiglas filter may be used as a light shield.

Proper adjustment of the intensity control is necessary for proper definition of the range marks, which are applied as intensified dots. This adjustment is particularly essential on the 200,000-yd sweep since the 2000-yd markers are so close together.   The maximum intensity of
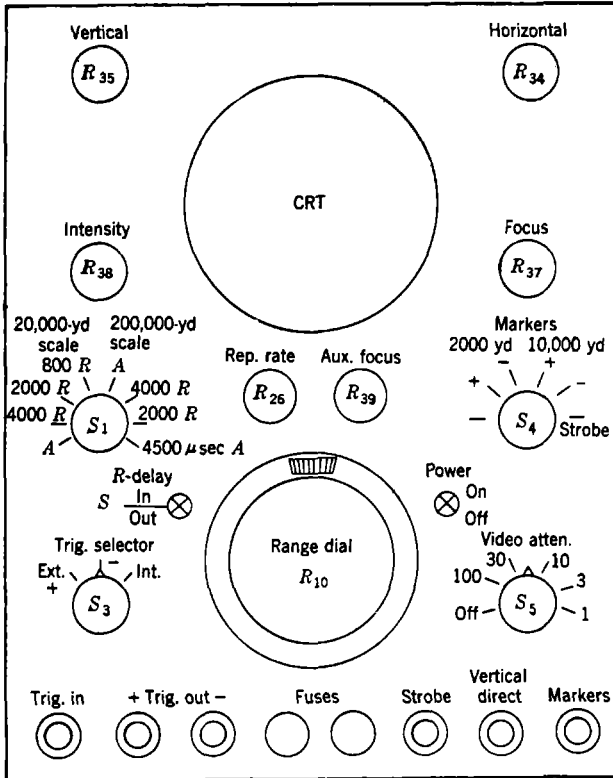


FIG. 7·20.—A/R-scope front-panel controls.

these markers is set at a low level to prevent blooming on the cathode-ray tube.   The proper setting of both focus controls is also necessary.

*Focus Controls.*—The auxiliary focus control $R_{39}$ (astigmatism adjustment) on the front panel is useful when observing small details.   It need not be adjusted frequently but its optimum adjustment does shift with changes in the intensity control.   Proper adjustment of the auxiliary focus control is obtained by first turning it completely to the left and then focusing the tube by means of the normal control $R_{37}$.   Then, especially

on a long sweep like the 200,000-yd one, the middle 2 in. of the trace are in focus but the edges are not. To remedy this, the auxiliary focus control may be turned up slightly and the normal control readjusted. As this process is continued, more of the edges clear up. Eventually, when the auxiliary focus control is at maximum the edges will be sharp and the middle portion will not be. The optimum setting of the auxiliary focus control depends on the nature of the waveform being viewed. Inability to achieve a proper auxiliary focus condition is an indication of a faulty cathode-ray tube or of wrong acceleration voltages.

*Sweep-length Selector Switch.*—Two A-sweeps, namely 20,000 yd and 200,000 yd, are provided. An expanded portion of either of these two scales is obtained by using the R-sweeps associated with them. Thus the four left switch positions are for the 20,000-yd scale, whereas the four right ones are for the 200,000-yd scale.

The R-sweeps, appearing at two places in the labeling on the panel, are so tied in with the 7-gang 8-position sweep-selector switch that they have the proper repetition rate and also show the region indicated by the strobe marker on the associated A-sweep. The 8th position of this switch is a long A-sweep of 4500-$\mu$sec duration; therefore the entire duty ratio between triggers can be seen. The gangs on this switch are used to select: $A$ the zero and slope controls for the delay potentiometer, $B$ the repetition rate range, $C$ the charging condenser for the sweep sawtooth wave, $D$ the length of the long rectangular wave, $E$ the gating pulse for the sweep clamp, $F$ the slope of the delay sawtooth, and $G$ the intensifier for the cathode-ray tube.

*R-sweep Delay Toggle Switch.*—When $S_2$ is turned to the UNDELAYED position, the R-sweep starts with the initial trigger, and the strobe marker appears only at the beginning of the A-sweep.

*Marker Selector.*—Switch $S_4$ permits either the crystal-controlled markers or the strobe to appear as an intensification along the A-scope sweeps. Both positive and negative markers are provided for convenience in separating signals from markers. Usually the positive (blanking) markers are preferred if extreme accuracy is not necessary.

These markers are available externally on the marker output connector. Although this is labelled MARKERS, the signals presented depend on the position of the switch. There is also a separate output terminal connected directly to the strobe so as to provide an external delayed trigger.

This external delayed trigger (or marker) is 24 $\mu$sec wide (that is, 4000-yd R-scope gate). A shorter pulse may be obtained by changing the time constant on the grid of $V_{6b}$ or by differentiation of the gate.

*Trigger-selector Switch.*—Switch $S_3$ connects the sweep and range delay circuits to either (1) the internal repetition-rate generator $V_{11}$,

which is driven from the crystal, or (2) any external trigger coming in the lower left panel connector. In either case, these triggers connect to the trigger amplifier and shaper $V_{12}$.

*Video Attenuator Switch.*—A front-panel knob is connected by a flexible coupling to the attenuator switch $S_6$ mounted on the amplifier at the rear of the chassis. In the OFF position, $S_5$ connects one vertical deflection plate to a front panel connector marked VERTICAL DIRECT.

**7·7. High-speed Oscilloscope.** *Introduction.*—Two limitations of synchroscopes, typified by the Model 5, which made necessary the development of a new synchroscope are (1) transit-time distortion in the cathode-ray tube, and (2) slow sweep speed (of the order of 5 in./μsec). Prior to the development of this new scope, writing speeds greater than 20 to 30 in./μsec were obtained by using a DuFour-type oscillograph. The difficulties of building, operating, and maintaining a DuFour-type scope were realized and efforts were bent toward finding a sealed tube from which high-speed sweeps could be photographed.[1] A new tube (Du Mont type K1017) (see Sec. 2·9) was developed to reduce transit time to less than $3 \times 10^{-10}$ sec while good deflection sensitivity was maintained. Techniques used in radar pulsers are employed to produce high-speed sweeps.

*Photographic Recording.*—In the study of repeating transients, such as sparking and starting time in magnetrons, it is often desirable to observe the variations occurring in successive transients. Each transient must be photographically recorded and the following three major factors become important: (1) single-trace writing speed; (2) short trace persistence; and (3) optical means for taking a series of pictures at the rate of 2000 per sec or higher.

If it is assumed that it is possible to measure the difference between two spot diameters[2] each equal to 0.005 in., then 0.05 in. can be measured to a precision of $\pm 10$ per cent. With a sweep speed of 50 in./μsec it is thus possible to resolve time intervals of $10^{-9}$ sec to a precision of $\pm 10$ per cent for a single transient, or to measure the time interval between two points in a single transient to $\pm 10^{-10}$ sec. It is important to have a jitter-free sweep because it is necessary that the sweep be synchronized with the transient to be studied. In order to measure differences in successive pulses to $10^{-9}$ sec it is necessary to keep the jitter between sweep and transients no greater than 1 or $2 \times 10^{-9}$ sec.

The screen used in the K1017 tube has a decay time of less than $10^{-4}$

---

[1] For data concerning maximum writing speeds available from conventional methods see: R. Feldt, "Photographing Patterns on Cathode-ray Tubes," *Electronics*, **17**, p. 130 (Feb. 1944); also Goldstein and Bales, "High-speed Photography of the Cathode-ray Tube," *RSI* (March 1946).

[2] In practice, smaller intervals can be measured.

sec and gives a trace sufficiently bright to allow photographing a single trace with writing speeds as high as 300 in./μsec. Successive transients at frequencies up to 4000 cps can be photographed[1] by using one of the commercially available high-speed movie cameras with a modified shutter. The higher writing speeds yield photographs that are sharp enough for measurements of waveforms, but which are not of high enough contrast for good photo reproduction. At lower sweep speeds a modulated carrier of 3000 Mc/sec can be recorded to show the modulation envelope.
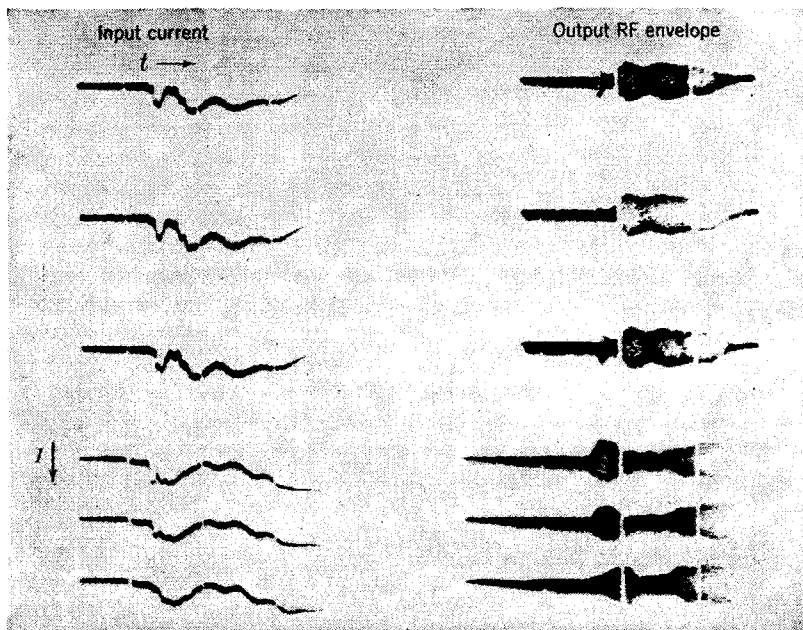


FIG. 7·21.—Successive pulses of a 3000-Mc/sec pulsed oscillator. The upper three sets of photographs were taken with a sweep of 1 in./μsec; the lower three with a sweep of 8 in./μsec.

Figure 7·21 shows the input current and the output r-f envelope of a 3000 Mc/sec oscillator for three successive pulses photographed with sweep speeds of 1 in./μsec and 8 in./μsec.

*Block Diagram.*—(See Fig. 7·22.) The cathode and post-accelerator supplies are conventional 60-cps rectifiers with good filtering. The control-grid bias should have less then 3 volts of ripple for the best photographic results because the grid is driven to about −4 volts bias and the light output of the screen is a rapidly varying function of grid

[1] Goldstein and Bales, *loc. cit.*

voltage in this region. This requirement is especially important in studying successive transients with very fast writing speeds.

*Sweep Circuit.*—The operation of the sweep circuit may be understood by reference to Fig. 7·23. The initial charge on condenser $C_1$ is $q_0$, whereas $C_2$ is initially uncharged. Switch $S_1$ is then closed, allowing $C_1$ to discharge through $R_1$, $L_1$, $R_2$, and $L_2$ into $C_2$. The general equation
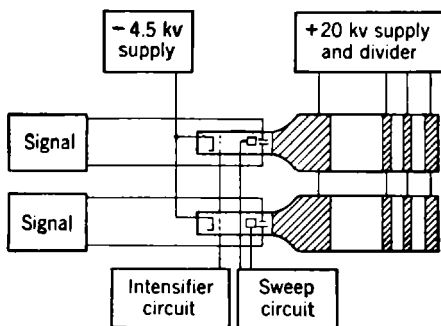


Fig. 7·22.—Block diagram for high-speed oscilloscope.

for the change in voltage across $R_1$, $L_1$, and $R_2$, $L_2$, is

$$e = e_1 - e_2 - E_0 = -E_0 \left[ 1 + E^{-\frac{t}{2RC}} \left( \frac{\sin \frac{2Zt}{RC}}{4Z} - \cos \frac{2Zt}{RC} \right) \right],$$

where $Z$

$$= \sqrt{\frac{1}{2k} - \frac{1}{16}}, \ K = \frac{2L}{R^2 C}, \ R = R_1 = R_2, \ L = L_1 = L_2, \ C = C_1 = C_2.$$

If $L$ becomes infinite, with finite values for $R$, the voltage is an exponential. If $R$ becomes infinite, with finite values for $L$, the voltage is a sine function. If $-e$ is plotted against $t/RC$ for various values of $K$, a family of curves that all have an initial $de/dt = E_0/RC$ will be obtained (see Fig. 7·24). The voltage $e$ is negative in this circuit but, for convenience, $-e$ is plotted against
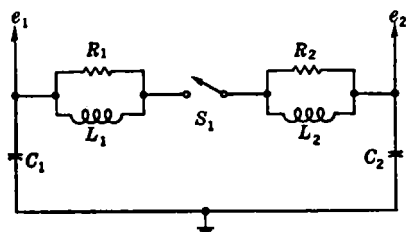


Fig. 7·23.—Simplified sweep circuit.

$t/RC$ to give a universal curve in which $R$, $C$, $L$, and $t$ can have any value. For values of $K$ between 0.7 and 0.9 the value of $de/dt$ will remain practically constant up to 70 or 80 per cent of $E_0$, and an essentially linear voltage can therefore be generated. The curve for $K = 0.7$ shows that it is within 4 per cent of being perfectly linear up to $-e = E_0$ whereas the

curve for $K \to \infty$ (the ordinary $RC$-circuit) has departed 9 per cent from the straight line when the voltage has a value $-0.1E_0$.  This difference plus the use of d-c resonant charging reduces the sweep power-supply voltage to approximately $\frac{1}{18}$ of that needed in a standard $RC$-circuit to obtain the same degree of linearity in the sweep.    By virtue of the balanced cir
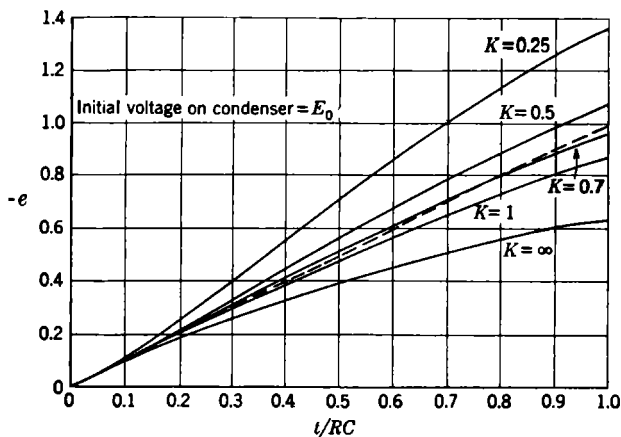


Fig. 7·24.—Voltage across $R_1$ or $R_2$ in Fig. 7·23.

cuit, push-pull voltage changes are obtained which may be applied to opposite deflecting plates of the cathode-ray tube to produce a linear sweep.

*Intensifier Circuit.*—The pulse-forming network[1] shown in Fig. 7·25 is charged by suitable means to a voltage $E_0$.    This network is designed to produce a pulse with a very fast rise and flat top.  The pulse length $\delta$ is determined from the slowest sweep speed for which the scope is intended and from the size of the cathode-ray tube.  For example, a 2 in./$\mu$sec sweep speed on a 5-in. scope should have an intensifier pulse length of at least 2.5 $\mu$sec.  The impedance $Z_0$ is determined by considerations of



Fig. 7·25.—Intensifier circuit.

switch characteristics, power dissipation, etc.    For the best match, $R_1$ is made numerically equal to $Z_0$.    A pulse voltage whose shape is determined by the network design and whose peak amplitude is $E_0/2$ appears across $R_1$ when the switch is closed.    All or part of this pulse voltage may be applied to the cathode-ray-tube control grid for intensification.

[1] See Vol. 5 of the Radiation Laboratory Series.

A summary of important relations pertaining to lumped-parameter delay lines is given here:

$$Z = \sqrt{\frac{L}{C}},$$

where $Z$ = surge impedance in ohms, $L$ = total inductance in henrys, $C$ = total capacitance in farads, and $\delta$ = pulse length.

$$\delta = 2\sqrt{LC}$$

$$C_1 = C_2 = \cdots C_{n-1} = C_n = \frac{C}{n}$$

$$L_2 = L_3 = \cdots = L_{n-2} = L_{n-1} = \frac{L}{n}$$

Inductances $L_1$ and $L_n$ are increased slightly ($\approx 1.2L/n$) to make a flatter-topped pulse by preventing overshoot. The inductance may be a continuously wound solenoid tapped at the proper points. A ratio of

$$\frac{\text{Coil length per section}}{\text{Coil diameter}} = 1.35 \text{ to } 1.5$$

gives a satisfactory value of mutual inductance. This value is approximate and serves only as a guide. A little experimentation is usually necessary in order to determine the exact number of turns. In general, the more sections for a given pulse length, the more nearly the pulse shape approaches a rectangular wave.

The intensifier pulse and sweep voltages start simultaneously; and hence for very fast sweeps (50 in. to 100 in./µsec) the intensifier pulse must reach full amplitude in the shortest possible time in order that the first part of the sweep may be visible. Since conventional pulse-forming-network designs have an inductive output impedance, their output pulses rise too slowly or overshoot. This difficulty has been overcome by adding and $RC$ output section $R_0C_0$ (Fig. 7·25) to the conventional network. This addition causes the pulse to rise in about $4 \times 10^{-8}$ sec but not to overshoot if the value of $R_0$ is made equal to the load resistor. A further improvement may be made by adding between the thyratron plate and ground a small condenser that will balance the distributed capacity between the cathode and ground.

Figure 7·26 shows how the sweep (Fig. 7·23) and intensifier (Fig. 7·25) circuits are combined to use the same charging voltage and switch tube, $V_6$.

The resonant charging of the pulse-forming network and $C_1$ is accomplished through a choke and the diode in series with it. A positive trigger pulse from a fixed- or variable-delay trigger-pulse generator fires the hydrogen thyratron switch $V_6$.

Fig. 7·26.—Schematic diagram of high-speed synchroscope.

To reduce background light from electrons sprayed on the screen when the beam hits the side of the tube, a clamp circuit ($V_1$) is provided on the intensifier. The time at which the clamp fires may be adjusted by varying the bias on the screen grid.

A modification of this circuit, which allows the intensifier pulse to be applied a discrete interval of time before the sweep, is shown in Fig. 7·27. Separate switch tubes are used for the intensifier and sweep circuits in this scheme. A lower-voltage pulse-forming network may then be used with a resultant saving in power in the intensifier circuit since the required sweep voltage may be several times larger than that needed for intensify-
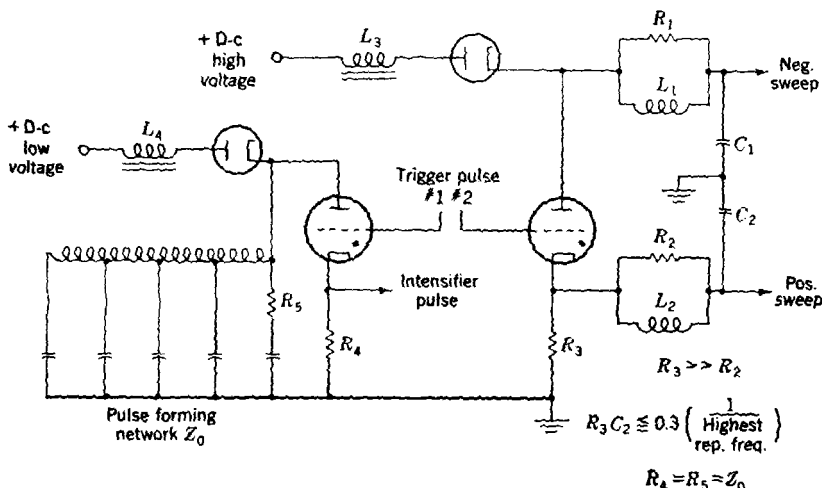


FIG. 7·27.—Scheme for intensifying before the sweep starts. Trigger pulse No. 1 precedes No. 2.

ing the trace. Although an extra switch tube and hold-off diode are necessary, this circuit may be justified by the saving in power and its ability to use less expensive switch tubes with lower power ratings.

*Sweep Phasing.*—It is important that any time variations between the start of the scope sweep and the trigger pulse applied to the apparatus under examination should not be larger than the smallest unit of time to be measured ($10^{-9}$ sec). It is further desirable to be able to phase the sweep and the output trigger pulse relative to one another. A variation of several hundredths of a microsecond in the interpulse interval is permissible provided that the trigger pulse applied to the apparatus under examination and to the sweep are stable to $10^{-9}$ sec relative to one another. Hence a crystal-controlled oscillator is not needed. An ordinary audio oscillator of the Wien-bridge type followed by amplifying and

differentiating stages is used to produce a pulse that rises to full amplitude in about 3 $\mu$sec and lasts for about 5 $\mu$sec (Fig. 7·26). This pulse is applied through $J_1$ to two lumped-constant delay lines, one of variable length and one fixed. The fixed line delays the pulse by approximately 2.5 $\mu$sec. By varying the inductance of the first section of the second line, both its impedance and delay are varied. This continuous variation in delay plus taps along the 5-$\mu$sec lumped-constant line provide a trigger pulse that is continuously variable for $\pm 2.5$ $\mu$sec about the position of the fixed-delay trigger pulse first mentioned. Both lines feed identical triggered blocking oscillators that produce pulses that rise to 1000 volts in $3 \times 10^{-8}$ sec with a duration of 0.7 $\mu$sec. The fixed trigger fires the thyratron switch in the sweep-intensifier circuit while the variable-delay trigger is sent to the pulse generator (or other apparatus) that is being studied (available on $J_2$).

In order to reduce time jitter between the two trigger pulses, the following precautions need to be taken: All d-c circuits supplying plate and grid voltages should be isolated from the trigger circuits by means of r-f chokes and bypass condensers; separate filament transformers with built-in Faraday shields should be used in each trigger circuit because capacity coupling between heater and cathode of one blocking oscillator causes random firing of the other blocking oscillator. This condition is especially bothersome when the two trigger pulses occur at approximately the same time. Good filtering in the d-c supplies also helps to reduce jitter. A d-c heater supply helps further.

Other sources of jitter are the hydrogen thyratron in the sweep circuit and the switch tube in the instrument that is to be studied. By applying a fast-rising (20 kv/$\mu$sec) high-voltage (500 to 1000 volts) trigger pulse to the thyratron grid, it can be made to fire consistently. A further reduction in jitter may be realized by using d-c power in the thyratron heaters.

*Signal Input.*—In the ordinary cathode-ray tube, coupling between the two pairs of deflecting plates becomes increasingly undesirable as the impressed frequency increases. The deflecting-plate leads must be brought out directly through the sides of the tube rather than through the base for frequencies in the megacycle range; and for frequencies of the order of magnitude of 1000 Mc/sec, it is imperative that a coaxial-type input be employed.

In the Du Mont tube (type K1017) coupling between signal-input circuits and external disturbances has been minimized by careful shielding of the separate deflecting plate circuits. Direct current centering and calibrating voltages are introduced to the shielded signal-input circuits through isolating resistors and bypass condensers to prevent r-f voltage induced in the various leads from appearing on the deflecting plates.

Wires carrying direct current and alternating current are run in separate cables and shielded where it is necessary.

**7·8. J-scope.**[1]—The use of a J-scope is recommended for accurate measurements of time intervals ranging from 0 to 300 μsec. This type of indication, briefly discussed in Sec. 1·3, employs a cathode ray tube of the radial deflection type, described in Sec. 2·9. The time base is a circular trace on the face of this tube, produced by crystal-controlled sine and cosine voltages on the two pairs of deflection plates. The signals to be measured are applied to a central electrode which results in a radial deflection from the time base circle. A trigger pulse is accurately synchronized with the time base, always occurring at 0°, so that the angular position of the radial signal measures the time elapsed between the trigger pulse and the signal observed. By proper choice of the crystal frequency, one complete cycle of the base circle may be made to correspond to an integral number of microseconds (for example, 1 or 10 μsec), or for radar use, to 1 land mile or to 2000 yd. For measurements of time intervals greater than that corresponding to one revolution of the time base circle, the appropriate subsequent cycle which includes the signal to be measured is brightened by a calibrated delay circuit. A single example of such a J-scope will be here described, and others will be found in Chap. 7 of Vol. 20 this series.

*Model III Range Calibrator—General Information.*—The Model III range calibrator[2] was designed for laboratory use in the measurement of time intervals up to 300 μsec. Its chief characteristics are as follows:

1. *Time base speed.* Three versions of the calibrator are available, with time base speeds corresponding to 10 μsec, 1 land mile, or 2000 yd per complete circle.

2. *Triggers.* Since the time base is generated by a crystal oscillator, an external trigger may not be used to start the sweep. However, the J-scope provides both positive and negative triggers of 100 volts across resistances of 1000 ohms, for external use.

3. *Repetition rates.* Five pulse repetition rates of nominal values, 400, 800, 1200, 2000, and 2300 pps, are available.

4. *Signal input.* The signal may be applied to the central deflection electrode of the cathode ray tube either directly or through a single-stage video amplifier having a gain of approximately 18, constant within ±3 db between 50 cps and 4 Mc/sec. The input impedance is 750,000 ohms paralleled by about 30 μμf with the amplifier in, and about 40 μμf with the amplifier out. An input signal greater than 3.5 volts will overload the amplifier.

[1] By T. Soller.

[2] This instrument was designed by the Radiation Laboratory and the F. W. Sickles Co., Chicopee, Mass., and is manufactured by the latter.

5. *Accuracy.* When properly adjusted, the accuracy of time measurement is ±0.1 μsec (see also Sec. 7·9).

The schematic diagram of the calibrator is shown in Fig. 7·28.

*Circuits—Sweep Generators.*—The triode-connected pentode $V_1$ is used to generate a sinusoidal voltage of stable frequency controlled by the crystal in the grid circuit. The voltages in the secondaries of the transformer in the plate circuit of $V_1$ may be adjusted by condensers $C_7$ and
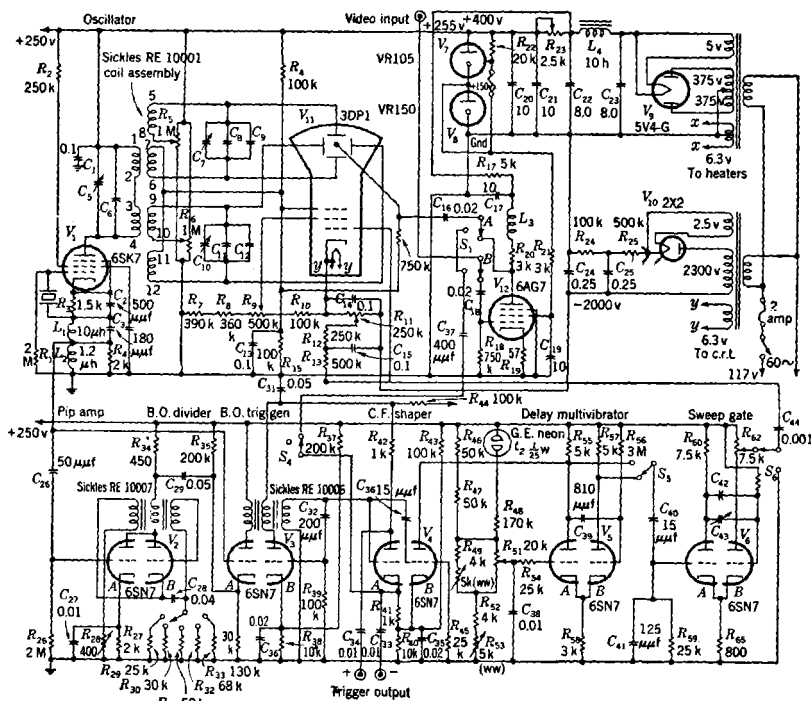


FIG. 7·28.—Model III range calibrator.

$C_{10}$ to give sinusoidal voltages which are 90° out of phase and which are applied to the two orthogonal pairs of deflection plates of the cathode ray tube $V_{11}$, producing the time-base circle. The diameter of the circle is controlled by the primary tuning condenser $C_5$.

*Trigger Generator.*—Pips of 15 volts amplitude, at crystal frequency, are generated across the damped choke $L_2$ in the cathode circuit of $V_1$. These are amplified by $V_2a$, and are then used to trigger the blocking oscillator frequency divider $V_2b$ which produces rectangular pulses approximately 18 μsec long at any of five audio-frequency rates controlled

by $S_2$ in the grid circuit. $V_3a$ is a coincidence amplifier, used to produce a trigger whose phase does not vary. To accomplish this, the long pulses from the divider $V_2b$ are applied to the cathode, and the short pulses from the crystal oscillator are applied to the grid. The quiescent grid bias of $V_3a$ is 30 volts, and $V_3a$ is kept below cutoff even during the time of application of the frequency divider pulse by adjusting the 400-ohm variable resistor in the cathode return circuit of $V_2b$. During this time interval, the next crystal oscillator pulse following the one that triggered the frequency divider drives the grid of $V_3a$ above cutoff, and fires $V_3b$, a blocking-oscillator trigger generator, from which positive and negative triggers of 100 volts, and of 0.6 $\mu$sec duration, are derived by the paraphase amplifier $V_4$.

These triggers are available for external use. The positive trigger may be connected internally to the signal electrode of the cathode ray tube through switch $S_4$.

The variable-ratio frequency-division scheme for pip selection is used instead of a continuously variable frequency oscillator both because it is economical and because it assures that the selected crystal oscillator pip always lies on the flat top of the longer pulse and thus assures stable operation.

*Delay Circuits and Intensifying Gate.*—When measurements of time intervals beyond that required for the first revolution of the circular time base are to be made, means must be provided for indicating exactly which of the succeeding revolutions is occupied by the observed signal, by brightening on the cathode ray tube any one of the first 30 successive sweeps following a given trigger.

This is done by using a trigger shaper $V_4b$ and two multivibrators $V_5$ and $V_6$ in cascade. The first of these multivibrators produces a pulse of variable calibrated duration, controlled by $R_{51}$, which varies the bias of the normally "off" tube, $V_5a$. The pulse length is made to agree with the calibration by adjusting the slope control $R_{50}$ and the zero control $R_{53}$. The neon tube in the delay-control bleeder circuit is introduced to reduce the effect of plate voltage changes on the gate length.

The second multivibrator, $V_6$, produces a positive pulse whose duration is somewhat less than 10 $\mu$sec, but adjustable by means of $C_{43}$. This pulse is applied to the grid of the cathode ray tube through the coupling condenser $C_{44}$, which must be a high-voltage condenser, since the cathode-ray-tube grid is at $-2000$ volts.

The first revolution of the trace on the cathode ray tube is brightened by this pulse when switch $S_5$ is in the upper position, since the action of the multivibrator $V_6$ is then initiated by the positive rise of the pulse at the plate of $V_4b$, coupled to the grid of $V_6a$ by the differentiating circuit comprising $C_{40}$, $C_{41}$, and $R_{59}$. When switch $S_5$ is in the lower position, the

multivibrator $V_6$ is actuated by the positive fall of the end of the pulse at the plate of $V_5b$, and a delayed narrow pulse results, the amount of the delay being determined by the setting of the calibrated control $R_{51}$.   This pulse may also be used externally by coupling to the plate of $V_{6b}$ through a 0.01-$\mu f$ condenser.

*Signal Amplifier.*—A single low-gain stage of amplification (voltage gain 18) is provided by $V_7$, with shunt peaking in the plate circuit to extend the bandwidth to 4 Mc/sec.   Switch $S_1$ allows the input signal to bypass the amplifier and to be applied directly to the central electrode of the cathode ray tube if its amplitude is sufficient.

*Cathode-ray-tube Control Circuits.*—The accelerating voltage on the cathode ray tube is 2000 volts, and the method of focus- and intensity-control is conventional.   Centering of the circular time base is provided by adjustment of the potential of one of the plates of each pair by means of $R_5$ and $R_6$.

*Power Supply.*—The power supply is designed to provide 35 ma at +400 volts, 6.3 volts for heaters, and −2000 volts for an external sweep-oscilloscope unit which operates at a time-base speed of 1 $\mu sec$ per revolution.

**7·9. The Precision and Accuracy of Time Measurements Made with a Circular Sweep or J-scope.**[1]—The J-scope[2] is useful for measuring the time interval between two events only when one of them, the "trigger," recurs at constant frequency.   As with an ordinary electric clock, the measurement of time interval is reduced to the measurement of a phase angle.   It is necessary therefore to examine with what accuracy the cathode-ray tube can maintain the angle of position of its fluorescent spot proportional to the phase angle of the driving voltage.

*Errors Due to Nonorthogonality of the Deflection Electrodes and Their Driving Voltages.*—The $x$ and $y$ sets of deflection electrodes, which are intended to produce beam deflections at right angles, may not in practice do so because of faulty tube construction.   Moreover their respective driving voltages may not be in exact quadrature.   It is evident that either or both of these conditions can cause the "circular" sweep to become elliptical, thereby producing a periodic departure from the desired condition of proportionality.

Let the deflection factors of the $x$- and $y$-plates be respectively $k_1$ and $k_2$, and let the $y$-plates produce a deflection of the beam which lacks $\phi_0°$ of being perpendicular to the $x$-deflection, as shown in Fig. 7·29.   Let the voltages applied to the two sets of plates be out of quadrature by the

[1] By G. E. Valley.

[2] Davenport and Warner, "Errors in Range Measurement with a Circular Sweep," RL Report No. 9, Jan. 24, 1942; Hales, "Errors in Circular Sweeps Due to Decentering and Ellipticity of the Circle," RL Report No. 328, Feb. 13, 1943.

angle $\theta_0$.  Then the actual deflections in the $x$ and $y$ directions will be

$$x = k_1 V_1 \cos \omega t - k_2 V_2 \sin (\omega t + \theta_0) \sin \theta_0,$$
$$y = k_2 V_2 \sin (\omega t + \theta_0) \cos \phi_0,$$

where $\omega$ is the constant driving frequency.  If $\phi = \tan^{-1} (y/x)$ is the **angular displacement** of the spot on the screen, its angular velocity is

$$\frac{d\phi}{dt} = \frac{x \dfrac{dy}{dt} - y \dfrac{dx}{dt}}{x^2 + y^2}$$

and it follows immediately that when $\phi_0$ and $\theta_0$ are each zero and $V_1$ and $V_2$ are adjusted so that $k_1 V_1 = k_2 V_2$, $d\phi/dt = \omega$.  The spot then travels in a circle with constant velocity.  In general, however,

$$\frac{d\phi}{dt} = \frac{k_1 k_2 V_1 V_2 \cos \phi_0 \cos \theta_0}{\begin{array}{l} k_2^2 V_2^2 \cos^2 \theta_0 + \sin 2\omega t[\frac{1}{2}k_2^2 V_2^2 \sin 2\theta_0 - k_1 k_2 V_1 V_2 \cos \theta_0 \sin \phi_1] \\ + \cos^2 \omega t[k_1^2 V_1^2 - 2k_1 k_2 V_1 V_2 \sin \theta_0 \sin \phi_0 + k_2^2 V_2^2 (\sin^2 \theta_0 - \cos^2 \theta_0)] \end{array}}$$

If $k_1 V_1 = k_2 V_2$ and if $\theta_0 = \phi_0 \neq 0$, then again

$$\frac{d\phi}{dt} = \omega.$$

Since the denominator of the above equation is just $x^2 + y^2 = r^2$, it is easily shown that when $\theta_0 = \phi_0 \neq 0$, the radius of the sweep is given by



Fig. 7·29.—Nonorthogonality of deflection plates.

$r = k_1 V_1 \cos \theta_0$.  Thus the condition for constant $d\phi/dt$, when the deflection plates are not orthogonal, is that the phase angle between the voltages applied to the $x$ and $y$ sets of plates be so adjusted as to make the sweep precisely circular.

*Error Due to Eccentricity of the Sweep Circle.*—In a clock, it is necessary that the graduated dial circle be concentric with the shaft on which the hands are mounted. Similarly the shaft of the rotary cursor and the central deflection electrode of a J-scope must be concentric with the sweep circle.

Let the error in centering the sweep circle be $\Delta$, in the direction of the $x$ axis; then the instantaneous position of the spot is

$$x = \Delta + a \cos \omega t$$
$$y = a \sin \omega t.$$

The position angle of the spot at a time $t$ will be $\phi = \omega t$ (neglecting increments of $2\pi$) if the scale is linear; let there be deviation from linearity

$\alpha$ such that $\phi = \omega t + \alpha$. Then

$$\tan \phi = \tan (\omega t + \alpha) = \frac{y}{x} = \frac{a \sin \omega t}{\Delta + a \cos \omega t}$$

and

$$\tan \alpha = - \frac{\Delta \sin \omega t}{a + \Delta \cos \omega t}.$$

It is seen that $\alpha$ oscillates with frequency $\omega$ and thus passes through one maximum and one minimum value as the sweep scans the circle once. Its maximum value occurs when $\sin \omega t = 1$, at which point $\alpha_{max} = \tan^{-1} (\Delta/a)$. If $\epsilon_{\infty}$ is the maximum error in microseconds and $\tau$ is the number of microseconds per revolution ($\tau = 2\pi/\omega$), then for small errors

$$\epsilon_{\infty} = \frac{\Delta}{2\pi a} \tau.$$

*Error Due to Sweep Ellipticity.*—If for any reason the sweep is elliptical, although the center of the ellipse is concentric with the cursor shaft and the central deflection electrode, so that the minor axis of the ellipse is $a$ and the major axis is $a + \Delta$, the spot trajectory may be described by

$$x = a \cos \omega t$$
$$y = (a + \Delta) \sin \omega t;$$

then, defining $\alpha$ as in the previous case,

$$\tan \alpha = \frac{\Delta \sin 2\omega t}{2a + \Delta - \Delta \cos 2\omega t}.$$

This error is doubly periodic, and its maximum value is approximately $\alpha_{max} = \Delta/2a$. The error in microseconds is approximately $\epsilon_{el} = (\Delta/4\pi a)\tau$.

Errors due to ellipticity of the circle are not great in practice since even small ellipticities are easily detected by the eye. Conversely, parallax between the standard comparison circle and the sweep circle often causes sizable eccentricities to be unnoticed.

All the foregoing discussion assumes the driving voltages to be pure sinusoids. If harmonics are present whose amplitude is only a few per cent of the fundamental, a substantial departure of $d\phi/dt$ from constancy ensues.

### A TEST OF THE LINEARITY OF A CIRCULAR SWEEP

A circular sweep was arranged[1] so that $\tau = 12.2\ \mu\text{sec}$; upon the intensifying grid of the tube there were impressed a series of short pulses regularly spaced and $0.61\ \mu\text{sec}$ apart. These pulses were derived from another oscillator whose frequency was locked at twenty times that of the sweep

[1] Hales, loc. cit.

oscillator. The angular position of each of the pulses was read from a rotatable radial cursor. These readings, after being reduced to yield relative error in microseconds, are plotted in Fig. 7·30.

In Fig. 7·30 Curve *a* shows the performance of the J-scope where the eccentricity and ellipticity of the circle (whose radius was 27.7 mm) were reduced to a minimum. Curve *b* shows the error resulting from decenter-
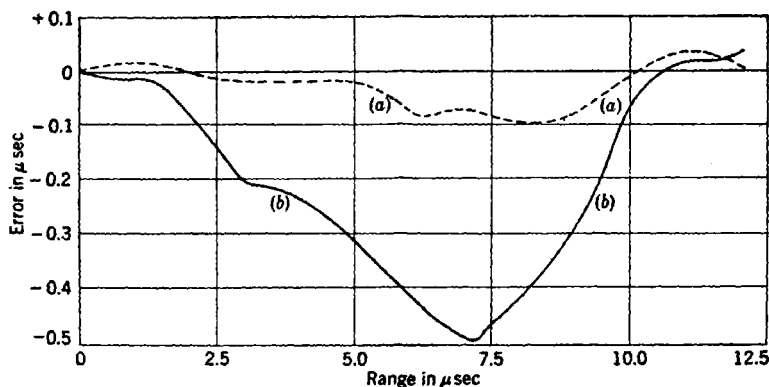


Fig. 7·30.—Experimental error in a J-scope.

ing the sweep circle by 3 mm ($\Delta = 3$ mm). It will be noted that the errors are not plotted so as to lie symmetrically about the line of zero error.

Curve *a* indicates that the device can be adjusted to yield data more accurate than $\pm 1$ per cent of the time interval $\tau$ represented by 360° on the tube face. Curve *b* indicates an error about 25 per cent greater than would be expected from the pertinent formula given above.

# CHAPTER 8

## DEFLECTION COILS

### By Ralph Dressel

#### GENERAL PROPERTIES OF DEFLECTION COILS

A deflection coil is an electromagnetic device for generating a magnetic field across the neck of a cathode-ray tube so that electrons will be deflected as they pass from gun to screen. The amount of deflection is controlled by the current in the coil and with an ideal coil would, for any point on the tube screen, be exactly proportional to this current. Moreover, various parts of an ideal coil would be free from electric and magnetic interaction, which give rise to oscillations whose effects appear as crooked sweep lines. Finally, the ideal coil would preserve the focus of an initially focused electron beam. Practical coils fall somewhat short of the performance postulated for ideal coils, but, through careful design, can be made to have a satisfactory minimum of imperfections.

**8·1. Theory of Deflection.—** The path of an electron through a magnetic deflecting field is shown in Fig. 8.1. It is assumed that the magnetic field is uniform and normal to the plane of the paper, and that the magnetic-flux density has the value $H$ in the region



Fig. 8·1.—Path of an electron through a uniform magnetic deflecting field.

between Boundaries 1 and 2 but is zero everywhere else. An electron with mass $m$, charge $e$, and initial velocity $v$ is deflected through an angle $\theta$ in passing through this magnetic field.

The general expression for the force on a charged body moving in a magnetic field is

$$\mathbf{F} = e(\mathbf{v} \times \mathbf{H}). \tag{1}$$

Since the only component of $\mathbf{H}$ is that normal to the paper, the force $\mathbf{F}$ must always lie in the plane of the paper. Moreover, $\mathbf{F}$ is constant in magnitude and is directed perpendicular to the instantaneous velocity $\mathbf{v}$ of the electron. These conditions cause the electron to move in a circular

path while it traverses the magnetic field. The magnitude of the centripetal force $F$ is simply equal to $Hev$, which equals the reaction due to acceleration of the electron. Therefore, $Hev = mv^2/r$, where $r$ is the radius of curvature of the circular path. Solving for $r$,

$$r = \frac{mv}{He}. \tag{2}$$

The incident electron enters normal to the boundary of the magnetic field marked by Line 1 and, emerging from Boundary 2, travels in a straight line after having been deflected through an angle $\theta$ relative to its initial direction. The center of curvature of the electron path lies on Line 1. It is simple to prove from Fig. 8·1 that angle $\phi$ equals the deflection angle $\theta$, and

$$\frac{l}{r} = \sin \theta, \tag{3}$$

where $l$ is the distance between Boundaries 1 and 2, or the axial length of the deflecting field. Substituting the value of $r$ from Eq. (2),

$$\sin \theta = \frac{lHe}{mv}. \tag{4}$$

The speed of the electron can be stated to a close approximation in terms of the accelerating anode potential, $E_b$. Thus, $E_b e = \frac{1}{2}mv^2$, or $v = \sqrt{2E_b e/m}$. Substituting this value of $v$ in Eq. (4),

$$\sin \theta = Hl \sqrt{\frac{e}{2E_b m}}. \tag{5}$$

Equation (5) holds for any angle less than 90° and is adequate for this study of beam deflection. A clearer insight into the behavior of a deflection coil can be gained if the general relationships expressed in Eq. (5) are stated separately. The sine of the angle of deflection is—

1. Proportional to the magnitude $H$ of the deflecting flux and reverses sign with $H$.
2. Proportional to the length $l$ of the deflecting field.
3. Inversely proportional to the square root of the accelerating voltage $E_b$.
4. Proportional to the square root of the ratio of charge to mass $e/m$ of the deflected particle. Therefore, ions are not deflected as much as electrons.

Inserting the numerical value of $e/m$ for an electron in Eq. (5), and expressing $l$ in centimeters, $E_b$ in volts and $H$ in gauss,

$$\sin \theta = 0.30 \frac{Hl}{\sqrt{E_b}}. \tag{6}$$

If the actual path of an electron through the field of a deflection coil is traced, it may be seen from Fig. 8·1 that the electron behaves as if it traveled into the magnetic field in a straight line up to the point $O$, was then deflected sharply through the angle $\theta$, and continued again in a straight line.    It is useful to regard the point $O$ as a center of deflection that may shift slightly as the deflection angle increases.    This shift is not more than about 10 per cent of the length $l$ of the magnetic field and is negligible when compared to the distance from deflection coil to the screen of the cathode-ray tube.    Since the concept of a center of deflection is used only in conjunction with the pattern on the tube screen, the approximation is valid.

The magnetic field generated by practical deflection coils is never so abruptly bounded as was assumed in this ideal case.    The axial field distributions of ideal and physical deflection coils are compared in Fig. 8·2.    This diagram illustrates clearly the large amount of fringing field extending beyond the ends of the coil.    These fields contribute materially to the actual deflection of the electron beam.    Therefore, if it is desired to calculate the deflection angle from a known field distribution, a numerical integration must be performed.    The relation corresponding to Eq. (6) is then

$$\sin\,\theta \,=\, \frac{0.30}{\sqrt{E_b}} \int_{-\infty}^{\infty} H\,dl. \quad (7)$$
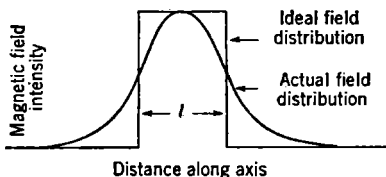
Fig. 8·2.—Comparison of axial field distributions of ideal and physical deflection coils.

The integration limits are interpreted to be sufficiently far away from the ends of the coil so that the field remaining beyond these limits is negligible.

It is also seen from Fig. 8·2 that a practical deflection coil has no definite magnetic length because the field tapers off infinitely far in both directions.    An effective length can, however, be defined as being the length of an ideal coil that will give the same angle of deflection as the practical coil.    Therefore,

$$\frac{\int_{-\infty}^{\infty} H\,dl}{H_0} \,=\, l_0, \quad (8)$$

where $H_0$ is the peak value of magnetic-field intensity, and $l_0$ is the effective length of the coil.    The integral is the same that appears in Eq. (7).

The equations in the preceding paragraphs are intended not for calculating the deflection angle, but simply to indicate the factors that are important in magnetic deflection and their relationships to the deflection angle.    Actually, the simplest and most accurate way of finding the

deflection angle is to put the coil on a cathode-ray tube and measure the deflection.

**8·2. Maximum Length of Deflection Coils.**—As illustrated in Fig. 8·3, the maximum length of a deflection coil is governed both by the internal neck diameter of the cathode-ray tube and by the maximum allowable deflection angle. The latter is the angle at which the electron beam just grazes the neck of the tube. The cross section of the electron beam is appreciable and varies with the current. Consequently, at the point of contact with the glass, the central axis of the beam is removed a distance approximately equal to the beam radius.
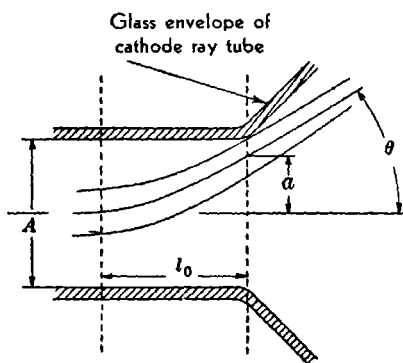


Fig. 8·3.—Limitation of deflection angle by internal neck diameter of tube.

From Fig. 8·1 it can be seen that $a = r(1 - \cos \theta)$. Dividing this by $l_0$, the effective length of the coil,

$$\frac{a}{l_0} = \frac{r}{l_0} (1 - \cos \theta).$$

But since $r/l_0 = 1/\sin \theta$, $a/l_0 = \tan \theta/2$, or

$$l_0 = \frac{a}{\tan \dfrac{\theta}{2}}. \qquad (9)$$

A typical magnetic cathode-ray tube may have an internal neck diameter $A = 1.140$ in. Under average operating conditions, the beam radius is approximately 0.1 in., and $a$ is therefore 0.47 in. The magnetic tube is generally designed for a maximum deflection angle of 26°. Substituting these values into Eq. (9), the maximum effective length of a coil to be used with this tube is found to be

$$l_0 = 2.0 \text{ in.}$$

Because long deflection coils have a high deflection efficiency, it is desirable to build the coil as long as the tube will allow. There are however at least two practical difficulties: unless rather large tolerances are allowed to account for variations in the tube-neck diameter, electron-beam diameter, and position of the coil on the tube neck, there is a large probability that the electron beam will strike the glass envelope; also, a long coil is not always possible since the length of the tube neck is finite and since other units in addition to the deflection coil must fit in this limited length.

**8·3. Deflection Efficiency.**—Although the neck of the cathode-ray tube limits the effective length of the magnetic deflecting field to the

value given by Eq. (9), the deflection does not require that any field exist outside of the region enclosed by the glass walls of the tube. However, a practical deflection coil always has stray fields, which do not contribute to the deflection of the electron beam but which simply add to the total magnetic energy stored in the coil. The deflection efficiency of a practical coil may be defined as the ratio of the energy stored in the field of an ideal coil to the energy stored in the field of the practical coil.

Since, in most cases, the energy stored in the coil must be essentially dissipated before the start of the next sweep, the time required to dissipate this energy will depend upon the total amount stored. A high deflection efficiency will minimize this time. The recovery time usually is long enough so that it is the limiting factor in determining the sweep-repetition frequency.

The energy stored in the magnetic field of an ideal coil may easily be calculated. If it is assumed that the field generated by an ideal coil is uniform and exists only in the region enclosed by the glass walls of the tube neck, and that the length of the ideal coil is the same as the effective length $l_0$ of the physical coil with which it is compared, then the volume in which this field exists is $V = \pi a^2 l_0$, where $a$ is the radius of the tube neck. The energy density of magnetic field is $w = BH/8\pi$, or, since the medium is air, $w = H^2/8\pi$. The total energy of the uniform magnetic field will be the product of the energy density and the volume of the field,

$$W = \frac{H^2}{8\pi} \pi a^2 l_0, \tag{10}$$

where $W$ = total energy in ergs, $a$ = radius of tube neck in cm, $l_0$ = effective length of coil in cm. Equation (6) furnishes the value of $H$ in terms of the deflection angle.

$$H = \frac{\sin \theta \sqrt{E_b}}{0.30 l_0}.$$

Substituting this value of $H$ in Eq. (10), the total energy stored in the magnetic field of the ideal deflection coil for a given angle of deflection is

$$W = \frac{a^2 \sin^2 \theta E_b}{0.72 l_0} \qquad \text{ergs.} \tag{11}$$

A practical coil offers a different problem because the fringing fields are difficult to integrate. The energy stored in the magnetic field is, therefore, much more easily measured experimentally than calculated. It is given by the familiar expression

$$W = \tfrac{1}{2} L i^2 \qquad \text{joules,} \tag{12}$$

where $L$ is the inductance of the coil in henrys and $i$ is the current in amperes flowing through the coil. To determine how effective the practi-

cal coil is in deflecting the electron beam it must be compared with an ideal coil that will deflect the electron beam through the same angle. Consequently, if the reference angle is $\theta_0$, then $I_0$ will be the current that must flow through the coil to deflect the electron beam by this angle.

These values of $\theta_0$ and the corresponding $I_0$ may be substituted in Eqs. (11) and (12) to obtain the total energies stored in the ideal and physical coils. Accordingly, the deflection efficiency will be

$$\text{Deflection efficiency} = \frac{\dfrac{a^2 \sin^2 \theta_0 E_b}{0.72 l_0} \times 10^{-7}}{\frac{1}{2} L I_0^2} = \frac{2.78 a^2 \sin^2 \theta_0 E_b \times 10^{-7}}{L I_0^2 l_0}. \tag{13}$$

Although $E_b$ appears in Eq. (13), the deflection efficiency of a coil is independent of the accelerating voltage applied to the cathode-ray tube because $I_0^2$ is also proportional to $E_b$. It should be pointed out that deflection efficiency is simply a measure of how effective the magnetic field of a given coil is in deflecting an electron beam.

All the important factors that affect the deflection efficiency of a coil may be grouped together and labeled "form." In general, any increase in length, decrease in cross-sectional area, or the introduction of an iron core will tend to increase the deflection efficiency by an amount that is difficult to compute. An important fact, however, is that the deflection efficiency is completely independent of the number of turns in the windings. Therefore, the fundamental problem in designing deflection coils to meet certain current and voltage specifications is first to determine the form that will give the required deflection efficiency and then to wind on the proper number of turns to satisfy the current or voltage specifications. The types of deflection coil described in this book have efficiencies of about 50 per cent, but new designs may possibly improve this figure.

**8·4. Deflection Sensitivity.**—The deflection sensitivity is the ratio of the deflection of the electron beam to the current flowing in the coil. Deflection may be measured either by the angular deflection of the beam or by the distance the illuminated spot has moved across the tube face. The latter method is both simple and direct, but the deflection sensitivity as so measured depends upon the dimensions of the cathode-ray tube as well as upon the deflection coil. With the former method, the sensitivity depends only on the coil, but it is usually necessary to calculate the deflection angle. A convenient way to combine the advantages of these two methods is to use one radius of the cathode-ray tube as the unit of deflection.[4] Magnetic cathode-ray tubes such as the 5FP7, 7BP7, and the 12DP7 are designed to give a deflection of one radius when the deflection

angle is 26°; thus, a deflection of one radius specifies a deflection angle of 26° for all of these tubes.

It is much more convenient to use the deflection factor rather than its reciprocal, the deflection sensitivity, to describe the performance of a coil. The deflection factor is the current required to produce a unit deflection, in this case one radius. This is exactly the information a circuit designer needs to know. It must be remembered, however, that no measurement of deflection factor is meaningful unless the acceleration voltage on the cathode-ray tube is also stated.

The two important quantities that influence the deflection factor of a coil are the form and the number of turns. If the number of turns in the windings is assumed to be fixed, then the deflection factor is inversely proportional to the effective length of the coil. Also, if the coil cross section perpendicular to its axis is magnified by a chosen amount so that the relative dimensions remain unchanged, then the deflection factor will be increased by the same ratio. This relationship may be symbolized as follows:

$$\frac{I_0'}{I_0} = M \frac{l_0}{l_0'}, \tag{14}$$

where $I_0$ is the deflection factor, $M$ is the cross-section magnification factor, and $l_0$ is the effective length. From Eq. (14) it is obvious that if all the coil dimensions are multiplied by the same amount $M$ then the deflection factor will not be changed. On the other hand, if the form is held constant, the deflection factor will be inversely proportional to the number of turns in the windings:

$$\frac{I_0'}{I_0} = \frac{N}{N'}. \tag{15}$$

Equations (14) and (15) may be combined to form one complete equation:

$$\frac{I_0'}{I_0} = M \frac{l_0}{l_0'} \frac{N}{N'}. \tag{16}$$

**8·5. Resistance.**—Every practical deflection coil has resistance, which is usually important both from the standpoint of driving voltage and of power loss. The factors that influence coil resistance are again form and number of turns. Usually, the winding space available on a given coil is limited. If the coil is wound so as always to fill the available space, then, for a given form, the same amount of copper will be wound regardless of the number of turns. The resistance will thus be directly proportional to the square of the number of turns.

$$\frac{R'}{R} = \frac{N'^2}{N^2}. \tag{17}$$

Moreover, if the number of turns is fixed, but all the physical dimensions of the form are multiplied by a factor $f$, the resistance will also be decreased by this factor

$$\frac{R'}{R} = \frac{1}{f} \tag{18}$$

Again, these two equations may be combined to give

$$\frac{R'}{R} = \frac{1}{f} \cdot \frac{N'^2}{N^2}. \tag{19}$$

One of the objections to coil resistance stems from the temperature rise in windings. The relationship between the $I^2R$ loss and the number of turns in a coil may be found by combining the results expressed in Eqs. (16) and (19).

$$\frac{I_0'^2 R'}{I_0^2 R} = \frac{1}{f} M^2 \frac{l_0^2}{l_0'^2}. \tag{20}$$

This equation clearly indicates that the power loss is independent of the number of turns. Also, since $f$ is a factor multiplying all dimensions of the coil, then to be consistent $f = M$, and $l_0/l_0' = 1/f$. When these values are substituted into Eq. (20), $I_0'^2 R'/I_0^2 R = 1/f$. All dimensions of a coil must therefore be increased by a factor $f$ to obtain a corresponding decrease in power loss.

**8·6. Inductance.**—Form and the number of turns also govern the inductance of a coil. Since the field inside a deflection coil is nearly uniform, the inductance of the coil is to a fair approximation independent of the magnification of the cross section, but it is directly proportional to the effective length of the coil,

$$\frac{L'}{L} = \frac{l_0'}{l_0}.$$

If the form is fixed, the coil inductance is also directly proportional to the square of the number of turns in the windings. The complete relationship is

$$\frac{L'}{L} = \frac{l_0'}{l_0} \frac{N'^2}{N^2}. \tag{21}$$

**8·7. Voltage Drive.**—The voltage required to drive a coil may be expressed in terms of the form and the number of turns through the use of the equations in Secs. 8·4, 8·5, and 8·6. If it is assumed that the input current has a sawtooth waveform and that the sweep starts from the center of the tube screen, traveling one radius in a time $t$, the portion of the total voltage drop due to inductance will be

$$L \frac{di}{dt} = L \frac{I_0}{t}.$$

Adding to this the drop across the resistance, the total drop is

$$E = L \frac{I_0}{t} + I_0 R.$$

Now, if the form and the number of turns are changed to a new value, the effect of these changes on the total voltage drop can be calculated from the relations expressed in Eqs. (16), (19), and (21). The new voltage drop will be

$$E' = L \frac{l_0'}{l_0} \frac{N'^2}{N^2} \left( \frac{I_0 M \frac{l_0}{l_0'} \frac{N}{N'}}{t} \right) + I_0 M \frac{l_0}{l_0'} \frac{N_0}{N_0'} R \frac{1}{f} \frac{N'^2}{N^2}.$$
$$= L \frac{I_0}{t} M \frac{N'}{N} + I_0 R \frac{1}{f} M \frac{l_0}{l_0'} \frac{N'}{N}.$$

For a given form this equation becomes

$$E' = \frac{N'}{N} \left( L \frac{I_0}{t} + I_0 R \right). \tag{22}$$

Since the quantity in the parentheses is exactly equal to the original voltage drop, the total voltage drop is directly proportional to the number of turns. However, if the form is changed by multiplying all dimensions by the factor $f$, then again $M = f$ and $l_0/l_0' = 1/f$. Therefore

$$E' = \frac{N'}{N} \left( f \frac{LI_0}{t} + \frac{1}{f} I_0 R \right). \tag{23}$$

It should be remembered that Eq. (23) has been derived under the assumption made in Sec. 8·6—namely, that the inductance of a coil is not affected by a change in its cross-sectional dimensions. For all square iron-core deflection coils this assumption is true, but for most other types the inductance does change with the cross section. The change is slight, however, and Eq. (23) applies to all deflection coils to a reasonably good approximation.

**8·8. Recovery Time.**—The recovery time of a deflection coil is the time required for the coil to dissipate at the end of a single sweep essentially all the energy stored in it. In some instances where the sweep-repetition frequency is high, the time interval between the end of one sweep and the beginning of the next is so short that the coil cannot recover. In such a case, the origin of the sweep shifts to a new position somewhat removed from the initial position.

Any change in the coil form that tends to increase the deflection efficiency will also shorten the recovery time, but such a change is not always possible. The other solution is to dissipate the stored energy

as rapidly as possible.  A critically damped coil dissipates its energy most rapidly, and a resistor equal to $\frac{1}{2}\sqrt{L/C}$ connected across the coil provides this damping.  Such a damping resistor prevents large induced voltages at the end of a sweep.  The recovery time can also be reduced by decreasing the distributed capacitance $C$ of the coil, since the time constant of the coil is equal to $\sqrt{LC}$.  The capacitance of a coil may be reduced by separating the windings, by pie winding, or by the use of insulation having a lower dielectric constant.

**8·9. Defects in Magnetic Deflecting Fields.**—The characteristics of a deflection coil should be such as to produce an undistorted deflection pattern and a uniform focus over the entire tube screen.  Pattern distortion is treated extensively in Chap. 9.  In general, the quality of the focus of a pattern on a cathode-ray tube varies considerably from the center to the edge of the tube.  If the focus adjustment is so made that spots are in good focus near the center of the screen, they will become larger and blurred near the edges, and will frequently be distorted in shape.  The most common shape is an ellipse whose major axis is oriented either parallel with or perpendicular to the line of deflection.  Thus, a sweep line may be narrow near the center of the screen and wider near the edges.  However, not all of the focus distortion is due to the deflection coil; some can be traced to the change in focal length due to flat-face tubes, as is explained in Chap. 9, or to the focus coil itself.  Only those distortions directly due to the deflecting field (usually designated as "deflection defocusing") will be considered here.



Fig. 8·4.—Field pattern in plane through geometric axis of typical iron-core deflection coil, showing region traversed by the electron beam.

Almost all of the causes of defocusing can be traced to nonuniformities in the deflecting field.  Figure 8·4 shows the field pattern in a plane through the geometric axis of a typical iron-core deflection coil.  Because of the symmetry of the coil, the flux lines all cross at right angles to the coil axis.  An electron beam whose initial direction coincides with the coil axis is deflected in a plane passing through the axis and perpendicular to the lines of force; but since the electron bundle has a definite cross section, as indicated in the figure, not all of the electrons in the beam are deflected by the same amount.  The electrons above and below the axis are deflected through a slightly smaller angle than those on the axis; therefore a beam cross section originally round is squeezed into an oval.

Fortunately, nonuniformity in the fringing fields, over which the designer has little control, causes much less defocusing than lack of uniformity in the main deflecting field of a coil, which can be controlled to some extent. The magnetic-field intensity within a coil may increase, decrease, or remain constant in the direction of deflection. Each of these distributions has a characteristic effect on the beam cross section.

A magnetic field that increases in intensity along the line of deflection tends to distort the cross section of a circular electron beam into an oval with the pointed end in the direction of deflection. This type of magnetic field has been called a "pincushion" field from the shape suggested by the flux lines. Figure 8·5a shows the field pattern in a plane perpen-



(a)                                         (b)
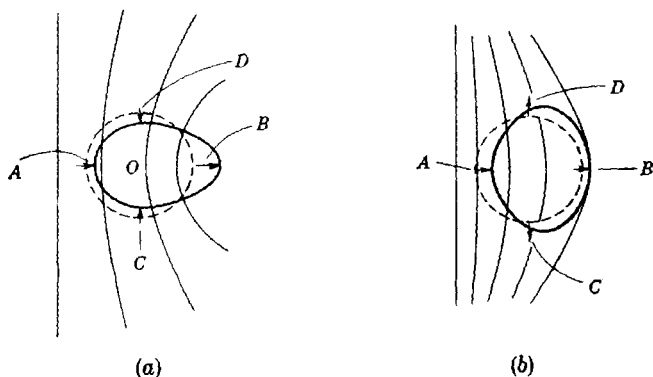
Fig. 8·5.—Distortions of circular cross section of electron beam produced by non-uniform fields. (a) Change produced by coil having a "pincushion" field. (b) Change produced by coil having a "barrel" field.

dicular to the axis of a coil having a pincushion field. The dashed circle represents the circular cross section of an electron beam. Electrons at the beam edge marked $A$ are deflected less than those at $B$ because the magnetic field is stronger at $B$ than at $A$. Also electrons at $D$ are deflected down and those at $C$ are deflected up because of the horizontal components of magnetic field. These distortions change the beam cross section into the shape shown by the solid line.

A magnetic field that decreases in intensity along the line of deflection causes a circular cross section to be changed, roughly, into an elliptical shape with the major axis perpendicular to the line of deflection as in Fig. 8·5b. A "barrel" field such as this causes electrons at $A$ to be deflected more than those at $B$. Horizontal field components now cause electrons at $D$ to be deflected up and those at $C$, down. The squeezing and pulling effect gives rise to the illustrated cross section.

None of these distortions are present when the electron beam is deflected by a uniform field because all the electrons are deflected by the

same amount. Consequently, the main deflecting field should be as uniform as possible if good focus is desired.

A given field distribution in a deflection coil may be studied to determine its effect on focus if the current in the focus coil is reduced so that the illuminated spot appearing on the screen of the cathode-ray tube is about one-quarter to one-half inch in diameter. The focal point then lies beyond the tube screen and the illuminated spot, which may be thought of as an underfocused spot, is an image of a cross section of the converging electron beam. The undeflected spot is round but, as the electron beam is deflected, the spot may gradually change to one of the shapes illustrated in Fig. 8·5. If the beam cross section remains round as it is deflected, then, if the focus coil is perfect, the electrons of the beam will converge at a single point. When the beam cross section is distorted, those electrons that are pulled out of the original circle will converge beyond, and those electrons that are squeezed into the circle will converge on, the near side of the original focal point. Thus, more information may be obtained about the defocusing properties of a coil through a study of the unfocused spot than by measuring spot size.

It is not easy to generate a uniform magnetic field with a small coil. The magnetic field must, therefore, be shaped either with magnetic pole pieces or by the distribution of turns in the windings. Of these two methods, the latter is preferred because it gives a much finer control of the field and is less cumbersome. A convenient way to determine the proper winding distribution for a deflection coil is to divide the winding into several sections, each of an accurately known number of turns, with separate leads brought out. Then, with the deflection coil on a cathode-ray tube, the currents through each section may be adjusted until the underfocused spot can be deflected without altering its cross section. From the values of the products of turns times current, the proper distribution of turns among the sections when they are connected in series may be determined.

**8·10. Methods of Producing Deflecting Fields.**—The relationships that have been indicated in the discussion thus far apply to deflection coils of all types and sizes. In the following sections, some of the known deflection-coil types will be treated in detail, but each of these types falls into one or the other of two general classes. In the first class are all deflection coils whose windings are placed so that they generate the magnetic field in parallel, each winding contributing an equal share of the magnetic flux. The second class contains all those coils whose windings generate a magnetic field in series, each winding sharing the same magnetic flux. Coil types that do not fit into these two classes are unimportant because they are intrinsically inferior.

A pair of short solenoid windings placed side by side but sufficiently

far apart to allow the neck of the cathode-ray tube to pass between them will generate a magnetic field in parallel if the proper direction of current is chosen.   Such an arrangement together with the magnetic field is
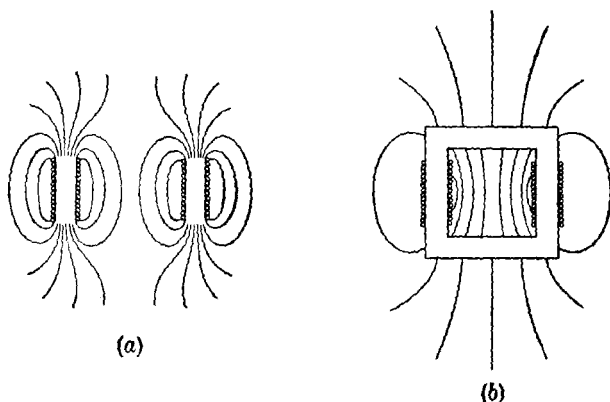


FIG. 8·6.—Magnetic field surrounding a pair of parallel windings (electron beam perpendicular to paper).   (a) Not joined by an iron core.   (b) Joined by an iron core.

shown in Fig. 8·6a.   Because of the symmetrical arrangement of the windings, the magnetic field is also symmetrical and is nearly uniform in the region of the tube neck.   However, a large part of the magnetic field generated is not useful in deflecting the electron beam.   If an iron core is used as shown in Fig. 8·6b it not only increases the total magnetic flux but also helps to guide the flux to the region where it is needed.   Although even with the iron core only about 30 per cent of the total flux generated is useful in deflecting the electron beam, the method of Fig. 8·6 is one of the most efficient ways of generating a deflecting field.

Deflection coils of the second class have a pair of windings placed one above the other on opposite sides of the tube neck and are so connected that they generate the magnetic field in series.   A pair of series windings



FIG. 8·7.—Magnetic field surrounding a pair of series windings.

is shown in Fig. 8·7.   With this type of coil, most of the flux generated is useful in deflection, but the current required to set up this flux is so large

that the deflection efficiency is very nearly the same as that of coils of the first class.  Nevertheless, the deflection efficiency can be considerably improved if a tight-fitting magnetic iron shell is placed around the outside of the windings.  This iron shell provides a low-permeability return path for the flux passing around the outside of the coil, and thereby increases the deflection efficiency.  Another useful characteristic of coils of the second class is the fact that the magnetic-field distribution within the coil is governed almost entirely by the distribution of windings.  Figure 8·7 shows a coil with two lumped windings, but if the wires were distributed over a cylindrical surface, a much more uniform field would result.

## IRON-CORE DEFLECTION COILS

The square iron-core deflection coil is a practical example of the class of coil in which the magnetic field is generated by two coils in parallel.

**8·11.  Deflecting Field of a Square Iron-core Coil.**—Two views of a typical square iron-core coil together with its magnetic field are shown
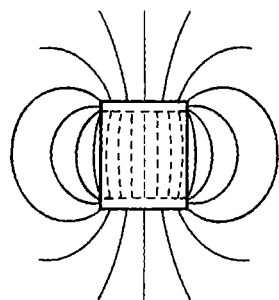


FIG. 8·8.—Axial magnetic-field distribution of a typical square iron-core coil.

in Figs. 8·6b and 8·8.  The magnetomotive force is in the same direction in both legs of the core, and the top of the core is therefore raised to a higher magnetic potential than the bottom.  This difference of magnetic potential causes flux to pass more or less uniformly across the air gap within the core, but approximately two-thirds of the total flux passes around the outside where it is of no use for deflection.  Although the square iron-core coil therefore has a low deflection efficiency, the efficiency of most other deflection-coil types used at the present time is no better.

In a coil of this type, it is important that the core have a permeability of 500 or more for the following reasons:

1. To minimize the drop in magnetomotive force along the core length, so that the top and bottom of the coil may be equipotential surfaces and may thus set up the most uniform field in the air gap.

2. To minimize the effect of changes in the magnetic properties of the core.  All of the flux passing across the air gap also passes through the core.  If the permeability is high, then the reluctance of the iron path will be negligible compared to that of the air path; consequently, even large changes in the core permeability will not affect the deflecting field.

Not only should the core material have a high permeability but it should also have a low retentivity so that the field of the coil will collapse to zero at the end of a sweep. If the core retains its magnetism, the residual field will tend to cause a shift in the origin of the sweep.

It is not difficult to find satisfactory core materials, since the flux density in the core rarely is greater than 15 per cent of the amount needed for saturation. Better grades of silicon steel, Hipersil, and Permalloy all make excellent cores. The magnetic properties of these materials depend upon the annealing process to which they are subjected in the course of manufacture, and particular care must be exercised to prevent magnetic "hard spots," which cause distortions in the magnetic field.

**8·12. Eddy Currents in the Core.**—Sweep currents induce eddy currents in any metal parts in or near the deflection coil. If the losses associated with eddy currents are to be minimized, the iron core must be laminated. These losses are all dissipative and have practically the same effect as a resistor shunted across the windings. The value of this effective shunt resistance increases as the thickness of the laminations decreases and is approximately 100,000 ohms for laminations 0.014 in. thick. Except in special applications, this value of shunt resistance will not appreciably interfere with the coil performance; therefore, 0.014-in. laminations are satisfactory.

Eddy currents in the core tend to slow the start of the sweep. When the magnetic deflecting field starts to increase at the beginning of a sweep, these currents oppose it and cause it to increase at a much slower rate, but as time increases, the effect of the eddy currents becomes less significant, with the result that the sweep is nonlinear. Additional power must be supplied at the start of the sweep by the driving circuits in order to counteract the effects of these eddy currents.

One type of lamination used in square iron cores is an L-shaped piece stamped from 0.014-in. silicon steel. One leg is $2\frac{1}{4}$ in. and the other is 2 in. long. These laminations are usually stacked, alternating the long and short legs, to a height of $1\frac{1}{2}$ in. If the joints are arranged on only one pair of diagonally opposite corners, the core may be opened to permit the windings to be slipped onto the legs. Another type of laminated core occasionally used is made with Hipersil tape, $1\frac{1}{2}$ in. wide and 0.002 in. thick. This tape is wound on a square form until a core thickness of approximately $\frac{1}{4}$ in. has been built up. After it has been wound, the core is varnished to hold it together and then cut apart with a fine saw so that the windings may be placed on it. The cut edges are etched and finished so that they will fit together tightly.[1]

Because of the excellent properties of iron-dust cores at high fre-

[1] More information about these cores may be obtained from the Westinghouse Electric and Manufacturing Co., Sharon, Pa.

quencies, an attempt was made to use them in deflection coils.    Unfortunately, however, they did not prove satisfactory because of their low permeability.

A ribbon-wound core exhibits stronger eddy-current effects than does a core having L-shaped laminations.    This difference occurs because the laminations at the top and bottom of a ribbon-wound core are not in the proper orientation to minimize eddy currents.    The curves of Fig. 8·9 show how laminations affect the response of a deflection coil to a voltage step.    Each of these curves has an initial slope that is determined by the magnitude of the eddy currents, but in a short time this effect disappears and the curves become linear.    If the linear portion is extrapolated back
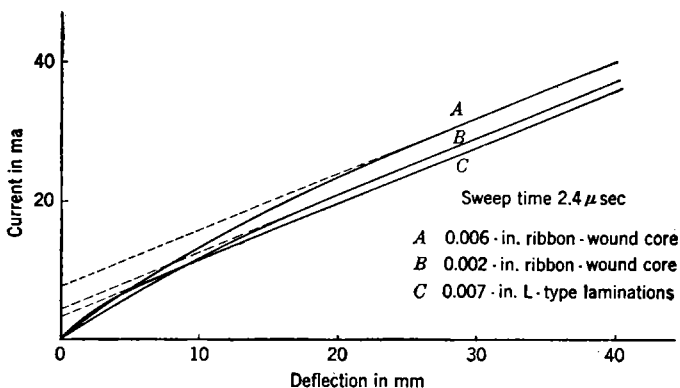


Fig. 8·9.—Effect of laminations on response of an iron-core deflection coil to a voltage step.

to the current axis, then the current at the point of intersection will be inversely proportional to the resistance reflected into the windings by the eddy currents in the core.    This resistance, which is effectively shunted across the windings, is about 100,000 ohms for the L-type laminations but is only about 50,000 ohms for the 0.006-in. ribbon-wound core.    In most ordinary applications of deflection coils these differences are not important, but, when very fast sweeps are used, the delay in the start of the sweep may be objectionable enough to warrant care in the choice of core laminations.

**8·13. Windings.**—The windings of an iron-core coil may be very simple because the magnetic field is chiefly determined by the core. Therefore, a multiple-layer solenoid may be wound on a base of rectangular fiber tubing according to conventional coil-winding practice. The dimensions of the fiber tubing are chosen so that the coil will fit snugly on the core and so that it will extend over the length of the leg. Similarly, the winding depth is also fixed by the core dimensions because

the windings can occupy only the space between the core and the glass wall of the cathode-ray-tube neck.

Deflection coils may be wound for either single-ended or push-pull operation. For single-ended operation, two identical coils are fitted on opposite legs of the core and connected, usually in series, so that their magnetic fields are in the proper direction to produce a deflecting field. The series connection is preferred because the same current will then flow through both windings and small differences in the resistance of the windings will not be significant. A push-pull coil, on the other hand, has two



FIG. 8·10.—Connections for push-pull deflection coil. Heavy line indicates winding adjacent to core.

windings on each leg, one wound on top of the other. The inside winding of one leg is connected in series with the outside winding of the other leg in the manner illustrated in Fig. 8·10. With this connection, the field due to the quiescent current of the push-pull tubes is balanced out, but any differential in the plate currents of these tubes will produce a deflecting field and the electron beam will be deflected either to the right or left depending upon which tube is conducting the greater current.

A deflection coil with windings on only one pair of legs will be able to deflect the electron beam along one coordinate axis. If a similar set of windings is placed on the remaining two legs of a square core (see Fig. 8·11), it is possible to deflect the beam both horizontally and vertically. The set of windings giving horizontal deflections need not have the same number of turns as the set giving
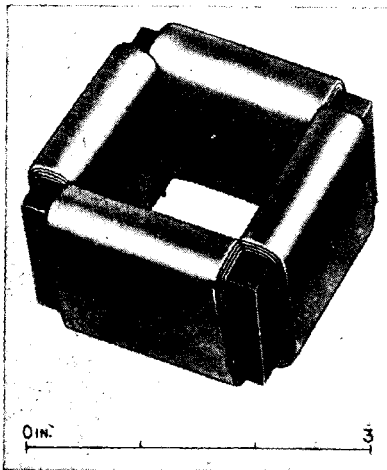


FIG. 8·11.—Iron-core deflection coil with two sets of windings.

vertical deflections. Each set of windings may be designed to fit the circuits used to drive it, if the ratio of the turns is not greater than 3 or 4. It is important that the windings be accurately centered on the core in order to minimize inductive coupling. It may be seen in Fig. 8·6*b* that the magnetic field generated by one set of windings is

perfectly symmetrical if the windings are centered.   If a second set of
windings is added to the legs at the top and bottom of the coil illustrated
and if these windings are centered, then the magnetic flux from the first
set will cut half the turns of the added set in one direction and half in the
other, so that the total emf induced in the second set will be zero.   Practi-
cal coils, nevertheless, always exhibit some inductive coupling between the
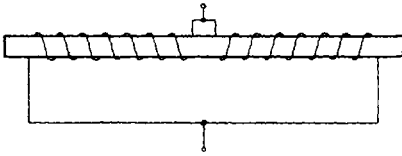


Fig. 8·12.—Balanced winding.

windings.

Inductive coupling between
the two sets of windings causes
one set to oscillate at its natural
frequency while the other set is
being driven.   The effect of this
oscillation appears in the sweep as
a wiggly line instead of the desired straight line.   To reduce still further
the inductive coupling present in deflection coils having conventional
solenoid windings, a type of winding known as a "balanced winding" (see
Fig. 8·12) has been used.[1]   In this case, the winding is divided in half;
one half is wound in one direction and the other in the opposite direction.
The inside leads of each half are connected together to form one terminal
of the balanced winding, whereas the two leads at the ends are connected
together to form the second terminal.   With this type of winding, the
current enters at the middle and flows toward both ends.   Since the ends

are connected together, the
balanced winding cannot oscillate
as does an ordinary solenoid and
consequently it is less sensitive to
a small asymmetry of the winding
with respect to the geometrical
center of the core.

**8·14. Pie Windings.**—Pie
winding offers the possibility of
reducing the recovery time of a
coil by reducing its distributed
capacitance.   (See Sec. 8·8.)



Fig. 8·13.—An iron-core deflection coil with
pie windings.

A pie-wound iron-core deflection coil is illustrated in Fig. 8·13.   The
windings of this coil are divided into eight sections or pies, each pie being
separated from the others by an insulating wall.   All of the sections are
random-wound and all are connected in series.   Such a coil is suitable
only for single-ended drive since the benefits of pie winding are lost in a
push-pull coil.   As is indicated by the curve of Fig. 8·14, the number of
sections directly influences the distributed capacitance.   This curve
tapers off at 10 $\mu\mu$f, indicating that no matter how many sections are

[1] Mr. W. H. Pratt, Research Construction Co., personal communication.

included the distributed capacitance for a 2400-turn winding will not fall much below 10 $\mu\mu$f. Therefore, it is not worth while to use more than the eight sections illustrated in Fig. 8·13 because the difficulties in winding increase more rapidly than the capacitance decreases.

Pie winding is also particularly well suited to the correction of high-frequency sectional oscillations in the windings of deflection coils. Sectional oscillation is a descriptive term applied to cases in which a coil is oscillating in a mode higher than the fundamental. The mode of oscillation most frequently encountered is one in which the ends of the coil remain at a fixed potential, but the middle swings up and down in much the same manner as a vibrating string. A damping resistor



FIG. 8·14.—Variation of distributed capacitance with number of sections in pie-wound coil.

placed across the ends of the coil will, in this case, have no effect on the oscillation. However, if the coil is divided into two parts and if a resistor is connected across each part, this mode can be effectively damped. Similarly, by properly dividing the coil, any mode of oscillation can be damped.

**8·15. Deflection-coil Shields.** In order to improve the deflection efficiency by reducing the large amount of the magnetic field that passes around the outside of the core and is not useful in deflecting the electron beam, tight-fitting copper or aluminum shields have been placed around square iron-core deflection coils. Eddy currents that circulate in the shield oppose the "buildup" of the magnetic field around the outside of the core and effectively eliminate it for the duration of the sweep.



FIG. 8·15.—Copper shield for an iron-core deflection coil.

A type of copper shield commonly used is illustrated in Fig. 8·15. This shield surrounds the deflection coil, but has two holes just large

enough to accommodate the neck of the cathode-ray tube. Normally, the magnetic field that fringes out along the axis and beyond the ends of the coil makes a substantial contribution to the deflection of the electron beam, but this field also is cut off to a large degree by the end plates of the copper shield. The curves of Fig. 8·16 show the extent to which the axial field distribution is affected. Because the shielding effect is greater at the higher frequencies, the effective length of the deflection coil
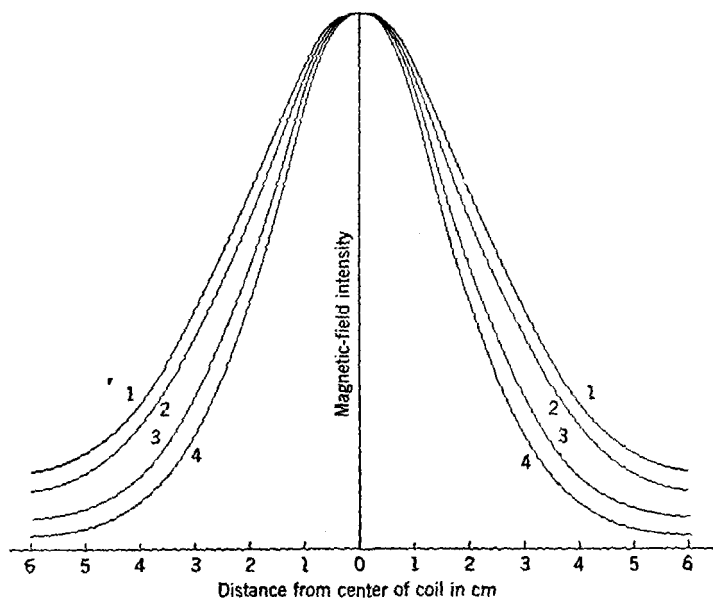


Fig. 8·16.—Axial field distribution of an iron-core coil with and without copper shield. 1. Coil without case. 2. With case—100 cps excitation. 3. With case—1000 cps excitation. 4. With case—10,000 cps excitation.

is frequency dependent, as is the sensitivity, which decreases at high frequencies to about 80 per cent of its value with direct current. Such a variation of sensitivity with frequency causes nonlinearity in a sweep whose duration is of the order of 200 μsec. Slower sweeps exhibit a slow start, whereas very fast sweeps are linear but require a larger driving current. It is possible to avoid all of the troubles caused by the end plates if a shield similar to that illustrated in Fig. 8·17 is used. Stray fields around the sides of the coil are then effectively shielded but the fringing fields at the ends are relatively unaffected.

Since the magnetic field around a deflection coil is reduced by the addition of a copper shield, the inductance is also decreased by an amount that depends upon the frequency at which it is measured. The change

in inductance affects the input-voltage waveform and may cause a nonlinear sweep if the proper waveform is not supplied.

A typical inductance curve for an iron-core deflection coil fitted with a copper shield of the type illustrated in Fig. 8·15 is shown in Fig. 8·18. At very low frequencies, eddy currents in the shield are not strong and the inductance is therefore not much affected; but, as the frequency increases, the eddy currents increase until the shielding is complete.
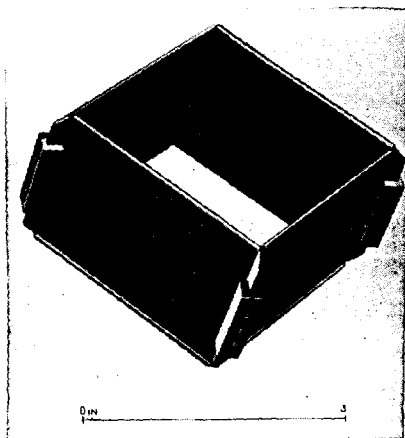


Fig. 8·17.—Copper shield without end plates.
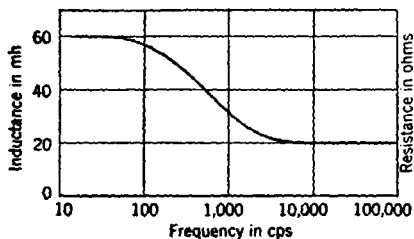


Fig. 8·18.—Variation of inductance of a typical iron-core deflection coil.
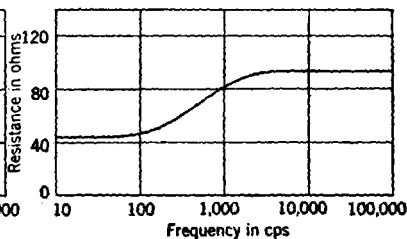
Fig. 8·19.—Variation of resistance of a typical iron-core deflection coil.

In the frequency range where the shielding is complete, the inductance is constant but is considerably reduced from its value at low frequencies. For most ordinary coil shields the shielding is nearly complete at 1000 cps. Consequently, the inductance of a deflection coil will be almost constant for all sweeps whose duration is 1000 $\mu$sec or less. If a longer sweep time is employed, then the inductance will change during the course of the sweep.

Eddy currents in the shield reflect an apparent resistance into the windings as do the eddy currents in the core. However, since the mag-

netic coupling between the windings and the shield is very much looser
than the coupling between the windings and the core, the effect is different
from that of a simple shunt resistance.    The resistance reflected into the
windings grows in magnitude as the eddy currents in the shield increase
and finally reaches a maximum value as shown in the curve of Fig. 8·19.
The initial value of the resistance in this curve is the d-c resistance of the
wire in the windings.    The increase in resistance corresponds at each
frequency to the decrease in inductance of the coil.

**8·16. Equivalent Circuit of an Iron-core Deflection Coil.**—The elec-
trical response of a deflection coil can be closely approximated at all
frequencies by an equivalent circuit composed of resistive, inductive,
and capacitive elements.    Two such equivalent circuits are shown in
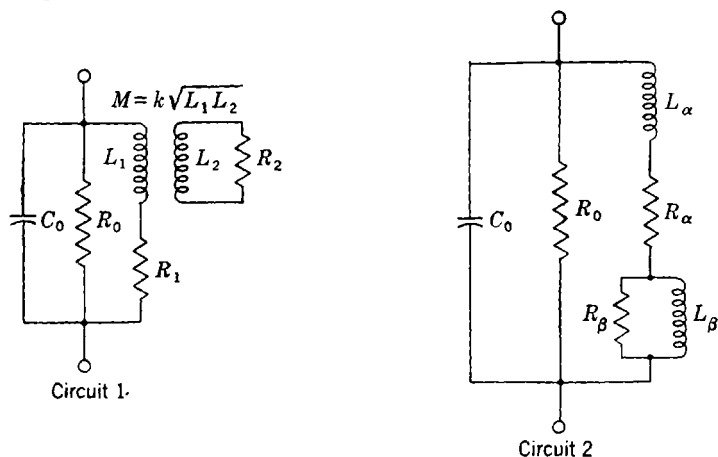


Fig. 8·20.—Equivalent circuits of an iron-core deflection coil.

Fig. 8·20.    Although they both present exactly the same impedance, the
arrangement of the elements is different.    The first circuit is useful in
visualizing the coil behavior because the elements correspond closely to
the physical concept of a deflection coil.    On the other hand, it is much
simpler to evaluate the elements of the second equivalent circuit although
these elements do not have physical counterparts in an actual coil.
For this reason, the relationships between the elements of Circuit 1 and
a physical coil will be described and then the elements of Circuit 2 will
be defined in terms of the elements of Circuit 1.

The elements of Circuit 1 are related to a physical deflection coil as
follows: $C_0$ is the lumped equivalent of the distributed capacitance of the
windings; $R_0$ corresponds to the effective resistance of the core lamina-
tions and is the shunt resistance described in Sec. 8·12; $L_1$ is the self-
inductance of the windings; $R_1$ is the resistance of the wire; $L_2$ represents

the effective inductance of the metal shield surrounding the core; $R_2$ represents the effective resistance of the shield; $M$ is the mutual inductance between the shield and windings, and is equal to $k\sqrt{L_1 L_2}$ where $k$ is the coupling coefficient.

Of the total input current to the coil, only the portion that flows through $L_1$ is effective in generating a deflecting field. All the rest of the current is either used to counteract losses or shunted by the distributed capacitance. Consequently, the deflection produced by a practical coil will not be exactly proportional to the input current. Therefore, in order to generate a linear sweep, either the proper waveform must be supplied at the terminals of the coil or else the deflection coil must be designed so that the distortions produced by its losses are negligible.[1] The latter alternative is the more practical.

The relationship between the elements of Circuit 1 and Circuit 2 are: $L_\alpha = L_1(1 - k^2)$, $L_\beta = k^2 L_1$, $C_0 = C_0$, $R_\alpha = R_1$, $R_\beta = k^2 \dfrac{L_1}{L_2} R_2$, and $R_0 = R_0$, where $k = M/\sqrt{L_1 L_2}$.

**8·17. Measurement of the Circuit Constants.** Because an inductance bridge measures the inductive reactance of a coil rather than its inductance, the indicated inductance of a coil measured on such a device will, in general, increase with the measuring frequency. Although the assumption that this reactance is caused by a pure inductance is valid for low frequencies, is it not true at higher frequencies where the effect of the distributed capacitance becomes significant. If, however,



Fig. 8·21.—Right-hand branch of equivalent circuit of iron-core deflection coil.

measurements are confined to the frequency range in which the assumption is valid, then an inductance bridge will serve adequately for measuring the variation of inductance with frequency of a deflection coil. In determining the values of other circuit constants also, advantage is taken of the fact that at certain frequencies the effect of all the other elements on the one measured is negligible.

The impedance function of a deflection coil may be simplified by examining the right-hand branch impedance of the equivalent circuit (see Fig. 8·21). The impedance of this branch is

$$Z_a = R_a + j\omega L_a + \frac{j\omega L_\beta R_\beta}{R_\beta + j\omega L_\beta},$$

[1] For derivation of equations for current through a deflection coil based on the equivalent circuit, see Chap. 10.

or

$$Z_a = \left[ R_\alpha + \frac{\omega^2 L_\beta^2 R_\beta}{R_\beta^2 + \omega^2 L_\beta^2} \right] + j\omega \left[ L_\alpha + \frac{L_\beta R_\beta^2}{R_\beta^2 + \omega^2 L_\beta^2} \right]. \tag{24}$$

The impedance $Z_a$ expressed by Eq. (24) may be regarded as an apparent resistance,

$$R_a = R_\alpha + \frac{\omega^2 L_\beta^2 R_\beta}{R_\beta^2 + \omega^2 L_\beta^2}, \tag{25}$$

in series with an apparent inductance,

$$L_a = L_\alpha + \frac{L_\beta R_\beta^2}{R_\beta^2 + \omega^2 L_\beta^2}, \tag{26}$$

where both $R_a$ and $L_a$ are functions of frequency. The branch impedance then becomes $Z_a = R_a + j\omega L_a$.

As a result of the simplification, the impedance of the complete equivalent circuit may be written in terms of the variables defined by Eqs. (25) and (26). Then,

$$Z = \frac{(R_a + j\omega L_a)\left[ \dfrac{R_0(1 - j\omega C_0 R_0)}{1 + \omega^2 C_0^2 R_0^2} \right]}{R_a + j\omega L_a + \left[ \dfrac{R_0(1 - j\omega C_0 R_0)}{1 + \omega^2 C_0^2 R_0^2} \right]},$$

which reduces to

$$Z = R + jX,$$

where

$$R = \frac{\dfrac{1}{R_0}(R_a^2 + R_0 R_a + \omega^2 L_a^2)}{(1 - \omega^2 L_a C_0)^2 + 2\dfrac{R_a}{R_0} + \dfrac{R_a^2}{R_0^2}(1 + \omega^2 C_0^2 R_0^2) + \dfrac{\omega^2 L_a^2}{R_0^2}}, \tag{27a}$$

and

$$X = \frac{\omega(L_a - C_0 R_a^2 - \omega^2 C_0 L_a^2)}{(1 - \omega^2 L_a C_0)^2 + 2\dfrac{R_a}{R_0} + \dfrac{R_a^2}{R_0^2}(1 + \omega^2 C_0^2 R_0^2)}. \tag{27b}$$

Because an inductance bridge measures the inductive reactance of a coil, the indicated reading will be

$$L_{\text{measured}} = \frac{X}{\omega},$$

where $X$ is the actual reactance of the coil at the measuring frequency $\omega$. Consequently, the measured inductance of a deflection coil will be

$$L_{\text{measured}} = \frac{L_a - C_0 R_a^2 - \omega^2 C_0 L_a^2}{(1 - \omega^2 L_a C_0)^2 + 2\dfrac{R_a}{R_0} + \dfrac{R_a^2}{R_0^2}(1 + \omega^2 C_0^2 R_0^2)}.$$

However, in the frequency range from 0 to 5000 cps, the capacitance $C_0$ is usually small enough so that all terms containing it may be neglected, and $R_a \ll R_0$. The measured inductance is then given by the approximate equation

$$L_{\text{measured}} \approx L_a \qquad \text{(from 0 to 5000 cps)}.$$

Values of $L_\alpha$, $L_\beta$, and $R_\beta$ in the equivalent circuit can be determined from a curve of $L_a$ plotted against frequency as in Fig. 8·22. The curve is flat and horizontal at low frequencies, then goes through an inflection, and again becomes flat and horizontal at the higher frequencies. The inductance $L_a$ at these flat portions of the curve is labeled $L_{a_1}$ and $L_{a_2}$. Now, from Eq. (26), it is easy to see that at low frequencies



Fig. 8·22.—Curve of the apparent inductance $L_a$ of an iron-core deflection coil.

$$L_a = L_{a_1} \approx L_\alpha + L_\beta, \qquad (28)$$

and at the higher frequencies,

$$L_a = L_{a_2} \approx L_\alpha. \qquad (29)$$

Also, at the frequency $\omega_0 = R_\beta / L_\beta$,

$$L_a = L_\alpha + (\tfrac{1}{2})L_\beta. \qquad (30)$$

Equations (28), (29), and (30) may be solved for $L_\alpha$, $L_\beta$, and $R_\beta$, giving

$$L_\alpha = L_{a_2},$$
$$L_\beta = L_{a_1} - L_{a_2},$$
$$R_\beta = \omega_0(L_{a_1} - L_{a_2}).$$

After the inductance of a deflection coil has been determined, the distributed capacitance can be found. The presence of this capacitance will cause the coil, when driven by a voltage applied to its terminals, to antiresonate at a frequency determined by the relation

$$\omega^2 = \frac{1}{L_a C_0} - \frac{R_0^2}{L_a^2}.$$



Fig. 8·23.—Connection for additional condenser across deflection coil.

The shunt resistance $R_0$ does not affect the antiresonant frequency. If another condenser $C$ of known

value is placed across the coil, as in Fig. 8·23, then the antiresonant frequency will be changed to a new frequency given by

$$\omega^2 = \frac{1}{L_a(C + C_0)} - \frac{R_0^2}{L_a^2}.$$

Rearranging this expression gives

$$\frac{1}{\omega^2} \frac{Q^2}{Q^2 + 1} = L_a(C + C_0), \tag{31}$$

where $Q = \omega L_a/R_a$. If several values of $C$ are placed across the deflection coil, there will be a separate antiresonant frequency for each value of $C$. Thus, when $\dfrac{1}{\omega^2} \dfrac{Q^2}{Q^2 + 1}$ is plotted against $C$ the resulting curve will appear as in Fig. 8·24. As indicated in Eq. (31) the slope at any point of this



curve is $L_a$. At the higher frequencies, $L_a$ becomes constant; consequently, the curve may be extrapolated as a straight line until it intersects the axis of $C$. The value of $1/\omega^2$ at this intersection is zero; therefore, from Eq. (31), $C_0 = -C$. Generally, $Q$ is high enough so that the factor $Q^2/(Q^2 + 1)$ is approximately 1. Then $C$ may be plotted against only $1/\omega^2$.

Fig. 8·24.—Curve of $F = (1/\omega^2)$ $[Q^2/(Q^2 + 1)]$ plotted against $C$, showing the value of distributed capacitance $C_0$.

The shunt resistance $R_0$ may be measured directly at the antiresonant frequency of the deflection coil. At this frequency the reactance of Eq. (27b) is zero, and the impedance of the coil is therefore all resistive. Equation (27a) reduces to

$$R = \frac{1}{\dfrac{1}{R_0} + \dfrac{R_a C_0}{L_a}},$$

TABLE 8·1.—TYPICAL VALUES OF ELEMENTS IN EQUIVALENT CIRCUIT OF AN IRON-CORE* DEFLECTION COIL†

| $N$, turns/leg | $R_\alpha$, ohms | $L_\alpha$, mh | $R_\beta$, ohms | $L_\beta$, mh | $R_0$, ohms | $C_0$, $\mu\mu f$ |
|---|---|---|---|---|---|---|
| 500 | 11.2 | 4.8 | 14.4 | 8.6 | 19,900 | 704 |
| 1000 | 45 | 20.6 | 50 | 32.2 | 51,700 | 450 |
| 1600 | 161 | 52.0 | 123 | 91.0 | 114,000 | 246 |

\* Core—L-type laminations of 0.014-in. silicon steel.

† Windings on opposite legs are connected in parallel; copper shield as in Fig. 8·15.

and, except where $R_a$ is very large, this equation reduces to

$$R \approx R_0.$$

Typical values for the elements in the equivalent circuit of an iron-core deflection coil are given in Table 8·1.   These values were measured according to the methods outlined above.

**8·18. Toroidal Iron-core Deflection Coils.**—A deflection coil, rotated mechanically, has frequently been used to rotate the sweep in a radial-time-base display (PPI).   For simplicity in mounting, this coil should be round.   Although an iron-core coil can be made in this form, the winding must be done on a toroidal winding machine and constructional difficulties are thereby considerably increased.   A simplification results, however, from the fact that only one pair of windings is required.   In Fig. 8·25, the general construction of a toroidal coil is shown.
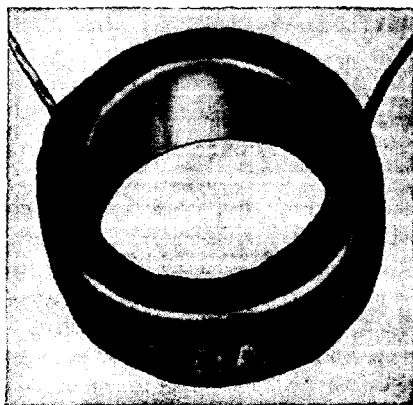


FIG. 8·25.—Toroidal deflection coil.

If the required sweep speed is not so fast that the delay due to eddy currents is objectionable, the cores of these coils can be ribbon-wound. Otherwise, circular punchings may be used.   A core thickness of $\frac{1}{8}$ in. is adequate to carry the flux.   It may be necessary to limit the core height to 1 in. to allow space for the slip rings and bearings required for a rotating-coil mount.

The winding of toroidal coils is rather critical and the number of turns in each section must be accurately held to one turn.   The windings must also be positioned on the core as accurately as possible.   If every effort is not made to make the winding smooth (i.e., as nearly layer-wound as is possible) the sweep produced is likely to be crooked.   A photograph of such a sweep is shown in Fig. 9·12b.

For a coil $1\frac{11}{16}$ in. ID by $1\frac{1}{8}$ in. high, wound with a total of 4000 turns,

a current of approximately 100 ma is required to produce a one-radius deflection at 5-kv accelerating voltage[1] when the two sections are connected in parallel. The inductance varies with the degree of shielding afforded by the case in which the coil is mounted, but will be approximately 100 millihenrys.

Toroidal iron-core coils have been used extensively in the past few years for radial-time-base sweeps. It is probable, however, that they will be replaced entirely by air-core coils because the latter are less likely to produce crooked sweeps. The focus obtainable with the air-core coil is definitely superior to that obtainable with the toroidal type, and the efficiencies of the two types are not very different.

### AIR-CORE AND MOTOR-STATOR TYPES OF DEFLECTION COIL

Air-core deflection coils along with a few coils having iron cores, notably the motor-stator type, form a class distinct from the parallel-field type described in the previous sections, since their windings generate a magnetic field in series.

**8·19. Advantages of Air-core Design.**—There are four important advantages that may be gained through the use of an air-core deflection coil. First, since an air-core coil has no iron, it will not interfere with or distort the magnetic field generated by surrounding coils or magnets. Therefore, it is possible to build a deflection system consisting of an air-core coil surrounded by a larger, iron-core coil. The air-core coil may be rotated mechanically to provide a radial-time-base display whereas the larger coil may be used to set the center of the display at any point on the tube screen. Second, an air-core coil, because of its low distributed capacitance and also because it does not tend to produce sectional oscillations, may be driven at much faster sweep speeds than an iron-core coil. Third, the air-core coil is lighter; and fourth, the magnetic-field distribution can be readily controlled by the winding distribution so that a pincushion, barrel, or uniform field may be produced at will.

On the other hand, a good air-core deflection coil is difficult to build. Techniques other than those used in standard coil-winding practice must be employed.

**8·20. Coils with Lumped Windings.**—The simplest type of air-core coil has lumped windings and has two separate but identical halves as shown in Fig. 8·26. These halves are shaped to fit a cylindrical surface and are made so that they will just pass over the neck of the cathode-ray tube. A coil such as this can be made by winding two hanks of wire on a rectangular form of the proper dimensions and bending it by hand into the required cylindrical shape after wrapping each hank with silk or cotton tape.

[1] See Appendix B·1.
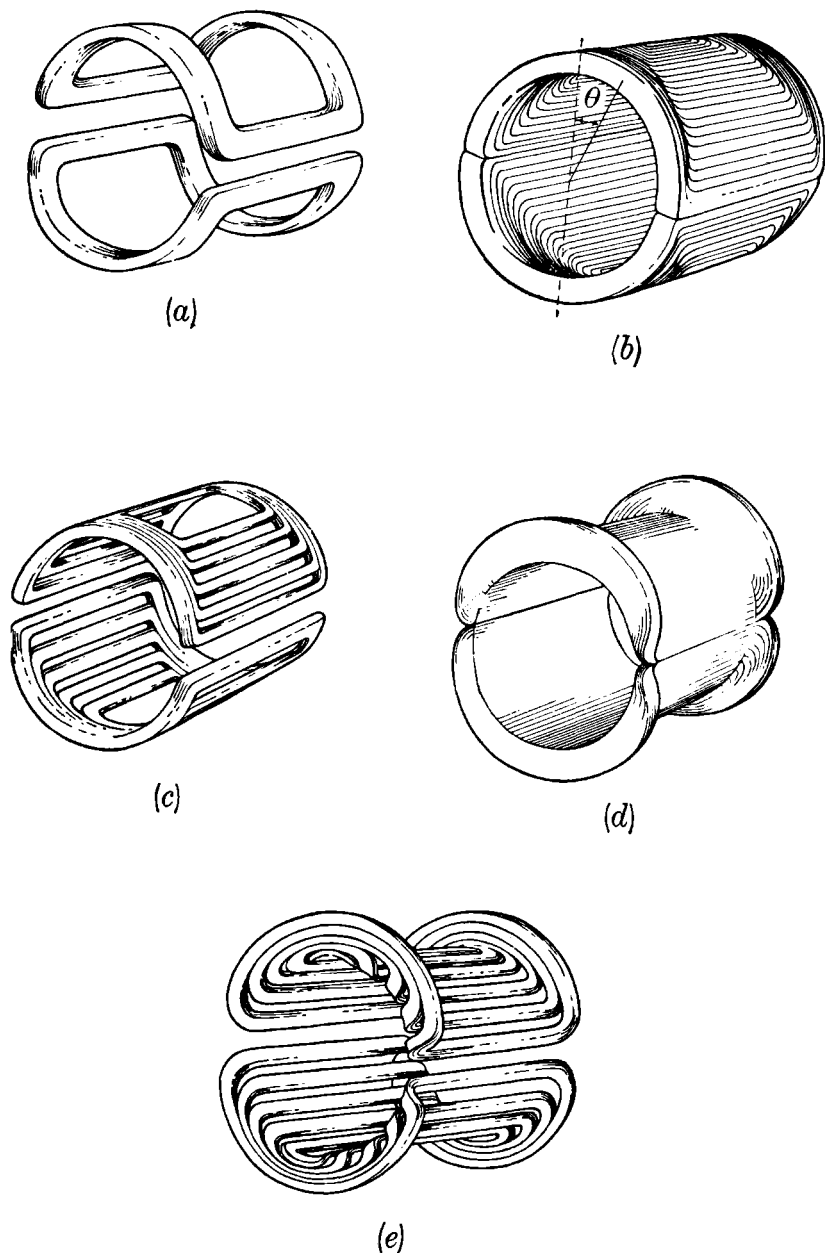
FIG. 8·26.—Types of air-core coils.  (a) Lumped winding.  (b) Distributed winding. (c) Semidistributed winding.  (d) Distributed winding with bent-up ends.  (e) Semidistributed winding with bent-up ends.

The magnetic field generated by a coil with lumped windings is illustrated in Fig. 8·27. This field distribution, particularly the fringing fields, applies not only to a lumped winding but to all air-core coils in general. The fringing field of an air-core coil is entirely different from that of the iron-core coil described in the previous sections because the return flux passes down around the coil ends and is directed opposite to the main deflecting field. Interference between the main field and the
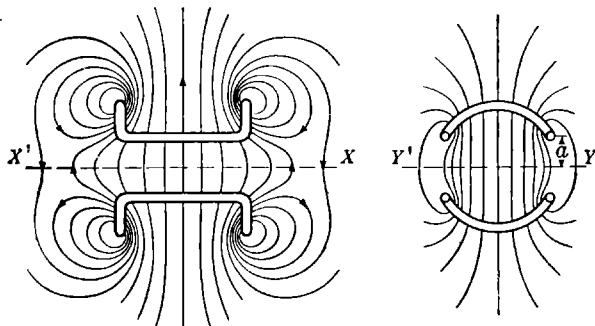


FIG. 8·27.—Magnetic field about an air-core coil with lumped windings.

fringing field creates a null at both ends of the coil, thus sharply terminating the main field.

The variation of field intensity along the coil axis marked $XX'$ in Fig. 8·27 is shown in Fig. 8·28. This curve clearly shows the position of the nulls and also shows the relative magnitudes of the main deflecting field and the reverse fringing fields. Because the fringing fields are reversed with respect to the main deflecting field, the electron beam follows an S-curve as it passes through the coil. When an air-core coil is used alone, the serpentine deflection is very slight since the integral of the reverse field along the axis is less than 10 per cent of the main field. A small amount of reverse field does not interfere with the deflection pattern on the screen of the cathode-ray tube, nor does it cause any noticeable defocusing of the beam, but large amounts produce characteristic distortions.



FIG. 8·28.—Axial field distribution of an air-core coil. Ends of the coil are marked by dashed lines.

The uniformity of the magnetic field throughout the central portion of a lumped air-core deflection coil is governed to some extent by the spacing of the two half sections. Because the sides of the coil are straight and parallel, the field in the central portion is similar to the field between

four long parallel wires. This field will be most uniform if the wires are spaced on the surface of a cylinder of radius $C$ such that the distance marked $a$ in Fig. 8·27 is $\frac{1}{2}C$. The field in the central portion of a lumped deflection coil will also be most uniform if the two half sections are so spaced. Even with this adjustment, the main deflecting field is not completely uniform since it is impossible to generate a uniform field except with distributed windings. Consequently, a coil with lumped windings always contributes to the defocusing of the electron beam. (See Sec. 8·9.)

**8·21. Distributed Windings.**—A deflection coil of the type shown in Fig. 8·26b will generate a very nearly uniform field in its interior if the windings are properly distributed.
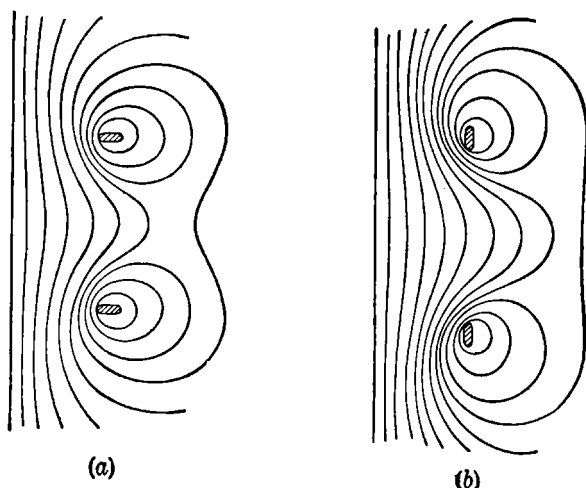


FIG. 8·29.—Field patterns about one end of an air-core deflection coil, showing the effect of bent-up ends. (a) Coil with flat ends. (b) Coil with bent-up ends.

If any surface is built up of plane loops of wire carrying the same current $I$, arranged parallel to each other and spaced so that the number of loops per unit length along the normal to the planes of the loops is constant, the magnetic field inside this surface will be uniform if the surface is of the second degree.[1] An ellipsoid of revolution may be chosen as the surface because the deflection coil is similar to the central portion of a very long ellipsoid. The winding distribution on the deflection coil, in order to approximate a uniform field, should be the same as the winding distribution in the central portion of the ellipsoid.

The winding distribution of a deflection coil can be more conveniently

[1] E. Mascart and J. Joubert, *Leçons sur l'Electricité et le Magnétisme*, Vol. I, Masson, Paris, 1882, 1896, p. 545.

expressed in terms of the angular position of the loops. If the number of turns per degree at the circumference of the circular cross section is made proportional to the sine of the vertical angle (Fig. 8·26b), then the winding distribution will be exactly as described above. Such a distribution of turns will be referred to as a sine distribution.

Although the ends of the coil interfere to some extent with the uniformity of the internal field, their effect can be minimized by binding them up at right angles as in Fig. 8·26d. This construction carries the strongly curving fields farther away from the coil axis and consequently improves the performance of the coil with respect to defocusing the electron beam. Field patterns about the ends of two deflection coils that are identical except that one has its ends bent up are shown in Fig. 8·29. These figures indicate the extent to which the fringing field can be modified by a simple change. It should be noticed that bending up the coil ends moves the position of the null farther out along the axis and thus broadens the main deflecting field.

If the windings of a distributed coil are gathered into four or five separate hanks as in Figs. 8·26c or 8·26e no significant change will take place in its magnetic field; the construction,[1] however, is tremendously simplified by such an arrangement.

**8·22. Coils with an Iron Return Path.**—The deflection efficiency of an air-core coil may be improved considerably by placing a cylindrical, closely fitting, laminated iron shell around the outside of the coil. This shell provides a low reluctance path for the flux passing around the outside, and thereby increases the ratio of the energy of the magnetic field inside the coil to the energy outside. Although surrounding the coil by an iron shell increases its inductance, the gain in deflection efficiency allows a reduction in the number of turns on the coil so that the inductance may be brought back to its original value.

An iron return path does not affect the magnetic-field distribution inside the deflection coil, but it does change considerably the fringing fields around the ends. The reverse field is eliminated for all practical purposes and the strongly curving fields at the coil ends are withdrawn from the axis as well as reduced in magnitude. These changes all improve the deflection-coil performance with respect to defocusing the electron beam.

**8·23. Compound Coils.**—Both horizontal and vertical deflection may be provided by one unit if two air-core coils are mounted concentrically and oriented at 90° to each other. This assembly may be equipped with an iron shell to secure the benefits of an iron return path. Such a compound coil is illustrated in Fig. 8·30.

[1] The technique of constructing such a coil is given in Appendix B·2.

A deflection coil of this type has several features that make it superior
to most other deflection coils and particularly suited to television.    It has
a deflection efficiency of approximately 40 per cent, which is slightly
better than the efficiency of a square iron-core coil without a copper
shield.    In addition, because of its concentric construction, it can be
adjusted to minimize or even eliminate the magnetic interaction between
the horizontal and vertical coils.    As in the case of iron-core coils, any
inductive coupling between the horizontal and vertical coils will give
rise to transient oscillations that result in a wiggly sweep.    Concentric
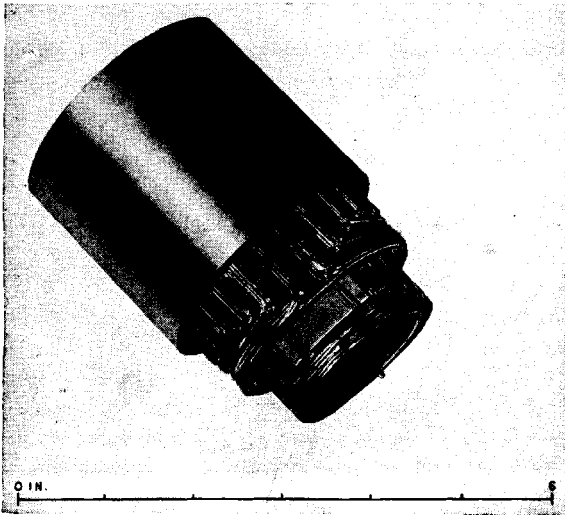


FIG. 8·30.—Compound deflection coil, extended to show construction.

construction allows one coil to be rotated within the other so that any
inductive coupling can be canceled.    If the coils are well made, the can-
cellation is very sharp and the null occurs when the coils are oriented
at exactly 90°.    A displacement from the 90° position by as little as
1/10° may be easily detected.

Even if all inductive coupling between the two coils is balanced out,
there still may exist an interaction due to capacitive coupling.    This
interaction is not serious at low sweep speeds but it becomes increasingly
important as the sweep speed increases.    When the sweep duration is
approximately 10 $\mu$sec, wiggles again become noticeable.    The operating
range of the coil may be extended if an electrostatic shield is placed
between the two windings.    This shield must be designed so that it will
not support eddy currents that would lessen the deflection sensitivity of
the coil.    It may be constructed by close-winding with a small-gauge

enameled wire a single-layer solenoid on a cylindrical form whose diameter equals the outside diameter of the inner coil. The length of the solenoid should equal the length of the coil. After this solenoid has been varnished to hold it together it may be split along its length, creating a sheet of parallel insulated wires that can easily be lifted from the form. A connecting lead may be soldered along one side of the cut, thereby joining all of the wires together at one end to complete the shield.

With its iron shell providing a return path for the flux, the compound air-core coil preserves the focus of an electron beam far better than any of the other coil types mentioned. It is possible to maintain good focus when the electron beam is deflected because of the uniformity of the main deflecting field and because the fringing fields are minimized by the iron return path. Although the quality of the coil depends to a large extent upon the care used in its construction, the defocusing for a reasonably good coil is so slight that the diameter of the illuminated spot is only 1 or 2 per cent greater at the edge of the tube screen than at the center. The corresponding increase for other coils is about 50 per cent.

Another advantage offered by the air-core design is the possibility of altering the winding distribution to obtain any desired magnetic-field distribution. Any departure from a uniform deflecting field will correspondingly increase the defocusing action, but in some cases it may be desirable to sacrifice focus in order to gain a particular deflection pattern. For instance, Sec. 9·1 deals with the distortions caused by a flat-faced tube, pointing out that a square deflection pattern is distorted into a pincushion pattern. This distortion may be corrected if the deflecting field can be made to increase in strength as the deflection angle increases. Since the winding distribution directly determines the field of an air-core coil, this distribution can be varied to determine experimentally the proper function to correct a given distortion.

Each type of cathode-ray tube will require a deflection coil designed to correct the distortion produced by that particular tube type because the distance from the center of deflection to the screen, together with the radius of curvature of the screen, changes with the tube type. A 7BP7 requires approximately a sine-squared winding distribution to correct for a square pattern whereas a 12DP7 displays a square pattern with a sine distribution. The proper distribution for other types can be judged from these examples.

**8·24. Deflection Coils Wound on Motor-stator Cores.**—The idea of an iron-return path may be extended to include motor stator cores as shown in Fig. 8·31. The slots in the core receive the wires in much the same manner as the slotted form described in Appendix B·2. The deflection efficiency of such a construction is about 20 per cent higher than that of other core types mentioned. A motor-stator coil owes its high efficiency

to the short air gap inside.    The pole pieces may be designed to come very close to the glass wall of the tube neck and therefore a large portion of the magnetic field generated will be concentrated in the region where it is most useful for deflection.    Ordinary motor laminations are not of sufficiently high quality for deflection coils so that special punchings from highgrade silicon steel, Hipersil, or Permalloy are necessary.

Coils may be wound flat between a pair of winding disks and then placed on the core.    Both horizontal and vertical windings may be added to the same core but there is no way completely to balance out the inductive coupling.    However, the windings are oriented by the position of
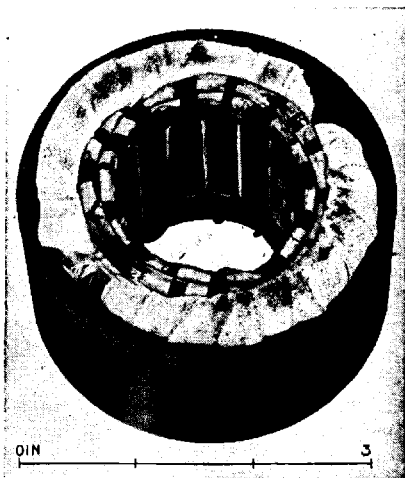


Fig. 8·31.—Motor-stator deflection coil wound for push-pull horizontal and vertical deflection.

the slots so that the inductive coupling is small and is not serious except at the higher sweep speeds.    It is also possible to put push-pull windings on the core, but the problem of finding room for the wire is difficult.

One serious difficulty encountered in motor-stator deflection coils is the large amount of distributed capacitance, which is of the order of millimicrofarads, as compared to the small value of 25 $\mu\mu$f for ordinary air-core coils.    Because the distributed capacitance shunts the deflection coil, most of the input current is bypassed at the beginning of a sweep, causing a slow start.    However, the distributed capacitance can be reduced by using insulation with a low dielectric constant between the wires and the core.    The high efficiency of a motor-stator deflection coil justifies its further development.

# CHAPTER 9

## PATTERN DISTORTIONS ON MAGNETIC CATHODE-RAY TUBES

### By R. D. Rawcliffe

In order to produce a satisfactory pattern on a cathode-ray-tube screen, the deflection coil must be carefully designed and the focus coil must be carefully aligned with the tube. Otherwise, a number of distortions occur, including the following: "pincushion," rhombic, or trapezoidal-shaped patterns; wiggly or bowed sweeps, and sweeps that are split into two lines.

The causes of these distortions fall into several categories:

1. The cathode-ray tube itself tends to produce a pincushion pattern, which can be largely corrected by the proper magnetic-field distribution in the deflection coil.
2. Nonuniformities in the deflecting field also distort the pattern. These nonuniformities may be due either to an improper distribution of the windings and poorly placed magnetic material in the deflection coil, or they may be due to high-frequency effects such as oscillations in the windings, coupling (cross-talk) between different windings, or coupling to metallic parts of the mount near the coil. The former cause distorts the pattern at all sweep speeds but the high-frequency effects become increasingly worse as the sweep speed increases.
3. Distortion may arise from the interaction between the deflecting and focus fields.

**9·1. Distortions Due to the "Flat"-faced Cathode-ray Tube.**—In order to facilitate making measurements on the faces of cathode-ray tubes, these are made as flat as is consistent with the mechanical-strength limitations. The distance from the center of the deflection coil to the screen is then smaller than the radius of curvature of the screen by a factor of between 2 and 5 depending on the tube type.

If these two distances were equal, the deflection distance ($d_1$ in Fig. 9·1) would be proportional to the sine of the deflection angle. It has already been shown in Sec. 8·1 that the magnetic field and hence the current through the deflection coil are also proportional to the sine of the

deflection angle. Therefore, the deflection would be directly proportional to the deflection current. Since horizontal and vertical deflecting fields combine vectorially when both are used, the deflection components would also combine vectorially. Hence the horizontal and vertical components of the resultant deflection would be independent of each other—that is, a change in the vertical deflection would have no effect on the horizontal deflection. Therefore, if the tube were viewed from far enough away so that the spherical screen itself did not cause an appreciable distortion of the image formed by the eye, the pattern seen would be undistorted.

With flat-faced tubes, however, the deflection distance ($d_2$ in Fig. 9·1) is proportional to the tangent, not the sine, of the deflection angle, and

$$d = K \tan \theta = K \frac{\sin \theta}{\sqrt{1 - \sin^2 \theta}} = \frac{aI}{\sqrt{1 - bI^2}} = a(I + cI^3 \cdots),$$

where $d$ is the deflection distance, $K$ is the distance from the center of the deflection coil to the screen, $\theta$ is the deflection angle, $I$ is the deflection current, and $a$, $b$, $c$ are constants. This equation may be rewritten

$$d = d_0 + Ad_0^3 \cdots, \qquad (1)$$

where $d_0$ is the deflection that would occur if it were proportional to the current, and $A$ is a constant. Because of the cubic term the deflection increases somewhat faster than the current. If both horizontal and vertical fields are used, the fields add vectorially as before but the deflection components do not. The two deflec-



FIG. 9·1.—Pattern distortion due to flat-faced cathode-ray tubes: $A$, Spherical face of radius equal to $k$; $B$, plane face; $C$, spherical face of radius equal to $3k$; $d_1 = k \sin \theta$; $d_2 = k \tan \theta$; $k \tan \theta > d_3 > k \sin \theta$.

tion components are no longer independent of each other, and increasing the horizontal deflecting current causes the vertical deflection to increase also. The result is the familiar pincushion distortion shown in Fig. 9·2 in which a straight line, $y = y_0$, a constant, becomes distorted into a parabola $y = y_0[1 + A(x^2 + y^2)]$, where $x$ and $y$ are the two deflection components. A circular pattern with center at the origin remains a circle, but its radius is enlarged from $r = r_0$ to $r = r_0(1 + Ar_0^2)$.

In actual cathode-ray tubes the faces are not perfectly flat but have a rather large radius of curvature. The deflection ($d_3$ in Fig. 9·1) is then proportional to a function whose values lie between the sine and the tangent of the deflection angle. This function can be approximated by

decreasing the constant $A$ in Eq. (1).   This constant is approximately

equal to $\dfrac{\left(1 - \dfrac{K}{\rho}\right)\left(2 - \dfrac{K}{\rho}\right)}{2\left(\dfrac{K}{\rho}\right)^2}$, where $\rho$ is the radius of curvature of the

screen.   Approximate values of $K/\rho$ for various tube types are 0.19
(5FP7), 0.28 (7BP7), and 0.57 (12DP7).   For these values, $A$ becomes
0.024, 0.014, and 0.0023 respectively.
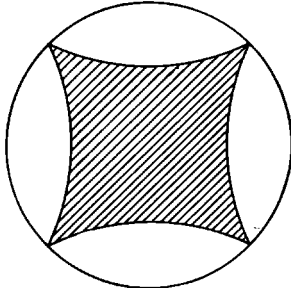


FIG. 9·2.—Typical pincushion distortion produced by flat-faced tube.

If centered radial sweeps (PPI) are used, the distortion caused by flat-faced tubes is of the same sort as that produced by nonlinearity in the driving current, and it can therefore be corrected by making the current properly nonlinear.   If, however, an off-centered radial sweep or a rectangular scan with independent $x$ and $y$ sweeps is used, it is impossible to correct the pattern distortion by adjusting the sweep current waveform.   In such a case the correction is effected by making the deflecting field itself nonuniform in the proper manner.   Although nonuniform deflecting fields tend to defocus the electron beam, the amount of nonuniformity needed is small, and the little defocusing produced is outweighed by the advantage of an undistorted pattern.   The deflection pattern produced by a deflection coil is associated with the distribution of its mag-



(a)                                      (b)
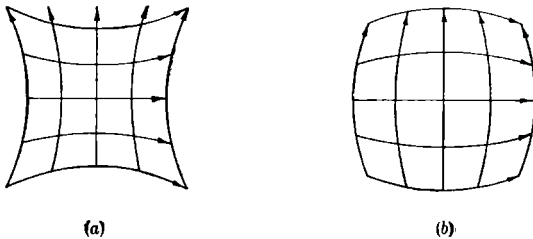
FIG. 9·3.—Pincushion and barrel field distributions.   (a) Pincushion.   (b) Barrel.

netic field.   This distribution is measured in a plane passing through the coil center and perpendicular to its axis.   A pincushion-shaped field distribution tends to correct the distortion produced by a flat-faced tube, and a "barrel-shaped" distribution has the opposite effect.

The action of the field in controlling the pattern shape is illustrated in Fig. 9·3.   In both field distributions shown, an electron beam entering the paper would be deflected toward the upper left corner.   Since the two

fields in Fig. 9·3a make an oblique angle in the region into which the electron is deflected, their vector sum is less than it would be if the fields were perpendicular to each other.    Hence the electron will be deflected •
less in the case illustrated in Fig. 9·3a than in the case of a uniform rectangular field.    In the case of a barrel-shaped field, illustrated in Fig. 9·3b, the two fields make an acute angle in the region into which the electron is deflected, and consequently this field shape deflects the electron more in this region than in the case of the uniform rectangular field.

In addition, if one component of the pincushion field (for example, the horizontal component) becomes equal to zero at some time, the electron beam will be deflected to the left along the center line into a region of greater field strength, and its deflection will be greater than it would have been in the case of a uniform field.    The net result of a pincushion field on a nominally square pattern is that the centers of the sides are pushed out at the same time that the corners are pulled in.    The reverse is true for the barrel field.

Although it might be expected that pattern correction by means of a nonuniform deflecting field would distort circles into squares, experiment shows that with the amount of correction needed for standard tubes the distortion of the circles is very small.

With a square iron-core coil the amount of correction is very simply controlled by the length of the windings on the legs of the core.    If the windings extend over the full length of the legs, the field will be nearly uniform in the cross section through the center of the coil.    As the winding length is shortened, the field becomes more and more pincushioned. Measurements of the amount of distortion for various winding lengths are shown in Fig. 9·4.    The distortion plotted is the maximum deviation from a straight line of one side of a "square" pattern as projected on a plane perpendicular to the axis of the tube.    The lengths of the sides of the squares are 3 in. for the 5FP7, $4\frac{1}{4}$ in. for the 7BP7, and 7 in. for the 12DP7.    These lengths correspond approximately to the largest usable square area on each tube.    The coils were assembled on a core with a $2\frac{1}{8}$-in. inside window and a $1\frac{1}{2}$-in. stack height.

Thus far in the discussion, it has been assumed that the axial field is uniform along the length of the coil, and zero elsewhere.    Actually the fringing fields are important, and they cause the cross-sectional fields near the front and rear of the coil to be more pincushion than the field in the center.    In some cases, as illustrated for the 12DP7 in Fig. 9·4, the field behaves as if it were pincushion even when the longest possible winding is used.    In practice it is not possible to wind the full length of the core because the windings on adjacent legs interfere at the corners, and hence a simple layer-wound coil will not correct the pattern on a 12DP7.

Approximately the same effect as lengthening the winding can be

obtained, however, by omitting a section of the winding from the center
of the leg.    The winding then consists of two separate sections.    A better
coil can be obtained with the pie-sectional construction shown in Appen-
dix B.    Different numbers of turns are then used in the various sections
to obtain the proper pattern correction.    With the coil dimensions shown
in Fig. B·3, lines are straight if viewed from a point directly in front of
the line.    If the whole pattern were viewed from a point on the axis of
the tube at the normal viewing distance from the screen, the lines would
still show an outward bowing because of the curvature of the screen.
Correction of this bowing would require a large change in winding dis-
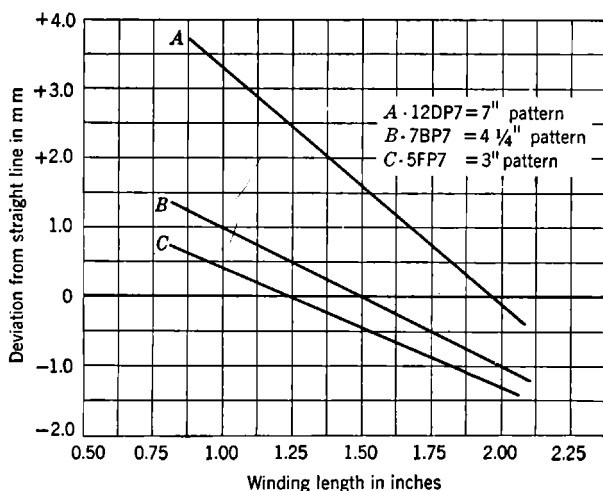


FIG. 9·4.—Pattern distortion plotted against winding length on a square iron-core
deflection coil.

tribution, with perhaps some sections in the center wound in the reverse
direction, and would therefore probably result in considerable deteriora-
tion of the focus.

For a 7BP7, a uniform distribution of turns in the pie-section form
gives a corrected pattern.

Although the curves of Fig. 9·4 cannot be converted to other core
sizes by a simple scaling process, they can be used as a rough guide, so
that the proper distribution may be obtained after a few trials.

**9·2. Precentering.**—If a nonuniform deflecting field is used to correct
for pattern distortion, it is essential that the undeflected electron beam
pass down the central axis of this field.    Otherwise, the pattern will be
overcorrected on one side and undercorrected on the other.    Because the
electron guns are not always perfectly aligned, however, the electron
beam may not always initially be directed toward the center of the screen.

On a type 12DP7 tube, for instance, the beam may hit anywhere within a 2-in. diameter circle about the center of the screen.   Therefore, if it is assumed that the focus coil does not deflect the beam axis, the beam may enter the deflecting field approximately $\frac{3}{16}$ in. from its center.

A simple device for correcting for the misalignment of an electron gun is illustrated in Fig. 9·5.[1]   The small circular magnet $A$ is magnetized to give a transverse field similar to that of a deflection coil.   It is mounted on a cylindrical brass support $E$ on which it can be rotated to adjust the
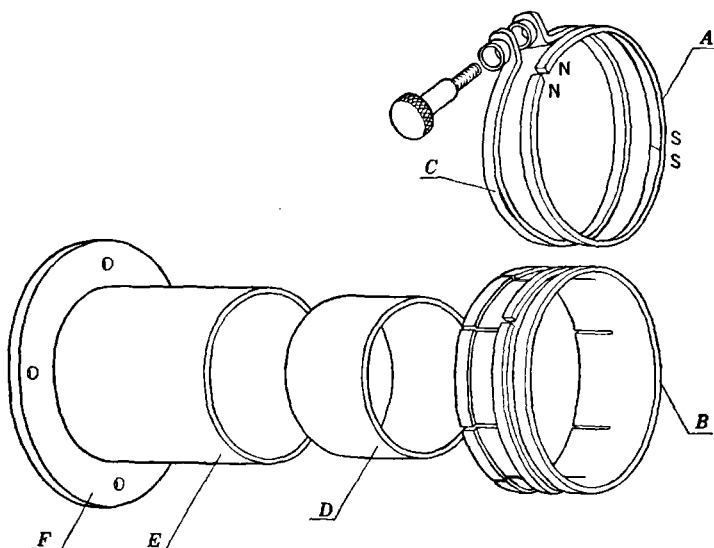


FIG. 9·5.—Precentering assembly.   $A$, the magnet—GE "Cunife" alloy 0.120 × 0.050 strip, rolled into 2-in. ID circle; $B$, brass ring; $C$, brass clamping ring; $D$, soft iron shunt to be soldered into rear end of supporting cylinder; $E$, brass supporting cylinder; $F$, mounting flange.

direction of its field.   It also can be moved parallel to the axis of the supporting cylinder.   Inside the rear half of this cylinder is a soft iron shunt $D$.   If the magnet is located over this shunt, practically no field reaches the interior of the tube.   Hence the position of the magnet controls the field strength.

The precentering assembly is mounted over the cathode-ray tube so that its field passes through the tube just ahead of the electron gun. The direction of the electron beam as it leaves the gun can thus be adjusted at will, thereby correcting for gun misalignments.   If the electron beam starts a small distance from the tube axis, the precentering field can deflect it back toward the axis.   The beam, as it enters the

[1] R. B. Gethman, General Electric Co., personal communication.

focus field, then, is heading toward the axis and is probably never more than $\frac{1}{32}$ in. from it.    If, by some such means as that described in Sec. 3·6 and Fig. 3·15, the focus coil can be adjusted so that the axis of its field coincides with that of the electron beam, then the focus field will cause no deflection of the electron beam, and the beam will still be approximately in coincidence with the tube axis when it enters the deflection coil.    If the deflection coil is centered on the tube, as it easily can be, the deflecting field nonuniformities are symmetrical about the beam, and pattern corrections may then be applied to optimum advantage.

Another significant advantage that arises from the use of precentering is the possibility of employing longer deflection coils.    It was shown in Sec. 8·2 that the axial length of a deflection coil is limited by "neck shadow," which occurs because the electrons are deflected too soon by a long coil, and they therefore cannot be deflected to the edge of the screen without hitting the tube neck.    If the electron beam entering the deflecting field is displaced from the tube axis, then, when the beam is deflected in the same direction as this displacement, neck shadow occurs earlier than it would if the beam were coincident with the tube axis.    However, if the beam is precentered so as to enter the deflecting field along the tube axis, neck shadow occurs symmetrically and a longer coil can be used before the shadow appears.    The energy saving resulting from the use of the longer coil may amount to 20 per cent.

**9·3. Pattern Rotation Due to Focus–deflection Interaction.**—A rotation of the whole pattern on the screen can arise from an interaction of the focus and deflecting fields.    The deflection of the electron beam then starts before the focusing is complete, and the electrons are given a radial component of velocity.    The axial component of the focus field then causes the electrons to spiral through a small angle around the axis. Fortunately this angle is very nearly independent of the deflection distance—that is, a straight sweep remains a straight sweep, and the pattern as a whole is merely rotated through an angle without much distortion. The deflection coil is mounted in such a way that it may be rotated through the same angle but in the reverse direction to bring the pattern back to its original position.    The amount of rotation varies with the focus-field strength; hence it varies by a small amount as the focus field is adjusted.    Therefore, the position of the deflection coil should be determined after the focus has been attained.

The magnitude of the pattern rotation depends on the distributions of the focus and deflecting fields and also on the amount by which the two overlap.    If a focus coil such as that shown in Fig. A·1 and a square iron-core deflection coil are used in their customary positions (Fig. 16·3) on a tube such as the type 7BP7, the pattern rotation is about 12°.    Because the coils are usually mounted considerably further apart on the type

12DP7 tube, the rotation with this tube is considerably smaller. The rotation is also somewhat smaller with an air-core deflection coil because of its different field distribution. If a focus magnet such as that shown in Fig. 3·17 is used, the rotation is approximately equal to that produced by a coil; whereas, if a shielded magnet (Fig. 3·20) is used, the rotation is only approximately one degree. Because the rotation reverses when the focus field is reversed, a simple method of determining the angle of rotation is to measure the change in the direction of the sweep (twice the rotation angle) when the current through the focus coil is reversed. Determination of this angle with a focus magnet is much more difficult because the field cannot be reversed. The magnet must be removed from the tube without disturbing the deflection-coil alignment. The angular position of the unfocused sweep can then be roughly measured and compared with the position of the focused sweep.

The pattern rotation is not in itself a pattern distortion because it can be compensated by adjusting the deflection coil. However, if the rotation is affected by the magnitude of the deflection, by the sweep speed, or by the direction of the sweep, definite pattern distortions arise, which can frequently be traced to this focus-deflection interaction. The effects are complicated and not too well understood, and similar effects can be produced by distortions of the deflecting field itself. In the next sections two of these effects, "jump" and "line splitting," will be discussed as they both arise from focus-deflection interactions and deflecting-field distortions. Variations in the rotation with the magnitude of the deflection would cause the sweep to be curved rather than straight.[1]

**9·4. Jump.**—Jump is measured by the change in sweep direction with sweep speed. Factors causing jump are of universal occurrence but fortunately they frequently cause no trouble because they tend to cancel. The residual amount of jump can be as much as 5°, although this value is exceptional. The jump must be very nearly eliminated if the bearing readings on a PPI pattern are to be accurate to 1° or even less. The toroidal PPI coil described in Sec. 8·18 has caused a great deal of trouble because of the difficulty of reducing the jump below 1°.

Both types of jump frequently exist simultaneously, but they can easily be distinguished because reversing the focus field reverses the focus-deflection interaction but does not affect the deflecting-field distortions. From the change in magnitude and sign of the jump when the focus field is reversed, the relative magnitude of the two general types of jump can be roughly determined.

The simplest type of jump arises from the use between the deflection and focus coils of a shield made of nonmagnetic material such as copper.

---

[1] This is probably a contributing factor to the errors in the off-center PPI pattern discussed under Sec. 12·5.

The effectiveness of this shield increases with frequency and, therefore, the faster the sweep the more effective is this shield in preventing the deflecting field from penetrating the focus field.   As it is this interpenetration that causes the pattern rotation, faster sweeps are rotated through a smaller angle than are slow ones.    If the nonmagnetic shield is replaced by iron, the jump is in the opposite direction—that is, slower sweeps are rotated through the smaller angle.    This effect is probably produced by a combination of magnetic and eddy-current shielding with hysteresis effects playing an important role.    If both iron and copper shielding are placed between the coils, the two shields produce jumps in opposite directions which tend to counteract each other.    In practice, iron-core deflection coils are enclosed in cases of copper or aluminum, whereas the focus coils are enclosed in iron.    Therefore, both types of shielding are present between the coils.    The magnitude of the resultant jump depends on the position of the shielding—that is, the separation of the two coils.    Experiments show that if the cases are of the types shown in Fig. 16·3 the two effects balance and there is no jump when the two coils are about 0.3 in. apart.

Although the shielded focus magnet of Fig. 3·20 causes a pattern rotation of only about 1°, a jump of over 2° is often produced; whereas the unshielded magnet of Fig. 3·17, which causes about 12° of pattern rotation, produces only a few tenths of a degree of jump.    This difference is due to the characteristic field distribution (Fig. 3·21) of the focus magnet.    This field has three sections.    It is positive in one of these sections and negative in the other two.    The net rotation of the pattern is the algebraic sum of the three rotations in the individual sections. The region of deflection is toward the left in Fig. 3·21.    Because the deflecting field is cut off rather sharply at the front of the focus magnet (indicated by the tick-mark) by the shielding action of the iron, the focus field to the right of the tick-mark has little effect on the pattern rotation. The positive and negative contributions of the focus field to the left of the tick-mark are essentially balanced in the case of the shielded magnet $A$, and therefore a very small pattern rotation results.    Since they are unequal in the case of the unshielded magnet $B$, the pattern rotation will be considerably greater.    Jump occurs as a result of changes in the distribution of the deflecting field with change in sweep speed.    These changes are due to the shielding action of the front face of the focus magnet, which alters the field distribution in its vicinity.    In this region the average field strength of the magnet's field is considerably less when the shield is not used, and consequently the jump observed will be less in this case.

Jump arising in the deflecting field itself is probably due entirely to asymmetrical shielding about the coil.   A toroidal coil, for instance, is

customarily mounted in a cylindrical copper or aluminum case. If the coil is not accurately centered in this case, the shielding will be asymmetrical. The effective inductance of the section of the coil more tightly coupled to the case will be lower than that of other sections. Current will therefore tend to build up faster in that section, and a change in sweep direction will result. Because this shielding effect varies with frequency, the change in sweep direction depends on sweep speed, i.e., the sweep jumps.

Asymmetrical shielding whether due to copper or iron is likely to cause other undesirable effects such as crooked sweeps and distortion of the rectangular scan. Hence it is important to reduce asymmetries to a minimum.

**9·5. Line Splitting.**—If an alternating current is passed through a deflection coil the resulting sweep should be a straight line, the forward



Field enters here

Normal rotation

S

N

Field emerges here    *(a)*                    *(b)*                    *(c)*    Unrotated sweep direction
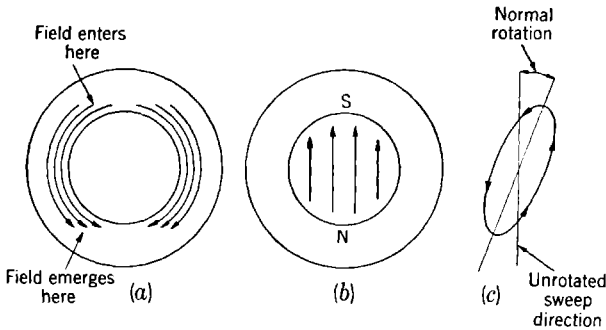
Fig. 9·6.—Line splitting as caused by hysteresis effects in the focus-coil case.

sweep being accurately superimposed on the return sweep. Frequently these two traces are separated so that the straight line is distorted into an approximately elliptical figure. Even if the return sweep is blanked out, the remaining sweep appears as an elliptical arc. Under normal circumstances the minor axis of this ellipse is not more than about 3 per cent of the major axis, but it is easily possible to produce ellipses that are nearly circles. Line splitting is caused by a number of factors including unbalance in the windings of the deflection coils, asymmetrical shielding around the deflection coil, and hysteresis and eddy-current effects in the focus-coil case. A few of the factors of this complicated problem which can be isolated are presented here.

The pattern rotation due to the overlapping of the focus and deflecting fields is the underlying cause of line splitting. Figure 9·6a shows the general contours of the field set up in the front face of the focus-coil case by the deflection coil. The field remaining after the deflecting field has been removed is shown in Fig. 9·6b. This residual field is in the direction

opposite to that of the field that caused it.    Consequently, as the deflecting field decreases from its maximum value, it is further weakened in the vicinity of the focus coil by the residual field of the case, and the rotation of the sweep is therefore reduced.    As the deflecting field reaches zero and increases in the opposite direction, the residual field aids the deflecting field so that the rotation is now larger than normal.    In a complete cycle the pattern shown in Fig. 9·6c is obtained.    Because hysteresis is independent of frequency, at least for reasonably low frequencies, this splitting also should be independent of frequency.

If the iron of the focus-coil case is replaced by a piece of copper or other nonmagnetic material, line splitting occurs in almost the same manner,
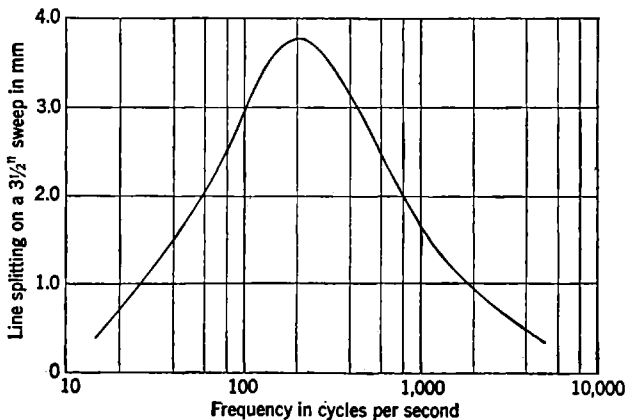


Fig. 9·7.—Line splitting vs. frequency, for uncased focus and deflection coils separated by 0.15 in., with a copper shield between coils.

but is due to eddy currents that act to maintain the existing flux within the metal.    If the sweep frequency is low the eddy currents are too small to cause an appreciable splitting.    If the frequency is high the shielding action of the metal is so complete that only a small amount of the deflecting field gets beyond the metal to interact with the focus field, and once again the line splitting is small.    At intermediate frequencies of the same order of magnitude as the reciprocal of the time constant of the metal, however, the eddy currents lag about 90° behind the impressed field and cause a maximum amount of splitting.

Measurements of line splitting due to a $\frac{1}{16}$-in.-thick copper washer between the deflection and focus coils follow the general behavior shown in Fig. 9·7.    The splitting measured in this figure was the maximum separation of the two sides of the ellipse, i.e., its minor axis.    The deflection coil used was a square iron-core coil with windings on only two of the legs.    No cases were used on the coils nor was there any other shielding in

the neighborhood. The deflection coil was driven by a variable-frequency oscillator whose output voltage was adjusted to maintain a $3\frac{1}{2}$-in. sweep on a 5FP7 tube. The maximum splitting occurs at about 200 cps. It is interesting to note that copper deflection-coil shield
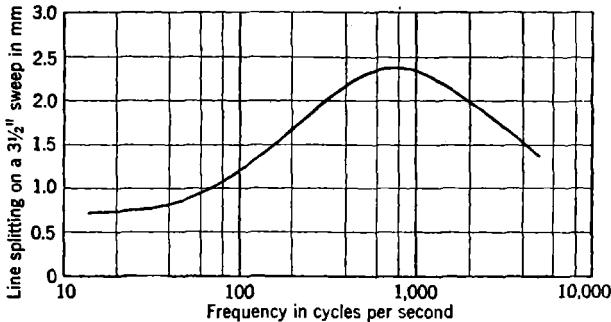


FIG. 9·8.—Line splitting vs. frequency with an iron case around the focus coil, and 0.15 in. between coils.

cases have a time constant for the decay of eddy currents of about $\frac{1}{200}$ sec.

A similar curve illustrating the line splitting obtained with an iron case around the focus coil instead of the copper washer between the coils is shown in Fig. 9·8, the splitting being due to a combination of eddy currents and hysteresis. At low frequencies the amount of line splitting is about 0.75 mm. This amount of splitting is caused by hysteresis, upon which is superimposed the line splitting caused by eddy currents. The frequency of maximum splitting is higher for iron than for copper by a factor of about 4, which is roughly the ratio of the resistivities of iron and copper.

The magnitude of the splitting also falls off as the distance between the coils is increased as shown in Fig. 9·9 in which the splitting at 1000 cps is plotted for various positions of an iron-cased focus coil. If the splitting were plotted against the distance between the centers of the gap and the deflection coil, the curve would very nearly follow an inverse square law.



FIG. 9·9.—Line splitting for various focus-coil positions.

A second simple type of line splitting arises from cross coupling

between the horizontal and vertical windings on the deflection coil. If this coupling is not balanced out, a net voltage is induced in one set of windings from the current in the other. If a reasonably low impedance path exists for current flow, this voltage causes a current that has in-phase and out-of-phase components to flow in the winding. The in-phase component causes a rotation of the sweep line—i.e., the sweep jumps —whereas the out-of-phase component causes a splitting of the sweep line into an ellipse. These effects are shown in Fig. 9·10 for a badly misaligned deflection coil. Measured values of line splitting are shown as triangles near the calculated curve $A$. The circles are measured values
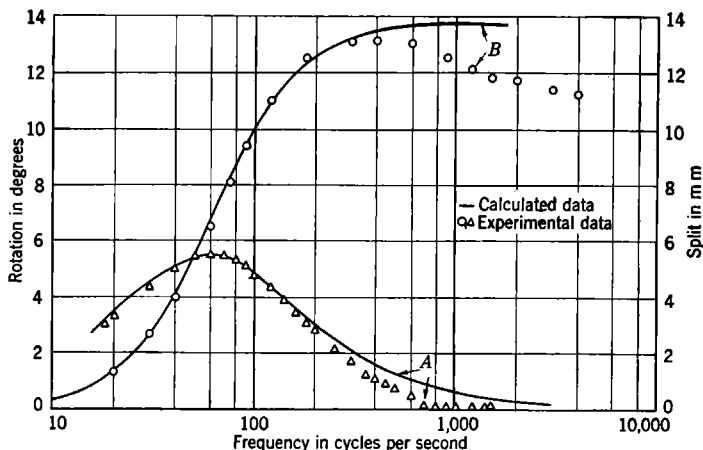


Fig. 9·10.—Line splitting and rotation due to coupling between the two sets of windings on a square iron-core deflection coil plotted against frequency. Curve $A$, line splitting. Curve $B$, sweep-line rotation.

of the rotation of the sweep line whose calculated values are shown in curve $B$. A voltage applied to one pair of windings from a variable-frequency oscillator was adjusted as before to maintain a $3\frac{1}{2}$-in. sweep on a type 5FP7 tube. The other pair of windings was short-circuited. Splitting due to the focus coil was eliminated by removing its case. In the calculation it was assumed that the distributed capacity in the short-circuited winding had a negligible effect. Both calculated curves were adjusted in amplitude to match the experimental curves. The frequency for maximum splitting in the calculated curves was set at 60 cps to coincide with the measured peak. This is also the frequency for a rotation of half the maximum amount. The calculated curves depart from the measured points at the higher frequencies, at which the distributed capacity becomes important.

Since the misalignment of the windings of the deflection coil used in

these measurements was much more severe than that normally encountered, the splitting and rotation are larger than might be expected from this cause alone.   However, coils can be unbalanced by other factors as well.   One such factor is the joints in the core when L-shaped laminations are used.   The fields produced by the two sets of windings are not perpendicular to each other because of the air gaps introduced in the magnetic circuit by the joints; hence, coupling between the windings can cause a certain amount of splitting.   Other effects of these joints are discussed in more detail in the next section.   Unsymmetrical shielding can also produce a large amount of splitting.   A piece of iron, for instance, if properly placed along one corner of the core, can produce a splitting so severe that the ellipse approaches a circle.   A similarly placed piece of copper also produces a splitting but of considerably smaller magnitude.

Line splitting in itself is not often a serious distortion.   However, the unbalance that causes the worst splitting is also an important cause of other more serious types of distortion.

**9·6. Other Distortions Due to Asymmetries in Iron-core Coils.**—In addition to the line splitting and jump described in the previous sections, other distortions due to asymmetries in the deflection coil take on two general aspects: (1) that in which a square pattern or "raster" is distorted into a figure resembling a rhombus, trapezoid, or some other sort of irregular quadrilateral, and (2) that in which the sweep lines are crooked. If the sweeps are very slow, the line will usually be straight, except perhaps for a gentle bowing such as might be due to the flat-faced tube, but the raster as a whole may be badly distorted.   As the sweep speed is increased, the raster distortion is usually not much affected, but the sweep lines themselves develop irregularities, known colloquially as "wiggle," "hook," or "dog leg," which are caused by oscillations in the individual windings or cross-talk between windings.   The raster distortion is usually relatively simple to understand, although it is not always easy to rectify, whereas the oscillations that can occur in a deflection coil are often complex, and they become more and more difficult to deal with as the sweep speed increases.

One of the more troublesome asymmetries to correct is that caused by the method of stacking square iron cores.   These cores are customarily stacked of L-shaped laminations in such a way that lap joints are formed at two diagonally opposite corners and the iron pieces at the other two corners are continuous.   At each of these joints there is inherently a gap in the magnetic laminations whereas there is no such gap at the other two corners.   The effect of this asymmetrical reluctance is to rotate the deflecting field through an angle of about one degree toward the diagonal joining the two joints.   Because both the horizontal and vertical fields are rotated in this manner, they are no longer perpendicular but are

approximately 88° apart. A square raster is distorted into a rhombus by this rotation. The rhombus diagonal that is parallel to the line joining the joints in the core is about 2 per cent shorter than the other diagonal.

Although the core would be symmetrical if I-shaped laminations stacked to give a lap joint at each corner were used, it would not then be mechanically rigid because there would be four joints instead of two, and it could itself be squeezed into a rhombus. It is so difficult to maintain the squareness of the core when it is made of I-shaped laminations that it is not feasible to construct cores in this manner.

A second scheme[1] for eliminating this distortion consists of stacking the L-shaped laminations in such a way as to distribute the joints, "half" a joint occurring at each corner. In order to do this, the laminations are assembled within two windings that are to be opposite each other in the finished coil. Into each of these windings short legs of the laminations are pushed alternately from the opposite sides of the winding so that each section when completed is U-shaped. The other two windings are next placed over the two bare legs on one of the U's and the two U's are then pushed together to complete the assembly. In this final operation it is necessary that the laminations of the two U's be interleaved simultaneously on both sides. Because the loose ends of these laminations do not interleave easily, and because the laminations on one U are nearly covered by windings, this final assembly is extremely tedious.

A third method of correcting this distortion consists of punching the L-shaped laminations with the two legs at an angle somewhat greater than 90°. The square core itself then becomes rhombic by a small, accurately controlled amount. This shaped coil causes distortion of the fields in a direction opposite to that produced by the joints, and the joint distortion can therefore be balanced out by properly designing the lamination. The angle between the legs is determined by the effective air gap at the joints—that is, by the amount of insulating material on the laminations.

Because the positions of the windings on the legs of the core have an analogous effect on the pattern, the distortion introduced by the joints in the core could be corrected by off-centering the windings by the proper amount. Unfortunately the required displacement is larger than is acceptable as the windings interfere with each other in the corners; hence this simple correction method is ruled out.

Accurate winding alignment is important in maintaining pattern precision. In order to illustrate the effects of misalignments in the windings, the windings on a coil were purposely displaced, and the resulting distortions were photographed. In Fig. 9·11 the displacements

[1] R. B. Gethman, GE, private communication.

of the windings together with the resultant field distributions are indicated in the sketches (1) at the left.   In the first set of photographs (2), distortion produced in a rectangular scan is shown.   To obtain these patterns, a 60-cps current was passed through one set of windings on the coil while a 400-cps current was passed through the other.   The second set of photographs (3) shows, by the amount of line splitting present the relative amounts of coupling between the windings in each case.   A 60-
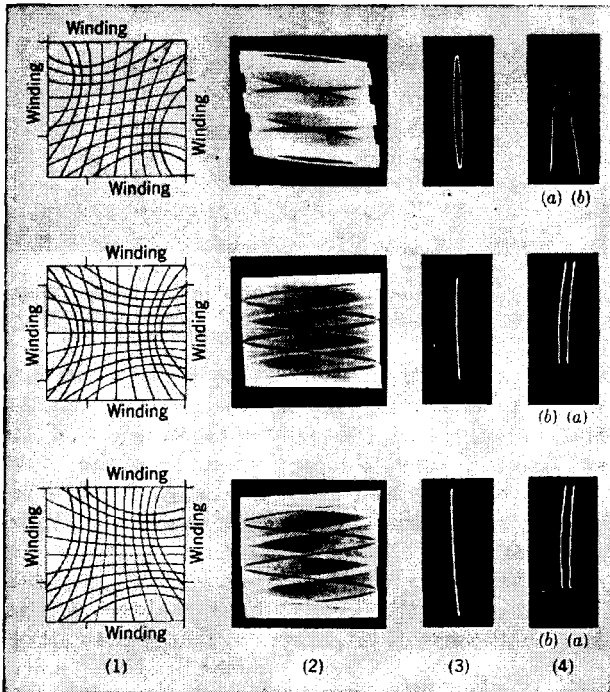


FIG. 9·11.—Distortion in sweep and pattern produced by misplaced windings.

cps current was passed through one winding while the other winding was short-circuited.   The third set of photographs (4) was obtained with a fast sweep (30 μsec) applied to one winding while the other winding was either open-circuited (a), or short-circuited (b).   The crookedness of these sweeps is accentuated, but they are typical examples of sweeps frequently produced by inaccurately wound coils.

The coil used to obtain the pictures shown in Fig. 9·11 had a single winding on each of the four legs of the core.   When two windings are used on each leg, another type of distortion sometimes occurs (Fig. 9·12a) in which the sweep oscillates and the peak of each oscillation is out of

focus.     This distortion is caused by oscillations in segments of the second set of windings.     This type of oscillation can often be reduced by changing the interconnections between windings within the coil, the best connections being found by experiment.

A somewhat similar oscillation (Fig. 9·12b) frequently occurs in the sweep produced by a toroidal coil (see Sec. 8·18).     In this case the defocusing does not occur.     The remedy again is accurate winding.



(a)                    (b)                                        (c)

FIG. 9·12.—Typical sweep distortions.     (a) Defocusing and curvature due to sectional oscillation of the deflection coil.     (b) Curvature produced by oscillations in a toroidal deflection coil.     (c) Sweeps showing effect of insufficient recovery time.

**9·7. Distortions in the Start of the Sweep.**—The sweep should start smoothly from a given starting position—that is, from a given base line in a rectangular scan, or from the center of the tube in a PPI.

Sufficient time must be allowed for the recovery of the deflection coil. To minimize the recovery time the coil is usually critically damped (see Sec. 8·8) so that the current in the coil dies down exponentially after the sweep is terminated.     No matter how accurately the coil is constructed, oscillations in the windings or segments of the windings cause a "hook" in the start of the sweep if the allowed recovery time is too short.     Then the current has not decayed to zero by the start of the next sweep and the sweep does not start from the designated point.     These effects are illustrated in Fig. 9·12c, which shows photographs of the sweep at a series of different repetition rates.     If, now, the repetition rate is unstable, as it might well be if a blocking oscillator or a free-running multivibrator were used to trigger the sweep, the time between sweeps is not fixed, but varies in a random manner.     Therefore, the starting position of the sweep also jumps around at random—that is, the sweep "jitters."     This jitter and the hook previously mentioned are the two most serious difficulties encountered in attempting to increase the repetition rate or the sweep duration to the limit.

In a rectangular scan, if the sweep current does not get back to zero, this shift in the start of the sweep can be corrected with the "centering" adjustment if the shift in center does not vary.     In a PPI it cannot be

corrected so easily because it causes a "hole" in the center of the pattern which cannot be removed by shifting the whole pattern.

Factors other than the sweep shift resulting from insufficient recovery time for the coil may cause the hole in the PPI pattern.    One of these factors is traceable to the fact that a rotating coil must be supported on bearings that, if made of magnetic materials, can become magnetized by the stray field of the deflection coil itself or by other stray fields.    It is not easy to substitute nonmagnetic bearings because the latter are difficult to make, are expensive, and are not nearly so good mechanically as steel bearings.[1]    If the inner race of a bearing is magnetized, it deflects the electron beam in the same manner as does the coil itself.    The bearing rotates with the coil, and the start of the sweep therefore traces out a circle that is perhaps a half-inch in diameter on a 5-in. tube.    Since this magnetization may be in any direction relative to the sweep field, the sweep may start out tangent to this small circle.    As the outer race does not rotate, any field it produces displaces the pattern as a whole, but this displacement can be corrected.    The balls in the bearing are small and, therefore, they cannot produce a large deflection.    However, the field they produce is very unsatisfactory because the balls rotate much faster than the coil, with the result that little irregular waves are superimposed on the markers on the sweep.

An effect similar to that due to the magnetization of the inner race is produced if the core of the deflection coil becomes magnetized.    To minimize this, any iron used in the core (or in the return path if an air-core coil is used) should be well annealed to produce minimum retentivity. A similar effect is produced if the deflection coil is mounted off-center so that it rotates eccentrically.    The iron of its core alters the field distribution of the focus coil in such manner as to cause a small deflection of the beam.    This deflection rotates with the coil and causes, in the center of the pattern, a hole that will probably never exceed $\frac{1}{16}$-in. in diameter.

Because of persistent eddy currents or of magnetization, metallic parts near the deflection coil may also cause a hole in the PPI pattern. These effects can be minimized by careful placement of parts.    Iron and copper shielding sometimes act in opposite directions, copper producing an open center and iron producing a hole that is inverted—i.e., a hole with a "negative" radius; therefore if iron and copper are properly placed together their effects can be balanced.

[1] For available nonmagnetic bearings, see Sec. 16·3.

# CHAPTER 10

## SWEEP AMPLIFIERS FOR REACTIVE LOADS

By C. W. Sherwin, Robert M. Walker, and F. N. Gillette

**10·1. Deflection Coils.**—In display circuits the reactive load most commonly encountered is the deflection coil of a magnetically deflected cathode-ray tube. The coil is employed to create across the tube neck a magnetic field that varies with time in some stipulated way, and that, in turn, produces a proportional deflection of the electron beam. The complete equivalent circuit of the coil (see Fig. 8·20) contains elements that represent leakage flux, iron losses, coil resistance, stray capacitance, eddy-current losses, and self-inductance. If the values of these elements are known, it is possible to calculate the voltage waveform that must be applied across the deflection coil in order to produce a given current waveform. If a voltage waveform of this shape can be generated, it may be used as the input wave for a voltage-feedback circuit that drives the coil.

The accuracy with which the assumed current wave is duplicated depends upon (1) the correctness of the equivalent circuit used in the calculation, (2) the precision with which the waveform generator duplicates the calculated wave, and (3) the distortion introduced by the feedback amplifier. This method can be made very accurate.
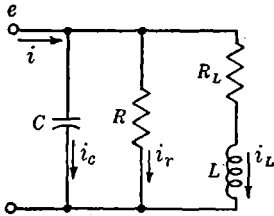
Fig. 10·1.—Simplified equivalent circuit of a deflection coil.

Usually extreme accuracy is not required and the problem may be simplified by deleting from the equivalent circuit all elements that contribute only second-order effects. The circuit that remains is shown in Fig. 10·1. An external damping resistance, not part of the coil, is represented by $R$.

For a linear sweep, it is required in the equivalent circuit of Fig. 10·1 that

$$i_L = kt. \tag{1}$$

Then $e$, the voltage across the deflection coil, must be

$$e = L\frac{di_L}{dt} + R_L i_L = Lk + R_L kt. \tag{2}$$

356

which is a step-plus-sawtooth waveform. This voltage causes a current $i_R$ to flow in the shunting resistor $R$,

$$i_R = \frac{Lk + R_L kt}{R},\tag{3}$$

and a current $i_C$ in the condenser $C$,

$$i_C = LkC[\delta(t)] + kR_L C,\tag{4}$$

where $\delta(t)$ is a delta or impulse function of infinite amplitude and infinitesimal duration. This function can only be approximated in practice since all practical sources of the required voltage waveform $e$ have a limited current capacity. The total input current to the deflection coil is, from Eqs. (1), (3), and (4),

$$i = k\left\{\underbrace{LC[\delta(t)]}_{\text{Impulse}} + \underbrace{R_L C}_{\text{Step}} + \underbrace{\frac{L}{R} + \left(1 + \frac{R_L}{R}\right)t}_{\text{Sawtooth}}\right\}.\tag{5}$$

Equations (2) and (5) give the input voltage $e$ and the input current $i$ necessary to cause a linear sawtooth current $i_L = kt$ to flow in the inductance of the equivalent circuit.

Because the impulse function is difficult to simulate in practice it may be useful to determine what $i_L$ will be with this impulse term missing. It is then required that the current $i$ have the form

$$i = k\left[\frac{L}{R} + R_L C + \left(1 + \frac{R_L}{R}\right)t\right].\tag{6}$$

From this equation $i_L$ can be calculated. From Fig. 10·1 it is evident that the following equations are true:

$$i = i_C + i_R + i_L\tag{7}$$

$$i_C = C\frac{de}{dt}\tag{8}$$

$$i_R = \frac{e}{R}\tag{9}$$

$$L\frac{di_L}{dt} + R_L i_L = e.\tag{10}$$

All currents and voltages are required to be zero when $t < 0$. The solution of these equations involves a third-order differential equation[1] in $i_L$ and $t$. Oscillatory terms in the solution are small and are critically

[1] For methods of solving such equations see Philip, Franklin, *Differential Equations for Electrical Engineers*, Wiley, New York, 1933.

damped under certain conditions that can be approximated by putting $R = \frac{1}{2}\sqrt{L/C}$. They will be neglected. The remaining terms give

$$i_L = kt\,(1 - e^{-\frac{t}{\sqrt{LC}}}). \qquad (11)$$

For large values of $t$ compared with $\sqrt{LC}$, $i_L = kt$, and consequently there is no extrapolated delay in the start of the sweep. At $t = \sqrt{LC}$ there is a maximum deviation of $0.7k\sqrt{LC}$ between the actual value of $i_L$ and the ideal value $kt$. Equation (11) is plotted in Fig. 10·2, which illustrates the general shape of the current waveform in the inductance.

If a short pulse of current charging $C$ occurs at the start of the sweep, it can greatly aid in reducing the temporary lag in $i_L$. This short pulse may be either artificially generated or automatically obtained by driving the deflection coil from a low-impedance generator that has its source voltage given by Eq. (2).
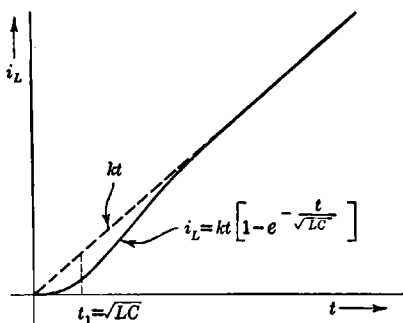


Fig. 10·2.—Current in a deflection coil.

Deflection coils should be designed with as short leads and as low distributed capacity as practicable to make the resonant frequency as high as possible at the required deflection sensitivity. The resonant frequency can be made high by reducing the number of turns, but the deflection sensitivity is thereby reduced. This solution to the resonant-frequency problem requires large deflection currents that cannot be cheaply obtained directly from vacuum tubes. Transformers may, of course, be used, but they have limitations at both high and low frequencies. Because sensitive coils can be used for very slow sweeps, the driving power can also be kept low in this case. However, many displays will involve a wide range of sweep speeds and duty ratios. It is in such cases that driving the sweep becomes expensive. The supply voltage and coil inductance are determined by the fast sweeps, the peak current by the maximum displacement, and the average current by the long-duty-ratio sweeps. Thus a driving stage consisting of several 807 tubes in parallel is not uncommon.

Table B·1, Appendix B, lists the principal operating characteristics of some typical deflection coils used in radar applications. The sweep speeds obtainable with these coils range from about 20 to 50 $\mu$sec/diameter to several seconds per diameter of the cathode-ray-tube screen. Faster sweeps can be obtained by reducing the number of turns on the coils and increasing the current. In obtaining fast-starting linear sweeps

free from wiggles, raising the applied voltage is not so effective as reducing the number of turns and increasing the current.

**10·2. Amplifiers for Applying a Given Voltage Waveform to a Deflection Coil.**—One of the simplest ways of driving a linear sawtooth current through a deflection coil is to connect it to a low-impedance generator that produces the step-plus-sawtooth input voltage required by Eq. (2). Several amplifiers of this type will be described in this section.

*The Cathode Follower.*—Figure 10·3 shows a cathode follower driving an inductive load. The output impedance of a cathode follower is approximately $1/g_m$. The condenser current flows through the cathode-follower output impedance, but this current is unimportant in practice
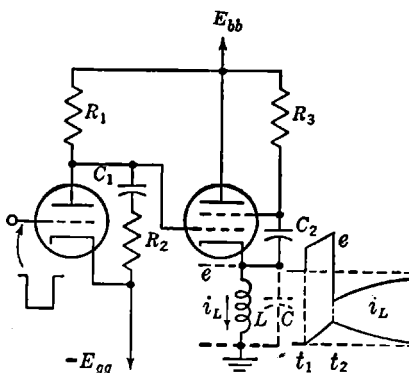


FIG. 10·3.—Cathode follower driving an inductive load.

except during the "step" part of the voltage. The step across the inductance is really a fast-rising exponential of time constant approximately equal to $(1/g_m)C$. This time constant is very short compared with the time constant of the inductance and its series resistance, $\dfrac{L}{(1/g_m) + R_L}$; therefore, the current in the inductance is only a small fraction of its final value at the time $(1/g_m)C$. Thus almost all the voltage drop in the cathode-follower output impedance during and shortly following the step is due to the condenser alone. This time constant $(1/g_m)C$ is approximately equal to the delay in getting a linear sawtooth current started in the inductance.

In computing the sawtooth part of the generator source voltage, Eq. (2), it is necessary to add $1/g_m$ in series with $R_L$. The condenser current through $1/g_m$ is unimportant after the step is completed, and there is no damping-resistor current.

The "overshoot" of the voltage across the inductance following time $t_2$ is necessary since the average voltage across an inductance with series

resistance $R_L$ must be $R_L(i_L)_{av}$.   The voltage $R_L(i_L)_{av}$ is small compared with the size of the applied voltage waveform in most practical cases.

The overshoot actually causes the cathode follower to continue to conduct during the time following $t_2$, and the current in the inductance decays with a time constant of $\dfrac{L}{(1/g_m) + R_L}$.   This slow recovery makes a circuit of this type useful only for those cases where adequate recovery time is available.   Because of the damping action of the continuously conducting cathode follower, no extra damping resistor is needed.

If the step-plus-sawtooth waveform on the grid of the cathode follower in Fig. 10·3 is followed by a large negative signal, the cathode follower will cut off after time $t_2$.   If the inductance is almost critically damped, a fairly rapid recovery of the inductance to the quiescent current point (zero, in this case) will be possible.   A rather large negative signal is needed, however, to do much good.



FIG. 10·4.—Voltage feedback for driving a deflection coil.

The simple circuit in Fig. 10·3 is very useful for fast-starting low-duty-ratio sweeps.   It is capable of good linearity provided that the input waveform is accurately generated and the cathode follower is not too heavily loaded.   An additional cathode follower inserted in the grid of the deflection-coil driver permits it to produce higher peak currents in the condenser at time $t_1$ and thus aids in speeding up the start.

*Amplifiers Using a Series R-C Circuit in the Feedback Loop.*—Another simple circuit that applies a predetermined voltage waveform to a deflection coil is shown in Fig. 10·4.   If the amplifier $V_2$ is assumed to have an infinitely large $g_m$ so that the output voltage $e_p$ across any finite load can be obtained by an infinitesimal grid signal $e_g$, the operation of the circuit is as follows.   At time $t_1$ a constant current, $i_0 = (E + E_{gg})/R_2$, starts to flow into $C_1$ and $R_1$ because the clamping circuit is opened at this instant.   The negative feedback from plate to grid of $V_2$ keeps the grid at an essentially constant voltage level.   The output voltage $e_p$ must therefore be the voltage across $R_1$ and $C_1$,

$$e_p = -\left(\frac{i_0 t}{C_1} + R_1 i_0\right),\tag{12}$$

which is a step voltage $R_1i_0$ plus a sawtooth voltage $(i_0/C_1)t$. The overshoot following $t_2$ is as shown·if $R$ is set for critical damping. It is now required that the current $i_L$ in the deflection coil be equal to $kt$. Equation (2) gives the step-plus-sawtooth voltage waveform,

$$e = -[Lk + R_Lkt],$$

needed across the deflection coil to produce this current. The voltage waveforms in Eqs. (2) and (12) must be identical for all values of $t$. Then $Lk = R_1i_0$ and $i_0/C_1 = R_Lk$. A combination of these expressions gives the condition for operation of this type:

$$R_1C_1 = \frac{L}{R_L}. \tag{13}$$

Thus if Eq. (13) is satisfied and an infinite $g_m$ is assumed for the amplifier tube $V_2$, a constant input current $i_0$ will cause a current $i_L = kt$ to flow in the inductance $L$, where

$$k = \frac{i_0}{C_1R_L} = \frac{i_0}{\dfrac{L}{R_1}}. \tag{14}$$

Because of the finite $g_m$ and·limited maximum output current from $V_2$, the step voltage is not perfect but rises as rapidly as the circuit can deliver charge to the distributed capacity that is always present across a practical coil.

To make the best possible use of the limited output current capabilities of $V_2$, an inductance $L_s$, shunted with a resistance $R_s$, may be inserted in series with $R_1$ and $C_1$. The resistance $R_s$ has such a value that, at time $t_1$ when the sweep starts, the grid of $V_2$ goes to zero bias rather than only part way. The voltage across $L_s$ and $R_s$ starts out with the value $i_0R_s$ and exponentially approaches zero with a time constant $L_s/R_s$. The value of the inductance should be experimentally adjusted for the best-appearing start as seen on the cathode-ray-tube display.

Very large values of effective $g_m$ can be readily obtained by using several tubes in parallel, or better, by interposing a voltage amplifier in the grid lead to $V_2$. However, a single tube is often used in the circuit shown in Fig. 10·4 and the effective $g_m$ is not very great. It is therefore of interest to determine the conditions that must be satisfied if $g_m$ is not infinite. The effect of capacity across the deflection coil can be neglected because the current to the capacity is small after the initial step is completed. A damped inductance in series with $R_1$ and $C_1$ may be added to aid in speeding up the start of the sweep.

An analysis, similar to that given for the ideal case, gives to a good

approximation the following values of the feedback elements $C_1$ and $R_1$ which cause $i_L$ to be a sawtooth wave:

$$R_1 = \frac{kL}{i_0}\left(1 + \frac{1}{g'_m R}\right) + \frac{1}{g'_m}, \tag{15}$$

$$C_1 = \frac{i_0}{k\left[\dfrac{1}{g'_m}\left(1 + \dfrac{R_L}{R} + \dfrac{R_1}{R_2}\right) + R_L\right]}, \tag{16}$$

where, as before, $i_0 = \dfrac{(E + E_{gg})}{R_2}$ and where $g'_m = \dfrac{g_m}{1 + g_m R_k}$, the effective transconductance of $V_2$ with the cathode resistor $R_k$ in place. As $g_m$ approaches infinity, Eqs. (15) and (16) approach the values of $R_1$ and $C_1$ given by Eqs. (13) and (14). Since in all practical cases $R_L$ is much smaller than $R$, Eq. (16) becomes, solving for $k$,

$$k \approx \frac{i_0}{C_1\left(1 + \dfrac{R_1}{R_2}\right)} \cdot \frac{g'_m}{1 + g'_m\dfrac{R_L}{\left(1 + \dfrac{R_1}{R_2}\right)}}. \tag{17}$$

Thus the slope $k$ of the current in the inductance is independent of $g'_m$ only if $g'_m R_L/(1 + R_1/R_2) \gg 1$. If $g'_m = 6 \times 10^{-3}$ mhos, $R_1/R_2 = 0.3$, and $R_L = 650$ ohms, a 20 per cent change in $g'_m$ will cause a 5 per cent change in the slope $k$. It is important always to have $R_L$ and $R_2$ as large as is practicable in order to get the greatest possible independence of $k$ from the effective $g_m$ of the amplifier. Usually a resistance is added in series with the inductance to make the value of $R_L$ large enough. Besides the desired effect, this resistance causes some additional delay in the start of the sweep because the distributed capacity of the coil is charged through this extra resistance.

A deflection amplifier of the type shown in Fig. 10·4 is very useful. The circuit is simple and fairly independent of the driver-tube characteristics if the tube does not operate too close to cutoff. The cathode resistor $R_k$ is added to stabilize the quiescent current level with respect to changes in heater voltage. It has the advantage, over the cathode-follower driver shown in Fig. 10·3, that at the termination of the sweep the deflection coil is free to execute a damped oscillation and to recover rapidly. One disadvantage of this circuit is the fact that any ripple or other disturbance on $E_{bb}$ is coupled to the grid of $V_2$ through $R_1$ and $C_1$ during the time the clamp is open and causes a noticeable fluctuation of the display.

**10·3. Amplifiers for Applying a Given Current Waveform to a Deflection Coil.**—In order to cause a sawtooth current waveform to flow through

the inductive part of the deflection-coil equivalent circuit, the total input current must be as specified by Eq. (5). A voltage waveform that approximates the shape of this current waveform can be generated (by a circuit such as the one shown in Fig. 10·5), and an amplifier using feedback may then be used to convert this voltage into a similar current waveform.

It is convenient to distinguish between two types of feedback amplifier, the distinction depending upon whether the deflection coil is in the cathode or the plate circuit of the output tube. In both amplifiers the feedback signal is obtained from a current-sampling resistor $R_0$. The output tube has transconductance $g_m$, plate resistance $r_p$, and amplification factor $\mu$. The generalized formula for the gain of a feedback amplifier is $\mathcal{G} = \alpha/(1 - \beta\alpha)$, where $\mathcal{G}$ is voltage gain with feedback, $\alpha$ is voltage gain without feedback, and $\beta$ is the fraction of the output voltage fed back into the circuit.



Fɪɢ. 10·5.—Circuit for generating a waveform $e_0$ which has the approximate shape required to produce a linear current in an inductive load.

When the deflection coil is in the cathode circuit, as in the circuit shown in Fig. 10·11,

$$\mathcal{G} = \frac{i_0 R_0}{e_i} = \frac{\alpha \dfrac{\mu}{\mu + 1} \dfrac{R_0}{\dfrac{r_p}{\mu + 1} + Z_L + R_0}}{1 - \beta\alpha \dfrac{\mu}{\mu + 1} \dfrac{R_0}{\dfrac{r_p}{\mu + 1} + Z_L + R_0}}, \tag{18}$$

ꜱn expression which can be solved for $i_0$ (using $\mu = r_p g_m$) as follows:

$$i_0 = e_i \cdot \frac{\alpha g_m}{1 - \beta\alpha g_m R_0} \cdot \frac{1}{1 + g_m \dfrac{\mu + 1}{\mu} \dfrac{Z_L + R_0}{1 - \beta\alpha g_m R_0}}. \tag{19}$$

If $i_0$ is to be independent of $g_m$ and $\alpha$, it is required that $|\beta\alpha g_m R_0| \gg 1$ (In a typical case $\alpha = 200$, $g_m = 5 \times 10^{-3}$ mhos, $R_0 = 100$ ohms, $\beta = -\frac{1}{2}$; hence $|\beta\alpha g_m R_0| = 50$.) Then using the approximation

$$\frac{\mu + 1}{\mu} = 1,$$

the last term becomes $\dfrac{1}{1 - \dfrac{Z_L + R_0}{\beta \alpha R_0}}$. Since $Z_L$ varies with frequency,

$i_0$ will not be proportional to $e_i$ unless

$$|\beta \alpha R_0| \gg Z_L. \tag{20}$$

(In the example above $\beta \alpha R_0 = -10^4$ ohms.)

When the deflection coil is in the plate circuit,

$$\mathsf{G} = \frac{i_0 R_0}{e_i} = \frac{\alpha \mu \dfrac{R_0}{r_p + Z_L + R_0}}{1 + \beta \alpha \mu \dfrac{R_0}{r_p + Z_L + R_0}}, \tag{21}$$

and

$$i_0 = -e_i \frac{\alpha g_m}{1 + \beta \alpha g_m R_0} \frac{1}{1 + \dfrac{Z_L + R_0}{r_p (1 + \beta \alpha g_m R_0)}}. \tag{22}$$

As for Eq. (19), it is required that $|\beta \alpha g_m R_0| \gg 1$. The last term is independent of $Z_L$ only if

$$|r_p \beta \alpha g_m R_0| \gg Z_L. \tag{23}$$

This requirement is much less stringent than Eq. (20), and indicates that a plate-driven coil will give results more independent of amplifier changes than those obtained with a cathode-driven coil. The cathode drive is preferable, however, in those cases in which the capacity of the line to the coil is large, or in which ripple in the plate supply voltage becomes noticeable with plate drive.

Both Eq. (19) and Eq. (22) reduce to the simple form

$$i_0 = -\frac{e_i}{\beta R_0} \tag{24}$$

when the condition $|\beta \alpha g_m R_0| \gg 1$ and the restrictions of Eqs. (20) and (23) are satisfied. The usual stability requirements (see Vol. 18) for feedback amplifiers must be met so that oscillations will not occur.

*Generation of Sweep Waveform as a Voltage.*—Figure 10·5 shows a typical circuit useful for generating a waveform that has a "spike"-plus-step-plus-sawtooth voltage. An essentially constant current $i_0$ is obtained from the large voltage $+E$. (The end of $R_1$ connected to $E$ may be "bootstrapped" to maintain $i_0$ almost exactly constant. See, for example, Fig. 10·7.) The cathode-follower-diode switch circuit ($V_1$ and $V_2$) opens at time $t_1$. A rectangular wave, differentiated by $C_2$ and $R_4$ and applied through diode $V_3$ to $R_2$, produces a "spike" at the start of the sweep. The step-plus-sawtooth part of the waveform is

formed by $R_2$ and $C_1$. At time $t_2$, the cathode follower cuts off and thereby allows a very smooth return of $e_0$ to its quiescent level since $C_1$ discharges principally through $R_2$, $R_3$, and the diode resistance, all in series. The negative "spike" at $t_2$ is prevented from getting through to $R_2$ by the diode $V_3$.

It is often very important that there be no overshoot or "spike" at time $t_2$ since in some circuits the feedback in the amplifier disappears after time $t_2$ (because of the cutting off of the output tube $V_7$ in Fig. 10·7). The overshoot or "spike" is then greatly amplified and charges the coupling condensers; this situation is very undesirable. The cathode-
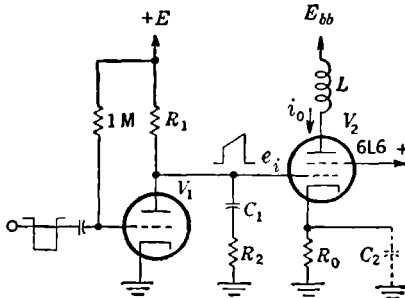


FIG. 10·6.—The simple tetrode deflection coil driver with cathode degeneration.

follower-diode switch is ideal for use in generating waveforms of the required type since the closed impedance is low and constant. There is no overshoot whatever. A simple triode or pentode switch has some overshoot at time $t_2$ and this condition causes serious difficulty in many cases.

The operation of several types of amplifier, which force a given current through a deflection coil, will now be examined.

*The Simple Pentode or Tetrode Amplifier.*—A simple one-tube amplifier that has been widely used in radar applications is shown in Fig. 10·6. As long as the plate of the tetrode (or pentode) stays above the "knee" in the plate-characteristic curve (i.e., above 50 to 80 volts), the screen takes approximately a constant fraction of the cathode current. For this condition, the circuit operates in accordance with the following equation:

$$i_0 \approx e_i \frac{g_m}{1 + g_m R_0},  \tag{25}$$

where $g_m$ is the transconductance of $V_2$ and the capacity $C_2$ is neglected.

The grid voltage $e_i$ is generated to have the step-plus-sawtooth form of Eq. (2), and it will cause a linear sawtooth current to flow in $L$ after a time large compared with the resonant period of the deflection coil. Faster starting sweeps may be produced by adding a condenser $C_2$

across $R_0$.  The time constant $R_0C_2$ should have a value that is of the order of magnitude of $\sqrt{LC}$, but it will usually have to be adjusted for best results.

If $R_0$ is made larger, the effective transconductance

$$[(g_m)_e = g_m/(1 + g_mR_0)]$$

becomes smaller and larger grid signals are needed to produce the required output current $i_0$.  Large signals on the cathode of $V_2$ also reduce the plate-to-cathode voltage.  Therefore, $E_{bb}$ must be higher than would otherwise be necessary.  If $R_0 = 500$ ohms, and when $V_2$ is a 6L6, good linearity results.  This linearity is further improved by operating in
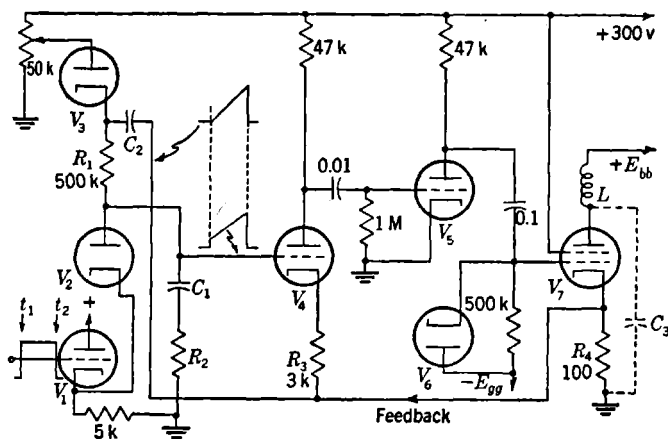


Fig. 10·7.—Three-stage feedback amplifier.

push-pull two amplifiers like the one shown in Fig. 10·6.  A deflection coil that has a separate winding for each of the amplifiers is then required, and push-pull grid signals are needed.  The second-harmonic distortion in the amplifier tubes is canceled by this process.

*Three-stage Feedback Amplifier with the Deflection Coil in the Plate Circuit of the Output Tube.*—A widely used sweep amplifier circuit is shown in Fig. 10·7.  The clamp circuit consisting of $V_1$ and $V_2$ is opened by a rectangular voltage waveform on the grid of $V_1$ at time $t_1$.  The step-plus-sawtooth voltage is generated at the grid of $V_4$.  The amplifier causes this sweep signal to appear across the sampling resistor $R_4$ in the cathode circuit of the output tube.  The sampled voltage is fed back to the cathode of $V_4$ and there it is compared with the input signal.  The feedback operates to make the generated waveform and the sampled waveform across $R_4$ as nearly identical as possible.  A compensation network in the amplifier loop may be necessary to stabilize the circuit.

If the plate of $V_7$ stays at least 50 to 80 volts above the cathode, the screen current is essentially a constant fraction of the cathode current. For higher accuracy, however, the effect of changes in screen current should be compensated. (See Fig. 10·8 for one method of doing this.)

The value of $E_{gg}$ is set for cutoff of $V_7$. The ability of this circuit to operate with $V_7$ conducting only during sweeps is one of its chief advantages. Diode $V_6$ causes the grid waveform always to start from the fixed level of $-E_{gg}$ for sweeps of any duty ratio. The voltage $E_{bb}$ must be large enough to supply the required step voltage, $Lk$, as well as the sawtooth voltage, $R_L kt$.

The feedback to the diode $V_3$ serves to "bootstrap" the positive end of the sweep-generating resistor $R_1$, and thus to keep the voltage across $R_1$ constant during the entire sweep (if condenser $C_2$ is sufficiently large). An alternate method for bootstrapping the sweep generator is to omit $V_3$ entirely, and to connect the positive end of $R_1$ to a selected point on $R_4$ which has a sawtooth voltage of approximately the correct amplitude. This method is not so flexible or so accurate as the one shown, but it is cheap, and is good enough for many applications.

The effective transconductance of $V_7$ is approximately

$$g_m = \frac{(g_m)_7}{1 + (g_m)_7 R_4}, \tag{26}$$

where $(g_m)_7$ is the transconductance of $V_7$ with no cathode resistor. Thus if $\alpha$ is the voltage gain without feedback from the grid of $V_4$ to the grid of $V_7$, the effective transconductance of the amplifier in Fig. 10·7 is

$$(g_m)_e = \alpha g_m. \tag{27}$$

To determine the value of $\beta$, the feedback-network transfer characteristic, it is necessary to take into account the difference in the gain of the first tube $V_4$ with a signal $e_i$ on the grid as compared with the gain with a signal $e_k$ inserted in series with the cathode circuit. With the feedback loop broken by connecting the lower end of $R_3$ to ground rather than to the cathode of $V_7$, $e_i$ and $e_k$ produce identical currents in $V_4$ only if $e_i = -e_k \frac{\mu + 1}{\mu}$, where $\mu$ is the amplification factor of $V_4$. Thus the feedback signal from the cathode of $V_7$ can be considered to be added to the input signal on the grid of $V_4$ only when multiplied by $-\left(\frac{\mu + 1}{\mu}\right)$. Thus,

$$\beta = -\left(\frac{\mu + 1}{\mu}\right). \tag{28}$$

When the values of $g_m$ and $\beta$ are substituted from Eqs. (26) and (28) in Eq. (22), the output current $i_0$ into resister $R_4$ is

$$i_0 = -e_j \frac{\alpha \left[ \dfrac{(g_m)_7}{1 + (g_m)_7 R_4} \right]}{1 - \left( \dfrac{\mu + 1}{\mu} \right) R_4 \alpha \left[ \dfrac{(g_m)_7}{1 + (g_m)_7 R_4} \right]}. \tag{29}$$

The dependence of Eq. (29) on $(g_m)_e$ [Eq. (27)] and on $\mu$ can be calculated. For $\dfrac{\mu + 1}{\mu} R_4 (g_m)_e \gg 1$, $i_0$ is directly proportional to $\dfrac{\mu}{\mu + 1}$. This dependence is not a serious defect of the amplifier since $\mu$ is very nearly constant and is large. For the circuit shown in Fig. 10·7, $\alpha \approx -60$,
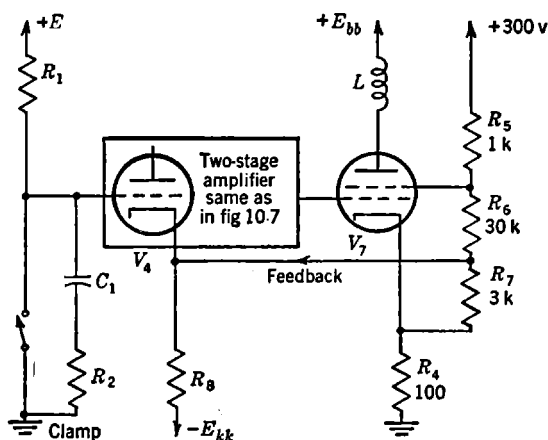


Fig. 10·8.—Method of compensating the feedback signal for screen current.

$g_m$ of $V_7$(6L6) varies from 0 up to $5 \times 10^{-3}$ during the sawtooth wave (for computation a value of $4 \times 10^{-3}$ is taken), $R_4 = 100$ ohms, $\mu = 20$; and $\dfrac{\mu + 1}{\mu} R_4 (g_m)_e \approx -16 = $ loop gain. A 17 per cent change in the loop gain will change $i_0$ by only 1 per cent.

Only a fraction of the cathode current $i_0$ goes through the deflection coil because part of the current is screen current in $V_7$. This effect is usually not serious because the screen current is a small and essentially constant fraction of the plate current as long as the plate voltage is high enough. However it is possible to cancel the effect of changes in screen current by use of the circuit shown in Fig. 10·8. A resistance $R_5$ is inserted in the screen circuit so that the signal that appears at the screen

and is due to screen current is −10 times that part of the signal that appears at the cathode and is due to screen current. The divider consisting of $R_6$ and $R_7$ samples both signals in such a manner that the net contribution of the screen current is zero, and a signal proportional only to the plate current is used for feedback. The d-c level of the cathode of $V_4$ is set at the correct operating point by means of $R_8$, a large resistor (compared with $R_7$) returned to a negative d-c source.

In the circuit of Fig. 10·7 or Fig. 10·8, the current to the plate-circuit output capacity (which may include the capacity of a cable and be rather large) goes through $R_4$ and must be compensated for by an extra "spike" just as must the distributed capacity $C$ of the deflection coil.

Another modification of the amplifier shown in Fig. 10·7 is shown in Fig. 10·9. For an amplifier having a very large effective transconductance, the input voltage $e_i$ to the amplifier is very small compared
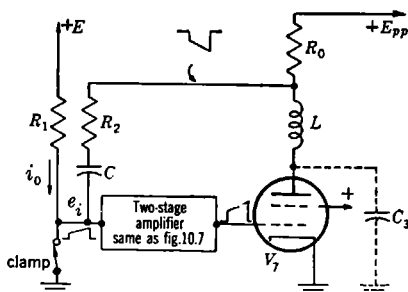


Fig. 10·9.—Three-stage feedback amplifier.

with the signal across $R_0$. The constant current $i_0$, starting at time $t_1$, causes a step-plus-sawtooth voltage to appear across $R_0$ because of the action of the feedback. The step voltage is approximately equal to $i_0R_2$ and the sawtooth voltage is approximately equal to $i_0t/C$. Because of the large voltage gain of the two-stage amplifier, the effective $g_m$ is large enough to make these simple calculations accurate. Allowance for finite amplifier transconductance can be made by using an analysis similar to that applied to the circuit of Fig. 10·4 (which resembles that of Fig. 10·9 except that a current sample rather than a voltage sample is used for feedback purposes).

This circuit has the advantage that the current to $C_3$ does not appear in $R_0$ and thus the feedback amplifier automatically corrects for the presence of $C_3$. Also the screen current does not flow through the sampling resistor $R_0$.

Figure 10·10 shows another circuit of the same general type as Fig. 10·7. The pentodes may be 6AC7's or 6SJ7's. The current

$$i_0 \approx \frac{e_i}{2\left(\dfrac{\mu}{\mu+1}\right)} \frac{g_m}{1 - \beta g_m R_0}, \tag{30}$$

where

$$\beta = 1,$$

$$g_m = \mathfrak{A} \frac{(g_m)_3}{1 + R_0(g_m)_3}, \tag{31}$$

$\mathfrak{A}$ = voltage gain from the grid of $V_2$ to the grid of $V_3$ with the grid of $V_1$ fixed, and

$\mu$ = grid-screen amplification factor of $V_2$.

Since there is only one $RC$-coupling in the feedback loop, the circuit is particularly easy to stabilize against oscillations due to feedback.



*Three-stage Amplifiers with the Deflection Coil in the Cathode Circuit of the Output Tube.*—A current-sampling feedback amplifier with a cathode follower in the final stage is shown in Fig. 10·11. The operation of this circuit is described by Eq. (19) where $\beta = -\dfrac{\mu+1}{\mu}$ as in Eq. (28). The voltage gain (with the lower end of $R_3$ grounded) from the grid of $V_1$ to the grid of $V_3$ is given by $\mathfrak{A}$. Resistor $R_1$ is made equal to $1/(g_m)_3$ where $(g_m)_3$ is the transconductance of $V_3$.

FIG. 10·10.—Another variety of feedback amplifier that causes a current waveform of the same shape as $e_i$ to flow through the deflection coil.

When the clamp opens, the feedback forces a sawtooth current to flow in $L$, and the necessary voltage across the deflection coil is thus generated. At time $t_2$, when the clamp closes, the inductance overshoots but the rapidly decreasing input signal on the grid of $V_1$ causes a signal to go through the amplifier. This signal turns off $V_3$ and allows the current in the coil to recover at a rate governed by its $L/R$ time constant. The current feedback thus removes one of the difficulties associated with the simple voltage-feedback cathode-follower circuit of Fig. 10·3. The current to $C_3$ does not go through $R_0$, and both the screen and plate currents contribute to the deflection current. Tube $V_3$ operates from cutoff.

**10·4. Direct-coupled Amplifiers for Producing a Given Current Waveform in a Deflection Coil.**—Often it is desirable for amplifiers

driving deflection coils to pass direct current.[1]   The coil acts like a
resistor for very slow sweeps since the induced voltage in the inductance
is negligible.   The distinction between amplifiers that apply given volt-
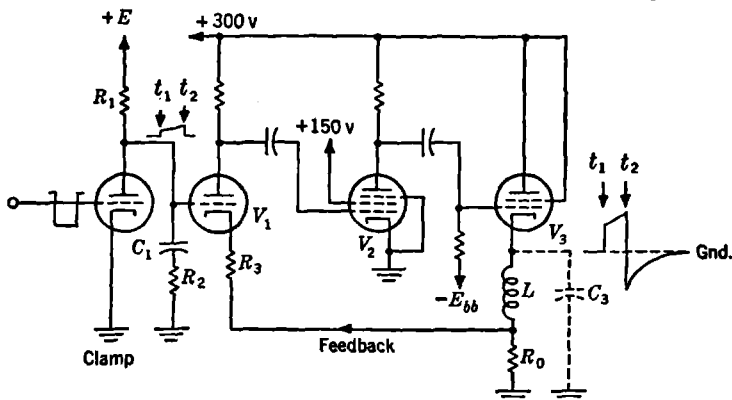


Fig. 10·11.—Feedback amplifier with deflection coil as cathode load.

ages and those that apply given currents to the deflection coil disappears.
In these circuits the feedback network must operate at zero frequency.

Although the simple output
amplifier shown in Fig. 10·6 has
almost constant feedback for all
frequencies to zero, it may not be
linear enough or have constant
enough effective $g_m$ to be satis-
factory.   An improved amplifier
is shown in Fig. 10·12, where an
extra tube with feedback is added
to increase both the effective $g_m$
and the linearity.   A sweep volt-
age may be inserted at one input
terminal and a d-c off-centering
voltage at the other.   By means
of a switching circuit, the sweep
wave-forms can be forced to have
a fixed d-c level during the "wait"
time.   They can then be directly



Fig. 10·12.—Direct-coupled feedback cir-
cuit for producing an output current $i_0$ pro-
portional to $e_1 + e_2$.   $R \gg R_0$.

added to the off-centering voltages at the input terminal of the amplifier.
The following equations can be derived:

$$i_0 \approx \frac{(e_1 + e_2)}{R_0} \frac{\alpha}{1 - \alpha} \qquad \text{or} \qquad \frac{i_0}{e_1 + e_2} \approx \frac{1}{R_0} \frac{\alpha}{1 - \alpha} \qquad (32)$$

[1] The circuits discussed in Sec. 11·3 and Sec. 13·7 exemplify this need.

and

$$\alpha \approx \frac{\mathcal{G}_1}{3} \frac{g_m R_0}{1 + R_0 g_m}. \tag{33}$$

Here, $\alpha$ is the loop gain of the amplifier, $g_m$ is the transconductance of $V_2$, and $\mathcal{G}_1$ is the voltage gain from the grid of $V_1$ to the grid of $V_2$. The quantity $(1 - \alpha)$ is the factor by which nonlinearities or spurious signals introduced inside the feedback loop are reduced.[1]   An example of this type of circuit is the case where $V_1$ is a 6AC7, $\mathcal{G}_1 = -50$, $V_2$ is a 6L6 with
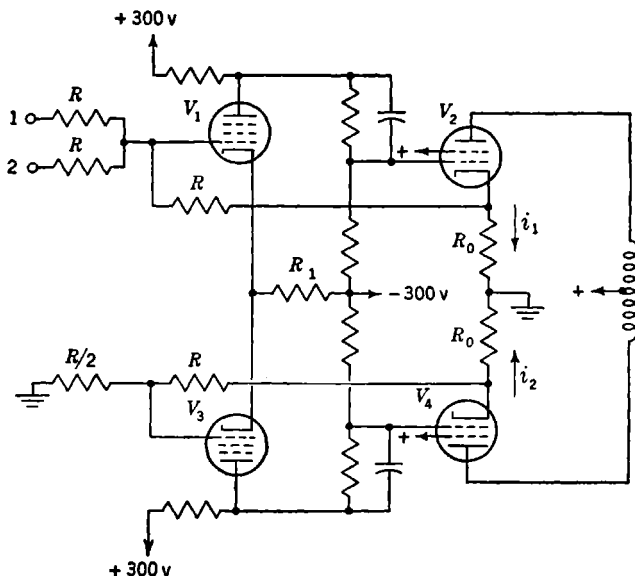


FIG. 10·13.—Direct-coupled feedback circuit to produce an output current difference $(i_1 - i_2)$ proportional to $(e_1 + e_2)$.  $R \ll R_0$.

$g_m = 5 \times 10^{-3}$ mhos, and $R_0 = 200$ ohms.   Equation (33) gives $\alpha \approx -8$, The effective $g_m \approx 4.5 \times 10^{-3}$ mhos, and depends very little on $\alpha$.   To maintain high-frequency response, small condensers may be added between the plate of $V_1$ and the grid of $V_2$, and also, if necessary, across the mixing resistors $R$.

Figure 10·13 shows an extension of the circuit shown in Fig. 10·12, in which a push-pull output signal can be obtained with a single combined input signal.   The deflection is proportional to $i_1 - i_2$, and

$$i_1 - i_2 = \frac{e_1 + e_2}{R_0} \frac{\alpha}{1 - \alpha} \tag{34}$$

[1] *Feedback Amplifiers*, Vol. 18 of the Series.

where

$$\alpha = \frac{1}{3}\left[\frac{\mathcal{G}_1}{2}\frac{(g_m)_2 R_0}{1+(g_m)_2 R_0} + \frac{\mathcal{G}_2}{2}\frac{(g_m)_4 R_0}{1+(g_m)_4 R_0}\right], \tag{35}$$

in which equation

$\mathcal{G}_1 =$ voltage gain from grid of $V_1$ to grid of $V_2$ with the cathode of $V_1$ fixed in potential;

$\mathcal{G}_2 =$ voltage gain from grid of $V_3$ to grid of $V_4$ with the cathode of $V_3$ fixed in potential;

$(g_m)_2 =$ transconductance of $V_2$; and

$(g_m)_4 =$ transconductance of $V_4$.

If, for example, $\mathcal{G}_1 = \mathcal{G}_2 = -50$, $(g_m)_2 = (g_m)_4 = 5 \times 10^{-3}$ mhos, and $R_0 = 200$ ohms, the value of $\alpha$ is $-8$ and the effective $g_m = 4.5 \times 10^{-3}$ mhos as in the case of the example for Fig. 10·12. There is one important difference between the two circuits, however. In the first the effect on the operating point of $V_2$ of drift in the values of the resistors at the plate of $V_1$ and the grid of $V_2$ is reduced by the factor $(1 - \alpha)$. In the push-pull circuit, however, the feedback does not act to stabilize the operating points of $V_2$ and $V_4$ although it does act to stabilize the effective $g_m$ of the circuit. As a result, it is necessary to adjust $R_1$ carefully so that $V_2$ and $V_4$ operate at the desired quiescent level.
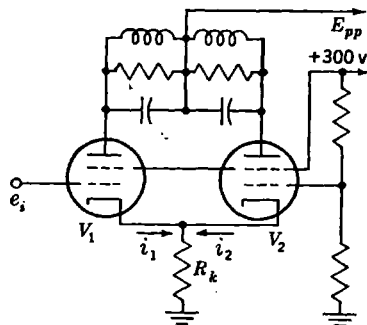


FIG. 10·14.—Cathode-coupled deflection-coil-driver circuit.

The push-pull circuit does have an advantage that is apparent from Eq. (35). If $(g_m)_2$ or $(g_m)_4$ should go to zero, the value of $\alpha$ changes by only a factor of 2 and the change in $i_1 - i_2$ [Eq. (34)] is small if $\alpha$ is large. Thus there is no discontinuity of operation when one of the output tubes· cuts off but only a relatively small change in the effective $g_m$ of the amplifier.

*Cathode-coupled Push-pull Amplifier.*—A simple but not very accurate direct-coupled amplifier is shown in Fig. 10·14. The relation between the input signal $e_i$ and the difference of the cathode currents (which is proportional to the deflecting magnetic field except for small screen-current corrections) is

$$i_1 - i_2 = e_i(g_m)_1 \frac{1 + 2R_k\frac{\mu+1}{\mu}(g_m)_2}{1 + R_k\left[(g_m)_1 + \frac{\mu+1}{\mu}(g_m)_2\right]}, \tag{36}$$

where

   $(g_m)_1$ = transconductance of $V_1$,

   $(g_m)_2$ = transconductance of $V_2$,

     $\mu$ = grid-to-screen amplification factor of $V_2$, and

   $R_k$ = common cathode resistance.

When $R_k$ is large compared with $1/(g_m)_1$ and $1/(g_m)_2$, and when $\mu \gg 1$, Eq. (36) reduces to

$$i_1 - i_2 \approx e_i \frac{2(g_m)_1(g_m)_2}{(g_m)_1 + (g_m)_2}. \tag{37}$$

Therefore, there is a strong dependence of the effective transconductance

$$\left[ (g_m)_e \approx \frac{2(g_m)_1(g_m)_2}{(g_m)_1 + (g_m)_2} \right]$$

on both $(g_m)_1$ and $(g_m)_2$. There is no effective feedback, and the non-linearity of both $V_1$ and $V_2$ causes important errors. For example, if either $(g_m)_1$ or $(g_m)_2$ approaches zero, $(g_m)_e$ approaches zero. Making
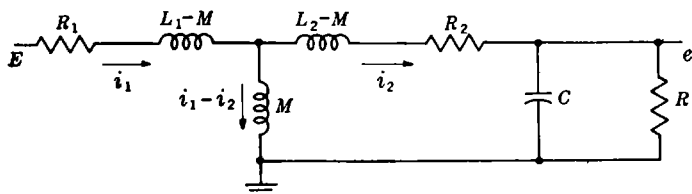


Fig. 10·15.—Equivalent circuit for a synchro.

$R_k$ large does not appreciably affect the accuracy, but merely causes the two currents $i_1$ and $i_2$ to have more nearly the same magnitude.

Another disadvantage of the circuit of Fig. 10·14 is the power lost by dissipation in $R_k$. Resistors inserted in the cathode leads to each of the tubes will improve the linearity of each at the expense of a lower value of $(g_m)_e$ and the necessity of a larger value of $R_k$ if the same ratio of $i_1/i_2$ is required.

**10·5. Transient Response of a Synchro.**—An equivalent circuit[1] for a synchro, simplified to include but one stator winding, is shown in Fig. 10·15. Other stator windings would be represented by adding identical circuits, with all the circuits connected in parallel at their input terminals and ground. A linear sawtooth voltage waveform $E$ applied to the rotor would produce at the stator output terminal a waveform distorted,

---

[1] This is a circuit synthesized for transformers with constant components and sinusoidal voltages. The equivalence is not exact, especially at high frequencies, but it will serve in calculating first-order correction terms for the input and output voltages of a synchro.

as shown in Fig. 10·16, and having an amplitude depending on the sine of the shaft angle. Although the delay varies as a function of the shaft position, and hence cannot be corrected uniformly for all angles, it is not an important factor except for a very-fast-rising sawtooth waveform.

*Low-frequency Response.*—If the distributed capacity $C$ is neglected, the input voltage $E$ required to produce a linear saw-tooth output voltage $e = kt$ is readily calculated. All voltages and currents are zero up to $t = 0$.
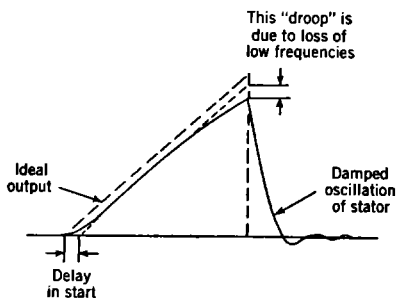


FIG. 10·16.—Distortion of sawtooth voltage waveform when transmitted through a synchro.

The voltage across $M$ in Fig. 10·15 is

$$M \frac{d}{dt}(i_1 - i_2) = (L_2 - M)\frac{di_2}{dt} + R_2 i_2 + kt. \tag{38}$$

Since

$$i_2 = \frac{e}{R} = \frac{kt}{R}, \tag{39}$$

then

$$M \frac{di_1}{dt} = \frac{L_2 k}{R} + \frac{R_2}{R} kt + kt, \tag{40}$$

and

$$i_1 = \frac{k}{M}\left[\frac{L_2 t}{R} + \left(\frac{R_2}{R} + 1\right)\frac{t^2}{2}\right]. \tag{41}$$

$$E = R_1 i_1 + (L_1 - M)\frac{di_1}{dt} + M\frac{d}{dt}(i_1 - i_2). \tag{42}$$

In practice, $R$ is usually very much larger than $R_1$ or $R_2$; hence Eq. (42) reduces to

$$E = \frac{k}{M}\left[\frac{R_1 t^2}{2} + L_1 t + \frac{L_1 L_2 - M^2}{R}\right]. \tag{43}$$

The rotor-stator coupling coefficient is $k_0 = M/\sqrt{L_1 L_2}$. It varies with angle from 0 to a maximum of about 0.9 for the types of synchro suitable for resolving sawtooth waveforms. Putting this term in Eq. (43) gives

$$E = \frac{k}{M} L_1\left[\frac{R_1 t^2}{2L_1} + t + \frac{L_2(1 - k_0^2)}{R}\right]. \tag{44}$$

The first term, in $t^2$, is required to prevent the "droop" in the response at large values of $t$. For a sawtooth voltage of short time duration, or for a

synchro with extremely low rotor resistance, it can be omitted. The last term is a step voltage that is required to reduce the delay. For a sawtooth wave of long duration and for large $R$, it can be omitted. A large value of $R$, however, may reduce the permissible duty ratio because of the time required for oscillations set up by the termination of the sawtooth wave to die away. The expression $L_2(1 - k_0^2)$ is the stator leakage inductance. It varies from $L_2$ for the rotor position of zero coupling to approximately $0.2L_2$ for the position of maximum coupling.

*High-frequency Response.*—At high frequencies the effect of the distributed capacity is appreciable, and it must be left in the equivalent circuit. As shown by Eq. (44), $R_1$ may be omitted. For an output voltage $e = kt$, the stator current is then

$$i_2 = i_R + i_C = \frac{kt}{R} + Ck. \tag{45}$$

Since $i_2 = 0$ for $t < 0$, its derivative involves the impulse function $\delta(t)$,

$$\frac{di_2}{dt} = \frac{k}{R} + Ck\delta(t). \tag{46}$$

The voltage across $M$ is

$$M \frac{d}{dt}(i_1 - i_2) = (L_2 - M)\frac{di_2}{dt} + R_2 i_2 + kt. \tag{47}$$

From Eqs. (45), (46), and (47)

$$\frac{di_1}{dt} = \frac{k}{M}\left[\frac{L_2}{R} + R_2 C + \left(\frac{R_2}{R} + 1\right)t + L_2 C\delta(t)\right]. \tag{48}$$

$$E = (L_1 - M)\frac{di_1}{dt} + M\frac{d}{dt}(i_1 - i_2). \tag{49}$$

From Eqs. (46), (48), and (49), with $L_2(1 - k_0^2)$ set equal to L,

$$E = L_1 \frac{k}{M}\left[\frac{L}{R} + R_2 C + \left(\frac{R_2}{R} + 1\right)t + LC\delta(t)\right]. \tag{50}$$

This equation is the same as Eq. (5) derived for the current through a deflection coil, except that it is for a voltage rather than a current waveform, and that $L$ is not constant. If the impulse function is omitted from the input voltage, the output voltage will be of the same form as the current in Eq. (11) plotted in Fig. 10·2:

$$e = kt\left(1 - e^{-\frac{t}{\sqrt{LC}}}\right). \tag{51}$$

The damping resistor and the step voltage are usually chosen to match the condition of maximum coupling. As the coupling is reduced,

the value of $L$ increases and the point $t_1$ moves to the right. Finally, for the condition of zero coupling, $t_1$ reaches a value equal to a little more than twice its original value. Since the change in delay is different for the resolved phase components from the synchro, it leads, for a short time after the start of the sawtooth wave, to angular distortion of the vector sum of the components, as well as to waveform distortion. After a time long enough for the exponential term to vanish, there is no longer any distortion.

**10·6. Circuits for Driving Sweep Waveforms through a Synchro.—** Some of the circuits used for deflection coils are suitable, with short- and medium-length sawtooth wave-forms, for applying voltage waveforms to a synchro. One precaution must be observed. The rotor-winding insulation in many synchros is not sufficient to withstand the plate supply voltage; hence condenser or transformer coupling must be used if the load is in the plate circuit of the amplifier. There will then be a loss in frequency response. Slight modifications make possible the addition of the $t^2$ term of Eq. (44) required for a long sawtooth waveform.

Reasonably linear output voltages may be obtained with the



FIG. 10·17.—Miller-rundown sawtooth-voltage driving circuit for a synchro.

circuit shown in Fig. 10·17. The slope of the sawtooth voltage on the plate depends primarily on $E_0$, $R$, and $C$, and is largely independent of the voltage gain of $V_1$ and therefore of the plate load impedance.[1]

After every sweep, the energy is dissipated in the damping resistors across the synchro windings. A clamp circuit (such as the one shown in Fig. 4·35) must hold the grid of $V_1$ to the bias voltage $-E_{gg}$ after the sweep is completed, even though the plate is executing a damped oscillation. The bias is so chosen that the tube passes a small quiescent current. Since the series resistance of $L_1$ is small, the average voltage across $L_1$ must be very nearly equal to zero. Therefore, the positive overshoot must have an amplitude that is large enough and a duration long enough to ensure that the area of the waveform above $E_{pp}$ is the same as the area below $E_{pp}$. This characteristic of an inductance is used in generating balanced waveforms (see Sec. 13·10). If the stator

[1] See *Sweep Generators*, Vol. 19 of the Radiation Laboratory Series.

leads of the synchro in Fig. 10·17 are applied directly to the plates of an electrostatic cathode-ray tube and if there is time enough between sweeps for the damped oscillation to reach a negligible amplitude, the sweep on the cathode-ray tube will rotate about the point corresponding to $T_1$. The time required for damping can be estimated by the rate at which a transient is damped out in a circuit where $L_1$, $R_1$, and $C$ are in parallel. If $R_1 \geqq \frac{1}{2} \sqrt{L_1/C}$, the value for critical damping, the amplitude of the oscillation decreases with $e^{-\frac{t}{2R_1C}}$. Thus at a time large compared with $2R_1C$, the voltage at the plate equals $E_{pp}$. In practice, a value of $R_1$ slightly greater than the value for critical damping returns the synchro rotor to its quiescent state in the shortest time. The amplitude of the overshoot may be very great if $C$ is small and if the period of
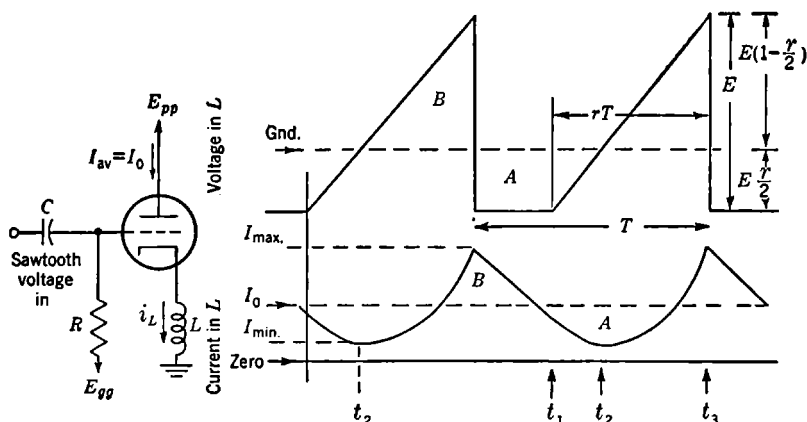


FIG. 10·18.—Voltage and current in an inductance driven by an ideal cathode follower.

oscillation is short. In fact this reverse overshoot voltage may reach an amplitude greater than the plate supply voltage and may need to be reduced in order to prevent insulation breakdown. If extra capacity is added across $L_1$ to reduce this amplitude, the period of the damped oscillation is increased.

Another simple circuit for applying a sweep voltage to a synchro is a cathode follower shown in Fig. 10·18 with voltage and current waveforms. In this circuit the energy is not extracted from the synchro rotor after each sweep as in the circuit of Fig. 10·17. Because of the low resistance of the inductance $L$, the average value of the voltage waveform applied to the synchro rotor is about equal to ground potential. The current through the synchro has a constant average value $I_0$ for all sweeps no matter what fraction of the recurrence period is used for the actual sweep.

Thus there is actually a small average voltage $E_0 = I_0 R_L$, which appears across $L$.

The voltage across $L$ is $e = L \dfrac{di_L}{dt}$ (neglecting $E_0$). At $t_2$, $e = 0$ and

therefore $L \dfrac{di_L}{dt} = 0$, and $i_L$ is a minimum. The areas $B$ and $A$ of the current waveform must be equal. Since the cathode follower must always have some current flowing through it in order to maintain damping action across $L$, it is necessary to draw an average current $I_0$ large
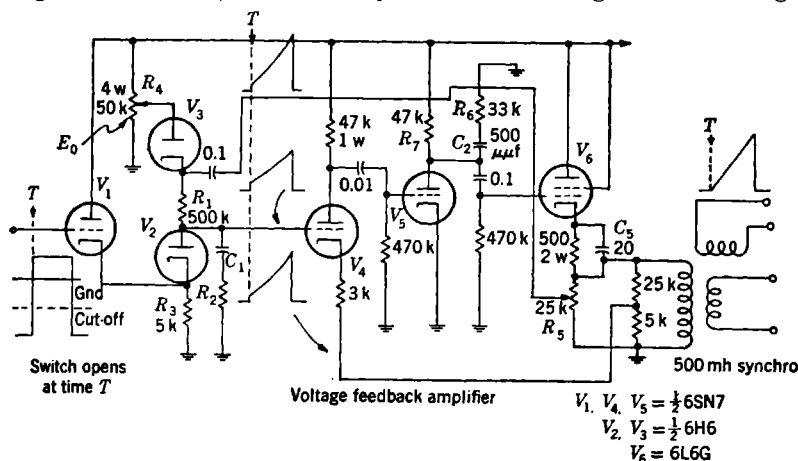


Fig. 10·19.—Typical circuit for applying a voltage waveform such as that of Fig. 10·5, across a synchro. The output tetrode can handle peak currents of about 150 ma at maximum waveform voltages of about 150 volts. $R_2$ and $C_1$ are chosen to give respectively the step and slope desired for the sweep waveform. $R_4$ also adjusts the sweep slope. $R_5$ controls the correction for low-frequency losses in the synchro.

enough to keep $I_{min}$ always positive. In order to design the amplifier output circuit so that it has adequate quiescent current $I_0$ and is capable of delivering $I_{max}$ without drawing grid current, it is useful to know the values of $I_0$ and $I_{max}$. The following symbols will be used:

$T$ = period of repetition,

$r$ = fraction of total time during which sawtooth is rising,

$E$ = amplitude of sawtooth voltage across $L$.

The average current is

$$I_0 = \frac{ErT}{L}\left(\frac{r^2}{8} - \frac{r}{3} + \frac{1}{4}\right) + I_{min}. \tag{52}$$

The maximum current is

$$I_{max} = \frac{ErT}{2L}\left(\frac{r^2}{4} - r + 1\right) + I_{min}. \tag{53}$$

$I_{min}$ may be set equal to zero.

A circuit that provides low output impedance with the aid of voltage feedback is shown in Fig. 10·19.

The midfrequency loop gain of this amplifier is about 10, and the normal output impedance of the 6L6G (about 200 ohms) is therefore reduced to less than 20 ohms. Nevertheless, there are appreciable low-frequency losses due to the finite resistance of the rotor. Therefore the circuit using the bootstrap principle has been designed to generate a sawtooth voltage of constantly increasing slope (i.e., with a $t^2$ correction term) by causing the voltage of the positive end of $R_1$ to increase faster than that of the negative end. It may be shown by calculating the value of $e_c$, the voltage across $C_1$, as a function of time that this inserts the $t^2$ term necessary for a linear output voltage. If the step resistor $R_2$ is zero and the current through $R_1$ is $i_{R_1}$,

$$e_c = \frac{1}{C_1} \int_0^t i_{R_1} \, dt. \tag{54}$$

But

$$i_{R_1} = \frac{E_0 + \mathcal{G}e_c - e_c}{R_1}, \tag{55}$$

where $\mathcal{G}$, the voltage gain of the amplified signal being applied to the positive end of the resistance $R_1$, is greater than one. When Eq. (55) is substituted in Eq. (54) and the resulting equation is solved for $e_c$, under the conditions that $e_c = 0$ when $t = 0$,

$$e_c = \frac{E_0}{\mathcal{G} - 1} \left( e^{\frac{(\mathcal{G}-1)t}{R_1 C_1}} - 1 \right). \tag{56}$$

When the exponential is expanded to a power series,

$$e_c = \frac{E_0}{R_1 C_1} t + \frac{E_0(\mathcal{G} - 1)}{2R_1^2 C_1^2} t^2 + \cdots . \tag{57}$$

Thus, to a first approximation, the correction term added by the extra gain in the feedback signal to the positive end of $R_1$ produces the required $t^2$ term. For any given $R_1$, $C_1$, and $E_0$, $\mathcal{G}$ can be adjusted by means of potentiometer $R_5$ to produce the desired magnitude of the $t^2$ coefficient. The resistor $R_2$ forms a step of amplitude $\dfrac{R_2}{R_1 + R_2} E_0$, which can be adjusted to form correctly the constant term in Eq. (44).

The switch circuit, which uses a diode and a cathode follower, has an advantage over the simple triode or pentode switch; namely, that there is no negative "*spike*" following the sawtooth waveform. When condenser coupling is used, this "*spike*" may otherwise be caused by the exceptionally low triode or pentode switch impedance at the time when

the grid waveform ends and large grid current is flowing.   Furthermore, the capacity "feedthrough" of the switching rectangular wave through $V_2$ is in the right direction to aid the start of the sweep waveform.

Another circuit capable of performing the same function is shown in Fig. 10·20.   Here all the low-frequency correction and some of the high-frequency correction to the sweep waveform is introduced directly[1] by the feedback circuit.   An extra winding on the rotor samples the flux in very nearly the same manner as the stator windings sample it.   The feedback circuit causes the voltage on this extra winding to be a step-plus-sawtooth voltage identical with the input voltage.   This method
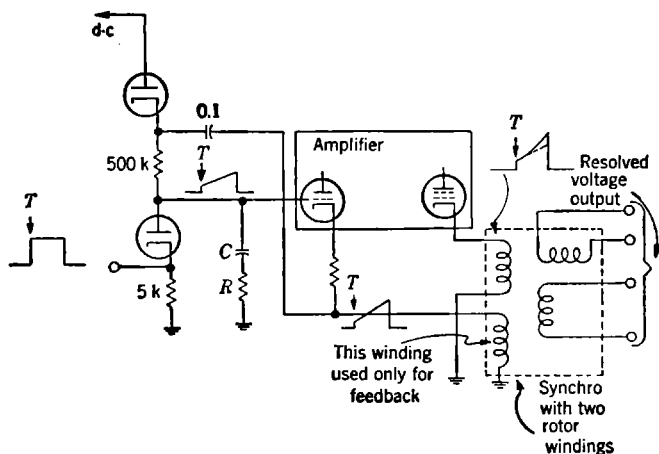


Fig. 10·20.—Method of correcting output-voltage waveform for low-frequency losses due to the finite output impedance of the amplifier and the resistance of the rotor.

corrects almost exactly for low-frequency losses, but corrects for only part of the high-frequency losses because the coupling coefficient of the two rotor windings is higher than that from the rotor to stator, and the distributed capacities are different.   The voltage on the stator winding has the same appearance as was shown in Fig. 10·19.   Some compensation for the frequency response between the two windings on the synchro rotor is usually necessary to prevent instability.   The $R_6$, $C_2$ network in the plate circuit of $V_5$ (see Fig. 10·19) performs this function.

A third method of correcting for low-frequency loss in the synchro is shown in Fig. 13·10.   Here an $RC$-network is inserted in the feedback lead from the synchro rotor.   This network peaks the low-frequency gain of the amplifier by reducing the negative feedback at low frequencies.

**10·7. Synchro Driving a Deflection Coil.**—In some applications, deflection-coil currents are obtained directly from a synchro.   The input

[1] Personal correspondence from General Electric Company, Receiver Division.

waveform to the synchro is of the same form as that used when a voltage output waveform is desired, but the coefficients of the various terms are different.    Figure 10·21 shows the equivalent circuit for a synchro and deflection coil with the distributed capacity transformed to the rotor winding.    In order to produce a linear deflection current $i_2 = kt$, the voltage across $M$ must be similar to Eq. (38):

$$M \frac{d}{dt}(i_1 - i_2) = (L_2 - M + L_3)\frac{di_2}{dt} + (R_2 + R_3)i_2. \qquad (58)$$

Neglecting the effect of $C$, the rotor current $i_1$ calculated from Eq. (58) is

$$i_1 = \frac{k}{M}\left[ (L_2 + L_3)t + \left(\frac{R_2 + R_3}{2}\right)t^2 \right] \qquad (59)$$

under the conditions that $i_1 = 0$ when $t = 0$.
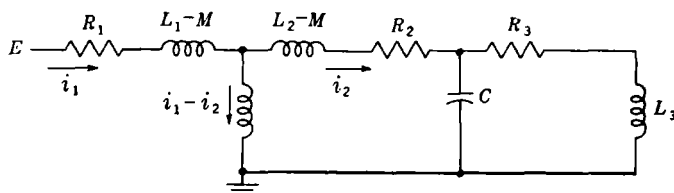


FIG. 10·21.—Equivalent circuit of a synchro driving a deflection coil $L_3$, $R_3$.

The input current, therefore, must be a sawtooth waveform plus a $t^2$ term.    The $t^2$ term is small compared with the $t$ term only when

$$t \ll 2\frac{(L_2 + L_3)}{(R_2 + R_3)}.$$

With the types of synchros and deflection coils available, this condition is not fulfilled for sweeps of more than 500 to 1000 $\mu$sec in length.    The circuit shown in Fig. 10·19 is an example of a circuit providing correction of this type.    In general, the same types of sawtooth amplifier circuits already discussed are applicable here.

Since there is some capacity, often as much as about 0.001 $\mu$f, across the synchro rotor and stator, there will be a delay in the start of the output waveform and it is usually necessary to damp out transient oscillations initiated by changes in input current.    In practice, damping resistors must be added across only the rotor of the synchro.    An approximate value of the rotor damping resistor may be determined by assuming the synchro to be an ideal transformer.    Then the stator capacity may be transformed to the rotor.    If $L$ is the total deflection-system inductance as measured at the rotor, and $C$ is the total equivalent capacity at

the rotor, the value of damping resistor needed for critical damping may be calculated from

$$R_{\text{critical}} = \frac{1}{2}\sqrt{\frac{L}{C}}. \tag{60}$$

If $L_1 = L_2 = 13$ mh, and $L_3 = 5$ mh, then $L \approx 5$ mh. If there is a capacity of 0.001 $\mu$f on both rotor and stator, $R_{\text{critical}} = 800$ ohms. This value is approximately what is required in an actual circuit (for Diehl synchro type FP). These damping resistors are sometimes added not across the rotor itself, but on the primary of the transformer driving the rotor (see Fig. 13·22). It is not desirable to have the damping resistors across the deflection coils because, in that case, their current would have to be supplied through the leakage inductance of the synchro, and an additional delay in the start of the sweeps would result.

# CHAPTER 11

## RECTANGULAR-COORDINATE DISPLAYS

### By L. D. Ellsworth

Rectangular-coordinate displays include three general types: the B-scan, the C-scan, and the television scan. The B-scan is characterized by a plot of the time interval against an independent variable; the C-scan gives a plot of two independently controlled variables, and the television scan presents two synchronized time-base sweeps. Signals are presented on the display by means of intensity modulation. For reference and increased accuracy in reading the graph, electronic markers may be used. The same results may be achieved by means of an overlay on the tube face, but care must then be taken to keep a fixed dimensional relationship between the electronic presentation and the overlay.

In order to obtain a display that has both low power consumption and a small number of circuit elements, an electrostatically focused, electrostatically deflected cathode-ray tube may be used. A tube of this type may also be employed wherever an extremely fast sweep, such as a fast-time-base sweep, is desired. If, however, better contrast, greater luminescence, and more nearly orthogonal traces are required, electromagnetically deflected tubes are superior.

## THE B-SCAN

**11·1. General Characteristics.**—The B-scan display is a plot of time interval against an independent variable. Basically, a B-scan unit consists of a cathode-ray tube and of some associated circuits having, in all, three input terminals. One input signal, a synchronizing trigger, which usually occurs at regular time intervals, initiates the time-base sweep. This sweep is generally oriented vertically on the tube face (display units made with the time-base sweep horizontal have been designated as E-scans). Another input signal is a voltage proportional to a function $f(x)$ of an independent variable $x$. It controls the horizontal sweep, and hence the lateral position of the vertical sweep. In order to obtain a recurring pattern, $f(x)$ must be periodic. The period of the function of the independent variable is, in general, much greater than the time interval between synchronizing triggers. In fact, the vertical sweep is obtained from a-c–coupled circuits whereas the horizontal sweep, because of its relatively low periodicity and because of the possibility

384

that it may assume a stationary value, is obtained from direct-coupled circuits. Under these circumstances, the vertical traces are straight lines and are sufficiently close together to give an essentially solid picture (Fig. 6·1). The signals and reference marks that intensity-modulate the scan are applied to the third input terminal.

The independent variable $x$ may be any physical quantity, such as an angle, a distance, or a voltage. In radar displays the quantity $x$ is an angle, and $f(x)$ is equal either to $x$ or to sin $x$. The resultant display of angle against time maps in rectangular coordinates an area that has been scanned in polar coordinates as shown in Fig. 11·1 (see Chap. 13). Here distortion is introduced as shown in Fig. 11·2, and vectors between
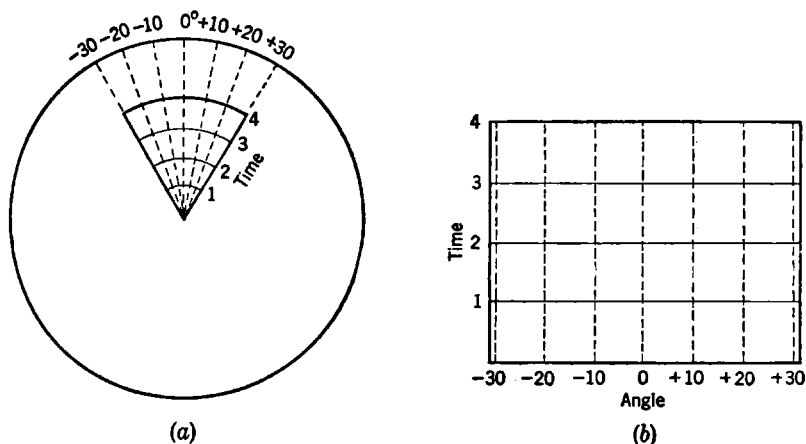


Fig. 11·1.—Distortion of a sector when presented in a B-scan. Equal areas present (a) on a true sector and (b) on a B-scan.

points are changed both in magnitude and in direction; nevertheless, signal position may be determined by interpolation between angle and time indices such as those shown in Fig. 11·1. The simplest B-scope unit has the following features: (1) The time-base sweep begins at zero time (time is measured from the synchronizing trigger); (2) the speed of the vertical sweep may be fixed or variable; (3) the value of $f(x)$ at the center of the tube, $f(a)$, is arbitrarily chosen and fixed; (4) the horizontal sweep represents a fixed or a variable range of $f(x)$ centered about $f(a)$.

A more flexible unit may be designed by adding to these features a circuit to delay the start of the time-base sweep, which then includes the time interval between $t_1$ and $t_2$, where $0 \leqq t_1 < t_2$ and $t_2$ is the maximum value of time to be plotted. As $t_1$ becomes greater, the distortion of a B-scan that represents a polar-coordinate sector decreases (Fig. 11·3).

Additional versatility is obtained from a movable display in which

any value of $f(x)$ may be centered on the tube.    This feature is partic-
ularly useful if successively different intervals of the complete cycle of
$f(x)$ are to be plotted.



(a)                                                  (b)
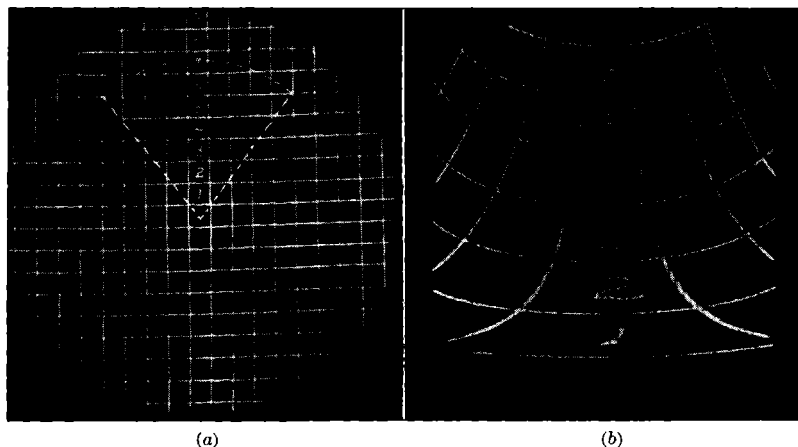
FIG. 11·2.—Distortions produced by a B-scan used as a map sector: (a) shows grid
squares which may be superimposed on a true map; (b) shows the corresponding squares as
distorted by a B-scan.



(a)                                                  (b)
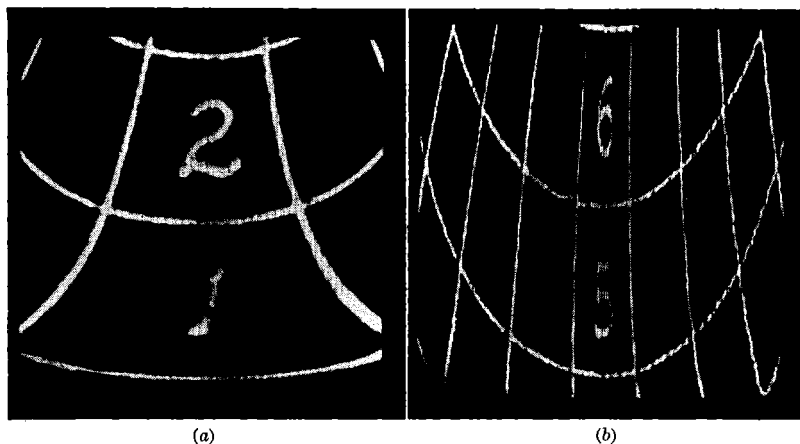
FIG. 11·3.—Pattern of a B-scan with no range normalization.    (a) 50-mile B-scan, zero
delay.    (b) 50-mile B-scan, 4-unit delay.

**11·2. Methods of Producing a B-scan.**—A block diagram of a typical
B-scope is shown in Fig. 11·4.    In the time-base-sweep block, a trigger
is applied to a selective buffer amplifier that is intended to prevent any
other information that may be present on the same transmission line
from also acting as a trigger signal.    The output signal of the buffer
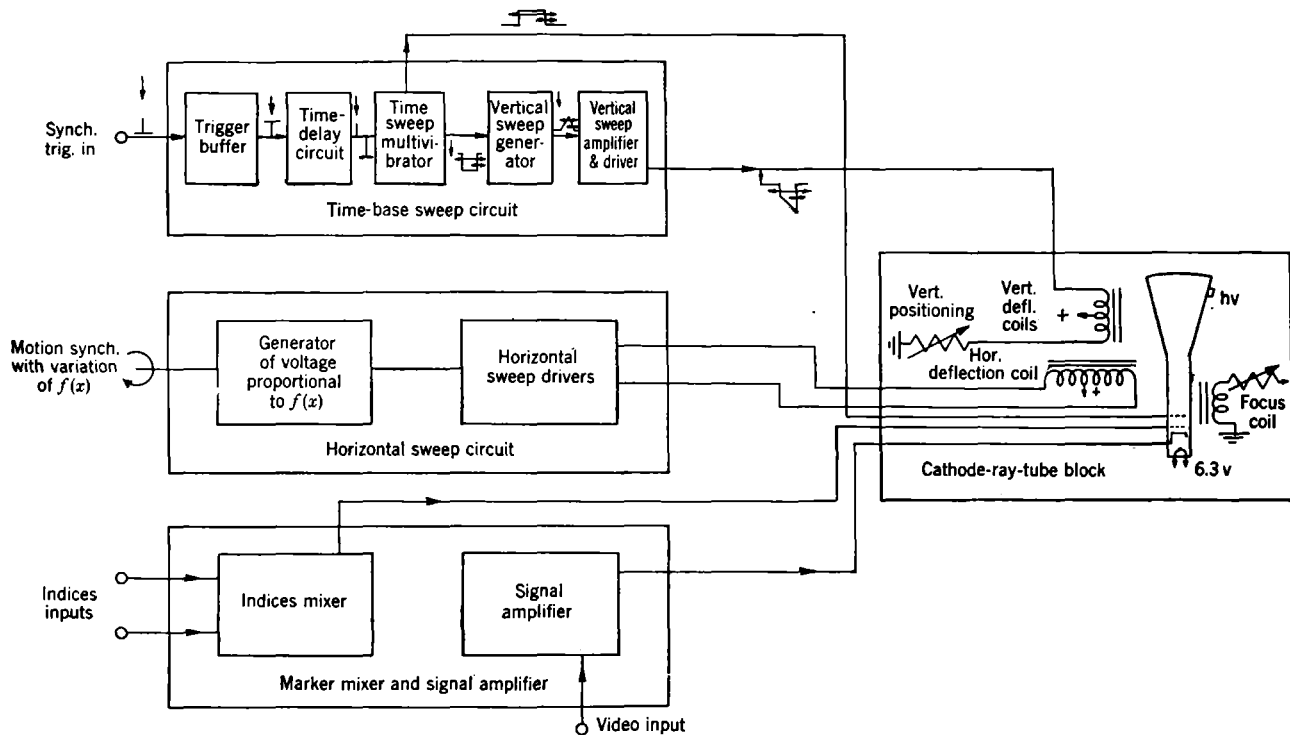
FIG. 11·4.—Block diagram of typical B-scan unit.

amplifier triggers a time-delay circuit, which furnishes a delayed trigger to the master multivibrator. This circuit produces positive and negative square waves having the desired time duration. The positive square wave, applied to the first anode of the cathode-ray tube, brightens the trace during the time of the sweep. The negative square wave opens the electronic switch associated with a voltage-sawtooth-waveform generator. By means of the amplifier and sweep driver, a similar current waveform is driven through one of the vertical deflection windings. Vertical positioning of the trace is controlled by the direct current through a second vertical deflection winding.

The horizontal-sweep block contains a source of voltage proportional to the value of the function of the independent variable $f(x)$, and sweep drivers that produce currents through the horizontal deflection windings proportional to this voltage. The voltage source may be any of those mentioned in Chap. 5. A movable display may be made if some mechanical or electrical means of orienting the voltage source with respect to the input shaft is available. This orientation may be done mechanically either by rotation of the potentiometer, condenser, or synchro-stator frame, or by the insertion of a mechanical differential between the driving shaft and the voltage source; or it may be done electrically by the use of a differential synchro.

The choice as to whether potentiometer, synchro-carrier, or condenser-carrier methods of obtaining voltage information should be used depends upon the desired horizontal-sweep speed, the permissible phase lag in $f(x)$ (especially important when scanning back and forth over an interval of $f(x)$ or when scanning at variable rates), the required filtering of ripple voltage, and the expected life of the equipment. For high scanning speeds (about 10 cps) the condenser-carrier method is most suitable because (1) the condenser can be operated at higher rotational speeds than the potentiometers and synchros now available, (2) the carrier frequency may be relatively high (1 Mc/sec or more) requiring little filtering of the detected output and hence small phase lag, and (3) the life is quite long. Synchros may be operated at slower speeds (up to about 1 cps) and lower values of carrier frequency (maximum of 25 kc/sec). Advantages of this method are that the data are free from noise, and the life is long. On the other hand, the potentiometer method is certainly the easiest and cheapest, and recently developed potentiometers have long lives (10 million revolutions). However, the data tend to be noisy; sufficient filtering minimizes this effect but phase lags may then become excessive.

The signal and marker amplifiers included in the complete circuit are usually fairly wide bandpass circuits (1 to 10 Mc/sec) in which the selection of the pass band depends upon several factors (such as resolu-

tion, sweep speed, and tube spot size) discussed in Sec. 4·8; and in which the gain depends upon the voltage level of the input signals. It is desirable to apply signals of at least 35 to 40 volts to the cathode-ray tube. Sometimes the markers are mixed with the signals, but often it is found much easier to insert them on different elements of the tube. If more than one type of electronic marker is to be shown on the tube face, they are mixed first.

The cathode-ray-tube block includes the tube itself, deflection and focus coils, and intensity and focus controls.

If the scanner rotates continuously in one direction, the horizontal sweep must be blanked out during its return time or the return time must



(a)                                        (b)
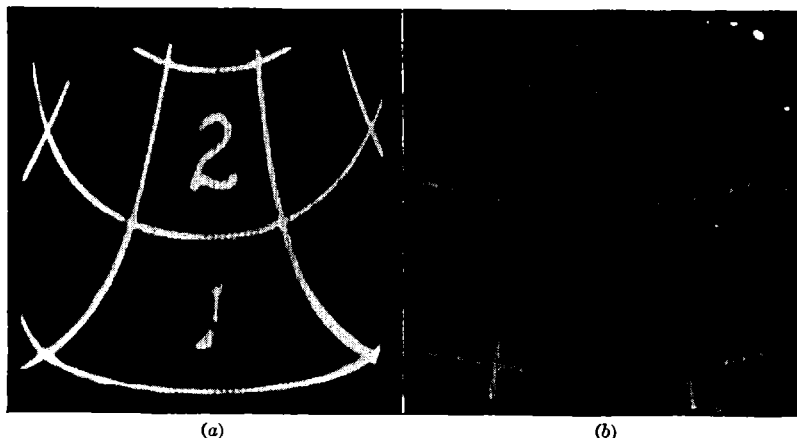
FIG. 11·5.—Pattern of B-scan with range normalization. (a) 50-mile B-scan, 0 delay. (b) 50-mile B-scan, 3-unit delay, range normalization.

be so short as to leave no visible trace on the tube. Otherwise two sets of data will be presented for two different values of $f(x)$. For an oscillating scanner it is necessary only to insure that $f(x)$ is a single-valued function of the scanner angle.

One variation of a B-scan should be considered in connection with the reproduction of a sector of a polar-coordinate sweep with a radial time base (in radar, a map sector). If the vertical sweep is delayed in time so that later time intervals may be presented, the conventional B-display preserves nearly constant spacing between angle indices with increasing delay. This effect increases the lateral-distance scale factor with increasing time as is evident in Fig. 11·3 where the lateral spacing of angle marks is much less in *b* than in *a*. At times it is desirable to preserve the lateral scale factor. This can be done if the horizontal sweep speed is increased in proportion to the time delay of the start of the sweep, a process known as "range normalization." The vertical time sweep must

be fairly short because only an average normalization can be introduced. In Fig. 11·5 the average distance between angle marks with range normalization is more nearly the same for $a$ and $b$ than is the case without normalization shown in Fig. 11·3$a$ and $b$. With a range-normalized scan, an overlay using a fixed scale factor may be placed over the display to determine distance between points with a reasonable degree of accuracy.

**11·3. Examples of B-scopes.**—A typical B-scope is described in block form in Fig. 11·6, and the corresponding circuit diagram is shown in Fig. 11·7.

The independent variable controlling the horizontal sweep is the angular position of a scanner; the voltage supplied to the sweep drivers is proportional to the sine of the scanner angle, as measured from a fixed reference point. This particular B-scope includes a movable sector obtained by employing two synchros so that, by adjustment of the rotor of the type 1CT synchro (Fig. 11·7), any angle may be set at the center of the cathode-ray tube.

A 1500-cps carrier of 200 volts peak-to-peak amplitude is generated by the oscillator circuit, consisting of $V_1$ and the tank circuit, a 0.05-$\mu$f condenser $C_1$ in parallel with the rotor of a size-5G synchro that rotates synchronously with the scanner. If the size-5G synchro is rotating at constant angular velocity, and if the shaft of the type 1CT synchro is stationary, the rotor output from the 1CT synchro is a modulated carrier such that the modulation envelope consists of two symmetrical sine waves, 180° out of phase, in which the period $T$ is the same as that of the variation of angle (2 to 10 rpm), (refer to waveforms on block diagram, Fig. 11·6). The output waveform of the 1CT synchro, after passing through a cathode follower $V_2$, is demodulated by a phase-sensitive rectifier $V_3$ in such a way as to obtain only one of the sine waves making up the envelope. This rectified voltage, applied to the cathode-coupled horizontal-sweep drivers $V_4$ and $V_5$, controls the current through the horizontal deflection coils.

Except for the known voltage change in the cathode follower, the d-c voltage level placed on the modulated carrier by the potentiometer $R_1$ (which is also the voltage at points $A$ and $B$ on the waveform shown in Fig. 11·6) is maintained through the following circuits and applied to the input grid of one of the horizontal drivers. The voltage of the other driver grid is adjusted by potentiometer $R_2$ so that the two drivers are drawing equal currents at angles corresponding to the null points $A$ and $B$ of the modulated carrier. Because the deflection coils are connected in push-pull, the trace is then centered horizontally.

The null points are determined by the orientations of the rotors of the 5G and 1CT synchros relative to their respective stators. By turning

FIG. 11·6.—Block diagram, B-scan.

FIG. 11·7.—Circuit diagram, B-scan.

the 1CT rotor, the null positions are changed, and accordingly the azimuthal angles appearing at the center of the tube are changed. It must be noted that the null points are located at two azimuthal positions, 180° apart. Furthermore, the slope of the voltage curve at one null is positive, whereas that at the other is negative and gives rise to sweeps in different directions at each 180°. Since the scanner rotates continuously in one direction, it is desirable to blank out one of the two sweeps, the "reverse azimuth sweep," to avoid presenting two sets of information on the scope.

During the time of the reverse azimuth sweep, the "flop-over" $V_8$ provides positive blanking pulses on the cathode of the cathode-ray tube. The output voltage of the phase-sensitive rectifier is applied to one grid of $V_8$, with the result that only one section conducts at a given time. The section that conducts is determined partly by the value of the input grid voltage, but mostly by the sign of the slope of the voltage curve at that point. Figure 11·8 makes this clear.

The vertical sweep, or range sweep, uses no feedback to linearize the current through the vertical deflection coil; the simplicity is permitted by the relatively slow time sweeps (250 to 1000 $\mu$sec) that were needed and by the low requirements on linearity. A more complicated circuit, using current feedback for increased linearity, could be used for the range sweep (see Chap. 10).



Fig. 11·8.—Method of blanking return azimuth sweep in a B-scan. (a) Azimuth sweep voltage sine wave applied to grid of azimuth sweep-blanking tube $V_{8a}$. (b) Square-wave blanking pulse on plate of $V_{8,b}$ which is used to blank the cathode-ray tube during the positive interval, *EF*, corresponding to the time of the reverse sweep control about *B*. Dashed portion of (a) represents reverse azimuth sweep.

The synchronizing trigger, about 40 volts positive, is buffered by a trigger discriminator tube $V_{11}$, which is so biased that only the inverted trigger will appear on the output terminal. A time-delay "flip-flop" $V_{12}$ is used to delay the time of the start of the sweep by an arbitrary amount. The positive rectangular wave from the delay circuit is differentiated, and the resulting positive and negative pulses are applied to the master flip-flop, which is fired only by negative triggers. Hence, the sweep flip-flop is triggered only by the falling edge of the delay gate. To eliminate jitter of the time-base sweep, it is important that the delayed

FIG. 11·9.—Block diagram of B-scope.

trigger represent a stable time delay, with a minimum of pickup.   For this reason the VR-150 voltage-regulator tube $V_{13}$ is used to supply d-c voltage with very low ripple to the cathode-coupled delay flip-flop.   The master flip-flop, producing negative and positive rectangular waves of the desired time duration, supplies the positive rectangular wave to the first anode of the cathode-ray tube to brighten the trace during the time of the sweep.   The negative rectangular wave operates the switch tube $V_{15a}$ to provide in the plate circuit a voltage sawtooth waveform.   The positive sawtooth voltage is a-c coupled, and d-c restored to the proper bias level, to the grid of the single-ended vertical sweep driver $V_{16}$ to give an approximately linear current through one vertical deflection winding.   Direct current through the other vertical deflection winding, controlled by $R_3$, determines vertical positioning of the trace.   The sweep driver $V_{16}$ is biased nearly to cutoff between sweeps so that, without centering current, the vertical sweep will begin at about the center of the tube.

Video signals, 6 to 10 volts in amplitude, are amplified in one stage, $V_6$, and a-c coupled to the cathode of the cathode-ray tube.   The cathode is d-c restored to a selected bias controlling the brightness of the trace. Angle and time indices are mixed nonadditively in a cathode-follower and inserted on the grid of the cathode-ray tube.   The focus is controlled by $R_4$.

An extremely simple B-scope may be designed by combining the vertical sweep circuit in the preceding unit with the horizontal sweep circuit used in the example of a C-scan (Sec. 11·5).

A block diagram of another typical B-scope is given in Fig. 11·9 and a circuit diagram in Fig. 11·10.   Particular features of this instrument include: (1) a very fast time-base sweep, 15 $\mu$sec in duration, which may start at zero time or at any accurately controlled delayed time; (2) a fast azimuth sweep (16 sweeps per second), which is greatly expanded (covering about 5° in azimuth) and in addition is range-normalized so that distances on the scope will be preserved regardless of the time delay; (3)

TABLE 11·1.—ADDITIONAL INFORMATION REGARDING PARTS INCLUDED IN FIG. 11·10

| Part no. | No. of turns | Wire size | Form, in. |
| --- | --- | --- | --- |
| $L_1$ | 50* | #18 | 2 |
| $L_2$ | 50 | #28 | $\frac{1}{8}$ |
| $L_4$ | 51 | #28 | $\frac{1}{8}$ |
| $L_5$ | 55 | #32 | $\frac{1}{8}$ |
| $L_6$ | 52 | #28 | $\frac{5}{16}$ |
| $L_7$ | 55 | #28 | $\frac{5}{16}$ |

* Tapped 9½ turns.
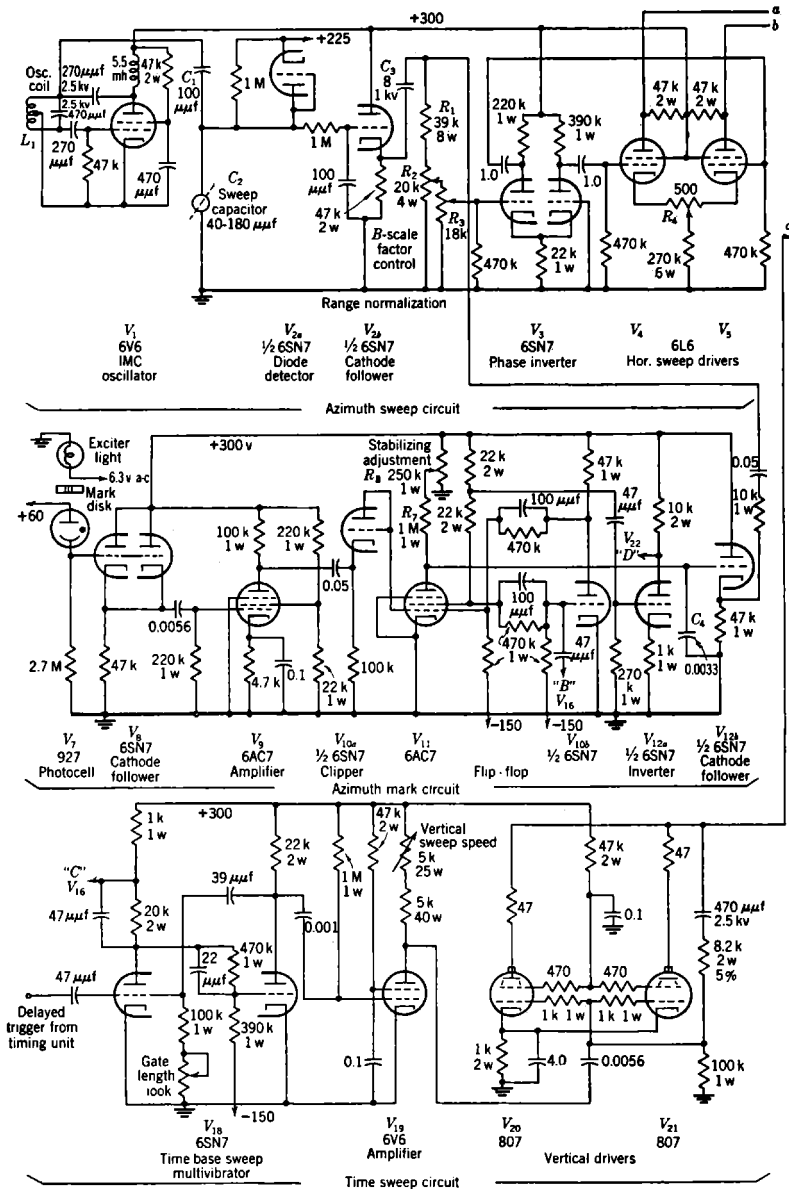
FIG. 11·10.—Circuit diagram of B-scope. See
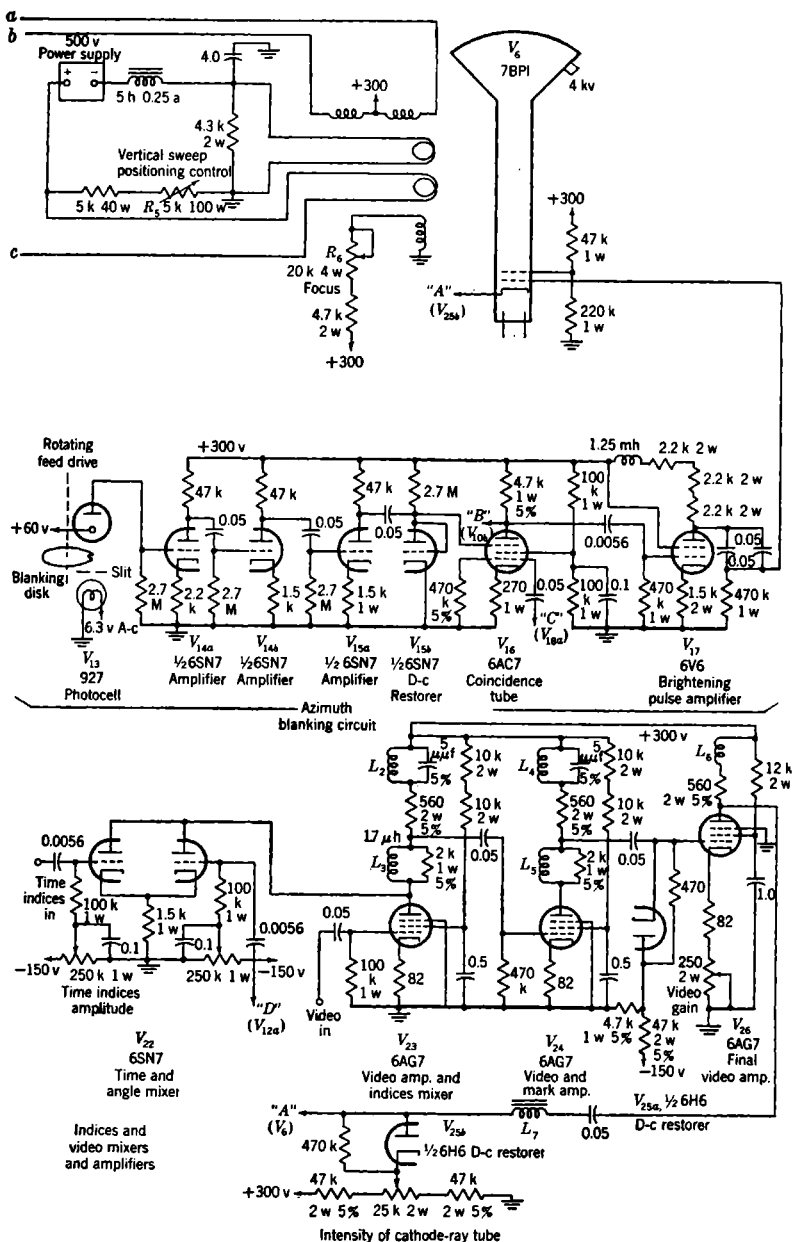
Table 11·1 for additional information.

three accurate 1° electronic angle markers centered in the display; and
(4) blanking of the cathode-ray tube by means of a photoelectric-cell
switch at all azimuth angles except those to be presented on the tube.

Voltage for driving the horizontal sweep is obtained by the condenser
method of data transmission. The sweep condenser is effectively geared
to the scanner so that 320° rotation of the condenser corresponds to 10°
variation in azimuth. During the remaining 40° rotation of the con-
denser, the azimuth sweep is restored to its initial position (see Fig. 11·11).

The output from a 1-Mc/sec oscillator $V_1$ (Fig. 11·10) is applied to a
voltage divider, consisting of $C_1$ in series with the sweep capacitor $C_2$
whose capacity varies linearly with the angle of rotation. The values of
the two capacities at all angles are such that the fraction of the carrier
voltage that appears across the
sweep condenser is proportional to
the angle of rotation of the con-
denser rotor. This modulated
carrier voltage is then detected by
$V_{2a}$, and the demodulated carrier
is filtered and inserted into a
cathode-follower stage $V_{2b}$ to lower
the driving impedance. Because
the azimuth sweep is relatively
fast compared with the one used
in the B-scope previously de-
scribed, the azimuth voltage from
the cathode follower is a-c coupled
to the driving stage. Potentiometer $R_2$, the scale-factor control, con-
nected across the azimuth voltage, determines the amount of that
voltage to be supplied to the driving circuits and therefore determines
the azimuth scale. To compensate for the change of lateral scale
factor with time delay of the vertical sweep, the range-normalization
potentiometer $R_3$ is added. This potentiometer is mechanically con-
nected to the manual control that determines the time of delay of the
start of the vertical sweep, so that, as the time delay is increased, the
amount of available azimuth voltage at the brush of $R_3$ to be supplied
to the sweep drivers is proportionally increased. The range-normalized
azimuth voltage is split into two phases, 180° apart, by the phase inverter
$V_3$, to provide push-pull voltages to the two horizontal sweep drivers $V_4$
and $V_5$. The horizontal deflection coils are driven in push-pull from the
plates of these tubes. By proper adjustment of the tapped resistor
(potentiometer $R_4$) between the two cathodes of the drivers, the tubes
are made to draw equal currents when their grids are at the same poten-
tial, thereby centering the horizontal sweep.



FIG. 11·11.—Relation between rotation
of the azimuth sweep condenser and azimuth
position.

The "stabilization sawtooth" voltage, which is coupled into the azimuth sweep voltage at the junction of $C_3$ and $R_1$, is added to the horizontal sweep voltage only at the three positions where angle indices are to appear on the tube.[1]   At these positions, this superimposed waveform stops the horizontal sweep always at the same voltage for a given mark just long enough to ensure that the angle marks will be located at the same positions for successive scans.

The azimuth-mark circuit performs two functions: (1) It provides the three azimuth marks to intensity-modulate the tube; and (2) it supplies the stabilization sawtooth waveform. A disk, rotating synchronously at 16 cps, intercepts the light to a photocell $V_7$ except when one of the three slots that are effectively 1° apart in azimuth is passing through the beam. Positive impulses generated at these three points are applied to a cathode follower $V_8$ and are then inverted and amplified in $V_9$. The negative output signal from the amplifier is clipped by $V_{10a}$ and used to trigger the flip-flop multivibrator, $V_{11}$ and $V_{10b}$. To the other input terminal of the flip-flop is applied a negative range gate 4000 times a second (since the repetition rate of the trigger is 4 kc/sec). This gate coincides with the time interval of the vertical sweep. The flip-flop is insensitive



Fig. 11·12.—Production of azimuth mark and stabilization of azimuth sweeps at the time of the mark. Shaded area in (e) represents time interval of azimuth mark during which the azimuth sweep voltage is practically constant. The horizontal scale is greatly compressed as compared with the vertical scale. (a) Positive square wave on screen of $V_{11}$. (b) Waveform (a) differentiated. (c) Inversion and amplification of (b). The positive square wave is the angle mark that coincides with a range sweep. (d) Stabilization sawtooth voltage generated on plate of $V_{11}$. (e) Stabilized azimuth voltage.

to these negative pulses except for the first one that occurs immediately after an angle pip has "triggered" the flip-flop. The net result is that there appears on the screen of the $V_{11}$ section of the flip-flop a positive square wave, which begins with the azimuth-mark pulse and ends at the beginning of the range sweep (see Fig. 11·12). This positive square wave is differentiated, inverted, and clipped to produce a leading negative pip and a lagging positive pip that occurs at the time of start

[1] See Sec. 6·2, Fig. 6·8, sweep-stopping circuit.

of the vertical sweep and that is about 16 μsec wide. The information is applied to a mixer stage $V_{22}$, which is sensitive only to the positive pip, and there it is mixed with time indices and ultimately with the video signals to intensity-modulate the cathode beam of the cathode-ray tube.

The stabilization sawtooth waveform is produced on the plate of the $V_{11}$ section of the flip-flop. Actually it ends right at the time of the start of the intensified vertical sweep corresponding to the angle mark, but the azimuth sweep voltage returns to its normal level so slowly in comparison with the 16-μsec time duration of the sweep that the shift is not noticeable. The $RC$ sawtooth circuit consists of $R_7$ and $C_4$; the amplitude of the stabilization sawtooth waveform is controlled by potentiometer $R_8$. A cathode-follower driver $V_{12b}$ is used to mix the sawtooth waveform with the normal azimuth sweep voltage.

The azimuth blanking circuit prevents a positive gate, coincident in time with the vertical sweep, from raising the grid of the cathode-ray tube to conduction level during the time of the reverse azimuth sweep. Whether or not the positive brightening pulse is transmitted to the tube through the part of the blanking circuit consisting of the coincidence tube $V_{16}$ and the amplifier $V_{17}$ depends upon the voltage on the suppressor grid of $V_{16}$. During the 320° when the associated blanking disk is interrupting the light to the photocell $V_{13}$, this grid is at ground level, the brightening pulse is transmitted, and a sweep is visible on the tube. This 320° is the angle through which the sweep condenser rotates to produce the normal 10° azimuth sweep. During the remaining 40° rotation, the suppressor grid of the coincidence tube is sufficiently negative (because of the impulse received from the photocell) to cut off $V_{16}$. Therefore, the reverse sweep is blanked.

In the vertical sweep circuit, the time-sweep multivibrator $V_{18}$ is triggered by the delayed trigger from a timing unit. A positive time gate from the plate of $V_{18a}$ is coupled to the coincidence tube $V_{16}$. A negative time gate from $V_{18b}$ is amplified and inverted by $V_{19}$ to supply a positive pulse to the two grids of the vertical sweep drivers $V_{20}$ and $V_{21}$ operating in parallel. It is necessary to apply a large rectangular wave of voltage across the deflection coil to produce the fast vertical sweep. Voltage feedback from the deflection coil to the grids of the sweep drivers acts to start the vertical sweep faster, and to make it more linear.[1]

The vertical position is determined by the direct current through the other vertical deflection coil; rheostat $R_5$ is used to control this current. The focus-coil current is adjusted by rheostat $R_6$. The first anode of the cathode-ray tube is tied to a fixed potential.

Another part of the complete circuit includes marker and video mixers and amplifiers to intensity-modulate the cathode-ray tube.

[1] For a more complete discussion of this type of feedback, see Sec. 10·2.

Time and angle indices and video signals are mixed in the two halves of $V_{22}$, and in $V_{23}$, respectively, since these three sections contain a common plate load.

## THE C-SCOPE

**11·4. General Principles.**—A C-scan is a rectangular display in which each of the two coordinates is a function of an independent variable. The points are plotted on this coordinate system by applying an intensifying signal to the cathode-ray tube whenever the values of independent variables are such that the phenomenon under investigation occurs. The two coordinate axes are generated by the horizontal and vertical sweeps from voltages proportional to the desired functions of the two independent variables.

To emphasize the general features of this display, an example will be cited which illustrates its fundamental graphical properties more clearly than does the radar example. In order to obtain a plot of the characteristics of a triode vacuum tube, a deflection-modulated display (Chap. 7) could be used to show the variation of $i_p$ with either $e_g$ or $e_p$, provided that one of these variables was held constant. However, with a C-scan, a plot may be obtained of all the combinations of $e_g$ and $e_p$



Fig. 11·13.—Curves of variation of plate current with plate voltage and grid voltage.

which correspond to a given value of $i_p$. The vertical position of the cathode-ray-tube beam could be controlled by $e_g$ whereas the horizontal position could be controlled by $e_p$. Then, the proper circuits could be set up to give an intensifying pip any time that $i_p$ reached a given value such as zero.

Figure 11·13 shows the resultant display. The line $i_p = 0$ (the cut-off point for the tube) is shown as a solid line. Similar plots of $i_p = I_1$, or $i_p = I_2$, could also be presented. In order to give continuous information, it is desirable for one of the independent variables to go through its range of values much more rapidly than the other.

Figure 11·14 illustrates the advantages of this method of proportioning sweep speeds. To develop the display of Fig. 11·13 it would be simplest to vary the grid voltage through its range of values while the plate voltage changed slightly.

In radar, the C-scope is used to present azimuth vs. elevation angle

of a radar beam that is sweeping systematically (in azimuth and eleva-tion) through a given sector of space. At certain combinations of the two variables, targets are located and appear on the screen as intensity-modulated echoes.

If this were the whole story, designing a C-scan would involve only altering the vertical sweep of a B-scan so that it, like the horizontal sweep, would be controlled by an independent variable. But a compli-cating factor is added in pulsed systems, including radar, because of the time factor that must be considered. The time-base sweep, which nor-mally resolves signals and noise, tends to add a third dimension to the two-dimensional display of azimuth vs. elevation angle. To be consist-
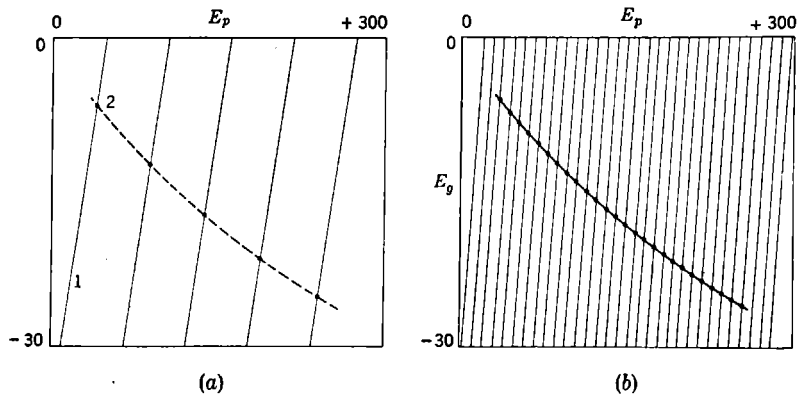


FIG. 11·14.—Effect of increasing vertical sweep speed relative to horizontal sweep speed. (a) Horizontal sweep speed about ½ vertical sweep speed. The vertical sweep is shown at 1; the intensity modulated signal at 2. (b) Horizontal sweep very slow com-pared with vertical sweep.

ent with the constraints imposed by the two dimensions, the time-base line must be compressed to a dot, and all the information appearing along that time-base line integrated to make up the total intensity of the dot. However, if the information of interest occupies but a small time interval of the total time-base line, as is usually the case in pulsed systems, its signal contributes but a small incremental effect to the integrated intensity. Physically this means that it would be very difficult to differentiate between a spot in which the signal occurs and one in which only noise occurs.

The only effective way to gain the needed contrast between a position in azimuth and elevation containing a signal and one without a signal is to locate in range a small pedestal on the target, and to bias the cathode-ray tube so that only during the short time interval represented by the width of the pedestal is the screen of the cathode-ray tube brightened, regardless of the azimuth-elevation position of the antenna. The noise

and signal are integrated only over the brief time corresponding to the pedestal This, then, is a condition for satisfactory operation of a C-scope in pulsed systems to distinguish signals from noise. To fulfill the condition, it is almost a necessity to operate simultaneously another type of display, such as an A-scope, in which the time base is resolved into a line on which the pedestal may be located over the target. This range pedestal restricts the space area that can be presented on the display; therefore the C-scope is a plot of azimuth and elevation only over a small interval of range. The size of this range interval must be kept small if weak signals are to be recognized in the midst of noise.
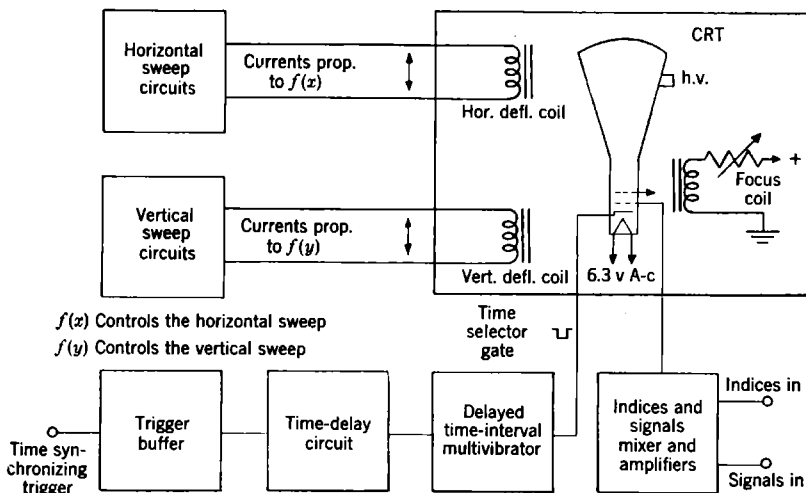


FIG. 11·15.—Simplified block diagram of C-scope.

A simplified block diagram of a C-scope is shown in Figure 11·15. The horizontal and vertical sweep circuits are similar to those used for the horizontal sweep of a B-scope; in fact, they may be identical. The signal-amplifier and marker-mixer block and the cathode-ray-tube block also resemble corresponding parts in a B-scope. The only addition in the case of the C-scope is a time-selection circuit, which provides for a time pedestal to brighten the cathode-ray tube only during the time interval occupied by the signal of interest. This time-pedestal feature is necessary only for pulsed systems. For a simple system, in which one is interested in plotting only the variation of a phenomenon with respect to two independent variables regardless of a time consideration, a C-scope may be extremely simple and may involve no electronic components except for signal amplifiers and the cathode-ray tube.

The time-selector circuit consists fundamentally of a time-delay

circuit that gives sufficient delay to locate the pedestal on the signal and a delayed-time-interval multivibrator to produce a delayed square wave. This delayed waveform may be connected directly to some element of the cathode-ray tube to brighten the tube, or it may be inserted into the signal amplifier so that signals will be transmitted to the tube only during the time interval of the pedestal. It is important to remember that the time-selection pedestal is operating no matter what the values of the two independent variables may be.

**11·5. Example of a C-scope.**—The circuit diagram of a typical C-scope is shown in Fig. 11·16.

The azimuth and elevation sweep circuits are identical, and of the type that could equally well be used to provide the horizontal sweep of a simplified B-scope. Each circuit consists only of a deflection coil connected directly across two contact arms (180° apart) of a full-circled potentiometer (see Chap. 5). The potentiometer is connected from the +24-volt d-c source to ground as shown. When the contact arms are each at the half-way voltage point between 24 volts and ground, no current flows through the coil, and the trace is centered. Rotation of the contact arms in one direction or the other from the central position deflects the beam in the corresponding direction from the center of the tube.

There are some objections to this method. If the winding of the potentiometer is linear, then the current drawn by the potentiometer from the power source must be large compared with the current through the deflection coil. Otherwise, the deflections would not be linear. To obtain a low-resistance potentiometer, the wire used must be rather large, and, consequently, poor continuity of data transmission or large potentiometer noise will result. Although the linearity may be improved by properly tapering the winding, the current taken from the potentiometer by the deflection coil will usually still be sufficient to require wire size large enough to cause considerable noise and short life. These factors must be balanced against the accompanying circuit simplicity to determine whether the potentiometer method, as used in this circuit, is suitable for a particular case.

Control of the horizontal and vertical positioning is obtained by two air-core coils on the same form, placed inside of the focus coil. Dual potentiometer $R_3$ determines the vertical centering and dual potentiometer $R_4$ determines the horizontal centering. The current through the focus coil is controlled by $R_5$.[1]

---

[1] Alternatively, the centering coil may be a square coil similar to the deflection coil, but with a stack height of only $\frac{1}{4}$ in., interposed between the focus and deflection coils. Neither of these methods of centering is so satisfactory from the standpoint of performance as that of centering by means of extra windings on the deflection coil itself.
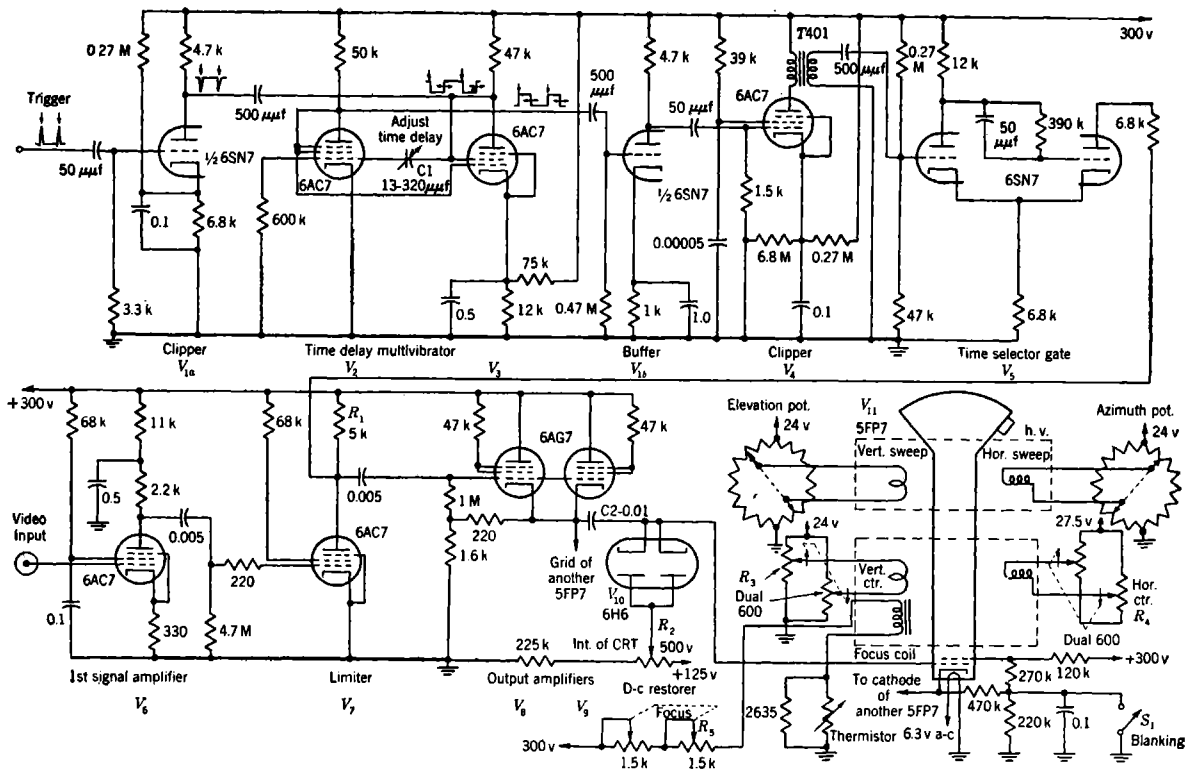
Fig. 11·16.—Circuit diagram of C-scope.

The circuit used to obtain the delayed time-selector gate could be simplified for some applications by omitting some of the clipper and buffer stages.   In this circuit, a positive trigger is amplified and inverted by $V_{1a}$, and the negative output pulse is used to trigger the time-delay flip-flop consisting of $V_2$ and $V_3$.   The amount of delay is controlled by the value of the variable condenser $C_1$.   The positive rectangular wave from this flip-flop is buffered from the gate circuit and amplified by $V_{1b}$. The output of the buffer is a positive pulse at the delayed time (end of flip-flop waveform).   This pulse is differentiated and applied to a clipper tube $V_4$, which is so biased as to transmit only the positive differentiated pip.   By transformer coupling to the plate of the buffer tube, the delayed positive trigger is applied to a cathode-coupled multivibrator, the time-selector gate generator $V_5$.   Part $(R_1)$ of the plate resistance of the section that gives a positive gate is common with the limiter section $V_7$ of the video-amplifier circuit; thus a video signal that occurs during the time interval of the time-selector gate is placed on top of that pedestal. The mixed output of the time-selector gate and the video signal is then applied through cathode followers $V_8$ and $V_9$ to drive a low-impedance cable.   Before this information is applied to the grid of the cathode-ray tube, it is connected through $C_2$ to a d-c restorer that restores the voltage level to a value set by $R_2$ so that only the video information will intensify the tube.

The cathode of the cathode-ray tube is held at ground potential during the normal sweep intervals because $S_1$ is closed.   At the time of the return sweep, however, $S_1$ is opened to put the cathode at a positive level and, therefore, to blank the tube.   The first anode is held at a fixed, positive potential.

### TELEVISION DISPLAYS

**11·6. General Principles.**—The third type included under rectangular-coordinate displays is the television scan.   Here the two sweeps are functions of time, and both are synchronized to give a stable and recurring pattern.   The sweeps are usually linear with time.   The horizontal sweep, the fast sweep, is $k_1t$, and the vertical sweep $k_2t$, where $k_1/k_2$ is a constant.   If $k_1/k_2$ is an integer, the pattern is exactly duplicated for each complete vertical scan.   If $k_1/k_2$ is a half integer, the pattern requires two vertical scans to give a complete picture.   In television, this latter case is known as "interlacing."

The use of the television display in radar has been limited to that of producing rasters on cathode-ray tubes for testing and checking such characteristics of the tubes as light output from the screen, decay time of the phosphors, buildup factor of the phosphor, and spot size.[1]

Except for the need of a unit that synchronizes the triggers to the

[1] These factors are discussed in detail in Chap. 18.

vertical and horizontal sweep channels, the problems in designing a television scope are similar to those encountered in designing the time sweep in a B-scope. Since, in both cases, it is very desirable to produce sweeps that are linear, the same types of coils and driving circuits are applicable. There is one important feature of the fast horizontal sweep of a television scan, however, that requires more attention, and that is the very short recovery time between the end of one horizontal sweep and the start of the next. In B-scans, and in fact in all time-base sweeps used in radar, it has been customary to let the deflection coils fully
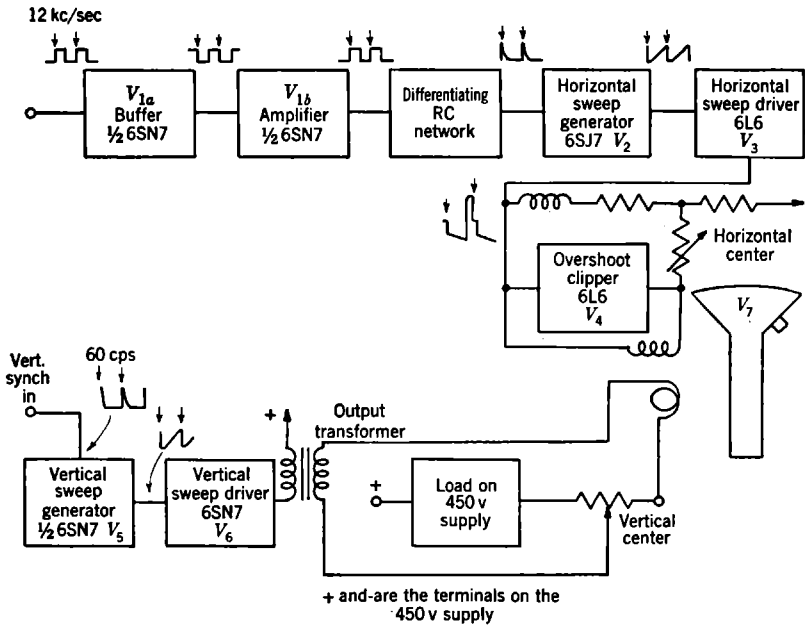


Fig. 11·17.—Block diagram of the sweep circuits used in television display.

recover between sweeps. In this way, it has been possible to avoid the sweep "jitter" that would be present with any variation in the timing of the trigger if successive sweeps started at varying initial flux conditions in the deflection coils. This practice has meant that, for the types of deflection coils commonly used, at least 200 $\mu$sec is allotted for coil recovery, and that the time between synchronizing triggers must be enough greater than the longest time sweep desired to give the 200-$\mu$sec difference.

By contrast, the 525 horizontal sweeps per scan, occurring 30 times a second according to present television standards, require a time interval between horizontal triggers of 65 $\mu$sec. Of this time, $\frac{1}{7}$, or about 10 $\mu$sec,
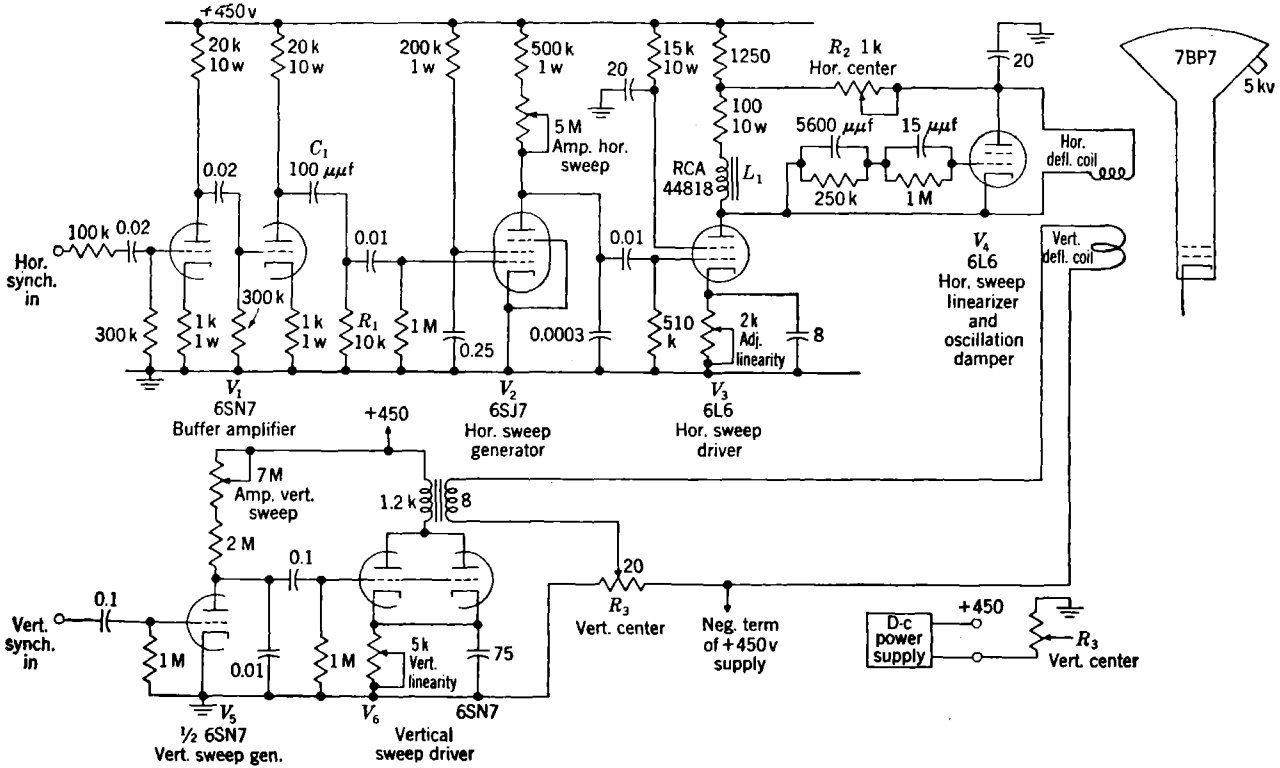
FIG. 11·18.—Circuit diagram of the sweep circuits in a television display.

is allotted to the return time. It is necessary, therefore, to resort to special methods of damping the oscillations that tend to occur in the deflection coil after the horizontal sweep is terminated. Furthermore, the sweep coil does not completely recover to its initial flux condition. instead, since the triggers occur at exactly spaced time intervals, the horizontal sweep is always started at the same flux intensity of the coil.

**11·7. Methods of Obtaining a Television Display.**—A typical circuit, used in cathode-ray-tube test equipment, is shown in Figs. 11·17 and
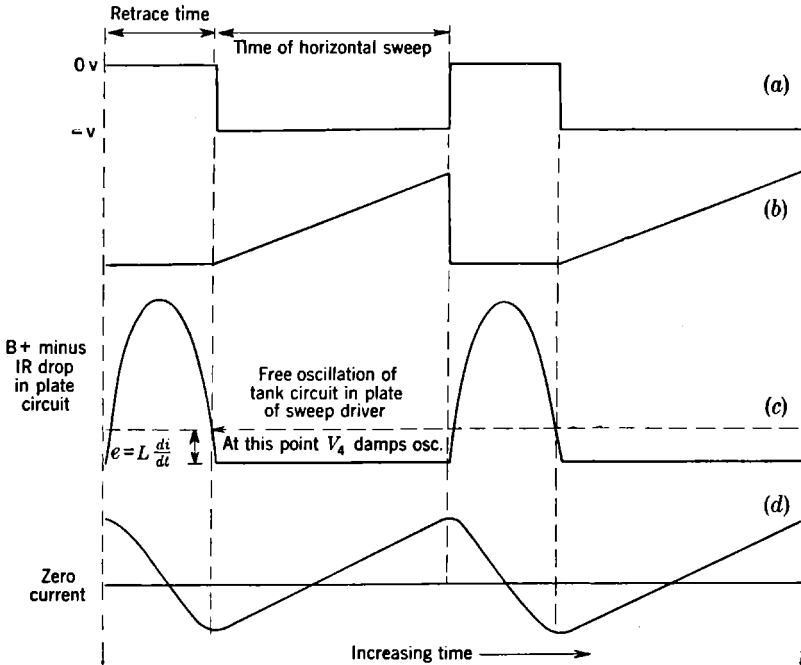


FIG. 11·19.—Waveform of horizontal television sweep circuit. (a) Switching square wave to input (grid $V_2$) of horizontal sweep generator. (b) Voltage input to grid of horizontal sweep driver $V_3$. (c) Voltage waveform on plate of sweep driver. (d) Current through deflecting coil.

11·18. A positive 12-kc/sec horizontal synchronization pulse is put through two stages of amplification $V_1$ and differentiated by $R_1$ and $C_1$ to give a switching waveform to the horizontal sweep generator $V_2$. The sawtooth voltage from the plate of $V_2$ is applied to the grid of the horizontal sweep driver $V_3$. In the plate circuit are connected three units in parallel: (1) a large choke of low distributed capacity, (2) $V_4$, and (3) the deflection coil. The combined action of the sawtooth voltage waveform on the grid of $V_3$, acting through the tube, and of $V_4$,

with the special network connected between the grid and cathode, is to provide a fairly linear sweep through the deflection coil. Tube $V_4$ also serves to damp the free oscillations initiated in the inductances and associated distributed capacities, as shown in Fig. 11·19. After the horizontal sweep driver is turned off at the end of the input sawtooth voltage, the voltage on the plate returns quickly to $B+$ and overshoots above $B+$; $V_4$ acts as an open circuit and thus does not tend to decrease the $Q$ value. When the voltage on the plate returns to a value just below $B+$ (because of the $IR$ drop in the plate circuit), $V_4$ becomes conducting and damps out the oscillation.

In this case, horizontal positioning of the trace is accomplished by a method not previously discussed. A simplified, but not complete, explanation of this method is that the deflection coil is effectively a-c coupled to the driving circuit so that the sawtooth waveform of current passing through it is centered about zero average current in the coil. Accordingly the current is negative at the start of the sweep and the beginning of the horizontal trace is shifted about as far to the left of the center as the end of the sweep is to the right.

Actually, some direct current flows through the deflection coil, but it is only a small amount because of the relatively low resistance of $L_1$ and $V_4$ in parallel with the deflection coil. The value of this small direct current may be controlled by rheostat $R_2$ which, therefore, is the horizontal centering control.

The vertical sweep is so slow that the load of the plate circuit of the drivers $V_6$ looks almost like a resistance load. In this case, the vertical deflection coil is transformer-coupled to the sweep driver tubes so that negative centering currents may be supplied, as shown by Fig. 11·18. The centering is controlled by the rheostat $R_3$.

# CHAPTER 12

## SPECIAL DEFLECTION COILS FOR OFF-CENTERING

### By R. D. Rawcliffe and R. W. Dressel

Frequently, it is desirable to locate the origin of a display at some definite position with respect to the center of the cathode-ray-tube screen. The process of setting the origin accurately at the center of the screen is called "centering"; whereas the process of locating the origin of the display at some position other than the center is termed "off-centering." Usually, centering involves only the small deflections necessary to correct inaccuracies in the electron-gun alignment, but off-centering requires large deflections since the origin may be off-centered by one or more radii. The usual methods for centering cannot, as a rule, be used for off-centering because of this difference in the magnitude of deflection.

The large deflections for off-centering may be achieved by a separate deflection coil, permanent magnets, special driving-circuit design, or a special winding on the deflection coil itself. The particular method chosen will depend upon the requirements and limitations of the system in which it is to be used.

**12·1. Centering Systems Using Separate Coils Displaced Axially from the Sweep Coil.**—One of the simplest arrangements for centering consists of a thin, square, iron-core coil inserted between the standard focus and deflection coils. The focus coil must be pushed back from its optimum position to make room for this coil, and therefore an increase in spot size, which can be estimated from the curves of Fig. 3·6, results. The core-lamination stack thickness of the centering coil should be less than $\frac{1}{2}$ in. to minimize the focus-coil displacement.

Defocusing can be reduced if the centering coil is mounted inside the focus coil. An air-core centering coil should be used and the inside diameter of the focus coil must be enlarged to accommodate it. This change considerably increases the power required for focusing; however, such a centering system operates satisfactorily with the additional advantage that it requires very little room.

A separate centering coil can be placed between the screen and the sweep coil on tubes such as types 7BP7 or 12DP7. The glass envelope of these tubes is so shaped that there is room for a large centering coil in this position. Such an arrangement may also be used for off-centering

by a limited amount, the limit being approximately one-quarter radius of the tube screen.    If the display is off-centered a distance greater than one-quarter radius, the electron beam will be intercepted by the tube neck in the course of its complicated deflection, and a portion of the screen will be left in shadow.    The magnetic-field distribution of this coil should be strongly "pincushion" to preclude pattern distortion.[1]    A large toroidal deflection coil having two sets of windings for both horizontal and vertical deflection works well in this application.    To produce the necessary pincushion field each winding should cover an arc of only 80° on the toroidal core.    Within their limits of deflection, these coils give satisfactory performance and require very little current.

**12·2. Off-centering Field Provided by a Separate Winding on the Deflection Coil.**—The field for off-centering a display may be generated by a separate set of windings on the core of the deflection coil.    These additional windings are similar to the push-pull windings described in Sec. 8·13, and, in fact, a push-pull coil may be used for this purpose. However, the presence of the extra winding significantly affects the performance of the windings used for deflection.

The two sets of windings are tightly coupled magnetically since they are wound one over the other on the same core.    As a result, the distributed capacitance of the off-centering winding, multiplied by the square of the ratio of the off-centering to deflection turns, is reflected into the deflection winding.    Since the distributed capacitance of a layer-wound solenoid is large, the off-centering winding should have fewer turns than the deflection winding to avoid enormous values of shunt capacitance.    Another reason for keeping the turns ratio at unity or less is to prevent large induced voltages in the off-centering windings. These limits on the number of turns make it necessary to have an off-centering current rather large compared to the average deflection current. In addition, the windings are sensitive to oscillations, the effects of which appear as crooked sweeps.    For these reasons, an off-centering system of this type should be used only for slow sweeps where the effects of distributed capacitance and oscillation are small.

**12·3. Permanent-magnet Off-centering with an External Magnet.**— One arrangement[2] for permanent-magnet off-centering consists of an air-core sweep coil surrounded by a square yoke, two legs of which are permanent magnets.    The other two legs are of soft iron or some high-permeability alloy, as shown in Fig. 12·1.    The field of this magnet is almost equivalent to that of a square iron-core deflection coil and is essentially uniform if the magnets extend the full length of one side of the square.    Shortening the length of the magnets and replacing the

---

[1] See Chap. 9.

[2] A. M. Skellett, Bell Telephone Laboratories, personal communication.

sections removed with soft iron causes the field to become pincushion in the same manner that the field in a square iron-core coil becomes pincushion if the winding length is decreased.    The amount of off-centering can be adjusted by changing the degree of magnetization of the bar magnets, or by the use of adjustable soft-iron shunts placed parallel to the magnets along their outer surfaces.    These shunts can be mounted to swing back from the magnets to vary the field strength.    In this manner, a variation in the off-centering by a factor of about 3 can be achieved.

The deflection coil used with this off-centering yoke is necessarily of the air-core type.    The only iron return path permissible around this coil is that provided by the permanent-magnet yoke,



FIG. 12·1.—Permanent-magnet off-centering with external magnet.

which adds very little to the efficiency of the deflection coil.    It does, however, tend to distort the field of the coil if the coil is not accurately aligned in the yoke.    Because of the poor return path, the deflection coil
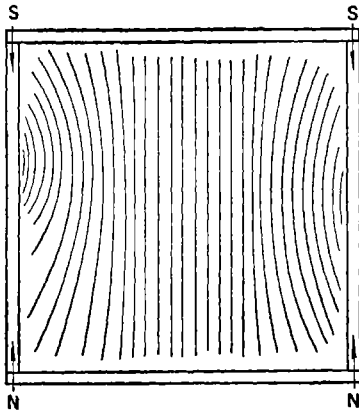


FIG. 12·2.—Typical field distortion in permanent-magnet off-centering yoke.

requires nearly twice as much driving power as it would if there were a close-fitting soft-iron return path around it.

The permanent magnet provides an off-centering field in only one direction.    Off-centering in any other direction must be provided by passing a current through the deflection coils.

One of the disadvantages of this type of off-centering is the pattern distortion produced.    Iron-filing patterns of the fields produced by permanent magnets nearly always indicate a nonuniform magnetization.    In particular, if two magnets are placed so that their fields oppose as is the case of the magnet yoke considered here, one magnet seems always to be sufficiently stronger than the other to reduce the uniformity of magnetization of the weaker magnet.

One typical field distortion is shown in Fig. 12·2. The resulting pattern distortion is small, but it is large enough to be troublesome in precision systems. The distortion varies in a random manner from unit to unit, and hence it cannot be easily corrected. The field distortion is usually not abrupt enough to cause noticeable defocusing.

A better off-centering yoke could probably be made if the magnets were used only to produce a magnetomotive force in such a way that they did not determine the field distribution. Soft-iron pole pieces could be used to shape the field. One possible arrangement of permanent magnets is shown in Fig. 12·3. It has the fundamental advantage that the two magnets furnish fields that aid instead of oppose each other. Slight unbalances in the strengths of the two magnets have negligible effects on the field. Because the magnets are small, they must have a large coercive force. Alnico II is one of the best materials now available for this purpose. The obvious disadvantage of an off-centering yoke of this type is its large physical size, but this difficulty may well be offset by its improved performance.



FIG. 12·3.—Improved permanent-magnet off-centering yoke.

**12·4. Permanent-magnet Off-centering with Internal Magnets.**—A permanent-magnet off-centering field can be produced by small magnets inserted in the core of a square iron-core deflection coil. As shown in Fig. 12·4, two small magnets are required in each of two opposite legs of the core to produce the off-centering field. The windings are placed over these legs covering the magnets as well. An additional set of windings may be placed on the remaining two legs of the core.

The field produced by the magnets, also shown in Fig. 12·4, is similar to that produced by a coil. However, fringing fields around the short magnets distort the field somewhat, so that it is not uniform, and cause a small amount of pattern and focus distortion. In order to prevent extremely nonuniform fields the magnets need not be uniformly magnetized but the effective strength of the four magnets must be equal.

The field distribution is controlled by the separation $A$ between the magnets. By adjustment of $A$, the field can be made very pincushion- or slightly barrel-shaped. This distance plays the same role as the wind-

ing length on a square coil.   The field distribution required for minimum pattern distortion will depend on the type of cathode-ray tube used.

The field produced by the windings over the magnets should be carefully matched to that of the magnets since the net deflecting field is the
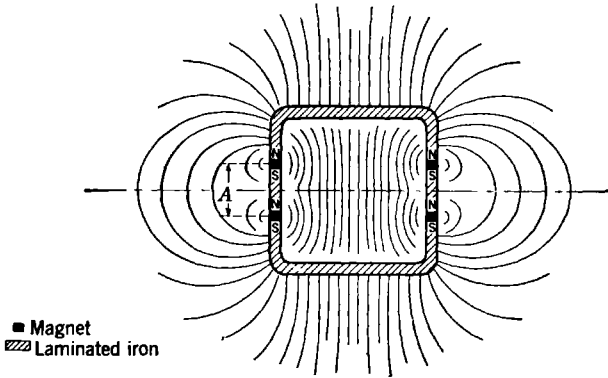


FIG. 12·4.—Core of deflection coil with permanent-magnet off-centering, showing the field of the magnets.
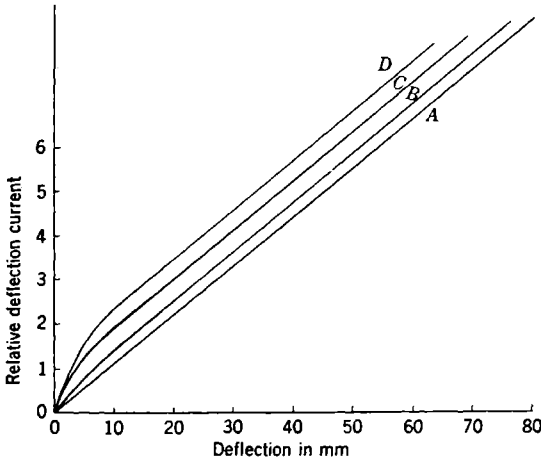


FIG. 12·5.—Deflection versus deflection current for deflection coils with permanent-magnet off-centering.   Curve A, slow sweep; Curve B, 200-μsec sweep; Curve C, 50-μsec sweep; Curve D, 12-μsec sweep.

vector difference between these two fields.   If the two fields have different distributions, the net field will be distorted, particularly when the two fields are nearly equal.   Serious irregular pattern distortions result, accompanied by a deterioration of focus.   The winding distribution needed to match the fields is best found by trial.   Pie winding (see

Sec. 8·14) should be used for this winding because of the ease and accuracy with which the winding distribution can be controlled.    Adequate control of the magnetic field is not possible with simple layer windings.

The core of a deflection coil using internal magnets is cut into four pieces, two I-sections and two U-sections, and the magnets are inserted at the cuts.    A ribbon-wound core (see Sec. 8·13) is satisfactory, but U- and I-shaped lamination punchings may be stacked to form a core.    The windings cannot be separately wound and slipped onto the core because of the shape of the U pieces; instead they must be wound directly upon the core section held in a winding machine.

The magnets themselves support stronger eddy currents than does the ribbon-wound core. These eddy currents act to slow the start of the sweep and to prolong the recovery time when the sweep has been completed.    The series of graphs in Fig. 12·5 shows the effect of these eddy currents upon the input current to the coil. The voltage waveforms in Fig. 12·6 illustrate how the magnets retard by approximately 30 $\mu$sec the recovery time of the coil at the end of a sweep.    The magnets also reduce the peak of the oscillation by a factor of 2.



Fig.    12·6.—Recovery of permanent-magnet off-centering deflection coils.    Time measured from end of sweep—Curve *A*, no magnets in core; Curve *B*, with magnets.

Since the current in the coils tends to demagnetize these small magnets, they must be made of a material having a high coercive force if they are to produce a sufficient and steady off-centering field.    There are a number of suitable magnetic materials that have a coercive force high enough to withstand this demagnetizing action if it is limited to that produced by the sweep current.    However, if the plate end of the coil should be accidentally short-circuited to ground, as might frequently occur during testing, thus connecting the whole power supply directly across the coil, a much larger current will pass through the coils.    No known magnetic material will withstand this current surge, but the best available is the type 426 alloy.[1]    Alnico V has a very much higher energy

[1] Type 426 alloy magnets are manufactured by the General Electric Co., Schenectady, N.Y.    G.E. Drawing No. K-71D730.

content but is less satisfactory, as shown in the curves of Fig. 12·7. The operating point is at such a low flux density that the demagnetizing force for the 426 alloy is considerably larger than that for the Alnico V.

After the fields $H_1$ or $H_2$ of Fig. 12·7 have been applied, any weaker field will not disturb the magnetization, but a stronger field will further reduce it. The current that can safely be passed through the coil is therefore limited. The current can be limited to this value in case the plate side of the coil is short-circuited to ground by inserting a small resistance in series with the coil on its positive side. Because the 426-alloy magnets can stand about ten times the demagnetizing field pro-
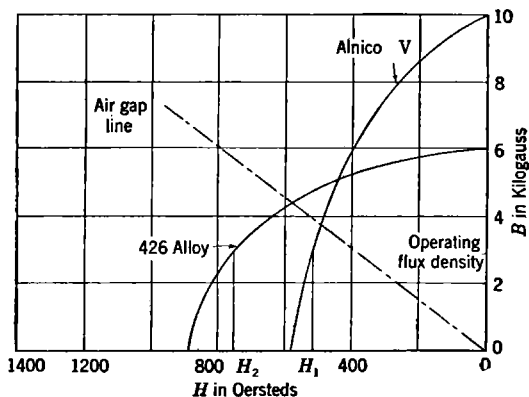


FIG. 12·7.—Demagnetization curves of Alnico V and 426 alloy. Demagnetization fields needed to attain desired operating point are shown as $H_1$ (Alnico V) and $H_2$ (426 alloy). (These curves are not quantitatively to scale.)

duced by the sweep current, the current-limiting resistor may be small so that the voltage drop across it during the sweep may not be serious.

The magnetization of the magnets must be done in such a manner as to attain the maximum possible stability. First, they must be thoroughly saturated in the direction in which the field is desired. The magnetization must then be reduced to the desired operating point by passing current through the windings themselves. The saturating operation can be satisfactorily accomplished with the field of a strong electromagnet. The "knockdown" or partial demagnetization cannot, however, be so accomplished. Because it is usually most convenient to do both operations with one setup, an electromagnet need not be used at all. Frequently magnets are magnetized by discharging a condenser through a coil, but this method is not advisable in this case because the voltage rises so rapidly when the condenser is connected across the coils that the distributed capacity shunts out most of the winding at the start of the pulse. The first few turns then take all the load for an instant and burn out.

The circuit shown in Fig. 12·8 will force the necessary current through the coil without allowing such a steep wavefront as to damage the winding.   The inductance of the Variac and transformer in series with the coil prevent this steepness.   The current through the coil consists of a pulse of rectified half cycles of the 60-cps voltage, and the length of this pulse is determined by the length of time the push button is held down.   Since a very few half cycles are adequate, the push button should be given only a short tap.   The amplitude of the current is set to the desired value by the Variac.   Approximately 5,000 ampere-turns through each leg of the coil are required for saturating the magnets.   For reducing the magnetization to the operating point, approximately a third of the above field is required in the reverse direction.
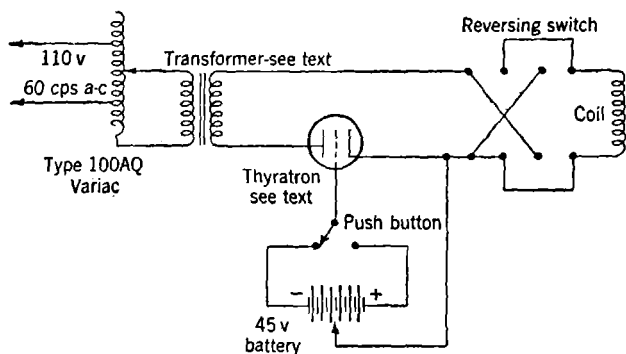


Fig. 12·8.—Magnetizing circuit.

The thyratron must be capable of standing surge currents of about 25 amp (for a 200-turn coil) and a voltage of about 1500 volts (for coils with about 1000 turns).   A GE Type 3C45 tube was found to operate very well for coils within this range.   The required grid voltage for this tube is supplied by the 45-volt battery shown.

The voltage required across the coil is essentially equal to the $IR$-drop, which is proportional to the number of turns.   A stepup transformer is needed for coils with more than about 200 turns.   This transformer need be rated for only a fraction of the peak current required, but its resistance should be small compared with that of the coil being magnetized.   It should have adequate insulation to allow for surges that may occur when the thyratron circuit opens.   For coils with 200 turns or less, the transformer should be omitted.

A permanent-magnet off-centering deflection coil of this type is useful principally for the production of a rectangular scan, one sweep of which is fast (10 to 50 $\mu$sec) and the other slow.   The obvious advantage is the large saving in off-centering power, which might amount to more

than 100 watts in coils wound for fast sweeps. The disadvantages include somewhat poorer focus and a small amount of pattern distortion. Eddy currents in the magnets cause a small amount of sweep distortion, but the over-all performance at higher sweep speeds is probably at least as good as that of the conventional square iron-core coil although not as good as that of an air-core coil. It is much cheaper to operate than the air-core type of coil.

**12·5. Off-centering for a Radial–time-base Display.**—Two deflection coils combined as in Fig. 12·9 may be used to off-center a radial–time-base display. The larger of these two, a square iron-core deflection coil, generates a fixed magnetic field that serves to set the origin of the display at any desired position, whereas the inner air-core coil carries the sweep currents and is rotated mechanically to provide the radial display. Sweep power may be applied to the rotating coil through a pair of slip rings.

If the magnetic fields of the two coils were identical, it would be possible to move the sweep origin any number of radii from the center of the tube screen. However, it is impossible to build two coils so widely different in shape and achieve identical field distributions. For this reason,



Fig. 12·9.—Off-centering coil and air-core deflection coil in combination.

the origin may be off-centered a maximum distance of about three radii by this scheme before the focus deteriorates and the pattern distortion becomes unacceptable.

Axial field distributions of the sweep coil and off-centering coil, together with the resultant field distribution when these two are superimposed, are shown in Fig. 12·10. Because of its large size, the field from the off-centering coil is broad, whereas that of the sweep coil is comparatively narrow. Consequently, the resultant field of these coils in combination is complicated, having two reversals along the coil axis.

An electron in passing through such a field is deflected first in one direction and then in another, following the peculiar serpentine path illustrated in Fig. 12·11. An idea of how scanning occurs may be gained by examining the three electron paths shown. When the off-centering system is in operation, the field generated by the off-centering coil is fixed while that of the sweep coil (here assumed to be stationary) increases linearly with time from zero to its maximum value. In Fig. 12·11, the field due

to the sweep coil is in a direction opposite to that of the off-centering coil. Accordingly, the resultant field distribution passes through all values between the limits marked *a* and *c* in the diagram. Deflection paths for three particular values illustrate the progressive deflection of single electrons.

A beam of electrons is deflected in a similar fashion, but because of the complex field distribution with its attendant nonuniformities, the beam becomes defocused. The defocusing action of the deflecting field increases more and more rapidly as the sweep origin is carried off the screen, three radii off-center representing a practi-
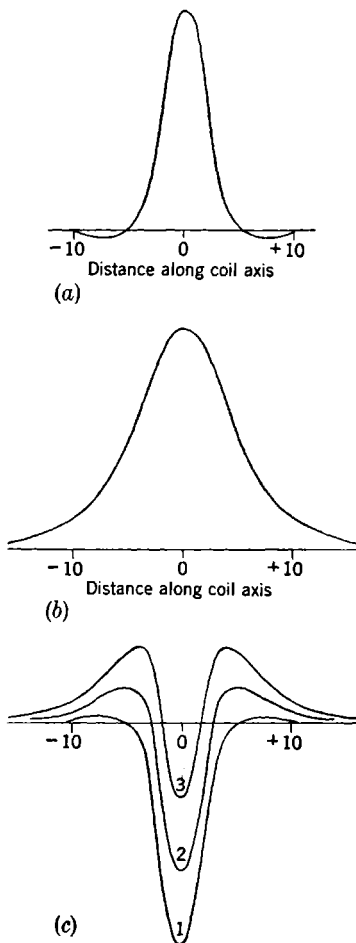


Fig. 12·10.

Fig. 12·11.

Fig. 12·10.—Axial field distribution of coils used in off-centered display. (*a*) Field of sweep coil. (*b*) Field of off-centering coil. (*c*) Resultant field when sweep and off-centering fields are in opposition: (1) no off-centering, (2) 1-radius off-centering, (3) 2-radii off-centering.

Fig. 12·11.—Electron paths (*A, B, C*) through field distribution (*a, b, c*), showing how scanning takes place.
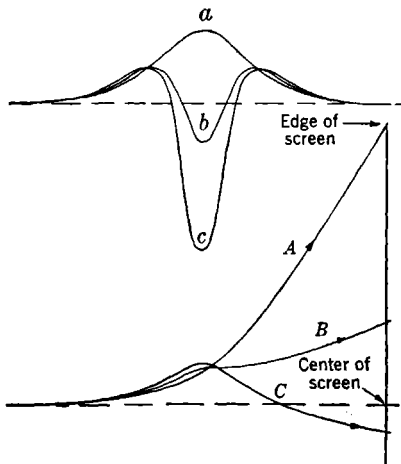
cal limit. Not only does the illuminated spot on the screen become defocused, but it also is distorted in shape as shown in Fig. 12·12.

These distortions are characteristic of the field distribution because they do not occur if the fields of the two coils are identical.

The deflection pattern also is distorted in the manner illustrated in Fig. 12·13. This diagram shows four views of a cathode-ray tube in which the sweep origin is off-centered 0, 1, 2, and 3 radii. These four views are joined together so that the whole length of the sweep may be seen as one continuous line. Solid lines indicate the actual sweep, and the dotted lines indicate the position that the sweep would have had if
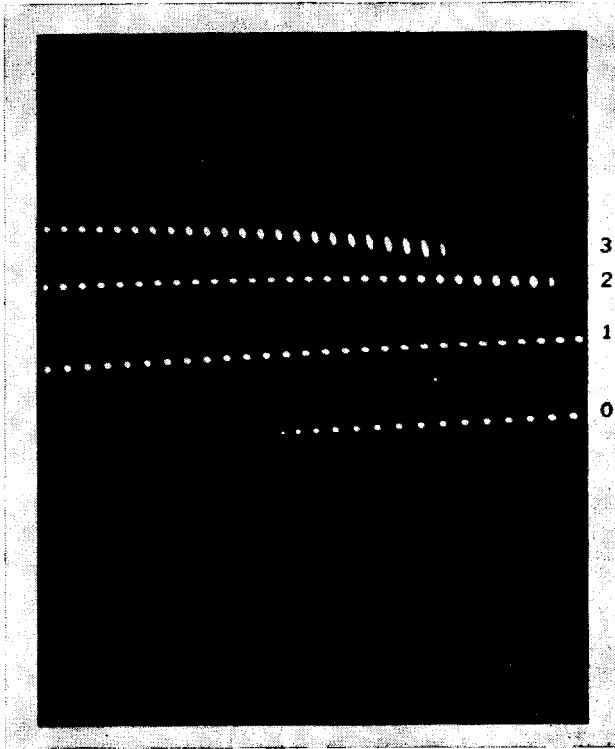


Fig. 12·12.—Distortion of spots and sweep with off-centering of 0, 1, 2, and 3 radii.

it were straight. A distortion as great as this may be serious if accurate measurements are to be taken directly from the tube face, but the pattern in any one of the off-centered positions is not objectionably distorted in appearance. A better idea of the appearance of such a display may be obtained from the series of photographs in Fig. 12·14.

Since the magnetic field generated by the sweep coil in this deflection system is four times as great as that generated in ordinary deflection, eddy currents induced in surrounding metal parts can become much more troublesome. These currents continue to circulate for 2000 to 5000

μsec after the sweep has ended.    Moreover, they have sufficient strength
in metal parts close to the tube neck to cause a small deflection of the
beam.    Consequently, the time required for the decay of eddy currents
in the tube mount may limit the sweep repetition frequency in a manner
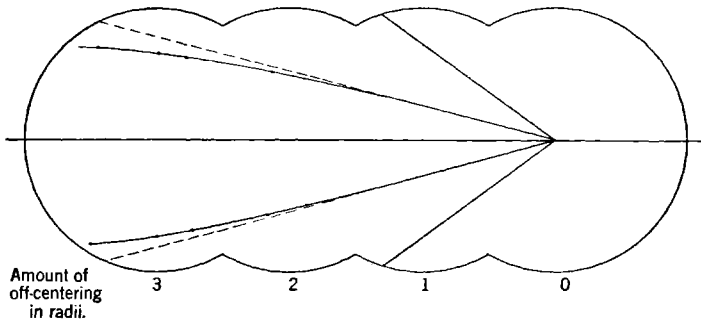


FIG. 12·13.—Composite showing traces for four conditions of off-centered radial sweep.

similar to the limitations imposed by the recovery time of the deflection
coil.    The only remedy is to replace the offending parts with nonmetallic
material.

Strong magnetic fields that tend to magnetize permanently any iron
parts of the mount are set up by the off-centering coil.    This permanent
magnetism is particularly undesirable when the radial display is shifted
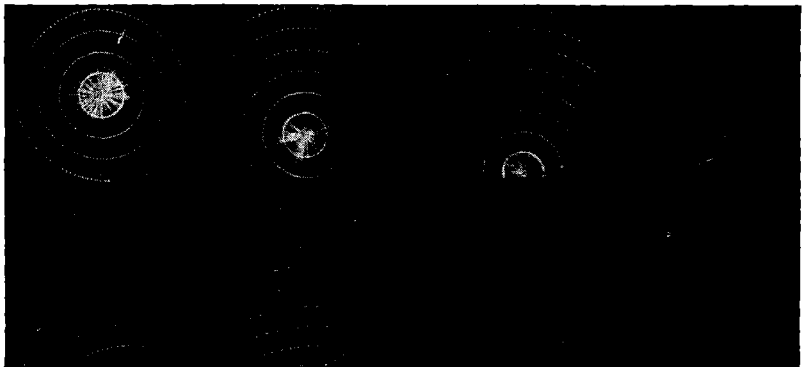


FIG. 12·14.—Radial–time-base display in various off-centered positions.

to various off-center positions because it may cause an error of as much
as 1 in. in the location of the origin.    The cure for this condition is again
to remove the iron parts.    In addition, the iron core of the coil itself
tends to become permanently magnetized, and care should therefore be
exercised to select a core iron having low retentivity.

The physical construction of the air-core coil is discussed in Appendix B.  A semidistributed coil with bent-up ends (as illustrated in Fig. 8·26e) fits this application better than any other air-core coil because of its comparatively broad axial field distribution, its uniform field, and its reduced fringing fields.

The problem of construction of the large off-centering coil, however, is unique because of the requirements of the coil.   Since this coil is external to and encloses the sweep coil, its aperture is much larger than that of the sweep coil.   Thus, the number of ampere-turns required to produce a given deflecting field is higher.   Further, since the currents that must be maintained in the off-centering coil are essentially constant, the power
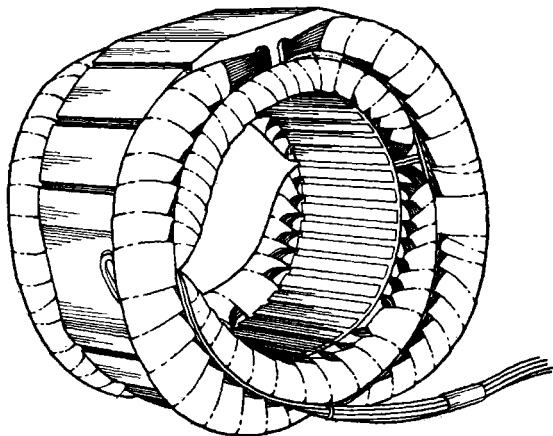


Fig. 12·15.—Motor-stator type of off-centering coil.

required to hold the origin of the trace several tube radii off-center may be high.  Usually, then, in order to reduce the current required, one would like to use as many turns of wire as possible on this coil.   Unfortunately, this method increases the magnetic coupling between the fixed and rotating coils, and causes difficulties to be described later.   The stack height of the core should be short in order to keep the axial field distribution as narrow as possible, but here again a short stack height requires a large driving power.   About one inch is a good compromise height.[1]   Even if the off-centering coil carries only direct current, the iron core should be laminated because of its proximity to the sweep coil. Windings may be center-tapped and placed on four legs to give both horizontal and vertical deflection.   With this type of winding the origin of the radial display may be located in any of the four quadrants.   An alternative design is to build a mount rotatable through 360° and capable

[1] For constructional details see Fig. B·4.

of holding the large, square coil.   A mount of this type is illustrated and discussed in Sec. 16·3.   Single-ended windings may be placed on all four legs and connected in series to give a magnetic field directed across one diagonal of the coil.   In this case the origin may be located in polar coordinates.[1]

An off-centering coil may also follow the motor-stator type of design illustrated in Fig. 12·15.   Such a coil is twice as efficient as the square-core coil and otherwise equals its performance in every respect.   However, the windings require considerably more wire than the square-core type, and thus weight and size are significantly increased.

Two-coil deflection systems are limited in compactness by the magnetic coupling between the two coils.   If the coupling coefficient is greater than 0.2, the off-centering coil will absorb enough power to reduce the sensitivity of the sweep coil by a significant amount.   Since the coupling between the coils varies as the sweep coil rotates, the sensitivity of the sweep coil will also vary.   As a result, circles in the sweep pattern are distorted into ellipses, the major axes of which lie along the direction corresponding to minimum coupling and the minor axes of which correspond to maximum coupling.   The best remedy for such coupling is a larger separation between the two coils.

Because of this same magnetic coupling, the rapid decay of the deflecting field at the end of a sweep induces a high voltage in the off-centering coil, which then oscillates until its energy has been dissipated.   Consequently the sweep-repetition rate in a two-coil system is usually limited by the recovery time of the off-centering coil.   Even with the relatively efficient (40 ma/radius per leg) bulky coil illustrated in Fig. 12·15, the recovery time is approximately 800 $\mu$sec.   The recovery time may be reduced by one or all of three different methods.   First, the efficiency of the off-centering coil may be increased.   This method is not always practicable in view of the restrictions upon inductive coupling and upon the physical length of the coil.   Second, the coil may be critically damped.   This method is a simple and effective improvement; in some cases, however, it may be necessary to resort to sectional damping.   Third, if a coil is already critically damped, the time constant will be proportional to $\sqrt{LC}$, consequently, its recovery time may be reduced by decreasing the number of turns, or the distributed capacitance, or both.

[1] Sec. 13·2.

# CHAPTER 13

## RADIAL–TIME–BASE DISPLAY

### By P. Axel, C. W. Sherwin, and G. M. Glasford

An accurate plan view of signals, showing them in their proper spatial relation throughout 360° of azimuth, may be generated by presenting intensity-modulated signals in polar coordinates. At each trigger pulse a linear time-base sweep is started, and moves the cathode-ray beam from the center of the tube to the edge in a direction corresponding to the direction assumed by the scanning device. The radius vector to any given signal will depend upon the distance of the target and the speed of the sweep. As the scanning device rotates in azimuth, various targets will come into view. Their corresponding signals will be "painted" on the display tube at properly scaled distances from the center of the tube at the time when the line of sight passes over each target.

In order to avoid a spoked appearance in the display, the rate of change of the azimuth angle must be slow compared to the repetition time. For radar displays the time required for a complete revolution is a number of seconds; hence, if the whole picture is to be preserved, a long-persistence screen must be used in the cathode-ray tube. Figure 1·3 shows the appearance of such a display, often called a PPI display (plan-position indicator), or RTB display (radial time-base).

The straightforward method of developing a radial–time-base display is by the use of a single deflection coil that can be rotated about the neck of the cathode-ray tube in synchronism with the scanner. The amplifier circuit must include clamps or some other provision to insure that the current in the deflection coil is zero at the start of each sweep.

It is also possible to develop a radial–time-base display using a fixed deflection coil with two or more deflection axes if the magnetic sweep field is made to rotate in harmony with the desired display angle. There are two methods of rotating the sweep field. In one method, a time base or sweep waveform is first generated and then resolved into components according to the deflection-coil axes and the angle. The components are individually amplified, if amplification is necessary, and recombined in the deflection coil to reproduce the original waveform at the angle set into the resolving device. In the other method a carrier voltage is passed through a resolving device and the several component voltages used to control the amplitudes of as many identical waveform

generators. The resulting component sweep waveforms may then be treated as in the previous case.

### ROTATING-COIL METHOD

In a display of this type the radial deflection is dependent only on a single current through the deflection coil, and the azimuth position of the trace is dependent solely on the mechanical orientation of the coil. The sweep circuits are therefore simplified at the expense of the additional mechanical complexity required to rotate the deflection coil. Considerably less power is required for this method than for the fixed-coil method of producing a radial–time-base display.

The rotating-coil method of generating a polar display can be studied most conveniently by considering separately the tube mount with its coil-rotating features and the display circuit. In general, any of the rotating-coil tube mounts (see Secs. 16·3 and 5·1) can be used in conjunction with any of the display circuits to be described.

To maintain angular correspondence between the trace on the display and the signal source, the deflection coil must rotate in synchronism with the signal source. The coil is, therefore, mounted in a rotatable housing that has two slip rings and brushes for electrical connection and a gear that can be driven to give the correct mechanical rotation.

In addition to errors that affect the mechanical position of the coil (see Sec. 5·5), this method may produce a very small electrical error in the coil, evidenced by a change in angular position of the trace when the sweep speed is varied, and caused by magnetic interaction between the coil and other parts of the mount (see Sec. 9·4). Some error will also be introduced in visual estimation of azimuth position because of the reference markers used. Although mechanical markers can be inscribed on an overlay or directly on the tube face, this method can neither compensate for all errors nor be used conveniently in off-centering operation; therefore, electronic azimuth markers are often used. In cases where the accuracy of reading angle is limited by interpolation between fixed reference markers, a single, phasable, precision marker may be used. When it is required that the azimuth position locate an expanded display on a signal area, it is convenient to move a radial mechanical strobe over the signal and have this motion geared to the phasing device on a display indicator.

By using the proper data-transmission system, tube mount, and marker technique, a rotating-coil radial–time-base display can be designed to have an azimuth accuracy that is limited only by the resolution of the cathode-ray tube.

**13·1. General Circuit Considerations.**—The rotating-coil radial–time-base display requires comparatively simple circuits since only

unidirectional current, independent of azimuth position, is needed for the deflection coil.

A block diagram of the essential electrical circuits is shown in Fig. 13·1a. A trigger pulse from the signal source synchronizes the start of each cycle. This pulse fires a rectangular-wave generator. The rectangular waveform from this generator is used to activate the sweep
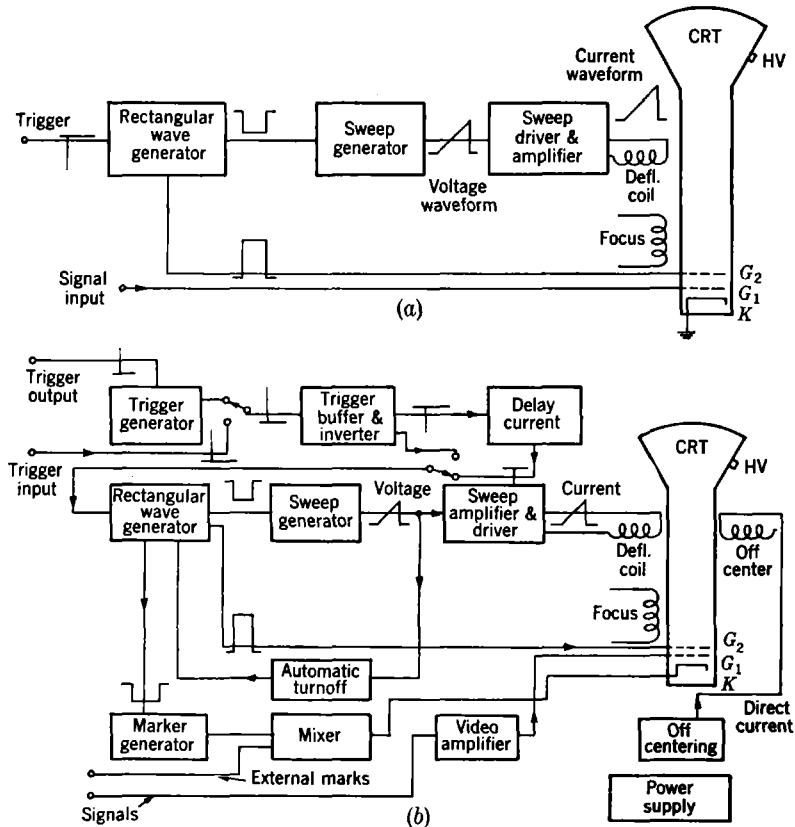


FIG. 13·1.—Block diagram of radial–time-base display.

generator and to intensify the cathode-ray tube. The sweep generator produces a sweep voltage that is converted by the driver to a sweep current through the deflection coil.

In addition to these essential circuits there are often some useful associated circuits, as illustrated by Fig. 13·1b. To synchronize the start of each cycle of the display circuit with that of the source, a common trigger pulse is used for both units. When this pulse is available from

the source, it is put through an isolating buffer stage, which may also be used as an inverter. If, however, a trigger pulse is needed *for* the source, a trigger generator may be incorporated in the display circuits. The input terminal of the trigger buffer may be switched to either the internal or the external trigger generator. The output signal from this stage is usually a negative trigger pulse whose exact requirements depend on the rectangular-wave generator whose action it is to initiate. The trigger pulse may then be used directly or it may be delayed by a variable time-delay circuit. Usually, this delay circuit need only satisfy a maximum jitter specification and its accuracy, linearity, and constancy with time are of only secondary importance. In some cases, however, it may also serve as an accurate timing circuit, its output pulse being used as a precision time marker on the display; it must then, of course, be carefully designed.

The rectangular-wave generator must be stable and capable of recovering rapidly enough to respond to each input trigger pulse. Since its output voltage is used for gating the sweep generator and for intensifying the cathode-ray tube, if rapid time bases are used, the rise time of the rectangular output wave must be short, particularly if a large intensifying waveform is necessary for the cathode-ray tube. If the rectangular waveform is also used to gate the time-marker circuit (which may be done only if no delay is used), it must be particularly large and fast, and usually must be from a low-impedance source. The time duration of the rectangular wave is usually made a little longer than the time interval that is being displayed. If the display is not going to be off-centered it is most convenient to have the rectangular-wave generator shut off automatically when the trace reaches the edge of the tube (see Sec. 4·7). The automatic gate turnoff obviates the necessity of changing the length of the rectangular wave manually for each change in sweep speed. Since the back edge of the rectangular waveform is beyond the time interval being displayed, jitter or long-time drifts in this back edge are not usually critical. Hence, most types of rectangular-wave generators discussed in Sec. 4·4 may be used.

The sweep generator usually forms a linear sawtooth voltage, but for special applications hyperbolic, square-law, or other waveforms may be desired (refer to Vol. 19, Chap. 8). The voltage waveform is generated by using a gated switch tube across an *RC*-network. This waveform must be such as to put the desired current waveform through the deflection coil. Therefore, its exact shape depends on the deflection coil and the deflection-coil driver as well as on the required sweep characteristics. The driver stage converts the voltage waveform of the sweep generator into the properly varying current through the deflection coil. To overcome the nonlinearity inherent in power tubes, inverse feedback is used

to insure the proper current waveform through the deflection coil. The complexity of the resultant feedback-amplifier circuit depends on the accuracy desired in the display. Because of the interdependence of the various parts of the sweep channel (sweep generator, sweep driver amplifier, and deflection coil) its design must be accomplished as a whole rather than as three individual circuits.

The factors contributing to time errors are of two different types— "jitter" and distortion. A jittering pattern is caused by relative motion between the sweep trace and the fixed signal, caused either by jitter of the trigger pulses, the delay circuit, or the sweep generator, or by ripple in the sweep channel. Excessive high-voltage ripple will cause variation in the deflection sensitivity, and this variation will also result in pattern jitter. On the other hand, distortion in the pattern may be caused by the sweep amplifier or by the inherent distortion of cathode-ray tubes (see Sec. 9·1). When extreme accuracy is necessary, the sweep amplifier may be designed to compensate for tube distortion.

The display circuits have several functions in addition to the generation of the proper deflection current. An intensifying pulse obtained from the rectangular-wave generator is used to insure the appearance of signals only during the time intervals being studied. In addition, a video amplifier might be required for the amplification of input signals to the levels necessary for the cathode-ray tubes. Often there are other circuits, such as marker generators or mixer, which are incorporated in this unit.

**13·2. Expanded Displays.**—There are two common methods of increasing the resolving power of a rotating-coil polar display at long range. The simpler method introduces a time delay between the trigger pulse and the start of the radial sweep, so that a fast sweep will include the area of interest. Angles and distances are badly distorted in the display. The other method requires a second coil (see Sec. 12·4) for producing an off-centering magnetic field and a fast sweep that begins with the trigger pulse. Although there is theoretically no geometrical distortion in off-centering, some distortion due to the large magnetic fields required is found in practice. Figure 13·2 shows several photographs of an off-centered and of a delayed-sweep polar display illustrating the distortion due to delays and off-centering. A discussion of off-centering coils will be found in Chap. 12. Off-centering a rotating-coil polar display is more expensive than off-centering other sector displays (see Chap. 14) since, mechanically, it entails two deflection coils and, electrically, two large magnetic fields.

The off-centering can be accomplished radially, with the angular position of the off-centering coil determining the direction, or it may be accomplished using $x$ and $y$ off-centering controls and a fixed coil. Figure
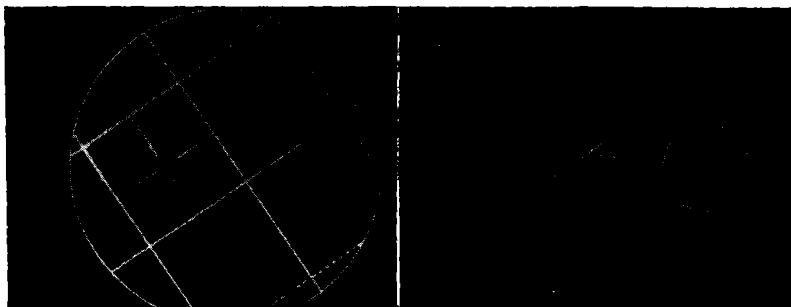
(a) R/2 off center.                    (d) normal 150-mile sweep RTB.
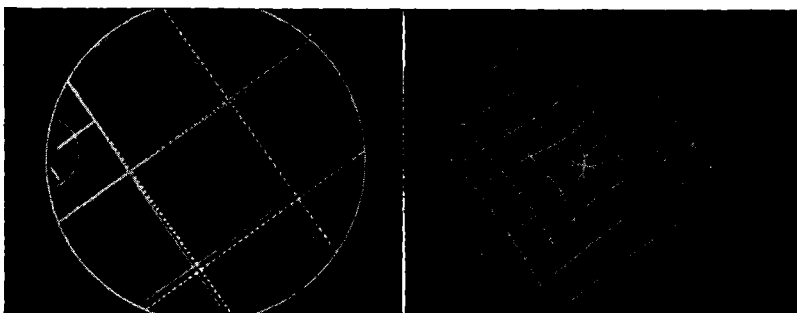
(b) R off center.                    (e) 20-mile delay in start of 150-mile sweep.
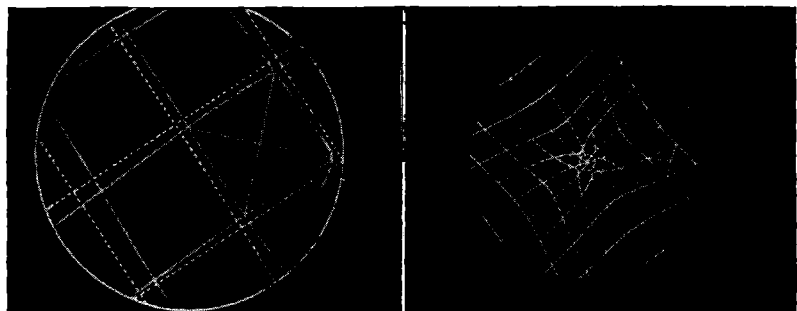
(c) 2R off center                    (f) 40-mile delay in start of 150-mile sweep.

FIG. 13·2.—Distortions produced in off-centered display and in delayed-sweep RTB display.   The circles are 10-mile range marks.   The grid lines are produced by the method of video mapping explained in Chap. 16.   Dashed lines in the off-centered display show the amount of distortion.

13·3 shows these two methods for obtaining the off-centering magnetic fields.

The radial off-centering coil connection, with all four legs in series, gives a resultant field proportional to $i_r \sqrt{2}$.   In the $x$- and $y$-deflection

system, the off-centering in the $x$- and $y$-directions is proportional to $i_x$ and $i_y$ respectively. Hence, to insure with the $x$, $y$ system an amount of off-centering in any direction equivalent to that available with $i_r$ in the radial system, each current must be variable from 0 to $i_r \sqrt{2}$. The total current necessary for maximum deflection would vary from $i_r \sqrt{2}$ to $2i_r$, dependent on the direction of off-centering. Since $i_r$ is approxi-
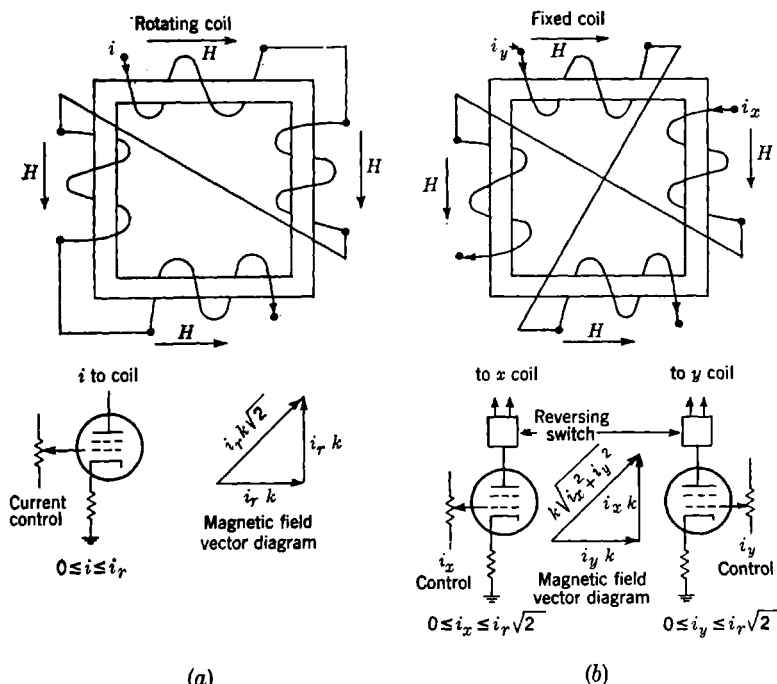


FIG. 13·3.—Off-centering coils. (a) The current $i$ is variable and it flows through all four legs of the coil; the deflection is proportional to $i \sqrt{2}$ and is perpendicular to the magnetic field vector; the coil is rotated to change the direction of off-centering. (b) The currents $i_x$ and $i_y$ are independently variable and reversible; the magnetic fields in the $x$- and $y$-directions are proportional to the currents that generate them.

mately 100 ma, the current control is usually put in the grid circuit of a power tube, rather than in series with the coil. Thus, the $x$, $y$ system uses one extra power tube. On the other hand, the radial off-centering method requires a rotatable off-centering coil.

COMPLETE DISPLAY CIRCUITS

Three circuits will be used as illustrations of this method of generating a radial time base. The first of these is a very simple, inexpensive circuit in which linearity and versatility have been sacrificed for economy. The

second is a much more reliable and versatile circuit, which employs many of the latest techniques. The third is also a reliable circuit, which uses regulated power throughout because it was designed for use where power and size were not limited. This model contains the off-centering feature.

All these display circuits have been built in production, and hence the circuits have been engineered to operate satisfactorily with any components that are within standard tolerance ratings. The various components have been conservatively rated, with a safety factor of about 2.5 over the rated dissipation values for resistors.

It should be noted that any of these indicator circuits can be used with any rotating-coil tube mount (see Chap. 16). The only two interconnecting links that may vary for different systems are the off-centering feature and the data-transmission circuit. Either of the two basic off-centering circuits (shown in Fig. 13·3) may be added to any of the displays and any desired data-transmission circuit (see Chap. 5) may be used. The only data-transmission system of which the circuits are at all complicated is the servo system.

**13·3. A Simple Rotating-coil System.**—This display circuit, shown schematically in Fig. 13·4, is a very economical one. It has five sweep speeds with four markers per sweep.

| Sweep-speed factor, $\mu$sec/radius | Time-marker interval, $\mu$sec. |
|---|---|
| 50 | 12.5 |
| 125 | 31.25 |
| 250 | 62.5 |
| 1250 | 312.5 |
| 2500 | 625 |

*Trigger Inverter.*—Although this tube, $V_{1a}$, is normally biased below cutoff, the positive input trigger drives the grid to zero bias. A grid-limiting resistor $R_1$ is used to limit the grid current. This resistor is bypassed by a small condenser $C_1$ to prevent slowing down of the trigger rise because of the distributed capacity to ground. The positive input trigger is inverted, appearing on the plate as a negative trigger. The plate of the inverter is connected directly to the plate of the "off" tube of the rectangular-wave generator, thereby eliminating the necessity of a separate plate resistor and coupling condenser.

*Rectangular-wave Generator and Cathode Follower.*—Tubes $V_{1b}$ and $V_{2a}$ are used as a cathode-biased d-c coupled "flip-flop" circuit (see Chap. 4). In the absence of a trigger, this circuit is in a stable condition and $V_{2a}$ is at zero bias, thus drawing enough current to keep the cathode at about +55 volts. The grid of $V_{1b}$, which is d-c–connected to the plate of $V_{2a}$, is below cutoff and rests at about +35 volts (or 20 volts below the cathode potential). However, if the resistors in the circuit had values outside the specified tolerance limits, or if the tubes used varied by amounts
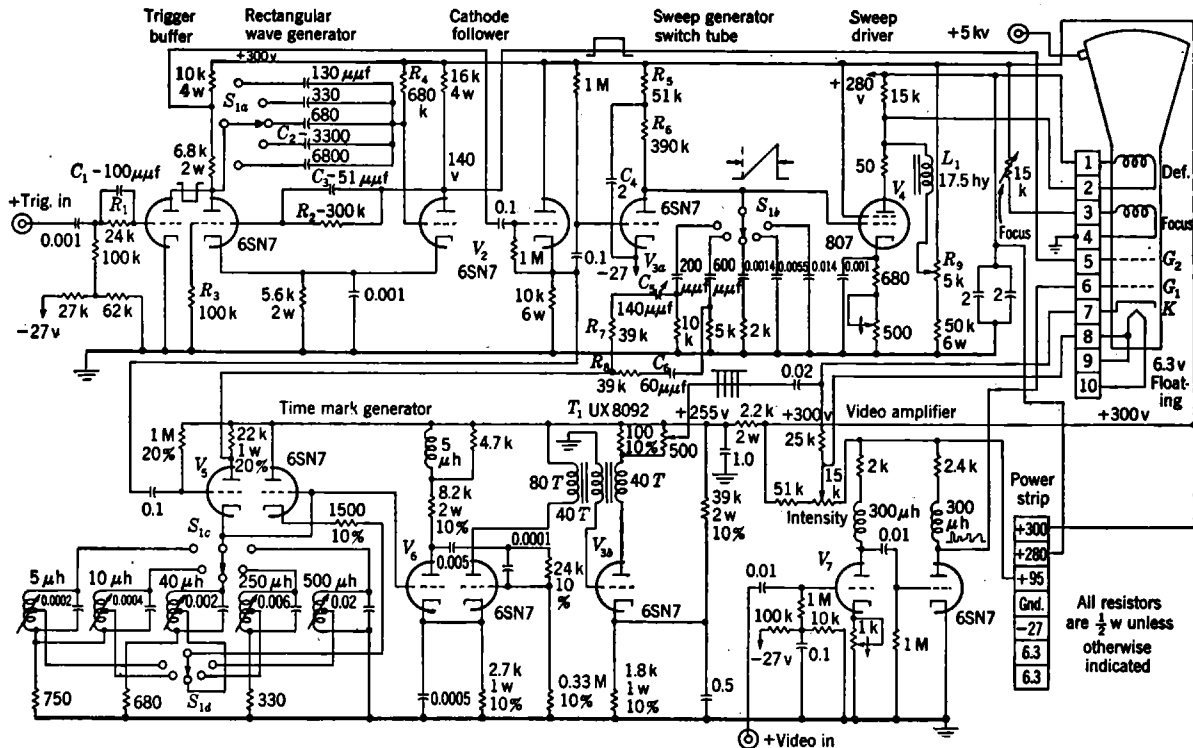
Fig. 13·4.—Simple rotating-coil system.

greater than those prescribed in the JAN tube specifications, the flip-flop might begin to act as a free-running multivibrator. The insertion of a potentiometer control in the cathode circuit (for example, a 4700-ohm resistor in series with a 2000-ohm potentiometer instead of the 5600-ohm resistor) would make the tolerance on the components less critical in so far as stability is concerned.

The time constant of the grid return circuit of $V_{2a}$ is so chosen that the minimum time duration of the rectangular voltage wave is the time of the sweep. If there is no time-duration control, the circuit constants and their tolerances must be such as to insure this minimum time under all possible combinations of component values that are within the specified tolerances. Thus, the normal time duration will be longer than the desired sweep length, and the maximum value may be about 20 per cent larger than this sweep length. Because the trace is not on the cathode-ray-tube screen during the extra time period, the increased time of the gate does not become important unless a repetition rate that is high enough to require rapid recovery of the sweep circuit after every sweep is to be used. If adjustable time duration were required, a potentiometer and a smaller resistor could be inserted in place of $R_4$, the grid-return resistor. This control would vary the time duration for all the ranges. If separate controls for each range were desirable, it would be best to use a single condenser for all ranges and to switch resistor-potentiometer series combinations as is done in the circuits shown in Figs. 13·5 and 13·6.

The output signal from the rectangular-wave generator has three functions. The positive output signal (from the plate of $V_{2a}$) is connected directly to the second grid of the cathode-ray tube, and acts as an intensifying pulse for the duration of the sweep. After the sweep is over, the second grid of the cathode-ray tube is kept at $+140$ volts. This voltage is not low enough to insure adequate blanking for all signals unless the cathode is biased above this point. However, when the cathode is biased that high, the first accelerating voltage (for example, the voltage between the second grid and the cathode) is too low. The accelerating voltage as it exists in this indicator is much lower than it should be for optimum operation. Thus, the spot size could be reduced by a factor of 2 if the second grid were biased higher. The second grid could remain at a fixed potential, which could be obtained from a point on the high-voltage bleeder resistor, if blanking were done on the cathode or first grid of the cathode-ray tube and the video and the range marks were mixed.

The negative output of the rectangular-wave generator is used to gate both the sweep generator and the marker circuit. Since these circuits would excessively load the gate generator, a cathode follower $V_{2b}$ is used to couple the waveforms to them. The negative output is

obtained from a tap in the plate load resistor of $V_{1b}$.   Since the cathode follower is at zero bias and it rests at $+160$ volts, the negative gating pulse will not cut it off.

*Sweep Generator.*—The sweep generator uses a triode clamp $V_{3a}$ which keeps the grid of the driver at about $-22$ volts.   When the negative gating pulse is applied, this clamping action ceases and the potential of the grid rises.   The rise is exponential, with the time constant determined by $R_6$ and the condenser that is selected by the switch $S_{1B}$. Because this sawtooth voltage is not amplified, a large one must be generated so that degeneration can be used in the driver cathode.   The sawtooth waveform that is generated is 100 volts in amplitude, more than 30 per cent of the amplitude of the exponential.   The linearity of the sawtooth voltage is therefore distorted because the voltage increase during the final 25 per cent of time is only 70 per cent of the increase during the first 25 per cent of time.   However, the final distortion on the display is less than that which would result if a smaller, more linear sawtooth waveform were used, and the degeneration were decreased. The ripple filter network $R_5$, $C_4$ tends to improve this linearity slightly for the slower sweeps.   On the faster sweeps, part of a positive rectangular wave is coupled into the sweep generator (through $R_7$, $C_5$ and $R_8$, $C_6$) to give a rapid start (see Sec. 10·1).

*Driver.*—The driver stage consists of an 807 tube $V_4$ with the deflection coil in the plate circuit.   The coil used in this case requires 110 ma for a deflection of one radius.   Degeneration is used in the 807 cathode circuit to compensate for the nonlinearity of the 807 characteristics. The potentiometer in the cathode circuit acts as an amplitude adjustment of the sweep by changing the amount of degeneration.   Even with the degeneration, it is necessary to operate the 807 at a quiescent current that is removed from the very nonlinear low-current region near cutoff. If this quiescent current were to flow through the deflection coil the trace would be deflected before the start of the sweep and the display would show a circle rather than a spot at zero time.   To compensate for this quiescent current, the deflection coil is returned to $+280$ volts rather than to $+300$ volts.   Then, the quiescent current can be supplied through $L_1$ and $R_9$ rather than through the deflection coil.   However, this necessary compensation setting on $R_9$ varies as the range is changed, since the change in range changes the voltage levels of $B+$ and plate of the clamp.   Hence, as the range is shifted, there is some change in the position of the start of the sweep.   This difficulty is not present in the circuits shown in Figs. 13·5 and 13·6 because both of these have no quiescent current in the driver stage.

*Marker Generator.*—The marker generator is a simple shock-excited sine-wave oscillator $V_5$.   The tank circuit connected to the cathode of

$V_{5a}$ begins to oscillate when the tube is cut off by the gating pulse; $V_{5b}$ acts as the oscillator and sustains the oscillations. The resistor in the cathode of this tube limits the amplitude of the oscillation to that of the natural amplitude of the first half cycle.

*Cathode-coupled Flip-flop.*—In the stable position of this flip-flop, $V_{6a}$ conducts enough current to keep the cathode of $V_{6b}$ above its cutoff voltage. When the grid of $V_{6a}$ goes negative, its plate goes positive and regeneration turns $V_{6b}$ on and $V_{6a}$ off. During the positive half cycle of the input sine wave the grid of $V_{6a}$ returns to its conducting position, $V_{6b}$ is cut off, and the flip-flop is ready for the next negative-going half cycle. Since the return of the flip-flop to its stable position is determined by a change of input voltage, rather than the time constant, the circuit is actually being used as a flopover. If the input voltage to the flopover is not high enough for proper operation, the cathode of $V_{3b}$ may be returned to a tap on the cathode resistor of the flopover.

*Video Amplifier.*—The video amplifier $V_7$ has a maximum gain of about 23, a bandwidth of about 1 Mc/sec, and a 20-volt maximum output signal. The positive video signal is inverted twice through two shunt-peaked stages and reappears amplified on the grid of the cathode-ray tube. The first stage $V_{7a}$ has a variable cathode resistor that is used as a gain control. The negative output signal of this stage is d-c–restored by the grid current of the second stage. The output of the second stage is directly coupled to the grid of the cathode-ray tube, thereby eliminating the need for a coupling condenser, biasing resistors, and a d-c restorer. However, this coupling results in the detrimental CRT biasing conditions described in the early part of this section.

**13·4. A Display Circuit Incorporating Current Feedback.**—The performance of this display circuit is relatively independent of line voltage and duty ratio, and its sweeps are linear (Fig. 13·5). The expense of the circuit in terms of both component parts and power is justified by the sweep speeds attainable, the accuracy of the display, and the relative freedom from restrictive tolerances.

The circuit has 5 sweep speeds with 4 markers per sweep.

| Sweep-speed factor, μsec/radius | Time-marker interval, μsec. |
|---|---|
| 25 | 6.25 |
| 50 | 12.5 |
| 250 | 62.5 |
| 1000 | 250 |
| 2500 | 625 |

*Trigger Inverter.*—The input trigger is a +7.5-volt pulse transmitted on a 72-ohm cable. The trigger inverter $V_1$ uses two halves of a 6SN7 in parallel to insure enough gain to fire the following rectangular-wave generator.
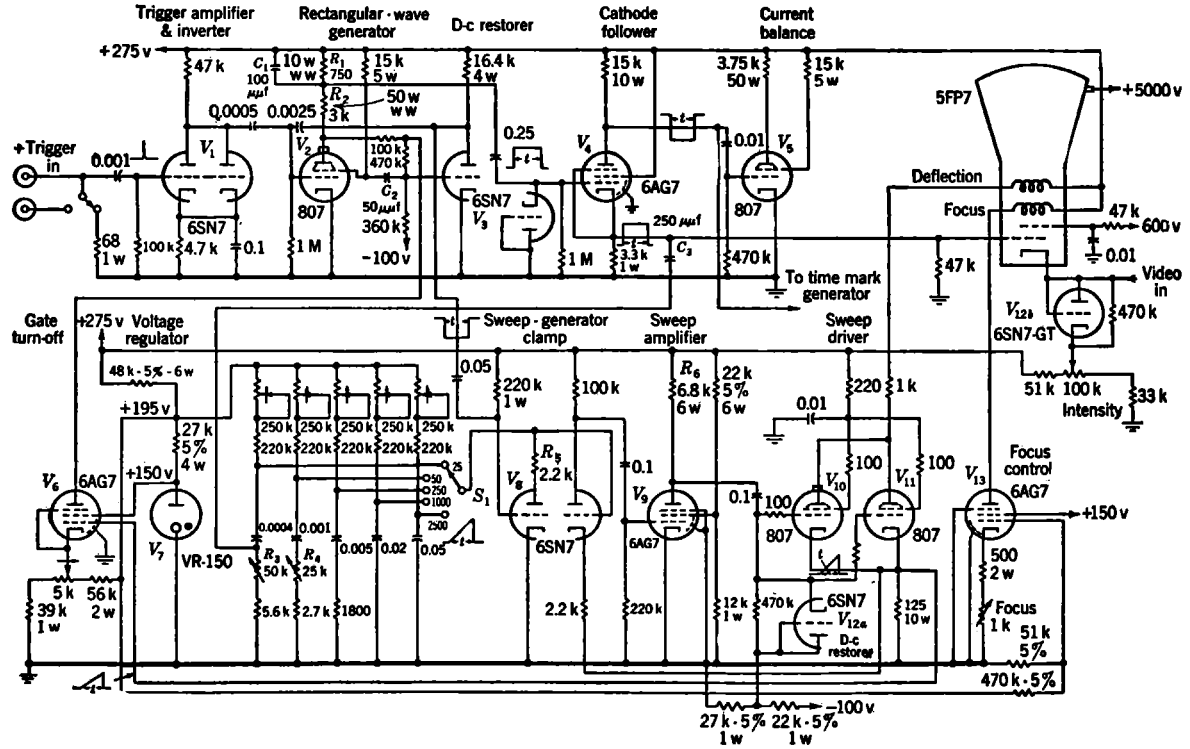
FIG. 13·5.—Rotating-coil radial–time-base display with current feedback.

*Rectangular-wave Generator (Flip-flop).*—The flip-flop $(V_2, V_{3a})$ is actually used as a flopover because the automatic turnoff rather than the time constant determines the length of the gating pulse. In the stable condition $V_2$ is conducting and the grid of $V_{3a}$ is held below cutoff. A rapidly rising gate is insured by keeping the resistance in the plate circuit of $V_2$ low. The 100-$\mu\mu$f condenser $C_1$ across $R_1$ is put there to compensate for the distributed capacity of $R_2$, and its exact value will depend on the particular brand of wire-wound resistor used. The regenerative action of the gate generator, which is initiated by the negative trigger, is speeded by the coupling condenser $C_2$ from the screen grid of $V_2$ to the grid of $V_{3a}$.

The negative gating pulse for the sweep generator is taken directly from the plate of $V_{3a}$. Part of the rapidly rising positive rectangular wave of $V_2$ is coupled to the cathode-follower stage $V_4$.

*Cathode Follower with Plate Load.*—The positive rectangular-wave input to the cathode follower $V_4$ is d-c–restored to ground by $V_{3b}$, thereby making the d-c level of the grid of the cathode follower independent of duty ratio. The positive output pulse of the cathode follower is connected directly to the first grid of the cathode-ray tube and acts as the intensifying pulse. The positive wave is also coupled, through $C_3$, to the sweep-generator circuit in order to start the sweep quickly. The negative rectangular wave from the plate of the cathode follower is used as a gating pulse. It cuts off both the current balancing tube $V_5$ and the clamp in the range-mark circuit.

*Current-balance Tube.*—This 807, $V_5$, is added to equalize the current drawn during the sweep and the current drawn between sweeps, in order to make the operation of the unit independent of duty ratio. When these currents are different, the voltage from the unregulated power supply will vary in so far as changes in duty ratio change the average current. If the voltage did change with duty ratio, then for a given sweep length, changes in repetition rate would change the intensity, the sweep sensitivity, the focus adjustment, and the length of the gating pulse. In this case, the current-balance tube must draw 75 ma during the off time of the sweep, in order to equalize the current drains. If an electronically regulated power supply were used this compensation would not be necessary.

*Voltage-regulator Tube.*—The voltage-regulator tube $V_7$ is used to compensate for any changes in line voltage. If no precautions were taken, then when the line voltage changed, the deflection current, the focus current, and the high voltage would all change proportionally. However, in order to stabilize the display, it is necessary for the deflection current and the focus current to change as the square root of the high voltage. When the voltage change is small, it is a close approximation to use one-half the change rather than the square root. A voltage of

+195 volts on the bleeder from +275 volts to the plate of the VR 150 was found to give the best compensation.

*Sweep Generator.*—On all ranges a sawtooth voltage of approximately 30 volts is generated. This sawtooth represents the first 15 per cent of an exponential voltage rise and is thus fairly linear; the voltage increase in the last 25 per cent of the sweep time is 95 per cent of the increase in the first 25 per cent. The voltage is generated from the +195-volt line-voltage-compensated point by using an $RC$-network and a clamp $V_{8a}$. The 25-$\mu$sec sweep is peaked with a portion of the positive pulse that is coupled through $C_3$ from the cathode follower $V_4$. The step resistors ($R_3$ and $R_4$) in both the 25-$\mu$sec and the 50-$\mu$sec sweep-generating networks are variable so that the start of these sweeps can be made linear and fast. This adjustment is necessary in order to compensate for variations in the cathode-ray-tube mount and in the associated distributed capacity with production models. If it is feasible to select these step resistors after the display circuit is operating with its cathode-ray-tube mount, these controls may be eliminated. There is also a separate control in the sweep-generating networks to adjust the speed of each sweep independently. These controls have a nominal range of $\pm 25$ per cent, which is adequate to compensate for the variation in all of the components that affect the sweep speed. The 2200-ohm resistor $R_5$ in the plate circuit of the clamp increases the impedance of the clamp. If this resistor were not present, the sawtooth voltage would be brought down very quickly at the end of the sweep and there would be some negative overshoot.

*Feedback Amplifier and Drivers.*—The feedback-amplifier–driver combination ($V_{8b}$, $V_9$, $V_{10}$, $V_{11}$, and $V_{12a}$) is in principle the same as the one described in Sec. 10·3. The driver stage is held below cutoff before the sweep begins. When the driver stage is cut off, the gain through the first two stages is approximately 800. The actual gain with feedback is only about one.

To increase the rapidity of response of the amplifier the second stage consists of a 6AG7 with the relatively low plate load of 6800 ohms ($R_6$). Because the peak current necessary for generating the deflection field is 220 ma, two 807's in parallel are used as the driver stage. The grids of these tubes are held at −55 volts between sweeps by a d-c restorer $V_{12a}$. Since the d-c restorer keeps the most negative point of the voltage waveform at −55 volts, negative overshoot will shift the actual bias level of the grid at the start of the sawtooth waveform. Since a very small negative overshoot at the end of the input sawtooth waveform would be amplified without degeneration, it is important to prevent overshoot of this input wave. There is a tendency for the amplifier and the driver stages to oscillate; in order to prevent these high-frequency oscillations,

small resistors are put in series with the control and screen grids of the drivers.

*Gate Turnoff.*—The gate-turnoff tube $V_6$ is biased below cutoff. The grid is connected directly to the cathode of the driver stage and when the driver current reaches the value necessary for a deflection of one radius, the current through the turnoff tube turns the rectangular-wave generator off. This turnoff point is adjusted by the potentiometer control in the cathode circuit of the turnoff tube. To keep this cutoff point constant with changes in line voltage, it is necessary to obtain the biasing voltage from the same +195-volt point that is used for generating the sweep voltage. When this is done, it is necessary to keep the screen grid at the constant +150 volts available at the VR tube $V_7$. ·

*Range-mark Generator.*—The range-mark circuit is not shown since it can be identical with that described in Sec. 13·3.

*Focus-compensating Pentode.*—This 6AG7, $V_{13}$, with the variable-cathode-resistor focus adjustment, automatically adjusts the focus current to compensate for changes in line voltage. This compensation is accomplished by biasing the grid from the +195-volt compensated point in the VR-150 circuit.

*Cathode-ray Tube.*—The cathode-ray tube operates with the anode at 5 kv. The intensifying pulse of 50 volts is applied to the grid. The control grid is biased by the cathode of $V_4$ whereas the cathode bias is variable from 50 to 200 volts in order to accommodate the wide CRT tolerances. The video signals are applied to the cathode. The second grid is at a potential of 600 volts (obtained from the high-voltage bleeder). Setting this voltage at 600 volts rather than at 275 volts decreases the spot size by a factor of 0.6.

**13·5. Rotating-coil Radial–time-base Display with Off-centering.**— Because size and economy of power were not primary considerations in the design, this unit (Fig. 13·6) uses electronically regulated power. There are three adjustable sweep ranges; in each case the beam can be deflected at least four radii.

The sweep-speed factors ($\mu$sec/radius) are: $2880 \pm 2440$ $\mu$sec., $1280 \pm 1000$ $\mu$sec., and $760 \pm 620$ $\mu$sec.

The limiting duty ratio is usually determined by the time required for recovery of the off-centering coil, and this time is at least 700 $\mu$sec.

The signal amplifier accepts two separate +1 volt ($\pm \frac{1}{2}$ volt) video signals and mixes them. It has a maximum gain of about 40, a pass band 2 Mc/sec, and a low output impedance.

There is a nonadditive marker mixer with a gain of 1, which accepts external positive angle and time markers and applies them to the grid of the cathode-ray tube. There is also an off-centering circuit, capable of off-centering the sweep trace up to a distance of three radii.

FIG. 13·6.—Rotating-coil radial-time-base display with off-centering.

*Trigger Buffer.*—This tube, $V_1$, is cut off until the positive input trigger is applied. The trigger is amplified, inverted, and applied directly to the off tube of the delay circuit by using a common plate resistor for $V_1$ and $V_{2a}$.

*Voltage Regulator.*—A very well regulated voltage is necessary for the delay circuit in order to keep the jitter in the delay at a minimum. To obtain this voltage, the regulated $+300$ volts is filtered and further regulated by the VR tube $V_3$. The $RC$-network ($R_1$ and $C_1$) helps in the filtering and prevents the VR tube from oscillating as it would if the condenser were placed directly across it.

*Delay Circuit.*—The delay circuit is a conventional cathode-coupled flip-flop $V_2$. Special precautions are necessary to minimize the jitter for long delays. One of these is the special $+150$-volt power obtained from $V_3$. Another is a separate filament transformer for $V_1$ and $V_2$ exclusively. This is a simple 1-to-1 transformer $T_1$ whose primary is connected to the regular filament supply. In addition, it is necessary to take special care in wiring the delay circuit, particularly near the "on" grid of the flip-flop. The duration of the delay is determined by the potentiometer $R_4$. The maximum-delay control $R_2$ is used to set the delay rate so that the delay can be normalized to coincide with a direct-reading dial on the delay-length control. The resistor $R_3$ in series with the delay control prevents the delay circuit from loading the trigger excessively when the delay control is set at a minimum. This resistor prevents the delay from going to zero, but this difficulty is not at all important with the long sweep lengths involved. The switch $S_1$ connects either the negative trigger or the positive rectangular wave (whose back edge is shaped into a trigger) to the input of the trigger sharpener.

*Clipper and Sharpener.*—When the delay is not being used this circuit acts as a two-stage amplifier, both amplifying and sharpening the negative input trigger. When the delay circuit is being used, the positive rectangular pulse is differentiated at the input terminal. The positive pulse resulting from the front edge is sharply attenuated by $V_{4a}$ which is at zero bias. The small portion of the front edge which is present at the plate of $V_{4a}$ appears there as a negative pulse. Since $V_{4b}$ is cut off, this negative pulse has no effect on it. On the other hand, the negative pulse that results from the back edge of the input rectangular wave is amplified and inverted by $V_{4a}$. It then appears on the grid of $V_{4b}$ as a positive pulse and drives this tube into the conducting region. A positive delayed trigger for external use may be obtained from the cathode resistor of $V_{4b}$. The plate of $V_{4b}$, at which the negative trigger appears, is connected directly to the plate of the "off" tube of the following flip-flop.

*Rectangular-wave Generator.*—The rectangular wave is generated by a combination cathode-coupled, d-c–coupled flip-flop $V_5$. Since the dura-

tion of the gating pulse is kept the same for all three sweep ranges, unnecessary power dissipation results when the faster sweeps are being used. It is therefore suggested that a second gang be added to the range switch to provide independent adjustment of the gate length. For each range, the gate length should be adjusted so that the sweep has time to deflect the beam over four radii. The negative rectangular output wave from the plate of the off tube $V_{5a}$ is used to cut off the switch tube and the intensifier tube.

*Sweep Generator.*—The switch tube $V_8$ is a pentode clamp that operates across the $RC$-network chosen by the range switch $S_2$. Rather than accept the distortion due to the exponential rise of the voltage on the condenser, an inexpensive feedback system is used to linearize the sawtooth waveform. A voltage waveform that is approximately the same as the waveform at the charging condenser ($C_2$) is applied to the top of the charging resistor $R_5$. This feedback voltage is obtained from the second stage of the following amplifier, and therefore tends to keep the voltage across the charging resistor constant, and hence maintains a constant charging current.

*Amplifier and Driver.*—The amplifier-driver system ($V_9$, $V_{10}$, $V_{11}$, and $V_{12}$) is similar to the one described in Sec. 13·4. Between sweeps the two drivers ($V_{11}$ and $V_{12}$) are cut off because their grids are d-c–restored to $-60$ volts. The gain of the amplifier up to the driver grids is 100. When the drivers begin to conduct, the degenerative feedback reduces this gain so that the over-all gain from the input grid to the cathode of the drivers is about one.

The sensitivity of the deflection coil is approximately 55 ma per radius. During off-center operation, a deflection of between three and four radii might be desirable. To supply the necessary current at the voltage available, two 807's are used. Even with the two drivers the deflection available is a function of the sweep speed. As faster sweeps are used, the voltage across the coil $[L\ (di/dt) + iR]$ becomes greater and hence the voltage across the driver decreases. This decrease in tube voltage results in a decrease in the current available from the tube at zero bias. From the constants of the coil used in this circuit ($L = 335$ mh, $R = 610$ ohms), it can be determined that the fastest sweep that can be driven four radii is one whose sweep-speed factor is 400 $\mu$sec/radius. If it is not necessary to off-center the sweep by as much as three radii, a faster sweep can be used.

*Sweep Intensifier.*—To obtain proper blanking of the cathode-ray tube using the first anode, it is necessary to keep the anode potential below that of the cathode. To insure this, an 807 ($V_6$), whose plate is connected directly to the first anode, is used for blanking. Between sweeps the plate of the 807 rests at about $-10$ volts. Its cathode is

held at about $-40$ volts by the unregulated negative output of the power supply. When the tube is cut off the plate rises to $+300$ volts, thereby intensifying the cathode-ray tube.

*Off-centering Control Tube.*—A tube rather than a rheostat is used to control off-centering because of the large amount of current that is required. For a maximum off-centering of three radii a current variable from 0 to 100 ma is necessary. This control is made fairly linear by putting it in the grid circuit of an 807, $V_7$, and using cathode degeneration. The direction of the off-centering is controlled by the position of the off-centering coil in its rotatable housing. Although this coil need only pass direct current, it should not have too long a time constant, for there are transients that exist in it. These transients occur because of the overshoot that is inductively coupled from the deflection coil at the end of each sweep. Even with critical damping, the off-centering coil requires an appreciable time to recover from the transients. When this unit was run at a repetition frequency of about 350 cps, the maximum duty ratio that could be obtained without the center's moving was about 70 per cent. This is equivalent to the recovery time of 700 $\mu$sec required by the off-centering coil.

*Marker Mixer.*—Time and angle markers are mixed nonadditively in the double cathode follower $V_{16}$. The marker-intensity controls shift the bias of the grids of the cathode follower so as to cut off the lower portion of the input waveform. This type of intensity control will change the relative amplitude of the input markers. Hence, when the input marks are not of uniform size (for example, if every fifth time marker is of increased amplitude), an attenuator is more desirable than the bias-changing intensity control. The angle markers consist of a gated pulse of high-frequency oscillation; therefore a relatively low time constant can be used in applying them to the grid of the cathode-ray tube.

*Video Amplifier.*—Tubes $V_{13}$ and $V_{14}$ are two identical video amplifiers whose output signals are additively mixed in the plate circuit. They each have an independent gain control and an independent off-on switch. The low-frequency response is improved by the screen bypass condensers $(C_3, C_5)$ and the large condenser $(C_4)$ in the plate circuit; the high-frequency response is improved by conventional shunt peaking. The positive input signal to either of these tubes is amplified and inverted. The negative output is then applied to the cathode-ray tube through a cathode follower $V_{15}$. The cathode follower decreases the capacitive load on the video amplifier, thereby improving the high-frequency response. It also drives directly the low impedance (100,000 ohms) of the cathode-ray tube, eliminating the large condenser that would be required if the low-frequency response were to be preserved while using a-c coupling. The negative-going cathode follower at zero bias, or $+80$

volts with a 5000-ohm load ($R_6$) in the cathode circuit, is fast enough to respond to the video signals from the amplifier stage (2 Mc/sec). It also acts at its own d-c restorer.

*Focus.*—The focus coil used in this instrument is of the low-voltage type and hence it requires special power at 30 volts d-c. The current through this coil can be reversed so that the focus coil may be positioned properly.

### RESOLVED–TIME-BASE METHOD

If a radar antenna is pointed at an angle $\theta$ (with respect to a reference angle $\theta = 0$) and the distance to a signal is a function of time $f(t)$, Fig. 13·7 shows that the signal can be displayed in proper orientation if

$$x = f(t) \sin \theta \tag{1}$$

is plotted horizontally, and

$$y = f(t) \cos \theta \tag{2}$$

is plotted vertically.

Devices using resistance (sine-cosine potentiometers), capacitance (sine-cosine condensers), and inductance (synchros) have all been employed to resolve the constant-amplitude sweep waveform $f(t)$ into sine and cosine components according to the angle information put into the device (see Chap. 5). As resolvers for sweep waveforms, the principal limitations of the sine-cosine potentiometers are roughness of output data, and limited life. The limitations of the condenser are poor low-frequency response and errors in the output data caused by unbalance in the capacity loading. The limitation of the synchro is its poor low- and high-frequency response. Nevertheless,



Fig. 13·7.—Sine and cosine components of $f(t)$.

because of its mechanical dependability, its ability to operate at low impedance levels, its ability to transmit power directly to deflection coils, and because of the smoothness of its output data, the synchro has proved to be the most useful resolver.

**13·6. Zero Reference Level.**—Usually the sweep wave, represented by $f(t)$, remains at zero during the "wait" interval between sweeps; during the remainder of the sweep cycle, it varies linearly to some maximum value. Since a purely reactive device such as an inductive or capacitive resolver cannot transmit the d-c component of the waveform required to make it zero during the wait interval, the output wave of such a device will be as represented in Fig. 13·8a. The d-c reference level is therefore lost and the resolver output wave is not represented by Eqs. (1) and (2). The only points on the sweep waveform which do not change level with rotation of the resolver are points, such as $P$ in

Fig. 13·8a, which lie on the average-level line. In a fixed-deflection-coil system, however,[1] the sweep rotates about that point on the display which corresponds to the zero level of the a-c components of the current through the deflection coil. In a radial–time-base display it is necessary to have the central fixed point of the pattern occur at zero time. Thus, at zero time it is necessary for the a-c current through the deflection coil to be at zero level. If the current waveform through the coil corresponds to the waveform shown in Fig. 13·8a, the sweep would rotate about *P*, rather than about *S*, which is the start of the sweep waveform. Thus, only that part of the sweep from *P* to *F* would be useful. An additional disadvantage that is evident from Fig. 13·8a is the fact that
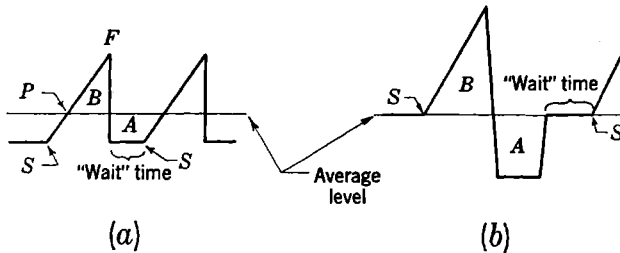


FIG. 13·8.—Output waveforms from inductive-coupled or capacitive-coupled resolver. Area *A* = area *B* in each case. (a) Sweep waveform with no correction. (b) Area-balanced waveform.

the time delay between *S* and *P* depends on the shape of the sweep waveforms [that is, on $f(t)$]. This dependence of the time delay on $f(t)$ prevents the use of simple time-delay circuits to generate a zero-time trigger at *P* from the master trigger at *S*.

There are several methods of compensating for the loss of d-c level. One is to balance the input sweep waveform with a "balancing waveform" of equal area as in Fig. 13·8b. This balancing waveform may conveniently follow directly after the sweep waveform, and then terminate shortly before the next sweep waveform is expected. The area of the balancing waveform is adjusted so that the "wait" level corresponds to the average level and thus the start of the sweep waveform occurs at this level. The sweep will then rotate about the point *S*, Fig. 13·8b, no matter how long the wait time may be.

A second method of correcting for the loss of d-c level is to insert a d-c potential by means of electronic switches or clamps in order to force the waveform to have a fixed d-c value during the wait time (see Sec. 4·1). The switch is then opened so that the linear rise of the waveform can pass undisturbed to the deflecting system. This method works best with voltage waveforms. Examples are shown in Sec. 13·10. The

---

[1] If electrostatic tubes are used the same considerations apply.

corresponding process for clamping current waveforms is discussed in Sec. 13·12.

The third method of coping with the loss of d-c level is to make no effort to overcome the effect directly, but to design the timing circuits to accommodate the situation. This method may be used most easily when it is possible for the display circuits to control the basic timing of the system associated with the display. For example, if a trigger pulse at the time corresponding to $S$ in Fig. 13·8a is allowed to be the fundamental timer for the complete system, it is then possible to generate a trigger pulse at $P$ by a delay circuit of some sort. An example of this is shown in Fig. 13·21 where the sweep waveform itself is used to generate a trigger pulse at the point at which it crosses the average level.

RADIAL–TIME-BASE DISPLAYS USING VOLTAGE WAVEFORMS THROUGH RESOLVING DEVICES

**13·7. Complete RTB Displays in which the Sweep Waveform Is Transmitted through a Synchro.**—Display circuits, employing synchros through which voltage waveforms are transmitted, vary from simple units, in which the synchro drives the plates of an electrostatic cathode-ray tube directly, to complex units that operate magnetic-deflection cathode-ray tubes through amplifiers. These circuits all allow off-centering of the pattern a distance of several radii from the normal centered position by shifting the d-c levels of the "wait" time from zero.

*RTB Display in Which a Synchro Drives an Electrostatic CRT.*— Probably the simplest display using a synchro can be made with the circuit of Fig. 10·16 to supply the sawtooth voltages to the deflection plates. The "overshoot" following the sweep waveform does not have to go through an amplifier and can therefore be large compared with the amplitude of the sawtooth waveform. The area-balanced waveform-generator circuit shown in Fig. 13·15,[1] where the inductance $L$ in this case is the rotor of a synchro, can also be used for this purpose. Figure 13·9 shows the next stage of complexity of this type of display. In this circuit switch tubes are used to restore the d-c level of the sweep waveform. Therefore, a high-duty-ratio sweep, in which the sweep waveform can occupy 80 to 90 per cent of the total time between sweeps, may be used. The transformers have different ratios of primary to secondary turns, or have attenuation on the output voltage to correct for the difference in deflection-plate characteristics. They can be eliminated

---

[1] Much of the initial work in using inductances to generate area-balanced waveforms was done at Telecommunications Research Establishment, Malvern, Eng. See F. C. Williams, TRE report, "Magslip PPI Time base for Magnetic Tubes;" and F. C. Williams and B. H. Briggs, "Magnetic PPI Circuit," submitted at I. E. E. convention, Mar. 1946.

if the synchro output voltage is high enough.   If vacuum-tube voltage amplifiers were used between the synchro stators and the deflection plates, a low-inductance synchro with good high-frequency response could be used, and the necessity of having either amplifying transformers or high-inductance stator windings would be avoided.

*The Use of Synchro-derived Voltage Waveforms to Operate a Magnetic-deflection Cathode-ray Tube.*—If simple amplifiers are inserted between
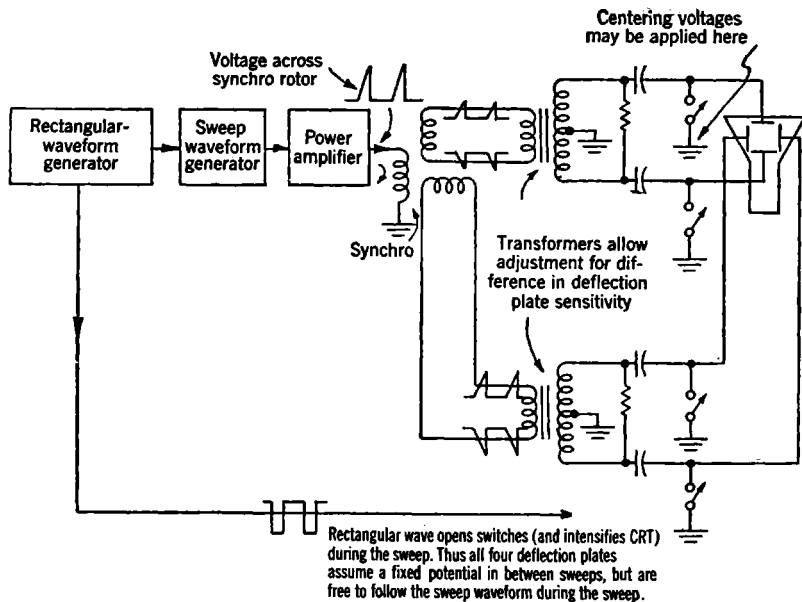


FIG. 13·9.—Block diagram of RTB display in which a synchro drives an electrostatic cathode-ray tube directly.   Typical sweep generators and power amplifiers are shown in Chap. 10.   Typical switch circuits are shown in Chap. 4.

the synchro stators and the deflection coil, as in Fig. 13·10, the voltage waveform through the synchro appears as a nearly identical current waveform in the deflection coil.   With these simple amplifiers, accuracies of $\pm 1$ degree and $\pm 2$ per cent in range are obtainable.   The principle of operation of the deflection-coil driver-amplifier ($V_{16}$ through $V_{19}$) has been described in Chap. 10.   The current through the tube is determined almost exclusively by the grid voltage and is almost independent of the plate voltage.   This operation is greatly aided by the 500-ohm cathode resistors.   The fraction of the cathode current taken by the screen is nearly constant as long as the plate voltage is greater than about 80 volts.

The free-running period of the multivibrator ($V_2, V_3$) is large com-
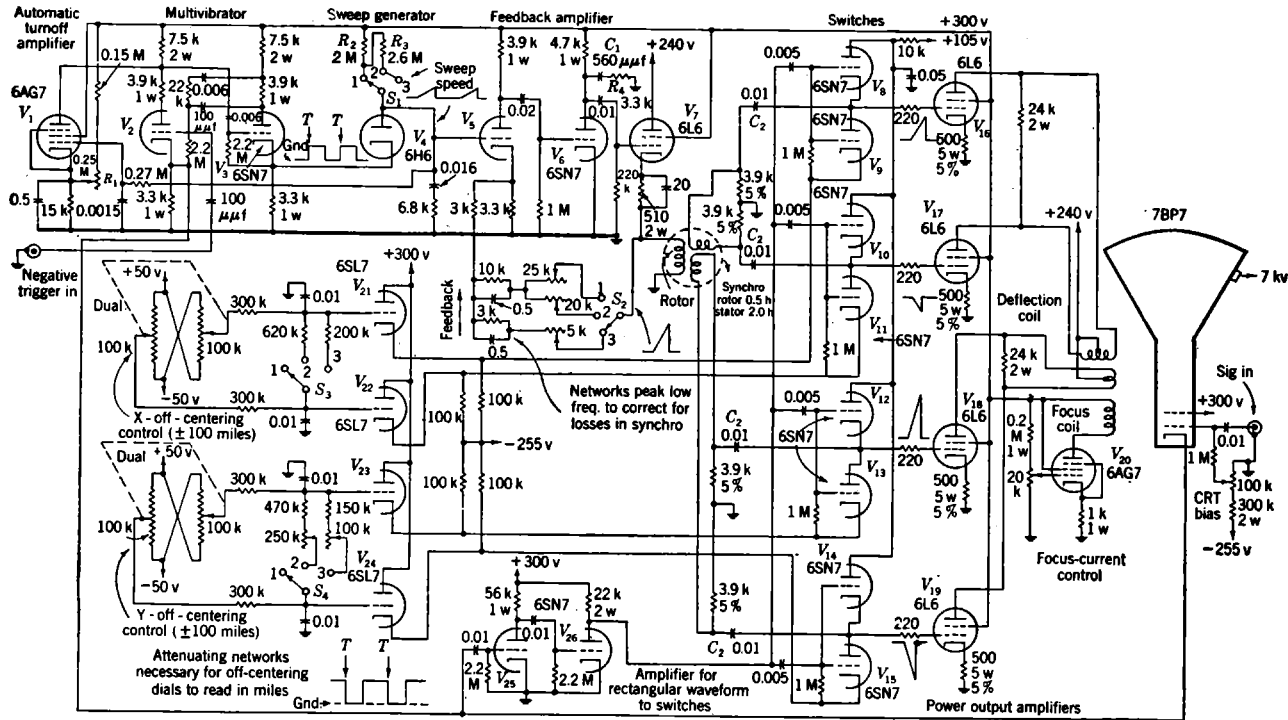
Fig. 13·10.—Off-center RTB display. The sweep voltage waveform is modulated by the synchro, and amplifiers change the synchro–stator voltage waveforms into current waveforms in the deflection coil; Switch Position 1 = 150-mile duration, 3-radii amplitude; Switch Position 2 = 200-mile duration, 2-radii amplitude; Switch Position 3 = 200-mile duration, 1-radius amplitude.

pared with the period of the input trigger and with the sweep duration. The voltage at which the generated sweeps are automatically turned off is set by $R_1$, and $R_2$ and $R_3$ control the slope (and therefore the duration of the sweeps). Thus the rectangular waveform is started by the input trigger and stopped by the sweep, which causes $V_1$, the turnoff tube, to conduct. The feedback amplifier ($V_5$, $V_6$, $V_7$) contains the high-frequency stabilizing network $C_1$ and $R_4$. The low-frequency peaking networks in the feedback lead from the synchro rotor increase the amplifier gain at low frequencies and thus approximately correct for low-frequency losses in the synchro. It is necessary to amplify the cathode waveform that controls the switches, since it is impractical to use the large waveform on the plate of the multivibrator tube $V_3$ because of the heavy load presented by the grids of the switch tubes. In order to control the centering of the RTB display from high-impedance potentiometers, it is necessary to add the cathode followers $V_{21}$ through $V_{24}$. These tubes provide low-impedance points to shift the d-c level of the switch tubes. With the off-centering distances possible with the circuit of Fig. 13·10, the grids of the output tubes do not draw current during the time between sweeps. This circuit can off-center the pattern by two radii and can therefore put on the cathode-ray tube a 50-mile-per-radius sweep covering an area within a 150-mile radius. If larger off-center distances are desired, it is necessary to insert cathode followers between the switch tubes and the driver grid resistors, and at the same time to increase these resistors from 220 ohms to some larger value such as 50,000 ohms. This change in the circuit will prevent output-amplifier grid current from charging condensers $C_2$.

An intensifying waveform, which coincides with the time that the spot is visible on the tube face, is sometimes required. A simple circuit performing this function can be added. This circuit includes four diodes, each of which has its plate connected to the cathode of one of the output tubes ($V_{16}$ through $V_{19}$). The four diode cathodes are connected together and through a resistor to a fixed d-c level that is just equal to the level reached by any one of the power-tube cathodes when the cathode-ray-tube spot is at the edge of the screen. Thus if any one of the output amplifiers exceeds the specified deflection current, a signal appears across the common cathode resistor of the four diodes. This signal may be amplified and used to blank the tube whenever the spot leaves a square region that must be centered about the center of the screen. This signal can also be used to identify the location of the particular sector under observation on another display connected to the same timing and angle data.

**13·8. RTB Display Using a Sine–cosine Potentiometer.**—Figure 13·11 is a diagram of a resolved–time-base display circuit using a sine-

Fig. 13·11.—RTB display circuit employing a sine-cosine potentiometer and an electrostatic-deflection cathode-ray tube.

cosine potentiometer.    The plates of the electrostatic-deflection cathode-ray tubes are directly connected to the brushes of the potentiometer. Because the two sweep generators are also directly coupled to the potentiometer, there is no loss of d-c level in this system.    Therefore, the sweep on the tubes rotates about the point corresponding to the start of the sweep waveform.    This circuit can produce RTB sweeps of 50 or more $\mu$sec per tube radius.

The two 400-volt power supplies are off-set with respect to ground so that the voltage across the sine-cosine potentiometer is zero during the wait time.    The quiescent currents that flow in $V_4$ and $V_6$ during the wait time go through resistors $R_1$ and $R_2$.    Because there is no current flowing through the sine-cosine potentiometer during the wait time, rotation of the potentiometer causes no deflection of the cathode-ray-tube beam during this time.    Thus the starting point of the sweep is fixed on the screen of the cathode-ray tube.    Adjustment of $R_3$ can, however, cause a current to flow in the sine-cosine potentiometer during the time between sweeps, and thus cause the locus of the sweep-starting points to lie on a circle, whose center is the previous starting point, producing an "open center" display.

The attenuators in the leads between the brushes of the sine-cosine potentiometer and the deflecting plates correct for the difference in deflection sensitivity of the two sets of plates, and also permit the insertion of d-c voltages for centering the pattern on the tube face.    Brush noise, much of which is due to contact potentials and is essentially independent of the voltage on the potentiometer, causes small irregularities in the pattern.    The amplitude of this noise is small compared to the relatively large (200-volt) sweep waveforms.

Because the resistance from each brush to ground is fairly high, the leads from the sine-cosine potentiometer must be shielded and limited in length if high sweep speeds are required.    The effect of the capacity loading on the brushes is most noticeable near the 45° point where both brushes are loading the same point on the potentiometer card.    When 5 ft of shielded low-capacity cable is employed it is possible to transmit sweep waveforms as fast as 50 $\mu$sec per tube radius without appreciable distortion.

**13·9. RTB Displays with Sweep Waveforms Transmitted through a Sine-cosine Condenser.**—A sine-cosine condenser has the advantage, compared to a synchro, of good high-frequency response.    A circuit for an RTB display using a condenser of this type (Cardwell, Type KS8534) is shown in Fig. 13·12.    The capacities from one rotor to each of its two stators have the form $C_0 + C_m \sin \theta$ and $C_0 - C_m \sin \theta$.    The capacities from the other rotor to its two stators have the form $C_0 + C_m \cos \theta$ and $C_0 - C_m \cos \theta$ $(C_0 > C_m)$.    If the amplitude $C_m$ of the sinusoidal varia-

tions is small compared with $(C_0 + C)$, the difference in the voltages occurring on a pair of stators is proportional to sin $\theta$. This difference signal is amplified by a difference amplifier, and the output is in push-pull form, ready for direct application either to the plates of a cathode-ray tube or to an amplifier capable of driving a deflection coil. It is necessary to d-c–restore the sweep levels by switch tubes if the sweep is to rotate about the point corresponding to $T$, Fig. 13·12.
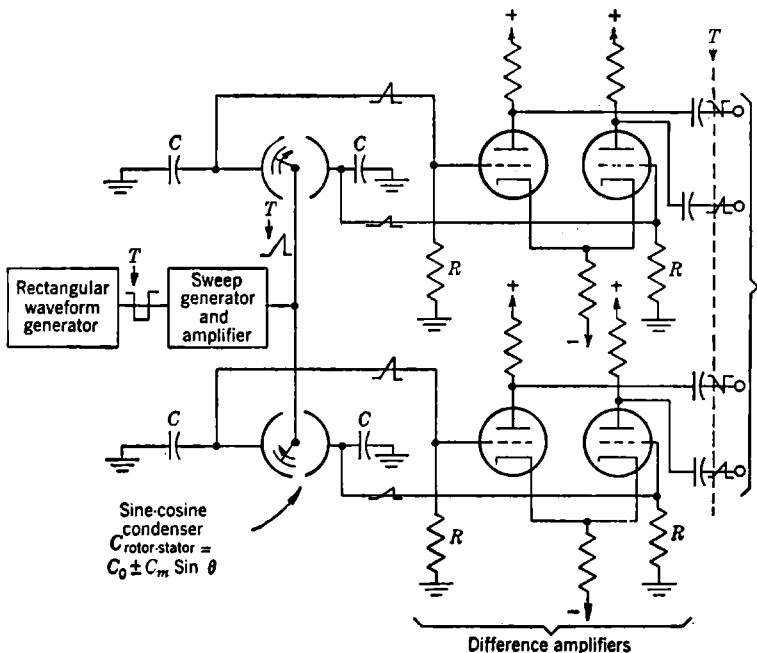


Fig. 13·12.—RTB display using a sine-cosine condenser. $C + C_0$ must be large compared to $C_m$ if the capacity from a rotor to a stator has the form $C_0 + C_m \sin \theta$. $(C_m < C_0)$.

To compute the deviation from a sine curve of the voltage difference on a pair of stators, consider the circuit of Fig. 13·13. The source of $e_i$ has negligible impedance and the resistors $R$ (Fig. 13·12), which affect only the low-frequency response, are neglected.

$$e_2 - e_1 = e_i \left( \frac{\dfrac{1}{C}}{\dfrac{1}{C_2} + \dfrac{1}{C}} - \frac{\dfrac{1}{C}}{\dfrac{1}{C_1} + \dfrac{1}{C}} \right), \tag{3}$$

$$e_2 - e_1 = e_i \frac{2CC_m \sin \theta}{(C + C_0)^2 - C_m^2 \sin^2 \theta}, \tag{4}$$

where $C_1 = C_0 - C_m \sin \theta$ and $C_2 = C_0 + C_m \sin \theta$. Examination of Eq.

(4) indicates that the unwanted $\sin^2 \theta$ term in the denominator is negligible only if $C_m < C + C_0$. The output signals will then be much smaller than the input signals.

A further limitation of the circuit of Fig. 13·13 is that the condensers $C$ must be exactly equal. If they are not, additional errors are introduced into Eq. (4). Long leads on the stators can be used only if they have exactly equal capacities to ground. Since the output voltage is approximately inversely proportional to $C$, a change in length of cable will also affect the amplitude.

The problem of low-frequency losses due to the presence of the resistors $R$ shunted across the condensers $C$ can be solved for sweep lengths appreciably less than the time $RC$ by distorting the input waveform with the addition of a $t^2$ term as in Fig. 10·18.
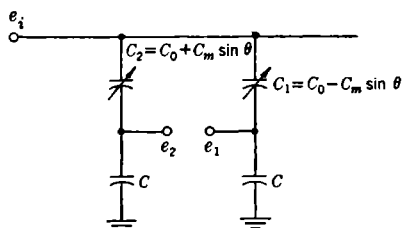
FIG. 13·13.—Sine-cosine condenser used in a voltage divider.

The difference amplifiers are not perfect and they produce signals that are not exactly equal in magnitude. Therefore it is necessary to depend on the linearity of the following push-pull amplifier to equalize the sweep waveforms.

In spite of the good high-frequency response, the limitations of this type of sine-cosine condenser have caused it to be used very seldom.

RTB DISPLAYS USING CURRENT WAVEFORMS THROUGH A SYNCHRO

A motor-stator deflection coil may be driven directly by a synchro through which a sawtooth waveform is resolved. The synchro acts like a set of variable transformers, and the current waveforms in the coil will center about an average value of zero, with a portion of the sawtooth current going in the negative direction (see Fig. 13·8a). The current during the "wait" time can be made equal to zero by the use of the proper area-balanced waveform or by means of switching and clamping circuits. Since the clamp must pass a high peak current (as much as 0.9 amp) as well

FIG. 13·14.—Three types of area-balanced waveforms.

as have a very low forward resistance, selenium rectifiers are more suitable than vacuum tubes for this use.

**13·10. Methods of Generating Area-balanced Waveforms.**—Three types of area-balanced waveforms are shown in Fig. 13·14. In each case the waveform is generated as a voltage and then transformed into a

current waveform by a feedback amplifier. In practice, each of the types of waveform shown in Fig. 13·14 limit the useful sweeps to about 50 per cent of the total recurrence period.

The "step plus sawtooth" wave in Fig. 13·14a is generated by an ordinary $RC$ sawtooth-voltage generator that has a resistor in series with the condenser being charged. A trigger may be generated at the instant the rising sawtooth part of the waveform crosses the zero line. (Figure 13·21 shows a circuit using this method of area-balancing and output-trigger generation.)

An ordinary $RC$-generator produces the sawtooth waveform of Fig. 13·14b, and the rectangular balancing waveform is produced by a resistor and a switch tube. The duration of the balancing waveform is usually fixed (for any given recurrence period) and its amplitude is automatically varied in proportion to the area of the sweep waveform. A voltage proportional to the area of the sawtooth waveform is derived by using an $RC$ integration filter, and is used to set the amplitude of the balancing waveform. (This type of generator is used in the circuit of Fig. 13·22.)



FIG. 13·15.—Balanced waveform generator using an inductance.

The generation of the balanced waveform shown in Figs. 13·14c and 13·16 is accomplished by the action of the inductance $L$ shown in Fig. 13·15. Because the inductance contains only a very small amount of series resistance, the average voltage across it must be very nearly zero no matter what the shape of the waveform. The "Miller run-down" sawtooth generator is essentially independent of the impedance of the plate load. Therefore, when the switch tube is opened at time $t_1$ (see Fig. 13·16), the voltage on the grid of $V_1$ starts to rise, and the plate voltage drops in the usual manner. The nonlinear current in $L$ and the extra current in $R_2$ do not appreciably affect the waveform. After the sawtooth waveform has reached the required amplitude $E_1$ at time $t_2$, the switch is closed and the current through $V_1$ is stopped. The inductance and the two shunting capacities $C_1$ and $C_2$ are completely free to follow the sinusoidal oscillation that is necessary in a free $LC$-circuit in which energy has been stored. After the first positive half cycle, the plate of $V_1$ tries to go below the 200-volt point and continue its oscillation. It is interrupted, however, at time $t_5$ by the diodes $V_2$ and $V_3$, which

present a low impedance to the inductance as long as the inductance current $i_{(t_5)}$ is not in excess of that flowing through $R_2$ (that is, as long as they both conduct).

The current $i_{(t_5)}$ can be readily determined from the energy $\frac{1}{2}CE_2^2$ stored in the condenser at the peak of the oscillation. Equating this energy to $\frac{1}{2}Li_{(t_5)}^2$ the value of $i_{(t_5)}$ is

$$i_{(t_5)} = \sqrt{\frac{CE_2^2}{L}}, \tag{5}$$

where $E_2$ = the amplitude of the sinusoidal oscillation and $C = C_1 + C_2$.
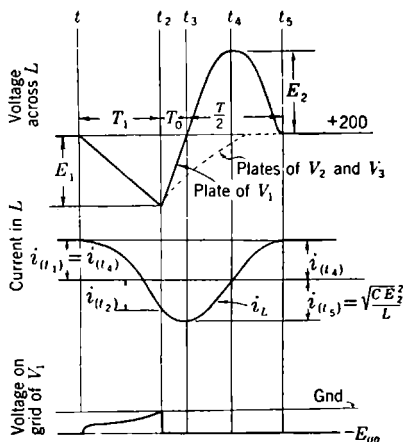


FIG. 13·16.—Waveforms in Fig. 13·15. The positive direction of the current in the inductance $i_L$ is shown in Fig. 13·15.

The inductance will be unable to swing below the 200-volt level only if the current through $R_2$ $[i_{R_2} = (300 - 200)/R_2]$ exceeds $i_L$ and the diodes both remain conducting. The current $i_L$ decreases exponentially during the "wait" time following $t_5$ with a time constant $L/R_{\text{diodes}}$.

To examine the operation of this circuit in more detail, it is assumed as before that the resistance $R$ associated with the inductor $L$ is so small that the voltage drop across it is negligible compared with the total voltage across $L$. This relationship will always hold if the inductance time constant $L/R$ is much greater than the duration of the longest waveform.

The first useful relation in determining the amplitude and phase of the balancing sine waveform is that involving the energy. If $i_{(t_2)}$ is the current in $L$, and $E_1$ the voltage across $L$ at time $t_2$, then

$$\tfrac{1}{2}Li_{(t_2)}^2 + \tfrac{1}{2}CE_1^2 = CE_2^2, \tag{6}$$

where $E_2$ is the amplitude of a sinusoid with the same energy as the total energy stored in $L$ and $C$ at time $t_1$. Thus, if $i_{(t_2)}$ and $E_1$ are known, it is possible to compute the maximum amplitude of the sinusoidal segment of period $T = 2\pi\sqrt{LC}$, which begins at $t_2$ and terminates at $t_5$. If $T_0$ is equal to the time interval between $t_2$ and $t_3$ then

$$\sin\frac{2\pi T_0}{T} = \frac{E_1}{E_2}. \tag{7}$$

It is thus possible to compute the phase of the sine wave with respect to the termination of the sweep waveform.

The conclusion that the sweep and balancing waveforms are equal follows from the general argument that the average voltage across the inductance, which has very small series resistance, must be very nearly zero; that is, the average voltage of the plate of $V_1$ (Fig. 13·16) is 200 volts no matter what the waveform shape. In the circuit of Fig. 13·15 the inductance is clamped at the 200-volt point during the "wait" time; therefore the voltage during the "wait" time coincides with the average value of the waveform.

Actually, it is usually necessary slightly to correct the generated waveform because of second-order effects in the deflection coil. These second-order effects produce an overlapping center circle on the radial–time-base display. Therefore, the cathode of $V_3$ is set at a voltage $\Delta V$ less than 200 volts. The sweep part of the waveform can then start at a voltage level $\Delta V$ volts below the 200-volt level; that is, the sweep starts below the level with respect to which the average voltage must be zero. The appearance of this voltage $\Delta V$ across the inductance, following time $t_5$, causes a current $i_{LL}$ to build up in $L$ (opposite to $i_{(t_5)}$, which is already flowing at time $t_5$) according to the law

$$L \frac{di_{LL}}{dt} = \Delta V, \tag{8}$$

or

$$(i_{LL})_t = \frac{\Delta V \cdot t}{L}, \tag{9}$$

where $t$ = time elapsed since the application of $\Delta V$ to the inductance, that is, the time measured from $t_5$. When $i_{LL}$ gets large enough to equal $i_{(t_5)}$ the current in $L$ is zero. At this instant the diode $V_2$ opens and the inductance is free to oscillate sinusoidally with an amplitude $\Delta V$ about the 200-volt level. If, however, the product $\Delta V \cdot t$ is small enough, $V_2$ does not open and the inductance remains at a voltage $\Delta V$ below the 200-volt average level during the "wait" time. This action tends to produce the open circle necessary for compensation in the RTB display.

The balancing characteristic of the circuit of Fig. 13·15 does not depend on the amplitude $E_2$ of the balancing sinusoid if there is adequate time for the sinusoid to complete the positive half cycle. If this voltage waveform goes directly through a synchro to the deflecting plates of an electrostatic-deflection CRT, a high amplitude of the balancing wave is not an important limitation. However, in driving magnetic-deflection cathode-ray tubes it is necessary to pass this voltage waveform through an amplifier and finally to cause it to appear as a current waveform in the inductance of a synchro rotor (for example, Fig. 13·20).

An alternative method of using an inductance to generate an area-balanced waveform is shown in Fig. 13·17. The sweep part of the wave-

form starting at $t_1$ is generated in the same manner as in Fig. 13·15, but the type of balancing waveform is different.    The inductance $L$ is shunted by a damping resistor $R$ whose value is slightly less than that needed for critical damping, that is, $\frac{1}{2}\sqrt{L/C}$.  Consequently, at time $t_2$, when the current in the pentode tube $V_1$ is cut off, the plate executes a critically damped overshoot that has the initial energy $W_{(t_2)}$.

$$W_{(t_2)} = \tfrac{1}{2}Li_{(t_2)}^2 + \tfrac{1}{2}CE_1^2. \tag{10}$$

The value of $i_{(t_2)}$ is readily determined by integrating the sweep-voltage waveform $E(t)$ from $t_1$ to $t_2$.  Because all the energy $W_{(t_2)}$ is completely extracted from the circuit, mainly through the action of the damping
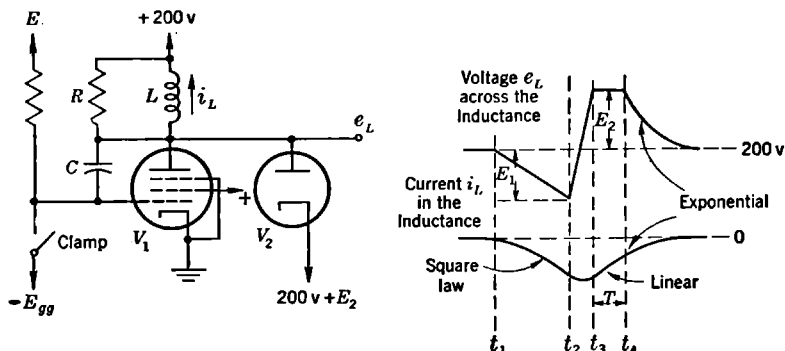


Fig. 13·17.—Circuit for generating an area-balanced waveform.

resistor $R$, before the next sweep starts, the initial current in the inductance is zero.    Therefore:

$$i_{(t_2)} = \frac{1}{L}\int_{t_1}^{t_2} E(t)\,dt. \tag{11}$$

Following time $t_2$, the $LC$-circuit is continually losing the energy being dissipated in the damping resistor.

From $t_3$ to $t_4$ the diode holds the inductance at the $(200\text{-volt} + E_2)$ level, and the total energy lost during this time is $T\ (E_2^2/R)$ where $T$ is equal to $t_4 - t_3$.

At time $t_4$ the current in the inductance has been reduced until the diode no longer conducts and the circuit has the energy

$$W_{(t_4)} = \frac{1}{2}L\left(\frac{E_2}{R}\right)^2 + \frac{1}{2}\,CE_2^2. \tag{12}$$

Following time $t_4$, the voltage and current decay exponentially with a time constant $L/R$ until both reach negligible values and all the energy stored in the circuit at time $t_2$ has been dissipated.

In order to determine the approximate duration $T$ of the flat part of the voltage waveform, the energy lost during the short time $t_2$ to $t_3$ is assumed to be small compared to the total energy. The energy at time $t_2$, $W_{(t_2)}$, then approximately equals that at time $t_3$. Therefore:

$$T \frac{E_2^2}{R} = W_{(t_2)} - W_{(t_4)}. \tag{13}$$

Since $W_{(t_4)}$ and $W_{(t_2)}$ are known from Eqs. (10) and (12), $T$ can be calculated.

The current waveform in Fig. 13·17 shows how the current in the inductance varies with time.

When the voltage waveform in Fig. 13·17 is changed into a current waveform in the inductance of a synchro rotor, somewhat higher voltages are needed in the plate supply of the final amplifiers than in the case of the waveform of the circuit in Fig. 13·15. Push-pull output amplifiers operate successfully with this type of waveform, however.

Figure 13·18[1] shows the output amplifier with the reflected deflection-system inductance $L_1$ in the plate circuit. The grid of this amplifier goes negative during the sweep part of the waveform, and the decreasing current in $L_1$ causes a positive voltage $L_1 I_1 / T_1$ to appear on the plate. This voltage



FIG. 13·18.—Current and voltage waveforms for the rotor of the synchro in an RTB display. $L_1$ is the total inductance of the deflection system as measured at the synchro rotor or at the primary of a transformer driving the rotor.

may be very great if $i_L$ is reduced rapidly and thus the speed of the sweeps is not limited by the plate supply voltage. In the circuit of Fig. 13·18, feedback (not shown) is used to cause the grid signal to have the shape that is needed to produce the required current in $i_L$. The quiescent current $I_0$ must be large enough so that the tube does not cut off near the peak of the sawtooth, i.e., $I_0 > I_1$. The voltage $E_{pp}$ must be larger than $L_1 I_2 (2\pi/T)$ so that the maximum rate of change of current at time $t_3$ can be attained. The power in the output stage must be at least as great as $L_1 I_1 I_2 (2\pi/T)$. For fixed $L_1$, $I_1$, and $T$ this power is directly proportional to $I_2$. In practice, sweep duty ratios above 50 per cent are uneconomical.

If a condenser $C$ is placed in series with $L_1$ (between $E_{pp}$ and $L_1$,

[1] F. C. Williams, Telecommunications Research Establishment Report, "Magslip PPI Time Base for Magnetic Tubes."

Fig. 13·18) the voltage needed at $E_{pp}$ can be appreciably reduced with a consequent reduction in power. The condenser $C$ must be shunted by a large inductance $L_2$ to provide a d-c path for the current $I_1$, as in Fig. 13·19. The saving effected in the $E_{pp}$ voltage may be qualitatively seen by noting that during the time from $t_1$ to $t_3$ (Fig. 13·19) the decreasing current in $L_1$ causes the voltage across $C$ to rise (proportionally to $t^2$ if $t = 0$ at $t_1$). The current causing the increase in voltage across $C$ comes from the large, and therefore essentially constant-current, inductance
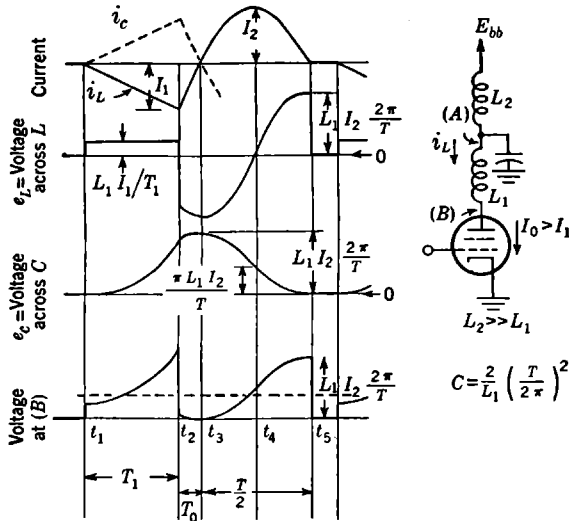


Fig. 13·19.—Operation of the driving circuit of an area-balanced current waveform in an inductance $L_1$. The inductance $L_2$ is much larger than $L_1$ and therefore maintains a constant current. The condenser $C$ aids the plate supply $E_{bb}$ by providing extra voltage at time $t_3$.

shunting $C$. The current in $C$ is actually increasing when the current in $L$ is decreasing because the net current to point $A$ must be constant. As a consequence, the effective plate voltage for the tube continues to increase during the entire time that the current in $L$ is decreasing.

If a sinusoidal current $i_c = -I_2 \sin \dfrac{2\pi t}{T}$ is forced through $C$ ($t = 0$ at the time $t_3$, Fig. 13·17), then the voltage $e_c$ across $C$ is

$$e_c = \frac{1}{C} \int_0^t i_c \, dt = +\frac{I_2 T}{2\pi C} \cos \frac{2\pi t}{T} + \text{constant}. \tag{14}$$

If it is required that $e_c = 0$ when $t = T/2$ (at time $t_5$, Fig. 13·19) and if $C$ is given the particular value

$$C = \frac{2}{L_1}\left(\frac{T}{2\pi}\right)^2, \tag{15}$$

then

$$e_c = \frac{\pi I_2 L_1}{T}\left(\cos\frac{2\pi t}{T} + 1\right). \tag{16}$$

This curve is plotted in Fig. 13·19 from $t_2$ to $t_5$. The voltage across the condenser must have the same value at time $t_5$ as it had at time $t_1$ since the current waveform $i_c$ has a net value of zero from $t_1$ to $t_5$. Thus the $t^2$ rise in $e_c$ from $t_1$ to $t_2$ is just the right value to join the sinusoidal part of $e_c$ at time $t_2$.

Since the voltage across the condenser and the voltage across the inductance are known, they may be added to obtain the total voltage on the plate of the driver tube (voltage curve for point $B$, Fig. 13·19). The relation of this voltage curve for point $B$ to the plate supply voltage $E_{pp}$ depends on the duty ratio of the complete waveform. Because there is negligible resistance between $B$ and $E_{pp}$, the average voltage for any long period at point $B$ must always be $E_{pp}$. The case requiring the greatest value of $E_{pp}$ occurs when a new waveform starts just after the previous one has finished. In this case, inspection of the voltage waveform at $B$ shows that $E_{pp}$ is somewhere near the inflection point of the sinusoid (dashed line in waveform $B$, Fig. 13·19). This value is about half that required if only $L_1$ is in the plate circuit of the power output tube. In equipment where light weight is important, this saving is appreciable.

**13·11. Practical Circuits for RTB Displays Using Area-balanced Current Waveforms.**—The simplest display of this type is the one using the sinusoidal area-balancing waveform generated with the aid of an inductance. Figure 13·20 shows such a circuit.[1]

The rectangular-waveform generator is a stable cathode-coupled flip-flop; $V_2$ conducts in the absence of trigger pulses. In the initial stable condition, the sweep-generating tube $V_5$ is not conducting because its grid is held just below cutoff through $V_4$. The trigger pulse causes $V_1$ to conduct, and the flip-flop regenerates as the plate voltage of $V_2$ rises. The rising plate voltage of $V_2$ also causes diode $V_4$ to open, allowing the grid of the sweep-generator tube $V_5$ to charge in a positive direction.

[1] This is a modification of a circuit given in the TRE report, "Magslip PPI Time Base for Magnetic Tubes." Different types of vacuum tubes were used in the original British circuit. A "flashback control" circuit that limits the maximum speed with which the waveform shifts from the sweep to the area-balancing part has been omitted in Fig. 13·20 in the interest of simplicity. This control circuit permits a further reduction in the power in the output tube $V_{10}$ by reducing the necessary plate supply voltage. Consequently the circuit of Fig. 13·20 has not been operated in the exact form shown.
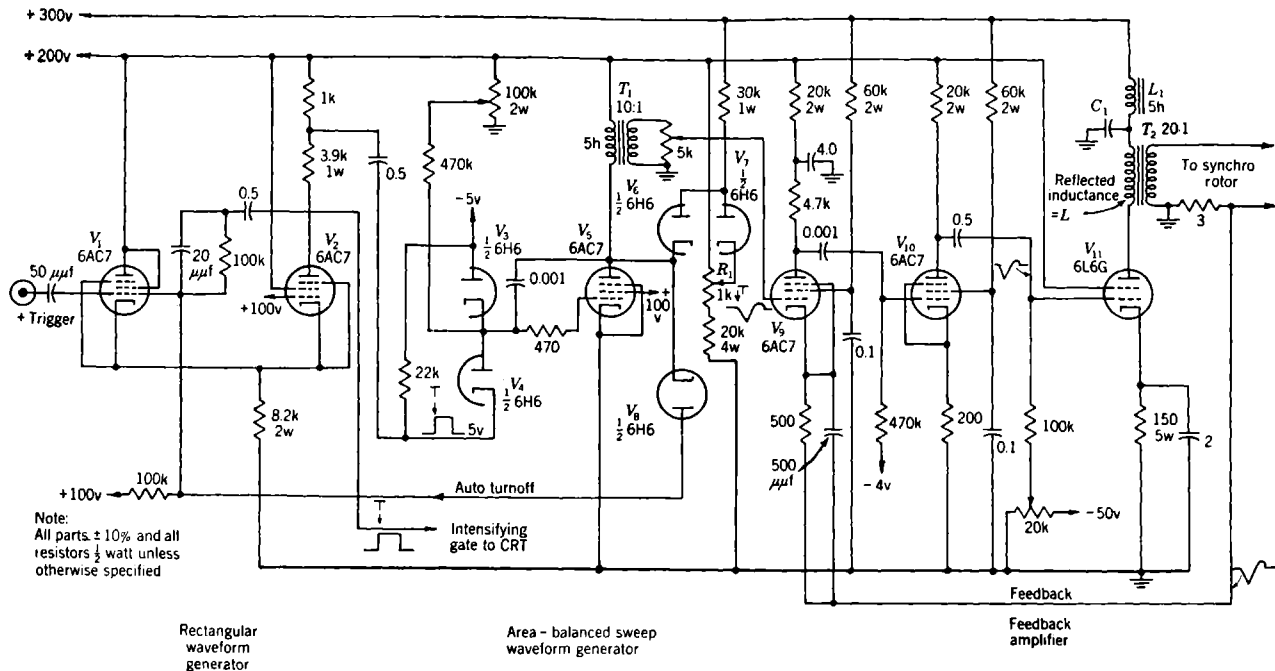
FIG. 13·20.—Driving circuit for RTB display using area-balanced waveform. The compensation in the feedback amplifier depends very strongly on the frequency of the output transformer.

This generates the negative sawtooth sweep waveform at the plate of $V_6$ in the manner described in Fig. 13·15.   When the plate of $V_5$ goes below 100 volts, diode $V_8$ conducts, returning the flip-flop to its stable initial condition.   Then the diode switch in the grid circuit of $V_5$ closes, and the current in $V_5$ ceases.   The plate of $V_5$ goes through one positive half cycle of sinusoidal oscillation and is then stopped by the diode switch $V_6$ and $V_7$ at a point near the 200-volt level, controlled by $R_1$.   The complete waveform is picked up on the secondary of $T_1$ and transmitted through the compensated feedback amplifier consisting of $V_9$, $V_{10}$, and $V_{11}$.   If $C_1 = (2/L)(T/2\pi)^2$, the voltage for the plate supply of $V_{11}$ can be reduced to approximately one-half the value that would be required if $L_1$ and $C_1$ were not used.   $T$ is the period of the sinusoidal balancing waveform and $L$ is the inductance of the deflection system as measured at the plate of $V_{11}$.   Fast-starting sweep waveforms (as in ground-range sweeps) require high voltage across the primary of $T_2$. In the circuit as shown, these sweep voltages are generated by simply cutting off the current in $V_{11}$ at the required rate.   The feedback loop of the output amplifier includes the output transformer.   The extra attenuation introduced by the transformer at both low and high frequencies requires additional compensation in the amplifier in order to maintain stability.   For good performance the transformer must be made with very-thin–lamination iron and be designed for the closest possible coupling between primary and secondary.

Another type of circuit employing area-balanced waveforms is shown in Fig. 13·21.   The waveform used is of the type shown in Fig. 13·14a. The rectangular-waveform generator is started by a trigger pulse from the constant-frequency trigger generator that sets the period of the sweeps.   The sweep generator then generates a sawtooth waveform, which must have a shorter duration than the time between the basic triggers.   This voltage waveform is transformed by the feedback amplifier into a current waveform in the synchro rotor.   In this case a high-inductance rotor (about 275 mh) is used so that waveforms of about 40 to 1000 $\mu$sec may be applied directly to the rotor by a vacuum tube. In order to obtain an output trigger at the time that the current waveform in the deflection coil is passing through zero, it is necessary first to distort the waveform appearing in the cathode of the synchro-driving tube to approximate the distortion caused by the synchro and deflection coils.   This distorted, and thereby corrected, waveform is inserted into an amplifier that amplifies only above a fixed d-c level (in this case, ground).   A rectangular intensification waveform and an output trigger are produced by this amplifier.   Changes in the slope or period of the initial sawtooth (or "step plus sawtooth") waveform do not affect the operation of this circuit, provided that the sawtooth is always completed
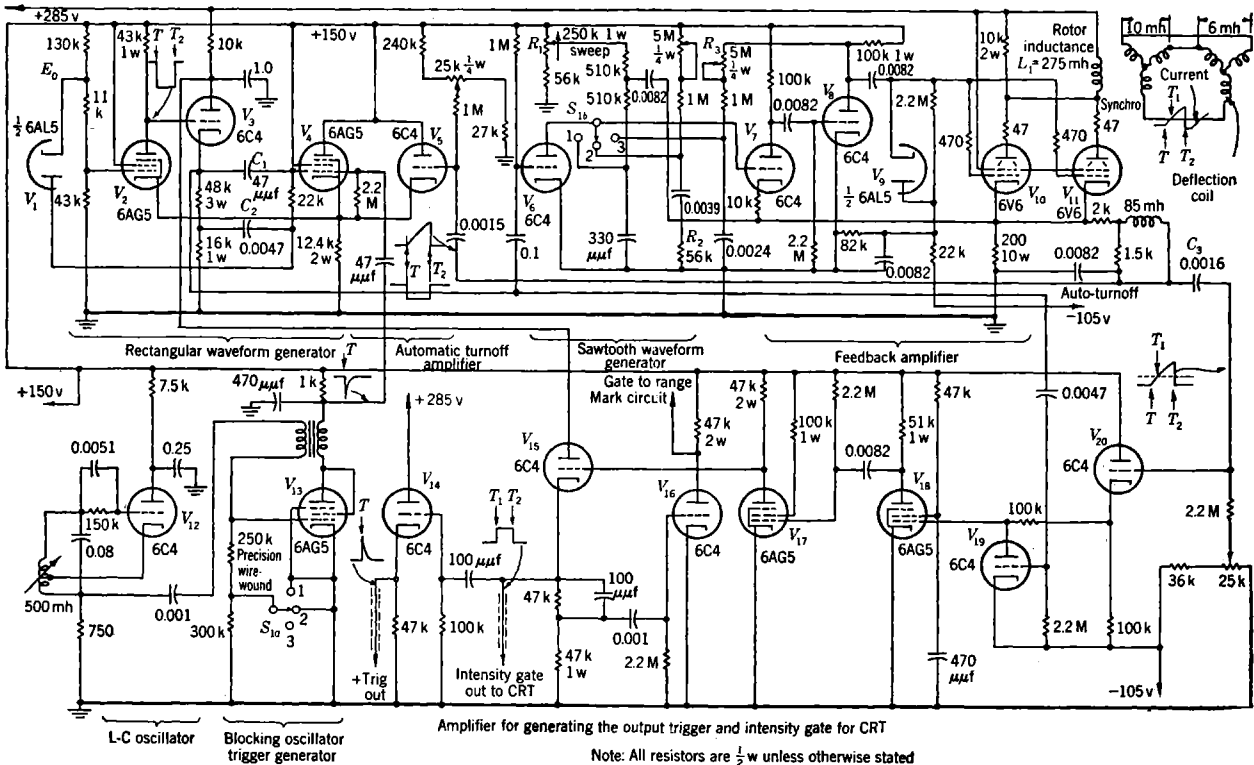
FIG. 13·21.—RTB display circuit using area-balanced sweep waveforms. A trigger is automatically sent out from this circuit at the time the spot on the CRT passes through the point of rotation.

before the next trigger occurs. The trigger and intensification pulse always start at the instant the spot on the cathode-ray tube is crossing through the point of rotation.

The operation of the circuit of Fig. 13·21 may be summarized as follows.

The $LC$-oscillator $V_{12}$ runs at 800 cps. It controls a blocking oscillator, $V_{13}$, which operates either at 800 cps on Positions 1 and 2 of $S_{1A}$, or at 400 cps on Position 3. The trigger from this blocking oscillator starts the cathode-coupled flip-flop circuit.

The presence of the cathode follower $V_3$, which charges condensers $C_1$ and $C_2$ rapidly at the end of the sweep (time $T_2$), enables the flip-flop circuit consisting of $V_1$ through $V_4$ to operate in a stable manner at very high duty ratios. The diode $V_1$ is used in place of the large resistor that would normally be present in the grid circuit of $V_4$. This diode causes the grid of $V_4$ to assume, very accurately, the voltage level $E_0$ from time $T_2$ to the start of the next sweep. This voltage is higher than that of the grid of $V_2$, and therefore $V_2$ is cut off during this time. The automatic-turnoff cathode follower $V_5$ causes the flip-flop to return to its initial condition at time $T_2$ because of the presence of the corrected sweep waveform a-c coupled to its grid. Since the corrected waveform is a-c–coupled to the grid of $V_5$, the amplitude of the useful sweep on the cathode-ray tube is constant. The sawtooth generator is of the conventional type. On Position 1 of $S_{1B}$ a sweep adjustable by potentiometer $R_1$ from 35 $\mu$sec/radius to about 200 $\mu$sec/radius is generated. On Position 2 of $S_{1B}$ a sweep of about 540 $\mu$sec out of a recurrence period of 1200 $\mu$sec is generated. The step resistor $R_2$ aids in making this sweep duty ratio easier to obtain. Switch Position 3 gives a 1100 $\mu$sec sweep at a recurrence period of 2400 $\mu$sec. Low-frequency correction is provided by using the plate of $V_8$ as a source of a large feedback voltage to $R_3$ causing a time-squared term to appear in the sweep waveform. The feedback amplifier allows the output tubes $V_{10}$ and $V_{11}$ to operate from cutoff. Their average current in the rotor of the synchro is not zero and therefore there is a slight open circle in the pattern when the synchro is rapidly rotated, because of the generator action of the synchro. This effect limits the rotation speed possible without interposing a transformer between the output amplifiers and the synchro to cause the average current in the synchro rotor to be zero. A speed of 30 rpm is feasible without a transformer.

The deflection coil is the slightly modified stator of a 3-phase size-1 synchro (see Appendix B, Table B·1).

The correction network causes the voltage on the grid of $V_{20}$ to be very similar to the current waveform in the deflection coil. The cathode follower $V_{20}$ prevents any charge from being stored on the coupling con-

denser $C_3$. This charge would upset the d-c level of the input to the trigger-generating amplifier. At time $T_2$ a clamp tube $V_{19}$ causes the grid of $V_{18}$ to be pulled in the negative direction faster than the corrected sweep waveform itself. The intensification waveform is therefore terminated a little sooner than the actual sweep waveform in the deflection coils and the backtrace is thus prevented from being visible. The rest of the amplifier for the output gate and trigger is of conventional design.

A circuit using the type of area-balanced waveform of Fig. 13·14b is outlined in Fig. 13·22. The sawtooth and balancing rectangular wave are generated separately and after going through two essentially identical amplifiers are applied to the primary of the output transformer. At time $T_1$ the diode clamping tube $V_1$ is opened and the sweep appears on its plate. The sweep is overcompensated because the large signal is applied to the positive end of the sweep-generating resistor $R_1$ through amplifier $V_{17}$. The feedback amplifier is conventional except for the cathode follower $V_6$ which allows the grids of the output tubes $V_7$ and $V_8$ to be driven positive, producing high peak currents.

The voltage waveform on the cathodes of the sweep driver tubes $V_7$ and $V_8$ is averaged by the $RC$-filter $R_2$ and $C_1$. This voltage determines the amplitude of the rectangular balancing waveform that appears on the grid of $V_{11}$. A capacity of 240 $\mu\mu$f on the grid of $V_{11}$ slows up the start of the balancing waveform to reduce the size of the voltage peak occurring across the output transformer at time $T_2$. The 740-volt plate supply for the output tubes is necessary for 60 $\mu$sec/diameter sweeps.

The 2-phase deflection coils are slightly modified stators of 2-phase synchros (Diehl Type PD). For off-centering the pattern, they have extra windings, with twice as many turns as the sweep windings. This circuit will operate two cathode-ray tubes that are off-centered one radius and have a radial time base one diameter in amplitude.

For recurrence frequencies of 200 to 800 cps, sweeps having a 50 per cent duty ratio are possible with this circuit.

**13·12. The Use of Selenium Rectifiers for Maintaining Unidirectional Currents in Deflection Coils.**—It is apparent from the foregoing discussion that the area-balanced waveform scheme has numerous disadvantages, not the least of which is the limitation of the useful sweep to about 50 per cent of the total recurrence period. If rectifiers of suitable characteristics, such as selenium units, are inserted in series with the deflection coils, essentially unidirectional current will flow in the deflection coil even though the source of current is a synchro stator winding. Figure 13·23 shows the equivalent circuit for this case where $R_f$ and $R_b$ are the forward and back resistance of the rectifier, respectively. The imaginary switch $S$ must be considered to be in the appropriate position corresponding to the instantaneous direction of the current.
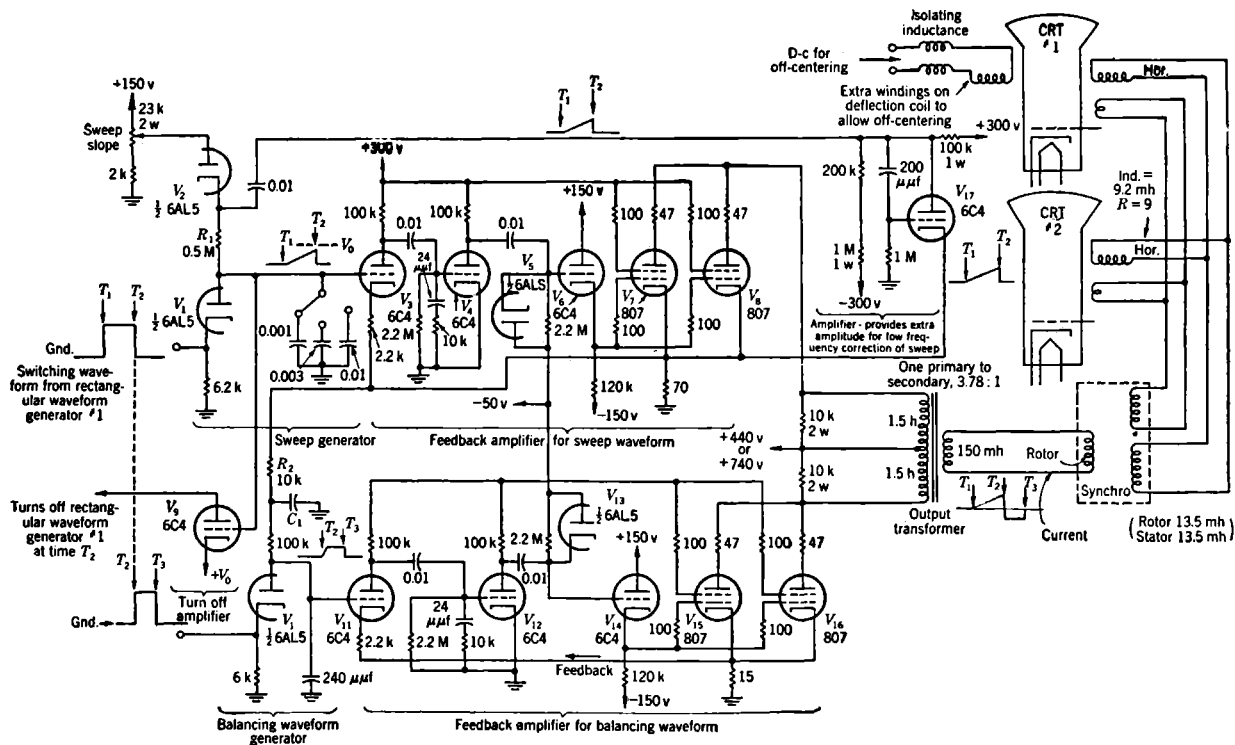
FIG. 13·22.—Area-balanced driving circuit for RTB display. Two magnetic deflection CRT's can be operated in parallel. One radius off-centering is possible.

When a synchro is driving the deflection coil, it is necessary to reverse the polarity of the rectifier at every null point of the stator used because the current waveform reverses sign at the null. Such reversal may be obtained by means of cams and switches or a commutator attached to the synchro shaft. There should be a short interval, corresponding to no more than $\frac{1}{2}°$ of rotation, during which the switch short-circuits the rectifier before effecting the reversal. This switch action makes a smoother transition, which is almost unnoticeable on a cathode-ray screen using a magnetic-deflection tube with normal resolution. A
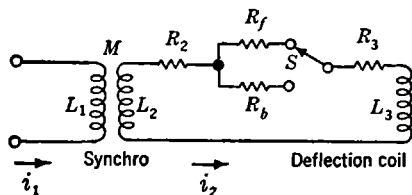


FIG. 13·23.—Equivalent circuit for a synchro driving a deflection coil through a rectifier unit. $R_f$ = forward resistance and $R_b$ = back resistance of the rectifier. The switch $S$ is thrown at the instant the current reverses.

resistor whose value is several times that of the back resistance of the rectifier at low currents should be used across the reversing switch. This resistor reduces the effect of transients due to the action of the reversing switch.

It is of interest to determine the manner in which the rectifier causes the unidirectional current to flow in the stator circuit (Fig. 13·23). The actual forward and back resistances of the selenium rectifier are not constant but vary rapidly with current (see Table 13·1, also Fig. 4·72). The analysis of the rectifier operation is, however, greatly simplified by assuming constant resistances, and an allowance for their variation

TABLE 13·1.—RESISTANCE OF SINGLE SELENIUM-RECTIFIER DISK ($1\frac{3}{4}''$ OD)

| Forward direction | | Reversed direction | |
|---|---|---|---|
| $I$, ma | $R$, ohms | $I$, ma | $R$, ohms |
| 2 | 140 | 0.6 | 3,500 |
| 4 | 80 | 1.8 | 2,200 |
| 10 | 44 | 6.6 | 1,200 |
| 20 | 25 | 12.2 | 820 |
| 40 | 14 | 56.0 | 270 |
| 80 | 7 | .... | ..... |
| 100 | 5.7 | .... | ..... |
| 300 | 2.5 | .... | ..... |
| 500 | 1.7 | .... | ..... |

can be made after the operation with constant values of $R_f$ and $R_b$ is approximated.

To produce a linear current sweep in the stator circuit of Fig. 13·23 it is necessary to cause a current made up of a sawtooth waveform plus a $t^2$ correction term to flow in the rotor (see Sec. 10·7). The rotor current $i_1$ necessary to produce a sawtooth stator current $i_2 = k_1t$ in the stator
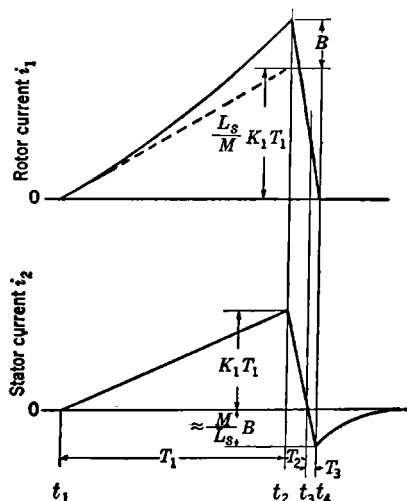


FIG. 13·24.—Current waveforms in the rotor and stator of the synchro in Fig. 13·23. The "overshoot" in the stator current, caused by low-frequency losses, recovers rapidly because of the high back resistance of the rectifier.

circuit is (from Eq. 10·59; it is required that both $i_1$ and $i_2$ are zero at $t = 0$)

$$i_1 = \frac{k_1}{M}(L_2 + L_3)t + \frac{k_1}{M}\frac{R_2 + R_. + R_f}{2}t^2. \tag{17}$$

The rectifier reversing switch (not shown in Fig. 13·23) is always thrown so that the forward resistance is used during the sweep. Figure 13·24 shows the current waveforms in the rotor and stator circuits of Fig. 13·23 where both $i_1$ and $i_2$ are assumed to be zero at time $t_1$. To simplify the writing of the equations, the following substitutions will be made.

$$L_. = L_2 + L_3. \tag{18}$$

$$R'_f = R_2 + R_3 + R_f. \tag{19}$$

$$R'_b = R_2 + R_3 + R_b. \tag{20}$$

$$B \equiv \frac{k_1}{M}\frac{(R_2 + R_3 + R_f)T_1^2}{2}, \tag{21}$$

where $T_1$ is the duration of the sweep sawtooth waveform in Fig. 13·24,

and where $B$ is the time-squared term in the rotor current waveform in Eq. (17).

The magnitude of overshoot of the stator current $i_2$ is readily determined if the first part of the return time $T_2$ required to reduce the stator current to zero (Fig. 13·24) is small compared to $L_s/R_f'$ and if the remainder of the return time $T_3$ is small compared to $L_s/R_b'$. If these two conditions are met (they are readily met in practice) then the $t^2$ correction term can be completely neglected for the case of the return-time waveform itself. If the return-time waveform in the stator is required to be a sawtooth waveform of slope $k_2$, then the rotor current necessary to produce this has a slope $(L_s/m)k_2$, as may be seen from Eq. (17). Since the amplitude of the rotor return waveform is $(L_s k_1 T_1/M) + B$, the amplitude of the stator return-time waveform is very nearly $k_1 T_1 + (MB/L_s)$. Thus, the stator overshoot is $MB/L_s$. At time $t_4$ the rotor current is forced to be zero by the rotor-driving circuit, and the stator current is allowed to decay toward zero with a time constant of $L_s/R_b'$, according to the equation

$$i_2 = \frac{MB}{L_s}\,(1 - e^{\frac{R_b' t}{L_s}}),\tag{22}$$

where $t = 0$ at time $t_4$ in Fig. 13·24. If adequate time is not allowed for $i_2$ to get back to zero, the sweep will not rotate exactly about one end because $i_2$ will still be negative at the start of the next sweep. Note that the rate of recovery is essentially constant for a given synchro deflection coil and selenium rectifier. The amount of recovery necessary is directly proportional to the magnitude $B$ of the time-squared correction term in the rotor. For sweeps short compared to the forward-resistance stator time constant $L_s/R_f'$ the amount of overshoot is small.

An example will illustrate the time required for recovery of a typical system. Let $L_1 = L_2 = 10$ mh, $L_3 = 5$ mh, $k_0 = 0.92$ $(k_0 = M/\sqrt{L_1 L_2})$, $R_2 + R_3 = 15$ ohms. For the selenium rectifier used, $R_f = 5$ ohms at 125 ma, which is the current needed for about half a radius deflection. For an approximate calculation this value may be taken as the average forward resistance. Then, from Eq. (21) the ratio of $B$ to the amplitude of the sawtooth part of the input current waveform $(L_s/M)k_1 T_1$ (see Fig. 13·24), may be obtained.

$$\frac{B}{\dfrac{L_s}{M}\,k_1 T_1} = \frac{(R_2 + R_3 + R_f)T_1}{2L_s}.\tag{23}$$

**Using the constants given above and a sweep of duration $T_1 = 1000$ $\mu$sec,**

$$\frac{B}{\dfrac{L_s}{M}\,k_1 T_1} = 0.66,$$

which shows that the value of the $t^2$ term $B$ in the input waveform is nearly as large as the sawtooth part. Therefore, the overshoot is large and the time for complete recovery is longer. The time constant of the recovery waveform (following $t_4$, Fig. 13·24) is $L_s/R_b'$, according to Eq. (22). If the input waveform has a peak value of 166 ma, then the overshoot will be $MB/L_s$, or 40 ma in the case of the above example. The selenium rectifier has about 400 ohms back resistance at a current of 40 ma. With this value of $R_b$, the overshoot will decay to 36 per cent of its original amplitude in 36 $\mu$sec. In practice, the deflection coils described here can recover from a one-radius 1000-$\mu$sec sweep in about 200 $\mu$sec and have no noticeable defect in the centering of the RTB pattern. A much higher useful sweep duty ratio thus is possible than could be used with area-balancing displays. The sweep-driving circuit of Fig. 13·22 is useful for exciting the rotor of a synchro with selenium rectifiers in series with the stator. Because the stator current, for all practical purposes, recovers to zero current after each individual sweep, any rate of change of sweep amplitude is permissible. Rapid rotation rates of the synchro therefore have no deleterious effect on the RTB pattern.

The major limitations of this type of RTB display are:

1. Poor performance on long sweeps because of the distortions caused by the nonlinear resistance of the rectifiers (particularly noticeable near a null point where the small-amplitude sweep component has an appreciably different shape from the large-amplitude one). In this respect a 3-phase system should give better results than a 2-phase system.
2. The necessity of a long-life low-resistance rectifier-reversing switch that will throw rapidly and accurately in a small angle. With further development of rectifiers and switches, this method should be useful in many applications of RTB displays.

### RESOLUTION BEFORE TIME-BASE GENERATION

This method of producing a radial–time-base display uses a resolving device to operate on a carrier voltage (sometimes a d-c voltage and sometimes a sinusoidal voltage) other than the sweep waveform itself. This carrier voltage is then resolved into components whose amplitudes are respectively proportional to the sine and cosine of the angle of rotation of the rotor of the resolving device. Sweep waveforms proportional in amplitude to these voltages are then generated. The primary advantage of this method is that it eliminates the necessity either of passing the sweep waveform through the resolving device or of transmitting it over long distances. The high-frequency-transmission characteristics of the

resolving device, of transmission lines, and of their associated driving circuits are therefore not required to be of such a degree of excellence as in the previously described schemes.

**13·13. General Description.**—The general nature of a resolution-before-time-base generation system depends somewhat on the type of resolving device used.    The simplest device is a sinusoidal potentiometer to which are applied d-c voltages.

Another system applies an a-c carrier to the resolving device, which is usually a synchro but is sometimes a sinusoidal condenser or potentiom-
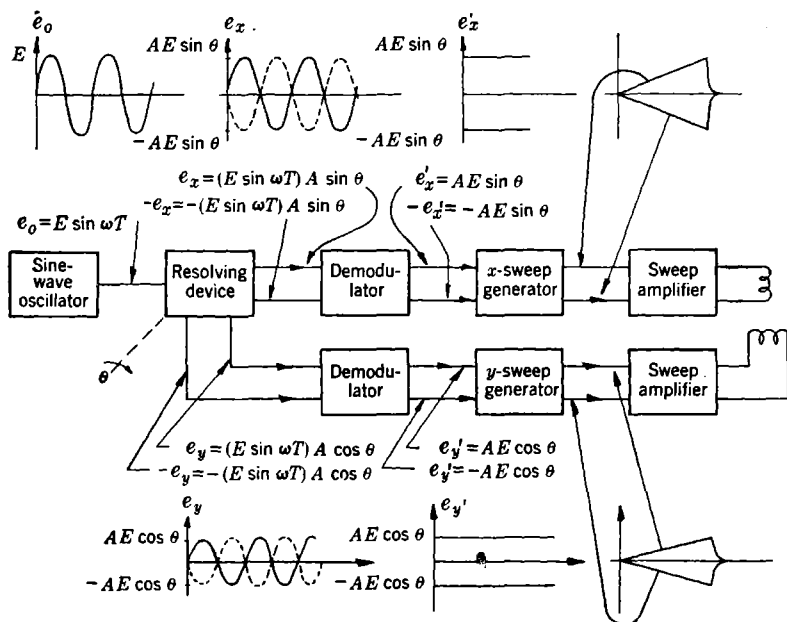


FIG. 13·25.—Elements of a radial–time-base display using pre-time-base resolution.

eter.    A block diagram of this system is shown in Fig. 13·25.    The frequency of the sinusoidal carrier wave used depends on the speed of rotation of the resolving device, the sweep repetition rate, and the ease with which that frequency may be sent over the available transmission lines.    For most practical systems this frequency is between 400 and 5000 cps for synchro resolvers and may be as great as 1 Mc/sec for sinusoidal-condenser resolvers.

The output voltage of the sine-wave oscillator may be written as

$$e_0 = E \sin \omega t.$$

This voltage is applied to the resolving device and the following two components are obtained:

$$e_x = (E \sin \omega t)A \sin \theta,$$

and

$$e_y = (E \sin \omega t)A \cos \theta,$$

where $\theta$ is the angle of rotation of the resolver. The demodulator removes the a-c carrier frequency leaving

$$c'_x = \pm AE \sin \theta$$

and

$$c'_y = \pm AE \cos \theta.$$

Generally, as indicated in Fig. 13·25, both positive and negative voltages are generated because it is advantageous to use push-pull drive.[1] There are two methods of obtaining push-pull drive for the driver stage. One of these is to generate push-pull voltage sawtooth waveforms directly from the resolver output voltages. This method requires a two-way clamp and voltages on the resolver which are both positive and negative with respect to the clamping point. These positive and negative output voltages are available from synchros and from some potentiometers, but are usually not available from condensers. The other method of generating push-pull voltages is to use a difference amplifier. In the electrostatic case, when the current requirements on the driver are not high, it is usually possible to develop the push-pull voltages in the driver stage itself. However, in the magnetic sweep generators, the drivers cannot serve as good differential amplifiers. Thus, undirectional sawtooth waves can be used only if an intermediate difference-amplifier stage is inserted. The signals from this amplifier will then have to be d-c–coupled to the driver grids. If a-c coupling were used, two-way clamps would be necessary on the driver grids.

Because of the lack of stability of d-c amplifiers it is generally more desirable to generate push-pull sawtooth waves from the resolver itself. This is most satisfactorily done using double-diode clamps and voltage feedback (Fig. 13·30). If insufficient input voltage is available to the driver grid from this type of clamp circuit, one-way clamps followed by differential amplification should be used.

**13·14. Time-base Generators.** *One-way Clamp Combined with Differential Amplifier.*—In this case, only positive sawtooth waveforms are generated and these are then combined in a differential amplifier to

---

[1] Push-pull drive has very definite advantages in both magnetic and electrostatic deflection systems. In the magnetic case, the grid swing on the drivers is usually so large that the output wave is nonlinear, but push-pull drive will compensate for this nonlinearity of the tubes. In the electrostatic case, anything but push-pull drive will badly defocus the spot.

obtain the desired deflection. A circuit diagram for such a system is shown in Fig. 13·26.

A sinusoidal potentiometer (see Vol. 17, Chap. 8) is used as a resolving device. If a single positive voltage $E$ is impressed on a sinusoidal potentiometer that has four rotating brushes 90° apart, from one brush is
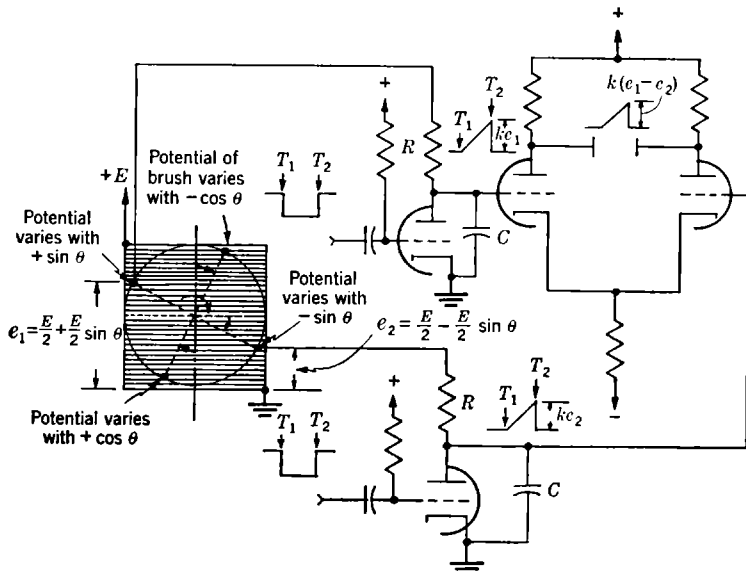


Fig. 13·26.—Pre-time-base–resolution system using one-way clamps with differential amplifier.

obtained a d-c potential

$$e_1 = \frac{E}{2} + \frac{E}{2} \sin \theta,$$

and from the one 180° away is obtained

$$e_2 = \frac{E}{2} - \frac{E}{2} \sin \theta.$$

Since both of these voltages are positive, a one-way clamp can be used together with an $RC$ charging circuit to generate positive sweep waveforms. If only a small portion of the charging curve is used, these sweep waveforms will be nearly linear and of amplitudes equal to $ke_1$ and $ke_2$ respectively. The differential amplifier combines them in such a way that the peak voltage $k(e_1 - e_2) = \mathcal{G}kE \sin \theta$ (where $\mathcal{G}$ is the gain of the amplifier) appears between deflecting plates. A vertical linear sweep whose maximum amplitude is proportional to $\sin \theta$ can thereby be obtained on an electrostatic cathode-ray tube.

The output voltage from the other pair of brushes of the sinusoidal potentiometer can be treated in a similar manner and a deflection of amplitude $\mathcal{G}kE \cos \theta$ can be obtained on the horizontal plates of the cathode-ray tube.

*Two-way Clamp.*—A system such as the one illustrated in Fig. 13·25 has sweep waveforms that go both positive and negative. The most common type of two-way clamp used for generation of these waveforms is shown in Fig. 13·27.

A complete PPI of this type requires four such clamps, one for each sweep component generated. There are four sweep components gen-
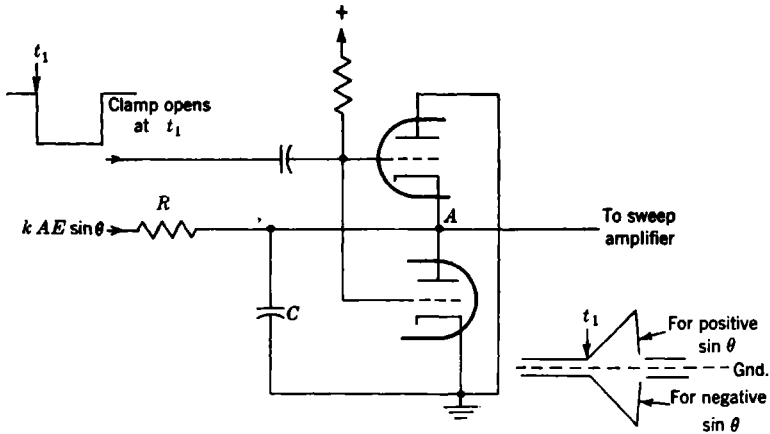


Fig. 13·27.—Sawtooth generator with two-way two-triode clamp.

erated since both horizontal and vertical deflection coils are driven in push-pull; therefore two sweep generators of opposite phase are needed for both horizontal and vertical channels.

The double-triode two-way clamp is subject to the trouble of "gate feedthrough"; that is, a small negative pip appears at the beginning of the sweep because of the capacity between the grids of the clamp tube and the point $A$ at which the sweep waveform is generated. This voltage is always of the same sign and in a push-pull system tends to balance out; however, this balancing action is not complete.

In order to reduce such capacity effects, the diode-bridge type of clamp may be used. There are several variations of this but the one shown in Fig. 13·28 is most common. If the diode capacities are equal, there will be no voltage developed at the junction of $R$ and $C$ due to the gates, provided that the gates are of the same size and have equal rise times. The two gates must therefore be balanced and be obtained from very low or equal impedance sources. A clamp of this type appears at

first to be costly in comparison with the double-triode clamp. However, the two grounded diodes ($V_1$ and $V_3$) of Fig. 13·28 can be common to all four sweep generators and therefore ten diodes are required for a complete system as compared to eight triodes with the double-triode-clamp system.

In either type, the "gate feedthrough" may be reduced by slowing the rise of the gate and by making the gate as small as possible. In a clamp of the diode-bridge type, it may be completely balanced out by adding a small variable capacitance across the diodes, thereby equalizing
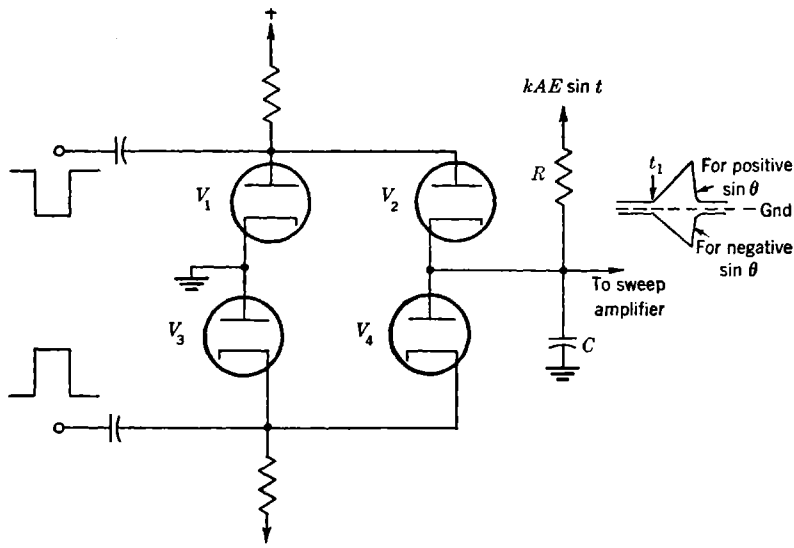


FIG. 13·28.—Four-diode clamp for generation of either positive or negative sawtooth waveforms.

the total capacitances. Actually it is sufficient to equalize the capacitances across $V_2$ and $V_4$.

*Sweep-amplitude Adjustment.*—The over-all sweep amplitude can be adjusted by variation of the carrier-voltage amplitude, but this adjustment affects both the sine and cosine components of the sweep. Therefore, other means must be provided for controlling the relative amplitudes of the $x$- and $y$-sweeps to insure circularity of constant-time indices. Variation of the time constant in one of the sweep-generator circuits is one possible method.

Another possible method of sweep-amplitude adjustment is the variation of all the time constants in the sweep-generator circuits, generally by means of variable resistors. If simultaneous adjustment is desired, these resistors can be ganged together. However, if independent adjust-

ment of all the time constants is made, the circularity of the pattern may be controlled at the same time.

*Centering.*—Centering of the trace on the cathode-ray tube may be accomplished by returning the clamps in the sweep generators to some d-c level other than ground. By this means the amount of current which the sweep-driver tubes pass at the start of the sweep can be varied, and this variation, in turn, changes the position of the origin of the trace on the cathode-ray tube. The same idea may be extended to off-center displays, as illustrated in Fig. 13·10.

**13·15. A Practical System.**—A circuit for a complete pre-time-base–resolution indicator, using as a resolving device a sinusoidal potentiom-
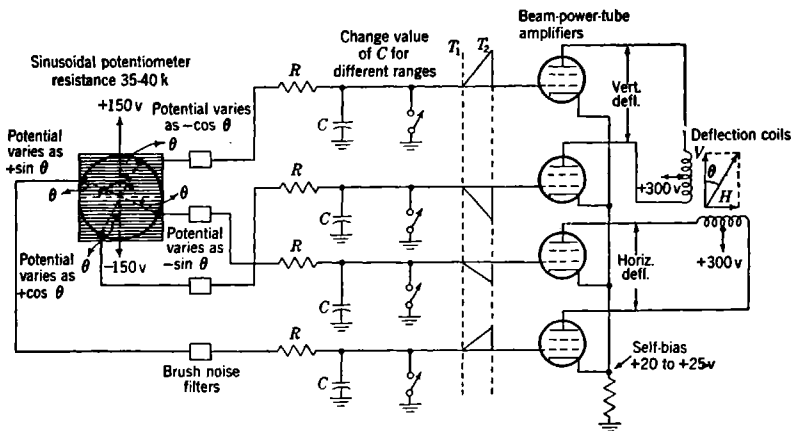


FIG. 13·29.—Simplified schematic of sweep circuit for radial–time-base display using potentiometer as resolving device. Electronic switches open at time $t_1$ close at time $t_2$. Condenser $C$ charges to 10 or 15 per cent of the brush potential, thus generating sawtooth waveforms.

eter with d-c–impressed voltages, is shown in Fig. 13·29. The system using this indicator has a pulse repetition rate of 2000 cps and the indicator tube provides radial rotating sweeps of 7.5, 15, and 30 miles.

The four output voltages from the brushes of the sine potentiometer shown in Fig. 13·29 are passed through high-frequency filters to remove noise generated as the brushes move from wire to wire on the potentiometer. The output waveforms from the brushes of the potentiometer are low-frequency a-c voltages whose frequencies are equal to the speed of rotation of the potentiometer shaft. The filter time constants must therefore be small enough to prevent phase shift at this frequency and the resultant angular errors.

As indicated in Fig. 13·29, the output voltages from the filters are used to control the slopes of four independent sawtooth generators com-

Fig. 13·30.—Complete radial–time-base display

To dropping resistor at $V_6$, $V_7$

+250v  $V_{13}$

1 M

0.01

6V6

300
2 w

0.02

820 k

C  D

$V_9$

6SN7

500
μμf  0.001  0.002

30 k  15 k  5.1 k

500 k  500 k  500 k

68 k
1 w

0.25

22 k

1 M
6V6
$V_{14}$

22 k  1 M

0.01

0.25

$V_{10}$

E

6SN7

100
$R_3$  2 w

300
2 w

50
10 w

47
2 w

500
μμf  0.001  0.002

30 k  15 k  5.1 k

1 M
$V_{15}$
6V6

100
$R_4$

47
2 w

0.01

a

22 k  1 M

0.25

$V_{11}$

F

6SN7

300
2 w

0.02

68 k
1 w

0.001  0.002  0.003

30 k  15 k  5.1 k

To cathode  $V_{7a}$

1 M
$V_{16}$
6V6

0.01

22 k  1 M

0.25

$V_{12}$

G

6SN7

300
2 w

+300v

0.001  0.002  0.003

30 k  15 k  5.1 k

Clamps  Sweep amplifiers

0.02  300
2 w

+300v

+Video

−150v

b
c

+150v

F
E
D
C
B
A

−150v

using potentiometer with d-c impressed voltages.

posed of the $RC$-circuits together with the clamps that are indicated as switches. These clamps are of the two-way variety illustrated in Fig. 13·27. They perform the function of starting and stopping the sweeps at the proper time; and also of starting the sweep at the proper d-c level. This level is maintained regardless of the amplitudes of the sweeps, which vary in synchronism with the rotation of the potentiometer shaft. The two push-pull sweep voltages whose amplitudes are controlled by the $\cos \theta$ voltages are applied to a push-pull amplifier that drives the vertical sweep coil. In a similar manner, the sine components are used to drive the horizontal sweep coil.

In Fig. 13·30, $V_1$ and $V_2$ comprise the trigger generator circuit, with $V_{1a}$ being a blocking oscillator whose repetition rate is controlled by $R_1$. The generated trigger pulse is then applied to $V_{1b}$, which supplies the trigger to the radar modulator. It is also applied through $V_2$ and transformer $T_2$ to the flip-flop $V_5$ and to the delay circuit $V_3$. From the plate of $V_{5a}$ is taken a negative rectangular wave that is applied to the grid of $V_{6a}$. Tubes $V_6$ and $V_7$ comprise the fixed range-mark generator which is discussed in Chap. 6.

The negative trigger pulse is supplied to $V_{3b}$ which with $V_{3a}$ is a flip-flop that generates a variable-width rectangular wave. The end of the positive wave from $V_{3b}$ is developed by the blocking oscillator $V_{4a}$ into a movable marker pip whose position is controlled by $R_2$.

This marker and the range marks from $V_7$ are mixed in $V_8$ and applied to the cathode of the cathode-ray tube. A positive pulse from the plate of $V_{5b}$ is applied to the first anode of the cathode-ray tube for intensification of the sweep. Positive video signals are applied to the grid of the cathode-ray tube.

The clamp circuits, comprising $V_9$, $V_{10}$, $V_{11}$, and $V_{12}$, form the sweep-waveform–generating circuits. The tubes $V_{13}$, $V_{14}$, $V_{15}$, and $V_{16}$ are the sweep drivers.

The gang switch selects one of three positions for ranges of 7.5, 15, and 30 miles. Sections $D$, $E$, $F$, and $G$ are used to switch condensers in the sweep-generating circuits. The resistors in series with the charging condensers cause a trapezoidal rather than a sawtooth waveform to be generated; this waveform is necessary to force a sawtooth waveform of current through the deflection coils. Section $C$ is used to switch one of three variable charging resistors into one of the four channels. Circularity correction for the pattern is thus provided by making up for variability of resistors and condensers and for variation in gain of different driver tubes. Section $A$ is used to switch from 2-mile marks on the 7.5-mile sweep to 5-mile marks on the 15- and 30-mile sweeps. Section $B$ is used to change the length of the gating pulse from the main flip-flop for the various ranges.

In the sweep driving circuits, $R_3$ and $R_4$ are controls for properly centering the pattern on the cathode-ray tube. These are merely bias controls for the clamps on the driver grids which allow the sweep to start with either more or less initial current in the deflection coils.

The sweep driving tubes are of the beam-tetrode type 6V6. Separate cathode degeneration is used for each one to improve linearity and stability. The condensers at the cathodes of the driver tubes $V_{13}$ to $V_{16}$ are peaking condensers that are just large enough to present low impedance for the higher-frequency components associated with the start of the sweep. The sweep can therefore start with less delay than it otherwise would.

The main advantage of a display of this type over other pre-time-base–resolution circuits, such as that using an a-c carrier passed through a resolving device and then demodulated, is its simplicity. However, it has some limitations that are due almost entirely to the potentiometer itself. One of these is the limited potentiometer life, which is dependent upon the speed of rotation of the shaft. Another is a spoking effect in the display due to the irregular angular information as the brushes move from one wire to the next.

# CHAPTER 14

## SECTOR-DISPLAY INDICATORS

### By R. W. Lee

**14·1. Introduction.**—The sector display is a magnified section of a radial–time-base display in which the center of rotation may or may not be at the center of the cathode-ray tube. Figure 14·1a shows a



(a)                                    (b)

(c)                                    (d)
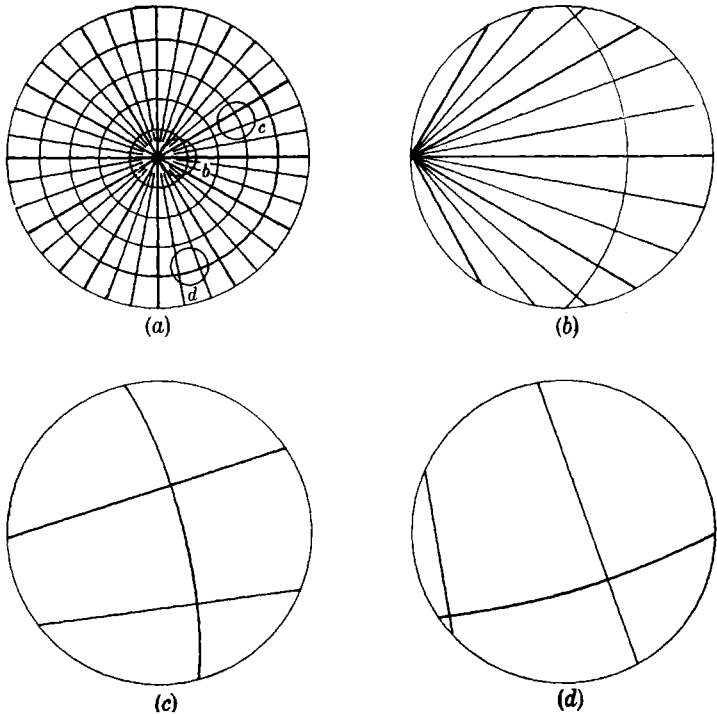
Fig. 14·1.—Sector displays.  Examples (b), (c), and (d) are the various sections indicated in (a) enlarged eight times.

radial–time-base display with time and angle indices.  Figures 14·1b, c, and d show magnified regions of this display as they would appear on a sector-display indicator.  Resolution in the picture is determined by the trace speed and the size of the spot of light on the cathode-ray-tube screen.  Since, ideally, the spot size remains constant as the pattern

is expanded to obtain a sector display, the resolution of the display increases linearly with the magnification until it is limited by the signal pulse length or the repetition rate.

The sector display is free from the inherent distortion of the expanded B-scope; in addition, the proper orientation of the picture is maintained. North is always a definite direction on the tube face regardless of the manipulations that result in the display of the sector. Thus, relative ranges and vectors may be read directly from the tube by means of overlays and other plotting aids (see Chap. 16).

The information required for the generation of such a display is the same as for most other types. It includes (1) a voltage pulse to synchronize the sweeps in time; (2) polar-angle information, preferably in the form of a shaft rotation provided by a servomechanism, for synchronization of the polar coordinates; (3) signals to be displayed, usually voltage pulses involving video frequencies.

In principle, the simplest method of deriving a sector display is to generate a highly expanded radial-time-base trace, which may be of



FIG. 14·2.—Generation of sector display.

either the fixed or rotating-coil variety. By means of constant currents in an external coil, or in the sweep coil itself, if it is of the stationary type, a deflecting field that can move the origin of the trace off-center may be created. If the off-centering coil system is orthogonal, the trace may be moved independently in $x$- and $y$-coordinates. A rotatable off-centering coil lends itself naturally to $r$ and $\theta$ coordinate selection.

It is also feasible to simulate the sector without actually generating the complete picture. To clarify this statement, consider Fig. 14·2. The cathode-ray-tube face is defined by the circle passing through points $B$ and $C$. If the trace is off-centered to point $A$, the time-base deflection brings it back to the tube along the line $ABC$. The appearance of the sector display can also be obtained by holding the trace just off the edge of the tube and then causing deflection along the line $BC$ at the appropriate time. However, the synchronization must be perfect; that is, the spot must appear at $B$ at exactly the same time after the trigger pulse that it would have appeared there if it had been pulled off to $A$ and then driven back. In this way the deflection produced need never be much in excess of one diameter of the tube face.

#### SECTOR DISPLAYS DERIVED FROM RADIAL-TIME-BASE DISPLAYS

**14·2. Rotating-coil Methods.**—The inherent limitations of this method[1] lie in the deflection system, which has been treated in Chap. 12.

[1] This subject has already been discussed in Chapter 13.

Creating a sector display with a rotating-coil radial–time-base sweep and an off-centering coil requires the least complicated circuits of any off-centering method. If not extended beyond two radii off-center, it is possibly the most feasible and practical method. For greater displacements, however, fundamental limitations in the coil system impose difficulties with spot size, pattern distortion, and retrace time, which are not economically overcome.

**14·3. Fixed-coil Methods.**—It is possible to generate a sector display with a two-coil system, whether the sweep coil is fixed or rotatable.
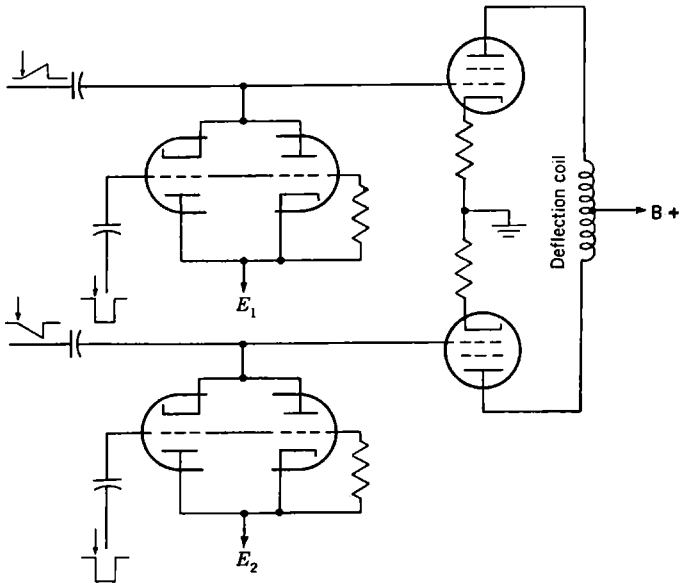


FIG. 14·3.—Typical sweep-amplifier circuit.

However, the limitations of the field-addition method are just as applicable in the case where the inner coil is fixed as in that where it is rotatable (see Chap. 12).

In another method both sweep and off-centering fields are generated in the same coil. A sweep-amplifier circuit, similar to some of those discussed in Chap. 13, is shown in Fig. 14·3 for one coordinate only. Resolved linear sweep voltages are applied to the grids of the amplifiers that drive the deflection coil. The position of the origin of the trace is determined by the direct currents in the output stages, and thus by their grid biases $E_1$ and $E_2$. If these bias levels are variable, the trace may be off-centered in an orthogonal $x$- and $y$-coordinate system. If the gain of the amplifier is sufficiently high, and the output stage does not limit, it

is possible by this means to generate a radial–time-base display that is highly expanded and that may be off-centered many radii.

The limitations of field addition in a two-coil system are circumvented by this method. However, the coil requirements are still stringent. The large magnetic fields that must be generated, and the large amount of energy stored in the field which must be dissipated between cycles, require that a large amount of copper be used to reduce the power and prevent overheating, and to provide a sufficiently low retrace time. On the other hand, spot size on the cathode-ray tube does not suffer because the off-centering and sweep fields are exactly superimposed. Inherent pattern distortions due to asymmetries in the deflection system will be magnified in the same ratio as the picture magnification.

Actually, in any fixed-coil system, it is not necessary to generate large off-centering fields to pull the origin of the trace many radii off the center of the tube face and then to drive the sweep all the way back again. Voltage addition on the grids of the amplifiers may replace the field addition of other methods because the sweep amplifiers are essentially null instruments. In the diagram of Fig. 14·4 illustrating the waveform in the sweep-amplifier grid circuit, time is plotted horizontally. If the grid sawtooth waveform is made to shift vertically with respect to the cutoff level, the sweep may be made to start at an earlier or later time according to the range to the sector area to be displayed. The spot is held off the edge of the tube face by clamping the driver-tube grids to the necessary voltages, and the sweep is made to start at the proper time by adding an appropriate d-c voltage to the grid sawtooth waveform. As soon as the spot has reached the opposite side of the tube, the amplifier may be allowed to 'reach saturation. If it is assumed that the current gain of the amplifier remains constant for all grid voltages, the cutoff level may be moved up or down at will, and (when the amplifier is conducting) the current through the amplifier remains the same for any given grid bias. Hence the sweep speed is controlled only by the sawtooth waveform and not by the grid bias. In other words, field addition of the two-coil method has been replaced by voltage addition on the input grid of an amplifier. If the amplifier were linear from cutoff to zero bias, it would never be necessary to drive the spot off-center farther than the edge of the tube, where it would wait until the proper time to start moving.

The simple case discussed, however, has several practical difficulties. Mixing of a centering voltage and the sweep voltage waveform on the grid of the output amplifier is not advisable. The sawtooth waveform is usually condenser-coupled into this grid, and d-c restored by a clamp tube. This restoration is not practical unless the baseline of the sweep is below zero bias, for at zero bias the output-tube grid current makes

that stage look like a diode, and it will pull against whatever d-c restorer is used. A better method of mixing is a direct-coupled scheme using resistor networks. The off-center display described in Sec. 14·4 (Fig. 14·10) uses this method. Between the mixing point and the output amplifier, there is a degenerative feedback amplifier.

It should be pointed out that this amplifier is critical to the accurate generation of a sector display. The linearity must be good, both for a-c and d-c signals. In other words, it is essential that this direct-coupled amplifier have an almost flat frequency response over the region 0 to 100,000 cps because it is necessary to generate sector displays with high expansions, where no more than the first microsecond of the trace should
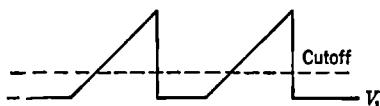


FIG. 14·4.—Waveform in sweep-amplifier grid circuit.

be lost because of poor high-frequency response. Further, since this is a high-gain amplifier, the necessary peaking to obtain the required frequency response must be done carefully because of the danger of regeneration at high frequencies. The operating level of the push-pull amplifier is sensitive to the value of the plate resistors and voltage dividers. Careful normalization of the gains of the two pairs of amplifiers is necessary to insure pattern circularity.

Although the circuits associated with this scheme are more complicated than several others, it is definitely more practical than the "brute-force" schemes if an off-centering of more than three radii is desired. The fundamental limitations, those imposed by the deflection system, are no longer present.

These voltage-addition methods are most applicable to fixed-coil displays, and therefore lend themselves naturally to $x$- and $y$-coordinate off-centering. One advantage of centering in these coordinates is the ease with which this system is adapted to component addition. In many cases, it is convenient to have the total displacement of the trace represent the sum of several separate displacements. All such displacements are vectors, and their components in a rectangular-coordinate system add as scalars. This is a real advantage, for voltage addition of several quantities that are slowly varying is easy in resistor networks. If the off-centering system worked in polar coordinates, there would be no simple way of adding in the external centering voltages.

### SECTOR DISPLAYS THAT ARE NOT DERIVED FROM RADIAL-TIME-BASE DISPLAYS

Thus far, the problem of generating a sector display has been solved by magnetic field addition or by voltage addition on the grids of sweep

amplifiers. Both of these methods represent modifications of existing radial–time-base displays and are geometrically exact. However, if the sector display does not have to be able to generate a complete centered radial–time-base display, there are simpler circuits that can be used to give expansion of sectors. These sectors can be generated by using delayed sweeps. Figure 14·5 shows a radial vector on a radial–time-base display.

The circled sector could be synthesized by resolving the sweeps into two components, one parallel to the vector **R**, and the other perpendicular to it. Any vector **R'** then has a vertical component $\mathbf{R'} \cos \theta$ and a horizontal component $\mathbf{R'} \sin \theta$. The vertical component $\mathbf{R'} \cos \theta$ could further be divided into a delay $\mathbf{R'_1} \cos \theta$ and a sweep $(\mathbf{R'} - \mathbf{R'_1}) \cos \theta$.

For many applications, approximations to these components can be made on the sector display. The B-scan represents an inexact expanded sector in which **R'** is used for **R'** $\cos \theta$ and $\theta$ is used for $\mathbf{R'} \sin \theta$. The following sections will deal with the geometry of other approximate sector displays and the circuits necessary for generating them. As the approximations become more exact, the circuits become more complex.

**14·4. Micro-B Scope with Range Normalization.**—The simplest of these approximate sector displays, for which the approximation is fair, especially at long range, is an adaptation of the B-scope discussed in Chap. 11. The Micro-B scope is a display that combines a delayed time-base of arbitrary duration with a controlled sweep of very low frequency,



FIG. 14·5.—Off-centered display; **R'** can be synthesized by two vectors: one parallel to **R** and equal to $\mathbf{R'_1} \cos \theta$ + $(\mathbf{R'} - \mathbf{R'_1}) \cos \theta$, and one perpendicular to **R** and equal to $\mathbf{R'} \sin \theta$; $\mathbf{R'_1} \cos \theta$ is a time delay.

in which the control coordinate usually is an angle, perhaps the azimuth position of an antenna. The ordinary Micro-B scope suffers from a huge distortion of the scale factor. In the direction of the trace, the scale factor may be 10 miles in 5 inches; but perpendicular to this direction it is a function of range, since a constant number of degrees of angle is presented on the tube face regardless of the range delay of the display. Since the width of the sector displayed is constant in angle, the width of the sector *in miles* is directly proportional to range, as may be seen from Fig. 14·6. To minimize the distortion, the scale of the display in miles per inch must be the same in all directions on the tube face. Therefore, the number of degrees displayed in a given number of inches

on the tube face must be *inversely* proportional to range, or the deflection of the controlled sweep must be made directly proportional to the product of the delay range and the angle. This deduction is borne out by the geometry of Fig. 14·6. Here, the rectangle is matched to the sector $ABCD$ at the points $EF$, and the half-width is

$$\frac{EF}{2} = R_0 \tan \frac{\theta}{2}.$$

If it is desired to present a sector of length $r$ in range, then to minimize the distortions it is necessary to set $r = EF$. Therefore, $r = 2R_0 \tan \frac{\theta}{2}$, and $\Theta = 2 \tan^{-1}(r/2R_0)$ will be the width of the required sector in angle.
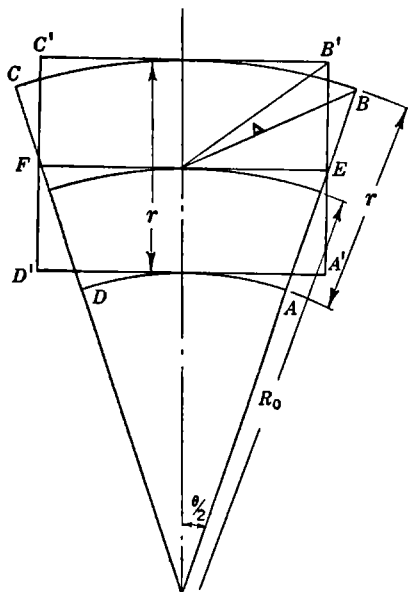


FIG. 14·6.—Geometry of range-normalized Micro-B sector.

The sector $ABCD$ is approximated by the rectangle $A'B'C'D'$. The resulting distortion is not great, except at very close range. For example, if $R_0$ is greater than $2r$, $\theta$ will be less than about 30°. For such an approximation, $\tan \theta$ and $\sin \theta$ may be replaced by $\theta$ itself. Then,

$$BB' \approx \frac{r}{2} \times \frac{\theta}{2} = \frac{r\theta}{4}.$$

To obtain the maximum position error, its maximum value $\Theta$ is substituted for $\theta$, and the following quantity obtained:

$$\epsilon = \frac{r}{4R_0}.$$

The vector error between any two points in the display will be equal to the deviation between the direction line joining them in the true sector and the direction line that joins them in the normalized Micro-B scope.    This error is a maximum for the case of the points $C$ and $D$, or $A$ and $B$.    The vector error is just the angle between $CD$ and $C'D'$, or

$$\alpha = \frac{\theta}{2}.$$

The second case of interest occurs when one of the points is at the center of the tube, and the other at one of the corners.    Since

$$OB = \frac{r\sqrt{2}}{2},$$

$$\Delta \approx \frac{\epsilon}{OB} \approx \frac{\dfrac{r\theta}{4}}{\dfrac{\sqrt{2}\,r}{2}} = \frac{\theta}{2\sqrt{2}} \approx \frac{\theta}{3}.$$

Inspection of the figure shows that other cases are even less important. Note that $AD$ and $A'D'$, $BD$ and $B'D'$, etc., are all nearly parallel, with the result that the vector error is nearly zero.

If it is assumed that a 10-mile sector is to be displayed, then $\theta$ is about 6° at 100 miles and the maximum vector error is only 3°.    At 50 miles, this maximum error is about 6°, and it becomes correspondingly larger as the delay is decreased.

Since the controlled sweep is varying slowly in the case of the Micro-B scope,



Fig.    14·7.—Range-normalization network.

the method of getting a deflection proportional to $R_0$ is simple.    In Fig. 14·7, $R_2$ is a linear potentiometer ganged with the delay knob. As the range increases, the fraction of signal picked off by the divider increases linearly with $R_0$.    If the input voltage is proportional to sin $\theta$, the voltage out of the divider is proportional to $R_0$ sin $\theta$.    (The use of sin $\theta$ instead of tan $\theta$ is justified since it has already been assumed that the angles dealt with are small.)    It is, furthermore, convenient because most resolver devices put out sin $\theta$ rather than tan $\theta$.    In the figure, $R_1$ is simply a slope adjustment to provide the proper normalization.

The second serious defect of the Micro-B scope is that it does not present the proper orientation of the pattern; the sector presented is centered in azimuth about any arbitrarily preselected angle.    A differential gear in the drive of the reference generator producing the sin $\theta$ reference voltage serves to select the angle at which this reference voltage

goes to zero. Figure 14·8 shows how the azimuth-selection crank can be used to rotate the deflection coil so that the orientation of the pattern will be correct.

Since sin $\theta$ has two zeros in every complete cycle, it is necessary to prevent the pattern from appearing on the tube every other time; that is, the unwanted pattern occurring 180° out of phase with the desired pattern must be "blanked out." When a differential gear is used to drive the data generator, a simple device like a cam on the data-generator shaft, actuating a Microswitch, can be used to get rid of the unwanted null point.



FIG. 14·8.—Mechanical schematic diagram for Micro-B scope. Hand crank turns deflection coil directly and phases data from data synchro. Servomechanism gives out control-data information of shaft motion.

In this fashion, a very fair approximation to a true sector may be displayed at a minimum of cost electrically. Mechanically, the scheme is somewhat more complicated than fixed-coil methods, but the coil does not have to be rotated with the antenna; it is rotated only by hand power in the process of sector selection.
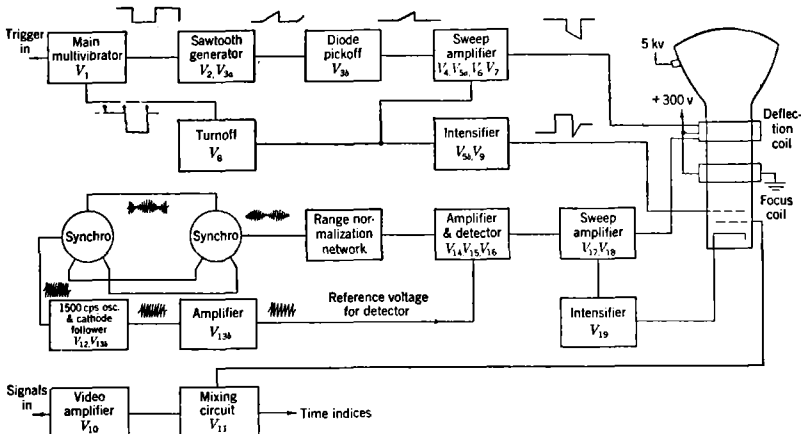


FIG. 14·9.—Block diagram of range-normalized Micro-B sector.

Range-normalization of a B-scope has been mentioned briefly in Chap. 11. Figure 14·9 is the complete block diagram of an experimental sector display of this type, and Fig. 14·10 is the schematic diagram. The tubes $V_2$ and $V_3$ form a linear sawtooth-waveform generator and
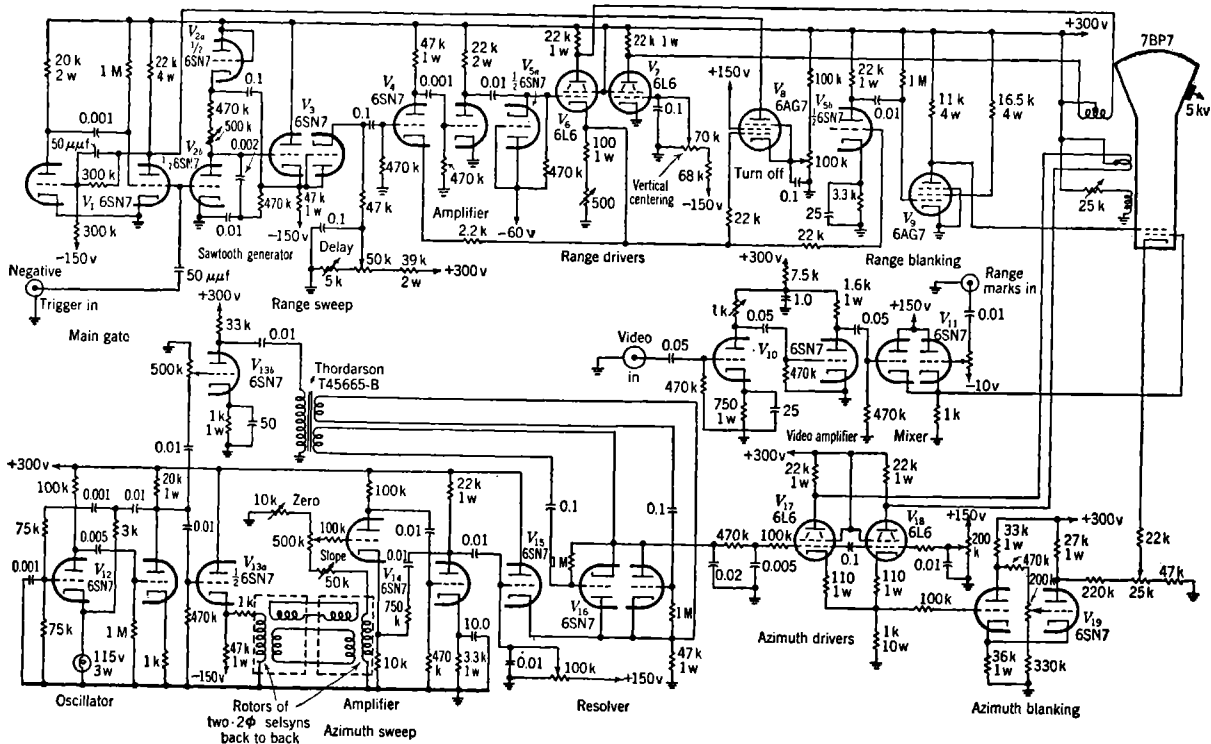
FIG. 14·10.—Schematic diagram of range-normalized Micro-B scope.

diode pickoff circuit similar to that used in many time-delay circuits. However, instead of developing a delayed pulse to trigger a multivibrator gating circuit for the range sweep, the picked-off sawtooth waveform is condenser-coupled into the sweep amplifier and used directly for the time-base waveform. The main rectangular waveform generator is of the "flip-flop" variety with a long time constant, and is turned off at the end of the sweep by the action of a pentode ($V_8$) that conducts only when the current through the output stage of the sweep amplifier reaches a certain predetermined level. It should also be pointed out that this circuit, instead of using a differential gear for phasing the angle reference voltage, utilizes two synchros. One synchro, the rotor of which is turned by hand, replaces the differential gear. The second synchro is turned by the servomechanism, and the stators of the two synchros are tied together. Under these conditions, it is not possible to use a cam and Microswitch for angle intensification of the display, and a "flop-over" circuit ($V_{19}$), acting on the d-c reference voltage, is necessary for this purpose.



Fig. 14·11.—Geometry of rotating-coil range-normalized Micro-B scope. *ABEF* is the sector to be displayed with *O* at the center of the cathode-ray tube. $R_0$ is the range to the sector center, and $r$ the sweep length on the tube.

**14·5. Range-normalized Micro-B Scope of the Rotating-coil Type.**—The approximation treated in the previous section is good at long range (that is, for values of $R_0$ greater than $2r$). The chief cause of error is the fact that the trace does not rotate with the antenna and therefore does not point in the direction of the beam at every instant. However, it is possible to preserve orientation approximately because the trace is lined up with the beam when it is at the center of the tube.

If, however, the coil is rotated with the antenna and the sweeps applied are the same as those used in the range-normalized B-scope, an interesting type of display results. The range sweep, the starting time of which may be delayed by an adjustable amount, is a synchronized time-base of duration $r$, of constant amplitude about equal to the tube diameter. The trace is off-centered by means of direct current until the origin is about at the edge of the tube face. The controlled sweep,

applied at right angles to the range sweep, is a d-c voltage proportional to the sine of the control coordinate (usually an azimuth angle).   Its amplitude is further modulated by means of resistor networks to be proportional to the range delay.   The geometry resulting from this arrangement is shown in Fig. 14·11.   The mechanical schematic diagram of Fig. 14·12 shows the arrangement of the mechanical components required to drive the deflection coil and generate the data for the azimuth sweep.  ·As can be seen from the figure, the setting of the hand crank will determine the position of the coil at which the data voltage will go to zero.   The trace will then be at the center of the tube face, pointing in a direction determined solely by the position of the antenna, as transmitted by the servomechanism.   As the coil rotates through an angle $\theta/2$, the range trace will rotate also about a center that coincides with the center of the tube face.   Simultaneous with this rotation there is a displacement of the trace perpendicular to itself due to the controlled sweep.   From the figure, the displacement
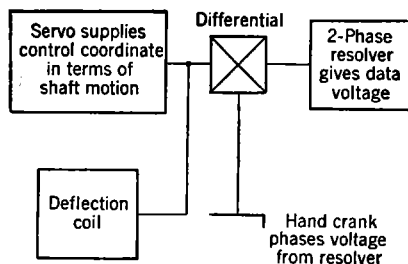


FIG. 14·12.—Mechanical schematic diagram for rotating-coil Micro-B scope.

must be equal to the length $OG$, if the position of the trace is to coincide as nearly as possible with the desired position $BA$.   But

$$OG = R_0 \sin \frac{\theta}{2},$$

which is exactly equal to the output voltage of the range-normalized azimuth sweep.

Figure 14·11 illustrates the errors involved.   The extreme position errors occur at the corners of the pattern.   A signal that should appear at point $A$, for example, will appear at $A'$ in this picture.

Now, since $AB = A'B'$, and $DA$, $OH$, $CB$ are arcs of concentric circles,

$$AA' = BB' = GH = JG - JH.$$

But

$$JG = R_0 \left( \sec \frac{\theta}{2} - \cos \frac{\theta}{2} \right),$$

$$JH = R_0 \left( \sec \frac{\theta}{2} - 1 \right),$$

$$\therefore GH = R_0 \left( 1 - \cos \frac{\theta}{2} \right)$$

$$\approx R_0 \frac{\theta^2}{8}.$$

To find the angular width $\Theta$ of the pattern presented on the tube face, it is necessary to equate

$$R_0 \sin \frac{\Theta}{2} \approx \frac{r}{2}.$$

$$\Theta \approx \frac{r}{R_0}.$$

Therefore, the maximum possible error (which occurs at the edge of the tube face) is

$$\epsilon = GH_{\text{max}} \approx \frac{r^2}{8R_0},$$

which is about half the error encountered with the ordinary range-normalized Micro-B scope. Vector errors between two points in the display are similarly decreased. For example, the angle

$$\alpha = \tan^{-1} \frac{R_0(1 - \cos \theta/2)}{R_0 \sin \theta/2}$$

$$\approx \frac{\theta^2/8}{\theta/2} \approx \frac{\theta}{4},$$

and

$$\alpha_{\text{max}} \approx \frac{\Theta}{4} \approx \frac{r}{4R_0}.$$

Thus, in presenting a delayed 10-mile sector, the center of which is at 50 miles, the number of degrees presented is

$$\Theta \approx 11°.$$

The maximum position error is then

$$\epsilon \approx \frac{r^2}{8R_0} \approx \frac{1}{4} \text{ mile,}$$

and the maximum vector error is

$$\alpha_{\text{max}} \approx 3°.$$

One disadvantage of this scheme lies in the extreme distortions that are produced when the delay is small; that is, when $r/2 < R_2 < r$. As the angle presented becomes larger, the motion of the trace becomes very complicated. The trace displacement is the sum of a rotation about the center of the tube and a sidewise motion proportional to $R_0 \sin \theta/2$. Therefore, for short delays and when large angles are presented, the position of the trace is not a single-valued function of the control coordinate.

The block diagram for a model of this type of sector display is given in Fig. 14·13 and the corresponding circuit diagram in Fig. 14·14. The circuit is essentially the same as that given in Sec. 14·4, but there are

differences in detail.   For example, tubes $V_1$ through $V_5$ form a conventional linear sawtooth delay network that generates a trigger pulse at any arbitrary delay up to about 1000 $\mu$sec.   This delayed pulse

+6 kv

+300

Peaking amplifier $V_{4b}, V_5$

Pickoff diode $V_{3b}$

Sawtooth generator $V_2, V_{3a}, V_{4a}$

Wide gate generator $V_{1b}, V_{2a}$

Trigger amplifier $V_{1a}$

Trig. in

Deflection coils

Focus coil

Time-base sweep amplifier $V_9, V_{10}, V_{11}, V_{12}$

Sawtooth generator $V_8$

Delayed gate generator $V_6, V_{7a}$

1500 cps Osc. & cathode follower $V_{18}, V_{19a}$

Controlled sweep amplifier $V_{16}, V_{17}$

Amplifier & detector $V_{20}, V_{21a}, V_{15}$

Range form. network

1CT Synchro

Reference voltage

Isolating amplifier $V_{19b}$

Angle blanking $V_{23a}$ +cam.

D-c restorer $V_{22}$

Video amplifier $V_{13}, V_{14}$

Time mark amp. $V_{23b}, V_{24}$

Signals in

Time marks in

FIG. 14·13.—Block diagram for circuit of rotating-coil range-normalized Micro-B scope.

initiates a time-base of a speed equal to about 100 $\mu$sec per tube diameter. Another important difference is that, in this case, only one resolver, a 1CT synchro, is used.   Because this resolver is driven by a differential gear, the angle-blanking of the picture is done by a cam and Microswitch
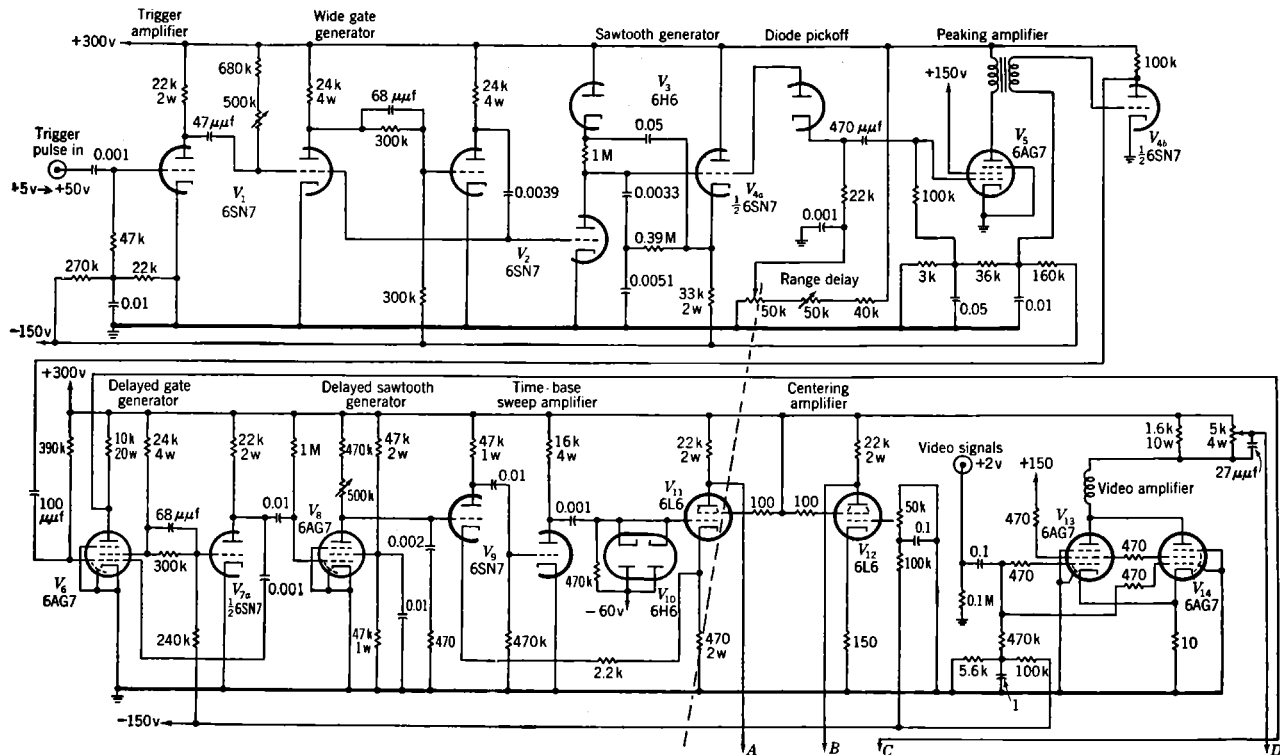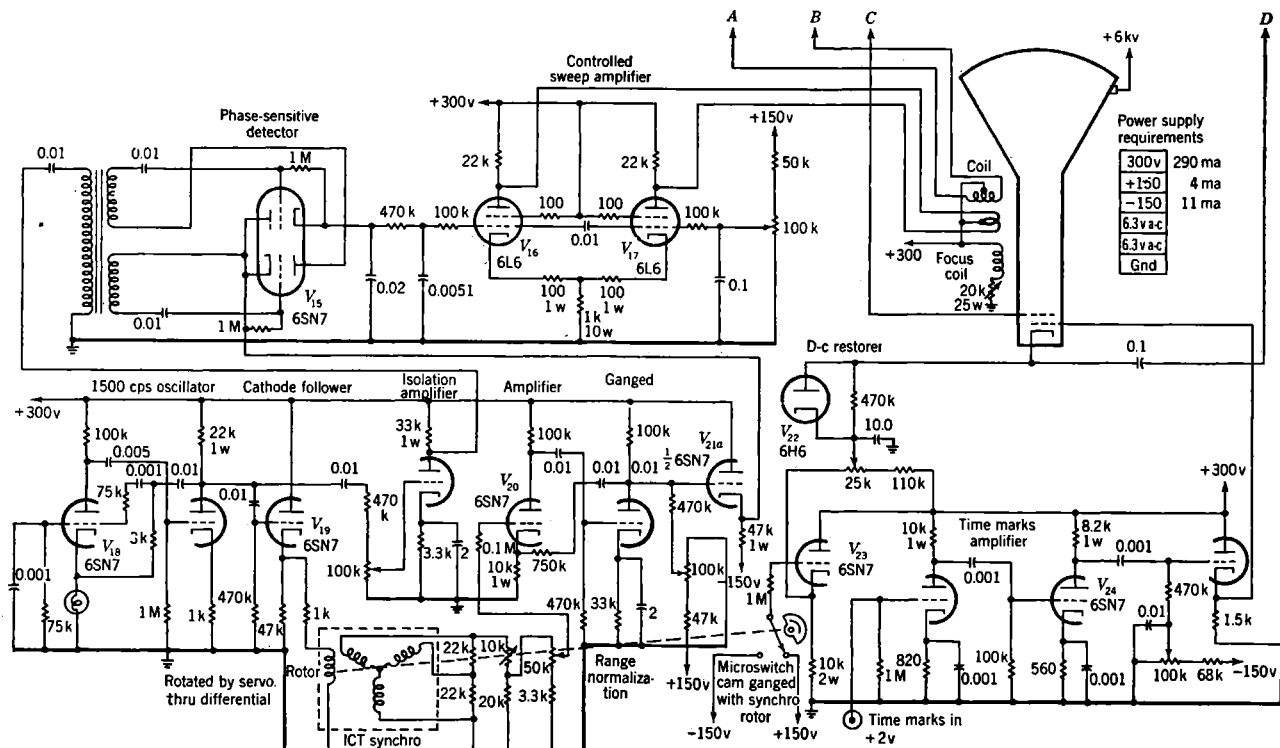
Fig. 14·14.—Electrical schematic diagram for rotating-coil range-normalized Micro-B scope.

arrangement rather than by a flop-over circuit as in the previous example. This method is possible because the use of the differential gear preserves, on a shaft, a motion that always represents the difference between the position of the hand crank and the position of the synchro shaft. A cam on this shaft can be positioned so that it will intensify only the desired sector symmetrical about the center of the tube, and reject all other sectors, including the second null 180° away.

Since both the signals to be displayed and the time markers are inserted into this system at a low level (about two volts peak, positive polarity), a video amplifier is needed for both sets of signals. The signal amplifier $(V_{13}, V_{14})$ has a maximum voltage gain of about 40, and a pass band approximately 3 Mc/sec wide. (This corresponds to a rise time of about 0.1 $\mu$sec.)

**14·6. Approach to True Sector.**—The sector displays discussed in the two previous sections have consisted of one unmodulated time base and a controlled sweep similar to that used in the Micro-B scope. The displacement of the trace from the center of the tube has been made proportional to $R_0 \sin \theta$, where $R_0$ is the range to the center of the delayed sector. Thus, in the method of Sec. 14·4, the displacement from the zero position is the same for all points on the trace at any given value of $R_0$. By rotating the coil, as in the method of Sec. 14·5, the trace can be kept pointing in the proper direction, but the picture is overcorrected; lines of constant range, for example, trace out paths that have too much curvature. If, instead of either of these methods, a time base, the amplitude of which is modulated by $\sin \theta$, is used for the $x$-deflection, the display is improved in several respects. The displacement due to such a sweep is everywhere proportional to $t \sin \theta$, where $t$ is time measured from the pulse that starts the sweep. Since, in the geometry of a radar display, range and time are equivalent, the displacement due to a sine-modulated time base is $R \sin \theta$ (*not* $R_0 \sin \theta$).

One point that should be emphasized is that the displacement in one coordinate of an orthogonal coil system is completely independent of the deflection, or lack of it, in the other. Figure 14·15 illustrates how this fact applies to the method of this section. By means of direct current in one of the windings of the deflection system, the spot is off-centered to position $A$. At the time of the trigger pulse, the sine-modu-lated time base starts deflection of the spot along the line $AB$. At the end of the delay time, the range sweep is started, and the spot moves along the line $BC$. This range sweep is linear in time and unmodulated. The trace is intensified only during the range sweep; thus $BC$ is the only portion that is visible. The sweep therefore *appears* to originate at the point $O$. The important point is that the sine-modulated time base continues deflection in the same direction at the same rate after the

delayed time base starts.    Hence,

$$AB = OB \sin \theta,$$
$$DC = OC \sin \theta, \text{ etc.}$$

Therefore, the displacement of the sweep at every point is proportional to the *range at that point*, rather than to the average range of the sector, $R_0$.

In Chap. 13, methods of deriving angle-modulated time bases have been discussed.    Here, only the most-used alternatives will be mentioned.



FIG. 14·15.—Sector display generation: two time bases.  For any angle $\theta$, the sweep moves along $AB$ in the time corresponding to the range $OA$; then it moves along $BC$ at the end of the time delay that gives $OA$. The line $BC$ is the resultant of two motions, one in the direction $AB$, the other in the direction $AD$.

1. Resolution of a linear time base into sine and cosine components by transmission of a linear-sweep waveform through a synchro.

2. Direct use of d-c voltages proportional to sine and cosine of the reference angle to generate the necessary modulated time bases. This d-c voltage may be available from a sine potentiometer, or an a-c carrier voltage may be transmitted through a synchro resolver, the modulated carrier detected, and the detected waveform used in the same fashion.
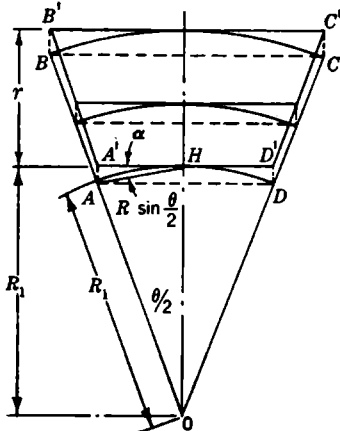


FIG. 14·16.—Geometry of time-base modulation.  $ABCD$ is the true sector represented on the tube face by $A'B'C'D'$.  $R_1$ is the range to the near edge of the sector and $r$ is the sweep length on the tube.

In the approximations to be treated, it is assumed that the angles involved are so small that $\cos \theta$ is essentially equal to one, and therefore only the sine voltage is used.    When $R$ is of the same order of magnitude as $r$, the duration of the "range" sweep, this approximation is very poor because the number of degrees displayed on the tube face is then large.

The geometry of this approximation is shown in Fig. 14·16.    The sector $ABCD$ is represented by $A'B'C'D'$.    The error $AA'$ is

$$AA' = R\left(1 - \cos \frac{\theta}{2}\right).$$
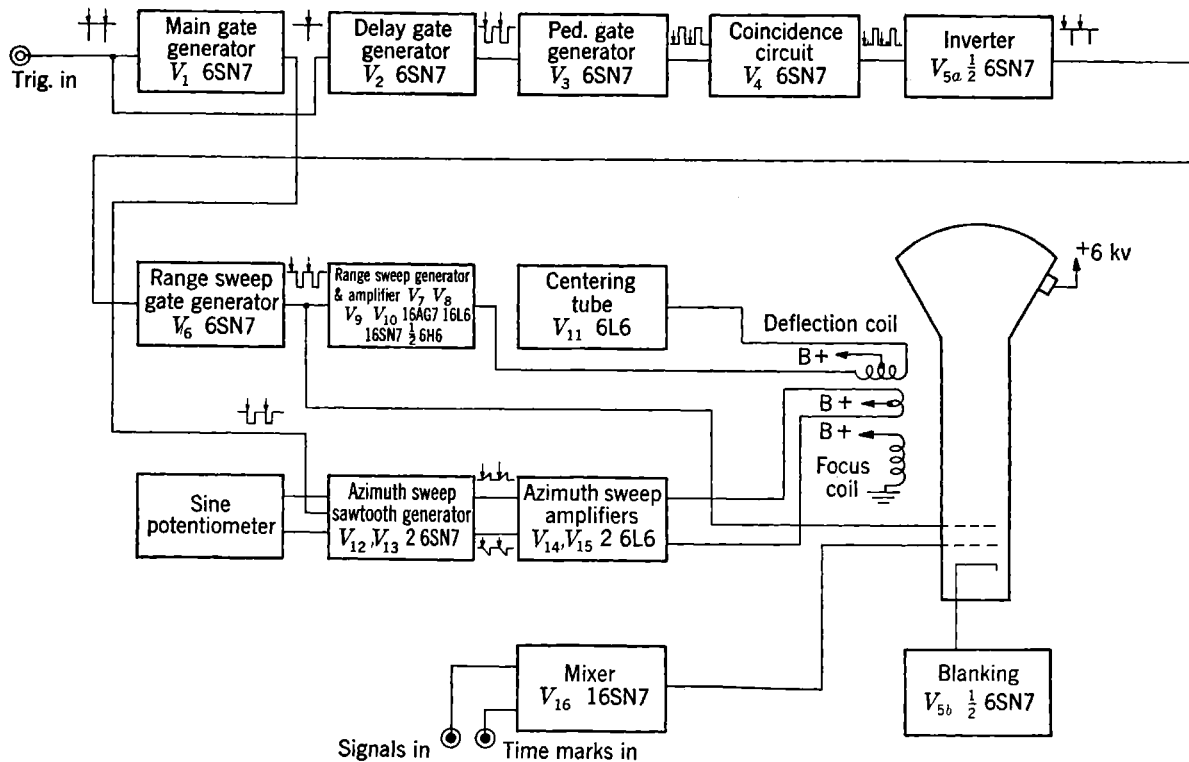
FIG. 14·17.—Block diagram for double-time-base sector.

FIG. 14·18.—Electrical schematic diagram for sector produced by two time bases.

The angle displayed on the tube, at any range $R$, is again

$$\theta = \frac{r}{R}.$$

The maximum displacement error (at the edge of the tube) is therefore

$$\epsilon = \frac{r^2}{8R},$$

and the maximum vector error $\alpha = \dfrac{r}{4R}.$

Errors in the display can be reduced somewhat by proper normalization. The deflection $HA'$ is smaller than it need be to produce closest possible superposition of $AB$ and $A'B'$ because $HA'$ is proportional to $R$ sin $\theta$, rather than $R$ tan $\theta$. It is possible to reduce the error by correcting this relationship at some particular angle. However, the equalization holds at only this one value of $\theta$ because this process amounts to setting $k_1 \sin \theta = k_2 \tan \theta$, and this equation can be true only at a particular value of $\theta$.

The block diagram and the corresponding circuit diagram are given in Figs. 14·17 and 14·18, respectively. A mechanical schematic diagram, Fig. 14·19, is also included. It should be noticed that in this system it is again necessary, in order to preserve proper orientation of the pattern, to rotate the deflection coil with the hand crank that selects the sector. This requirement is always present in methods in which the coil does not rotate with the radar antenna, or in which time bases are resolved in a coordinate system that is *rotated* by a differential mechanism.

FIG. 14·19.—Mechanical schematic diagram for display of double-time-base sector. Servomechanism puts out a shaft motion duplicating antenna rotation.

The delay circuit, which includes tubes $V_2$, $V_3$, $V_4$, and $V_{5a}$, is somewhat different from those considered heretofore. A stepped delay is provided, instead of a continuously variable delay. These steps are made to coincide with the time markers applied to the circuit (from an external source, in this case). The input trigger pulse initiates a delay gate ($V_2$), the length of which is just slightly shorter than the required time. From the trailing edge of this delay gate is generated a pedestal gate, which serves to pick out the desired range marker in a coincidence circuit. This range mark, thus selected, is inverted and used for the

trigger pulse that initiates the range sweep.   The sine-modulated azimuth sweep is derived from a sine potentiometer, which furnishes d-c voltages proportional to the sine of the azimuth angle.   The d-c voltages are used as sources for the generation of modulated sawtooth time bases in tubes $V_{12}$ and $V_{13}$.   These waveforms are applied to the push-pull amplifier circuit of $V_{14}$ and $V_{15}$.

**14·7. A Better Approximation.**—An important defect common to all the approximate methods discussed thus far lies in the extreme distortion near zero delay.   The elimination of this distortion from the display of Sec. 14·6, for example, would be a very desirable improvement.

It must be remembered that the generation of any true radial-time base sweep requires resolution into two orthogonal components —one of which is modulated by the cosine of a direction angle, and the other by the sine of the same angle.   Angle modulation of the "range" sweep is the factor that has been lacking in the methods described.   Section 14·3 discusses the case where the rectangular coordinate axes along which resolution takes place are fixed in space, usually N-S, E-W axes. Such a method leads to $x$, $y$ sector-selection methods.   In subsequently discussed methods, a differential gear or differential



FIG.   14·20.—Geometry   of   range-normalized double-time-base sector.   $A'B'C'D'$ is the approximation of the true sector $ABCD$.   $R_1$ is the range to the start of the sweep $r$.

synchro has been used to rotate the coordinate axes by allowing an arbitrary fixed angle to be inserted in the data by means of a hand crank. These methods lead to $r$, $\theta$ selection of the sector display.

In all of the systems it has been assumed that the angles in question are small, and therefore that $\cos \theta$ is approximately equal to one.   However, in the case of a sector display of the type shown in Fig. 14·20, it is possible to generate a pattern that is reasonably accurate even when the angle presented is large.   Although it is necessary for perfect reproduction of the true geometry to modulate both the range delay and the "range" sweep, the modulation of the delay is unimportant, *if the delay is zero*.   When the delay is not zero, there is some distortion, but it will always be smaller than that of the method presented in Sec. 14·6.

An estimate of the magnitude of the errors involved may be gained

from an inspection of the geometry of Fig. 14·20. It differs from the
case of Sec. 14·6 only in that the range sweep is cosine-modulated. The
sector $ABCD$ is approximated by the figure $A'B'C'D'$. If $R_1$ is the range
to the start of the sweep, or the delay, and if $R_2 = R_1 + r$, the range to
the end of the sweep, then

$$AA' = HJ = R_1\left(1 - \cos\frac{\theta}{2}\right),$$
$$BB' = EF = GF - GE.$$

But

$$GF = R_2\left(1 - \cos\frac{\theta}{2}\right),$$
$$GE = r\left(1 - \cos\frac{\theta}{2}\right).$$

Therefore,

$$EF = (R_2 - r)\left(1 - \cos\frac{\theta}{2}\right),$$

and

$$AA' = BB' = R_1\left(1 - \cos\frac{\theta}{2}\right).$$

As before, the total number of degrees displayed on the tube face is

$$\theta \approx \frac{r}{R}.$$

Therefore, the maximum error is

$$\epsilon \approx \frac{R_1 r^2}{8R^2},$$

which approaches zero as $R_1$ approaches zero.

Likewise, the maximum vector error at any range $R$ is

$$\alpha \approx \frac{\dfrac{R_1}{R}\dfrac{r^2}{8R}}{\dfrac{r}{2}} = \frac{R_1 r}{4R^2},$$

which also goes to zero as $R_1$ approaches zero.

One curious feature is that, although the error is zero when $R_1$ is zero,
it becomes finite when $R_1$ is not zero, and then eventually becomes smaller
again as $R_1$ continues to increase. It would be interesting to find out
where the maximum value as a function of $R_1$ occurs. If $R$ is assumed to
be equal to $R_1 + \dfrac{r}{2}$, the maximum error at any range becomes

$$\epsilon = \frac{R_1 r^2}{8(R_1 + r/2)^2}.$$

Differentiating this equation with respect to $R_1$, and setting the result equal to zero, the range at which the error is a maximum is

$$R_1 = \frac{r}{2}.$$

The method of deriving the cosine-modulated sweep is shown in Fig. 14·21. The waveform that is available on the second winding of
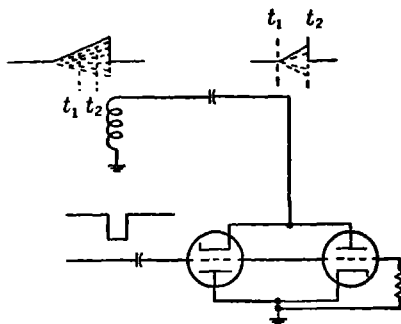


Fig. 14·21.—Method of deriving cosine-modulated sweep.
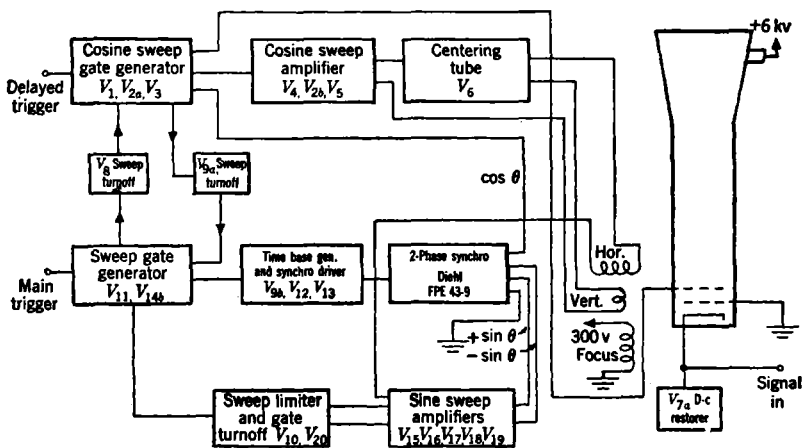


Fig. 14·22.—Block diagram of sector scan with cosine-modulated range sweep.

the data synchro is condenser-coupled into a clamping circuit at the input terminal of the sweep amplifier. The clamp is opened by a square wave, the leading edge of which is delayed by the desired amount. This square wave can be generated by triggering a suitable flip-flop circuit with the already available delayed trigger pulse. If the input wave is assumed to be of the form

$$E = kR \cos \theta = Kt \cos \theta,$$

All resistors ½ w unless specified
All condensers < 0.01 μf are mica
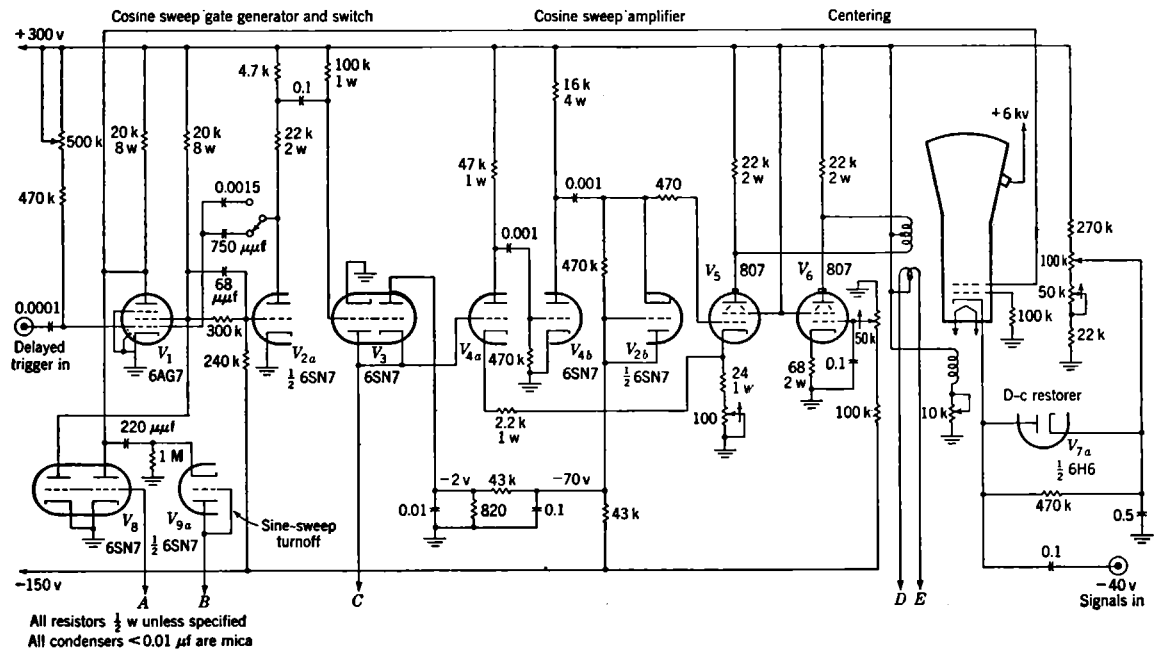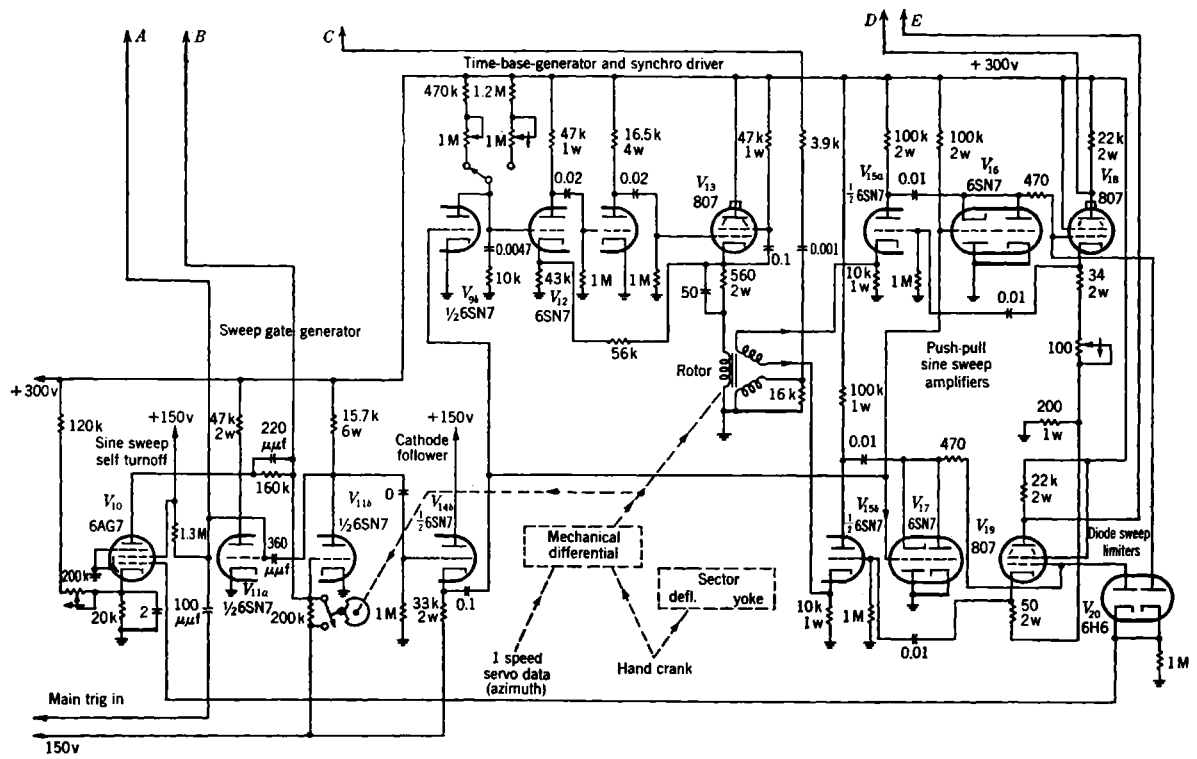
FIG. 14·23.—Sector-scan circuit diagram with cosine-modulated range sweep.

then, if the clamp opens at time $t_1$, the value of the voltage is

$$E_1 = Kt_1 \cos \theta.$$

When it closes at a time $t_2$,

$$E_2 = Kt_2 \cos \theta.$$

Therefore,

$$E_2 - E_1 = K(t_2 - t_1) \cos \theta$$
$$= Kr \cos \theta,$$

which is the value that is required.

This approximation, which neglects only the cosine modulation of the time delay, has been used with considerable success because it possesses the accuracy of other methods when the delay is large, and in addition is distortion-free when the delay is zero. The block diagram of a typical circuit is given in Fig. 14·22, and the corresponding schematic diagram in Fig. 14·23. The mechanical schematic diagram is the same as that of Fig. 14·19 except that a synchro is substituted for the sine potentiometer, and a cam is attached to the synchro shaft for turning off the sweep gate generator during all angles of rotation except those included in the desired sector.

The sweep-generation method illustrated in Fig. 14·23 is different from those discussed heretofore in that angular resolution takes place after the time base has been generated. The circuit for accomplishing time-base generation is composed of tubes $V_{9b}$, $V_{12}$, and $V_{13}$, a feedback amplifier that compares the voltage across the rotor of the synchro with the input linear time base. The modulated-time-base output signals of the 2-phase synchro resolver are used to drive the sweeps. From one of the resolver stators, signals of opposite polarity are applied to a push-pull amplifier pair, each half utilizing one stage of degenerative feedback. This set of amplifiers is called the "sine-sweep amplifier" (tubes $V_{15}$, $V_{16}$, $V_{17}$, $V_{18}$, and $V_{19}$). From the other stator, a cosine-modulated time base is applied to the delayed clamping circuit $V_3$, which samples this signal in the manner illustrated in Fig. 14·21. The output signal is used as the input voltage waveform for the cosine-sweep amplifier, $V_4$ and $V_5$, which will be recognized as of the conventional two-stage current-feedback variety.

A notable feature of this circuit is the number of automatic-shutoff devices. These are used to prevent overdrive of the amplifiers that drive the deflection coil. There is one diode on each grid of the output amplifiers $V_{18}$ and $V_{19}$; therefore, the effect is to cut off the sweep at each edge of the tube. The signal picked off by either diode is amplified by $V_{10}$, and used to shut off the main gate generator $V_{11}$. However, since the cosine-sweep gate generator is used to intensify the trace, it is necessary to see that this gate generator is shut off when the trace is

stopped. This shutoff is accomplished by the coincidence tube $V_8$, which prevents triggering of the delayed gate if the main-sweep gate generator has been turned off. Moreover, to insure that the sine sweep never lasts longer than the cosine sweep, the trailing edge of the cosine-sweep gate is differentiated and used as a trigger to turn off the main sweep gate simultaneously.

**14·8. True Sector.**—It has been stated in Sec. 14·7 that in order to obtain a true sector it is necessary to cosine-modulate both the time delay and the "range" sweep. This has been done in the method illustrated in Fig. 14·24.
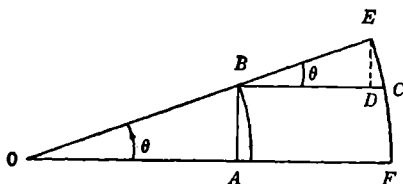


FIG. 14·24.—Geometry of "true sector." The sweep moves along $AB$, then is intensified while it moves along $BE$. In the direction $AB$, the sweep speed is proportional to the range from $O$ multiplied by $\sin \theta$. In the direction $BD$ the sweep is modulated by the factor $\cos \theta$.

If $R$ is the range delay when $\theta$ is zero,

$$OA = kR.$$

Then, for some other value of $\theta$, the delay will not be $R$, but will have a new value $R'$, where

$$R' = \frac{OB}{k}.$$

At the time of the input trigger pulse, the deflection starts out along the line $AB$. Since the time base is sine-modulated, the deflection will be

$$d = kR' \sin \theta.$$

But

$$kR' = \frac{OA}{\cos \theta} = \frac{kR}{\cos \theta},$$

and therefore

$$d = kR \tan \theta = OA \tan \theta,$$

or

$$d = AB.$$
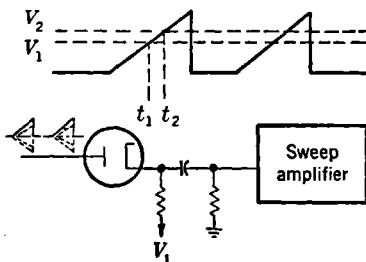


FIG. 14·25.—Diode pickoff circuit.

If it is assumed that the trace will be of duration $r$, the vertical deflection will be $kr = AF$ when $\theta$ is zero. When $\theta$ is not zero, the deflection vertically, starting at a time $R'$ from the point $B$, must be equal to $BD$.
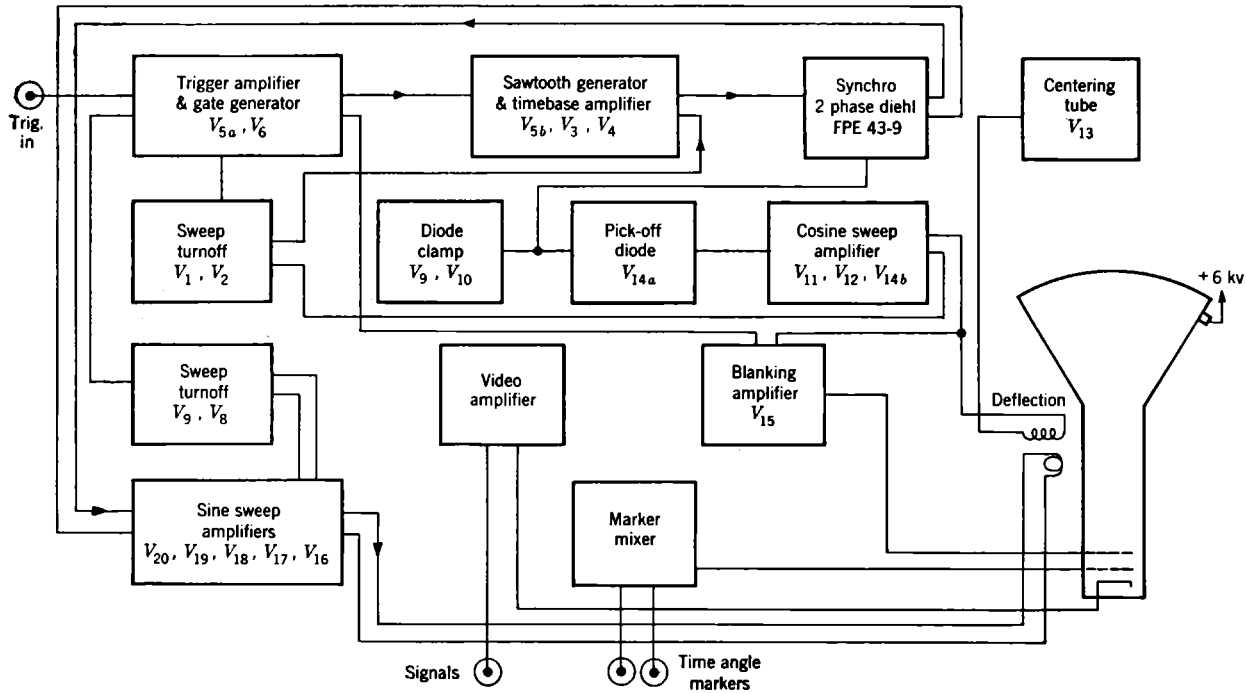
FIG. 14·26.—Block diagram for true-sector display.

But

$$BD = BE \cos \theta$$
$$= kr \cos \theta.$$

Therefore, the requirements for a true sector are that (1) one time base shall be sine-modulated; (2) the delay in starting the orthogonal time base shall be $R' = R/\cos \theta$, where $R$ is the time delay when $\theta$ is zero; (3) amplitude of the second time base shall be cosine-modulated. Conditions 2 and 3 are easily realized by using a diode pickoff circuit similar to those used in ordinary delay circuits (see Fig. 14·25). If the input sawtooth voltage is of the form

$$E = kt \cos \theta,$$

and the pickoff voltage is set at a value $V_1$, then the time $t_1$ required for this voltage to reach the value $V_1$ is

$$t_1 = \frac{V_1}{k \cos \theta}.$$

The amplitude of the signal picked off, at any time $t_2$ after $t_1$, will be

$$V_2 - V_1 = k(t_2 - t_1) \cos \theta.$$

Therefore, the delay time and time-base amplitude behave exactly as required. From another viewpoint, this behavior is exactly what should be expected, because the same principles of voltage addition that were discussed in Sec. 14·3 for another type of fixed-coil sector display have been applied here. The diode used here is not strictly necessary; the effect could as well be simulated with resistor-mixing on the grid of an amplifier. Diode cutoff gives the same effect as one cutoff limit of an amplifier.

Figure 14·26 gives the block diagram for such a display, which is actually very similar to the circuit of Fig. 14·22. The corresponding circuit diagram is given in Fig. 14·27. The mechanical schematic diagram is again like that of Secs. 14·6 and 14·7, with the substitution of a 2-phase synchro resolver for the potentiometer shown in Fig. 14·19.

It has probably been noted that as the approximations used come closer to the true sector, the circuits become more complicated. The true sector itself, however, is essentially no more complicated than the approximation discussed in the last section. The same circuit as in Fig. 14·23, but involving tubes $V_3$, $V_4$, and $V_5$ in this case, is used for driving a linear time-base voltage into the 2-phase synchro. The diode pickoff method of deriving the cosine-modulated delay and time base is essentially that demonstrated in Fig. 14·23. However, in this case, instead of having the diode returned to a variable bias, the diode is returned to a
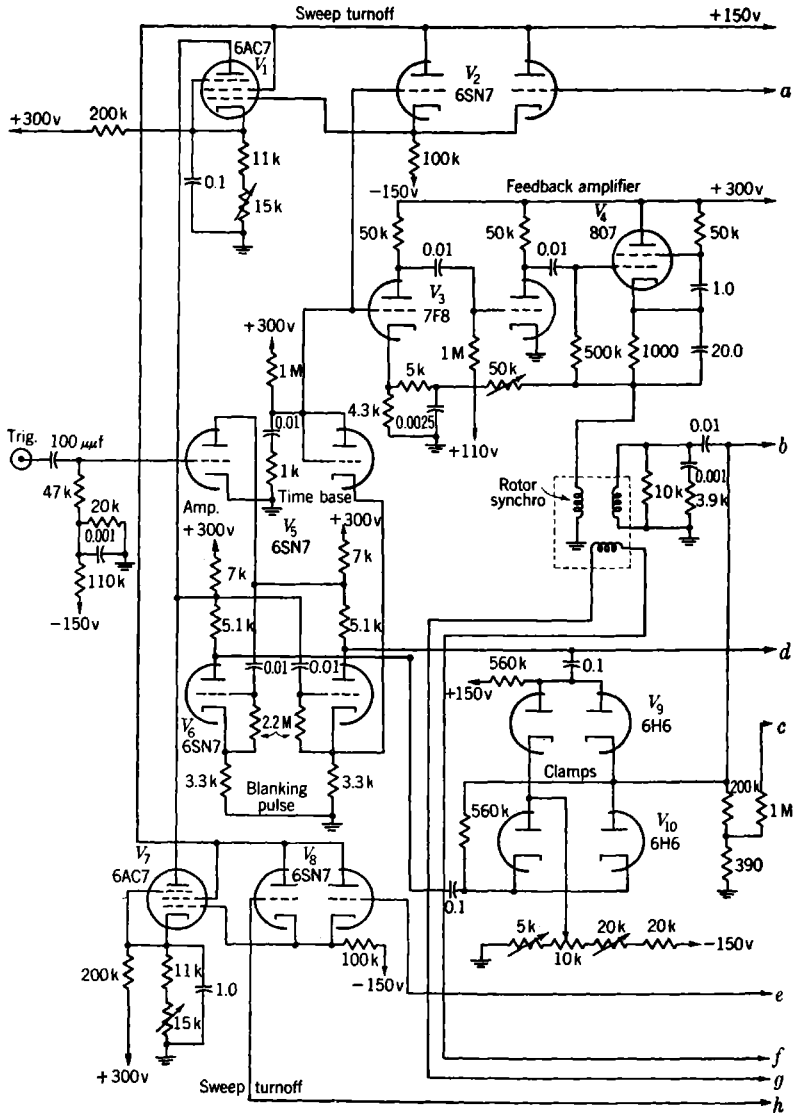
Fig. 14·27.—True-sector
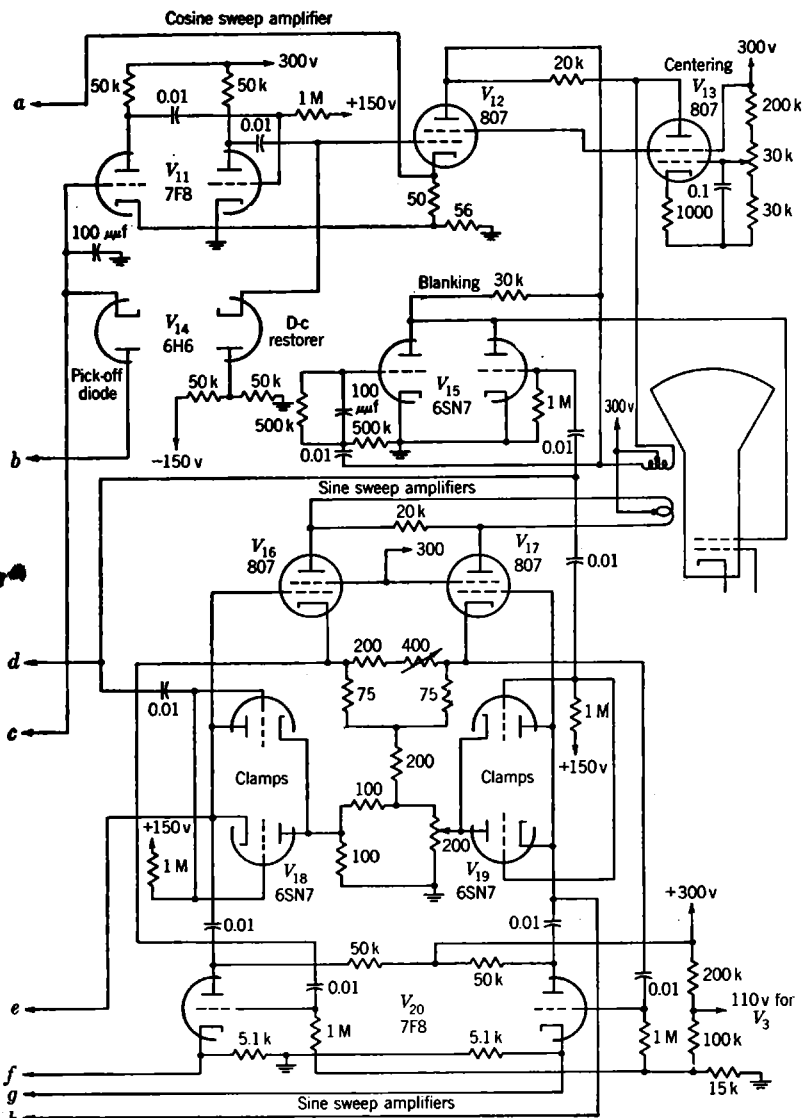
schematic diagram.

fixed bias.    The time base, condenser-coupled out of the synchro, is
d-c restored by diode clamps $V_9$, $V_{10}$ to a bias that may be varied.    Thus,
instead of moving the diode up and down with respect to the sawtooth
waveform, the time base is moved up and down relative to the diode
bias.    The same general types of sweep turnoff are applied as before in
order to limit the possibility of overdriving the amplifiers.    In this
circuit, however, there is no delayed trigger pulse, and hence no delayed
gate generator.    It is therefore necessary to use the deflection-coil wave-
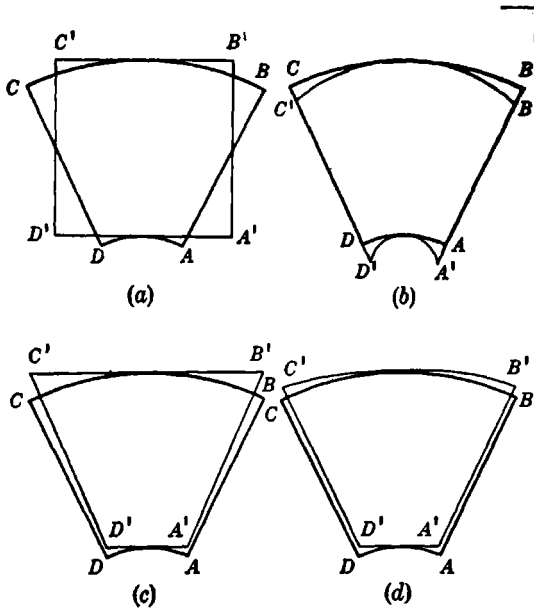


Fig. 14·28.—Comparison of approximations to true sector as obtained by the four
methods.    $A'B'C'D'$ is the appearance on the cathode-ray tube of the sector $ABCD$.
(a) Rectangular B-scan.    (b) Rotating-coil with range-normalized sweep.    (c) Double-
time-base B-scan.    (d) Double-time-base range-normalized B-scan.

form to intensify the cathode ray.    The cosine sweep starts approxi-
mately at the edge of the tube face at the proper delayed time.    Hence,
use of the deflection-coil square wave to cut off one half of the coincidence
blanking amplifier, $V_{15}$, insures that the beam is intensified only at the
proper time.    The sine-sweep amplifiers are the same as the push-pull
pair shown in Fig. 14·23.

**14·9. Summary.**—Figure 14·28 indicates the distortions inherent in
each of several approximate methods that have been discussed.    Each
of the small figures there is drawn in such a way that the delay time is
about equal to the duration of the sector.

Rotating-coil "brute force" off-centering systems are generally free of distortions. Although more complex mechanically, they are generally the simplest systems electronically. They can be made exceedingly reliable and free of servicing troubles. There is also the feeling that "in a mechanically rotated PPI the range marks are always circles." On the other hand, such a scheme is, in general, limited to three radii off-center. However, if the maximum amount of off-centering desired is two radii, this is probably the most feasible method of obtaining a sector display.

Fixed-coil schemes are better adapted to very large expansions, and the simplest of these is the range-normalized Micro-B scope. In this display, only one (unmodulated) time base is used, and the inductance of the deflection coil is the only practical limit on the expansion that may be obtained. The really serious defect of this sector display is the extreme distortion that is present when the delay time is small.

Fixed-coil methods having a higher inherent accuracy than the range-normalized Micro-B scope involve more complicated circuits. Usually they have been generated by using a 2-phase synchro as a time-base resolver. This synchro is probably the limiting factor for the expansions that may be attained.

Fixed-coil systems can be divided into two classes: (1) those in which resolution of the time base is performed in a coordinate system that is fixed in space; (2) those in which resolution of the time base is performed in a rectangular coordinate system, the axes of which are rotated in the act of selecting the sector to be displayed. Class 1 lends itself to $x$, $y$ sector selection. Class 2 is adapted to $r$, $\theta$ sector selection. If it is necessary that the total off-centering be the sum of several displacements, as is often the case, then a sector of Class 1 is necessary, for $x$, $y$ components of vector displacements add directly, whereas $r$, $\theta$ components do not. If such addition is not required, a sector display of Class 2 is probably preferable. Although sectors of this type are mechanically more complex (they require a differential mechanism and a means of rotating the deflection coil) they do not have the difficulties with d-c amplifiers which are inherent in Class 1 sector displays. Synchro problems are equally important to both types.

CHAPTER 15

## RANGE-HEIGHT DISPLAYS

By P. Axel

**15·1. Introduction.**—A display in which one dimension of a rectangular portion of a polar display is expanded is illustrated in Fig. 15·1. The area in Fig. 15·1b is an expanded display of the shaded area in



(a)                                        (b)

(c)
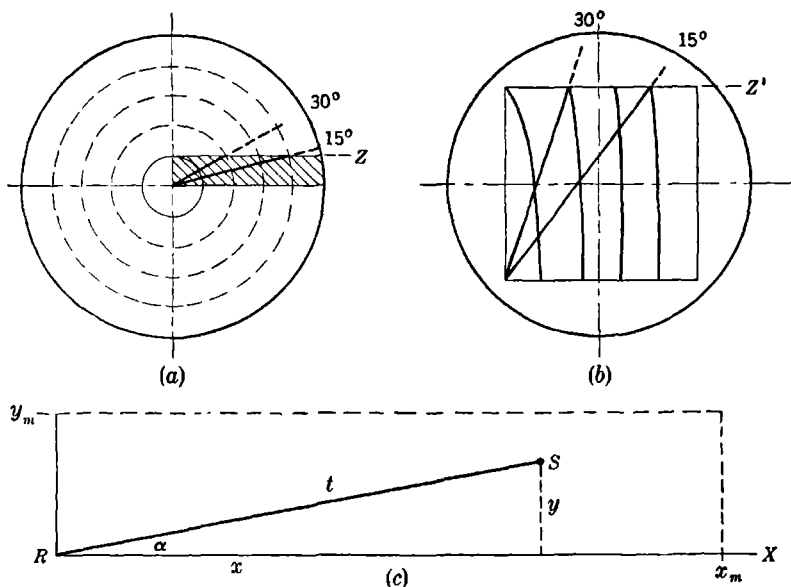
Fig. 15·1.—Radial–time-base display.  (a) The rectangular area to be investigated is shown.  Circles are constant time loci.  Angles of 15° and 30° are drawn in.  (b) The vertical component of the rectangle of (a) is shown expanded by a factor of 5.  The constant time loci are distorted to the ellipses shown.  The 15° and 30° angles are reproduced. Note that line $Z'$ is the reproduction on the new scale of line $Z$.  (c) Rectangular area bounded by $y_m$ and $x_m$.  The vector of magnitude $t$ and angle $\alpha$ positions any point in this area.  The components of $S$ are given by $x = t \cos \alpha$, $y = t \sin \alpha$.

Fig. 15·1a.  The expansion results in geometrical distortion as is evidenced by the ellipses shown in Fig. 15·1b which correspond to the normally circular contours of constant time or distance.  However, a straight line parallel to the horizontal radial reference line remains parallel ($Z'$ of Fig. 15·1b corresponds to $Z$ of Fig. 15·1a).  Therefore, a

516

display of this type is particularly useful for displaying a rectangular region if the information required is the vertical distance from a target to a horizontal reference line.

Figure 15·1c shows a rectangular area bounded by the coordinates $y_m$ and $x_m$, where $y_m$ is considerably smaller than $x_m$. Because of the relation between these two boundary values, it is desirable to expand the $y$-direction with respect to the $x$-direction to make more efficient use of the cathode-ray-tube screen. It is obvious from Fig. 15·1c that the vertical distance $(y)$ of any signal $(S)$ from the reference line $(x)$ can be obtained if the vector from the origin to $S$ is known. A display of this type was used in radar for height measurements, where the expected height of the target was restricted to values considerably less than the expected range. There are many other display problems that have similar geometry and which can be treated in the same way.

*Generation of the Display.*—There are several methods of producing a vertically expanded display. Since the signal-position data is in the form of polar coordinates, one obvious method is to modify a rotating-coil polar-coordinate display. By rotating the coil at a speed faster than the signal source, and by incorporating a permanent-magnet off-centering system, an acceptable presentation can be developed. However, this method has many disadvantages. This presentation would be an angular expansion and the geometry of it would be rather involved. It also is mechanically difficult to apply this technique to rapidly scanning systems. The angular stepup in gearing would be a source of error and impair the accuracy of the display. Since it was required that the height displays that were developed be accurate and have rapid scan rates, this method was not deemed feasible.

A better way to generate a height display is to resolve the polar information into $x$- and $y$-components and to use these with a fixed-deflection-coil system. From Fig. 15·1c it is seen that to reproduce the geometry accurately would require plotting $t \cos \alpha$ horizontally and $t \sin \alpha$ vertically. To obtain the desired vertical expansion, the $t \sin \alpha$ term can then simply be multiplied by a constant. The methods of obtaining a voltage proportional to an angle or a function of that angle are discussed in Chap. 5, and it will be assumed here that a d-c voltage that is a function of the angle is available.

*Geometry of the Display.*—The angular occurrence of signals is such that only a small angle need be displayed to cover most of the rectangular area. Therefore sufficient accuracy may often be obtained by using $t$ as the horizontal coordinate (setting $\cos \alpha = 1$) and $t\alpha$ as the vertical coordinate (setting $\sin \alpha = \alpha$). The distortion caused by these approximations is shown in Fig. 15·2. In radar experience the substitution of $t$ for $t \cos \alpha$ has always been made. The reading of time data is thereby

simplified by maintaining the constant-time contours as vertical lines, and this advantage outweighs the resultant distortion. However, the choice of $t\alpha$ or $t \sin \alpha$ for the vertical component would give a less distorted pattern. As shown in Fig. 15·2b, the geometrical difference between these two vertical components is rather small. From the point of view of the sweep circuits it is immaterial which information is used.[1] Therefore, the choice is usually made on the basis of the data generation and transmission system.
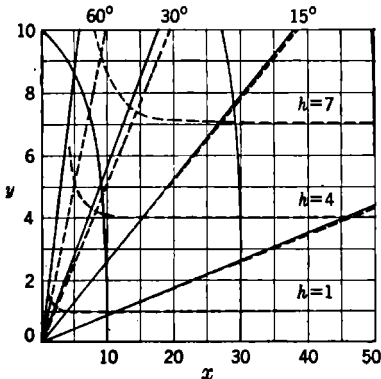


FIG 15·2a.—Distortion due to approximations $\cos \alpha = 1$ and $\sin \alpha = \alpha$. ———— $y = t \sin \alpha$, $x = t \cos \alpha$; lines of constant $t$ and constant $\alpha$ are shown; lines of constant height are horizontal. — — — $y = t\alpha$, $x = t$; lines of constant $h$ and constant $\alpha$ are shown; lines of constant $t$ are vertical.
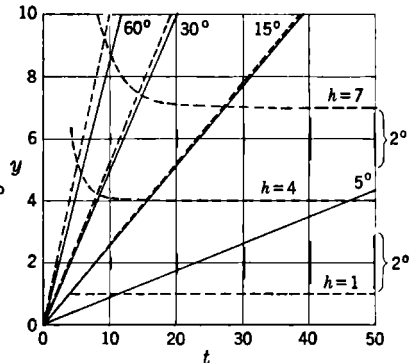
FIG. 15·2b.—Comparison of $\sin \alpha$ and $\alpha$ as elevation input information. — — — $y = t\alpha$, $x = t$; lines of constant $h$ and $\alpha$ are shown. ———— $y = t \sin \alpha$, $x = t$; lines of constant $\alpha$ are shown; lines of constant $h$ are horizontal; the height of a 2° signal is shown at various values of $t$.

*Evaluation of Display Geometry.*—Although this section is primarily concerned with the circuits necessary to generate a range-height display, the study of another display method of presenting the same area will help emphasize the advantages and limitations of the RHI (range-height indicator). This other display, called the E-scope, plots elevation angle vertically and time horizontally as shown in Fig. 15·3. The E-scope maintains the horizontal linearity of lines of constant angle, whereas a constant-height line becomes a hyperbola. The RHI, however, maintains the horizontal linearity of constant-height lines, and it is therefore more convenient for use in height determination (just as the E-scope would be more convenient for angular determination). However, considerations of the resolution and accuracy limitations may outweigh these conveniences.

[1] If it were necessary to use $t \cos \alpha$ rather than $t$ as the horizontal component, the sweep circuits would have to be changed to provide for the inclusion of this angular data.

Because the signal size is determined by the beamwidth of the source, it covers a constant angle on either display. Therefore, the size of the signal on the display is proportional to $t$ on the RHI, whereas it is constant on the E-scope. For very small values of $t$ on the RHI the signals are compressed to a point where spot size begins to limit resolution. At large values of $t$, the increased signal size does not seriously limit the precision because large signals can be bisected accurately. The change of signal size with $t$ does have one slight advantage in that the signal size is proportional to the possible error in height.[1]

In the E-scope, on the other hand, the signals maintain a constant size over the entire display and are, therefore, easily resolved at either small or large values of $t$. The constant signal size also helps to reduce the minimum discernible signal at large values of $t$ by concentrating the light on the cathode-ray-tube screen. However, the E-scope has the disadvantage that the height lines are crowded at large values of $t$, and the precision of the height reading is thereby limited.
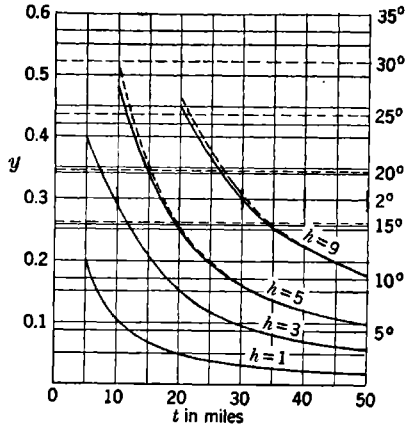


FIG. 15·3.—E-scope. $- - - y = \alpha$, $x = t$; the height of the 2° signals remain constant. —— $y = \sin \alpha$, $x = t$; lines of constant angle are horizontal; lines of constant height are shown.

Another factor that enters into the evaluation of a display is the efficiency with which the screen area is used. After an upper limit has been set on the height coverage desired, and the angular coverage is known, height and angle contours may be sketched on the two types of displays. After various different scale factors have been used and signal sizes sketched in, the decision as to which display to use can be made. It will be noted that, for large angles, neither display is very satisfactory. The RHI crowds the area above 30°, very seriously limiting the precision and resolution of the unit. The E-scope, operating over large angles, will also excessively crowd the signals as $t$ is increased. Therefore, the circuits that were designed and will be discussed as height indicators give limited angular coverage. In this chapter two examples of the RHI and one of the hybrid RHI–E-scope, illustrated in

---

[1] This advantage holds only if the limiting factor in the height determination is the accuracy of the angular data (as is usually the case). Since this accuracy is independent of time, and the height $H$ equals $t \sin \alpha$, the error in height for a given error in angle is proportional to $t$.

Fig. 15·4, will be described in detail.  The E-scopes represent, as far as circuits are concerned, a very simple modification of the B-scopes described in Chap. 11.

*Height Determination.*—When the signals are displayed, either an overlay with height lines, a series of electronic height lines, or a single precision electronic height marker can be used for actual height determination.  A precision electronic marker is capable of being set to $\pm 2$ per cent on a 1-in. signal, and this accuracy is much better than that obtained with either of the other two methods.  Fixed electronic height lines are limited in precision by the interpolation that is necessary in reading height.  When an overlay can be used, it is usually simpler to normalize the sweeps to that overlay, thereby avoiding the electronic complication inherent in the generation of height marks. If the area covered by the display is to be varied, however, it is necessary to use electronic marks. The precision marker is illustrated in the second of the following examples, whereas the first and third examples use overlays.



Fig. 15·4.—Hybrid RHI-E-scope; $y = \alpha + \dfrac{t\alpha}{50}$, $x = t$; lines of constant $\alpha$ and $h$ are shown.

**15·2. Circuits.**—A block diagram of the RHI is shown in Fig. 15·5.  The input trigger pulse is put through a buffer stage, the negative output of which is used for both the range and the height channels.  The trigger into the range channel may then be delayed.  If no delay is used, the range and height rectangular-wave generators may be combined.  If a delay is necessary, a simple delay circuit that is relatively free from jitter may be used.  The main rectangular-wave generator is then triggered by the output of the delay circuit, and ·its output, in turn, is used both for sweep generation and blanking.  The gate waveform is thus critical only in so far as short rise time and short recovery time are required by the duty ratio.  The time sweep generator is turned on by the main gate and generates a unidirectional linearly increasing sawtooth waveform.  When a distortionless picture is required, this sawtooth wave is modulated by $\cos \alpha$, in the same manner as the height modulation.  The output voltage from the sawtooth generator is then converted by the amplifier and driver stages into a current through the deflection coil.  Associated with the horizontal sweep circuit is the

horizontal centering tube, which sets the horizontal zero position of the display.

The height circuit is essentially the same as the time circuit. The height rectangular-wave generator may have an automatic-turnoff feature to prevent excessive vertical deflection current at large angles. The height sweep generator is controlled by the height gate, and it generates a linear sawtooth wave, whose maximum amplitude is determined by the angle input data. The resultant waveform, which is pro-
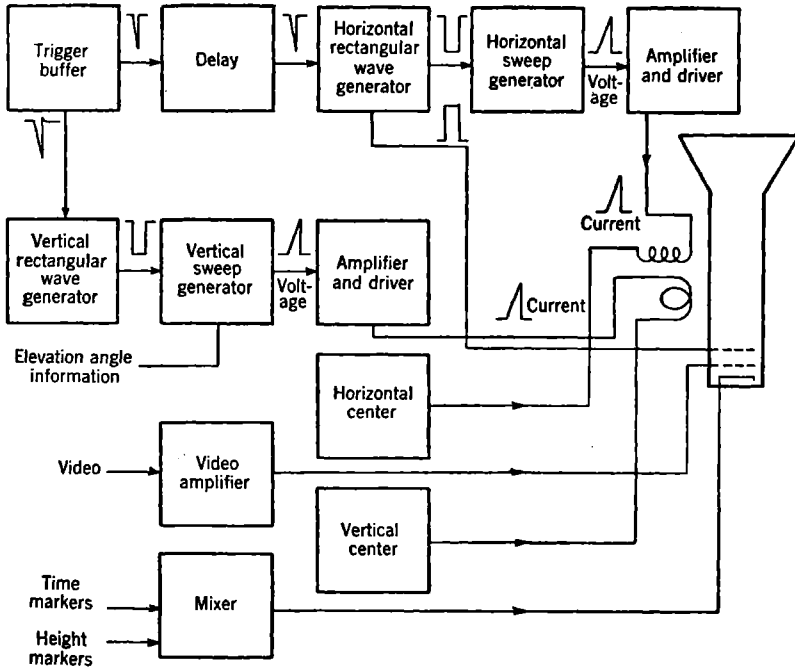


FIG. 15·5.—RHI block diagram.

portional to $t\alpha$ (or possibly $t \sin \alpha$), is put through the amplifier-driver stage and the proper current is then sent through the vertical deflection coil. The vertical centering circuit is the same as the one used for horizontal centering.

A mixer is necessary for time and height marks if both types of electronic markers are being used. The time markers may be of the conventional type and may very well be derived from an external source that is synchronized by the timing trigger. The height markers, however, represent a more complicated problem because they must be generated from a varying control voltage. The height markers are generated

by using a variation of the sawtooth delay circuit, in which the sawtooth wave is modulated by the angle. The complete discussion of the generation of these markers can be found in Chap. 6. If the signal source is designed to give information only when the angle is increasing, it is necessary to provide a circuit to blank out the signals while the angle is returning to zero after having reached its maximum value.

**15·3. RHI, First Example.**—This circuit (Fig. 15·6) is a relatively inexpensive one whose design characteristics were predominantly dictated by power and size limitations. The displayed area goes from $-2°$ to $+23°$, and out to 67 miles in range, with $y = t \sin \alpha$ and $x = t$. The angle information is obtained by passing the sweep sawtooth voltage through a synchro whose rotor moves with the elevation angle. The height determination is made by using a horizontal cursor that is geared to a direct-reading height dial.

In addition to the sweep channel, the video channel, and the marker circuit, this unit contains the master multivibrator that determines the repetition rate of the entire system, as well as circuits for generating a delayed trigger for the signal source. The nature of the sweep circuits makes it convenient to delay the source trigger. The repetition rate of the system is 1000 cps; its over-all absolute accuracy is about $\pm0.3$ mile and its relative accuracy is about $\pm0.1$ mile. The video circuit accepts negative video signals of about 1 volt and amplifiers them to $+40$ volts for application to the grid of the cathode-ray tube, and has a high-frequency response of 1.6 Mc/sec.

*Master Multivibrator.*—This free-running multivibrator $V_1$ has a natural repetition rate of 1000 cps. Tube $V_{1b}$ is on for three-quarters of the recurrence period, and it is during this 750-$\mu$sec period that the sweep is generated. The output of the multivibrator is taken from the plate circuit of $V_{1b}$. The large output signal taken directly from the plate is used to gate both sets of vertical clamps ($V_5$ and $V_7$). The smaller output signal obtained from part of the load resistor ($R_1$) is used to gate the delay circuit and the "bootstrap" sawtooth generator.

*Bootstrap Sawtooth Generator.*—The clamp ($V_{2a}$) conducts until the negative gating pulse cuts it off. In order to obtain the proper bias for the cathode follower, the sawtooth waveform for the cathode follower is taken from a tap on the charging resistor. The cathode-follower bootstrap action is made less effective by this method of obtaining bias (by the ratio of $R_3$ to $R_2$ plus $R_3$) but the final sawtooth linearity is acceptable for this application. The output waveform of the sawtooth generator is then used in both the horizontal and vertical channels.

*Elevation Synchro Driver.*—The vertical sweep must be modulated by the sine of the angle of elevation. To accomplish this, the sawtooth voltage is applied to the rotor of a 2-phase synchro that is moving in

synchronism with the elevation data (1 cps). The output of the Diehl type FJE41-5 synchro is taken from the sine winding and applied in push-pull to the following amplifier. The synchro rotor resistance is 100 ohms and its inductance is 500 mh. The inductance of the secondary is 2 henrys and hence there is a voltage stepup of 2. The synchro rotor is driven by the cathode of $V_3$. The tube attains self-bias by drawing grid current at the positive peak of the input sawtooth waveform. This biasing method is acceptable only when the sawtooth amplitude requires driving the tube from near cutoff to zero bias. This method would be very undesirable if the sawtooth waveform to the grid were interrupted because the tube would then continually operate at zero bias.

*Vertical-sweep Amplifiers.*—The sine output voltage of the synchro appears across the damping resistors ($R_4$ and $R_5$), and is biased to about $+50$ volts. It is then applied push-pull to $V_4$, which is connected as a degenerative amplifier. The potentiometer between the cathodes decreases the degeneration and thereby acts as a gain control. The push-pull output signal from the plates is a-c coupled to the two sweep drivers.

*Vertical Clamps.*—The clamps ($V_5, V_7$) return the grids of the drivers to a fixed voltage between sweeps. Since the displayed angle is sometimes negative, both positive and negative sawtooth voltages appear on the grid of each driver. Hence, it is necessary to use a two-way clamp for proper biasing with either sign of the input voltage. One of the clamps is returned to ground whereas the other is returned to a positive potential that controls the vertical centering of the trace.

*Vertical-sweep Drivers.*—The quiescent current through the drivers ($V_6, V_8$) is such as to produce a field between sweeps which keeps the vertical position well below the center of the cathode-ray tube. This vertical deflection is set by the potentiometer $R_6$ in the clamp circuit that clamps the grid of $V_8$. The coil is so connected that quiescent current through it will deflect the trace below the center of the tube. Even with this quiescent current and the push-pull drive, the start of the sweep is very nonlinear. To eliminate this nonlinear region, the trigger pulse starting the source (and therefore representing zero time) is delayed, so that the sweeps will be linear by the time the intensifying pulse is applied and signals appear.

At large angles, the grid voltage of the vertical driver $V_6$ is limited by grid current while the negative-going wave for $V_8$ goes below cutoff. Turning off the gate to prevent excessive power dissipation is unnecessary because the normal operation is such as to drive the grids to zero bias without harmful results. The current difference required to deflect the trace across the diameter of the tube is about 100 ma.
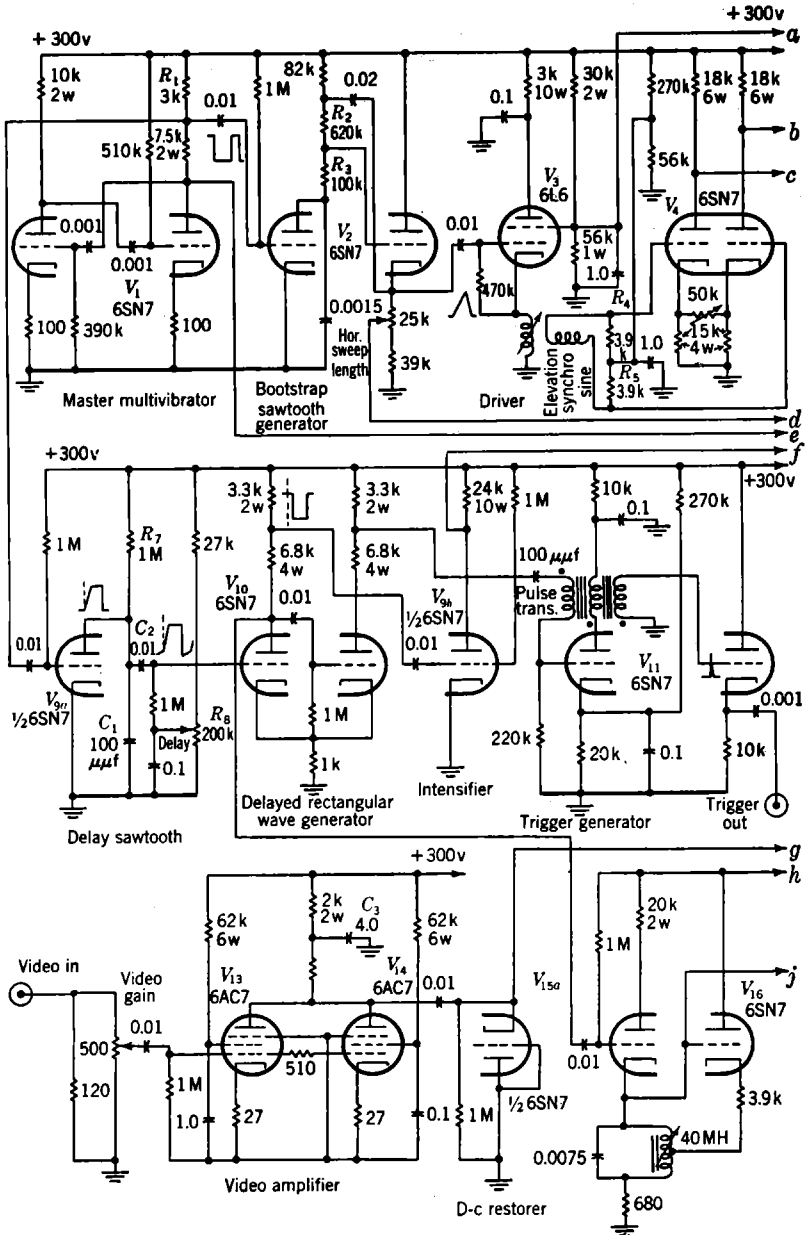
Fig. 15·6.—Range-height
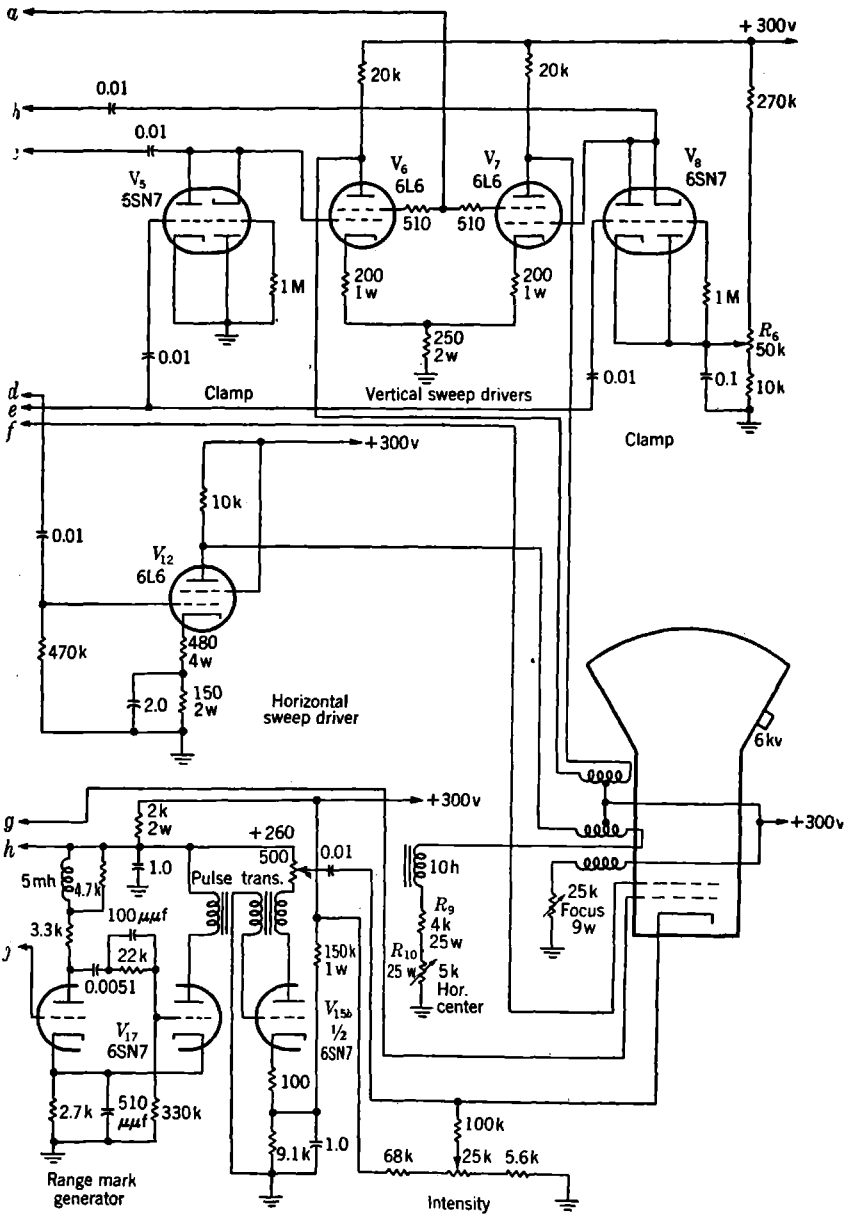
indicator, first example.

*Horizontal-sweep Driver.*—An adjustable fraction of the original sawtooth voltage is coupled from the potentiometer in the cathode-follower circuit $V_{2b}$ to the grid of the horizontal driver $V_{12}$. This driver is biased by the combination of a bypass cathode resistor and a degenerative cathode resistor. The input sawtooth voltage is nominally variable from 85 to 140 volts, and therefore the 100 ma necessary for deflection is insured regardless of the variations within specified tolerance of the circuit parameters. The horizontal-positioning control, which determines the horizontal-deflecting field between sweeps, consists of a variable resistor $R_{10}$, which is in series with a 10-henry choke, a fixed resistor $R_9$, and the deflection coil. Since the resistance of the deflection coil is about 300 ohms, and the current required is about 60 ma, this control has enough range to compensate for variations within the prescribed tolerances.

*Delay Sawtooth Generator.*—The delay is set so that the spacing from the time origin (which occurs before the intensifying pulse) and the first marker is the same as the spacing between subsequent markers. Thus, at the start, the sweep travels the distance corresponding to the normal distance between 100-$\mu$sec markers, in the delay time (from 10 to 50 $\mu$sec) plus 100 $\mu$sec. After this period, the sweeps are essentially linear; hence the only serious distortion in the display occurs within the first 10 miles.

The delay sawtooth generator $V_{9a}$ is a simple triode clamp operating across an $RC$-network $(R_7, C_1)$. This clamp is gated by the master multivibrator. Since the time constant of the exponential generated is 100 $\mu$sec and the delay required is from 10 to 50 $\mu$sec, as much as 0.4 of the total height of the exponential may be used.

*Delayed-rectangular-wave Generator.*—This circuit is a "flopover" that is triggered by the delay sawtooth waveform. When $V_{10a}$ draws grid current, the rapid rise of the plate of $V_{9a}$ is stopped and the time constant of 100 $\mu$sec is changed to 10,000 $\mu$sec, because $C_2$ now limits the rise. The duration of the delay is determined by the bias on the off grid $(V_{10a})$ of the flopover. Since the upper limit of the grid waveform is determined by the zero-bias condition, the determining factor in the delay becomes the voltage change on the coupling condenser $(C_2)$ between sweep cycles. This voltage change is determined by the setting of $R_8$.

When the master-multivibrator gating pulse drives the clamp $V_{9a}$ into conduction, ending the sawtooth waveform, the grid of $V_{10a}$ is pulled down and the regenerative action causes $V_{10b}$ to conduct again. It is to be noted that the time constant in the grid circuit of $V_{10b}$ is much too large to enable it to operate as a "flip-flop" at the 1000-cps repetition frequency of the master multivibrator.

*Intensifier Circuit.*—The negative output of the delayed rectangular wave is used to gate the intensifier tube $V_{9b}$, and it permits the plate of this tube (and therefore the second grid of the cathode-ray tube) to rise from about +85 volts to +300 volts. This variation of second-grid voltage is not enough to insure proper blanking at all times, when the cathode and first-grid bias are as shown.

*Blocking Oscillator.*—The front edge of the delayed rectangular wave fires the cathode-biased blocking oscillator $V_{11a}$. A positive output trigger is obtained from the third winding of the blocking-oscillator transformer.

*Cathode Follower.*—The positive trigger is transmitted to the signal source and any other external circuits at a low impedance level through the cathode follower $V_{11b}$.

*Video Amplifiers.*—The input signal is at a −1-volt level and must be amplified to a +40-volt level. To obtain this amplification and maintain the bandwidth required (1.6 Mc/sec) two 6AC7's ($V_{13}, V_{14}$) are used. The positive output voltage of the video amplifier is a-c coupled to the grid of the cathode-ray tube, which is d-c restored to ground by $V_{15a}$. The large bypass condenser $C_3$ in the plate circuit improves the low-frequency response of the amplifier.

*Range-mark Circuit.*—The oscillator $V_{16b}$ is overdamped by $V_{16a}$ between sweeps. The delayed rectangular wave is used to start the time-marker generation at the same time that the delayed trigger starts the source. The sine-wave output of the oscillator controls the action of the flopover ($V_{17}$), which in turn fires the blocking oscillator $V_{15b}$. Negative time markers are coupled from the plate of the blocking oscillator to an output terminal and to the cathode of the cathode-ray tube. The cathode of the CRT may be biased from about +15 volts to +90 volts with respect to the grid.

**15·4. RHI, Second Example.**—This circuit is a precise RHI that uses an electronic marker to determine height. It has been designed to display heights up to 8 miles with an accuracy of ±0.02 mile. The elevation angle varies from 0 to 12°, and height data is generated as a d-c voltage, 4 volts per degree. The elevation angle increases linearly from 0 to 12° and then quickly drops to zero again. This cycle is repeated 10 times per second. On the 20- and 50-mile ranges, a system repetition frequency of 1170 cps is used. For the 100-mile range this repetition rate is changed to 585 cps.

The schematic diagram (Fig. 15·7) contains only the range circuit, the height circuit, the precision-height-marker circuit and the height-blanking circuit. The video amplifier, range-mark generator, and the trigger buffers are not included because they have been illustrated elsewhere in this volume. There are three range sweep lengths available:

20, 50, and 100 miles.    The 20-mile range can be delayed so that it covers any 20 of the first 50 miles.

A deflection coil of 1320 turns on a $2\frac{1}{8}$-in. window is used.    This coil has an approximate sensitivity of 70 ma per radius when the potential of the CRT anode is 7 kv.

*Range "Flip-flop."*—This is a direct-coupled, electron-coupled circuit $(V_1, V_{2a})$ that receives a negative trigger that may be delayed.    It is this delay feature that necessitates a separate rectangular-wave generator for each of the two sweep channels.    On the 20- and 100-mile ranges, the duration of the rectangular wave may be determined by the time constant of the flip-flop.    On the 50-mile range, and sometimes on the other two, the end of the height rectangular pulse operates the range turnoff $V_7$, thereby causing the range flip-flop to return to its stable position.    This interacting turnoff is necessary because the range flip-flop supplies the intensifying pulse for the cathode-ray tube.    The intensifying pulse is obtained from the plate of the "on" tube $(V_1)$ of the flip-flop, which normally rests at $+15$ volts and rises to $+300$ volts with the input trigger. The negative gating pulse for the sweep-generator clamp is obtained directly from the grid of this "on" tube.

*Range Sweep-generator Clamp.*—A standard pentode clamp $V_3$ is switched across the proper $RC$-network for any of the three sweep speeds. An 80-volt sawtooth wave, which is about 0.25 of the exponential amplitude, is generated.    The distortion caused by generating this large sawtooth voltage is not serious (the voltage increase in the last 25 per cent of time is 82 per cent of the rise in the first 25 per cent).

*Cathode Follower.*—The cathode follower $V_{2b}$ is used as a buffer and also provides proper bias for the following driver stage.

*Range Driver.*—A sawtooth wave of about 50 volts is applied to the grid of the driver $V_4$, which is biased at about $-25$ volts.    This bias provides enough quiescent current to insure fairly linear operation of the 807.    A peak of 100 ma of deflection current is necessary to generate the sweep for the coil that has been used.

*Horizontal Centering.*—Tube $V_5$ provides the steady-state current (70 ma) required to keep the spot deflected at the left side of the cathode-ray tube between sweeps (despite the quiescent current in the driver).

*Height Flip-flop.*—The height flip-flop $V_6$ is a d-c–coupled circuit that generates the negative rectangular gating pulse for the height channel.    On both the 20- and 50-mile ranges, the duration of the pulse must be 50 miles because a delayed 20-mile range sweep must be accommodated.    The flip-flop is turned off automatically when the height is above the 8-mile coverage desired, in order to limit the power that must be dissipated in the height circuit and to make a neater presentation. The negative rectangular wave from the plate of the "off" tube $(V_{6b})$

is condenser-coupled to the earth's-curvature and intensity-compensation circuits. This same wave is transformer-coupled to the height-sawtooth triode clamp and the height-marker clamp. A negative gating pulse is also obtained directly from the "on" grid, for both the range-turnoff tube and the height-sawtooth pentode clamp.

*Range Turnoff.*—A pentode clamp $V_7$ turns off the range flip-flop whenever the height flip-flop is turned off. This action is necessary in order to blank the height-sweep retrace, since the height sweep collapses when the height flip-flop is turned off. A turnoff function of this type can often be accomplished more cheaply by deriving a negative trigger from the back edge of the height rectangular wave and applying it to the grid of $V_{2a}$, which is conducting when the range sweep is on.

*Height-gate Turnoff.*—A portion of the height sawtooth wave is fed back to the grid of the normally nonconducting tube $V_{14}$. When this tube conducts, it lowers the plate potential of the "on" tube ($V_{6a}$) of the height flip-flop, thereby ending the rectangular wave. The potentiometer control $R_2$, which determines the amplitude and bias of the feedback sawtooth wave, sets the maximum height coverage of the display.

*Height-sawtooth Pentode Clamp.*—This tube ($V_8$) clamps the condenser ($C_1$) until the negative height gating pulse on the grid permits the condenser to charge exponentially toward the value of the height input data. Since the height input data is at a very low level at low angles, precautions must be taken to insure proper clamping and freedom from ripple at the plate of the clamp.

*Bootstrap Diode.*—The height information is in the form of a d-c potential that increases 4 volts per degree increase in elevation angle. Between sweeps the diode $V_{9b}$ supplies current for the charging resistor $R_1$ and the bootstrap condenser $C_2$. While the height sweep is being generated, the bootstrap condenser cuts the diode off.

*Triode Clamp.*—When the height data has passed its maximum and returns to its minimum value, the cathode of the diode remains more positive than the plate until the charge on the bootstrap condenser can change. To produce a low-impedance path that will enable the charge on this condenser to change rapidly, a triode clamp $V_{9a}$ is necessary. This clamp functions only when the height input potential decreases more than the bootstrap condenser potential during the sweep time. The level of this clamp shifts with the height data and hence a transformer-coupled gating pulse is used.

*Bootstrap Cathode Follower.*—The cathode follower $V_{10a}$ takes part in the bootstrap action of the sawtooth generator. It also distributes the height sawtooth wave to three different circuits. The entire sawtooth wave from the cathode is coupled to the height-marker circuit. Thus,

Fig. 15·7.—Range-height
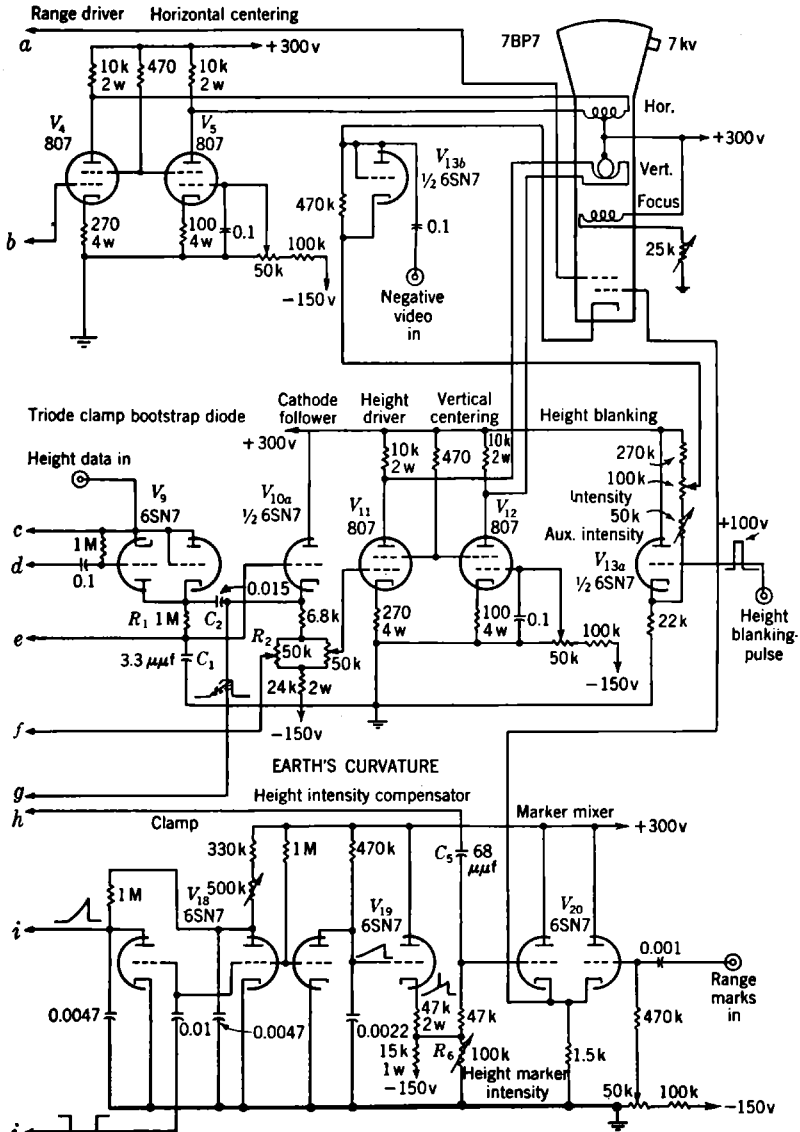
indicator, second example.

any display distortion that occurs past this point (in the driver or in the deflection coil) will not impair the accuracy of the height determination. If the accuracy attainable with this circuit requires improvement, the height sawtooth wave should be linearized by using feedback integration.[1]

A variable portion of the height sawtooth wave is applied to the grid of the height turnoff tube. The third output signal, which is coupled directly to the grid of the height driver, is variable so that the vertical expansion can be controlled. Changing the expansion results in a slight change of the quiescent current in the driver, and hence there is a shift in the vertical centering.

*Height Driver.*—This tube ($V_{11}$) draws a small amount of quiescent current and thereby operates in a fairly linear region of its characteristic. A maximum deflection current of approximately 100 ma is supplied by a 50-volt input sawtooth wave on the grid.

*Vertical Centering.*—The vertical centering tube $V_{12}$ draws about 70 ma and thereby keeps the spot below the center of the tube between sweeps.

*Height-blanking Cathode Follower.*—The height input data is derived from a unidirectional source. Some provision is therefore necessary for blanking the display when the input is returning to zero after having reached its maximum value. A positive pulse (going from 0 to 100 volts) is made available from the source for this purpose. This pulse is applied to the grid of a cathode follower $V_{13a}$, whose cathode is part of the cathode-ray-tube biasing arrangement. Hence, the blanking pulse raises the voltage of the cathode of the cathode-ray tube, thereby blanking it, and $V_{13b}$ is used to d-c restore the negative video signals applied to the cathode of the cathode-ray tube.

*Marker Clamp.*—The height sawtooth wave is condenser-coupled from the cathode of the bootstrap cathode follower $V_{10a}$ to the grid of the marker cathode follower $V_{16a}$. This grid is biased at the potential set by the height-marker control. This potential must control the d-c level of the base of the sawtooth waveform. The combination triode clamp and d-c restorer $V_{15}$ fixes this level independent of the sawtooth waveform. Since the level varies with the height-marker control, the triode clamp must shift its level and is therefore gated through the transformer. The height rate control $R_3$ fixes the potential gradient across the marker-control potentiometer and thereby permits calibration of this control to coincide with an external direct-reading height dial.

*Marker Flopover.*—The resistor coupling ($R_4$) to the grid of the flopover $V_{17}$ limits the grid current, whereas the condenser ($C_3$) across it prevents integration due to distributed capacity from the grid to ground.

[1] Such integration is used in the sweep circuit included in Fig. 7·17 (A/R scope).

Normally, $V_{17b}$ is conducting while $V_{17a}$ is cut off. As the grid of $V_{17a}$ rises because of the impressed height sawtooth wave, it reaches the conduction point and the regenerative action of the flopover turns $V_{17a}$ on, and $V_{17b}$ off. The potential at which the flopover regenerates is determined by the potential of the "on" grid $V_{17b}$. For a given value of this grid potential the time between the start of the sweep and the flopover point depends on the time it takes the height sawtooth wave to reach this regeneration potential. The height marker is derived by differentiating the front edge of the rectangular wave formed by the regenerative action of the flopover. Because of the curvature of the earth, height above the earth is given by $h \approx r \sin \alpha + kr^2$, where $r =$ range, $\alpha =$ elevation angle, $k =$ a constant. To correct for this curvature, the regeneration potential of the flopover must decrease as the range increases. To decrease this potential, a negative correction waveform is applied to the "on" grid of the flopover.

*Earth's-curvature Correction.*—To obtain the square-law curve necessary for the earth's-curvature correction, two clamps, $V_{18a}$ and $V_{18b}$, are used. When these clamps are released, an approximate sawtooth waveform is generated at the plate of $V_{18b}$. This waveform is used for the charging voltage of $V_{18a}$ and an approximate square-law curve is then generated at the plate of $V_{18a}$. This waveform is inverted by the amplifier $V_{16b}$ and direct-coupled to the grid of the flopover. The small condenser $C_4$, across the coupling resistor $R_5$, prevents integration by distributed capacity, which would result in a cubic rather than a square-law correction.

*Height-marker-intensity Compensation.*—Since the sweep traces are diverging from the origin, there are less sweeps per unit display area at the longer ranges. The light output of the tube is a function of the number of times the electron beam impinges on a spot as well as on the number of electrons in the beam and their energy. To compensate for the reduction in the number of sweeps per unit area, the intensity of the height marker is increased at longer ranges by adding the height marker to a sawtooth waveform generated by the triode clamp $V_{19a}$. A portion of this sawtooth wave is coupled to the marker mixer by means of a cathode follower $V_{19b}$, and the sawtooth voltage becomes part of the bias of the marker-mixer grid.

*Nonadditive Marker Mixer.*—The bias of the grid of $V_{20a}$, which is normally cut off, determines the intensity of the height marker and can be controlled by the setting of $R_6$. The marker is coupled to the grid of $V_{20a}$ from the height flopover through $C_5$.

The other half of the mixer $V_{20b}$ is used for positive range marks. The intensity control is in the form of a bias adjustment rather than an attenuator.

*Cathode-ray Tube.*—The cathode-ray-tube anode is operated at 7 kv. The second-grid voltage is only 300 volts and this voltage should be increased if the resolution needs improvement. A higher second-grid voltage could be obtained from the high-voltage bleeder, provided that the blanking was done on another electrode.

**15·5. Hybrid RHI–E-Scope.**—In this indicator the height determination is accomplished by using a set of height lines inscribed on an overlay. The pattern formed by this type of presentation is shown in Fig. 15·4.

This indicator gives a pattern of 50° at 10 miles and 20° at 140 miles, and increases the precision attainable at 140 miles by a factor of 2.5 as compared to an E-scope presentation. The height information is derived from a precision potentiometer and varies from 50 to 140 volts as the elevation angle goes from 0 to 60°.

The presentation is set to cover a range of 140 miles in two 70-mile steps: (1) from 10 to 80 miles, (2) from 70 to 140 miles. The use of these two ranges increases the range resolution but also necessitates the use of two different height scales.[1]

To obtain maximum height accuracy and precision from a system using a mechanical-height scale, the normal distortion of a fixed-deflection-coil pattern must be reduced. To minimize the standard "barrel" distortion that exists on a 12-in. cathode-ray tube, a special deflection yoke is used. The coil used in this indicator is illustrated in Fig. B·3.[2] Another method of improving the pattern is the accurate mechanical adjustment of the focus coil, as described in Sec. 3·6. The low-voltage focus coil and the switch shown in the schematic diagram make possible the use of alternating current for lineup.

Another factor that contributes to the accuracy of the displayed pattern is the absence of the first ten miles. This allows 100 μsec in which to obtain linear sweeps. It is particularly difficult to start the fast vertical sweep quickly and linearly when the elevation angle is small. To insure the stability of the pattern, all bleeder resistors and driver-degenerating resistors are wire-wound. With the indicator as shown, the limiting factor in reading height accurately is interpolation of the midpoint of a signal between the height lines.

The range-sweep circuit, the video amplifier, and the marker mixer are shown as blocks in the schematic diagram (Fig. 15·8) and require 15

[1] See Sec. 16·7, Fig. 16·19.

[2] The sectional winding of this coil permits the use of many damping resistors per coil, provided that they are mounted on the coil. If these damping resistors are used, it is necessary to omit the damping resistors that are shown in Fig. 15·8 connected between B+ and the plates of the sweep-current tubes.

tubes.   The circuits are the same as those shown in Fig. 13·6, except for the following necessary modifications:

1. The delay switch must switch the scale lights on the overlay.
2. Only one driver is required.
3. The off-centering current tube must be connected to the deflection coil to be used for horizontal centering.
4. Only one sweep (of 80 miles) need be generated.   This sweep is then either undelayed or delayed by 60 miles.
5. A negative trigger must be provided to the height flip-flop from the screen of the trigger buffer.
6. The trigger buffer is biased so that a blanking voltage will prevent the trigger from reaching the circuits.   This blanking voltage is supplied from the elevation data-take-off system by using a cam and Microswitch arrangement.

*Elevation-data Cathode Follower.*—The height-input data is used to generate a "slow" vertical sweep, that is, a sweep proportional to the elevation angle $\alpha$, and a "fast" vertical sweep, proportional to $t\alpha$. Because the slowly varying component must be direct-coupled to the driver $V_2$, the d-c level of the input data determines the operating region of the driver.   Hence, the input-data level must be chosen high enough to insure operation in a satisfactory region of the tube characteristic. This unit uses an input voltage that varies from $+50$ volts to $+140$ volts.

This input data must be available at a low-impedance level for the generation of the fast vertical sweep.   Hence, the cathode follower $V_{4a}$ is used.   To compensate for the $+50$-volt level at $0°$, it is necessary to have a fixed reference voltage of approximately $+50$ volts.   This low-impedance point ($V_{4b}$) is used as the clamp-biasing voltage and insures a zero-voltage sawtooth waveform at $0°$.   The voltage of this reference point is set by a potentiometer $R_3$.

As the current through the data-transmission cathode follower increases, the $\mu$ of the tube changes so as to increase the gain of the cathode follower.   To compensate for this source of error in the data transmission, negative feedback is used.   Feedback is accomplished by obtaining the potential for the data potentiometer from the plate of the cathode follower.   Thus when the cathode-follower gain increases, this potential decreases.   The compensation linearizes the cathode-follower output voltage with respect to changes in angle so that it produces negligible error.

The phase shift introduced by the filter network connected to the arm of the potentiometer is negligible at the slow elevation-scanning

Range
centering

807

Trigger
shaper

6SN7

Rectangular
wave
generator

6SN7

Sweep
intensifier

807

Sweep
generator

6SJ7

Sweep
amplifier

6SN7

Range
driver

807

Delay

6SN7

Voltage
regulator

VR150

D-c
restorer

6H6

Positive
trigger

Trigger
buffer

6AC7

Markers in

Marker
mixer

6SN7

Video in

Video
amplifier

2-6AG7

Cathode
follower

6SN7

Hor.

Vert.

Switch
A-c

D-c

2.0

Focus

1800  300

+30v

120v A-c

120v A-c

25

a

b

c

FIG. 15·8.—Hybrid RHI-E-scope.

rate used. To increase the precision of the electrical input data the potentiometer is run at 3-speed with respect to the actual elevation motion. To prevent signals from appearing when the source is not in the proper 50° angular interval, a cam and Microswitch on the 1-speed shaft are used to render the trigger buffer inoperative.

The output signal from the cathode follower for the slow vertical sweep is obtained from a potentiometer $R_4$. Since this potentiometer is connected between the two cathode followers, the vertical-centering zero adjustment is independent of the amplitude of the slow vertical sweep. The output signal for the fast vertical sweep is obtained through the bootstrap diode $V_{5a}$.

*Bootstrap Sawtooth Generator.*—At small angles, the sawtooth voltage that is generated by $V_6$ and $V_{5a}$ is very small, and negative-gate feedthrough in the clamp would be very objectionable. To minimize this feedthrough, only a small portion of the rectangular wave is used as the gating pulse. If the first 10 miles were to be used, further feedthrough precautions (in the form of an integrating network for the gating pulse) would be necessary.[1]

*Sweep Amplifier, D-c Restorer and Sweep Driver.*—The 807 driver $V_9$ is cut off between sweeps (its waveform is d-c restored to the −60-volt bias point available at the range driver). The gain without feedback is about 1000 whereas the over-all gain with feedback from input grid to driver cathode is 1. In order to have the driver start conducting quickly it is necessary to use cathode bias in the second stage ($V_8$) of the amplifier. Without this bias, the grid of this stage would be conducting and hence present a low impedance to the first stage. This impedance would decrease the gain of the amplifier (from 1000 to 50) and excessively delay the start of the small-amplitude vertical sweeps. The fast-sweep current and the slow-sweep current are added by connecting the plates of the corresponding drivers.

*Slow Vertical Driver and Vertical Centering.*—The slow vertical sweep is applied to the grid of the driver $V_2$. The 1000-ohm degenerating resistor $R_1$ increases the linearity of this stage. The common 100-ohm resistor $R_2$ is a form of cathode coupling which gives some push-pull action, further aiding the linearity and decreasing the necessary driving voltage. Both these resistors serve to bias the 807's ($V_2, V_3$) properly and at the same time to supply degeneration. Hence these resistors are wire-wound to give pattern stability.

[1] It is difficult to use a pentode clamp because the screen-grid current that would have to come from the reference cathode would change the reference voltage between sweeps.

# CHAPTER 16

## MECHANICAL AND OPTICAL DEVICES

By T. Soller, R. W. Dressel and C. W. Sherwin

### MOUNTS AND MAGNETIC SHIELDS FOR CATHODE-RAY TUBES[1]

Cathode-ray-tube mounts consist basically of a support for the cathode-ray tube, the driving coils, and other control elements, plus a support for the entire assembly mounted independently or in combination with related components.

The electrostatic type of cathode-ray tube is usually shielded by its support from outside magnetic interference. This assembly is most often mounted in the same box with other apparatus.

The magnetic tube, used more extensively as a radar indicator, is mounted in a tube mount containing a deflection coil, which may be fixed or rotatable depending upon the application, a focus coil or magnet, and other necessary control elements. The tube must be accurately positioned with respect to the external coils, and this position, once obtained, should be rigid and lasting. However, the position of the coils with respect to various tubes differs, and, since the cathode-ray tube is a fragile unit that must be replaced, the position of the coils in their housing must be adjusted to get the most efficient performance from any one tube. These adjustments must be made for any new tube or for the original tube when the output characteristics vary because of changing electrical characteristics. They must be accomplished simply and easily whether the tube mount is a separate mount that can be reached from all sides, or whether it is mounted in a console and can be reached only from the front.

Tube mounts have been designed for three basic uses: airborne, shipborne, and stationary installations.

The airborne mounts are designed to have minimum size and weight and yet be rigid enough to withstand the applied vibrations. A supporting frame, containing vibration-isolation mounts, is then added when the mount is supported independently in the plane. A mount of this type can also be used in a panel installation. However, if the installation is close to the magnetic compass, magnetic shielding is necessary in order to eliminate the effect on the compass of the magnetic fields of the various coils.

Shipborne mounts are the same in principle but are constructed to withstand the great shock to which they may be subjected during gunfire.    A more rigid and weighty structure is therefore necessary.    Indicator tube mounts used in shipborne work are almost always built into the indicator-circuit consoles, which are properly shock-mounted. Thus the tube mount itself does not need a separate shock-mounting frame.

In stationary work the shock and vibration problem is not a primary consideration and no special mountings are necessary.   However, the mounts must be capable of withstanding rough treatment in shipment. They must also be compact since they are built into the indicator-circuit consoles, which must be easily transportable.

**16·1. Tube Mounts for Electrostatic Cathode-ray Tubes.**—A mount to support an electrostatic cathode-ray tube is generally a relatively
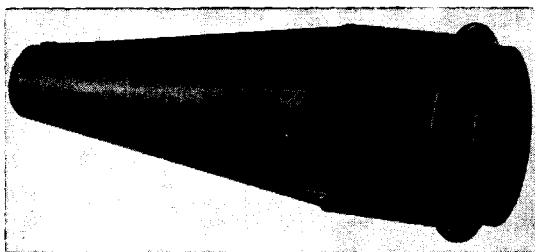


FIG. 16·1.—Support and magnetic shield for 5-in. electrostatic tube.

simple device.    These tubes are almost always located in a box containing the driving circuits and various controls.    The mount usually consists of a conical or cylindrical part and a front cover.    The conical or cylindrical part extends over the entire length of the cathode-ray tube and is mounted behind a hole in the front panel of the instrument.    The front cover accommodates a ruled scale, either on a clear plastic or on one that is a color filter, and it usually has provision for attaching a viewing hood.

Figure 16·1 illustrates a typical support for a 5-in. tube.    The cylindrical front part is made of well-annealed soft iron, and the conical part of a high-permeability alloy that extends over the entire region occupied by the electron gun and the deflection plates.    Such a magnetic shield is almost always required, especially if transformers, etc. are located in the vicinity of the cathode-ray tube.    The shape of such magnetic shielding should be kept as simple as possible because the high-permeability alloys are not easily fabricated into complicated shapes.    The tube socket (not shown in Fig. 16·1), is usually mounted on a separate bracket. Figure 16·2 illustrates a tube mount for a 3-in. cathode-ray tube that

can be mounted directly on the instrument panel with the tube socket held by the clamping arrangement at the rear of the mount.

**16·2. Mounts for Fixed-coil Magnetic Cathode-ray Tubes.**—One of the most important classes of mounts used in radar indicators is the mount for the fixed-coil magnetic cathode-ray tube. The fixed coil refers to the deflection coil, which is kept fixed in position while the tube is operated. The deflection of the electron beam is accomplished by properly varying applied voltages. The mount consists of the following: a cathode-ray tube, properly supported in medium-hard sponge-rubber mountings designed to absorb the applied shock and yet keep the tube properly positioned; a deflection coil, fixed in position except for a slotted mounting that is used to get proper initial azimuth orientation; a focus coil or focus magnet for properly focusing and aligning the electron beam.
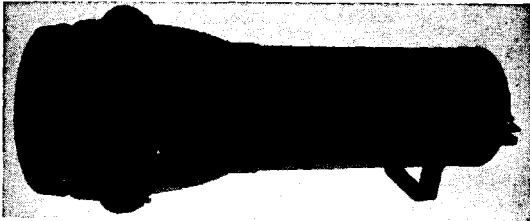


FIG. 16·2.—Tube mount and shield for 3-in. electrostatic tube.

When the focus coil is used it is necessary to have a method of tilting and clamping the coil in order to align the electron beam. When the focus magnet is used, a method of externally adjusting the focus shunt to get the proper magnetic field strength for focusing, and a method of moving a centering plate in the *x*- and *y*-axis to align the electron beam properly are necessary. In front of the cathode-ray tube is placed a reference scale marked on a transparent overlay. This scale is either edge-illuminated or darkened so as to be in contrast with the tube face. The scale is designed to be either fixed or rotated in azimuth depending upon the application.

A typical example of a simple fixed-coil mount is shown in Fig. 16·3. This mount consists of a case spinning that houses the deflection coil *D*, the focus coil *F*, a rear terminal strip *T*, and the rubber supports for the tube, which consist of the front sponge-rubber support *R*, and the back tube grommet *G*. The high voltage for the cathode-ray tube is brought in on a high-voltage cable that passes through the fitting *H*. The extrusion *E* on the spinning allows the leads from the front edge-illuminating bulb socket *L* and leads from the deflection coil to pass over the focus coil and be connected to the terminal strip without interfering with the motion of the focus coil. The leads from the focus coil are also connected

to the back terminal strip.    External power is brought in on a cable,
passes through the fitting $C$, and is terminated on the back terminal
strip.    The tube socket is also wired to this back terminal strip.    An
end cap is used to close up the back of the mount.    The front section of
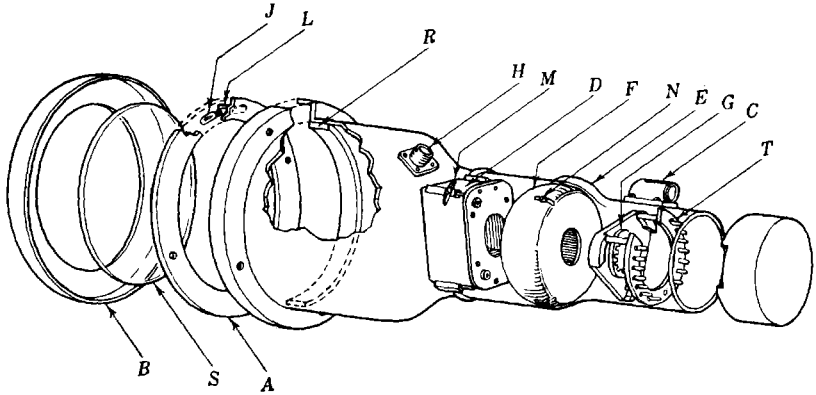


Fig. 16·3.—Cathode-ray tube mount (exploded view).

the mount consists of a transparent overlay $S$ set in a supporting ring $A$.
This assembly is then covered by a ring-spinning $B$ forming the necessary
light box to house the edge-illuminating bulbs $J$, and to shield the light
from the operator.    The deflection coil is positioned in azimuth by
loosening the screws $M$, rotating the coil in the slots, and then fastening
the screws.    The focus-coil position is adjusted by loosening the screws
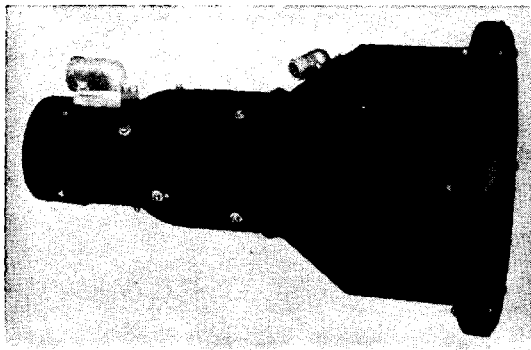


Fig. 16·4.—Fixed-coil mount for 7-in. magnetic tube.

$N$, tilting the spherical-contoured coil by means of these screws in the
spherical section of the tube-mount spinning, and then tightening the
screws.    To install a tube, the front spinning and the overlay assembly
must be removed.    The tube is then inserted in the main spinning and
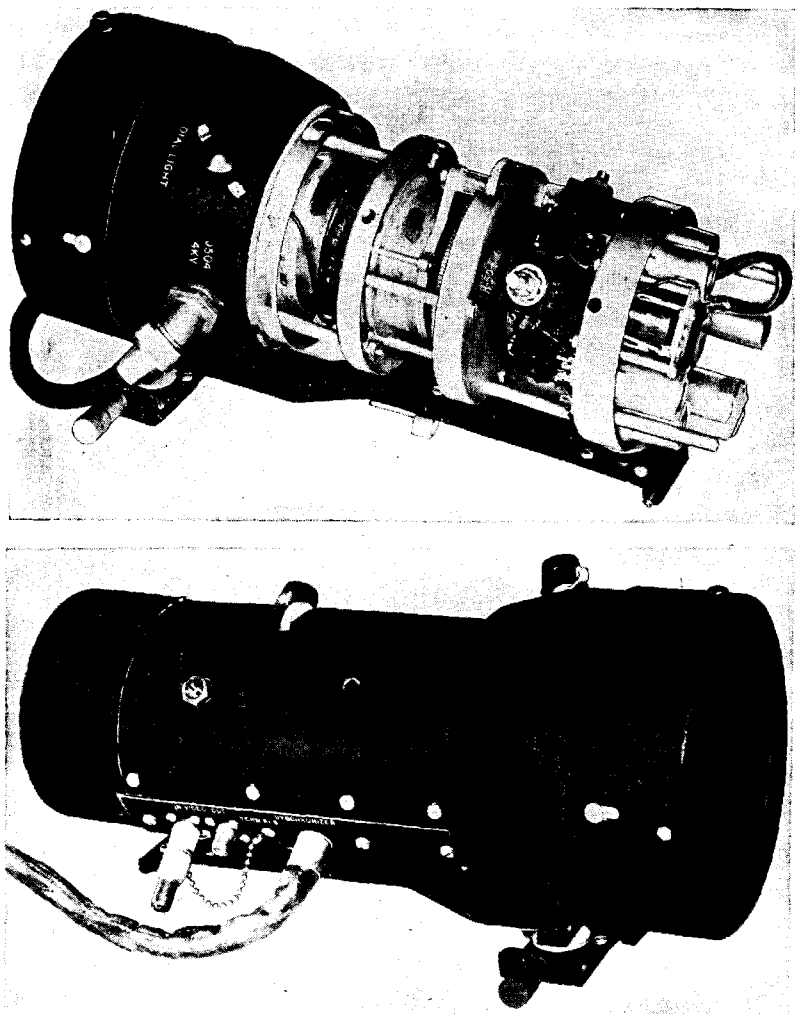
FIG. 16·5.—Fixed-coil mount for 5-in. magnetic tube, with permanent-magnet focusing and including amplifier.   Top figure shows unit exposed.

pushed back until the reference line of the tube is in line with the front edge of the deflection coil and the glass is brought into contact with the flat sponge-rubber ring mounted on the front of the deflection coil. Since, in normal tubes, there is a variation of about a quarter of an inch in the length from the reference line to the front face of the tube, the front assembly is telescoped into the mount to compensate for this

variation and to put axial pressure on the tube face through the front rubber cushion. Figure 16·4 shows a photograph of such a mount for a 7-in. cathode-ray tube.

Another example of a fixed-coil mount is the mount shown in Fig. 16·5. This mount varies from the spinning type in that it is made up of mounting plates and spacers instead of a spun container. This
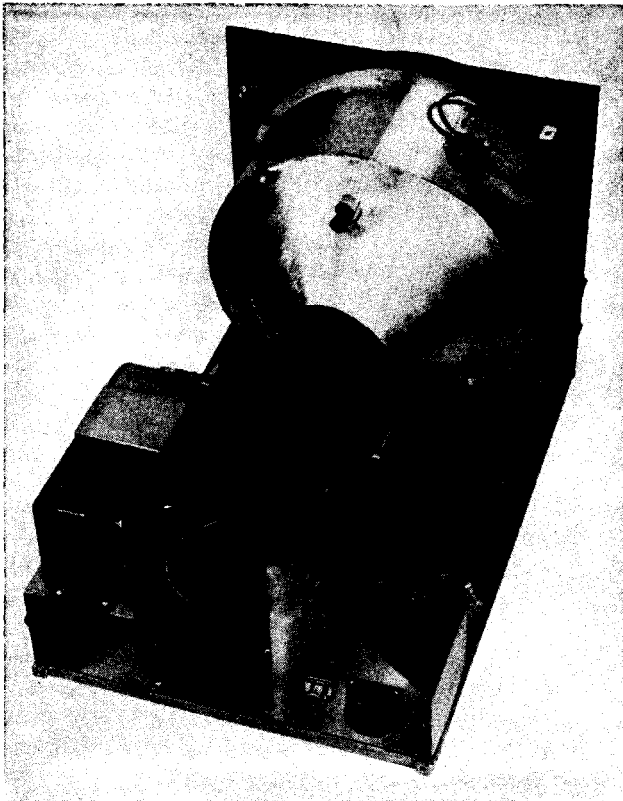


FIG. 16·6.—Fixed-coil mount for 12-in. magnetic tube with provision for accurate focus-coil adjustment.

method of construction is especially suited to this application because the apparatus contains a focus-magnet assembly that acts as a part of the structural section of the mount because it may be kept fixed in position and does not have to be tilted. Separate vibration mounts are incorporated in the framework because this mount is a separately installed unit. Aside from these changes the mount does not differ greatly from the simple spinning type.

In Fig. 16·6 is a third example of a fixed-coil magnetic-tube mount designed to house a 12-in. cathode-ray tube. To allow for the variation in critical dimensions from tube to tube, the section that contains the deflection and focus coils is arranged to slide forward or backward on the base plate. However, the greatest difference in this particular mount is the use of a focusing-coil arrangement that allows the coil both to be adjusted accurately in the $x$- and $y$-axes and to be tilted about these axes. This motion is necessary in order to get the proper adjustment of the coil and to get the best performance from the 12-in. cathode-ray tubes. The uses of this type of focus-coil mount are discussed in detail in Sec. 3·6.

16·3. Rotating-coil Mounts for Magnetic Cathode-ray Tubes.—A rotating-coil magnetic cathode-ray-tube mount is one designed to cause the sweep on the face of the cathode-ray tube to rotate by mechanically rotating the deflection coil, in synchronization with the scanner unit, about the center line of the tube neck. A mount of this type finds greatest application when used as a plan position indicator.

This mount presents a more complex mechanical-design problem than the fixed-coil magnetic cathode-ray-tube mount because a rigid frame must be built up to support a ball-bearing–mounted coil housing, a gearing arrangement, and a driving unit. The design of the rotating mechanism must be governed by the following mechanical and electrical considerations.

1. The deflection coil must be freely rotating because of the limited torque available in the smaller-sized positioning devices and the increasing errors of positioning with increased loads of many of these devices such as synchros and flexible shafts. It is also necessary, therefore, to have the torque as constant as possible in order to eliminate any variations in pattern during rotation.
2. The deflection-coil assembly must be compact in order that there may be sufficient room along the tube neck for the proper location of the focusing coil or magnet.
3. Except for properly designed coil housings, as much of the materials used around the deflection coil and focus coil as possible should be nonmagnetic in order to eliminate stray permanent magnetic fields which affect the performance of the cathode-ray tube.
4. The slip-ring contacts should be designed to give a minimum of electrical resistance and long operational life. The brush contacts must also be constructed to give minimum electrical resistance plus proper contact at any speed of rotation of the deflection coil. Proper surface-leakage paths and insulation for the peak voltages encountered must also be provided between individual slip rings

and ground as well as between individual brush arms and ground. However, all this must be accomplished with the lightest brush pressure possible in order not to increase materially the torque necessary to drive the deflection-coil assembly.

5. A precision or other compensating gear train is needed between the positioning unit and the deflection coil to decrease the error introduced by backlash or looseness in the gear train, and in order to eliminate as much as possible any variations in torque caused by the local binding of eccentric or improperly mounted gears.

6. Magnetic shielding is required for the electromechanical drive units, when they are mounted close to the tube neck, to diminish the effect of magnetic pickup from these units by the electron beam. However, an effort is made to have the drive unit mounted as far from the tube neck as possible and as far in back of the gun structure in the tube as possible.[1]

7. The rotating-coil mount must be structurally rigid and compact, and have provision for supporting the focusing coil or magnet as well as a means of centering and rigidly supporting the cathode-ray tube.

*Bearings.*—One of the major difficulties encountered in the design of a rotating-coil mount is the proper choice of bearing arrangement for the rotating deflection coil. The conventional use of a precision steel ball bearing of the aircraft type has been most common. Although this type of ball bearing, if properly mounted, is capable of doing a splendid job as far as torque and rotation is concerned, it can easily be magnetized either by passing a d-c field through the deflection coil or before assembly by coming in contact with a magnet or magnetized instrument. Therefore, in production, a careful check is made of each ball bearing before installation.

To eliminate the difficulty of magnetization of the bearings that support the deflection coil, a means of supporting the coil with non-magnetic materials has been used. The various methods include the use of V-shaped roller disks running in a groove cut in the deflection-coil housing, the use of large-diameter V-grooved raceways attached to the deflection-coil case with monel-metal balls, or a conventional bearing made of nonmagnetic materials. The use of the V-shaped roller and the large V-grooved ball bearings requires a large-size servomechanism to supply sufficient torque for rotation. In most cases, however, a low-power servomechanism or a low-power synchro follow-up system is used to rotate the deflection coil. Therefore, it has been necessary to develop

---

[1] A further discussion of magnetic shielding of magnetic cathode-ray tubes from driving units can be found in Sec 8·15.

a low-torque nonmagnetic ball bearing. Such bearings have been designed and built using bronze or other composition raceways, and stainless-steel or monel-metal balls. The design of these bearings follows conventional bearing designs as far as shape and size of raceways and balls is concerned. Because high load capacities are not needed in a ball bearing used to support a rotating deflection coil, it is possible to use softer raceways and balls than those found in the conventional hardened-steel precision ball bearings. Materials such as tobin bronze, "Ampco-21,"[1] stainless steel (18-8), and beryllium copper, which are nonmagnetic, have been used for raceways. Materials such as K monel metal, monel metal, stainless steel, and even glass have been used for the ball materials. The most satisfactory bearings to date have been those in which the raceway material has been made of "Ampco-21" and the balls of K monel metal. The "Ampco-21" has a Brinell hardness of 285-311 and a Rockwell hardness of 30-33C. The K-monel-metal balls have a Brinell hardness of 290-300. These materials have been made into ball bearings of conventional form in sizes similar to the Fafnir or Norma-Hoffmann A545 and A544, and similar to the Marlin Rockwell 0015.[2] When mounted these bearings have given torque measurements equivalent to the standard steel ball bearings, and have been capable of withstanding the shock and vibration encountered in aircraft, ship, and stationary installations for rotating-coil work.

*Synchro-driven Mount.*—The mount[3] shown in Fig. 16·7 is a typical rotating-coil mount designed for general application. Two sizes are available, one to house a 5-in. cathode-ray tube and another to house a 7-in. cathode-ray tube. However, the mount has been designed in such a way that sections can be removed and separately mounted to take care of larger sizes of cathode-ray tubes. This mount is designed to be driven by a 10-speed synchro follower; that is, the gear ratio between the deflection-coil gear and the drive pinion is 1 to 10. The deflection coil is mounted in a housing that is in turn supported by two ball bearings similar to Norma-Hoffmann bearing No. A545. The deflection-coil gear is fastened to this housing. On the outside surface of the deflection-coil housing is mounted a slip-ring assembly. This assembly consists of an insulated tube of paper phenolic on which two coin-silver slip rings are fastened and insulated from the case and from each other by about $\frac{5}{16}$ in. of surface path and $\frac{5}{32}$ in. of solid insulating material. This insulation is sufficient to withstand 500 volts of constantly applied voltage under high-humidity conditions. The deflection coil, however,

<hr>

[1] "Ampco-21" is supplied by Ampco Metal Inc. Milwaukee, Wis.

[2] These sizes are available from Howe Engr. Co., 1503 E. Michigan St., Indianapolis, Ind.

[3] Sanborn Co., Cambridge, Mass.

has peak voltages of about 700–800 volts, but these are of extremely short duration and have not caused "arc-over" under usual operating conditions.

This assembly is housed in the deflection-coil outside casting and end plate. The casting supports the brush blocks and the pinion-gear ball-bearing assembly. The pinion-gear assembly consists of the pinion and shaft set into two ball bearings and supported by the outside pinion sleeve. The sleeve is turned so that the outside diameter is 0.005 in. eccentric with the bore. The eccentricity allows for variation in the
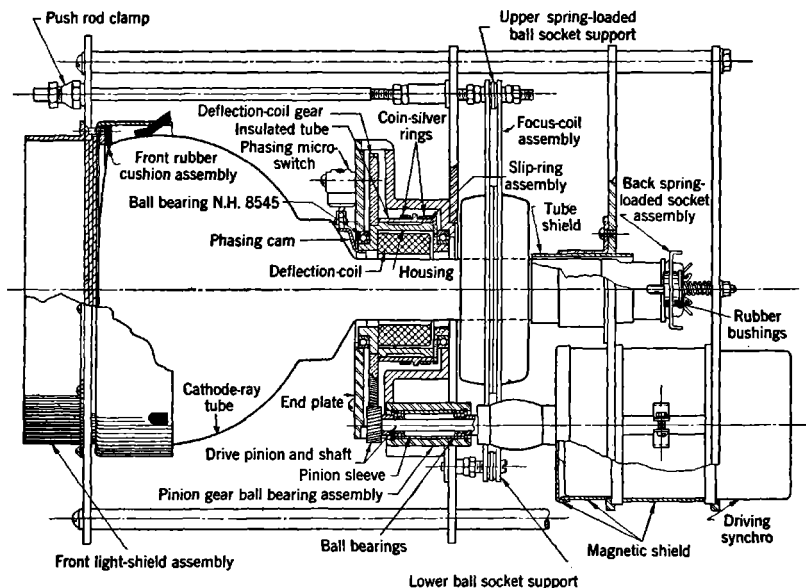


FIG. 16·7.—Rotating-coil cathode-ray-tube mount.

gear-center distance between the pinion and drive gear and forms a means of adjusting the pinion with respect to the deflection-coil gear to get minimum backlash with free rotation. The gears themselves are precision gears cut to a tolerance of ±0.0003 in. They are helical gears of 48 normal diamentral pitch with a helix angle of 17° 51' and a 20° normal pressure angle.

Attached to the plate supporting the deflection-coil housing is the focus-coil assembly. This assembly is fixed to the main plate by three spring-loaded ball-socket supports. The lower support is fixed in position, and tilting is accomplished by the adjustment of the two upper push-rod and socket supports. Tilt in all directions can be obtained by moving each push rod independently or both simultaneously.

A clamp arrangement, mounted on the front panel, is tightened to keep the coil fixed in position.

A tube shield is then mounted on the second mounting plate to minimize the effect of the magnetic field of the driving synchro.

The driving synchro is a Size 5F, supported by the second and third mounting plates and surrounded with a magnetic shield. The Size 5F when energized will supply 0.402 oz-in. of torque per degree of lag. The absolute accuracy of the synchro, however, is no better than $\frac{1}{2}°$ because this value represents the accuracy of the windings in the synchro itself. The tube is supported by the front rubber-cushion assembly and the back spring-loaded socket assembly. The socket plate is mounted on vibration-absorbing rubber bushings.

The specifications on the mount require that a maximum of 12 oz-in. of torque, applied at the 1-speed or deflection-coil axis, will rotate the deflection-coil gear, meshed with the pinion-drive gear and the driving synchro, which is attached but not energized. From this torque figure the accuracy of rotational following which may be expected can be calculated. With 12 oz-in. of torque at the 1-speed shaft, 1.2 oz-in. of torque is required at the 10-speed or pinion shaft if the gear efficiency is assumed to be 100 per cent. This assumption is approximately true for a precision spur or a helical gear, for which the efficiency of transmission is about 98 to 99 per cent in a single mesh. Since the synchro motor supplies 0.4 oz-in. of torque per degree of lag, the synchro will lag approximately 3°. However, 3° of lag at the 10-speed shaft reflects only 0.3° at the 1-speed shaft. But, 3° at the driving synchro should be considered 4° absolute accuracy since the synchro windings are no more accurate than $\frac{1}{2}°$. Now, if about 1° of inaccuracy, which may be attributed to backlash between the meshing gears, is included, there is a total of 5° of inaccuracy at the pinion shaft. Then 0.5° will be reflected at the deflection coil. Thus the mount can be said to be accurate to within 0.5° in following. Similar considerations can be used to evaluate the accuracy of follow-up for similar type mounts with synchro–drive followers.

Since the mount is driven with a 10-speed synchro, there are 10 stable positions in which the mount may be driven by the driving 10-speed synchro generator mounted on the rotating antenna. To eliminate this uncertainty of azimuth positioning a phasing scheme that incorporates two cams, two switches, and a relay is used (see Fig. 16·8). One cam and one switch are mounted on the coil mount, whereas the other cam and switch are mounted on the antenna base. The cams rotate at one speed and are so designed that the tube mount and antenna, once aligned, will always operate from the same azimuth reference. The cam on the indicator is 25° in width acting on a normally open switch, and the cam on the antenna is about 30° in width with a normally

closed switch.  If both units are operating in synchronism the antenna switch will open and remain open while the indicator switch is closed. Since these switches are in series, there will be no voltage applied to the relay.  If the two units get out of synchronism the indicator switch will close the relay, thus short-circuiting two legs of the stator of the driven 5F synchro and causing the coil to stop with the switch closed.  The coil will remain in this position until the antenna switch is opened by the cam and the relay circuit is again broken.  At this point, the indicator unit will again start rotation and will rotate in synchronism with the antenna. This scheme requires that the driven and the driver synchros be properly
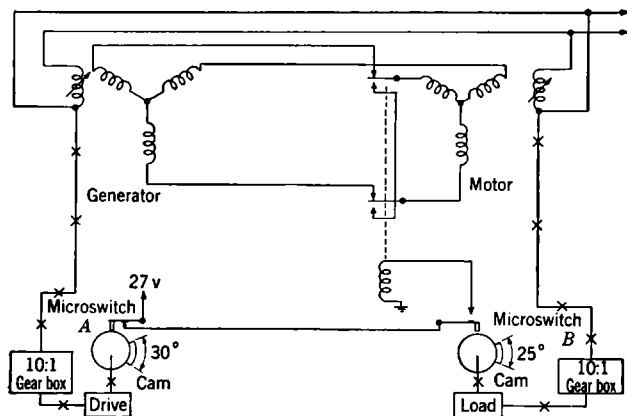


Fig. 16·8.—Microswitch phasing circuit.

"zeroed" or phased so that the indicator synchro will not again jump out of phase.

Another important consideration in keeping the torque small is the proper choice of brush-contact and slip-ring material.  In the mounts described a $\frac{3}{16}$-in.-wide, coin-silver slip ring is used.  The surface is turned and polished with as few ripples as possible.  The brush contact is of silver graphite material containing about 45 per cent graphite.  By using these materials it is possible to get sufficiently low electrical resistance and long operational life with a brush pressure of about 10 oz per square inch of contact area.

*Servomechanism-driven Mount.*—In Fig. 16·9 is shown a rotating-coil magnetic-tube mount designed to be driven by a servomechanism,[1] and to house a 7-in. cathode ray tube.

The deflection-coil assembly *A* is similar to that used in the mount previously described except that it is designed to be somewhat more

[1] Sanborn Company, Cambridge, Mass.
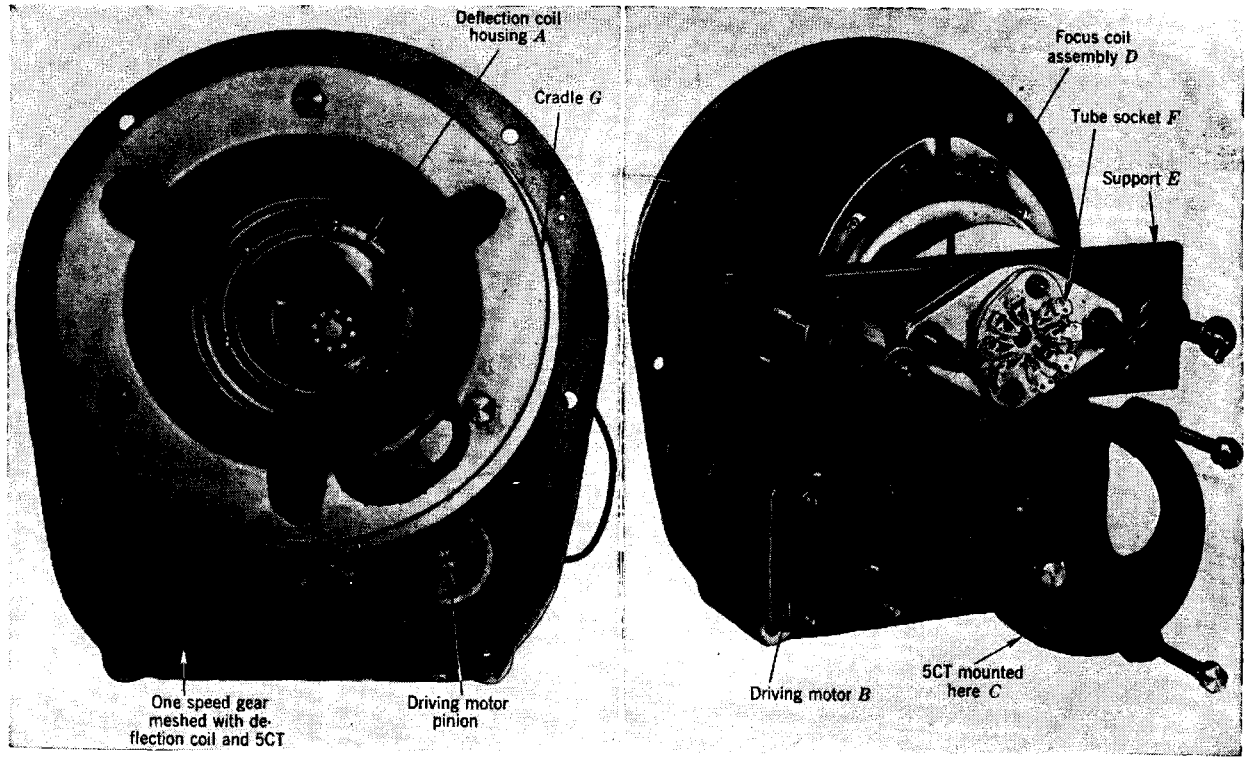
Fig. 16·9.—Rotating-coil mount for 7-in. magnetic tube with provision for servomechanism drive.

rugged.    This deflection-coil assembly is supported by two ball bearings, Marlin Rockwell No. 0015.

The deflection-coil gear is meshed in a train with a 5CT synchro. This synchro is the positioning-control device but not the drive unit. Meshed by gears to the synchro and deflection-coil gear is a drive motor *B*, which supplies the drive power to the train but is controlled by information from the 5CT synchro fed through an amplifier back to the drive motor.    This drive motor is a low-inertia Diehl FPE 25-11.    The overall accuracy of the mount is controlled by the amount of backlash between the 5CT synchro *C* and the deflection-coil gear, the accuracy of the control transformer, the regulation of the drive motor, and the proper design of the servomechanism amplifier.

In this mount a 1-speed servomechanism system is used, that is, the control element, the 5CT synchro in this case, is geared 1-to-1 with the deflection-coil gear.    Other systems may use one or more control synchros running at the same or higher speeds.    Typical ratios between deflection-coil gears and control synchros consist of a 1-speed deflection coil coupled with the single 1-speed control synchro, or a 1-speed deflection coil coupled with two synchros, one running at unit speed and the other running at 36-speed, where the 1-speed synchro is used for synchronism and the 36-speed synchro for greater azimuth accuracy.

The gear train in the mount is precision-cut and precision-mounted to get minimum torque and minimum backlash.    Although minimum backlash between the drive motor and the rest of the gear train does not influence the accuracy of follow-up, it does materially account for the amount of oscillation or "hunt effect" appearing in the drive motor. Therefore, the amount of backlash between the drive-motor pinion and the first driven gear should be kept small.    The couplings between the drive motor and its gear shaft, and the control transformer and its gear shaft, are of an antibacklash type to eliminate added errors.

The rear of the mount consists of a focus-coil assembly *D* mounted on the back of the main casting, a tube support *E*, and a spring-loaded tube socket *F*.

A spring-loaded tube-support cradle *G* is mounted in front of the main casting and exerts axial support pressure on the bulb of the cathode-ray tube.

*Rotating-coil Mount with Provision for Off-centering.*—In Figs. 16·10 and 16·11 are shown an off-center PPI rotating-coil mechanism mounted on a chassis *A*, which contains the indicator circuits, and a front panel *B* on which are built front tube supports *C*.    The overlay assembly *D* attaches to the front panel and puts axial pressure on the tube face by means of a sponge-rubber ring.    The tube bulb is in turn forced forward by the spring cradle *E*.    This cradle exerts axial pressure but does little
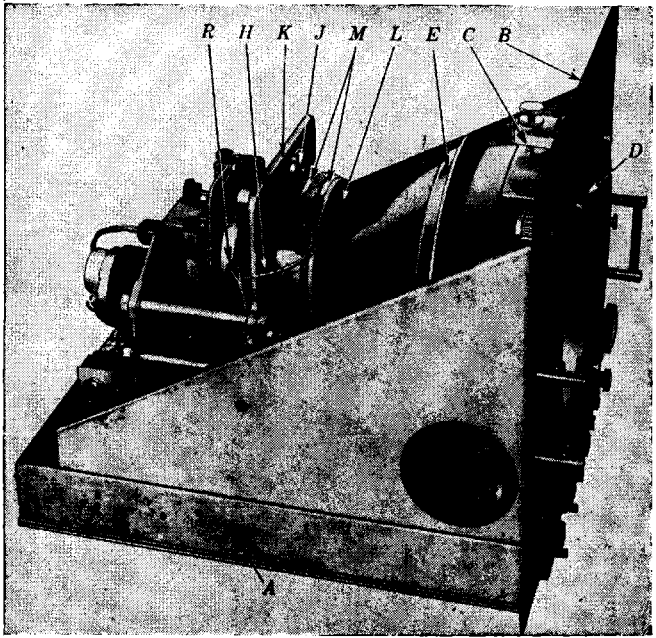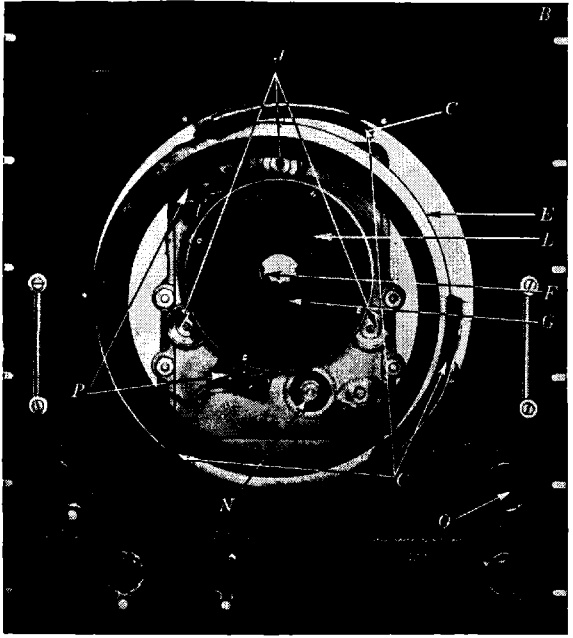
FIG. 16·10.—Rotating-coil tube mount with off-centering.

in the way of centering the bulb.    The tube is centered by means of the
back grommet *F*, and the adjustable front tube clamps *C*.    These front
tube clamps allow for variations in perpendicularity between the front
tube face and center axis of the tube neck.
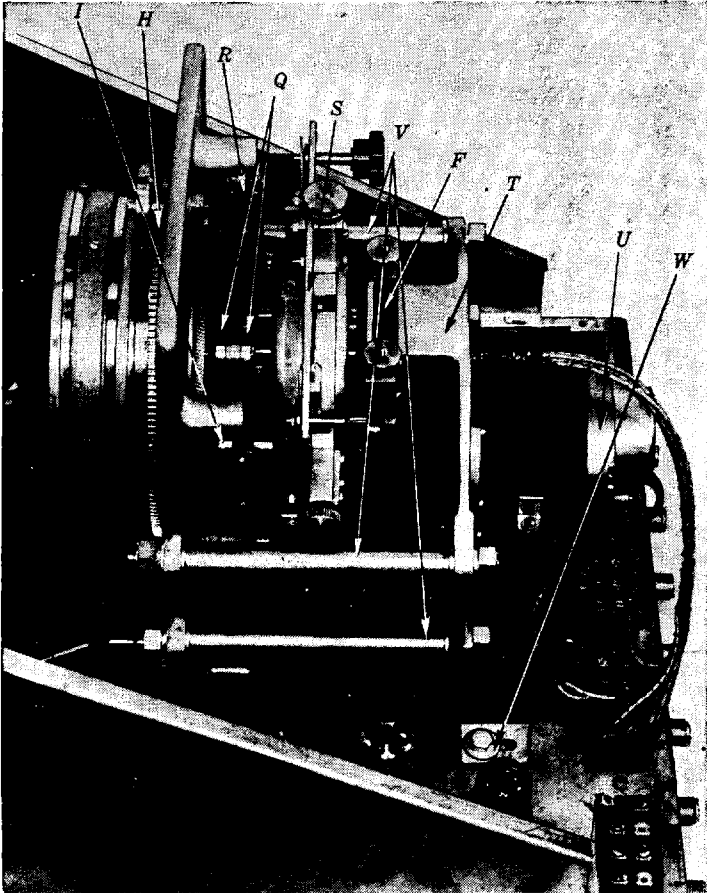


FIG. 16·11—Detail of rotating-coil mount for 12-in. magnetic tube showing slip rings and
focus-coil adjustment.

The rotating deflection coil *G* is an air-core coil supported by a single
nonmagnetic ball bearing similar in size to a Marlin Rockwell 0015.
The rotating-coil gear *H* is similar to the gear in the mount previously
described and meshes with a similar pinion-gear assembly (*I*, Fig. 16·11).

Included in this mount is an off-centering coil assembly that is

mounted on roller disks $J$ attached to the main front casting $K$. The off-centering assembly includes an off-centering coil in an outside case $L$, two insulated slip rings $M$, and an off-centering gear $N$. This gear is positioned by a knob and shaft assembly $O$ from the front panel. Two insulated brush blocks $P$ are mounted from the main front casting and contain brush contact arms for the two outside slip rings.

The internal rotating deflection coil leads are brought out to two coin-silver slip rings $Q$ and through two brush contacts $R$ (Fig. 16·11).

Attached to the back of the front casting is a focus-coil assembly $S$. This assembly allows the focusing coil to be tilted as well as to be moved in the $x$- and $y$-axes to get best performance from the cathode-ray tube.

The back casting $T$ contains a rear tube-support grommet $F$ and a method of supporting the 5F driving synchro $U$. A servomechanism has been designed to drive this mount and has been made to fit into the space allotted to the 5F synchro. This servomechanism unit uses a FPE-25-11 Diehl motor and a size-1CT control-transformer synchro.

To compensate for variation in the length of the cathode-ray tube, the front and back casting assemblies, which are tied together by the support rods $V$, can be adjusted forward and backward on the supporting chassis by means of slots in the casting base $W$.

**16·4. Magnetic Shielding of Cathode-ray Tubes.**—The electron beam in both electrostatic and magnetic cathode-ray tubes is subject to unwanted deflection by stray magnetic fields. One of these, the earth's magnetic field, produces a steady deflection, the magnitude of which depends upon the geographical location. In the case of magnetic tubes with an applied accelerating potential of 5 kv, this deflection may amount to one-tenth the screen radius. Power transformers, motors, and other similar equipment constitute a second source of stray fields, which are particularly annoying because the deflections they produce are not steady. Field intensities as high as 0.1 gauss are frequently encountered and these are capable of introducing into the deflection pattern a ripple whose amplitude is approximately one per cent of the screen radius.

Not only do magnetic fields from surrounding apparatus cause spurious deflections of the electron beam, but the fields generated by the coils on a magnetic tube, particularly the deflection coil, may similarly affect other coils and instruments in their vicinity. If the deflection coil is of the square iron-core type, its magnetic field decreases with the cube of the distance from the coil center; nevertheless, its field is strong enough so that the maximum intensity 8 in. away is about one gauss. Ordinary eddy-current shielding will adequately stop the deflecting field if the sweep duration is less than 500 $\mu$sec, but it is not effective for a sweep whose duration is 1000 $\mu$sec or longer. A suitable magnetic shield solves both the problem of shielding a cathode-ray tube from external

superposed on the display. The cathode-ray tube must be tilted downward if the plotting surface is to be at a convenient angle for viewing and plotting. In order to keep the apparent brightness of the signals on the cathode-ray-tube screen as high as possible, the mirror $M$ has an almost totally reflecting upper surface that allows the transmission of only about 10 to 20 per cent of the light coming from the plotting surface $P$, which consequently must be brightly illuminated. The cathode-ray-tube pattern as viewed from $A$ is reversed because of the single reflection. This difficulty is readily overcome by connecting the circuits so that the sense is correct when viewed with one reflection.

**16·8. Double-mirror Device.**—An arrangement that allows direct viewing of the cathode-ray tube and the superposition of a map or plot



Fig. 16·21.—Cross-section of double-mirror unit illustrated in Fig. 16·22. $HH'$, light shield; $L$, lamp; $T$, cathode-ray tube; $CC'$, chart table; $M$, mirror; $G$, partially reflecting glass; $E$, eye of operator; $P$, chart point; $P'$, virtual image of $P$; $II'$, virtual image of chart $CC'$.

without reversal is shown in Fig. 16·21. The operator views the cathode-ray-tube screen through a sheet of glass $G$, whose front surface is partially reflecting (10 to 20 per cent) and whose back surface (toward the cathode-ray-tube screen) is nonreflecting. Plotting is done on surface $C'C$, which is viewed by reflection from $G$ and from the mirror $M$. Because the observer views the plotting surface $CC'$ after it has been reflected twice, it appears in the correct right-left sense. A map or other pattern may be placed on the plotting surface $CC'$ and illuminated by an ordinary lamp $L$, so that its virtual image is visible on the cathode-ray-tube screen at $II'$. Excessive background light obscures the cathode-ray-tube pattern, particularly if the signals are weak. It is important for best performance, therefore, that the lines of the map be white and the paper on which they are drawn be black. Illumination of the map will then make the lines visible but not cause appreciable background light from the paper on which the map is drawn. Figure 16·22 shows a unit of

sometimes with the addition of a small amount of copper. The greater effectiveness of the high-nickel-content alloys for shielding in the region of low magnetic fields is apparent from Fig. 16·12.

Joints and holes used in the construction of a shield seriously affect its shielding efficiency. Joints parallel to the flux direction in the shield decrease somewhat the efficiency at low field intensities but have little effect at high intensities. There is apparently no gain in increasing the number of spot welds along the joint. On the other hand, joints normal to the direction of flux cause an enormous drop in shielding efficiency, the decrease being contingent upon the shield dimensions.



FIG. 16·12.—Magnetization curves for magnetic metals suitable for shields.

Any necessary holes should be as small as possible.

For the shielding of electrostatic cathode-ray tubes, a cylindrical or conical form of shield is usually employed, as illustrated in Figs. 16·1 and 16·2. The shield should fit the tube as closely as is practicable. Shielding of magnetic tubes is less frequently required. In some cases, when alternating fields in the vicinity of the gun of a magnetic cathode-ray tube cause trouble, a small cylindrical shield may be placed closely around the tube neck in the region covering the gun. If large fields extend throughout the volume occupied by the tube, a cylindrical shield extending over the entire tube length may be required.

If the disturbance of the cathode-ray-tube trace is due to the field of a transformer in the



FIG. 16·13.—Shielding efficiency of one, two, and three concentric cylinders (for zero frequency). Shielding efficiency = 20 $\log_{10}$ $H_e/H_i$, where $H_e$ = field intensity without shield, and $H_i$ = field intensity with shield. $\mu = 5000$, $R_1/r_1 = r_2/R_1 = R_2/r_2 = r_3/R_2 = R_3/r_3$. Curve *A*—one cylinder $R_n/r_1 = R_1/r_1$; Curve *B*—two cylinders $R_n/r_1 = R_2/R_1$; Curve *C*—three cylinders $R_n/r_1 = R_3/r_1$. Cylinders considered infinitely long. Direction of flux perpendicular to axis of cylinders. (*Courtesy of Bell System Technical Journal.*)

vicinity, the addition of a shield around the transformer may be advisable, provided that the transformer is appreciably smaller in size than the cathode-ray tube.
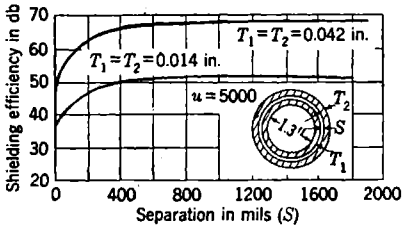


Fig. 16·14.—Shielding efficiency of two concentric cylinders vs. the air gap between them. Thickness of the wall of each cylinder kept constant. Zero frequency. (*Courtesy of Bell System Technical Journal.*)

Single shields of the type discussed above are usually adequate in shielding efficiency. In cases where the best single shield is inadequate, a more complicated form may be required. Except for very thin shields, the effectiveness of a magnetic shield can be considerably improved by building it of several concentric layers of magnetic material separated by air or copper.[1]    The shielding efficiency of one, two, and three concentric cylinders is shown in Fig. 16·13.    When a shield of this type is fixed in size, that is, when the inside and outside radii are specified, it will be most efficient when the radii of the successive surfaces follow a geometrical progression,

$$\frac{R_1}{r_1} = \frac{r_2}{R_1} = \frac{R_2}{r_2} = \frac{r_3}{R_2} = \frac{R_3}{r_3}.$$

Spacing and thickness, however, of consecutive layers is not very critical as shown in Figs. 16·14 and 16·15.    The broad, flat maxima of these curves indicate that there is considerable latitude in the shield dimensions.

In general, then, the shielding efficiency of a multiple-layer shield increases with the initial permeability of the metal, with the thickness of the shield, and with the number of separate layers.    In addition, there is an optimum



Fig. 16·15.—Shielding efficiency of two concentric cylinders vs. the air gap between them.    The total thickness of the shield $P$ is kept constant.    (*Courtesy of Bell System Technical Journal.*)

although not very critical spacing between layers.

**16·5. Simple Overlays and Filters for Cathode-ray Tubes.**—A transparent or selectively transparent overlay is generally placed over the face of the cathode-ray tube to perform any or all of the following functions.

[1] W. G. Gustafson, "Magnetic Shielding of Transformers at Audio Frequencies," *Bell Sys. Tech. J.*, **17**, 416 (1938).

1. Protection of the observer from flying glass in case of breakage of the cathode-ray tube.
2. Provision of coordinate or other reference scales for interpretation of signals appearing on the cathode-ray-tube screen.
3. Elimination of pattern distortion on screen due to electrostatic effects.
4. Control, by means of a filter, of the wavelength distribution of the light leaving the cathode-ray-tube face.

*Overlays for Protection.*—Protection against the results of cathode-ray-tube breakage or implosion, which sometimes results in the gun's forward propulsion through the glass tube face, is usually obtained by covering the face of the tube with a circular transparent plastic or safety-glass overlay attached to the tube mount. Such overlays are usually curved to conform to the radius of curvature of the tube face in order to reduce the magnitude of parallax errors when the overlay contains reference scales. When laminated glass is used, the thickness is usually $\frac{1}{4}$ in., whereas plastic overlays[1] vary between $\frac{1}{16}$ and $\frac{1}{4}$ in. in thickness, with $\frac{1}{8}$ in. as the usual thickness.

*Scales.*—Coordinate or other reference scales are almost always required for oscillographs or radar indicators. For those applications in which the accuracy called for will tolerate a reasonable amount of parallax, these scales are either engraved in the plastic overlay, or are applied to the surface of the glass overlay by a photolithographic or other transfer process. Scales having circular symmetry may be engraved on plastics while they are flat, and the overlay subsequently molded to conform to the shape of the tube face, thus reducing the parallax in the outer region of the pattern. Scales involving rectangular coordinates are usually placed only on flat overlays, for obvious reasons. For use with 5-in. and smaller electrostatic tubes that are to be used as oscillographs, it is usually satisfactory to place in contact with the tube face a thin flat overlay with the scale engraved on the side away from the observer because the thickness of the blown face of this type of tube is less than $\frac{1}{8}$ in., and the curvature not too great.

Magnetic tubes of 5-in. and larger diameter have pressed glass faces whose curvature is much less than could be attained with blown bulbs. Their thickness is about 0.2 in. for the 5- and 7-in. sizes, and 0.25 in. for the 9- and 12-in. sizes. Hence the distance between engraved scale and the cathode-ray-tube screen is greater than $\frac{1}{4}$ in., even if the overlay is curved to match the tube face. Parallax therefore is serious if the scale is placed immediately in front of the tube.

[1] Usually made of Plexiglas: Rohm and Haas, Philadelphia, Pa., Lucite: E. I. du Pont de Nemours and Co., Plastics Division, Arlington, N.J.

In order to eliminate this parallax, an image of the reference scale may be superposed optically upon the cathode-ray tube screen,[1] or a system of reference marks may be applied directly to the screen by suitable modulation of the cathode-ray beam.[2]

The scales engraved on plastics may conveniently be made self-luminous by what is known as edge lighting. One or several small lamps are placed as near the edge of the plastic as possible, preferably with their filaments between the planes of the plastic surfaces. Light from these lamps passes through the overlay readily, and escapes only by scattering from engraved lines or other scattering areas, such as crayon marks, in optical contact with the surface. The brightness of such lines is greatest when the lines are on the side of the plastic away from the observer. Color contrast between scale and signals from the tube face may be obtained by covering the lamps with filters transmitting any desired color.

*Overlays for Electrostatic Shielding of Tube Screens.*—The trace on the screen of a cathode-ray tube may be objectionably distorted, especially when the screen is not at ground potential, by contact of the observer's hand with the glass, by capacity effects due to the motion of the observer's hand in plotting, or by the similar effect produced when a reference scale is moved in front of the face. In such cases it is necessary to provide electrostatic shielding for the cathode-ray-tube screen. One method of accomplishing this shielding is to coat the surface of the glass or plastic overlay nearest the tube face with an evaporated metal film. Chromium is a very good metal to use for this purpose because it forms a very hard, tenacious film. Adequate conductivity for the purpose of electrostatic shielding is provided by a film that reduces the transmission of the overlay by only 10 to 20 per cent in the visible region.[3] A transparent plastic material that will not maintain an electrostatic charge is also available.[4] A third material that is applied to the surface to reduce reflection is a special film that also possesses antielectrostatic properties.[5]

**16·6. Filters.**—The use of a filter of appropriate transmission characteristics is generally recommended because, by such a device, it is possible to increase the contrast when the intensity of the ambient light is high, or to improve the performance by elimination of unwanted light from the signal, for either visual observation or photographic recording.

The most practical color filters for use with cathode-ray tubes are plastics that embody a dye. A wide variety of dyed plastics is available

[1] See Secs. 16·7, 16·8.

[2] See Sec. 16·12 and Chap. 6.

[3] Evaporated Metal Films, Inc., Ithaca, N.Y. are equipped to perform this process.

[4] Material BT-48-306, The Bakelite Corp., 300 Madison Ave., New York, N.Y.

[5] The American Optical Co., Southbridge, Mass.

from several manufacturers.[1] For some applications, a selectively reflecting film on glass has been used.

*Filter for Improvement of Contrast.*—A filter may be used with a cathode-ray tube to improve the ease of seeing a pattern by increasing the contrast, when the tube must be used in the presence of high ambient illumination. The case of a green filter placed before the face of a cathode-ray tube having a P1 (green) screen is a practical illustration of the use of such a filter. The distribution in wavelength of the emission
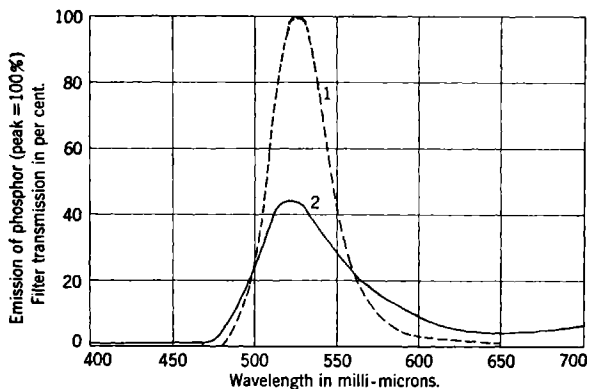


FIG. 16·16.—Transmission of green filter for use with P1 screen. Curve 1, emission from P1 screen (relative). Curve 2, Plexiglas filter No. 260.

of the excited P1 phosphor is illustrated in Curve 1 of Fig. 16·16, and that of the transmission of a specific filter commercially available[2] in Curve 2 of the same figure. The light from the trace is selectively absorbed by this filter, and calculations combining the data of these two curves with that of the photopic eye lead to the result that the visual brightness of the P1 trace when viewed through the filter is 36 per cent of its brightness when viewed directly. Similarly, calculations show that the brightness of the screen surrounding the trace, due to light incident upon it from the room, will be reduced to 6 per cent of its original value by the interposition of this filter. This result is caused by a two-fold absorption of the filter, for light traveling toward the screen and for that scattered by the screen.

The net result of the use of this filter therefore is a reduction in trace brightness by approximately a factor of 3, but coupled with a sixfold increase in ratio of trace to surrounding brightness. The quantitative

[1] Rohm and Haas, Philadelphia, Pa.

E. I. du Pont de Nemours Co., Plastics Div., Arlington, N.J.

Monsanto Chemical Co., Plastics Div., Springfield, Mass.

[2] Plexiglas No. 260.

evaluation of the degree of improvement in ease of seeing and recognizing the features of a given trace, due to this change in objective conditions, is difficult.    If a constant trace brightness is assumed, the improvement depends upon sharpness of the trace, the amount of detail requiring recognition, the magnitude of the surrounding illumination, and the exact characteristics of the filter.    Relatively meager experimental data at hand indicate that the maximum amount of improvement is obtained at the higher levels of illumination (i.e., over 50 foot-candles), and may amount to a change from a condition of being visible but with difficulty to one of being visible with ease, or to making visible a trace that previously was unrecognizable.    A filter having a higher maximum transmission, with a steeper attenuation on both sides of the maximum, would seem to result in further improvement in visibility.    The possibilities of improvement by the use of such filters obviously need further investigation.

*Filters for Use with* P7 *Screens.*—Most screens for intensity-modulated radar displays are of the two-layer or cascade type.    The principal one is the P7 screen that is described in detail in Chap. 18.    It has a blue excitation layer of very short persistence, and next to the glass is an excited phosphor layer of long persistence, which appears yellow.    It is the radiation from this yellow layer which is of primary importance to the radar observer.    The distributions in wavelength of the blue and yellow components of the P7 screen are indicated in the dashed curves of Fig. 16·17.    Absolute intensity levels are not given, but the curves are normalized to 100 per cent at the wavelength of peak excitation. Figures for the relative visual brightness due to the blue and to the yellow and longer wavelengths are not available.    In the photography of P7 screens, where a panchromatic emulsion[1] and an exposure time of about three seconds has been used, it has been found that the yellow persistent image contributed about one third of the total exposure.

Filters for use with the P7 screen are of two general classes; those that eliminate one of the components more or less completely without serious change in the wavelength distribution of the other component; and those that shift the distribution of the long-persistent component significantly toward the red end of the spectrum.

*Removal of Blue-component Radiation.*—The radiation from the blue layer is very intense at the instant of excitation.    For long-time observation, this intensity undoubtedly contributes appreciably to the fatigue of the operator.    Filters that reduce the contribution of the blue component to practical insignificance without reducing appreciably the brightness of the yellow are those whose transmission curves are given in Curves 1, 2, and 3 of Fig. 16·17.    It should be pointed out, however,

[1] Eastman Super XX.

that the matter of fatigue varies from operator to operator, and for the detection of very weak signals, which are often detectable only in the "flash," no filter should be used.

For the motion-picture photography of radar displays involving the use of the P7 screen, the most satisfactory filter to date is that given in Curve 1 of Fig. 16·17.

*Removal of Yellow Component.*—For visual observation of rapid fluctuations in the intensity of signals, as for example in the observation of pulsed-doppler effects, the long-persistence radiation is detrimental, and hence a blue-transmitting filter is desirable. Unfortunately, no
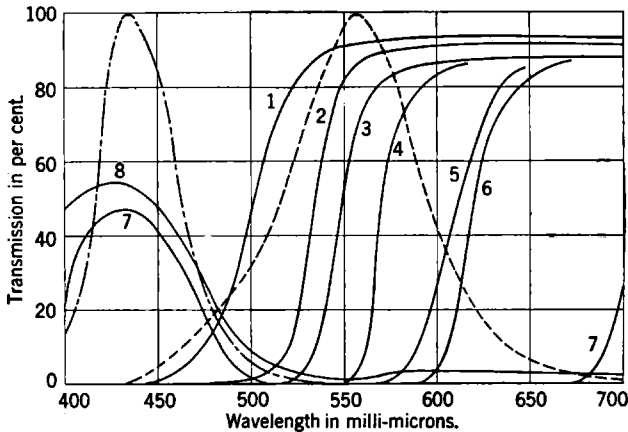


FIG. 16·17.—Transmission of various plastic filters. Curve 1, Plexiglas No. 106; Curve 2, Lucite No. H-10016; Curve 3, Plexiglas No. 121; Curve 4, Plexiglas No. 108; Curve 5, Plexiglas No. 159; Curve 6, Polaroid XDA8FAP; Curve 7, Polaroid X815 (0.003 in.); Curve 8, Monsanto A74592TVA (0.125 in.)

dyed filter is available which has a high percentage transmission in the blue with a relatively sharp cutoff at longer wavelengths. A good dyed filter is that given in Curve 8, of Fig. 16·17, but this filter is available only in thin acetate films. When laminated between clear sheets of acetate, the transmission is reduced still further. A somewhat lighter filter is that indicated in Curve 7. Other filters, particularly useful for photographic work, in sizes to fit over camera lenses, are Corning No. 5543 and Wratten No. 39. Another application that calls for the elimination of the long-persistent component is the stop-frame photography of a single scan of the tube face, in which the fainter image remaining from the previous scan is to be removed. A blue-sensitive emulsion, together with a blue filter similar to that of Curve 7 over the camera lens, is satisfactory for this purpose.

A further similar use of a blue filter is in the process of video mapping[1] where such a filter placed in front of the phototube picking up signals from the P7 screen is helpful.

*Filters for Dark-adaptation Use.*—When the P7 screen is to be used for nighttime observation, and the operator is required to preserve his dark adaptation for other observation as well, it is imperative that the energy received from the cathode-ray tube be predominantly in the region of long wavelengths. It is not within the scope of this volume to discuss adequately the factors that influence dark adaptation, or the performance of the scotopic eye.[2] For use with P7 screens, as deep a red filter should be used as can be tolerated while still preserving a brightness of the information on the tube face adequate for recognition by the scotopic observer. The filter represented by Curve 4 of Fig. 16·17 is useful for this purpose. Curves 5 and 6 represent two versions of "dark adaptation" filters, which, however, are probably not too useful for use over cathode-ray tubes with P7 screens.

### OPTICAL-SUPERPOSITION DEVICES

The simplest means for superimposing a reference scale upon the cathode-ray-tube screen, in order to reduce errors of parallax, utilizes a plane partially reflecting mirror. Double-mirror devices are generally used when the orientation of the pattern is important. Since the elimination of parallax is resorted to only to obtain increased accuracy of measurement, good stability of the display pattern, which often requires extra care in the regulation of supply voltages, is also necessary to obtain the desired accuracy.



Fig. 16·18.—Method of superposing an edge-lighted scale on a CRT pattern.

### 16·7. Single-mirror Devices.

One form of superposition device is illustrated in Fig. 16·18. In this, the observer views the tube face normally. Interposed between the observer and the screen is a partially reflecting glass plate placed at an angle of 45° to the tube axis. The reference scale is usually engraved on an edge-lighted transparent plastic plate orthogonal to the tube face, located at such a distance from the 45° mirror that its virtual image, as seen by the

---

[1] See Sec. 16·12.

[2] For a discussion of this subject, see: Charles Sheard, 'Dark Adaptation: Some Physical, Physiological, Chemical and Aeromedical Considerations," *J. Opt. Soc. Am.,* **34,** 464 (1944). See also Sec. 18·10.

observer, is at the surface of the phosphor.   Since most cathode-ray-tube
faces have some curvature, complete elimination of parallax is not possi-
ble over the entire face of the tube, and the usual adjustment is to pro-



Cathode ray tube
12DP7

Height scales

4 section
light box
Scale lights

Scale positioning knob
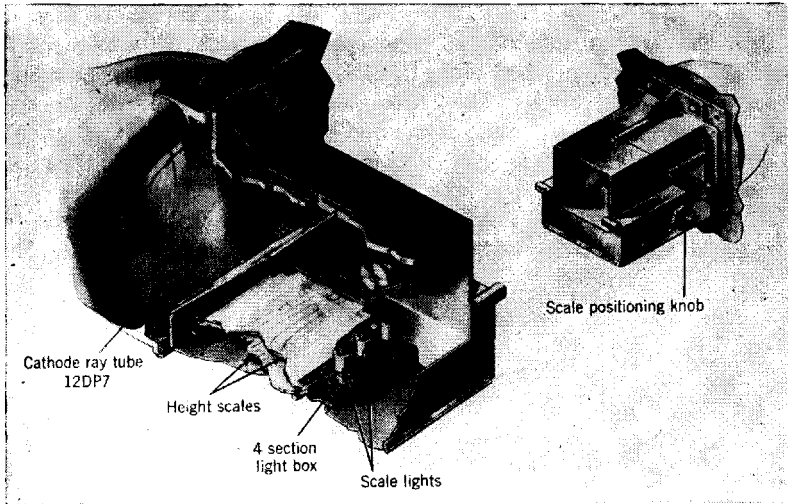
FIG. 16·19.—Height-indicator scale box, cut-away view.

duce exact superposition on a centered circle whose diameter is one-third
to one-half that of the tube face.

Figure 16·19 shows a cut-away view of this type of optical super-
position device used for height deter-
mination.[1]  Two  edge-illuminated
scales are so arranged that their
images may be viewed vertically on
the face of the cathode-ray tube.
Separate lights are used to illuminate
the two scales, and these are
switched by the same knob that con-
trols the range-switching.   The two
pieces of Plexiglas on which the scales
are engraved are separated by $\frac{1}{32}$ in.,
and the scales are located on the
adjacent surfaces, in order to mini-
mize parallax.   When unilluminated,
the scale not in use is almost invisible.



$P'$        $A$

10 to 20% trans-
mission mirror

$M$

$P$
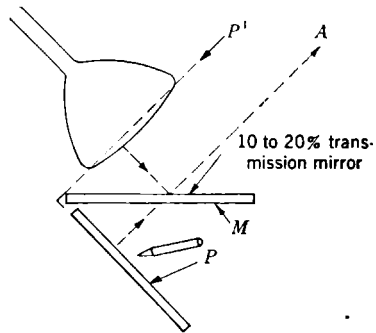
FIG. 16·20.—Method of superposing maps
or plots on a CRT.

A slightly different arrangement using a partially reflecting mirror, is
shown in Fig. 16·20.   This device is useful when a map or a plot is to be

[1] See Sec. 15·5.

superposed on the display.    The cathode-ray tube must be tilted down-
ward if the plotting surface is to be at a convenient angle for viewing and
plotting.    In order to keep the apparent brightness of the signals on
the cathode-ray-tube screen as high as possible, the mirror $M$ has an
almost totally reflecting upper surface that allows the transmission of
only about 10 to 20 per cent of the light coming from the plotting surface
$P$, which consequently must be brightly illuminated.    The cathode-ray-
tube pattern as viewed from $A$ is reversed because of the single reflection.
This difficulty is readily overcome by connecting the circuits so that the
sense is correct when viewed with one reflection.

**16·8. Double-mirror Device.**—An arrangement that allows direct
viewing of the cathode-ray tube and the superposition of a map or plot



Fig. 16·21.—Cross-section of double-mirror unit illustrated in Fig. 16·22.   $HH'$, light
shield; $L$, lamp; $T$, cathode-ray tube; $CC'$, chart table; $M$, mirror; $G$, partially reflecting
glass; $E$, eye of operator; $P$, chart point; $P'$, virtual image of $P$; $II'$, virtual image of
chart $CC'$.

without reversal is shown in Fig. 16·21.    The operator views the cathode-
ray-tube screen through a sheet of glass $G$, whose front surface is partially
reflecting (10 to 20 per cent) and whose back surface (toward the cathode-
ray-tube screen) is nonreflecting.    Plotting is done on surface $C'C$,
which is viewed by reflection from $G$ and from the mirror $M$.    Because
the observer views the plotting surface $CC'$ after it has been reflected
twice, it appears in the correct right-left sense.    A map or other pattern
may be placed on the plotting surface $CC'$ and illuminated by an ordinary
lamp $L$, so that its virtual image is visible on the cathode-ray-tube screen
at $II'$.    Excessive background light obscures the cathode-ray-tube
pattern, particularly if the signals are weak.    It is important for best
performance, therefore, that the lines of the map be white and the paper
on which they are drawn be black.    Illumination of the map will then
make the lines visible but not cause appreciable background light from
the paper on which the map is drawn.    Figure 16·22 shows a unit of

this type attached to a 5-in. cathode-ray tube.    Maps can be placed on the adjustable table and moved by the screw mechanism until they match the cathode-ray-tube pattern.    In one important shipborne radar application, the PPI pattern visible in coastal waters is matched to a printed chart.    The center of the PPI display can then be exactly located on the chart to give the position of the ship.    The ship can determine its position with high accuracy because the best match between the map and the PPI pattern effectively averages the contributions of many different signals in determining the position.
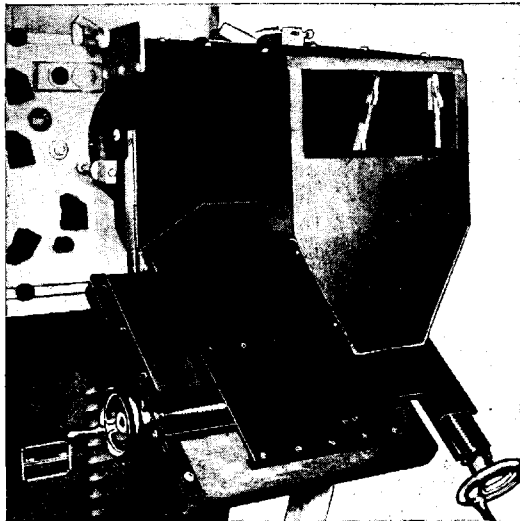


FIG. 16·22.—A double-mirror unit for superposing a map or plot on a 5-in. CRT.    The optical paths are indicated in Fig. 16·21.

The disadvantages of a device of this type, when used as a plotting aid, are (1) its size and mechanical complexity, (2) the relatively large distance from which the operator must view the cathode-ray-tube screen, and (3) the fact that, when plotting, the point of contact of the pencil is not visible.

A modification of this device uses maps recorded on 35-mm film. A real image of the film is projected from below on the translucent plotting surface (*CC'* of Fig. 16·21).    The film can easily be moved to produce the desired matching between the PPI pattern and the map.[1]

## PLOTTING

The recording of a transient signal or waveform on a persistent screen is only temporary, lasting for a few seconds or minutes at most, and often

---

[1] A variety of optical superposition devices are described in greater detail in "Radar Aids to Navigation," Vol. 2 of the Radiation Laboratory Series.

some method of easily plotting the shape of a transient waveform or the location of a signal on a radar display is of great practical value. Slow changes in the display pattern are often best followed by plotting.

One important requirement for any plotting operation is that the display pattern be stable over the entire time required for plotting. Therefore, carefully designed sweep circuits and amplifiers, and regulated high-voltage and focus supplies for the CRT are often necessary.

**16·9. Direct Plotting.**—Making marks directly on a cathode-ray tube (or on a thin shield over the cathode-ray tube) with glass-marking pencils or with a pen is the simplest way of plotting. There are several disadvantages to this method, however.

1. There is parallax between the plotting surface and the actual screen; this parallax is accentuated if a protective shield must be interposed between the plotter and the cathode-ray tube.
2. There is generally a distortion of the pattern because of local changes in the high screen potential caused by contact of the plotter's hand with the glass. This distortion can be greatly reduced by operating the cathode-ray-tube screen at ground potential, or by interposing between the plotter and the screen a transparent sheet of material with the surface on the side of the cathode-ray tube thinly covered with conducting material.[1]
3. The bluntness of the pencil point makes accurate plotting difficult.

Transparent overlays, which are inscribed with fixed lines on the side next to the cathode-ray tube and are illuminated by edge lighting, preferably of a different color than the light from the cathode-ray tube, are found most desirable. They are, however, limited to fixed patterns since they are not easily altered.

**16·10. Plotting by Optical Superposition.**—Most of the disadvantages of direct plotting are overcome by the optical superposition method illustrated by Fig. 16·23. A mirror, whose upper surface is partially reflecting (10 to 20 per cent) and whose lower surface is nonreflecting, is interposed between an edge-lighted plotting surface and the cathode-ray-tube screen. The position of the mirror (or plotting surface) is adjusted so that the optical distances $A$ and $B$ are equal. The virtual image of the mark is made to appear on a plane that best approximates the curved cathode-ray-tube screen surface. The lighting makes the marks of the plotting pencil much brighter when viewed from the bottom side of the plotting surface than when viewed from the top side, thereby making a mirror of low reflection coefficient practical.

The plotting points can be viewed either directly or in the mirror, and the actual point of contact of the pencil is visible as soon as it touches

[1] See Section 16·5.

the plotting surface. The illuminated plot is in a readily available position for study and measurement. There is much less parallax than in the direct-plotting method, and there is no electrostatic interference with the cathode-ray-tube pattern.

There are some disadvantages to this method of plotting also.

1. There is a limit to the density of plots that can be "looked through." Since every line of the plot is visible in two places—directly, and through the mirror—there are twice as many obscuring marks as in the case of direct plotting. If the distances $A$ and $B$ (Fig. 16·23) are each about one inch, the 2 in. between the direct and reflected plots makes it easy to distinguish these plots, however. Even with the edge lighting turned off and the eyes focused on the
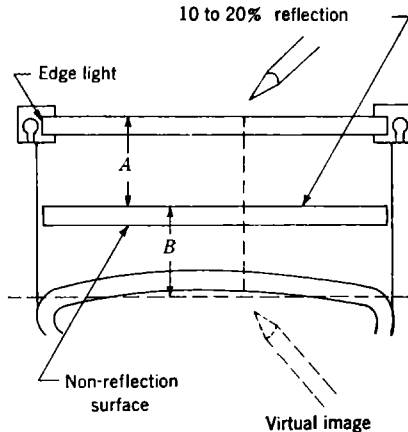


FIG. 16·23.—Method of plotting using optical superposition.

cathode-ray-tube screen rather than on the plotting surface, a point is reached where the plots seriously interfere with the display.

2. All plots and maps must be drawn on transparent material and be capable of being edge-lighted. This limitation does not exist in the devices illustrated in Figs. 16·20 and 16·21.

3. With complete absence of ambient light it is sometimes difficult to get the pencil to the right region for plotting before it actually touches the plotting surface and thereby becomes visible. A series of quick touches, without bearing down on the point so as to make a permanent mark, greatly aids in the location of the exact plotting point.

**16·11. Remote Plotting.**—In radar-systems operation, central plotting boards are often used to collect the information from several differ-

ent displays that may be remotely located. The transfer to a plotting board of data from a remote display is a difficult problem. The simplest solution is to have the display operator call out the coordinates of each point that should be plotted. A plotter then records these points on the central plotting board. A good plotter can plot ten points per minute in $R$ and $\theta$ coordinates, but at best this is a slow and clumsy process.

A second method of remote plotting uses a servomechanism. The servomechanism is controlled by an operator who moves a marker (for example, with the aid of one of the virtual-image plotting aids discussed in the previous section) to the point to be plotted. The operator pushes a switch and a solenoid-operated plunger makes a plot on the large board. This method has not been used much because of the complexity and limited transient response of the servomechanism and the fact that the servomechanism can take orders from only one cathode-ray-tube operator at a time.

A third method of plotting on a large surface some distance from an indicator is to use photographic projection of a PPI.[1] This method has the advantage, over plotting on a persistent cathode-ray-tube screen, that all the echoes are constantly present and are not continually fading out during the time that one frame is being projected. It has the disadvantage that there is a delay between the actual appearance of an echo and the time it is visible for plotting. It is thus primarily useful on displays where the changes of a moving signal from one complete frame to the next are not very large (1 or 2 per cent of the pattern diameter, for example) and where the developing time (10 to 20 sec) does not cause a serious delay.

## VIDEO MAPPING

**16·12. General Principles of Video Mapping.**—A method called "video mapping" is a very useful means of displaying on an ordinary indicator cathode-ray tube pertinent information such as maps or fiducial marks mixed with the regular video signals. With simple precautions, the plotting of moving points is also possible.

The transmitting unit of the video mapper consists of a modified indicator, such as a PPI. In order to secure proper register of the information to be transmitted, the transmitting unit is first used as an ordinary indicator on which ordinary video signals are visible. Plots, maps, or other marks may be drawn during this time on a transparent surface that is located as close to the cathode-ray-tube screen as possible. The indicator unit is then used to scan the map with a constant-intensity moving spot using exactly the same scanning pattern employed in locat-

[1] See Sec. 16·17.

ing or drawing the map or plot.    The modulated light from this scan is picked up photoelectrically (see Fig. 16·26) and transmitted to remote indicators as video signals that are there presented along with ordinary



(a)                                    (b)

(c)                                    (d)
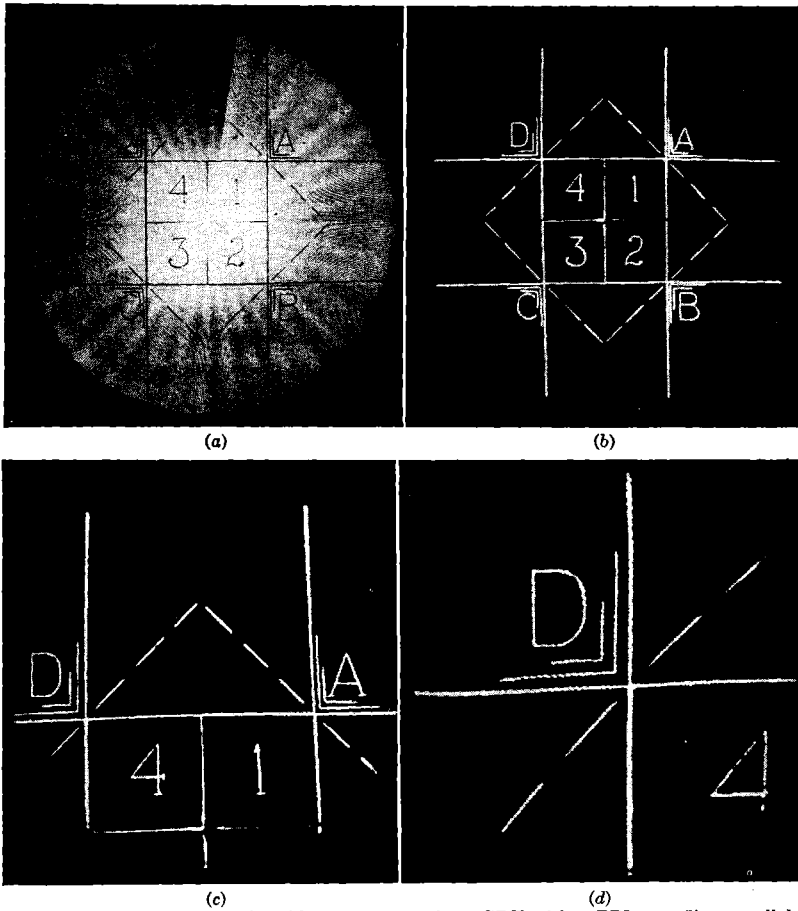
Fig. 16·24.—Photographs of a video-map transmitter CRT with a PPI scan (linear radial trace 1800 μsec/radius) and of several receiving displays with the same type of scan.

video signals.    Circuits designed for video-mapping transmission are described in Sec. 16·13.

One of the advantages of this system is the ability of the receiving display to receive video map signals from a large number of different transmitter units.    Since the video map signals from a stable transmitter unit are locked to the regular synchronizing pulses, they remain fixed in

time with respect to any ordinary video signals present. Thus, another advantage is that the map is always correctly located with respect to the ordinary video presentation on the receiver display no matter how it is off-centered or distorted.



(a)                                    (b)

(c)                                    (d)
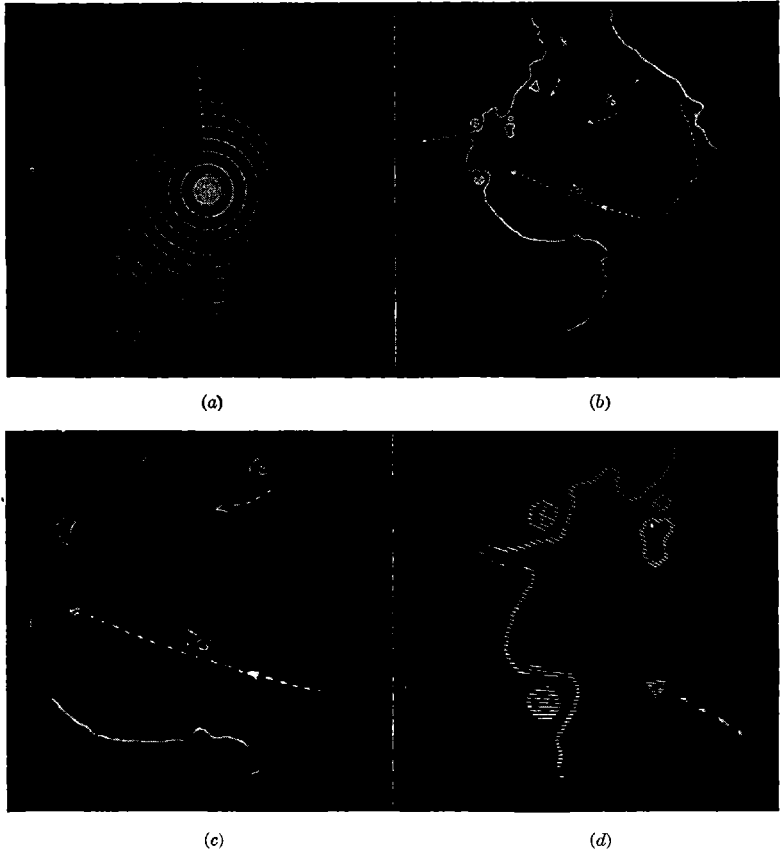
FIG. 16·25.—Photographs of a video-map transmitter CRT with a PPI scan (linear radial trace, 1800 μsec/radius) and of several receiving displays with the same type of scan. The transmitting tube transmits map video only on every fourth radial sweep.

Figure 16·24 shows photographs of the operation of a video-mapping unit connected to a PPI. Figure 16·24a shows the appearance of the screen of the transmitting cathode-ray tube during one complete rotation of the radial sweep as viewed from a point close to the phototube (Aperture B, Fig. 16·26). The map is clearly visible as dark lines against the constant-intensity cathode-ray-tube sweeps. Figures 16·24b, c, and d show the receiving PPI with various degrees of magnification.

The appearance of the received display is very similar if the map being transmitted is drawn with transparent lines on opaque material (lines scratched in a thin coat of Aquadag, for example), provided that the sign of the map video is such that the map lines appear bright on the receiving cathode-ray tube.   Because of the opaque material, it is difficult to use the same transmitter cathode-ray tube for essentially simultaneous reception of ordinary video signals and transmission of map video signals.   A method of using alternate time-base sweeps for the two different functions has had limited trial.   Figure 16·25 shows operation of this sort where three consecutive sweeps are used for receiving ordinary video signals (in this case the video signals consist of marks spaced 120 $\mu$sec apart), and one sweep is used to transmit map video signals.   The receiving displays present only the map video.   Since the map video signals appear on only every fourth sweep, the map lines appear coarser than usual, although they are still legible.   The light from the constant-intensity mapping sweeps excites the persistent screen of the transmitter tube somewhat.   Extra background light is therefore added to that already present due to the noise on the regular video sweeps.   As long as the individual making the plots does not get his hand between the scanning spot and the phototube he does not interfere with the transmission of the map video.   Figure 16·26 shows the geometrical arrangement of a typical video-mapping transmitter.   The aperture $A$ may be about $\frac{1}{2}$ in. square and still pass enough light to actuate a type 931A or 1P21 photomultiplier tube located about 15 in. from the cathode-ray-tube screen.   For high accuracy and sharp signals the cathode-ray tube must have good focus; and an accelerating voltage of 5 to 7 kv is recommended. The decay time of the blue light from the screen should be short compared to the time for the spot to move one spot diameter.   The intensity of the light from the blue layer of the P7 screen under short pulse excitation decays to half intensity within less than 10 $\mu$sec.   This decay time allows good mapping with 1000 $\mu$sec/diameter sweeps.   A curved plotting surface decreases parallax but is less convenient for holding prepared maps. The error between a map drawn on the cathode-ray-tube screen itself and a map on the flat plotting surface is not very great if the phototube is far enough from the cathode-ray tube.   For example, in the case of a typical 12-in. cathode-ray tube, the useful screen surface is inside a circle 5 in. in radius.   The radius of curvature of the cathode-ray-tube screen surface is 20 in. and the shortest distance from the screen itself to the plotting surface is about $\frac{3}{8}$ in.   If the cathode-ray-tube pattern is normalized to a prepared, undistorted map at about 4 in. from the center of the cathode-ray tube, and the phototube is 15 in. from the plotting surface, a maximum error of about 1.5 per cent in the radial location of any point will occur.   If the cathode-ray tube has a radial–time-base

display centered at the center of the cathode-ray-tube screen, the sweep waveform may be readily distorted to remove all the geometrical error. If plots are made (by an operator looking through the viewing aperture, Fig. 16·26) with respect to real video signals on the display, then the plots will have an exact relation to the location of the real video signals no matter what the distortion of the display may be, because the phototube views the plots from essentially the same aspect and with identical display sweeps as does the operator.

In addition to the simple geometrical arrangement of Fig. 16·26, another scheme, in which a real image of the scanning spot is focused on the map, has been successfully used.[1]  The principal objection to this system is the size and necessary high quality of the optical system.  Since the image of the spot and the map are in the same plane there is no parallax to cause errors.  In this case a condensing lens, which picks up a large fraction of the light from the image of the spot, can precede the phototube unit.  The over-all optical efficiency can be made about the same as in the system of Fig. 16·26.



FIG. 16·26.—Geometrical arrangement of a video-mapping transmitter. The aperture *A* is small enough so that the parallax between the spot on the CRT screen and the marks on the plotting surface is small.

**16·13. Circuits for a Video-mapping Transmitter.**—Figure 16·27 shows a complete circuit for a video-mapping transmitter.  The phototube is followed by a cathode follower $V_2$ so that the phototube pickup unit may be remote from the rest of the circuit.  The negative 600-volt supply for the phototube should be regulated (four VR 150 tubes in series are good enough) to maintain constant gain in the phototube itself.  This unit is required to transmit signals obtained from either opaque lines on a transparent sheet of material ("positive" map data) or transparent lines on an opaque sheet of material ("negative" map data).  In the former case, care must be taken that both the cathode-ray-tube face and the plotting surface be clean to prevent "noise" or interference.  The switch $S_1$ is used to allow for the reversal of sign of the input video mapping signals so that signals on the plate of $V_3$ will always have the same sign.  The signals on the plate of $V_3$ are always negative because it is required that the final output signals be positive, and 5 to 10 volts in magnitude, across a 75-ohm line.  Peaking of high frequencies

[1] See Vol. 2, Sec. 7·12.
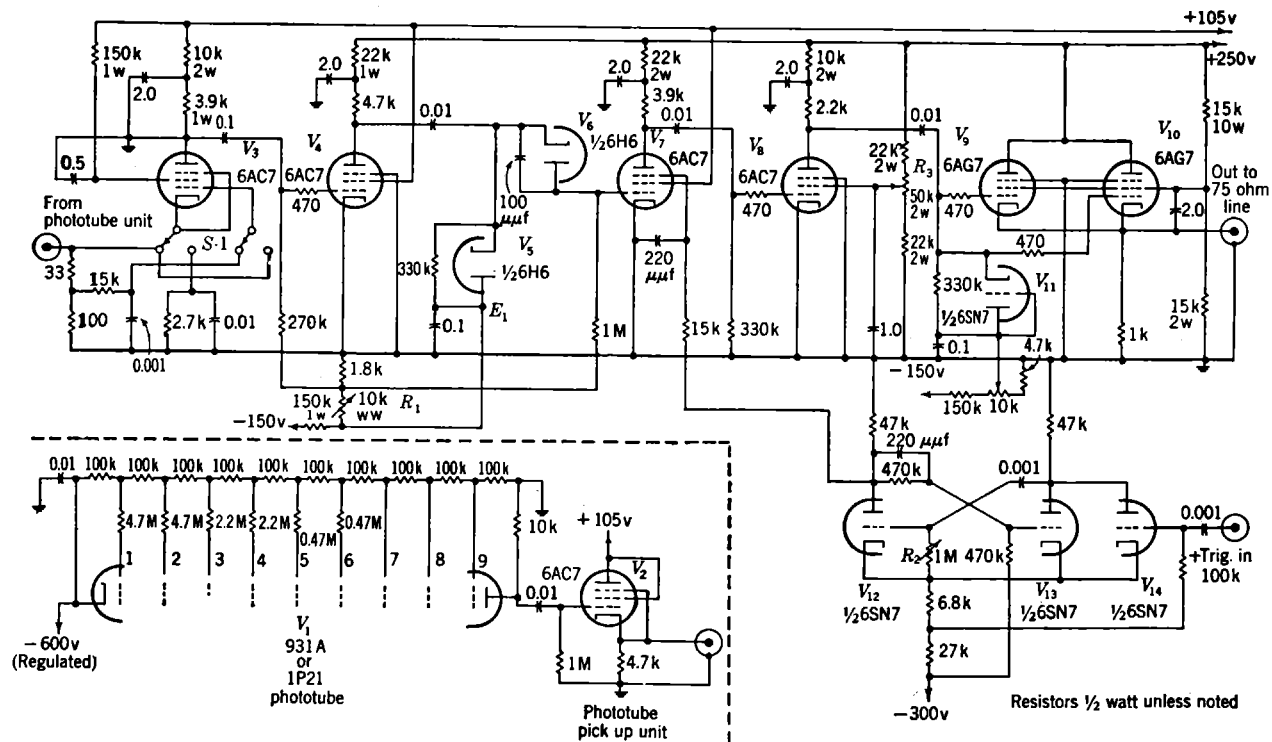
Fig. 16·27.—Circuit for a video-mapping transmitter.   The phototube picks up the light variations from a flying-spot cathode-ray-tube scanner. The amplifier transmits these signals to remote indicators.

is introduced by the R-C network in the cathode or grid circuit of $V_3$, and low-frequency compensation in the plate circuit.

The signals on the plate of $V_4$, an inverter tube, should be about 3 volts in amplitude so that the "clipper" tube $V_7$ can operate from slightly below cutoff (set by potentiometer $R_1$). Diode $V_5$ sets the base of the signals at the voltage $E_1$. Diode $V_6$ prevents the long positive signal occurring between sweeps from causing $V_7$ to draw grid current. The flip-flop circuit, composed of $V_{12}$ and $V_{13}$ and triggered through amplifier $V_{14}$, gates the suppressor of amplifier $V_7$ so that map video signals may pass through only during the time starting with the input trigger (which also starts the cathode-ray-tube sweeps) and ending with termination of the flip-flop (set by $R_2$). Other gating signals, such as the gating signals that identify the location of the fixed-deflection-coil off-center PPI in Sec. 13·7, may be applied to the suppressor of $V_7$. This gating is usually needed, in the case of a "positive" map, to remove the long positive output signal corresponding to the time the spot is off the cathode-ray-tube screen. Since the grid of $V_7$ operates from cutoff the gating of the suppressor produces no pedestal in the plate signal.

Amplifier $V_8$ limits the signals at a level controlled by $R_3$, which also acts as a gain control. The output cathode followers operate from below cutoff and remove the signal base line.

### PROJECTION SYSTEMS

Large images are desirable in television and in radar in order to permit greater comfort in viewing and to permit several observers to see or work at a single display. In radar, a large display on a flat surface is often desirable for quick and accurate plotting.

**16·14. Direct Projection of Bright-trace Cathode-ray Tubes.**—The optical system used to form the enlarged image may be either a projection lens or a reflective optical system. The optical quality of the projection systems must be high, in order not to sacrifice resolution. Glass projection lenses having an aperature of f/2 to f/1.5 have been designed for this purpose, but they are relatively expensive. A reflective optical system currently being used has an effective aperture of approximately f/1.0 or better, and is an adaptation of the Schmidt camera developed for astronomical use. It employs a spherical concave mirror, in conjunction with a correction plate or lens designed to reduce to a negligible amount the spherical aberration introduced by the use of the spherical mirror. Suitable processes have been developed for the mass production of the correction plates, which must have an aspherical surface, and these are now producible in the form of either a clear plastic or a glass plate.[1]

[1] For a discussion of the use of reflective optics in projection television, see I. G. Maloff and D. W. Epstein, *Electronics*, **17**, No. 12, page 98 (Dec. 1944).

In addition to the use of a high-aperture optical system, it is necessary that the intrinsic brilliance of the cathode-ray-tube screen be made as high as possible in order to achieve image brightnesses that will be satisfactory when used under conditions of appreciable ambient illumination. To this end, the accelerating voltages used on projection tubes range from 25 to 50 kv, necessitating the use of considerable power in the deflection circuits.

At low accelerating voltages, the luminosity of a spot on a cathode-ray-tube screen increases roughly as the square of the accelerating voltage; but, as the potential is increased, a condition is approached where there is little additional gain in luminosity because the screen reaches a limiting potential, known as its "sticking" potential. The recent introduction[1] of a thin reflecting aluminum backing on the screen serves both to eliminate the restriction caused by this sticking potential, and to increase by a factor of approximately 2 the amount of light proceeding in the forward direction from the tube face.

The combination of the use of reflective optics and of a projection tube employing a metal-backed screen results in television images of high brightness and adequate resolution. Because the entire television pattern is scanned at a frequency higher than the critical flicker frequency of the eye, the screen does not have to have any appreciable persistence since the integration into a continuous picture is performed by the eye.

In attempting to project the image of a radar display, a very serious difficulty arises because of the very long time that elapses between successive excitations of a given area. This time may amount to as much as 15 to 30 sec; therefore, if a continuous presentation of the entire field is desired, the screen of the cathode-ray tube must perform the function of integration which the eye accomplishes in the television case. A long-persistence screen is therefore a necessity.

Two attempts have been made to use a bright-trace projection tube employing the cascade type of long persistent screen described in detail in Chap. 18. The first involved the use of the two-layer screen in the projection tube itself. The second method, which from theoretical considerations should be more efficient than the first, used only the blue component in the cathode-ray tube, and placed the long-persistent yellow component on the projection screen. Even this second method failed to yield an adequate persistent image brightness.

**16·15. Projection of Televised Long-persistent Display.**—The sensitivity of some pickup tubes, such as the RCA Image Orthicon, is such that even the very low luminosity of the P7 radar screen 10 to 15 sec after excitation may be sufficient to yield a usable signal from the Orthicon. This idea was tried as a joint project by the Watson Laboratories

---

[1] See Sec. 2·6.

of the Army Air Forces and the Radio Corporation of America, and involved the use of the techniques of television. The face of a normal P7 long-persistent cathode-ray tube, on which the radar signal appeared, was scanned by means of a camera employing an Image Orthicon as the pickup tube. The scanning was done at a rate of 40 frames per second, and the signals from this unit were applied directly to a television receiver and projected by means of a reflective-optical system originally designed for theater projection of television images. Thus adequate brightness of the projected image, even up to a 12-ft diameter, was available.

The tests showed that although the sensitivity of the pickup unit was sufficient to yield a signal from the PPI traces many seconds after their excitation, the extreme range in signal brightness, from the initial flash to that of the persistent image 10 to 15 sec after excitation, was so great that the Image Orthicon and the associated equipment could not accommodate the entire range of signals at a single setting of the controls. When adjusted to give satisfactory reproduction of the low-brightness signal, the peak light of the PPI "spoke" overloaded and paralyzed the device; conversely, if the device was adjusted so that it was not overloaded at the peak, the signal level of the persistent image was insufficient to show.

The obvious advantages of this system are that standard television equipment may be used, and that the desired information may be transmitted over great distances if desired. However, considerable research and development of the pickup tube, or other means of obtaining signal storage, will be necessary before the method becomes feasible for use.

**16·16. Direct Projection of Dark-trace Cathode-ray Tube.**—The characteristics of the so-called dark-trace cathode-ray tube adapt it especially to the projection of radar images. The screen of the dark-trace tube is composed of an alkali halide, usually KCl, evaporated onto the face plate of the tube from an evaporator cup inside the tube.[1] When illuminated by white light, the unexcited screen appears white, whereas the regions struck by the electron beam are caused by this beam to develop an absorption band extending throughout the visible portion of the spectrum, with its peak at approximately 5600 Å. As a result of this, the signals appear on the tubes as a magenta-colored darkening.

In order to project an image of the face of a cathode-ray tube of this type, it is only necessary to illuminate the tube by means of an external light source to a level sufficiently high to yield the desired image brightness of the projection screen. This level will depend upon the type of optical system used for projection.

[1] For a more complete description of this type of screen and its properties, see Chap. 18.

The persistence time of the darkening of such a screen depends upon the signal strength, the number of times the signal is repeated on the same area, and the illumination level and the temperature of the face plate.   Unlike the P7 luminescent screen, in which the rate of decay of luminosity increases with increasing excitation, the rate of decay of the darkening of strong signals on a dark-trace screen is less than that of weak signals.   The persistence of the darkening can vary from a fraction of a second to an indefinite period (years) depending on the four conditions mentioned above.
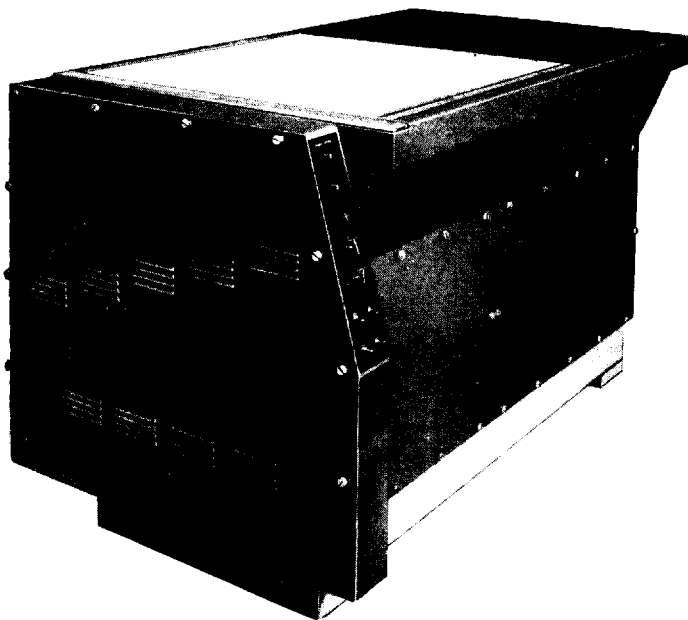


FIG. 16·28.—Projection indicator.

The idea of using the dark-trace tube in a projection indicator for displaying radar echoes apparently came from England, and an early development of the method occurred there.   The device as there developed employed a lens system for projection, and used a number of high-pressure mercury lamps to illuminate the face of the tube.

In the United States, the development of this form of projection indicator has centered around the use of a reflective-optical system. A photograph of an experimental model of such a rotating-coil projection-PPI indicator is shown in Fig. 16·28.   The plotting and projection surface is 25 in. in diameter, and the optical system is folded in

order to conserve space. This unit serves as a remote indicator, requiring a 2-volt video input signal, a 20-volt trigger pulse, and information as to the instantaneous direction of the radar antenna, in the form of synchro voltages.

The principal circuits and controls of this indicator are located in a shallow end box, which permits ready access to the various components for test and adjustment. This feature is illustrated in Fig. 16·29.
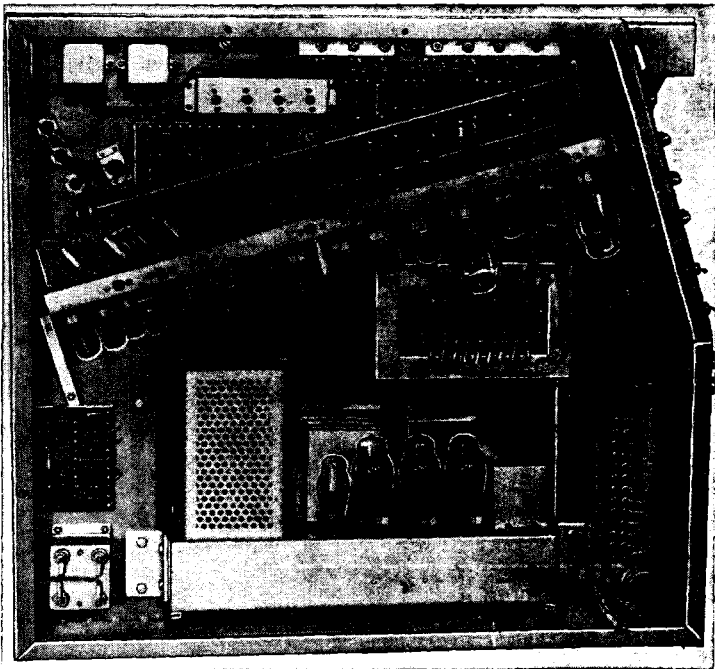


FIG. 16·29.—End view of control box.

This view also shows the power-supply chassis, which furnishes 9 kv for the cathode-ray tube, as well as +300-volt and bias supplies. Besides the video amplifier, range-mark generator, and sweep amplifiers, the circuits employed in this indicator contain two additional features necessitated by the use of the dark-trace type of cathode-ray tube. These are

1. An automatic video-gain control, energized by a tachometer generator geared to the shaft that rotates the deflection coil. This control varies the gain of the video amplifier from 0 at zero rotational speed to full gain at a speed of 4 rpm in order to prevent the excessive long-persistence darkening of the trace which would

otherwise occur in case the antenna stopped rotating.   Therefore this type of indicator can be used only for continuous scanning.

2.  A modulation of video gain with range, so that points near the periphery of the tube face receive a higher signal level than those
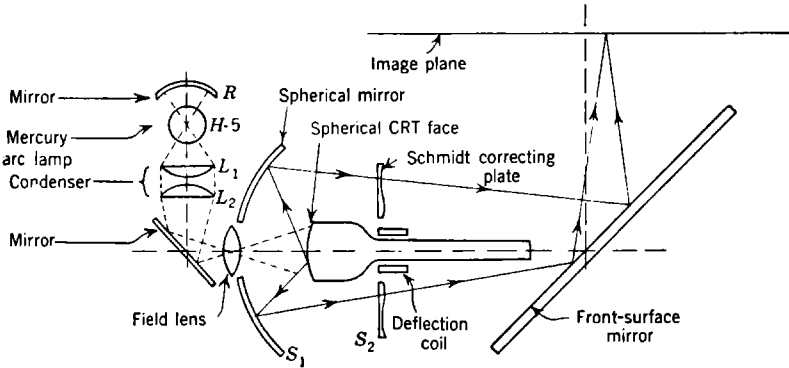


FIG. 16·30.—Projection and illumination optics used in dark-trace projection indicators.
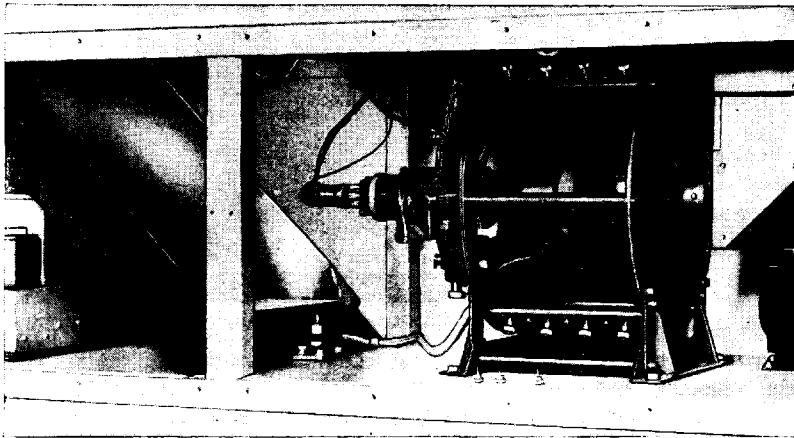


FIG. 16·31.—Side view of illumination and projection system.

near the center of the tube, in order to compensate for the geometry of the PPI display.

The projection and illumination optics employed in this indicator are shown diagrammatically in Fig. 16·30.   A side view of the illuminating and projection system is shown in Fig. 16·31.   Although the illuminating system illustrated in Figs. 16·30 and 16·31 employs a high-pressure mercury lamp whose light is projected vertically downward to the plane mirror near the field lens, a 1-kw tungsten lamp has been used to advan-

tage in other models of this equipment.  In this case, the light path from the source to the mirror is made horizontal instead of vertical.

The projection system is designed for a magnification of approximately 6.5, producing a 25-in.-diameter image from the type 4AP10 cathode-ray tube, whose face has a nominal diameter of 4 in.  With either of these illumination systems, the illumination level of the cathode-ray-tube face should be approximately 8,000 to 10,000 foot-candles in order to yield an image brightness sufficient to be used in an ambient illumination on the projection surface of 1 to 2 foot-candles.

Fig. 16.32 illustrates the method of supporting the cathode-ray tube and associated equipment in the optical system.  Since all of the light
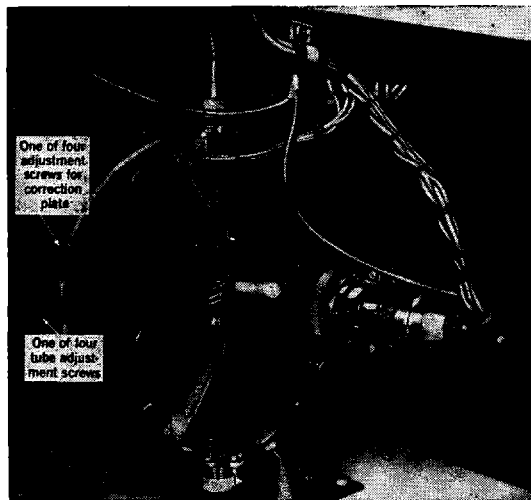


FIG. 16·32.—Detail of tube mount and drive.

that reaches the projection screen must pass through the correction plate that encircles the deflection coil, it is important that the support for the tube, as well as the deflection and focus coils, be designed so as to intercept the minimum possible amount of light.  Figure 16·32 also indicates the methods of adjustment of the correction plate to secure its accurate location on the optic axis, and of the positioning of the cathode-ray tube. The adjusting screws provide independent lateral adjustments for both the correction plate and for the spider that supports the tube and associated equipment.  The axial position of the cathode-ray tube is controlled by the knurled ring near the tube clamp.  The adjustment of both the correction plate and the tube face itself must be carefully done because the high-aperture optical system has only a small depth of focus.

Figure 16·32 shows one method of driving the deflection coil, using a

10-to-1 worm gear driven by a 10-speed size-5 synchro located in the compartment above.   In this case, a microswitch (not shown) is used to secure proper phasing of the deflection coil.   A more satisfactory although more complex method of drive uses a 1-speed servo system. In this system, it is still desirable to use a worm gear to drive the coil, because this type of drive intercepts a minimum of light.   The driving shaft in this case has the geared-up driving motor at one end, and the geared-down 1-speed comparison synchro at the other, both being outside the optical path.

Although this type of projection indicator, as developed, is far from being completely satisfactory, it is the only method that at the present time permits the instantaneous projection of large radar images.   The shortcomings of the device as described are a low contrast of relatively weak echoes, and an excessive persistence of strong or often repeated signals, which leave a dark trail behind slowly moving strong targets, or tend to smudge up the entire picture when a change of sweep range is made.

These persistent signals may be removed by the application of heat or of a diffuse electron beam.   Used together, the two methods are capable of removing badly burned-in signals within a few minutes, but this process makes the unit inoperative for the reception of information during this clean-up period.   If a mercury arc lamp is used as the source of illumination, the controlled radiation from one or more infra-red sources such as cone heaters directed obliquely toward the tube face may be used to raise the temperature of the screen to such a point as to secure satisfactory decay time.   If a 1-kw tungsten lamp is used, the large amount of infra-red energy in such a source will raise the temperature of the tube face well over 100°C, unless heat-absorbing filters are interposed in the illuminating path.   By this means, plus the use of a hot or cold air blast on the tube face, a wide range in the operating temperature of the screen is possible.

The use of 15 kv instead of 9 kv as the accelerating voltage on the cathode-ray tube would increase the image contrast and the resolution, but at the expense of an aggravation of the difficulty caused by the burning-in of oft-repeated signals.   Although raising the temperature of the tube face to 150°C will eliminate this burning-in, this high temperature will also cause weak signals to disappear very rapidly.   It is advisable to have a wide range of control on the screen temperature, so that the decay rate may be adjusted to meet the needs of any given situation.

Another approach to the solution of the problem of burn-in and decay rate necessitates the development of a cathode-ray-tube gun and associated focusing and deflecting equipment to create a considerably higher

contrast gradient in the excited area of the screen than is possible with the present equipment. If this can be achieved, a lower peak contrast may suffice to make the presence of a signal detectable for an entire scanning period. If a satisfactory reduction of the burn-in problem is to result,[1] the beam-modulating circuits must be so designed that the peak screen excitation is properly limited to allow no more than a safe upper limit to this excitation. It should also be noted that the adoption of this method would necessitate a reeducation of operators to the acceptance of a low-contrast display as opposed to the higher-contrast but otherwise unsatisfactory presentation now available.

**16·17. Photographic Projection.**—Another method for obtaining a large image of the display of radar echoes on a cathode-ray tube, which does not suffer from the decay of signal strength with time but presents a picture of an entire scan at a constant brightness, involves the projection of the developed photographic image of an indicator cathode-ray tube. This method obviously does not permit the instant availability of the information on the projection screen since there is a maximum delay in presentation of information of the time required for one whole frame or scan plus that required for developing the image. Since it is important that this time interval be as small as possible, a reduction of the processing time to a minimum is desirable.

An automatic photographic projection equipment of this sort was designed and built by the Eastman Kodak Company in cooperation with the Radiation Laboratory. This equipment contains a camera for photographing the screen of a cathode-ray tube, means for rapid processing of the photographic film, and an optical system for projecting the processed image. In addition, there is provision for the repetition of the entire process in synchronism with the antenna rotation.

The use of special film, developer, and a high processing temperature (170°F) produces an image of high contrast but low fog and graininess which is ready for projection 10 sec after the development process begins. The diameter of the image is 0.285 in. on 16-mm film. The resolution and contrast of the projected image, which may be 6 or 8 ft. in diameter, are remarkably good, considering the high magnification involved.

A photograph of the apparatus is shown in Fig. 16·33. The various steps of the complete cycle are controlled by a series of cams that operate microswitches, which in turn control the various functions by operating solenoids or clutches. The cam timing chart illustrated in Fig. 16·34 indicates the sequence of the various steps and their duration. The apparatus also includes a vacuum line that serves to remove the developer and fixer from the film after use, and compressed air for cooling the film

[1] See Sec. 18·14 *et seq.*

during projection.   The processing of the film takes place in a small cup just large enough in diameter to include the area of the film on which the cathode-ray-tube image is formed.   A detail of this processing cup, as well as a diagrammatic sketch in elevation of the processing system, is shown in Fig. 16·35.   The film passes horizontally under the processing cup with the emulsion side up.   It is held stationary during the time of one complete scan of the radar antenna, during which time the camera lens and prism system located below the film project a greatly reduced
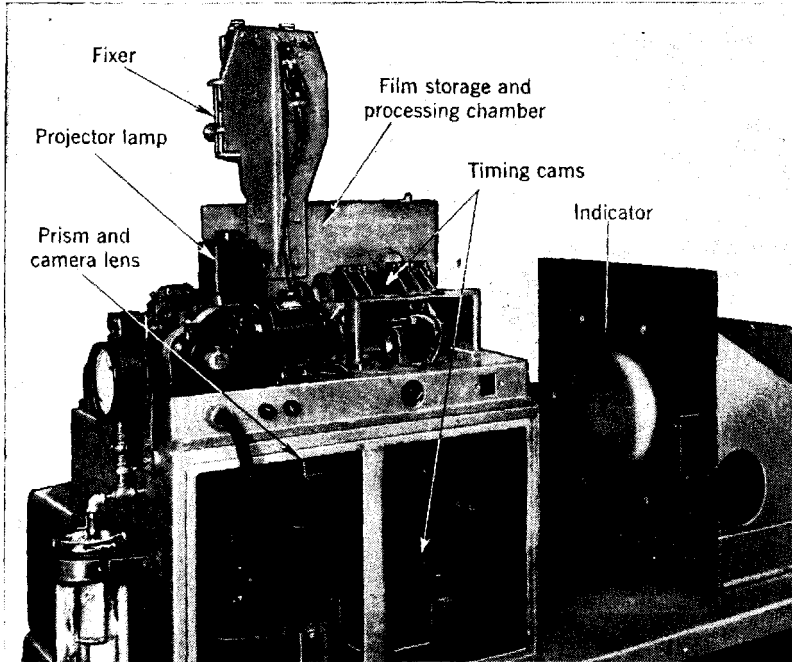


Fig. 16·33.—Photographic processing and projection equipment.   (*Photograph courtesy of Eastman Kodak Company.*)

image of the cathode-ray-tube screen through the film base onto the emulsion.   This image is centered on the axis of the processing cup. Upon the completion of one rotation of the PPI, the processing cycle of Fig. 16·34 commences with the energizing of a solenoid controlling a cam-shaft clutch, and a continuously running motor engages the cam shaft for one revolution.   Developer is poured into the cup, and after 2.7 sec is removed by suction applied to the annular space in the cup. At 3.1 sec, fixer is poured into the cup and continues in action until 6.6 sec, whereupon it in turn is removed from the cup.   A short rinse of developer follows in order to eliminate the corrosive action of the acid

fixer on parts of the projection apparatus. This developer is then removed and suction applied in order to dry the film from 7.5 sec until 9 sec. At this time a solenoid lifts the cup from contact with the film and shortly thereafter the film is quickly advanced by a pull-down sprocket to the projection position, which is 1.5 in. (5 sprocket holes) from the taking and developing position, and the next exposure may begin.

It is not necessary to close the camera shutter during the development process because the desensitizing action of the developer prevents the recording of additional data once the development cycle has begun.
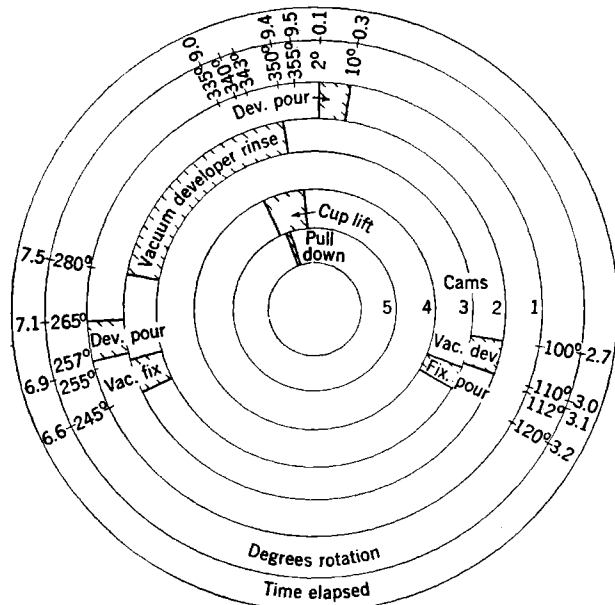


FIG. 16·34.—Cam timing chart; 10-sec cam-shaft cycle.

If the apparatus is adjusted to project a new picture once every 30 sec (for example when photographing alternate scans of 15-sec period), 24 hr of operation will result in approximately 2900 pictures, and will require 360 ft of film. Only one fifth of this film will contain data, but the space between taking and projection cannot be reduced much beyond the 1.5 in. used in this equipment. The amount of developing and fixing solutions required is moderate since only the area actually receiving photographic exposure is developed. A little over one-half gallon of developer and half this amount of fixer will process 3000 pictures.

The accuracy of both the pull-down sprocket and of the perforation

in the film must be of a high order if the wandering of supposedly "fixed" spots in the projected image is not to be excessive. In the apparatus here described, such fixed spots will lie within a circle of ¼-in. diameter on the projection screen, when the projected image is 8 ft in diameter.

The screen used in photographing the cathode-ray-tube traces may be either the double-layer P7 screen or the blue P11 screen. The latter is preferable since the thinner screen layer results in somewhat greater
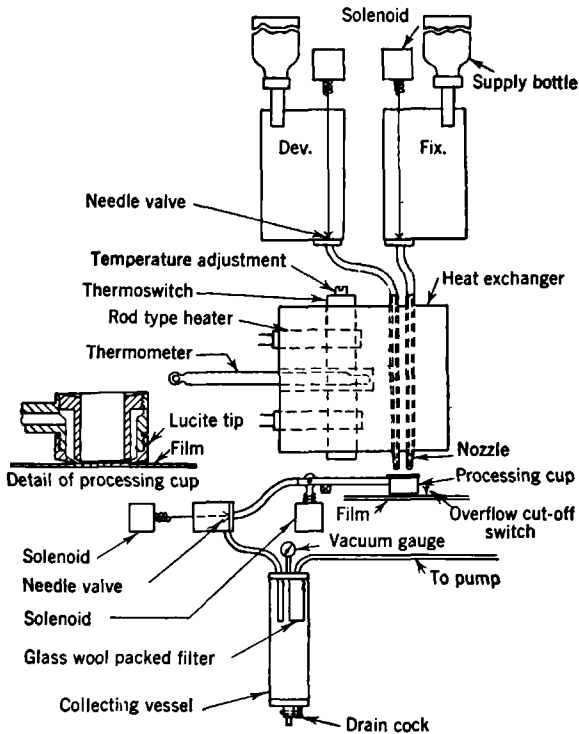


FIG. 16·35.—Diagram in elevation of processing system.

resolution. Although this equipment embodied an f/1.4-aperture 1-in.-focal-length camera lens, an opening of f/4 was found sufficient for good exposure for normal tube operation.

In projecting the image, an f/2 projection lens is used in conjunction with a 300-watt lamp. The light is directed vertically through the horizontal film, and a prism is used to project the beam horizontally onto a vertical plotting surface.

To make use of this device as a means for plotting on a large scale, two methods of plotting may be used. One of these employs front

projection with plotting from the rear of the screen, and the other uses front projection as well as plotting from the front of the screen.

For front projection and rear plotting, the projected photographic image is formed on a diffusing, partially transparent sheet in close but not optical contact with the front face of a clear plastic or glass plate. The projected image is visible from both sides of the screen. The plots are made on the back surface of the clear plate by plotters who record the position of signals by using china-marking pencils of various colors. These marks are made visible by edge illumination of the plate by a series of enclosed lamps along its vertical edges.

The thin screen receiving the projected image must be such that it will scatter the light from the projector enough so that observers viewing the screen from the front will not see the projection source reflected in the screen; on the other hand the degree of diffusion cannot be so great as to blur the plots located behind this surface. To minimize this effect, the thickness of the edge-illuminated plate should be kept as small as possible ($\frac{1}{4}$ to $\frac{3}{8}$ in.), and the separation between screen and plate should be negligible. To achieve the latter requirement, it is advantageous to curve the plotting plate to form a section of a cylinder of large radius of curvature. A 2- or 3-in. bow in the 8-ft width is sufficient to provide mechanical contact between plate and screen over the entire area by applying tensile stress to the screen along its vertical edges. Although the mechanical contact so achieved is good, the natural roughness of the screen material provides only a very small number of points of optical contact. Such optical contact is undesirable because the light flux in the clear plate would be transmitted at these contact points, and would make the projection screen self-luminous if extensive optical contact took place. It is for this reason that the projection screen is not made an integral part of the plotting plate. To date, no completely satisfactory material has been found for the diffusing projection screen.

The problem of the previous paragraph can be overcome and the space behind the projection surface for the plotters can be saved if projection and plotting are both done from the front of the screen. Then a conventional type of beaded motion-picture screen may be employed. This method involves the use. of separate projectors at the front for adding auxiliary grid squares and other markings, as well as an opaque projector for each plotter. In principle, this method is not difficult, but the details of this apparatus have not been carried to completion.

Tests have been made to determine what percentage of the signals appearing on the original PPI will be recorded by this photographic-projection plotting method. A separate camera photographed a PPI

continuously for 10 min.    During this time plotters behind the screen recorded what they saw.    At the end of the 10-min interval, the large screen containing the plotters' tracks was photographed, and this was compared with the 10-min direct exposure of the PPI tube itself.    This comparison indicated that approximately 90 per cent of the signals actually present were plotted on the screen.

# CHAPTER 17

## SPOT SIZE

### By R. D. Rawcliffe and T. Soller

The size of the luminescent spot on an operating cathode-ray tube is an important factor in determining the resolution, or fineness of detail, which can be distinguished in a radar or television display, but it is by no means the only factor. In radar, the beam width and pulse length, the i-f bandwidth of the receiver, the sweep speed, spot size, and luminance level of the cathode-ray tube, and the characteristics of the human eye all enter into the determination of the over-all resolution in any given case.[1] The factors that affect the contrast and resolution in television are discussed by various authors.[2] It should be noted that, in the cathode-ray tube itself, the contrast and resolution are affected by factors other than the current distribution in the spot itself, such as internal reflections in the glass face plate and the use of metal-backed screens. Internal reflections may be significantly altered by varying the thickness of the face plate, and by the application of a nonreflecting film to the outer face.

The present chapter is limited to a discussion of various methods that have been devised to measure spot size, and to the conditions of operation which produce a minimum spot size in a given cathode-ray tube.

**17·1. Meaning of Spot Size.**—One of the major difficulties in the measurement of spot size is due to the indefinite nature of the spot. In the ideal case in which there are no aberrations or defocusing of the beam due to imperfect electron lenses and deflecting systems, the distribution of charge in the beam falls off exponentially with the square of the distance from the center of the beam. If the response of the fluorescent screen is assumed to be linear, the light in the spot falls off in the same manner, and the spot then has no sharp boundary. The decision as to what constitutes the boundary of the spot must therefore be arbitrary. The usual definition of the edge of the spot is that it is the contour for which the brightness has fallen to some fraction $K$ of that at the center of the spot. In most methods of measurement, $K$ is so chosen that if the

---

[1] See Secs. 1·11, 1·12, 18·10, and 18·11 for a further discussion of these various factors.

[2] V. K. Zworykin and G. A. Morton, *Television*, Wiley, New York, 1940.

C. H. Bachman, *General Electric Review*, **48**, 13–19, September, 1945.

centers of two spots are one spot "diameter" apart, the two spots can just be resolved.

In practical cathode-ray tubes, imperfections in the electron optics cause spot deformations that considerably complicate spot-size measurements.  The spot frequently is not round, especially near the edge of the tube.  In the case of electrostatic focus and deflection cathode-ray tubes, the asymmetry usually takes the form of an astigmatic spot, an ellipse with a large ratio of major to minor axes, with the entire area more or less uniformly bright.  For magnetic focus and deflection cathode-ray tubes, the energy distribution in the distorted spot may be much more complicated.  For example, the spot may have "tails," such as are illustrated in the first few photographs of Fig. 3·4.  A measurement of spot size which has real significance is extremely difficult under these circumstances.  It is usually true that the brightness of the tails is enough less than that of the center of the spot so that the tails have negligible effect on ordinary measurements of the minimum resolvable separation of the two spots.  The tails do not, however, have negligible effect on the true resolution, particularly in the resolution of two spots of unequal intensity, because the tail from the strong spot may be nearly as bright as the weaker spot itself.  Tails also degrade the over-all contrast on the screen.  With spots that are not round, spot size cannot be expressed by a single number, and resolution measurements become more complicated.

The methods of spot-size measurement to be discussed in this chapter are applicable to both electrostatic and magnetic tubes.  However, the analysis of the performance of electrostatic tubes has been made almost entirely on the basis of the shrinking-raster method,[1] and the typical values of line width for such tubes, which were mentioned in Sec. 2·8, refer to this method.  The discussion of other methods mentioned refers specifically to magnetic tubes.

**17·2. Spot-size Measurements with a Microscope.**—The simplest and probably also the least accurate method of measuring spot size is that of direct measurement with a microscope.  The best type of microscope for this purpose is one that contains a reticule scale so that the image of the spot may be superposed on the reticule for measurement.  A magnification of about ten is best for most measurements unless the spot size is less than about 0.1 mm.  For ease of measurement, a microscope mount such as that shown in Fig. 17·1 is useful.  With this mount, the microscope can be moved independently in two coordinates, each motion being measured by means of the vernier scales shown.  This "cross motion" is also very convenient for many other types of measurement, notably pattern distortion and sweep linearity.

[1] Discussed in Sec. 17·4.

In direct measurements with a microscope, the edge of the spot is determined by the judgment of the observer. The reproducibility is fair, perhaps ±10 per cent with a given observer under controlled conditions, but there is at least twice that variation from observer to observer. The ambient light should be kept constant and should be noted, because it seriously affects these spot-size measurements. These measurements do not agree with those made by other methods, but are larger by a factor of about two than those made by methods in which spots or lines are shrunk together until just resolved. Although the latter measure-
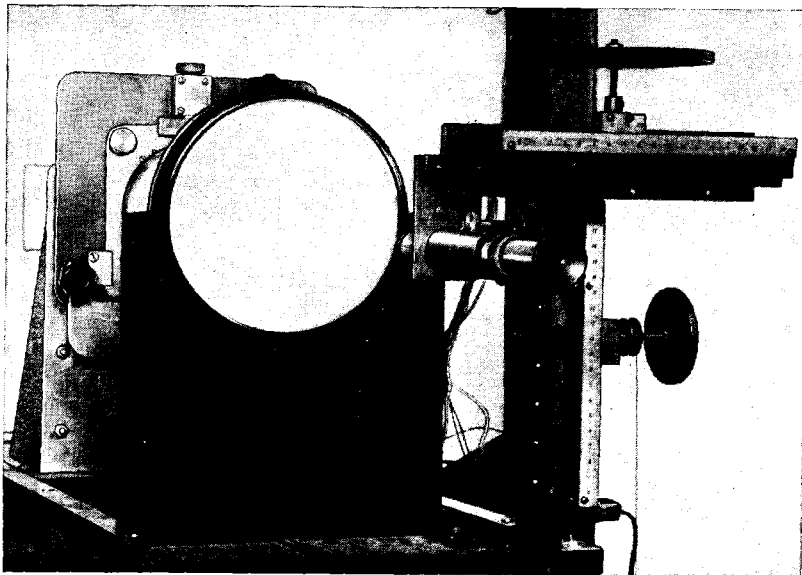


Fig. 17·1.—Microscope and cross motion for measurement of spot size.

ments correspond more nearly to actual operating conditions, the microscope measurements are useful for rapid comparisons of tubes and coils. In addition to the speed with which the measurements can be made, this method has the added advantage that the spot itself is seen. An experienced observer can often infer from the spot distortion observed the type of correction needed in the deflecting and focusing fields to reduce the distortion.

The beam current and duty ratio at the time of spot-size measurement should reproduce actual operating conditions of the tube under test if a satisfactory correlation of results is to be obtained. The beam should therefore be "pulsed" during the microscope observation.

**17·3. Spot Measurements by the Double-pulse Method.**—The double-pulse method is particularly well-suited to the measurement of

spot size on a rotating-coil PPI pattern, although it can be used with other scans as well.   A block diagram of the circuits required is shown in Fig. 17·2.   A synchronizer provides a trigger to start the sweep through the deflection coil; a second trigger, delayed by a variable amount after the sweep trigger, to start the double-pulse generator; and a linear sweep for the A-scope, the start of which coincides with the second trigger. The sweep driver provides a linear sweep current through the rotating deflection coil as well as a suitable square-wave voltage for brightening the trace on the cathode-ray tube.   The double-pulse generator pro-
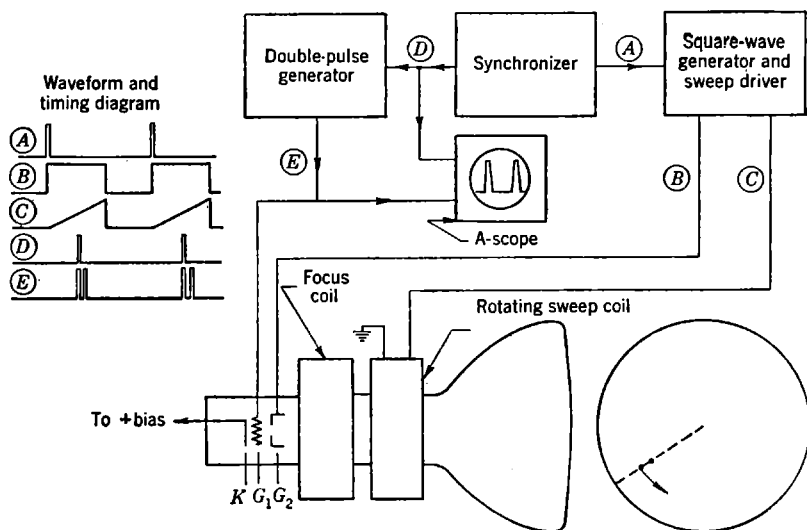


FIG. 17·2.—Block diagram of apparatus for spot-size measurement by the double-pulse method.

duces two square waves adjustable from about $\frac{1}{2}$ to 10 $\mu$sec in duration whose rise and fall are as fast as possible (less than 0.1 $\mu$sec).   These pulses are delayed by times that are independently adjustable so that one can be run through the other.   They are mixed and applied to the cathode-ray-tube grid in such a way that the grid is at ground potential during either pulse and is biased negatively at other times.   These pulses may be observed on the A-scope.   The sweeps on both cathode-ray tubes are so calibrated that the separation of the spots on the PPI tube can be determined by measuring their separation on the A-scope.   The operation, then, consists of varying the delay of one of the pulses until the two spots on the PPI tube are just resolvable, and then calculating their separation from the separation on the A-scope.

The double-pulse method is especially useful for measurements on tubes with long-persistence screens because the spot measurements can be made in the persistence instead of the "flash" as must be done with most other methods. Since the flash is usually filtered out as well as possible in the operation of long-persistence tubes, measurements in the persistence involve one less step in the application of measured data to practice. In measurements on dark-trace tubes (P10 screen) the double-pulse method is one of the few permissible because other methods cause too severe an excitation of relatively large areas of the screen. In the double-pulse method, only a very small area need be darkened at a time.

When a PPI type of scan is used, this method has the advantage that a visual inspection of the appearance of the rotating pair of dots, well-separated, gives an indication of any asymmetry due to misalignment of parts of the electron gun. It must be remembered that in order to isolate the effects due to the tube itself, adequate care must be exercised in the alignment of the focus and deflection coils with respect to the tube. Quantitative measurement of spot size as a function of angular position may then be made.

**17·4. Shrinking-raster Method of Measurement of Resolution (Line Width).**—The method commonly used by manufacturers of cathode-ray tubes to specify the performance of tubes with regard to spot size is the "shrinking-raster" method. A television-scan pattern, known as a raster and composed of a large number of equally spaced lines, is applied to the tube under test. These lines are produced by sawtooth scanning at a frequency of 60 cps along one axis and at 35 to 105 times this frequency along the perpendicular axis. Figure 17·3 is a simplified block diagram of apparatus for this method of measurement, which uses frequencies that give a 100-line pattern.

The amplitude of the fast scan is first adjusted until the length of the lines is approximately 90 per cent of the maximum screen diameter. The low-frequency scanning amplitude is then expanded until the lines are clearly separated. After suitable adjustment of current and optimum focus have been achieved, the pattern is slowly "shrunk" until the line structure first disappears at the center of the screen. The width of the pattern at this time, divided by the number of lines in the pattern, is called the "line width." A single measurement does not suffice because the resolution near the edge of the tube is usually inferior to that at the center, and, furthermore, the astigmatic effects in electrostatic tubes may make the relative line widths in perpendicular directions dependent on the focus adjustment.

In measuring electrostatic tubes, two measurements are made as follows:

1. Adjust for best focus at the *center* of the pattern and measure at this point, called Position "A."
2. Without readjusting the focus, interchange the low- and high-frequency scans and make the measurement at a point that is a distance of three-eighths of the maximum bulb diameter along the direction of high-frequency scan. This point is known as Position "B," and the measurement is made at the less favorable of the two alternative B positions.

This procedure is designed to give a measure of the astigmatic effects in a given tube. If these effects are serious, the ratio of the two measure-
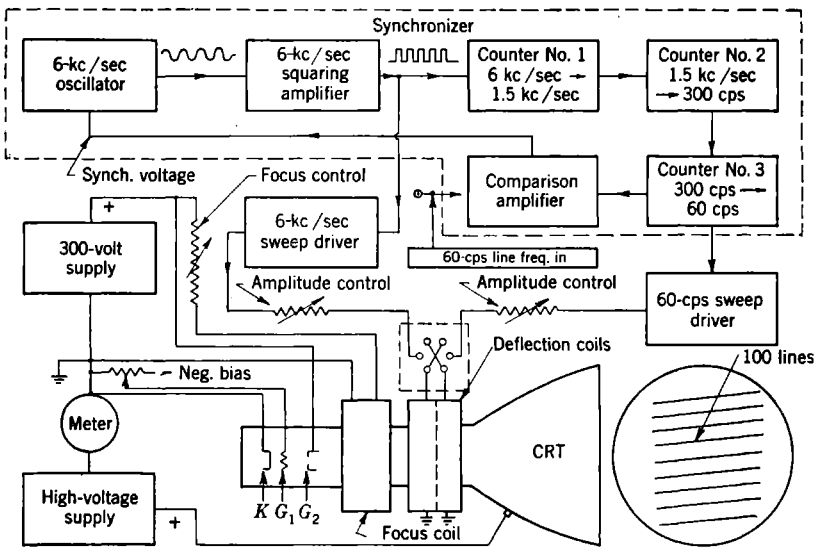


FIG. 17·3.—Simplified block diagram of apparatus for the shrinking-raster method of line-width measurements.

ments will be large. For a good tube, the ratio will be near unity. In any case, in actual operation the focus adjustment will be so made as to give the best average spot size and this value will be between the values found for Positions A and B.

In magnetic tubes, astigmatic effects are usually much smaller than in electrostatic tubes. Measurements are therefore made at Position A, i.e., at the center of the high-frequency scanning line, and at Position "C," the less favorable of the two alternative positions three-eighths of the maximum bulb diameter along this same line. These measurements are markedly influenced by the quality, dimensions, and location of the

focus and deflection coils used, and therefore these conditions must also be specified in order that the measurements may have significance.

A photometric investigation[1] of the raster lines applied in the shrinking-raster method of measuring line width has been made for the case of a magnetic type 5FP7 cathode-ray tube operated at $E_b = 4$ kv. Photographs of the raster, with the lines well separated, were taken at four different beam currents and were analyzed by the use of a Moll microphotometer. Contours were obtained for several values of the beam current. These contours can be very closely represented by Gaussian distributions.



| Current µa | Beam line width, mm | |
|---|---|---|
| | Raster | 1/e of peak |
| 30 | 0.24 ± 0.01 | 0.25 ± 0.015 |
| 60 | 0.26 ± 0.01 | 0.29 ± 0.01 |
| 150 | 0.32 ± 0.01 | 0.34 ± 0.008 |
| 200 | 0.36 ± 0.01 | 0.36 ± 0.008 |
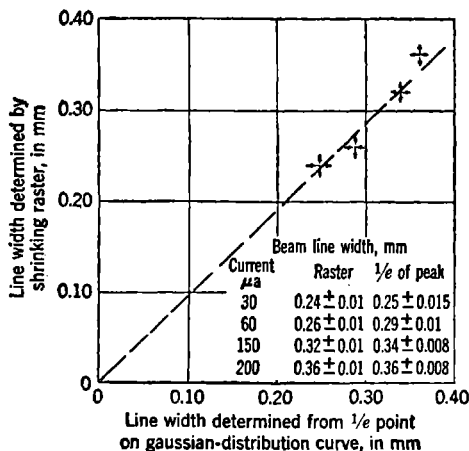
FIG. 17·4.—Comparison of line-width measurements.

Line widths were determined visually for each beam current by shrinking the raster until the lines were just unresolvable. A comparison of the line widths so obtained and the contours determined by the microphotometer reading shows that at each current the intensity at the edges of a line defined by the shrinking-raster method is about 40 per cent of the peak intensity. A photometric analysis over the raster as shrunk to measure line width shows that the minima are only 10 to 15 per cent lower in intensity than the maxima, and that these maxima are at the peaks of the individual lines.

By the use of the Gaussian curve best fitted to each line, the width of the line at the intensity points that are $1/e$ of the peak intensity was calculated for each of the beam currents used. The graph and table shown in Fig. 17·4 compares these line widths with those found by the shrinking-raster method. It is evident from this figure that there is a

[1] Measurements by A. Crampton and B. Cherry at the Radiation Laboratory, M.I.T.

definite linear correlation between the two sets of results, so that the shrinking-raster method yields line widths proportional to the actual width of the lines reckoned at a definite percentage intensity.

**17·5. Polka-dot-raster Method.**—In order to avoid some of the objections to the shrinking-raster method, the "polka-dot raster" method was devised. The two methods are similar except that in the latter spots instead of lines are measured, and complete measurements can be made at any point on the tube face. A block diagram of the apparatus is shown in Fig. 17·5. The synchronizer, which is similar to that shown in Fig. 17·3, provides trigger pulses at 60, 300, and 4800 cps, all of which
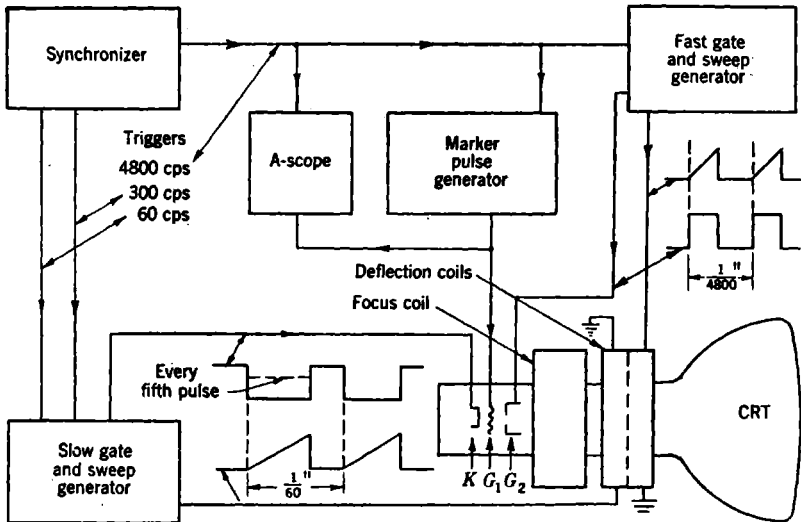


FIG. 17·5.—Block diagram of apparatus for the polka-dot-raster method of spot-size measurement.

are "locked in" with the 60-cps line frequency. The 60- and 4800-cps trigger pulses are used to initiate slow and fast sweeps that form a raster on the cathode-ray-tube screen similar to the "shrinking"-raster except that it appears in one quadrant only, and is considerably smaller. The marker pulse generator provides fast, sharp, voltage pulses, which are applied to the cathode-ray-tube grid in order to produce a row of spots on the screen for each fast sweep. The pattern, then, consists of a number of rows of these spots, as illustrated in Fig. 17·6. In order to make the illustration clearer, the size of the spots in this photograph is considerably larger than that occurring under most operating conditions. The pulse generator must be extremely good in order to produce pulses that are so short that the motion of the sweep during the pulse duration

is negligible compared with the spot size. The generator used in the
original equipment produced pulses resembling a half sine wave about
0.05-μsec wide, of adjustable separation down to about 0.3 μsec, and
variable in amplitude from 0 to 100 volts. Both sweep circuits are also
used to generate square waves to gate the cathode-ray tube. One such
wave from the fast sweep generator is applied to the second grid to blank
the tube between fast sweeps. A second such wave from the slow sweep
generator is applied to the cathode to suppress the return of the slow
sweep. Superimposed on this second square wave is an intensifying
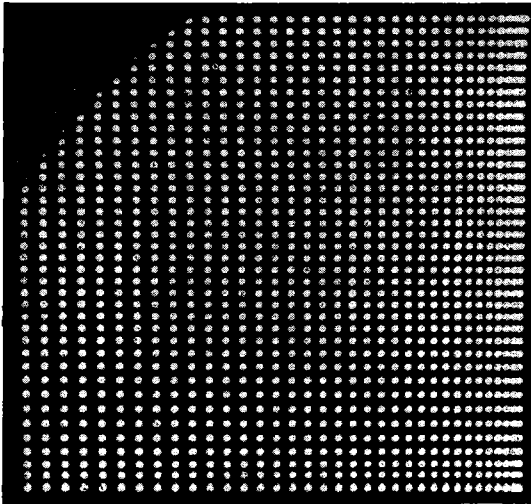


Fig. 17·6.—Photograph of section of cathode-ray-tube face showing polka-dot pattern.

square wave initiated by the 300-cps trigger pulse to brighten every
sixteenth fast sweep. The A-scope is used to observe the marker pulses
on a fast sweep, whose start can be delayed by a variable time after the
4800-cps trigger pulse so that pulses on any portion of the raster may be
measured.

The spot-size determination, then, consists of two steps:

1. As in the shrinking-raster method the slow sweep is shrunk down
   to the minimum resolvable separation of two spots at any given
   point on the screen. The spot "diameter" in the direction of the
   slow sweep is measured with the microscope (Fig. 17·1) as $\frac{1}{16}$ of
   the separation of two intensified lines.
2. The other dimension of the spot is measured along the fast sweep.
   The spots themselves are shrunk together to minimum resolution,

their separation is determined on the A-scope, and the spot diameter is calculated from the known sweep speeds on the A-scope and on the tube being tested.

Only a small raster is needed because measurements are made on a small area approximately a centimeter in diameter. The raster is moved around to various positions on the screen by superimposing direct current on the sweep current through the coil in the same direction as the sweep current. Reversing switches are needed in the leads to the deflection coils to allow measurements in all four quadrants of the screen.

An obvious modification of this method is the application of the intensity-modulated high-speed sweep to a rotating deflection coil, producing a PPI type of pattern. This pattern is then contracted until the limit of resolution is reached, and the spot size is determined by measuring the width of the pattern and dividing by the number of "dots." This method is very similar to the double-dot method described in Sec. 17·3, but avoids the necessity of measurement of sweep speed and time separation of pulses.

**17·6. Other Methods of Measurement of Line Width or Spot Size.—** This section briefly mentions several methods for the determination of line width or spot size which have not been directly investigated, and for which no quantitative data are on hand. The list is not complete, however, for the number of methods used for these determinations is almost as great as the number of investigators in this field.

One method uses a double-image prism the thickness of which is such as to give a separation a little greater than the widest line that is to be measured. A single line is scanned across the face of the cathode-ray tube and examined by means of an instrument that contains the prism and a lens giving suitable magnification. The prism is rotated until the two images just begin to merge. A calibrated scale on the mount gives a direct reading of line width. The results obtained with this device should correlate closely with those obtained by the shrinking-raster method.

Another method involves covering a given line on the cathode-ray tube with one of a series of fairly closely spaced opaque lines whose width increases from line to line by an arbitrary ratio. The lines are formed on a clear film base by a photographic process. The known width of the particular line that is judged to just cover the line on the cathode-ray tube is taken as a measure of its width. Obvious difficulties with this method include the parallax between the line observed and the "covering" line, and the different intensity distributions of the lines produced by various tubes.

Other methods involve the direct measurement of the energy distribution in a single spot.  One technique is to produce, by means of a high-quality lens, a greatly enlarged (20 to 40 times) image of the spot to be measured and then to measure the energy distribution in this enlarged image.[1]  A box containing a high-sensitivity photo-multiplier, e.g., a 931 tube, placed directly behind a small circular aperture, is made to move across the image in such a manner that the aperture is exactly in the image plane, and the motion is accurately controlled.  The size of the aperture depends upon the degree of resolution desired and the sensitivity and stability of the photo-multiplier circuit.  In general, an aperture of dimensions between 2 per cent and 10 per cent of that of the enlarged image may be used.

The entire contour of a spot can be obtained by a series of equally spaced traversals across the spot image.  This method is slow, and unless the spot shape is exceedingly irregular, two traversals at right angles through the estimated center of the spot, along the major and minor axes of symmetry, will yield equivalent information.  A direct record of the distribution may be obtained by synchronizing the motion of the aperture with that of a pen-and-ink recorder.  A simple apparatus of this type has been built, and indicates that the method affords a rapid quantitative assessment of energy distribution across a spot.  A versatile instrument, incorporating adjustments that make it possible to measure a spot located at any position on the tube face, and with the direction of travel of the pickup aperture variable at will, would be a very useful tool for an investigation of this type.

**17·7. Comparison of the Various Methods of Spot-size Measurement.** Because of the many uncertainties connected with spot measurements, the conditions of measurement should duplicate operating conditions as closely as possible.

No techniques of measuring spot size are completely satisfactory. Gross defects in the focus are usually shown up reasonably well but small variations are often not detected.  Measurements of limiting resolution usually rate tubes producing diffuse spots as being equal to those producing clean, sharp spots.  However, when the tubes are inserted in operating equipment, there is usually unanimous agreement that the tubes producing the sharp spots afford better resolution.  A particular case in which this phenomenon occurred repeatedly was in the comparison between magnetic tubes containing standard guns and some tubes that had limiting-aperture guns.  It is felt that hidden among the many variables that affect spot size there must be some important ones that are not being adequately measured or controlled in any of the existing spot-measurement methods.

[1] R. B. Windsor, Radiation Laboratory, M.I.T.

One variable that must be carefully controlled is the beam current, since the spot size changes rapidly with this current. If the cathode-ray tube is deflection-modulated (A-scope), the beam current is steady and may be read with an ordinary d-c meter. Measurements by the shrinking-raster method are then close to operating conditions. If, however, the cathode-ray tube is to be intensity-modulated (television scan; PPI), the measurements should be made with a pulsed beam and with sweep speeds approximately equal to those to be used under operating conditions. The polka-dot-raster method is definitely better than the ordinary shrinking-raster method for these measurements.

When the beam is pulsed, measurements of beam current are difficult to make because of the high frequencies involved. It is nearly impossible to measure the beam current accurately by observing the voltage across a known sampling resistor by means of an oscilloscope because the distributed capacity in the oscilloscope and in the cathode-ray tube is so large that a very small sampling resistor must be used. The voltage drop across the resistor is then very small and the deflection on the oscilloscope is almost unreadable. A video amplifier might be used, except that the difficulties connected with calibrating and operating such an amplifier would prevent accurate measurements.

The best method consists of measuring the instantaneous grid-to-cathode voltage on the tube with an oscilloscope and then reading off the instantaneous current from a grid-voltage–beam-current characteristic curve previously measured with steady voltages on the tube. It is assumed that the high-frequency and low-frequency characteristics of the tube are the same.

This scheme runs into trouble, as do all others, if limiting-aperture guns are used. Because the limiting aperture is connected internally to the anode, there is no method of separating current to the screen from that masked off by the aperture. Spot-size measurements in terms of light output would be more useful than those in terms of beam-current values. These measurements could be made independently of the current masked off by the aperture. However, because the response of existing light meters is given by the total light output of the screen, and because the response of the screen is not linear with beam current, light measurements are also difficult.

**17·8. Effect of Various Parameters on Spot Size.**—The performance of a cathode-ray tube is the result of the interplay of a large number of factors, most of which have already been discussed in earlier chapters. The present section will point out the effects on the spot size of varying (1) certain electrical parameters, such as the anode voltage $E_b$ and the second-grid voltage $E_{c_2}$, (2) the beam current $i_{sn}$, and (3) the tube size.

*Effect of Anode Voltage $E_b$ on Spot Size.*—Theoretical considerations for an ideal gun involving simplifying assumptions have led Zworykin and Morton[1] to the conclusion that the spot size should be inversely proportional to $E_b$ and should be independent of the potential of the crossover. In their analysis, they assume a two-lens system, in which the second lens forms an image of the crossover. On the other hand, Liebmann,[2] assuming that three and not two lenses are actually involved in the image formation, and that the cathode and not the crossover is imaged on the screen, finds that the spot size should be practically independent of the final-anode voltage. Liebmann also gives experimental data supporting this conclusion.

Figure 17·7 indicates the relation between spot size and $E_b$ as determined by the polka-dot-raster method discussed in Sec. 17·5. This
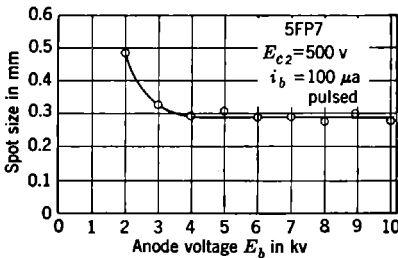


FIG. 17·7.—Relation between spot size and accelerating voltage.

curve indicates that within the limits of experimental error the spot size is independent of $E_b$ in the range between 3 to 10 kv. The measurement at 2 kv is not significant because the intensity of the pulsed spot at this voltage is too low to permit accurate measurement.

Line-width-measurement data using the shrinking-raster method for various values of $E_b$ are not very extensive. They indicate a slight improvement of line width with increasing $E_b$, but not nearly great enough to satisfy the inverse $\sqrt{E_b}$ relation.

It is not true, however, that no gain in performance will accrue by raising the value of $E_b$; later discussion will indicate the advantages of making $E_b$ as high as practicable.

*Effect of Second-grid Voltage $E_{c_2}$ on Spot Size.*—Figure 17·8 indicates typical experimental data obtained on a 7BP7 tube in which both spot size and $E_{c_2}$ voltage are plotted logarithmically. The polka-dot method of measurement was used with a final anode voltage $E_b = 5.5$ kv, a beam current, $i_{an} = 100 \mu a$ (peak of pulses), and the second-grid voltage $E_{c_2}$ variable. The focus-coil gap was $2\frac{3}{4}$ in. from the reference line.

Similar curves for other tubes, having the same type of gun and varying in size from 5 in. to 12 in., indicate that neither the break at 500 volts nor the exact slope of the curve illustrated are significant because some other tubes measured show a break at various lower values of $E_{c_2}$, whereas

[1] V. K. Zworykin and G. A. Morton, *Television*, Wiley, New York, 1940, pp. 369 ff.

[2] G. Liebmann, *Proc. I.R.E.*, **33** (1945), pp. 381–389.

others have no break.   Also, the slopes of the curves vary considerably, and in general they are less steep than the curve illustrated.   From the relatively meager data at hand, it appears that the spot size of tetrode magnetic cathode-ray tubes operated at constant current and total voltage varies with second-grid voltage in the range of useful operating values according to the relation

$$\text{S.S.} = \text{const. } E_{c_2}^{-n},$$

where the value of $n$ has been found to vary between 0.32 and 0.65 from tube to tube.   Since an average value of $n = 0.5$ is probably reasonable, these measurements indicate in a general way that the spot size varies inversely as the square root of the second-grid voltage.

Measurements of this sort, using the shrinking-raster method, have not been very extensive or too reliable.   The variation found is in the same direction, but much smaller in amount.   A great number of additional data are obviously needed to establish more quantitatively the relation between spot size and second-grid voltage.

*Effect of Beam Current on Spot Size.*—The spot size for any given cathode-ray tube operated at a



FIG. 17·8.—Spot size as a function of second-grid voltage.

constant accelerating voltage increases with increasing beam current. This increase in spot size is primarily due to two factors: (1) The increase in "object size" with increasing beam current, whether this "object" be considered as the emitting area of the cathode or as the size of the cross-over; and (2) the increasing aberration due to the focusing lens since the diameter of the electron bundle also increases with increasing beam current (see Sec. 2·12).

Extensive experimental determinations of the relation between spot size and beam current, under well-controlled conditions, are not available. A great many measurements have been made by the various methods previously described, but not under identical conditions of voltage and coil position.   All of these results seem to indicate that, whatever method of measurement is adopted, the experimentally determined points can be associated with straight lines as indicated by sample plots shown in Fig. 17·9.   These are not intended to represent average performance for the tube sizes indicated as far as absolute value of spot size is concerned.

FIG. 17·9.—Typical plots of line width as a function of beam current. *A*, 5FP7, shrinking-raster method; *B*, 7BP7, double-pulse method; *C*, 12DP7, double-pulse method; *D*, 7BP7, microscope method.

They do, however, indicate the general relation between spot size and beam current for any given tube. The fluctuations from tube to tube are considerable. In general there is a somewhat greater difference between 5 in. and 7 in. tubes than Fig. 17·9 indicates. Measurements at beam currents as low as 30 $\mu$a indicate that the curves seem to continue toward the axis of ordinates along the line followed at higher beam currents. The curves extend to values of beam current far beyond what can be considered to be the useful operating range. In the useful operating range of the cathode-ray tube, namely between 50 and 300 $\mu$a, the ratio of the spot size at 300 $\mu$a to that at 50 $\mu$a varies with tube size, and has approximate values of 1.8, 1.5, and 1.3 for 12DP7, 7BP7, and 5FP7 tubes, respectively. It should be noted that the spot size as determined by the microscope method is approximately twice that measured by the other methods. Also, in making the measurements the procedure adopted was to adjust
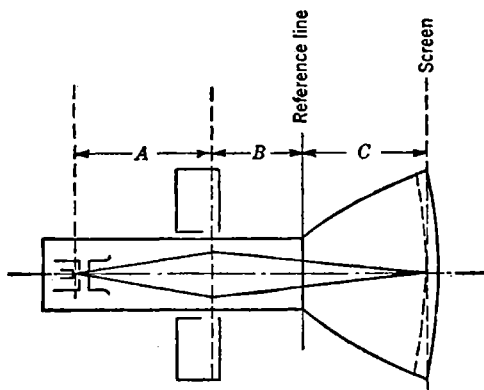


FIG. 17·10.—Illustration of geometrical magnification of focusing lens (see Table 17·1).

the focusing current so as to obtain the best focus at each value of beam current. In practice the focus current would probably remain constant and set at the best "average" value so that the spot size for currents other than that corresponding to the "average" would be appreciably larger than indicated by these curves.

*Effect of Tube Size on Spot Size.*—With a given gun type and constant operating conditions in tubes of various sizes, the relative spot sizes for the various sizes of tubes should be calculable from the object-to-image distances and the location of the focusing lens, if aberrations are neglected. Figure 17·10 indicates the object-image geometry; and Table 17·1 gives

TABLE 17·1.—GEOMETRICAL MAGNIFICATION OF FOCUSING LENS FOR COMMON TUBE TYPES

| Tube type | A | B | C | Magnification $\left(\dfrac{B + C}{A}\right)$ |
|---|---|---|---|---|
| 3HP7 | 2.25 | 2.75 | 2.20 | 2.20 |
| 5FP7 | 2.25 | 2.75 | 3.45 | 2.75 |
| 7BP7 | 2.25 | 2.75 | 5.50 | 3.67 |
| 12DP7 | 3.75 | 2.75 | 10.25 | 3.47 |
|  | 3.0 | 3.5 | 10.25 | 4.58 |
|  | 2.38 | 4.12 | 10.25 | 6.03 |

numerical data for the common tube types used in radar. Table 17·2 indicates the ratios of spot size as calculated from the data given in Table 17·1, and also presents some experimental values determined by the various methods of spot-size measurement.

TABLE 17·2.—CALCULATED AND OBSERVED VALUES OF SPOT-SIZE RATIO, R, FOR THREE COMMON TUBE SIZES

| Tubes compared | 7BP7 : 5FP7 | | 12DP7 | | : 5FP7 |
|---|---|---|---|---|---|
| Dimension A, Fig. 17·10 | 2.25 | 2.25 | 3.75   3.0   2.38 | | 2.25 |
| Calculated R from Fig. 17·10 | 1.33 | | 1.26 | 1.67 | 2.19 |
| Observed values of R: | | | | | |
| Shrinking-raster method | 1.25 | | 1.5 | | |
| Microscope method | 1.36 | | 2.4 | | |
| Polka-dot method | 1.50 | | 2.2 | 2.4 | 2.7 |

The data indicate that the experimentally determined spot-size ratio agrees fairly well with the calculated values for the 7BP7 and 5FP7 types, in which the object-lens geometry (Dimension A in Fig. 17·10) is

identical for the two types, but that for the 12DP7 and 5FP7 comparison the correlation is poor. The reason for this is that the aberrations resulting from the larger beam across section at the focusing lens in the case of the 12DP7 type make the experimentally determined spot size larger than would be expected from the tube geometry. The discrepancy between experimental and calculated values decreases as the focus coil is moved nearer the gun of the 12DP7 and the beam across section at the focusing lens is thus reduced.

It is safe to assume that the ratio of the spot sizes is approximately equal to the ratio of the screen diameters, i.e., 1.4 for the ratio of 7- to 5-in. tubes, and 2.4 for the ratio of 12- to 5-in. tubes. In other words, for a given type of gun and associated components, the resolution, as determined by the maximum number of resolvable dots, is independent of the size of tube used.

**17·9. Conclusions Regarding the Attainment of Optimum Resolution from Cathode-ray Tubes.** *Magnetic Cathode-ray Tube.*—From the preceding discussions, it is evident that many factors must be considered to achieve the best performance from a cathode-ray tube. Some of these factors relate to the electrical conditions of operation, whereas others pertain to the quality and adjustment of external parts, such as focus and deflection coils. Often the optimum adjustment of one of the components, for example the focus coil, must be a compromise between geometrical magnification and lens aberrations.

In operating magnetic tubes it is desirable from the standpoint of brightness and resolution to use as high an accelerating voltage, $E_b$, as possible. The light output as a function of $E_b$ at constant current density is of the form $L.O. = KE_b^n$, in which the value of $n$ varies with screen material and conditions of excitation. In general, $n$ decreases with increasing current density. Typical values of $n$ are $n \approx 1.5$ for willemite (P1) screens for values of $E_b$ in the range of 4 to 10 kv, and $n \approx 2$ for the long-persistence cascade (P7) screens in the range of 4 to 10 kv. For radar work involving the use of long-persistence screens, then, the light output goes up roughly as the square of the total applied voltage.[1] If gain in brightness is primarily desired, a fourfold increase is attainable by raising $E_b$ from 4 to 8 kv, if it is assumed that beam current and spot size do not change (same current density as at 4 kv). However, a significant reduction in beam current at the higher voltage is possible and desirable, because improvement in both brightness and spot size may still be attained at the higher voltage by this method. For example, compared with a beam current of 200 $\mu$a at $E_b = 4$ kv, a beam current of only 50 $\mu$a at $E_b = 8$ kv will result in a reduction in

[1] For a discussion of the behavior of screens under various conditions of excitation, see Chap. 18.

spot size of roughly one-third (from Fig. 17·9), with a corresponding spot area a little less than one-half as great as at 200 $\mu$a.    The current density $j = i/A$ corresponding to the 50 $\mu$a condition will therefore be approximately one-half that associated with a beam current of 200 $\mu$a at 4 kv.    Hence, a twofold increase in brightness coupled with a 50 per cent gain in the number of resolvable spots may be achieved by doubling the accelerating voltage.    It must be remembered that additional power will also be required to drive the deflection coil at the higher voltage. Although the driving current increases only as the square root of the accelerating voltage, the power goes up linearly.

It is also very advantageous from the standpoint of spot size to operate the cathode-ray-tube with as high a voltage on the screen grid ($E_{c_2}$) as possible, as indicated by the results shown in Fig. 17·8.    The added increase in resolution so achieved is again coupled with an increase in brightness just as in the discussion of the previous paragraph.    As was discussed in Sec. 2·12, an increase in $E_{c_2}$ not only changes the cutoff bias of the tube, but also decreases the slope of the modulation character- istic so that a higher grid drive is necessary to achieve a given beam current.    The possibility of reducing the beam current necessary at the higher accelerating voltage $E_b$ is therefore advantageous in terms of video output voltage required when $E_{c_2}$ is also raised in order to improve spot size.

In addition to the electrical conditions of operation, the location of the focus coil along the tube neck should be adjusted until the best compromise between increasing magnification and increasing aberrations is reached, as was discussed in Sec. 3·4.    Also, it is important that the mechanical adjustment of the focus coil to make its axis coincide with that of the electron beam be properly made, as was discussed in Sec. 3·6.

The quality of the deflection coil also affects the tube performance, particularly near the periphery of the screen.    The factors involved in deflection-coil performance are discussed in Secs. 8·9 and 8·10.    It is to be noted that the deflection defocusing for any given deflection coil is decreased as $E_b$ is increased.    The curves of Fig. 2·32 indicate that, for a given beam current, the cross section of the electron bundle is decreased as $E_b$ is increased.    This cross section, for a given nonuniformity of field produced by the deflection coil, determines the amount of deflection defocusing.

*Electrostatic Cathode-ray Tube.*—The factors that affect the perform- ance of electrostatic cathode-ray tubes have already been discussed in Chap. 2.

The same considerations that obtain for magnetic tubes in regard to the use of as high an accelerating voltage as possible hold also for electro- static tubes.    In tubes that have a postdeflection acceleration electrode,

the ratio of total voltage to second-anode voltage must be kept below a certain maximum, however.

The deflecting circuits for electrostatic tubes should provide push-pull voltages, rather than single-sided voltages; and an "astigmatism-control" adjustment should be available to adjust the mean potentials of the two pairs of deflection plates to the optimum values with respect to the second-anode potentials.  In addition, if the trace is intensity-modulated, pulsing of the focusing anode $A_1$ will also be advantageous in order to adjust the focus at all values of beam current.

The elimination of stray electrostatic and magnetic fields,[1] particularly a-c fields, from the region occupied by the cathode-ray tube is very necessary for best performance.

[1] Sec. 16·4.

# CHAPTER 18

## SCREENS FOR CATHODE-RAY TUBES

By W. B. Nottingham

**18·1. General Introduction.**—All the cathode-ray-tube screens to be described in this chapter were designed for visual observation and are of two types: (1) light-emitting screens and (2) light-absorbing screens. These will be discussed in the order named.

*Luminescence and Phosphorescence.*—All luminescent materials useful as cathode-ray-tube phosphors emit light subsequent to the termination of the actual electronic excitation, as illustrated by Fig. 18·1. It is assumed that the electron excitation of the screen is constant over the period of time from $t_1$ to $t_2$ and is off until time $t_3$. Prior to $t_1$, there is no light output but, during the period $t_1$ to $t_2$, the light increases according to a curve that is characteristic of the type of phosphor used. As soon as the excitation is discontinued at time



Fig. 18·1.—The rise and fall of screen luminance under pulse excitation.

$t_2$, the light output starts to fall, and the light then emitted is called "phosphorescent light."

Screens are rated according to the persistence of phosphorescence as "short," "medium," and "long." In general, a short-persistence screen will have a period of phosphorescence comparable to the time required to excite the screen to a reasonably constant luminance level. This period may be as short as a few microseconds or as long as one millisecond. If the period of useful phosphorescence is greater than about twenty milliseconds and less than two seconds, the screen is considered to have medium or intermediate persistence. Useful luminance may be obtained from long-persistence screens for some minutes after excitation has ceased.

The precise nature of the rise of luminescence depends on the composition of the luminescent material, those details of manufacturing procedure which influence crystal size, the impurity content, and the method of excitation. The excitation may be by direct electron impact or by the absorption of light. Excitation of a phosphor by light in a

cathode-ray tube is generally associated with a multiple-layer screen, in which the layer bombarded by the electrons emits radiant power that is absorbed by the layer in contact with the inner surface of the tube face. This layer emits the light seen by the observer.

*Test Equipment.*—Three major pieces of test equipment have been used to study the screen properties described here. In the first[1] the screen is excited by accurately controlled pulses of electron current lasting from a few microseconds to 200 μsec, and occurring in sequences of 2 to 20 at 500 μsec intervals. An associated equipment was capable of measuring the radiant power as a function of the time, both during and after excitation. The data were recorded photographically.

This equipment was later supplanted by one in which the cathode-ray-tube screen was excited by a television-type raster generated by a high-speed horizontal sweep and a low-speed vertical sweep. By means of this pair of sweeps, a rectangular area of the cathode-ray-tube screen was excited by electrons in $\frac{1}{60}$ sec. Earlier investigation had shown that luminance measurements made a few tenths of a second after the excitation just described could be interpreted without detailed attention to the fact that one part of the screen had been excited 16 msec earlier than another part.

The third piece of equipment employed the raster method of exciting the screen but was very different in detail and was used to evaluate light absorption on the "dark trace" screen. The measuring procedure followed the plan of illuminating the tube face by suitably controlled lamps and then measuring directly on a pen-and-ink recorder[2] the decrease in reflectance that followed the electronic excitation of a small rectangular area on the tube face.

**18·2. Electronic Structure of Matter.**—Screen materials of particular interest may be grouped into four categories: (1) the silicates, (2) the sulfides, (3) the fluorides, and (4) the alkali halides, particularly potassium chloride. The most important sulphides are those associated with solid solutions of zinc sulfide and cadmium sulfide. A very brief and qualitative discussion of the nature of the electronic structure[3] of zinc and sulfur atoms and some of the electronic properties of the zinc sulfide crystals is given here.

[1] W. B. Nottingham, "Excitation and Decay of Luminescence under Electron Bombardment," RL Report No. 6-4S, Jan. 22, 1942.

[2] General Electric High-speed Photoelectric Recorder. Catalog No. 32C77, nearest equivalent described in GEA2394A as Model No. 8CEIGK27.

[3] G. Herzberg, *Atomic Spectra and Atomic Structure*, Prentice-Hall, New York, 1937.

N. F. Mott, and R. W. Gurney, *Electronic Processes in Ionic Crystals*, Clarendon Press, Oxford, 1940.

F. Seitz, *The Modern Theory of Solids*, McGraw-Hill, New York, 1940.

*Electronic Structure of Zinc Atoms.*—Of the 30 electrons associated with a normal zinc atom, 28 are in the K-, L-, and M-levels. The two remaining electrons are known as "valence electrons" and are associated with the N-level. If zinc is vaporized and then excited by intense heat or electron bombardment, radiant power that is largely concentrated close to a specific set of wavelengths is emitted.

Some of these wavelengths are in the ultraviolet, others are in the visible, and still others are in the infrared part of the spectrum. An analysis of these "spectrum lines" yields information concerning the electronic levels associated with the zinc atom which normally are not occupied by electrons, but which are available to hold electrons for very short periods of time in case sufficient energy is given to an individual atom to cause one of the valence electrons to make a transition from its normal state of lowest total energy to one of the excited states. The emission of radiant power is associated with the return of the atom as a whole to its normal unexcited state. The sharpness of the energy levels into which the electrons are able to go is a direct indication of the fact that the valence electrons cannot absorb energy of small and arbitrarily chosen amounts, but can absorb only relatively large steps of energy equal to those required to transfer the atom as a whole from one state of energy to another.

*The Electronic Structure of the Sulfide.*—The sulfur atom has a nuclear charge of 16 and is therefore surrounded by 16 electrons, of which two are in the K-shell, eight are in the L-shell, and six are in the M-shell. Thus, the valence of sulfur might be considered to be $-2$ since the M-shell has a particularly symmetrical configuration when it is accommodating eight electrons. Hence, in a crystal formed by a combination of zinc and sulfur, each atom of the former tends to yield its two valence electrons to fill the gap in the outer shell of sulfur. In the crystal there are normally just as many zinc atoms as there are sulfur atoms, and the crystal structure is such that each zinc atom is surrounded by four sulfur atoms and each sulfur atom is surrounded by four zinc atoms. The valence electrons are in a region of strong electric fields very different from those associated with the isolated atoms. Although some of the character of the original occupied and unoccupied levels of the atoms is still maintained, the fact that such a large number of electrons must be accommodated in a geometrical space so small compared with that available when the atoms were all separated gives rise to a new distribution of the occupied electronic energy levels which can be described better as occupied bands. It is one of the properties of a perfect crystal of zinc sulfide that the energy levels associated with the filled band are just sufficient to accommodate all the electrons and that there is a gap in the energy level system between the uppermost level of the filled band and the lowest level of the nearest unoccupied band.

*Electronic Band System.*—Figure 18·2*b* illustrates this band system in a very qualitative way.   In Fig. 18·2*a* the curved lines represent potential energy differences shown along the vertical scale as a function of the radial distance out from an individual atom in free space, whereas in Fig. 18·2*b* they show the potential as a function of the distance through a crystal with each atomic nucleus indicated by the plus sign.   Note that there are two classes of electronic levels, namely, filled levels and unoccupied levels, and that there is a gap in the system of levels in which there are no places available for electrons.   Insulating crystals are thus differentiated from conducting crystals, which differ from the system shown in Fig. 18·2*b* in that no gap exists between the occupied and the unoccupied levels.   Conductivity is associated with the ease with which electrons can be given a very small amount of energy from the external
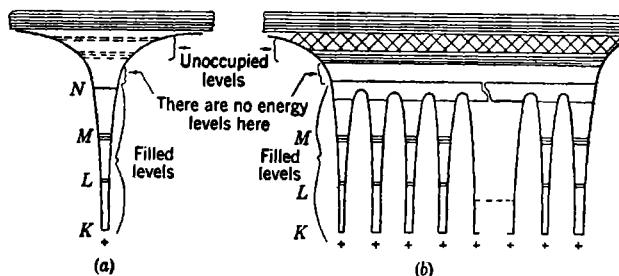


Fig. 18·2.—Idealized energy levels of a single atom and of an insulator.   (*a*) Single atom.
(*b*) Insulator.

field and caused to migrate through the lattice of the solid with very little resistance being offered by the presence of the atoms.   In the idealized crystal shown, there can be no electron conductivity unless, for some reason, electrons can be given sufficient energy to lift them from the filled band into the unoccupied or "conduction" band.   If such energy is given, then the crystal becomes electronically conducting.

No crystal is as perfect as the one illustrated in Fig. 18·2*b* because of the presence of irregularities and impurities in the lattice.   Even a minute excess of zinc atoms over the number required to be exactly equal to the sulfur atoms present can be considered to be an impurity in the zinc sulfide lattice.   The introduction of copper atoms or silver atoms may also make important modifications in the system of energy levels and thus alter the luminescent properties of the crystal.

*Impurity Levels.*—Three forms of irregularity are illustrated in Fig. 18·3 for nonionic crystals, such as the sulfide.   The irregularities of the first type, shown dark to indicate the presence of electrons in the "localized" states, are thought to be due to metallic impurities.   The second

type, shown schematically with an open circle to indicate the presence of vacant electronic levels, is associated with an excess of the nonmetallic element. The third type of localized impurity level assumes that a partially filled electronic level is available.

Consider now a few of the possible transitions that may be expected to take place in a solid characterized by all the features illustrated in Fig. 18·3. A convenient unit of energy is that associated with the displacement of an electron through a difference of potential of one volt. That unit of energy is known as "one electron-volt." The average kinetic energy associated with the motion of particles at room temperature is about 0.03 electron-volt (ev).

The difference in energy between the highest level of the filled band and the lowest level of the conduction band is likely to be 2.5 to 4 ev.
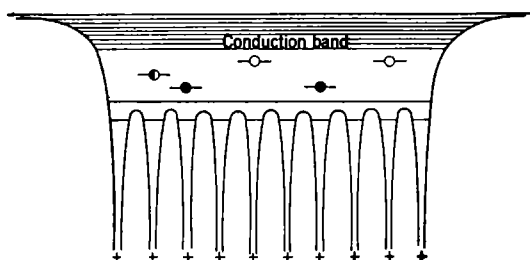


Fig. 18·3.—Electronic structure of an insulator with three types of localized impurity shown. Type 1 —●— impurity center with electronic states filled; type 2 —○— impurity center with unoccupied electronic states; type 3 —◐— impurity center with both filled and unfilled electronic energy level.

If high-energy electrons bombard a crystal, some of them deliver energy to the electrons in the filled band and excite them into the conduction band. Thus during the excitation and a short time thereafter, vacancies will exist in the filled band and mobile electrons will be found in the conduction band. In order for the electrons of the conduction band to return to the vacant levels, a sort of recombination process must take place. Such recombination without the aid of the so-called "trapping" states is, however, not particularly efficient.

*Electron and Hole Traps.*—The vacancies in the filled band have considerable mobility and are likely to be attracted to the impurity levels shown schematically as being of the type 1 in Fig. 18·3. These impurity levels yield electrons to fill the vacancies in the normally filled band and thus trap the vacancy, giving rise to a process known as the "trapping of the electron holes." This trapping of the electron holes is likely to

take place in a very short time and afterwards an electron from the conduction band can refill the hole by falling from the conduction band into the trapped hole. Associated with this transition, light is very often emitted.

Since an impurity atom in the presence of a lattice may be there in a variety of different ways, the impurity levels that are capable of trapping the holes, as just described, will probably not all be equally spaced with respect to the lowest level of the conduction band. As a consequence, the light emitted will not be confined to a narrow range of wavelengths but is likely to extend over a rather considerable range in wavelength depending on the distribution of the relative levels that constitute the hole traps.

It is also possible that in certain structures there may be localized impurity levels like that shown schematically as type 3. The implication here is that such an impurity level already has in it a hole capable of receiving an electron from the conduction band, and it may also be partially occupied so that it is capable of receiving another hole by delivering an electron from that localized state into the filled level whenever a deficiency has been produced there following excitation. It is impossible to show all the "dynamic features" of these various possible impurity systems since it is expected that, following each change in the population of electrons in the neighborhood of an impurity level, the level itself changes because of the local readjustment of the atoms in case the changed condition lasts long enough for the neighboring atoms to take up new equilibrium positions.

If the crystal contains impurity levels of the kind indicated as type 2, these may serve as traps for the electrons that have been excited into the conduction band. They are called "traps" because once an electron finds its way into such a localized level it is not easy for it to make a direct transition to the normally filled band or into a hole trap. During the time that the electron is finding its way to the electron trap, most of the holes of the filled band will have been occupied by transitions from impurity levels of the types 1 and 3. Thus the holes as well as the electrons will have been trapped. Associated with the trapping process, energy may be stored within the crystal and held for hours if the crystal is maintained at a very low temperature. Once an electron is trapped in a localized state of type 2, it is very improbable that it will make a transition out of that state without first being reintroduced to the conduction band. If the trapping state lies only a few tenths of an electron-volt below the lowest level of the conduction band, then even at room temperature there will be a finite probability that the electron will jump from the trapping level into the conduction band. In case this jump takes place, the electron is free to travel through the crystal until

it is again trapped in another high-level trap or in a low-level trap. There must be some tendency for the electrons to be attracted locally toward the "holes" because these are local centers of excess positive charge. The second alternative corresponds to a transition from the conduction band into one of the levels in which a hole is trapped and energy is emitted in the form of light.

*Excitation and Emission.*—The sequence of six sketches in Fig. 18·4 may be used to summarize this discussion. The normal state of the crystal is shown in block *a*. The excitation transition is shown in block *b*. Here an electron is lifted from the filled band into the conduction
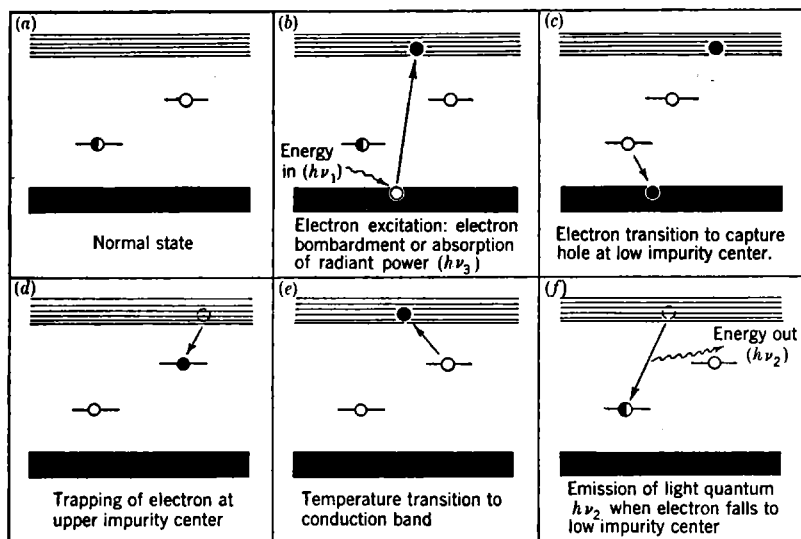


FIG. 18·4.—Block illustration of sequence of steps from excitation to phosphorescence.

band by the absorption of energy from a bombarding electron or from absorbed radiant energy. Block *c* shows the capture of the hole in the lower impurity center. Block *d* shows the capture of the electron in the upper impurity center. Block *e* shows the transition of the electron from the upper impurity center back to the conduction band as a result of a statistical fluctuation in the temperature energy. The absorption of energy from an infrared source or even from further electron bombardment constitutes another means of inducing the transition of block *e*. The final transition is that of block *f*, in which the electron falls from the conduction band into the lower impurity center with a consequent emission of light $h\nu_2$. It is evident from these diagrams that $h\nu_2$ will always be less than $h\nu_1$, which is the limiting quantum energy required to excite the phosphor.

The sequence of excitation and emission shown by Fig. 18·4 represents only one of the many possible sequences likely to be encountered in different luminescent materials. Innumerable experiments may be performed which will yield information concerning the electronic levels and the transition probabilities that determine the behavior of screen materials. Only a small fraction of these experiments has been performed and very few of them have been coordinated in such a way as to yield the information that is required concerning a single phosphor. The experimental results to be reported in this chapter are therefore inconclusive although they do contribute some new and useful information concerning the phosphors investigated.

*Surface Traps.*—It is not certain that all the upper trapping centers are confined to irregularities localized within the crystal at impurities of the type 2 such as would be associated with the presence in the lattice of a sulfur atom with only three zinc atoms in its immediate proximity instead of four. It has been suggested[1] that crystal surfaces are capable of trapping electrons. It is assumed that surface-trapped electrons have surface mobility so that they may interact on each other as would be the case for a two-dimensional "electron gas." The quantum theory of such a gas is analogous to the Fermi theory of electrons within a conductor. If this assumption is made and a calculation is carried through for the emission of radiant power in phosphorescence, theory and experiment are in reasonably satisfactory agreement. The agreement is not conclusive, however, for it is possible to postulate a suitable distribution of "volume" traps in contrast to the "surface" traps that would yield the same luminance-decay curve. The important point is that the experimental phenomena that have been observed demand that the trapping levels are not all of equal depth as expressed in the energy units required to reexcite an electron from a trapping center to the conduction band.[2]

*Nomenclature.*—There is general agreement concerning the use of the word "phosphorescence" to describe the luminance of the phosphor that is observed a considerable time after the cessation of excitation. The word "fluorescence" is likely to mean either one of two phenomena. The common use of the word is associated with the luminance of a phosphor during the period of excitation. A detailed consideration of the probable mechanism involved shows that internal electronic processes associated with phosphorescence contribute to the luminance of a phosphor even during the period of excitation. Therefore, it has been advo-

[1] Unpublished results of theoretical analysis by H. M. James of the M.I.T. Radiation Laboratory.

[2] J. T. Randall and M. H. F. Wilkins, "Phosphorescence and Electron Traps," *Proc. Royal Soc.*, **33**, 50 (May 20, 1940) (RC(C)22); **168**, 209 (March 30, 1941). G. F. J. Garlick and M. H. F. Wilkins, "Short Period Phosphorescence and Electron Traps," *Proc. Royal Soc.*, **303**, 328 (Feb. 29, 1944).

cated by Leverenz and others that the term "luminescence" be used to identify the luminance associated with the excitation period of a phosphor and that the word "fluorescence" be used to identify those processes in which the electron returns from the conduction band to a lower electronic level without first having been held in any sort of localized trapping center.  It is evident that, as thus defined, fluorescence may extend a short interval of time after the cessation of excitation, although the time element may be a fraction of a microsecond.  A clear distinction between fluorescence and luminescence is made so seldom that it may be necessary to misuse the word fluorescence in this chapter on occasion, in order not to confuse readers who have firmly associated with the word its more general meaning rather than its specific meaning.  The word luminescence will be applied in the strict sense in which it is defined as being associated with the emission of light during the actual period of excitation. This use avoids the necessity of distinguishing between the fluorescent process and the phosphorescent process as being responsible for the luminance observed during the excitation period.

*Spectral Absorption.*—Investigation of the spectral absorption and emission characteristics of phosphors yields information important to the understanding of the electronic processes involved in the excitation of phosphors.  It is, however, difficult to perform experiments that give good quantitative information.

Crystals of all phosphors show absorption in the violet and ultra-violet part of the wavelength spectrum.  The absorption curves[1] for three phosphors of interest are shown in Fig. 18·5a.  The curve for zinc sulfide shows a maximum in the relative absorptance at approximately 320 m$\mu$ and a long-wavelength threshold in the absorptance at approximately 440 m$\mu$.  The location of the threshold has not been accurately determined, but in terms of the models described in the previous section, the threshold may be interpreted measuring the energy difference between the highest occupied level of the electron band and the lowest unoccupied level of the "conduction band."  This energy difference is approximately 2.8 ev.  It is possible that the 2.8 ev represents the difference in level between an occupied impurity state and the conduction band.  An investigation of the details of the absorption characteristic in the neighborhood of the threshold could answer such a question.  The peak in the absorption is a measure of the energy most likely to be absorbed and probably gives the order of magnitude of the energy difference between the middle of the normal occupied band and a part of the conduction band to which transitions are most easily made.  In the case of zinc sulfide, this energy difference is approximately 4.0 ev.

[1] H. W. Leverenz, "Research and Development Leading to New and Improved Radar Indicators," NDRC 14-498, RCA, June 30, 1945.
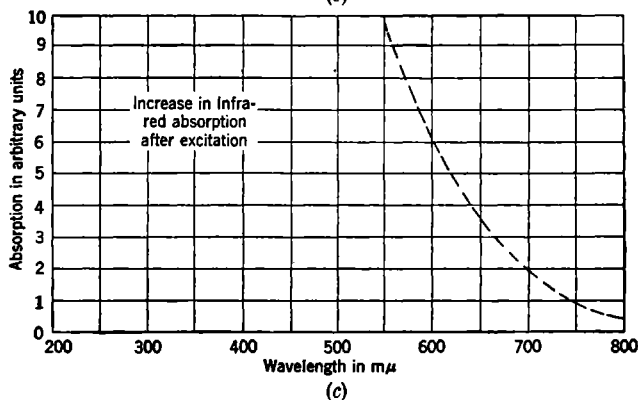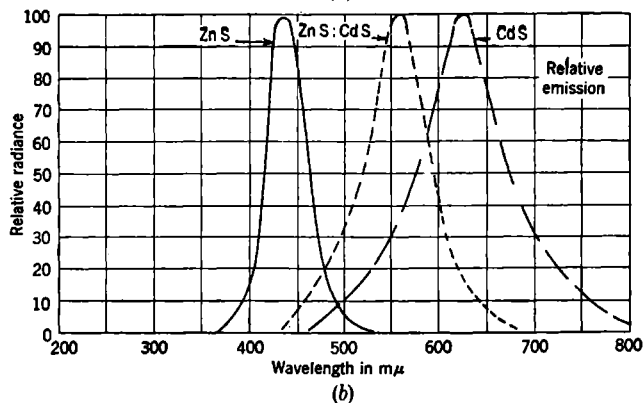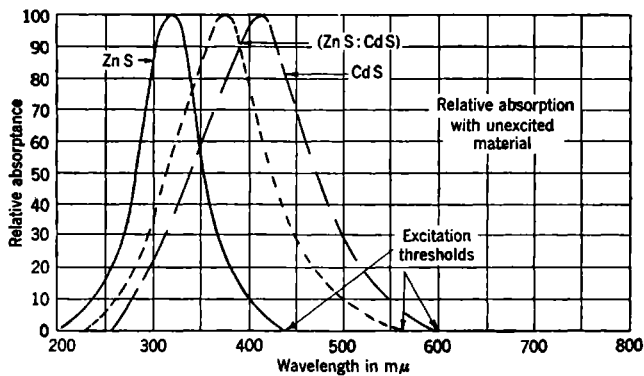
FIG. 18·5.—Absorption and emission curves for sulfide phosphors. (a) Relative absorption bands for zinc and cadmium sulfides. (b) Relative emission bands for zinc and sulfides. (c) Assumed increase in infrared absorption after electronic excitation of a long-persistent sulfide phosphor.

Crystals of cadmium sulfide are very similar in structure to those of zinc sulfide, as would be expected since the cadmium atom bears a close resemblance to the zinc atom with the exception that there are 48 electrons required to balance the nuclear charge on the cadium nucleus and the two valence electrons are in the O-shell instead of the N-shell. In either zinc or cadmium, the electronic structure of the shell just inside the valence shell is one that accommodates 18 electrons. As a consequence of the need to accommodate more electrons, the interatomic spacing in the cadmium sulfide crystal is 7 per cent greater than that of the zinc sulfide crystal.

The energy levels of the zinc and cadmium atoms are very similar in general structure, with the actual energy differences somewhat less throughout for cadmium than for zinc. It is therefore to be expected that a cadmium sulfide crystal would have energy bands, both occupied and unoccupied, similar to those of zinc sulfide, and that the differences in energy between corresponding bands would in all probability be less for cadmium sulfide.

Since the structures of these sulfides are so nearly the same, it is possible to have "solid solutions" of almost any proportions from 100 per cent zinc sulfide to 100 per cent cadmium sulfide. As the proportion of cadmium sulfide increases, the lattice constants increase almost linearly in proportion to the atomic fractions of the two constituents, zinc and cadmium. The absorptance and the emission properties change in the way that is qualitatively illustrated in Figs. 18·5a and 18·5b.

*Glow Curves and Infrared Excitation.*—Two types of experiment in addition to those already mentioned yield information concerning the electronic transitions after the phosphor has been excited (see footnote 1, page 623). The first shows that, at the temperature of liquid nitrogen (78°K), there is almost no phosphorescence, but that, as the temperature increases, the crystal becomes luminous. At the present time such experiments are only qualitative. Quantitative observations of the luminance as a function of the temperature and the time would yield significant data that might be analyzed to give information concerning the distribution of the electron-trapping levels in crystals prepared to have specific structural properties and impurity content. The second class of experiment shows that the decay of luminance at a particular temperature is accelerated if the crystal is irradiated by power associated with wavelengths longer than the threshold for excitation. For example,[1] the luminance of a phosphor may be observed quantitatively to be falling with time along a certain reproducible line, as indicated in Fig. 18·6. The line $a$-$a'$ represents the normal decay characteristic after a specific

[1] H. E. Ives, and M. Luckiesh, "The Effects of Red and Infra-red on the Decay of Phosphorescence in Zinc Sulfide," *Astrophys. Jour.*, **34**, 173 (1911).

excitation at a specific temperature.   If the phosphor is irradiated by an infrared source beginning at the time $t_1$, then the luminance rises suddenly to a sharp maximum indicated at $b$, after which it falls very rapidly to $b'$, which may be only a very small fraction of the luminance that would have been present at the time $t_2$, had the infrared exposure been absent. The enhancement of phosphorescence in the presence of infrared has been of much practical and theoretical interest.   It would be of interest to try to observe an increase in the spectral absorptance factor in the infrared as a function of the wavelength and the degree of excitation of the phosphor crystal, but such experiments have not been performed in detail.   In view of the general observation that the shorter the wave-



length of the infrared used to stimulate phosphorescence the more effective it is, it might be assumed that the increase in infrared absorptance after excitation would follow a curve like that of Fig. 18·5c.   On the other hand, it would be worth investigating in more detail with the phosphor at a low temperature because it might be possible to get new information on the energy levels into which the electrons have become trapped and the transition probabilities associated with the removal of the electrons from the traps into the conduction band.

Fig. 18·6.—Influence of infrared energy applied at $t_1$ on phosphorescent decay.

**18·3. Screen Transmittance and Absorptance.**—It is evident from a comparison of Figs. 18·5a and 18·5b that sulfide crystals are fairly transparent to their own emission spectra.   Practical cathode-ray-tube screens are usually prepared by depositing millions of individual crystal grains onto the glass face-plate surface by a suitable manufacturing procedure.   The most commonly used method for the sulfides is that of allowing the crystals of material to settle from a liquid suspension under the influence of gravity.   This method produces a very uniform screen with the larger crystals in direct contact with the glass and the smaller ones, which settle somewhat later in time, filling in the interstices between the larger crystals.   The excitation of a screen of this kind by the absorption of radiant power is a maximum at the surface that first receives the incident irradiance.   Figure 18·7 shows qualitatively a much magnified section of the coating of screen material on a glass surface as though the coating were actually a two-layer system of crystals.   The irradiant flux per unit area decreases as a function of the distance through the polycrystalline screen, as indicated in the sketch above the crystalline section

shown.    The two factors largely influential in determining the decrease in radiant flux are (1) the multiple and diffuse scattering that takes place at the crystal boundaries and results in a considerable back reflection of the incident radiant flux and (2) the absorption of the radiant flux as it is propagated through individual crystals and is absorbed in the excitation process.    The general shape of this curve indicates that the volume concentration of excitation will be more or less proportional to the radiant flux present at each depth within the screen structure.    Luminescence or phosphorescence, as the case may be, will have a volume distribution determined by the exciting irradiant flux density, but the observer who is interested in the luminance of the surface as seen through the glass must consider the attenuation of the light as it is transmitted through the screen material.    Luminance that originates near the glass surface is transmitted more efficiently than that originating deeper in the screen material as is shown by the transmissivity diagram in Fig. 18·7.



FIG. 18·7.—Magnified sectional view of a luminescent screen on glass.  Curves show decrease in exciting irradiance with penetration distance and change in transmissivity of emitted radiance at various distances from glass.

The quantitative data shown in Figs. 18·8 and 18·9 apply to phosphors of the zinc sulfide–cadmium sulfide family.    Screens were prepared in the usual way using proportions of these phosphors in sufficient quantity to put 5, 10, and 15 mg/cm² onto the different face plates, and the main body of the blank was removed after the screens were completely processed so that spectral transmission curves could be obtained.    Figure 18·8a shows the three curves that apply for 7 per cent cadmium sulfide, and Fig. 18·8b shows the three curves that apply for 25 per cent cadmium sulfide.    These curves indicate that the threshold of the absorption band is close to 490 mµ for Fig. 18·8a and 530 mµ for Fig. 18·8b.

Among the phenomena which influence the transmissions are the reflections occurring at the two phosphor surfaces and the two glass surfaces, and the absorption in the glass.    These effects are independent of the thickness of screen material for the range of thicknesses included in the experimental data.    The transmission is also affected by the diffuse

scattering at the crystal boundaries within the screen itself and by the optical absorption within the individual crystals. These effects depend on thickness in such a way that there is a linear relationship between the logarithm of the transmittance and the screen thickness as shown for the selected wavelengths specified in Figs. 18·9a and 18·9b. The fact that all three straight lines on each figure extrapolate back to a common
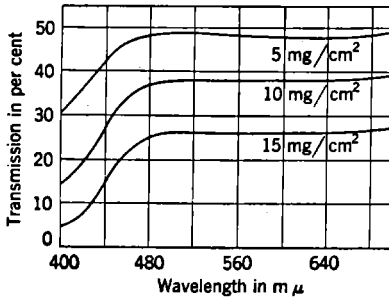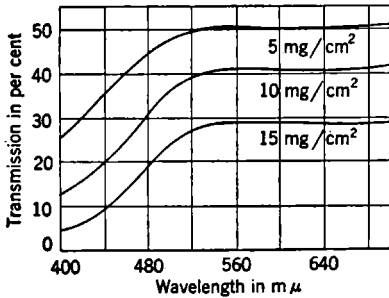


Fig. 18·8.—Spectral transmissivities of two phosphor types and three screen thicknesses. (a) (93)ZnS:(7)CdS:Cu. (b) (75)-ZnS:(25)CdS:Cu.
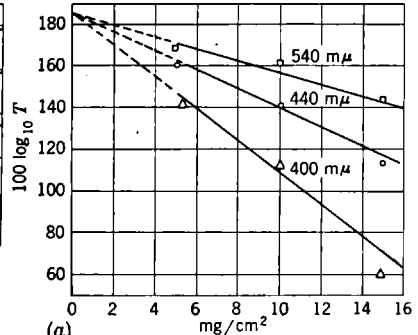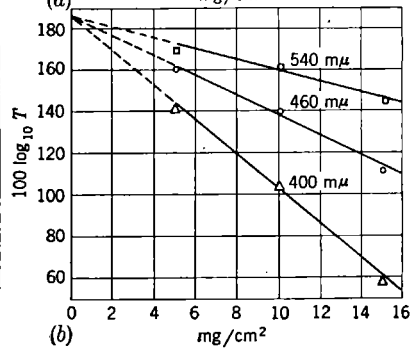
Fig. 18·9.—Plots to determine absorption coefficients at wavelengths shown for two screen materials. $T$ is the transmission in per cent. (a) (93)ZnS:(7)CdS:Cu. (b) (75)ZnS:(25)CdS:Cu.

value of 71 per cent at zero thickness is of considerable interest. If the transmission of the glass is assumed to be 86 per cent when two reflection surfaces and the absorption in the thick face plate are allowed for, then a diffuse reflectance at each surface of the phosphor of approximately 8·5 per cent will account for the observed over-all transmissivity.

For normal screen thicknesses of approximately 10 mg/cm², the light emitted from crystals farthest away from the observer will probably suffer an attenuation of approximately 50 per cent in comparison with

the light emitted from the crystals nearest the observer. The nonuniformity of excitation must be considered since, if the excitation is by means of absorbed radiant power (although the most effective radiant power is no doubt in the ultraviolet range, not shown in Fig. 18·9), the excitation density in the crystals farthest from the observer will be greater, by a factor of 10 or more, than that of the crystals near the observer.

*Optimum Screen Thickness.*—These considerations make it evident that for any given case there must be an optimum thickness of screen coating material for the production of cathode-ray tubes of maximum luminance output per unit of excitation energy. This optimum thickness will depend on the duration of excitation, the time after excitation at which observations are made, the details of the excitation cycle, and the magnitude of the excitation. If these factors can be specified, the screen thickness for optimum performance can be easily determined. If a tube is to be designed to fit a very wide range of excitation conditions, however, it is more difficult to choose the best screen thickness for optimum over-all performance.

Since most instruments for measuring the luminance of a cathode-ray tube do not differentiate between the contributions from the crystals near the measuring equipment and those from the crystals that are more highly excited but farther away, it is evident that a theoretical analysis of decay of luminance, or radiance, with time, will not be easy. Over certain ranges of excitation, a factor of 10 plays a very important part in determining the precise nature of the decay characteristics.

**18·4. Excitation by Pulsed Light.**—In the double-layer cathode-ray-tube screen (see Sec. 18·9), the radiant excitation enters the screen material from the side that is opposite to the one viewed. Researches may be made, however, on screens in such a manner as to minimize the nonuniformity of the excitation by irradiating the crystals to be excited from the same side as they are viewed. Also, a filter can be used ·to confine the exciting radiation to wavelengths fairly near the threshold wavelength and thus reduce the absorption. Since it is by means of the absorption that the crystals are excited, a practical balance must be achieved between the intensity of the exciting radiation and the degree to which the crystals are to be excited.

The two sets of data presented in Fig. 18·10 show the buildup of radiance[1] of various cathode-ray-tube screens as a function of the number

---

[1] Throughout this chapter, radiance is expressed in logarithmic units, the unit employed being the "centibel" (abbreviated cb). This unit is defined by the equation $100 \log_{10} (P_1/P_2) = \Delta$ cb. The zero level of the centibel scale was arbitrarily set at $10^{-15}$ w $\times$ cm$^{-2}$ $\times$ m$\mu^{-1}$. For cathode-ray-tube screens having a wavelength distribution similar to that of P7 screens (see Fig. 18·32) the conversion between radiance

of repeated excitations by radiant energy. The upper set of curves applies to measurements of radiance taken 1 sec after each application of the excitation, whereas the lower set of curves shows the radiance 10 sec after each application of excitation. The time interval between excitations was 10 sec for both sets. For all the data shown, the exciting irradiance per excitation was held constant. In the plots shown the horizontal and vertical scales are so proportioned that, if the radiance increases in direct proportion to the number of pulses applied, the slope of the curve drawn through the experimental points will be unity. Thus the slopes greater than 45°, which are particularly prominent in phosphor 2005 for the 10-sec observations, indicate that four times as much radiance is observed after the second pulse as is observed after the first pulse.



FIG. 18·10.—Buildup under excitation by radiant energy of various relative levels. Screen excited at 10-sec intervals, with observations at 1 sec and 10 sec after each excitation.

TABLE 18·1.—CHARACTERISTICS OF VARIOUS PHOSPHORS

| Code | EX | Weight, mg/cm$^2$ | Composition | Description of phosphor |
|---|---|---|---|---|
| 21 | EX1921 | 14.4 | (85)ZnS:(15)CdS:Cu | P7 yellow component |
| 22 | EX1922 | 24.4 | (85)ZnS:(15)CdS:Cu | P7 yellow component |
| O2 | EX2002 | 14.4 | (100)ZnS:Ag | P7 fluor |
| O4 | EX2004 | 14.4 | (77.5)ZnS:(22.5)CdS:Cu | Orange phosphor |
| O5 | EX2005 | 14.4 | (75)ZnS:(25)CdS:Cu | Deep orange phosphor |
| O6 | EX2006 | 14.4 | (93)ZnS:(7)CdS:Cu | Blue-green phosphor |
| P7 | ........ | .... | (88)ZnS:(12)CdS:Cu | P7 screen |

The increase in radiance after approximately twenty excitations is very small, but it is measurable for practically all phosphors up to fifty

expressed in centibels and luminance expressed in foot-lamberts or equivalent foot-candles ($B$) is

$$B = 2.27 \times 10^{-6} \times 10^{cb/100}.$$

For further details, see W. B. Nottingham, "Notes on Photometry, Colorimetry, and an Explanation of the Centibel Scale," RL Report No. 804, Dec. 17, 1945.

excitations.   In some cases hundreds of excitations are required before the observed radiance no longer increases.

The copper-activated zinc sulfide–cadmium sulfide phosphor with 25 per cent cadmium sulfide (EX2005 in Table 18·1) was studied in some detail, to determine the influence of the intensity of the irradiance on the buildup characteristic over a total range approximately 20 to 1.   In order to establish the irradiance level used to excite this screen, a freshly prepared magnesium oxide surface was substituted for the fluorescent screen, and measurements were made of the integral of all the photoelectric current produced at the cathode of a 931 multiplier phototube as a result of its irradiation by the light from the magnesium block.   The absolute intensity values associated with each curve have no particular significance, although the differences indicated are an accurate measure of the *relative* energies associated with each excitation represented.   Figure 18·11 shows the buildup of radiance in the 2005 screen as a function of the number of excitations at the different irradiation levels shown and observed 1 sec after each excitation.   The time interval between excitations is 10 sec.   Measurements of the buildup observed
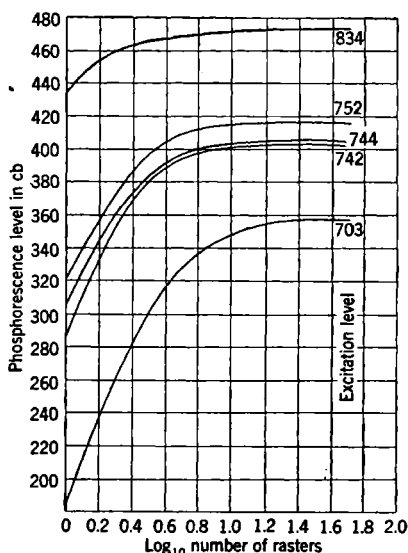


FIG. 18·11.—Buildup under excitation by radiant energy of various relative levels. Tube No. EX2005, Phosphor: (75)ZnS: (25)-CdS:Cu, deep-orange emission.   Screen excited at 10-sec intervals, with observations 1 sec after each excitation.

10 sec after excitation are shown in Fig. 18·12.   Again the scales are so chosen that linear increases in radiance with pulse number show as a slope angle of 45°.   The words "superproportional" and "subproportional" are associated with slopes respectively above and below 45°. At the lowest level of irradiance, shown in Fig. 18·11, superproportionality continues up to five excitations.   When the observations are made 10 sec after each excitation, superproportionality continues up to nine excitations.   In both cases, the higher the excitation level, the quicker subproportionality sets in.   Double-layer cathode-ray-tube screens that are constructed according to procedures that give perfect separation of the two layers of the phosphor are certain to exhibit characteristics similar to those of Figs. 18·11 and 18·12.

**18·5. Persistent Screens in Radar Displays.**—For many types of operation, particularly those in which long persistence is needed, screens that are excited by radiant energy using the cascade principle have advantages over those excited directly by electrons.   The most satisfactory long-persistence screens seem usually to exhibit at least some superproportionality but this may be a related and not a causal phenomenon.   In any case the observational effects of superproportionality are not well understood.
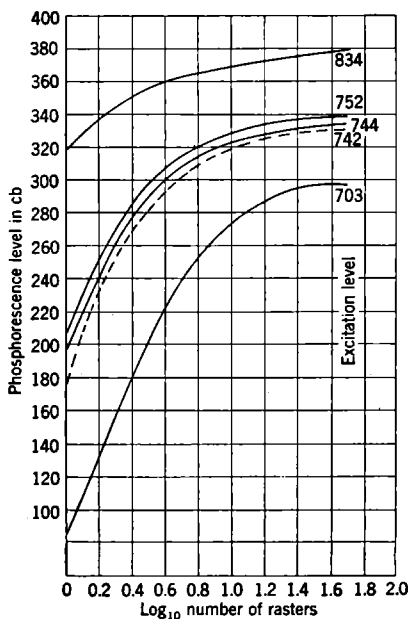


FIG. 18·12.—Buildup under excitation by radiant energy of various relative levels. Tube No. EX2005, Phosphor: (75)ZnS:(25)-CdS:Cu, deep-orange emission.   Screen excited at 10-sec intervals, with observations 10 sec after each excitation.

Although the cascade screen has found its greatest usefulness in intensity-modulated displays requiring long persistence it was originally applied as an aid in detecting signals on an A-scope, particularly in the presence of man-made interference (jamming).   Many types of interference are met with but nearly all are characterized by the fact that the jamming signals are not synchronized with the radar set and therefore have no fixed pattern on a display involving range. The benefit derived from the persistent screen is, therefore, due to the fact that through its integrating or averaging properties it assists the operator in distinguishing a signal that appears at the same position on each sweep. Particularly in the presence of certain forms of strong pulsed interference the benefits derived are extremely great.

The use of a cascade screen in an A-scope sometimes also results in an enhancement of the signal-to-thermal-noise discernibility.   If the signals dealt with are very weak, the receiver gain must be set so high that random displacements of the electron beam occur at all points along the range sweep.   If averaged over a long time, these fluctuations will, in the absence of a signal, give rise to a continuous band of luminance on which is superposed the bright flash of the electron beam as it sweeps across the tube face.   If a moderately strong signal is present, the average vertical position of the band will be appreciably higher at the range of the signal

than at other points, a fact that is easy to recognize even without long-time averaging.   If, however, the signal is very weak, its principal effect is an enhancement of the average luminance at the position of the signal. As stated in Chap. 1, a practiced operator is able to perform visual and mental averaging processes over periods of several seconds and thereby detect very weak signals by virtue of this change in luminosity even when using a short-persistence tube.   It has been found, however, that in certain cases the ability to recognize such a weak signal is slightly enhanced by the use of selected tubes having long-persistence cascade screens. Only a small fraction of the cascade-screen cathode-ray tubes made for use as A-scopes showed the enhancement of luminance at the location of a weak signal to a sufficient degree to be particularly noteworthy as a means of distinguishing between the signal and the noise unless, shortly after the A-scope had been operating for a few seconds, the electron beam were cut to zero and the observer made the evaluation on the basis of phosphorescence only.   Such tubes were described as having a significant degree of "smoothing," and experiments indicated that, for these, an improvement in signal-to-noise discrimination of about 3 db was likely and, indeed, a maximum improvement of 6 db has been reported.   The particular physical properties of the screen that exhibited this improvement were never identified.   The indications were that the phenomenon of superproportionality was necessary but not sufficient to insure success.

In the United States, in the development of the cascade screen, the emphasis was placed upon its use in intensity-modulated displays, rather than in A-scopes, since the detection of weak signals on the latter is relatively unimportant in modern equipments.   In intensity-modulated displays, especially those associated with slow scanning rates, cascade screens are superior to single-layer screens because of their reduced initial flash and their increased luminance at relatively long times after excitation.   The assistance in detecting weak signals that can be derived from the integrating properties has been discussed in Sec. 1·11.   Direct experiments have failed to show any benefits deriving directly from the phenomenon of superproportionality, but this phenomenon is without doubt intimately associated with those properties that do make this type of screen superior.   Operational and physiological investigations have not been sufficiently well coordinated with the physical properties of the cathode-ray-tube screens themselves to permit clear understanding of the really significant features that should be developed to yield an improvement in the performance of a specific radar indicator.

**18·6. Some Electrical Properties of Screen Materials and Glass.—** Cathode-ray-tube screen materials are generally very poor conductors at the temperatures at which they normally operate.   To deliver an

electron current to the cathode-ray-tube screen, an *exactly* equal number of other electrons must be removed from the screen, in order that it not charge up negatively and finally stop the continued arrival of electrons. The fact that the secondary electrons leave with a very much lower average kinetic energy than that of the primary ones means that the difference in energy is supplied to the screen material and must be dissipated as radiant power or conducted away as heat.

High-energy electrons that strike crystals of the phosphor penetrate a considerable number of interatomic distances before they have lost all of their kinetic energy. If the electrons within the crystal are distributed as shown in schematic form in Fig. 18·4a, the arrival of a high-speed electron within the crystal can be expected to give rise to a large number of transitions comparable with that shown in Fig. 18·4b. Although the minimum energy that is absorbed by one of the electrons in the normally filled band is probably 2.5 to 3 ev, it is more probable that an energy of about 10 ev will be absorbed and a great many electrons may absorb even as much as 25 or 30 ev. Those with high energy which are excited within a few atomic distances ($10^{-7}$ cm) of the surface are likely to escape from the crystal into the evacuated space. For Pyrex glass, two or three electrons are ejected from the surface of the glass[1] for each bombarding electron that arrives with an energy of 400 ev. Although measurements have not been made on zinc sulfide or cadmium sulfide crystals, it is almost certain that at least four or five electrons are ejected from the crystal for each electron that bombards the screen. On the average, only one of the four or five electrons ejected reaches the anode coating used to collect the secondary electrons.

All the electrons that are excited are considered to be secondary electrons. Those that escape may be classified as external secondary electrons and those that remain within the crystal are classified as internal secondary electrons. For each internal secondary electron, there is a hole in the normally occupied band which will diffuse through the crystal until it is captured, as was explained in connection with Fig. 18·4c. Prior to the capture of either the hole or the secondary electron, they diffuse through the crystal with equal average velocities. Any tendency for either the holes or the electrons to diffuse at different velocities is counteracted by the electric forces of attraction that exist between them.

*Penetration of High-energy Electrons.*—Theoretical considerations lead to the conclusion that the electron penetration into a solid substance is proportional to the square of the kinetic energy of the bombarding electron. For practical purposes, the kinetic energy may be taken to be directly proportional to the difference in potential between the anode

[1] C. W. Mueller, "Secondary Electron Emission of Pyrex Glass," *Jour. App. Phys.*, **16**, 453 (1945).

and the cathode of a cathode-ray tube. Leverenz[1] has computed the proportionality constant that relates maximum range to the electron energy. These constants of proportionality are lised in Table 18·2. The maximum penetrations computed for 4000-volt electrons are shown in

TABLE 18·2.—THEORETICAL PENETRATION OF 4000-VOLT ELECTRONS FOR VARIOUS PHOSPHORS

| Phosphor | $a$ | $x_{4000}^*$, m$\mu$ |
|----------|-----|------------------|
| $Zn_2SiO_4$ | $25.0 \times 10^{-6}$ | 400 |
| $Be_2SiO_4$ | 26.8 | 429 |
| $CaWO_4$ | 24.6 | 394 |
| ZnS | 28.3 | 452 |
| CdS | 32.4 | 519 |
| $ZnF_2$ | 22.8 | 365 |
| KCl | 46.5 | 744 |

* Theoretical maximum penetration distances $x$ expressed in m$\mu$ by formula: $x = aV^2$ where $V$ is electron energy in ev.

Column 3. For zinc sulfide, the maximum penetration is thus competed as 452 m$\mu$. If one considers the interatomic spacing found in most of these crystals, it is evident that 4000-volt electrons penetrate approximately 1000 atom diameters. As a very rough approximation, it may be assumed that the number of internal electrons produced per unit of pathlength is more or less constant and independent of the primary electron energy. This statement is based on the observed relationship between the radiance produced in a phosphor and the electron energy. In most cases studied, the radiance increases with the square of the voltage. There are some examples in which the "square law" is very accurately the best representation of the experimental results.[2]

*Insulator and Screen Potentials.*—For all cathode-ray-tubes, some consideration must be given to the "sticking" or "limiting" potential of all insulating surfaces that are likely to be bombarded by electrons. In Fig. 18·13 the difference in potential between the phosphor and the second anode is plotted as a function of the anode potential for a $Zn_2SiO_4$ phosphor. Above 6000 volts, a difference in potential between the screen

[1] H. W. Leverenz, "Problems Concerning the Production of Cathode-ray-tube Screens," *J.O.S.A.*, **27**, 25 (1937); and H. W. Leverenz, "Final Report on Research and Development Leading to New and Improved Radar Indicators," NDRC 14-498, p. 128, June 30, 1945.

[2] W. B. Nottingham, "Electrical and Luminescent Properties of Willemite under Electron Bombardment," *Jour. App. Phys.*, **8**, 762 (1937).

W. B. Nottingham, "Electrical and Luminescent Properties of Phosphors under Electron Bombardment," *Jour. App. Phys.*, **10**, 73 (1939).

S. T. Martin and L. B. Headrick, "Light Output and Secondary Emission Characteristics of Luminescent Materials," *Jour. App. Phys.*, **10**, 116 (1939).

and the anode develops and continues to rise in such a way as to indicate that the screen potential is not changing, even though the anode potential continues to increase. This behavior arises from the fact that for the particular phosphor studied 6400-volt electrons produce on the average just one *external* secondary electron for each primary electron.

The maximum potential at which at least one external secondary is produced per primary electron is dependent both upon the phosphor material itself and upon the condition of its surface. It is possible to influence the secondary emission by covering the surface with a very thin layer of electropositive material, such as barium "getter," and in that way to increase the sticking potential. Calcium tungstate ($CaWO_4$) has the lowest sticking potential (4000 volts) of all phosphors that have been investigated quantitatively. The sticking potential of clean
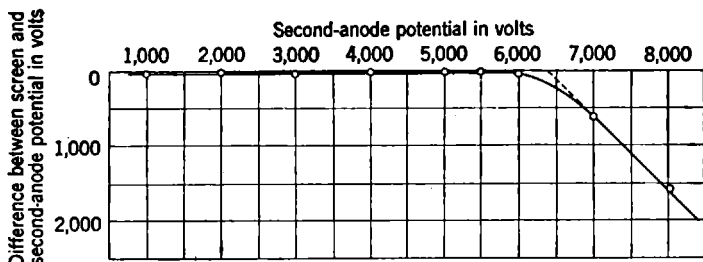


FIG. 18·13.—Screen-to-anode potential as a function of the second-anode potential. Willemite $ZnSiO_4$: Mn. [*Courtesy of J. Appl. Phys.*, **8**, 762 (1937).]

willemite ($Zn_2SiO_4$) is approximately 6500 volts. Although Martin and Headrick[1] have reported zinc sulfide sticking potentials as low as 7 kv, no examples of sticking potentials below 10 kv were observed at the Radiation Laboratory. The sticking potential can be determined by investigation of the dependence of the luminescence on anode voltage or by an examination of the raster distortion or lack of raster compression that is associated with the maintenance of constant sweep fields and the increase in the anode voltage. Both methods, although indirect and not very accurate, seem to be sufficient for the discovery of any major difficulty that may arise from an insufficiency in the yield of external secondary electrons.

Mueller's[2] measurements of the secondary emission from Pyrex glass show that its potential must be close to 2500 volts. The sticking potentials for most glass surfaces likely to be used in cathode-ray tubes will probably not exceed 3 or 4 kv. In some cathode-ray tubes a considerable length of uncoated glass is permitted between the anode coating

[1] S. T. Martin and L. B. Headrick, *op. cit.*

[2] C. W. Mueller, *op. cit.*

nearest the face plate and the screen itself.    If the magnitude of the
electron sweep is sufficient to drive the electron beam out to the glass
wall, then it would seem that there would be a tendency for this surface
to become very negative with respect to the anode.    The fact that no
trouble from this source has ever been reported probably depends upon
two factors.    The first consideration is that the quoted sticking poten-
tials apply to glass bombardment
with normal incidence, and the
secondary-emission yield resulting
from bombardment with grazing
incidence is higher than that ob-
tained with normal incidence.
This effect would go far to mini-
mize the likelihood of finding the
glass wall some thousands of volts
more negative than the anode
when high-voltage operation is
attempted.    The second factor is



FIG. 18·14.—Buildup under repeated elec-
tron excitation.    Screen excited at 10-sec
intervals, with observation 1 sec after ex-
citation.    $Q = 20$ m$\mu$c/cm$^2$ per raster.    See
Table 18·1 for screen compositions.

the influence of the surface and volume conductivity of the glass, in the
sense that if the number of electrons that strike the glass per unit area is
small, the actual surface and volume conductivity may play a useful part
in the discharge of the uncoated area.    There is also a possibility that
enough sulfide sticks to the uncoated glass to alter its secondary emission.



FIG. 18·15.—Buildup under repeated elec-
tron excitation.    Screen excited at 10-sec
intervals with observations 10 sec after each
excitation.    $Q = 20$ m$\mu$c/cm$^2$ per raster.
See Table 18·1 for screen compositions.

**18·7. Single-layer Sulfide
Screen Excited by Electrons.**—
Extensive studies have been made
of the luminescent and phospho-
rescent properties of single-layer
zinc sulfide and zinc sulfide–
cadmium sulfide screens during
and after excitation by electrons.
Figures 18·14 and 18·15 illustrate
the buildup of phosphorescence
that results from repeated appli-
cations of raster excitation[1] on six
different single-layer screens.
The curves of Figs. 18·14 and

18·15 for electron excitation are very similar in character to those
shown in Fig. 18·10 for excitation by light and apply to the same
phosphors.    Although there are small differences between the results

[1] The charge density per unit area per raster or per excitation is the determining
factor that governs the excitation if the time at which the observation of phosphores-
cence is made is long compared with the time used to excite the screen

obtained on the different phosphors, all the former curves are uniformly less steep than those of Fig. 18·10.   Before the physical explanation for these properties is discussed, it would be well to examine the decay that follows electron excitation.

*Phosphorescent Decay.*—Figures 18·16 to 18·21, inclusive, show the change in phosphorescence as a function of the time following the last of a series of either electronic or radiant excitations.   Observations apply
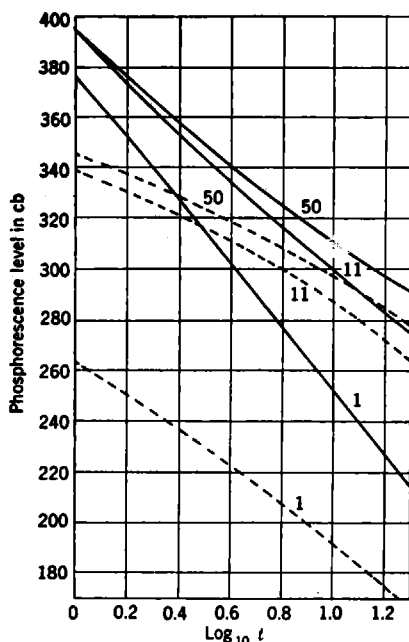


FIG. 18·16.—Phosphorescent decay after radiant—or electronic—excitation.   Yellow component of P7 screen (85)ZnS:(15)CdS:Cu.   Screen thickness 14.4 mg/cm².   Time *t* in seconds.

to phosphorescence following 1, 11, or 50 excitations.   The time of observation extends from 1 to 20 sec.   In the first five figures, the data for electronic excitation are shown as solid lines, and the dashed lines show the results following excitation by radiant energy.   The coordinate scales are so chosen that the slope of the curve at any time is the exponent S of the inverse time decay law that may be used to represent any small segment of the actual decay curve.

*Decay Laws.*—The first type of decay is generally known as "monomolecular" decay and is associated with conditions in which the number of transitions that take place per unit of time is directly proportional to

the number of active particles.   Thus if $n$ is the number of electrons in a conduction level,

$$\frac{dn}{dt} = -\alpha n. \tag{1}$$

The further assumption is made that the phosphorescence observed at
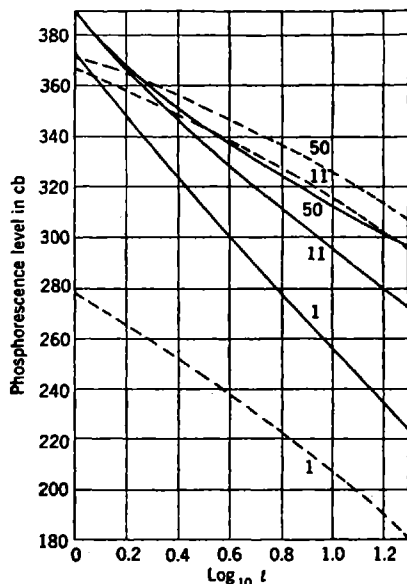


FIG. 18·17.—Phosphorescent decay after radiant—or electronic—excitation.   Yellow component of P7 screen (85)ZnS:(15)CdS:Cu.   Screen thickness 24.4 mg/cm².   Time $t$ in seconds.

any particular time is directly proportional to the time rate of change of electron population in the conduction band:

$$P = -c\frac{dn}{dt}. \tag{2}$$

The method of plotting experimental data is that in which a number proportional to the logarithm of the phosphorescence $P$, which may be denoted as $(cb)_P$, is plotted as a function of the logarithm of the time.   It follows from Eq. (2) that the slope of such a logarithmic curve is given by Eq. (3) or simply by Eq. (4).

$$\frac{d(\log_{10} P)}{d(\log_{10} t)} = \frac{d(\log_{10} n)}{d(\log_{10} t)} = \frac{t}{n}\frac{dn}{dt} \tag{3}$$

$$\frac{d(\log_{10} P)}{d(\log_{10} t)} = -\alpha t. \tag{4}$$

The reciprocal of $\alpha$ is defined by Eq. (5) as $\bar{t}$.

$$\bar{t} = \frac{1}{\alpha}. \tag{5}$$

The tangent to the curve plotted as described would have a slope of $-1$ at the time $\bar{t}$.
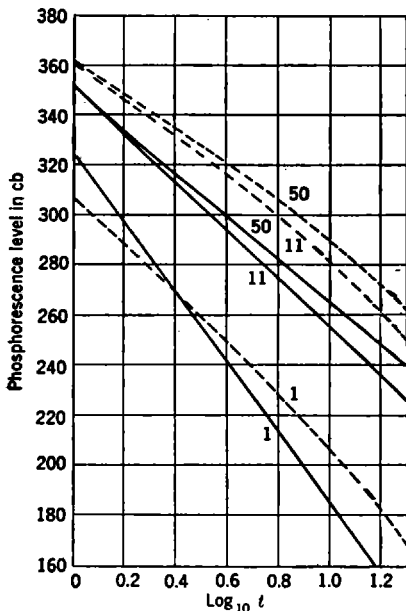


FIG. 18·18.—Phosphorescent decay after radiant-- or electronic—excitation. Phosphor composition (77.5)ZnS:(22.5)CdS:Cu. Screen thickness 14.4 mg/cm². Time $t$ in seconds.

The average lifetime in the excited state is equal to $\bar{t}$. It may be seen from the equation

$$(\text{cb})_P = (\text{cb})_0 - 43.43 \frac{t}{\bar{t}}, \tag{6}$$

that if, instead of plotting $(\text{cb})_P$ as a function of log $t$, $(\text{cb})_P$ were plotted as a function of the time, then a phosphor that decays according to the monomolecular law would have a characteristic decay curve that is a straight line of the slope $-43.43/\bar{t}$. The average value for $\bar{t}$ for any part of such a curve can be obtained by drawing the best straight line through the experimental points and determining the increment of time required for a change in the value of $(\text{cb})_P$ of 43.43 cb.

The second law of decay, commonly found in reactions that involve the recombination of separated entities, is known as the bimolecular law. It is evident that if there are no more electron holes at the lower electronic levels than there are electrons in the conduction level, the probability of an electron's finding a hole will be directly proportional to the number of electrons that are in the conduction level. It follows that
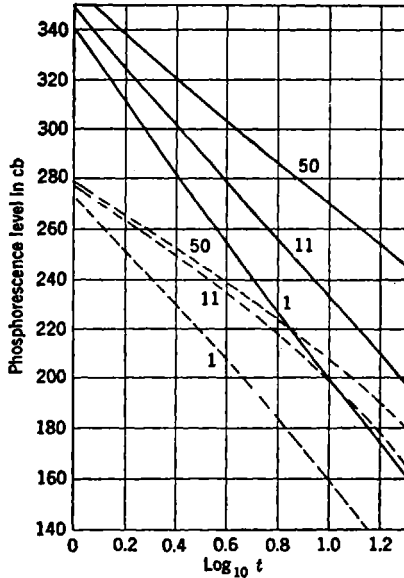


Fig. 18·19.—Phosphorescent decay after radiant—or electronic—excitation. Phosphor composition (75)ZnS: (25)CdS: Cu.   Screen thickness 14.4 mg/cm². Time *t* in seconds.

the time rate of change of electrons in the conduction level should be proportional to the square of the number of electrons there:

$$\frac{dn}{dt} = -\beta n^2. \tag{7}$$

The solution of this equation is

$$n = \frac{n_0}{1 + n_0\beta t}, \tag{8}$$

in which $n_0$ represents the number of electrons in the conduction band at the time $t = 0$.   Again, if the phosphorescence is proportional to the time rate of change of electrons in the conduction band, Eq. (9) shows the expected variation with the time.

$$P = c\beta \frac{n_0^2}{(1 + n_0\beta t)^2}. \tag{9}$$

If the logarithm of the phosphorescence is plotted as a function of the logarithm of the time, it is evident that the slope of such a curve will
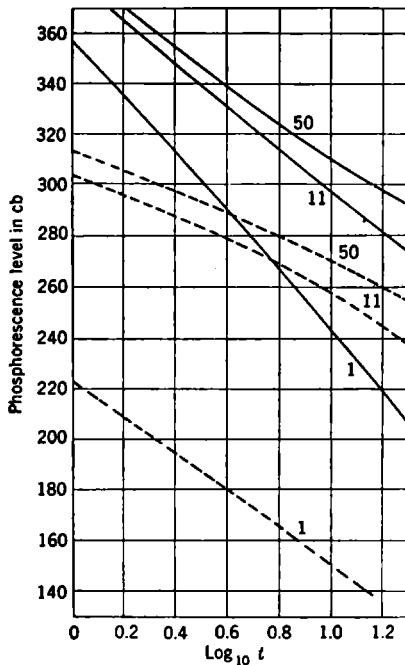


FIG. 18·20.—Phosphorescent decay after radiant -- or electronic–excitation. Phosphor composition $(93)ZnS:(7)CdS:Cu$. Screen thickness 14.4 mg/cm². Time $t$ in seconds.

not be constant, but will start out at zero, just as was the case for the exponential decay:

$$\frac{d(\log_{10} P)}{d(\log_{10} t)} = -2 \frac{t}{t + \dfrac{1}{n_0\beta}}. \tag{10}$$

Again there is a time $t_1$ at which the slope of the curve is unity:

$$t_1 = \frac{1}{n_0\beta}. \tag{11}$$

The time $t_1$ is dependent not only on the proportionality factor, $\beta$, but also on the extent to which the excitation has taken place, that is, on the value of $n_0$.

It is also evident from Eq. (10) that for times large compared with $t_1$,

the slope of the curve approaches but does not exceed $-2$. The equation relating $(cb)_P$ and time is

$$(cb)_P = (cb)_0 - 200 \log_{10}\left(1 + \frac{t}{t_1}\right). \tag{12}$$

The observed decay in phosphorescence for the sulfide is not well represented by either of the preceding two reaction formulas. None of
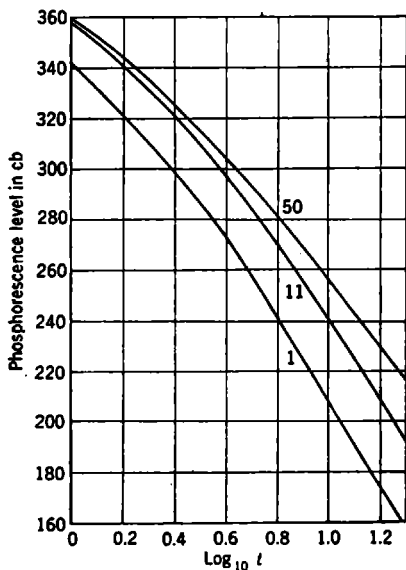


FIG. 18·21.—Phosphorescent decay after electronic excitation.  Phosphor composition (ZnS:Ag).   Screen thickness 14.4 mg/cm².   Time $t$ in seconds.

the curves shown has an absolute value of slope as great as 2 and most of them have slopes that range between about 0.7 and 1.4.

The fact that the observed decay characteristics differ so radically from those expected on the basis of either of the two decay laws indicates that the concentration of electrons in the conduction levels continues to be replenished by the feeding of electrons up from the traps into the conduction level.    The problem may be approached from either of two points of view.   One might start with the observed phosphorescence as a function of the time and try to work back to find the corresponding concentration of electrons in the conduction level, and then analyze the distribution in trapping levels and the corresponding transition probability that would yield the required conduction-level concentration.   The second approach might be to make a direct study of the distribution of

trapping levels by observing the stimulated phosphorescence obtained under the influence of infrared irradiation when the phosphor is held at a very low temperature.
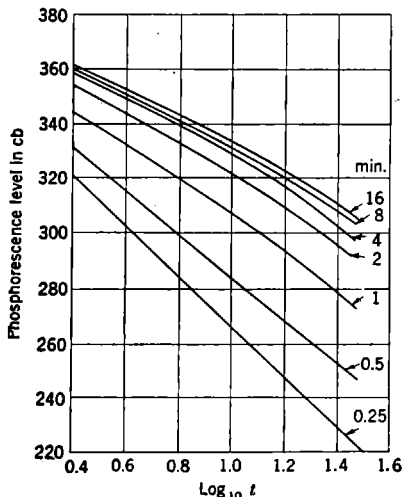


FIG. 18·22.—Phosphorescent decay after raster excitation at $(cb)_f = 500$ for times shown.   Time $t$ in seconds.

*Deexcitation of Screens.*— Almost all the experimental observations reported in this chapter have followed the complete deexcitation of the phosphor since experience shows this to be the surest way of obtaining reproducible results.   The phosphor was deactivated by irradiating it with a strong beam of radiant power obtained from an incandescent lamp and passed through a filter that absorbed all the radiant power confined to the wave lengths shorter than 590 m$\mu$. The length of time required to deactivate a screen in this way is approximately one minute. Following such deactivation, the phosphorescence observed subsequent to a definite excitation is always accurately reproducible.   The curves of Figs. 18·22 and 18·23 illustrate how the screen properties change with time of excitation.   In Fig. 18·22, there are seven curves showing the decay in phosphorescence for the period of time from 2.5 to 30 sec, following excitation lasting from 0.25 min to 16 min.   The luminance observed at 30 sec after 16 min of excitation is 83 cb higher than that observed at 30 sec after 0.25 min of excitation.   The slope of the decay curve changes from 0.95 for the short excitation to 0.50 for the long excitation.   It follows from these observations that wide differences in the apparent properties of the screen will be observed if the extent of excitation is not accurately known.



FIG. 18·23.—Change in phosphorescent levels after varying periods of raster excitation at 500 cb, observed at times indicated. Duration of excitation $t_f$ in minutes.

If the screen is thoroughly deactivated by means of red light before the application of the continuous raster, the results obtained will be

reproducible but dependent upon the exact time that the continuous raster is allowed to play upon the surface of the phosphor.    For the data shown in Fig. 18·22, the luminance level during the excitation period was constant at 500 cb for all the curves.    These data are plotted in a different way in Fig. 18·23, in which the abscissa is the logarithm of the time of excitation.    It will be noted that the rise in all curves is more or less uniform with the logarithm of the time of excitation up to about 2 min, after which the rise is less rapid.    Even up to 16 min, the observed
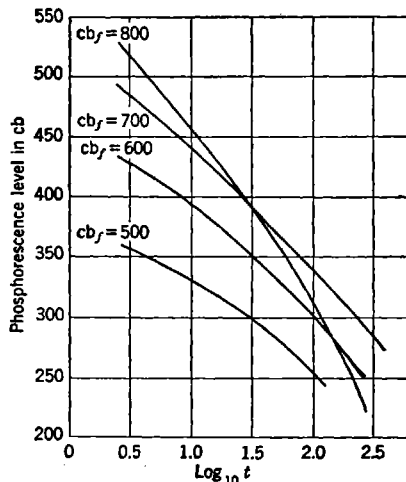


FIG. 18·24.—Phosphorescent decay after 5 min of raster excitation at cb; levels shown. Time *t* in seconds.

phosphorescence level at any specified time is still increasing with the time of excitation.

The curves shown in Fig. 18·24 are of interest because they illustrate the unexpected fact that the luminance 5 min after excitation to the very high initial luminescence of 800 cb is less than that obtained when the initial level of luminescence is only 600 cb or a factor of 100 less than in the previous case.    All the curves shown there follow an excitation period of 5 min during which 18,000 rasters were applied to the phosphor.

*Four General Conclusions.*—Four general conclusions that may be drawn from an inspection of Figs. 18·16 to 18·21 may be listed as follows.

1. Slopes of all curves decrease as the number of the excitations used is increased.
2. For repeated electronic excitation, the slope of the decay curve may decrease to 50 per cent of its single excitation value, whereas, for radiant excitation, it seldom falls to less than 75 per cent.

3. The slopes of curves following extended electronic excitation gradually approach those for radiant excitation if the levels of radiance are comparable.

4. Many of the observed slopes over the entire range over which they have been investigated are less than 1. It is necessary to conclude that outside the range of observation the slopes will ultimately exceed 1 since, if this were not true, the integral of all the power radiated would not remain finite.

There is nothing fundamentally different about electronic excitation compared with excitation by radiant power except for the excitation density. The absorption coefficient for electrons is so much greater than that for radiant power that at 4 or 6 kv practically all the excitation is confined to a depth of 500 to 1000 $m\mu$. Since the average thickness of the usual single-layer sulfide screen is between 20 and 30 $\mu$, all the excitation that yields light to the observer is contained in a very thin shell on the phosphor surface which is probably not more than 5 per cent of the entire volume of crystalline material. For the experiments described here, the transmissivity of the screen as a whole was so great that it is reasonable to consider that the irradiation excited the entire volume of the screen to a sufficient level to have a comparable radiance when one considers a comparison between the electronic and the radiant excitation shown.



FIG. 18·25.—Phosphorescent decay following single pulse excitation and current density of $j = 4$ ma/cm². Time $t$ in seconds. Excitation period 30 $\mu$sec —; 50 $\mu$sec – – –; 200 $\mu$sec ——. Screen type: (88)ZnS: (12)-CdS:Cu.

Thus the volume density of excitation for electron bombardment was probably 20 to 50 times as great as that encountered for the radiant excitation.

*Short-time Decay of Phosphorescence.*—The data available on the decay characteristic of sulfide phosphors less than 1 sec after excitation are very incomplete. The curves shown in Fig. 18·25 are typical of those that are available. These curves show the decay of phosphorescence following excitation under electron bombardment with a voltage of 6 kv and an approximate current density of 4 ma/cm². The three curves show the decay in phosphorescence following excitation for three different lengths of time—30, 50, and 200 $\mu$sec. In each case, a single pulse of

electrons at the specified current density and voltage was used to excite a fully deexcited screen. The logarithm of the time of observation after the termination of the excitation period is shown as the abscissa, and the ordinate is the radiance expressed in centibels.[1]

Much of the theoretical significance of the curves of Fig. 18·25 is lost because of the fact that the pulse length used to excite the screen was far too long. The observed variation in radiance covered a range of 4,000,000-fold in value and it is very likely that the actual variation for a particular crystal was no less than 10,000,000- and probably no greater than 50,000,000-fold. All curves show a slope that is less than 1.0, out to 10 msec, and greater than 1.0 beyond this time. To show the radiance per unit of charge, relative to the solid line, the dotted curve should be displaced upward 82 cb and the dashed curve 40 cb. Such a displacement would put the dotted curve above the solid line throughout the entire range of observation whereas the dashed line would be higher at some points than the dotted line and at other points would be lower than the solid line. The accuracy of the measurements was such that the width of the line used to represent the results in Fig. 18·25 is greater than the uncertainty of the values obtained. The small variations are not an indication of experimental error, but are probably determined by the statistical distribution in depths of the trapping levels.

*Short-time Luminescence.*—Additional complexities concerning the excitation of phosphors are illustrated in Fig. 18·26, which shows six conditions of excitation involving the bombardment of a phosphor by a given number of electrons. These electrons were first distributed over such a large area that the average current density was 1.0 ma/cm$^2$, later distributed over a smaller area to give a density of 4 ma/cm$^2$, and finally concentrated into such a sharply focused beam that the density was 30 ma/cm$^2$. Pulse lengths of 50 and 200 $\mu$sec were used. The luminescence increases more rapidly for the high current density than it does for the low current density. At the end of 50 $\mu$sec the total luminescence produced by the electrons delivered at a low current density is higher

---

[1] In order to make intercomparison of observed data as valid as it can be under the circumstances, corrections have been made, whenever possible, to indicate the results that would have been obtained from a 50 cm$^2$ raster or excited area even though the actual area used may have been much less.

For pulse excitation, the number of pulses in a group is given by $N$; the length of each current pulse is expressed in microseconds as $L$, and the current density in milliamperes per square centimeter is $j$. The product $N \cdot L \cdot j = Q$ and the unit is millimicrocoulombs per square centimeter. With excitation by a raster of overlapping lines the value of $Q$ is given in the same units as above by $Q = (iT)/A$ where $i$ is the electron beam current in microamperes; $T$ is the time required to apply the raster in milliseconds (16.7 msec for $\frac{1}{60}$ sec); and $A$ is the raster area in square centimeters.

than that produced with a higher current density. There is very little increase in luminescence for the ensuing 150 μsec, in the case of the highest current density studied; whereas for the curve, $j = 1$, the luminescence is still increasing very noticeably at 200 μsec. A very short time decay after either the 50- or the 200-μsec excitation with $j = 30$ is independent of the time of excitation between these limits. Data not shown here, however, indicate that after a long period of observation of the phosphorescence the 200-μsec excitation is measurably higher in radiance level than is the 50-μsec excitation. The curves for $j = 4$ ma/cm² are also very similar although not identical, and represent the phosphorescent decay curves already shown in Fig. 18·25.
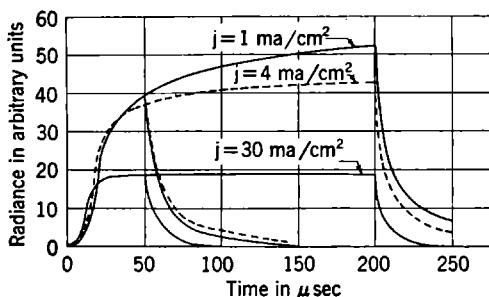


Fig. 18·26.—Time curves of luminescence and phosphorescence for pulse lengths of 50 and 200 μsec. Three current densities shown. Phosphor: (88)ZnS:(12)CdS:Cu.

The inverse relations between the curves over the first 20 μsec is an exhibition of the phenomenon of superproportionality; whereas, at 25 μsec, the superproportionality is followed by subproportionality or saturation. The curves of both Figs. 18·25 and 18·26 serve to illustrate the extreme complexity of the detailed behavior of both the rise in luminescence and the fall in phosphorescence, during and subsequent to electron excitation.

If the integral of the power radiated during the first tenth of a second is very high, then the screen is said to exhibit high "flash." There are two approaches to the problem of flash reduction. One solution involves the use of a cascade screen that functions first to convert the electronic excitation to radiant power that in turn excites the layer next to the glass to emit radiant power largely confined to wavelengths associated with yellow or orange light. A filter may be used to absorb the blue light transmitted through the "glass" layer. The second method used for the reduction of flash depends upon the development of single-layer phosphors that have very nearly exponential decay characteristics of moderately long duration.

**18·8. Properties of Other Single-layer Light-emitting Screens.**—Two classes of phosphors known as the "silicates" and the "fluorides" were investigated to some extent. The most commonly used silicate is known as "willemite" or "zinc silicate" ($Zn_2SiO_4$:Mn). Willemite has an approximately exponential type of decay with a time constant of approximately 14 msec. If the decay in phosphorescence were accurately represented by the exponential law, then a plot of $(cb)_P$ as a function of the time would yield a straight line of constant slope. Actually the line is slightly convex downward and over different small segments of the curves the characteristic time $\bar{t}$ varies between 8 and 16 msec.

*Time Constants for Silicates and Fluorides.*—Magnesium silicate (MgSiO$_3$:Mn) and cadmium silicate (CdSiO$_3$:Mn) have also been found to yield quasi-expo-



FIG. 18·27.—Phosphorescence of two silicates as a function of time.

nential decay of phosphorescence. Typical results for these two phosphors are shown in Fig. 18·27. An analysis of the curves gives a value for $\bar{t}$ for the MgSiO$_3$ of approximately 80 msec; and for CdSiO$_3$, $\bar{t}$ varies from 25 to 35 msec, as the time at which the slope is measured is increased.

The investigation of the fluorides, namely, zinc fluoride (ZnF$_2$:Mn)



FIG. 18·28.—Phosphorescence of three fluorides as a function of time.

and zinc magnesium fluoride (ZnF$_2$:MgF$_2$:Mn), shows that the decay of phosphorescence following electronic excitation of these phosphors is also essentially exponential. Some typical results are illustrated in Fig. 18·28. The three curves shown are for different proportions of MgF$_2$ and ZnF$_2$. The proportions of ZnF$_2$ are 100, 90, and 50 per cent. It is evident that there is a small tendency toward higher time constants as the proportion of magnesium fluoride is increased. The total range of time constants is approximately 80 to 1000 msec.

The phosphorescent characteristics of the fluorides are subject to alteration as a result of electron bombardment. The changes are

illustrated by Figs. 18·29 and 18·30.   The abscissa scales of these figures
and also of Fig. 18·31 represent the logarithm of the total quantity of
charge used to bombard the screen in life-test experiments.   Since the
charge put into the screen by the application of a single raster was 20
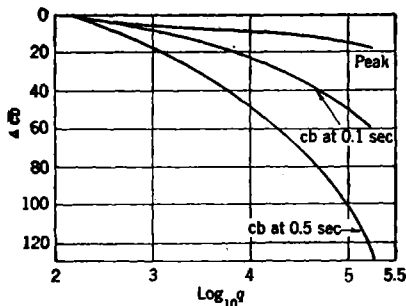


FIG. 18·29.—Change in radiance levels
of ZnF₂: Mn phosphor following excitations
repeated at the rate of 60 per second with
charge density per excitation of 20 mμc/cm².
Total q in microcoulombs per square centi-
meter.
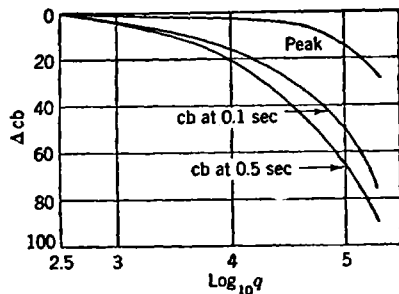
FIG. 18·30.—Change in radiance levels of
(50) ZngF₂: (50) MgF₂: Mn phosphor follow-
ing excitations repeated at a rate of 60 per
second, with charge density per excitation of
20 mμc/cm².   Total q in microcoulombs per
square centimeter.

millimicrocoulombs (mμc) per square centimeter per raster, and the total
extent of the aging summed to 0.2 coulomb per cm², it is evident that
the aging shown is the equivalent of the application of ten million rasters.
The bombarding and measuring voltage was 4 kv.   The luminescence
observed at the termination of an excitation is identified as the "peak"
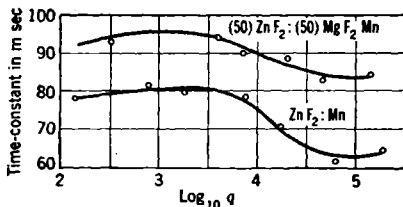


FIG. 18·31.—Time constants for phos-
phorescent decay (exponential) for two
phosphors shown as a function of total charge
q (μc/cm²) applied at a rate of 60 excitations
per second at 20 mμc/cm² per raster.

value, and the phosphorescence
observed at the end of 0.1 sec and
0.5 sec is so indicated.   In all
cases, the phosphorescence de-
creased in consequence of the
aging, and the amount of this
decrease ($\Delta$ cb) is shown as the
ordinate in Figs. 18·29 and 18·30.
Figure 18·29 applies to a typical
zinc fluoride (ZnF₂:Mn), and Fig.
18·30 corresponds to a zinc
fluoride–magnesium fluoride [(50)-

ZnF₂:(50)MgF₂:Mn)].   The spreading of the curves of Figs. 18·29 and
18·30 is a direct indication that the exponential time constant has
decreased.   The extent of this decrease in the time constant is illustrated
in the two curves of Fig. 18·31, in which the time constants in milliseconds
that apply from 0.1 to 0.3 sec are plotted as the ordinates.

The fact that the changes in the properties of $ZnF_2$ are noticeably greater than the changes for the $ZnF_2MgF_2$ phosphor is a point in favor of the latter, and in addition its longer time constant is also an advantage for some purposes.   This phosphor has been used for a small lot of production tubes and has received the RMA designation P12.   An explanation of the phenomenon of phosphor aging under electron bambardment has not been discovered.

**18·9. Properties of Double-layer Sulfide Screens.**—The principal distinguishing feature of the double-layer or cascade cathode-ray-tube screen is well indicated by its name.   The word "cascade" in this particular application indicates that the electrons bombard the "electron layer" to excite it to a high level of radiance, and that the radiant power emitted by this layer is absorbed to a considerable extent in the neighboring layer (often identified as the "glass layer"), which becomes excited throughout its volume and reemits radiant power in the form of a time-delayed phosphorescence.   Although the time of excitation in certain extreme cases may be as short as 1 $\mu$sec, the time interval over which the luminance may be observed may extend to some tens of seconds.   It is not absolutely necessary to use a cascade screen to get this extension in time of observation, but experience shows that if luminance is required 10 sec after the excitation has taken place, it can be obtained with less high-intensity flash with the cascade screen than with the single-layer screen.

In order to construct a screen of the cascade type, a glass blank is prepared by suitable cleaning processes for the deposition of the "glass layer," which is usually a zinc sulfide–cadmium sulfide phosphor, copper-activated.   The most common method of applying this layer is by gravitational settling from a water suspension of suitably prepared crystals.   The weight of material deposited generally falls within the limits of 8 to 15 mg/cm². There are other methods of applying the phosphor layer to the cathode-ray-tube blank, and there are many technical details that influence to some extent the efficiency and other properties of the phosphor screens.   It is beyond the scope of this presentation to discuss them.   It has already been indicated that if the glass layer is excited only by the absorption of radiant energy, then its buildup properties are enhanced to the highest extent, and, associated with this condition, the luminance produced by a single excitation is low.   It is possible to guarantee that almost no excitation of the glass layer is produced by the direct electron bombardment by the introduction of an optically transparent "barrier layer" that is sufficiently thick to absorb any electrons that might possibly have found their way between the individual crystals of the electron layer.   Although many experimental tubes have been produced with a barrier layer to separate the electron

layer from the glass layer, it is not considered necessary in order to meet the normal specifications associated with the P7 screen type.

*Luminance Characteristics of P7 Components.*—After the glass layer has been applied, an electron layer of comparable thickness is applied to the cathode-ray-tube face plate. Zinc sulfide activated with silver is generally used for the electron layer because this phosphor is very efficient in terms of the radiant power that it emits within the wavelength band that gives rise to excitation in the glass-layer phosphor. The relative spectral power distribution associated with the radiant emittance of the usual electron layer is shown in Fig. 18·32, along with



the relative power distribution associated with the radiance of a typical glass-layer phosphor.

The electron layer just described is often known as the "blue screen" and sometimes as the "blue fluor." A color analysis of the spectral power distribution shown in Fig. 18·32 shows that the dominant wavelength[1] is 451 $m\mu$ and that the excitation purity is 98.4 per cent, when referred to

FIG. 18·32.—Relative spectral power distributions of radiance from yellow and blue phosphors of P7 screen.

the equal-energy source as the achromatic spectrum. Computation shows that the glass-layer spectral power distribution of Fig. 18·32 yields a dominant wavelength of 563.2 $m\mu$ and an excitation purity of 76.3 per cent. This component of the cascade screen is often called the "yellow layer" since it is both yellow in color and yellow in its radiant emittance. For many applications, the P7 screen is viewed through a filter that absorbs practically all the blue and blue-green light. The transmission characteristic of this filter is very close to that of the Wratten filter No. 15, which has a negligible transmission for wavelengths shorter than 500 $m\mu$ and is very transparent for wavelengths longer than 550 $m\mu$. With this filter in place, almost all the blue light that is not absorbed in the glass-layer phosphor is absorbed in the filter. Therefore, the high-intensity flash associated with the electron bombardment of the electron layer is practically eliminated. An analysis of the

[1] W. B. Nottingham, "Notes on Photometry, Colorimetry, and an Explanation of the Centibel Scale," RL Report No. 804, Dec. 17, 1945. The dominant wavelength is obtained by the drawing of a straight line on a chromaticity diagram (Fig. 18·47) from an achromatic point such as $E$ through the sample point such as $G$ to intersect the spectrum locus. The dominant wavelength may be read off the wavelength scale indicated along the spectrum locus. The excitation purity measures the fractional distance from the achromatic point to the sample point with the total distance to the boundary of the domain of realizable colors taken as unit distance.

spectral power distribution associated with the radiance as viewed through the filter yields a new dominant wavelength of 571.2 m$\mu$ and a purity of 99.8 per cent.

*Liminal Contrast Determined by Luminance Level and Object Size.*— Cathode-ray-tube screens to be used in intensity-modulated indicators must be evaluated with respect to two important properties, (1) signal recognizability and (2) signal resolution. Both these properties depend on physical and electrical properties of the radar system, and also upon the characteristics of the cathode-ray-tube screen itself. In addition to the physical factors that must be considered, there are also the physiological and the psychological limitations of the observer. Figure 18·33 presents important physiological data obtained by an NDRC project operated as the "Tiffany Foundation."[1] The curves of Fig. 18·33 show the liminal contrast required for the observer to see various-sized objects as a function of the adaption level of the observer ex-



Fig. 18·33.—Liminal contrasts (50 per cent certainty) for surfaces, with subtending angles shown, for observers adapted to luminance levels indicated. Adaptation luminance in foot-lamberts. (Reprinted from OSRD Report 6401, Tiffany Foundation.)

pressed in foot-lamberts. The liminal observational conditions are such that the observer is 50 per cent certain of seeing the object that subtends the angle indicated in minutes of arc.

Although these data do not bear directly on cathode-ray-tube screens as such, they do yield quantitative information that is of very great importance for the designer of cathode-ray tubes and cathode-ray-tube equipment. For most applications of the cascade screen, the adaption level is between $10^{-4}$ and $10^{-2}$ foot-lamberts. Small target patterns of interest, as observed from the normal distance of approximately 30 cm, subtend angles of about 20 min. Therefore the curve designated 18.2′ is of most interest. The adaption level of the observer is determined partly by the light present in the observation room and partly by the light given off by the cathode-ray tube. In the PPI display, the luminance of the cathode-ray tube is not constant but is likely to vary considerably, depending on the nature of the pattern of radar echoes being displayed. If the number of echoes present is negligible, then under normal operating conditions the observer sees a faint luminance over the entire face of the tube, and a rotating "spoke" of luminance that indicates the position of the range sweep. The luminance produced by this spoke is largely due to signals created by receiver noise and such other disturb-

[1] OSRD, Report No. 6401, Fig. 37.

ances as may be present. The screen surface therefore exhibits a very nonuniform appearance because of the statistical nature of the excitation that it is receiving. If the screen excitation were perfectly uniform, and equal to that of the adaption level of the observer, then an increase in luminance of 10 per cent would be required for an observer to be more than 50 per cent certain that the signal from a radar echo were present. The problem in practice is not so simple as this because of the random nature of the noise (see Sec. 1·11).

Signal resolution also depends upon all these factors. Although the curves shown in Fig. 18·33 cannot be said to be directly applicable to a quantitative analysis of the physiological and psychological problems of resolution, it is easy to see from these curves that the lower the level of luminance and the lower the level of retinal adaption, the poorer the resolution sensibility of the observer.

Certain radar applications have no dearth of signal strength but do depend upon the ability of the system to display small differences in signal strength. Again, the cathode-ray-tube screen plays a very important part in the determination of the ultimate resolution capability of a system. Uniformity of screen response is an obvious and very important requirement. The data shown in the curves of Fig. 18·33 apply to regions that have such sharp boundaries that any further increase in contrast gradient cannot be detected by the observer.

*Contrast Gradient.*—It is well known that if two regions differ in luminance it will be difficult or impossible for an observer to recognize this difference unless the luminance gradient or contrast gradient is sufficiently great. Best results are obtained with sharp boundary lines. It is easily demonstrated qualitatively, and experience with television displays indicates, that picture quality depends more on contrast gradient up to a certain limit than it does on contrast itself. Cathode-ray tubes that are viewed directly by the observer, and not indirectly by means of an optical system, are subject to reduction in contrast gradient by the scattering of light within the screen material. The normal P7 screen is probably one of the coarsest screens used commonly in cathode-ray-tube displays. The gross thickness of this screen may range from 50 to 150 $\mu$. With moderately high accelerating voltages, useful electron beams may be focused so sharply that the screen material and structure are limiting factors in the control of resolution and contrast gradient. It is therefore to be expected that for applications where the signal strength is always adequate some sacrifice in luminous efficiency would be justified if, in return, a better screen were produced from the point of view of uniformity and reduction in internal scattering of light so as to increase resolution.

*Short-time Luminescence of P7 Screens.*—The rise in luminescence under pulse excitation is illustrated in Fig. 18·34 in which the curves

correspond to the excitation of a P7 screen with a single 200-$\mu$sec pulse applied at a charge density of 2 ma/cm$^2$ for the solid curve and 11 ma/cm$^2$ for the dashed curve. The marked difference in shape of these curves when they are compared with those of Fig. 18·26 is demonstrated by the replotting of one of the curves from Fig. 18·26 on the graph of Fig. 18·34. This curve is shown dashed. Three points may be noted. (1) the initial luminance seems to rise very fast; (2) it is followed by a very much slower increase in luminance with somewhat less tendency for the P7 screen, compared with the yellow sulfide, to "saturate" when bombarded by electrons; and (3) the



Fig. 18·34.—Time variation of radiance from P7 screen, excited by 200-$\mu$sec square-wave pulse at two current densities indicated. (Dashed curve is for single-layer screen, from Fig. 18·26).

decay in phosphorescence immediately following the period of excitation is distinctly slower for the P7 than for the single-layer screen. For the two P7 curves shown, the total amount of current used was the same, but the area excited was $5\frac{1}{2}$ times larger fo the 2 ma/cm$^2$ curve as compared with the other. Over the first few microseconds of excitation, super-proportionality is very evident, whereas over the greater portion of the illustrated curves the luminance (per unit area) is sub-proportionally related to the current density.



Fig. 18·35.—Short-time decay of phosphorescence following 2-$\mu$sec pulse excitation at current densities shown. Curves computed by Eq. (14) with $t_1 = 3.6$ $\mu$sec and 2.1 $\mu$sec.

*Short-time Phosphorescence of P7 Screens.*—In Fig. 18·35 the centibel value of the phosphorescence is plotted as a function of the time following the termination of the excitation period of 2 $\mu$sec.

Equation 10 may be rewritten to make it more applicable to Fig. 18·35.

$$\text{Slope} = \frac{d(nP)}{dt} = -\frac{2}{t + t_1}. \tag{13}$$

Although Eq. (13) shows that the magnitude of the slope can be expected to decrease with the time, the observed decrease in slope is more rapid than that computed by this equation. It has already been stated that

the slope of the long-time decay characteristic is much nearer to 1.0 than it is to 2.0 and, therefore, it is worth while to see whether or not a modified form of Eq. (12) might come nearer to fitting the observed data of Fig. 18·35. The equation chosen is the following:

$$(cb)_P = (cb)_0 - 100 \log_{10}\left(1 + \frac{t}{t_1}\right). \tag{14}$$

Values of $t_1$ have been chosen as 3.6 $\mu$sec and 2.1 $\mu$sec for the two curves of Fig. 18·35. The experimental points are shown as the dots
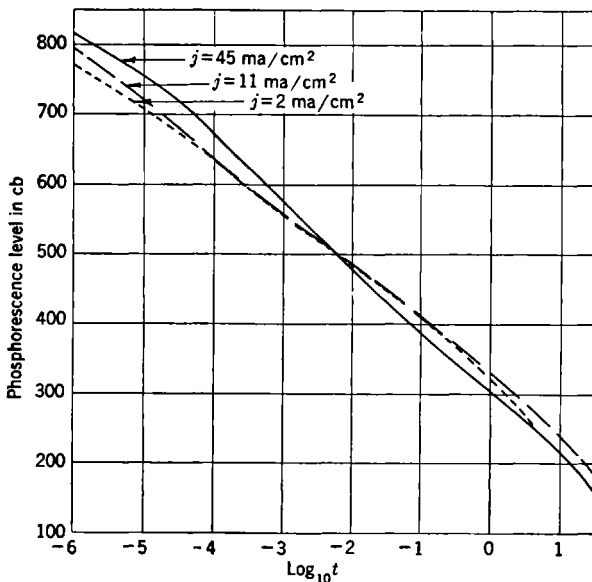


Fig. 18·36.—Phosphorescent decay of typical P7 screen following 12.5-$\mu$sec pulse excitation with three current densities shown. Time $t$ in seconds.

and circles for the two current densities of 2 ma/cm² and 11 ma/cm², respectively, and the lines shown were computed by means of Eq. (14).

*Short- and Long-time Phosphorescence of P7 Screens.*—The long-time decay curves of a typical P7 screen are shown in Fig. 18·36. Here again, the observations are to be associated with a given amount of the exciting current applied as a single pulse of 12.5-$\mu$sec duration and focused to give the three current densities of 2, 11, and 45 mc/cm² as indicated. It is evident that the general trend of the curves corresponds to a decay that is even slower than $1/t$. On the average the decay is represented by $(1/t)^{0.8}$. The actual luminance differences between the curves are greater than might be thought at first glance, since there are so many orders of magnitude of luminance represented in this plot. The greatest separa-

tion between the curves is approximately 50 cb, which is a factor slightly greater than 3. Since the details of the decay in phosphorescence during short intervals of time are far less important from the practical point of view, more attention was given to the measurement of phosphorescent decay within the range of time from 0.2 to 20 sec and very extensive data have been taken at the 1-sec point.

*Raster Excitation.*—In order to establish a definite routine for screen excitation, the tube-testing equipment was designed to apply a single raster to a given part of the screen and to repeat its application at intervals of 1 sec, for eleven consecutive applications. Figure 11·37 is a reproduction of a typical pen and ink pattern. At the time $t = 0$ the first raster was applied and the record shows that a very sudden increase in luminance took place and was followed within a few tenths of a second by the phosphorescent decay curve. At $t = 1$, 2, and 3, the second, third, and fourth rasters were applied, as shown. Between the third and the fourth seconds, the amplifier gain was reduced by 50 cb or $10^{0.5}$. An additional decrease in gain of 50 cb is shown to have taken place between 8 and 9 sec. The long-time decay of phosphorescence is shown with two increases of amplifier gain, each of 50 cb, which occur between 11 and 12 sec and between 14 and 15 sec. For routine measurements, the luminances indicated at the three points $a$, $b$, and $c$, are of particular interest and when these are converted to their corresponding centibel levels are noted respectively as $(cb)_1$, $(cb)_5$, and $(cb)_{10}$. These luminance levels are those observed 1 sec after the first, fifth, and tenth rasters respectively. For all measurements, the gain level was established prior to the measurement in terms of a suitably adjusted standard lamp. It was an easy matter of computation to take into account the gain used for a given experiment and combine it with the observed deflection of a recording instrument, as indicated at point $b$ for example. The property of superproportionality is clearly demonstrated by the record of Fig. 18·37. The symbol $G_{5:1}$ is defined as the ratio of the luminance observed 1 sec after the fifth raster to that 1 sec after the first raster and the symbol $G_{10:1}$ is the ratio of the luminance 1 sec after the tenth raster to that observed 1 sec after the first raster. In the case shown, the superproportionality is demonstrated by the $G$ values, which are $G_{5:1} = 7.2$ and $G_{10:1} = 14.1$. These values are typical of P7 screens when excited by a charge density of 20 m$\mu$c/cm$^2$ in each raster.

The phenomenon of superproportionality is the most characteristic feature of the cascade screen and serves as a relatively simple means of distinguishing cascade from a single-layer construction. Although the superproportionality phenomenon identifies a cascade screen most clearly, no direct correlation has ever been established between the buildup ratios and operational superiority.

In addition to the radiance levels, $(cb)_1$, $(cb)_5$, and $(cb)_{10}$, routine measurements generally include observations of two other quantities, $(cb)_f$ and $(cb)_i$.   The radiance obtained during the period of excitation, $(cb)_f$, is determined by measurements when rasters are repeated 60 times per second.   The quantity $(cb)_i$ is much more involved and is an indication of the *integrated* radiant emittance observed over a specified time. In the actual experiment the integral of all the photoelectric current obtained over a total period of 1 sec is used, including the radiance emitted during the single-raster excitation and the phosphorescence that followed. It was customary to have the screen in the completely deexcited state
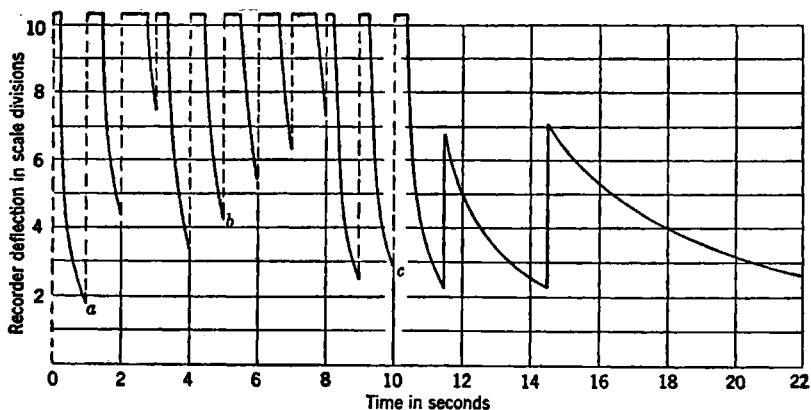


FIG. 18·37.—Reproduction of pen and ink recording of P7 phosphorescence during and after application of 11 single rasters applied at 1-sec intervals.   Readings $a$, $b$, and $c$ proportional to luminance after first, fifth, and tenth excitation.   Gain changes 50 cb at 3, 8, 11.5, and 14.5 sec.

before the application of the single raster.   The computational procedure that has been followed expresses $(cb)_i$ as the radiance level that, if maintained constant for a period of 0.1 sec, would yield an integrated radiant emittance exactly equal to the actual integrated emittance that was observed over a period of 1 sec.

All the quantities just described and also the decay characteristics depend on the charge density used for the excitation, the electron energy expressed in terms of the anode-to-cathode potential difference, the physical and chemical structure of the phosphors, and the constructional procedure used for the manufacture of the screen.   In the paragraphs that are to follow, a selection of the best-established phenomena will be described and numerical data presented.

*One-second Buildup Properties of Six Cascade Screens.*—The buildup properties of six different cascade screens are illustrated by Fig. 18·38. In all cases, the charge density per raster was 20 mμc/cm² and the anode

voltage was 4000 volts. The centibel levels indicated are those observed 1 sec after the pulse number indicated along the abscissa. The logarithm of this pulse number is plotted on a scale such that if the slope of the line for a given tube exceeds unity then superproportionality is indicated, but, if the slope is less than unity, subproportionality is indicated. It is evident that for all the tubes shown, with one exception, superproportionality is present for the first few applications of the raster. The three curves identified by $G$ correspond to the three proportions of zinc sulfide to cadmium sulfide, where the symbol (80):(20) gives the respective percentages. These curves indicate a systematic trend related to composition, in that the buildup decreases very markedly as the cadmium content increases. This same trend is shown by the three curves that have the common letter $R$. The one designated (88):(12) is the RCA version of the P7 screen. Differences in manufacturing technique are responsible for the fact that the trend in the curves is not given strictly by the zinc-to-cadmium proportions.



FIG. 18·38.—Buildup properties of six different cascade screens. Measurements made 1 sec after excitation. $V_a = 4000$ volts; $Q = 20$ m$\mu$c/cm$^2$ per raster.

*Phosphorescent Decay for Six Cascade Screens.*—The decay curves following selected numbers of raster excitations are shown in Figs. 18·39a to f. In all cases, the decay following a single raster is faster than the decay covering the same period of time following 11 or 100 rasters. It is to be noted that the rasters referred to were applied singly with a 1-sec interval between rasters until the last one had been applied, and the decay curve corresponds to the change in phosphorescence with the time starting the instant that the last of the series of rasters was applied.

The vertical separation between curves is a direct indication of the magnitude of the buildup factor as determined at any arbitrarily chosen time represented in Fig. 18·39. There seems to be a general trend toward lower buildup values as the cadmium content of the phosphor is increased. It is interesting to note that there is relatively little difference in the decay characteristics as one screen is compared with another when all are excited by a single application of the exciting raster. The fact that the buildup of the (70):(30) phosphor is so small, as compared with the P7 phosphor, is just another way of stating that the decay of phosphorescence following repeated excitation is very nearly the same as the decay in

Fig. 18·39.—Phosphorescent decay for six different cascade screens. Excitation: 1, 11, and 100 rasters. 1-sec interval. $Q = 20$ m$\mu$c/cm$^2$, per raster. $V_a = 4000$ volts. Time $t$ in seconds.

phosphorescence after a single excitation. In contrast, for the P7 screen, the decay in phosphorescence is extremely slow following extended excitation in comparison with a single excitation. It is evident from these curves that if, for some particular application, the phosphorescence following extensive excitation is required to fall off rapidly, then a high concentration of cadmium content is called for.

*Single-layer Compared to Cascade Screens.*—Data are not available for satisfactory comparisons between the results obtained for single-layer screens and the various cascade screens just described. Such data as can be offered are presented in Fig. 18·40. In this figure, the solid lines are a reproduction of Fig. 18·39f whereas the dotted lines are a reproduction of the data of Fig. 18·16 and the dashed line shows data obtained on a single-layer screen following an excitation of 100 rasters. It would have made the comparison more significant if complete data were available for the decay after a single raster and after 11 rasters for the same tube as the one for which the 100-raster data are at hand. It may be concluded from the comparison that the decay characteristics of a cascade screen that has a (70):(30) glass layer is steeper even after 100 excitations than is the decay characteristic of



R(88): (12) single layer
D(85): (15) single layer
G(70): (30) cascade
Figures on curves indicate number of rasters used to excite screen.

FIG. 18·40.—Comparison of phosphorescent decay from selected cascade and single layer screens. Time $t$ in seconds.

a single-layer P7 type of screen material when excited directly by electrons. The two single-layer screens represented in Fig. 18·40 involve two slightly different screen compositions. The upper curve shows the decay of an RCA single-layer phosphor of composition (88):(12) after excitation by 100 rasters. The phosphor represented by the dashed curves was a Du Mont single-layer screen of composition (85):(15). It follows from the comparison of data, Figs. 18·39a to f, that cascade screens have a wide range of decay characteristics which overlap satisfactorily with the characteristics of single-layer screens. Detailed analysis of application problems combined with an investigation of screen properties should yield improvement of operating equipment designed to meet specific indicator demands.

Operating conditions are not such that the charge density per excita-

tion is constant.   It is likely to vary over two or three orders of magnitude from about 1 to 1000 m$\mu$c/cm$^2$ per excitation.   This wide range makes it exceedingly difficult to make any simple statements concerning the performance characteristics of a given cascade screen.

*Properties Dependent on Charge Density.*—A few of the properties of a cascade screen of the P7 type have been studied over a wide range of charge density per excitation (see footnote 1, page 631).    Figures 18·41 and 18·42 present some of these data.   In Fig. 18·41, $S_1$ represents the initial slope of a buildup curve such as that of Fig. 18·38, in which the luminance is expressed as a function of the logarithm of the number
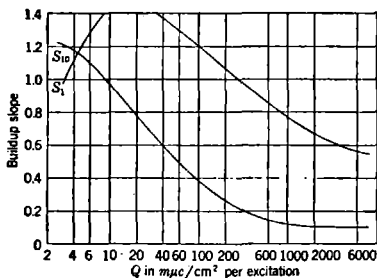


Fig. 18·41.—Slopes of buildup curves for typical P7 cascade screens, for excitations repeated at 1-sec intervals, for the $Q$ values shown.    $S_1$ = initial slope; $S_{10}$ = slope at tenth excitation.

of repeated excitations, and $S_{10}$ represents the slope at the time of the tenth excitation.   Within the range of $Q$ shown, which extends from 4 m$\mu$c to 6000 m$\mu$c, the slopes represented by $S_1$ are greater than 1.0 up to 300 m$\mu$c.   The indication is that the slope for charge densities less than 4 m$\mu$c is definitely less than 1. Thus the buildup curve for very low current densities is one that starts off slowly and finally gains in such a manner that after 10 excitations at 1-sec intervals have been applied, the observed phosphorescence increases superproportionally with the number of excitations given.    The slope $S_{10}$ falls very rapidly as the $Q$ is increased and has fallen to the very low value of 0.1 at approximately 1000 m$\mu$c.

The ratio of the phosphorescences indicated by $G_{10:1}$ is very dependent on the charge density per excitation and is indicated in Fig. 18·42.    It may be seen there that the phosphorescent output 1 sec after the tenth excitation is barely more than 2 times the phosphorescent output 1 sec after the first excitation, if the charge density is 1000 m$\mu$c/cm$^2$ or more; whereas, with a charge density of 10 m$\mu$c/cm$^2$, the ratio of phosphorescences is approximately 19.   The exact value of this ratio for a given charge density is very dependent on the particular phosphor and the production procedure by which the screen was created.   Maximum values of $G_{10:1}$ of over 30 have been observed whereas, in other cases, the maximum value at the optimum $Q$ does not exceed 12.

*Properties Dependent on Anode Voltage.*—Experimental determinations have been made of the luminescence (during electron excitation) as a function of the electron energy expressed in volts.   If the luminescence in arbitrary units is $L$ and the electron energy in volts is $V_e$, it has been

found that the following equation represents the experimentally determined results.[1]

$$L = K(V_e - V_0)^n. \tag{15}$$

In Eq. (15), $K$ is a constant of proportionality, and $V_0$ is the so-called "dead voltage." For most cases observed, $V_0 = 0$ and therefore may
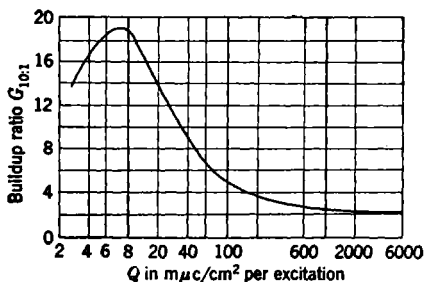


FIG. 18·42.—Buildup ratio $G_{10:1}$ for typical P7 screen as a function of charge density per excitation.

be omitted but, in a few cases, a better fit of the experimental data at low voltages is obtained by assigning a small value to $V_0$. The exponent $n$ has been observed to vary from approximately 1.4 to 3.0 with many cases on record of values that are approximately 2.
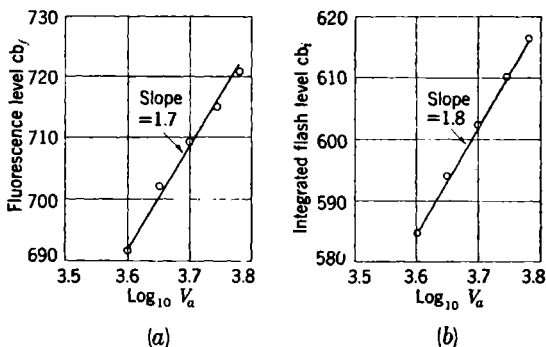


FIG. 18·43.—Dependence of fluorescence and integrated flash levels on anode potential $V_a$ in volts.

The relation between phosphorescent output and voltage has been investigated over a very limited range of electron energy. The results

[1] W. B. Nottingham, "Electrical and Luminescent Properties of Willemite Under Electron Bombardment," *J. App. Phys.*, **8**, 762 (1937).

W. B. Nottingham, "Electrical and Luminescent Properties of Phosphors Under Electron Bombardment," *J. App. Phys.*, **10**, 73 (1939)
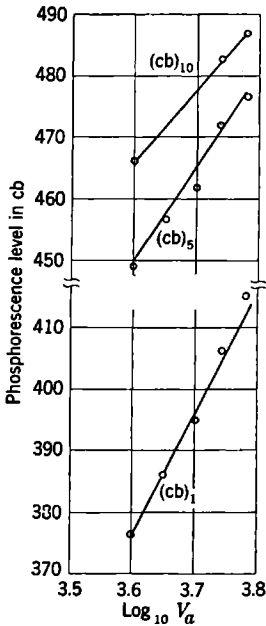
FIG. 18·44.—Dependence of phosphorescence levels on anode potential $V_a$ in volts. Slope $(cb)_1 = 2.0$; slope $(cb)_5 = 1.7$; slope $(cb)_{10} = 1.2$.

obtained with a charge density of 20 m$\mu$c/cm$^2$ per raster are shown in Figs. 18·43 to 18·45 inclusive. The centibel level of "fluorescence," which measures the luminance level attained by the screen area when bombarded by applications of the raster repeated 60 times per second, is designated by $(cb)_f$. Figure 18·43a shows that $L_f$ is approximately proportional to the 1.7 power of the electron energy. The luminance level described as the "integrated flash" has been defined above and is represented by $(cb)_i$. The exponent $n$ (Fig. 18·43b) for the dependence of $(cb)_i$ on electron energy is 1.8. The three lines of Fig. 18·44 show the phosphorescent levels, $(cb)_1$, $(cb)_5$, and $(cb)_{10}$. They are measures of the phosphorescent luminance 1 sec after the first, the fifth, and the tenth repeated raster with a repetition period of 1 sec. The corresponding exponents $n$ of Eq. (15) are 2.0, 1.7, and 1.2. The fact that the increase in $(cb)_{10}$ is very definitely less rapid with voltage is further illustrated by the lines of Fig. 18·45, in which the $G$ ratios are plotted as a function of the logarithm of the electron energy and show that the buildup ratios decrease as the voltage increases. All the data of Figs. 18·43 to 18·45 apply to a particular 5FP7 cathode-ray tube, and therefore to a cascade screen that has a glass layer composition represented approximately by the formula (88)ZnS:(12)CdS:Cu. Insufficient data has been taken to insure that these results are typical of the voltage characteristics of P7 screens in general.

**18·10. Properties of Triple-component and Other Special Screens.**—A cathode-ray-tube screen was desired which would register in one color if the tube area in question were bombarded repeatedly and if the area received only a few bombardments would yield luminance of a distinguishably different color. Although none of the tubes produced was successful enough to be of any practical use in the particular application for which they
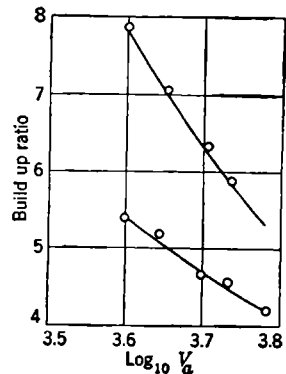


FIG. 18·45.—Dependence of buildup ratio on anode potential in volts.

were designed, some discussion of the principles and difficulties involved will be of value.

The psychological interpretation of the sensations created when the retina of the eye is illuminated involves considerations that cannot be clearly evaluated in terms of available published information.    In spite of this lack of detailed quantitative information, some of the qualitative aspects deserve discussion.    The International Commission on Illumination (I.C.I.) system of color specification offers an excellent means for the quantitative expression of color appearance of individual sources of known relative spectral power distributions.    Furthermore, if two or more sources are viewed simultaneously, it is possible to evaluate the color appearance of the mixture in terms of the relative proportions of the mixed components.

*Some Properties of the Human Eye.*—The sensation attributes of light are brightness, hue, and hue saturation, and the corresponding quantitative attributes are luminance, dominant wavelength, and excitation purity (see footnote 1, page 646).    The human eye has two classes of light-sensitive receptors, known as "cones" and "rods."    At the very low levels of retinal illuminance, the rods gain in sensitivity as the eye becomes dark-adapted and become so sensitive in comparison with the cones that the psychological interpretation of the sensations produced is dominated by their properties.    The rods are capable of delivering only the sensation of brightness and do not yield any sensation of color.    Thus if the phosphor of the cathode-ray tube is excited to a high state of luminance, the eye may identify the color as being yellow, but if a given area is allowed to decay to a sufficient extent that the sensations produced are dominated by the response of the rods, then even though the relative spectral power distribution remains unaltered, the sense of the hue will be lost completely and the observer will only be able to state that he recognizes a sensation of brightness.

When the eye is in the state of dark adaption and the levels of retinal illuminance are very low, the response is said to be "scotopic."    This implies a total lack of hue discrimination, a considerable reduction in visual acuity, and a wavelength-sensitivity curve that is shifted toward the shorter-wavelength part of the visible spectrum.    Curve $A$ of Fig. 18·46 expresses the variation in the level of retinal irradiance as a function of the wavelength that is required to stimulate a constant sensation of brightness.    This curve shows that a given amount of power concentrated near 510 m$\mu$ will be just as effective in the production of the sensation of brightness as 10 times that amount of power concentrated near the wavelength 580 m$\mu$.    At high levels of retinal illumination, the eye is said to be in a state of "photopic vision."    The photopic properties include all the sensation attributes that involve hue and hue saturation in

addition to the sensation of brightness.    At high levels of retinal illumination, a contrast of 0.5 per cent between adjacent fields of luminance can be detected if the boundary line between them is sufficiently sharp.    As the level of retinal illumination falls, a greater contrast between the fields must be present in order for the observer to recognize differences in luminance (see Fig. 18·33).    The power of the eye to discriminate between equally luminous surfaces that differ slightly in dominant wavelength or excitation purity is also a function of the level of retinal illumination. Thus hue or color discrimination is dependent not only on the relative spectral power distribution but also on the state of dark adaption of the eye and the level of retinal illumination used in the observation.    In normal operation, cathode-ray tubes are observed under conditions for which the eye is in an intermediate state of adaption, called "mesopic," between that for scotopic vision and that for photopic vision.



FIG.   18·46.—Relative   spectral   power levels   for   constant   brightness   sensation. Curve   *A*—scotopic    vision    (dark-adapted eye);   Curve   *B*—photopic   vision   (I.C.I. standard   luminosity   curve),   approximate threshold of cone vision.

Curve *B* of Fig. 18·46 is a plot of the "standard luminosity curve" so placed with respect to curve *A* as to locate the threshold of cone response relative to the threshold of rod response.    If the radiance level required to stimulate the rods to yield a sensation of brightness is exceeded by an amount that is less than the vertical separation between curves *A* and *B* of Fig. 18·46, the sensation stimulated will be devoid of any sensation of hue, and the level of retinal illumination is said to fall within the "photochromatic interval."

The conclusions that must be drawn from this discussion are (1) that the higher the level of retinal illuminance used, the smaller is the difference in dominant wavelength or excitation purity which can be detected, the better is the sensitivity of the observer to small contrasts, and the better is the observer's ability to resolve small details in the presentation; and (2) that for a color-discrimination tube to be successful, it must be operated under such conditions that a high retinal-illumination level is used.

*Two-color Screens.*—There are very few examples of homogeneous phosphors that undergo any change in their relative spectral power distribution with time during phosphorescence.   Also, there are no known homogeneous phosphors that change their emitted spectral power distribution an appreciable amount with the number of repetitions of the exciting pulse of electrons, where these excitations take place with a repetition period of 0.1 sec or greater.   If the luminances obtained from sources of differing relative spectral power distribution are superimposed, the normal eye will not be able to identify the individual components of the compound stimulus but will see the color as a stimulus having a hue intermediate between the hues of the components that make up the stimulus.   It follows, therefore, that if the relative proportions of stimulus components vary with the time, the sensation of hue and possibly the sensation of hue saturation will vary with the time or past history of excitation only if the cathode-ray tube has been produced with a screen that contains two or more components.

Assume that one component of the screen can be excited to a moderately high state of luminance as a result of a single application of the electron beam, while the other component is excited very feebly by a single pulse of electrons.   Suppose, furthermore, that the easily excited screen component gives off a relative spectral power distribution with a dominant wavelength of 600 m$\mu$ and an excitation purity of 99 per cent.   The normal observer will identify the hue associated with such a stimulus as *light red*.   Suppose that the phosphor that has a comparatively weak luminance for a single pulse of electron excitation has a dominant wavelength of 510 m$\mu$ and an excitation purity of 90 per cent.   The hue associated with this stimulus will generally be identified as *green*.

The representative points that identify these two stimuli are shown as $R$ and $G$ in the I.C.I. chromaticity diagram of Fig. 18·47.   Let $B_R$ represent the luminance of the red phosphor at any instant of time at which the corresponding luminance of the green phosphor is $B_G$.   The location of the representative point that is obtained as a result of the superposition of these two luminances in the proportions defined can be computed as the fractional distance along the straight line from $R$ to $G$ with the help of the following equation:

$$\frac{RX}{RG} = \frac{\dfrac{B_G}{y_G}}{\dfrac{B_G}{y_G} + \dfrac{B_R}{y_R}}. \tag{16}$$

In this equation, the linear distance from $R$ to $G$ is represented by $RG$ and the distance from $R$ to $X$ is represented by $RX$.   The ordinates of $R$ and $G$ respectively are $y_R = 0.372$ and $y_G = 0.707$.

Consider the case in which the luminance excited in the green phosphor by a single electronic pulse is one unit while, at the same time, a single pulse excites ten units of luminance in the red phosphor.    From Eq. (16) the representative point of the compound stimulus is $X_1$.    Suppose that



FIG. 18·47.—I.C.I. chromaticity diagram and its use for the specification of phosphor colors and color mixtures.   Component phosphors represented by points $G$ and $R$.   Specific mixtures represented by points $X_1$, $X$, and $X_{50}$.   $E$ is representative point for equal energy white.   Excitation purities calculated with respect to point $E$ as achromatic point.

the buildup of the red phosphor following a large number of repeated excitations results in a luminance of 14 units, whereas the buildup of the green phosphor luminance may reach a value of 20 units.    Under these circumstances, the representative point of the combined stimuli will fall at $X_{50}$.    The screen areas that receive repeated excitations are likely to be represented on the chromaticity diagram by points on the straight

line $RG$ which are close to the one marked $X_{50}$.   The diagram shows that the dominant wavelength for this stimulus is 544 m$\mu$ and the excitation purity is 58 per cent.   Other areas of the screen which have received very few repeated electronic excitations will be represented by points near $X_1$. The dominant wavelength here is 596 m$\mu$ and the excitation purity is 96 per cent.

If the luminance level is sufficiently high so that the observer's vision is photopic, then the difference in color sensation or hue associated with the representative points $X_1$ and $X_{50}$ will be easily recognized.   If, on the other hand, the luminance level is so low that the observer's vision is scotopic, then, in the extreme case, there will be no detectable difference in hue.   There will be some tendency for the red phosphor used in this illustration to maintain its ability to stimulate the sensation of hue until its luminance level is very nearly that of the threshold of visibility.   This conclusion is supported by the fact, as illustrated in Fig. 18·46, that the photochromatic interval at 600 m$\mu$ is only about 30 cb.   In making this statement, the problem is definitely oversimplified because phosphors generally do not emit their radiance over such a small range in wavelength that they can be considered to be monochromatic, even though at high luminance levels they may be matched in color appearance perfectly by monochromatic stimuli.

The need for high luminance in order to make the color discrimination strong indicates that the exciting beam should deliver as much electronic charge to the screen per excitation as is possible.   In conflict with this desire is the need for high buildup of the luminance of one of the phosphors.   This change in luminance with repeated excitation must be depended upon to create a color discrimination that indicates a difference between an area of repeated excitation and a nonrepeated one.   Figure 18·42 illustrates the fact that the buildup produced by high $Q$ excitation is likely to be very small.   It is therefore necessary to strike a balance between high luminance and high buildup.   It is also necessary to select phosphors that have a wide difference in color, and that have other desirable characteristics including phosphorescence.

Although research was undertaken to create a suitable color-discrimination tube, the project was discontinued before a reasonably complete understanding of the problem and its difficulties was available. The more promising screens that were produced involved three components.   The construction of a screen using the phosphors described above would involve placing the green-emitting phosphor on the glass and creating a layer to be bombarded by electrons that was composed of a good red-emitting phosphor and one that had strong emission within the optical absorption band of the green-emitting phosphor.   The latter material would be used to excite the green by the absorption of radiant

power from the electron-excited layer. It has been demonstrated that it is principally by this method of excitation that one can hope to generate a fairly high luminance and at the same time obtain a high buildup by repeated excitations.

**18·11. The Dark-trace Cathode-ray-tube Screen and its Development.**—Goldstein[1] is generally credited with the discovery that certain crystals develop absorption bands for light within the visible range of wavelength subsequent to bombardment by electrons. The phenomenon of induced absorption bands is invariably associated with ionic crystals, of which potassium chloride is typical. The principal absorption center is associated with the occupancy by an electron of a vacant negative-ion site. Throughout the interior of a potassium chloride crystal, for example, it is to be expected that a finite number of crystallographic faults will exist which correspond to the omission of the chlorine ion that would normally be there. In spite of these faults in the crystal structure of potassium chloride, it is very transparent to radiant power within the band of visible wavelengths 380 m$\mu$ to 750 m$\mu$. The maximum of the induced absorption band, usually denoted by the letter "$F$" for "farben" or "Farbzentren," is close to 560 m$\mu$. Although the absorption is less for the shorter and the longer wavelengths, it is appreciable throughout the entire range of the visible spectrum. A potassium chloride surface prior to excitation has such a uniform diffuse reflectance that it looks very white when viewed with white light. After the absorption band has been created, the enhanced absorption of green light causes the diffusely reflected light to be rich in red and blue, and therefore to appear magenta.

Practical cathode-ray tubes produced by evaporating potassium chloride onto the inside surface of a tube face plate are generally viewed by white light and show the effect of electron bombardment as a darkening of the surface; hence the name "dark trace" or DT tube. Other names applied to this type of tube are "color trace tube" and "Skiatron."

The possibility of using a dark-trace tube as a radar indicator was demonstrated in England.[2] The developments that are reported in this chapter are largely due to Radiation Laboratory activity and are directed toward the solution of problems associated with the production of this screen and the investigation of the properties of screens produced under standardized conditions, so that suitable operational limitations could be determined.

---

[1] E. Goldstein, *Mon-ber. Berliner Ak.* S 225 (1891); "Action of Cathode-rays on Salts," *Ann. d. Physik und Chemie*, **54**, 371 (1895); "Coloration of Salts by Cathode-rays," *Ann. d. Physik und Chemie*, **60**, 491 (1897); "On Salts Colored by Cathode-rays," *Nature*, **94**, 494 (1914).

[2] Much work in the development of the tube was done under the direction of R. W. Sutton at the Admiralty Signal Establishment Extension, Bristol, England.

*Sensitivity of the Eye to Contrast and the Importance of Contrast Gradient.*
In the case of luminescent material, the light output of a screen must
exceed the threshold required for visual observation; or, for photographic
recording, the radiant energy must be sufficient to yield a detectable
contrast in the emulsion.   A similar limitation exists for the dark-trace
screen in that a sufficient number of electrons must be delivered to the
cathode-ray-tube screen to develop a detectable contrast.   Figure
18·33 shows that the liminal contrast that can be detected when the eye
is adapted to a luminance of one foot-lambert is about 0.4 per cent for
relatively large surface areas if the gradient is very sharp.   Since the
eye is able to resolve two point sources that are separated from each
other by slightly less than one minute of arc, it seems reasonable to
suppose that a step in contrast of 0.5 per cent in a linear distance of 0.1
mm would represent the required contrast gradient for viewing at 30-cm
distance.   Middleton[1] has reported some experimental results that may
be interpreted to indicate that, for contrast in the range of 2 to 10 per
cent, the contrast gradient required is probably 0.3 per cent per minute
of arc.   Thus, if the contrast difference is 10 per cent and the gradation
takes place over a distance of 2.6 mm the fact that a difference in con-
trast exists will be just detectable with reasonable certainty.   It follows
that, in order to detect a trace on a DT tube, it is not sufficient to have a
contrast difference of a few per cent but it is necessary that the boundary
have a contrast gradient of at least 0.3 per cent per minute of arc and
preferably 0.5 per cent per minute of arc.

*A Comparison Between Certain Characteristics of DT and P7 Screens.*
Dark-trace tubes that have been developed serve best in applications
where a moderately long persistent pattern is desired.   It is therefore
appropriate to compare the properties of the DT tube with those of the
cascade screen type such as the P7.   For the range of charge density per
excitation of most interest in connection with the use of the P7 tube, it
has been demonstrated above that high-intensity excitation tends to be
followed by a more rapid decay in luminance than does lower-intensity
excitation.   In the case of the PPI indicator the usual adjustment of the
associated amplifiers results in a continuous excitation of the screen due
to the random noise impulses that are applied to the grid of the cathode-
ray tube.   A weak signal applied to the grid in addition to the noise
modifies the distribution of noise and tends to increase the luminance
of the tube screen at the localized point of application.   Within a few
tenths of a second after the signal has been applied, the visual contrast
between the signal area and the surrounding region is higher than at any
other time until the next excitation takes place.   Two factors enter here,

[1] W. E. K. Middleton, "Photometric Discrimination with a Diffuse Boundary,"
*J.O.S.A.*, **27**, 112 (1937).

both of which have been mentioned above: (1) the faster decay for stronger signals, and (2) the loss in recognizability of a given contrast as the level of luminance decreases. The performance of the DT screen will be shown to differ from the P7 screen in that traces following weak excitation disappear faster than those resulting from strong excitation. This DT characteristic is both advantageous and disadvantageous. Even though the contrast over a specific excitation area is decreasing with·the time, the fact that the contrast in the unexcited area decreases more rapidly makes the contrast gradient decrease more slowly than would otherwise be the case. Since signal recognizability depends both upon the contrast and the contrast gradient the differential decay in contrast will tend to keep signal recognizability more constant. The disadvantage associated with the slowness of the decay of contrast following strong excitation is the so-called "burn in" difficulty. If a given area of the screen is bombarded so heavily that a contrast of 25 per cent or more is developed, then it may be so difficult to remove the trace that its presence on the tube will be detrimental to its further usefulness.

**18·12. Test Methods and Terminology.**—The electron beam in each of the tubes investigated was magnetically focused and deflected. A rectangular raster was used. The high-speed sweep frequency was 12 kc/sec and the low-speed sweep was 60 cps. Excitation was generally by means of a single raster applied intermittently with a period between rasters of 10 sec. The notations to be described identify the excitation procedure.

Contrast measurements were made with the help of a 931 multiplier phototube and a pen-and-ink recorder. The circuits were arranged so that a recorded deflection could be made directly proportional to the light flux entering the phototube. However, by means of suitable switching the recorder could be made to indicate the *decrease* in light flux entering the phototube. The advantage of this arrangement is that a direct measure of the diffusely scattered radiant power could be obtained so as to determine the reflectivity of the coating in the absence of absorption bands. With the circuit reconnected to measure changes in reflectivity, the recorded deflection was directly proportional to the induced contrast. From these two data the contrast could be computed.

Since the excited region of the screen was small compared with the entire tube face it was necessary to use a lens to project an image of the screen surface onto a slit behind which the phototube was located. In order to use the method described as a means of measuring contrast three criteria must be satisfied: (1) the amount of light that enters the slit as a result of scattering from parts of the screen other than the area imaged by the lens must be negligible in comparison with the light being measured; (2) the lamps used to illuminate the screen must yield a con-

stant amount of light throughout the entire time over which a given contrast measurement is made; and (3) the area outside the region of measurement must be unexcited and must have the same diffuse reflect-
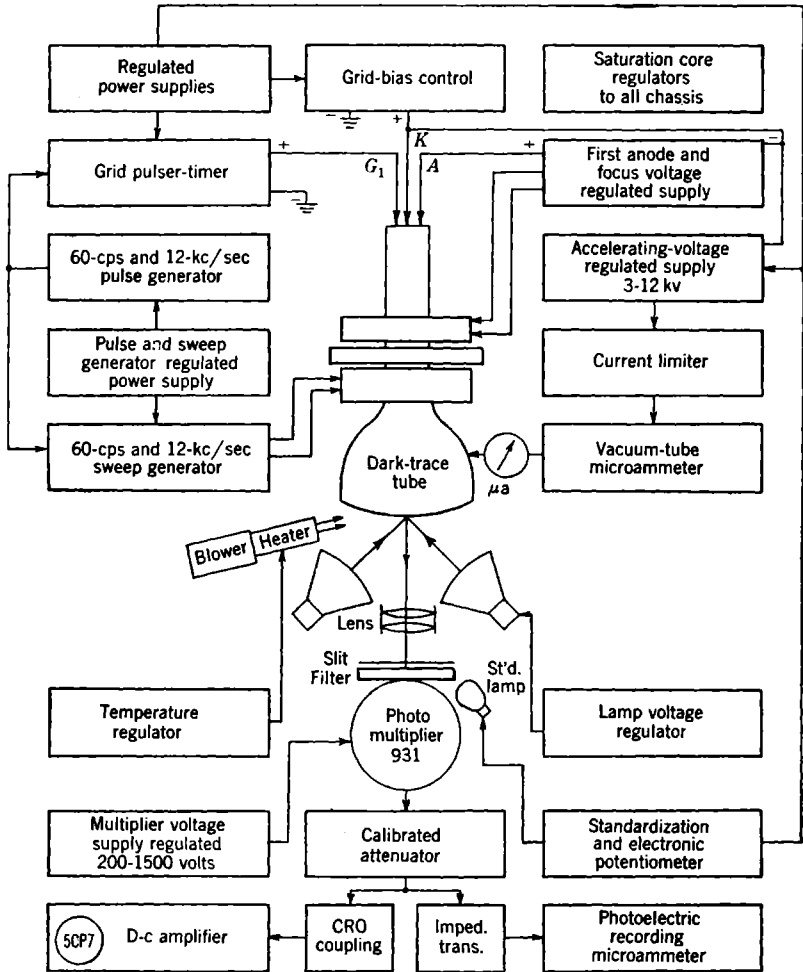


FIG. 18·48.—Block diagram of dark-trace test equipment.

ance as the area over which the induced absorptance is generated following electron bombardment.

If the phototube current is directly proportional to the instantaneous luminance of the area under investigation, then

$$100 \frac{B_0 - B_t}{B_0} = 100 \frac{i_0 - i_t}{i_0} = \text{contrast expressed in per cent.}$$

In the above equation $B_0$ is the diffuse luminance of the cathode-ray-tube screen when it is free from induced absorption, and $B_t$ is the luminance at any chosen time at which knowledge of the induced contrast is desired. The currents $i_0$ and $i_t$ are the corresponding phototube currents that are actually measured.

The production and decay of contrast are very complex functions of the screen properties and of the controllable operating parameters. The principal parameters are the following:

1. Charge density per excitation in terms of current density and excitation time.
2. Sequence of excitation in terms of time intervals and the number of excitations applied prior to observation.
3. Sequence and nature of weak beam bombardment sometimes used to stimulate the decay of contrast.
4. Electron energy expressed in terms of cathode-to-anode voltage.
5. Temperature of the screen.
6. Relative spectral power distribution of the illuminant used for viewing or measurement.
7. Intensity of illuminating radiation.
8. Time of observation subsequent to last previous excitation.

The block diagram of Fig. 18·48 shows the general organization of the equipment used to operate and test dark-trace cathode-ray tubes. The two diagrams of Fig. 18·49 serve to define the symbols used for the identification of contrasts most likely to be of interest. Figure 18·49a shows the excitation and decay of contrast on a time scale that is fast enough to show that the measured contrast rises during the $\frac{1}{60}$ sec occupied by the excitation. The maximum contrast at the end of an excitation period is designated by the letter $M$, preceded by a number telling the order number of the excitation, and followed by a number describing the time interval between excitations. Thus the symbol 2M10 represents the contrast at the end of the *second* excitation in a sequence of excitations separated by *10 sec*. For measurements of decay, the letter $D$ is preceded by the order number of the last excitation and followed by the decay time since that excitation. Thus the symbol 2D5 represents the contrast *5 sec* after the *second* excitation.

The contrast produced on the screen of a DT tube decreases with time depending on the initial contrast, the means by which that initial contrast was produced, the temperature of the screen, and the intensity of the radiance used to illuminate the screen. No simple decay law has

been discovered which represents the change in contrast with the time. In studying the decay, the time most often chosen has been the 10-sec point.    Data will be presented later giving the results of observations made after a number of arbitrarily chosen periods of time.    Although the maximum contrast $M$ depends to some extent upon the number of excitations that have been applied, it is most dependent upon the charge density per excitation and is only slightly dependent upon the temperature and the illumination.

A single number, known as "the contrast ratio" indicates the bleaching rate under standardized operating conditions.    The contrast ratio is the contrast ($1M$) divided by the contrast ($1D10$) that is observed after excitation with a $Q$ of 1.0 $\mu c/cm^2$.    The standardized final-anode potential was 9000 volts and the standard illumination on the face of the tube was rated at 8000 foot-candles.    The illumination was derived from two
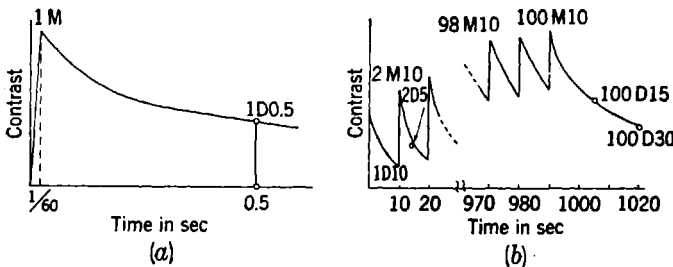


FIG. 18·49.—Illustration of nomenclature.    (*a*) Single pulse.    (*b*) Multiple pulse.

150-watt incandescent projector spot lamps operated from a regulated d-c power line.    The light from the lamps was passed through water cells 3 in. in thickness in order to remove much of the heat radiation. Automatically controlled air blasts kept the temperature of the screen at 35°C while under measurement.    Under these conditions pure potassium chloride screens, when first produced, have a contrast ratio close to 12. It may be pointed out here that subsequent to extensive operation of pure potassium chloride screens, the contrast ratio generally decreases and approaches 6 or 7 after the total charge per square centimeter delivered to the screen is approximately 1 coulomb.

Two methods were used for the determination of the maximum contrast obtainable immediately after screen excitation.    The older of the two methods involved the reading of the maximum swing of the pen-and-ink recorder and was subject to considerable inaccuracy.    All later measurements of the maximum contrast depended on examination of contrast as a function of the time by means of a cathode-ray oscilloscope having a P7 long-persistence screen and a synchronized time sweep, so

arranged that the observer could obtain an accurate determination of the contrast immediately following excitation.

*The Universal (1M) Curve and the Screen-sensitivity Index.*—Under a given set of conditions the curves that represent the contrast (1M) as a function of the excitation $Q$ are all of very nearly the same general shape when plotted on logarithmic scales. When the logarithm of the contrast is plotted as the ordinate and the logarithm of the charge density per excitation is plotted as the abscissa, and curves for various screens compared, it is found that the points can be made to fall very closely on a single "universal" curve if each set of data is displaced by a proper amount only along the $Q$ axis (horizontal). Thus the factor by which it is necessary to change $Q$ to change the contrast (1M) by a given factor depends not upon the $Q$ required to give the initial contrast but only upon
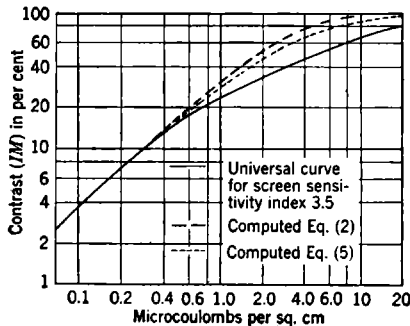


FIG. 18·50.—Observed universal curve compared with theory.

the contrast itself.[1] Figure 18·50 shows (1) the "universal" (1M)-$Q$ curve and (2) two theoretical curves that will be discussed in more detail in a later section. The form of the universal curve shown in Fig. 18·50 was established by a very careful investigation of 10 typical good-quality· dark-trace screens made with pure potassium chloride.

The universal curve represents the data so faithfully that a nomographic chart was developed (Fig. 18·51) which provides an accurate prediction of the contrast to be expected from any chosen value of $Q$ if the contrast at some other arbitrarily chosen $Q$ is known.

In order to make use of the $QM$ nomograph it is necessary to define a number known as "the screen-sensitivity index." This index is equal numerically to the reciprocal of the $Q$ value required to generate a contrast (1M) equal to 10 per cent. In order to use the nomograph, it is not

[1] R. B. Windsor, "Production and Properties of Skiatron Dark-trace Cathode-ray Tube with Microcrystalline Alkali Halide Screens," Thesis, Radiation Laboratory and Dept. of Physics, M.I.T., 1944.

necessary to make the initial measurement with the exact value of $Q$ that generates a 10 per cent contrast, but any $Q$ value may be used if the contrast produced is within the range for which the accurate data may be obtained.    Experience indicates this range to be between 5 and 25
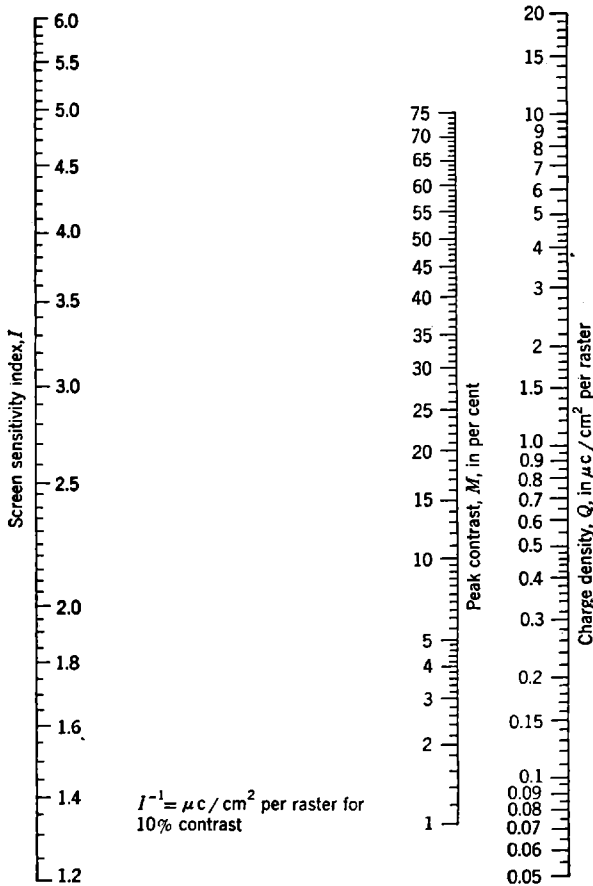


FIG. 18·51.—*QM* nomograph.

per cent.    For example, a contrast of 19 per cent has been observed on a particular tube to be generated by a charge density per raster of 0.7 $\mu c/cm^2$.    A straight line that joins the observed $Q$ value and the observed contrast ($1M$) extrapolates to intersect the screen-sensitivity index line at 3.4.    This particular tube therefore is characterized by the index number 3.4 and will yield a contrast of 10 per cent if a $Q$ value equal to

the reciprocal of 3.4 is applied.    This reciprocal value in the case under discussion is 0.293 $\mu c/cm^2$ per raster.    In the example cited a straight line drawn from the index number 3.4 to the charge density scale at 1 $\mu c$ intersects the contrast scale at 24.    This result shows that the expected contrast for the tube in question will be 24 per cent for a $Q$ value of 1 $\mu c/cm^2$.

It is evident from Fig. 18·50 that over the range of contrast from 1 per cent to approximately 15 per cent the contrast is almost directly proportional to the first power, and between 20 per cent and 35 per cent to the square root of the charge density per raster.

**18·13. Dependence of Maximum Contrast on Anode Voltage, Temperature, and Illumination.**—The dependence of the maximum contrast ($1M$) on the electron energy has been investigated in the range from 1500 to 14,000 volts.    Typical results are illustrated in Fig. 18·52 for three values of charge density ($Q$).    It is evident from the plotted curves that the lower the value of $Q$ the greater the increase in contrast with voltage.    The scales of the plot shown in Fig. 18·52 have been so chosen that the slope of the curve is the exponent of the contrast dependence on voltage.    For example, on the low-voltage range and for the low-$Q$ value of 0.5 $\mu c/cm^2$, the slope of the curve seems to be close to 2, and therefore the contrast increases with the square of the voltage.    The curve for highest value of $Q$ has an increase in contrast with voltage that is less than linear over the entire range.    Very early in the development of the dark-trace tube the normal operating voltage of the tubes was more or less determined to lie within the range 8 to 10 kv, and this chosen range seems to be reasonably well supported by the data of Fig. 18·52. There are other considerations that make the determination of the optimum operating voltage difficult to establish.    For the tubes to be used in optical projection systems, it is desirable to have the best possible focus of the electron beam and experience shows that the higher the voltage used the higher the current density obtainable and therefore the higher the contrast gradient.    For tubes that are to be viewed directly, the focus requirement would not demand potentials in excess of 8000 volts. In all cases consideration should be given to the more complex details of the voltage dependence of contrast decay under specified conditions of initial contrast, operational temperatures, and light intensity used for viewing. The data now available are insufficient for the establishment of the most suitable operating voltage to suit the operational requirements likely to be met.

An increase in light intensity or an increase in temperature of the screen causes a dark-trace pattern to bleach more rapidly.    Up to a temperature of 150°C and up to an illumination level of the order of 10,000 foot-candles there is very little decrease on the maximum contrast

$(1M)$.[1]   When the screen is operated at high temperature and under high illumination the decay in contrast that takes place during $\frac{1}{60}$ sec is appreciable and therefore the measured maximum $(1M)$ is more and more in error as an indication of the true physical phenomena being investigated as the light and heat are increased.
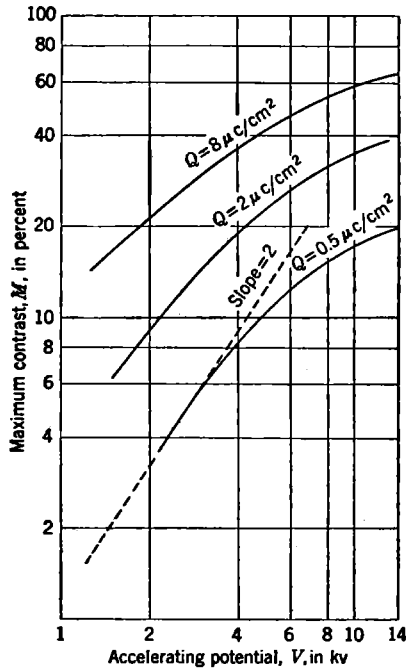


FIG. 18·52.—Maximum contrast as a function of accelerating potential.

**18·14. Persistence of Contrast.**—The changes of contrast with time following excitation are of far more direct interest to the observer of the dark-trace tube than is the maximum contrast generated at the instant of excitation, since the pattern (1) must last long enough for the observer to make use of it, and (2) must be capable of being erased or bleached sufficiently quickly so that the old pattern does not interfere with the new. These two requirements combined with the inherent physical properties of dark-trace screens make it necessary for the user of this cathode-ray tube to devise schemes for driving the control grid of the tube sufficiently far to give the required minimum excitation current and yet

[1] H. F. Ivey, "Optical and Electronic Properties of Polycrystalline Potassium Chloride Spectron Screens," Thesis, Radiation Laboratory and Dept. of Physics, M.I.T., 1944.

to avoid overdriving the grid and thus generating such a high contrast in localized regions of the screen that it is difficult to remove the consequent trace.

All attempts that have been made to find a useful formula to describe the decay in contrast as a function of time have failed.   It has therefore been necessary to devise graphical methods for summarizing experimental data that represent the decay properties of dark-trace screens.   Figures 18·53 and 18·54 represent a method of presentation that has been found to be useful although not sufficient for all purposes.   The curves shown in Fig. 18·53 show the contrast as a function of the charge density per raster, with each curve corresponding to the time in seconds after a single excitation.   The curve designated $(1M)$ is the maximum contrast
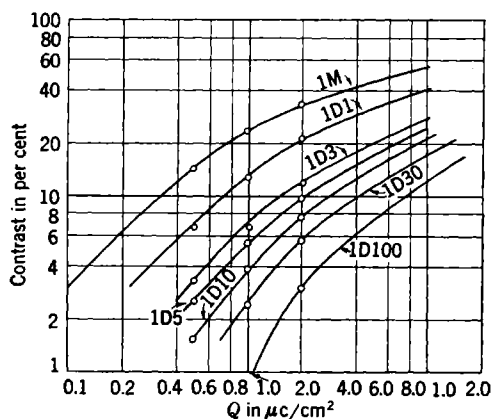


Fig. 18·53.—Decay of contrast from a single pulse as a function of exciting charge density $Q$.

observed on the particular tube to which the data applies.   The $(1M)$ characteristic for this tube is well represented by the universal curve, the screen sensitivity index being 3.1.

These decay curves are similar to although not identical with the universal curve described above.   In the range of contrast from 5 per cent to 1 per cent the slope of the $1D10$ curve is greater than unity.   This curve shows that if the charge density per excitation is $0.6 \ \mu c/cm^2$ the contrast will fall in the first 10 sec from approximately 17 per cent to 2 per cent.   If the contrast gradient is sufficiently high, then such a signal will be visible for the entire period of 10 sec.

The data shown in Fig. 18·53 apply to observations made subsequent to a single excitation.   In the practical application of dark-trace tubes, it is often necessary to excite some localized region of the screen over and over again, during which time the contrast increases as a result of this repetition.   It was decided arbitrarily to investigate the decay in contrast

following 360 excitations. Typical results are shown on Fig. 18·54. For a $Q$ of 0.6 $\mu$c/cm², the maximum contrast observed at the end of the 360th excitation is approximately 21 per cent, and 10 sec later the contrast is 8 per cent. After 300 sec of bleaching the contrast is 3.6 per cent and is therefore well above the minimum required for a signal to be observable if the contrast gradient is adequate.

*Decay in Contrast Related to Maximum Contrast.*—A second general method for the presentation of information concerning the decay of contrast is that in which the $Q$ required to generate the contrast is not expressed explicitly. In Fig. 18·55 the maximum contrast $(1M)$ is plotted along the abscissa of the coordinate system and the decay contrast $(1D\text{-})$ is plotted as the ordinate. The eight curves shown in Fig. 18·55 apply to observations taken at different times following the excitation by a single raster.



FIG. 18·54.—Decay of contrast after 360 pulses repeated at 10-sec intervals, as a function of exciting charge density $Q$.

Quantitative data on the decay of contrast after repeated excitations are presented in Fig. 18·56, which is similar to Fig. 18·55 except that the
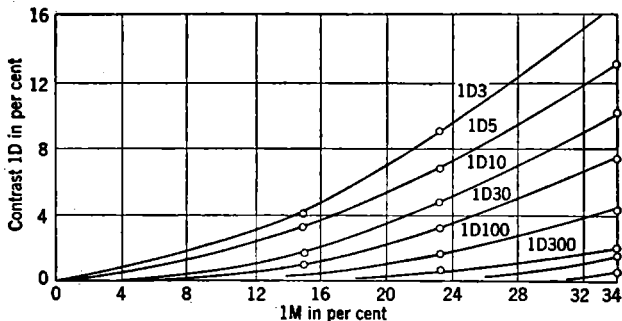


FIG. 18·55.—Decay of contrast (tube R-220) from a single pulse in screen condensed at 35°C and operated at 35°C.

contrast $(360M10)$ is plotted in place of $(1M)$ and the decay contrast $(360D\text{-})$ is plotted in place of $(1D\text{-})$. The eight curves shown in this figure apply to times of observations from 3 sec after the 360th excitation

to 1000 sec after that excitation.    In order to make the fullest use of Figs. 18·55 and 18·56 the curve that relates the maximum contrast (360$M$10) to the maximum contrast (1$M$) is needed.    This curve is shown in Fig. 18·57.    The solid line gives the relation between (1$M$) and (360$M$10) for the same tube and data as were used for Figs. 18·55 and 18·56.    The screen-sensitivity index for that particular tube was 4.3.

In order to illustrate the use of these curves, an example will be discussed in which the requirement is made that the contrast developed from a single excitation and observed 10 sec after this excitation shall be equal to 1 per cent.    This requirement is sufficient to establish the value of (1$M$) as 12 per cent.    The curve of Fig. 18·57 may be used to determine
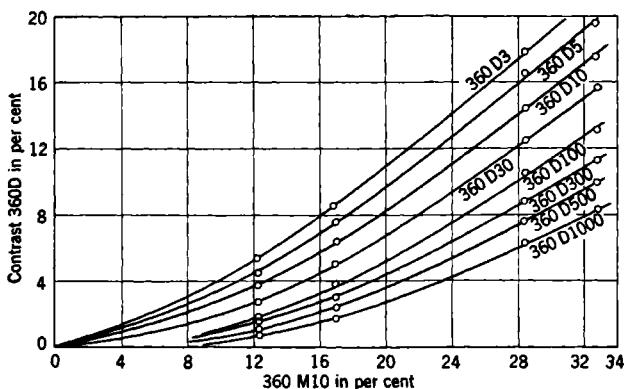


Fig. 18·56.—Decay of contrast (tube R-220) after repeated pulses in screen condensed at 35°C and operated at 35°C.

the corresponding value of (360$M$10) as 13 per cent.    By use of the nomographic chart of Fig. 18·51 and the sensitivity index of 4.3, the current density per raster required to generate this contrast is known to be 0.29 $\mu$c/cm$^2$.    Under these conditions of operation, the contrast over an area that has been bombarded 360 consecutive times with an interval of 10 sec between bombardments will exceed 1 per cent for a time of 500 sec and will fall from 13 per cent at the maximum of each additional excitation down to 4.2 per cent between successive excitations.

One may conclude from these figures that if the grid drive is limited so that 0.3 $\mu$c/cm$^2$ is the maximum $Q$ that can be delivered near the periphery of a dark-trace tube that may be used in a PPI radar indicator, then signals will be visible and "burn-in" will not be serious.

In an ideal indicator the pulse repetition period and the minimum spot diameter of the cathode-ray-tube beam are so related that adjacent radial sweeps of the electron beam overlay at the periphery of the tube face.    If this condition is not satisfied, the effective contrast for signals

at the periphery of the tube will be appreciably reduced because of the intermixture throughout the signal area of excited and unexcited regions of the screen.    If this first criterion for good tube operation is satisfied, then it is evident that the effective $Q$ value used to excite other parts of the tube will be inversely proportional to the radius.    Compensation for this undesirable increase in $Q$ should be possible by synchronized electronic control of the limiting.    The maximum $Q$ value at any part of the tube may be made to remain practically constant when full consideration for the overlapping of the excited regions is incorporated. It may not be practical to bring about perfect compensation because of the nonlinear relation between the electron beam current density and the grid drive. If synchronized limiting and gain control are not included in the receiver used to operate a dark-trace tube on a PPI indicator, objectionable burn-in is almost certain to follow.



FIG. 18·57.—Relation between (1 *M*) and (360 *M* 10) for tube R-220.

The decay in contrast that follows many hours of bombardment is slower than that shown by the data of Fig. 18·56.    No quantitative data are available that can be used to predict the decay after many hours of operation.

**18·15. Dark-trace-tube Operation at 100°C.**—Extensive researches have been undertaken in order to make better use of dark-trace tubes:

1. The investigation of the properties of pure potassium chloride screens operated at relatively high temperatures.
2. The investigation of the properties of pure potassium chloride screens that had been produced by condensation of the potassium chloride onto the inner surface of the tube while it was maintained at a low temperature.
3. The investigation of the properties of screen into which impurities were intentionally introduced.

The curves of Figs. 18·58 and 18·59 are typical of the response and decay characteristics of pure potassium chloride screens operated at 100°C.    The dotted lines on each of the figures indicated the decay curves for an operating temperature of 35°C.    Figure 18·58 illustrates

that high-temperature operation causes a marked increase in decay of contrast for any given initial contrast $(1M)$. The contrast $(1D)$ was observed to fall in 10 sec, when the tube was operated at 100°C, to about the same value as that observed at 30 sec for the tube operated at 35°C.
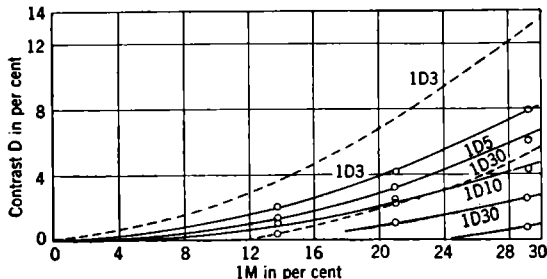


FIG. 18·58.—Decay of contrast (tube R-194) after single pulse in screen condensed at 35°C and operated at 100°C. Dotted curves represent operation at 35°C.

Even though Figs. 18·53 to 18·57 apply to a different tube from that used for Figs. 18·58 and 18·59 the minor differences in performance may be taken as typical of tubes produced under standard controlled conditions. The increased rate of screen bleaching following excitation is well illustrated in Fig. 18·59. The contrast observed 30 sec after 360 excitations, with operation at 100°C, is almost identical with that obtained 500 sec after the last previous excitation if the operation is at 35°C.
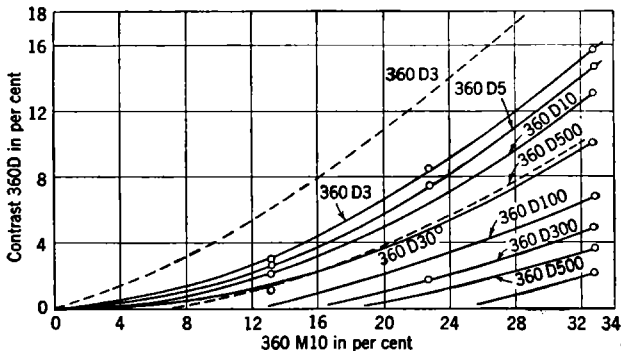


FIG. 18·59.—Decay of contrast (tube R-194) after repeated pulses in screen condensed at 35°C and operated at 100°C. Dotted curves represent operation at 35°C.

The curve shown in Fig. 18·57 relates $(360M10)$ to $(1M)$ and the universal curve and the nomographic chart of Figs. 18·50 and 18·51 relate $(1M)$ to the $Q$ value. This procedure is justified because the maximum contrast is almost independent of the temperature of operation.

The small decrease in contrast that may exist becomes important only if one becomes interested in the detailed behavior of a particular tube.

An example was given above in which it was required that the tube be operated in such a manner that $(1D10)$ should be 1 per cent. If this is repeated for high-temperature operation the corresponding values $(1M)$ and $(360M10)$ can be determined from the curves given and from the knowledge that for the particular tube in question the screen-sensitivity index is 2.85. For the contrast $(1D10)$ of 1 per cent, the maximum contrast $(1M)$ must be 16 per cent and will be obtained if the $Q$ value is 0.64 $\mu c/cm^2$. The corresponding value of $(360M10)$ is 18 per cent. Under these conditions of operation, the value of contrast is at least 1 per cent for approximately 125 sec following the 360th excitation. This figure of 125 sec is to be compared with the figure of 500 sec found above for operation at 35°C. The particular tube investigated had a lower screen-sensitivity index than the one used in the previous example, which accounts for about 50 per cent of the increase in $Q$ (above 0.3 $\mu c/cm^2$) for comparable operation. On the average, tubes operated at 100°C will require an increase of 50 to 75 per cent in charge density per excitation, as compared with operation at 35°C. Thus, although operation at high temperature minimizes the objectionable burn-up, it has the disadvantage that higher current densities are required to produce a given contrast. It generally follows that the use of a high current density yields a lower contrast gradient and, unless the gradient is as much as 0.5 per cent per minute of arc, a lowering of the gradient will lower the signal discernibility. Although it is not difficult to obtain a gradient slightly better than 0.5 per cent per minute of arc on the face of the tube, a projection system with a magnification of 5 reduces the contrast gradient by an amount at least equal to the magnification factor. Thus to attain a gradient of 0.5 per cent per minute of arc of the projected image, a gradient on the tube face would have to be higher than 2.5 per cent per minute of arc. Such a high gradient would be exceedingly difficult to attain and improvements in gun design that would increase current density at the expense of total current would be beneficial.

**18·16. Influence of Screen-condensation Temperature.**—Investigations have been made of the properties of screens condensed at various temperatures down to approximately −170°C. Ralph Johnson of the General Electric Company experimented in the development of the dark-trace tube with the condensation of potassium chloride films on glass surfaces held at temperatures both well above and well below room temperature.[1] He did not investigate the properties of the films thus produced except to describe their physical appearance. The first experi-

---

[1] S. Dushman, "Report on Progress of Work on Dark-trace Tubes," NDRC 14-147, GE Co., March 1, 1943. (See Figs. 4 and 5 therein.)

ments undertaken at the Radiation Laboratory covered the range of temperature down to $-50°C$ and yielded tubes for which the performance curves indicate a reduction of the burn-in.

As the condensation temperature is lowered, the weight of potassium chloride that must be deposited on the screen in order to create a diffuse reflection factor sufficiently high for efficient tube operation increases very noticeably. A screen of "normal" thickness (about 12 microns) deposited at a temperature of $-100°C$ is so transparent that it is hardly visible. Over a range of temperature between $-115°C$ and $-135°C$ a given weight of potassium chloride gives a screen with very noticeably higher back reflectance than that found for tubes made at both higher
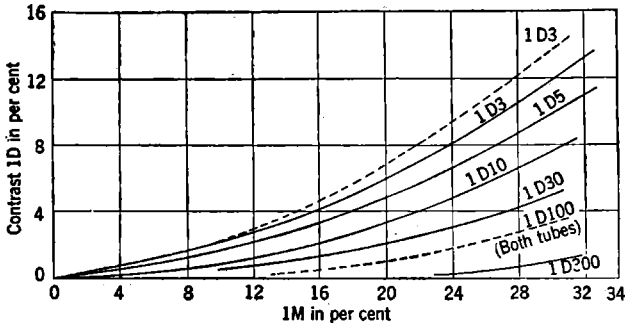


FIG. 18·60.—Decay of contrast (tube R-212) after single pulse in screen condensed at $-50°C$ and operated at 35°C. Dotted curves apply to tube R-220, condensed at 35°C.

and lower temperatures. The properties of tubes having screens condensed at approximately $-125°C$ were found to be unfavorable since the screen-sensitivity index was low and the burn-in more objectionable than tubes made at somewhat higher temperature. The best condensation temperature for creating a tube that is efficient and for minimizing the burn-in is approximately $-70°C$. Over the range of temperature from $+25°C$ to $-70°C$ it is more and more difficult to obtain a screen of uniform back reflectance as the temperature is lowered. Satisfactorily uniform screens were produced in the laboratory down to $-50°C$ with very little change in method except to use a larger weight of potassium chloride in the evaporator cup. Little research has been undertaken to develop satisfactory techniques for the mass production of uniform screens at very low temperatures.

*Comparison between Low- and High-temperature Screens in Operation.*—The tube designated by the number R-212 was produced by the condensation of potassium chloride onto a face plate maintained at $-50°C$. The screen-sensitivity index for this tube is 3.10. The curves presented in Fig. 18·60 should be compared with those of Figs. 18·55 and 18·58.

The close similarity between the curves of Figs. 18·60 and 18·55 show that the decay characteristics of the low-temperature tube when excited by a single raster are almost identical with those of the room-temperature tube. It has already been demonstrated in connection with Fig. 18·58 that the systems operation of a tube at high temperature alters the decay of contrast following a single excitation. Figure 18·61 shows the decay following 360 excitations repeated with a time interval of 10 sec. This figure is therefore similar to Figs. 18·56 and 18·59 and should be compared with them. The important fact to note is that the decay of contrast following repeated excitation is very definitely faster for tube R-212 than
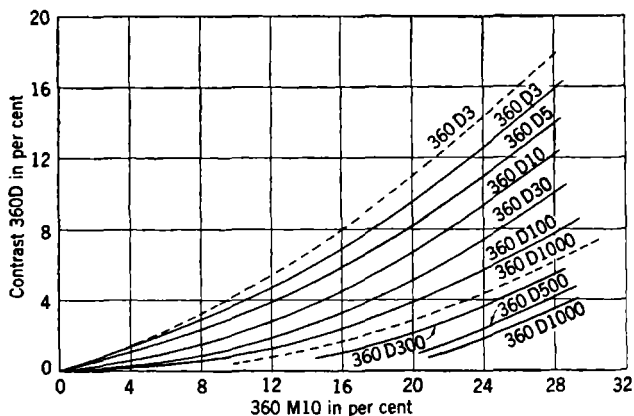


Fig. 18·61.—Decay of contrast (tube R-212) after repeated pulses in screen condensed at −50°C and operated at 35°C. Dashed curves apply to tube R-220, condensed at 35°C.

was the case for the tube R-220 when both tubes were operated at the same temperatures. The dashed curves show two selected decay characteristics that were observed at 3 sec and 1000 sec after the 360th excitation. Note in particular that the 1000-sec decay curve of R-220 coincides with the probable location of the 200-sec curve of the low-temperature tube R-212. The comparison of Figs. 18·59 and 18·61 shows that the 100-sec curve of Fig. 18·59 coincides reasonably well with the 300-sec curve of Fig. 18·61. Thus it may be concluded that the operation of the low-temperature tube at 35°C is comparable with the operation of the other tube at 100°C, although its bleaching following repeated excitation is not so fast. Although data are not at hand to establish curves for the high-temperature operation of tube R-212, enough experience was obtained to establish the fact that a moderate increase in temperature above 35°C, for the operating value, would give tube R-212 an increased bleaching rate and make it equal to that exhibited in Fig. 18·59.

The numerical examples of tube operation given above required that

the contrast following a single excitation remain above 1 per cent for 10 sec.   From the curves of Fig. 18·60 it is evident that if the contrast ($1M$) is 11.5 per cent, the contrast ($1D10$) will be 1 per cent.   Since the screen-sensitivity index is 3.1, Fig. 18·51 shows that the charge density per single excitation must be 0.38 $\mu c/cm^2$.   Figure 18·57 shows that the corresponding value of ($360M10$) will be 12.5 per cent.   From Fig. 18·61 it is evident that with the excitation as described, the contrast of a repeated signal will drop to 1 per cent in 125 sec.   This final result is in exact agreement with that obtained for the "normal" tube operated at 100°C, and was obtained with an excitation charge density of 0.38 $\mu c/cm^2$ excitation, which is advantageous.   At the relatively low charge density required for this tube, there is a better chance of realizing a high contrast gradient than there is when the charge density has to be raised to 0.64 $\mu c/cm^2$ as is necessary for high-temperature tube operation as illustrated above.

A summary of the numerical examples that have been worked out in the above discussion is incorporated in Table 18·3.   It was arbitrar-

TABLE 18·3.—INFLUENCE OF CONDENSATION AND OPERATING TEMPERATURES ON
SCREEN CHARACTERISTICS

| Characteristic | Tube no. | | |
| --- | --- | --- | --- |
| | R-220 | R-196 | R-212 |
| Cond. temp..................... | 35°C | 35°C | −50°C |
| Oper. temp..................... | 35°C | 100°C | 35°C |
| Index......................... | 4.30 | 2.85 | 3.10 |
| ($1M$) for 1 % ($1D10$)............ | 12% | 16% | 11.5% |
| $360M10$....................... | 13% | 18% | 12.5% |
| Time for decay to 1 %........... | 500 sec | 125 sec | 125 sec |
| $Q$............................. | 0.29 $c/cm^2$ | 0.64 $c/cm^2$ | 0.38 $c/cm^2$ |

ily decided in advance of the preparation of Table 18·3 that the contrast following a single excitation should hold above 1 per cent for 10 sec and that the criterion for bleaching after 360 excitations should also be the 1 per cent contrast value.   Although these are reasonable choices, experience with a particular cathode-ray tube indicator might make a slightly different choice of limiting numbers more appropriate.   If the family of curves for typical tubes and for typical operating conditions is available, the problem can be worked out for choices of the limits of signal discernibility after a single excitation and of limiting contrast following extended excitation.

Although the advantage of using dark-trace screens condensed at low temperature is unmistakable, the use of such screens is not warranted

unless electron guns capable of giving the highest contrast gradient possible under operating conditions are also obtained.    In case the image is projected, great care must be exercised in the electron-beam and optical focusing and in the design and construction of the optical system so as to minimize the loss in contrast gradient.

The final point to be emphasized is the need for synchronized limiting and gain control if the dark-trace tube is to be used on a PPI radar indicator.    It is important that the maximum charge density per unit area be as uniform as possible and be held within the range that produces a maximum contrast of not more than about 18 per cent.    If contrasts exceed this value, more strenuous methods must be used to bleach such areas after repeated excitations have been applied (see Sec. 16·16).

**18·17. Influence of Metallic Impurities.**—The introduction of metallic aluminum into the evaporator cup along with the normal charge of potas-

TABLE 18·4.—EFFECT OF METALLIC IMPURITIES ON CERTAIN DARK-TRACE SCREEN
CHARACTERISTICS

| Metal* | %† | $(\%/A) \times 10^5$‡ | $\Delta H$§ | $(1M)\|$ | $I$¶ |
|--------|------|------|------|------|------|
| Th | 0.006 | 3 | 2 | 27 | 4.25 |
| Mg | 0.006 | 30 | 24 | 26 | 4.10 |
| Al | 0.2 | 700 | 44 | 27 | 4.25 |
| Mn | 0.3 | 600 | 45 | 24 | 3.45 |
| Cu | 0.8 | 1200 | 68 | 21 | 2.78 |
| Sb | 2.0 | 1600 | 69 | 23 | 3.18 |

* Metals used, generally in the form of fine powder of small particles.

† Per cent (by weight inserted in evaporator cup) required to obtain screens with a contrast ratio of 25.   (The average ratio for pure potassium chloride is 12.)

‡ A number proportional to the number of metallic atoms used as the impurity.   It is $10^5$ times the percentage shown in Column 2 divided by the atomic weight of the metal.

§ The quantity $\Delta H$ is the difference between the heat of formation of potassium chloride and the heat of formation per chlorine ion of the metallic salt.   The heat of formation of potassium chloride is approximately 100 kilocalories per mole.

|| The symbol $(1M)$ here indicates the contrast expressed in per cent produced by a single raster with a charge density $Q$ of 1 $\mu c/cm$.

¶ The screen sensitivity index is represented by $I$.   Figure 18·51 may be used for the computation of contrast with any other $Q$ value.

sium chloride results in the production of dark-trace screens that exhibit a marked increase in the bleaching rate following nonrepeated excitation.[1]    Very extended researches were undertaken with the hope that screens with improved operating characteristics would be so created. Since this effort failed in its objective, only a brief summary of results and conclusions will be presented here.

Experiments soon showed that some metals were decidedly more effective than others in altering the contrast ratio (1M/1D10).    The

[1] ASEE progress reports, Bristol, England.

heat of reaction per chlorine atom when a salt is formed is a rough measure of the tenacity of one metal atom compared with another to take or hold the chlorine. The amount of heat evolved upon the formation of potassium chloride, KCl, is larger than that evolved upon the formation of the chlorides of other common metals. The difference between the heat formation of thorium chloride, ThCl$_4$, and of KCl is small, and thorium was found to be the most active of all the metals investigated. Table 18·4 summarizes the results obtained on six of the metals studied.

It would be incorrect to interpret the results recorded in Columns 5 and 6 as an indication that there is a systematic trend in the maximum contrast ($1M$) for standard excitation. Relatively minor alterations in production technique, including such factors as the exact amount of potassium chloride used to produce a given screen, alter the contrast ($1M$) as much as 4 or 5 per cent, and it is considered likely that more efficient tubes than those used for the tabular data could be produced in cases where the screen-sensitivity index is less than 4. Magnesium and thorium are definitely more active than aluminum for the production of screens with high contrast ratio. Strontium should be expected to be comparable with thorium, but the results of an attempted test of this point were not conclusive because the strontium used was very highly oxidized and was considered very impure.

Just after the screen condensation the physical appearance of the screens formed with added thorium yielded information that explains the nature of the chemical reactions that take place when metallic impurities are used. Many years ago the researches on the coloration of alkali halide crystals established the experimental fact that the presence of excess potassium within a KCl crystal produces coloration.[1]

*Initial Coloration of Screens Containing Metal Impurity.*—The physical appearance of a pure potassium chloride screen immediately upon evaporation, or during evaporation, is that of a very nonselective diffuse reflector. A freshly produced screen, created by the evaporation of a charge of potassium chloride into which thorium or magnesium metal has been mixed, is generally not white as viewed with white light, but has a distinct magenta appearance. A spectral examination of the back reflectance as a function of the wavelength shows that the absorption is essentially identical with that induced by electron bombardment. Although the screen appears colored when first produced, this absorption band bleaches out under the action of light and heat so that the final condition of the screen is more or less indistinguishable in physical appearance from that of a pure potassium chloride deposit.

The explanation of the initial coloration of adulterated screens

[1] R. W. Pohl, "Electron Conductivity and Photochemical Processes in Alkali Halide Crystals," *Proc. Phys. Soc.*, London, **49**, 3 (1937). (A review article.)

involves a consideration of the steps of screen production. The material from which the screen is condensed is normally pressed in the form of a pill and put in an evaporator cup. The cup is heated by a high-frequency induction heater until the potassium chloride melts. While at the melting point, or slightly above, it is assumed that a chemical reaction takes place in which some of the potassium chloride is reduced by the presence of the active metal impurity that has been incorporated in the pill for the purpose. In the case of thorium, a certain amount of thorium chloride is produced and free potassium is liberated. At the temperature involved, potassium chloride, free potassium, and thorium chloride evaporate and condense on the cathode-ray-tube face plate. The freshly produced screen, therefore, contains free potassium so located in positions in the individual crystals of the condensed screen that the absorption band characteristic of excess potassium is unmistakably present. At a temperature of 100°C or less, and in the presence of strong light (8000 foot-candles) from an incandescent source, the screen may be bleached so that almost no traces of the original absorption band remain. It is presumed that under these conditions the potassium combines with the chlorine of the thorium chloride and leaves a crystal of potassium chloride with almost no excess of free potassium but with a very definite excess of free thorium.

It is possible that when aluminum metal is used for the impurity, a similar reaction takes place. Since aluminum is so much less active than thorium, the amount of free potassium produced is probably insufficient to create noticeable coloring. If the amount of aluminum put in is less than 0.5 per cent by weight, the physical appearance of this screen is almost indistinguishable from that of a pure potassium chloride screen. As the proportion of aluminum is increased, the screen takes on a "brown" appearance when viewed in white light. A brown screen of this kind cannot be bleached by the application of moderate heat and strong light. That this brown appearance is the result of light absorption by particles of aluminum is suggested by an experiment in which pure potassium chloride was deposited by evaporation from an evaporator cup, while simultaneously pure aluminum was evaporated from the surface of a nearby tungsten filament. The screen thus produced showed the characteristic brown appearance associated with the excess use of aluminum, and at the same time the decay in contrast following a single excitation was almost identical with that usually obtained from pure potassium chloride. The conclusion from this experiment is that the aluminum must be incorporated into the crystals of which the screen is made by a process that segregates the aluminum atoms from each other more effectively than can be accomplished by the simultaneous condensation of aluminum atoms and potassium chloride molecules.

**18·18. Changes of Contrast Ratio with Use.**—Even though high contrast ratios can be produced by the introduction of metallic impurities, some physical transformation of the screen takes place as a consequence of electron bombardment during use.   Figure 18·62 illustrates the extent of the observed alteration in contrast ratio with electron bombardment for pure potassium chloride and for this salt with three different metallic impurities.   The impurity percentages indicated are the weight of metal introduced into the evaporating cup and do not give an easily interpreted measure of the actual amount of the impurity properly situated within the cathode-ray-tube screen investigated.   It is interesting to note that following 1,000,000 applica-
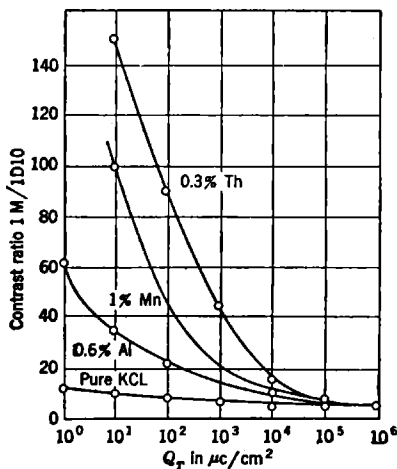


FIG. 18·62.—Aging effect in screens adulterated with various metals.

tions of a raster having a charge density of 1 $\mu c/cm^2$, the contrast ratios of all screens were essentially equal.   Although the great reduction in contrast ratio observed is the most evident effect of extended electron bombardment, small changes in the screen-sensitivity index and in the diffuse reflectance factor have been observed but not extensively investigated.

For the radar application for which these tubes were developed, the alterations brought about by metallic impurity is exactly opposite to that desired.   Even though the screens produced with metallic impurities have found no useful application at present, research in this field should not be terminated before many of the unexplored phenomena have been investigated. Thorium, strontium, and magnesium are probably the most active metals and the influence of the condensation temperature on the performance of the screens using various amounts of these impurities should be investigated with the hope that screen properties useful in some application might be discovered.

**18·19. Influence of Metallic Salts as Impurities.**—The main difficulty in the tubes in which metallic salts have been added to potassium chloride is that, if the screen is found to have modified characteristics, the thermionic cathode of the cathode-ray tube is invariably unsteady and poor in its emission properties.   Certain salts and experimental procedures have been used on occasion to produce screens in tubes that have had good thermionic cathodes, but in these examples the screens themselves

showed no characteristics different from those obtained with pure potassium chloride.   If modified screen properties do result from a given procedure, the chemical reaction evolves chlorine as a result of the decomposition of the metallic salt.   The free metal then reacts to decompose potassium chloride to yield some free potassium that in turn evaporates over with the other molecules.   The liberated chlorine reacts unfavorably with the cathode and yields an insensitive and unsteady thermionic emitter.   If this reaction does not take place, then the cathode is not poisoned and the screen does not seem to be influenced by the presence of the metallic salt introduced as an impurity.

**18·20. Physical Structure of Dark-trace Screens.**—The physical structure of the condensed film as a whole plays an important part in the determination of the efficiency of a dark-trace cathode-ray-tube screen. Before any potassium chloride is condensed, reflections of light from the internal and external surfaces of the cathode-ray-tube face plate are almost equal in intensity.   After the evaporator cup has been maintained hot enough for some evaporation to take place the first evidence of condensation is the gradual coloration of the light reflected from the inner surface.   Later the film reaches a thickness for which practically no visible light is reflected at that surface and, finally, the surface begins to take on a "milky" appearance and the diffuse reflectance factor increases as the amount of potassium chloride deposited increases.   For optimum screen efficiency it has been found that a diffuse reflectance factor of about 23 per cent relative to that of a thick coating of freshly prepared magnesium oxide is needed.

There are two broad overlapping classifications of diffuse reflectors, and, therefore, it is difficult to give precise definitions.   These are "volume reflectors" and "surface reflectors."   Light penetrates into the interior of all crystalline solids.   In the case of metals the absorption of light is so great that the depth of penetration is generally negligible. In the case of nonconductors, however, the light may penetrate with almost undiminished intensity until an inhomogeneity in the structure is encountered.   Imbedded particles within a glass or a surface boundary across which there is change in the index of refraction would constitute such an inhomogeneity.   Snow constitutes a diffuse reflector in which reflections take place at the crystal boundaries throughout the volume of the bulk material.   A similar situation is associated with the diffuse reflection from a thick coating of magnesium oxide and from a thick coating of potassium chloride.   For the want of a better name, diffuse reflectance of this type is referred to as "volume" reflectance; and, in choosing this term, the bulk volume is referred to and not just the internal structure of a single crystal.   A second form of diffuse reflectance is illustrated by a sand-blasted or etched glass surface.   In this case, the

reflected rays of light are returned to the observer as a result of one or more reflections that have occurred at the interface between the solid substance and the surrounding air or vacuum. If the angle of incidence between the light ray and the roughened surface of the glass is just right, then two "total reflections" may take place and return the light ray in the general direction of the observer. Experiment shows that with suitable roughened surfaces as much as 20 per cent of the incident light may be diffusely scattered back to the observer by this phenomenon.

There are a number of related experiments that indicate the importance of so making the surface of a dark-trace tube screen that the major part of the diffusely scattered light comes to the observer as a result of surface scattering. Electron bombardment of a potassium chloride crystal gives rise to an induced absorption band that has a depth of penetration within the crystal of approximately three microns for a screen voltage relative to the cathode of 9 kv (see Table 18·2). From a consideration of these phenomena it would seem that the efficiency of a dark-trace screen in terms of contrast per unit of anode current would be strongly influenced by the physical structure, and high efficiency would be associated with a surface structure in which most of the light rays returned to the observer would have passed through as much of the absorption region as possible. Diffuse reflection offers the best means of using the induced absorption because the light rays as they pass into the thin film of potassium chloride become totally reflected at the crystal-to-vacuum interface. After the first reflections the light travels some distance more or less parallel to the crystal surface, through a region of high concentration of absorption centers, and finally after a second reflection is received by the observer. There are at least five factors that influence the character of the vacuum-to-screen interface: (1) the amount of material (weight) deposited per unit area; (2) the temperature of the surface upon which the potassium chloride is condensed; (3) the angle of incidence between the molecular beam of potassium chloride issuing from the evaporator cup and the surface of the cathode ray tube face plate; (4) the rate of evaporation; and (5) the mean free path of the potassium chloride atoms during evaporation. These five factors are evidently not independent variables.

Experience has shown that "volume scattering" of the diffusely reflected light is less prevalent if a single evaporator cup is used as the source of potassium chloride. It therefore follows that the angle of incidence of the potassium chloride molecular beam varies over the surface of the face plate. As a result of this variation in the angle of incidence, it is found that different amounts of potassium chloride are required in each locality for the completed screen to have a reasonably uniform distribution of diffusely reflecting surfaces. Although consider-

able research has been devoted to the design of an evaporator cup capable of delivering a nonuniform thickness of screen material to compensate for the systematic variation in the average angle of incidence, it is thought that the one described later in this chapter is best only for the production of screens in the 4AP10 cathode-ray-tube blank and for screens condensed at temperatures within the range 0°C to 35°C. Larger tube-face sur-
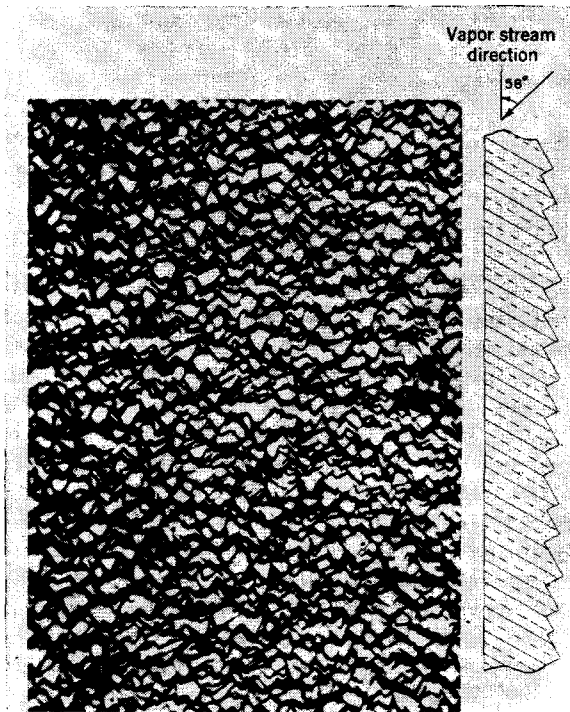


FIG. 18·63.—Evaporated KCl screen structure. *(Courtesy of Johnson and Grams, GE Research Laboratory.)*

faces and lower condensation temperatures would make it desirable to study means of improving the evaporator cup design.

Although the photomicrograph shown in Fig. 18·63 was not taken with a screen produced by condensation from an evaporator cup of the design finally adopted for 4AP10 production, it shows very clearly the physical structure of the screen-to-vacuum interface found with a condensed potassium chloride surface. Note that the crystalline plates have linear dimensions of approximately 2 to 4 microns. The fact that there is such a systematic orientation of these crystals leads to the con-

clusion that there are surface structures that have developed on a more or less amorphous film in direct contact with the glass. As the light used for viewing a dark-trace screen is transmitted first through the glass of the face plate and into the screen, it suffers almost no reflection at the interface between the glass and the transparent amorphous layer of potassium chloride. Since the film was constructed by the condensation of potassium chloride molecules, crystalline structure develops and becomes evident during condensation by the fact that increased diffuse reflectance gradually develops. If too much potassium chloride is used or if the conditions of condensation are not suitably adjusted, the diffuse reflectance factor can be increased well above the optimum of approximately 23 per cent. Such increases in the diffuse reflectance factor are associated with the "volume" diffuse reflection because material so deposited creates "layers" of small crystals and light may be scattered at interfaces that receive very little electron bombardment.

One of the qualitative methods of judging a potassium chloride screen after it has been formed is to illuminate the cathode-ray-tube gun with a strong light and try to recognize the parts as they are viewed through the screen. A good screen, in terms of contrast efficiency, is sufficiently transparent so that the electron gun parts can be seen clearly but very faintly. Experiments undertaken to evaluate the transmissivity of a typical potassium chloride screen at first yielded inconsistent results. The potassium chloride screen is such a very efficient diffuse transmitter that it is difficult to construct an optical system with sufficiently narrow slits to obtain a direct measure of the image-forming rays. The best results so far obtained indicate that the transmission factor of a normal potassium chloride screen is approximately 0.02 per cent. Approximately 23 per cent of the light that falls upon a potassium chloride screen is diffusely back-reflected. It is diffusely transmitted to the extent of approximately 70 per cent and "regular" transmittance is approximately 0.02 per cent. The fact that the crystals that are responsible for the efficient diffuse scattering have dimensions of the order of magnitude of the wavelength of light is further substantiated by the fact that "regularly" transmitted light (image-forming) is selectively transmitted, with red light being more efficiently transmitted than blue light. For screens in which the induced color absorbing centers are absent, both the diffuse reflectance and the diffuse transmittance are very nearly perfectly nonselective.

**18·21. Construction and Mounting of Evaporator Cup.**—Figure 18·64 illustrates the construction of the evaporator cup which has been found to give the most uniform screens of all of those tested. The assembled cup and all of the individual parts are shown. The *evaporating cup e* and the *aperture structure b* were pressed in the same die. The *cover*

*plate c* with its gauze of fine mesh nickel wire has the same diameter ($\frac{9}{16}$ in.) as the flange of the cup and the aperture structure. The procedure for the assembly of the unit involves first spot-welding the baffle
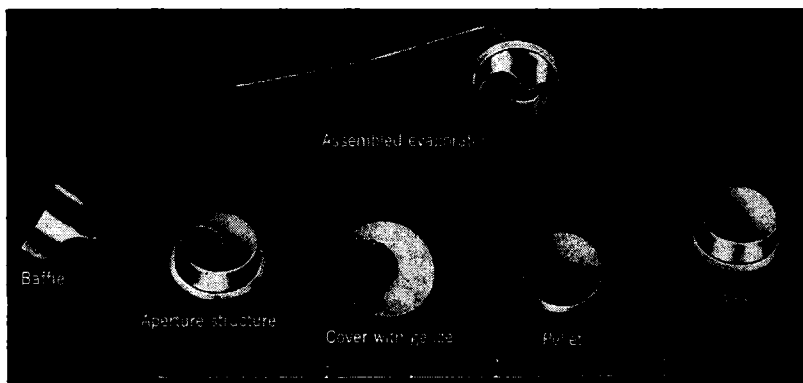


FIG. 18·64.—Assembly and parts of evaporator cup.
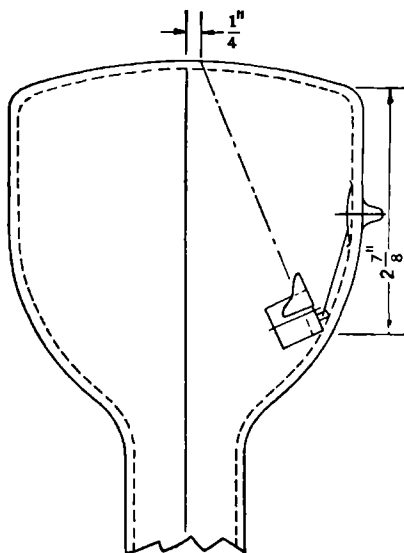


FIG. 18·65 —Evaporator mounting.

to the aperture structure. The support wire is welded to the cup flange and then the cup cover and aperture structure are fastened together with a few welds along the flanges of the cup and the aperture structure. It was standard practice to heat this assembly in an atmosphere of pure hydrogen for 10 min at a temperature of 1100°C by induced high-fre-

quency currents. Immediately after this outgassing procedure and just prior to the final assembly and evacuation of the cathode-ray tube, the pellet of potassium chloride *d* was inserted into the cup by springing it open just sufficiently to insert the pellet. Great care was exercised to see that the flanges of the cup and the aperture structure were spot-welded perfectly. It was necessary to confine the pellet to a cup enclosed by a fine mesh screen in order to eliminate the possibility of having loose potassium chloride in the cathode-ray tube. The aperture structure and the baffle *a* were designed from experience gained in the construction of many tubes. The mounting of the evaporator cup is illustrated by Fig. 18·65.

**18·22. Some Theoretical Aspects of Dark-trace Screens.**—The electronic structure of the solids used as fluorescent screens was discussed briefly in Sec. 18·2. Figures 18·2 and 18·3 illustrate the fact that the assembly of such a large number of atoms in a given volume, as is required to form a solid, distorts the normal electron energy states associated with the individual atoms and creates in a perfect crystal a situation that is reasonably well approximated by the band structure of Fig. 18·2*b*. Any inhomogeneity in the arrangement of the atoms of a single crystal causes a localized disturbance in the system of occupied and unoccupied electron levels.

At the temperature at which the potassium chloride is evaporated, decomposition of the pure salt is negligible. The first molecules to arrive at the face plate become attached to the glass surface by strong adhesive forces. As more and more molecules arrive, the influence of the glass becomes vanishingly small. The molecules tend to orient themselves with respect to those already condensed, and in so doing naturally start the formation of small crystals. Some of the crystals tend to absorb their more minute neighbors to form larger and larger crystals. At the temperature involved the extent of this absorption of one crystal by another is limited and comes to an abrupt stop when the crystal boundaries of two relatively large (1-micron linear dimension) crystals meet. It is thought that at this stage the crystals grow only by the absorption of the additional molecules condensed on the screen. The plate-like structure of Fig. 18·63 clearly shows the nature of the crystals that form a normal potassium chloride screen.

*Two Types of Crystal Fault.*—Figure 18·66 illustrates by means of a two-dimensional approximation the way in which a faulty crystalline structure becomes "frozen" into the individual crystals of potassium chloride. This diagram shows that there are two types of structural faults that can occur. Each negative sign in the diagram represents a chlorine ion ionically bonded to a potassium ion in the original molecule. The assumed pairing of the atoms is shown by the lines around them.

The grouping that is indicated there is intended only to show the orientation of the molecules as they condense onto the crystal lattice that already existed before the arrival of the additional potassium chloride molecules.   It is evident that a fault in the crystal structure, represented by an open circle, is a region in which the chlorine atom is missing, and a fault represented by an open square is a region in which a potassium atom is missing. In the absence of metallic impurities it is to be expected that throughout a given crystal there will be exactly as many open-circle faults as there are open-square faults and that these will be randomly and more or less uniformly distributed throughout the volume of a given crystal.  Experiment has established that potassium ions are more mobile than chlorine ions.  It is therefore to be expected that with some stimulation due to electronic excitation, heat, or electrical fields, a potassium ion such as the one shown at $A$ may move into the ion vacancy $B$.  The appearance of the diagram will remain much as it was except for the fact that the open square at $B$ will have moved to position



FIG. 18·66.—Illustration of two types of crystal faults.  ○-chlorine vacancy; □-potassium vacancy.

$A$.   It must be assumed that the open-square faults have some degree of mobility and may tend to take up positions near the surface of the individual crystal or, in some cases, become grouped in some other manner that disturbs the original randomness of their distribution.   The experimental support for this supposition will become more evident later.
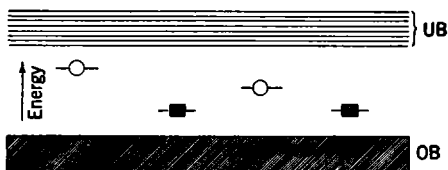


FIG. 18·67.—Energy-level system with localized chlorine vacancy at —○— and potassium vacancy at —■—.   Occupied band (OB); unoccupied band (UB).

The energy level diagram of Fig. 18·67 is very similar to the diagrams of Figs. 18·3 and 18·4 except that in Fig. 18·67 the chlorine vacancies are identified by open circles.  The potassium vacancies are represented in

the diagram by filled-in squares. The difference in the representation is associated with the fact that a crystal fault in which there is a chlorine vacancy is one that has an electron affinity and is therefore a localized region capable of trapping an electron. Associated with a potassium vacancy there is an excess electron and therefore this may be considered to be a localized region capable of trapping an electron "hole."

*Trapping of Electrons and Holes.*—The early experiments on the coloration of potassium chloride crystals established the fact that the trapping of an electron in a chlorine vacancy is the mechanism by which induced light absorption is developed within the crystal. The trapped electron becomes identified as the *F*-center since this electron is capable of absorbing light. The center of the absorption band lies at 560 m$\mu$. If Fig. 18·67 represents the distribution of the electrons in the occupied band and in the various localized levels, then Fig. 18·68 may be taken to represent the situation following the electron excitation of the crystal. The bombardment of a crystal by high-energy electrons excites many internal secondary electrons from the occupied band (OB) into the unoccupied band (UB). This latter band is often known as the "conduction band." After an electron is excited in an ionic crystal it has a considerable degree of mobility in the conduction band but it cannot
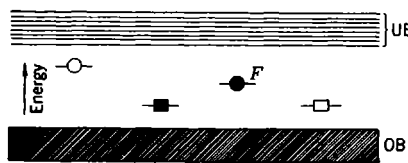


Fig. 18·68.—Energy-level system with electron trapped at *F* and hole trapped at ─■─.

move entirely independently of the "hole" that is created in the occupied band. The electron is a negatively charged body and the hole is effectively a region in which there is an average positive charge density equal in magnitude to that of the electron. Strong electric fields would be set up in the crystal if the electrons did not flow more or less simultaneously with the holes. After an electron is excited it is possible for it to recombine with its hole before the ions in the lattice have had an opportunity to readjust themselves to the altered condition of the electric field. If instantaneous recombination does not take place then it seems likely that the hole in the occupied band will be filled by an electron associated with one of the localized potassium vacancies. Thus, in effect, the hole is trapped at a potassium-ion site and this trapping is illustrated in Fig. 18·68 by the open square. As soon as the hole is trapped, an electron in the conduction band finds itself held to that neighborhood by the moderately long-range forces of the trapped hole. The electron may become trapped in a chlorine-ion vacancy as shown by the letter *F* in Fig. 18·68 or it may recombine with a trapped hole. In the absence of strong light, heat, or additional electron excitation, the new distribution of electrons

and holes becomes "frozen."   If a weak light is used to view the excited screen, the presence of the induced absorption in all regions that have been bombarded sufficiently by high-energy electrons is very evident, and if a tube is kept in the dark even at room temperature, the number of transitions from the $F$-centers that take place spontaneously is so small that almost no reduction in the absorbtance takes place in weeks.

If the essential features of the structural aspects of a pure potassium chloride dark-trace screen are simplified just as far as possible, the complexities will be greater rather than less than those associated with the simplified models described above.   For example the $F$ absorption band is not the only induced band associated with the coloration and bleaching of pure potassium chloride screens.   There are others, sometimes known as the $R$ bands and the $M$ bands, which in all probability correspond to electron traps of a much more complex nature than that just described as a "chlorine vacancy."[1]

**18·23. Qualitative Explanation of Universal Curve for (1M).**—Many of the experimental results already described can be explained qualitatively in terms of a simplified model.   It is of interest to give consideration to the factors that determine the universal curve shown in Fig. 18·57 that relates contrast (1M) to the charge density for a single excitation.   If it were true that each light ray reaching the observer had passed through a definite thickness ($l$) of the absorption region, then the amount of light that reached the observer is given by the following equation:

$$I = I_0 e^{-nal} \tag{17}$$

The symbol $I$ represents the light received by the observer when the density of $F$-centers is constant, and equal to $n$ per unit volume, and the letter $I_o$ represents the light received by the observer when the density of absorbing centers is zero.   The constant $a$ measures the probability that a light quantum will be absorbed as it passes a unit distance through a unit concentration of $F$-centers.   If this formula were valid then the contrast would be given as a function of $n$ as follows:

$$C = (1 - e^{-nal}). \tag{18}$$

In order to compare Eq. (18) with experiment, the assumption is made that $n$ is proportional to the charge density $Q$.   Since Eq. (18) yields a contrast that is directly proportional to $n$ (or, after substitution has been made, to $Q$) when the value of ($nal$) is small compared to unity, Eq. (18) agrees with experiment over the range of small $Q$ values, that is, for

[1] F. Seitz, O. Stern, I. Estermann, R. J. Maurer, S. Lasof, and G. I. Kirkland, "Theory of Dark-trace Tubes," NDRC 14-131, Apr. 1943; 14-172, Sept. 1943; 14-257, Apr. 1944; 14-265, May 1944; "Darkening and Bleaching of Potassium Chloride," NDRC 14-177, Sept. 1943; 14-205, Nov. 1943; Carnegie Inst. of Tech.

contrast values less than 10 per cent.    As the value $(nal)$ becomes greater than 0.2, the equation predicts a more rapid increase in contrast than experiment shows.    The assumptions upon which this equation was based are likely to be invalid for three reasons: (1) the path length for those rays that pass through the region of induced absorption and arrive at the observing phototube are not all equal to a constant value $(l)$; (2) the concentration of absorption centers may not be constant all along the length of the path; (3) the concentration of absorption centers is very likely not proportional to $Q$ over the entire range of observation because electrons are capable not only of creating the absorption centers but also of destroying them.    Therefore, although for small $Q$ values the number of absorption centers generated is likely to be proportional to $Q$, there will certainly be a tendency for the number $(n)$ to increase less rapidly as $Q$ increases.

Although it is impossible to give precise formulation to correct for the objections raised, there are two formulas that might be of interest because they are based on simple assumptions that attempt to take into account a distribution in possible path lengths.    The first of these is based on the assumption that the rays received by the observer may be thought of as being subdivided among travel distances from zero to a certain maximum distance $l_m$.    It is further assumed that the amount of light associated with a unit range in $l$ shall be constant.    On this assumption the contrast is given by

$$C = 1 - \frac{1 - e^{-nal_m}}{nal_m}. \tag{19}$$

If it is assumed that $n$ is proportional to $Q$, then the form of the curve given by Eq. (19) is more nearly that observed than that given by Eq. (18).

There is still a third assumption that is easily worked out, for which the distribution of light rays per unit range in length is given by the following formula:

$$\frac{dI_0}{dl} = kle^{-\frac{l}{L}}. \tag{20}$$

In this equation, $k$ is a proportionality constant that does not come into the calculation of the contrast, and $L$ is a constant that determines the distribution in possible path lengths.    If this form of the equation is used, then the contrast is

$$C = 1 - \frac{1}{(1 - naL)^2}. \tag{21}$$

The curve obtained by using Eq. (21) is nearly the same as that given by Eq. (19), and both agree very well with the universal curve up to a

contrast of approximately 30 per cent; hence it cannot be said that the experimental results favor one assumption more than the other. In addition to the fact that both curves have approximately the right shape, the functions also indicate that if the $Q$ required to produce any given contrast is known, then to generate some new specified contrast the $Q$ will be obtained by multiplying the first one by a definite factor. It was the experimental support of this fact that made the universal curve and the screen-sensitivity index useful as means of describing dark-trace-screen properties.

*The Screen-efficiency Index Determined Largely by the Mechanical Structure of the Screen.*—The physical structure of the bulk screen material, and especially of the interface between the screen and the vacuum of the cathode ray tube, has more influence than any other known factor on the screen efficiency as measured by the contrast $(1M)$. This fact supports the simplified picture of a potassium chloride screen developed in the preceding paragraphs. The contrast $(1M)$ is almost independent of (1) the presence of a small amount of impurity in the screen, (2) the actual thickness of the screen as long as the interface structure is "normal," (3) the temperature at which the screen is operated, (4) the light intensity used to bleach the screen, and (5) the precise details of excitation so long as the total charge is introduced into the screen in a time shorter than a few milliseconds. The meaning of Statement 2 is that the actual screen coating in terms of milligrams per square centimeter is dependent on the angle of incidence and upon the temperature at which the screen is condensed. Low-temperature screens require as much as twice the weight of potassium chloride per unit area as is demanded for screens condensed at room temperature.

**18·24. Factors That Influence Contrast Decay.**—It is impossible to formulate a satisfactory and yet reasonably simple theory to explain the phenomena associated with the decay in contrast. Known factors that influence the decay in contrast are the following:

1. Impurities contained in the potassium chloride screens.
2. The condensation temperature used for the screen production.
3. The operating temperature of the screen.
4. The spectral power distribution and the magnitude of the illuminance used for observing the screen.
5. The sequence of excitations used to produce a given contrast.
6. The magnitude of the charge per unit area used to create the contrast.
7. The electron energy.
8. The age of the tube in terms of previous excitation and operating conditions, particularly as regards the effect of the operating temperature and total electronic charge put into the screen.

If a given contrast is excited on a completely bleached screen by a single raster, the decay in contrast is very much more rapid than the decay that follows the generation of the same initial contrast as a result of repeated excitations that are individually smaller but sufficient to excite the specified contrast value. It is assumed that a potassium chloride screen that has not been used extensively will have a random distribution of chlorine and potassium vacancies, and that these will be equal in number. Immediately after the screen is excited the chlorine vacancies that are filled by internal secondary electrons become $F$ centers and the electron holes become trapped at the potassium-ion vacancies. The trapping of the electrons and the hole occurs in a very short time after the excitation; and, in the absence of additional excitation either from electrons, light, or heat, the population of $F$ centers remain almost constant. In the presence of light the electrons that absorb the light in the $F$-centers are excited to higher electronic energy states and become mobile to a limited extent. Electrons in the excited state are likely to combine with the trapped electron holes since these trapped holes are electrostatically attractive to the free electrons as a result of coulomb forces. Unoccupied chlorine vacancies also attract electrons and the mobile electrons may become retrapped in a chlorine vacancy and thereby return to recreate an $F$-center. Although the absorption of light within the $F$-band always involves the excitation of an electron in an $F$-center, it does not necessarily follow that the $F$-center has been annihilated. Removal of $F$-center electrons is associated only with the return of the electron to a captured electron hole. The complete bleaching of the screen is identified with the return of almost all the electrons to captured electron holes.

In all practical cases the number of chlorine vacancies generally far exceeds the number of trapped holes. Therefore, although the force of attraction between the mobile electron and trapped hole is greater than that between an electron and a chlorine vacancy, many of the electrons will go to chlorine vacancies. It seems certain that those $F$-centers nearest electron hole traps will yield their electrons to recombine with the holes and that after the initial fairly rapid decay in the concentration of $F$-centers, the decay will become progressively slower and slower. This decrease in the probability of recombination accounts for the fact that the accumulated concentration of $F$-centers after repeated excitation becomes progressively harder and harder to bleach.

*Movement of Ions under Electron Bombardment and Heat.*—The electron bombardment of the potassium chloride screen increases the likelihood that a potassium-ion vacancy will move through the crystal by the displacement of individual potassium atoms to fill the vacancy. Throughout the crystal there must be sites created by the surface struc-

ture, crystalline faults, or random assemblies of ion vacancies that correspond to conditions of lower vacancy mobility. If the original distribution of chlorine and potassium vacancies was random and reasonably uniform, the final distribution is presumably less uniform, and although there still is a sum total of potassium vacancies equal to the sum total of chlorine vacancies, the capturing of the potassium vacancies at localized regions results in a small increase in the average short-range distance between the potassium and the chlorine vacancies. Thus if the holes are always trapped at potassium vacancies a definite decrease in the bleaching rate for a given excitation should be expected and, in fact, is observed. The application of heat to an unused screen also reduces the bleaching rate although the effect of heat is not identical in every respect to the effect of electron bombardment.

The presence of metallic impurities within the lattice increases the number of electron hole traps without increasing the number of chlorine vacancies. Thus although the contrast $(1M)$ is independent of the impurity content over the practical range, the decay contrast $(1D10)$, and therefore also the contrast ratio $(1M)/(1D10)$, are strongly influenced by the presence of metallic impurities because they increase the density of hole traps above the density of chlorine ion vacancies. Figure 18·62 shows that extended use of a dark-trace screen finally results in a rearrangement of the distribution of the impurities in the crystalline material such that the contrast ratio after many hours of service is approximately the same as for pure potassium chloride. An adulterated screen changes contrast ratio by heat alone and again the effect is not exactly the same as that produced by high-energy electrons.

**18·25. Standardized Test Equipment.**—The test equipment used for the investigation and quality control of luminescent and dark-trace cathode-ray tubes can be represented by the similar block diagrams of Fig. 18·48 and 18·69. There are many detailed differences between the two pieces of equipment which do not show up in block diagrams because in the "P7 test equipment" the anode voltage generally used was much lower and therefore the sweep circuits differed considerably in their details. The "DT test equipment" was arranged to make a direct measurement of luminance and also of contrast. The cathode-ray-tube mounts were very different because all the DT tubes ranged in face-plate size from 3 to 4 in., and provision was made for the application of heat so that the face plate could be raised to a temperature as high as 200°C. For the luminescent tubes provision was made for the operation of tubes of many varieties that included both electrostatically deflected and magnetically deflected electron beams and a range in face-plate diameter from 2 to 12 in. In the "P7 equipment" it was necessary to have a strong source of infrared and red light to assist in the deexcitation of

long-persistence screens.　The high-speed sweep ran at 12 kc/sec and was accurately synchronized to the 60-cps 115-volt a-c line used to furnish power to the entire system.　The 60-cps sweep was synchronized directly to the 60-cps line.　In the dark-trace-tube equipment provision
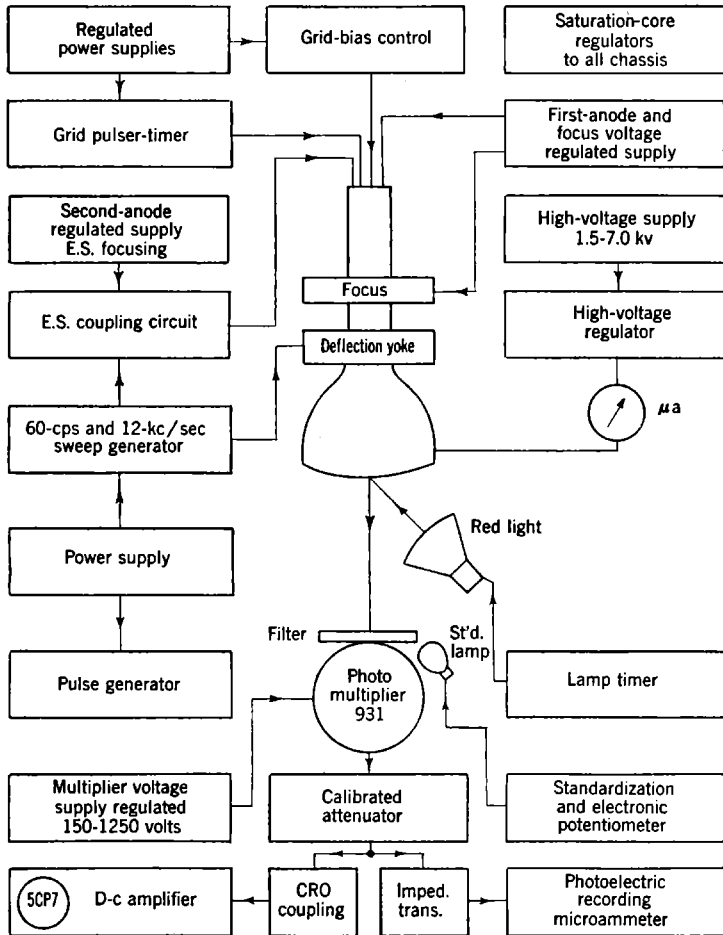


FIG. 18·69.—Block diagram of P7 cathode-ray-tube test equipment.

was made only for magnetic deflection of the electron beam.　Focusing currents or voltages were furnished by regulated supplies.　The current in the electron beam was measured either directly on a suitably constructed and shielded microammeter or on a vacuum-tube microammeter. In the dark-trace test equipment a current limiter was needed in order to
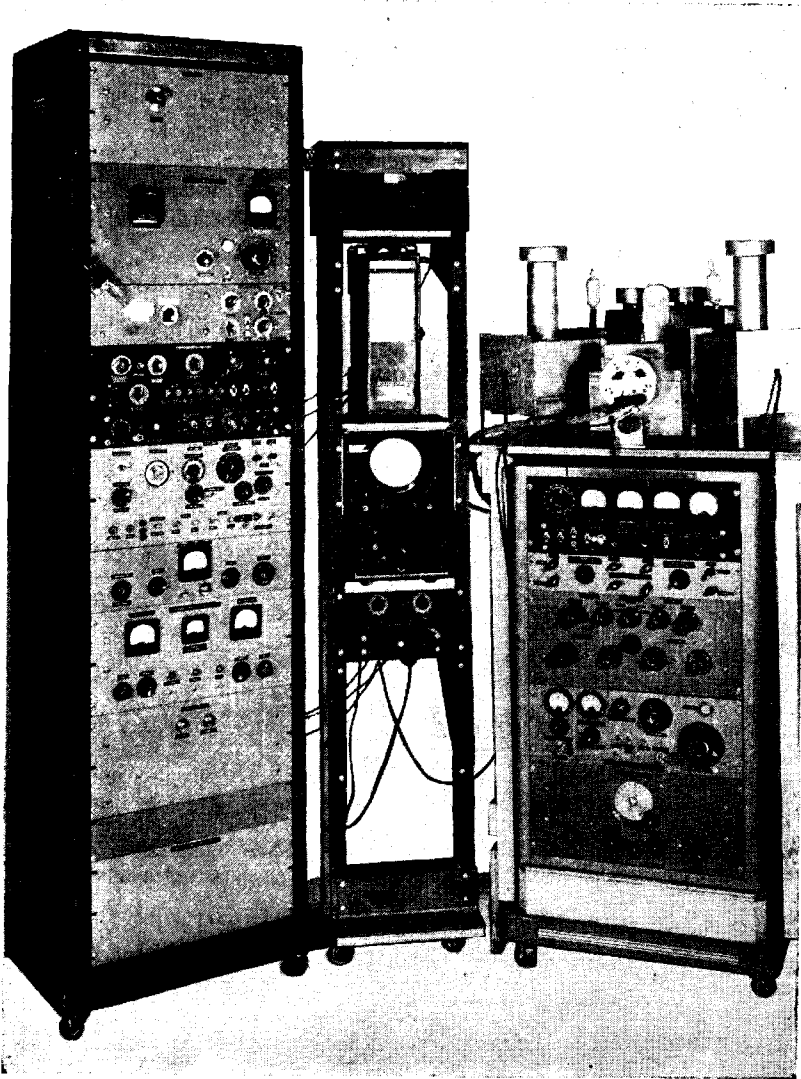
FIG. 18·70.—General view of dark-trace test equipment.

protect the measuring instruments against the flow of excess currents in cases in which tubes sparked over unexpectedly.

The photometric measurements were made by the use of selected type 931 multiplier phototubes.   It was necessary to select these tubes in order to obtain the ones suitable for photometric work, which demanded

(1) sensitivity, (2) long-time stability, and (3) freedom from short-time instability or noise.   Power was supplied to the phototube from a very carefully regulated power unit that served also as a means of establishing definite and preassigned amplification values.   For both the P7 and the DT test equipment, provision was made for recording the variation in photocurrent either by means of a pen-and-ink recorder or by means of a cathode-ray oscilloscope in which a long-persistence cathode-ray tube was ·installed.   The two methods of recording permitted the range in
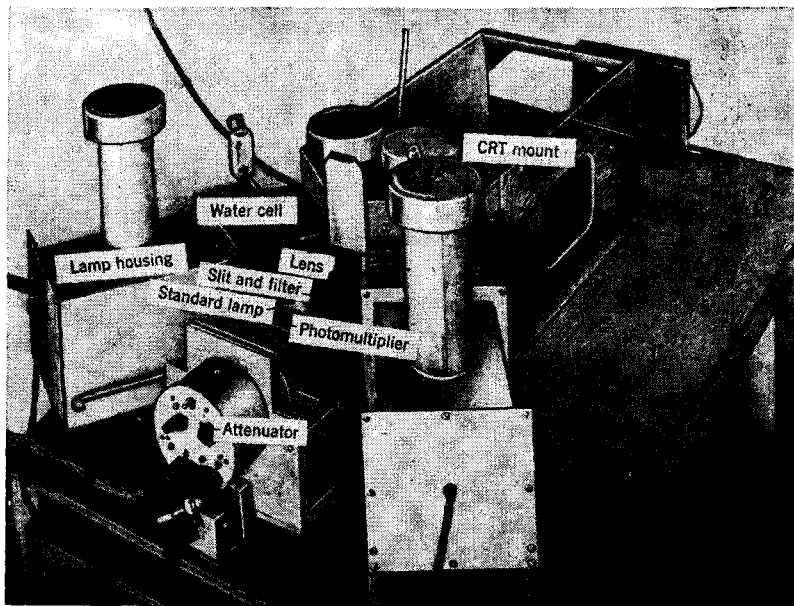


FIG. 18·71.—Detailed view of tube mount, lamp housing, and 931-phototube mount.

time investigated to extend from 1 msec to many minutes or even hours when necessary.   An important part of the test equipment for DT tubes was the lamp assembly that furnished a constant source of illumination on the face of the cathode-ray tube under test.   The intensity of the illumination on the face was thought to be approximately 8000 foot-candles.   The 115-volt lamps were run from a 220-volt d-c line and were very accurately regulated.

In order to maintain the temperature of the screen at a preassigned value, an automatic regulator controlled the heating of an air blast. For the measurement of contrast it was necessary to deal with a very definite area on the tube face and therefore a lens was used to project that area onto a slit directly in front of the cathode of the multiplier
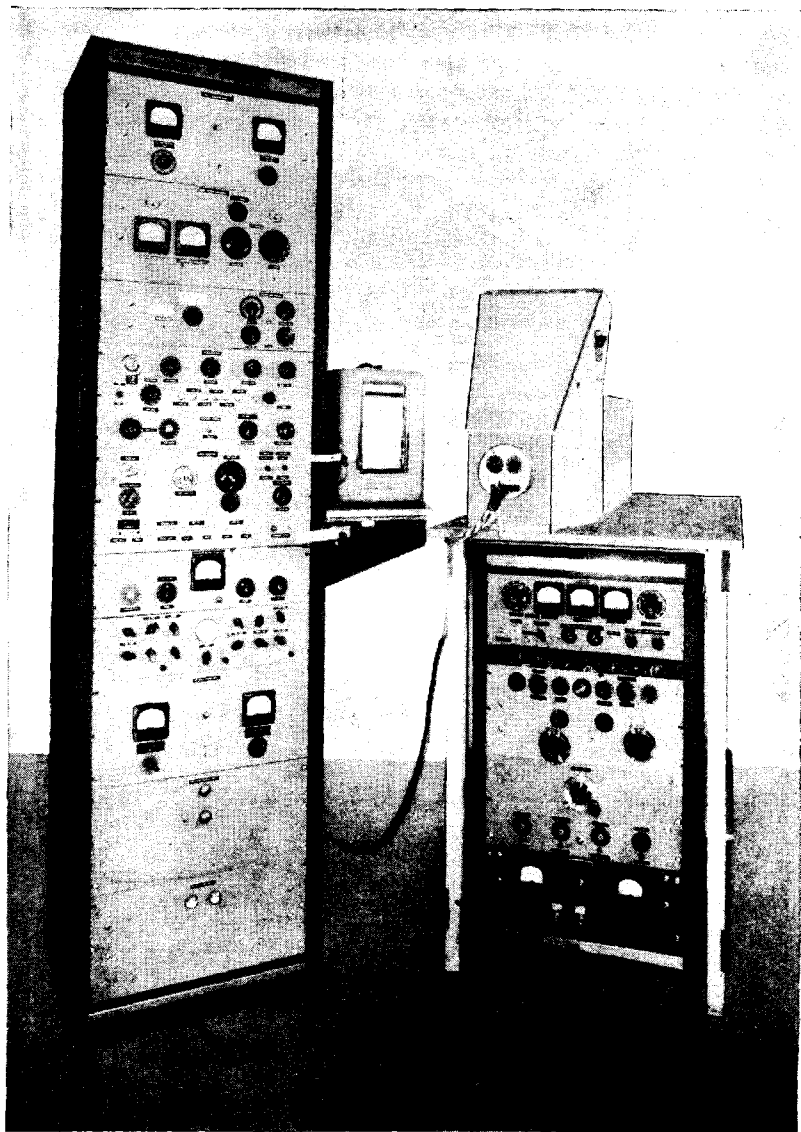
FIG. 18·72.—General view of P7 test equipment.
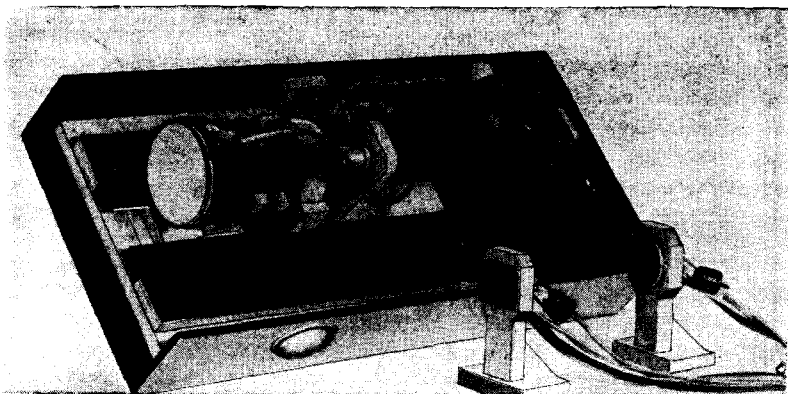
FIG. 18·73.—Detailed view of tube mount and cover.
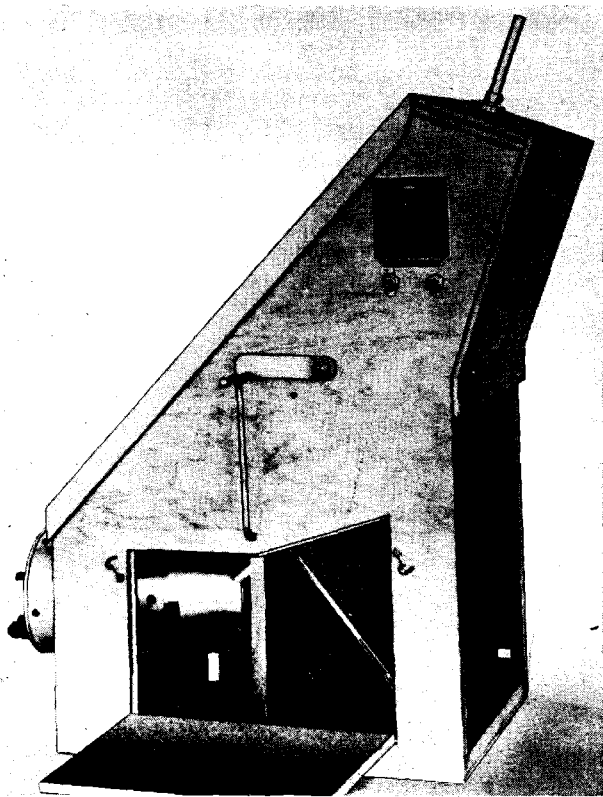


FIG. 18·74.—Detailed view of light-tight box for 931 phototube mount, red light, and lamp timer.

phototube.   A filter, the equivalent of a Wratten No. 15 filter, was used to reduce the sensitivity of the receiver as a whole in the short-wavelength range of the spectrum and thus make it more responsive to changes in luminance associated with the center of the $F$ absorption band near 560 m$\mu$.   For the P7 test equipment it was not necessary to use a lens since the luminance calibrations were worked out in terms of a standard distance of 30 cm from the multiplier phototube to the screen under test.[1]

The photographs shown in Figs. 18·70 and 18·71 illustrate the arrangement of the dark-trace equipment.   In Fig. 18·70 the relay rack to the right is largely associated with the sweep circuit and the controls for focusing the electron beam.   On the table above the sweep panel may be seen the 931 multipler phototube mount and the lamp housing.   In the center the pen-and-ink recorder and the cathode-ray-tube recorder are evident.   The tall left-hand rack of panels are power supplies and standardization control equipment.   Figure 18·71 shows a more detailed view of the lamp housing and the water cells used to remove a large proportion of the heat rays normally emitted by the lamp.   Part of the cathode-ray-tube mount is also shown.

Figures 18·72, 18·73, and 18·74 show the P7 test equipment.   The arrangement of panels and standardizing equipment is very similar to that just described in connection with the DT equipment.   Figure 18·73 shows the details of the cathode-ray-tube mount and Fig. 18·74 shows the housing in which the phototube is located.

[1] All the details that had to be worked out in order to maintain standards of photometry have been explained in "Notes on Photometry, Colorimetry, and an Explanation of the Centibel Scale," RL Report No. 804, Dec. 17, 1945.
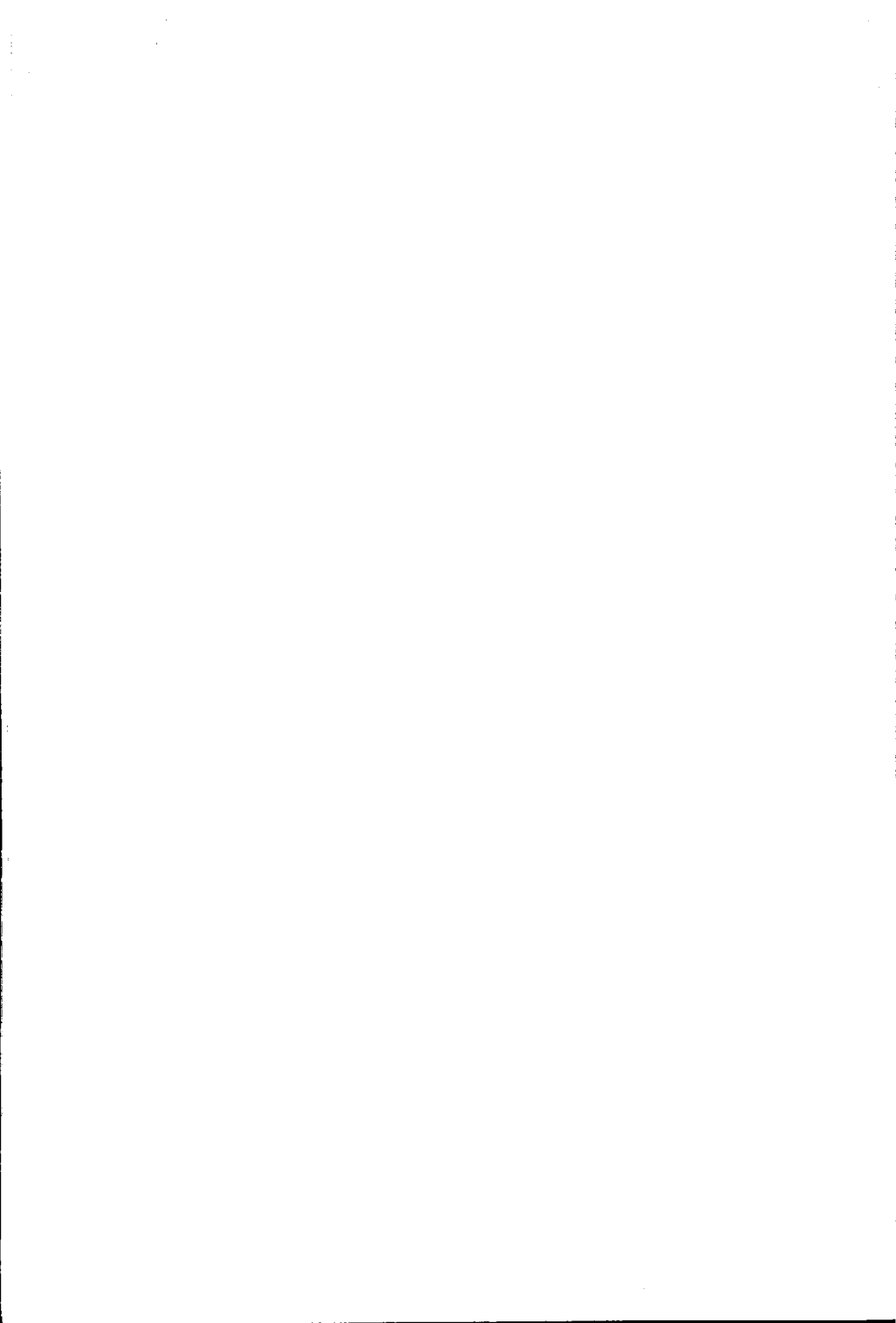
# APPENDIX A

## CONSTRUCTION OF FOCUSING DEVICES

### By R. D. Rawcliffe

**A·1. Focus Coil.**—A method of construction of a simple focus coil of the type illustrated in Fig. 3·1c is shown in Fig. A·1. This coil was designed specifically to fit the tube mount illustrated in Fig. 16·3. The dimensions and shape may be altered, and it may be desirable to attach to the case other means for adjusting the position of the coil with respect to the cathode-ray tube. For optimum performance, it is necessary that
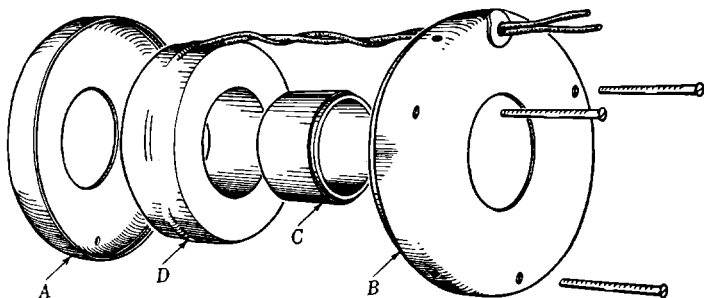


Fig. A·1.—Construction of simple focus coil. Focus coil and case. $A$, front half shell (0.062″); $B$, rear half shell (0.062″); $C$, center tubing, $1\frac{1}{2}$ in. ID, $1\frac{3}{4}$ in. OD, with turned shoulder, to be peened into $B$; $D$, coil, $1\frac{3}{4}$ in. ID, $3\frac{1}{4}$ in. OD, $1\frac{1}{4}$ in. long.

high-quality, well-annealed iron be used, that the parts be accurately aligned, and that the air gap be uniform. The specifications for the coil illustrated are as follows:

*Case*

1. *Material.* SAE 1015 soft steel, to be annealed after fabrication to eliminate all strains.
2. *Dimensions.* Shell, No. 16 U.S.S. gauge; flat out to a diameter of $3\frac{1}{2}$ in., and beyond this spun so that outer surface of the completed shell will form a spherical section of $2\frac{1}{8}$ in. radius of curvature. After spinning, corresponding shoulders are turned in the adjacent edges of parts $A$ and $B$ so that they will be accurately centered. Completed housing: inside diameter, $1\frac{1}{2}$ in.; maximum outside diameter, $4\frac{1}{4}$ in.; axial length, $1\frac{1}{2}$ in.; air gap, $\frac{1}{4}$ in.

3. *Annealing.*  After fabrication is completed, heat to 1700°F for one hour; cool not faster than 200°F/hr to 400°F; protect from oxidation during annealing.  (Annealing is recommended to avoid magnetic nonuniformities due to fabrication.)

4. *Plating.*  Cadmium-plate after annealing.

*Coil*

1. *Dimensions.*  After impregnation, dimensions should be: minimum ID, $1\frac{3}{4}$ in.; nominal OD, $3\frac{1}{4}$ in.; maximum length, $1\frac{1}{4}$ in.  Wire is usually wound on a spool of thin fiber or Kraft paper.  After winding, the coil is wrapped with linen or fiberglas tape, and impregnated.

2. *Turns data.*  Wire size to be chosen to fit application.  With no allowance for impregnation, approximately 40,000 turns of No. 38 enameled wire, having a resistance of 18,000 ohms, can be wound on a spool to fit the enclosure.  If impregnation is required, 80 to 90 per cent of the above number will be possible.  See Fig. 3·8 for current and voltage required to focus, for this and other wire sizes, for the condition that the wire used will always fill the same volume.

3. *Impregnation.*  The impregnation required depends on the severity of the atmospheric conditions that the coil will encounter.  For ordinary use, a single vacuum impregnation, following the technique of Appendix C, will be sufficient.  The complete treatment will be necessary for protection under severe atmospheric conditions.  In this case it may be more satisfactory to use a hermetically sealed type of construction, in which the gap in the magnetic circuit is filled by a ring of cadmium-plated brass, and the ring and other joints are soldered to make an airtight enclosure.  The leads are brought through the case through Kovar glass seals.

**A·2. Focus Magnet.**—The construction of one type of focus magnet is illustrated in Fig. A·2.  Because some redesign work will be necessary to adapt this magnet to particular circumstances, the information given is of a general nature.  Dimensions are given to serve as a guide for the redesign work.  Letters refer to parts so designated on the drawing.

The magnetic parts of the unit (except for the magnet itself) are best made of soft steel (SAE 1010 or 1015) and should be well annealed after machining to reduce residual magnetization.  If the shunt *B* has (magnetic) hard spots it becomes magnetized and distorts the field so that the focus deteriorates.  The magnetization of the shunt has a deflecting action.  The direction of the magnetization tends to be aligned with the asymmetry introduced in the field by the centering ring.  If the hys-

teresis of the iron is large because of poor annealing, however, the shunt can be turned through a rather large angle with no readjustment of the magnetization. The pattern on the screen of the cathode-ray tube, then, does not drift appreciably as the focus is adjusted in one direction. If the direction of focusing is reversed, however, the position of the pattern suddenly jumps by perhaps an inch. Magnetization of the shunt causes the most trouble; magnetization in other parts has a smaller effect.
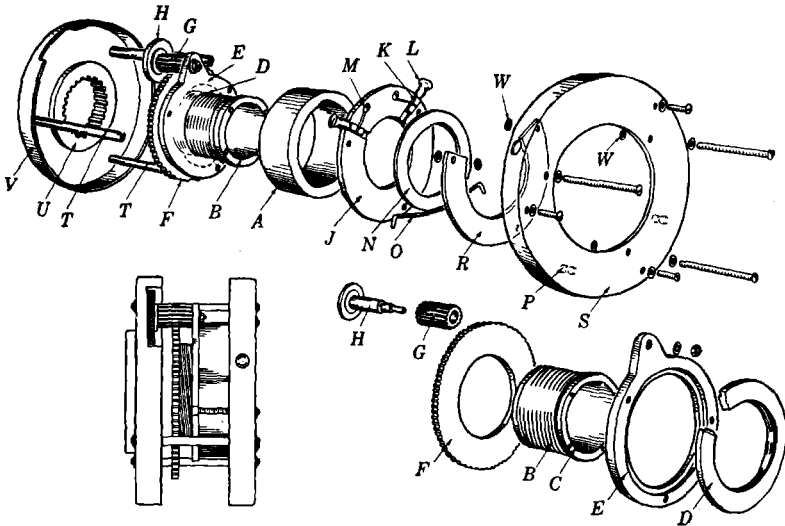


Fig. A·2.—Details of focus-magnet construction. *A*, Alnico magnet; *B*, magnetic shunt—soft steel; *C*, brass pins; *D*, steel insert for *E*, threaded to accommodate *B*; *E*, rear plate—brass; *F*, aluminum gear for turning *B*; *G*, brass pinion gear; *H*, knurled thumb knob; *J*, steel front plate; *K*, brass cam for adjusting centering ring *N*; *L*, brass adjusting screw for driving cam—head of screw is cup-shaped for holding screw driver; *M*, spring for holding cam in groove; *N*, steel centering ring; *O*, spring for centering ring; *P*, support for spring *O*; *R*, aluminum plate to hold centering ring in place; *S*, front end cover—aluminum; *T*, aluminum spacing pillar; *U*, rubber grommet; *V*, back end cover; *W*, spacing washers. ·

Soft steel rusts badly, and it should, therefore, be given some sort of protection. It is difficult to protect the shunt and rear ring *D* because of the threading. A plating of nonmagnetic material a few thousandths of an inch thick will not interfere appreciably with the field distribution.

The fit of the threaded joint should be good. The shunt should turn freely, but the amount of wobble should be kept to a minimum. The range of motion of the shunt should be about half an inch, closing to a minimum gap of about $\frac{1}{32}$ in. The gap should not be allowed to close completely because this disturbs the magnetization. The four brass pins, *C*, press-fitted into the end of the shunt, prevent complete closure of the gap. The threading should not extend to the front end of the shunt

because the threaded ends will produce an asymmetry in the field that rotates with the shunt.

An effort should be made to preserve axial symmetry of all magnetic parts. The rear plate $(D,E)$ is divided into two parts, the inner one of steel, the outer one of brass so that the protruding-ear support for the pinion gear will not be magnetic. If economy is required, the whole rear plate can be made of steel, provided that the ear is kept small and that no other magnetic material is near it. The front plate $J$ and the centering ring $N$ are symmetrical. The spring $O$ and spring supports $P$ are of steel. They are small enough, however, to cause no appreciable distortion.

Considerable care is needed in preparing the magnet, which is made of Alnico V. Appropriate dimensions are $2\frac{1}{2}$ in. OD, and 2 in. ID by $\frac{3}{4}$ in. length. The ends should be ground smooth and parallel. This grinding should preferably be done by the manufacturer[1] of the magnets because it requires a special technique. Alnico is extremely brittle and, if improperly ground, chips and breaks. The magnet should be free of chipped edges, cracks, and blow holes.

The magnet should be annealed for a field parallel to the axis. Considerable care is required in the annealing. A number of magnets have had small sectors that have been considerably weaker than the remainder of the magnet, probably because of nonuniform cooling in the annealing process. With use, the magnetization of the weak sector has become reversed and the field has been badly distorted. A more careful annealing corrected this.

The rubber grommet[2] $U$ is a convenient support for the rear of the cathode-ray tube. All machine screws should be of brass, plated to avoid corrosion with the aluminum. The remaining parts, including the end covers $S$ and $V$, the large gear $F$, and the miscellaneous spacers $R$, $T$, and $W$ are all made of aluminum.

Magnetization of the focus magnets requires a very strong field. It should be done after the assembly of all magnetic parts is completed, but preferably before the end cover $V$, the pinion gear $G$, and knurled screw $H$ have been added. The centering ring should be centered by eye by means of the adjusting screws $L$. The gap should then be opened as far as it will go, and the unit placed between the pole pieces of a magnetizing magnet. The focus magnet should be saturated. The field of the magnetizer should then be reversed and the magnetization reduced to the desired operating point. If it is not reduced far enough at the first trial, it can be reduced further a second time. However, if

---

[1] Obtainable from General Electric Company, Schenectady, N.Y.; Indiana Steel Company, Valparaiso, Ind.

[2] Part No, MD3368, Canfield Rubber Company, Bridgeport, Conn,

it is too weak, it must be resaturated before the second trial.    Otherwise the magnetization will not be stable.

A convenient instrument for testing the field strength of a focus magnet is a fluxmeter with a special pickup coil.    The fluxmeter reading depends on the exact position of the coil in the magnet.    Therefore, a standard position must be defined.    The particular fluxmeter-coil combination must be calibrated against a standard focus magnet, that is, a magnet that has been tested in the mount in which it is to be used. The standard should be adjusted so that the anode voltages for focus with maximum and minimum gap widths should center (geometrically) about the anode voltage at which the cathode-ray tube is to operate. There is sufficient range of control of the field so that a tolerance of $\pm 10$ per cent in the fluxmeter reading will be satisfactory for production magnets.

# APPENDIX B

## CONSTRUCTION AND CHARACTERISTICS
## OF DEFLECTION COILS

By R. Dressel and T. Soller

This appendix contains a compilation of information concerning the mechanical and electrical characteristics of the various types of deflection coils discussed in this volume, in tabular and diagrammatic form. More specific information pertaining to the actual technique of construction of air-core coils with distributed windings is also included.

**B·1 Mechanical and Electrical Characteristics of Various Types of Deflection Coils.** These are given in Figs. B·1 through B·5, and in Table B·1.
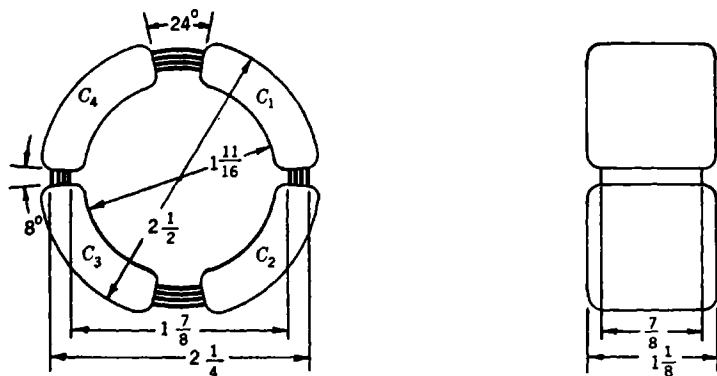


Fig. B·1.—Toroidal deflection coil. *Core:* Ribbon-wound silicon steel, annealed. *Coils:* $C_1$, $C_2$, $C_3$ and $C_4$—layer-wound without paper insulation between layers. For wire size and electrical characteristics see Table B·1.

**B·2. Construction of Air-core Coils With Distributed Windings.**— A slotted form such as is illustrated in Fig. B·5 serves to support the windings and at the same time fixes the geometrical properties of the coil. The slots are radial and are equally spaced around the circumference of the cylindrical form. Because of this equal spacing, the number of wires in each slot must be proportional to the sine of the vertical angle of the slot if the coil is to be wound with a sine distribution. The illustrated forms have two slots missing on top, and two slots missing on the bottom. Since the number of wires which ordinarily would fit into these slots is very small compared with the number of wires in the other

712

TABLE B·1.—DEFLECTION COIL CHARACTERISTICS

| Coil, type | Fig. no. | Core, Window, in. | Stack height, in. | Clear opening, in. | No. of coils on each leg | Total no. of coils | Type of connection | Wire size | No. of turns on each coil | $L$, inductance, millihenrys, (measured at 1000 cps) | $R$, resistance, ohms | $I_0$, current in ma to produce 26° defl. at 5 kv* | $C_s$, effective shunt cap, μμf | $\sqrt{LC_s}$, μsec | $R_e = \frac{1}{2}\sqrt{L/C_s}$ approx. critical damping shunt resistance, ohms |
|---|---|---|---|---|---|---|---|---|---|---|---|---|---|---|---|
| Toroid | B·1 | 1¼ | 1 | 1¾ | ....... | 4 | series / series-par. / parallel | 36E | 1000 | 380 / 96 / 23.5 | 344 / 86 / 21.5 | 49 / 98 / 196 | 300 | 5.4 | 9,000 |
| Square iron | B·2a | 1 11/16 | 1½ | 1 1/16 + | 2 | 8 | 2 in series, on opposite legs | 38E / 37E / 37E / 37E | 1600 / 1100 / 750 / 500 | 580† / 280 / 130 / 58 | 700 / 340 / 250 / 167 | 36 / 52 / 76 / 115 | 160 / 200 / 225 / 250 | 10 / 7 / 5 / 4 | 30,000 / 19,000 / 12,000 / 8,000 |
| Square iron | B·2b | 2¼ | 1½ | 1½ | 2 | 8 | 2 in series, on opposite legs | 33E / 33E / 33E / 33E | 1500 / 1300 / 1100 / 550 | 520† / 390 / 280 / 70 | 200 / 173 / 146 / 73 | 47 / 54 / 63 / 125 | 158 / 180 / 200 / 250 | 9 / 8 / 7 / 4 | 29,000 / 23,000 / 19,000 / 8,000 |
| Square iron | B·3 | 2¼ | 1½ | 1½ | 2 8-section pies | 8 | 2 in series, on opposite legs | 34E | 1500 | 510 | 283 | 47 | .... | ... | ...... |
| Square iron | B·4 | 3¼ | 1 | 2 11/16 | 1 | 4 | .......... | 28E | 4380 | ..... | 90 (each coil) | 15§ | These two coils used in conjunction for rotating coil off-center, PPI. | | |
| Air-core | B·5a | ... | .. | 1¾ | ....... | 2 | series, aiding | 34E | 1600‡ | 335 | 610 | 50 | | | |
| Air-core | B·5b | ... | .. | 1½ | ....... | H 2 / V 2 | series, aiding / series, aiding | 38E / 36E | 2000‡ / 829‡ | 555 / 97 | 2300 / 408 | 35 / 84 | 25 | 1.5 | 8,000 |
| Synchro stator | ..... | 1½ | 1½ | 1½ | ....... | .... | .......... | .... | ..... | 400 / 200 / 100 | 800 / 400 / 200 | 34 / 48 / 68 | 1500 / 1500 / 1500 | 24 / 17 / 12 | 20,000 / 15,000 / 11,000 |

* For push-pull connected coils, this is the differential current in the windings.
† These figures are for an uncased coil.  A close-fitting shield, Fig. 8·15, will reduce $L$ by a factor of 2.3 at 1000 cps.
‡ Five-section distribution:

2000 turns: 207, 329, 428, 499, 536.
1600  " : 166, 264, 342, 400, 428.
829  " : 85, 136, 179, 209, 220.

§ Windings connected for diagonal field.

slots, they may be neglected without serious resultant distortion of the magnetic field.   The form dimensions are governed by the diameter of the cathode-ray-tube neck over which the coil must fit and by the maximum angle of deflection required.   The maximum angle, in turn, is determined by the relationships between form dimensions and coil performance discussed in Chap. 8.
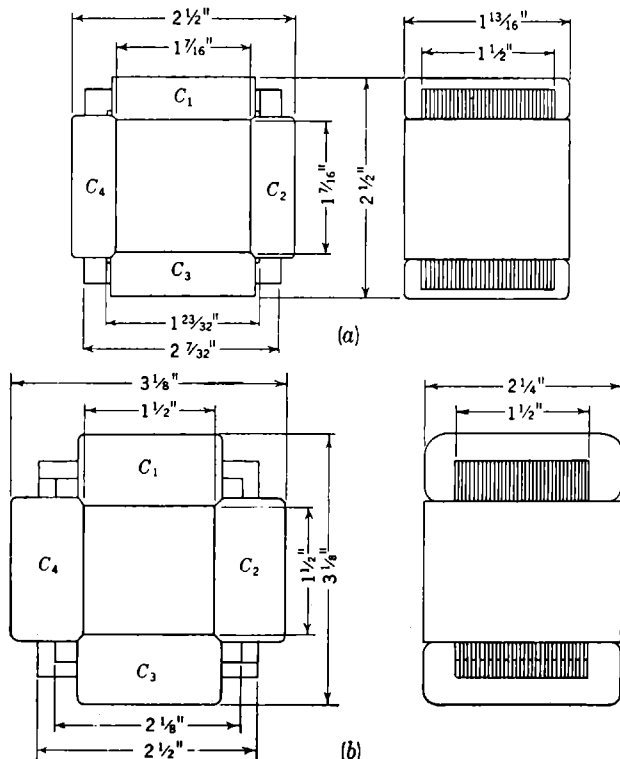


B·2.—Two sizes of square iron-core deflection coils.   *Core:* Interleaved 0.014-in. or 0.007-in. silicon steel $L$ punchings annealed.   *Coils:* $C_1$ and $C_3$ form one pair for vertical deflection.   $C_2$ and $C_4$ form one pair for horizontal deflection.   Coils layer-wound, with paper insulation between layers.   For wire size and electrical characteristics see Table B·1.

Windings to fit the slots on the form are made between two flat disks (Fig. B·6b and c).   These disks are drilled so that wire pins can be pushed easily through the holes in one disk, across the space between the disks, and out the corresponding holes in the other disk.   For winding, the disks are mounted on a shaft held in a winding machine so that they may be rotated.   Four pins, forming a small rectangle, are pushed into the set of holes nearest the shaft.   The proper number of turns of insulated
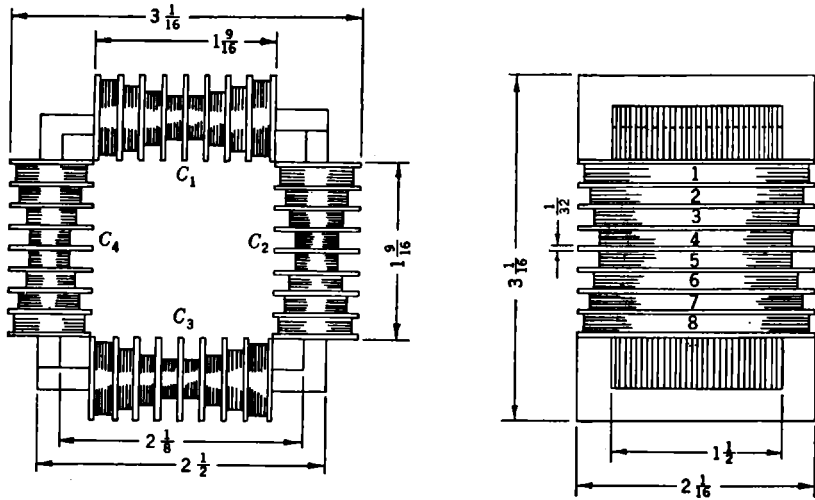
Fig. B·3.—Square iron-core deflection coil designed to present a square deflection pattern on a 12DP7 tube.   *Core:* Laminated silicon steel.   *Coils:* $C_1$ and $C_3$ form a pair for vertical deflection.   $C_2$ and $C_4$ form a pair for horizontal deflection.   Wound and connected for push-pull operation.   Two separate windings of 1500 turns each are placed on each coil, one over the other.   Winding distribution: 264, 213, 162, 111, 111, 162, 213, 264 turns.   For wire size and electrical characteristics see Table B·1.
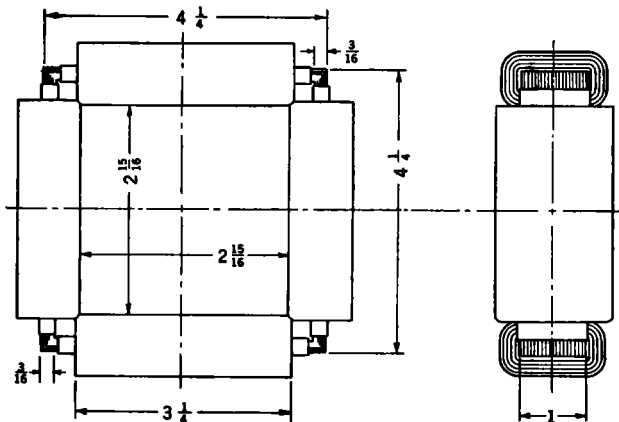


Fig. B·4.—Square iron-core off-centering coil.   *Core:* Laminated silicon steel.   *Coils:* Layer-wound, No. 28 enameled wire.   Paper insulation between layers.   First ten layers: 220 $T$/layer, 3-in. winding length; second ten layers: 200 $T$/layer, 2.9-in. winding length; last layer: 180 $T$/layer, 2.8-in. winding length.   Total turns = 4380.
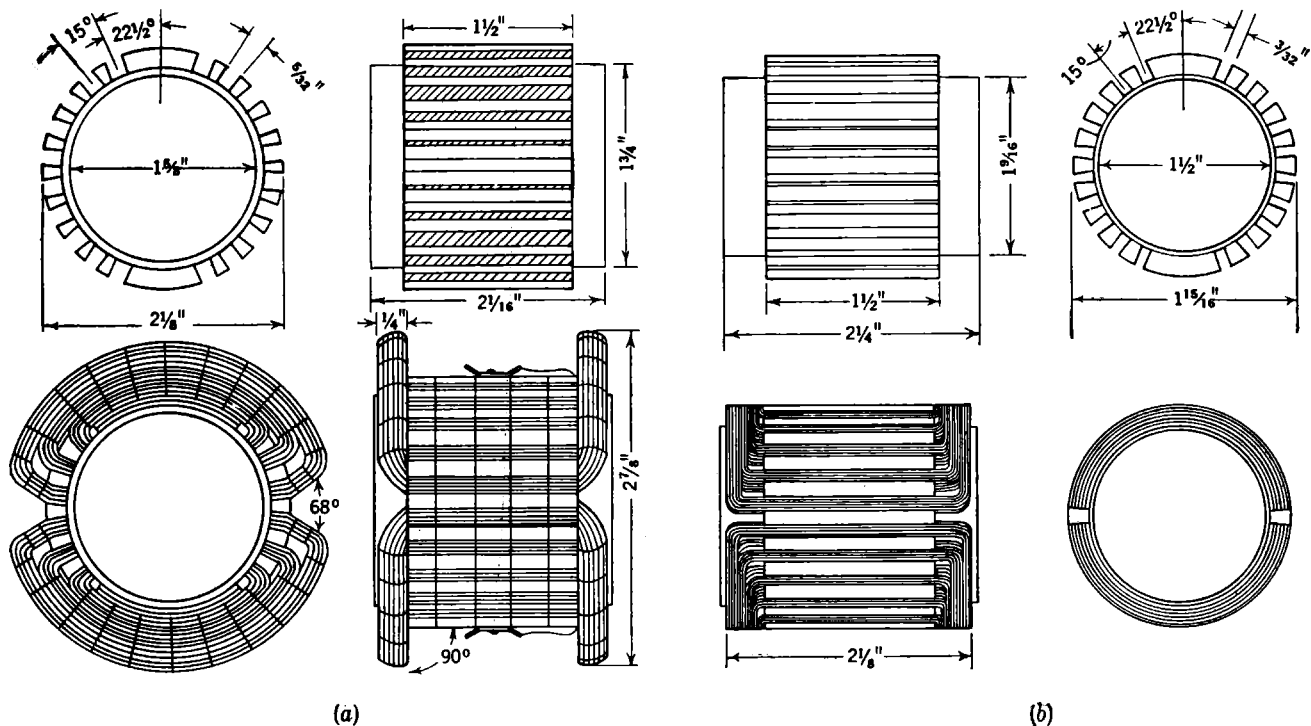
FIG. B·5.—Air-core deflection coils with sine distribution of windings.　Forms are machined or molded plastic.　Shape *a* is particularly adapted to off-centering applications when used in conjunction with the coil shown in Fig. B·4.　For wire size and electrical characteristics, see Table B·1.

(a) Slotted coil form on which windings are placed

(b) Face view of winding disks showing holes for pins

(c) Side view of winding disks showing position of slanting pins

(d) Cross-section of coil after winding



(e) Coil after winding and tying

(f) Coil bent to cylindrical shape

(g) Coil placed on slotted form
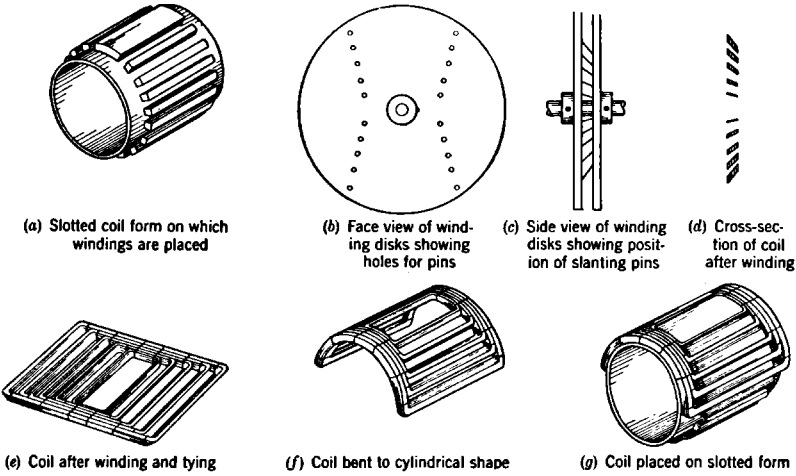
FIG. B·6.—Steps in building a semidistributed air-core coil.



(a) Winding disk showing position of holes

(b) Winding disk with pins in place

(c) Cross-section of winding

(d) Bending block

(e) Coil after winding and tying



(f) Coil in bending block

(g) Coil with ends bent ready for fitting on form

(h) Coil in place on form
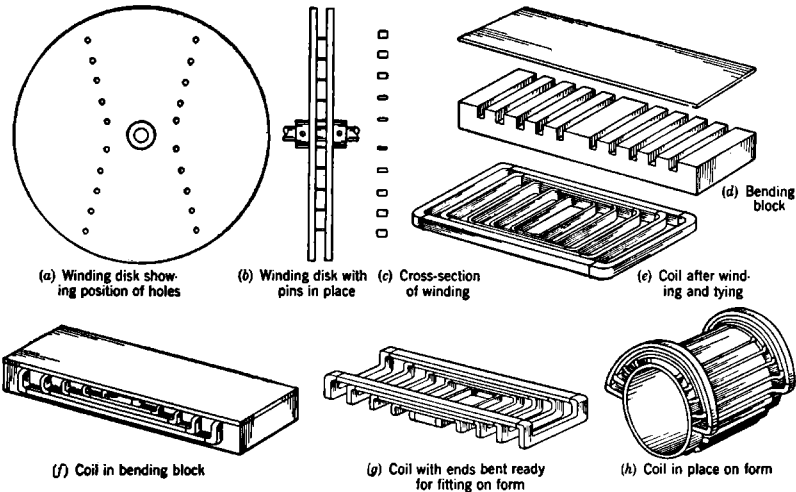
FIG. B·7.—Steps in building an air-core coil with bent-up ends.

copper wire may be wound over these pins to form the first hank; then without breaking the wire, the winding machine is stopped, four more pins are pushed into the second set of holes and the winding is continued until the proper number of turns have been wound on the second hank. The third, fourth, and fifth hanks are wound in the same manner.

Every size of coil form must have its own winding disks because the holes are drilled so that the finished winding just fits on the slotted form.

In order that the windings may fit into the radial slots of the coil form, slanting holes are used so that the finished winding will have one long side and one short side, corresponding to the different arc lengths.    Winding should start at the bottom of the pin and then gradually work up the side until the required number of turns have been wound (Fig. B·6d), in order to prevent slippage.

After winding, the disks may be slid off the shaft and the pins pulled out of the holes.    The winding is thus freed and it should then be tied with thread or fine string as shown (Fig. B·6e).    The completely tied coil may then be bent with the fingers into a cylindrical shape (Fig. B·6f) and fitted onto the slotted form (Fig. B·6g).    An adhesive tape may be used to keep it in place.

Another winding, identical in every respect to the first, is placed on the bottom half of the form to complete the coil.    These halves are connected in series so that they will aid each other in generating the magnetic field.

The construction of a deflection coil with bent-up ends requires a somewhat different technique, as shown in Fig. B·7.    The same type of slotted coil form is used but the holes in the winding disks are spaced differently to allow for bent-up ends.    These holes are not slanted because the manner in which the ends are formed allows the windings to fit into radial slots.    The same steps as those described for the coil in Fig. B·6 are followed in winding the coil; but, after the hanks are tied to prevent their being tangled, the winding is placed in a bending block so that the ends may be bent up at right angles.    When this step is finished, the winding may be placed on the slotted form and secured as before.

# APPENDIX C

## IMPREGNATION OF DEFLECTION AND FOCUS COILS

### By R. D. Rawcliffe

Electronic equipment used under adverse climatic conditions frequently fails because of moisture penetration, fungus growth, corrosion, etc. More or less satisfactory techniques of protecting apparatus against the weather have been worked out. The protection of deflection and focus coils is a difficult problem because, unlike transformers, they cannot be hermetically sealed in a can. However, a number of techniques and materials have been developed for this purpose. The following treatment, although long and tedious, has been found to be one of the best. The extra trouble is worth while, however, if the coils must stand up under tropical conditions.

**C·1. Material Used.** *Impregnation Compound.*—The impregnation compound consists of Irvington Varnish and Insulator Company's "Harvel 612C" varnish, or its equivalent, thinned approximately 10 per cent by volume with V.M. and P. naphtha, having a distillation range from 104° to 160°C. The consistency of the impregnate should be 50 $\pm 5$ sec when measured with a 0.10 in. ASTM cup (ASTM-D333-40).

*Coating Compound.*—One gallon of Irvington Varnish and Insulator Company "Harvel 612C" Varnish, or the equivalent, is mixed with $3\frac{1}{2}$ lb of Whittaker, Clark, and Daniels No. 492 talc, or the equivalent, by adding small quantities of talc to the varnish and agitating thoroughly. The mixture is allowed to stand for 2 to 3 hr until all bubbling and foaming has ceased, and then it is stirred again to ensure that the talc has not settled. The talc should have a maximum water extract conductivity of 1.5 $(10^{-5})$ $\mu$ohms/gram. The consistency of the mixture when measured at any temperature between 21.1° and 37.8°C should be adjusted to 49 $\pm$ 4 sec in a 0.20 in. cup (similar to standard ASTM cups) by evaporating thinner from the mixture if the consistency is too low or adding thinner if the consistency is too high. The V.M. and P. naphtha as required for the impregnation compound is the only acceptable thinner.

**C·2. Condition of Coils.**—Before impregnation, the coils should be in the following condition:

1. Not treated with wax.
2. In assembled condition with the leads firmly fastened.

3. Assembly cleaned.
4. Assembly holes plugged.

### C-3. Method of Impregnation. *First Impregnation.—*

1. *Vacuum Drying.* The assembly is placed in a vacuum tank and the pressure reduced until a vacuum of not less than 29 in. of mercury is obtained. Drying is accomplished in 4 hr ± 15 min at a temperature between 104° and 116°C.
2. *Vacuum Cooling.* The assembly is then immediately placed in a second unheated vacuum tank and the pressure reduced until a vacuum of not less than 29 in. of mercury is obtained. The assembly is allowed to remain under this vacuum and cool for 1 hr ± 10 min.
3. *Impregnating.* The vacuum pump is then shut off and an amount of impregnating compound sufficient to completely cover the assembly is drawn into the tank so that the previously established vacuum is not reduced to less than 28 in. of mercury. The vacuum is broken after 15 min and the assembly allowed to remain immersed in the varnish for a period of 45 ± 10 min.
4. *Air Drying and Draining.* The assembly is then air dried and drained for 1 hr ± 10 min. During this draining period the assembly should be suspended in a vertical position.
5. *Baking.* The assembly is then baked at a temperature of 130° to 135°C, with the coil windings maintained at the baking temperature, for a period of 8 to 10 hr. During this baking period the assembly should be suspended from metal hooks with the winding assembly in the same vertical position as it was during the draining process.

*Second Impregnation.—*The process used for the first impregnation, starting with (2) vacuum cooling, is then repeated. In suspending the coil by hooks during draining and baking, the position should be opposite to that used in first impregnation.

**C-4. Coating.**—All coatings and air drying should be done at an ambient temperature between 21 and 38°C.

1. *First Coating.* Immediately after baking, the assembly is allowed to cool to a temperature of not over 9°C above room temperature. The assembly is then completely immersed in the coating compound, and allowed to remain in the solution for a minimum of 10 min.
2. *Air Drying and Draining.* The assembly is withdrawn from the compound and allowed to air dry and drain with the mounting

surface at the bottom for a period of 5 to 6 hr.  Approximately 2 hr after the start of the air-drying period, excessive lumps and streamers of the coating material should be removed from the assembly and spots smoothed over.

3. *Baking.*   The assembly is baked for a period of 5 hr ± 30 min at a temperature of 93 ± 6°C.

4. *Cooling.*   The assembly is removed from the baking oven and allowed to cool for a period of 3 to 4 hr.

5. *Second Coating.*   The process used to apply the first coating is repeated except that the baking time is extended to 11 to 12 hr instead of 5 hr, as previously.

**C·5. Final Preparation.**—At the conclusion of the second baking and cooling the assembly is examined for pin holes, bubbles, or other signs of defective coating.   If defects in the coating are found, the assembly should be recoated.   When the final coating is completed, the terminals and mounting surfaces should be scraped clean of all impregnating and coating materials.   Solvents should not be used in the cleaning procedure, and care should be taken in handling the assembly to assure that the coating is not damaged.

# APPENDIX D

## CATHODE-RAY-TUBE CHARACTERISTICS

### By T. Soller and A. Y. Bentley

The following tables of data covering cathode-ray-tube characteristics have been compiled partially from the "Joint Army-Navy Specification JAN-1A for Electron Tubes," and descriptive material covering ratings is largely paraphrased from this specification. See Chap. 2 for a further discussion of electrical characteristics of tubes, and Chap. 18 for screens.

*Note* 1.—The tubes listed may be obtained from the tube manufacturers with screen materials other than those indicated. Operating conditions for screen materials are listed in Table D·4.

In Table D·1 there are numerous "A" tube types. Mechanically the "A" type and the "non-A" type are interchangeable but electrically it will be noted that maximum Anode No. 1 current (or focus current) is negligible for the "A" types. Thus if the power supply for the cathode-ray-tube is designed for negligible focus current it will be overloaded when a "non-A" type is used. Wherever the two types differ, the values for the "A" type follow the shilling bar.

*Note* 2.—Grid No. 1 cutoff voltage is the voltage applied to that electrode to extinguish, visually, the undeflected, focused spot. Grid No. 1 cutoff ratings are subject to ±50 per cent variation, and are valid only when the other electrode voltages are as indicated.

*Note* 3.—Grid No. 2 voltage is the normal operating voltage applied to that electrode. Ratings for Grid No. 1 cutoff voltage, Anode No. 1 or focus voltage, or focus ampere-turns apply when Grid No. 2 voltage is as indicated. Maximum Grid No. 2 voltage is +220 volts for the 3HP type, +330 volts for the 7CP1 type, and +750 volts for all other types. Grid No. 2 can be used for blanking of the return trace because a change in Grid No. 2 voltage changes the Grid No. 1 cutoff voltage. In general, an improvement in spot size can be obtained if $E_{c2}$ is made more positive than the nominal value of +250 volts. Increasing $E_{c2}$ results in an increase in $E_{c0}$ also. The value of $E_{c0}$ for a voltage on the second grid, designated as $(E_{c0})_{c2}$, is given approximately by the expression

$$(E_{c0})_{c2} = (E_{c0})_{250} \cdot \left(\frac{E_{c2} + 75}{325}\right).$$

Increasing $E_{c2}$ also increases the amount of grid drive ($\Delta E_{c1}$) required to produce a given beam current.

*Note* 4.—When the Grid No. 1 voltage is adjusted to 75 per cent of the cutoff rating and all other voltages are as indicated, the Anode No. 1 voltage is that which must be applied to the first anode in order to bring the electron beam to focus on the luminescent screen. Anode No. 1 voltage or focus voltage ratings are subject to $\pm 20$ per cent variation.

*Note* 5.—Anode voltages (other than Anode No. 1 voltages) are nominal values and may be increased or decreased as indicated by the tube manufacturer. Higher voltages produce smaller spot size, higher light output, and decreased deflection sensitivity. For a minimum amount of aberration in the spot in the case of electrostatic-deflection types, a maximum ratio between Anode No. 2 voltage and Anode No. 3 voltage should not be exceeded. For electrostatic-deflection types, Anode No. 2 is the final anode when there is no Anode No. 3.

*Note* 6.—Modulation characteristic is the maximum Grid No. 1 drive (or change in Grid No. 1 voltage from the cutoff value) necessary to produce the indicated light output or anode current.

*Note* 7.—Deflection factor is the reciprocal of deflection sensitivity and is the ratio of the instantaneous voltage applied to the deflection plates to the corresponding deflection on the indicated deflection axis. Deflection factor ratings are subject to $\pm 20$ per cent variation, and apply only when the other electrode voltages are as indicated.

*Note* 8.—Deflection angle is twice the angle of deflection from the axis.

*Note* 9.—Focus-coil position is the distance from the center of the focus-coil gap to the reference line. See *Note* 16.

*Note* 10.—Focus-coil ampere-turns ratings are nominal values for a focus coil enclosed in a soft iron shell of $1\frac{1}{2}$ in. axial length, $1\frac{5}{8}$ in. inside diameter, and an air-gap width of $\frac{5}{16}$ in.

*Note* 11.—The test pattern used for light-output and shrinking-raster line-width determinations is a 35- to 105-line pattern provided by 60-cps sawtooth scanning on one axis and 2100- to 6300-cps sawtooth scanning on the other axis. In the case of electrostatic-deflection types, the mean potential of free deflecting plates should be that of Anode No. 2.

For light-output measurements, the pattern size should be adjusted to 2 in. by 2 in.

For line-width or spot-size measurements (see also Chap. 17) the pattern should first be adjusted to the size used in the measurement of light output, and the light output or anode current set to the indicated value by adjusting the Grid No. 1 voltage. After this adjustment, the high-frequency scanning amplitude (applied to the deflecting plates nearest the screen for electrostatic types) should be adjusted to give a

TABLE D·1.—ELECTRICAL AND MECHANICAL CHARACTERISTICS OF ELECTROSTATIC CRT

| Tube type (see also *Note* 1) | See note | 913 | 902 902A | 2AP1 2AP1A | 2BP1 | 3AP1 3AP1A | 3BP1 3BP1A | 3DP1 3DP1A | 3EP1 | 3FP7 3FP7A | 3GP1 | 3JP1 | 3KP1 | 905 905A |
|---|---|---|---|---|---|---|---|---|---|---|---|---|---|---|
| **Electrical characteristics:** | | | | | | | | | | | | | | |
| Heater voltage | | | 6.3 | 6.3 | 6.3 | 2.5 | 6.3 | 6.3 | 6.3 | 6.3 | 6.3 | 6.3 | 6.3 | 2.5 |
| Max. $E_{b2}$ | | 500 | 600 | 1100 | 2750 | 1650 | 2200 | 2200 | 2200 | 2200 | 1650 | 2200 | 2750 | 2200 |
| Max. $E_{b3}$ | | | | | | | | | | 4400 | | 4400 | | |
| Max. $E_{b2}/E_{b3}$ | 5 | | | | | | | | | 2.3 | | 2.3 | | |
| **Typical operating conditions:** | | | | | | | | | | | | | | |
| $E_{co}$-$V_{d-c}$ | 2 | −32 | −60 | −60 | −45 | −50 | −45 | −45 | −45 | −60 | −50 | −60 | −60 | −26 |
| $E_{b1}$-$V_{d-c}$ | 4 | 80 | 150 | 250 | 215 | 430 | 430 | 430 | 430 | 575 | 350 | 575 | 460 | 378 |
| $E_{b2}$-$V_{d-c}$ | 5 | 400 | 600 | 1000 | 1000 | 1500 | 1500 | 1500 | 1500 | 2000 | 1500 | 2000 | 2000 | 1500 |
| $E_{b3}$-$V_{d-c}$ | 6 | | | | | | | | | 4000 | | 4000 | | |
| Modul. charact. — $I_{b3}$-µa, d-c | 6, 11 | | | | | | | | | 150 | 150 | | | |
| Modul. charact. — Light output, ft. I. | 6 | | 1 | 2 | | 1 | 5 | 7.5 | 5 | | 1.5 | | | 2 |
| Modul. charact. — $\Delta E_{c1}$-$V_{d-c}$ from $E_{co}$ | | | 60 | 50 | | 45 | 40 | 40 | 40 | 50 | 45 | | | 25 |
| Deflection factor, $V_{d-c}$/in. — $D_1D_2$ | 7 | 240 | 139 | 230/217 | 135 | 114 | 150 | 40 | 166 | 250 | 120 | 198 | 118 | 86 |
| Deflection factor, $V_{d-c}$/in. — $D_3D_4$ | 7 | 176 | 117 | 196 | 87 | 109 | 111 | 150 | 124 | 180 | 105 | 145 | 90 | 73 |
| Max. electrode current, µa d-c — cathode | 12 | | 1000 | 1000 | −15, +10 | 1000 | 1000 | 1000 | 1000 | 1500 | 1000 | 1500 | | 1000 |
| Max. electrode current, µa d-c — anode No. 1 | 12 | | 200/10 | 150/10 | | 400/10 | 200/10 | 500/10 | 300 | 600/10 | 400 | 10 | | 200/10 |
| Spot size, mm. — Position $A$ | 11 | | 0.75 | 0.5/0.45 | | 0.45 | 0.7/0.6 | 0.75 | 0.7 | 0.75 | 0.35 | 0.75 | | 1.3/0.9 |
| Spot size, mm. — Position $B$ | 11 | | 1.0 | 0.65/0.55 | | 0.65 | 0.75/0.70 | 1.05/0.8 | 1.0 | 1.1/0.9 | 0.45 | 0.9 | | 1.5/0.9 |
| Interelectrode capacitance, µµf. — $K$ to all | 13 | | | 6 | | | 7 | 5–10.5 | | 7 | | 5 | | |
| Interelectrode capacitance, µµf. — $g_1$ to all | | 8 | 7 | 8 | 8 | 9 | 8 | 3.7–10.5 | 8 | 7 | 9 | 5 | 7 | 9 |
| Interelectrode capacitance, µµf. — $D_1$ to $D_2$ | | 3 | 4 | 1 | 2 | | 2 | 0.5–4 | 1 | 2 | 2 | 3 | 2 | 2 |
| Interelectrode capacitance, µµf. — $D_2$ to $D_4$ | | 3 | 3 | 1 | 2 | | 2 | 0.5–4 | 1 | 2 | 2 | 2 | 3 | 1 |
| Interelectrode capacitance, µµf. — $D_1$ to all | | | | 9 | 10 | | 9 | 5–15 | 7 | 9 | 13 | | 8 | |
| Interelectrode capacitance, µµf. — $D_3$ to all | | | | 9 | 7 | | 7 | 4–12 | 8 | 7 | 8 | | 8 | |
| Interelectrode capacitance, µµf. — $D_1$ to all except $D_2$ | | | | 8 | | | 7 | 3–13 | 6 | 7 | 11 | 6 | 7 | |
| Interelectrode capacitance, µµf. — $D_2$ " " " $D_1$ | | | | 5 | | | 7 | 3–13 | 5 | 7 | 12 | 6 | 8 | |
| Interelectrode capacitance, µµf. — $D_3$ " " " $D_4$ | | | | 8 | | | 5 | 3–12 | | 5 | 6 | 5 | | |
| Interelectrode capacitance, µµf. — $D_4$ " " " $D_3$ | | | | 4 | | | 6 | 3–8.3 | | 6 | 7 | 5 | | |
| Interelectrode capacitance, µµf. — $D_3$ to anode #2 | | | | | | | | 1–3.5 | | | | | | |
| **Mechanical characteristics:** | | | | | | | | | | | | | | |
| Min. useful screen diam., inches | 14 | 0.8 | 1.75 | 1.75 | 1.75 | 2.75 | 2.75 | 2.75 | 2.75 | 2.75 | 2.75 | 2.75 | 2.75 | 4.5 |
| Nom. screen rad. curvature, in. | 15 | | 8 | 8 | 8 | 8 | 8 | 8 | 8 | 8 | 8 | 8 | 8 | 8 |
| Bulb diameter, inches | 16 | 1.31 | 2.0 | 2.0 | 2.0 | 3.0 | 3.0 | 3.0 | 3.0 | 3.0 | 3.0 | 3.0 | 3.0 | 5.25 |
| Tolerance, ± | | | 0.06 | 0.06 | 0.06 | 0.06 | 0.06 | 0.06 | 0.06 | 0.06 | 0.06 | 0.06 | 0.06 | 0.06 |
| Over-all length, inches | 16 | 4.75 | 7.44 | 7.44 | 7.62 | 11.5 | 10.0 | 10.44 | 9.94 | 10.0 | 11.5 | 10.0 | 11.5 | 16.5 |
| Tolerance, ± | | | 0.19 | 0.19 | 0.19 | 0.37 | 0.25 | 0.31/0.27 | 0.25 | 0.25 | 0.37 | 0.25 | 0.25 | 0.37 |
| Basing and base type | 18 | 3 | 3 | 6 | 14 | 2 | 16 | 16 | 7 | 16 | 7 | 16 | 10 | 1 |

| Tube type (see also *Note* 1) | See note | 5AP1 | 5BP1 5BP1A | 5CP1 5CP1A | 5GP1 | 5JP1 | 5LP1 | 5MP1 | 5RP1 | 5SP1 | DuM. K-1017 | 7EP4 | 7GP4 | 12GP7 | 20AP1 |
|---|---|---|---|---|---|---|---|---|---|---|---|---|---|---|---|
| **Electrical characteristics:** | | | | | | | | | | | | | | | |
| Heater voltage | | 6.3 | 6.3 | 6.3 | 6.3 | 6.3 | 6.3 | 2.5 | 6.3 | 6.3 | 6.3 | 6.3 | 6.3 | 6.3 | 2.5 |
| Max. $E_{b2}$ | | 2000 | 2000 | 2200 | 2200 | 2200 | 2200 | | 3850 | 2200 | 4500 | 3300 | 4400 | 4400 | 4000 |
| Max. $E_{b1}$ | | | | 4400 | | 4400 | 4400 | | 25,850 | 4400 | 37,500 | | | 6600 | 8000 |
| Max. $E_{b2}/E_{b3}$ | 5 | | | 2.3 | | 2.0 | 2.0 | | 10.0 | 3.0 | | | | | |
| **Typical operating conditions:** | | | | | | | | | | | | | | | |
| $E_{co}-V_{d-c}$ | 2 | −43 | −30 | −45 | −30 | −56 | −45 | −50 | −60 | −60 | −90 | −60 | −60 | −140 | −80 |
| $E_{b1}-V_{d-c}$ | 4 | 432 | 337 | 431 | 337 | 390 | 375 | 375 | 575 | 575 | 865 | 650 | 1000 | 1230 | 1000 |
| $E_{b2}-V_{d-c}$ | 5 | 1500 | 1500 | 1500 | 1500 | 1500 | 1500 | 1500 | 2000 | 2000 | 3000 | 2500 | 3000 | 4300 | 4000 |
| $E_{b3}-V_{d-c}$ | 5 | | | 3000 | | 3000 | 3000 | | 10,000 | 4000 | 15,000 | | | 5500 | 8000 |
| Modul. charact. { $I_{b3}$-μa, d-c | 6 | | | | | | | | | | | | | 60 | |
| { Light output, ft. I. | 6, 11 | 2 | 2 | 7.5/15 | 2 | 3 | 4 | | | | | 5 | | | | |
| { $\Delta E_{c1}-V_{d-c}$ from $E_{co}$ | 6 | 35 | 35 | 40/45 | 35 | 40 | 35 | | | | | 38 | | 80 | |
| Deflection factor, $V_{d-c}$/in. { $D_1D_2$ | 7 | 93 | 63 | 69 | 27 | 77 | 77 | 66 | 128 | 92 | 130 | 110 | 108 | 112 | 110 |
| { $D_3D_4$ | 7 | 90 | 56 | 59 | 54 | 68 | 68 | 60 | 121 | 79 | 140 | 95 | 90 | 103 | 110 |
| Max. electrode current, μa-d-c { cathode | 12 | 1000 | 1000 | 1000 | 1000 | 1000 | 1000 | 1000 | | | | | | 1500 | |
| { anode No. 1 | 12 | 300 | 350/10 | 500/10 | 350 | 400 | 400 | 400 | | | | −50, +10 | −15, +10 | 600 | |
| Spot size, mm. { Position A | 11 | 1.0 | 0.7/0.65 | 0.65/0.75 | 0.7 | 0.6 | 0.6 | 0.7 | | | | | | 1.2 | |
| { " B | 11 | 1.2 | 1.0/0.65 | 0.9/0.75 | 1.0 | 0.7 | 0.9 | 1.1 | | | | | | 1.8 | |
| Interelectrode capacitance, μμf. { K to all | 13 | | | | | | | | 5 | <1 | | | 10 | 8−11.5 | |
| { $g_1$ to all | " | 9 | 9 | 7 | 7−12 | 8 | 10 | 8 | 6 | 2 | | 6 | 9 | 8.5−11.5 | 6 |
| { $D_1$ to $D_2$ | " | 1 | 1 | 2 | 0.5−5 | 1.4 | 2 | | 2 | 2 | 0.7 | 2 | 4 | 1.5−5 | 2 |
| { $D_3$ to $D_4$ | " | 1 | 1 | 2 | 0.2−3 | 1.2 | 2 | | 2 | 2 | 0.4 | 2 | 2 | 1.5−5 | 1 |
| { $D_1$ to all | " | 11 | 14 | 9 | 5−15 | 4 | 13 | 7 | | | | | 11 | 5−13 | 9 |
| { $D_3$ to all | " | 7 | 9 | 7 | 5−15 | 4 | 9 | 6 | | | | | 8 | 5−13 | 7 |
| { $D_1$ to all except $D_2$ | " | 11 | 12 | 7 | 5−13 | 2.5 | 12 | | 3 | 2 | 4.7 | 7 | | 5−10 | 7 |
| { $D_2$ " " " $D_1$ | " | 10 | 12 | 7 | 3−13 | 2.5 | 12 | | 3 | 2 | 4.7 | 7 | | 5−10 | 7 |
| { $D_3$ " " " $D_4$ | " | 5 | 8 | 5 | 3−15 | 2.1 | 7 | | 2 | 2 | 4.2 | 5 | | 3−9 | 6 |
| { $D_4$ " " " $D_3$ | " | 4 | 7 | 6 | 4−12 | 2.2 | 6 | | 2 | 2 | 4.4 | 5 | | 3−9 | 6 |
| { $D_5$ to anode #2 | " | | | | | | | | | | | | | | |
| **Mechanical characteristics-** | | | | | | | | | | | | | | | |
| Min. useful screen diam., inches | 14 | 4.5 | 4.5 | 4.5 | 4.5 | 4.5 | 4.5 | 4.5 | 4.5 | 4.5 | 4.5 | 6.0 | 6.0 | 10 | 17 |
| Nom. screen rad. curvature, in. | 15 | 9 | 8 | 8 | 8 | 10 | 10 | 10 | ∞ | ∞ | ∞ | 15 | 20 | 20 | 26 |
| Bulb diameter, inches | 16 | 5.25 | 5.25 | 5.25 | 5.25 | 5.31 | 5.31 | 5.31 | 5.25 | 5.28 | 5.25 | 7.0 | 7.0 | 12 | 20 |
| Tolerance, ± | | 0.06 | 0.06 | 0.06 | 0.06 | 0.06 | 0.06 | 0.06 | 0.09 | 0.09 | 0.09 | 0.12 | 0.12 | 0.19 | 0.37 |
| Over-all length, inches | 16 | 13.0 | 16.75 | 16.75 | 16.75 | 16.75 | 16.75 | 15.87 | 16.75 | 18.25 | 19.5 | 15.5 | 14.5 | 22 | 27.87 |
| Tolerance, ± | | 0.37 | 0.37 | 0.37 | 0.37 | 0.37 | 0.37 | 0.37 | 0.37 | 0.37 | 0.5 | 0.37 | 0.37 | 0.5 | 0.75 |
| Basing and base type | 18 | 7 | 7 | 16 | 7 | 9 | 8 | 2 | 17 | 18 | 17 | 7 | 16 | 18 | 15 |

TABLE D·2.—ELECTRICAL AND MECHANICAL CHARACTERISTICS OF MAGNETIC CRT

| Tube type (see also *Note* 1) | See note | 3HP7 | 4AP10 | 5FP7 | 5TP4 | 7BP7 | 7CP1 | 7DP4 | 9GP7 | 9LP7 | 10BP4 10EP4 | 12DP7 | 12JP4 | 15AP4 | 20BP4 |
|---|---|---|---|---|---|---|---|---|---|---|---|---|---|---|---|
| **Electrical characteristics:** | | | | | | | | | | | | | | | |
| Heater voltage | | 6.3 | 6.3 | 6.3 | 6.3 | 6.3 | 6.3 | 6.3 | 6.3 | 6.3 | 6.3 | 6.3 | 6.3 | 6.3 | 6.3 |
| Maximum $E_b$ | | 5500 | 9900 | 7700 | 30,000 | 7700 | 7700 | 8800 | 7700 | 7700 | 10,000 | 7700 | 13,200 | 13,200 | 16,500 |
| **Typical operating conditions:** | | | | | | | | | | | | | | | |
| $E_{co}$-$V$d-c | 2 | -27 | -45 | -45 | -70 | -45 | -45 | -45 | -45 | -80 | -45 | -45 | -45 | -45 | -45 |
| $E_{c1}$-$V$d-c | 3 | 150 | 300 | 250 | 200 | 250 | 250 | 250 | 250 | 250 | 250 | 250 | 250 | 250 | 250 |
| $E_b$-$V$d-c | 5 | 4000 | 9000 | 4000 | 27,000 | 4000 | 4000 | 6000 | 4000 | 4000 | 9000 | 4000 | 10,000 | 10,000 | 15,000 |
| Modul. charact. { $I_b$-$\mu$a, d-c | 6 | 200 | 600 | 200 | | 200 | | | 200 | 200 | | 200 | 200 | | 200 |
| { $\Delta E_{c1}$-$V$d-c from $E_{co}$ | 6, 11 | 38 | 35 | 38 | | 38 | | | 38 | 38 | | 38 | 38 | | 38 |
| Deflection angle, degrees | 8 | 39 | 40 | 55 | 50 | 55 | 55 | 50 | 55 | 55 | 50 | 55 | 50.5 | 52.5 | 50.5 |
| $E_{b1}$-$V$d-c | 4, 12 | | | | 4900 | | 780 | 1430 | | | | | | | |
| Focus coil position, inches | 9 | 2.75 | 2.75 | 2.75 | | 2.75 | | | 4.12 | 2.75 | | 4.12 | 2.75 | 2.75 | 2.75 |
| Focus ampere-turns | 10 | 398 | 450 | 398 | | 398 | | | 398 | 398 | | 398 | 650 | 625 | 550 |
| Spot size, mm. { Position A | 11 | 0.5 | 0.28 | 0.5 | | 0.75 | 0.5 | | 1.0 | 1.3 | | 1.35 | | | |
| { Position C | 11 | 0.6 | 0.28 | 0.6 | | 0.85 | 0.65 | | 1.2 | 1.5 | | 1.5 | | | |
| Interelec. capac., $\mu\mu$f. { $k$ to all | 13 | 9 | | 6.5 | 5 | 6.5 | | 5 | | | 5 | | | | 6.5 |
| { $g_1$ to all | 13 | | | 8 | 7.5 | 8 | | 6.5 | | | 6.5 | | | | 8 |
| { $g_2$ to all | 13 | | | 9 | | 9 | | | | | | | | | 9 |
| Ion trap in gun | 13 | | | | | | | ✓ | | | ✓ | | | | |
| Metal-backed screen | | | | | ✓ | | | | | | | | | | |
| **Mechanical characteristics:** | | | | | | | | | | | | | | | |
| Min. useful screen diam., inches | 14 | 2.5 | 3.38 | 4.25 | 4.25 | 6.0 | 6.5 | 6.0 | 7.62 | 8.5 | 9.0 | 10.0 | 10.0 | 13.5 | 18.0 |
| Nom. screen rad. curvature, in. | 15 | 8 | 5.8 | 24 | 7.100 | 24 | 20 | 24 | 20 | 18 | 42 | 20 | 20 | 60 | 30 |
| Bulb diameter, inches | 16 | 3.0 | 4.0 | 4.94 | 5.0 | 7.0 | 7.0 | 7.19 | 9.0 | 9.0 | 10.5 | 12.0 | 12.0 | 15.62 | 20.0 |
| Tolerance, ± | | 0.06 | 0.12 | 0.09 | 0.12 | 0.12 | 0.12 | 0.12 | 0.12 | 0.12 | 0.12 | 0.19 | 0.19 | 0.25 | 0.37 |
| Over-all length, inches | 16 | 9.81 | 14.75 | 11.12 | 11.75 | 13.25 | 13.44 | 14.06 | 17.0 | 14.97 | 17.62 | 20.12 | 17.5 | 20.19 | 28.75 |
| Tolerance, ± | | 0.25 | 0.37 | 0.37 | 0.37 | 0.37 | 0.37 | 0.37 | 1.0 | 0.35 | 0.37 | 1.0 | 0.5 | 0.62 | 0.75 |
| Reference line to face, inches | 16 | 2.28 | 4.25 | 3.62 | 4.81 | 5.75 | 6.0 | 5.94 | 7.37 | 7.5 | 9.44 | 8.62 | 10.5 | 13.56 | 20.0 |
| Tolerance, ± | | 0.09 | 0.19 | 0.12 | 0.09 | 0.25 | 0.25 | 0.19 | 0.25 | 0.25 | 0.19 | 0.25 | 0.25 | 0.25 | 0.50 |
| Neck diameter, inches | 16, 17 | 1.37 | 1.37 | 1.37 | 1.44 | 1.37 | 1.37 | 1.44 | 1.37 | 1.37 | 1.44 | 1.37 | 1.37 | 1.44 | 1.37 |
| Tolerance, ± | | 0.06 | 0.06 | 0.06 | 0.06 | 0.06 | 0.06 | 0.06 | 0.06 | 0.06 | 0.06 | 0.06 | 0.06 | 0.06 | 0.06 |
| Basing and base type | 18 | 4 | 4A | 4 | 11 | 4 | 5 | 11 | 4 | 4 | 12 | 4 | 12 | 13 | 13 |
| Anode terminal type | 19 | A | C | A | B | A | A | B | C | C | 10B-"B" 10E-"A" | C | A | A | C |

TABLE D·3.—BASE TYPES AND BASING OF CRT IN TABLES D-1 AND D-2

| Basing, No. (see note 18) | Base type | Pin numbers | | | | | | | | | | | | | |
|---|---|---|---|---|---|---|---|---|---|---|---|---|---|---|---|
| | | 1 | 2 | 3 | 4 | 5 | 6 | 7 | 8 | 9 | 10 | 11 | 12 | 13 | 14 |
| 1 | Medium 5-pin | $h$ | $p_1$ | $p_2$ | $g_1$ | $h, k$ | | | | | | | | | |
| 2 | Medium 7-pin | $h$ | $g$ | $D_2$ | $p_1$ | $D_1$ | $p_2, D_2, D_4$ | $h, k$ | | | | | | | |
| 3 | Octal 8-pin | $p_2, D_2, D_3$ | $h, k$ | $p_1$ | $D_1$ | $g_1$ | $D_4$ | $h$ | $nc$ | | | | | | |
| 4 | "      " | $nc$ | $h$ | $g_2$ | $nc$ | $g_1$ | $nc$ | $k$ | $h$ | | | | | | |
| 4a | "      " | $ic$ to 6 | $h$ | $g_2$ | $nc$ | $g_1$ | $ic$ to 1 | $k$ | $h$ | | | | | | |
| 5 | "      " | $nc$ | $p_1$ | $nc$ | $g_2$ | $k$ | $k$ | $h$ | $h$ | | | | | | |
| 6 | Magnal 11-pin | $h$ | $k$ | $D_1$ | $p_1$ | $nc$ | $D_4$ | $p_2$ | $D_2$ | $D_3$ | $g$ | $h$ | | | |
| 7 | "      " | $h$ | $nc$ | $D_1$ | $p_1$ | $ic$ | $D_4$ | $p_2$ | $D_2$ | $D_3$ | $g$ | $h, k$ | | | |
| 8 | "      " | $h$ | $nc$ | $D_1$ | $p_1$ | $nc$ | $D_4$ | $p_2$ | $D_2$ | $D_3$ | $g$ | $h, k$ | | | |
| 9 | "      " | $h$ | $nc$ | $nc$ | $p_1$ | $ic$ | $nc$ | $p_2$ | $nc$ | $nc$ | $g$ | $h, k$ | | | |
| 10 | "      " | $h$ | $g_1$ | $k$ | $p_1$ | $D_3$ | $D_4$ | $p_2, g_2$ | $D_2$ | $D_1$ | $ic$ | $h$ | | | |
| 11 | Duodical 7-pin | $h$ | $g_1$ | | | | $p_1$ | $ic$ | | | $g_2$ | $k$ | $h$ | | |
| 12 | "      " | $h$ | $g_1$ | | | | $nc$ | $nc$ | | | $g_2$ | $k$ | $h$ | | |
| 13 | "      " | $h$ | $g_1$ | | | | $ic$ | $ic$ | | | $g_2$ | $k$ | $h$ | | |
| 14 | Duodical 12-pin | $h$ | $g$ | $k$ | $p_1$ | $ic$ | $D_3$ | $D_4$ | $p_2$ | $D_2$ | $D_1$ | $ic$ | $h$ | | |
| 15 | 12-contact peripheral | $nc$ | $g$ | $h, k$ | $h$ | $nc$ | $p_1$ | $p_3$ | $D_4$ | $D_2$ | $p_2$ | $D_1$ | $D_3$ | | |
| 16 | Diheptal 12-pin | $h$ | $k$ | $g$ | $ic$ | $p_1$ | | $D_3$ | $D_4$ | $p_2$ | $D_2$ | $D_1$ | $nc$ | | $h$ |
| 17 | "      " | $h$ | $k$ | $g$ | $ic$ | $p_1$ | | $nc$ | $nc$ | $nc$ | $nc$ | $nc$ | $nc$ | | $h$ |
| 18 | "      " | $h$ | $k$ | $g$ | $ic$ | $p_1$ | | $h$ | $h$ | $k$ | $g$ | $nc$ | $p_1$ | | $h$ |

$h$ = heater; $k$ = cathode; $g$, $g_1$ = control grid; $g_2$ = accelerator grid (grid No. 2); $p_1$ = focusing electrode (anode No. 1); $p_2$ = anode No. 2; $p_3$ = intensifier electrode; $ic$ = internal connection, DO NOT USE!; $nc$ = no connection.

line length of approximately 90 per cent of the maximum tube diameter. The low-frequency scanning amplitude should be increased to make the line structure clearly visible and adjustment should be made for best focus at the center of the pattern. The pattern should then be compressed until the line structure first disappears or begins to overlap at the center of the screen. The line width at Position $A$ is then given by the quotient of the width of the compressed pattern transverse to the line structure divided by the number of scanning lines.

For Position $B$ (for electrostatic-deflection types) the connection of deflection elements to the low- and high-frequency scanning supplies should be interchanged from that of Position $A$ and the determination

TABLE D·4.—CATHODE-RAY-TUBE SCREEN CHARACTERISTICS

| Characteristic | See note | Screen designation (see *Note* 20) | | | | | | | | | | | |
|---|---|---|---|---|---|---|---|---|---|---|---|---|---|
| | | P1 | P2 | P3 | P4 | P5 | P6 | P7 | P10 | P11 | P12 | P13 | P14 |
| Number of layers | 21 | 1 | 1 | 1 | 1 | 1 | 1 | 2 | 1 | 1 | 1 | 1 | 2 |
| Luminescence | 22 | G | LBG | LGY | W | LV | W | BW | | LB | LO | LR | PW |
| Main peak λ | | 5250 | 5140 | 5500 | 4500 | 4300 | 4400 | 4400 | | 4580 | 5870 | 6740 | 4400 |
| Phosphorescence | 23 | G | LBG | LGY | W | LV | W | LY | | LB | LO | LR | LO |
| Main peak λ | | | | | | | | 5600 | | | | | 6090 |
| Tenebrescence | 24 | | | | | | | | M | | | | |
| Main peak λ | | | | | | | | | 5570 | | | | |
| Persistence, sec. (to 1 % of peak) | 25 | .05 | 0.5 | .06 | .06 | $10^{-5}$ | .005 | 3.0 | $10$–$10^2$ | .005 | 0.4 | 0.1 | 1.0 |
| Decay type | 26 | $e^{-t}$ | $t^{-n}$ | $e^{-t}$ | $e^{-t}, t^{-n}$ | $e^{-t}$ | $t^{-n}$ | $t^{-n}$ | $t^{-n}$ | $t^{-n}$ | $e^{-t}$ | $e^{-t}$ | $t^{-n}$ |
| Rel. lum. efficiency (P1 = 100%) | | 100 | 135 | 84 | 80 | 6 | 150 | | | 72 | 90 | 5 | |
| Minimum anode V. | 27 | 500 | 1000 | 500 | 500 | 500 | 500 | 4000 | 9000 | 500 | 4000 | 4000 | 4000 |
| Principal use | 28 | O, R | L, R | O, T | T | P | C, T | R, L | R, L | P | R | D,R | D, R, L |

(Color brace labels: Luminescence, Main peak λ, Phosphorescence, Main peak λ, Tenebrescence, Main peak λ.)

of line width repeated without adjustment of focus. In this case the line-structure disappearance or overlap should be determined at the less favorable of the two alternative $B$ positions (the points along the direction of high-frequency scanning, distant from the center of the screen by three-eighths of the maximum bulb diameter).

For Position $C$ (for magnetic-deflection types) there is no interchange of connections to the deflecting elements and line-width determination is made at the less favorable of the two alternative $C$ positions (same point location as $B$ position) without adjustment of focus.

The values for shrinking-raster line width or spot size are maximum values and for average tubes are about 50 per cent of this value. The actual "spot size" is approximately twice this value.

*Note* 12.—Maximum electrode currents are given for electrostatic types only for power-supply–design considerations. In magnetic types

no appreciable portion of the cathode current is collected by electrodes other than the final anode in the types where magnetic focusing is used; for the three electrostatic focus types listed, the focus electrode currents are as follows: 5TP4, 75 $\mu$a max. for 200 $\mu$a to $A_2$; 7CP1, 200 $\mu$a max.; 7DP4, between $-15$ and $+10$ $\mu$a.

*Note* 13.—The capacitance between the designated combinations of elements should be measured by any of the methods described in the 1938 Report of the Standards Committee of the Institute of Radio Engineers or by an equivalent method as exemplified by the direct-capacitance high-frequency bridge-type circuit, or the direct-capacitance high-frequency transmission-type circuit as shown by RMA Standards Proposal No. 140 dated 27 April 1943.

Average values of capacitance are given, where figures are available. In some cases the minimum to maximum range is given.

*Note* 14.—Minimum useful screen diameter is indicative of the extent of uniformly coated screen. It is possible to use a small portion of the screen outside of the screen size indicated but the uniformity of screen is not guaranteed by tube manufacturers.

*Note* 15.—Nominal screen radius of curvature is indicative of the "flatness" of the face plate.

*Note* 16.—Mechanical dimensions are for mounting design consider-ations. The reference line is determined by the position at which a 2 in. long cylinder will rest on the bulb cone. For tubes having a neck diameter of 1.37 in., this cylinder has an ID of 1.430 in. $+$ 0.003 in., $-0.000$ in.; for 1.44 in. tubes, the ID is 1.500 in., $+0.003$ in., $-0.000$ in.

*Note* 17.—Focus and deflection elements must be so designed that their inside diameters will adequately clear the maximum-size tube neck.

*Note* 18.—Basing and base types are shown in Table D·3.

*Note* 19.—Various shapes and sizes of anode terminals are used.

Type A: Recessed button.

Type B: Recessed small cavity.

Type C: Medium cap ($\frac{9}{16}$-in. diam, $\frac{1}{2}$ in. high cylinder).

*Note* 20.—Cathode-ray-tube screen properties. "P" numbers (P1, P2, P7, etc.) are RMA assigned numbers and are reasonably uniform among manufacturers. This table is of necessity brief and incomplete and is intended to convey only partially the differences between the various screen materials and the requirements for satisfactory operation.

*Note* 21.—Two-layer screens are referred to as "cascade" types. These have two adjacent layers of different phosphors.

The P10 is an evaporated screen and is not used as a phosphor. See also Note 24.

*Note* 22.—Luminescent color is the color of the light emitted by the screen material during excitation by the electron beam. $V =$ violet,

$B.$ = blue, $G$ = green, $Y$ = yellow, $R$ = red, $P$ = purple, $W$ = white, and $L$ = light, or pale.

*Note* 23.—Phosphorescent color is the color of light emitted by the screen material after cessation of electron excitation.

*Note* 24.—Tenebrescent color is the color of the darkening of the screen material due to excitation by the electron beam.   Cathode-ray tubes having tenebrescent screens are intended to be viewed by reflected light.   The color of a fresh trace is magenta $(M)$.

*Note* 25.—The approximate time in seconds to decay to 1 per cent of the peak excitation value is given.   Values may vary considerably from those given, since they depend upon current density used, especially in the case of phosphors that have $t^{-n}$ type of decay.

*Note* 26.—Screens are listed as following an exponential $(e^{-t})$ or power-law $(t^{-n})$ decay if the approximate behavior over the interval of time usually associated with the use of the screen is either exponential or power law in form.

No simple statement will adequately describe the complete decay characteristics of the screen.

*Note* 27.—Minimum anode voltage is the minimum recommended anode voltage at which reasonably satisfactory performance will be attained.

*Note* 28.—There are obviously other uses than the customary ones indicated by the following symbols: $C$, color television; $D$, dark adaptation retention; $L$, transient oscillograph; $O$, oscillograph or general purpose; $P$, photographic oscillograph and high-speed scanning; $R$, radar; $T$, television.

# APPENDIX E

## VIDEO AMPLIFIERS

### By P. Axel

| Fig. no. | Input signal, volts | Output signal, volts | Power supply | | Rise time, $\mu$sec, $\tau$ | Time for 10 % droop, $\mu$sec | Bandwidth $f = 0.35/\tau$, Mc/sec |
|---|---|---|---|---|---|---|---|
| | | | volts | ma | | | |
| E·1 | +1 | −50 | 120 | 75 | 0.06 | 1000 | 6 |
| E·2 | +1 | −35 | 150 | 22 | 0.06 | 470 | 6 |
| E·3 | +1 | −40 | 150 | 12 | 0.07 | ∞ | 5 |
| E·4 | −0.9 | −40 | 150 | 30 | 0.09 | 200 | 4 |
| E·5 | −0.9 | −36 | 250 | 43 | 0.043 | 500 | 8.3 |
| E·6 | +1.3 | −40 | 300 | 85 | 0.03 | 1000 | 12 |
| E·7 | +1 | −40 | { 300 | 40 | 1.6 | 2500 | 2.3 |
| | | | { 150 | 16 | | | |
| E·8 | ±0.5 | ±50 | { 300 | 50 | 1.3 | 470 | 2.8 |
| | | | { 150 | 70 | | | |

* See also Figs. 7·5, 7·6a, and 7·12 for other video amplifiers.
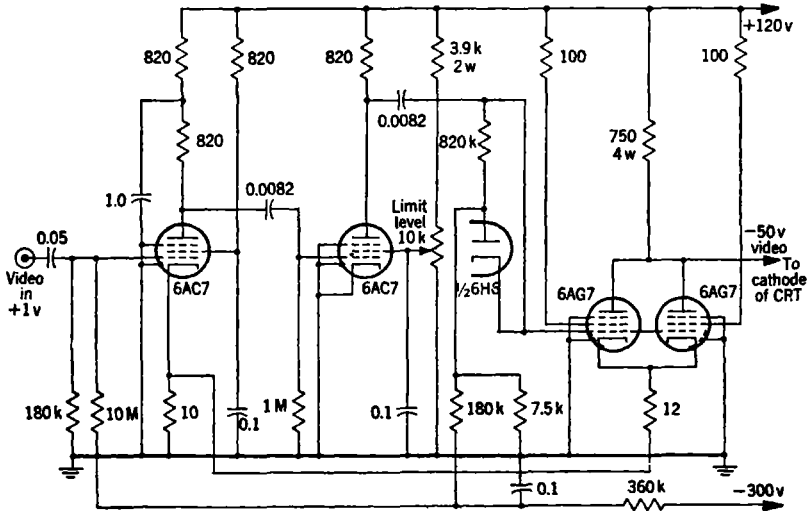


Fig. E·1.—Simple video amplifier with feedback.

731
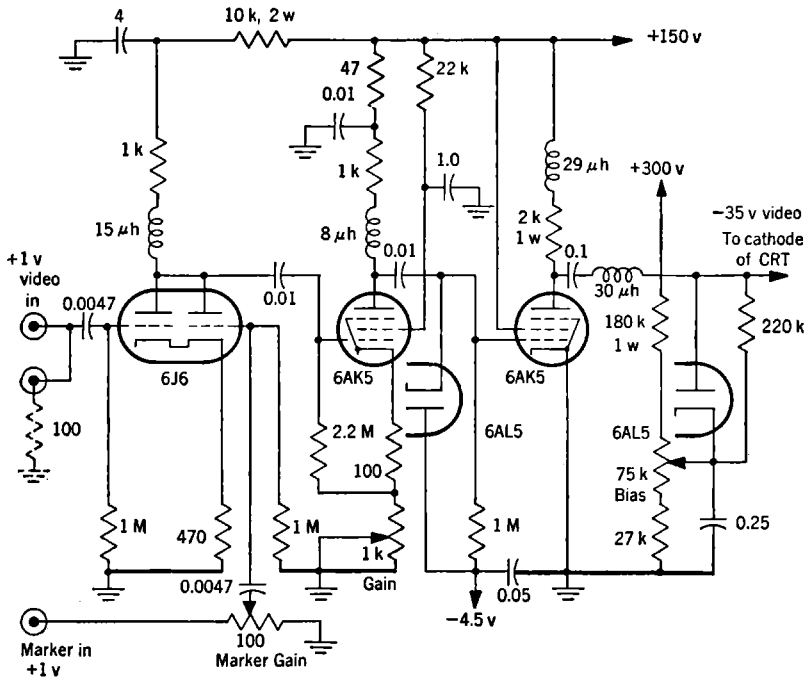
FIG. E-2.—Shunt-peaked amplifier.
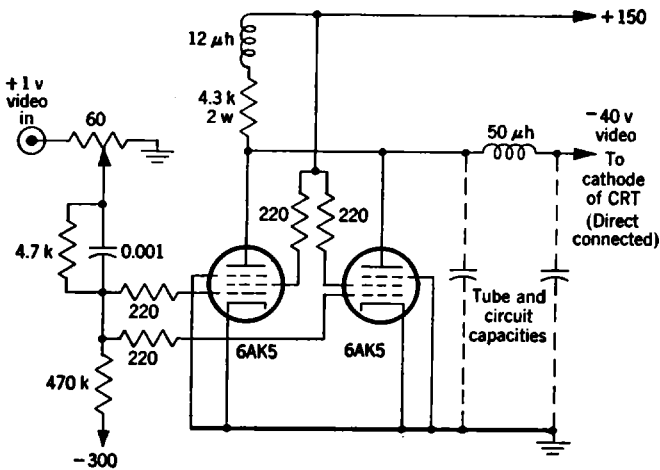


FIG. E-3.—Low-capacity tubes mounted at cathode-ray tube.
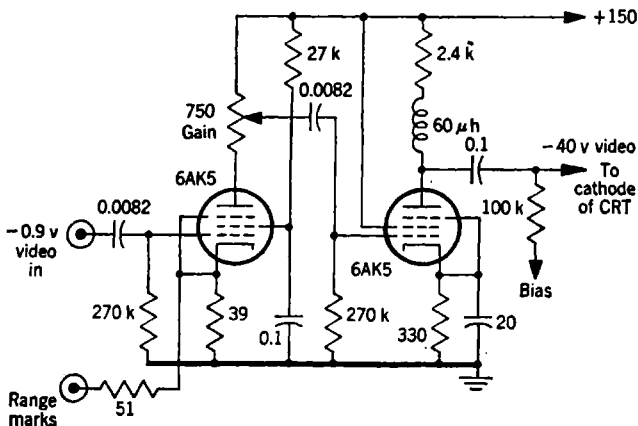
Fig. E·4.—Amplifier with two input channels.
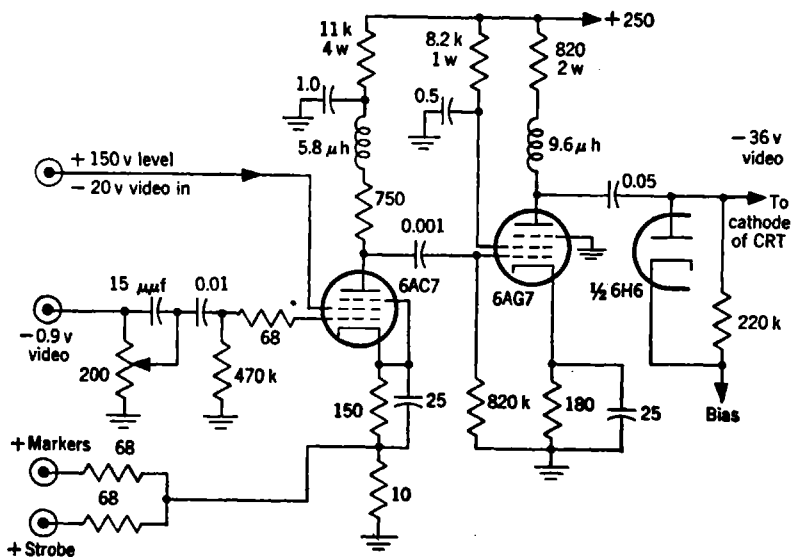


Fig. E·5.—Amplifier with three input channels.
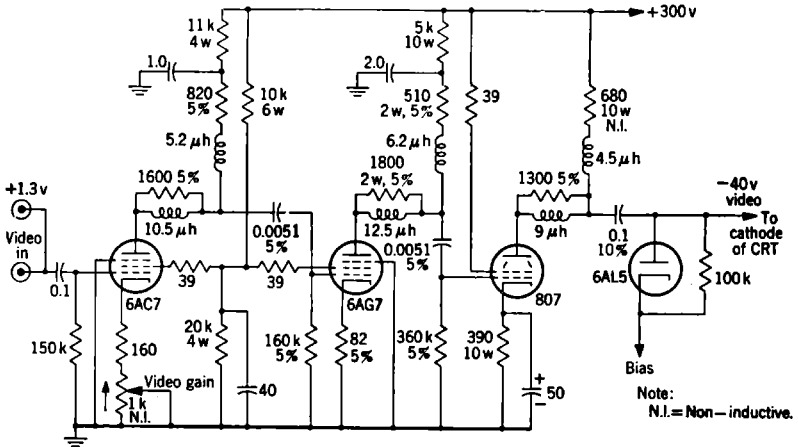
FIG. E·6.—Shunt and series peaking to obtain wide pass band with high gain.
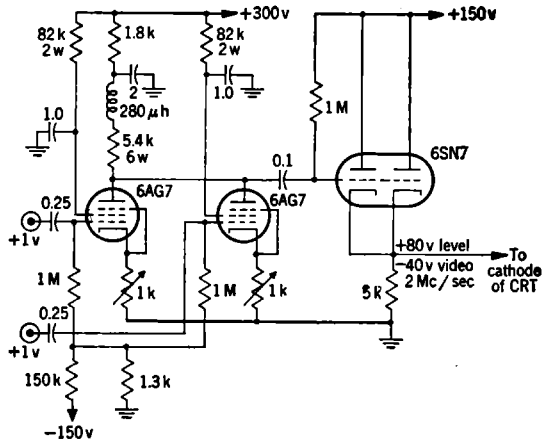


FIG. E·7.—Two identical amplifiers with common plate for mixing, cathode-follower low-impedance output.

FIG. E·8.—Push-pull output with single-ended input.

# *Index*